

**ADIWES INTERNATIONAL SERIES
IN THE PHYSICAL SCIENCES**

This book is in the
ADDISON-WESLEY SERIES IN
ADVANCED CHEMISTRY
Sidney Golden, Consulting Editor

Chemical Kinetics of Gas Reactions

BY

V. N. KONDRA'TEV

*Member of the Academy of Sciences
of the U.S.S.R.*

TRANSLATED FROM THE RUSSIAN

BY

J. M. CRABTREE

AND

S. N. CARRUTHERS

TRANSLATION EDITED BY

N. B. SLATER

*Professor of Applied Mathematics
University of Hull*

PERGAMON PRESS

OXFORD · LONDON · NEW YORK · PARIS

ADDISON-WESLEY PUBLISHING COMPANY INC.

READING, MASSACHUSETTS · PALO ALTO · LONDON

Copyright © 1964
PERGAMON PRESS LTD.

U.S.A. edition distributed by
ADDISON-WESLEY PUBLISHING COMPANY INC.
READING, MASSACHUSETTS . PALO ALTO . LONDON

This edition translated from
Kinetika Khimicheskikh Gazovkh Reaktsii
by V. N. Kondrat'ev, published by the Academy of Sciences
of the U.S.S.R., Moscow

Library of Congress Catalog Card. No. 62-11554

Set in Monotype Times 10 on 12 pt. and printed in Great Britain by
J. W. Arrowsmith Ltd., Bristol

FOREWORD

THIS monograph on the chemical kinetics of gas reactions is a survey of the present state of this important and rapidly developing branch of physical and theoretical chemistry. Not only to thermal reactions, but also photochemical reactions, reactions taking place in electrical discharge and, in part, radiation chemical reactions are discussed. The large amount of material that is continuously being accumulated in gas kinetics requires synthesizing in order to clarify progress in the various fields and to prepare the way for further developments. This task of synthesis—the main purpose of the monograph—has not always been fully accomplished. In certain cases the author has had to limit himself as far as possible to an objective account of points which require fuller experimental and theoretical treatment. This approach is a result of a critical survey of the available data, which reveals definite inadequacies in certain standard ideas and methods of treatment of the chemical processes.

This particularly applies to the elementary chemical process in thermal reactions, which is considered in a separate chapter of the monograph and a considerable part of other chapters. The elementary processes of photochemical reactions and electrical discharge reactions are considered in appropriate chapters in which special attention is given to photochemical and electrical activation of molecules.

It must be observed that the elementary chemical process or "act of reaction," has been insufficiently studied experimentally and theoretically. The activated complex theory as applied to reaction taking place without activation, where the very idea of the activated complex loses its usual meaning, is particularly unsatisfactory. The experimental investigation of the nature and rate of the elementary processes in the overwhelming majority of reactions is also in an unsatisfactory condition.

Further, a more detailed study is still needed of the theory of unimolecular reactions, especially the problem of activation and deactivation of molecules during collisions, and the problem of conservation of the Maxwell-Boltzmann energy distribution in reacting gases.

The modern theory of chain reactions is complete and logical in its formal kinetic part, but in applications to the chemical mechanism of particular reactions it has met with a series of difficulties. This is a result of the inadequate study of such questions as the role of the heterogeneous factor in the propagation of chain reactions, the nature of homogeneous catalysis and

degenerate branching, and the rates of individual elementary processes. All these points require further experimental study.

It is clear that both the kinetics and mechanism of combustion reactions with regard to the theory of flame propagation, and also the problem of equilibria in flames are in an unsatisfactory state.

This English edition is somewhat different from the Russian. Since the manuscript of the latter went to press much work has appeared in the literature supplementing, and more accurately defining, the facts and ideas discussed in this monograph; as far as possible this work has been taken into account in preparing the new edition. Certain inaccuracies and errors in the first edition have also been corrected. Finally the author has tried to make the account more compact. All this has required a series of changes which should improve the account of many problems.

The third chapter of the monograph, and also small sections of the fourth, fifth, sixth and eighth chapters were written by N. D. Sokolov.

V. N. KONDRAT'EV.

Professor Kondrat'ev also added a considerable amount of further new material when we were going through the typescript of the translation. The corresponding additional references to recent literature have been placed in the body of the text.

N. B. SLATER.

CHAPTER 1

GENERAL KINETIC RULES FOR CHEMICAL REACTIONS

§1. Rate of Reaction. Kinetic Types of Simple Reactions

Rate of Reaction

The rate of a chemical reaction is determined by the change in concentration of the reacting substances (or reaction products) with time. Concentration is usually measured by v , the number of moles of the given substance, divided by the volume V in cm^3 , i.e. as the quantity

$$c = \frac{v}{V} \text{ moles/cm}^3 \quad (1.1)$$

or by the number of molecules in unit volume

$$n = cN_A \text{ molecules/cm}^3 \quad (1.2)$$

($N_A = 6.02 \times 10^{23}$ molecules per mole, namely Avagadro's number). Sometimes the concentration is measured by the number of grams of the given substance in unit volume, i.e. the density

$$\rho = mn = cM \quad (1.3)$$

(m is the mass of a molecule of the substance, $M = mN_A$ is its molecular weight), and sometimes by the partial pressure of the substance, namely

$$p = nkT = cRT = \frac{\rho}{M}RT. \quad (1.4)$$

Suppose the concentration of any one of the reacting substances is c at a certain time t and at the next moment of time $t + \Delta t$ is $c + \Delta c$; then the mean rate of reaction for the time interval t to $t + \Delta t$ can be expressed by the quantity

$$\bar{w} = -\frac{\Delta c}{\Delta t}.$$

The rate of reaction at a given moment of time is given by the limit to which this expression converges when $\Delta t \rightarrow 0$:

$$w = -\frac{dc}{dt}. \quad (1.5)$$

If the rate of reaction is measured by the change in concentration c' of any one of the reaction products, then instead of (1.5) we have

$$w = \frac{dc'}{dt}. \quad (1.6)$$

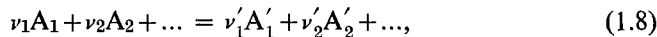
Expressions (1.5) and (1.6) represent the change in concentration per unit volume. The change in amount of a given substance in the total volume V (in unit time) is called the *overall rate of reaction* and is defined by the equation

$$W = - \int \frac{dc}{dt} dV, \quad (1.7)$$

which, if the reaction rate is uniform throughout every part of the volume considered, reduces to the form

$$W = - \frac{dc}{dt} V = wV. \quad (1.7a)$$

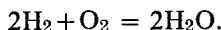
The rate of a reaction may also be measured by the change in concentration of any of the reaction products. Let us consider the reaction of the substances A_1, A_2, \dots (initial substances) being converted into substances A'_1, A'_2, \dots (reaction products). This reaction may be written down in the following form, which is known as the stoichiometric equation:



or

$$\sum v_i A_i = \sum v'_k A'_k. \quad (1.8a)$$

The quantities v_i and v'_k are called the *stoichiometric coefficients of the reaction* and are numbers proportional to the number of moles of the corresponding initial substance (v_i) consumed in the reaction and to the number of moles of the corresponding reaction product formed (v'_k).⁽¹⁾ Thus the stoichiometric equation for the formation of water from its elements may be written in the form



Then the stoichiometric coefficients of hydrogen, oxygen and water will be⁽²⁾

$$v_{H_2} = 2, v_{O_2} = 1 \text{ and } v_{H_2O} = 2.$$

(1) The stoichiometric coefficients are also proportional to the volumes of the reacting substances (and reaction products) $v_i(v'_k)$. In fact, assuming $p_i V = Pv_i$ (P is the overall pressure), since $p_i V = v_i RT$ and $PV = \sum v_i RT$, we have $v_i = (\sum v_i/V)v_i$, i.e. $v_i \sim v_i$. The symbol \sim here and elsewhere is used to denote proportionality.

(2) Writing the equation for the reaction in the form $H_2 + \frac{1}{2}O_2 = H_2O$, we obtain different values for the stoichiometric coefficients, namely $v_{H_2} = v_{H_2O} = 1$ and $v_{O_2} = \frac{1}{2}$.

A mixture containing two moles (or two volumes) of hydrogen to one mole (volume) of oxygen, or in the general case the number of moles of the initial substances being in the ratio $v_1:v_2:\dots$, is called a *stoichiometric mixture* and the initial concentrations of the initial substances in such a mixture are called the *stoichiometric concentrations*. In the case of a stoichiometric mixture, in contrast to a mixture of different composition (for example, an equimolecular mixture H_2+O_2), practically complete conversion of all the initial substances into reaction products is often possible under definite reaction conditions.

From the above stoichiometric relation between the coefficients v_i and v'_k of the reaction, it follows that the change in concentration of the initial substances and the resulting change in concentration of the reaction products must be proportional to the corresponding stoichiometric coefficients, i.e.

$$-\Delta c_1 : -\Delta c_2 : \dots : \Delta c'_1 : \Delta c'_2 : \dots = v_1 : v_2 : \dots : v'_1 : v'_2 : \dots ;$$

from which it follows that

$$-\frac{\Delta c_i}{v_i} = \frac{\Delta c'_k}{v'_k},$$

which allows us to express the rate of reaction in the form

$$w = w_i = w_k = -\frac{1}{v_i} \frac{dc_i}{dt} = \frac{1}{v'_k} \frac{dc'_k}{dt}. \quad (1.9)$$

The expressions (1.9) differ from (1.5) and (1.6) only by the constant factor $1/v_i$ or $1/v'_k$, and therefore each of them is a measure of the rate of this reaction. It follows from (1.9) that determination of the reaction rate as a change in concentration of any one of the initial substances or reaction products, which is related to the corresponding stoichiometric coefficient, is independent of the substance chosen and leads to the same value for the reaction rate.

The rate of a given chemical reaction depends on the concentration of the reacting substances, the temperature and pressure, the physical and chemical properties of the environment (for example, the properties of the solvent in the case of reactions taking place in solution), and on other conditions. The relationship between rate of reaction and concentration of the reacting substances is given by the *law of mass action*. According to this law, first clearly formulated by Guldberg and Waage [36] (1867), the rate of a chemical reaction is directly proportional to the product of the concentrations of the reacting substances; this gives for the reaction expressed by the stoichiometric equation (1.8)

$$w = kc_1^{v_1} c_2^{v_2} \dots = k \prod_i c_i^{v_i}. \quad (1.10)$$

The coefficient of proportionality k is called the *reaction rate constant* or the *specific reaction rate*, i.e. the rate for unit concentration of each of the reacting substances.

Independently of Guldberg and Waage the law of mass action was obtained by Pfaundler [36] (1867) by means of a calculation of the number of collisions between molecules on the basis of the kinetic theory of gases. According to this theory, the number of simultaneous collisions of v_1 molecules of substance A₁ (concentration c_1) with v_2 molecules of substance A₂ (concentration c_2) and so on, is proportional to the product $c_1^{v_1} c_2^{v_2} \dots$, i.e. to the quantity (1.10). Hence it is possible to come to the converse proposition: the rate of a reaction taking place in *one step*, and consisting of the simultaneous interaction of $v_1 + v_2 + \dots = v$ molecules on their collision, must be expressed by the law of mass action. We shall call such reactions *simple reactions*. Accordingly, simple reactions may be defined as reactions whose rates are expressed by the law of mass action. However, as we shall see below, this indication of the simplicity of a reaction is necessary but not in itself sufficient, as not infrequently there are cases when the law of mass action is obeyed by reactions taking place in several steps (*complex reactions*).

The number v of molecules taking part simultaneously in a reaction determines its *stoichiometric order*. When $v = 1$ the reaction is *first order*, when $v = 2$, *second order*, when $v = 3$, *third order*, etc. According to the "natural classification of reactions" put forward by van't Hoff [36] (1884), reactions of first order are called *unimolecular*, reactions of second order *bimolecular*, of third order *termolecular*.

The order of a reaction is determined experimentally by studying the dependence of reaction rate on the concentration of each of the reacting substances. One or another variant of the following method is used. The concentration of one of the substances, for example substance A₁, is made small compared to the concentrations of the other substances, i.e. $c_1 \ll c_2, c_3, \dots$. In this case the concentrations of the substances taken in excess are practically constant throughout the course of the reaction and the reaction rate may be written as $w_1 = k_1 c_1^{v_1}$, where

$$k_1 = k c_2^{v_2} c_3^{v_3} \dots = \text{const.}$$

Measuring the values of w_1 for various concentrations c_1 (and at constant concentrations of the remaining substances A₂, A₃, ...) a value for v_1 is found and is called the *order of the reaction with respect to substance A₁*. Furthermore, for a reaction with $c_2 \ll c_1, c_3, \dots$ by measuring the reaction rate $w_2 = k_2 c_2^{v_2}$ ($k_2 = k c_1^{v_1} c_3^{v_3} \dots = \text{const}$) for various concentrations c_2 , the order of the reaction with respect to substance A₂, equal to v_2 , is obtained, and so on. In consequence the *absolute* or *overall* order of the reaction $v = v_1 + v_2 + \dots$ is found [859, 871a, 1033a].

Often there are cases where the actual (kinetic) order of reaction does not coincide with its stoichiometric order found from the stoichiometric equation of the reaction. As we shall see later, non-coincidence of the actual order of a reaction with the stoichiometric order is evidence of the non-applicability of the law of mass action, i.e. of a *complex mechanism* for the reaction, due to its *multistage character*. The following are examples of reactions whose actual and stoichiometric orders do not coincide. According to the stoichiometric equations $2\text{N}_2\text{O} = 2\text{N}_2 + \text{O}_2$ and $2\text{N}_2\text{O}_5 = 2\text{N}_2\text{O}_4 + \text{O}_2$, the decompositions of nitrous oxide N_2O and nitrogen pentoxide N_2O_5 should be second order reactions but in fact they are first order. Also the reaction $\text{H}_2 + \text{Br}_2 = 2\text{HBr}$ has stoichiometric order 2 but its actual order is 3/2. A fractional order of a reaction is itself a rather frequent occurrence. Finally, reactions are known whose order with respect to some of the reacting substances is negative. For example, the rate of oxidation of acetylene falls with increasing oxygen concentration [1171].

Kinetic Types of Simple Reactions

Leaving aside for the present these and similar complex reactions, let us consider the kinetic rules which govern simple reactions of various orders. Since we have in view formal kinetic rules, i.e. rules which do not touch on the actual mechanism of a reaction, we may also include in this survey such reactions whose actual order differs from the stoichiometric order.

According to the law of mass action the rate of a first order reaction is expressed by the formula

$$w = -\frac{dc}{dt} = kc. \quad (1.11)$$

Integrating (1.11) and denoting the initial concentration at $t = 0$ by c_0 , we obtain

$$c = c_0 \exp(-kt) = c_0 \exp(-t/\tau). \quad (1.12)$$

The quantity

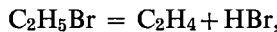
$$\tau = 1/k \quad (1.13)$$

is known as the *characteristic time of the reaction*; in a time τ the concentration of the reacting substance decreases by a factor e .

From (1.12) we obtain an expression for the rate constant of a first order reaction

$$k = \frac{1}{t} \ln \frac{c_0}{c} \text{ sec}^{-1}. \quad (1.14)$$

Examples of first order reactions are the unimolecular decomposition of ethyl bromide C_2H_5Br taking place according to the equation



and of vinyl bromide C_2H_3Br with the equation



[293]. Another example is the decomposition of a saturated molecule into a molecule and a biradical or into two radicals: the decomposition of nitrous oxide N_2O into N_2 and an O atom (see p. 313 *et seq.*) and the decomposition of a molecule of ethyl chloride C_2H_5Cl into a C_2H_5 radical and a Cl atom [293]. Yet another example is the unimolecular decomposition of a radical: $C_3H_7 = CH_3 + C_2H_4$ [907].

We may note that examples of processes which follow the first order reaction law (1.12) are furnished by the predissociation of a molecule, and also by a series of physical processes such as the radiation of light from an excited atom or molecule, or radioactive alpha- and beta-decay.

The rate of a second order reaction is given by the formula

$$w = -\frac{dc_1}{dt} = -\frac{dc_2}{dt} = kc_1c_2. \quad (1.15)$$

On integrating (1.15) with the initial conditions $c_1 = c_1^0$ and $c_2 = c_2^0$ when $t = 0$, we obtain

$$c_1 = c_1^0 \frac{(c_2^0 - c_1^0) \exp[-(c_2^0 - c_1^0)kt]}{c_2^0 - c_1^0 \exp[-(c_2^0 - c_1^0)kt]}$$

and

$$c_2 = c_2^0 \frac{c_2^0 - c_1^0}{c_2^0 - c_1^0 \exp[-(c_2^0 - c_1^0)kt]}. \quad (1.16)$$

From (1.16) we find

$$\frac{c_1}{c_2} = \frac{c_1^0}{c_2^0} \exp[-(c_2^0 - c_1^0)kt], \quad (1.17)$$

and hence

$$k = \frac{1}{t} \frac{1}{c_2^0 - c_1^0} \ln \frac{c_2c_1^0}{c_2^0c_1} \text{ cm}^3 \text{ sec}^{-1}. \quad (1.18)$$

In the particular case where $c_1^0 = c_2^0 = c^0$ and consequently $c_1 = c_2 = c$, the equation (1.15) takes the form

$$w = -\frac{dc}{dt} = kc^2. \quad (1.19)$$

Integrating this equation we obtain

$$\frac{1}{c} = \frac{1}{c^0} + kt \quad (1.20)$$

and

$$k = \frac{1}{c^0 t} \left(\frac{c^0}{c} - 1 \right) \text{ cm}^3 \text{ sec}^{-1}. \quad (1.21)$$

Equation (1.15) may also be reduced to (1.19) in the general case when $c_1 \neq c_2$. In fact, expressing c_2 in terms of c_1 using equation (1.17) and writing

$$\frac{c_2^0}{c_1^0} \exp\{(c_2^0 - c_1^0)kt\} dt = d\theta, \quad (1.22)$$

we may put (1.15) in the form

$$-\frac{dc_1}{d\theta} = kc_1^2$$

similar to (1.19). Integrating this equation, we find

$$\frac{1}{c_1} = \frac{1}{c_1^0} + k\theta$$

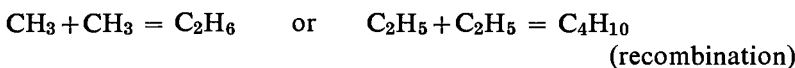
and

$$k = \frac{1}{c_1^0 \theta} \left(\frac{c_1^0}{c_1} - 1 \right),$$

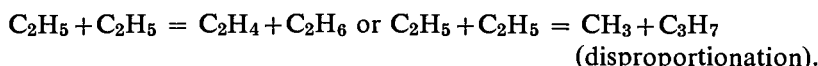
which are formulae similar to (1.20) and (1.21). Substituting in them the quantity θ on the basis of (1.22) (or using (1.22) directly) we may express θ in terms of t by the formula

$$\theta = \frac{1}{k} \frac{c_2^0}{c_1^0} \frac{1}{c_2^0 - c_1^0} \{ \exp [(c_2^0 - c_1^0) kt] - 1 \}.$$

An example of a second order reaction is the reaction $\text{H}_2 + \text{I}_2 = 2\text{HI}$ (see Table 20). This reaction is one of the few adequately studied bimolecular gas reactions between saturated molecules. One of the less studied reactions is the decomposition of gaseous nitrosyl chloride $2\text{NOCl} = 2\text{NO} + \text{Cl}_2$ (see Table 20). The recombination and disproportionation of radicals are also second order reactions and are very important in the kinetics of radical reactions, for example:



and



We shall now consider third order reactions. In the general case the expression for the rate of a third order reaction has the form

$$w = -\frac{dc_1}{dt} = -\frac{dc_2}{dt} = -\frac{dc_3}{dt} = kc_1c_2c_3. \quad (1.23)$$

Without solving these equations for the general case we shall limit ourselves to the particular case of the reaction $A_1 + 2A_2$ with a stoichiometric ratio of the reagent concentrations so that $c_3 = c_2 = c$ and $c_1 = c/2$. Integrating the equation obtained in this case, namely,

$$w = -\frac{dc}{dt} = kc^3, \quad (1.24)$$

we obtain

$$\frac{1}{c^2} = \frac{1}{c_0^2} + 2kt, \quad (1.25)$$

and hence

$$k = \frac{1}{2c_0^2 t} \left(\frac{c_0^2}{c^2} - 1 \right) \text{ cm}^6 \text{ sec}^{-1}. \quad (1.26)$$

The termolecular reaction $O_2 + 2NO = 2NO_2$ may serve as an example of a third order reaction.⁽³⁾ In Chapter 5 we shall deal with another process, triple or *ternary collision*, which is basically a gas-phase combination of atoms, e.g. $H + H + M = H_2 + M$ (M denotes any molecule taking part in the triple collision but not entering into the reaction). Since in the latter case the concentration of M molecules remains unchanged, it is possible to include it in the rate constant, setting $k' = kc_M$, which leads to an apparently bimolecular law for the rate of the reaction, namely

$$w = -\frac{1}{2} \frac{dc_H}{dt} = k'c_H^2.$$

The actual termolecular law for the reaction may be clearly established by the dependence of the "bimolecular constant" k' on the concentration c_M .

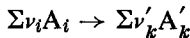
§2. Chemical Equilibrium

Equilibrium Constant

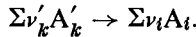
In the preceding paragraph we tacitly assumed that each of the reactions studied went only in one direction. However every elementary reaction is *reversible*, i.e. it can also go in the reverse direction. In other words,

⁽³⁾ In Table 19 there is the reverse of this reaction, the bimolecular reaction $2NO_2 = 2NO + O_2$.

together with the *forward reaction* corresponding to the stoichiometric equation (1.8a)



(the arrow indicates the direction of the reaction), its *reverse reaction* also takes place, corresponding to the equation



Combining both these formulae, we obtain



Considering both reactions (forward and reverse) and expressing the rate of each of them in terms of the law of mass action in the form (1.9), we obtain the following expression for the overall reaction rate:

$$w = -\frac{1}{\nu_i} \frac{dc_i}{dt} = \frac{1}{\nu'_k} \frac{dc'_k}{dt} = kc_1^{\nu_1} c_2^{\nu_2} \dots - k' c'_1^{\nu'_1} c'_2^{\nu'_2} \dots \quad (2.2)$$

In (2.2) k and k' are the rate constants for the forward and reverse reactions respectively.

Each of these constants, generally speaking, can be measured independently. Actually, if we take A_1, A_2, \dots as the initial substances, in the first phase of the reaction (when the reaction products have not yet accumulated in noticeable quantities) the reaction rate will be

$$w = -\frac{1}{\nu_i} \frac{dc_i}{dt} = kc_1^{\nu_1} c_2^{\nu_2} \dots$$

By measuring this quantity it is possible to determine k . It is possible, however, to take the products of the forward reaction A'_1, \dots as the initial substances. In this case the reaction rate in the first phase will be

$$w = -\frac{1}{\nu'_k} \frac{dc'_k}{dt} = k' c'_1^{\nu'_1} c'_2^{\nu'_2} \dots$$

The rate constant for the reverse reaction k' may be found from this equation.

The last two equations give approximately the rates of the forward and reverse reactions only for the initial phase of the corresponding reaction. An exact expression for the reaction rate, valid for any moment of time, is given by the expression (2.2). It follows from this equation that the rate of reaction has a *maximum value* when $t = 0$, when there are no reaction products present in the system. As time passes, owing to the decrease in concentrations of the initial substances (c_1, c_2, \dots) and the increase in concentrations of the reaction products (c'_1, c'_2, \dots), the rate of reaction steadily decreases, converging to the limiting value $w = 0$. This limit is

reached when the rate of the reverse reaction becomes equal to the rate of the forward reaction and indicates the establishment of *equilibrium* between the initial substances and the reaction products. Denoting the *equilibrium concentrations* by the capital letters C_i and C'_k , we find from the *equilibrium condition* that

$$w = - \frac{1}{v_i} \frac{dc_i}{dt} = 0, \quad (2.3)$$

or

$$k C_1^{v_1} C_2^{v_2} \dots = k' C_1'^{v'_1} C_2'^{v'_2} \dots \quad (2.3a)$$

We shall introduce the quantity

$$K_c = \frac{k}{k'} = \frac{C_1'^{v'_1} C_2'^{v'_2} \dots}{C_1^{v_1} C_2^{v_2} \dots} = \frac{\prod C_k'^{v_k}}{\prod C_i^{v_i}}. \quad (2.3b)$$

The quantity K_c is called the *equilibrium constant*. From the first and second laws of thermodynamics it can be shown that the equilibrium constant is a function of both temperature and the heat of reaction Q .

It follows from many experiments that the equilibrium state, which is characterized by the *definite values* of the equilibrium concentrations, is

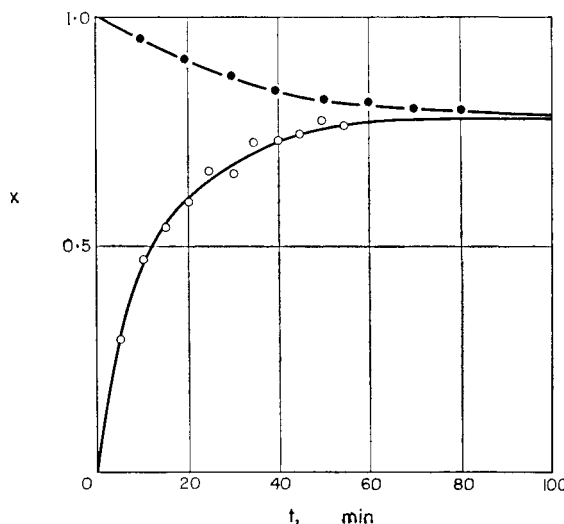


FIG. 1. The formation and decomposition of hydrogen iodide HI according to Bodenstein [414]:

$$x = \frac{(HI)}{(HI) + 2(I_2)}; \quad 448^\circ C;$$

lower curve: formation of HI; upper curve: decomposition of HI.

reached in approaching equilibrium both from the side of the initial substances (A_1, A_2, \dots) and also from the side of the final substances (A'_1, A'_2, \dots) (provided the initial concentrations in both cases correspond to the same number of atoms of each given sort). The simplest reaction here is the reaction $H_2 + I_2 = 2HI$ studied by Bodenstein [414] (1894-98). The course of this reaction in the directions from $H_2 + I_2$ to HI and from HI to $H_2 + I_2$ is shown in Fig. 1. It is clear that in each case, with the attainment of equilibrium, a mixture is formed containing the same amounts of H_2 , I_2 and HI (corresponding to the equilibrium $H_2 + I_2 \rightleftharpoons 2HI$ at the temperature of the experiment).

This result follows directly from a consideration of the kinetic equation of the reaction. In fact, using the general expression for the reaction rate⁽⁴⁾

$$w = \frac{1}{2} \frac{d(HI)}{dt} = - \frac{d(H_2)}{dt} = - \frac{d(I_2)}{dt} = k(H_2)(I_2) - k'(HI)^2$$

(k and k' are the rate constants for the forward and reverse reactions), and the equations for the rate of formation of HI in the mixture, which originally contained only H_2 and I_2 , namely

$$(HI) = 2(H_2)_0 - 2(H_2) = 2(I_2)_0 - 2(I_2)$$

(the subscript 0 denotes initial concentrations) we obtain

$$\frac{1}{2} \frac{d(HI)}{dt} = \frac{1}{2} k [2(H_2)_0 - (HI)] [2(I_2)_0 - (HI)] - k'(HI)^2$$

Similarly, for the rate of decomposition of HI , from the equations

$$(HI)_0 - (HI) = 2(H_2) = 2(I_2)$$

we have

$$-\frac{1}{2} \frac{d(HI)}{dt} = k'(HI)^2 - \frac{k}{4} [(HI)_0 - (HI)]^2.$$

It is not difficult to see that when $(H_2)_0 = (I_2)_0$ and $(H_2)_0 + (I_2)_0 = (HI)_0$, i.e. when the numbers of H and I atoms in the system are equal, both the foregoing expressions for the reaction rate coincide. Hence it follows that in both cases the same equilibrium concentration of hydrogen iodide is obtained, namely

$$(HI)_{eq} = (HI)_0 / (1 + 2K^{1/2}), \quad K = k'/k$$

(and consequently the equilibrium concentrations of H_2 and I_2 also); this is determined by the *equilibrium condition*

$$\frac{d(HI)}{dt} = 0.$$

⁽⁴⁾ (H_2) , (I_2) , (HI) denote the concentrations of H_2 , I_2 , and HI respectively, expressed in molecules per cm^3 (n_{H_2} , n_{I_2} , n_{HI}).

Introducing the notations $a = (\text{HI})_0$, $x = (\text{HI})/a$ and $\gamma = 2akK^{1/2}$, we may write the foregoing equation in the form

$$-4K^{1/2}\gamma^{-1}(dx/dt) = 4Kx^2 - (1-x)^2. \quad (2.4)$$

Carrying out the integration under the initial conditions that $x = 0$ when $t = 0$ in the case of the forward reaction $\text{H}_2 + \text{I}_2 = 2\text{HI}$, and $x = 1$ when $t = 0$ in the case of the reverse reaction $2\text{HI} = \text{H}_2 + \text{I}_2$, for the two reactions we find

$$x = \frac{f(t)}{f(t) + 2K^{1/2}} \quad (\text{forward reaction}) \quad (2.5)$$

and

$$x = [1 + 2f(t)K^{1/2}]^{-1} \quad (\text{reverse reaction}), \quad (2.6)$$

where

$$f(t) = [1 - \exp(-\gamma t)]/[1 + \exp(-\gamma t)] = \tanh(\frac{1}{2}\gamma t). \quad (2.7)$$

Introducing the equilibrium constant for hydrogen iodide

$$(\text{HI})_{\text{equilib}} = ax_e = a/(1 + 2K^{1/2}),$$

the expressions obtained for x may also be put in the form

$$x = x_e \frac{f(t)}{1 - x_e + x_e f(t)} \quad (2.5a)$$

and

$$x = x_e \frac{1}{(1 - x_e)f(t) + x_e}. \quad (2.6a)$$

It can be seen from these equations that when $t \rightarrow \infty$, since $f(\infty) = 1$, both the limiting values of x are equal to the equilibrium value x_e .

The relative concentrations of HI (2.5a) and (2.6a) as functions of the quantity $f(t)$ for $x_e = 0.786$ (corresponding to $T = 448^\circ\text{C}$) are shown graphically in Fig. 2. A comparison of Figs. 1 and 2 shows their close agreement.

Equilibrium constants are usually determined experimentally by measuring the equilibrium concentrations. The rate constants for the forward and reverse reactions may be determined from the reaction rate in the initial phase of the reaction (see p. 9). Moreover, if the equilibrium constant is known, the rate constants may be calculated from the measured values for x at different times. Thus, we obtain the following expression from formula (2.4) for calculation of the constants k and k' :

$$k' = Kk = (K^{1/2}/2at) \ln \frac{1 + (2K^{1/2} - 1)x}{1 - (2K^{1/2} + 1)x}. \quad (2.8)$$

The values of $\log k$ and $\log k'$ as functions of $1/T$, calculated from equation (2.8), are shown in Fig. 3.

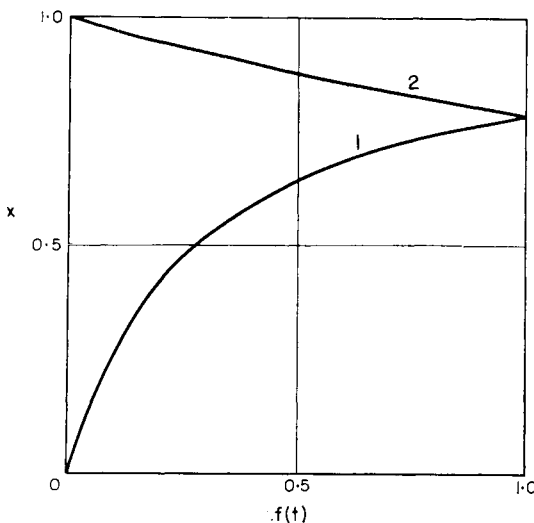


FIG. 2. The formation and decomposition of hydrogen iodide as functions of the quantity $f(t)$ at 448°C (see text, p. 12).
(1) Formation of HI; (2) decomposition of HI.

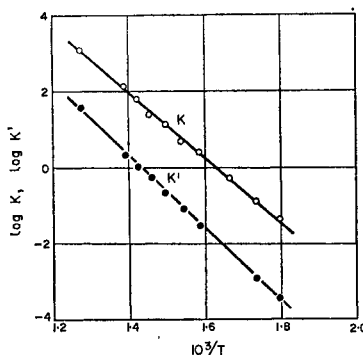


FIG. 3. The temperature dependence of the reaction rate constants for the formation (k) and decomposition (k') of hydrogen iodide HI (according to Bodenstein [414]).

The fact that the equilibrium concentrations are independent of the side from which equilibrium is approached has a basis in thermodynamics, according to which equilibrium is reached when the free energy of the reaction products becomes equal to the free energy of the initial substances. This condition, as well as the kinetic condition for equilibrium that the rate of the overall reaction should be zero, is clearly independent of the direction of approach to equilibrium.

The Arrhenius Equation

The equilibrium constant is an exponential function of temperature. As first realized by van't Hoff (1884) there is also an exponential relation between temperature and the rate constant of a reaction. Actually, following van't Hoff, we may assume that the quantity Q (the heat of reaction) in the formula

$$\frac{d \ln K}{dT} = -\frac{Q}{RT^2}$$

is equal to the difference between certain quantities E and E' , i.e.

$$Q = E' - E, \quad (2.9)$$

which allows us to rewrite the formula, since $K = k/k'$, in the form of the two following formulae

$$\frac{d \ln k}{dT} = \frac{E}{RT^2} + b \quad \text{and} \quad \frac{d \ln k'}{dT} = \frac{E'}{RT^2} + b. \quad (2.10)$$

If we assume that the quantities b and E are not dependent, or are only weakly dependent, on temperature, then an approximately exponential relationship between the rate constants of the forward (k) and reverse (k') reactions and temperature, which takes the form $k \sim \exp(-E/RT)$, is obtained from these formulae.

Such a relationship was actually established experimentally for a series of reactions by van't Hoff himself and also by certain of his predecessors. However the physical idea behind this relationship was discovered by Arrhenius [329] (1889) who gave it a sound interpretation on the basis of kinetic theory. According to Arrhenius only *active molecules* take part in reaction, i.e. molecules which possess a certain excess energy $E(E')$ called the *activation energy*.

Accordingly, Arrhenius proposed a formula of the following type for the rate constant:

$$k = k_0 \exp \left[\frac{E(T - T_0)}{RTT_0} \right]. \quad (2.11)$$

This formula, which may also be written in the simpler form

$$k = A \exp(-E/RT) \quad (2.11a)$$

expresses the *Arrhenius equation*, according to which the rate constant for a simple chemical reaction is an exponential function of temperature. It is not difficult to see that formulae (2.11) and (2.11a) are given by the appropriate van't Hoff formula (2.10) when $b = 0$ and when the quantity E is independent of temperature.

The dependence of the rate of a chemical reaction on temperature is a well-known experimental fact. Usually the reaction rate increases with increase in temperature. As an example, Fig. 3 shows the dependence on temperature of the rates of the forward and reverse reactions $H_2 + I_2 \rightleftharpoons 2HI$ over the temperature range 283–508°C (according to Bodenstein [414]). With the coordinates $\log k$ and $1/T$ the experimental points lie on straight lines, showing that the Arrhenius equation is followed in this case. From the slope of the lines Bodenstein calculated the following values for the energies of activation⁽⁵⁾: E (forward reaction) = 40,000 cal/mole and E' (reverse reaction) = 44,000 cal/mole.

The dependence of reaction rate on temperature is often described by a *temperature coefficient* which is defined as the ratio of the reaction rate constants at two temperatures differing by 10°, i.e. the quantity

$$\eta_T = \frac{k_{T+5}}{k_{T-5}}. \quad (2.12)$$

Calculating the temperature coefficient from formula (2.10) or its equivalent (2.11), we obtain

$$\eta_T = \exp \left[\frac{10E}{R(T^2 - 5^2)} \right] \approx \exp \left[\frac{10E}{RT^2} \right]. \quad (2.13)$$

It can be seen from these formulae that the temperature coefficient of simple reactions must always be greater than 1 (since $E > 0$) and must decrease with an increase in temperature, converging to 1 as $T \rightarrow \infty$. The values of the temperature coefficients of the reaction $H_2 + I_2 \rightarrow 2HI$ at temperatures 600, 650 and 700°K are equal to 1.78, 1.65 and 1.51, respectively.

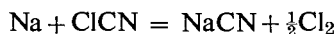
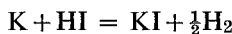
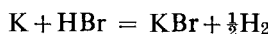
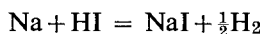
The temperature coefficient of a reaction as defined by formula (2.13) suffers from a definite drawback as a result of its sharp dependence on temperature. For this reason the quantity η , defined by the following formula, is often used as a characteristic of the temperature dependence of a reaction rate:

$$\eta = \frac{d(\ln k)}{d(1/T)} = \frac{E}{R}; \quad (2.14)$$

this also follows from (2.10) or (2.11a). According to formula (2.14) the temperature coefficient η of a reaction is constant to the same extent as the energy of activation E is independent of temperature. In future we shall use both of the quantities η (2.14) and η_T (2.13).

⁽⁵⁾ In future, in the case of all energy quantities referring to molar quantities, instead of cal/mole or kcal/mole we shall write cal or kcal respectively.

The temperature coefficients of different reactions are fairly widely spread. Apparently the largest temperature coefficients belong to certain reactions which have a measurable rate at low temperatures. The value of η_T for these reactions is often between 5 and 7 at room temperature. At the same time the temperature coefficient of some other reactions is 1, so that the rate of reaction is independent of temperature, and E is zero. Examples of such "inertia-less" or "activationless" reactions are provided by certain reactions of alkali metal atoms which were studied by Polanyi and his associates [1030]. According to Polanyi's data, the following reactions in particular belong to this type:



and so on (in fact here it is clearly preferable to talk about reactions of low inertia rather than "inertia-less" reactions; see Chapter 2, §6).

An activation energy of zero is clearly only possible for exothermic reactions, i.e. reactions taking place with the evolution of heat, or for thermoneutral reactions. Endothermic reactions must have an activation energy not less than the heat of the reaction (its "endothermicity"). However, exothermic reactions with $E = 0$ and endothermic reactions with $E' = Q$ (Q is the heat absorbed) are quite rare, and the activation energy of exothermic reactions is usually greater than zero. Since $Q = E' - E > 0$ (2.9), we have in this case $E' = E + Q > Q$. The activation energy of a reaction going in an exothermic direction will often be called the *true* (or *exothermic*) *activation energy*. According to (2.9) the activation energy of an endothermic reaction E' is equal to the true energy of activation E plus the "endothermicity" of the reaction, a measure of which is given by the heat of reaction Q .

As we shall see below, even with an energy of activation (which is allowed for by the Arrhenius factor $\exp(-E/RT)$), an actual reaction is by no means an inevitable consequence of every collision of active molecules. The reasons for this non-correspondence between the number of actual reactions and the number of collisions of active molecules will be considered in Chap. 3. The ratio of these two numbers (clearly always less than 1) is called the *steric factor*. In rare cases the steric factor may have a value close to 1.

§3. Complex Reactions

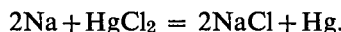
A reaction whose stoichiometric order agrees with its actual order and whose rate obeys the law of mass action is called a *simple* chemical reaction. Accordingly, the decomposition of a molecule into any of its component parts by breaking or redistribution of the intramolecular bonds is always a simple (elementary) reaction of the first order. Similarly, reactions taking place as the result of a collision of two or three molecules, and proceeding in the one direction, are always simple reactions of the second or third order respectively.

Coincidence of the observed order of a reaction with its stoichiometric order is a necessary but not sufficient condition for the reaction to be simple (see p. 43). Any deviation of the observed order of reaction from the stoichiometric order is an indisputable indication that the reaction is not simple but is complex. From the point of view of its internal chemical mechanism, a complex reaction is a *collection* of simple reactions or *elementary processes* following one after the other or taking place in parallel.

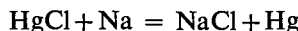
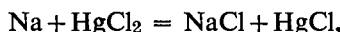
Reactions with Consecutive Steps

A characteristic feature of the kinetics of many complex reactions is the occurrence of two or more steps following one another and for this reason often appearing separate in time. Such reactions may be called *reactions with consecutive steps*. Reactions are clearly two- or many-step reactions if, in the first step a substance is formed which is capable of further chemical change taking place in the subsequent steps. Such substances are called *intermediate substances*.

It is possible to quote a large number of examples of reactions with a clearly defined sequence of individual steps. One of these is the reaction between sodium vapour and mercuric chloride vapour which is observed in the so-called highly-rarefied flames (see §6), namely the reaction



Detailed study of this and similar reactions leads to the conclusion that its *mechanism* is a combination of two consecutive steps



(see pp. 84–85). The two-step nature of these reactions is clearly shown by the existence of *two zones* of reaction: a zone with maximum yield of reaction products and a zone with maximum light yield (see p. 85). The intermediate in this reaction is the univalent radical HgCl .

An example of a more complex reaction with consecutive steps is the

oxidation of acetaldehyde vapour [175]. Figure 4 shows the kinetic curves for this reaction, i.e. graphs of the time-dependence of the partial pressures of the initial substances (acetaldehyde, CH_3CHO , and oxygen) and of the substances formed in the course of the reaction, acetyl hydroperoxide (peracetic acid), CH_3COOOH , and acetic acid, CH_3COOH , and also the

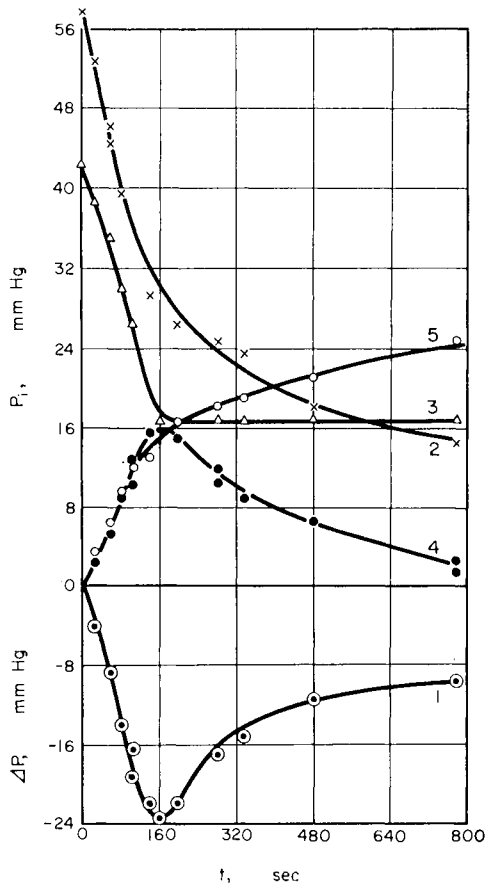
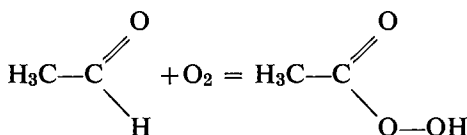


FIG. 4. Kinetic curves for the oxidation of acetaldehyde vapour CH_3CHO (according to Maizus and Emanuel' [176]).

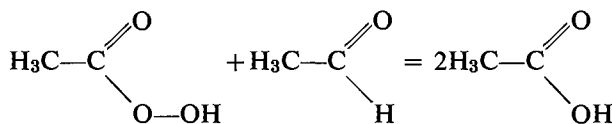
P_0 , 100 mm Hg, 170°C ; 1, ΔP ; 2, CH_3CHO ; 3, O_2 ;
4, CH_3COOOH ; 5, CH_3COOH .

kinetic curve of pressure of the mixture. It is clear from this figure that two steps can be distinguished in the course of the reaction: a step characterized by the consumption of oxygen, fall in pressure and increase in concentration (partial pressure) of the hydroperoxide, and a step characterized by a decrease in this concentration, and an increase in pressure,

taking place with a constant partial pressure of oxygen. It may be concluded from study of the kinetic curves in Fig. 4 that in the first step the main role is played by the reaction



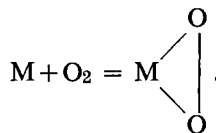
leading to formation of the hydroperoxide, which is the intermediate substance, and in the second step by the reaction



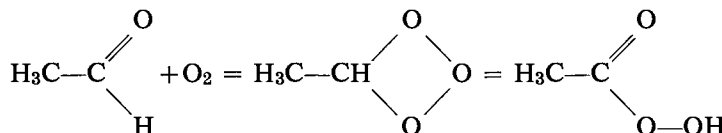
resulting in the conversion of the intermediate into the reaction product—acetic acid.

The drop in pressure in the first step of the reaction results from the fact that this step goes with a decrease in the number of molecules (two molecules—an aldehyde molecule and an oxygen molecule—are converted into one molecule of hydroperoxide and, correspondingly, three molecules—two aldehyde molecules and one oxygen molecule—are converted into two molecules of acetic acid). The second step of the reaction (in the part concerning the conversion of the hydroperoxide to the acid) goes without change in the number of molecules. However, since at the same time as the formation of the acetic acid CH_3COOH in the second step of the reaction, further oxidation takes place leading to the formation of analytically detectable CO , CO_2 and H_2O , this second step is usually accompanied by an increase in pressure because on the whole the number of new molecules formed exceeds the number reacting. The constancy of the oxygen pressure in the second step of the reaction shows that the conversion of the hydroperoxide into acetic acid (and into the products of further oxidation) takes place in this step of the reaction without the participation of free oxygen.

The description of the above reaction scheme for the oxidation of acetaldehyde to the acid formally corresponds to one of the oxidation schemes appearing in the *peroxide oxidation theory* of Bach and Engler [298] (1897). According to this theory the first step of an oxidation reaction is the formation of a “moloxide” MO_2 , which is the product of the direct addition of a molecule of oxygen to the fuel molecule:



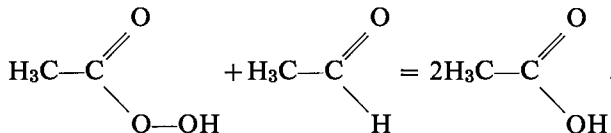
The "moloxide" changes into the usual peroxide as a result of isomerization, for example,



The second step of the oxidation reaction, according to Engler [298], follows the scheme



corresponding in our example to the reaction



Regarding the actual mechanism of the oxidation of acetaldehyde, it may be asserted on the basis of a more detailed study that it does not correspond to the above stoichiometric equations. In particular the formation of acetyl hydroperoxide does not appear to be the result of a simple interaction of acetaldehyde and oxygen. Free radicals play a substantial part in the mechanism of this reaction [39, 939].

As an example of a complex reaction with clearly defined steps let us consider the oxidation of hydrogen occurring in a fast flow. According to the analytical data the products of this reaction are water and hydrogen peroxide; the amount of the latter remaining in the reaction products falls sharply with increase in the time (τ) the mixture spends in the reaction zone, as is particularly clear from Fig. 5 [133]. For sufficiently small times τ the H_2O_2 content reaches 85 per cent, from which it may be concluded that the primary product of oxidation of hydrogen under these experimental conditions is hydrogen peroxide, which is converted into water in subsequent steps of the reaction. The mechanism of the oxidation of hydrogen will be considered later (§38).

To explain the kinetic features of reactions with consecutive steps we shall consider the general case of a reaction which consists first of the conversion of substance A into substance B which in its turn is converted into the reaction product C: $A \rightarrow B \rightarrow C$. The details of the kinetics of

reactions of this type depend of course on their mechanism. However, since we are attempting to obtain the general characteristics of the kinetics of reactions taking place via consecutive steps, we shall confine ourselves to the simplest case in which each of the two reaction steps is itself a unimolecular process. A good example of consecutive processes, each of which obeys a unimolecular law, is given by the processes of radioactive conversion observed in the radioactive series.

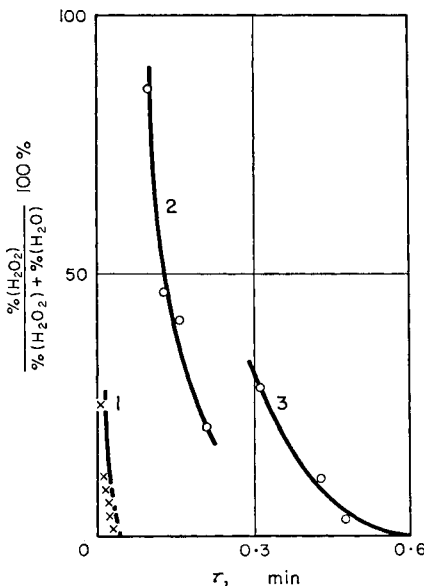


FIG. 5. Dependence of hydrogen peroxide H_2O_2 yield on reaction time τ in the slow oxidation of hydrogen using three different vessels [133].

- (1) Molybdenum glass, $(\text{H}_2)_0 : (\text{O}_2)_0 = 2.45$; 827°K ;
- (2) Pyrex, $(\text{H}_2)_0 : (\text{O}_2)_0 = 1.75$; 823°K ;
- (3) Quartz, $(\text{H}_2)_0 : (\text{O}_2)_0 = 2.50$; 795°K .

Denoting the rate constants for the unimolecular conversion of A into B and B into C by k_1 and k_2 respectively, we may write the equations for the reaction in the form⁽⁶⁾

$$\left. \begin{aligned} -\frac{d(A)}{dt} &= k_1(A), \\ \frac{d(B)}{dt} &= k_1(A) - k_2(B), \\ \frac{d(C)}{dt} &= k_2(B). \end{aligned} \right\} \quad (3.1)$$

⁽⁶⁾ Here (A), (B) and (C) denote the concentrations of the substances A, B, and C.

Further, introducing the symbols $x = (A)/(A)_0$, $y = (B)/(A)_0$ and $z = (C)/(A)_0$, where $(A)_0$ is the original concentration of the initial substance (A), we may rewrite these equations in the simpler form

$$-\frac{dx}{dt} = k_1 x, \quad \frac{dy}{dt} = k_1 x - k_2 y, \quad \frac{dz}{dt} = k_2 y. \quad (3.2)$$

Solving these equations, we obtain

$$\left. \begin{aligned} x &= \exp(-k_1 t), \\ y &= \frac{k_1}{k_2 - k_1} [\exp(-k_1 t) - \exp(-k_2 t)], \\ z &= 1 - \frac{k_2}{k_2 - k_1} \exp(-k_1 t) + \frac{k_1}{k_2 - k_1} \exp(-k_2 t). \end{aligned} \right\} \quad (3.3)$$

When $k_1 = k_2 = k$ these formulae take the simpler form:

$$x = \exp(-t'), \quad y = t' \exp(-t'), \quad z = 1 - (1 + t') \exp(-t'), \quad (3.3a)$$

where $t' = kt$. The quantities x , y and z expressed by the formulae (3.3) are shown graphically in Fig. 6 (for $k_1:k_2 = 10^{-1}$, 1 and 10).

It is not difficult to satisfy oneself that for any ratio of the constants k_1 and k_2 the equations $dy/dt = 0$ and $d^2z/dt^2 = 0$ are satisfied for one and the same time t . This means that the curve $y = y(t)$ has a maximum at the same value of t for which the curve $z = z(t)$ has a point of inflection. The time to reach the maximum is $t_{\max} = [\ln(k_2/k_1)]/[k_2 - k_1]$. Substituting t_{\max} in the expression for the relative concentration of intermediate B, we obtain

$$y_{\max} = \left(\frac{k_1}{k_2} \right)^{k_2/(k_2 - k_1)}. \quad (3.4)$$

It follows from an analysis of this expression that the quantity y_{\max} , which is small for small values of the ratio $k_1:k_2$, increases when the value of this ratio increases and passes through the value e^{-1} when $k_1:k_2 = 1$ and approaches indefinitely near to 1 for larger $k_1:k_2$ (see also Fig. 6). In the latter case, as a result of the large rate of the first step of this reaction ($A \rightarrow B$) and of the low rate of the second step ($B \rightarrow C$), both steps are almost separate in time; the reaction takes place so that at first all, or practically all, of the initial substance A is converted into the intermediate substance B which is then converted into the reaction product C. As a consequence, the rate of formation of the reaction product, which characterizes the overall reaction rate, is determined in this case by the rate of the slower second step of the reaction (since $k_1 \gg k_2$). The limiting role of the slower step of the reaction is also shown in the reverse case when

$k_1 \ll k_2$. Indeed, from (3.3) we have

$$w_2 = k_2 y = \frac{k_2}{k_2 - k_1} \{1 - \exp[-(k_2 - k_1)t]\} w_1,$$

and hence when $k_1 \ll k_2$ we obtain

$$w_2 = [1 - \exp(-k_2 t)] w_1,$$

i.e. $w_2 < w_1$. Consequently in this case the rate of formation of the reaction product, i.e. the rate of the overall reaction, is determined by the rate of its slow step. This rule is general for all complex reactions taking place with two or more consecutive steps.

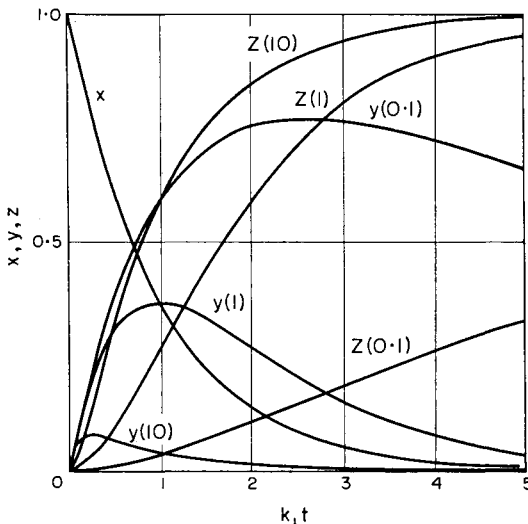


FIG. 6. Kinetic curves for the reaction $A \xrightarrow{k_1} B \xrightarrow{k_2} C$ when $k_1 : k_2 = 0.1, 1$ and 10 .

Defining the rate of reaction as the rate of formation of the reaction product C , we see from the relation $w = k_2 y$ and Fig. 6 that the quantity w , which is equal to zero at the start of the reaction ($t = 0$), increases according to the accumulation of the intermediate substance y , and at t_{\max} reaches its maximum (as also does the concentration of the substance y). This acceleration of the reaction (in the time from 0 to t_{\max}) is also reflected in the S-shaped curve of the growth law for the reaction product C . Such a course for the reaction rate (and also for the shape of the reaction product growth curve) is itself an indication of a complex reaction, since a simple reaction obeying the law of mass action has a maximum

rate at the initial moment of time when the concentration of reacting substances is a maximum.

However, owing to high chemical reactivity of the intermediate substance B (compared with the initial substance A), so that $k_2 \gg k_1$, reactions with consecutive steps are usually such that the maximum reaction rate is reached in the first stages of the reaction, i.e. practically at the initial moment of time $t = 0$. For this reason the kinetics of the accumulation of the product of a reaction with consecutive steps usually corresponds to a steady *decrease* in the rate of reaction from its maximum value (at $t \approx 0$), i.e. to an absence of a noticeable inflection in the curve $z = z(t)$.

Steady State Method

The second term in the expression for the rate of change of concentration of the intermediate substance, $dy/dt = k_1x - k_2y$, is equal to zero at the start of a reaction and increases with time (since $dy/dt > 0$), becoming *equal* to the first term (which decreases with consumption of the initial substance A) at a definite moment of time. At this moment of time (t_{\max}) we have $dy/dt = 0$. From this moment the concentration of the intermediate substance B decreases parallel to the decrease in concentration of the initial substance and the value of dy/dt is *automatically* kept close to zero. For this reason it is possible to reckon that for $t > t_{\max}$ the equation $dy/dt = 0$ is approximately fulfilled; owing to this, one of the two independent differential equations of the reaction (3.2) (the third equation is not independent since $\dot{x} + \dot{y} + \dot{z} = 0$), namely the equation $\dot{y} = k_1x - k_2y$, may be replaced by the algebraic equation $k_1x = k_2y$. This leads to an important simplification of the mathematical task of calculating the concentrations x , y and z as functions of time. In the case we are considering, the approximate values for the concentrations may be written in the form

$$x = \exp(-k_1t), \quad y = \frac{k_1}{k_2} \exp(-k_1t), \quad z = 1 - \exp(-k_1t). \quad (3.5)$$

Comparing (3.5) with (3.3), it is easy to see that these approximate values for the concentrations are closer to the accurate values (3.3) the more the constant k_2 exceeds k_1 . When $k_2 \gg k_1$ both sets coincide.

The procedure used here is very common in chemical kinetics and is known as *the steady state method*, or *method of quasi-stationary concentrations*. This method of approximately solving kinetic equations was first clearly formulated by Bodenstein [415], although it was used by other authors in earlier times in an imprecise form. The method was developed further and put to general use by Semenov [235] and his school. The generalized method of Semenov is sometimes called *the method of*

partial stationary concentrations. The steady state method has been particularly fruitful in investigations of chain reactions (Chap. 9).

The present discussion indicates an important limitation on the use of the earlier relations (1.9) concerning the rate of reaction. According to (1.9) as applied to the present case of a complex two-step reaction $A \rightarrow B \rightarrow C$, the reaction rate may be determined by the equation

$$w = -\frac{dx}{dt} = \frac{dz}{dt},$$

which is contradicted by the accurate equation

$$\frac{dx}{dt} + \frac{dy}{dt} + \frac{dz}{dt} = 0.$$

It follows from this equation that the earlier definition of the rate of reaction is only an approximation, valid to the same extent as $y \approx 0$, or more accurately,

$$\frac{dy}{dt} \ll -\frac{dx}{dt} - \frac{dz}{dt}.$$

Consequently we must conclude that the relationships (1.9) are strictly fulfilled only in the case of simple reactions. In contrast to the latter, in the case of complex reactions these relationships are of an approximate character and express (approximately) only the rate of the *stationary reaction*. Thus, a stationary reaction is one which fulfills the condition

$$\frac{dy}{dt} = 0$$

or the relations (1.9) equivalent to it, to a sufficient degree of accuracy.

In addition, the (approximate) fulfilment of the relations (1.9) when $k_2 \gg k_1$ may also be considered as evidence of a low concentration of the intermediate compared to the concentrations of the initial substance and the reaction product. In fact, considering in the equation $x+y+z=1$ (obtained from $\dot{x}+\dot{y}+\dot{z}=0$) the relative concentration of the intermediate substance y to be negligible small ($y \ll x, z$) we have the approximation $x+z=1$, from which it follows that $\dot{x}+\dot{z}=0$, which is a relationship of the same type as (1.9).⁽⁷⁾

Parallel Reactions

As well as reactions taking place with consecutive steps it is necessary to distinguish *parallel reactions*. The simplest type of parallel reactions are those in which the same initial substance A can react in two or more

⁽⁷⁾ The accuracy of the steady state method was recently examined by Bakhareva [23] for the kinetics of the chain cracking of paraffin hydrocarbons. The author concludes that the method is a good approximation. See also [767], [228a], [674], [310a].

independent ways leading to the same or different reaction products



Reactions taking place in parallel may be uni- or bimolecular or reactions of a mixed character (one uni-, the other bimolecular). We shall consider first two parallel unimolecular reactions. Denoting the rate constants for these reactions by k_1 and k_2 we have

$$\frac{d(C_1)}{dt} = k_1(A) \text{ and } \frac{d(C_2)}{dt} = k_2(A). \quad (3.7)$$

Dividing one of these equations by the other and integrating, we find

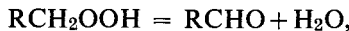
$$\frac{(C_1)}{(C_2)} = \frac{k_1}{k_2}, \quad (3.7a)$$

from which it follows that the concentrations (yields) of the products of the reactions taking place in parallel are related in the same way as the rate constants of these reactions. Since substances C_1 and C_2 are formed as a result of the disappearance of the initial substance A we have

$$-\frac{d(A)}{dt} = \frac{d(C_1)}{dt} + \frac{d(C_2)}{dt} = (k_1 + k_2)(A) = k(A). \quad (3.8)$$

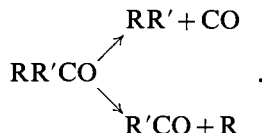
Consequently the rate constant k for the overall reaction with two or more parallel reactions taking place is equal to the sum of the rate constants of these reactions: $k = k_1 + k_2$ (or $k = \sum k_i$).

An example of parallel unimolecular reactions is the decomposition of the hydroperoxide RCH_2OOH , which may decompose either with the elimination of a water molecule to form the aldehyde



or by rupture of the O—O bond. In the latter case a free hydroxyl and alkoxy RCH_2O radical are formed, the alkoxy later being converted into alcohol.

Parallel unimolecular reactions are apparently most frequently met in photochemical reactions. Thus there are reasons for assuming (p. 421) that the photochemical decomposition of ketones $\text{RR}'\text{CO}$ may be accomplished in the following two ways:



The simplest cases of parallel bimolecular reactions are reactions between the same substances; for example



Regarding the yield of products, such reactions are somewhat similar to the parallel unimolecular reactions considered above. In this case we have

$$\frac{d(C_1)}{dt} = k_1(A)(B) \text{ and } \frac{d(C_2)}{dt} = k_2(A)(B), \quad (3.10)$$

where k_1 and k_2 are rate constants for the two reactions. As in the previous case it follows from these equations that

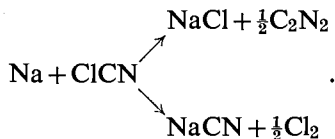
$$\frac{(C_1)}{(C_2)} = \frac{k_1}{k_2}. \quad (3.10a)$$

Further we have

$$-\frac{d(A)}{dt} = -\frac{d(B)}{dt} = \frac{d(C_1)}{dt} + \frac{d(C_2)}{dt} = (k_1 + k_2)(A)(B) = k(A)(B), \quad (3.11)$$

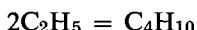
i.e. $k = k_1 + k_2$. The time dependence of the concentrations of substances A and B in this case is expressed by the formulae (1.16) obtained earlier for the bimolecular reactions.

One of the simplest examples of reactions of this type is the reaction between sodium atoms and cyanogen chloride, ClCN ,



The study of these reactions shows that the rate of the first reaction increases with temperature and the rate of the second is temperature independent [733].

As a second example we may take the recombination of radicals and the parallel reaction of disproportionation, for example:



and



A more complex case is given by the parallel reactions of a given substance A with different substances:

$$A + B_1 = C_1 \text{ and } A + B_2 = C_2. \quad (3.12)$$

In this case we have

$$\left. \begin{aligned} -\frac{d(B_1)}{dt} &= \frac{d(C_1)}{dt} = k_1(A)(B_1), \\ -\frac{d(B_2)}{dt} &= \frac{d(C_2)}{dt} = k_2(A)(B_2), \\ -\frac{d(A)}{dt} &= -\frac{d(B_1)}{dt} - \frac{d(B_2)}{dt} = [k_1(B_1) + k_2(B_2)](A). \end{aligned} \right\} \quad (3.13)$$

Solving these equations we find $(C_1) = (B_1)_0 - (B_1)$, $(C_2) = (B_2)_0 - (B_2)$ and $(A) = (A)_0 - (C_1) - (C_2)$ [$(B_1)_0$, $(B_2)_0$ and $(A)_0$ are the initial concentrations of substances B_1 , B_2 and A], and also

$$\left[1 - \frac{(C_1)}{(B_1)_0} \right]^{k_2} = \left[1 - \frac{(C_2)}{(B_2)_0} \right]^{k_1}. \quad (3.14)$$

The kinetic equations in this case are a system of non-linear differential equations, and the analytical expressions for the concentrations of A , B_1 , B_2 , C_1 and C_2 as functions of time may be obtained only for definite ratios of the constants k_1 and k_2 . Thus when $k_1 = k_2$ it follows from the foregoing expression that

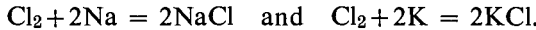
$$\frac{(C_1)}{(C_2)} = \frac{(B_1)_0}{(B_2)_0} \quad (3.15)$$

and further, from the above relationships

$$\frac{(B_1)}{(B_2)} = \frac{(B_1)_0}{(B_2)_0} \text{ and } (A) = (A)_0 - (B_1)_0 - (B_2)_0 + (B_1) + (B_2).$$

It is not difficult to satisfy oneself that in this case the kinetic equations are easily integrated.⁽⁸⁾

A simple example of parallel reactions of this type which have been studied in detail is the pair

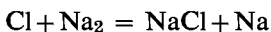
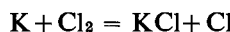
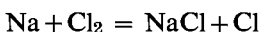


A more complex example is given by the oxidation reactions of a mixture of two or more substances, in particular a mixture of hydrocarbons.

⁽⁸⁾ It is also easy to integrate the kinetic equations for the initial period of the reaction (for any k_1 and k_2) since in this case the concentrations sought follow an approximately linear relationship. Actually, in the initial period of the reaction, when the concentrations of the substances C_1 and C_2 are small compared with the initial concentrations of the substances B_1 and B_2 , the general equation (3.14) gives as a first approximation

$$\frac{(C_1)}{(C_2)} = \frac{k_1 (B_1)_0}{k_2 (B_2)_0}.$$

It should be pointed out however that in none of these examples does the mechanism of the reaction correspond to the above simple scheme of two parallel bi- or termolecular reactions. Disregarding the complex mechanism of the latter reaction we note that, according to investigations on the reactions of alkali metal vapours with halogens, the main part in the mechanism of the first of the above reactions is played by the following pairs of parallel processes:



Coupled Reactions. Chemical Induction

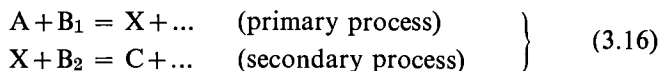
Among parallel reactions of especial interest are the so-called *coupled reactions*; their special characteristic is that even if one of the set of parallel reactions, for example the reaction $\text{A} + \text{B}_1$, goes independently of the other, then the latter ($\text{A} + \text{B}_2$) may take place only in the presence of the first reaction. In chemistry this phenomenon has received the name *chemical induction*. The first, or inducing, reaction ($\text{A} + \text{B}_1$) is called the *primary reaction* and the reaction ($\text{A} + \text{B}_2$) induced by it or coupled with it is called the *secondary reaction*. The substance A which takes part in both reactions is called the *actor*, and substance B_1 whose interaction with A induces the secondary reaction is called the *inductor*, and substance B_2 the *acceptor*. The ratio of the amount of substance A taking part in the conversion of substance B_2 (the acceptor) to the amount taking part in the conversion of substance B_1 (the inductor) is called the *induction factor* [893].

Coupled (induced) reactions are very widely encountered in chemistry. As an example let us consider the joint oxidation of carbon monoxide and hydrogen. Unlike the reaction $2\text{H}_2 + \text{O}_2 = 2\text{H}_2$ the reaction $2\text{CO} + \text{O}_2 = 2\text{CO}_2$ with pure substances (in the absence of an admixture) does not proceed, even up to very high temperatures, but in the presence of hydrogen it is easily accomplished [135]. In this way, the hydrogen here is the inductor, CO is the acceptor, and the oxygen itself taking part in the reactions with the H_2 and CO is the actor. The induction factor is equal to the ratio of the quantities of CO_2 and H_2O formed.

Another good example is the reaction in the ternary mixture $\text{Na} + \text{Cl}_2 + \text{H}_2$ [423]. At $150\text{--}250^\circ\text{C}$ the rate of the reaction of chlorine with hydrogen in the absence of sodium vapour is negligibly small. However in the presence of the parallel reaction of chlorine with sodium vapour the hydrogen readily reacts with the chlorine and for each molecule of NaCl about 10^4 molecules of HCl are formed. It follows that in this case the induction factor is 10^4 .

The basic features of the mechanism and kinetic characteristics of coupled reactions were discovered as a result of work on oxidation reactions in solutions, which give a particularly large number of examples of coupled reactions. It was established that the basis of the phenomenon of coupling or chemical induction, expressing itself in the interlinking of parallel reactions, lies in the formation of *intermediate substances*, which arise as a result of the primary reaction and appear as direct *carriers* of the inductive effect of the primary reaction to the secondary reaction as a *binding link* between the two reactions [1002].

As a result of these ideas, a coupled reaction in the simplest possible case may be represented as a combination of two elementary processes:



where A, B₁ and B₂ are the initial substances (A the actor, B₁ the inductor, B₂ the acceptor), X an intermediate substance and C the reaction product. Introducing the rate constants *k*₁ and *k*₂ for these processes we write the kinetic equations of the reaction as

$$\left. \begin{array}{l} -\frac{d(A)}{dt} = -\frac{d(B_1)}{dt} = k_1(A)(B_1), \\ \frac{d(X)}{dt} = k_1(A)(B_1) - k_2(B_2)(X), \\ -\frac{d(B_2)}{dt} = \frac{d(C)}{dt} = k_2(B_2)(X). \end{array} \right\} \quad (3.17)$$

Owing to the non-linearity of these equations their solution in the general case cannot be obtained in analytical form. For this reason we shall limit ourselves to the special case when *k*₁ = *k*₂ = *k* and the initial concentrations of all three initial substances are equal, i.e.

$$(A)_0 = (B_1)_0 = (B_2)_0 = a.$$

In this case the foregoing equations may be reformulated as

$$\left. \begin{array}{l} -\frac{d(A)}{dt} = k(A)^2, \\ \frac{d(X)}{dt} = k\{(A)^2 - [(A) + (X)](X)\}, \\ (B_1) = (A), \\ (B_2) = (A) + (X), \\ (C) = a - (A) - (X). \end{array} \right\} \quad (3.18)$$

Solving the differential equations we find

$$\left. \begin{aligned} (A) &= (B_1) = \frac{a}{1+t'}, \\ (B_2) &= \frac{2a^2(A)}{a^2+(A)^2} = 2a \frac{1+t'}{2+2t'+t'^2}, \\ (C) &= \frac{[a-(A)]^2}{a^2+(A)^2} = a \frac{t'^2}{2+2t'+t'^2}, \\ (X) &= \frac{a^2-(A)^2}{a^2+(A)^2}(A) = \frac{a}{1+t'} \frac{2t'+t'^2}{2+2t'+t'^2}, \end{aligned} \right\} \quad (3.18a)$$

where $t' = akt$.

The concentrations of substances A, B₁, B₂, C and X expressed by these formulae are shown as functions of time in Fig. 7 (here the quantity a is taken as 1). The substance B₂ (the acceptor) is used up more slowly than the substances A and B₁ taking part in the primary reaction. This indicates

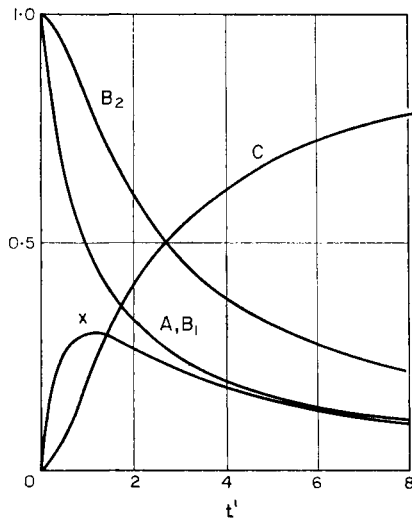


FIG. 7. Kinetic curves of two coupled reactions in the system A + B₁ + B₂.

that B₂ is involved in the reaction only through an intermediate substance X whose concentration is small in the initial period of the reaction. This is also in accord with the S-shape of the reaction product (C) yield curve. It can be seen that the initial acceleration of the reaction expressed by this curve is of the same kind as the initial acceleration established for reactions with consecutive steps (see p. 23); the acceleration in both cases is connected with the formation and accumulation of an intermediate substance with whose assistance the reaction product is formed.

It was noted earlier in connection with consecutive reactions that initial acceleration of these reactions can only rarely be observed in practice since, as a result of the great activity of the intermediate substance, its stationary concentration and consequently the maximum rate of reaction is established practically at $t = 0$. This note also applies to coupled reactions for the same reason ($k_2 \gg k_1$).

The similarity in the kinetics of both reactions, those with consecutive steps and the coupled reactions considered here, is based on the fact that the latter are only formally parallel reactions and are in fact also reactions with consecutive steps as is clear from their mechanism. The only difference between these reactions and those studied earlier is that the participants are at least three initial substances whereas in reactions with consecutive steps two substances only are usually involved.

Starting with the time when the concentration of the intermediate substance reaches its maximum value, and using the steady state method, we may assume that approximately $d(X)/dt = 0$, i.e. $k_1(A)(B_1) = k_2(B_2)(X)$, from which it follows that

$$-\frac{d(A)}{dt} = -\frac{d(B_1)}{dt} = -\frac{d(B_2)}{dt} = \frac{d(C)}{dt},$$

i.e. the rates of disappearance of all three initial substances and the rate of formation of the reaction product are equal, which is an indication that the reaction is stationary (see p. 25).

Homogeneous Catalysis

Catalytic reactions are those reactions which are accelerated in the presence of a foreign substance (the catalyst) which is not consumed in the process of reaction and which is usually present in small quantities in a chemical system. If the reaction takes place in the gas or liquid phase and the catalyst is in a state of molecular or atomic dispersion, then the process is called homogeneous catalysis, as distinct from heterogeneous catalysis in which the catalyst is a solid (for gas reactions a liquid catalyst is also heterogeneous).

According to all the information we have accumulated on homogeneous catalytic reactions, the catalyst in this case is a substance which *directly participates* in the chemical reaction differing, however, from the other substances in that it is not consumed as a result of the reaction. Homogeneous catalytic reactions in the customary sense may be considered as the limiting case of coupled reactions. Both types have in common the formation of an active intermediate substance as a result of the primary process of interaction of the actor with the inductor (in the case of catalytic

reactions the catalyst serves as the inductor). This intermediate substance enters into the secondary process of chemical interaction with the relatively inert acceptor, drawing it into the reaction. It is characteristic of homogeneous catalytic reactions that the catalyst-inductor undergoes a closed cycle of conversions and is regenerated (restored) at the end of the reaction.

The idea that the basis of the mechanism of catalytic reactions lies in the formation of intermediate substances had been expressed even at the beginning of the nineteenth century. For example, Clément and Desormes [1307] (1806), in connection with their study of the catalytic action⁽⁹⁾ of nitric oxide NO on the oxidation of sulphur dioxide SO₂, suggested that the nitric oxide removes oxygen from the atmospheric air and forms with it a definite intermediate compound which, interacting with the sulphur dioxide, transfers oxygen to it and is changed back to nitric oxide. The latter is again oxidized by air and again transfers oxygen to the sulphur dioxide. In this way the homogeneous catalytic reaction becomes a combination of alternating oxidation and reduction processes. A definite chemical mechanism for this reaction has been proposed by a series of authors. The closest to the ideas of Clément and Desormes is the mechanism proposed by Berzelius [1307] (1835). This mechanism is an alternation of two processes,



and



As we can see, in Berzelius' mechanism the proposed active intermediate substance, which transfers oxygen from the air to the sulphur dioxide, is the sesquioxide of nitrogen N₂O₃.

An attempt to systematize coupled oxidation-reduction reactions, in which catalytic reactions were considered as a special case, was made by Luther and Shilov [893] (1903). Material relating to this was given further general treatment by Shilov [298] (1905). Here a detailed study was made of the relation between the induction factor and the behaviour of the inductor in the course of the reaction. Regarding the coupling as "the mutual influence of two reactions taking place in one medium" Shilov distinguished between the following three types of coupled reactions:

(1) Reactions in which the concentration of the inductor *decreases* in the course of the reaction; this type is characterized by a definite *constant* limiting value of the induction factor; (2) coupled reactions in which the concentration of the inductor remains *constant* and consequently the induction factor is *infinite*; homogeneous catalytic reactions in which the catalyst

⁽⁹⁾ The term *catalysis* was introduced by Berzelius in 1835.

(inductor) is completely regenerated belong to this type;⁽¹⁰⁾ (3) coupled reactions in which the concentration of the inductor *increases* and the induction factor has a *negative* value; Shilov placed self-induced reactions, which are characterized by an initial acceleration, in this category.

In Shilov's classification, as in his subsequent work, there is no clear definition of homogeneous catalysis. Thus, he placed in the category of reactions in which the concentration of the inductor decreases, not only coupled reactions in the usual (Ostwald's) sense but also catalytic reactions in which the catalyst is consumed whatever the reason for its consumption. It is possible that, effectively or formally, these types of reaction do not differ in their kinetic features or are distinguished only with difficulty. However, ordinary coupled reactions and homogeneous catalytic reactions must be sharply differentiated according to their nature. Here we call coupled reactions those reactions in which the inductor (independent of the fact whether it is called an inductor or catalyst) is consumed in the formation of the reaction products and is not regenerated at the end or during the course of the reaction. We call catalytic reactions those reactions in which the catalyst is not consumed in the formation of the reaction product, independently of whether it is regenerated completely or partially. It is essential that losses of the catalyst are not directly connected with stoichiometry of the reaction.

As we saw earlier (pp. 23, 31) the initial acceleration is a characteristic feature of reactions taking place with the formation of an intermediate substance. This category of reactions includes both reactions with consecutive steps and coupled reactions, since in the course of both of these an intermediate substance is formed. However, in the case of both types of reaction the initial acceleration is usually confined to a negligibly small time interval near $t = 0$ and is therefore not observed in practice (or observed only in exceptional cases). In self-induced or autocatalytic reactions, which include reactions catalysed by the end products, the maximum rate is observed after considerable conversion of the initial substances, so that the effect of self-induction or self-acceleration of the reactions is then very clear. We shall consider reactions of this type later.

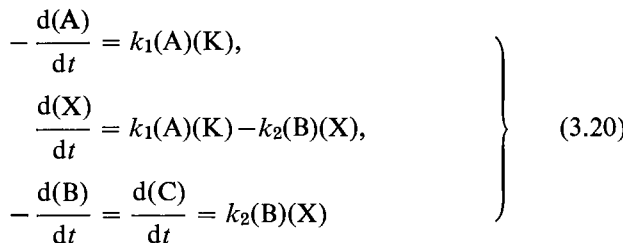
In spite of the great theoretical and practical importance of homogeneous catalytic reactions and the amount of work that has been devoted to them, the mechanism of such reactions has been studied very

⁽¹⁰⁾ Actually part of the catalyst is usually lost for some reason or other, and its regeneration is never complete. For example it has been established that during the combustion of carbon monoxide in the presence of water as a homogeneous catalyst, because hydrogen is absorbed by the walls of the reaction vessel, the quantity of water found at the end of the reaction is less than that contained in the mixture at the start of the reaction [135]. The expression "complete regeneration of the catalyst" in the text is used in the sense that the catalyst is not used up in the formation of the reaction product (in the foregoing example, in the formation of carbon dioxide CO_2).

little so far. Apparently the type of homogeneous catalytic reaction most commonly met is the reaction whose course, as we have noted above, is determined by the formation (with participation of the catalyst) of an active intermediate substance. On the basis of this idea it may be assumed that as a result of the interaction of the catalyst (K) with one of the initial substances an active intermediate substance (X) is formed, the further conversion of which leads to formation of the reaction product (C), and the catalyst is regenerated. This scheme may be represented in a very general form by a combination of processes



similar to the processes (3.16). Introducing the rate constants k_1 and k_2 for these processes, we may write the kinetic equations of the reaction as



and assuming that the stationary state condition $d(X)/dt = 0$ is applicable, we obtain for the rate of the catalytic reaction:

$$w_k = \frac{d(C)}{dt} = k_1(A)(K). \quad (3.21)$$

Comparing the quantity w_k with the rate of the non-catalytic reaction which is expressed by the formula

$$w = k(A)(B),$$

we see that for the display of catalytic action, i.e. for the catalytic reaction to predominate over the non-catalytic reaction, the condition $k_1(K) > k(B)$ must be fulfilled. When the concentration of the catalyst is small compared with the concentration of the initial substances, this condition is equivalent to the condition $k_1 \gg k$. Consequently if homogeneous catalytic reactions of the type considered are to occur, it is necessary that the catalyst itself should possess significant chemical reactivity.

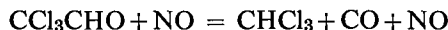
The above formal scheme for an homogeneous catalytic reaction is supported by experiment in that over a definite concentration range the rate of the homogeneous catalytic reaction is often directly proportional to the concentration of catalyst. For example, Hinshelwood, Clusius and

Hadman [764] found that acetaldehyde vapour is decomposed at a significant rate only at temperatures above 500°C, the reaction following a bimolecular law. In the presence of iodine vapour—the homogeneous catalyst—a fast catalytic reaction takes place even at 400°C and the kinetics are expressed by the equation

$$-\frac{d(\text{CH}_3\text{CHO})}{dt} = k(\text{CH}_3\text{CHO})(\text{I}_2).$$

The main products of the catalytic reaction are CH₄ and CO, corresponding to the stoichiometric equation $\text{CH}_3\text{CHO} = \text{CH}_4 + \text{CO}$. Particular experiments have established that in the course of the reaction the concentration of iodine vapour is *unchanged*.

According to the measurements of Verhoek [1250], the decomposition of trichloracetaldehyde vapour CCl₃CHO in the presence of nitric oxide as an homogeneous catalyst.



may be represented approximately by the rate formula

$$-\frac{d(\text{CCl}_3\text{CHO})}{dt} = k(\text{CCl}_3\text{CHO})(\text{NO}).$$

In the same way the rate of combustion of moist carbon monoxide, according to Zel'dovich and Semenov [87], may be expressed by the formula

$$-\frac{d(\text{CO})}{dt} = \frac{d(\text{CO}_2)}{dt} = k(\text{CO})(\text{H}_2\text{O}).$$

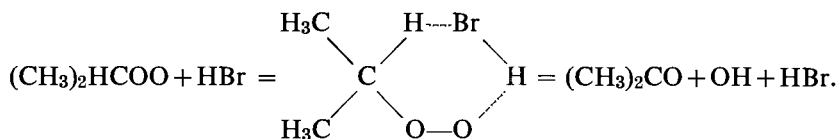
However, it must be emphasized that the agreement of the overall kinetic law in the above examples with formula (3.21), which was obtained from the formal scheme for a homogeneous catalytic reaction, must not be considered as proving the correctness of this scheme for the reaction mechanism as applied to the reactions studied. This applies especially to the combustion of carbon monoxide, the mechanism for which indicates that the catalytic action of water is connected with its participation in the formation of very reactive forms of matter—atoms of O and H and OH radicals. This has nothing in common with the direct interaction of CO and H₂O molecules [135, 463].

In addition the complexity of the actual mechanism of homogeneous catalytic reactions is indicated by the different action of catalysts in the initial period of the reaction and at later stages; this is shown by the

frequent resolution of a reaction into macroscopic steps clearly separated in time (see §37).

The idea of the role of the catalyst as a source of active intermediate substances also embraces those cases of homogeneous catalysis where these active substances are formed as a result of decomposition of the catalyst. In particular, nitrogen dioxide NO_2 (at sufficiently high temperatures and under certain conditions) may be such a catalyst; it dissociates comparatively easily (taking up 71.8 kcal instead of the 118.0 kcal for the dissociation of O_2) into NO and an O atom which is one of the most reactive particles. The ease of the reaction $2\text{NO} + \text{O}_2 = 2\text{NO}_2$ ensures regeneration of NO_2 in the presence of oxygen, i.e. the catalytic character of the process. However, it must be said that cases similar to this are very rare, since as a result of their great reactivity, the radicals formed by dissociation of an initial substance (which acts as a radical source) are combined in molecules of the reaction products or other substances, and this eliminates the possibility of regeneration of the catalyst. A typical example is that of reactions taking place in the presence of easily dissociated organic peroxides, in particular polymerization reactions. Analysis of the products of these reactions shows that RO radicals, which are formed by dissociation of the initial peroxide ROOR , enter into a molecule of the reaction product (a polymer) as an integral part of it [101, 395a]. It follows from this, that in this case we do not have a homogeneous catalytic reaction but a typical coupled reaction taking place in a system such that one of its components is a peroxide stimulating the reaction. The peroxide thus acts as an inductor, not a catalyst.

In the examples of homogeneous catalytic reactions considered in this section, a trace of catalyst (in this case called a *positive* catalyst) accelerates the reaction. A large number of cases are also known in which the catalyst not only accelerates the reaction but also changes its direction, i.e. causes preferential formation of a particular product. For example, the products of the oxidation of propane C_3H_8 in pure propane–oxygen or propane–air mixtures at about 350°C are water, carbon monoxide, carbon dioxide, methyl alcohol CH_3OH , formaldehyde HCHO and acetaldehyde CH_3CHO , acids, peroxides, and also products of cracking—propylene C_3H_6 , methane CH_4 and hydrogen; in the presence of an homogeneous catalyst—hydrogen bromide—the main reaction product is acetone $(\text{CH}_3)_2\text{CO}$ which is formed from about 70 per cent of the oxidized propane [176, 177]. The mechanism of the catalytic action of the HBr directing the reaction has so far not been explained. However it may be assumed that it is connected with the interaction of HBr molecules with the peroxide radical $\text{C}_3\text{H}_7\text{OO}$ which is formed in the course of the oxidation reaction (see p. 628), resulting in the formation of a molecule of acetone, an OH radical and the regeneration of an HBr molecule [100]:



Another example of the guiding action of an homogeneous catalyst is the oxidation of methane in the presence of oxides of nitrogen. Here in a pure mixture of methane and oxygen at about 650°C carbon monoxide is preferentially formed; but in the presence of oxides of nitrogen the main product is formaldehyde HCHO [103] (see Fig. 8). The guiding catalytic action of the oxides of nitrogen is possibly connected, to a considerable extent, with reactions taking place on the walls of the reaction vessel.

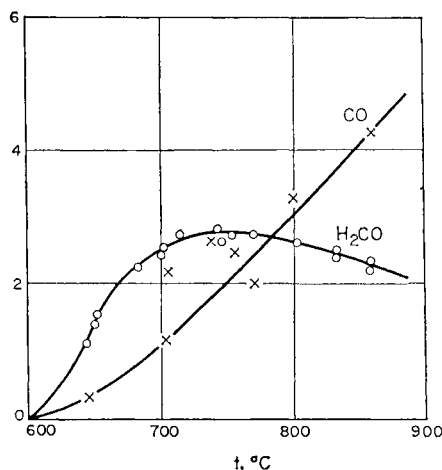


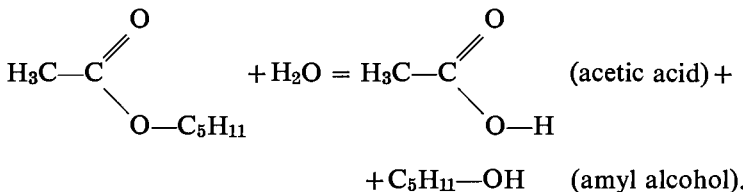
FIG. 8. Yield of formaldehyde HCHO and carbon monoxide CO during the thermal oxidation of methane CH_4 in the presence of nitric oxide at various temperatures (according to Karmilova [103]).

As well as homogeneous catalytic reactions in which the catalyst acts as an accelerating agent (positive catalysis), a large number of reactions are known which are retarded by admixtures. Such admixtures are called *negative catalysts* or *inhibitors*. An example of a negative catalyst is iodine, whose vapour retards the combustion of hydrogen [201], or oxygen, which retards the reaction $H_2 + Cl_2 = 2HCl$ [24]. In these and similar cases the reason for the retarding action of the admixture (inhibitor) is its interaction with reactive intermediate substances (see below, p. 571).

Catalysis by End Products

As already noted, cases are possible where the catalyst is formed in the reaction itself and appears as its product. Accumulation of this product

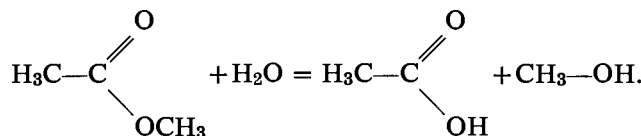
in the course of the reaction accompanies the self-acceleration which is characteristic of this type of reaction. One of the first reactions discovered, that of bromine with lactose $C_{12}H_{22}O_{11}$, belongs to this category. Baeyer (1857) showed [342] that in this case the accelerating action belongs to the reaction products (according to Shilov, to the hydrogen bromide [298]). Another example of a reaction of this type is the decomposition of tertiary amyl acetate studied by Menshutkin [189] (1882):



As Konovalov showed later [156], the accelerating action in this reaction is caused by the acetic acid. Konovalov expressed the rate of this reaction by an equation which can be written in the form

$$\frac{dx}{dt} = k(x + x_0)(1 - x), \quad (3.22)$$

where x is the relative amount of amyl acetate decomposed and x_0 is the original (relative) concentration of acetic acid. A similar equation was obtained earlier by Ostwald [1000] (1883) for the saponification of methyl acetate $\text{CH}_3\text{COOCH}_3$:



A formula of the form of (3.22) was also obtained by Ostwald, by theoretical calculation [1001]. We assume that the reaction proceeds by two parallel independent routes, namely (i) a unimolecular conversion of the initial substance taking place with rate $k_1a(1 - x)$ where k_1 is the rate constant, a the original concentration of the initial substance, and x the concentration of the reaction product relative to a ; and (ii) the interaction of the initial substance with the reaction product taking place at a rate $k_2a^2x(1 - x)$. Then, by adding the rates of processes (i) and (ii), we obtain the formula

$$\frac{dx}{dt} = (k_1 + k_2ax)(1 - x), \quad (3.22a)$$

which can be reduced to a form identical with the empirical formula (3.22) if we introduce the notation $k = k_2a$ and $x_0 = k_1/k$.

Formulae of the form (3.22) were also obtained by Shilov [298] in his studies of the reaction $2\text{HBrO}_3 + 3\text{As}_2\text{O}_3 = 3\text{As}_2\text{O}_5 + 2\text{HBr}$. He set up a formal kinetic law for this and similar autocatalytic reactions by assuming that the slowest step, the rate of which determines the rate of the overall reaction (cf. p. 22), is the interaction of one of the initial substances with the catalyst, i.e. in this example, a molecule of bromic acid HBrO_3 with hydrogen bromide HBr . In the general case, denoting the concentration of the initial substance by (A) and the concentration of the catalyst by (K), according to the foregoing assumption, we have

$$-\frac{d(A)}{dt} = \frac{d(K)}{dt} = k'(A)(K).$$

These equations may be replaced by one equation. For by writing $(K) = a - (A)$, where a is the initial concentration of substance A and introducing the notation $(K) = ax$ (x is the relative concentration of the reaction product), we obtain

$$\frac{dx}{dt} = kx(1-x) \quad (3.23)$$

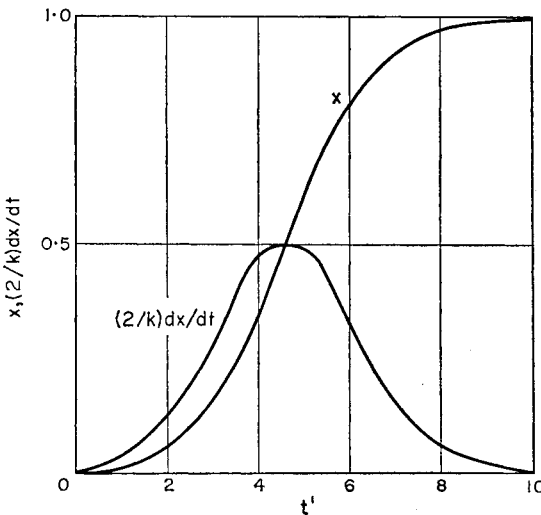
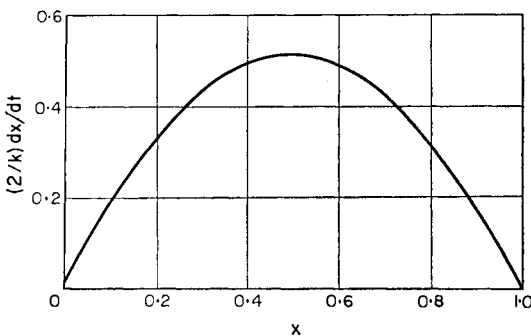
where $k = k'a$. In the case of a catalyst added beforehand, namely the reaction product in quantity ax_0 , formula (3.23) becomes the Ostwald-Konovalov formula (3.22).

Equations (3.22) and (3.23) express the basic law of autocatalysis. It is not difficult to see, however, that equation (3.23) is unsuitable for describing the autocatalytic process in the initial period of the reaction. In fact, according to (3.23), since initially $x = 0$ and the rate of reaction is zero, the reaction cannot start. As we have seen earlier, the way out of this difficulty, according to Ostwald, lies in the assumption that, besides the main autocatalytic reaction, a slow reaction of direct conversion of the initial substance A into the reaction product K is possible; this leads to an equation of the form (3.22).

Integrating equation (3.22) with the initial condition $x = 0$ when $t = 0$, we obtain

$$x = x_0 \frac{\exp[(1+x_0)kt] - 1}{1 + x_0 \exp[(1+x_0)kt]} = x_0 \frac{1 - \exp(-t')}{x_0 + \exp(-t')} \quad (3.24)$$

where $t' = (1+x_0)kt$. From (3.24) it follows that $x = 1$ when $t = \infty$. The curve $x = x(t)$ has a point of inflection at $t = t_{\max} = -\ln x_0/[k(1+x_0)]$, and since $k_1 \ll k$, i.e. $x_0 \ll 1$, it follows that this curve is S-shaped. Substituting $t = t_{\max}$ in (3.24), we obtain $x_{\max} = (1-x_0)/2 \approx \frac{1}{2}$ (since $x_0 \ll 1$). At the same value of t the rate of reaction has its maximum value, $(\dot{x})_{\max} = \frac{1}{2}k(1+x_0)^2 \approx \frac{1}{2}k$. The dependence of x and dx/dt on t' is shown in Fig. 9 for $x_0 = 0.01$. In Fig. 10 the reaction rate dx/dt is

FIG. 9. Kinetic curves of an autocatalytic reaction ($x_0 = 0.01$).FIG. 10. The rate of an autocatalytic reaction as a function of the relative quantity of reacted substance (x).

shown as a function of x . Thus the maximum rate of autocatalytic reactions, of the type considered, occurs when half the initial substance has been consumed, i.e. long after the start of the reaction.

Study of the overall kinetics of various reactions shows that in a series of cases the kinetic law of the reaction may be expressed with a certain degree of accuracy by the formula

$$\frac{dx}{dt} = k(x+x_0)^n(1-x)^m, \quad (3.25)$$

of which formula (3.22) is a particular case. In the case corresponding to formula (3.25) it follows that $x_{\max} = (n-mx_0)/(n+m) \approx n/(n+m)$ from

the condition that at the maximum rate of reaction $\dot{x} = 0$. In particular, when $n = 1$ and $m = 2$, $x_{\max} \approx 1/3$, i.e. the maximum rate is reached when one third of the initial substance has been converted.

An example of a reaction following a kinetic law of form (3.25) is the slow oxidation of hydrogen in a mixture of $2\text{H}_2 + \text{O}_2$. According to Chirkov's measurements [287], the rate of this reaction is expressed by the empirical equation

$$w = k'(\text{H}_2)^2(\text{H}_2\text{O}),$$

which indicates the autocatalytic action of water which is practically the only product of this reaction. Noting that $(\text{H}_2) = (\text{H}_2)_0 - (\text{H}_2\text{O})$ and introducing the notation $(\text{H}_2\text{O}) / (\text{H}_2)_0 = x$ and $k'[(\text{H}_2)_0]^3 = k$, we may reformulate the previous equation as

$$w = kx(1-x)^2,$$

which agrees closely with equation (3.25) in the particular case when $n = 1$, $m = 2$, and $x_0 = 0$. According to this law the maximum reaction rate is observed when x is close to $1/3$. We may note that, as in all the previous examples, the actual mechanism of the slow oxidation of hydrogen is far from the formal scheme from which it would be possible to obtain the foregoing formula, which expresses the overall law of this reaction.

The mechanism of reactions for which the autocatalytic law (3.22) or (3.23) has been established has received quite inadequate study. However, there is no doubt that the formal scheme of Ostwald and the scheme of Shilov (p. 40), from which the law of autocatalysis is obtained, are very far from the actual mechanism of these and similar reactions.⁽¹¹⁾ This circumstance was clearly recognized by Shilov himself who wrote in connection with his study of the reaction of arsenious and bromic acids: "The interaction of arsenious and bromic acids is one of the most graphic examples of the phenomenon that the gross equation expresses only the final result of the process but does not give any idea as to the actual path of the reaction or the intermediate processes which specify its course."

Autocatalytic reactions are one of the many types of complex reactions whose overall law has nothing in common with the rate law obtained from

(11) Semenov [236] has shown that the law of autocatalysis (3.23) expresses sufficiently accurately the rate of branched chain reactions which are characterized by a very complex mechanism. A suitable example is the oxidation of hydrogen (p. 623) and also the oxidation of formaldehyde. Snowden and Style [1160] found that for the latter reaction the rate follows an autocatalytic law of the following form throughout the whole time of the reaction save for a short period of initial acceleration:

$$-\frac{dF}{dt} = kF(F - C),$$

where F is the concentration of formaldehyde and k and C are constants. See also [1108].

the stoichiometric equation of the reaction. As already indicated (p. 17) the non-correspondence of the observed and stoichiometric rate laws of a reaction is also clear evidence that the actual mechanism is considerably more complex than the simple scheme which is expressed by the stoichiometric equation of the reaction.

Cases are not uncommon, however, for which, under certain conditions which determine the features of the chemical mechanism of the reaction, the kinetic law of a complex reaction coincides with the formal law obtained from the stoichiometric equation of the reaction. One suitable example of this type is the oxidation of methane CH_4 which is a complex chain reaction. Under definite conditions the rate of this reaction may be expressed by the simple formula $w = k(\text{CH}_4)(\text{O}_2)^2$, corresponding to the stoichiometric equation of the reaction [71]. Semenov has shown that very often decomposition reactions taking place according to a complex chain mechanism follow the unimolecular law obtained from the stoichiometric equation of the reaction. It follows from all this that the coincidence of the observed and stoichiometric rate laws of a reaction cannot be used to decide if a given reaction is simple or complex. A detailed study of the kinetics and chemical mechanism of a reaction is necessary to solve this problem.

CHAPTER 2

CHEMICAL MECHANISM OF REACTIONS

§4. Experimental Methods for Studying Chemical Reaction Mechanisms

Homogeneous and Heterogeneous Stages of Chemical Reactions

In order to explain the mechanism of a chemical reaction and the nature of its individual elementary processes it is very important to consider whether the reaction takes place completely in a homogeneous (gas) phase or whether heterogeneous factors have an influence on the course of the reaction. In the case of gas reactions this factor is usually the wall of the reaction vessel. The importance of the walls of the reaction vessel (especially their nature and relative surface areas) in the kinetics of chemical gas reactions was first noticed by van't Hoff [37] (1884) although individual observations of the effect of the walls on a chemical reaction had been made even earlier. While studying the polymerization of cyanic acid HCNO in glass vessels with various surface areas, van't Hoff found that the reaction rate in a vessel with large surface area is appreciably greater than the rate in a vessel with smaller surface area. Furthermore, he established that a preliminary coating of the walls of the reaction vessel with cyamelide—the product of cyanic acid polymerization—leads to an increase in the rate of reaction by more than three times. He also noticed the strong influence of the nature of the walls on reaction rate in the case of oxidation of the detonating mixture $2\text{H}_2 + \text{O}_2$ (at 440°C). In subsequent years the influence of the surface area and nature (composition and processing) of the walls on the rate of a chemical reaction was established for many gas reactions. It was shown that in certain cases the wall retards a reaction and in others it accelerates it. Cases are also known in which the wall exerts a double action, both favouring and retarding a reaction. The action of the wall on the combustion of hydrogen may serve as an example here. Nalbandyan and Shubina [204] detected a strong retardation of the reaction on introducing fine rods of various substances into the combustion zone. On the other hand, Alyea and Haber [315] showed that ignition of hydrogen at the junction of hot streams of hydrogen and oxygen (heated to $T \leq 540^\circ\text{C}$) at a pressure of several tenths of a millimetre of mercury takes place only on the introduction of a fine quartz rod into the gas.⁽¹⁾ Thus one may conclude that a solid surface favours the

⁽¹⁾ A similar effect was observed by Thompson [1221] for the reaction of carbon disulphide CS_2 and oxygen. He found that at the junction of streams of CS_2 and O_2

initiation of the combustion of hydrogen and retards the reaction as it proceeds. According to chain theory the double action of a surface in similar cases is connected with the initiation and termination of the reaction chains (see Chapter 9).⁽²⁾

One of the widely used methods for estimating the action of the walls on a chemical reaction is to study the reaction in vessels with different ratios S/V of the surface area of the walls to the volume of the vessel (for example in cylindrical or spherical vessels of various diameters). A variation of this method is to fill the reaction vessel with solid fragments (usually of the same material as the walls of the vessel), which greatly increase the surface to volume ratio, and to make a comparative study of the reaction in the filled and empty vessels. If it is shown that the rate of reaction or composition of products is dependent on the ratio S/V , then it may be concluded that heterogeneous reaction stages occur, i.e. stages (processes) taking place at the wall of the reaction vessel. If the reaction rate is not changed on changing the ratio S/V , then this constancy of the rate (and the composition of the products) is taken as an indication of the homogeneous character of the reaction.

However, Rice and Herzfeld [1063] showed that, as a result of the double action of the wall, cases are possible in which the rate is independent of the ratio S/V in spite of the occurrence of heterogeneous reaction stages. Therefore we conclude that this method gives an unambiguous indication of the influence of the heterogeneous factor on the course of the reaction only when the reaction rate is shown to be dependent on the ratio of the surface area of the walls of the reaction vessel to its volume. When the reaction rate is independent of the ratio S/V , the conclusion that the reaction proceeds in an homogeneous (gas) phase in all its stages may not always be accurate; for this reason the problem of the influence of the heterogeneous factor on the reaction requires additional study.

The method of differential calorimetry developed by Koval'skii [29] is much more satisfactory both in regard to the unambiguity of interpretation of the results and in regard to quantitative calculation of the influence of the heterogeneous factor. The essence of the method lies in the use of two fine thermocouples enclosed in glass or quartz capillaries, one of which is placed at the centre of the reaction vessel and the other at its wall; the temperature is measured at appropriate points in the reaction zone. The difference in the readings of the thermocouples gives in this way a measure

continued from page 44

the carbon disulphide does not ignite if the temperature of the gases is lower than 290°C. On the introduction of a small glass rod at the junction ignition takes place even at 160°C.

(2) This does not rule out the possibility that the action of the rod in ignition of the gas in the combined streams is due to the gas-dynamic effect.

of the initial temperature rise ΔT of the gas in the centre of the vessel relative to its walls. The quantity ΔT may also be calculated from the equation for thermal conductivity. If the reaction is entirely homogeneous (with no heterogeneous stages) then the initial temperature rise in the case of a cylindrical reaction vessel should be

$$\Delta T_g = q_g / 4\pi\lambda, \quad (4.1)$$

where q_g is the heat liberated by the reaction per second and λ is the coefficient of thermal conductivity of the gas. If the reaction takes place only at the walls of the reaction vessel (and of the capillaries), then in this case the following expression for the heating effect is obtained from the thermal conductivity equation:

$$\Delta T_w = \frac{q_w}{2\pi\lambda} \frac{r \ln(R/r)}{r + R}, \quad (4.2)$$

where q_w is the heat liberated by the reaction, R is the radius of the reaction vessel and r is the radius of the capillary. Finally, when the reaction takes place partly homogeneously and partly at the walls, it is necessary to use the equation

$$\Delta T = \Delta T_g + \Delta T_w = \frac{1}{4\pi\lambda} \left[q_g + q_w \frac{2r \ln(R/r)}{r + R} \right]. \quad (4.3)$$

We shall consider the particular case when two parallel reactions take place, one homogeneous and the other at the walls of the reaction vessel. In this case, denoting the rates of these reactions by the letters W_g and W_w respectively, we have for the overall reaction rate $W = W_g + W_w$. Hence the quantity of heat liberated by the reactions will be equal to $q_g = W_g Q$ and $q_w = W_w Q$, where Q is the molar heat of reaction. Denoting the contribution of heterogeneous stages by α , we obtain $W_g = (1 - \alpha)W$ and $W_w = \alpha W$ and further, $q_g = (1 - \alpha)WQ$ and $q_w = \alpha WQ$. Substituting these values of q_g and q_w in formula (4.3), we may rewrite it

$$\Delta T = \frac{WQ}{4\pi\lambda} \left(1 - \alpha + \alpha \frac{2r}{r + R} \ln \frac{R}{r} \right). \quad (4.4)$$

Using this formula and measured values of the temperature rise ΔT , the overall reaction rate W , and λ , the coefficient of thermal conductivity, it is possible to calculate α , i.e. the portion of the complete reaction relating to its heterogeneous part. Measurements of this kind were made by Markevich [183] for the thermal reaction $\text{H}_2 + \text{Cl}_2 = 2\text{HCl}$ (at pressures of the stoichiometric mixture of 8–100 mm Hg and temperatures of 270–370°C). He found that under the conditions of his experiments (in the absence of admixtures) this reaction is homogeneous ($\alpha = 0$), taking place throughout the entire space of the reaction vessel at a uniform rate. By

also studying the reaction in the presence of oxygen, which has a strong retarding effect, he established (from the decrease in the quantity $\Delta T/W$ compared with its value for the pure mixture of H_2 and Cl_2) that it is a chain reaction in which the chains are initiated at the wall of the reaction vessel.⁽³⁾

Recently Maizus, Markevich and Emanuel' [175] used Koval'skii's method to study the oxidation of propane C_3H_8 in the presence of HBr and NO_2 . As a result of this and similar experiments Emanuel' [306] concluded that there were *macroscopic stages*, separate in time, of a complex chemical reaction (see §37). Urizko and Polyakov [268] used Koval'skii's method to study the role of the walls in the oxidation of methane CH_4 to formaldehyde H_2CO . They found that under the conditions of their experiments the formaldehyde is formed in the gas phase and is oxidized at the walls. Coating the walls of the reaction vessel with potassium tetraborate $K_2B_4O_7$ leads to retardation of the heterogeneous formaldehyde oxidation.

Koval'skii's method is of especial interest from the point of view of studying the mechanism of heterogeneous catalytic reactions of gases. One modification of this method specially adapted for the study of reactions taking place in the presence of a heterogeneous catalyst is characterized by the fact that two series of experiments are made: in the first, the catalyst in the form of a fine layer is applied to the wall of the reaction vessel and in the second, to the thermocouple capillary placed on the axis of the cylindrical reaction vessel. If, simultaneously with the reaction at the surface of the catalyst which liberates a quantity of heat q_c , there takes place a gas phase reaction with liberation of heat q_g , then in the first case (with the catalyst on the walls of the reactor), as a consequence of the fact that the gas is not heated since the reaction is taking place only at the walls, the observed heating up, i.e. the difference in the readings of the thermocouples placed on the axis and at the wall of the reaction vessel, will be governed by the gas phase reaction and consequently will be expressed by the formula $\Delta T_1 = q_g/4\pi\lambda$, similar to formula (4.1). In the second series of experiments (the catalyst on the capillary) the heating up is expressed by the formula

$$\Delta T_2 = \frac{q_g}{4\pi\lambda} + \frac{q_c}{2\pi\lambda} \ln \frac{R}{r}, \quad (4.5)$$

similar to formula (4.3). From these two formulae, eliminating the coefficient λ of thermal conductivity, we obtain for the ratio of the quantities of heat liberated at the surface and in the gas phase

$$\frac{q_c}{q_g} = \frac{\Delta T_2 - \Delta T_1}{2\Delta T_1 \ln(R/r)}. \quad (4.6)$$

⁽³⁾ See also Chaikin [285] and Markevich [184].

Applying this formula to the reduction of sulphur dioxide vapour by carbon monoxide $3\text{CO} + \text{SO}_2 = 2\text{CO}_2 + \text{COS}$, which is catalysed by aluminium oxide Al_2O_3 , Bogoyavlenskaya and Koval'skii [29] found that only 3–4 per cent of the heat of the reaction (at $570^\circ\text{--}615^\circ\text{C}$) is liberated on the catalyst. From this they conclude that under the conditions of their experiments this reaction is homogeneous and takes place in its basic stages in the gas phase, and is only initiated at the surface of the solid catalyst. According to the experiments of Bogoyavlenskaya and Koval'skii the reduction of sulphur dioxide by hydrogen, which also is catalysed by aluminium oxide, is also homogeneous. However, in contrast with the previous reaction, here the heterogeneous stage of initiation of the reaction is endothermic, as is indicated by the cooling of the catalyst during the course of the reaction. In contrast with these reactions, the oxidation of sulphur dioxide on platinum at a temperature of about 500°C and a pressure of 100 mm Hg takes place solely at the surface of the catalyst, and so is completely heterogeneous.

The presence of heterogeneous stages in certain homogeneous reactions and also of homogeneous stages in heterogeneous catalytic reactions, i.e. the homogeneous–heterogeneous character of these reactions, was also established by Polyakov and his co-workers [218].

The nature of the initiating action of solid surfaces and also the nature of their retarding action will be considered in Chapter 9.

Labelled Atom (Tracer) Method

By "labelled atoms" are meant here radioactive isotopes or stable but rare isotopes of a given element, by means of which we may distinguish isotopic molecules of any compound containing this element. For example, using isotopes of hydrogen, carbon and nitrogen we can distinguish isotopic molecules of hydrogen cyanide: $\text{H}^1\text{C}^{12}\text{N}^{14}$, $\text{D}^2\text{C}^{12}\text{N}^{14}$, $\text{H}^1\text{C}^{13}\text{N}^{14}$, $\text{D}^2\text{C}^{13}\text{N}^{14}$, $\text{H}^1\text{C}^{14}\text{N}^{14}$, $\text{D}^2\text{C}^{14}\text{N}^{14}$, $\text{H}^1\text{C}^{12}\text{N}^{15}$, $\text{D}^2\text{C}^{12}\text{N}^{15}$, etc. In tracer investigations isotopic molecules are normally labelled with isotopes of one element, or more rarely of two.

Of the above-mentioned isotopes only the carbon isotope C^{14} is radioactive, the remainder being stable. When using radioactive isotopes as labelled atoms the isotopic composition of a compound (the distribution of isotopes of the appropriate element in the compound) is determined by measuring its concentration, i.e. the overall concentration c of inactive and \check{c} of active isotopes, and its activity, i.e. the quantity which determines \check{c} . In this way it is possible to determine both the quantities c and \check{c} and also the percentage composition, $100\check{c}/(c + \check{c})$ ($\approx 100\check{c}/c$, if $\check{c} \ll c$), of the active isotope of the compound in question. The distribution of stable isotopes of an element between isotopic molecules of the appropriate compound is usually determined by mass-spectrometric analysis which

gives the ratio of the concentrations of the isotopic molecules. In experiments with the hydrogen isotopes H and D the isotopic composition is often determined by combustion of the mixture of isotopic molecules and measuring the density of the water obtained [180].

The tracer method was initially used to study the mobility or reactivity of various atoms in a molecule of a given compound or in molecules of various compounds, as shown in particular in *isotopic exchange reactions*. The first investigations of these reactions were carried out by Hevesy and Paneth [756] who studied the exchange of isotopes of natural radioactive elements. However, systematic investigations of isotopic exchange reactions began with the discovery of deuterium and the production of artificial radioactive and stable isotopes of various other elements. The tracer method has proved to be a very effective method for studying the mechanism of other classes of chemical reactions also.

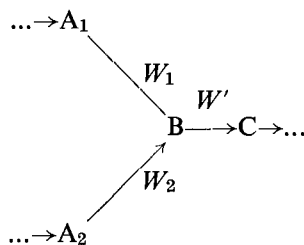
Study of the distribution of a given isotope in the reaction products, or in intermediates, when conducting a reaction in systems containing substances labelled with this isotope, makes it possible to solve such important points about the mechanism of the chemical reaction as (i) whether the reaction proceeds in an isolated molecule or in a molecular complex, (ii) which bonds are broken and thus give rise to intra- or intermolecular rearrangements, and (iii) which substances are the precursors of a substance formed in the course of the reaction. A valuable method for solving problem (iii) is the *kinetic tracer method* which was developed by Neiman and coworkers [210] for the study of the mechanism of complex chemical reactions.

The mechanism of these reactions is usually the combination of a large number of consecutive steps in which the initial substances are converted into the reaction products. For this reason, knowledge of the sequence in which the various substances are converted into other substances is an important step in establishing the chemical mechanism of the reaction. As shown by Neiman and his coworkers, the kinetic method may be used not only to establish the sequence of conversions of the various substances into others but also to measure the rates of formation and consumption, in the course of the reaction, of the various substances participating in it.

The kinetic tracer method involves the determination of the actual sequence of chemical conversions of substances in the reaction and the rate of conversion of these substances at various times in the course of the reaction; this is accomplished by adding to the reacting system at the initial or any other time a substance labelled with the appropriate isotope and then measuring the kinetics of the change in concentration and the specific activity of this substance⁽⁴⁾ and also of the substances which are the

⁽⁴⁾ When using stable isotopes their specific content in the appropriate substances is measured.

prospective products of the chemical conversion of the added substance. For example, let the assumed sequence of individual steps in the reaction be such that a certain intermediate substance B, which is produced from substances A_1 and A_2 in two different ways, is in its turn converted into substance (or substances) C in one or several ways, as is shown in the scheme:



(here W_1 , W_2 and W' denote the rates of the appropriate steps in the reaction). Adding to the reacting mixture a definite quantity of substance A_1 labelled with a radioactive isotope, we may express the change in specific activity of substance B , $\beta = \dot{b}/b$ (\dot{b} and b are the concentrations of radioactive and non-radioactive B at a definite time), by the differential equation

$$\frac{d\beta}{dt} = \frac{W_1}{b} \alpha_1 - \frac{W_1 + W_2}{b} \beta, \quad (4.7)$$

where α_1 is the specific activity of A_1 , which is equal to the ratio of the concentration of radioactive A_1 to the overall concentration of this substance, $\dot{a}_1/(a_1 + \dot{a}_1)$ ($\approx \dot{a}_1/a_1$, since $\dot{a}_1 \ll a_1$). A similar equation for the specific activity of substance A_1 takes the form

$$\frac{d\alpha_1}{dt} = - \left(W_1 + \frac{da_1}{dt} \right) \frac{\alpha_1}{a_1} = - \frac{\alpha_1}{a_1} W_{A_1}, \quad (4.8)$$

where W_{A_1} is the rate of formation of substance A_1 from its precursors. It is clear from this last equation that the specific activity of substance A_1 falls off continuously, this fall ceasing only when the formation of A_1 ceases. The specific activity of substance B , as is clear from equation (4.7), at first grows and reaches a maximum and then decreases. From the condition $d\beta/dt = 0$ for the maximum we obtain the expression for the ratio of the specific activities of substances B and A_1 , when the maximum is reached:

$$\frac{\beta}{\alpha_1} = \frac{W_1}{W_1 + W_2}. \quad (4.9)$$

By measuring the specific activities of A_1 and B in the course of the reaction it is possible to test the proposed reaction scheme on the basis of (4.9). For example, if the specific activities of A_1 and B at the maximum β are equal, which is possible only when $W_2 = 0$, then it may be concluded here that the substance B is formed in this reaction only as the result of conversion of substance A_1 , which is thus the only precursor of substance B . If $\beta < \alpha_1$ then consequently $W_2 \neq 0$ and the substance B is formed both via substance A_1 and also by other routes.

As an example of the use of the kinetic tracer method for studying the mechanism of complex chemical reactions we shall give the results obtained by Lukovnikov and Neiman [172] for the cool flame oxidation of butane. The question was whether CO_2 is formed only as a result of oxidation of the CO formed previously, or if there are other routes for the formation of CO_2 . To obtain the answer to this question a small quantity of CO labelled with C^{14} together with a small quantity of unlabelled CO_2 (so that at the moment of addition of CO the specific activity of the proposed

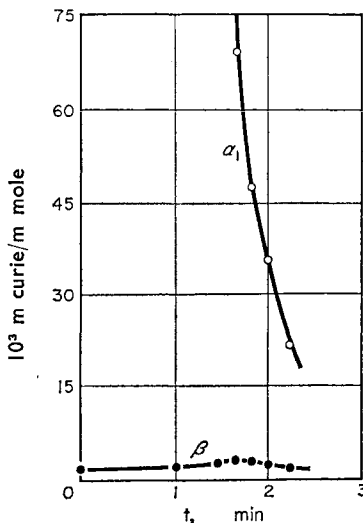
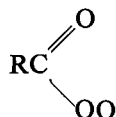


FIG. 11. Kinetic curves of the specific activities of CO (α) and CO_2 (β) in the oxidation of butane C_4H_{10} (with the addition of carbon monoxide labelled with C^{14}), according to Lukovnikov and Neiman [173].

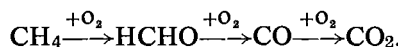
oxidation product of CO , namely carbon dioxide, was equal to zero) was added to the butane–oxygen mixture. The measured kinetic curves for the specific activities of CO (α_1) and CO_2 (β) are shown in Fig. 11. It can be seen from this figure that the specific activity of CO_2 is considerably less than that for CO throughout the reaction; it follows from this that during the cool flame oxidation of butane only an insignificant amount of CO_2 is formed as a result of the oxidation of CO . Measurements of ΣW_i , the

overall rate of formation of CO_2 , and W_1 , the rate of formation of CO_2 from CO , showed that at various reaction times the ratio $\Sigma W_i/W_1$ remains between 19 and 78, so that not more than 5.3–1.3 per cent of CO_2 is obtained from CO . We may add that in the opinion of Lukovnikov and Neiman the probable basic route for the formation of CO_2 in this reaction is connected with the decomposition of acyl peroxide radicals



which are formed in the course of the oxidation of butane, into CO_2 and alkoxy radicals RO .

Another example of use of the kinetic tracer method is given by the results obtained by Nalbandyan and Neiman and coworkers [18] during an investigation of the mechanism of the thermal oxidation of methane. This investigation supported the conclusion reached earlier by Nalbandyan [202] (from analysis of kinetic curves for the accumulation of formaldehyde and carbon monoxide which are formed during the photochemical oxidation of methane), namely that the various oxidation products of methane are formed in the sequence



In experiments with labelled atoms a small quantity of formaldehyde labelled with C^{14} , HC^{14}HO , and a small amount of ordinary carbon monoxide was added to a methane–air mixture. Fig. 12 shows the measured specific activities of formaldehyde (α) and carbon monoxide (β) as functions of the time t spent by the mixture in the reactor (the experiments were carried out with continuous circulation of the mixture through the reactor). Fig. 12 shows that at $t = 0.056$ sec the curves intersect which, according to the foregoing (p. 51), is an indication that in this reaction the CO is obtained exclusively from the oxidation of the formaldehyde formed in a previous stage of the reaction.

However, the kinetic method, which in principle solves the problem of the nature of the individual stages of a reaction and of the sequence of changes of the various substances into others in the course of the reaction, does not (in the form in which it has been used up to the present) give a complete solution to the problem of the chemical mechanism of a reaction, i.e. of the chemical nature of those elementary processes from which the mechanism of the gross reaction is composed. Knowing, for example, that during the oxidation of methane, carbon monoxide is obtained from formaldehyde, we still cannot write down the chemical equation which corresponds to the actual chemical mechanism of formaldehyde conversion

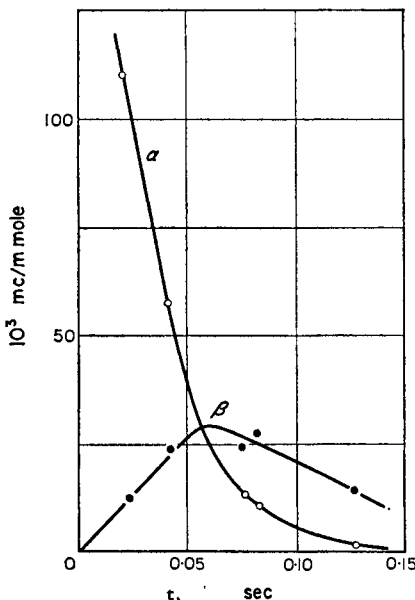


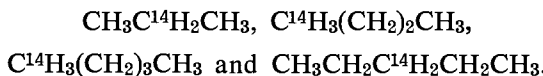
FIG. 12. Kinetic curves of the specific activities of formaldehyde HCHO (α) and carbon monoxide CO (β) in the oxidation of methane CH_4 (with the addition of formaldehyde labelled with C^{14}), according to Nalbandyan, Neiman *et al.* [18].

into CO , since we do not know the detailed chemical mechanism for the conversion of methane into formaldehyde. For a solution of this problem it is necessary to know, in particular, the nature of the particles which take part in the corresponding elementary processes and also the nature and location of the chemical bonds broken. Examples will now be given showing the use of the labelled atom method for solving the problem of the chemical mechanism of the individual stages of complex reactions taking place in the gas phase or in an inert solvent.⁽⁵⁾

Neiman, Lukovnikov and Feklisov [209] studied the oxidation of propane, *n*-butane and *n*-pentane in order to test the so-called theory of destructive oxidation of hydrocarbons; according to this theory in the oxidation of the normal hydrocarbon $\text{CH}_3(\text{CH}_2)_n\text{CH}_3$, formaldehyde H_2CO and acetaldehyde CH_3HCO may be obtained only from the end carbon atoms, i.e. from the C atoms in the CH_3 groups. To establish the

⁽⁵⁾ By an inert solvent we mean a solvent which does not take part in the reaction and does not give rise to electrolytic dissociation of the dissolved substances. The kinetics and mechanism of reactions in an inert solvent do not appear in the majority of cases to differ from the kinetics and mechanism of the same reactions in the gas phase. For example, the rate constant and activation energy for the decomposition of nitrogen pentoxide $\text{N}_2\text{O}_5 = \text{N}_2\text{O}_4 + \frac{1}{2}\text{O}_2$ in the gas phase and in solution in CCl_4 and in CHCl_3 are very close [187].

origin of the C atoms in the product aldehydes, the initial hydrocarbons were labelled with C¹⁴. The following compounds were studied:

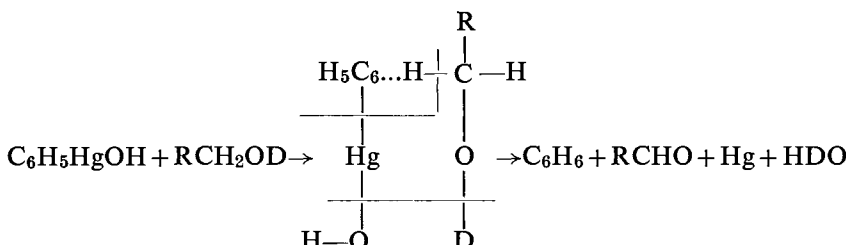


From measurements of the activity of the formaldehyde and acetaldehyde the above authors found that, in contrast with the theory of destructive oxidation, these products are formed from various parts of the hydrocarbon chain. It was inferred that the reaction follows a radical-chain mechanism (see Chap. 9, §39) under the conditions of these experiments (305–340°C) and that an essential role is played by decomposition of RCH₂O radicals into formaldehyde HCHO and an alkyl radical R. The high probability of decomposition of an alcoxyl radical at the temperature of the experiments follows from the comparatively low heat of the reaction



which is about 10 kcal.

A second example is provided by one of the results of Razuvaev, Petukhov, Rekasheva and Miklukhin [221], who studied the mechanism of the photochemical decomposition of the hydroxide of phenylmercury C₆H₅HgOH in methyl CH₃OD and ethyl C₂H₅OD alcohols labelled with deuterium in the hydroxide group. From the fact that benzene C₆H₆ obtained as one of the reaction products does not contain deuterium, the authors conclude that the phenyl group C₆H₅ does not accept the deuterium from the hydroxide group of the alcohol but an H atom from its alkyl group; they consider the most probable mechanism to be the following, in which an intermediate stage is the formation of a complex from two interacting molecules—a molecule of the hydroxide and a molecule of the alcohol:

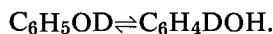


(R = H or CH₃).

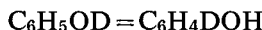
One of the most widely used methods for studying the mechanism of chemical reactions by means of labelled atoms is the method of *isotopic exchange* mentioned earlier. The possibility of exchange was pointed out by Mendeleev [188] who wrote in 1886: "With given particles AB and

BA, A from the first particle may cross over into the second and vice versa." This embodied the idea of mobile chemical equilibrium. The discovery of isotopes made possible the study of exchange reactions of this type. Without dwelling on the history of this problem [137] we shall adduce some examples of the use of the isotopic exchange method in studying the mechanism of chemical reactions.

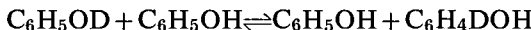
Brodskii and his co-workers [34] used the isotopic exchange method in the discovery of hydrogen rearrangement, which consists of the exchange of hydrogen between a side group of a mono-substituted benzene and the benzene nucleus, in particular the exchange in phenol



Study of isotopic exchange between phenol labelled with deuterium in the hydroxyl group $\text{C}_6\text{H}_5\text{OD}$ and anisole $\text{C}_6\text{H}_5\text{OCH}_3$, between $\text{C}_6\text{H}_5\text{OD}$ and phenetole $\text{C}_6\text{H}_5\text{OC}_2\text{H}_5$ and between phenol labelled with deuterium in the meta-position in the benzene ring $m\text{-C}_6\text{H}_4\text{DOH}$ and anisole, and also study of the kinetics of isotopic exchange in $\text{C}_6\text{H}_5\text{OD}$, have shown that of the two possible reaction mechanisms—the unimolecular



and the bimolecular



—it is the second which actually takes place. Let us consider the kinetics of this reaction.

Representing one form of the labelled molecule by AX and the second form by BX , the concentrations of these compounds by \check{a} and \check{b} , and the rate constants for the conversion of BX into AX and AX into BX by k and k' respectively, we may write the kinetic equation of the exchange in the case of the unimolecular reaction in the form

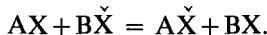
$$\frac{d\check{a}}{dt} = k\check{b} - k'\check{a} = kA - (k + k')\check{a},$$

where $A = \check{a} + \check{b}$ is a constant characterizing the content of the rare isotope in the system (the overall activity in the case of a radioactive isotope). Integrating the previous equation with the boundary conditions $\check{a} = 0$ when $t = 0$ and $\check{a} = \check{a}_e$ (the equilibrium concentration of labelled AX) when $t = \infty$, we obtain

$$\check{a} = \check{a}_e \{1 - \exp[-(k + k')t]\} = \check{a}_e \{1 - \exp[-(t/\tau)]\}, \quad (4.10)$$

where $\tau = 1/(k + k')$ is the characteristic time of the reaction. Equation (4.10) is the kinetic equation for the reversible reaction which follows a unimolecular law in the forward and reverse directions.

We shall now consider the bimolecular reaction, i.e. the reaction



Here AX and BX represent unlabelled compounds. Taking $a_0 = a + \check{a}$, $b_0 = b + \check{b}$ and retaining the symbols introduced earlier, we may write the kinetic equation for the reaction as

$$\frac{d\check{a}}{dt} = k\check{a}\check{b} - k'b\check{a} = kAa_0 - [(k - k')A + (ka_0 + k'b_0)]\check{a} + (k - k')\check{a}^2.$$

Since the systems $AX + BX$ and $A\check{X} + B\check{X}$ are very similar we may put $k' = k$ with sufficient accuracy. In this case the previous differential equation takes the form

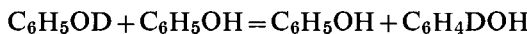
$$\frac{d\check{a}}{dt} = kAa_0 - k(a_0 + b_0)\check{a}.$$

Integrating this equation with the conditions that $\check{a} = 0$ when $t = 0$ and $\check{a} = \check{a}_e$ when $t = \infty$, we obtain the kinetic equation

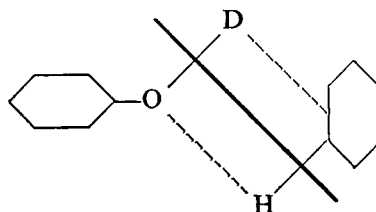
$$\check{a} = \check{a}_e \{1 - \exp[-k(a_0 + b_0)t]\} = \check{a}_e \{1 - \exp[-(t/\tau)]\}, \quad (4.11)$$

which differs from the equation of the first order reversible reaction (4.10) only in that the characteristic time of the reaction $\tau = 1/[k(a_0 + b_0)]$ is a function of the concentrations of the exchanging substances. This difference in the kinetic equations of the uni- and bimolecular reactions also makes it possible to establish the actual mechanism of the isotopic exchange reaction.

By determining the amount of deuterium transferred from the C_6H_5OD hydroxyl to the nucleus for various concentrations of heavy phenol in tetralin ($C_{10}H_{12}$), Brodskii and Kukhtenko [33] found that the value of τ does not remain constant but is inversely proportional to the concentration of phenol in solution—in accordance with the bimolecular law for the hydrogen rearrangement. According to Brodskii a necessary intermediate stage in the bimolecular hydrogen exchange reaction



is the formation of a complex with the structure:



The *kinetic isotope effect*, based on the influence of an isotope on the rate of reaction, is of considerable interest when studying the mechanism

of chemical reactions. Considering the interaction of two isotopic molecules, e.g. H_2 and D_2 , with the same particle, e.g. a halogen atom X , one must expect the rate constants of the reactions to be somewhat different. Actually even from simple collision theory (see Chap. 3, §9) we obtain for the ratio of the rate constants k_H and k_D of these reactions

$$\frac{k_H}{k_D} = \left[\frac{M_{D_2}(M_{H_2} + M_X)}{M_{H_2}(M_{D_2} + M_X)} \right]^{1/2} \simeq \left[\frac{M_{D_2}}{M_{H_2}} \right]^{1/2} = 1.41$$

(M = molecular weight), from which it follows that the mere difference in the mean velocities of thermal motion of the H_2 and D_2 molecule gives rise to a rate of reaction of H_2 with the halogen 1.4 times greater than the rate of reaction involving D_2 . In the case of heavier molecules with a smaller relative mass difference, the isotope effect, which is dependent on the difference in the mean thermal velocities, is less than this value (1.4) and in the limiting case of practically identical masses the effect is absent. The isotope effect does not, however, consist only in a difference in the pre-exponential factors in the equation for the rate constants but also gives rise to a difference in the activation energies of the reactions of the isotopic molecules, which makes a considerably greater difference in the rates of these reactions, especially at low temperatures. According to the activated complex theory (see Chap. 3, §12) the difference ΔE in activation energies of two reactions (in our example $H_2 + X$ and $D_2 + X$) may be expressed as the difference ΔE_0 in zero point energies of the systems $H_2 + X$ and $D_2 + X$ in the initial state minus the difference ΔE_0^\ddagger in zero point energies of these systems in the intermediate (activated) state corresponding to the configurations $H \dots H \dots X$ and $D \dots D \dots X$; thus

$$\Delta E = E_D - E_H = \Delta E_0 - \Delta E_0^\ddagger. \quad (4.12)$$

Since the zero point energy is the sum of the vibrational zero point energies of the components of the system, i.e.

$$E_0 = \sum \frac{h\omega_i}{2},$$

where ω_i is the natural vibration frequency of the i th component, then owing to the marked decrease in vibrational frequencies on conversion of the system into the activated state, arising from weakening of the interatomic bonds, one must consider the quantity ΔE_0^\ddagger to be appreciably less than ΔE_0 , from which it follows that

$$\Delta E \leq \Delta E_0. \quad (4.12a)$$

Since the zero point energy of the system containing the lighter isotopic molecules is greater than that of the second system (resulting from the corresponding difference in the vibration frequencies), we have $\Delta E > 0$.

Consequently both the difference in pre-exponential factors and the difference in activation energies give rise to an increase in the rate constant for the reaction in the lighter system compared to that in the heavier system ($k_D < k_H$).⁽⁶⁾

TABLE 1

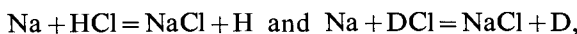
The ratios of rate constants and the differences in activation energies for reactions of stable isotopes of hydrogen

Reactions		T°, K	$k_H : k_D$	$Z_H : Z_D$	$\Delta E, kcal$	$\Delta E_0, kcal$
$H_2 + H$	$D_2 + D$	963	1.85	1.4	0.52	1.8
$H_2 + Cl$	$D_2 + Cl$	290	11.6	1.4	1.22	1.8
$H_2 + Br$	$D_2 + Br$	550	4.2	1.4	1.20	1.8
$H_2 + I_2$	$D_2 + I_2$	736	2.40	1.4	0.79	1.8
$H + HCl$	$H + DCl$	298	2.3	1.0	0.50	1.2
$H + HCl$	$D + HCl$	298	3.0	1.4	0.5	0.0

Table 1 is copied from Brodskii's book *Khimiya izotopov (Chemistry of Isotopes)* (p. 188) [34] and gives the ratios of rate constants and the differences in activation energies for a series of reactions involving atoms and molecules of hydrogen. The table also shows the mean temperature of the experiments, the ratio of the pre-exponential factors ($Z_H : Z_D$) and ΔE_0 values calculated from the vibrational zero point energy. It is apparent from Table 1 that in all cases save one the quantity ΔE is less than ΔE_0 in accordance with formula (4.12) and hence the quantity ΔE^\ddagger must not be disregarded.

As in the last example of Table 1 $\Delta E_0 = 0$ the quantity ΔE must have a negative value. The fact that its measured value is positive (0.5) clearly results from insufficiently accurate measurements of the activation energy.

Using the semi-empirical method of Polanyi and Eyring (see Chap. 3, §12) to calculate the quantities ΔE_0 and ΔE^\ddagger for the reactions



Bawn and Evans [365] found $\Delta E_0 = 1.20$ kcal (in complete agreement with the value obtained from the vibrational zero point energies of HCl and DCl) and $\Delta E^\ddagger = 0.75$ kcal, and hence $\Delta E = 0.45$ kcal, in good agreement with their measured difference in the activation energies for the above reactions, namely $\Delta E = E_D - E_H = 6.4 - 6.1 = 0.3$ kcal.

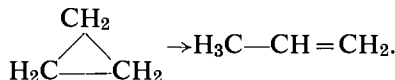
⁽⁶⁾ The opposite relation is obtained for the reactions of different isotopic atoms with the same molecule, for example $H + X_2$ and $D + X_2$. Since in this case the zero point energies of the initial state of both systems are the vibrational zero point energies of the X_2 molecule and so are identical, we have $\Delta E_0 = 0$ and $\Delta E = -E_0^\ddagger$; hence, as the zero point energy of the activated state of the lighter system is greater than that of the heavy system, i.e. $\Delta E_0^\ddagger > 0$, we obtain $\Delta E < 0$.

We give below figures for the hydrogen isotope effect taken from the work of Whittle and Steacie [1284] which involves more complex reactions. Thus for the reactions of methyl with a molecule of hydrogen these authors obtained the following data (in brackets are the energies of activation in kcal):



For the reactions $\text{CH}_3 + \text{acetone}$ and $\text{CD}_3 + \text{deutero-acetone}$ these authors found $E = 9.7$ and 11.6 kcal.

The difference in the rate constants for reactions of isotopic molecules due to the isotope effect clearly influences the rate of the overall reaction only when the effect occurs in the limiting step of the reaction, i.e. the step whose rate determines the overall rate of the reaction. For example it is known that in unimolecular reactions at sufficiently high pressures the limiting step of the reaction is the unimolecular decomposition of an activated molecule, whereas at low pressures the rate of reaction is determined by the rate of the bimolecular process of activation of the molecules of the initial substance (see Chap. 5, §18). For this reason one must expect that lowering the pressure will weaken the isotope effect in a unimolecular conversion, since it is natural to assume that the isotope effect must be particularly strong in the case of decomposition of an activated molecule as bonds are broken and new ones formed; the effect must be practically zero in the case of the bimolecular activation process connected with the physical process of energy transfer during the collision of molecules [388]. Such a case was evidently observed by Weston [1278] who studied the isomeric conversion of ordinary and tritium-labelled cyclopropane into propylene



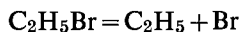
In Weston's experiments a marked isotope effect was observed at a pressure of about an atmosphere but decreased with decreasing pressure and had completely disappeared at pressures of about 0.5 mm Hg. In this way it is possible to use the isotope effect to establish the limiting step of a complex chemical reaction. We might add that a marked isotope effect in

this reaction may also be considered as an indication that here the conversion of activated molecules is due to the breaking of carbon–hydrogen bonds (along with C–C bonds); it may be concluded that the probable primary product of the conversion of the activated molecule is the final product of the reaction $\text{H}_3\text{C}-\text{CH}=\text{CH}_2$ and not the biradical

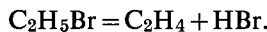


obtained by breaking a single C–C bond.

The previous example shows that the presence or absence (and in more general terms—the value) of the isotope effect depends on which bonds are broken in the course of the chemical reaction. A theoretical consideration of the kinetic isotope effect [1145] also leads to this conclusion. In particular it follows from the theoretical data that the ratio k/\bar{k} of the rate constants for the decomposition of the isotopic molecules of ethyl bromide $\text{CH}_3\text{C}^{12}\text{H}_2\text{Br}$ and $\text{CH}_3\text{C}^{13}\text{H}_2\text{Br}$ into an ethyl radical and a bromine atom cannot be less than the square root of the ratio of the reduced masses of these molecules, and hence $k/\bar{k} \geq 1.036$. For the decomposition of both ethyl bromides into ethylene $\text{CH}_2=\text{C}^{12}\text{H}_2$ and $\text{CH}_2=\text{C}^{13}\text{H}_2$ and a molecule of hydrogen bromide HBr, theory gives $k/\bar{k} \geq 1.003$. Thus by measuring the value of the isotope effect it is possible to decide whether the decomposition of ethyl bromide proceeds according to a radical or a molecular mechanism, i.e. according to the reaction scheme



or the scheme



This was used by Friedman, Bernstein and Gunning [632] in a study of the thermal decomposition of the ethyl bromides; they found that at 400°C , $k/\bar{k} \leq 1.016$. It follows from a comparison of this figure with the above theoretical values of k/\bar{k} for the two mechanisms that the actual reaction mechanism corresponds to the molecular scheme



This result is also obtained from the data of a study of the thermal decomposition of ethyl bromide using the so-called toluene method (see below, p. 79).⁽⁷⁾

Overall Formulae and Chemical Mechanisms of Reactions

One of the important properties of complex chemical reactions, which take place as a rule via a series of consecutive steps, is the fact that in the

⁽⁷⁾ See also the data concerning the pyrolysis of 1- C^{14} -propane $\text{C}^{14}\text{H}_3\text{C}^{12}\text{H}_2\text{C}^{12}\text{H}_3$ [630]. In this case it was found that the $\text{C}^{12}-\text{C}^{12}$ bond broke 1.08 times more frequently than the $\text{C}^{12}-\text{C}^{14}$ bond.

course of the reaction intermediate substances are formed which are capable of further conversion. The fact that these substances are not usually observed as final reaction products is evidence of their high chemical reactivity. The validity of this conclusion is supported by direct investigation of the nature of the intermediate substances (see next section) from which it follows that in the majority of reactions the intermediate substances are free atoms and radicals, i.e. extremely reactive and therefore unstable substances, which are at the same time of great interest from the point of view of the chemical mechanism of reactions. This property of the intermediate substances hinders their introduction in measured amounts into the reaction zone and is the chief reason for the practical impossibility of completely solving the problem of the chemical mechanism of reactions on the basis of a kinetic method alone.⁽⁸⁾

It follows from the above that one of the prerequisites for solving the problem of the chemical mechanism of a reaction must be the determination of the intermediate substances which are active participants in elementary processes involved in the reaction mechanism. Modern experimental methods of detecting chemically unstable (labile) intermediates and methods of measuring their concentration are considered in the following section. Here we shall confine ourselves to the general question how far the properties of the chemical reaction mechanism, assuming that it is known, are reflected in the overall formula for the reaction. This problem was discussed in the previous chapter in connection with the possible mechanism of coupled and autocatalytic reactions. It followed from this discussion that in general there is no well-defined link between the overall formula of a reaction and its mechanism. In particular we showed that the kinetic law of a series of complex chain reactions, in which labile intermediate substances—free atoms and radicals—take part, may sometimes be expressed by simple formulae which in no way reflect the complex mechanism of the reactions. For example the reactions of combustion and slow oxidation of hydrogen obey a kinetic rule which may be expressed by simple autocatalytic formulae which do not correspond to the complex mechanism of these reactions. It follows from these and similar examples that the overall formula in the general case does not give a correct assessment of the actual chemical mechanism of a complex reaction. Moreover, in many cases the same rule may be obtained from different assumed mechanisms for a reaction.

However it does not follow that experimental study of the macro-kinetic regularities of a reaction and in particular of its overall formula has no value in deciding the chemical mechanism of the reaction. Above

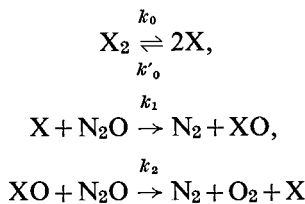
⁽⁸⁾ A kinetic method usually consists of measurements of the concentration of initial, final or stable intermediate substances and also of the overall pressure of the reacting mixture during the course of the reaction, i.e. as a function of time.

all it should be pointed out that the overall formula is the first touchstone for checking the accuracy of a mechanism proposed for a chemical reaction. Agreement between the experimentally obtained kinetic law of reaction and the theoretical law obtained from the reaction mechanism is the main criterion and is an essential but insufficient condition which must be satisfied by the chemical reaction mechanism. The absence of this agreement is a definite indication of the error or inadequacy of the proposed theoretical reaction mechanism.

Besides the general value of the overall formula for a reaction as a criterion of the reliability of the theoretical mechanism, it also frequently permits the detection of individual features of the chemical reaction mechanism. Here we may mention reactions of fractional order whose overall rate is proportional to the square root of the concentration of one of the reacting substances. If this relationship has been reliably established it may be considered as an unambiguous and direct indication that free atoms or radicals are taking part in the reaction. From a consideration of the possible reaction mechanisms in which free atoms and radicals take part, it follows that the power $\frac{1}{2}$ in the expression for the overall formula of reaction appears when the disappearance of these active particles is due to their recombination. We shall consider as an example the thermal decomposition of nitrous oxide N_2O in the presence of iodine or bromine vapour. According to the investigations of Volmer and Bogdan [1256] the overall formula of this reaction may be expressed as

$$-\frac{d(\text{N}_2\text{O})}{dt} = k(\text{N}_2\text{O})(\text{X}_2)^{1/2}$$

($\text{X} = \text{I}$ or Br). Assuming that the mechanism of this reaction consists of the following elementary processes:



(k_0 , $k'{}_0$, k_1 and k_2 are the rate constants of the appropriate elementary processes) and using the steady state conditions

$$\frac{d(\text{X})}{dt} = 2k_0(\text{X}_2) - 2k'{}_0(\text{X})^2 - k_1(\text{N}_2\text{O})(\text{X}) + k_2(\text{N}_2\text{O})(\text{XO}) = 0$$

and

$$\frac{d(\text{XO})}{dt} = k_1(\text{N}_2\text{O})(\text{X}) - k_2(\text{N}_2\text{O})(\text{XO}) = 0,$$

we find

$$(\text{X}) = \left[\frac{k_0}{k'{}_0} (\text{X}_2) \right]^{1/2} \text{ and } (\text{XO}) = \frac{k_1}{k_2} (\text{X}).$$

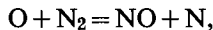
Substituting these values of the stationary concentrations of X and XO in the equation

$$- \frac{d(N_2O)}{dt} = k_1(N_2O)(X) + k_2(N_2O)(XO),$$

which expresses the overall formula of the reaction, and introducing the quantity $k = 2k_1(k_0/k'_0)^{1/2}$ we obtain a formula identical with the above empirical formula. The agreement in this case should be regarded as a weighty argument in favour of the accuracy of the postulated reaction mechanism, especially in the part which refers to the conception of the active form of the halogen as being atomic. The dependence of reaction rate on the square root of halogen concentration which is frequently observed in reactions of halogen compounds must also be ascribed to halogen atoms taking part in these reactions. This applies in particular to the photochemical reactions of halogen compounds (see Chap. 7). As a second example we shall use the oxidation reaction of nitrogen in hot flames. According to Zel'dovich, Sadovnikov and Frank-Kamenetskii [83, 86], the rate of this reaction (far from the equilibrium $N_2 + O_2 \rightleftharpoons 2NO$, i.e. without taking into account the reverse reaction) may be expressed by the formula

$$\frac{d(NO)}{dt} = k(N_2)(O_2)^{1/2}.$$

The same formula may be obtained from a reaction mechanism assuming that the controlling step of the reaction is the process



the reaction taking place in the equilibrium zone of the burnt gases and the oxygen atoms being at their equilibrium concentration, $(O) = [K_0(O_2)]^{1/2}$. The experimentally observed proportionality of the reaction rate to the square root of the oxygen concentration is a weighty argument in favour of the theoretical reaction mechanism in which the active role is played by the O atoms.

Further, according to Weiss and Shapiro [1273] the rate of hydrolysis of diborane B_2H_6 in the gas phase (at $50.5^\circ C$) is proportional to

$$(B_2H_6)^{1/2}(H_2O)$$

and it follows that one of the main steps of the reaction is the dissociation of the diborane molecule $B_2H_6 \rightleftharpoons 2BH_3$. In the proposed reaction mechanism the final products H_3BO_3 , HBO_2 and H_2 are formed as the result of successive substitution of hydrogen in BH_3 by hydroxyl.

As well as reactions whose rates have a fractional order with respect to one or other of the reacting substances, reactions are also frequently observed with rates independent of the concentration of some reacting substance. It may be concluded from general ideas on the kinetics of

complex reactions that reactions with consecutive steps may also be of this type. In order that the rate should not depend on the concentration of some one of the initial substances it is sufficient here for the rate of the limiting step of the reaction to be independent of the concentration of this substance. For example, in the simplest case of the reaction $A + B \rightarrow C$ taking place in the two stages:



for the rate of the stationary reaction, which satisfies the steady state condition

$$d(X)/dt = k_1(A) - k_2(X)(B) = 0,$$

we have

$$w = d(C)/dt = -d(A)/dt = k_1(A),$$

i.e. the rate of reaction is independent of the concentration of substance B. Reactions of this type must frequently be encountered in unimolecular reactions, in which the primary decomposition of one of the reacting substances is accompanied by fast secondary processes taking place in the presence of other substances in the reaction zone. Study of the kinetic law of these reactions is valuable in leading to definite ideas about the character of the individual elementary processes which contribute to a deeper understanding of the reaction mechanism.

In establishing the chemical mechanism of a reaction and checking experimentally the reliability of one or another of its modifications, great importance is attached not only to the kinetic formula describing the rate of change of concentration of the main reaction product but also to obtaining and checking experimentally the kinetic equations for side products and intermediate substances. Also important is a complete quantitative analysis of all substances formed in the course of the reaction with, of course, a check that the elements balance. The more complete the analytical data and the more detailed the kinetic study of the individual substances formed or consumed in the course of the reaction, the more rigid and definite are the conditions that must be satisfied by the reaction mechanism in question and the more reliable is the check on its accuracy.

The withdrawal of gas samples taken from the reaction zone at different times for subsequent analysis makes it possible to conduct kinetic investigations without interrupting the reactions. Besides normal chemical analysis, various physical and physico-chemical analytical methods have been used with success; we shall consider some of these methods in the following section in connection with the problem of intermediate substances in complex chemical reactions. Here we may note the recently developed mass-spectrometric method for studying the kinetics of fast gas reactions

[868] which permits registration of the mass spectra of the initial substances and reaction products every 5 msec in the course of the reaction. This method was used to study the kinetics of consumption of ether and oxygen in the cool-flame oxidation of diethyl ether $(C_2H_5)_2O$ and the kinetics of the accumulation of the reaction products C_2H_4 , CH_3HCO and CO_2 by the variation of the heights of the appropriate peaks in mass spectra.

The spectroscopic absorption method is very convenient, since it eliminates the use of complex techniques for taking out samples, which to a greater or lesser degree disturb the normal course of the reaction. Examples of the use of this method will be considered in the following section. Of the other physical methods let us mention the *rotating sector method* which has been used with success by various authors for the study of fast radical reactions. Thus, the rotating sector method in its simplest modification, which makes it possible to measure the rate of reaction at definite intervals of time after the formation of a certain initial quantity of radicals, was used by Oldenberg [996] and Kondrat'ev and Ziskin [141] to study the kinetics of recombination of hydroxyl HO obtained in an electric discharge in water vapour. In their experiments these authors determined the recombination rate by measuring the hydroxyl concentration spectroscopically.

Another modification of the rotating sector method consists of measuring the mean concentration of radicals as a function of the rate of rotation, which makes it possible to determine the lifetime of the radicals and also their concentration and the rate of their reaction (recombination). Gomer and Kistiakowsky [686], Dodd [544] and others have used this modification of the rotating sector method to study the reactions of the methyl radical, etc.⁽⁹⁾

A general method of studying the overall kinetics of complex chemical reactions which is of considerable interest is that recently developed by Vanpée [1242]; this consists of the simultaneous measurement of pressure (Δp) and of the heating factor (ΔT) of the reacting mixture in the course of the reaction. The use of this method to study the oxidation reactions of a series of hydrocarbons of various structures, formaldehyde $HCHO$, methyl alcohol CH_3OH , dimethyl ether $(CH_3)_2O$ and ethylene oxide $(CH_2)_2O$ (at 440°C) shows that in all cases the quantity ΔT , measured at different times, is proportional to the derivative of the quantity Δp with time (t); Vanpée concludes from this that the quantity $\Delta T(t)$ is a measure of the rate of reaction at different times. The author notes that measurements of the quantity ΔT are very convenient in order to establish the points of inflection and other characteristics of the plot of Δp against t . A similar method was developed by Emanuel' and co-workers (see Chap.

⁽⁹⁾ For the theory of the sector method see, for example, Melville and Burnett [949].

9, §38), in whose work the kinetic plots for separate individual substances are obtained as well as the parallel measurements of the quantities Δp and ΔT .

The so-called branched-chain reactions differ from other reactions by the presence of limiting effects which are expressed by a sharp change in reaction rate for insignificant changes in the composition of the reacting mixture, its pressure or its temperature; to establish or check experimentally the chemical mechanism of these reactions it is extremely important to derive from the reaction mechanism those regularities which are the quantitative characteristics of the above limiting effects, as well as the overall formula for the reaction. Below we shall see from examples how important are the regularities of the limiting effects in establishing the chemical mechanism of these reactions (see Chap. 9).

In connection with this short discussion of the various methods of studying the chemical mechanism of reactions we might mention that recently it has proved possible to solve, numerically, systems of differential kinetic equations by the use of electronic computing machines [486]; this should play a large part in the study of the mechanism of complex chemical reactions and also reactions taking place under non-isothermal conditions. We may note that methods of calculating the rates of reversible and irreversible reactions taking place under conditions of varying temperature (for example with cooling gases, in particular quenching a reaction mixture) have recently been put forward by Gaenslen and Mackenzie [645].

§5. Intermediate Substances

Stable Intermediates

One of the indications and criteria of the complexity of the mechanism of a chemical reaction is the formation of *intermediate substances* in the course of the reaction. Any substance may be called an intermediate substance if it is formed as a result of the reaction and its concentration tends to zero for an infinite reaction time. An accurate definition of the concept of an intermediate substance is necessary in view of the fact that frequently the chemical nature of a substance may not be a criterion as to whether the substance is an intermediate or a final product of the reaction; one and the same substance, depending on the reaction conditions, often behaves as an intermediate substance or as a reaction product. For example, hydrogen and carbon monoxide are detected in the reaction products of the slow oxidation of hydrocarbons along with water and carbon dioxide, and consequently must be included in the reaction products. H_2 and CO are also detected in the inner cone of the Bunsen flame (see below, p. 683) but are practically absent from the final combustion products of hydrocarbons, and so must be considered as intermediate substances in this

reaction. Another example is hydroperoxide, which is an intermediate substance in the slow (thermal) oxidation of hydrocarbons and is also the sole product of their oxidation near room temperature.

In many reactions it is possible to detect immediately the intermediate substances (using a chemical or any other analytical method) and to measure their concentration at different times in the reaction. In individual classes of reactions, for example coupled reactions (see p. 30), the formation of intermediate substances in the course of the reaction is very probable.

Different intermediate substances possess different degrees of stability depending on their reactivity, which in its turn depends on their chemical nature and the reaction conditions. Along with stable intermediate substances such as H_2 and CO in the above example of the combustion of hydrocarbons, or less stable intermediates such as aldehydes and peroxides which are detected in the same reaction, *labile* intermediate substances such as free atoms and radicals are observed whose chemical stability is negligibly small.

Intermediate substances which are stable at room temperature may be extracted from the reaction zone by any method and subjected to normal chemical or other analysis not limited by the lifetime of the substance to be analysed. Methods of analysing intermediate substances of this type do not differ in any way from methods of analysing the reaction products. One of the most customary methods for extracting an intermediate substance from the reaction zone is the *method of quenching*, consisting of a rapid lowering of the temperature of the gas taken from the reaction zone. The oxidation of hydrogen in a stream of detonating gas (see p. 20) serves as a suitable example. In this case owing to the short reaction time and the rapid lowering of temperature (quenching) it is possible to detect in the reaction products (along with water) hydrogen peroxide (see Fig. 5) which is one of the intermediate substances in this reaction; on increasing the time of the reaction, the concentration of H_2O_2 in the reaction products tends to zero. We may also cite sulphur monoxide S_2O_2 , which is one of the intermediate substances in the oxidation of hydrogen sulphide. According to Pavlov, Semenov and Emanuel' [216] H_2S is converted into S_2O_2 , up to 20 per cent, during the reaction process. The change in concentration of the sulphur monoxide in the course of the reaction is shown in Fig. 13. In these experiments the concentration of sulphur monoxide was measured by its characteristic absorption spectrum.⁽¹⁰⁾ The spectroscopic absorption method has also been used in the study of other reactions. For example Sprenger [1164] used this method to

⁽¹⁰⁾ There are indications that the compound taken as sulphur monoxide actually has the formula S_2O [950a] (D. J. Meschi, R. J. Myers, *J. Molecular Spectr.*, 3, 405 (1959)).

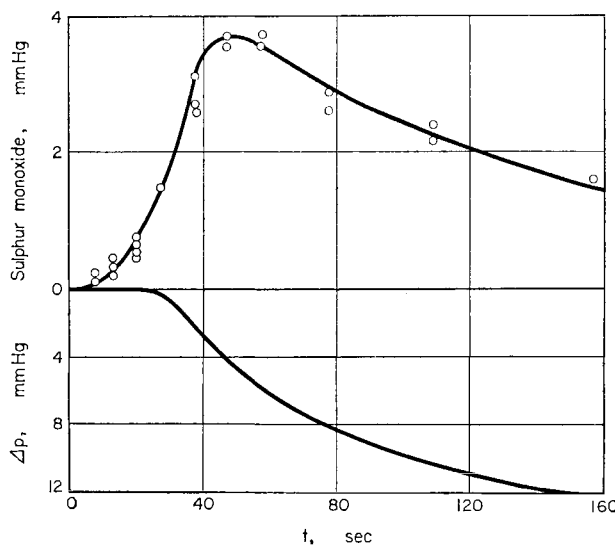


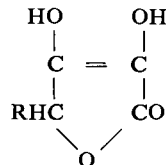
FIG. 13. Change in concentration of sulphur monoxide in the course of the slow oxidation of hydrogen sulphide H_2S (according to Pavlov, Semenov and Emanuel' [216]).

270°C ; $P_0 = 100 \text{ mm. Hg}$; $(\text{H}_2\text{S})_0/(\text{O}_2)_0 = 2/3$.

detect nitrogen trioxide, which is an intermediate in the reaction between ozone and nitrogen pentoxide. In the opinion of Sprenger the formation of NO_3 is connected with the reaction of nitrogen dioxide NO_2 , formed by the initial decomposition of N_2O_5 , with ozone, i.e. with the process $\text{NO}_2 + \text{O}_3 = \text{NO}_3 + \text{O}_2$.

Also noteworthy is the work of Egerton and Pidgeon [564], who studied the absorption spectra at different reaction times during the slow oxidation of mixtures of oxygen and butane, pentane, alcohols, etc. These authors found that in the first (initial) stage of the reaction the absorption spectra of all these mixtures contain a band of unknown origin⁽¹¹⁾ situated in the region 2800–2500 Å. After this band, which gradually weakens as the

(11) In the opinion of Ubbelohde [1234], who studied the absorption spectra of various substances in order to establish the chemical nature of the substance formed in the first stage of the oxidation ("substance X") which absorbs light in the 2800–2500 Å region, the structure of this substance must be close to that of ascorbic acid



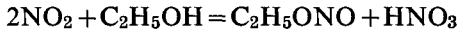
continued on page 69

reaction proceeds, absorption bands of aldehydes appear which in their turn give way to absorption bands of acids. Results similar to those of Egerton and Pidgeon were obtained by Thomas and Crandall [1220] and also Withrow and Rassweiler [1302] who studied the absorption spectra of gases in the cylinder of an internal combustion engine. In these experiments the step-wise nature of the oxidation is shown convincingly.

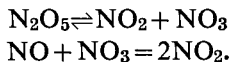
These examples of the use of the spectroscopic absorption method for studying the kinetics of chemical processes illustrate the application of electronic spectra for this purpose. Infrared absorption spectra have also been used successfully. Thus Cowan and coworkers [506] developed an infrared method with fast scanning which makes it possible to study the kinetics of fast gas reactions. This method was applied to the reaction



[505] and also the reaction



[975]. The results of the study of the first of these reactions, obtained by measuring the kinetics of the conversion of N_2O_5 into NO_2 using the intensities of the absorption spectra of these oxides, support the correctness of the reaction mechanism which involves the basic stages

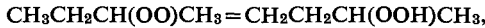


Karyakin and Nikitin [105] used the method of infrared absorption spectra to study the photochemical oxidation of various organic substances. Using the change in intensity of the bands corresponding to the frequencies of the C—H, O—H and O—O bonds it was possible to follow the formation of the hydroperoxide (the weakening of the C—H bands and the

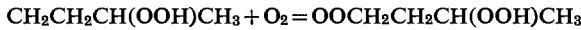
continued from page 68

Ubbelohde assumes that the "substance X" is formed as the result of the decomposition of an initially formed peroxide and is a secondary product of the oxidation reaction, apparently not influencing the course of the reaction.

According to the data of Barush *et al.* [350] "substance X" is *beta*-dicarbonyl $\text{HCOCH}_2\text{COCH}_3$ which is formed as the result of isomerization of the initially formed peroxide radical, for example



with the subsequent oxidation



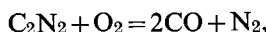
and dehydration. In the opinion of these authors a considerable part of the oxidized hydrocarbon passes through the *beta*-dicarbonyl stage. Thus in spite of the opinion of Ubbelohde "substance X" must play an important part in the mechanism of the oxidation of hydrocarbons.

appearance of O—H and O—O bands), which in its turn rapidly decomposed (with the disappearance of the O—O bands).

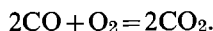
Pemsler [1021] used the infrared absorption method to study the chemical reaction between HF and ClF_3 . As he found the intensity of the absorption band at 2.57μ to be proportional to the product of the partial pressures of HF and ClF_3 , he ascribes this band to the molecular complex $\text{HF} \cdot \text{ClF}_3$ and finds that under the conditions of his experiments (close to room temperature) there is equilibrium between $\text{HF} + \text{ClF}_3$ and $\text{HF} \cdot \text{ClF}_3$ (see also [476, 1026]).

A method for the study of stable intermediate substances based on the step-wise nature of the reactions noted above was proposed by Teclu [1214] and Smithells and Ingle [1159]. This method consists in separating out the inner and outer cones of the flame of a Bunsen burner and using a gas analyser which makes it possible to analyse the intermediate substances formed as a result of the chemical processes taking place in the inner cone of the flame.

As an example let us use the results of Smithells and Dent [1158] from their studies of a cyanogen (C_2N_2) flame burning in air. Analysis of the inter-cone gas shows that when the air-to-cyanogen ratio is increased in the initial mixture from 3.31 to 4.06 the following change in its composition is observed: 65.8–69.2% N_2 , 25.5–24.4% CO, 7.4–3.8% C_2N_2 , 0.8–1.1% oxides of nitrogen and 0.5–1.5% of CO_2 . The large percentage of carbon monoxide CO, which changes little with increase of the oxygen content of the mixture, shows that the dominant overall process in the inner cone is



and in the outer cone



The visible signs of these two reactions are the rose colour of the inner-cone flame, which arises from the presence of excited C_2N_2 molecules, and the pale blue colour of the outer cone, characteristic of a carbon monoxide flame.

Subsequently Gaydon [50] perfected the separated flame method by cooling the inter-cone gases with running water and so effecting a quenching

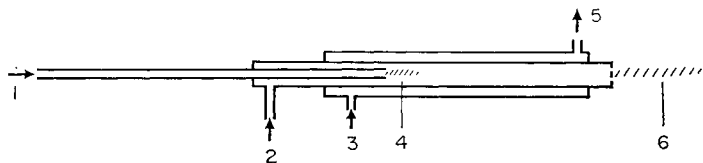


FIG. 14. Burner for the production of cooled flames with separated cones (according to Gaydon [50]). Gas and initial air feed (1); secondary air feed (2); water (3); inner cone (4); water (5); outer cone (6).

of the products ("cooled flame" method). The scheme shown in Fig. 14 is that used by Gaydon for the burner. An interesting result obtained by Gaydon in his study of the emission spectrum of the outer cone of the flame with simultaneous analysis of the inter-cone gases was that the intensity of the HCO radical bands increases with the peroxide concentration in the inter-cone gas. This is extremely important from the point of view of the mechanism of formation and conversion of organic peroxides in flames.

A method of analysis for stable substances that is extremely effective and widely used in kinetic studies is the *polarographic method* [51] for the analysis of substances dissolved in water or other solvents. The method consists of finding the current-voltage characteristics of a solution containing the substances to be analysed, using a dropping mercury electrode. The oxidation-reduction reactions of the substances present in solution, which take place at the electrode at certain voltages characteristic of a given substance, account for jumps in the current on the current-voltage curve. The size of the jump (step) is determined by the concentration of the given substance (usually being proportional to the concentration), while the position of the jump is determined by the nature of the substance. As an example Fig. 15 shows a polarogram illustrating the determination of aldehydes and peroxides in the oxidation products of acetaldehyde CH_3CHO [206]. Curve 1 shows the current-voltage characteristics of a basic electrolyte (in this case a 0.1 N solution of sodium hydroxide NaOH in water) on the addition of a certain quantity of acetaldehyde to it; curve 2 was obtained on the addition of formaldehyde H_2CO to the basic solution and curve 3 on the addition of diethyl peroxide $(\text{C}_2\text{H}_5)_2\text{OO}$. Curve 4 is the polarogram of a 2 per cent solution of the condensate obtained from the cool-flame oxidation of CH_3CHO . We see that the following steps are present on the last curve: CH_3CHO (at -1.62 V), H_2CO (at -1.47 V) and $(\text{C}_2\text{H}_5)_2\text{OO}$ (at -1.00 V); it follows that these substances are present in the condensate investigated, in quantities corresponding to the heights of the appropriate steps.

The sensitivity of the polarographic method of analysis is frequently greater than the sensitivity of normal chemical methods. Thus the sensitivity of the polarographic determination of organic substances, which are of the greatest interest with regard to the kinetics of gas- and liquid-phase reactions, is 1 g per 1000 l., so that to conduct an analysis it is sufficient to have a tenth of a drop of solution. The sensitivity in determining certain metals and other substances (in particular, alkaloids) reaches 1 g per 100,000 l. [51].

We shall now mention the *chromatographic method* of analysing gas (and also liquid) mixtures. This consists in filling an adsorption column with the mixture to be analysed so that different components of the mixture

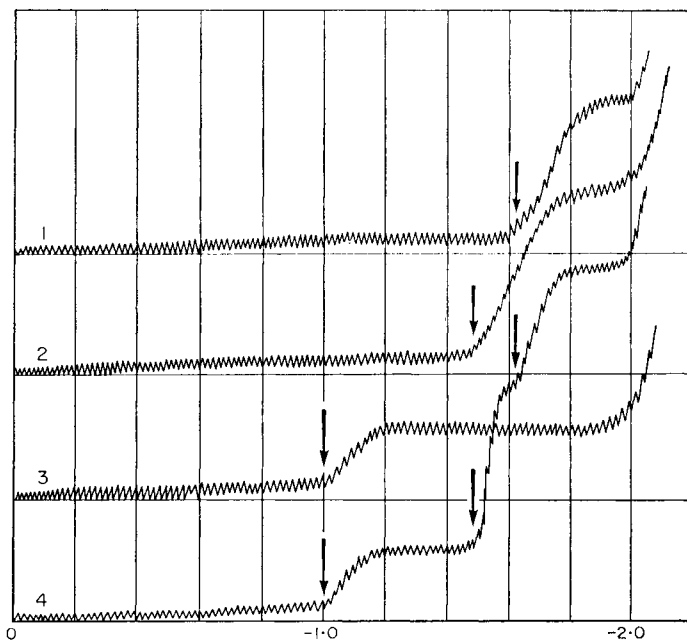


FIG. 15. Polarograms of various substances in 0.1 N NaOH (according to Neiman, Dobrinskaya and Gnyubkin [206]). (1) CH_3CHO (-1.62 V); (2) H_2CO (-1.47 V); (3) $(\text{C}_2\text{H}_5)_2\text{OO}$ (-1.00 V); (4) 2 per cent solution of the condensate obtained from the cool-flame oxidation of acetaldehyde CH_3CHO .

are adsorbed with different degrees of stability owing to the difference in their adsorption properties. Then the column is washed with a uniform stream of an inert gas "solvent" which extracts one after another the more and more strongly adsorbed substances so that in due course their separation is accomplished. Analysis of the extracted substances is carried out using normal methods, for example the interferometer method.

The chromatographic method (chromatography) discovered by the Russian botanist Tsvet (1903) was later developed in detail in its theoretical and experimental aspects and has received wide application in various scientific fields including chemical kinetics. We shall not dwell on a description of all the various methods of chromatographic analysis or on the theory of chromatographic processes⁽¹²⁾ but shall note only thermal chromatography [72] and radiochromatography [96]; the latter is a method based on the use of radioactive isotopes which greatly facilitates and simplifies the production and analysis of the distribution curves for the adsorbed substances on adsorption columns. As an example, Fig. 16

⁽¹²⁾ For literature see *Chromatography*, Moscow, FLPH, 1949 and [288, 866, 73, 283, 32].

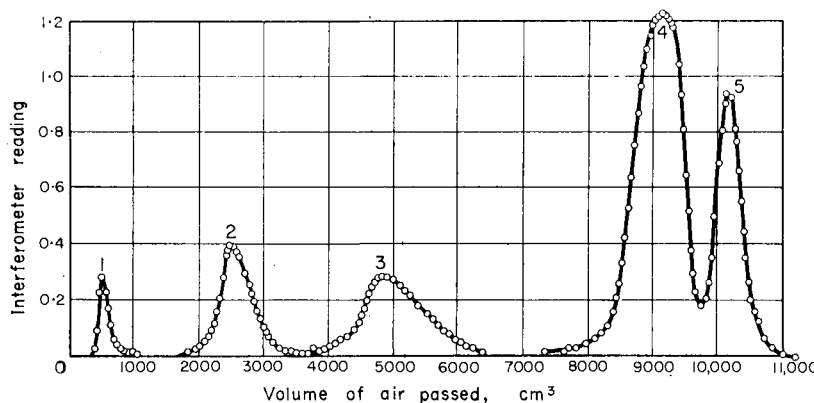


FIG. 16. Thermal chromatographic separation of a mixture of methane CH_4 (1), ethane C_2H_6 (2), ethylene C_2H_4 (3), propane C_3H_8 (4), and propylene C_3H_6 (5) (according to Medvedeva and Torsyeva [186]).

shows the curve for the thermal chromatographic separation of a mixture containing 9.2 cm^3 of methane CH_4 (1), 12.0 cm^3 of ethane C_2H_6 (2), 17.8 cm^3 of ethylene C_2H_4 (3), 31.8 cm^3 of propane C_3H_8 (4) and 12.3 cm^3 of propylene C_3H_6 (5) [186].

Labile Intermediates

The above analytical methods except spectroscopy, which is of some limited use, are not suitable for the detection and measurement of the concentration of labile intermediate substances which have a high chemical reactivity, and correspondingly very short lifetimes. Spectroscopic methods used to solve the analytical problems include both emission and absorption analysis. The following radicals (or radical-type substances) have been detected in various flames using emission analysis: CH , NH , OH , NO , PO , SO , BrO , CN , CS , CBr , C_2 , S_2 , HCO , NH_2 , C_2H , HO_2 , C_3 , CH_3O , $\text{C}_2\text{H}_5\text{O}$. The absorption spectra observed in flames during thermal dissociation and photodissociation of various substances and also in an electric discharge have been used to identify the radicals: BH , CH , NH , OH , PH , SH , SD , C_2 , CN , CF , CS , NO , ClO , S_2 , HCO , DCO , NH_2 , CF_2 , PH_2 , PD_2 , C_3 , N_3 , C_5H_5 , $\text{C}_6\text{H}_5\text{O}$, $\text{C}_6\text{H}_5\text{S}$, $\text{C}_6\text{H}_5\text{NH}$, etc.

We shall consider some of these radicals in more detail.

The bands of hydroxyl OH lying in the ultraviolet and partly in the visible regions (for emission spectra) of the spectrum are a characteristic property of the spectra of flames containing hydrogen and oxygen. Recently the infrared spectrum of OH emitted by vibrationally excited radicals was discovered in the reaction of atomic hydrogen with ozone [941, 482]. In this spectrum there are observed transitions from various

vibrational levels of OH down to $v = 9$ which corresponds to an energy of 80 kcal [782]. The infrared vibrational spectrum of OH was detected earlier in the spectrum of the night sky. The microwave spectrum of hydroxyl has recently been used for its detection in an electric discharge in water vapour [1101].

Fowler and Vaidya suggested that the characteristic bands discovered by Vaidya [1238] in the emission spectrum of hydrocarbon flames should be ascribed to the HCO radical. Confirmation of the correctness of this suggestion was obtained as a result of a detailed analysis of the structure of the absorption spectrum of HCO and DCO [751]. In particular a linear structure was established for this radical in the excited state and a bent structure with angle $\angle \text{HCO} = 120^\circ$ in the ground state. Even earlier Burton [470] had shown that the HCO radical is very stable and does not decompose even at 100°C.

It is assumed that the emission bands in the 5060–5700 Å wavelength region which are observed in the spectrum of a discharge in the vapour of various organic substances should be ascribed to the C₂H (and also C₂D) radical [1114].

The group of bands in the 4050 Å region, characteristic of the C₃ radical and observed in the spectrum of comets, was also detected by Herzberg [748, 749] in the spectrum of a discharge in CH₄ and was ascribed by him to the CH₂ radical. These bands were also later detected in the emission spectrum of a series of hydrocarbon flames [916]. That these bands belong to the C₃ molecule was shown by Douglas [549] as the result of an analysis of the rotational structure of the C₃¹² 4050 Å band and also of the C₃¹³ band.

The band of frequency 1305 cm⁻¹, which is detected in the infrared emission spectrum of flames, is ascribed to the HO₂ radical [255a].

We may also note that absorption bands of NH₂ (the so-called alpha-bands) are observed during photolysis of ammonia NH₃ and hydrazine N₂H₄ but NH bands only during photolysis of hydrazine [750]. However both bands are observed during a pulsed discharge in both ammonia NH₃ and in hydrazine N₂H₄ [968]. See also [343a].

Emission spectral analysis may be used in practice as only a qualitative method of investigating intermediate substances. By measuring the intensity of a spectrum it is possible to determine the concentration of excited molecules, which is always considerably less than the concentration of unexcited molecules. Determination of the number of unexcited molecules requires further study; it is of fundamental interest with regard to the kinetics and mechanism of the reaction. In the general case the following relationship can be established between the concentrations n' and n of excited and unexcited molecules of a substance:

$$n' = fn. \quad (5.1)$$

The quantity f may be called the *excitation factor*. This quantity is a complex function of the conditions of excitation and must be determined experimentally in each individual case. Here the only exception is the case of *thermal* or *equilibrium* radiation where the ratio f of the concentrations of excited and unexcited molecules is given by the Boltzmann distribution. In the simplest case of atomic radiation the excitation factor is

$$f = (g'/g) \exp(-A/RT)$$

where g and g' are the statistical weights of ground and excited states and A is the excitation energy of the atom.

Experimental determinations of the excitation factor show that in flames, i.e. for chemical excitation of luminescence (*chemiluminescence*), the quantity f is usually *considerably greater* than the thermal factor. This property of chemiluminescence is a consequence of the *non-equilibrium* nature of this type of radiation, the excitation of which is directly connected with the energy released as the result of an elementary chemical process. It follows that chemiluminescence is very important not only as a method of identifying labile intermediate substances but is also a delicate method of establishing the details of chemical reaction mechanisms. Consider the following example: measurements of the absolute intensity of hydroxyl bands in the spectrum of a rarefied hydrogen flame (pressure 10 mm Hg, temperature 1000°K) indicate that it exceeds by at least 10^{12} the intensity of equilibrium radiation under the conditions of this flame. Consideration of the various possible mechanisms of excitation of hydroxyl in the flame leads to the conclusion that the excited hydroxyl arises as a result of the recombination of H and O atoms; and this is in quantitative agreement with the data from studies of the properties of the radiation of hydroxyl and with the mechanism of combustion of hydrogen. Thus the fact that the non-equilibrium character of the hydroxyl radiation has been established serves as an indirect indication that H and O atoms are present in the hydrogen combustion zone. This conclusion is also supported by other data [133].

One of the widely used emission spectral methods is that for the determination of oxygen atom concentrations, based on measurements of the intensity of the spectrum emitted in process $O + NO = NO_2 + h\nu$ (M. L. Spealman and W. H. Rodebush, *J. Amer. Chem. Soc.* **57**, 1474, 1935; [654].) The intensity of this spectrum, as measured by James and Sugden [799], was found to be proportional to the concentration of O atoms and to that of added nitrogen oxide. Kaufman (F. Kaufman, *J. Chem. Phys.* **28**, 352, 1958) reports that it does not depend on admixtures of foreign gases. The rate constant of this process is of the order $10^{-18} \text{ cm}^3 \text{ molecule}^{-1} \text{ sec}^{-1}$.

Sugden and co-workers have put forward a series of spectroscopic methods for the determination of the concentration of H atoms in a

flame [463b] which are based on measurements of the intensity of radiation of the resonance doublets of alkali metals added to the combustible mixture, and on the equilibrium constant for the appropriate process (for example, $\text{Li} + \text{H}_2\text{O} = \text{LiOH} + \text{H}$); these authors also put forward a method for determining OH concentration according to the intensity of the continuous emission spectrum connected with the process $\text{Na} + \text{OH} = \text{NaOH} + h\nu$ [799a].

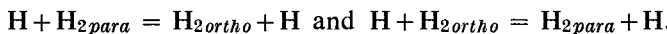
In contrast with the emission method, the absorption spectroscopic method makes it possible to determine directly the concentration of unexcited molecules. However the applicability of this method to detect a radical requires that the radical should have suitable energy levels which give absorption bands in an accessible spectral region and also an adequate concentration of light-absorbing radicals. The minimum measurable concentration is rarely less than that corresponding to a partial pressure of about 10^{-2} – 10^{-3} mm Hg (for an absorbing layer thickness of 10 cm). Table 2 shows the minimum quantities of various substances (including radicals) detected by their absorption spectra for an absorbing layer thickness of 10 cm [1286]. The concentrations of active intermediate substances are frequently of similar or even greater orders of magnitude (see for example p. 610). The limited use of the absorption method results mainly from the absence of absorption bands in the accessible region of the spectrum, so that this method is practicable only in certain cases. We should add that to measure absolute concentrations using this method one must also know the probabilities of the appropriate transitions, which are known for only a few molecules. Below we shall briefly consider some other methods for detecting and measuring the concentration of labile intermediate substances.

TABLE 2

The minimum concentrations of molecules and radicals (in g. mole/l) detected by their absorption spectra for an absorbing layer thickness of 10 cm (according to Wieland) [1286]. (λ is the wave length characterizing the absorption region)

Absorbing molecules or radicals	c , g. mole/l.	λ , Å
OH	$6 \cdot 10^{-8}$	3100
CN	$\sim 6 \cdot 10^{-10}$	3880
CdI	$< 3 \cdot 10^{-6}$	3400
HgI	$3 \cdot 10^{-7}$	3050
O ₃	$3 \cdot 10^{-6}$	2600
I ₂	$3 \cdot 10^{-5}$	5000
C ₆ H ₆	$1 \cdot 10^{-4}$	2550

Usually these methods are based on some chemical reaction of the intermediate substances (including also isotopic exchange reactions). In one of these, the method of *ortho-para conversion of hydrogen* (see Steacie [1169], pp. 59–61), *para*-hydrogen is mixed with the reacting gas and the degree of its conversion into *ortho*-hydrogen after a definite time interval is measured. The method is most accurate for the measurement of the concentration of atomic hydrogen in the absence of other radicals or atoms, since in this case the *ortho-para* conversion is based on only two processes, namely:



Introducing the rate constant k_H for these processes, we have

$$-d[(H_2)\text{para}]/dt = k_H(H)[(H_2)\text{para} - (H_2)\text{ortho}].$$

Considering the concentration of H atoms to be constant throughout the measurements and the overall quantity of hydrogen $(H_2\text{para}) + (H_2\text{ortho}) = (H_2)$ to be constant also, we obtain as a result of integrating the previous equation

$$(H) = -\frac{1}{2k_H t \ln(1-2\xi)}, \quad (5.2)$$

where

$$\xi = \frac{(H_2) - (H_2)\text{para}}{(H_2)}$$

is the quantity of *para*-hydrogen converted into *ortho*-hydrogen during the time t .

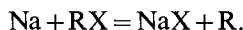
When the *ortho-para* conversion method is used to measure the concentration of any radical R, the reacting gas contains a mixture of active particles of at least two kinds: the radicals being studied, and H atoms formed by the interaction of the radical R with a hydrogen molecule. Considering that *ortho-para* conversion is based chiefly on the interaction of H atoms with molecules of *para*- or *ortho*-hydrogen [1011] and that H atoms disappear as a result of the reaction $H + RH = H_2 + R$, then when their concentration becomes stationary (according to the condition $d(H)/dt = 0$) the required concentration of radicals R is found to be

$$(R) = -\frac{1}{2k_H t \ln(1-2\xi)} \frac{k' (RH)}{k (H_2)}, \quad (5.3)$$

where k and k' are the rate constants for the processes $R + H_2 = RH + H$ and $H + RH = H_2 + R$ (or any other process leading to the disappearance of H atoms). From formula (5.3), knowing the quantities k_H , k , k' , (RH) and (H_2) , it is possible to find the concentration of R radicals. The method

of ortho-para conversion has most often been used to measure the concentration of H atoms and certain radicals in photochemical reactions and also in the thermal decomposition of a series of substances.

A method of studying labile intermediate substances which, like the ortho-para conversion method, consists of the introduction into the reaction zone of foreign admixtures, has been used with success by several authors to detect free atoms and radicals formed in various reactions. Thus Polanyi and co-workers [1033] added iodine vapour to a reaction mixture of an alkali-metal vapour (Na) and an alkyl halide RX (X=Cl, Br), thus forming R radicals according to the reaction



The presence of the radicals was shown by the formation of the alkyl iodide RI (which appears as the result of the reaction $\text{R} + \text{I}_2 = \text{RI} + \text{I}$). The "iodine method" for detecting free radicals was later used by Gorin [690] to detect H atoms (as HI) and various radicals (as RI) formed in the photolytic reactions of organic substances.⁽¹³⁾

A similar method has been developed by Medvedev and co-workers [185] and applied to the study of free radicals formed in polymerization processes. These authors used a titrimetric procedure to determine the products of the interaction of radicals with iodine, which was introduced into the reacting substance; and so they were able to measure the concentrations of radicals carrying the polymerization chain.

We might also mention Hinshelwood's method ([1169] p. 56) which consists of introducing oxides of nitrogen into the reaction zone and calculating the concentration of radicals by the inhibiting effect of the oxides introduced. The reason for this inhibiting action is the chemical interaction of a radical with a molecule of the oxide of nitrogen.

An idea of the nature of this interaction and of its products is given by the work of Bryce and Ingold [462] who studied the reaction of methyl, CH_3 , with NO. These authors found that for short reaction times (less than 5×10^{-2} sec) the only reaction product is CH_3NO , from which it follows that CH_3NO is the primary product. For a reaction time of 5×10^{-2} sec the reaction products are found also to include NH_3 , H_2O , HCN, CO, N_2 , CO_2 , CH_3CN , etc. At 480° and 900°C the rate of reaction of CH_3 with NO is the same, so that the activation energy of this reaction is zero.

According to Sleppy and Calvert's measurements (W. C. Sleppy, J. G. Calvert, *J. Amer. Chem. Soc.* **81**, 769, 1959) at pressures of 150–280 mm Hg the reaction between CH_3 and NO obeys the bimolecular law. At 25°C the rate constant of this reaction is $10^{-12} \text{ cm}^3 \text{ molecule}^{-1} \text{ sec}^{-1}$.

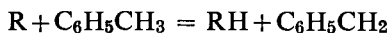
Fenimore and Jones (C. P. Fenimore, G. W. Jones, *J. Phys. Chem.* **62**,

⁽¹³⁾ Certain of Gorin's results have not been confirmed [1029, 918].

178, 1958) determined O atom concentrations in a flame from the yield of nitrogen oxide formed by the reaction $O + N_2O = 2NO$ on addition of nitrous oxide. The rate constant of this reaction was found to be

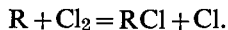
$$k = 3.3 \times 10^{-10} \exp(-32000/RT) \text{ cm}^3 \text{ molecule}^{-1} \text{ sec}^{-1}.$$

Recently Szwarc [1200] has developed and used with success the "toluene method" for detecting free radicals and solving the problem of the chemical mechanism of the pyrolytic splitting of molecules of various substances; the basis of this method is the great mobility of the hydrogen in the methyl group of toluene $C_6H_5CH_3$. When toluene is added to a reaction mixture the toluene reacts with radicals present in the mixture according to the scheme



and it is possible to decide whether free radicals are present in the mixture by the formation of dibenzyl ($C_6H_5CH_2$)₂ which is formed as a result of the recombination of $C_6H_5CH_2$ radicals.

An extremely sensitive method used by Bogdandy and Polanyi [423] consists of observations of the chain reaction in a mixture of chlorine and hydrogen. By adding hydrogen to chlorine, which reacts with the vapour of the alkali elements (and also with Cd, Zn, Mg, As and P vapour), these authors detected chlorine atoms, arising as a result of the above reactions, by the formation of large quantities of hydrogen chloride. This reaction of chlorine atoms with hydrogen was also used to detect CH_3 , C_2H_5 and C_6H_5 radicals which appear as a result of the reaction $Na + RBr = NaBr + R$ and which react with the Cl_2 molecules according to the scheme



Another method for detecting free radicals, based on essentially the same chemical principle, has been proposed and developed by Paneth [1006] (for this *mirror method* see also Steacie [1169], pp. 37-53). The method is based on the reactions of radicals (and atoms) with metallic mirrors placed in a stream of the gas issuing from the reaction vessel. As a result of these reactions volatile compounds are formed resulting in the obscuration of the metallic mirrors. It is possible to estimate the concentration of radicals by the rate of disappearance of the mirror and the nature of the radicals by analysis of the metallic compound formed. It has been established that different metals interact with different radicals in different ways. For example methylene radicals CH_2 "corrode" tellurium, antimony, selenium and arsenic mirrors and do not affect zinc, cadmium, bismuth, thallium and lead; methyl radicals CH_3 (and also other alkyl radicals), however, react with all these mirrors. It has also been found that hydrogen atoms react with germanium, tin, arsenic, antimony and

tellurium [1169] and also with carbon [4] but do not affect lead or bismuth [1169]. This specificity of interaction of radicals (and atoms) with various substances makes it possible to form an opinion of the nature of the radical. The mirror method has been used to establish the nature, and to measure the concentration, of radicals formed during the thermal and photochemical decomposition of various substances and also of radicals formed in certain electric-discharge reactions. A disadvantage of this method is the necessity for careful purification of the gases from traces of oxygen which dulls the mirror by the formation of an oxide film.⁽¹⁴⁾

To detect hydrogen atoms and to measure their concentration in various flames (H_2 , CO , C_2H_2) the method of catalytic recombination⁽¹⁵⁾ was developed; this method is based on the fact that the catalytic activity of different substances with regard to the recombination of atoms and radicals at their surfaces is extremely specific. One of these catalysts is the mixed oxide $ZnO \cdot Cr_2O_3$ which stimulates preferentially the recombination of H atoms. When this catalyst (as a thin film applied to the surface of a quartz capillary) is introduced into the flame zone it is observed to heat up as a result of the process $H + H \rightarrow H_2$ [149, 151]. In the case of stationary flames (streams) the heating-up factor ΔT , which is equal to the difference in the temperatures of the catalyst surface and the surrounding flame, must be constant. Assuming that the heat balance of the catalyst is determined by the evolution of heat as a result of the recombination of H atoms diffusing to its surface, and by the elimination of heat through transfer into the surrounding gas, the following expression [149] may be obtained from the equation of balance:

$$\Delta T = \frac{Q}{2C_v M} \frac{p_H}{p}, \quad (5.4)$$

where Q (103,000 cal/mole) is the dissociation energy of the H_2 molecule; C_v (5 cal/degree) is the molar heat capacity of the gas in the combustion zone; M (10) is the mean molecular weight of the gas; p is the pressure in the combustion zone and p_H is the partial pressure of atomic hydrogen. Introducing the known values of Q , C_v and M into formula (5.4) the coefficient of proportionality between the heating factor ΔT and the relative partial pressure $\pi_H = p_H/p$ of H is found to be about 1000.

⁽¹⁴⁾ Tellurium mirrors are an exception since they are not rendered passive by traces of oxygen; see Steacie [1169], pp. 42-43.

⁽¹⁵⁾ This method was first used by Bonhoeffer [425] to detect H atoms formed in an electric discharge. Other authors have used the catalytic recombination method in various modifications. For literature see Steacie [1169], pp. 64-65. Here we shall just mention that Harteck and Kopsch [728] have determined the concentration of oxygen atoms by the heating of a platinum wire due to the recombination of atoms at its surface, and that Schwab and Friess [1124] have measured the concentration of chlorine atoms by the heating of a copper-constantan thermocouple.

Thermocouple measurements of the heating effect for a pressure of several millimetres of mercury in the flame zone and for various hydrogen–oxygen mixtures show that the ΔT factor reaches several hundreds of degrees; it follows from this that the partial pressure of H atoms in the flame zone is some tenths of a millimetre of mercury and that the ratio of the partial pressures of atomic and molecular hydrogen is about 10 per cent.

Eltenton [569] has developed a *mass-spectrometric method* based on the fact that the appearance potential I_R of an ion R^+ during the bombardment of R radicals with electrons is less than the appearance potential I_M of the same ion during the bombardment of molecules containing this radical. It is not difficult to see that

$$I_M = D + I_R \quad (5.5)$$

where D is the energy of abstraction of the radical R from M. In the case of light hydrocarbons, D is about 4 eV, i.e. an easily measured value. By subjecting the gas passing from the reaction zone to electron bombardment in the ionization chamber of a mass spectrometer and by measuring the appearance potentials of the ions of appropriate masses, Eltenton detected CH_3 , C_2H_5 and other radicals formed in various reactions.

The mass-spectrometric method for detecting free atoms and radicals and for the study of radical reactions has been developed further by various authors. For example Ingold and Lossing [792] have identified the following radicals in various reactions: C_6H_5 , $C_6H_5CH_2$, C_6H_5O , C_6H_5CO , allyl $CH_2=CH-CH_2$ and vinyl $H_2C=CH$. Foner and Hudson [616] have detected H and O atoms and OH radicals in a hydrogen flame and the CH_3 radical in a methane–oxygen flame. The same authors [617] have detected HO_2 as the primary product of the interaction of atomic hydrogen with O_2 molecules and have measured the ionization potential of this radical (11.53 eV) and the bond energy of H– O_2 (47 ± 2 kcal) [618, 790]. Tsuchiya [1232] observed hydroxyl OH formed as a result of the thermal dissociation of water vapour heated to $1200^\circ C$ (see also Steacie [1169], pp. 66–67).

Another method is that of *isotopic exchange* which may be used in individual cases to establish the nature of radicals taking part in a reaction and to measure their concentration. This method was first used to measure the stationary concentration of H atoms in the gas resulting from an electric discharge in hydrogen. On adding deuterium to the gas an exchange reaction takes place, namely



The concentration of atomic hydrogen taking part in the reaction may be determined from the yield of HD [598].

New uses for hydrogen exchange in establishing the nature of radicals were proposed by Voevodskii, Lavrovskaya and Mardaleishvili [164, 160]. On the basis of their analysis and data from the literature, these authors came to the conclusion that in a gas containing aliphatic radicals and molecular deuterium, the radicals easily exchange hydrogen with the D_2 molecules although only those H atoms linked to a carbon atom possessing a free valency take part in the exchange.⁽¹⁶⁾ The most important fact established in these studies is that, when the reaction is carried out in the presence of molecular deuterium, exchange in the products serves as an indication that free radicals have taken part in the mechanism of the process. By this method it was established, in particular, that CH_3 and C_2H_5 radicals take part in the slow oxidation of propane. For other methods of detecting and identifying free atoms and radicals see Steacie [1169] (Chap. 2) and also [467 and 882].

It is found from measurements of the concentration of radicals in the reaction zone that in many cases these concentrations are very considerable. Thus it has already been shown (p. 81) that the concentration of H atoms in rarefied hydrogen flames may be over 10 per cent of the concentration of molecular hydrogen. Measurements of the concentration of hydroxyl in these flames also indicate high values [133]. The concentration of oxygen atoms in a carbon monoxide flame [152] and the concentration of CS radicals in a carbon disulphide flame [129, 130] are also high. These concentrations exceed by factors of thousands and tens of thousands the equilibrium concentrations of atoms and radicals under the conditions of the appropriate flames, and it follows that their origin is chemical and not thermal. It has been established in a series of cases that radicals play a leading role in the reaction. For example in the combustion of hydrogen [133] and in that of moist carbon monoxide [148] it has been shown that the overall rate of reaction is determined by the rate of interaction of fuel molecules with hydroxyl.

The leading part played by free atoms and radicals in reactions is also apparent from the fact that the introduction of these particles into the reaction zone considerably increases the rate of reaction. Many cases are known of this accelerating action of atoms and radicals. It has been established that reactions are often accelerated by irradiation of the reacting substances, thus creating free atoms and radicals, or by the introduction into the reaction zone of substances which yield free radicals on their decomposition. An especially large effect is obtained when free atoms are introduced directly into the reaction zone. An illustration of this is given by Fig. 17 which shows the yield of CO_2 in the $CO + O_2$ reaction for various temperatures on exposing the mixture to ultraviolet

⁽¹⁶⁾ This does not exclude the possibility that exchange reactions of this type take place at solid surfaces.

light (γ_ϕ) and the yield without exposure (γ_r) [147]. It is clear from this figure that exposure sharply increases the yield ($\gamma = P_{CO_2}/P_{CO}$). Figure 18 shows the effect of oxygen atoms on the self-ignition of detonating gas [198]. It can be seen that the introduction of O atoms into the reaction zone greatly enlarges the region of self-ignition.

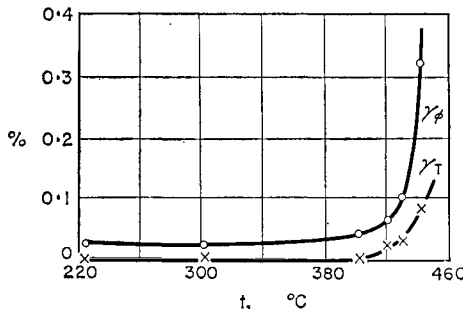


FIG. 17. The yields of carbon dioxide CO_2 in the dark (γ_r) and in the photochemical (γ_ϕ) reactions of $CO + O_2$ (according to Kondrat'eva and Kondrat'ev [147]).

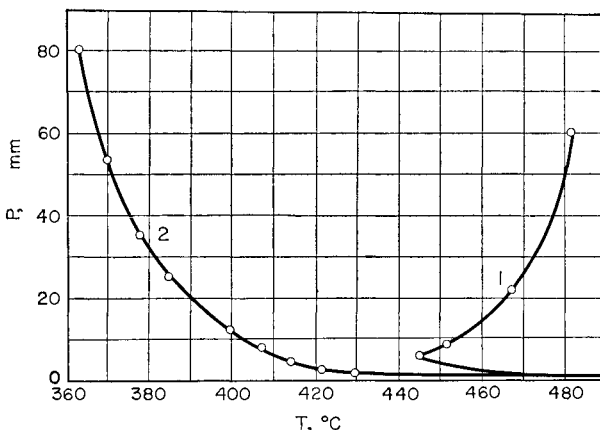


FIG. 18. Enlargement of the region of self-ignition of the mixture $2H_2 + O_2$ in the presence of oxygen atoms (according to Nalbandyan [198]). (1) Before the introduction of atomic oxygen; (2) in the presence of O atoms.

The accelerating action of free atoms and radicals is clearly based on the ease with which they enter into various reactions. According to experimental and theoretical data the high reactivity of free atoms and radicals is shown by the relatively low activation energy of reactions in which they participate. As free atoms and radicals play an important role in chemical reactions the study of elementary reactions in which they take part is of

exceptionally great interest with regard to the chemical mechanism of reactions. Reactions of free atoms and radicals constitute very important chapters in the study of the chemical process.

§6. Reactions of Free Atoms

Reactions in Highly-rarefied Flames

The reaction $M + HgCl_2$. In the study of the elementary reactions of free atoms and radicals, investigations of chemical reactions in so-called *highly-rarefied flames* have proved very important. These are a special class of flame which burn at very low pressures (about 0.1–0.001 mm Hg) and at relatively low temperatures (200–300°C). The low temperature of these flames shows that the chemical processes take place in them without much activation energy. Since highly-rarefied flames are observed at low pressures, processes which occur in them must be mainly bimolecular. For these reasons the mechanism of reactions in highly-rarefied flames is very simple and it has been finally established in almost all its details. In explaining this mechanism a not insignificant role has been played by studies on chemiluminescence.

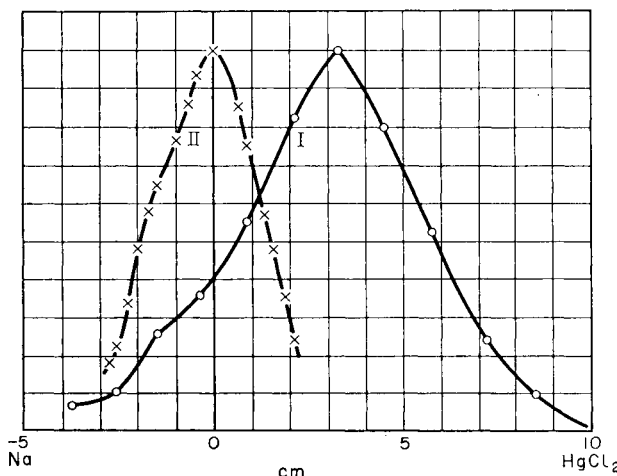


FIG. 19. The distribution of reaction product (zone I, circles) and of luminescence (zone II, crosses) in the reaction $Na + HgCl_2$ (according to Kondrat'ev [119]). Abscissa: distance along reaction tube.

The simplest way of obtaining these flames, which has been used to study the reactions of Na and K vapour with Cl_2 , Br_2 , I_2 , $HgCl_2$, $HgBr_2$ and HgI_2 vapour, is to permit the reagent vapours to stream counter to each other in an evacuated glass or quartz tube heated to 200–300°C. The reaction which takes place where the two streams mix by diffusion is

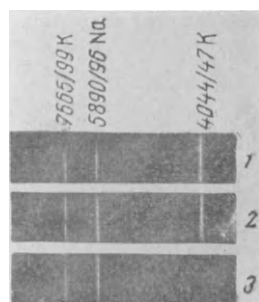
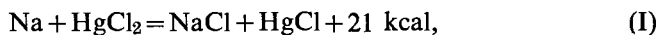


FIG. 20. Highly rarefied flame spectra, $K + HgCl_2$ (1), $K + HgBr_2$ (2), $K + HgI_2$ (3), (according to Kondrat'ev [122]).

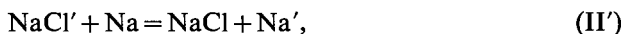
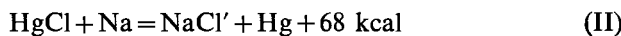
detected by the luminescence of the flame and by the deposition of a solid reaction product—the alkali-metal halide salt.

We shall consider in more detail the reaction between sodium vapour and the vapour of mercuric chloride HgCl_2 [1030]. In this reaction, as in the other reactions mentioned above, the intensity of luminescence of the flame is within one per cent determined by the sodium D-lines, and consequently the flame has a characteristic orange colour. The distribution of the intensity of chemiluminescence and of the reaction product (NaCl) along the reaction tube is shown in Fig. 19 [119]; it can be seen from the figure that the reaction zone falls into two parts: a zone with maximum yield of reaction product (I) and a zone with maximum yield of light (II); zone I is situated closer to the salt and zone II closer to the sodium.

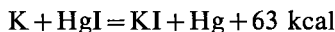
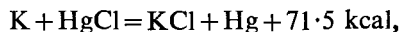
Separation of the reaction zone into two parts is explained by the fact that the reaction takes place in two stages: in zone I the following process takes place:



and in zone II



The excitation energy of the sodium D-lines is 48 kcal; consequently the heat of reaction II is quite sufficient to excite these lines. Moreover the excitation of other sodium lines requires a minimum of 73 kcal and this explains the predominance of the D-lines in the spectrum of the flame during this reaction. The accuracy of this conclusion is supported by other data. A comparative study of the flame spectra of $\text{K} + \text{HgCl}_2$, HgBr_2 and HgI_2 [121] shows that whereas the first and second terms of the principal series of potassium are of comparable intensity in the first two flame spectra, in the third flame spectrum the second term is vanishingly weak compared with the first (Fig. 20). Comparing the excitation energies of these terms in the principal series of potassium, 37.0 and 70.5 kcal, with the thermal effects for processes II:



we see that in the last case the thermal effect is sufficient to excite only the first term in the principal series of potassium whereas in the first two cases it is sufficient to excite both terms. A comparison of the intensities of these terms in the first two flames shows that both terms are excited in

process II and that practically all the energy liberated in process II is concentrated in the molecule MX' .⁽¹⁷⁾

These molecules may be either normal molecules MX in high vibrational levels, or excited molecules, possibly in a metastable electronic level. The latter hypothesis is more probable since the measurements of various authors show that the probability for process II, i.e. the probability for energy transfer from an MX' molecule to an M atom, is close to the probability for transfer of the electronic excitation energy, which is found to be nearly unity from data on the quenching of fluorescence. However, the first hypothesis must not be ruled out [862].

The reaction $M + X_2$. The reaction of atoms of alkali elements with halogens has many properties which distinguish it from the reaction $M + HgX_2$ [1030]. In contrast with the latter, the light-yield in $M + X_2$ reactions is a function of temperature, the light-yield decreasing with increase in temperature. According to Polanyi and Schay's measurements [1032] the negative temperature coefficient for the light-yield in the $Na + Cl_2$ reaction corresponds to an energy of 18.5 kcal, which is close to the dissociation energy for the Na_2 molecule (17.5 kcal) (see Roth and Schay [1091]). Hence it may be concluded that the excitation of light in $M + X_2$ reactions is connected with the participation of M_2 molecules in the reaction. The inclusion of M_2 molecules in the mechanism of $M + X_2$ reactions is also necessary because at low pressure, when ternary collisions are of very low probability, the interaction of a halogen atom (which appears in this reaction, see below) with a metal atom is possible only at the walls of the reaction tube; consequently the luminescence which is observed in the space of the reaction zone cannot be attributed to the reaction $M + X \rightarrow MX$. On the other hand it follows from a calculation of the equilibrium $2Na \rightleftharpoons Na_2$ that the ratio of the partial pressure of Na_2 and Na in saturated sodium vapour at 220°C is 0.003. Hence it is seen that the concentration of Na_2 molecules in the rarefied flame is so considerable that not only must the reaction of halogen atoms with M_2 molecules be taken into account but it should even be recognized as a fundamental homogeneous process in zone II. As we shall see below, the energy liberated in this process is the main source of the radiation of the flames considered.

Another property of $M + X_2$ reactions is that, as we have already

⁽¹⁷⁾ According to the data of Berger and Schay [384], in these reactions the $4p^2P$ level of the K atom (the first term of the principal series of potassium is connected with the transition from this level to the ground level $4s^2S$) is excited not directly but via the $3d^2D$ level whose excitation energy is 61.5 kcal. The transition from this level to the ground level is realized directly by the emission of the weak "forbidden" line $^2D - ^2S$ (which was detected by Berger and Schay in the flame spectrum) and also in two stages via the $4p^2P$ level—with the emission of an infrared line (a triplet) $^2D - ^2P$ and a red line (a doublet) $^2P - ^2S$, the first term of the principal series. This observation supports the conclusion that the energy liberated in process II is concentrated in the molecule MX' .

mentioned (p. 29), an admixture of hydrogen in an $\text{Na} + \text{Cl}_2$ flame results in the formation of a considerable quantity of HCl besides NaCl (the yield is as much as 10,000 HCl molecules to one NaCl molecule), whereas in an $\text{Na} + \text{HgCl}_2$ flame HCl is not formed at all. This is an indication of the presence of chlorine atoms in an $\text{Na} + \text{Cl}_2$ flame and of their absence in an $\text{Na} + \text{HgCl}_2$ flame; this is in complete agreement with the mechanism of these reactions. The mechanism of the $\text{M} + \text{X}_2$ reactions is the sum of the following processes which take into account the properties of these reactions:



Here, as in the $\text{M} + \text{HgX}_2$ reactions, the reaction zone falls into two parts. The energy liberated in process I in the case of the reaction $\text{Na} + \text{X}_2$ is not sufficient to excite an atom of sodium and in the case of the $\text{K} + \text{X}_2$ reaction is only sufficient to excite the first term in the principal series of the potassium atom. For this reason the source of the excitation energy of the sodium atom can only be process II, in which the energy liberated is in all cases greater than the excitation energy of the sodium atom; the source of excitation of the two terms of the principal series of potassium can also only be process II (only in the case of I_2 is the energy liberated in this process insufficient to excite both terms).

It might be assumed that the M atom formed in process II is directly excited by the energy liberated in this process. A series of factors are at variance, however, with this assumption. One should mention first the experiments of Ootuka [999] who studied the intensity of luminescence of $\text{K} + \text{Cl}_2$ and $\text{K} + \text{Br}_2$ flames with potassium containing 7 per cent sodium. Ootuka found that the intensity of *D*-luminescence in this case is in no way related to the sodium content of the potassium vapour, since the light-yield in the form of *D*-luminescence in the sodium-potassium mixture (with regard to the overall quantity of reacted sodium) is many times greater than the yield in the $\text{Na} + \text{X}_2$ reaction. Hence it follows that in Ootuka's experiments the overwhelming majority of sodium atoms are excited as a result of the reaction of Cl or Br atoms with K_2 molecules; this would not be the case if, as a result of process II, i.e. $\text{X} + \text{K}_2 = \text{KX} + \text{K}$, direct excitation of a potassium atom had taken place. Thus it must be assumed that the major part of the energy liberated in process II is concentrated in the MX molecule, while the excitation of the metal atom takes place as a result of process II'.

The following factors also support this hypothesis. Study of the influence of foreign gases on the intensity of chemiluminescence shows that the quenching of chemiluminescence in highly-rarefied flames is much stronger than that of appropriate metals (Na, K) by the same gases. If the excited atoms in the flame zone arose directly from process II then the quenching action of foreign gases would clearly have been identical in both the chemiluminescence and fluorescence. Since this is not so, the stronger quenching of the chemiluminescence must clearly be connected with deactivation of MX' molecules, i.e. we must again assume the primary excitation to be of the latter, which excludes direct excitation of metal atoms. Finally the basis for assuming primary excitation of MX molecules is the fact that in the spectra of highly-rarefied flames there are observed in almost every case, besides the main most intense lines (the first terms of the principal series of the metals), both higher terms of the principal series and also terms of other series whose excitation energy is considerably greater than the heat effect of process II. For example in the $Na + Cl_2$ flame there are observed very weak lines whose excitation energy is 113.5 kcal, whereas the heat effect of the reaction $Cl + Na_2 = NaCl + Na$ is equal to only 80.2 kcal. The heat of the process $Na + Cl \rightarrow NaCl$ (97.7 kcal), which takes place on ternary collision, and the overall energy of two excited sodium atoms ($2 \times 48 = 96$ kcal), which makes it possible for higher levels of the Na atom to be excited on the binary collision of these atoms, are both considerably less than 113.5 kcal; the possibility is not excluded that such a high level of the Na may be excited in the process $NaCl' + Na' = NaCl + Na''$ (the maximum energy of which is $80.2 + 48.0 = 128.2$ kcal); this last reaction must have a considerable probability when MX' is a molecule in a metastable or vibrationally-excited state.⁽¹⁸⁾

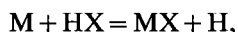
Experiments show that the yield of reaction products in highly-rarefied flames of both types, i.e. the reactions $M + X_2$ and $M + HgX_2$, are *independent of temperature*. This fact, and also the relatively small extent of the reaction zone, point to a high reaction rate and to the absence of a marked activation energy. This means that the individual elementary processes involved in the reaction mechanism take place on practically every collision of the appropriate particles. Beutler and Polanyi came to this conclusion [392] from a study of the dependence of the extent of the reaction zone on pressure of the reacting substances in the reaction $Na + I_2$. A similar result was obtained by Kondrat'ev [119] who showed that the number of $NaCl$ molecules formed in the reaction $Na + HgCl_2$ is of the

(18) In contrast to the above experimental data, Magee [899] using a theoretical method came to the conclusion that direct excitation of the sodium atom is also possible in process II. On the basis of a consideration of the potential surfaces of a system consisting of two sodium atoms and one chlorine atom, he found that sodium atoms in the reaction of sodium with chlorine are excited partly in process II' and partly in process II.

same order of magnitude as the number of collisions of molecules of the reacting substances.⁽¹⁹⁾ From subsequent calculations by Polanyi and co-workers [1030] it follows not only that the elementary processes in both types of flame considered take place on every collision of the appropriate particles, but also that the effective cross sections for these collisions are considerably (up to 10 times) *greater* than the gas-kinetic cross sections [1106]. Therefore in highly-rarefied flames of this type we have an example of reactions taking place without any activation. The main reason for the lack of inertia in these reactions is clearly the ionic character of the bonds in the reaction product molecules.

Points of resemblance with reactions of the type $M + X_2$ are displayed by reactions between the divalent metals Cd, Zn, Mg, or between As and P and the halogens in so far as these reactions take place with the splitting-off of a halogen atom. Actually, as Polanyi and co-workers [1030] have shown, these reactions are capable of inducing the $H_2 + Cl_2$ reaction which is an indicator for atomic chlorine (see p. 79). The formation of chlorine atoms indicates that the probable primary process here, as in reactions of the alkali metals, is the interaction of a metal atom (in the case of As and P, As_4 or As_2 molecules and P_4 or P_2 molecules respectively) with a halogen molecule, resulting in the formation of an MX radical and an X atom: $M + X_2 = MX + X$. Study of the reaction rates of $Zn + Cl_2$ and $Cd + Cl_2$ showed that this process in the reaction of Zn takes place on every 5000th collision of the metal atom with a chlorine atom and in the reaction of Cd on every 100,000th collision. According to Polanyi's calculations [1031], the activation energies of these processes are 8 kcal (Zn) and 12.5 kcal (Cd). This does not exclude the possibility that these activation energies are close to the heats of the appropriate processes and that consequently the "true" activation energies of these processes are close to zero.

The reaction $M + HX$. The third type of reaction in highly-rarefied flames involves alkali atoms and hydrogen halides. Among reactions of this type Schay [1107] and Hartel [730] studied the cases of Na and K with HCl , HBr and HI . On the basis of estimates of cross sections and activation energy, both authors come to the conclusion that the rate of these reactions is determined by the size and sign of the heat of the reaction

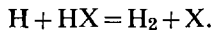


the activation energy of endothermic processes being equal to their heat,

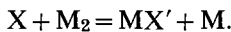
⁽¹⁹⁾ As in the previous case this result is obtained qualitatively from a comparison of the length of the reaction zone with the mean free path, which are of similar orders of magnitude. For example with a mean pressure in the zone of the $Na + Cl_2$ reaction of about 0.01 mm Hg the path length is about 1 cm and the half length of the reaction zone (the part at whose ends the reaction rate is half the maximum rate at the centre of the zone) is 4 cm.

and the activation energy of exothermic processes being practically zero. Thus comparing the reaction rate, i.e. the number of NaX molecules formed, with the number of gas-kinetic collisions between sodium atoms and HX molecules, Hartel finds that the activation energies of the processes $\text{Na} + \text{HCl}$, HBr , $\text{HI} = \text{NaCl}$, NaBr , $\text{NaI} + \text{H}$, are equal to 4.5, 1.9 and 0.2 kcal respectively. He compares these values with the heats of these processes which he puts at 5.1, 1.6 and 0.0 kcal respectively. Using a similar method for the first of these processes Schay found $E = 5$ kcal and Bawn and Evans [365] found $E = 6.1$ kcal. However, the conclusions of these authors concerning the lack of inertia in these reactions is apparently not supported by the latest data. This is clear from a comparison of Schay and Hartel's calculated activation energies with the more accurate values of the heats of reaction, and also from recent measurements of the rate constants for the reaction $\text{K} + \text{HBr} = \text{KBr} + \text{H}$. Studying this reaction in intersecting molecular beams of potassium and hydrogen bromide Taylor and Datz [1213] found that the activation energy $E = 3.4 \pm 0.1$ kcal and the steric factor⁽²⁰⁾ $P = 0.1$ with a heat of reaction +5.3 kcal. In contrast with these data, Schay finds that practically every gas-kinetic collision is effective for this reaction. Thus we should conclude that this reaction has a "true" activation energy of several kilocalories per mole. The accuracy of this conclusion is also supported by Hartel and Schay's data on the temperature dependence of the rate of the reaction $\text{Na} + \text{HCl} = \text{NaCl} + \text{H}$. From these data Hartel obtained $E = 6$ to 6.5 kcal. From similar measurements Schay finds that the ratio of the rate constant for this reaction to the effective number of gas-kinetic collisions is 0.01 at 600°K and 0.04 at 700°K and hence $E = 11.5$ kcal.

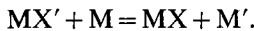
A characteristic property of flames of this type is the insignificant light yield compared with that of flames of the first two types; this is doubtlessly connected with the small heat of reactions which take place in flames of this type. According to Schay [1107] the excitation of light in these flames is based on two processes. The first is connected with the formation of X atoms as a result of the process



The X atoms react further with M_2 molecules according to the scheme



The excitation process in this case, as before, is the process

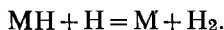


(20) From these data the following expression is obtained for the rate constant of the reaction $\text{K} + \text{HBr} = \text{KBr} + \text{H}$:

$$k = 3.0 \times 10^{-12} T^{1/2} \exp(-3400/RT) \text{ cm}^3 \text{ molecule}^{-1} \text{ sec}^{-1}.$$

An indication that these processes take place is given by the fact that halogen is detected in the reaction products frozen out by liquid air, and also by the negative temperature coefficient of the intensity of the flame which results from the dissociation of M_2 molecules at higher temperatures.

The second process of light excitation in these flames is connected with the formation of hydride molecules MH as a result of the reaction of H atoms with the metal; these molecules react further according to the scheme



The reaction $M + RX$ and other reactions. Reactions similar to those above are the reactions between Na atoms and molecules of XCN , C_2N_2 and also RX where R is an organic radical ($R = CH_3$, C_2H_5 , C_6H_5 , CH_2Cl , $CHCl_2$, etc.). These reactions have been studied [722, 732, 733, 741, 947, 1074a, 1169] by the following method: a reaction apparatus, consisting of a glass tube fitted with a nozzle by which sodium vapour is passed into an atmosphere of the second reagent, is illuminated from the side by the light of a sodium resonance lamp (Fig. 21). This light is absorbed by the

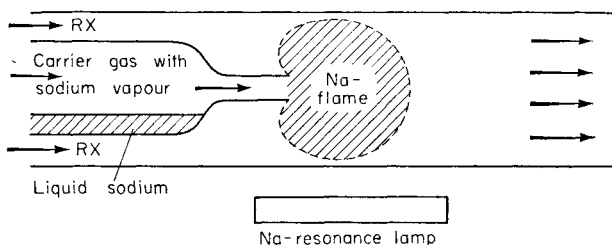


FIG. 21. The production of highly-rarefied diffuse flames.

sodium vapour and it is possible to see the shadow of the cloud of sodium vapour on a screen placed behind the reaction apparatus. The dimensions of the shadow are determined by the depth to which the sodium penetrates into the atmosphere of the gas reacting with it; these dimensions may be used to measure the reaction rate. In the same way as the retardation of the reaction in the method considered earlier leads to a broadening of the reaction zone, a decrease in the rate of reaction here allows the sodium vapour to penetrate to a greater depth into the atmosphere of the second reagent and this is directly shown by the size of the shadow. Hartel and Polanyi [947, 733] developed a quantitative method which makes it possible to determine more precisely the rate of reaction by the dimensions of the shadow on the screen. The exact theory of the method is given in reference [1057a]. Using this method it has been shown that most of the reactions studied have some degree of inertia, which is shown by the fact

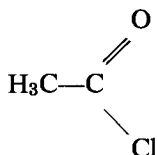
that reaction, as a rule, is by no means effected at every collision of the molecules of the reacting substances. This inertia in some cases is based on the presence of a "true" activation energy, i.e. the activation energy which is observed in the case of exothermic processes; in other cases the inertia of the reaction is connected with a low steric factor due to structural characteristics of the molecules. In the latter cases the reaction rate is not a function of temperature, in contrast with processes which take place with activation.

A characteristic example of the last type of reaction is the reaction $\text{Na} + \text{C}_2\text{N}_2$. According to Hartel and Polanyi's data [733] Na atoms react with C_2N_2 molecules on approximately every 15,000th collision, independently of the temperature of the reaction zone, and it follows that the inertia of the reaction in this case is based on a low steric factor. This effect is quite natural in this reaction, as the primary elementary process is the process $\text{Na} + \text{C}_2\text{N}_2 = \text{NaCN} + \text{CN}$. Here the screening of the vulnerable part of the cyanogen molecule by nitrogen atoms is clearly the cause of the inertia in the reaction.

The reaction $\text{Na} + \text{CICN}$ is also of interest in this respect [732, 733, 511]. Here the possible primary processes are: $\text{Na} + \text{CICN} = \text{NaCl} + \text{CN}$ and $\text{Na} + \text{CICN} = \text{NaCN} + \text{Cl}$. Study of these reactions shows that the first of these processes goes with an activation energy of 2 kcal and the second, being an "inert" process, has a rate which is independent of temperature. In accordance with the different causes of inertia in the two reactions the probability of the first process increases relatively to the probability of the second process on raising the temperature; this is detected by the change in composition of the reaction products.

Data relating to reactions of the type $\text{Na} + \text{RX}$ will be considered in Chap. 4, §17 and we shall therefore limit ourselves here to mentioning only some of characteristics of these reactions. The most important of these properties is the fact that the activation energy decreases with increase in length of the organic chain. For example according to Hartel, Meer and Polanyi [732] a sodium atom at 275°C reacts with a CH_3Cl molecule on every 10,000th collision, with a $\text{CH}_3\text{CH}_2\text{Cl}$ molecule on every 7000th collision and with a $\text{CH}_3\text{CH}_2\text{CH}_2\text{Cl}$ molecule on every 4400th collision, etc. The effect of a carbon-carbon double bond on the reactivity of the compounds is also of interest. It appears that a chlorine atom joined to a carbon atom bound by a double bond reacts less readily with sodium than a chlorine atom joined to a carbon atom bound by a single bond. Thus the reaction of Na with $\text{H}_2\text{C}=\text{CHCl}$ at 275°C takes place on every 11,000th collision, whereas the reaction of Na with $\text{H}_3\text{C}-\text{CH}_2\text{Cl}$ takes place on every 7000th collision. On the other hand, the presence of a double bond located next to a single bond decreases the inertia of a reaction: this is indicated by the result that the reaction

of Na with $\text{H}_2\text{C}=\text{CH}-\text{CH}_2\text{Cl}$ takes place on every 250th collision but the reaction of Na with $\text{H}_3\text{C}-\text{CH}_2-\text{CH}_2\text{Cl}$ takes place only on every 4400th collision (275°C). The presence of an oxygen atom bound to the same C atom as the chlorine atom also lowers the inertia of the reaction; this may be seen in particular from the following example: the reaction of Na with $\text{CH}_3\text{CH}_2\text{Cl}$, as we have seen, takes place on every 7000th collision, but the reaction of Na with



takes place approximately on every 100th collision (275°C).

Finally we should point out that the rate of reaction of a sodium atom with various halogen derivatives increases in the direction from fluorine to iodine. Thus according to the data of Hartel and Polanyi [732, 733] the activation energy for the reaction $\text{Na} + \text{CH}_3\text{X} = \text{NaX} + \text{CH}_3$, which may be calculated from a comparison of the number of atoms reacted with the number of gas-kinetic collisions, is greater than 25 kcal when $\text{X} = \text{F}$; when $\text{X} = \text{Cl}$, Br and I , the activation energy is 8.8,⁽²¹⁾ 3.2 and 0.3 kcal respectively. Fairbrother and Warhurst [594] studied the reactions of sodium atoms with $\text{C}_6\text{H}_5\text{Cl}$, $\text{C}_6\text{H}_5\text{Br}$ and $\text{C}_6\text{H}_5\text{I}$ molecules and found $E = 8.3$ kcal (Cl), 3.5 (Br) and 0.8 (I).⁽²²⁾

Reactions of Atomic Hydrogen

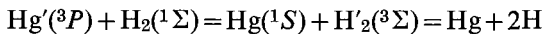
One of the methods most frequently used to obtain H atoms is the method of electric discharge. It was shown by Wood [1316] that a high percentage of atomic hydrogen is obtained as a result of a glow discharge in hydrogen at a pressure of 0.1 to 1 mm Hg. Wood's method is at present widely used to obtain atomic gases. For the study of the chemical properties of H atoms this method was first used by Bonhoeffer [426]. The electric discharge method for obtaining atomic hydrogen is usually applied in this way: a stream of hydrogen is passed through a discharge tube so that H atoms are formed, and then the stream is directed into a reaction vessel and a reagent mixed with it. The slow recombination of H atoms, which takes place either at the walls or as a result of ternary collision, makes it possible to extract atomic hydrogen from the discharge tube.

⁽²¹⁾ In this case Hartel and Polanyi find $E = 7.5$ cal from the temperature dependence of the reaction rate.

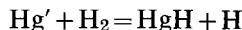
⁽²²⁾ For many other examples of the reactions of sodium atoms with various organic substances see Steacie's survey [1169] Chap. 13.

Because both these processes are slow under sufficiently favourable conditions (low pressure, poorly catalytic walls), the lifetime of atomic hydrogen may be quite considerable. Thus in a glass vessel at room temperature and a pressure of 0.1 mm Hg the lifetime of H atoms is about 1 sec. Such a long lifetime for the atomic hydrogen makes it possible to transport it a considerable distance (tens of centimetres from the discharge tube).

Another common method of producing atomic hydrogen is based on photochemical sensitization. By saturating hydrogen, or a mixture of hydrogen and another gas, with mercury vapour and illuminating this mixture with a quartz mercury arc, excited atoms of mercury $Hg' ({}^3P)$ are obtained as the result of the absorption of the resonance line 2537 Å by the mercury vapour. Excited Hg atoms interacting with H_2 molecules split them into H atoms. This interaction consists *either* of the transfer of the excitation energy to the H_2 molecule which then goes into the unstable state ${}^3\Sigma$ and splits into atoms



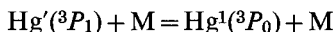
or of the formation of a mercury hydride HgH molecule and an H atom



(see p. 444).

In all probability both these mechanisms of formation of H atoms take place simultaneously. The mercury hydride molecule has a small dissociation energy (8.6 kcal) and readily decomposes into Hg and H atoms. Consequently the second mechanism, like the first, gives in the end two H atoms for every mercury atom reacting with an H_2 molecule [920].

At low pressures the yield of atomic hydrogen is considerably increased by the presence of nitrogen or water vapour. This is connected with the formation of metastable mercury atoms with long life, in consequence of which the probability of interaction with hydrogen is increased. The metastable atoms arise as a result of the process

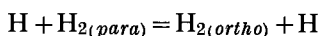


($M = N_2$ or H_2O). Gaviola [650] has shown that this process takes place on every collision in the presence of nitrogen. According to this author's measurements, the lifetime of the metastable atoms $Hg' ({}^3P_0)$ is 3×10^{-3} (the lifetime of atoms $Hg' ({}^3P_1)$ is 1.55×10^{-7} sec [454]).

Some experimenters have used, as a source of atomic hydrogen, substances which split off H atoms when illuminated. Thus in a study of the reaction $H_2 + O_2$, Farkas, Haber and Harteck [427] added to the detonating mixture ammonia, which decomposes photochemically according to the scheme $NH_3 + h\nu = NH_2 + H$. Ammonia is inconvenient, however, since NH_2 radicals are formed simultaneously with H atoms and take part in the reaction; this makes its mechanism more complex.

Hydrogen iodide has been found to be more convenient than ammonia and has been used by several authors in the study of various reactions. When exposed to ultraviolet light ($\lambda < 3100 \text{ \AA}$), hydrogen iodide decomposes according to the scheme $\text{HI} + h\nu = \text{H} + \text{I}$. Iodine atoms are considerably less reactive than hydrogen atoms and distort a reaction mechanism by a relatively small amount.

The simplest reaction of atomic hydrogen is its reaction with molecular hydrogen; this may be studied by the replacement of normal hydrogen, itself a mixture of the *para*- and *ortho*-modifications, by *para*-hydrogen or by the use of deuterium. It has already been shown (p. 77) that during collision of H atoms with *para*-hydrogen molecules, conversion of the latter into *ortho*-hydrogen takes place according to the scheme



(with the accumulation of *ortho*-hydrogen the reverse process—the conversion of *ortho*-hydrogen into the *para*-modification—begins to compete with this process). Measurements of the concentrations of *para*- and *ortho*-hydrogen in the course of the *para*-*ortho* conversion permit determination of the efficiency of collisions of H atoms with H_2 molecules. Such measurements show that at room temperature one in 5×10^5 collisions leads to conversion, and that the efficiency increases with temperature. These data lead to an estimation of the activation energy of *para*-*ortho* conversion at about 6 kcal [1119]. This value is practically identical with the activation energy obtained from measurements of the rate of conversion $\text{H} + \text{D}_2 = \text{HD} + \text{D}$.⁽²³⁾

For reactions of hydrogen atoms with oxygen the available data indicate that the interaction of H with O_2 takes place both as a bimolecular process



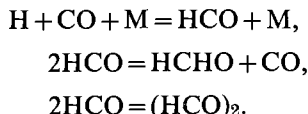
with an activation energy $E = 16$ kcal (the “true” activation energy is near zero) and also as a termolecular process [618]



(M denotes any particle). It follows from experiment (see §19) that the efficiency of the latter process is dependent on the nature of the third particle (M). Interaction of an HO_2 radical with a hydrogen molecule leads to the formation of H_2O_2 and H or of H_2O and OH. We shall see later that both reactions of an H atom with an O_2 molecule play a fundamental part in the mechanism of the combustion of hydrogen.

⁽²³⁾ For the reaction $\text{H} + \text{H}_2(\text{para}) = \text{H}_2(\text{ortho}) + \text{H}$, Farkas [600] gives $E = 6.2 \pm 1$ kcal and for the reaction $\text{H} + \text{D}_2 = \text{HD} + \text{D}$, Farkas and Farkas [597] give the figure $E = 6.55$ kcal.

Atomic hydrogen is also able to react with carbon monoxide. The main products of this reaction are formaldehyde HCHO and glyoxal (HCO)₂. According to Frankenburger [626], at room temperature and sufficiently high pressures the reaction takes place according to the scheme



At low pressures the yield of reaction products per H atom decreases sharply; according to Bonhoeffer and Harteck [30] this is connected with the predominance of the process $\text{HCO} + \text{H} = \text{H}_2 + \text{CO}$. Moreover according to the data of Farkas and Sachsse [601] the decomposition of the HCO radical has quite an important effect on the rate of reaction of H with CO.

Hydrogen atoms readily react with all hydrocarbons (only the reaction with methane is apparently slow). As early as 1928 Bonhoeffer and Harteck [428] used an analysis of the products of the interaction of H atoms with various hydrocarbons to establish that in this case processes of hydrogenation and dehydrogenation and also breaking of the carbon bonds in the molecules are possible. By now a large number of reactions of H atoms with different hydrocarbons and their derivatives has been studied. For many of these reactions approximate values of rate constants and activation energies have been established [1169]. In most experiments H atoms were obtained by using an electric discharge or a photochemical method; the reactions were studied at or near room temperature; sometimes deuterium was used. Tikhomirova and Voevodskii [266] have developed and used a new method for the study of the reactions of H atoms; the method is intended for high temperatures (about 400–500°C) and is based on measurements of the displacement of the ignition limits of a rich mixture of hydrogen with oxygen under the influence of small admixtures of the substance to be studied (see also [344]). A similar method was used earlier for a quantitative study of the mechanism of the combustion of carbon monoxide in the presence of admixtures of hydrogen [136].

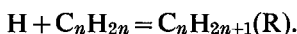
All our information concerning the reactions of H atoms with molecules of saturated hydrocarbons and their derivatives leads to the conclusion that at temperatures close to room temperature the main reaction is a splitting-off of an H atom from the molecule of the initial hydrocarbon (dehydrogenation) leading to the formation of an H₂ molecule and a radical R:



The activation energy of this process apparently seldom exceeds 10 kcal.

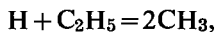
In the case of unsaturated hydrocarbons (in particular, olefins), along with the above reaction there also takes place the addition of the H atom

at the double bond of the hydrocarbon molecule (hydrogenation) resulting in the formation of a hydrocarbon radical (in the case of an olefin, an aliphatic radical):



This process apparently takes place with no energy of activation (see Steacie [1169] Chap. 5). According to the data of Allen, Melville and Robb [314] the addition of an H atom to an ethylene molecule C_2H_4 takes place on every 1300th collision, to a propylene molecule C_3H_8 on every 6000th collision and to a molecule of tetrafluoro-ethylene C_2F_4 on every 33,000th collision. H atoms are also capable of addition to molecules of aromatic compounds. According to Steacie [1169] an H atom is added to a benzene molecule C_6H_6 on every 7700th collision and to a toluene molecule $C_6H_5CH_3$ on every 50,000th collision. We should point out that the addition of an H atom to an olefin molecule makes it possible to obtain alkyl radicals R without contamination by other radicals; this is very important in the study of their chemical properties (see p. 106).

Reactions involving the rupture of a carbon-carbon bond (the splitting of a hydrocarbon molecule by interaction with an H atom) have been studied in less detail than the reactions mentioned above. On the basis of all the available experimental material, however, it may be concluded that the rate of these reactions is relatively small; this is apparently connected with a relatively large activation energy (see Steacie [1169] Chap. 5). In contrast with these, similar reactions of H atoms with radicals which lead to the splitting of the latter, i.e. reactions of the type



take place with great ease.

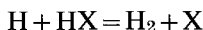
Other gas-phase reactions of atomic hydrogen that we shall consider are those with halogens, hydrogen halides and alkyl halides. The reaction of H atoms with halogens proceeds very rapidly. The primary process in these reactions is the exchange process



Comparing the data of various authors on the efficiency of the reactions $H + Cl_2 = HCl + Cl + 45.0$ kcal, $H + Br_2 = HBr + Br + 41.2$ kcal and $H + I_2 = HI + I + 34.9$ kcal, Schumacher [1119, p. 352] comes to the conclusion that the efficiencies are all close to unity. The activation energy of the last process is apparently zero; the activation energies of the first two processes differ somewhat from zero.

With bromine and iodine the reaction does not go to completion because of the comparative ease of secondary processes $H + HBr = H_2 + Br + 16.7$ kcal and $H + HI = H_2 + I + 32.8$ kcal (compared with the process $H + HCl = H_2 + Cl + 1.0$ kcal). These secondary processes lead to an

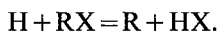
accumulation of Br and I atoms, respectively, the recombination of which results in the formation of the original halogen. According to Schumacher [1119] the efficiencies of these processes are about 0.1 and the activation energy is several kilocalories (the activation energy of the process $H + HCl = H_2 + Cl$ being some three kcal greater). The greater efficiency of the reactions $H + HBr$ and $H + HI$ compared with that of the reaction $H + HCl$ is also the reason why the products of the first two reactions contain a small quantity of halogen. The reaction



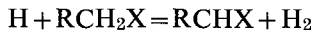
for all three halogens may be detected directly by the rapid disappearance of H atoms in the presence of hydrogen halides.

By reason of their low inertia, which is expressed by low activation energies and accordingly by a high efficiency, reactions of H atoms with halogens and with hydrogen halides are similar to the reactions of alkali metals. It is interesting that the "true" energy of activation for the exothermic reaction of an H atom with O_2 is also small (approximately zero).

It follows from the available experimental data that reactions of H atoms with alkyl halides proceed as rapidly as the reactions with halogens and with hydrogen halides. Here the main primary process is



This does not exclude the possibility that the reaction



takes place at the same time.

Atomic hydrogen reacts rapidly with gaseous H_2S and AsH_3 and also with certain solid and liquid metals, metalloids, metallic oxides, sulphides and halide salts: Na, K, Hg, Ag, P, As, Sb, S, CdS , CdI_2 , CuO , CuS , $CuCl_2$, PbO , etc. [426].

Reactions of Atomic Oxygen

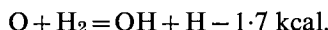
Let us now turn to the problem of the chemical properties of atomic oxygen. O atoms are usually obtained by the same methods as those used for H atoms, i.e. the electric discharge method and the photochemical method. Earlier studies of the reactions of oxygen atoms are those of Harteck and Kopsch [729], Geib and Harteck [663], Neuimin and Popov [213], Schenk and Jablonowsky [1109], Shekhter and Kushnerev [161] and others, referring to the period 1930–1941. These include the reactions of O atoms with certain of the simplest hydrocarbons, saturated and unsaturated, including benzene; methyl and ethyl alcohols; formaldehyde and formic acid; and also hydrogen. Most of these studies were unfortunately at high temperatures, with consequently a great extent of conversion and the presence of light characteristic of a hot flame. In these conditions the

primary products of the interaction escape observation to an important degree and the nature of the elementary processes may not be established with sufficient precision.

In this connection the studies of Avramenko and Kolesnikova (Lorentso) [7] have important advantages since they were carried out under conditions which exclude the possibility of the gas igniting. These studies are the most systematic investigations of the interaction of oxygen atoms with various organic substances, and have yielded rich qualitative material testifying to the great variety of chemical processes taking place with the participation of O atoms.

The experimental method which was developed by Avramenko and Kolesnikova for determining the sequence of elementary reactions, and applied to reactions of atomic oxygen, is of interest for the study of the mechanism of the interaction of atoms and radicals with various molecules. The method is based on a study of the yield of various products of the reaction as a function of the initial concentration of the fuel. It can be shown that under appropriate conditions, determined by the relationship between the rates of interaction of atoms with the initial and intermediate substances, the concentrations of various substances as functions of the initial concentration of the fuel are expressed by curves which differ markedly, depending on whether the substance is formed with the participation of one, two or more O atoms (in the terminology of Avramenko and Kolesnikova, the primary, quadratic, etc., products). From the form of these curves, according to Avramenko and Kolesnikova, it is possible to estimate the mechanism of formation of the various substances.

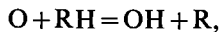
We shall consider the individual reactions which have been studied. The simplest is the reaction of an O atom with an H₂ molecule



The activation energy of this reaction according to Harteck and Kopsch [729] is 6 kcal; recent results of Azatyan, Voevodskii and Nalbandyan (V. V. Azatyan, V. V. Voevodskii, A. B. Nalbandyan, *Dokl. Akad. Nauk, SSSR*, 1962) give 12.1 ± 0.4 kcal. Neuimin and Popov [213] studied this reaction at low pressures (about 0.1 mm Hg) and found that the excited (metastable) atoms of oxygen O' (¹D) have a markedly large chemical reactivity as compared with normal atoms; a consequence of this is that the oxidation of hydrogen under the conditions of their experiments is due practically exclusively to metastable atoms (these are obtained by the photodissociation of O₂ molecules, at the same time as the normal atoms). The activation energy of the reaction O' (¹D) + H₂ = OH + H + 44.6 kcal according to Neuimin and Popov is less than 1.4 kcal.

A similar scheme is also followed by the reactions of an O atom with various molecules containing hydrogen. In its general form this scheme

may be described by the equation



where R is a univalent atom or radical. According to Harteck and Kopsch [729] the primary process in the reactions of O atoms with hydrogen halides, as a result of which H_2O and X_2 are formed, is the process $O + HX = OH + X$ which corresponds to the above scheme with $R = X$. The heat of this process for the three hydrogen halides is: -0.7 kcal (HCl), $+15.0$ kcal (HBr) and $+31.0$ kcal (HI). In accordance with the difference in the heats of these processes, their rates are different: calculations show that whereas in the case of the reaction $O + HCl$ only about one in 10^5 collisions of O and HCl leads to reaction (at room temperature), in the case of HBr and HI a minimum of one in 1000 collisions of O and HX is effective. The large rate of reaction is connected with a strong heating of the reaction zone which is observed in the case of the last two hydrogen halides. We should note that no ultraviolet OH bands are observed in any of the reactions $O + HX$; this is explained by the fact that the energy liberated in the individual elementary processes is not sufficient to excite the hydroxyl (the excitation energy of the lowest OH band is 92.5 kcal).

The scheme $O + RH = OH + R$ is also followed by reactions of O atoms with hydrocarbons, aldehydes and alcohols. In every case the activation energy is several kilocalories. However this reaction scheme is not the only one possible. It has been shown principally by Avramenko and Kolesnikova [7] that at a temperature of about $100^\circ C$ other reactions take place simultaneously. Thus the detection, in the reaction products, of substances containing less C atoms than the initial molecule (establishing their primary origin), leads to the conclusion that one of the main reactions involves breaking a C—C bond.⁽²⁴⁾ According to Avramenko and Kolesnikova the reaction $O + C_2H_6 = CH_3O + CH_3$ at $100^\circ C$ takes place three times as fast as the reaction $O + C_2H_6 = OH + C_2H_5$. From analysis of their experimental data these authors come to the conclusion that an oxygen atom may be taken up by the molecule at the C—H bond, as a result of which one primary elementary act of interaction of an O atom with a molecule of C_2H_6 , C_6H_6 or CH_3CHO respectively yields ethyl alcohol C_2H_5OH , phenol C_6H_5OH or acetic acid CH_3COOH .

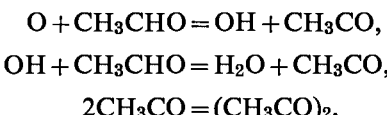
Avramenko and Kolesnikova [5] have also studied the reactions of atomic oxygen with the simplest olefins (C_2H_4 and C_3H_6). From analysis of the reaction products (using the method for determining the sequence

⁽²⁴⁾ From spectroscopic studies of flames obtained by interaction of atomic oxygen with various substances Geib [661] comes to the conclusion that O atoms (as well as H atoms) preferentially break the O—O bond (on interaction with H_2O_2) and the C—O bond (on interaction with alcohols), as these bonds are weaker than the C—H bond.

of the elementary processes; see p. 99) they come to the conclusion that, as well as reactions which take place on the interaction of O atoms with saturated hydrocarbons (breaking a C—C bond, splitting-off of an H atom, incorporation of O at a C—H bond), in the case of olefins the splitting of the molecule can take place in one elementary act at the double bond; this results in the formation of an aldehyde (for example $O + C_3H_6 = CH_2 + CH_3CHO$), which, according to Avramenko and Kolesnikova, is the primary product of the reaction.

The reaction of oxygen atoms with olefins was also studied by Cvetanović [515] who found that, whereas in the case of ethylene C_2H_4 the main reaction is connected with breaking the C=C bond, in the case of heavier olefins such as butene C_4H_8 decomposition plays a relatively small part and the reaction products are mainly the oxide of the olefin and its isomeric aldehyde or ketone. From the fact that, for example, in the reaction of an O atom with *cis*-but-2-ene $CH_3CH=CHCH_3$ the butene oxide is formed in both *cis*- $CH_3CHOCHCH_3$ and *trans*- $CH_3CHOCHCH_3$ modifications, and also from other data, the author concludes that the initial step in the reaction with an O atom is not the formation of an oxide but the formation of a biradical $CH_3CHO—CHCH_3$. Also see [620a].

Cvetanović [517] also studied the reaction of O atoms with acetaldehyde CH_3CHO . From the fact that the only important products in this case are H_2O and $(CH_3CO)_2$, the author proposes the mechanism



He estimates the activation energy for the first of these processes to be 3 kcal.

As a result of their experiments Avramenko and Kolesnikova come to the conclusion that reactions are possible in which an oxygen atom splits off simultaneously *two* H atoms with formation of an H_2O molecule and a second, also saturated, molecule. Avramenko and Kolesnikova connect reactions of this type with the formation of unsaturated compounds, for example, $O + C_2H_6 = H_2O + C_2H_4$ or $O + CH_3CH_2CH_3 = H_2O + C_3H_6$ and also the oxidation of formaldehyde by atomic oxygen $O + H_2CO = H_2O + CO$. The conclusion that it is possible to form two saturated molecules on the interaction of various compounds with an O atom is also found in studies by other authors. Thus Shekhter and Kushnerev [161] conclude that H_2CO is the primary product of the interaction of an O atom with a methane molecule $O + CH_4 = H_2CO + H_2$. Avramenko and Kolesnikova also arrive at this mechanism for the formation of H_2CO by the action of an O atom on methane. Even earlier Harteck and Kopsch [729]

had found that the action of atomic oxygen on carbon tetrachloride yields equal amounts of phosgene COCl_2 and chlorine. They came to the conclusion that this reaction takes place in one elementary step $\text{O} + \text{CCl}_4 = \text{COCl}_2 + \text{Cl}_2$. Similar schemes are possible for the reactions $\text{O} + \text{CH}_2\text{Cl}_2 = \text{COCl}_2 + \text{H}_2$ and $\text{O} + \text{CHCl}_3 = \text{COCl}_2 + \text{HCl}$, which were also studied by Harteck and Kopsch. We should also point out that Geib [660] takes the process $\text{O} + \text{HCOOH} = \text{CO}_2 + \text{H}_2\text{O}$ to be a possible mechanism for the interaction of an O atom with a molecule of formic acid.

The reactions of atomic oxygen with H_2O , H_2S , NH_3 , HCN , C_2N_2 , CS_2 , etc., have also been studied. The experimental data, however, are not sufficient to determine the mechanisms.

According to current ideas CO_2 is formed on the interaction of atomic oxygen with carbon monoxide according to the scheme



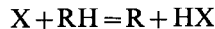
The formation of ozone $\text{O} + \text{O}_2 + \text{M} = \text{O}_3 + \text{M}$ follows a similar scheme, where M is an inert molecule. According to Groth [707] the first of these processes is 40 times slower than the second at room temperature. There are indications pointing to the bimolecular formation of CO_2 from CO and O at high temperatures [87, 542a, 634, 687, 137b].

Reactions of Atomic Halogens

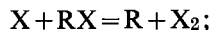
Let us now consider the reactions of atomic halogens. The methods for their production are basically the same as those for the production of H and O atoms, i.e. electric glow discharge and photodissociation. The latter is particularly suitable since X_2 (halogen) molecules have continuous spectra lying in the easily accessible visible and near ultraviolet region of the spectrum. We should also point out the method mentioned earlier that was developed by Bogdandy and Polanyi [423] which consists of the formation of halogen atoms by the reaction $\text{Na} + \text{X}_2 = \text{NaX} + \text{X}$.

Various authors have studied the reactions of atoms of chlorine, bromine and iodine with a large number of substances, including hydrogen, various hydrocarbons and their halide derivatives, aldehydes, ketones and acids (see Steacie [1169], Chaps. 10-12).

Study of these reactions leads to the following conclusions: with saturated compounds the main processes take place according to the scheme



or according to the scheme



in the case of unsaturated aromatic compounds the addition reaction $2\text{X} + \text{R} \rightarrow \text{RX}_2$ predominates.

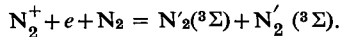
The activation energy as a rule is several kilocalories but sometimes reaches 15–20 kcal. For similar reactions (with the same RH or RX) the activation energy increases in the direction from chlorine to iodine. It should however be noted that here quantitative data are very scarce and often unreliable. Amongst recent quantitative studies on the reactions of chlorine atoms with hydrocarbons and their halide derivatives we shall mention the work of Pritchard, Pyke and Trotman-Dickenson [1050]. It follows from this work in particular that there is a decrease in the energy of activation (with a certain increase in the pre-exponential factor in the expression for the reaction-rate constant) on replacement of an H atom (or atoms) in methane CH_4 by an atom of chlorine or a CH_3 group (or groups). For the reaction $\text{Cl} + \text{CH}_4 = \text{HCl} + \text{CH}_3$ these authors found $E = 3.85$ kcal. Some of the data obtained by them are shown in Table 13 (p. 253).

We should mention also the fast reaction of chlorine atoms with oxygen molecules, as a result of which ClO_2 and ClO are formed. According to the data of Porter and Wright [1039] chlorine atoms in the presence of O_2 disappear 46 times faster than on recombination in the presence of nitrogen.

Reactions of Active and Atomic Nitrogen

Let us now consider the reactions of active nitrogen [110, 680] and of atomic nitrogen. Active nitrogen is obtained by electric discharge in nitrogen at a pressure of some millimetres of mercury and is a mixture of normal N_2 molecules, metastable N'_2 ($^3\Sigma$) molecules with an electronic excitation energy of about 140 kcal,⁽²⁵⁾ normal N atoms and metastable N' (3D and 3P) atoms with an excitation energy of 54.5 and 82 kcal [1186a]. N atoms have recently been detected in active nitrogen by Jackson and Schiff [797] using a mass-spectroscopic method. That there are considerable concentrations of nitrogen atoms in the discharge zone in nitrogen is also supported by the absorption of light in the region 400–800 Å [565] which for the most part must apparently be attributed to the atomic constituent of the discharge-zone gas. There are also indications that the chemical activity of nitrogen is based not on charged but neutral particles [1249, 956] and that recombination of nitrogen atoms is a source of the glow [1059, 386] and of the ionization of nitrogen (see also [995, 841a]). It is possible for this reason to suppose that atomic nitrogen is one of the components of active nitrogen (see also [340, 1301c]). The work of Anderson, Kavadas and McKay [321b], devoted to a study of the kinetics of the

⁽²⁵⁾ According to Sen Gupta [1130] these molecules may be in a high vibrational state ($v' = 11$ to 25) as a result of which their energy may reach a value of 220 kcal. Sen Gupta connects the excitation of high vibrational levels with the process



fading of the after-glow in nitrogen, shows that the maximal intensity of the glow immediately after the discharge is actually determined by recombination of nitrogen atoms in the ground state. The energy (9.6 eV) liberated on recombination of the atoms is very close to the excitation energy for the eleventh vibrational level of the excited state $B^3\Pi$, which gives the maximum contribution to the intensity of the glow.

The chemical activity of nitrogen lasts, however, for some time after the glow has ceased and corresponds to a larger number of active centres than the number of centres which give rise to the glow [1295a]. Evans and Winkler [577] assume that an important constituent of chemically active nitrogen is vibrationally excited molecules of N_2 in the electronic ground state.⁽²⁶⁾ The same conclusion is reached by Anderson [321a] from a study of the kinetics of fading of the weak glow in nitrogen. It is very probable that vibrationally excited N_2 molecules may give rise to the chemical activity of nitrogen although their energy is not sufficient to excite the $B^3\Pi$ state of one of the colliding N_2 molecules.

The great chemical reactivity of active nitrogen is shown by the enormous number of reactions in which it takes part and of reactions stimulated by it. Thus with the presence of oxygen in active nitrogen, nitric oxide is formed; with carbon disulphide active nitrogen gives nitrogen sulphide NS; with acetylene, benzene and other organic compounds it gives hydrogen cyanide HCN; with sulphur, H_2S or S_2Cl_2 it gives the nitride S_4N_4 ; in reactions with various metals and their salts, etc., it gives metallic nitrides; and NH_3 , HBr and HI rapidly decompose in contact with active nitrogen. A mixture of $H_2 + Cl_2$ is converted into HCl by the action of active nitrogen. Active nitrogen does not greatly affect H_2O , CO_2 and CO . (G. B. Kistiakowsky, G. G. Volpi, *J. Chem. Phys.* 27, 1141 (1957); 28, 665 (1958); [1249].)

Only in recent years have there been studies of the reactions of nitrogen atoms (formed by electric discharge in nitrogen) with various hydrocarbons (CH_4 , C_2H_6 , C_3H_8 , C_4H_{10} , C_2H_4 , C_3H_6 , C_4H_8 , C_2H_2 , etc.) and other organic compounds. In almost every case the reaction products were found to contain hydrogen cyanide HCN; this is formed, according to the proposed mechanisms for these reactions,⁽²⁷⁾ either in a primary step (in the case of saturated hydrocarbons and ethylene) or as a result of the subsequent decomposition of the radical first formed (for example, $N + C_3H_6 \rightarrow CH_2N + CH_3CH$, $CH_2N \rightarrow HCN + H$, or $N + C_2H_2 \rightarrow C_2H_2N \rightarrow HCN + CH$).⁽²⁸⁾ The activation energy of processes in which nitrogen

⁽²⁶⁾ See also [365a] (K. Dressler, *J. Chem. Phys.* 30, 1621 (1959); F. Kaufman, J. R. Kelso, *J. Chem. Phys.* 28, 510 (1958)).

⁽²⁷⁾ With the assumption that metastable nitrogen molecules do not take part in the reaction.

⁽²⁸⁾ See Steacie [1169] pp. 640-643, and also [576].

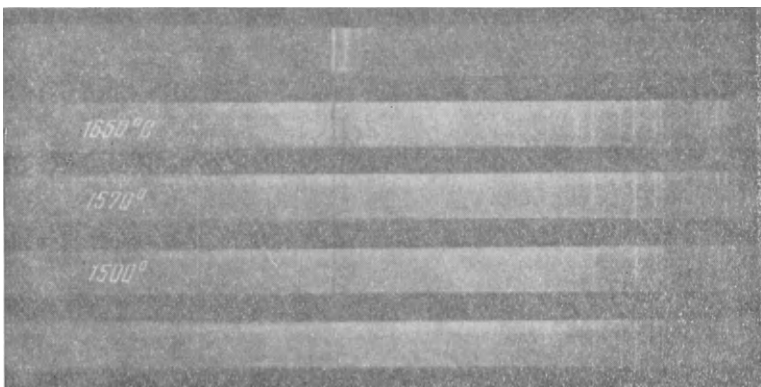


FIG. 22. The absorption spectrum of hydroxyl HO during thermal dissociation of water vapour (according to Bonhoeffer and Reichardt [429]).

atoms take part is usually several kilocalories per mole. Thus Back and Winkler [341] obtained an activation energy of 3.6 and 3.1 kcal for the reaction of nitrogen atoms with butane C_4H_{10} and iso-butane $(CH_3)_3CH$ respectively.

We should add that according to Zel'dovich, Sadovnikov and Frank-Kamenetskii [83, 86] nitrogen atoms react with molecular oxygen according to the scheme $N + O_2 = NO + O$. The activation energy for this process is 8.4 kcal according to the data of Kaufman and Kelso [826], and 6.2 kcal according to more recent results (R. E. Duff, N. Davidson, *J. Chem. Phys.*, **31**, 1018 (1959)).

§7. Free Radical Reactions⁽²⁹⁾

Production of Free Radicals

The great chemical reactivity of radicals which is observed in most cases is based on the fact that the electron shells of the appropriate atomic groups are incomplete; in consequence the properties of these groups are similar to the properties of atoms having the same number of outer electrons as the given atomic group. In this respect the similarity between the chemical properties of the hydrides of carbon, nitrogen, oxygen and fluorine and the chemical properties of the atoms with the same numbers of electrons is especially characteristic. Thus the CH (methenyl) radical is chemically similar to the N atom, CH_2 (methylene) and NH (imine) radicals are similar to the O atom, CH_3 (methyl), NH_2 (the amino-group) and OH (hydroxyl) radicals are similar to the F atom and finally the molecules CH_4 , NH_3 , H_2O and HF are in a certain sense (inertness) similar to the Ne atom. Because radicals are chemically unsaturated the activation energy of processes in which they take part is of the same order as the activation energy of atomic reactions. For this reason these processes as a rule proceed with approximately the same rate as that usual for atomic processes.

Chemically reactive radicals are observed in the free state only under certain specific conditions. Thermodynamically a high concentration of radicals corresponds to an increased free energy of the system; for this reason all factors which increase the free energy favour the formation of free radicals. In accordance with this, free radicals of various sorts are observed, for example, on raising the temperature. Thus Bonhoeffer and Reichardt [429] and also Avramenko and Kondrat'ev [9], Oldenberg and Dwyer [559] and others have obtained OH radicals in sufficient quantity for their detection by their absorption spectrum (Fig. 22) on heating water vapour, a mixture of $H_2 + O_2$ or of $H_2O + O_2$ to a temperature higher than $1000^\circ C$. Kistiakowsky and Gershinowitz [837] and White [1282] by the

⁽²⁹⁾ Also see Chap. 4.

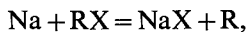
heating of cyanogen vapour to a temperature of 1256°C obtained CN radicals which were also detected by their absorption spectrum; Franck and Reichardt [622] have obtained NH radicals by heating ammonia NH₃. Free radicals are also obtained by heating various organic compounds. The decomposition (pyrolysis) of organic substances at high temperatures which takes place with formation of free radicals is one of the most widely used methods of obtaining various organic radicals (see for example [222, 1200]). A particularly convenient source of radicals is the decomposition of iodides RI, as the C—I bond is relatively weak at comparatively low temperatures; and as iodine atoms are not very reactive the R radicals are formed in a practically pure state.⁽³⁰⁾

The thermal decomposition of azo-compounds and organo-metallic compounds is a widely used source of free radicals. Thus CH₃ radicals are formed by the decomposition of azomethane H₃CN₂CH₃ or dimethyl mercury Hg(CH₃)₂. The methylene radical CH₂ is obtained by the thermal decomposition of diazomethane H₂CN₂.

A great variety of free radicals is observed when an electric discharge is passed through an atmosphere of various gases. These radicals are detected either spectroscopically or using a mass-spectrometer. We should add that Rice and Whaley [1066] have used the mirror method to detect a large number of radicals which are formed in an electric discharge in different organic substances. The electric discharge method, however, has the important disadvantage that it is practically impossible to obtain a given radical in sufficient concentration without substantial admixtures of other active particles. For example, H and O atoms are obtained simultaneously with hydroxyl during discharge in water vapour.

The following variant of the electric discharge method has been used with success to obtain aliphatic radicals [950]. H atoms are obtained directly by electric discharge in hydrogen. Since at room temperature the interaction of H atoms with olefins is practically exclusively the process H + C_nH_{2n} = C_nH_{2n+1}, i.e. the addition of an H atom to an olefin molecule with formation of an aliphatic radical, this radical may be obtained by introducing the appropriate olefin into the gas from the discharge which contains H atoms.

Radicals obtained in this way are the product of the chemical interaction of the primary atoms formed in the electric discharge with olefin molecules. Of other chemical methods for producing free radicals the most convenient is that developed by Polanyi and coworkers based on reactions of the type



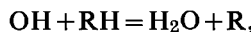
⁽³⁰⁾ See for example Polanyi and coworkers [472], and also Steacie [1169] Chap. 4, p. 53.

which take place in highly-rarefied flames (see p. 91 *et seq.*). Hartel [731] used this method to obtain a large number of free organic radicals. The chemical properties of CH_3 and C_2H_5 radicals have been studied by Horn, Polanyi and Style [1033].

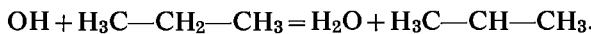
Finally, free radicals may be obtained photochemically. Thus OH radicals are formed on exposing H_2O_2 vapour to a zinc spark [1237]. Terenin and Neuimin [263] obtained these radicals directly by the photodissociation of molecules of H_2O , CH_3OH , etc. By exposing various alkyl halides to the appropriate spectral regions free radicals may be detected, for example CH_3 , CH_2Cl , CHCl_2 , etc. [753]. CN radicals are formed by exposing ICN vapour to an aluminium spark [310]. CH_3 radicals are formed by the photolysis of $\text{Hg}(\text{CH}_3)_2$ vapour in the region 2600 \AA [776]. A large number of different free radicals may be obtained by flash photolysis (see below, p. 413).

Reactions of Various Radicals

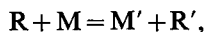
Let us now consider the reactions of individual radicals and in particular those of hydroxyl. Hydroxyl reacts with hydrogen according to the scheme $\text{OH} + \text{H}_2 = \text{H}_2\text{O} + \text{H}$. The rate constant for this process is given on p. 611. The reaction of hydroxyl with carbon monoxide follows the scheme $\text{OH} + \text{CO} = \text{CO}_2 + \text{H}$. The reactions of hydroxyl with several of the simplest hydrocarbons and aldehydes have been studied in addition to the reactions with H_2 and CO molecules. In all these reactions the main type of reaction corresponds to the scheme



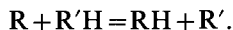
as is clear from analysis of the reaction products. For example, Avramenko and Kolesnikova (Lorentso) [10] found that the interaction of hydroxyl (obtained by photodissociation of hydrogen peroxide) with propane yields acetone as the main product; it is possible to conclude from this that the radical $\text{H}_3\text{C}-\text{CH}-\text{CH}_3$ is formed in the primary act of reaction, i.e. that the primary act is the process



It should be said, however, that in spite of a large amount of work, the reactions of radicals have so far been studied only very superficially. Owing to the particular importance of hydrocarbon-radical reactions the greatest amount of work has been devoted to the study of these reactions and above all to the study of reactions of hydrocarbon radicals with hydrocarbon molecules [1169]. It follows from this work that here the most common type of reaction is



where M and M' are saturated molecules. Among reactions of this type the most frequent are the reactions



It has been shown that reactions of this type play an important part not only in the cracking of hydrocarbons but also in their oxidation. Thus as a result of detailed analysis of products of oxidation of propane in the course of the reaction, Shtern and coworkers [299] showed that this reaction takes place in two ways, namely oxidation and cracking. Lukovnikov and Neiman [173] also concluded that cracking occurs in the oxidation reaction; they studied the cool-flame oxidation of pentane and propylene using the kinetic tracer method as well as normal chemical analysis. The large part played by cracking processes in the mechanism of high-temperature oxidation of organic substances was also noted earlier by several authors.

From many experiments the activation energy for processes $R + R'H = RH + R'$ is obtained as 5–10 kcal (for exothermic processes) [1169]. For example the activation energy for the process $CH_3 + C_2H_6 = CH_4 + C_2H_5$ was found by Steacie and coworkers [1169] to be 10.4 kcal. Volman and Brinton [1255] give $E = 7.5$ kcal for the activation energy of the process $CH_3 + C_2H_5CHO = CH_4 + C_2H_5CO$. A process which includes the breaking of a C–C bond, for example $CH_3 + RCH_3 = C_2H_6 + R$, clearly has a lower probability than the process $CH_3 + RCH_3 = CH_4 + RCH_2$ and is therefore more rare.

Alkyl radicals readily add on to molecules of olefins [1169] and other unsaturated (in particular, aromatic) compounds [874, 897]. Analysis of experimental data on the polymerization of olefins and other reactions shows that the activation energy for the process of addition of an alkyl radical to an olefin molecule is several kilocalories. Thus according to Steacie [1169] the probable activation energy for the process



is 1 to 3 kcal.

Different types of mutual interaction of radicals have been established and in individual cases have been studied quantitatively. These reactions are: *recombination* of radicals which leads to the formation of a saturated molecule, for example $CH_3 + CH_3 = C_2H_6$ or $CH_3 + C_2H_5 = C_3H_8$ and *disproportionation*, i.e. an interaction leading to the formation of two saturated molecules (the disappearance of free valencies) or of two new radicals, for example $C_2H_5 + C_2H_5 = C_2H_6 + C_2H_4$ or $H + C_3H_7 = CH_3 + C_2H_5$. Analysis of the experimental data leads to the conclusion that the recombination process is very efficient. Steacie and Ivin [796] found that the recombination of two methyls CH_3 , and also of two ethyls C_2H_5 , takes place on approximately every tenth collision. At low pressures the rate constant for the

recombination process is a function of pressure [1169] and it follows that it is termolecular in character (see Chap. 4, §14). In contrast with the recombination process disproportionation follows a bimolecular law at all pressures. According to Steacie and Ivin [796] the bimolecular rate constant for the disproportionation $C_2H_5 + C_2H_5 \rightarrow C_2H_6 + C_2H_4$ is close to that for the recombination $C_2H_5 + C_2H_5 \rightarrow C_4H_{10}$; but the activation energies differ, for $E_{\text{disp}} - E_{\text{recomb}} = 0.8 \pm 0.2$ kcal. The activation energy for the recombination process is usually taken as zero although one should not entirely exclude the possibility that $E_{\text{recomb}} \neq 0$ [793].⁽³¹⁾

Complex hydrocarbon radicals are also disposed towards unimolecular decomposition. This is supported by experimental studies on the mechanism of thermal decomposition of hydrocarbons and also by the fact that the energies for breaking C—C and C—H bonds in radicals are known from thermochemical data to be low, so that the thermal decomposition of a radical is thermodynamically very probable even at relatively low temperatures (see, for example, Trotman-Dickenson [1228], pp. 299–307).

Analysis of all the material relating to the cracking of hydrocarbons leads to the idea that one of the main processes of this reaction mechanism is the conversion of the complex radical into simpler particles as the result of either its interaction with other radicals or molecules, or its unimolecular decomposition. In the case of alkyl radicals, decomposition into a molecule of an olefin and a simpler alkyl radical is most probable energetically (see, for example [942]).⁽³²⁾ Thus, for example, the *n*-propyl radical decomposition by scheme $n-C_3H_7 \rightarrow CH_3 + C_2H_4$ is endothermic by 22 kcal, and that proceeding by $n-C_3H_7 \rightarrow H + C_3H_6$ by 35 kcal. Hence the first process would predominate at moderate temperatures. According to Kerr and Trotman-Dickenson (*loc. cit.*) the rate constants of these processes are

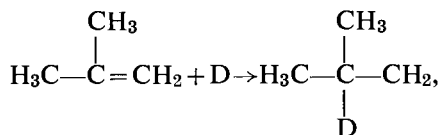
$$k = 10^{11.7} \exp(-25,200/RT) \text{ sec}^{-1} \text{ and } k = 10^{13.6} \exp(-35,000/RT) \text{ sec}^{-1}.$$

To explain the results of analysing the products of cracking, isomerization and oxidation of organic compounds several authors have assumed the possibility of the *isomerization* of radicals. For literature, see [164]. Direct evidence for this process has been given by Lavrovskaya, Mardaleishvili and Voevodskii [164]. By studying the isotopic exchange of hydrogen

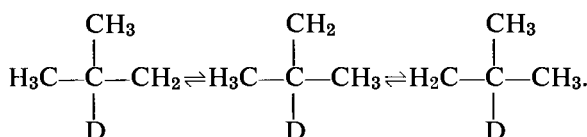
⁽³¹⁾ The ratio of the constants for disproportionation and recombination of *n*-propyl radicals (at 100°C) is 1 : 8 according to Whiteway and Masson [1283], and 1 : 6 according to Kerr and Trotman-Dickenson (J. A. Kerr and A. F. Trotman-Dickenson, *Trans. Faraday Soc.* **55**, 572, 1959). Krauss and Calvert (J. W. Krauss and J. G. Calvert, *J. Amer. Chem. Soc.* **79**, 5921, 1957) report the following ratios of constants for disproportionation and recombination of butyl radicals at 100°C: 4.6 for $(CH_3)_3C$, 2.3 for $(CH_3)_2CHCH_2$, and 0.4 for $CH_3CHC_2H_5$.

⁽³²⁾ We should add that according to Voevodskii [43] unsaturated radicals (for example, the radical $H_2C=CH-CH=CH_2$) are capable, besides disproportionation, also of converting an olefin molecule into an alkyl radical (in this case, the radical $H_3C-CH_2-CH=CH_2$) by the transfer of an H atom to the olefin.

between D_2 molecules and the primary isobutyl radicals which were obtained according to the reaction

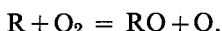


these authors found that the degree of deuteration in the product of the recombination of these radicals—namely octane C_8H_{18} —is considerably greater than the degree of deuteration that would be observed for exchange of only the H atom in the CH_2 group, which corresponds to the absence of isomeric conversion of isobutyl radicals. This result must be regarded as evidence for the isomerization of these radicals, which must clearly include migration of an H atom:

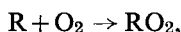


The conclusion regarding the possibility of radical isomerization is not inconsistent with the exchange mechanism proposed by these authors. In the case of heterogeneous exchange or of exchange in which D atoms take part according to the position of the free valency [1169] the results also lead to the conclusion that isomerization is occurring.

We know a good deal less about the reactions of radicals with oxygen which play a particularly important part in oxidation processes. By analogy with the well-studied reaction $H + O_2 = OH + O$ one may suggest a reaction

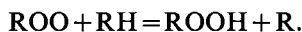


The presence of oxygen atoms in flames argues in favour of this reaction. This does not exclude the possibility, however, that the oxygen atoms in flames are the result of interaction between H and O₂. The probability of the reaction mentioned above is determined by its activation energy which is connected with the heat of reaction. The activation energy of this reaction when R=H is 16 kcal for a heat of reaction of -16 kcal. When R is an alkyl radical the heat of the reaction is -25 to -30 kcal and consequently the activation energy is more than 25-30 kcal. Such a large activation energy accounts for the low probability of this reaction and consequently even under flame conditions the following reaction may compete successfully with it:



which is similar to the reaction $H + O_2 + M \rightarrow HO_2 + M$.

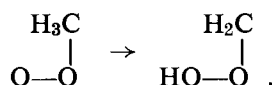
The possibility of the direct addition of the radical \mathbf{R} to the \mathbf{O}_2 molecule is apparent in particular from the experimental fact that, in the first stage of the oxidation of organic substances, peroxides are formed as the main reaction product. This fact was most strikingly demonstrated in the work of Fok and Nalbandyan [274] who found that at room temperature the main (and practically sole) product of the photochemical oxidation of propane is isopropyl hydroperoxide. According to the data of these authors, when the temperature is increased, aldehydes, acetone and products of further oxidation appear in the reaction products along with the hydroperoxide. These results obtain a natural explanation if one assumes that at low (room) temperatures the peroxide \mathbf{RO}_2 is so stable that it can react with the hydrocarbon (propane) and lead to the formation of the hydroperoxide:



It may be assumed that this reaction takes place with a low activation energy which also favours the formation of the hydroperoxide. That the activation energy is small may be judged from the data of Melville and Burnett [467], which show that liquid-phase reactions of this type have an activation energy of a few kilocalories. For example these authors obtained an activation energy of 1.8 kcal for the formation of benzoyl hydroperoxide $\mathbf{C}_6\mathbf{H}_5\mathbf{CO}\cdot\mathbf{OOH}$ during the interaction of the peroxide radical $\mathbf{C}_6\mathbf{H}_5\mathbf{CO}\cdot\mathbf{OO}$ with a benzaldehyde molecule $\mathbf{C}_6\mathbf{H}_5\mathbf{CHO}$. For other \mathbf{RH} they find $E = 4.2, 8.5$ kcal, etc. (See also V. F. Tzepalov, V. Ya. Shlyapintokh, *Dokl. Akad. Nauk, SSSR* **124**, 883, 1959; R. H. Burgess, J. C. Robb, *Trans. Faraday Soc.* **54**, 1015, 1958). At higher temperatures the stability of the peroxide radical \mathbf{RO}_2 decreases and accordingly the probability of its decomposition increases. The nature of the \mathbf{RO}_2 radical decomposition may be judged from results of Avramenko and Kolesnikova [10]. Using a spectroscopic absorption method they found that the products of the interaction of radicals obtained by the action of \mathbf{H} atoms on propane, i.e. $\mathbf{C}_3\mathbf{H}_7$ radicals, with molecular oxygen include free hydroxyl. This fact is explained if the formation of \mathbf{OH} is connected with the following process for the decomposition of the peroxide radical:



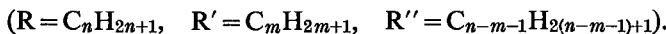
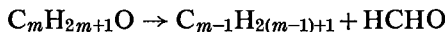
See also Burgess and Robb (*loc. cit.*). We should note that according to Semenov [241] this process must be preceded by isomerization of the peroxide radical, for example:



Other data also support the formation of a peroxide radical and the further possibility of its unimolecular decomposition. For example, from measurements on the activity distribution in formaldehyde HCHO and acetaldehyde CH_3CHO , which are formed on oxidation of 2C^{14} -propane $\text{H}_3\text{C}-\overset{\cdot}{\text{C}}\text{H}_2-\text{CH}_3$,⁽³³⁾ 1C^{14} -butane $\text{H}_3\overset{\cdot}{\text{C}}-\text{CH}_2-\text{CH}_2-\text{CH}_3$, 1C^{14} -pentane $\text{H}_3\overset{\cdot}{\text{C}}-(\text{CH}_2)_3-\text{CH}_3$ and 3C^{14} -pentane $\text{H}_3\text{C}-\text{CH}_2-\overset{\cdot}{\text{C}}\text{H}_2-\text{CH}_2-\text{CH}_3$ (at 305–340°C), Neiman, Lukovnikov and Feklisov [207] found that both aldehydes may be formed from the end and the centre carbon atoms of the initial hydrocarbon molecule. These authors show that the simplest explanation of their result (and also other facts established by a study of the slow oxidation of hydrocarbons) is on the basis of a radical-chain mechanism for the oxidation of hydrocarbons [238, 343]; the main role in the mechanism is played by decomposition of the peroxide radical ROO into an alcohol radical $\text{R}'\text{O}$ (or hydroxyl) and the corresponding aldehyde $\text{R}''\text{CHO}$. The authors also introduce into the mechanism a process of decomposition of the alcohol radical into a formaldehyde molecule and an alkyl radical in order to allow for the possibility of the formation of formaldehyde from *all* the carbon atoms. There is also assumed to be a parallel process of formation of the alcohol according to the scheme $\text{R}'\text{O} + \text{RH} = \text{R}'\text{OH} + \text{R}$. In this way the reaction stage considered may be represented as the following processes of decomposition of the peroxide and alcohol radicals:



and



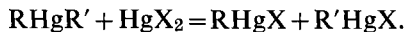
The products of the interaction of the methyl radical CH_3 with molecular oxygen have recently been studied by Ingold and Bryce [790] using a mass-spectrometric method. These authors detected the following radicals: CH_3O , CH_3O_2 , OH , HO_2 , CH_2 and CHO ?⁽³⁴⁾

Free alkyl radicals readily react with various solid metals and metalloids. For example, Paneth [1005] has detected a series of products from the interaction of CH_3 and C_2H_5 radicals with As, Sb and Bi such as $\text{As}(\text{CH}_3)_3$, $\text{As}(\text{C}_2\text{H}_5)_3$, etc. Razuvayev [220] has observed the different cases of the interaction of radicals with mercury and organo-mercury compounds in solution. According to the data of Rice [1061] the volatile dialkyl mercury compounds, formed as the result of the reaction of free radicals

⁽³³⁾ $\overset{\cdot}{\text{C}}$ denotes C^{14} .

⁽³⁴⁾ A more detailed summary of reactions of various free radicals is given by Steacie [1169]. See also *Disc. Faraday Soc.* No. 14, 1953 and Chap. 4 of this book.

with metallic mercury, react rapidly with mercury halides according to the equation



Complex Radicals

We have shown above that hydrogen atoms (p. 96) and also halogen atoms⁽³⁵⁾ (p. 102) and alkyl radicals (p. 108) readily add to olefin molecules to form new and more complex radicals. The addition of hydrogen atoms, chlorine atoms and alkyl and other radicals to the oxygen molecules takes place with similar readiness, since oxygen like olefins is to a certain extent unsaturated, and as a result the radicals HO_2 and ClO_2 and peroxide radicals ROO are formed. There are indications that hydroxyl HO and the oxides of nitrogen NO and NO_2 also possess the ability to add to unsaturated molecules. Thus Smith [1153], from analysis of the experimental data on photolysis of hydrogen peroxide H_2O_2 , comes to the conclusion that there might exist free radicals HO_3 and HO_4 of low activity, which are formed by the addition of HO and HO_2 radicals to an oxygen molecule. Similarly, from the study of the isotopic exchange of O^{18} between N_2O_5 and molecular oxygen and from the study of the oxidation of NO with oxygen labelled with O^{18} , Ogg [988] concludes that the mechanism of the first reaction must include the formation of an NO_4 radical [772] and that of the second reaction an NO_3 radical. We should add that investigation of the thermal decomposition of nitrogen pentoxide N_2O_5 also leads to the conclusion that the NO_3 radical exists.

Complex radicals formed by the addition of atoms or the simpler radicals to molecules of unsaturated structure have a lower chemical activity than the initial radicals and are therefore more stable. Considering the role of the stabilization of radicals in chemical kinetics, Szabó [1196] remarks that in some cases stabilization may retard a reaction and in other cases it may accelerate it. Retardation of a reaction is naturally connected with the above-mentioned low activity of complex radicals. Such a case is observed in the reaction of chlorine with hydrogen in which a sharp retardation of the reaction by oxygen is ascribed to the formation of ClO_2 and HO_2 radicals of low activity (see p. 571). The reaction of hydrogen with oxygen is retarded as a result of the formation of an inactive HO_2 radical on the interaction of H with O_2 (see p. 612). Moreover, the formation of stable radicals may favour the recombination of active radicals; according to Szabó, this must take place in the formation of the stabilized particles RNO (in the presence of nitric oxide NO as a "stabilizer"); owing to the low activity of RNO the probability

⁽³⁵⁾ This does not apply to iodine atoms since the endothermicity of the process $\text{I} + \text{C}_n\text{H}_{2n} = \text{C}_n\text{H}_{2n}\text{I}$, and hence its activation energy, reach a considerable value.

of the reaction of the R radical decreases and the probability of its recombination, which takes place according to the scheme $R + RNO = R_2 + NO$, increases.

The acceleration of a reaction by means of the stabilization of active radicals should be expected, since stabilization decreases the probability of their destruction. Reaction conditions are possible for which the increase in the lifetime of an active radical, due to its stabilization, favours the reaction. According to Szabó these conditions may be obtained in chain reactions. See also [71a].

In the literature there are indications of the formation of complex radicals involving saturated molecules. Thus, it follows from an approximate quantum-mechanical calculation for the system $CH_4 + H$ that it is possible to form a stable CH_5 complex which decomposes into $CH_4 + H$ with an activation energy of 8 kcal [689, 691, 1031a], (J. C. Polanyi, *J. Chem. Phys.* **24**, 493, 1956). In the opinion of Glasstone, Laidler and Eyring [57] the formation of the CH_5 complex (stabilization of H atoms) may be responsible for the inhibition of hydrogen para-ortho conversion by methane which has been observed by Farkas and Melville [599]. Farkas and Harteck [598] had explained the low concentration of atomic hydrogen during the photochemical decomposition of ammonia NH_3 by introducing into the mechanism of this reaction the process $H + NH_3 + M = NH_4 + M$ (M is any "third body") which leads to stabilization of the H atom in the NH_4 complex. Farkas and Harteck calculated the equilibrium constant for $H + NH_3 \rightleftharpoons NH_4$; and this indicates that at room temperature the equilibrium is completely displaced toward the NH_4 side and at $300^\circ C$ is completely displaced toward the $NH_3 + H$ side. The heat of the reaction $H + NH_3 = NH_4$ is 10 kcal. We should also point out that in order to explain the catalytic action of water vapour on the slow oxidation of hydrogen, Kondra'tev [133] has proposed a reaction mechanism including the process $H_2 + H_2O = H_3O + H$. The H_3O complex must clearly be considered as the analogue of the NH_4 and CH_5 complexes. However, it should be emphasized that the existence of these complexes has not been studied further, and at the present time the problem should be considered to be unsolved.⁽³⁶⁾

In a discussion of the mechanism of the $CO + O_2$ reaction near the so-called upper limit of ignition for a dry mixture of these gases, Lewis and von Elbe [174] consider possible the formation of a CO_3 complex by the interaction of ozone O_3 present in the reaction zone with carbon

⁽³⁶⁾ Regarding the H_3O complex, Voevodskii [41] has proposed a mechanism in which the part of the hypothetical process $H_2 + H_2O = H_3O + H$ is played by the process $HO_2 + H_2O = H_2O_2 + OH$ (this is a reversal of the process observed in a discharge in water vapour [643]) in order to explain the catalytic action of water on the oxidation of hydrogen.

monoxide. A suggestion of the formation of a CO_3 complex (in an excited or unstabilized state) in the reaction of dry CO and O_2 has recently been put forward by Knipe and Gordon [846] in connection with the flame spectrum of CO. In the opinion of these authors CO_3 is formed by the interaction of excited molecules of CO ($^3\Pi$), which are detected by their spectrum, with oxygen; on decomposition (into $\text{CO}_2 + \text{O}$ or into $\text{CO} + \text{O}_2$) the continuous spectrum characteristic of the CO flame is emitted. See also [255b].

CHAPTER 3

THEORY OF ELEMENTARY CHEMICAL PROCESSES

We shall call chemical reactions *elementary chemical processes* if they take place in one stage. For example, the reaction between hydrogen and iodine, $H_2 + I_2 \rightarrow 2HI$, is an elementary chemical process since it results directly from the collision of hydrogen and iodine molecules. It should be kept in view, however, that such an elementary chemical process is the statistical mean result of a large number of elementary changes which differ in the mutual orientation of the colliding molecules, and in the velocity, energy and state of the initial and final particles; essentially, however, all these elementary changes have a common feature in that they are all chemically similar, i.e. they lead to the same final substance.

The overwhelming majority of chemical reactions are complex processes taking place in several stages. Only very few reactions may be considered as elementary processes. Such reactions include, for example, the reaction mentioned above, the reverse reaction—the decomposition of hydrogen iodide—addition reactions of olefins to dienes and certain other reactions (see Chap. 4). However, a theoretical consideration of elementary processes is extremely important for complex reactions, as their individual stages are elementary chemical processes. A study of the mechanism and rate of individual stages makes it possible to predict the nature of a process as a whole. Often it is found that one of the stages is considerably slower than the others under certain conditions, and thus determines the rate and overall kinetics of the reaction. All this gives a basis for considering elementary chemical processes as an important object for study in their own right.

Elementary chemical processes are in essence inelastic molecular collisions accompanied by rearrangement of atoms. Various other forms of inelastic atomic and molecular collisions, although not leading directly to chemical change, may however play an important role in chemical gas reactions, by providing for an exchange of energy between colliding particles. These are the processes which give rise to the chemical activation of molecules, and in certain cases may even determine the rate of the overall reaction. On the other hand, the rate of attaining equilibrium distribution in the reacting system, departures from which may be reflected to a large extent in the reaction rate, is also dependent on these same

processes of energy exchange. (For classification of atomic and molecular collisions, see [189a]).

§8. Elements of the Statistical Theory of Elementary Chemical Processes

The theory of an elementary chemical process, strictly speaking, should be treated by quantum mechanics. The use of quantum ideas in the problem of the motion of several particles in a fixed potential field led to the creation of the quantum theory of collisions [193] which plays an important role in atomic physics. The quantum-mechanical treatment of chemical processes is, however, still in an early stage.

In the general case both the state of motion of the nuclei and the state of the electrons change simultaneously in an elementary chemical process. The motions of nuclei and electrons are intrinsically connected. This gives rise to serious mathematical difficulties in the treatment of the corresponding processes, since a wave equation must be solved containing the coordinates of electrons and nuclei. Analysis shows that under certain conditions the electronic and nuclear motions may be considered separately, i.e. by employing two equations, the first involving only the motion of the electrons and the second only that of the nuclei, instead of the usual single equation. Under these conditions displacement of the nuclei changes their potential energy continuously, without jumps. Processes in which nuclear motion of this type takes place are called *adiabatic*, and their quantum treatment is much simpler than for the general case.

It is found moreover that under certain conditions the motion of the nuclei (during an adiabatic process) may be treated to a first approximation by classical mechanics. This is a further great simplification of the problem of finding the probability of chemical conversion in a particular elementary process as a function of the energy, configuration and other characteristics of the colliding particles.

It is not possible, however, to treat all the degrees of freedom of the reacting molecules by classical mechanics; in certain cases, for example non-adiabatic processes, bimolecular decomposition reactions and certain others, classical mechanics is not applicable at all.

After the mechanical problem has been solved by some method, statistical methods may be used to calculate the mean (observable) rate of the elementary reaction. These calculations are usually based on classical statistics and assume that there is thermodynamic equilibrium in the system. Here the problem arises as to whether it is permissible to assume an equilibrium distribution (the Maxwell-Boltzmann distribution) when treating a non-equilibrium process, whatever the chemical reaction. Study of this problem has led to the conclusion that assuming an equilibrium

distribution in order to find the rate of a chemical process does not as a rule introduce a large error. Exceptions are certain types of reactions such as bimolecular decomposition reactions or fast reactions taking place at high temperatures.

In this way the rates of a large number of reactions may be calculated approximately on the basis of the following assumptions: that the process is adiabatic, that classical mechanics may be used in treating translational motion and that it is possible to use the Maxwell-Boltzmann distribution.

These assumptions will be considered in more detail below, and the methods of calculating reaction rates based on these assumptions will be discussed in subsequent sections (§§9-12). The fundamentals of the theory taking into account quantum characteristics of elementary chemical processes and the effect of disturbing the Maxwell-Boltzmann distribution will be considered separately (§13 and §16a).⁽¹⁾

Basic Ideas of Quantum Mechanics⁽²⁾

Direct experiments such as those on the diffraction of electrons and atoms lead to the conclusion that particles of matter have not only corpuscular properties, which are expressed by classical mechanics, but also wave properties, whose consideration is the object of quantum mechanics. The wave properties of a particle are characterized in quantum mechanics by a certain function $\Psi(x, y, z, t)$ of the coordinates of the particle and of time. This function is called the *wave function*, and in the general case is complex. The physical significance of this function is expressed by the fact that the square of its modulus multiplied by the volume element $d\tau = dx dy dz$, namely the expression $|\Psi|^2 d\tau$, represents the probability that at time t the particle will be at a point with coordinates inside the given volume element.

The wavelength, which according to quantum mechanics must be attributed to a moving particle, is given by the de Broglie relationship:

$$\lambda = h/mv, \quad (8.1)$$

where m is the mass of the particle, v is the velocity, and h is Planck's constant 6.62×10^{-27} erg sec. It follows from (8.1) that the wavelength corresponding to a moving particle may vary greatly depending on its mass and velocity. It is known from optical diffraction theory that diffraction may take place when the wavelength is of the same order of magnitude as the dimensions of the object causing the diffraction (a grating spacing for example). In just the same way, the wave properties of particles may be exhibited only when the wavelength characteristic of these particles

⁽¹⁾ For non-adiabatic processes see §13.

⁽²⁾ Only a very short schematic account of certain basic aspects of quantum mechanics will be given here. For a more detailed account see [28, 168].

is of the same order of magnitude as the dimensions of the object which causes the diffraction (for example, the dimensions of an atom). Thus for electrons ($m = 9.1 \times 10^{-28}$ g) moving with velocity 10^8 cm/sec (the order of electron velocities in an atom) we find from (8.1) that $\lambda \sim 6 \times 10^{-8}$ cm, i.e. a wavelength of the order of atomic dimensions. It follows that we are obliged to use quantum mechanics when treating the motion of electrons in an atom or molecule.

To determine the wave function mentioned above, the wave equation first obtained by Schrödinger is used; this has the following form for a particle of mass m moving in a potential field U (which in the general case is a function of the particle's coordinates and of the time):

$$-\frac{\hbar^2}{2m} \nabla^2 \Psi + U \Psi = i\hbar \frac{\partial \Psi}{\partial t}, \quad (8.2)$$

where $\hbar = h/2\pi = 1.054 \times 10^{-27}$ erg. sec. In this equation ∇^2 is a differential operator, which in Cartesian coordinates is equal to the sum of the second derivatives with respect to the coordinates of the particle,

$$\nabla^2 = \frac{\partial^2}{\partial x^2} + \frac{\partial^2}{\partial y^2} + \frac{\partial^2}{\partial z^2}.$$

Solving equation (8.2) gives the value of the function Ψ for any moment of time and at any point in space. As the equation is linear the function Ψ so found has an arbitrary factor. The value of this factor may be fixed by the following condition. According to the above, the expression $|\Psi|^2 dx dy dz$ represents the probability of finding the particle in the volume element $dx dy dz$ near the point with coordinates x, y, z . As the probability of finding the particle somewhere in space is unity, then according to the theorem of addition of probabilities we have

$$\int |\Psi|^2 dx dy dz = 1. \quad (8.3)$$

This is called the *normalization condition* and fixes (in modulus) the above-mentioned constant factor in the function.⁽⁸⁾ The equation (8.2) for the time-dependent wave function refers to the general case which includes transitions of the system from one state to another in the course of which the energy of the system has no definite value.

If the potential energy U is independent of time then the total energy of the system remains constant. The states of the system in which its energy has a definite constant value are called *stationary states*. It can be shown

⁽⁸⁾ If the energy values form a continuous spectrum then the normalization condition is formulated somewhat differently [28, 168].

[168] that for such states

$$i\hbar \frac{\partial \Psi}{\partial t} = E\Psi, \quad (8.4)$$

where E is the total energy of the particle. Integrating (8.4) we find that the wave function of a stationary state has the form:

$$\Psi = \exp(-iEt/\hbar)\psi(x, y, z). \quad (8.5)$$

The function $\psi(x, y, z)$ (sometimes called the amplitude wave function) is a function only of the coordinates of the particle. It follows from this expression that for stationary states the probability of finding the particle in a given region of space remains constant with time since, according to (8.5),⁽⁴⁾

$$|\Psi|^2 = \Psi\Psi^* = \psi\psi^* = |\psi(x, y, z)|^2.$$

In view of (8.4), the wave equation (8.2) for a stationary state may be written in the form

$$-\frac{\hbar^2}{2m}\nabla^2\psi + U\psi = E\psi. \quad (8.6)$$

The values of energy E for which this equation has finite, continuous and single-valued solutions are called *eigenvalues* of the energy of this system. For stable systems, i.e. those whose total energy is negative ($E < 0$), as for electrons in atoms and molecules, the energy eigenvalues form generally a *discrete* series (a so-called discrete spectrum). The complete set of eigenvalues of a system, however, usually includes also a region of positive energies ($E > 0$) in which the eigenvalues form a continuous spectrum (a continuous series). One or more eigenfunctions may be associated with each eigenvalue of a discrete or continuous spectrum. If there are two or more eigenfunctions the corresponding state is called *degenerate*.

It may be shown that two wave functions ψ_m and ψ_n referring to *different* energy eigenvalues ($E_m \neq E_n$) of a discrete spectrum are mutually orthogonal, i.e.

$$\int \psi_m \psi_n^* d\tau = 0, \quad (m \neq n).$$

In quantum mechanics an important role is played by the so-called *principle of superposition* which has the following meaning: If a given system may be in a state represented by the wave function ψ_1 and in another state ψ_2 , then in some conditions (for example, in an external field) the

⁽⁴⁾ The sign * after the function ψ signifies that the function ψ^* is the complex conjugate function of ψ .

state of the system may be represented by a wave function of the form

$$\psi = c_1\psi_1 + c_2\psi_2, \quad (8.7)$$

where c_1 and c_2 are constants. In the more general case, if the complete set of states of the system, which differ in a certain mechanical parameter (energy, momentum, etc.) corresponds to the set of functions $\psi_1, \psi_2, \psi_3, \dots$, then the wave function of any state of the system may be represented as a sum

$$\psi = \sum c_k \psi_k, \quad (8.8)$$

where the summation is over all k .

If both sides of equation (8.6) are multiplied by ψ^* and integrated over the total volume, we obtain

$$-\frac{\hbar^2}{2m} \int \psi^* \nabla^2 \psi \, d\tau + \int \psi^* U \psi \, d\tau = E \int \psi^* \psi \, d\tau.$$

In view of the normalization condition (8.3), the integral on the right-hand side is equal to unity. The integral

$$\int \psi^* U \psi \, d\tau$$

is the quantum-mechanical mean value of the potential energy.⁽⁵⁾ Introducing the notation

$$\bar{U} = \int \psi^* U \psi \, d\tau$$

and

$$\bar{T} = -\frac{\hbar^2}{2m} \int \psi^* \nabla^2 \psi \, d\tau,$$

we find

$$\bar{T} + \bar{U} = E.$$

Since E is the total energy of the particle then, according to the law of conservation of energy, \bar{T} should represent the mean kinetic energy of the particle. Accordingly the operator— $(\hbar^2/2m)\nabla^2$ —is called the *kinetic energy operator*.

⁽⁵⁾ According to quantum mechanics, if F is an operator corresponding to a certain physical quantity F , then the mean value of this quantity is

$$\bar{F} = \int \psi^* F \psi \, d\tau,$$

where ψ is the wave function of the state considered.

For a system of many particles, equations (8.2) and (8.6) must be generalized correspondingly. If m_j is the mass of the j th particle and U and Ψ denote the potential energy and wave function of the system and are functions of the coordinates of all the particles, then instead of (8.2) we have

$$-\frac{\hbar^2}{2} \sum \frac{1}{m_j} \nabla_j^2 \Psi + U\Psi = i\hbar \frac{\partial \Psi}{\partial t}, \quad (8.9)$$

where the summation is over all the particles; the subscript j on the operator ∇^2 signifies that the differentiation is carried out with respect to the coordinates of the j th particle. Similarly for a stationary state of a system of many particles we have

$$-\frac{\hbar^2}{2} \sum \frac{1}{m_j} \nabla_j^2 \psi + U\psi = E\psi, \quad (8.10)$$

where E is the total energy of the system.

If the system studied, or part of it, consists of identical particles, such as electrons, then an important additional condition, determined by the symmetry properties of the system, is imposed on the Ψ function. An important part in this additional condition is played by the spin of the electron (i.e. by its angular momentum). As the electron spin may be in one of two directions—along a magnetic field or counter to it (this field may result, for example, from another electron in the system)—a special spin coordinate is introduced which also has only two values. Thus the wave function of a system of electrons is a function of the four “coordinates” of each electron. The additional condition is that the wave function must be antisymmetric with regard to interchange of the coordinates of any two electrons, i.e. this operation must reverse the sign of the wave function. If for brevity we denote the combination of the four coordinates of an electron by one figure (1 or 2) then the condition of antisymmetry, which is the general form of the Pauli principle, may be written

$$\Psi(1, 2) = -\Psi(2, 1).$$

Solving the wave equation, i.e. finding the wave functions and energy values corresponding to different states of the system, involves serious mathematical difficulties except in the case of a small number of very simple systems. For stationary states, approximate solutions are usually sought in the following manner. First a wave equation which can be solved accurately or nearly accurately is obtained by using simplifying assumptions. For example, in the case of a polyatomic molecule the wave functions for the system of isolated atoms are found as a first approximation and then an approximate expression for the wave function ψ of the molecule is set up from these functions by using definite rules [304]. Next, both sides

of equation (8.10) are multiplied by ψ^* and integrated with respect to the coordinates of all the electrons, so that an approximate expression for the energy E of the system is obtained, namely

$$E = -\frac{\hbar^2}{2} \sum_i \frac{1}{m_i} \int \psi^* \nabla_i^2 \psi \, d\tau + \int \psi^* U \psi \, d\tau.$$

If in setting up an expression for ψ a series expansion is used in terms of the known eigenfunctions of any simplified wave equation, then the coefficients in this expansion may be determined from the variational principle that the energy E should have the lowest possible value.

For non-stationary states the problem is usually that of finding the probability of transition from one state to another. Calculation of this probability is in practice possible only if the perturbation causing the transition is sufficiently small.

Considering the case when the transition takes place under the action of a certain small time-independent perturbation energy U , and both initial and final states behave as a continuous spectrum. For example, this may be a transition caused by collision of an electron and an atom,⁽⁶⁾ and consisting of changes in the momenta (p) of the electron (the transition $p \rightarrow p'$) and the atom and in the internal energy of the atom (the transition $E_n \rightarrow E_k$). During collision the kinetic energy of the electron is partly used up in exciting the atom; according to the law of conservation of energy

$$\frac{p^2}{2m} + E_n = \frac{p'^2}{2m} + E_k.$$

As the kinetic energy of a free particle may take any value the terms $p^2/2m + E_n$ and $p'^2/2m + E_k$ behave as a continuous spectrum. The theory gives the following expression for the probability of this transition resulting in the electron moving in the elementary solid angle $d\Omega$ after collision:

$$P_{nk} d\Omega = \frac{2\pi}{h} \left| \int U \Phi_{n,p} \Phi_{k,p'} d\tau \right|^2 mp' d\Omega, \quad (8.11)$$

where $\Phi_{n,p}$ is the wave function of the system in the initial state and $\Phi_{k,p'}$ that in the final state and $d\tau$ is the product of the volume elements corresponding to the colliding particles. Equation (8.11) holds not only for collision of an electron and an atom but also for collision of two heavy particles, such as atoms or molecules, with the condition that the internal energy of only one of the particles varies. In the general case m is taken as the reduced mass of the particles.

⁽⁶⁾ In this case the perturbation energy U is the energy of the atom in the field of the electron and depends on the distance between them.

If the perturbation energy U is time-dependent, $U = U(t)$,⁽⁷⁾ then the probability of transition from the n th to the k th state will be equal to

$$P_{nk} = \frac{1}{\hbar^2} \left| \int_{-\infty}^{\infty} U_{kn} \exp(i\omega_{kn}t) dt \right|^2, \quad (8.12)$$

where

$$U_{kn} = \int U \Psi_k \Psi_n d\tau, \quad \omega_{kn} = \frac{1}{\hbar} (E_k - E_n). \quad (8.12a)$$

Here Ψ_k and Ψ_n are the wave functions of the k th and n th states and E_k and E_n are the energy eigenvalues of these states.

Adiabatic and Non-Adiabatic Processes

We have already noted that an “adiabatic” motion of nuclei is a process such that the motions of electrons and of nuclei are independent and the potential energy of the system varies continuously during nuclear motion, so that this motion is not accompanied by electronic transitions. We shall consider the conditions governing such motions [28, 1020].

Representing the sets of coordinates of nuclei and electrons by X and x respectively. For simplicity we shall assume that all the nuclei are identical. The Schrödinger equation for the whole system then takes the form

$$i\hbar \frac{\partial \Psi(X, x, t)}{\partial t} = \left[-\frac{\hbar^2}{2M} \nabla_X^2 - \frac{\hbar^2}{2m} \nabla_x^2 + U(X, x) \right] \Psi(X, x, t), \quad (8.13)$$

where M is the mass of the nucleus and m of the electron. The symbols ∇_x^2 and ∇_X^2 represent the sums of the kinetic energy operators for all the electrons and for all the nuclei respectively and $U(X, x)$ the potential energy of electrons and nuclei.

We shall first assume that the nuclei are at rest (the X coordinates fixed) and that the electrons are in a stationary state with energy ϵ . This assumption clearly holds for a system remote from the equilibrium state if the nuclear motion is much slower than the electronic motion, so that during each nuclear displacement the electrons “instantaneously” assume a configuration corresponding to the lowest energy of the system for the given electronic state and disposition of the nuclei. With this assumption we may neglect the operator $-(\hbar^2/2M)\nabla_X^2$ in equation (8.13) and then, using (8.4), we obtain instead of (8.13)

$$\left[-\frac{\hbar^2}{2m} \nabla_x^2 + U(X, x) \right] \psi = \epsilon \psi. \quad (8.14)$$

⁽⁷⁾ For example, in the case of the electric field of a light wave.

The eigenfunctions ψ_k and eigenvalues ϵ_k of (8.14) depend on the coordinates of the nuclei:

$$\psi_k = \psi_k(x, X), \quad \epsilon_k = \epsilon_k(X). \quad (8.15)$$

Each of the ψ_k functions characterizes the electronic state k for fixed values of the coordinates X of the nuclei.

Expressions (8.15) are required to find solutions of the equation (8.13). It is assumed that we know the ψ_k functions and the ϵ_k energy values. Expanding the required function $\Psi(X, x, t)$ in a series with respect to the ψ_k eigenfunctions:

$$\Psi(X, x, t) = \sum_k \varphi_k(X, t) \psi_k(x, X), \quad (8.16)$$

where $\varphi_k(X, t)$ are functions of coordinates X and time but do not depend on the coordinates of the electrons and therefore act as the coefficients c_k in formula (8.8). Substituting (8.16) into (8.13), multiply the latter by $\psi_j^*(x, X)$ and integrate with respect to x . Then, considering the ψ_k to be orthogonal and normalized, we obtain an equation for φ_j ($j = 1, 2, \dots$) which describes the motion of the nuclei,

$$i\hbar \frac{\partial \varphi_j(X, t)}{\partial t} = \left[-\frac{\hbar^2}{2M} \nabla_X^2 + \epsilon_j(X) \right] \varphi_j(X, t) - \frac{\hbar^2}{2M} \sum_k (2a_{jk} \nabla_X \varphi_k + b_{jk} \varphi_k), \quad (8.17)$$

where

$$a_{jk} = \int \psi_j^* \nabla_X \psi_k \, dx, \quad b_{jk} = \int \psi_j^* \nabla_X \psi_k \, dx. \quad (8.18)$$

Here, as in equation (8.13), the symbols ∇_X and ∇_X^2 represent the sums of the corresponding operators for all the nuclei. If we find φ_j functions which satisfy the equations (8.17) then the function (8.16) will be the required solution of equation (8.13).

We now assume that the eigenfunctions ψ_k of the electrons are weakly dependent on the coordinates of the nuclei. With this condition, according to (8.18), terms containing a_{jk} and b_{jk} in (8.17) may be neglected, so that instead of (8.17) we have

$$i\hbar \frac{\partial \varphi_j}{\partial t} = \left[-\frac{\hbar^2}{2M} \nabla_X^2 + \epsilon_j(X) \right] \varphi_j(X, t). \quad (8.19)$$

This equation represents the wave equation of the motion of the nuclei, whose potential energy ϵ_j refers to the j th electronic state and results from interaction of the nuclei with each other and with all the electrons and also from the kinetic energy of the electrons and their interaction with one another.

It is easy to see that, in this approximation, nuclear motion is not accompanied by change in the electronic state of the system, i.e. the motion is adiabatic. If, for example, at the initial instant the electrons are in the ψ_1 state and accordingly when $t = 0$, $\varphi_1 \neq 0$ and $\varphi_j = 0$ ($j = 2, 3, \dots$), then, according to (8.19), $d\varphi_1/dt \neq 0$ but $d\varphi_j/dt = 0$ ($j \neq 1$). In other words, electronic transitions do not occur, as when $j \neq 1$, $\varphi_j = 0$ throughout the process. During each nuclear displacement the electrons "instantaneously" assume a configuration corresponding to their minimum energy for the given electronic state and disposition of the nuclei; the electrons follow the nuclei without appreciable inertia. The nuclei move in the potential field $\epsilon_j(X)$ which depends only on the coordinates of the nuclei for each electronic state j . Consequently, the eigenvalue ϵ of the wave equation (8.14) for the electrons plays the part of the potential energy of the nuclei. If this function is known the problem consists of solving equation (8.19) to determine the nuclear motion in the given potential field.

Therefore, when the electronic wave functions are only weakly dependent on the disposition of the nuclei (i.e. when $a_{jk} = b_{jk} = 0$) the electronic and nuclear motions are actually separate, and nuclear motion is not accompanied by electronic transitions.

When the terms in a_{jk} and b_{jk} in (8.17) cannot be neglected it is easy to see that nuclear motion cannot be separated from the electronic motion and is accompanied by electronic transitions. Indeed, if, for example, the electrons are again in the state ψ_1 when $t = 0$, then, as above, this signifies that in equation (8.16) $\varphi_1 \neq 0$ and $\varphi_j = 0$ ($j \neq 1$). Now, however, as $a_{jk} \neq 0$ and $b_{jk} \neq 0$, then according to (8.17) $d\varphi_j/dt \neq 0$ for any j . This means that in the course of time the $\varphi(j \neq 1)$ functions differ from zero and, in accordance with (8.16), the electronic state of the system changes. In this case the motion of the nuclei will be non-adiabatic. To find the φ functions it is now necessary to solve the general equation (8.17) instead of (8.19).

The difference between adiabatic and non-adiabatic processes may be illustrated by the example of a system in which only one coordinate is varied, such as the internuclear distance in diatomic molecules. In this case adiabatic motion means that the system moves along the same potential curve corresponding to the given electronic state (Fig. 23, arrow *a*). On the other hand, for non-adiabatic motion the system undergoes transition from one potential curve to another corresponding to a different electronic state of the system (Fig. 23, arrow *b*) and, in contrast with optical transitions, this transition is not accompanied by the emission or absorption of light.

In §13 we shall give a more precise exposition of the conditions for motion to be an adiabatic process. We should mention here that one of

these conditions is that the nuclei should move with a sufficiently low velocity. This follows directly from the formula (8.12) for the probability of transition from the n th to the k th state if we take n and k as the corresponding electronic states and the quantity U (see (8.12a)) as the potential energy of the system, which depends on the internuclear distances, which themselves change with time. When the nuclei move slowly, U_{kn} will

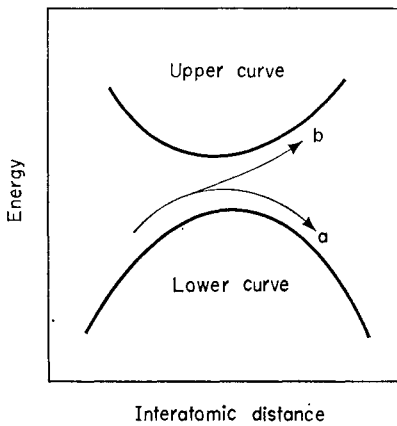


FIG. 23. Adiabatic (a) and non-adiabatic (b) motion in the region of closest approach of two potential curves.

depend only slightly on time. In this case U_{kn} may be placed outside the integral sign in (8.12) and the remaining integral becomes zero when $E_k \neq E_n$. This means that when the nuclei move slowly, electronic transition will be of low probability, i.e. the nuclear motion will be adiabatic. On the other hand, when the nuclei move rapidly the probability of non-adiabatic transitions is considerably increased.

Classical Treatment of Nuclear Motion

The general equation (8.19) of adiabatic nuclear motion is soluble only in certain simple cases. It is not difficult to show, however, that in adiabatic translational motion of nuclei in an elementary chemical process the wave equation may be replaced approximately by an equation of classical mechanics.

For simplicity we shall consider the one-dimensional relative motion of two nuclei with reduced mass μ and internuclear distance X . Then, omitting the subscript i , we obtain as representing (8.19)

$$-\frac{\hbar^2}{2\mu} \frac{\partial^2 \varphi}{\partial X^2} + \epsilon \varphi = i\hbar \frac{\partial \varphi}{\partial t}. \quad (8.20)$$

We shall make the substitution:

$$\varphi = \exp(iS/\hbar), \quad (8.21)$$

where $S = S(X, t)$ is a function (usually complex) of coordinates and time and has the dimensions of mechanical action (erg sec.). Substituting (8.21) into equation (8.20) we find

$$\frac{1}{2\mu} \left(\frac{\partial S}{\partial X} \right)^2 + \frac{i\hbar}{2\mu} \frac{\partial^2 S}{\partial X^2} + \epsilon(X) = - \frac{\partial S}{\partial t}. \quad (8.22)$$

If the potential energy ϵ of the system is independent of time then the motion is steady. It follows (see equation (8.6)) that in this case the function φ may be written

$$\varphi = \varphi_0 \exp\left(-\frac{iWt}{\hbar}\right) = \exp\left(\frac{i}{\hbar}S_0 - \frac{i}{\hbar}Wt\right), \quad (8.23)$$

where φ_0 and S_0 depend only on the coordinates, and the constant W is the total energy of the system. With this condition

$$\frac{\partial S}{\partial t} = -W, \quad (8.24)$$

and we have instead of equation (8.22)

$$\frac{1}{2\mu} \left(\frac{\partial S}{\partial X} \right)^2 + \frac{i\hbar}{2\mu} \frac{\partial^2 S}{\partial X^2} = W - \epsilon(X). \quad (8.25)$$

In order to explain the physical significance of the quantity S we shall first assume that it is only weakly dependent on X , so that the term in equation (8.25) containing the second derivative $\partial^2 S / \partial X^2$ may be neglected. With this condition we obtain

$$\frac{1}{2\mu} \left(\frac{\partial S}{\partial X} \right)^2 = W - \epsilon(X). \quad (8.26)$$

On the other hand, we have from the law of conservation of energy

$$\frac{1}{2\mu} p^2 = W - \epsilon(X),$$

where p is the momentum of a particle of mass μ . Comparing this equation with (8.26) we obtain

$$\frac{\partial S}{\partial X} = p. \quad (8.27)$$

It is assumed here that p is a function of X .⁽⁸⁾

⁽⁸⁾ To express p as a function of X is always easy if the time t is eliminated from the two functions $p(t)$ and $X(t)$ found by solving the mechanical problem.

Integrating (8.27) we obtain

$$S = \int p dX + f(t) \quad (8.28)$$

where $f(t)$ is a function of time only. On the basis of (8.24) we find that $f(t) = -Wt$ and therefore

$$S = \int p dX - Wt. \quad (8.29)$$

Hence in our approximation S is no other than the mechanical action of classical physics, and equation (8.26) is the Hamilton–Jacobi equation of classical mechanics when the potential energy ϵ is independent of time. The corresponding Hamilton–Jacobi equation for the general case is obtained from (8.22) by discarding the terms in $\partial^2 S / \partial t^2$.

The assumption that $\partial S / \partial X$ is only weakly dependent on X is a very special assumption, however, and may hold quite rarely, for example in the free motion of a particle (i.e. in the absence of external forces). It is therefore necessary to ascertain what more general physical assumptions are required if we are to be able to neglect the second term in the left-hand side of equation (8.25) and so to replace the wave equation by the equation of classical mechanics. It is not difficult to see that this requires

- (1) that for a given velocity $v [= (\partial S / \partial X) / \mu]$ the mass as is sufficiently great, or
- (2) that for a given mass μ the velocity is sufficiently great.

Note that on the basis of the de Broglie formula

$$\lambda = h / \mu v$$

these conditions are equivalent to assuming that the de Broglie wave length λ is sufficiently small; this is in accordance with the fact that for very small values of λ there are no diffraction effects. This result is obtained formally by assuming that $\hbar \rightarrow 0$, i.e. that the quantum of action is vanishingly small.

In these conditions we have instead of (8.25)

$$\frac{1}{2\mu} p^2 = W - \epsilon(X). \quad (8.30)$$

It is not difficult to see that in the case considered of one-dimensional motion this equation is equivalent to Newton's equation of motion. Indeed, differentiating the right- and left-hand sides of (8.30) with respect to X we find

$$\frac{p}{\mu} \frac{dp}{dX} = - \frac{d\epsilon}{dX}.$$

Noting that $p(dp/dX)/\mu = \mu v(dv/dX) = \mu(dv/dX)(dX/dt) = \mu(d^2X/dt^2)$ and that $d\epsilon/dX = -F$, where F is the effective force, we obtain Newton's equation

$$\mu(d^2X/dt^2) = F. \quad (8.31)$$

Therefore when the conditions indicated are fulfilled the motion of the nuclei may be approximately represented by using the laws of classical mechanics. We shall formulate these conditions quantitatively. Introducing for steady motion the notation $dS/dt = S'$ and $d^2S/dt^2 = S''$, we find from equation (8.25) that the second term in the left-hand side may be neglected if

$$\hbar S''/(S')^2 \ll 1. \quad (8.32)$$

Considering that, to a first approximation, according to (8.30)

$$S' = [2\mu(W - \epsilon)]^{1/2},$$

we find

$$S'' = -\mu(d\epsilon/dX)[2\mu(W - \epsilon)]^{-1/2} = \mu F/S'.$$

Consequently, instead of (8.32) we may write

$$\hbar\mu F/p^3 = (\hbar F)/(\mu^2 v^3) \ll 1. \quad (8.33)$$

Therefore a classical treatment of nuclear motion, in particular the motion in an elementary chemical process, is the more valid the higher the mass and velocity of the nuclei and the smaller the force acting on them.⁽⁹⁾

Consider, for example, a particle of mass μ moving with a finite velocity v over the top of a potential barrier (see §10 and §11); in this case a classical treatment is quite valid as $F = 0$ at the point of the potential energy maximum and condition (8.33) is fulfilled. We now suppose that a particle of mass $\mu = 1.66 \times 10^{-24}$ g (an H atom) approaches or leaves the top of the potential barrier, and the force acting on the particle (the force is the gradient of the barrier) is $F = 1$ eV/Å. If in this case the kinetic energy of the particle is 1 eV, then we find

$$(\hbar F)/(\mu^2 v^3) \simeq 2 \times 10^{-2},$$

and hence condition (8.33) is approximately fulfilled. If the energy of the particle is thermal ($\frac{1}{2}kT$) then at 300°K we find

$$(\hbar F)/(\mu^2 v^3) = 15.$$

In the latter case it is clear that a classical treatment is not applicable. The motion of atoms and molecules with such a small kinetic energy may

⁽⁹⁾ However, condition (8.33) which was obtained for one-dimensional motion is not always adequate for the general case of three-dimensional motion.

be treated on the basis of classical mechanics only if the forces acting on them are sufficiently weak, such as van der Waals forces.

A classical treatment of vibrational motion is applicable when the particle is close to the equilibrium point, where $F = 0$, and is not applicable close to the extreme positions of the particle, as its velocity at these points is zero.

It should be noted that in intermediate cases, where $\hbar F/\mu^2 v^3$, although less than one, is not sufficiently small for classical mechanics to be used with complete reliability, the quantum-mechanical solution of the problem may still be considerably simplified, as instead of the precise equation (8.20) we may use an approximate equation in a simpler form (the so-called quasi-classical approximation) [168].

Two statistical methods have been developed on the basis of a classical treatment of the translational motion of nuclei to calculate the rate of elementary chemical processes. The first is based on the gas-kinetic theory of molecular collisions and starts with the assumption that the molecules are hard spheres. The second method, which is called the activated complex or transition state method, considers the actual character of the dependence of the potential energy of the system on the disposition of the atoms. A common feature of both methods is the assumption that the equilibrium Maxwell-Boltzmann distribution in the system is not essentially disturbed in the reaction.

We shall consider in more detail the conditions for this assumption to be fulfilled.

Conditions for Conservation of the Maxwell-Boltzmann Distribution in a Reacting System

It is not difficult to see that the course of a chemical reaction perturbs the Maxwell-Boltzmann equilibrium distribution in the initial systems.⁽¹⁰⁾ Indeed, when the reacting substances are brought into contact with one another (by intermixing) and reaction begins, the reactant molecules with most energy continually undergo chemical conversion. Consequently the concentration of these molecules will decrease and the concentration of energy-rich product particles will increase. Deviations from an equilibrium distribution of product molecules also result from the heat effect of the reaction: a positive heat of reaction will increase their mean energy and a negative thermal effect will decrease it. The deviation from equilibrium of the distribution of energy among various degrees of freedom of a molecule may be especially great since, as a rule, exchange of energy between disparate degrees of freedom is more difficult than between similar degrees of freedom. At the end of the reaction, the system reaches thermodynamic

⁽¹⁰⁾ Review articles referring to this problem are given in [1136, 1044].

equilibrium after a certain time interval, owing to inelastic collisions of the molecules with one another and with the vessel walls and also due to radiation. The process of the system approaching the equilibrium state is called relaxation and the time which characterizes the rate of attaining equilibrium is called the relaxation time. The degree of deviation from equilibrium in the course of a reaction will depend on the relationship between the probabilities of the various elementary acts of energy exchange. If the probability of transfer of energy from one degree of freedom to another during an *elementary chemical conversion*⁽¹¹⁾ is much lower than the probability of energy exchange in the relaxation process, then the deviation from the Maxwell-Boltzmann distribution caused by the reaction will be small. If the converse holds, departures from the equilibrium distribution may be considerable. In this case statistical methods of calculating the reaction rate which assume that departures from the equilibrium distribution are small may lead to considerable errors.

In the general case, for a non-equilibrium distribution it is not possible to assign a definite temperature to the system. When there *is* equilibrium we may write the relative number of particles with energy ϵ_i , $f_i = n_i/n$, ($n = \sum n_i$), as

$$f_i = C \exp(-\epsilon_i/kT). \quad (8.34)$$

Consequently, T is the only parameter in the equilibrium distribution law. In this connection, the temperature T may be defined as the reciprocal of the slope of the straight line obtained by plotting $\log(f_i/f_0)$ against $(\epsilon_i - \epsilon_0)/k$ ($i = 1, 2, \dots$), where f_0 and ϵ_0 refer to the lowest energy level. In the absence of equilibrium, the number of particles in the i th quantum level in the general case will depend on the energies of all the remaining levels, on the probabilities of transitions between levels, and on time, i.e.

$$f_i = f_i(\epsilon_1, \epsilon_2, \dots, \epsilon_i, \dots, P_{12}, P_{13}, \dots, P_{i-1,i}, P_{i,i+1}, t), \quad (8.35)$$

where P_{ij} is the probability of transition from the i th to the j th state and t is time. In this case temperature is not a characteristic parameter of the distribution since the distribution law does not have the form of (8.34). In many non-equilibrium systems studied experimentally, however, it is apparently possible to introduce a characteristic parameter which corresponds to temperature. Thus, experiment shows that frequently plots of experimental values of $\log(f_i/f_0)$ against $(\epsilon_i - \epsilon_0)/k$ give an approximately straight line. We may define an effective temperature T^* by equating the slope of this line to $1/T^*$; this quantity, generally speaking, may be either

⁽¹¹⁾ We are considering the probability of a particular chemical process when the reacting particles are activated sufficiently. For rates of complex reactions in the absence of equilibrium see, for example, [C. A. Hollingsworth, *J. Chem. Phys.* **27**, 1346 (1957)]; [P. Van Rysselberghe, *J. Chem. Phys.* **29**, 640 (1959)].

higher or lower than the temperature at which the system reaches equilibrium. The distribution $f = C \exp(-\epsilon/kT^*)$ obtained in this way is called the *pseudo-Boltzmann distribution*. Theoretical studies of non-equilibrium distribution with respect to velocities [512, 1045, 1046, 1136] have shown that the introduction of an effective temperature is valid if the departure from the equilibrium distribution is small enough.

It is known that the energy of a molecule may be divided roughly into terms corresponding to the individual types of motion: translational, rotational, vibrational. With a pseudo-Boltzmann distribution the rate of energy exchange between individual degrees of freedom of a given type (for example, between rotational degrees of freedom) is much greater than that between degrees of freedom of different types (for example, rotational and vibrational degrees of freedom). Consequently, it is reasonable to talk about the effective temperature for degrees of freedom of a given type, such as "translational" temperature, "rotational" temperature, "vibrational" temperature and so on; under these conditions these temperatures are not equal. For this reason it is necessary when studying the distribution of molecules in a reacting system to consider the different character of the molecular distribution with respect to each type of energy: translational, rotational, vibrational and electronic. If the idea of temperature is not applicable, then the system may be characterized by the mean energy $\bar{\epsilon}$ per degree of freedom which becomes equal to $\frac{1}{2}kT$ in the limiting case of the Maxwell-Boltzmann distribution.

It is known that a Maxwellian distribution (the equilibrium distribution with respect to velocities) is established relatively rapidly, in a time of the same order as that of the free path of the molecules. Studies [853, 1046] (R. D. Present, *J. Chem. Phys.* **31**, 747 (1959)), show that appreciable departures from Maxwellian distribution may occur in the course of a reaction when $E/RT \leq 5$, where E is the activation energy of the reaction. When the temperature of a reaction does not exceed 1000°K, then for most reactions $E/RT > 5$ as usually $E \approx 10$ to 40 kcal. At higher temperatures this condition may not hold, especially in the case of reactions with very low activation energies such as those of atoms and radicals. Thus, the activation energy of the reaction $O + H_2 \rightarrow OH + H$ is 12 kcal and hence at the flame temperature ($\sim 3000^{\circ}\text{K}$) $E/RT \approx 2$. In similar cases we might expect appreciable departures from the equilibrium distribution with respect to velocities, considerably affecting the rate of reaction. According to Present (R. D. Present, *J. Chem. Phys.* **31**, 747, 1959), for example, at $E/kT = 5$ the reaction rate appears to be 8 per cent less than that following from the simple collision theory.

Deviations from the Boltzmann distribution with respect to vibrational degrees of freedom are related to reaction rates in a more complex manner.

The relaxation of vibrational motion of molecules has been studied

theoretically for the case of a system of harmonic oscillators in a heat bath, the molecules of which have a Maxwell-Boltzmann distribution [957, 1095]. Relaxation is different for different initial non-equilibrium distributions of harmonic oscillators with respect to vibrational levels. Thus, if we have an initial pseudo-Boltzmann distribution, then relaxation occurs through a continuous sequence of pseudo-Boltzmann distributions, and the effective temperature T^* gradually approaches the temperature T of the heat bath (Fig. 24) from the initial value T_0^* . If the initial distribution is such that

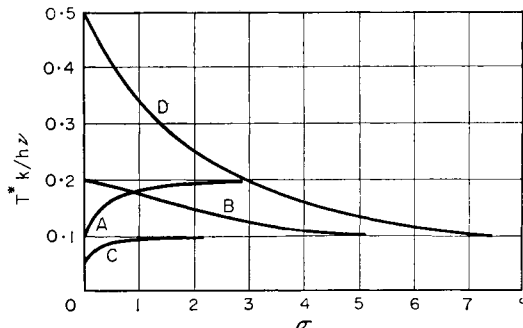


FIG. 24. Relaxation of vibrational temperature of a system of oscillators with an initial Boltzmann distribution for different initial (T_0) and final (T) temperatures.
 $A, T_0 = hv/10k, T = hv/5k$; $B, T_0 = hv/5k, T = hv/10k$; $C, T_0 = hv/20k, T = hv/10k$; $D, T_0 = hv/2k, T = hv/10k$; $\sigma = Z_0 n P_{10} (1 - \exp[-hv/kT]) t$ (according to Montroll and Shuler [957]).

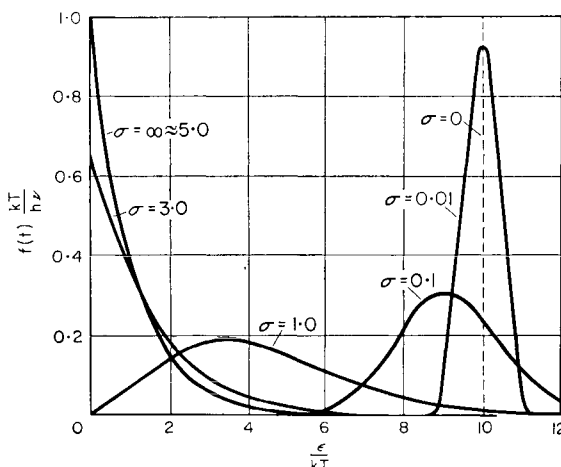


FIG. 25. Relaxation of a distribution (f) of oscillators with respect to energy (when $hv \ll kT$) when all the oscillators are initially in the same level (δ -distribution). The different curves refer to different times, $\sigma = (Z_0 n P_{10} hv/kT) t$ (according to Rubin and Shuler [1095]).

all the oscillators are in the same excited level (a so-called δ -distribution), then in the course of time the distribution "spreads" and its maximum moves toward the lower levels (Fig. 25). It is important to note, however, that the time of relaxation of the mean energy appears to be independent of the type of the initial distribution. If $\bar{\epsilon}(0)$, $\bar{\epsilon}(t)$ and $\bar{\epsilon}(\infty)$ are the mean energy of the system at the initial moment of time, at the time t and at $t = \infty$ (when equilibrium has been reached) respectively, then, assuming that the relaxation results from conversion of vibrational into translational energy on collision, we may write for this model [957, 1095]

$$\frac{\bar{\epsilon}(t) - \bar{\epsilon}(\infty)}{\bar{\epsilon}(0) - \bar{\epsilon}(\infty)} = \exp(-Z_0 n P_{10} t), \quad (8.36)$$

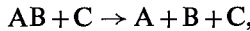
where P_{10} is the probability of the transition of the oscillator from the first excited vibrational level to the ground level, Z_0 is the collision number for a concentration of 1 molecule per cm^3 (see p. 143) and n is the number of molecules per cm^3 . It follows from formula (8.36) that the energy changes by a factor $1/e$ by the time t at which

$$Z_0 n P_{10} t = 1.$$

The time calculated from this condition may be defined as the *relaxation time* τ of the mean energy. Consequently,

$$\tau = \frac{1}{Z_0 n P_{10}}. \quad (8.37)$$

The change in the Boltzmann distribution with respect to vibrational levels, caused by thermal decomposition of diatomic molecules



has been studied by Nikitin [214a]. In order to simplify the calculations he represented the potential-energy curve of the AB molecule by the curve shown in Fig. 61 (p. 297). In this way the molecule AB is represented by a "harmonic" oscillator with a finite number of discrete levels of negative energy equidistant from one another and with a continuous positive-energy spectrum. These oscillators are in the above-mentioned heat bath.^(11a)

It is assumed that transitions in each oscillator may only occur between neighbouring levels, and that dissociation occurs during the transition of the oscillator from the last discrete level to one of the states of the continuous energy spectrum. The decrease, resulting from molecular decompositions, in the number of oscillators in an upper excited state disturbs the

^(11a) For the theory of relaxation of a system of anharmonic oscillators allowing for dissociation, see [E. E. Nikitin, *Dokl. Akad. Nauk, SSSR* **124**, 1085 (1959); K. E. Shuler, *J. Chem. Phys.* **31**, 1375 (1959)]. For general treatment of relaxation in an arbitrary system of molecules with many quantum states see [K. E. Shuler *Phys. Fluids* **2**, 442 (1959)].

Boltzmann distribution with respect to vibrational levels. Calculation shows that the relative number f_v of oscillators in the v th vibrational level decreases exponentially with time (with a rate independent of v) and is proportional to

$$f_v \sim \exp(-v\hbar\nu/kT) \times \times \left\{ 1 - \exp[-(v_0 - v)\hbar\nu/kT] \frac{v_0 + 1}{v + 1} \frac{p}{p + (1 - \exp[-\hbar\nu/kT])(v_0 + 1)} \right\}. \quad (8.38)$$

Here v_0 is the number of the uppermost discrete level, $\hbar\nu$ is the quantum of vibrational energy and $p = P_\infty/P_{10}$, where P_∞ is the probability of dissociation from the v_0 th level. It is apparent from (8.38) that a Boltzmann distribution with respect to vibrational levels holds only if the probability of dissociation of a molecule from the top vibrational level is very low, i.e. if $P_\infty \ll P_{10}$. Calculation of the rate constant gives

$$k = Z_0 P_\infty (1 - \exp[-\hbar\nu/kT]) \exp(-E_0/kT),$$

where E_0 is the dissociation energy of the molecule. Usually, however, $P_\infty \gg P_{10}$ (P_{10} usually varies from 10^{-2} to 10^{-12} and P_∞ is about 1). With this condition the distribution is disturbed and the probability of finding the oscillator in the $v \approx v_0$ levels is very small. Consequently, a decomposition reaction very strongly disturbs the Maxwell-Boltzmann distribution of vibrational levels near the dissociation limit. A similar disturbance should also occur in the case of polyatomic molecules (see §16).

Within the limits of Nikitin's simplified model these conclusions are applicable not only for dissociation of diatomic molecules but also qualitatively for bimolecular exchange reaction $AB + C \rightarrow A + BC$ (with the condition that the masses of atoms A and C are much greater than that of B). Here P_∞ is interpreted as the probability of transition of the system from the upper level of the first potential well (AB) to the upper level of the second potential well (BC). Approximate calculations (p. 206 *et seq.*) show that this probability is several powers of ten less than unity, and therefore, according to the above, it would be expected that in reactions of this type a disturbance of the equilibrium distribution with respect to vibrational levels of the initial molecule should occur only in exceptional cases. This problem, however, requires more study.

As vibrational relaxation is relatively slow, within the first moments the BC molecules will obviously be in vibrationally-excited states, and the energy of this excitation, E_{vib} , will in certain cases be very high. E_{vib} values for a number of exchange reactions, obtained by studying the spectra of reaction products, are given in Table 3 below.

The effect of the heat of a reaction on the degree of departure from equilibrium distribution and on the rate of the chemical reaction has been

TABLE 3
Excitation of vibrational levels in exchange reactions

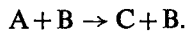
Reaction	Heat of reaction Q kcal	Highest (v) vibrational level observed	Highest E_{vib}	E_{vib}
				$\frac{Q}{Q}$
$H + Cl_2 = HCl^* + Cl$	[a, b]	45	6	1.00
$H + O_3 = HO^* + O_2$	[941]	80	9	0.94
$O + O_3 = O_2^* + O_2$	[940a]	93	17	0.68
$NO + O_3 = NO^* + O_2$	[c]	47.5	—	1.00
$O + ClO_2 = O_2^* + ClO$	[884]	61	8	0.56
$O + NO_2 = O_2^* + NO$	[884]	46	8	0.75
$Br + O_3 = BrO^* + O_2$	[940a]	19	4	0.41
$Cl + O_3 = ClO^* + O_2$	[940a]	40	5	0.28

a [J. K. Cashion, J. C. Polanyi, *J. Chem. Phys.* **29**, 455 (1958); **30**, 1097 (1959)].

b [J. C. Polanyi, *J. Chem. Phys.* **31**, 1338 (1959).]

c [J. C. Greaves, D. Garvin, *J. Chem. Phys.* **30**, 348 (1959).]

studied by Prigogine and Mahieu [1045] for the "chemical" quenching of fluorescence, i.e. the process in which the chemical reaction $A \rightarrow C$ takes place as the result of bimolecular collision of an electronically-excited molecule (A) and another molecule (B):



These authors obtained the following approximate expression for w , the initial rate of this process, at sufficiently high temperatures:

$$w = w_0 \left(1 + 1.2 x_A x_B \frac{Q}{E} \right). \quad (8.39)$$

where w_0 is the rate of the reaction calculated assuming an equilibrium distribution, Q is the heat of the reaction, E its activation energy and x_A and x_B are the mole fractions of substances A and B. If the reaction is exothermic ($Q > 0$) then it follows from (8.39) that perturbing the equilibrium distribution accelerates the reaction more, the greater the heat of reaction and the lower the activation energy. This is natural, since the higher the exothermicity of a reaction, the greater is the excess energy of molecules of the final substance which may be transferred to molecules of the initial substances and thus activate them. On the other hand, the effect of perturbing the equilibrium distribution should decrease with an increase in the activation energy, which tends to retard the reaction and consequently to restore the equilibrium distribution. Increase in rate due to the exothermicity of a process may obviously occur in other reactions, especially at high temperatures (see Chap. 10).

If the reaction is endothermic ($Q < 0$), then according to (8.39) the reaction rate decreases with an increase in the heat of the reaction, as when $Q < 0$ there is a decrease in the number of initial molecules with very large amounts of energy.⁽¹²⁾

On the whole it appears that for a large number of gas-phase chemical reactions the Maxwell–Boltzmann distribution is fairly well maintained and only for fast reactions proceeding at high temperatures is it necessary to allow for its disturbance.

In §42 (p. 684 *et seq.*) we give experimental data on non-equilibrium concentrations of particles formed for appreciable disturbances of the Maxwell–Boltzmann distribution as a result of chemical reactions in flames. In §16 we shall consider the kinetics of bimolecular decomposition reactions in which the equilibrium distribution of vibrational energy is strongly disturbed. Finally, in Chap. VI we give data on the rates of energy exchange, on which the degree of disturbance depends.

§9. Gas-Kinetic Collision Theory

We shall consider molecules as solid spheres as a first approximation. In this case it is easy, by using gas-kinetic theory, to calculate the number of binary collisions of molecules in unit time. When these collisions take place with sufficiently high energy it may be assumed that they lead to reaction. With this assumption, the theory does not then require that for an elementary chemical act to occur the energy must be completely redistributed among the various degrees of freedom in the colliding molecules; the probability of this redistribution may be much less than unity (see §11 and §12).

Effective Cross-Section

If molecules are represented as elastic solid spheres of a definite radius r , then the number of collisions will depend directly on the sum of their radii r_1 and r_2 and we may define a *collision cross section* $\sigma = \pi(r_1 + r_2)^2$. In reality molecules are not solid spheres, and their interaction at close range is determined by intermolecular forces which in the general case are governed by a complex law.

As we are usually interested not in the collision process itself but its result, such as the change in velocity and energy of each molecule, molecular collisions may be considered approximately as collisions of solid spheres. These collisions, however, will be characterized by an *effective cross section*

⁽¹²⁾ The effect of departures from equilibrium distribution on reaction rate has been studied qualitatively by Kramers [853]. His conclusion is that this effect should be small.

Zwolinsky and Eyring [1334], considering a simple model of the process of unimolecular decomposition, found that the true rate of reaction is approximately 20% less than the value obtained by assuming an equilibrium distribution.

whose value will depend on the nature of the forces between the molecules and also on the velocities of the colliding particles. The effective cross section for identical molecules may be different depending on the nature of the collision. For example, the cross section for elastic collision of two molecules (i.e. a collision which does not result in change in their internal energy) should in the general case be different from the cross section of a collision leading to chemical conversion. This difference mainly results from the fact that chemical conversions are always connected with inelastic collisions, whose efficiencies depend on the probability of energy redistribution among the various degrees of freedom of the molecules. This should be particularly evident in the case of reactions between complex molecules (see p. 198 *et seq.*).

Let us consider an *elastic collision* of two molecules A_1 and A_2 with velocities v_1 and v_2 . If we introduce the relative velocity $v = v_1 - v_2$, then we may consider that one of the molecules, A_1 say, is stationary and that the other (A_2) moves with a velocity v . We assume that A_1 is at the point O and the A_2 molecule has a velocity directed along the line MN (Fig. 26). We shall denote by q the distance OB by which the A_2 molecule would have passed A_1 were it not for their interaction. This distance q is called the *impact parameter*. In fact A_2 will not move along MN but along a curve shown by the broken line in Fig. 26; the line MN is an asymptote to this

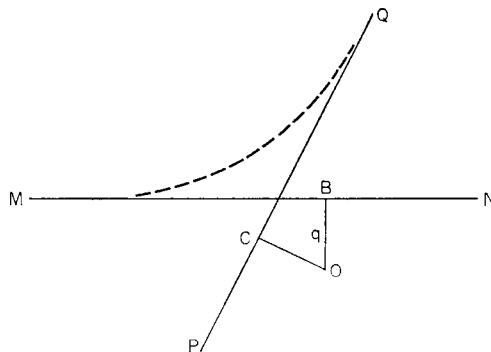


FIG. 26. Trajectory of a molecule colliding with a molecule at rest.

curve. The second asymptote (PQ) to this curve is the same distance from the point O , so that $OC = OB = q$. This follows from the laws of conservation of energy and momentum. In fact, as the collision is elastic, the relative velocity v' after collision (i.e. for sufficiently great separation of A_2 and A_1) is equal in its absolute magnitude to the velocity v before collision. From the law of conservation of momentum

$$\mu v q = \mu v' q'$$

(μ is the reduced mass of A_1 and A_2) and hence $q = q' = OC$.

We shall denote by θ the angle between the two asymptotes which is called the angle of deviation or dispersion. This angle is naturally a function of the impact parameter, determined by the nature of the forces acting between the particles.

Let us consider the plane perpendicular to MN and passing through the point O. We construct a ring with internal radius q and of width dq in this plane. The area of this ring

$$d\sigma = 2\pi q dq \quad (9.1)$$

is called the *differential cross section* of the A_1 molecule with respect to collisions with A_2 for which the angle of dispersion lies in the range θ to $\theta + d\theta$.⁽¹³⁾ When the potential energy of interaction of the particles is known, it is possible to find the function $q = f(\theta)$. Substituting this function in (9.1) we find

$$d\sigma = -2\pi f(\theta) f'(\theta) d\theta.$$

The minus sign is due to the fact that when $d\theta > 0$, $dq < 0$.

The total cross section σ may be defined as the area (πd_0^2) of the minimum circle such that on entering the circle the particle A_2 undergoes an appreciable deviation. In the general case σ may be found by integrating $d\sigma$ with respect to θ from 0 to π :

$$\sigma = -2\pi \int_0^\pi f(\theta) f'(\theta) d\theta = \pi \int_{\pi}^0 d[f(\theta)]^2 = \pi[f^2(0) - f^2(\pi)].$$

A deviation of $\theta = \pi$ is obtained when $q = 0$ (direct impact) and therefore $f^2(\pi) = 0$.

In the case of two solid spheres d_0 is clearly equal to the sum of their radii, $d_0 = r_1 + r_2$, and consequently

$$\sigma = \pi(r_1 + r_2)^2. \quad (9.2)$$

Number of Elastic Collisions in unit time [271, 1223]

Using the concept of the differential cross section it is not difficult to find the number of collisions in unit volume per unit time, leading to deviations of the A_2 molecules by an angle in the range θ to $\theta + d\theta$ if the components of the velocities of the colliding molecules A_1 and A_2 are in the ranges $(\dot{x}_1, \dot{x}_1 + d\dot{x}_1)$, $(\dot{y}_1, \dot{y}_1 + d\dot{y}_1)$, $(\dot{z}_1, \dot{z}_1 + d\dot{z}_1)$ and $(\dot{x}_2, \dot{x}_2 + d\dot{x}_2)$, $(\dot{y}_2, \dot{y}_2 + d\dot{y}_2)$, $(\dot{z}_2, \dot{z}_2 + d\dot{z}_2)$. We shall represent the number of A_1 molecules in unit volume with velocities in the ranges indicated by dn_1 and the corresponding number of A_2 molecules by dn_2 . We clearly find the required

⁽¹³⁾ In the more general case the differential cross section is defined by the expression $d\sigma = q dq d\varphi$, where φ is the angle in the plane mentioned between the direction of q and a certain reference direction.

number of collisions (dZ) if we multiply the number of impacts per second for the area $d\sigma$, which is the differential cross section of the A_1 molecule with respect to the A_2 molecule, by the number of A_1 molecules. Consequently dZ is equal to

$$dZ = dn_2 \cdot v \cdot d\sigma \cdot dn_1,$$

where v is the relative velocity of the A_1 and A_2 molecules, whose absolute velocities lie in the ranges indicated. Assuming a Maxwellian distribution of velocities, we may write

$$dn_1 = n_1 \left(\frac{m_1}{2\pi k T} \right)^{3/2} \exp[-m_1 v_1^2 / 2k T] d\dot{x}_1 d\dot{y}_1 d\dot{z}_1, \quad (9.3)$$

where v_1 is the velocity of the A_1 molecules:

$$v_1 = (\dot{x}_1^2 + \dot{y}_1^2 + \dot{z}_1^2)^{1/2}.$$

A similar expression is found for dn_2 . Consequently, the number of collisions in unit volume per unit time, for which the components of velocity lie in the limits defined above and the angle of deviation within the limits θ and $\theta + d\theta$, is

$$dZ = n_1 n_2 \frac{(m_1 m_2)^{3/2}}{(2\pi k T)^3} \exp[-(m_1 v_1^2 + m_2 v_2^2) / 2k T] d\sigma v d\dot{x}_1 d\dot{y}_1 d\dot{z}_1 d\dot{x}_2 d\dot{y}_2 d\dot{z}_2.$$

We shall determine $d\sigma$ for the case when the A_1 and A_2 molecules are solid spheres with radii r_1 and r_2 respectively. Without diminishing the validity of the argument, the A_2 molecule may be considered as a point and the A_1 molecule as a sphere of radius $d_0 = r_1 + r_2$. We shall represent by α the angle between the initial direction of the velocity of the A_2 molecule and the line joining the centres at the moment of impact (Fig. 27). It is not

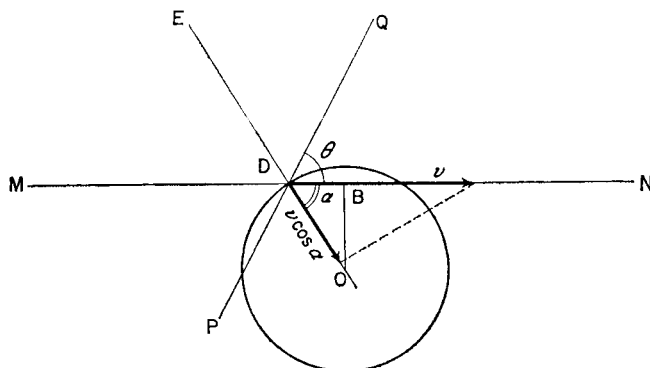


FIG. 27. Collision scheme of two molecules.

difficult to see that as the angle of incidence ($\angle MDE$) is equal to the angle of reflection ($\angle EDQ$), $2\alpha = \pi - \theta$. Therefore in place of the angle θ we shall in future use the angle α . As $OB = q$ in the triangle BOD, we find

$$q = (r_1 + r_2) \sin \alpha = (r_1 + r_2) \cos \frac{\theta}{2}. \quad (9.4)$$

Substituting this expression in (9.1) we obtain

$$d\sigma = 2\pi(r_1 + r_2)^2 \sin \alpha \cos \alpha \, d\alpha. \quad (9.5)$$

Consequently,

$$dZ = n_1 n_2 \frac{(m_1 m_2)^{3/2}}{(2\pi k T)^3} \exp[-(m_1 v_1^2 + m_2 v_2^2)/2kT] \times \\ \times v 2\pi(r_1 + r_2)^2 \sin \alpha \cos \alpha \, d\alpha \, d\dot{x}_1 \dots d\dot{z}_2. \quad (9.6)$$

We shall now determine the total number of collisions in unit volume per unit time. As independent variables we shall introduce the components of the velocity c of the centre of gravity of the two molecules, and the components of their relative velocity v :

$$c_x = \frac{m_1 \dot{x}_1 + m_2 \dot{x}_2}{m_1 + m_2}, \quad c_y = \frac{m_1 \dot{y}_1 + m_2 \dot{y}_2}{m_1 + m_2}, \quad c_z = \frac{m_1 \dot{z}_1 + m_2 \dot{z}_2}{m_1 + m_2}, \quad (9.7)$$

$$v_x = \dot{x}_2 - \dot{x}_1, \quad v_y = \dot{y}_2 - \dot{y}_1, \quad v_z = \dot{z}_2 - \dot{z}_1. \quad (9.8)$$

It is not difficult to show that

$$m_1 v_1^2 + m_2 v_2^2 = (m_1 + m_2) c^2 + \mu v^2; \quad (9.9)$$

$$d\dot{x}_1 d\dot{x}_2 = dc_x dv_x, \quad d\dot{y}_1 d\dot{y}_2 = dc_y dv_y, \quad d\dot{z}_1 d\dot{z}_2 = dc_z dv_z, \quad (9.10)$$

where

$$\mu = \frac{m_1 m_2}{m_1 + m_2} \quad (9.11)$$

is the reduced mass. Substituting (9.9) and (9.10) into (9.6), we find

$$dZ = n_1 n_2 \frac{(m_1 m_2)^{3/2}}{(2\pi k T)^3} 2\pi d_0^2 v \sin \alpha \cos \alpha \times \\ \times \exp[-\{(m_1 + m_2)c^2 + \mu v^2\}/2kT] \, d\alpha \, dc_x \, dc_y \, dc_z \, dv_x \, dv_y \, dv_z. \quad (9.12)$$

We shall integrate this expression with respect to all the velocity components c and v . For this purpose we introduce spherical coordinates in which $dc_x dc_y dc_z = c^2 dc \, d\omega_1$ and $dv_x dv_y dv_z = v^2 dv \, d\omega_2$, where $d\omega_1$ and $d\omega_2$ are elements of the corresponding solid angles. Integration with respect to the latter in the two cases gives factors 4π . Integrating further with respect to all the velocities c of the centre of gravity from zero to

infinity, we find the number of collisions, for which the relative velocity is within the limits v and $v+dv$ and the angle between it and the line of centres is within the limits α and $\alpha+d\alpha$, to be

$$n_1 n_2 \left(\frac{\mu}{2\pi k T} \right)^{3/2} \exp(-\mu v^2/2kT) 8\pi^2 d_0^2 v^3 \sin \alpha \cos \alpha d\alpha dv. \quad (9.13)$$

In order to determine the total number Z of collisions in unit volume per unit time, expression (9.13) should be integrated with respect to α from 0 to $\pi/2$ and with respect to v from 0 to infinity. These calculations lead to the expression:

$$Z = n_1 n_2 d_0^2 \left(\frac{8\pi k T}{\mu} \right)^{1/2}, \quad (9.14)$$

or

$$Z = n_1 n_2 Z_0,$$

where

$$Z_0 = d_0^2 \left(\frac{8\pi k T}{\mu} \right)^{1/2} = \sigma \left(\frac{8kT}{\pi\mu} \right)^{1/2}. \quad (9.15)$$

When the molecules are identical, (9.14) becomes

$$Z = n^{2\frac{1}{2}} d_0^2 \left(\frac{8\pi k T}{\mu} \right)^{1/2}. \quad (9.14a)$$

To estimate the order of magnitude of the number of binary collisions in unit volume per second we shall calculate Z for nitrogen at normal temperature and pressure. The effective cross section of N_2 molecules may be determined, for example from data on viscosity, as $\sigma \approx 7 \times 10^{-16} \text{ cm}^2$. Substituting this figure in (9.14a) and assuming $n = 2.7 \times 10^{19} \text{ cm}^{-3}$, $\mu = 2.4 \times 10^{-23} \text{ g}$, $T = 300^\circ\text{K}$, we find $Z \approx 1.7 \times 10^{28} \text{ cm}^{-3} \text{ sec}^{-1}$.

We shall now calculate the number of collisions for which the energy of relative motion along the line of centres is greater than a certain value ϵ^* .⁽¹⁴⁾ We shall represent by v^* the component of relative velocity $v \cos \alpha$ along the line of centres, which corresponds to this critical energy value (see Fig. 27). We are only interested in collisions for which $v \cos \alpha \geq v^*$.

It is not difficult to see that in accordance with this, expression (9.13) should be integrated with respect to α from 0 to $\text{arc cos}(v^*/v)$, and with respect to v from v^* to infinity. Therefore the number Z^* of collisions (in unit volume per unit time) having an energy of relative motion along the

⁽¹⁴⁾ In future we shall denote by ϵ^* the activation energy calculated per molecule. The sign \neq will be attached also to other quantities referring to the activated state (see §10 and §12).

line of centres which is greater than ϵ^* is equal to

$$Z^* = \int_{v^*}^{\infty} n_1 n_2 \left(\frac{\mu}{2\pi k T} \right)^{3/2} \times \\ \times \exp(-\mu v^2/2kT) 8\pi^2 d_0^2 v^3 dv \int_0^{\arccos v^*/v} \cos \alpha \sin \alpha d\alpha. \quad (9.16)$$

The integral with respect to α is equal to $\frac{1}{2}(1 - v^{*2}/v^2)$. Integrating with respect to v , we find

$$Z^* = n_1 n_2 \left(\frac{8\pi k T}{\mu} \right)^{1/2} d_0^2 \exp(-\mu v^{*2}/2kT), \quad (9.17)$$

or, according to (9.14) and (9.15),

$$Z^* = Z \exp(-\epsilon^*/kT) = n_1 n_2^2 Z_0 \exp(-\epsilon^*/kT), \quad (9.17a)$$

where

$$\epsilon^* = \frac{\mu v^{*2}}{2}.$$

On the basis of (9.17a), the number of collisions in unit volume per unit time for which the energy of relative motion along the line of centres is within the range ϵ and $\epsilon + d\epsilon$, is equal to

$$dZ = Z \exp(-\epsilon/kT) \frac{d\epsilon}{kT}, \quad (Z = Z_0 n_1 n_2). \quad (9.18)$$

Rate of Elementary Bimolecular Reaction

To calculate the rate of an elementary bimolecular reaction it is necessary to start from the number of collisions for which the energy of the system exceeds a certain given value. This is connected with the fact that for a chemical reaction to occur the energy of the colliding molecules should usually exceed a certain minimum value called the activation energy. The occurrence of an activation energy results from the nature of the chemical forces. It is known that a valence-saturated molecule does not usually add on an atom or radical, as when these particles approach there is a repulsion between them.⁽¹⁵⁾ The overcoming of this repulsion is also connected with the need for activating the molecules (see §10 and §11). Besides a sufficiently high energy of the colliding molecules, however, for

⁽¹⁵⁾ Here we are not considering the weak attraction resulting from van der Waals forces at large intermolecular distances, or donor-acceptor interaction between molecules.

reaction to occur there must also be a redistribution of the energy between the various degrees of freedom of the colliding molecules; this is not considered in the calculation of the collision number.⁽¹⁶⁾ We shall denote by P the probability that a collision of this type leads to chemical reaction. In the general case P is a function of the energy of the colliding particles (i.e. of the relative velocity v), of their mutual orientation (the angle α) and of the state of the molecules. Introducing P in the integrated expression (9.16) we have for the rate of a bimolecular reaction

$$w = n_1 n_2 \left(\frac{\mu}{2\pi k T} \right)^{3/2} 8\pi^2 d_0^2 \times$$

$$\times \int_{v^*}^{\infty} \exp(-\mu v^2/2kT) v^3 dv \int_0^{\arccos v^*/v} P \cos \alpha \sin \alpha d\alpha. \quad (9.19)$$

This formula is not of practical interest unless the dependence of P on the velocity, mutual orientation of the molecules, etc., is established. In simple collision theory it is assumed that this quantity is a constant. This means that the probability of energy redistribution between the various degrees of freedom of the molecules, which is necessary for reaction to occur, is taken to be independent of the energy and mutual orientation of the molecules. With this assumption P may be placed outside the integral sign, and (9.19) can then be evaluated. Considering (9.15), by analogy with (9.17) we may write for the rate constant of a bimolecular reaction

$$k = P Z_0 \exp(-\epsilon^*/kT), \quad (9.20)$$

or

$$k = P \sigma \left(\frac{8kT}{\pi\mu} \right)^{1/2} \exp(-\epsilon^*/kT). \quad (9.20a)$$

In this way the gas-kinetic collision theory gives an equation which enables us to calculate the rates of elementary reactions. For this we need to know the activation energy ϵ^* , the cross section σ and the probability factor P .

The activation energy is usually determined from experimental data (for theoretical calculations of activation energy see §10). Its values may be obtained from the experimental temperature dependence of the logarithm of the reaction rate constant. In this case the experimental data, which usually refer to a not very wide temperature range, are in good agreement with the Arrhenius equation

$$k = A \exp(-\epsilon_{\text{exper}}/kT), \quad (9.21)$$

⁽¹⁶⁾ For example, in a reaction of type $A + BC \rightarrow A + B + C$, the translational energy of the A atom is converted into vibrational energy of BC and as a result the BC molecule decomposes into atoms. For other examples see §11.

where A and ϵ_{exper} do not depend on temperature in the chosen range. To introduce ϵ_{exper} and write (9.20a) in the form of the Arrhenius equation it is necessary that, for a temperature T_0 inside the temperature range considered, the rate constants determined from equations (9.20a) and (9.21) should coincide and that the logarithmic derivatives with respect to temperature found from the same equations should also coincide. In other words it is necessary that

$$P\sigma\left(\frac{8kT_0}{\pi\mu}\right)^{1/2} \exp(-\epsilon^*/kT_0) = A \exp(-\epsilon_{\text{exper}}/kT_0)$$

and

$$\left(\frac{d \ln k}{dT}\right)_{T_0} \equiv (\epsilon^* + \frac{1}{2}kT_0)/(kT_0^2) = \epsilon_{\text{exper}}/kT_0^2.$$

It follows that

$$k = P\sigma\left(\frac{8kT_0e}{\pi\mu}\right)^{1/2} \exp(-\epsilon_{\text{exper}}/kT). \quad (9.22)$$

Values of the cross section σ are usually calculated from indirect data on the substances A and B , such as viscosity data. The values of σ found in this way or from other transport phenomena are called the *gas-kinetic cross sections* of the molecules.

The probability factor in the simple gas-kinetic theory cannot be calculated. If it is taken as equal to unity then it would be expected that the calculated rate constant would be greater than the experimental value, since the probability of energy transfer from one degree of freedom to another is always less than unity. Comparisons with experimental data support this. For some gas reactions the rate constants calculated from (9.22) assuming $P = 1$ are not very different from the experimental values. For example, Kistiakowsky's data [836] show that the rate constant of the reaction $\text{HI} + \text{HI} \rightarrow \text{H}_2 + \text{I}_2$ near 600°K may be expressed by the equation

$$k = 5.1 \times 10^{-10} \exp(-45900/RT) \text{ cm}^3 \text{molecule}^{-1} \text{sec}^{-1}.$$

If the collision diameter of HI molecules is taken as $3.2 \times 10^{-8} \text{ cm}$ (from viscosity data [255]) then $\sigma = 3.6 \times 10^{-15} \text{ cm}^2$ and by substituting this value and $P = 1$ in equation (9.22) we obtain a pre-exponential factor of $\sim 21 \times 10^{-10}$; this is only four times greater than the experimental value. Much the same results are obtained using equation (9.22) and $P = 1$ for certain other bimolecular reactions (see Chap. 4). In most cases, however, this equation (when $P = 1$) gives rate constants much greater than the actual values. For many reactions this difference is two, three or more powers of ten.

Differences of this type may be considered as an indication that an important part in the elementary reaction is played by energy redistribution

between the various degrees of freedom, and that this process is of low probability. Consequently the probability factor (also called the "steric" factor) P is less than unity in practice and allowance for this fact must always be made. Calculation of P , however, is only possible using the transition-state method (see §12).

Allowance for internal degrees of freedom [271]. So far we have not considered internal degrees of freedom of the colliding molecules. There is no doubt, however, that internal degrees of freedom make a definite contribution to the activation of molecules. For this reason attempts have been made to allow for internal degrees of freedom in the gas-kinetic collision theory. It is of primary interest to determine the number (Z') of collisions in unit time for which the sum of the energy of relative translational motion along the line of centres and the energy of the internal degrees of freedom (vibrational and rotational) is greater than a certain fixed value.

Vibrational degrees of freedom are easily allowed for if each of them is considered as a classical oscillator, i.e. it is considered that the quantum $h\nu$ of vibrational energy is much less than kT [271]. This assumption is a rather rough approximation and often untrue.⁽¹⁷⁾ On the other hand, for rotational degrees of freedom this condition usually holds as an adequate approximation. In future in this section we shall consider in particular vibrational degrees of freedom, although all the formulae obtained (9.24) to (9.32) also refer to rotational degrees of freedom.

When $h\nu \ll kT$ the probability that the energy of the i th oscillator is equal to or greater than a certain fixed value $\epsilon_i = n_i h\nu$ (n_i is the number of quanta) is proportional to $\exp(-\epsilon_i/kT)$. Consequently the probability that the energy of the i th oscillator is between ϵ_i and $\epsilon_i + d\epsilon_i$ is proportional to

$$\exp(-\epsilon_i/kT) \frac{d\epsilon_i}{kT}.$$

Hence the probability that the total energy

$$\epsilon = \sum_1^s \epsilon_i$$

of a system of s oscillators (in the general case a system having s internal degrees of freedom) is in the range $(\epsilon, \epsilon + d\epsilon)$, is equal to

$$C \int_{s-1} \dots \int \exp(-\epsilon/kT) d\epsilon_1 d\epsilon_2 \dots d\epsilon_s,$$

where C is a coefficient of proportionality. Here the integration should be

⁽¹⁷⁾ For a calculation, on the basis of quantum theory, of the case $h\nu \geq kT$ in the thermal decomposition of diatomic molecules see §16.

carried out with respect to $s-1$ degrees of freedom with

$$\epsilon = \sum_1^s \epsilon_i.$$

The factor C may be determined from the condition that the integral with respect to all the degrees of freedom is unity; this gives

$$C^{-1} = \int_s \dots \int \exp(-\epsilon/kT) d\epsilon_1 d\epsilon_2 \dots d\epsilon_s, \quad (\epsilon = \sum_1^s \epsilon_i). \quad (9.23)$$

Therefore the probability that s vibrations have a total energy between ϵ and $\epsilon + d\epsilon$ is

$$\frac{\int_{\epsilon-1}^{\epsilon} \dots \int \exp(-\epsilon/kT) d\epsilon_1 \dots d\epsilon_s}{\int_s \dots \int \exp(-\epsilon/kT) d\epsilon_1 \dots d\epsilon_s}, \quad (\epsilon = \sum_1^s \epsilon_i). \quad (9.24)$$

On substituting

$$\epsilon_1 = a_1^2 \epsilon, \quad \epsilon_2 = a_2^2 \epsilon, \dots, \quad \epsilon_s = a_s^2 \epsilon,$$

the condition

$$\sum_1^s \epsilon_i = \epsilon \quad \text{gives} \quad \sum_1^s a_i^2 = 1.$$

Expressing the product $d\epsilon_1 d\epsilon_2 d\epsilon_3 \dots d\epsilon_s$ in terms of the new variables ϵ and a_i ($i = 1, 2, \dots, s-1$) and cancelling the common factor in the numerator and denominator of (9.24) we obtain for the required probability [271]

$$\begin{aligned} & [\exp(-\epsilon/kT) \epsilon^{s-1} d\epsilon] / \left[\int_0^\infty \exp(-\epsilon/kT) \epsilon^{s-1} d\epsilon \right] \\ &= \frac{1}{(s-1)!} \left(\frac{\epsilon}{kT} \right)^{s-1} \exp(-\epsilon/kT) \frac{d\epsilon}{kT}. \end{aligned} \quad (9.25)$$

We now find the number of collisions in unit volume per unit time for which the kinetic energy of relative motion along the line of centres is between ϵ_{kin} and $\epsilon_{\text{kin}} + d\epsilon_{\text{kin}}$, and the energy of s definite vibrations, for one or both molecules, is between ϵ_{vib} and $\epsilon_{\text{vib}} + d\epsilon_{\text{vib}}$. Expression (9.18) is multiplied by the probability (9.25) that the energy of the s vibrations is

between ϵ_{vib} and $\epsilon_{\text{vib}} + d\epsilon_{\text{vib}}$ and we obtain for the required collision number

$$Z \exp(-\epsilon_{\text{kin}}/kT) \frac{d\epsilon_{\text{kin}}}{kT} \frac{1}{(s-1)!} \left(\frac{\epsilon_{\text{vib}}}{kT}\right)^{s-1} \exp(-\epsilon_{\text{vib}}/kT) \frac{d\epsilon_{\text{vib}}}{kT}. \quad (9.26)$$

Using the variables $\epsilon = \epsilon_{\text{kin}} + \epsilon_{\text{vib}}$ and ϵ_{vib} and integrating (9.26) with respect to ϵ_{vib} from 0 to ϵ , we find

$$Z \exp(-\epsilon/kT) \frac{1}{s!} \left(\frac{\epsilon}{kT}\right)^s \frac{d\epsilon}{kT}.$$

Then the number (Z') of collisions, in which the sum of the kinetic energy of relative motion along the line of centres and of the energy of the s vibrations is greater than the fixed value ϵ^* , is

$$\begin{aligned} Z' &= \int_{\epsilon^*}^{\infty} Z \exp(-\epsilon/kT) \frac{1}{s!} \left(\frac{\epsilon}{kT}\right)^s \frac{d\epsilon}{kT} \\ &= Z \exp(-\epsilon^*/kT) \sum_{\nu=1}^s \frac{1}{\nu!} \left(\frac{\epsilon^*}{kT}\right)^{\nu}. \end{aligned} \quad (9.27)$$

If the energy ϵ^* is sufficiently large, i.e. if $\epsilon^* \gg kT s$, then on the right-hand side of this equation only the last term is important and instead of (9.27) we may write

$$Z' = Z \exp(-\epsilon^*/kT) \frac{1}{s!} \left(\frac{\epsilon^*}{kT}\right)^s. \quad (9.27a)$$

Therefore the number of collisions in which the energy sum is as stipulated above may be much greater than the number of collisions as determined by expression (9.17a).⁽¹⁸⁾ For example, when $s = 3$ and $\epsilon^* = 20$ kcal, at 300°K we find

$$\frac{1}{s!} \left(\frac{\epsilon^*}{kT}\right)^s \approx 6 \times 10^3. \quad (9.28)$$

This quantity rapidly increases with s and ϵ^* .

In order to determine the rate of a bimolecular reaction it is necessary to know the probability that for a given collision a suitable redistribution of energy between the degrees of freedom takes place resulting in reaction. It is clear that this probability (P) is a function of the total energy ϵ of the

⁽¹⁸⁾ Compare with formula (16.7) which was obtained on the basis of quantum considerations.

molecules and of the energy ϵ_{vib} of their internal degrees of freedom. Strictly speaking, P is also a function of the structure and mutual orientation of the molecules; but in order to simplify calculation (as earlier) we shall consider that the two colliding molecules have spherical symmetry and therefore this dependence does not occur. Multiplying expression (9.26) by $P(\epsilon, \epsilon_{\text{vib}})$ we obtain an equation for the reaction rate which is analogous to (9.19)

$$w = \frac{Z}{(s-1)!} \int_{\epsilon \neq \epsilon_{\text{vib}}}^{\infty} \exp(-\epsilon/kT) \frac{d\epsilon}{kT} \int_0^{\epsilon} P(\epsilon, \epsilon_{\text{vib}}) \left(\frac{\epsilon_{\text{vib}}}{kT} \right)^{s-1} \frac{d\epsilon_{\text{vib}}}{kT}. \quad (9.29)$$

Again, as when we were considering only energy of relative motion (equation (9.19)), the gas-kinetic theory does not yield an exact expression for the function $P(\epsilon, \epsilon_{\text{vib}})$. In evaluating formula (9.29), therefore, we must confine ourselves to certain particular assumptions with regard to P .

We shall first assume that the probability factor P is independent of the energy of the colliding molecules. This means, for instance, that molecules in the ground vibrational state may react with the same probability as vibrationally-excited molecules; strictly speaking this does not occur in practice. Setting P outside the integral signs in (9.29) we may write by analogy with (9.27)

$$w = PZ \exp(-\epsilon^*/kT) \sum_{j=1}^s \frac{1}{j!} \left(\frac{\epsilon^*}{kT} \right)^j. \quad (9.30a)$$

When $\epsilon^* \gg skT$ this formula takes the form

$$k = PZ_0 \exp(-\epsilon^*/kT) \frac{1}{s!} \left(\frac{\epsilon^*}{kT} \right)^s. \quad (9.30b)$$

If now we introduce the experimental activation energy $E_{\text{exper}} = N_A \epsilon_{\text{exper}}$, then, analogous to (9.22), we find

$$k = \frac{PZ_0}{s!} \left[\frac{E_{\text{exper}} + (s - \frac{1}{2})RT}{RT} \right]^s \exp \left[\frac{1}{2} - \frac{E_{\text{exper}}}{RT} \right]. \quad (9.30c)$$

The practical application of this formula is made difficult by the fact that two parameters in it— P and s —are unknown. If, after Pritchard [1048], we assume $P \approx 1$, then for certain reactions it is possible by varying s over a wide range to obtain approximately correct values for the pre-exponential factor. For example, in the reactions of methane and isobutane with halogen atoms (chlorine and bromine) Pritchard obtains agreement with experiment by assuming in the first case $s = 3$ and in the second, $s = 10$. However, results of this type, based on a somewhat

arbitrary choice of the two parameters (P and s), can scarcely be regarded as significant.⁽¹⁹⁾

§10. Potential Energy of a System of Atoms

Potential-Energy Surfaces

We have considered above the gas-kinetic collision theory, in which the intermolecular forces acting between reacting molecules are not in fact allowed for. The initial stage of a more complete theory of elementary chemical processes consists in solving the problem of the dependence of the potential energy of the colliding molecules on the coordinates of all their component atoms. For example, in the case of reactions of a diatomic molecule AB with an atom C it is necessary to know the energy of the system A + B + C for any relative positions of the three atoms. In the general case this problem must be solved not only for the ground state but also for excited electronic states. If the total number of atoms in the system is N then the potential energy ϵ of their interaction will depend on $3N-6$ coordinates of the atoms (in the case of a linear system on $3N-5$ coordinates) which we shall represent by the letters $X_1, X_2, \dots, X_{3N-6}$. The problem, therefore, consists in finding the function

$$\epsilon = \epsilon(X_1, X_2, \dots, X_{3N-6}) \quad (10.1)$$

for each of the electronic states of interest in the system. From a geometrical point of view this equation represents the equation of a multidimensional surface. For this reason we frequently talk about *potential-energy surfaces*, having (10.1) in mind.

When the system consists of atoms able to interact chemically, a general feature of the potential-energy surfaces is that they contain potential wells corresponding to the formation of chemical bonds and separated from one another by more or less high barriers.

Solving the quantum-mechanical problem of determining the function (10.1) involves serious mathematical difficulties and has only been accomplished for systems of three and four hydrogen atoms. In spite of the approximate character of this solution it makes it possible to compose a general qualitative picture of the motion of atoms in the potential field ϵ and of the "mechanism" of energy transfer and conversion during collision of three atoms, and to determine which configuration of the system is energetically most favourable for reaction to occur. These qualitative conclusions were first made on the basis of London's formula [885] (formula (10.2)) using the so-called semi-empirical method (see below) for a system of three hydrogen atoms; these have subsequently been in effect confirmed

⁽¹⁹⁾ Kassel [106] used the expression $P = \alpha(\epsilon - \epsilon^*)^n/\epsilon^s$. However, as there are no grounds for this assumption, not much importance should be attached to the result obtained by Kassel.

by more precise calculations [1263, 701, 702]. For other atoms these precise calculations have not been made, and consequently the only information regarding their potential-energy surfaces has been obtained by using the semi-empirical method.

According to London [885], the energy of the ground state of a system of three hydrogen atoms is

$$\epsilon = A_1 + B_1 + C_1 - \{ \frac{1}{2} [(\alpha_1 - \beta_1)^2 + (\beta_1 - \gamma_1)^2 + (\gamma_1 - \alpha_1)^2] \}^{1/2}, \quad (10.2)$$

where A_1 , B_1 , and C_1 are the so-called coulombic integrals and α_1 , β_1 and γ_1 are the exchange integrals (Fig. 28). As these quantities depend on the three internuclear distances X_{AB} , X_{BC} and X_{AC} , expression (10.2) is an

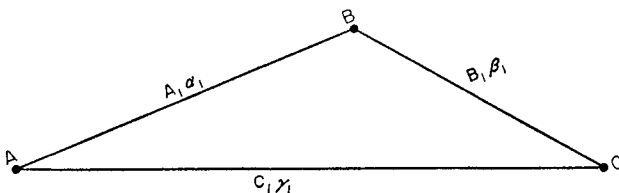


FIG. 28. Coulombic and exchange integrals in a system of three atoms.

approximate formula for the potential-energy surface (10.1) in the case of three H atoms. In order to simplify the calculation of ϵ as a function of the interatomic distances we shall use the approximation method of Eyring and Polanyi [591]. Using the Heitler-London method [741, 304] the energy of interaction of two hydrogen atoms may be represented in the approximate form:

$$\epsilon_{H_2} = A_1 + \alpha_1. \quad (10.3)$$

Alternatively, this energy may be expressed by a Morse function

$$\epsilon_{H_2} = D \{ \exp[-2a(X - X_0)] - 2 \exp[-a(X - X_0)] \}, \quad (10.4)$$

in which the constants D , a and X_0 are known from spectroscopic data. In order to use this function to calculate ϵ (10.2), Eyring and Polanyi assumed that the coulombic integral A_1 for all X_{AB} distances is a definite constant fraction n of the total energy of the bond. Assuming, therefore,

$$A_1 = n\epsilon_{H_2}, \quad \alpha_1 = (1-n)\epsilon_{H_2}, \quad (10.5)$$

we may use (10.4) to calculate these integrals for any interatomic distance. The same procedure may be applied to B_1 , C_1 , β_1 and γ_1 . It is not difficult to find from the results of Sugiura's calculations [1194] that near the equilibrium position of H_2 the number n is 0.12 to 0.14 [57]. If the values of the coulombic and exchange integrals found in this way are substituted in (10.2) we may calculate ϵ for any configuration of the hydrogen atoms.

This method of calculating a potential surface is called the *semi-empirical method* of Eyring and Polanyi.

Figure 29 shows the potential-energy surface for three atoms, A, B and C, in the particular case when the angle ABC is fixed, for example at 180° (Fig. 30). For this configuration the energy ϵ is a function of only two independent coordinates, such as X_{AB} and X_{BC} . The continuous curves

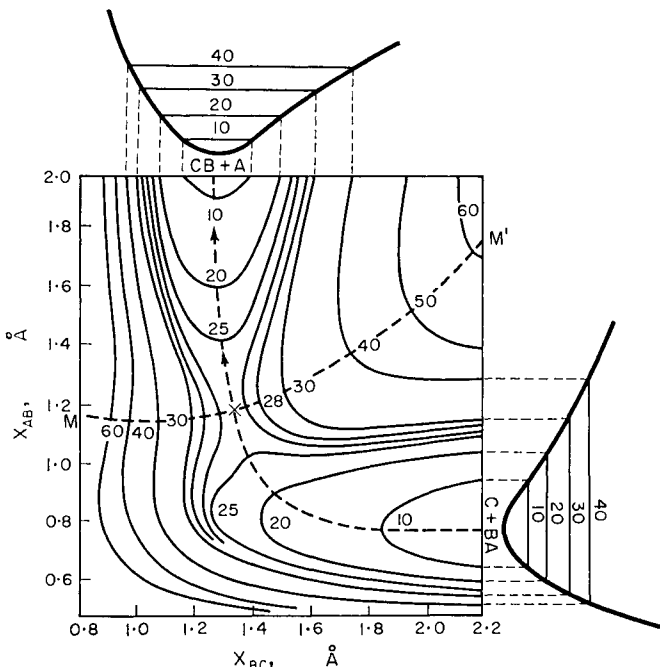


FIG. 29. Potential-energy surface for a three-atom system. The figures refer to levels of equal energy (in kcal).

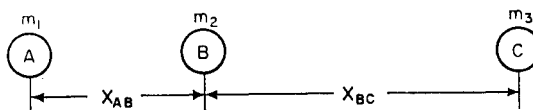


FIG. 30. Linear disposition of three atoms.

in Fig. 29 are lines of equal potential energy. The surface has two valleys separated by a pass, the top of which is the saddle point. The lower right-hand portion of the surface corresponds to the state where the atom C is far away from the molecule AB and there is no interaction between them. A section through the surface perpendicular to the abscissa axis ($X_{BC} = \text{const.}$) represents the usual potential curve of the diatomic molecule AB (shown to the right of Fig. 29). The upper left corner of the surface

corresponds to the state $A + BC$ and a section through the surface represents the potential curve of the molecule BC . The upper right corner corresponds to the state where all three atoms are far from one another (no interaction).

It is seen from Fig. 29 that when the atom C approaches the molecule AB (or the atom A approaches the molecule BC) the energy of the system increases. When X_{AB} remains constant and is not much greater than the equilibrium distance, the energy increases monotonically as X_{BC} changes. When X_{AB} is initially large the energy for constant X_{BC} varies similarly. When C approaches simultaneously with increase in the distance X_{AB} , the energy undergoes a certain increase and then begins to fall, corresponding to the occurrence of the exchange reaction



The reaction path requiring the least energy is indicated by the broken line in Fig. 29. This path passes through the saddle point (the cross in Fig. 29) which corresponds to the state of the system called the *activated* or *transition state*. The curve MM' which passes through the saddle point normal to the reaction coordinate and to the equipotential lines we call the *main diagonal*. The difference in the energies corresponding to the saddle point and the initial state of the system clearly represents the least energy required for reaction to occur, and consequently this difference is equal to the activation energy of the reaction.⁽²⁰⁾

If a section is made through the potential surface along the reaction path and the section is then drawn in one plane, we obtain a curve (*the profile of the reaction path*) as shown in Fig. 31. The so-called *reaction coordinate* is plotted as the abscissa and characterizes the degree of advancement of the system along the path of the reaction.

In the general case when the atoms A , B and C are different the reaction will be accompanied by energy liberation or absorption. Accordingly the initial and final levels of the profile of the reaction path will be at different heights. To emphasize the stable character of the initial and final states of a system the variation of potential energy during the course of a reaction is sometimes conventionally represented as shown in Fig. 32. The top of the potential barrier corresponds to the activated state in which the system is unstable. It is clear that the activated state will be the same for both forward (10.6) and reverse processes.

If the atoms obeyed perfectly the laws of classical physics then the activation energy of the elementary reaction would be given by the distance from the initial minimum of the potential curve to the top of the barrier

⁽²⁰⁾ Here we are concerned with the so-called classical activation energy (see below). The true activation energy at the absolute zero of temperature differs from the classical by the difference in zero-point energies of the activated and initial states (see Fig. 32).

(Fig. 32). This distance, marked E_{cl} in Figs. 31 and 32, is called the "classical" activation energy. In fact any atomic system capable of vibrating about an equilibrium position has a so-called *zero-point energy*; the energy of a system can in no circumstances fall below this value. Therefore the activation energy at the absolute zero of temperature should be given by

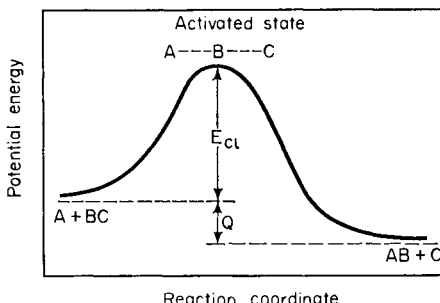


FIG. 31. Variation of energy during the course of the reaction $A + BC \rightarrow AB + C$ (the profile of the reaction path).

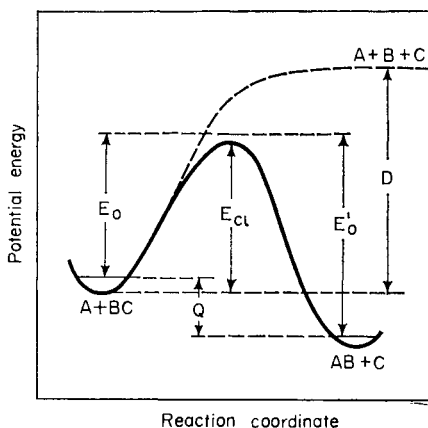


FIG. 32. Classical (E_{cl}) and true (E_0) activation energies of the reaction $A + BC \rightarrow AB + C$. The activation energy of the reverse (endothermic) reaction is equal to $E'_0 = E_0 + Q$.

the distance from the *zeroth* level of the initial state to the *zeroth* level of the activated complex (Fig. 32). For a diatomic system with one vibrational degree of freedom the zero-point energy is equal to $\frac{1}{2}h\nu$, where ν is the natural vibrational frequency. For a polyatomic system the zero-point energy is equal to the sum of these terms with respect to all the vibrational degrees of freedom. Bearing this in mind it is not difficult to see that the activation energy E_0 ($= N_A \epsilon^*$) corresponding to the absolute zero of

temperature is related to E_{cl} in the following way:

$$E_0 = E_{\text{cl}} - [\frac{1}{2} \sum h\nu - \frac{1}{2} \sum h\nu^*] N_A, \quad (10.7)$$

where the summation is over all vibrational degrees of freedom of the initial state (frequencies ν) and of the activated state (frequencies ν^*).⁽²¹⁾

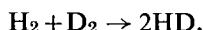
When the atoms involved in reaction (10.6) are identical the potential-energy surfaces will be completely symmetrical with respect to the main diagonal, which in this case will be represented by a straight line passing through the origin of the coordinates. In the case of three hydrogen atoms on a straight line the potential-energy surface is as shown in Fig. 40 (p. 172). In certain cases the potential-energy surface may have a basin (depression) in the region corresponding to the close approach of three atoms.⁽²²⁾ In this case the reaction coordinate will go through two barriers.

For the reaction involving three H atoms the most energetically favourable configuration of the activated complex is that in which the three atoms are collinear (see below). The problem of which configuration of the complex is most energetically favourable when many-electron atoms are involved in the reaction has not yet been finally solved as the calculations have only been made using the semi-empirical method [898].

An even more complex case is given by the exchange reaction involving four atoms



such as the reaction⁽²³⁾



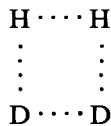
Graphical construction of the potential-energy surface as a function of the interatomic distances is made difficult in this case by the fact that there are always more than two coordinates varying in the course of the reaction. On the basis of London's equation, however, it is not difficult to see that, as in the case of three atoms, the potential surface has a barrier separating the initial and final states and as a rule there is a path for the reaction which requires the least energy consumption. In the case of the reaction of hydrogen (or deuterium) molecules it seems that of all the activated complex configurations which in principle may secure the exchange reaction in

(21) For a system of N atoms the number of vibrational degrees of freedom is equal to $3N - 6$ (in the case of a linear system, $3N - 5$). For the activated complex this number is one less, as one of the vibrational degrees of freedom is converted into the reaction coordinate (for more details see §11).

(22) There does not seem to be a depression of this type on the potential-energy surface of the H_3 system. See footnote⁽³⁶⁾ (p. 172).

(23) We have taken D_2 , and not H_2 , as the second molecule in order to show directly the nature of the reaction. The potential-energy surface does not, of course, depend on the isotopic composition of the system.

one act, the lowest energy corresponds to the rectangle [584]



Numerical Calculations of Activation Energy

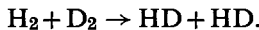
The semi-empirical method is approximate in nature and is therefore not suitable for quantitative calculations of activation energy. Indeed, besides the assumptions made in London's equation [885, 584] this method involves a series of other unjustifiable assumptions. For example, it is not valid to assume that the fraction n , which represents the coulombic integral in the total energy of the bond, is the same for all interatomic distances. In fact the exchange integral varies with interatomic distance much more rapidly than the coulombic integral. When the semi-empirical method is applied to reactions involving atoms with p -electrons, the choice of n is quite arbitrary. Thus, calculation of the interaction of two atoms with p -electrons (with the cloud axes along the length of the bond) shows that here the coulombic integral may even be greater numerically than the exchange integral; in the semi-empirical method it is arbitrarily assumed that $n \approx 0.14$ to 0.20 .

These and other inadequacies mean that the semi-empirical method is of value only for obtaining certain qualitative conclusions.

Use of the London formula enables us to make an approximate relative estimate of the activation energies of various elementary reactions involving hydrogen or deuterium atoms, such as



and



We assume first that the activated complex for the first of these reactions is linear. For simplicity we shall only consider those configurations where $X_{AB} = X_{BC}$, i.e. we shall only calculate the energy for points on the main diagonal OM (see Fig. 40). The activated state will clearly correspond to the lowest value of ϵ found in this way. For the above condition we have $\alpha_1 = \beta_1$ and $A_1 = B_1$, and in accordance with this we find from (10.2)

$$\epsilon = 2A_1 + C_1 + \alpha_1 - \gamma_1.$$

When $X_{BC} = \infty$ and $X_{AB} = X_{AB}^0$, where X_{AB}^0 is the equilibrium interatomic distance in the isolated AB molecule, we have $\epsilon_0 = A_1^0 + \alpha_1^0$, and therefore the activation energy is found to be⁽²⁴⁾

$$\epsilon^* \equiv \epsilon - \epsilon_0 = (A_1 - A_1^0) + (\alpha_1 - \alpha_1^0) + A_1 + C_1 - \gamma_1, \quad (10.9)$$

⁽²⁴⁾ In equation (10.9) and in subsequent formulae in this section we are considering the classical activation energy.

where the values of A_1 , C_1 , α_1 and γ_1 correspond to the point where the energy is a minimum on the line OM.

Formula (10.9) holds not only for a linear arrangement but also for any other disposition of the atoms (with the condition that $X_{AB} = X_{BC}$), such as when they are at the corners of a right-angled triangle (Fig. 33a). It is not difficult to see that in this case the integrals in (10.9) do not vary with the exception of C_1 and γ_1 , which increase in absolute magnitude owing to decrease in the X_{AC} distance. For hydrogen the exchange integral is much greater than the coulombic integral and consequently the main effect on ϵ^* will be given by the γ_1 integral, an increase in the absolute magnitude of which, according to (10.9), implies an increase in the activation energy. The semi-empirical method gives the following results. For the H_2 molecule it is necessary to assume $D = 108.5$ kcal and $a = 1.94 \text{ \AA}^{-1}$ in (10.4). Assuming that $n = 0.14$, calculation gives $X_{AB} = X_{BC} = 0.78 \text{ \AA}$ for the saddle point. Then for a linear model, considering that $X_{AB}^0 = X_{BC}^0 = 0.73 \text{ \AA}$, we find from (10.4) and formulae similar to (10.5) that $C_1 \approx -6$ kcal and $\gamma_1 \approx -34$ kcal, and for the right-angled model $C_1 \approx -11$ kcal and $\gamma_1 \approx -69$ kcal. Using these figures we find from (10.9) that the activation energy increases by approximately 30 kcal on passing from the first to the second model.

It may be said, therefore, that the activation energy for the triangular configuration of the transition (activated) complex $H.H.D$ is higher than that for the linear configuration, as the repulsion between the outer atoms in the first case is much greater than in the second case.

We shall now make a relative estimate of the activation energy for the reaction between H_2 and D_2 molecules. In the case of four H atoms the London equation has the form [57]:

$$\epsilon = Q - \left\{ \frac{1}{2} [(\alpha - \beta)^2 + (\beta - \gamma)^2 + (\gamma - \alpha)^2] \right\}^{1/2}, \quad (10.10)$$

where

$$Q = A_1 + A_2 + B_1 + B_2 + C_1 + C_2,$$

$$\alpha = \alpha_1 + \alpha_2, \quad \beta = \beta_1 + \beta_2, \quad \gamma = \gamma_1 + \gamma_2,$$

(Fig. 33b). We assume that the activated complex has a square configuration, so that

$$A_1 = A_2 = B_1 = B_2, \quad C_1 = C_2, \quad \alpha_1 = \alpha_2 = \beta_1 = \beta_2, \quad \gamma_1 = \gamma_2.$$

Consequently,

$$\epsilon = 4A_1 + 2C_1 + 2\alpha_1 - 2\gamma_1.$$

As the energy of the initial state is $2\epsilon_0 = 2A_1^0 + 2\alpha_1^0$, we find for the activation energy of the $H_2 + D_2 \rightarrow 2HD$ reaction

$$\epsilon^* = 2(A_1 - A_1^0) + 2(\alpha_1 - \alpha_1^0) + 2A_1 + 2C_1 - 2\gamma_1, \quad (10.11)$$

where the values of the integrals A_1 , C_1 , α_1 , and γ_1 are chosen for the point corresponding to the energy minimum, where

$$X_{AB} = X_{BC} = X_{CD} = X_{AD}.$$

Use of the semi-empirical method shows that this point corresponds to approximately the same interatomic distances as in the case of the right-angled arrangement of three atoms. Consequently, the values of all the integrals for the square complex of four atoms and the right-angled complex of three atoms are the same. From comparison of (10.9) and (10.11) we may conclude that the activation energy of the molecular reaction $H_2 + D_2$ is twice as large as that of the $H_2 + D$ reaction which

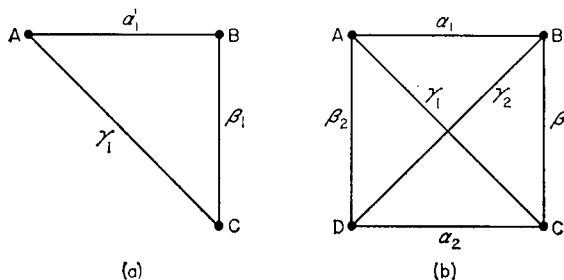


FIG. 33. Activated complex scheme: a—three atoms at the corners of a right-angled isosceles triangle, b—four atoms at the corners of a square.

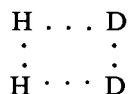
has a right-angled configuration of its transition complex. The energy of the linear complex $H.H.D$, as we have seen, is about 30 kcal below that of the right-angled complex. It follows that the activation energy (10.11) of the molecular reaction $H_2 + D_2$ is greater than the actual activation energy of the $H_2 + D$ reaction, not by a factor of two, but by a much larger factor. Calculation of the latter using the semi-empirical method and assuming $n = 0.14$ as before yields a value of 14 kcal [57]. Hence for the activation energy of the $H_2 + D_2$ reaction we find $\epsilon^* \simeq (14 + 30)2 = 88$ kcal (see also [57]). This fact may be used to explain the much greater prevalence of radical reactions compared with molecular reactions.

Our conclusions using the very approximate equation of London are supported by more precise calculations of the 3H and 4H systems using the method of electron pairs and the molecular orbital method. It has been shown [1263, 1143, 703] that if the energy of the $H.H.D$ [1263] and H_2 [1143] systems are calculated to the same approximation, using the method of molecular orbitals allowing for the wave functions being anti-symmetrical and for the so-called configuration interaction,⁽²⁵⁾ then the

⁽²⁵⁾ Allowance for "configuration interaction" is calculation of the energy of a system with a higher degree of approximation, where the wave function of many electrons is in the form of a linear combination of first-approximation wave functions which correspond to the different electronic states in the system.

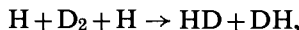
activation energy of the $H_2 + D$ reaction is obtained as 8.76 kcal [703], which is close to the experimental value of 7.7 kcal. In contrast, the activation energy of the reaction of two molecules, $H_2 + D_2$, is found to be greater than 100 kcal using the same method for a square model of the H.H.D.D complex.⁽²⁶⁾ This large increase in activation energy on passing from three to four atoms may be explained by the considerable increase in nuclear and electronic repulsions on passing from the linear to the square configuration, for which the atoms are closer to one another on average. This interpretation agrees in its essentials with the above explanation based on the London equation.

In most stable molecules the lowest state is the singlet, corresponding to a resultant spin of zero (certain molecules such as O_2 are exceptions). The molecular orbital calculation for the $H_2 + D_2$ system [701, 702] leads to the conclusion that in the complex

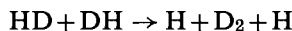


the singlet state is *higher* than the triplet. It is possible that this term sequence also holds for complexes of the type ABC which have a rectangular configuration and are the activated complexes of appropriate reactions (see §13).

It should be noted that according to quantum-mechanical calculations the reaction



which goes through the linear complex $H \dots D \dots D \dots H$, has rather a low activation energy (much lower than that for the square complex) which is comparable with the activation energy of the reaction $H_2 + D \rightarrow H + HD$. This result is also obtained both by using the London equation (see [241], appendix 1) and more precise calculations [704, 345]. It follows that the activation energy of the reverse reaction



is mainly due to the endothermicity of the process. As was suggested by Semenov [241], this type of reaction between molecules leading to formation of two atoms or radicals may, in certain cases, play a part in forming active centres in chain reactions (see §35).

In concluding this section we should mention that both the London equation and the semi-empirical method are suitable for making approximate relative estimates of activation energy, but only, it seems, if we are

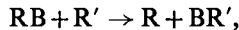
⁽²⁶⁾ See [701, 702]. In these articles the authors only estimate the effect of the interaction of certain configurations; they obtain the activation energy of the $H_2 + D_2$ reaction as about 170 kcal. A more complete allowance for the interaction of configurations should lower this value somewhat but probably by no more than 50 to 70 kcal.

concerned with the interaction of atoms with one valence *s*-electron. If the elementary process is assumed to involve electrons in *p*-orbitals or, especially, in hybridized orbitals⁽²⁷⁾ then part of the activation energy may result from the need to change the character of the hybridization. For example, the exothermic hydrogenation of ethylene possibly requires a certain expenditure of energy in changing the valence state of the carbon atoms (the transition from the trigonal to the tetrahedral configuration). In certain cases the presence of unshared electron pairs in the outer shell of a molecule may also have an effect on the activation energy. For example, in the reaction $\text{HCl} + \text{D} \rightarrow \text{H} + \text{ClD}$ the unshared *p*-electrons of the chlorine atom should play an important part in the atom-molecule interaction. According to the calculations of Magee [898], the semi-empirical method shows that the activated complex $\text{H} \dots \text{Cl} \dots \text{D}$ has a triangular structure.

None of these problems, however, has found a strict quantum-mechanical solution. The quantitative and even semiquantitative calculation of the activation energy of elementary chemical reactions involves serious mathematical difficulties which may possibly be overcome only by the extensive use of electronic calculating machines.

Relation between Activation Energy and Heat of Reaction [248]

Let us consider an adiabatic exchange reaction of type



where B is an atom and R and R' are atoms or radicals. It has been established empirically [989, 540, 580, 779, 579, 717, 374, 21, 266, 43, 57, 241] that for a series of reactions in which either R or R' is varied there is a simple linear relation between the activation energy (ϵ^*) and the heat of reaction (q).⁽²⁸⁾ For the exothermic direction this relation may be written in the form

$$\epsilon^* = a - bq, \quad (10.12)$$

where a and b are constants and $0 < b < 1$. We shall show that with certain assumptions this relation may be obtained theoretically.⁽²⁹⁾

⁽²⁷⁾ A hybridized atomic orbital is an atomic wave function constructed in the form of a linear combination of *s*-, *p*- or *d*-orbitals. The electronic distribution corresponding to it differs from the distribution of electrons in the isolated atoms (see, for example, [56]).

⁽²⁸⁾ We shall represent the heat of reaction per molecule by q .

⁽²⁹⁾ This relation has been analysed in most detail by Evans and Polanyi [581] but their argument is open to criticism. In order to obtain (10.12) these authors postulated that the heat of reaction and activation energy depend linearly on a certain parameter χ . The significance of this parameter should be understood as reflecting the nature of the molecular interaction in a series of reactions as a function of the structural characteristics of the reagents. It is extremely doubtful, however, whether in the general case we

To be specific let us assume that in the series of reactions under consideration R varies and R' remains the same. Similar arguments may be applied to the reverse case and also to the case where the atom B varies.

We shall choose a certain substituent R_0 as a standard and assume that the change in potential energy of the system $R.B.R'$ when R_0 is replaced by R is determined by the change in a parameter χ whose size depends on the nature of R . The physical significance of this parameter may vary and will not matter in the discussion. For example, it may be the effective charge (in the formula for the wave function) acting on the outer electrons of the atom or radical R , or it may be the potential of the outer electrons of the atom or radical R , or it may be the potential of the electric field near R , and so on. When replacing one R by another in the general case it is clear that the depth of the potential wells and the height of the potential barrier and the corresponding interatomic distances also change. It will be seen below, however, that to a first approximation the dependence of these distances on χ is not reflected in the position of these maxima and minima.

We shall denote by X_1 , X_2 , and X_3 the distances $R-B$, $B-R'$ and $R-R'$ respectively,⁽³⁰⁾ and by l the reaction coordinate. In the initial state $(RB+R')$ $X_1 = X_1^0$ is the equilibrium distance in the $R-B$ molecule; in the final state $(R+BR')$ $X_2 = X_2^0$ is the equilibrium distance in the $B-R'$ molecule; in the activated state $(R.B.R')$ $l = l^*$ is a certain combination of the corresponding values of the X_1^* , X_2^* and X_3^* coordinates. In this region l coincides with one of the normal coordinates⁽³¹⁾ of the activated

continued from page 161

can find a parameter which would satisfy this requirement and at the same time have such a simple connection with the heat of reaction and activation energy. If, for example, we take as the parameter χ the value of the potential field at a certain point near one of the molecules, then since this potential is a function of the coordinates in the corresponding wave equation, the dependence of the eigenenergy of the system on χ will be complex, generally speaking. To obtain a linear dependence between the energy and χ would only be possible using perturbation theory. The deduction of (10.12) given below is equivalent in its essentials to using this method.

⁽³⁰⁾ We shall take as the distance (X_1 or X_2) between the atom and radical the distance between the B atom and the atom of the radical directly connected with it. We shall take a corresponding value for the distance (X_3) between two radicals. We also assume that the normal coordinates of the system $R.B.R'$ are dependent only on X_1 , X_2 and X_3 .

⁽³¹⁾ The normal coordinates of a system of many particles are those coordinates in which the potential and kinetic energy of the system may be expressed as sums of squares of the coordinates and of their velocities respectively. Normal coordinates are independent and in the general case each of them is a linear combination of the coordinates of all the particles. If a system of bound atoms vibrates, then frequencies appear spectroscopically which correspond to the periodic changes in these normal coordinates, i.e. to normal vibrations. The number of normal vibrations is equal to the number of vibrational degrees of freedom of the system (see footnote ⁽²¹⁾ on p. 156) and their shape is determined by the system's geometrical shape (by the configuration of atoms and bonds in the molecule). For more details regarding normal vibrations see, for example, [48, 273, 53].

complex (if this is triangular then it has two other normal coordinates; in the case of a linear activated complex there is a fourth normal coordinate). Accordingly, the potential-energy surface $\epsilon(X_1, X_2, X_3, \chi)$ for reaction (10.12) has three extrema:

- I when $X_2 = X_3 = \infty, X_1 = X_1^0$ —minimum (RB + R'),
- II when $X_1 = X_3 = \infty, X_2 = X_2^0$ —minimum (R + BR'),
- III when $X_1 = X_1^*, X_2 = X_2^*, X_3 = X_3^*$ —maximum with respect to l and a minimum with respect to the other normal coordinates of (R.B.R').

At all these points

$$(\partial\epsilon/\partial X_1)_I = (\partial\epsilon/\partial X_2)_{II} = (\partial\epsilon/\partial X_3)_{III} = 0 \quad (i = 1, 2, 3), \quad (10.13)$$

where the subscripts I, II and III denote the values of the coordinates corresponding to the three extrema shown. It follows from these equations that $X_1^0, X_1^*, X_2^*, X_3^*$ are functions of χ , whereas X_2^0 clearly does not depend on χ .

We now assume that the change in the parameter χ with a change in the nature of R is small, i.e. $\Delta\chi \ll \chi$. This assumption can be fulfilled when R is a radical of type YZ and in this series of reactions only Y is changed and Z remains unchanged, which is the case in a homologous series of radicals. We shall introduce the notation $\lambda = \Delta\chi/\chi_0$ where χ_0 is the value of χ in the reaction with the R_0 radical taken as the standard. Expressing the energy ϵ and the coordinates X_1^0 and X_i^* ($i = 1, 2, 3$) as functions of λ , we expand ϵ into a series with respect to λ close to the extrema and confine ourselves to the linear terms

$$\epsilon_I = \epsilon_I^0 + \lambda \left(\frac{\partial \epsilon_I}{\partial \lambda} \right)_{\lambda=0} + \lambda \left(\frac{\partial \epsilon_I}{\partial X_1^0} \frac{d X_1^0}{d \lambda} \right)_{\lambda=0};$$

$$\epsilon_{II} = \epsilon_{II}^0;$$

and

$$\epsilon_{III} = \epsilon_{III}^0 + \lambda \left(\frac{\partial \epsilon_{III}}{\partial \lambda} \right)_{\lambda=0} + \lambda \sum_{i=1,2,3} \left(\frac{\partial \epsilon_{III}}{\partial X_i} \frac{d X_i^*}{d \lambda} \right)_{\lambda=0}.$$

Here $\epsilon_I^0, \epsilon_{II}^0$ and ϵ_{III}^0 are the values of $\epsilon_I, \epsilon_{II}$ and ϵ_{III} when $\lambda = 0$. Owing to the conditions (10.13), only the first two terms on the right-hand side in the first and third equations are not zero. Accordingly, the heat of the exothermic reaction and the activation energy (for an absolute temperature zero and neglecting the difference in zero-point energies) are found to be

$$q \equiv \epsilon_I - \epsilon_{II} = q_0 + \lambda G, \quad (10.14)$$

$$\epsilon^* \equiv \epsilon_{III} - \epsilon_I = \epsilon_0^* - \lambda G^*, \quad (10.15)$$

where

$$q_0 = \epsilon_I^0 - \epsilon_{II}^0 \quad \text{and} \quad \epsilon_0^* = \epsilon_{III}^0 - \epsilon_I^0$$

are the heat of reaction and activation energy for R_0 (the standard);

$$G = \left(\frac{\partial \epsilon_I}{\partial \lambda} \right)_{\lambda=0}, \quad G^* = \left(\frac{\partial \epsilon_I}{\partial \lambda} \right)_{\lambda=0} - \left(\frac{\partial \epsilon_{III}}{\partial \lambda} \right)_{\lambda=0}. \quad (10.16)$$

Eliminating λ from (10.14) and (10.15) we obtain equation (10.12), namely

$$\epsilon^* = a - bq,$$

in which

$$a = \epsilon_0^* + q_0 \frac{G^*}{G}, \quad b = \frac{G^*}{G}. \quad (10.17)$$

We now assume that replacing the standard R_0 by an arbitrary radical R displaces all the points of the potential surface in the same direction, at least in the part between the initial well and the barrier.⁽³²⁾ This assumption is quite natural when in a series of radicals $R = YZ$ the individual members differ only in the nature of the Y substituent.⁽³³⁾ With this assumption the derivatives $(\partial \epsilon_I / \partial \lambda)_{\lambda=0}$ and $(\partial \epsilon_{III} / \partial \lambda)_{\lambda=0}$ have the same sign. Moreover, as the effect on the potential-energy surface of changing R is mainly due to the direct interaction of the B atom with R , and $X_1^0 < X_0^*$, it is not difficult to see that

$$|(\partial \epsilon_I / \partial \lambda)_{\lambda=0}| > |(\partial \epsilon_{III} / \partial \lambda)_{\lambda=0}|.$$

Comparing (10.16) and (10.17) it follows that $0 < b < 1$, agreeing with the experimental data.

In deducing (10.12) it is essential to assume that the effect of R on the potential-energy surface is determined by the change in only one parameter, and that the change is quite small. As noted above, this assumption is admissible for the series of reactions $RB + R' \rightarrow R + BR'$ in which the radicals $R = YZ$ differ only in the nature of Y . This assumption is less justifiable for the series in which the R radicals differ in the nature of the Z atom, or in which the nature of the B atom varies, as the change in the parameter χ may then not be sufficiently small. It also follows from the method of deduction above that (10.12) cannot hold for the series of reactions in which two components (for example, R and B , or R and R') vary, or in which some of the members of the series have such an extensively branched Y substituent that there is strong direct interaction (such

⁽³²⁾ In other words it is assumed that the potential curves referring to different reacting substances and corresponding to the reaction path do not intersect in this section. For a discussion of this problem see, for example, [460].

⁽³³⁾ The assumption does not hold, for example, when one halogen atom acting as B is replaced by another [579].

as "steric repulsion") between B and Y. Under these conditions the change in the potential energy is, in the general case, determined by the change in more than one parameter.

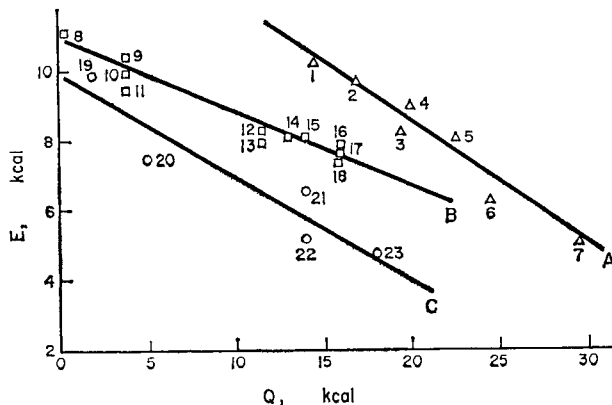


FIG. 34. The linear relation between the activation energy E and the heat of reaction Q .

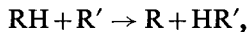
Line A: $\text{Na} + \text{Cl} - \text{R}$; R = 1, CH_3 ; 2, C_2H_5 ; 3, CH_2Cl ; 4, C_3H_7 ; 5, $(\text{CH}_3)_3\text{C}$; 6, CHCl_2 ; 7, CCl_3 [732, 1169].

Line B: $\text{CH}_3 + \text{H} - \text{R}$; R = 8, CH_3 ; 9, C_2H_5 ; 10, $\text{CH}_2\text{C}(\text{CH}_3)_3$; 11, $(\text{CH}_3)_3\text{CC}(\text{CH}_3)_2\text{CH}_2$; 12, *iso*- C_4H_9 ; 13, *iso*- C_5H_7 ; 14, *iso*- C_5H_{11} ; 15, *iso*- C_6H_{18} ; 16, $(\text{CH}_3)_2\text{CCH}(\text{CH}_3)\text{CH}(\text{CH}_3)_2$; 17, $(\text{CH}_3)_3\text{C}$; 18, $\text{CH}_3\text{C}(\text{CH}_3)\text{CH}(\text{CH}_3)\text{CH}_3$ [1229].

Line C: $\text{CF}_3 + \text{H} - \text{R}$; R = 19, CH_3 ; 20, C_2H_5 ; 21, *iso*- C_3H_7 ; 22, *iso*- C_4H_9 ; 23, $(\text{CH}_3)_3\text{C}$ [339, 603].

The experimental data support these conclusions (Fig. 34). When experimental activation energies ($E = \epsilon^* N_A$) and heats of reaction ($Q = qN$) are plotted, the points lie quite close to the same line when only the Y substituent is varied in the series of R (or R') radicals. This regularity is not so marked when the Z or B atom is varied in a series of reactions. If we plot the E and Q values for reactions of type $\text{RB} + \text{R}' \rightarrow \text{R} + \text{BR}'$ differing in the nature of two or even all three components (R, B, R'), the point does not lie on a straight line but mainly within a band of width ~ 3.5 kcal, and in certain cases fall outside these limits [241]. It would be expected from a theoretical point of view that with increased precision in the experimental data for E and Q the values of the constants a and b in the equation $E = a - bQ$ will be somewhat different for reactions differing in the nature of two radicals.

This idea is supported by the studies of Voevodskii [43] who found for a series of reactions of type



where R and R' are aliphatic radicals, the empirical relation (for the exothermic direction)

$$E = a - 0.27Q. \quad (10.18)$$

It seems that the constant a , which clearly has the significance of the activation energy when $Q = 0$ (i.e. the activation energy of the reaction in which R' and R differ only in isotopic composition), is definitely connected with the structure of the R' radical. The values of a adopted by Voevodskii [43] are shown in Table 4.

TABLE 4
Values of a for certain R' radicals

R'	a , kcal	R'	a , kcal
CH_3	11.5	$CH_3-CH-CH_3$	16.3
CH_2-CH_3	14.8	$CH_3-CH-C_2H_5$	17.0
$CH_2-C_2H_5$	15.5	CH_3-C-CH_3	18.0
$CH_2-C_3H_7$	15.6	CH_3	

As the heat of a reaction can always be expressed in terms of the bond dissociation energy, equation (10.12) makes it possible to relate the most important kinetic characteristic—the activation energy—to bond energies of a molecule. Relation (10.12) provides extensive opportunities for studying the connection between reactivity and molecular structure.

§11. Qualitative Consideration of Energy Changes in Three-atom Reactions

Introduction of Skewed Coordinates

Using a potential-energy surface we may follow qualitatively the exchanges of kinetic and potential energies in various reactions involving three atoms [57]. First it is necessary to introduce coordinates x and y such that the internal kinetic energy of the system may be expressed in the form

$$T = \frac{1}{2}\mu\dot{x}^2 + \frac{1}{2}\mu\dot{y}^2, \quad (11.1)$$

where μ is an effective (reduced) mass (see below). If the potential energy ϵ of the nuclei is expressed as a function of these coordinates, then the interconversions of their kinetic and potential energies in the course of an elementary act in a three-atom system may be likened to the corresponding conversions of the energy of a particle with mass μ sliding without friction under the influence of, for example, gravity on a surface with the same shape as the potential-energy surface $\epsilon(x, y)$. Analysis of the motion of such a

representative point makes it possible to explain certain features of the elementary chemical reactions of three atoms.

When the three atoms A, B and C with masses m_A , m_B and m_C lie on a straight line, the natural coordinates of the system are the distances X_{AB} and X_{BC} from the centre atom to the outer atoms (see Fig. 30, p. 153). In these coordinates the kinetic energy of the system has the form:⁽³⁴⁾

$$T = \frac{1}{2} \frac{m_A m_B}{m_A + m_B} \dot{X}_{AB}^2 + \frac{1}{2} \frac{m_C (m_A + m_B)^{-1}}{m_A + m_B + m_C} [(m_A + m_B) \dot{X}_{BC} + m_A \dot{X}_{AB}]^2,$$

or, after simplification

$$T = \frac{1}{2M} [m_A (m_B + m_C) \dot{X}_{AB}^2 + 2m_A m_C \dot{X}_{AB} \dot{X}_{BC} + m_C (m_A + m_B) \dot{X}_{BC}^2], \quad (11.2)$$

where

$$M = m_A + m_B + m_C.$$

The coordinates x and y for which the expression for T is in the form of (11.1) may be chosen in different ways. Thus, a transformation of the general type

$$\left. \begin{aligned} X_{AB} &= a_1 x + b_1 y, \\ X_{BC} &= a_2 x + b_2 y \end{aligned} \right\} \quad (11.3)$$

contains four unknown parameters (a_1 , a_2 , b_1 and b_2) which have only two conditions for their determination: (1) in the expression for T the coefficient of $\dot{x}\dot{y}$ should be equal to zero and (2) the coefficients of \dot{x}^2 and \dot{y}^2 should be equal. Choosing any two parameters and considering the simplest representation of the potential-energy surface we have $a_1 = 1$ and $a_2 = 0$. In this case it is not difficult to see that b_1 and b_2 should be chosen so that $b_1 = -\tan \theta$ and $b_2 = c/\cos \theta$, where θ is the angle between the y and X_{BC} axes. Then

$$\left. \begin{aligned} X_{AB} &= x - y \tan \theta, \\ X_{BC} &= c y \sec \theta. \end{aligned} \right\} \quad (11.4)$$

It is seen from Fig. 35 that this means that when condition (11.1) holds it is necessary to use skewed coordinates and reduce the scale along the X_{BC} axis c times to represent the potential-energy surface as a function of the old variables X_{AB} and X_{BC} . Calculation shows that the kinetic energy takes the form of (11.1) when

$$\cos \theta = \left[\frac{m_B M}{(m_A + m_B)(m_B + m_C)} \right]^{1/2}, \quad (11.5)$$

⁽³⁴⁾ This expression is easily obtained from the usual formula for the kinetic energy of three particles moving in one dimension by introducing the coordinates $X_B - X_A = X_{AB}$ and $X_C - X_B \equiv X_{BC}$ with the condition that the centre of gravity is stationary (X_A , X_B and X_C are the coordinates of the atoms A, B and C).

$$c = \left[\frac{m_A(m_B + m_C)}{m_C(m_A + m_B)} \right]^{1/2}, \quad (11.6)$$

and for μ we find

$$\mu = \frac{m_A(m_B + m_C)}{M}. \quad (11.7)$$

It is apparent from formulae (11.5) and (11.6) that the condition that $\theta = 0$, and consequently that the representative-point method may be used without skewed coordinates, is that $m_A/m_B \ll 1$, or $m_C/m_B \ll 1$. If the masses of all three atoms are equal ($m_A = m_B = m_C$) then $\theta = 30^\circ$ and $c = 1$.

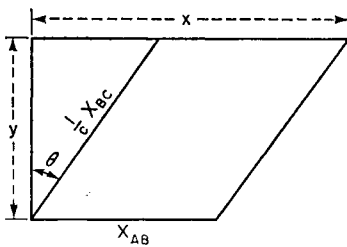


FIG. 35. Introduction of skewed coordinates.

The Reaction between a Diatomic Molecule and an Atom

If the potential-energy surface is represented in skewed coordinates (11.4) then, considering the motion of a representative point along this surface, we may follow qualitatively the conversions of translational and vibrational energies in a three-atom system.

We shall assume that an AB molecule collides with a C atom and before collision the molecule is in the ground vibrational state ($A \leftrightarrow B$ vibrations are absent). Then, initially the representative point will move parallel to the abscissa axis and if then the reaction path has a slight curvature the point will deviate somewhat from this direction. If the translational kinetic energy is not sufficient to surmount the barrier the point will begin to move back (Fig. 36). In this case, however, the point will clearly not move parallel to the abscissa axis but begin to vibrate in the direction of the second axis simultaneously with its translational motion. This means that after collision part of the translational energy of the particles is converted into vibrational energy of the AB molecule. If the AB molecule was vibrating before the collision then after collision the amplitude of the vibrations may increase.

In both cases we are concerned with *collisions of the first kind* where, as a result of the collision, translational energy is converted into internal energy (in this case, into energy of vibrational excitation) of the molecule.

The reverse process is also possible, i.e. *collisions of the second kind*, where vibrational energy (in the general case, internal energy) of the AB molecule is completely or partially converted into translational energy of the particles. This may be illustrated if we use Fig. 36 again but reverse the direction of the motion.

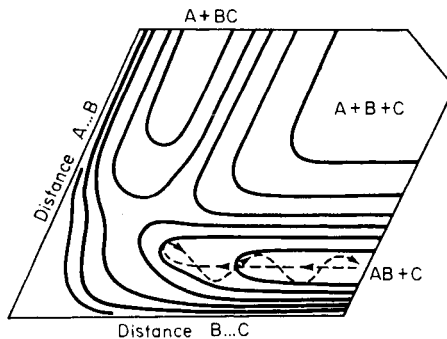


FIG. 36. Interconversion of relative translational and vibrational energy.

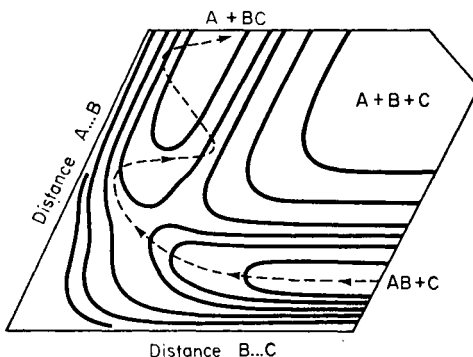


FIG. 37. Motion of the representative point crossing the barrier; part of the initial translational energy is converted into vibrational energy of the resulting molecule.

If the kinetic energy of the representative point is sufficiently great it may reach the top of the potential barrier and pass over; this means that the reaction $AB + C \rightarrow A + BC$ (Fig. 37) occurs. We should note that the kinetic energy of the representative point is the sum of the energy of relative translational motion of the atom and of the molecule, and of the vibrational energy of the latter. Consequently for reaction to occur it is necessary that this over-all energy of the colliding particles be greater than a certain critical value (cf. p. 147 *et seq.*). This means that vibrational energy makes a definite contribution to the activation energy.

In practice, however, reaction will not occur on every collision of this type. To explain this, we need to consider what degrees of freedom the activated complex has in our case. It is known that a linear system of three bound atoms (a linear triatomic molecule) has four internal degrees of freedom. In the case of a stable molecule they correspond to the four normal vibrations shown in Fig. 38. In the case of the activated complex

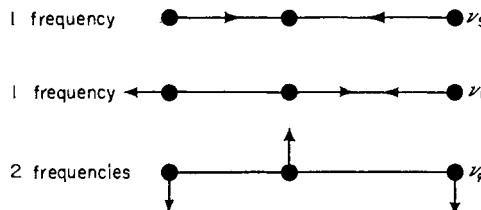


FIG. 38. Normal vibrations of a linear triatomic molecule.

one of the normal coordinates corresponds not to a minimum but to a maximum of potential energy, as the activated complex corresponds to the top of the potential barrier. It is not difficult to show that here the frequency of the corresponding vibration is imaginary;⁽³⁵⁾ this means that the vibrational motion is replaced by translational motion. In the case of the linear triatomic complex this "translational" normal coordinate (i.e. reaction coordinate) is a coordinate which corresponds to antisymmetric vibration in the molecule, as this vibration corresponds to the approach of two adjacent atoms with the simultaneous withdrawal of the third atom (Fig. 38, frequency ν_t). Reaction may evidently occur only if sufficient energy is concentrated in this translational degree of freedom of the activated complex. In other words, for reaction it is necessary that the C atom and the AB molecule should approach each other at a definite phase of the molecular vibration, namely the phase corresponding to the withdrawal of A and B from each other. It may happen, however, that, as a result of an unfavourable energy distribution in the initial state and an unfavourable shape of the surface near the top of the barrier, all the kinetic energy of the system near the top of the barrier is concentrated not into the degree of freedom corresponding to the reaction coordinate but into vibrational degrees of freedom of the activated complex. In this case the barrier is not crossed.

For a favourable energy distribution, giving the velocity of the representative point near the top of the barrier a finite component along the

⁽³⁵⁾ The frequency of the harmonic vibrations of a mass point m is determined by the well-known formula $\nu = [(d^2U/dx^2)_{x=0}]^{1/2}/2\pi m^{1/2}$, where U is the potential energy of the point. If, when $x = 0$, U has a maximum then $(d^2U/dx^2)_{x=0} < 0$ and consequently ν is an imaginary quantity.

reaction coordinate, the representative point will generally after the passage perform both translational and vibrational motion corresponding to the curvature of the reaction path (Fig. 37). This means that the BC molecule formed will be in an excited vibrational state. Moreover, there are cases when almost all the heat of exothermic exchange reactions will be at initial moments in the form of the vibrational energy of BC molecules. Indeed, experimental evidence shows that in all cases investigated the energy of vibrational excitation of molecules represents the major part of the heat of reaction (see Table 2). Smith (F. T. Smith, *J. Chem. Phys.* **31**, 1352, 1959) suggests that this part is the greater the smaller is the angle θ .

As the reaction path on the other side of the pass is more or less irregular, there is a finite probability that the representative point will return to the initial position even after it has crossed the barrier (Fig. 39). The

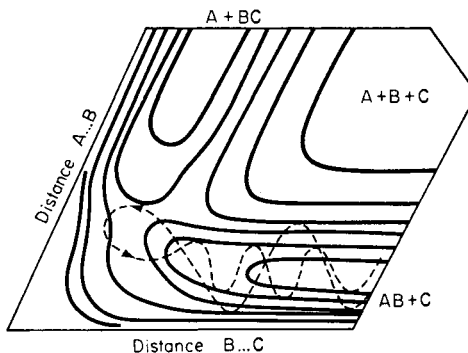


FIG. 39. The representative point crossing the barrier and then returning.

probability of such a return may be especially high when there is a basin near the top of the barrier. The representative point falling into it may perform a fair number of vibrations before leaving the basin. When the shape of this basin is symmetrical the probabilities of the point leaving in the forward or reverse directions are equal (see also [1259a]).

The H₂ + H reaction. The general picture given above for the interconversion of translational and vibrational energies during an exchange reaction involving three atoms may be applied to the interconversion of the *para*- and *ortho*-forms of hydrogen. The potential-energy surface for the system of three H atoms is shown in Fig. 40. This surface was obtained by using the semi-empirical method [587] and should therefore be regarded as merely approximate. For instance it is very probable that the small basin at the top of the barrier, which is obtained when this method of calculation is used, results from the roughness of the calculation and does not

correspond to reality.⁽³⁶⁾ Nevertheless the main features of the potential-energy surface are probably given correctly. For example, it appears that with a more precise calculation the saddle point, which corresponds to the activated complex, is at an X_{BC} distance which scarcely differs from the

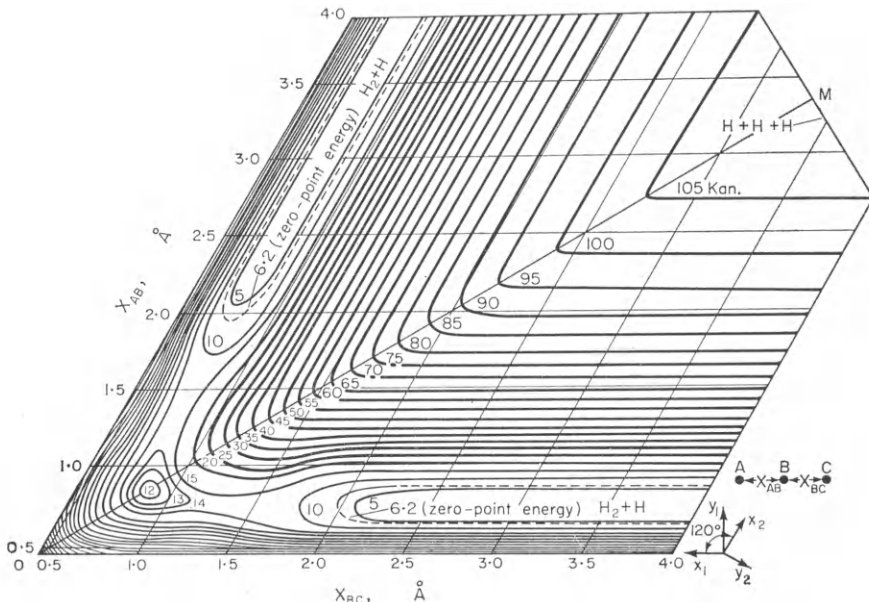


FIG. 40. Potential-energy surface for the system of three hydrogen atoms (according to Eyring, Gershinowitz and Sun [587]).

equilibrium interatomic distance in the H_2 molecule [1263]. It may be concluded from this that the activation energy of the *para-ortho* hydrogen conversion is mainly a *translational* energy.⁽³⁷⁾ Indeed, if the representative point at the top of the potential barrier is allowed to move freely in the

(36) According to Eyring and Polanyi [591], there is a small basin of 2.5 kcal depth at the top of the potential barrier in the $H.H.H$ system; accordingly the point of the pass is displaced somewhat to the side of the line OM. As follows from a semi-empirical calculation [E. P. Lippincott, A. Leiter, *J. Chem. Phys.* **28**, 769 (1958)], the potential energy surface has two basins located symmetrically with respect to the main diagonal. It will be noted, however, that there is no experimental confirmation of their occurrence nor is it substantiated theoretically, as the idea results from use of the very approximate semi-empirical method. Subsequent theoretical calculations for the system of three H atoms [770, 1263] do not support this result. In the new semi-empirical method put forward by Sato Shin [1102a] the basin at the top of the barrier is also lacking. See also [J. C. Polanyi, *J. Chem. Phys.* **23**, 1505 (1955); **24**, 493 (1956)].

(37) This conclusion clearly cannot be extended to the reactions of other molecules as their vibrational-energy quanta are smaller than those of hydrogen. It should be mentioned that all the reasoning in this section is approximate in nature, as the molecular vibrational motion is considered practically as non-quantized, i.e. it is assumed that $h\nu \ll kT$.

direction of the abscissa axis then its vibrational motion will be insignificant owing to the low curvature of the reaction path. This conclusion also follows from the fact that the height of the potential barrier in this reaction is less than the vibrational-energy quantum (about 7 kcal for the former, compared with 11.9 kcal for the latter). Accordingly, in order to surmount the potential barrier the kinetic energy should be nearly half the size of the vibrational quantum and consequently should be exclusively translational.

Another conclusion resulting from Fig. 40 is that on both sides of the diagonal there are parts of the potential surface in which the energy contours, starting with a certain energy, are almost parallel to the appropriate coordinate axis. According to the figure, this energy value is about 45 kcal. In these parts of the surface the potential energy may be represented as a function of only one coordinate. We shall represent by y_1 this coordinate for the part lying to the right of the diagonal and by y_2 that for the part to the left of the diagonal (Fig. 40). The coordinates perpendicular to y_1 and y_2 are represented by x_1 and x_2 respectively. The potential energy to the right of the diagonal depends only on the y_1 coordinate, which determines the vibrational energy of the representative point; the variation in the x_1 coordinate determines its translational motion. To the left of the diagonal there is a corresponding relationship with regard to y_2 and x_2 . It is clear that in each of these parts of the surface there is no transfer of energy between x and y .

If the representative point with energy greater than 45 kcal moves along the x_1 axis then its translational energy is not converted into vibrational energy (along y_1) until the point is near the diagonal, where $X_{AB} = X_{BC}$. Here there is a more or less rapid redistribution of translational energy among the vibrational and translational degrees of freedom. Suppose, for example, that the sum of the translational and vibrational energies of the $H_2 + H$ system is greater than the dissociation energy of H_2 . For dissociation to occur all (or nearly all) the energy must be concentrated in the vibrational coordinate. As stated above, this is impossible until the representative point reaches the diagonal line. After crossing this line the energy may be redistributed so that the vibrational energy, corresponding to the y_2 coordinate, is greater than the dissociation energy, and the representative point will be in the upper right-hand corner on the plateau, which corresponds to the state of three separate atoms. There is a finite probability, therefore, that as a result of an $H_2 + H$ collision an H_2 molecule will dissociate, leading to formation of the $H + H + H$ system (for more details, see §16).

Three-Atom Collisions

We now suppose that the initial state corresponds to three separate atoms A, B and C and we shall consider the reverse process to that above,

i.e. the formation of a diatomic molecule as a result of the ternary collision $A + B + C \rightarrow A + BC$. If the representative point leaves the plateau (Fig. 41), which represents the initial system, parallel to the abscissa axis (i.e.

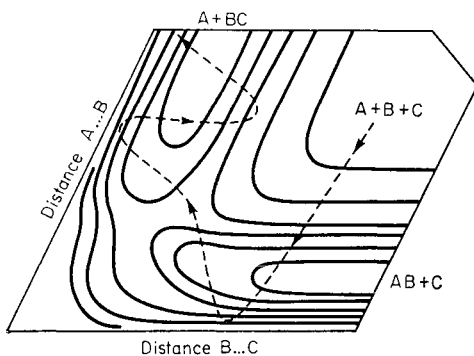


FIG. 41. Motion of the representative point corresponding to the atom-recombination reaction (when the atoms B and C are capable of interacting chemically).

parallel to the x_1 coordinate) then this clearly corresponds to the drawing together of only two atoms—B and C. Accordingly these two atoms cannot combine as there is no third particle present, which is necessary to remove the vibrational energy and stabilize the BC molecule. Ternary collision must occur for this molecule to be formed. It is apparent from Fig. 41 that in this case the representative point must leave the initial state at a quite definite angle, which will ensure that it crosses over the pass into the valley corresponding to the final state. Not every ternary atomic collision, therefore, is effective for molecule formation. It is very probable that in most cases the BC molecule is formed in a highly excited vibrational state (J. C. Polanyi, *J. Chem. Phys.* **31**, 1338, 1959).

§12. Transition-State (Activated-Complex) Method

Derivation of the Basic Equation

The statistical method of calculating the rates of elementary chemical reactions is called the activated-complex or transition-state method and is based on the same three main assumptions as collision theory. These assumptions have been discussed above (see §8). The first two are the assumptions that the motion of the nuclei is adiabatic and obeys the laws of classical mechanics.⁽³⁸⁾ Cases involving non-adiabatic transitions, which result in a discontinuous change of the potential energy of the atoms in the process of the reaction, require special consideration (see §13).

⁽³⁸⁾ This latter assumption is only applicable when treating the motion of the representative point along the reaction coordinate.

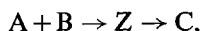
Deviations from classical mechanics are usually small and require only small corrections. (See p. 330 *et seq.*)

The third assumption is that the rate constant of the elementary reaction $X \rightarrow Y$ in the absence of chemical equilibrium scarcely differs from the rate constant of the same process calculated assuming chemical equilibrium between the initial and final substances, $X \rightleftharpoons{} Y$; in the latter case there is an equilibrium distribution, i.e. a Maxwell-Boltzmann distribution, with respect to energy of the initial and final particles and of the components of the system in its intermediate states.⁽³⁹⁾

The basic idea of the method under consideration is that of finding the number of representative points on the potential-energy surface which cross the main diagonal per second in the reaction direction. After introducing a certain correction factor this number is taken as the rate of reaction.

The main diagonal or "line of the pass" for this calculation is chosen on the following basis. We have already seen (§11) that when the line of the pass is crossed perpendicularly, the point representing the system will slide by inertia down towards the final state. It is true that on account of the curvature of the path the probability of reaching the final state should be less than unity, generally speaking. However, if we choose for the calculation of the number of crossings any other line on the potential surface, such as a line in front of the pass, then we would admit a much greater error, as some of the representative points crossing this line would not have sufficient kinetic energy to cross over the pass. In this case, moreover, the probability of reflection would be greater even when the kinetic energy of the representative point is sufficient to surmount the pass. If we calculate the number of crossings of any line on the other side of the pass then the calculation erroneously allows for representative points which leave the final state but return without reaching the top of the barrier. Therefore the line of the pass is the optimum choice.

Let us consider a bimolecular reaction of the type



where A and B are molecules of the initial substances, Z is the activated complex and C a molecule of the final substance. For a Maxwell-Boltzmann distribution, most of the representative points near the top of the potential barrier will move along the reaction coordinate, as significant deviations from this path require the expenditure of large amounts of energy. This greatly simplifies the calculation and allows us to consider only the immediate vicinity of the saddle point on the potential-energy surface.

⁽³⁹⁾ This has obtained confirmation recently for a reaction between iodine and hydrogen [J. H. Sullivan, *J. Chem. Phys.* **30**, 1577 (1959)].

We shall select at the top of the potential barrier an infinitesimal section dl of the reaction coordinate and consider that any representative point in this section corresponds to an *activated complex*. In this case the concentration of activated complexes is clearly proportional to the section length dl . We shall represent by dn_Z the number of activated complexes in unit volume for which the momentum p^* corresponding to the reaction coordinate is between p^* and $p^* + dp^*$. The lifetime of these activated complexes will be equal to the time in which a representative point of mass μ and with velocity $v^* = p^*/\mu$ traces out the length dl , i.e. it is equal to dl/v^* . Consequently, the number of representative points crossing the line of pass per second in the reaction direction and with momenta between p^* and $p^* + dp^*$ is equal to

$$v^* dn_Z/dl, \quad (v^* > 0).$$

However some of the systems in this number may not reach the final state but return as a result of reflection on account of the curvature of the reaction path, or react in another direction. For this reason the number of representative points of the type indicated crossing the line of the pass per second and reaching the final state will be less and is in fact

$$v^* \kappa(p^*) dn_Z/dl, \quad (12.1)$$

where $\kappa(p^*)$ is the probability that a representative point with momentum between p^* and $p^* + dp^*$ crosses the barrier and reaches the final state. This κ factor is called the *transmission coefficient*.

The total number of representative points crossing the line of the pass per second and reaching the final state will clearly be equal to the rate w of the forward reaction

$$w = \int v^* \kappa(p^*) dn_Z/dl.$$

Here the integration is carried out with respect to all the representative points crossing the line of the pass close to the activated state and with momenta between zero and infinity. On the other hand we may also write for w

$$w = k n_A n_B, \quad (12.2)$$

where k is the rate constant of the reaction $A + B \rightarrow C$. We have, therefore,

$$k n_A n_B = \int v^* \kappa(p^*) dn_Z/dl. \quad (12.3)$$

This equation holds for any conditions, such as when the reverse reaction $C \rightarrow A + B$ occurs and also for the state of chemical equilibrium $A + B \rightleftharpoons C$. In the latter case the concentrations of initial and final substances and of

the activated complexes will be the equilibrium values and (12.3) becomes

$$k_{\text{equilib}}(n_A)_{\text{equilib}}(n_B)_{\text{equilib}} = \int v^* \chi(p^*) (dn_Z)_{\text{equilib}}/dl. \quad (12.4)$$

Here the subscript "equilb" signifies that the relevant quantities refer to equilibrium conditions.

We now use the third assumption which is basic to the transition-state method. Applied to our derivation this assumption means that the rate constant k in (12.2), referring to the general, non-equilibrium case, scarcely differs from its value in the case of chemical (and consequently, general statistical) equilibrium, i.e.

$$k = k_{\text{equilib}}.$$

Let us determine k_{equilib} in an explicit form.

The equilibrium concentration of activated complexes may be expressed using the usual statistical relationship (where we take $p^* 70$)

$$(dn_Z)_{\text{equilib}} = \frac{Z'_*}{h Z'_A Z'_B} \exp[-p^{*2}/2\mu k T] dp^* dl (n_A)_{\text{equilib}} (n_B)_{\text{equilib}}, \quad (12.5)$$

where Z'_A and Z'_B are the partition functions of the initial substances A and B:

$$Z'_A = \sum_i \exp(-\epsilon_{ai}/kT), \quad Z'_B = \sum_i \exp(-\epsilon_{bi}/kT),$$

and Z'_* is the partition function of the activated complex

$$Z'_* = \sum_i \exp(-\epsilon_{zi}/kT),$$

allowing for all degrees of freedom save that corresponding to the reaction coordinate. The latter corresponds to the factor [in (12.5)]

$$h^{-1} \exp(-p^{*2}/2\mu k T) dp^* dl$$

where μ is the effective mass of the activated complex, corresponding to motion along the reaction coordinate. All the partition functions refer to unit volume and the energy is reckoned from a certain common level. In calculating the partition functions, however, it is more convenient to take the energy zero as the zero-level energy of the appropriate molecule or activated complex. In this way we replace Z'_A , Z'_B and Z'_* by

$$\left. \begin{aligned} Z_A &= \sum_i \exp[-(\epsilon_{ai} - \epsilon_{a0})/kT] = Z'_A \exp(\epsilon_{a0}/kT), \\ Z_B &= \sum_i \exp[-(\epsilon_{bi} - \epsilon_{b0})/kT] = Z'_B \exp(\epsilon_{b0}/kT), \\ Z_* &= \sum_i \exp[-(\epsilon_{zi} - \epsilon_{z0})/kT] = Z'_* \exp(\epsilon_{z0}/kT), \end{aligned} \right\} \quad (12.6)$$

where ϵ_{a0} , ϵ_{b0} and ϵ_{z0} are the zero-level energies of A, B and Z respectively. On the basis of (12.6) the ratio $Z'_\neq/Z'_A Z'_B$ may be written

$$\frac{Z'_\neq}{Z'_A Z'_B} = \frac{Z'_\neq \exp(-\epsilon_{z0}/kT)}{Z_A Z_B \exp[-(\epsilon_{a0} + \epsilon_{b0})/kT]} = \frac{Z'_\neq \exp(-\epsilon_0^\neq/kT)}{Z_A Z_B}, \quad (12.7)$$

where

$$\epsilon_0^\neq = \epsilon_{z0} - (\epsilon_{a0} + \epsilon_{b0}) \quad (12.8)$$

is the difference in zero-point energies of the initial substances and of the activated complex; this is clearly equal to the activation energy at the absolute temperature zero.

By substituting (12.5) and (12.7) in equation (12.4) and cancelling $(n_A)_{\text{equilib}} (n_B)_{\text{equilib}}$ from both sides of the equation, then since we have assumed $k = k_{\text{equilib}}$ we find

$$k = \frac{Z^\neq}{Z_A Z_B} \exp(-\epsilon_0^\neq/kT) \int_0^\infty \frac{p^\neq}{\mu h} \kappa(p^\neq) \exp(-p^{\neq 2}/2\mu kT) dp^\neq. \quad (12.9)$$

This integral is easily calculated assuming that $\kappa(p^\neq)$ is only weakly dependent on p^\neq .⁽⁴⁰⁾ Replacing the function $\kappa(p^\neq)$ by the mean value of κ and taking this outside the integral sign, we finally find for the rate constant of the reaction $A + B \rightarrow C$

$$k = \kappa \frac{kT}{h} \frac{Z^\neq}{Z_A Z_B} \exp(-\epsilon_0^\neq/kT). \quad (12.10)$$

When the initial system includes other substances besides A and B and they all enter into the same activated complex Z, then the denominator of (12.10) should include the partition functions of all the initial substances.

A few observations should be made with regard to the mechanism of establishing the equilibrium concentration of activated complexes for the chemical equilibrium $A + B \rightleftharpoons C$. The presence of this equilibrium concentration by no means signifies that there is an equilibrium between initial molecules and activated complexes of the type



where $w_1 = w'_1$. This is easily seen from the following considerations.

We first assume that $\kappa = 1$. In this case a representative point may return from the activated state (characterized by the section dl) to the initial state only on the condition that, when it reaches the top of the

⁽⁴⁰⁾ An attempt to allow for the dependence of κ on p^\neq has been made in an explicit form by Matsen [927] (see below, p. 195).

barrier, its momentum is infinitely close to zero. The number of representative points reaching the top of the barrier in unit time with momenta between 0 and dp^* is proportional to dp^* . Consequently the number of reverse crossings $Z \rightarrow A+B$ per second will also be proportional to dp^* and is therefore infinitesimal.⁽⁴¹⁾ But the total number of forward crossings $A+B \rightarrow Z$ per second, for which the representative points at the top of the barrier have all values of momentum greater than zero, is a finite number. The rate w_1 of formation of the activated complex, therefore, is infinitely greater than the rate w'_1 of the reverse decomposition; this is not compatible with the hypothesis regarding the presence of equilibrium (12.11).

If earlier we had not limited ourselves to the assumption that $\kappa = 1$ then, generally speaking, the equilibrium (12.11) may be realized on account of the strong reflection of the representative points due to the curvature of the reaction path near the activated state. For the equation $w_1 = w'_1$ to hold it must be assumed that $\kappa \ll 1$. As we shall see below, however, both comparison of the results of calculations, using the activated-complex method, with experimental data and direct numerical evaluations of κ show that in fact the transmission coefficient usually differs little from unity. This again leads to the conclusion that the equilibrium (12.11) is impossible.

With this condition it is clear that the equilibrium between initial and final substances may only occur according to the scheme [259, 258]:



where Z is any intermediate complex such as an activated complex. The symbols $+p^*$ and $-p^*$ show that in the one case the momentum of a representative point in the state Z has a positive value and in the other case a negative value. This mechanism of mobile equilibrium actually ensures the presence of an equilibrium concentration of activated complexes. As should occur in a statistical equilibrium, the number of activated complexes $Z(+p^*)$ formed per second as a result of $A+B$ collisions is equal to the number of complexes $Z(-p^*)$ formed from the final substance C , which decompose into $A+B$. This equality holds both for the total number of activated complexes and for complexes with an absolute momentum along the reaction coordinate between p^* and p^*+dp^* . It follows that (12.5) is valid.

Equation (12.10) was first obtained by Eyring [586] and, simultaneously but in a somewhat different form, by Evans and Polanyi [580]; the equation establishes a connection between the rate of reaction and the molecular

⁽⁴¹⁾ Cf. formula (12.5); it is apparent from this that the concentration of complexes with p^* between 0 and dp^* is proportional to dp^* and dl .

characteristics of the initial substances and of the activated complex. It is the basic equation of the transition-state method and is a very great improvement on the formula based on the classical collision theory.

In practice serious difficulties are encountered when equation (12.10) is used to calculate the absolute value of a rate constant. This is mainly caused by the difficulties involved in the theoretical calculation of the activation energy ϵ_0^* in the present state of calculating techniques (see §10). Practically, therefore, it is possible to calculate only the pre-exponential factor in (12.10) and even this is quite approximate as a rule, due mainly to the difficulty of calculating the transmission coefficient κ . Usually it is assumed that $\kappa = 1$ and this is apparently of the correct order of magnitude for most reactions which do not involve non-adiabatic transitions. Moreover, the configuration and characteristics of the activated complex, which are needed to calculate Z^* (see below), are usually unknown and can be evaluated only approximately using indirect data.

In the basic equation (12.10) there is the expression

$$\frac{Z^*}{Z_A Z_B} \exp(-E_0/RT) \equiv K^*, \quad (E_0 = N_A \epsilon_0^*), \quad (12.13)$$

which has the same form as the statistical expression for an equilibrium constant. For this reason the quantity K^* is frequently called the "equilibrium constant" for the equilibrium between the activated and initial states. As we have seen above, there is no such equilibrium in reality, as the fraction of representative points which return to the initial state due to reflection near the pass is small ($\kappa \approx 1$).⁽⁴²⁾ Nevertheless, treating K^* as an equilibrium constant has some basis in that when there is chemical equilibrium (i.e. the equilibrium $A + B \rightleftharpoons C$) the concentration of activated complexes may be determined from the appropriate partition functions, as we have seen. In essence K^* differs from a normal equilibrium constant only in that the factor corresponding to motion along the reaction coordinate is not included in the partition function of the activated complex. The remaining factors included in Z^* correspond to the same degrees of freedom as in any stable molecule.

By introducing K^* into equation (12.10) we find

$$k = \kappa h^{-1} k T K^*. \quad (12.14)$$

It should be mentioned that, in contrast with (12.10) in which the rate constant is expressed in concentration units, equation (12.14) is correct when the rate is expressed either in concentration units or in pressure

⁽⁴²⁾ We should note in connection with this that Benson [380] has attempted to treat bimolecular reactions in an analogous way to Slater's treatment [1142] (see §17) of the rate of unimolecular decomposition. This attempt should not be considered successful, however, as in it the author considers K^* as the constant of a true equilibrium ($A + B \rightleftharpoons Z$) between initial molecules and activated complexes, which is incorrect.

units; it is only necessary that the same units should be employed for k and K^* .

Using K^* we may introduce the concept of a "free energy of activation" characterizing the free-energy change of a system when it goes into the activated state, and accounting for all degrees of freedom except the reaction coordinate. If the process takes place at constant volume we have

$$\Delta F^* = RT \ln K^*. \quad (12.15)$$

For the change in "free energy at constant volume" we may write $\Delta F^* = \Delta E^* - T\Delta S^*$, where ΔE^* is the change in internal energy of the system on activation and ΔS^* is the corresponding change in entropy. Using these relationships we may rewrite (12.14) in the form:⁽⁴³⁾

$$k = \kappa(kT/h) \exp(-\Delta F^*/RT) = \kappa(kT/h) \exp(\Delta S^*/R) \exp(-\Delta E^*/RT). \quad (12.16)$$

Equation (12.16) shows that in the general case the rate of an elementary reaction is determined by the change in free energy of the system in the activation process. An essential point is that in certain cases the energy of activation ΔE^* and the entropy of activation ΔS^* may partially compensate one another. For example, condensation of a vapour, which may be considered as one case of molecular association, is a slow process because of the marked decrease of entropy, in spite of the fact that the heat of activation is low. In other cases the entropy of activation may give rise to a high rate of reaction in spite of a high heat of activation.

Introduction of Experimental Activation Energy

As a theoretical calculation of activation energy is difficult, this quantity is usually derived from experimental data. The task of theory then becomes that of calculating the pre-exponential factor in the Arrhenius equation starting from some assumptions regarding the character of the elementary process. For this purpose it is necessary to write equation (12.10) in a form containing the experimental activation energy determined from the temperature coefficient of the rate constant, i.e. from $d \ln k/dT$. The experimental data show that over a small temperature range this coefficient, like the pre-exponential factor A , remains approximately constant. To write (12.10) in the given temperature range approximately in the Arrhenius form

$$k = A \exp(-\epsilon^*_{\text{exper}}/kT) \quad (12.17)$$

it is necessary, as we said above, that at a temperature T_0 in this range, the

⁽⁴³⁾ In equation (12.16) it is assumed that ΔF^* , ΔE^* and ΔS^* refer to substances in their standard states.

values of k , and also of its logarithmic derivative with respect to temperature, should coincide for the forms (12.10) and (12.17). Let us introduce the notation

$$Z_1 = Z_a Z_b, \frac{\kappa k T Z^*(T)}{h Z_1(T)} = A'(T). \quad (12.18)$$

Then the first of the conditions indicated gives

$$\ln A'(T_0) - \frac{\epsilon_0^*}{k T_0} = \ln A - \frac{\epsilon^*_{\text{exper}}}{k T_0}.$$

According to the second,

$$\left(\frac{d \ln A'}{dT} \right)_{T_0} + \frac{\epsilon_0^*}{k T_0^2} = \frac{\epsilon^*_{\text{exper}}}{k T_0^2}.$$

Hence we find

$$\epsilon^*_{\text{exper}} = \epsilon_0^* + k T_0^2 \left(\frac{d \ln A'}{dT} \right)_{T_0} \quad (12.19)$$

and

$$A = A'(T_0) \exp \left[T_0 \left(\frac{\partial \ln A'}{\partial T} \right)_{T_0} \right]. \quad (12.20)$$

Substituting the last expression into (12.17) and bearing (12.18) in mind, we obtain

$$k = \kappa h^{-1} k T_0 e \frac{G^*(T_0)}{G_1(T_0)} \exp(-\epsilon^*_{\text{exper}}/kT), \quad (12.21)$$

where the following notations have been introduced (see [258]):

$$G^*(T_0) = Z^*(T_0) \exp \left[T_0 \left(\frac{d \ln Z^*}{dT} \right)_{T_0} \right], \quad (12.22)$$

$$G_1(T_0) = Z_1(T_0) \exp \left[T_0 \left(\frac{d \ln Z_1}{dT} \right)_{T_0} \right]. \quad (12.23)$$

If $\epsilon^*_{\text{exper}}$ is known, equation (12.21) makes it possible to determine the rate constant by calculating the partition functions (assuming that $\kappa = 1$).

It should be mentioned that the pre-exponential factors in (12.10) and (12.21) are numerically different. To explain the reason for this difference we shall determine the derivatives $d \ln Z_1/dT$ and $d \ln Z^*/dT$. Introducing the notation

$$\epsilon_{a0} + \epsilon_{b0} = \epsilon_{10} \quad (12.24)$$

and considering (12.6) we may write⁽⁴⁴⁾

$$\begin{aligned}
 \frac{d \ln Z_1}{dT} &= \frac{d \ln \sum_i \exp[-(\epsilon_{1i} - \epsilon_{10})/kT]}{dT} \\
 &= \frac{\sum_i (\epsilon_{1i} - \epsilon_{10}) \exp[-(\epsilon_{1i} - \epsilon_{10})/kT]}{kT^2 \sum_i \exp[-(\epsilon_{1i} - \epsilon_{10})/kT]} \\
 &= \frac{\bar{\epsilon}_1 - \epsilon_{10}}{kT^2}, \tag{12.25}
 \end{aligned}$$

where $\bar{\epsilon}_1$ is the mean energy of the initial molecules. In a similar way we find

$$\frac{d \ln Z^*}{dT} = \frac{\bar{\epsilon}_z - \epsilon_{z0}}{kT^2}. \tag{12.26}$$

Hence

$$\left. \begin{aligned}
 \exp \left[T \left(\frac{d \ln Z_1}{dT} \right) \right] &= \exp \left[\frac{\bar{\epsilon}_1 - \epsilon_{10}}{kT} \right], \\
 \exp \left[T \left(\frac{d \ln Z^*}{dT} \right) \right] &= \exp \left[\frac{\bar{\epsilon}_z - \epsilon_{z0}}{kT} \right].
 \end{aligned} \right\} \tag{12.27}$$

Therefore

$$G_1(T) = Z_1(T) \exp \left[\frac{\bar{\epsilon}_1 - \epsilon_{10}}{kT} \right] = \sum \exp[-(\epsilon_{1i} - \bar{\epsilon}_1)/kT]. \tag{12.28}$$

A similar expression is obtained for G^* . On the other hand, according to (12.18), (12.19) and (12.25) we have

$$\epsilon^*_{\text{exper}} = \epsilon_0^* + (\bar{\epsilon}_z - \epsilon_{z0}) - (\bar{\epsilon}_1 - \epsilon_{10}) + kT = \bar{\epsilon}_z - \bar{\epsilon}_1 + kT. \tag{12.29}$$

It is apparent from (12.29) that whereas the activation energy in equation (12.10) is defined, according to (12.6) and (12.8), as the difference in energy of the zeroth levels of activated complex and initial molecules, i.e.

⁽⁴⁴⁾ It should be borne in mind that

$$\begin{aligned}
 Z_1 &= Z_a Z_b = \sum_i \exp[-(\epsilon_{ai} - \epsilon_{a0})/kT] \cdot \sum_k \exp[-(\epsilon_{bk} - \epsilon_{b0})/kT] \\
 &= \sum_j \exp[-(\epsilon_{1j} - \epsilon_{10})/kT]
 \end{aligned}$$

where ϵ_{1j} is a typical sum $\epsilon_{ai} + \epsilon_{bk}$.

it is the activation energy at the temperature absolute zero, the activation energy ($\epsilon_{\text{exper}}^*$) in equation (12.21) is defined as a quantity depending on the difference in *mean* energies at the given temperature. Accordingly the energy in the partition functions G_1 and G^* is reckoned not from the zeroth levels of the molecule and the activated complex but from their mean energies [cf. (12.6) and (12.28)].

From formulae (12.21) it is easy to find expressions for G_1 and G^* if Z_1 and Z^* have been calculated previously. If, as is frequently the case, Z is of the form bT^γ , where b is temperature independent, then according to (12.22) or (12.23)

$$G = Ze^\gamma = b(Te)^\gamma. \quad (12.30)$$

When the temperature range in which the reaction rate is studied is changed, both the pre-exponential factor and the experimental activation energy also change. For example, if $A'(T)$ has the form $A'(T) = b_1 T^{\gamma_1}$, then according to (12.19) and (12.20) on passing from a temperature T_0 to T'_0

$$(\epsilon_{\text{exper}}^*)_{T'_0} - (\epsilon_{\text{exper}}^*)_{T_0} = \gamma_1 k (T'_0 - T_0), \quad (12.31)$$

$$(A)_{T'_0}/(A)_{T_0} = (T'_0/T_0)^{\gamma_1}. \quad (12.32)$$

Let us now rewrite (12.21) so that as well as $\epsilon_{\text{exper}}^*$ ($= E_{\text{exper}}^*/N_A$) it includes the entropy of activation instead of the partition functions. This is important when it can be assumed that the configuration of the activated complex is close to that of the final molecules (for example, in association reactions) and therefore we may take the entropy of the reaction as an approximation for the entropy of activation (this requires a certain correction connected with separating the degree of freedom corresponding to the reaction coordinate).

If the rate constant is measured in concentration units (i.e. at constant volume), then according to (12.16)

$$k = \kappa h^{-1} k T \exp(\Delta S^*/R) \exp(-\Delta E^*/RT). \quad (12.33)$$

The change ΔE^* in internal energy on activation is clearly equal to

$$\Delta E^* = N_A(\bar{\epsilon}_z - \bar{\epsilon}_1). \quad (12.34)$$

Consequently, according to (12.29), at a given temperature T_0

$$(\Delta E^*)_{T_0} = E_{\text{exper}} - RT_0. \quad (12.35)$$

Substituting this expression into (12.33) and combining it with the Arrhenius equation, we find

$$k = \kappa h^{-1} k T_0 e \exp(\Delta S^*/R) \exp(-E_{\text{exper}}/RT), \quad (12.36)$$

where ΔS^* refers to the temperature T_0 .

In practice the entropy for gas-phase reactions is frequently measured at constant pressure. In this case (12.33) is replaced by

$$k_p = \kappa h^{-1} k T \exp(\Delta S_p^\neq / R) \exp(-\Delta H^\neq / RT) \quad (12.16a)$$

The quantities ΔE^\neq and ΔH^\neq are related thermodynamically as follows:

$$\Delta H^\neq = \Delta E^\neq + P \Delta V^\neq, \quad (12.37)$$

where ΔV^\neq is the volume change in the same process. Using the equation of state of an ideal gas we may write

$$P \Delta V^\neq = (1-x)RT, \quad (12.38)$$

where x is the number of molecules included in the activated complex and $1-x$ is equal to the decrease in the number of particles on formation of the activated complex. In this way, using (12.35) we may write

$$(\Delta H^\neq)_{T_0} = E_{\text{exper}} - xRT_0. \quad (12.39)$$

As the order of an elementary reaction is the same as x , the number of molecules in the activated complex, we obtain the following relation from the general expression for the rate of reaction:

$$k = k_p(RT)^{x-1}, \quad (12.40)$$

where k , as above, is the rate constant expressed in concentration units. Substituting (12.39) and (12.40) into expression (12.16a) we find

$$k = \kappa h^{-1} k T_0 e^x (RT_0)^{x-1} \exp(\Delta S_p^\neq / R) \exp(-E_{\text{exper}}^\neq / RT), \quad (12.41)$$

where ΔS_p^\neq refers to the temperature T_0 . For example, in the case of bimolecular reaction ($x = 2$), according to (12.41) we find

$$k = \kappa h^{-1} k T_0 e^2 RT_0 \exp(\Delta S_p^\neq / R) \exp(-E_{\text{exper}}^\neq / RT). \quad (12.42)$$

If the experimental activation energy is measured at constant pressure and the rate constant is expressed in pressure units, then instead of (12.35) the following equation⁽⁴⁵⁾ holds:

$$(\Delta H^\neq)_{T_0} = E_{\text{exper}}^{(p)} + RT_0. \quad (12.43)$$

Substituting this equation into (12.16a) we obtain:

$$k_p = \kappa h^{-1} k T \exp(\Delta S_p^\neq / R) \exp(-E_{\text{exper}}^{(p)} / RT), \quad (12.44)$$

where the value of ΔS_p^\neq must be taken for the temperature T_0 .

⁽⁴⁵⁾ Equation (12.43) may be obtained using the same method as for (12.29). In this case it should be remembered that the partition function of each of the components of the reaction contains in the general case the factor $V = RT/P$, where V is the molar volume of the substance and P is the pressure which is assumed to be constant [cf. (12.46)]. On this condition, considering (12.37) and (12.38) we find

$$d \ln k_p / dT = [\Delta E^\neq + RT + RT(1-x)] / RT^2 = (\Delta H^\neq + RT) / RT^2,$$

and hence (12.43) follows.

As the gas system being considered is assumed to be ideal, the quantity ΔS_p^\neq does not depend on our choice of the standard state.

Formulae for Calculating the Pre-exponential Factor

Using partition-function formulae we are able to find a general approximate expression for the pre-exponential factor in the equation for the rate constant of an elementary reaction.⁽⁴⁶⁾

If the rate constant is calculated from equation (12.10) then the complete partition function Z is equal to the product of the partition functions for the different types of motion. These separate partition functions are usually expressed in the following manner:

1. For translational motion (three degrees of freedom) of an atom or molecule of mass m when the volume occupied by the gas is equal to unity,

$$Z_{\text{trans}} = h^{-3}(2\pi mkT)^{3/2}. \quad (12.45)$$

If the volume of gas is V then

$$Z_{\text{trans}} = h^{-3}(2\pi mkT)^{3/2}V = h^{-3}(2\pi mkT)^{3/2} \frac{RT}{P}. \quad (12.46)$$

2. For rotational motion:

linear molecules⁽⁴⁷⁾

$$Z_{\text{rot}} = g_{\text{el}}g_{\text{nuc}}8\pi^2IkTs^{-1}h^{-2}, \quad (12.47)$$

non-linear molecules⁽⁴⁷⁾

$$Z_{\text{rot}} = g_{\text{el}}g_{\text{nuc}}8\pi^2(8\pi^3ABC)^{1/2}(kT)^{3/2}s^{-1}h^{-3}. \quad (12.48)$$

Here g_{el} and g_{nuc} are the spin factors (statistical weights) of the electron states and nuclei, s is the symmetry number and A , B and C are the moments of inertia referred to the three principal axes of the molecule.

3. For vibrational motion (a harmonic oscillator)

$$Z_{\text{vib}} = [1 - \exp(-hv/kT)]^{-1}, \quad (12.49)$$

where v is the vibrational frequency. In the limiting case when $hv/kT \ll 1$, $Z_{\text{vib}} = kT/hv$. In the other limiting case when $hv/kT \gg 1$, $Z_{\text{vib}} = 1$.

If the rate constant is calculated from (12.21) the partition functions G for the separate types of motion may be obtained from the expressions for Z corresponding to these types of motion using the same formulae

⁽⁴⁶⁾ This is for reactions with non-zero activation energies. For deduction of the partition-function formulae for the individual degrees of freedom, see for example, [57, 304, 56].

⁽⁴⁷⁾ These formulae are obtained assuming that the separation of low rotational levels is small compared with kT .

(12.22) and (12.23) which relate the complete partition functions G and Z . As we have seen, Z_{trans} and Z_{rot} are of the form bT^γ [see (12.46)–(12.48)]. Then, according to (12.30), to find the appropriate G we must simply replace T by Te in the expression for Z . For example,

$$G_{\text{trans}} = (2\pi m k Te)^{3/2} h^{-3}. \quad (12.50)$$

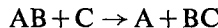
The vibrational partition function, according to (12.22) and (12.49) is now equal to

$$G_{\text{vib}} = [1 - \exp(-hv/kT)]^{-1} \exp\{-hv/[kT \exp(hv/kT) - kT]\}. \quad (12.51)$$

When $hv/kT \ll 1$, $G_{\text{vib}} = kTe/hv$; when $hv/kT \gg 1$, $G_{\text{vib}} = 1$. Comparing these values with the corresponding limiting values of Z_{vib} shows that G_{vib} and Z_{vib} usually differ by only a small amount.

In calculating the partition functions Z^* and G^* for the activated complex it should be remembered that the number of degrees of freedom to be considered is one less than for a stable molecule containing the same number of atoms. Consequently, an activated complex containing x atoms will have $3x - 7$ normal vibrations (in the case of a linear complex, $3x - 6$).

For a simple *bimolecular reaction* between a diatomic molecule and an atom



let us take the linear configuration as a possible configuration of the activated complex. As we have seen in §10, this configuration may be considered to be substantiated theoretically for atoms with a valence electron in an *s*-state.

Designating quantities referring to the activated state by $*$, to the AB molecule by the suffix 1 and to the C atom by the suffix 2, we find for the partition functions corresponding to this reaction⁽⁴⁸⁾

$$Z^* = \frac{(2\pi m^* k T)^{3/2}}{h^3} \frac{g^* 8\pi^2 I^* k T}{s^* h^2} \prod_{i=1}^3 [1 - \exp(-hv_i^*/kT)]^{-1}, \quad (12.52)$$

$$Z_1 = \frac{(2\pi m_1 k T)^{3/2}}{h^3} \frac{g_1 8\pi^2 I_1 k T}{s_1 h^2} [1 - \exp(-hv_1/kT)]^{-1}, \quad (12.53)$$

$$Z_2 = \frac{(2\pi m_2 k T)^{3/2}}{h^3} g_2. \quad (12.54)$$

Here g^* , g_1 and g_2 are the products of the appropriate electronic and nuclear factors. Substituting these expressions into (12.10), we obtain after

⁽⁴⁸⁾ In equation (12.52) m^* represents the actual mass of the activated complex which differs from its effective (reduced) mass in equations (12.5) and (12.9).

simple rearrangements

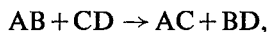
$$k = \kappa \frac{g^*}{g_1 g_2} \left(\frac{m^*}{m_1 m_2} \right)^{3/2} \frac{I^* s_1}{I_1 s^*} \times \times \frac{h^2}{(2\pi)^{3/2} (kT)^{1/2}} \frac{[1 - \exp(-h\nu_1/kT)] \exp(-E_0/kT)}{\prod_{i=2}^3 [1 - \exp(-h\nu_i^*/kT)]}. \quad (12.55)$$

In the two limiting cases the factors containing frequencies in this equation are simplified. When all the vibrational frequencies are very small or if the temperature is sufficiently high, i.e. when $h\nu_1 \ll kT$ and $h\nu^* \ll kT$, these factors become

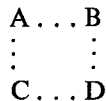
$$\left(\frac{kT}{h} \right)^2 \frac{\nu_1}{\prod_{i=2}^3 \nu_i^*}. \quad (12.56)$$

If, on the other hand, $h\nu_1 \gg kT$ and $h\nu^* \gg kT$, the total factor reduces to unity. In the two limiting cases when E_0 in (12.57) is replaced by E_{exper} the correct value of the pre-exponential factor is obtained by simply replacing T by T_e .

For a bimolecular reaction of the type



going through an activated complex of the type



the partition functions are expressed in the following way (the suffix 1 refers to the AB molecule and the suffix 2 to the CD molecule):

$$Z^* = \frac{(2\pi m^* k T)^{3/2}}{h^3} \times \times \frac{g^* 8\pi^2 (8\pi^3 A^* B^* C^*)^{1/2} (kT)^{3/2} \prod_{i=1}^5 [1 - \exp(-h\nu_i^*/kT)]^{-1}}{s^* h^3}, \quad (12.57)$$

$$Z_1 Z_2 = \frac{(2\pi m_1 k T)^{3/2}}{h^3} \frac{g_1 8\pi^2 I_1 k T}{s_1 h^2} [1 - \exp(-h\nu_1/kT)]^{-1} \times \times \frac{(2\pi m_2 k T)^{3/2}}{h^3} \frac{g_2 8\pi^2 I_2 k T}{s_2 h^2} [1 - \exp(-h\nu_2/kT)]^{-1}. \quad (12.58)$$

Substituting this expression into formula (12.10), we find the rate constant of the reaction under consideration.

Equation (12.10) may be applied directly to unimolecular reactions if it is assumed that the probability of activating the molecule by collision allows for the transmission coefficient; multiplying the remaining part of (12.10) by the concentration we obtain the rate of the reaction proper, i.e. the number (per second) of active molecules which concentrate in a definite bond sufficient energy for its rupture.

When the activated-complex method is used to calculate the rate of unimolecular decomposition (or the reverse reaction) the question frequently arises as to what is the transition state of the system. In fact, if we consider just the potential energy of the interaction of A and B in the decomposing AB molecule, the potential curve will not have a maximum as a rule, and consequently the position of the transition state will be indeterminate⁽⁴⁹⁾ (Fig. 42, curve I). The situation may be changed, however,

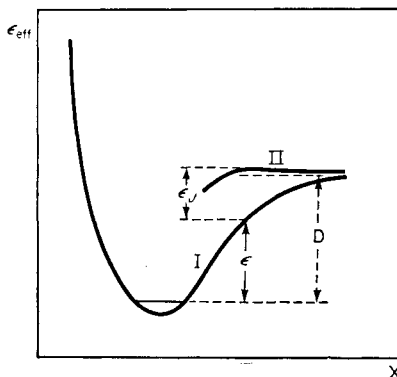


FIG. 42. Rotational barrier of the energy of a diatomic molecule.
I $\epsilon_{\text{eff}} = \epsilon$; II $\epsilon_{\text{eff}} = \epsilon + \epsilon_J$.

if, in addition to the potential energy (ϵ) of the interaction of the separate parts of the molecule, we allow for its rotational energy (ϵ_J). For a diatomic molecule AB this equals

$$\epsilon_J = \frac{\hbar^2 J(J+1)}{8\pi^2 I}, \quad (12.59)$$

where $I = \mu X^2$ is the moment of inertia, X is the interatomic distance A—B and μ is the reduced mass. Consequently, the rotational energy for each value of the rotational quantum number J depends on the distance

⁽⁴⁹⁾ The potential curve sometimes has a barrier in the case of a polyatomic molecule decomposing into two parts. There are also indications that there is a barrier present in the case of certain diatomic molecules (see, for example, [56]).

between A and B. If we plot along the ordinate axis the sum $\epsilon_{\text{eff}} = \epsilon + \epsilon_J$ as an "effective potential energy" we obtain an energy curve as shown in Fig. 42, curve II. It is seen from this figure, curve II, that, in contrast with the usual potential curve I, at a certain $X = X^*$ there is a gentle maximum which should be considered as the transition state of the unimolecular decomposition reaction $\text{AB} \rightarrow \text{A} + \text{B}$. It is evident that the activated state for the reverse reaction $\text{A} + \text{B} \rightarrow \text{AB}$ will be the same.

The value of X^* may be determined for each rotational quantum number from the condition $d\epsilon_{\text{eff}}/dX = 0$. For example, according to spectroscopic data [54], for the HgH molecule when $J = 20$, $X^* \approx 2.7 \text{ \AA}$ ($X_0 = 1.74 \text{ \AA}$) and the height of the barrier is about 1 kcal. To find the mean \bar{X}^* it is necessary to find the mean value of J (for the given temperature) and substitute it in the $X^*(J)$ function. The value of the interatomic distance \bar{X}^* obtained in this way for a recombination reaction is the effective collision diameter of A and B. Calculations [57] show that its value is a few times greater than the equilibrium interatomic distance in the AB molecule. For example, \bar{X}^* is between 4 and 5 \AA for two hydrogen atoms. On this basis it might be suggested that in an approximate calculation of the interatomic distance corresponding to the activated complex of a decomposition (or recombination) reaction we could use for $\epsilon(X)$ the expression for the energy of dispersion (or, in general, van der Waals) interaction [57].

Since the configuration of the activated complex corresponding to the top of the rotational barrier is similar to the configuration of the initial molecule, their partition functions (save that referring to the reaction coordinate) will have the same form and will differ only in moments of inertia and vibrational frequencies. Substituting the appropriate expression for Z into (12.10) for an initial molecule with N atoms and $3N-6$ vibrations, we find

$$k = \kappa \frac{s_1 (A^* B^* C^*)^{1/2}}{s^* (A_1 B_1 C_1)^{1/2}} \times \frac{\prod_{3N-6}^{3N-7} [1 - \exp(-h\nu_i/kT)]^{-1} kT}{\prod_{3N-6}^{3N-7} [1 - \exp(-h\nu_i/kT)]^{-1}} \frac{h}{\hbar} \exp(-E_0/RT). \quad (12.60)$$

As the height of the rotational barrier is usually quite small compared with the dissociation energy, here E_0 may be taken as the energy for dissociation of the molecule at the given bond (at the absolute temperature zero). This expression does not depend explicitly on the mass of the molecule as the translational partition functions of the initial and activated states cancel. The ratio of the symmetry numbers usually is not very different from

unity. On stretching the bond to be broken, as a rule, only one of the three principal moments of inertia, A say, may increase appreciably. For this reason, in the limiting case when $h\nu_1 \gg kT$ and $h\nu^* \gg kT$ we may replace (12.60) simply by

$$k = \kappa \frac{kT}{h} \left(\frac{A^*}{A_1} \right)^{1/2} \exp(-E_0/RT). \quad (12.61)$$

At ordinary temperatures $kT/h \approx 10^{13}$ sec⁻¹; in this case if $A^*/A_1 \approx 1$, then

$$k = 10^{13} \kappa \exp(-E_0/RT). \quad (12.62)$$

In the other limiting case when $h\nu_1 \ll kT$ and $h\nu^* \ll kT$, we find

$$k = \kappa \frac{\prod_{v=1}^{3N-6} v_1}{\prod_{v=1}^{3N-7} v^*} \left(\frac{A^*}{A_1} \right)^{1/2} \exp(-E_0/RT). \quad (12.63)$$

If the vibrational frequencies in the initial molecule and the activated complex are little different and, in addition, $A^*/A_1 \approx 1$, then this expression becomes

$$k = \kappa v_1 \exp(-E_0/RT), \quad (12.64)$$

where v_1 refers to the bond which is ruptured. At ordinary temperatures this may be valid when $v_1 \leq 10^{12}$ sec⁻¹.

When the bond to be broken is stretched considerably in forming the activated complex, the ratio of the moments of inertia in (12.61) and (12.63) will be somewhat greater than unity. However we cannot explain in this way cases where the pre-exponential factor in the equation for the rate of unimolecular decomposition is of the order 10^{15} to 10^{16} (for a more detailed treatment of unimolecular reactions, see Chap. 5).

It can be seen from (12.53) and (12.57) that the expression for the partition function of the activated complex also contains quantities such as moments of inertia, vibrational frequencies, effective mass and symmetry number, which are characteristic of its configuration. In principle these quantities, like the activation energy, might be calculated theoretically if the potential-energy surface were known well enough.

In practice, however, as we have noted, the activation energy must be derived from experimental data and for the other quantities we are limited to approximate evaluation based on assumptions regarding the configuration of the activated complex. In certain cases, such as unimolecular and Menshutkin reactions, there are grounds for considering the activated complex to have a configuration similar to the configurations of the initial or final molecules. The estimation of the characteristic parameters of the transition state is then easier.

Dependence of Reaction Rate on Isotopic Composition of the Reacting Molecules [396, 397]

Replacing one or several atoms in a molecule by their isotopes leads to a change in the rate of an elementary chemical reaction. Since the potential surface corresponding to a given elementary reaction does not depend on the masses of the atoms in the reacting molecules, the isotope effect is determined entirely by the fact that the rate constant depends on the masses of these atoms, either explicitly or through a vibrational frequency, moment of inertia or symmetry number.

To obtain a formula for the ratio of the rates of two reactions of type $A + B \rightarrow C$ which differ only in the isotopic composition of one of the molecules, A for example, we shall use equation (12.14). In this case we find

$$\frac{k_1}{k_2} = \frac{\kappa_1 K_1^*}{\kappa_2 K_2^*}, \quad (12.65)$$

where the suffixes 1 and 2 refer to the reactions which involve "light" and "heavy" A molecules respectively. The ratio of K_1^* and K_2^* may be written on the basis of (12.13):

$$\frac{K_1^*}{K_2^*} = \frac{Z_1^* Z_{A_1} \exp[-(\Sigma h\nu_1^* - \Sigma h\nu_1)/2kT]}{Z_2^* Z_{A_2} \exp[-(\Sigma h\nu_2^* - \Sigma h\nu_2)/2kT]}, \quad (12.66)$$

where $\frac{1}{2}\Sigma h\nu^*$ and $\frac{1}{2}\Sigma h\nu$ are the sums of the zero-point energies with respect to the vibrational degrees of freedom of the activated complex and the A molecule respectively. The "classical" activation energy E_{cl} , according to the above, does not depend on the isotopic masses and therefore falls out of expression (12.66).

If x is the total number of atoms contained in the reacting molecules ($x = x_A + x_B$), we find for the partition-function ratios

$$\frac{Z_1^*}{Z_2^*} = \left(\frac{M_{A_1}^*}{M_{A_2}^*} \right)^{3/2} \frac{(A_1^* B_1^* C_1^*)^{1/2} s_2^*}{(A_2^* B_2^* C_2^*)^{1/2} s_1^*} \frac{\prod_{3x-7} [1 - \exp(-h\nu_1^*/kT)]^{-1}}{\prod_{3x-7} [1 - \exp(-h\nu_2^*/kT)]^{-1}}, \quad (12.67)$$

$$\frac{Z_{A_1}}{Z_{A_2}} = \left(\frac{M_{A_1}}{M_{A_2}} \right)^{3/2} \frac{(A_{A_1} B_{A_1} C_{A_1})^{1/2} s_{A_2}}{(A_{A_2} B_{A_2} C_{A_2})^{1/2} s_{A_1}} \frac{\prod_{3x_A-6} [1 - \exp(-h\nu_1/kT)]^{-1}}{\prod_{3x_A-6} [1 - \exp(-h\nu_2/kT)]^{-1}}. \quad (12.68)$$

Here the symmetry number s also includes the statistical weights of the ground state of the nuclei. The quantities M_A and M^* are the molecular weights of the A molecule and activated complex; the symbol Π represents

the product with respect to all the vibrational degrees of freedom of the molecule or complex.

We shall now use the theorem of Redlich [1057] and Teller (see [53], p. 250), according to which the ratio

$$\frac{M^{3/2}(ABC)^{1/2}}{\prod_{i} \prod_{\nu_i} \prod_{k} m_k^{3/2}} \quad (12.69)$$

does not depend on the mass of the molecule (or activated complex) under consideration. In (12.69), $\prod_{i} \nu_i$ and $\prod_{k} m_k$ are, respectively, the product of all the normal vibrational frequencies and the product of all the atomic masses in the system considered. For the activated complex the "frequency" corresponding to the reaction coordinate should be taken as represented by the expression

$$\nu^* = \left(\frac{\partial^2 U}{\partial l^2} \right)_{\#}^{1/2} / (2\pi m^{\#1/2}), \quad (12.70)$$

where m^* is the reduced mass of the activated complex corresponding to motion along the reaction coordinate and $(\partial^2 U / \partial l^2)_{\#}$ is the second derivative of the potential energy with respect to this coordinate at the maximum. As $(\partial^2 U / \partial l^2)_{\#} < 0$, the frequency ν^* is an imaginary quantity.

Using (12.69), expression (12.67) may be rewritten:

$$\frac{Z_1^*}{Z_2^*} = \frac{\nu_1^* \prod_{i}^{3x-7} \nu_{i_1} \prod_{k}^{x} m_{k_1}^{3/2} s_2^* \prod_{i}^{3x-7} [1 - \exp(-h\nu_1^*/kT)]^{-1}}{\nu_2^* \prod_{i}^{3x-7} \nu_{i_2} \prod_{k}^{x} m_{k_2}^{3/2} s_1^* \prod_{i}^{3x-7} [1 - \exp(-h\nu_2^*/kT)]^{-1}}. \quad (12.71)$$

A similar equation may be written for Z_{A_1}/Z_{A_2} . Substituting all these expressions into (12.65) and introducing the notation

$$u = h\nu_2/kT, \quad \Delta u = (\nu_1 - \nu_2)h/kT,$$

we find from (12.66) after simple rearrangements

$$\begin{aligned} \frac{k_1}{k_2} &= \frac{\kappa_1 s_2^* s_{A_1}}{\kappa_2 s_1^* s_A} \left(\frac{m_2^*}{m_1^*} \right)^{1/2} \times \\ &\times \prod_{i}^{3x-6} \frac{u_i}{u_i + \Delta u_i} \exp(\Delta u_i/2) \frac{1 - \exp[-(u_i + \Delta u_i)]}{1 - \exp(-u_i)} \times \\ &\times \prod_{i}^{3x-7} \frac{u_i^* + \Delta u_i^*}{u_i^*} \exp(-\Delta u_i^*/2) \frac{1 - \exp(-u_i^*)}{1 - \exp[-(u_i^* + \Delta u_i^*)]}. \end{aligned} \quad (12.72)$$

As Δu is usually small compared with u , expression (12.72) may be expanded into a series with respect to Δu_i and Δu_i^* [398]. In the most interesting case of molecules containing hydrogen, however, the difference Δu in vibrational energies is so large that the corresponding formula is not applicable and expression (12.72) should be used as it stands.

The difficulty in applying formula (12.72) in practice is that the calculation of the effective mass m^* and of the vibrational frequencies of the activated complex is complicated. For certain three-atom reactions of type $A + BC \rightarrow AB + C$ Bigeleisen and Wolfsberg [399] have calculated possible values of m_2^*/m_1^* which allow us, by comparison with the measured values of k_1/k_2 , to come to certain conclusions regarding the mechanisms of the reactions considered. See also [809a, 1031a and review 1284a].

The Transmission Coefficient

As we mentioned above, the transmission coefficient κ in equation (12.10) is the probability that the system, having reached the activated state, actually reacts, i.e. proceeds to the final state. A qualitative picture has been given above (§11) showing the classical motion of a representative point over a potential-energy surface, and it was noted that for adiabatic reactions the possibility of a representative point returning to the initial state (i.e. the deviation of κ from unity) should be connected mainly with the curvature of the reaction path and also with the possible occurrence of a basin near the top of the pass (p. 171).

Quantitative treatment of the transmission coefficient is, strictly speaking, a quantum-mechanical problem requiring a knowledge of the equation of the potential-energy surface of the system. Owing to the mathematical difficulties, however, the problem has been solved only for a few of the simplest models.

As the potential surface near the line of the reaction path is approximately represented by part of the surface of a curved groove or channel, it is necessary to explain the influence on κ of the curvature of the cross-section of this groove, of the presence in it of a potential barrier and, finally, of the curvature of the groove itself (i.e. of the reaction path). Investigations show that the transmission coefficient is the smaller, the higher the curvature of the cross-section of the channel at the saddle point [1321]. In absolute magnitude, however, this influence is small: the deviation of κ from unity is apparently not more than 3% even for the $H_2 + H = H + H_2$ reaction, for which the greatest effect would be expected.

The effect of the reaction-path curvature on κ has been studied for the case where the groove contains a right-angled bend [304]. It was shown that, although this curvature also lowers the mean value of κ , the transmission coefficient in this case is also not very different from unity.

Matsen [927] has calculated the transmission coefficient for the

one-dimensional case assuming that the potential barrier has a rectangular shape (Fig. 43). In this case he was able to express κ in equation (12.9) as an explicit function of p^* . He showed that equation (12.10) retains its form but that the mean value of κ now depends on the temperature, activation energy and heat of reaction. Matsen found that with his assumptions the transmission coefficient is less than unity, increases with temperature and decreases with an increase in activation energy and heat of reaction (for the exothermic direction). On smoothing out the angles of the potential barrier, however, the effect of these factors decreases and the value of κ increases.

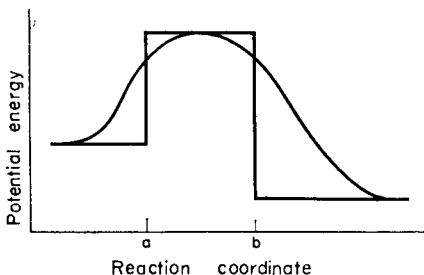


FIG. 43. Potential-energy barrier according to Matsen [927].

De Vogelaere and Boudart [1251] have calculated transmission coefficients for fast reactions of the type $AB + A \rightarrow A + BA$. Using classical mechanics to treat the motion of a representative point on a potential-energy surface with one saddle point, they found that at sufficiently high temperatures the transmission coefficient becomes much less than unity. In this case the temperature must be so high that the mean energy of the representative point is greater than the critical value

$$E^* = \frac{2(m_1 + m_2)}{2m_1 + m_2} E$$

(with the condition that $0 < E < 0.12D$, where D is the heat of dissociation of the A—B bond). This result does not depend on the particular shape of the potential surface, and may be important for reactions in flames.

The transmission coefficient of adiabatic reactions may show particularly large deviations from unity when two potential-energy surfaces, referring to different electronic states of the system, pass sufficiently close to each other in the neighbourhood of a certain point, i.e. when the difference in energy of two states of the system is small for a certain nuclear configuration. In this case a representative point moving with a certain velocity on one of these potential surfaces, the lower one for example, will

have a finite probability of jumping over to the other potential surface (non-adiabatic nuclear motion) (see Fig. 23 on p. 127). If the probability χ of such a transition is quite high the probability ($\rho = 1 - \chi$) of the converse event, i.e. the probability that the system remains on the lower surface (adiabatic nuclear motion), is very low. It is clear that this probability ρ should be included in the equation for the rate of the adiabatic reaction as a factor in the transmission coefficient. This problem will be considered in more detail in connection with non-adiabatic reactions (§13).

Comparison of Formulae from Gas-kinetic Theory and from the Transition-state Method

We have mentioned above, in §8, that simple collision theory and the activated-complex method proceed from substantially the same basic ideas. The most important of these is the idea that the rate of a given elementary process is the same whether there is statistical equilibrium (a Maxwell–Boltzmann distribution) or not. Thus in collision theory a Maxwellian distribution is used to determine the number of reacting molecules with a given velocity [equation (9.3)], while in the transition-state method partition functions are used in an expression [equation (12.4)] for the number of activated complexes. In simple collision theory, the collision number for the rate of reaction includes all collisions taking place with energy greater than a certain level. In the activated-complex method, however, by introducing partition functions account is taken only of such of these collisions as lead to the required redistribution of energy among the various degrees of freedom. This gives the transition-state method a certain advantage.

The rate-constant formula (9.22) provided by gas-kinetic theory and the formula (12.21) of the transition-state method are both in the form of an Arrhenius equation. As we have shown, however, the weakness of simple collision theory is that in practice it does not allow us to calculate the probability factor P , and it is therefore unable to explain the reason for the low rates of certain reactions. The advantage of the transition-state method is that it does enable us to calculate the absolute value of the pre-exponential factor apart from a transmission coefficient, which may usually be taken as equal to unity.

Comparison of formulae (9.22) and (12.21) shows that

$$PZ_0 = \kappa \frac{k T_0}{h} \frac{Z^*}{Z_A Z_B}. \quad (12.73)$$

It is possible to calculate P from this. As we shall see below, in certain cases this relation yields values of P much less than unity, and this enables us to explain the low values of the probability factor in “slow” reactions.

Let us first consider the simplest process—the collision of atoms A

and B. In this case, gas-kinetic theory gives us a precise formula (9.15) for the number of collisions per second in 1 cm³. The same number may be obtained using the activated-complex method if we take as the activated complex a complex A.B in which the atoms are in direct contact so that the internuclear distance is equal to the sum $r_A + r_B$ of their radii. A complex of this type has three translational degrees of freedom of the centre of gravity and two rotational degrees of freedom; the sixth degree of freedom of the complex, unlike that of a diatomic molecule, is not a vibration but a translational motion along the reaction coordinate, which coincides in this case with the interatomic distance. In accordance with (12.45) and (12.47), therefore, the partition function of the activated complex is

$$Z^* = \frac{[2\pi(m_A + m_B)kT]^{3/2}}{h^2} \frac{8\pi^2 I k T}{h^3}, \quad (12.74)$$

where m_A and m_B are the masses of atoms A and B. The moment of inertia of the diatomic complex A.B is

$$I = (r_A + r_B)^2 \frac{m_A m_B}{m_A + m_B}. \quad (12.75)$$

In the initial state, the atoms possess only translational degrees of freedom and hence

$$Z_A = \frac{(2\pi m_A k T)^{3/2}}{h^3}, \quad Z_B = \frac{(2\pi m_B k T)^{3/2}}{h^3}. \quad (12.76)$$

Substituting (12.74)–(12.76) in equation (12.10) and taking $\kappa = 1$ and $\epsilon_0^* = 0$, we find the number of collisions per second in 1 cm³, for $n_A = n_B = 1$, is

$$Z_0 = (r_A + r_B)^2 \left(\frac{8\pi k T}{\mu} \right)^{1/2}, \quad (12.77)$$

where $\mu = m_A m_B / (m_A + m_B)$. This expression is the same as the collision-theory equation (9.15) if we take $d_0 = r_A + r_B$. Thus both methods yield the same result for cases involving the simple collision of two atoms.⁽⁵⁰⁾

In order to compare these methods as applied to the calculation of the rates of reactions between two molecules or between a molecule and a radical, let us write the complete partition functions, Z , as the products of the partition functions for the individual degrees of freedom. For simplicity, we shall assume that the partition function for a given type of

⁽⁵⁰⁾ This agreement is sometimes regarded as evidence of the accuracy of the activated-complex method. We should note, however, that this agreement cannot in itself be used as a criterion of the accuracy of the fundamental premises of this method, as the same premises underlie simple collision theory.

motion has the same value for each of the initial molecules (or radicals) and for the activated complex.

Then in the case of two atoms we have

$$Z^* = \bar{Z}_{\text{trans}}^3 \bar{Z}_{\text{rot}}^2; \quad Z_A = Z_B = \bar{Z}_{\text{trans}}^3.$$

Consequently, if we take $\kappa \approx 1$, the pre-exponential factor in equation (12.10) will be

$$A = \frac{kT}{h} \frac{Z^*}{Z_A Z_B} \approx \frac{kT}{h} \frac{\bar{Z}_{\text{rot}}^2}{\bar{Z}_{\text{trans}}^3}. \quad (12.78)$$

As we have seen above, this expression agrees (within the limits of our approximation) with the collision number, Z_0 , of (12.77).

If the reacting molecules (or molecule and radical) A and B contain x_A and x_B atoms, their partition functions are written in the form (assuming a non-linear structure of the initial molecules):

$$Z_A = \bar{Z}_{\text{trans}}^3 \bar{Z}_{\text{rot}}^3 \bar{Z}_{\text{vib}}^{3x_A-6}; \quad Z_B = \bar{Z}_{\text{trans}}^3 \bar{Z}_{\text{rot}}^3 \bar{Z}_{\text{vib}}^{3x_B-6}; \quad (12.79)$$

$$Z^* = \bar{Z}_{\text{trans}}^3 \bar{Z}_{\text{rot}}^3 \bar{Z}_{\text{vib}}^{3(x_A+x_B)-7}. \quad (12.80)$$

The pre-exponential factor is equal to

$$A_1 \approx \frac{kT}{h} \frac{\bar{Z}_{\text{vib}}^5}{\bar{Z}_{\text{trans}}^3 \bar{Z}_{\text{rot}}^3}. \quad (12.81)$$

This expression differs from (12.78) and hence from Z_0 ; according to (9.20) it should be equal to the product PZ_0 . Assuming, therefore, that $A = Z_0$ and $A_1 = PZ_0$, equations (12.78) and (12.81) give

$$P \approx \left(\frac{\bar{Z}_{\text{vib}}}{\bar{Z}_{\text{rot}}} \right)^5. \quad (12.82)$$

The quantity \bar{Z}_{vib} is usually near unity and \bar{Z}_{rot} is usually of the order $10-100$.⁽⁵¹⁾ According to (12.82), therefore, the probability factor P for a reaction between complex molecules (or a molecule and radical) may vary within the limits 10^{-5} and 10^{-10} .

Expression (12.82) was obtained for two polyatomic, non-linear initial molecules. In other cases rather different values are obtained for the probability factor as shown in Table 5.

Since $\bar{Z}_{\text{vib}}/\bar{Z}_{\text{rot}} \approx 10^{-1}$ to 10^{-2} , we may conclude from this Table that the probability factor is near unity only in the case of reactions between atoms and simple molecules (or radicals) with small moments of inertia.

⁽⁵¹⁾ This follows, for example, from formula (12.47), according to which $\bar{Z}_{\text{rot}}^2 = 8\pi^2 k T I / h^2$. At normal temperatures $\bar{Z}_{\text{rot}}^2 \approx 2 \times 10^{41} I$. The moments of inertia of most molecules are between 3×10^{-40} and 5×10^{-38} gcm².

TABLE 5 [57]

PROBABILITY FACTORS FOR SOME TYPES OF REACTING PARTICLES

Types of reacting particles	P
I Two atoms	1
II Atom and diatomic molecule:	
(a) Non-linear complex	$Z_{\text{vib}}/Z_{\text{rot}}$
(b) Linear complex	$(Z_{\text{vib}}/Z_{\text{rot}})^2$
III Atom and polyatomic molecule	$(Z_{\text{vib}}/Z_{\text{rot}})^2$
IV Two diatomic molecules (or a diatomic radical and diatomic molecule):	
(a) Non-linear complex	$(Z_{\text{vib}}/Z_{\text{rot}})^3$
(b) Linear complex	$(Z_{\text{vib}}/Z_{\text{rot}})^4$
V Diatomic molecule (or radical) and polyatomic molecule (or radical)	$(Z_{\text{vib}}/Z_{\text{rot}})^4$
VI Two polyatomic molecules (or a polyatomic radical and polyatomic molecule)	$(Z_{\text{vib}}/Z_{\text{rot}})^5$

Table 5 shows that the greater the complexity of the reacting molecules (radicals) the smaller the probability factor, and when the initial particles are polyatomic, marked divergences from simple collision theory are to be expected. This conclusion is supported by experimental data. The experimental values of the pre-exponential factor A in the Arrhenius equation

TABLE 6 [1170]
PRE-EXPONENTIAL FACTORS FOR SOME RADICAL REACTIONS

Reaction	$A = PZ$
$H + H_2 \rightarrow H_2 + H$	3.5×10^{13}
$D + NH_3 \rightarrow H + NH_2D$	2.0×10^{13}
$D + PH_3 \rightarrow H + PH_2D$	1.5×10^{13}
$Br + CH_4 \rightarrow HBr + CH_3$	1.5×10^{12}
$Br + H_2 \rightarrow HBr + H$	1.1×10^{12}
$Br + CH_3Br \rightarrow HBr + CH_2Br$	1.3×10^{12}
$CH_3 + CH_3COCH_3 \rightarrow CH_4 + CH_2COCH_3$	5.0×10^{11}
$CH_3 + C_2H_6 \rightarrow CH_4 + C_2H_5$	2.0×10^{11}
$CH_3 + C_4H_{10} \rightarrow CH_4 + C_4H_9$	1.0×10^{11}
$CH_3 + C_5H_{12} \rightarrow CH_4 + C_5H_{11}$	2.0×10^{11}
$(C_6H_5 \cdot C_6H_4)_3C + C_6H_5CH_3 \rightarrow (C_6H_5 \cdot C_6H_4)_3CH + C_6H_5CH_2$	2.0×10^{10}
$(C_4H_9 \cdot C_6H_4)_3C + C_6H_5CH_3 \rightarrow (C_4H_9 \cdot C_6H_4)_3CH + C_6H_5CH_2$	5.0×10^9

are shown for a number of radical reactions in Table 6. It can be seen from this Table that, as was to be expected, the value of A shows a marked tendency to decrease for reacting particles of increasing complexity, and for the series in question there is a decrease in A of 10^4 . Considering that as the number of atoms in the colliding particles increases, the total diameters also increase, it is readily seen that the decrease in the P factor in the same series will be even more marked.

As we have mentioned, the deviation of P from unity in adiabatic reactions is mainly due to the fact that simple gas-kinetic theory makes no allowance for energy transfer from one degree of freedom of the colliding molecules to another. In point of fact, the conversion of part of the rotational degrees of freedom of the initial molecules into vibrational degrees of freedom of the activated complex has an important effect on the rate of the process. Usually, $\bar{Z}_{\text{vib}} < \bar{Z}_{\text{rot}}$, and so this process is slow. The higher the number of degrees of freedom involved in this kind of conversion, the slower is the process as a whole. According to (12.16), the pre-exponential factor may be expressed in terms of entropy change. We may say, therefore, that in the case of a reaction between atoms or simple molecules, the entropy change on formation of the activated complex is relatively slight, and simple collision theory is applicable. In the case of complex molecules, the entropy of activation is considerably less, mainly because of losses of rotational degrees of freedom. Thus, in reactions of complex molecules, by no means all collisions lead to formation of an activated complex, even when the kinetic or total energy of the colliding particles is sufficient. This demonstrates the inadequacy of simple gas-kinetic theory as applied to complex molecules.

It is seen from Table 5 that, for the same initial molecules, the conversion of rotational into vibrational motion involves different numbers of degrees of freedom when the configurations of the activated complex differ. This leads to different values of the probability factor P , depending on the orientation requirements for the colliding molecules. In this way the transition-state method gives a natural solution for the “steric factor” problem which remained unsolved by the methods of simple collision theory.

§13. Quantum-mechanical Treatment of the Rate of Elementary Processes

The use of quantum mechanics in calculating the rates of elementary physical processes—inelastic collisions not accompanied by rearrangement of atoms—has led to a well-developed theory with great scope for prediction [193]. In contrast, quantum mechanical calculations of elementary chemical processes are in a rudimentary state.

We shall give below the basis of quantum-mechanical calculation of the rates of elementary processes both for the adiabatic and for the non-adiabatic motion of nuclei.

Methods of Calculating the Probability of a Change of State on Collision

Calculations of the probabilities of transition from one state to another during an inelastic collision are based on the assumption that the perturbation causing the transition is sufficiently small. It is then possible to obtain

general formulae for the probabilities of transition, applicable alike to collisions of electrons and atoms and to collisions of atoms or molecules with each other [formulae (8.11), (8.12), p. 123, 124]. Several approximate methods of calculating the matrix elements involved in these formulae have been developed, the chief ones being *the Born method* and *the distorted wave method*. Both methods will be considered briefly here.

Born's approximate method (the Born approximation) is applicable when the potential energy of the colliding particles can be regarded as a slight perturbation, i.e. when the kinetic energy of their relative motion is sufficiently large. A close consideration of this problem (see [168], §45) leads to the conclusion that this assumption is justified when

$$|U_{\max}| \ll \frac{\hbar v}{a}. \quad (13.1)$$

Here a is the linear dimension of the region in which the potential energy U differs considerably from zero, and v is the relative velocity of the particles. Consequently the greater the relative velocity, the better the grounds for applying Born's perturbation theory. Note that the mass does not enter into (13.1).

When the particles interact according to Coulomb's law it is not possible to delimit a region where U differs from zero. In this case, taking $U = \alpha/r$ and replacing a by r , we find, instead of (13.1)

$$\hbar v/\alpha \gg 1. \quad (13.2)$$

Thus in this case too, if the relative velocity of the particles is sufficiently great, the potential energy of their interaction may be regarded as a slight perturbation.

Let us first consider a collision between an electron and an atom with Z electrons. As the mass of the atom is considerably greater than that of the electron, we may assume that the atom remains stationary during the process of collision. Let Ψ_n be the wave function of the electrons of the atom before collision, and Ψ_n' that after collision. The change in internal energy of the atom as a result of collision is equal to $E_n' - E_n$. According to the law of conservation of energy this difference must be equal to the change in the kinetic energy of the impinging electron, i.e.

$$E_n' - E_n = \frac{p^2}{2m} - \frac{p'^2}{2m}. \quad (13.3)$$

Here p and p' are the initial and final values of the momentum of the electron, and m is its mass.

Let us denote the wave functions of the electron before and after collision by $\chi_p(r)$ and $\chi_{p'}(r)$ respectively. We have agreed to regard $U(r)$, the potential energy of the electron in the field of the atom, as a small

perturbation, and so the χ wave functions may be treated to a first approximation, as eigenfunctions of the free electron, i.e.

$$\chi_p^0(\mathbf{r}) = (2\pi\hbar)^{-3/2} \exp\left(-\frac{i\mathbf{p}\cdot\mathbf{r}}{\hbar}\right), \quad (13.4)$$

$$\chi_{p'}^0(\mathbf{r}) = (2\pi\hbar)^{-3/2} \exp\left(-\frac{i\mathbf{p}'\cdot\mathbf{r}}{\hbar}\right). \quad (13.5)$$

Here function (13.5) is normalized in such a way that $\chi_{p'}^0(\mathbf{r})\chi_{p'}^{0*}(\mathbf{r}) dx dy dz$ gives the probability of an electron in the volume element $d\tau = dx dy dz$ having momentum p' with components p'_x , p'_y and p'_z .

In order to discuss inelastic collisions of an electron it is more convenient to normalize $\chi_p^0(\mathbf{r})$ in such a way that it is possible to find the probability of scattering the electron into a certain direction characterized by the elementary solid angle $d\Omega = 2\pi \sin \theta d\theta$. A necessary requirement for this is that the electron current over an area S per second per cm^2 should be equal to 1, i.e.

$$\int_{\Omega=1} v \chi_p^0(\mathbf{r}) \chi_p^{0*}(\mathbf{r}) dS = 1.$$

In this case, instead of (13.5), we find

$$\chi_p^0(\mathbf{r}) = v^{-1/2} \exp(-i\mathbf{p}'\cdot\mathbf{r}/\hbar). \quad (13.6)$$

The problem is now that of finding the probability of transition (per second) of the system from an initial state n , corresponding to the function

$$\Phi_n^0 = \Psi_n \chi_p^0(\mathbf{r}), \quad (13.7)$$

to a final state characterized by the function

$$\Phi_{n'}^0 = \Psi_{n'} \chi_{p'}^0(\mathbf{r}). \quad (13.8)$$

In this final state the electron has a momentum p' and moves within a solid angle $d\Omega = 2\pi \sin \theta d\theta$, while the atom is in the n' state.

To solve this problem, we shall use the theory of quantum transitions under time-independent perturbations (see p. 123). In our case, the perturbation is the energy $U(r)$. Applying (8.11) we find for the required probability

$$P_{nn'} d\Omega = \frac{2\pi}{\hbar} |U_{nn'}|^2 m p' d\Omega. \quad (13.9)$$

Here

$$U_{nn'} = \int \int \Phi_n^0 U \Phi_{n'}^{0*} d\tau d\tau', \quad (13.10)$$

and integrating with respect to τ means integrating with respect to the coordinates of all Z electrons of the atom, while integrating with respect to τ' means integrating with respect to the coordinates of the incident electron.

It is easy to see that if the functions χ_p^0 and $\chi_{p'}^0$ are normalized according to (13.4) and (13.6) the quantity $P_{nn'} d\Omega$ expressed by equation (13.9) has the dimensions of area; it represents an effective (differential) collision cross section, $d\sigma$. Substituting (13.4) and (13.6) in (13.9), therefore, and taking account of the relation $p = mv$, we find

$$d\sigma = \left(\frac{m}{2\pi\hbar^2} \right)^2 \frac{p'}{p} \left| \int \int U \exp(iqr) \Psi_n \Psi_{n'}^* d\tau d\tau' \right|^2 d\Omega, \quad (13.11)$$

where

$$q = \frac{\mathbf{p} - \mathbf{p}'}{\hbar}, \quad (13.12)$$

and p' is determined by the law of conservation of energy, (13.3).

The expression (13.11) for the effective cross section is valid not only for the collision of an electron and an atom, but also for the collision of any two particles, provided that (13.1) is satisfied. In the general case, m should be taken as the reduced mass of the colliding particles, and (13.11) will represent the probability of the process in a system of coordinates in which the mass centre of the particles is at rest.

According to (13.3), if the collision is elastic, i.e. if $E_n = E_{n'}$, then $p' = p$ and (13.11) takes the form

$$d\sigma_{\text{elast}} = \left(\frac{m}{2\pi\hbar^2} \right)^2 \left| \int \int U \exp(iqr) \Psi_n \Psi_{n'}^* d\tau d\tau' \right|^2 d\Omega. \quad (13.13)$$

For a non-elastic collision of an electron and an atom, formula (13.11) may be made a little more specific. The energy U in this case is

$$U = \frac{Ze^2}{r} - \sum_{l=1}^Z \frac{e^2}{r_l}, \quad (13.14)$$

where Ze is the charge of the nucleus, r is the distance of the incident electron from the nucleus, and r_l is the distance between this electron and the l th electron of the atom.

Substituting (13.14) in (13.11) and noting that, as the functions Ψ_n and $\Psi_{n'}$ are orthogonal, the integral containing Ze^2/r will be equal to zero, we obtain

$$d\sigma = \left(\frac{m}{2\pi\hbar^2} \right)^2 \frac{p'}{p} \left| \int \int \sum_{l=1}^Z \frac{e^2}{r_l} \exp(iqr) \Psi_n \Psi_{n'}^* d\tau d\tau' \right|^2 d\Omega. \quad (13.15)$$

Integrating with respect to τ' we find

$$d\sigma = \left(\frac{e^2 m}{\hbar^2} \right)^2 \frac{4k'}{q^4 k} \left| \int \sum_{l=1}^Z \exp(iqr_l) \Psi_n \Psi_{n'}^* d\tau \right|^2 d\Omega \quad (13.16)$$

(see, for example, [168]), where the momenta p and p' are replaced by vector wave numbers $\mathbf{k} = \mathbf{p}/\hbar$ and $\mathbf{k}' = \mathbf{p}'/\hbar$. Finally, integrating (13.16) with respect to all possible angles of scatter, we obtain the total effective cross section σ for the excitation of an atom from state n to state n' . Figure 91 (p. 468) shows the characteristic curves for the dependence of σ on the kinetic energy $K = p^2/2m$ of the bombarding electrons (the excitation function).

Into expression (13.16) instead of $d\Omega = 2\pi \sin \theta d\theta$ we may introduce dq , which is defined by the relation (cf. (13.12))

$$q^2 = k^2 + k'^2 - 2kk' \cos \theta.$$

The differential cross section will then be

$$d\sigma = 8\pi \left(\frac{e^2}{\hbar v} \right)^2 \frac{dq}{q^3} \left| \int \sum_l \exp(iqr_l) \Psi_n \Psi_{n'}^* d\tau \right|^2. \quad (13.17)$$

It follows from this that if q is about the same size as the reciprocal of the linear dimension of the atom, then

$$\sigma = \text{constant}/v^2, \quad (13.18)$$

i.e. σ is inversely proportional to the square of the relative velocity [168].

As formula (13.17) does not contain the masses of the colliding particles, it is applicable not only to electrons but to any charged particles. In the general case, when the charge on the incident particle is Ze , (13.17) takes the form

$$d\sigma = 8\pi \left(\frac{Ze^2}{\hbar v} \right)^2 \frac{dq}{q^3} \left| \int \sum_l \exp(iqr_l) \Psi_n \Psi_{n'}^* d\tau \right|^2. \quad (13.19)$$

It should be mentioned at this point that the application of collision theory to inelastic collisions of atoms and molecules encounters serious difficulties connected with the fact that the expressions for the potential energy of the interaction of particles are usually extremely complicated. Rough approximations have therefore to be made in the calculations and these decrease their validity.

In many important problems concerning the inelastic collision of particles, the relative velocity of the particles is small, and so their kinetic energy cannot be regarded as large in comparison with the interaction

energy. In these cases neither (13.1) nor (13.2) holds and the Born approximation is not applicable. One of the methods best suited to such cases is the *distorted wave method*.

The essence of this method is as follows. In the Born method, as a first approximation to the wave functions of the electron before and after collisions we use the solutions (13.4) and (13.5) of the Schrödinger equations for a freely moving particle,

$$\left(\frac{\hbar^2}{2m} \nabla^2 + \frac{p^2}{2m} \right) \chi_p^0(\mathbf{r}) = 0 \quad (13.20)$$

and

$$\left(\frac{\hbar^2}{2m} \nabla^2 + \frac{p'^2}{2m} \right) \chi_{p'}^0(\mathbf{r}) = 0, \quad (13.21)$$

where $p^2/2m$ and $p'^2/2m$ are the kinetic energies of the electron before and after collision. The solution will obviously be more precise if allowance is made for the effect of the atomic field on the wave function of the incident and scattered electron. The mean field in which the electron is situated before its collision with the atom corresponds to the energy

$$U_{nn} = \int \Psi_n U \Psi_n^* d\tau,$$

where Ψ_n is the wave function of the atom in the initial state. Similarly the mean field for the scattered electron will be characterized by the energy

$$U_{n'n'} = \int \Psi_{n'} U \Psi_{n'}^* d\tau.$$

Thus, for the incident and scattered wave functions we may replace⁽⁵²⁾ (13.20) and (13.21) by

$$\left(\frac{\hbar^2}{2m} \nabla^2 + \frac{p^2}{2m} - U_{nn} \right) \chi_p(\mathbf{r}) = 0 \quad (13.22)$$

and

$$\left(\frac{\hbar^2}{2m} \nabla^2 + \frac{p'^2}{2m} - U_{n'n'} \right) \chi_{p'}(\mathbf{r}) = 0. \quad (13.23)$$

Here $\chi_p(\mathbf{r})$ and $\chi_{p'}(\mathbf{r})$ are functions (now depending on the character of U_{nn} and $U_{n'n'}$) of the momentum and the relative coordinates of the colliding particles. After due normalization of the functions χ_p and $\chi_{p'}$ the effective cross section corresponding to the transition of the atom from

⁽⁵²⁾ A more rigorous foundation of the distorted-wave method is given in [193] Chap. 8.

state n to n' will be determined, in a way similar to (13.11), by the formula

$$d\sigma = \left(\frac{m}{2\pi\hbar^2} \right)^2 \frac{p'}{p} \left| \int \int U \chi_p(\mathbf{r}) \chi_{p'}^*(\mathbf{r}) \Psi_n \Psi_{n'}^* d\tau' d\tau \right|^2 d\Omega. \quad (13.24)$$

This expression, therefore, allows for the distortion of incident and reflected waves by the field of the atom undergoing bombardment.

As atoms and molecules have masses considerably greater than electrons, they satisfy the conditions for the applicability of the Born approximation less often than do electrons. In solving the problem of inelastic collisions of atoms and molecules, therefore, it is more usual to use more precise methods, such as the distorted wave method. Some results of calculations using these methods will be considered in Chap. 6 and Chap. 8.

Rate of a Metathetical Reaction

As we have mentioned (pp. 117, 174), an initial premise of both gas-kinetic collision theory and the transition-state method is the assumption that the motion of atoms obeys the laws of classical mechanics. In gas-kinetic theory this assumption refers to all degrees of freedom, whereas in the transition-state method it refers only to the translational degrees of freedom. As we have seen (p. 130), this assumption is not always strictly fulfilled. On the other hand, quantum mechanical calculations of the transmission coefficient (p. 194) and calculations of the tunnel effect correction provide evidence that the motion of a representative point along the reaction path does not, for the most part, deviate greatly from the laws of classical mechanics. This may be shown directly by carrying out a quantum-mechanical calculation of the rate of a model reaction.

The methods of calculating cross sections, developed in the quantum theory of atomic and molecular collisions, may in principle be applied to a collision which is accompanied by redistribution of the particles, i.e. an elementary chemical process. In practice, however, considerable difficulties occur in these calculations. Above all it is of the utmost difficulty to formulate the problem in such a way that we are justified in applying the quantum theory of transitions, which assumes that the perturbation is quite small. There are, moreover, difficulties connected with the lack of sufficiently precise data on the potential-energy surfaces of many-particle systems. Even if the potential surfaces were known, however, a precise calculation of the rate constant would still not be very easy in practice, because of the complicated character of the dependence of the potential energy of a polyatomic system on the coordinates of the atoms, and the associated mathematical difficulties. These circumstances force us to use simplified models which allow us to calculate, albeit very approximately, the effective cross-section of a collision leading to chemical reaction.

The simplest example of such a process is the exchange reaction



where A, B and C are atoms. As in other processes of inelastic collision, the problem is that of finding the probability of a redistribution of the energy of a system between different degrees of freedom. If, for simplicity, we disregard rotational degrees of freedom and take the process as adiabatic, we are concerned with the redistribution of energy between the translational and vibrational degrees of freedom. As a method of calculating the rate constant of the reaction, we may use the theory of quantum transition due to a time-independent perturbation (pp. 123, 202).

The calculation made by Bauer and Wu [364] is based on the assumption that the energy conversion necessary for the reaction $AB + C \rightarrow A + BC$ occurs near the saddle point z of the potential-energy surface (Fig. 44), so

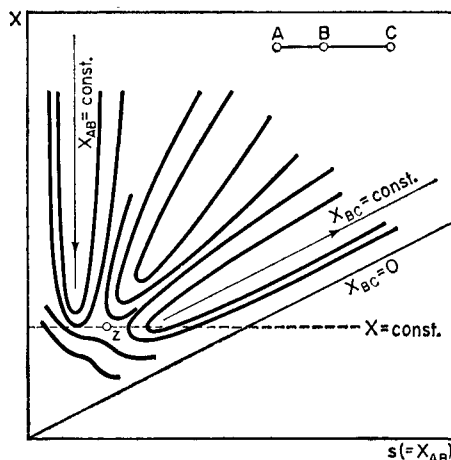


FIG. 44. Potential-energy surface for the reaction $AB + C \rightarrow A + BC$ (according to Bauer and Wu [364]).

that we can here introduce the small perturbation causing transition. In addition, Bauer and Wu assume that during the $AB + C$ collision, the atoms are in a straight line. It is convenient to use as independent coordinates the distance s between A and B, and the distance r between C and the centre of the masses of A and B, i.e.

$$\left. \begin{aligned} s &= r_{AB}; \\ r &= r_{BC} + \frac{m_A r_{AB}}{m_A + m_B}. \end{aligned} \right\} \quad (13.25)$$

With these coordinates the Schrödinger equation contains no cross-term

In order to separate the variables, the potential energy near the saddle point in the zeroth approximation, (W^0), is taken as a sum of two terms, one in each coordinate:

$$W^0(s, r) = U(s, r_z) + V(s_z, r). \quad (13.26)$$

The deviation from W^0 is considered as a perturbation $\Delta W(s, r)$ which is written

$$\Delta W(s, r) = \left[\frac{\partial U(s, r)}{\partial r} \right]_{r_z} (r - r_z) + \left[\frac{\partial V(s, r)}{\partial s} \right]_{s_z} (s - s_z), \quad (13.27)$$

where, as in (13.26), the suffix z refers to coordinates at the saddle point. In this way $W(s, r)$ is expressed as a series in $r - r_z$ and $s - s_z$, which may be approximated by the linear terms. If the functions $U(s, r_z)$ and $V(s_z, r)$ are chosen similarly the Schrödinger equation may be solved to a zeroth approximation. Then, using the resulting eigenfunctions $\phi_n(s)$ [for $U(s)$] and $\chi(r)$ [for $V(r)$], the probability of the transition $AB + C \rightarrow A + BC$ due to the perturbation ΔW may be determined. It is assumed here that the probability (α) of this transition is equal, apart from any transmission coefficient, to the probability of reaching the activated state z . The latter probability is proportional to

$$\left| \int \int \varphi_0 \chi_0 \Delta W \varphi_z \chi_z \, ds \, dr \right|^2, \quad (13.28)$$

where φ_0 and χ_0 are the wave functions of the initial state ($AB + C$) and φ_z and χ_z are those of the activated state ($A \dots B \dots C$).

For $U(s)$ we choose a function corresponding to a cross section through the potential surface parallel to the coordinate s and passing through point z (Fig. 44). This cross section is a curve with two minima (Fig. 45)

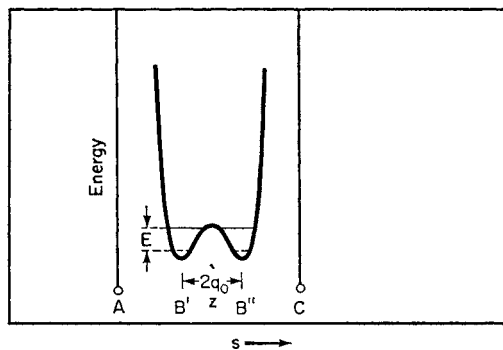


FIG. 45. Cross section of the potential energy surface along the line $X = \text{const.}$ (see Fig. 44).

which, for simplicity, is assumed to be symmetrical with respect to the maximum point (point z) and to correspond approximately to the formula

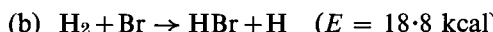
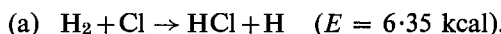
$$U(q) = \frac{1}{2}\mu_s \omega^2 \left[\frac{q^6}{12q_0^4} - \frac{q^2}{4} + \frac{q_0^2}{6} \right], \quad (13.29)$$

where $q = s - q_0 - AB'$ is the distance from the B atom to the point z (Fig. 45), μ_s is the reduced mass of the system A.B.C with respect to its motion parallel to the s coordinate, and ω is the fundamental vibration frequency for each of the potential wells.

The curve $V(r)$ corresponds to a section of the potential surface parallel to the r axis. Bauer and Wu take a Morse function for $V(r)$. This choice is, of course, a rather rough approximation, but this has little effect on the value of the rate constant.

In order to find the derivative $\partial U(r, s)/\partial r$ in (13.27) Bauer and Wu use the fact that near point z the s coordinate is a definite function of r . To evaluate $\partial V(r, s)/\partial s$ a much rougher approach has to be used, comparing the energy of interaction of hydrogen molecules ($s = s_0$) and the energy of interaction of helium atoms ($s = 0$).

With these assumptions, calculations have been made for two reactions:



(E is the activation energy). The rate constant may be calculated from the formula

$$k = \kappa v \sigma, \quad (13.30)$$

where κ is the transmission coefficient, v the relative velocity of the initial particles and σ the effective cross section of the reaction. The authors assume that σ depends on the initial energy of the relative motion of the particles in the following way:

$$\sigma = \begin{cases} 0 & \text{when } N_A \frac{\mu v^2}{2} < E; \\ \sigma_0 \alpha & \text{when } N_A \frac{\mu v^2}{2} \geq E. \end{cases} \quad (13.31)$$

Here σ_0 is the gas-kinetic effective cross-section and μ the corresponding effective mass. Calculation gives $\alpha = 1.37 \times 10^{-3}$ for reaction (a) and $\alpha = 2.58 \times 10^{-4}$ for reaction (b).

Averaging (13.30) with respect to all the initial energies yields

$$k = \kappa \sigma_0 \alpha E \left(\frac{8}{\mu \pi k T} \right)^{1/2} \exp(-E/RT). \quad (13.32)$$

On the other hand, according to (9.15) the number of binary collisions for unit concentrations ($n_1 = n_2 = 1$) is

$$Z_0 = \sigma_0 \left(\frac{8kT}{\pi\mu} \right)^{1/2}.$$

Comparing this expression with (13.32), we obtain for P , the probability factor,

$$P = \kappa\alpha E/kT. \quad (13.33)$$

At a temperature of 288°K, assuming that $\kappa = 1$, we find $P = 1.53 \times 10^{-2}$ for reaction (a) and $P = 1.77 \times 10^{-2}$ for reaction (b).⁽⁵²⁾ According to Jost's experimental data [811], $P = 3.84 \times 10^{-3}$ for reaction (b). In view of the extremely approximate nature of the calculation, this result should be considered satisfactory. It supports the conclusion reached earlier that in the case of a system moving along the reaction path, deviations from classical laws are insignificant.

These calculations of Bauer and Wu can, it seems, be regarded as an indication that in elementary metathetical reactions, $AB + C \rightarrow A + BC$, the energy redistribution necessary for reaction to take place actually occurs in the immediate vicinity of the transition state.⁽⁵³⁾

The Role of the Tunnel Effect

When deriving a basic equation for the rate constant using the transition-state method, it was assumed that adiabatic motion of nuclei along the reaction path obeys the laws of classical mechanics. This means, in particular, that for a representative point to cross a potential barrier it should have a kinetic energy at least equal to the height of the barrier. Substantially the same assumption is made in the quantum-mechanical calculation of the rate constant [equation (13.31)] given above. In fact, however, there is a finite probability that nuclei will cross the potential barrier even when this condition is not satisfied, by quantum-mechanical "leakage" through the barrier (the tunnel effect). A process of this kind added to the normal classical means of surmounting the barrier, should increase the rate of the elementary process.

In order to elucidate the possible role of the tunnel effect under various conditions, Bell [373a] represented the potential barrier by a section of a

⁽⁵²⁾ In their approximate calculation Bauer and Wu [364] assume $\kappa = \frac{1}{2}$, considering that only half the total number of systems reaching the transition state achieve the final state. As we have seen (§12) this assumption is unfounded.

⁽⁵³⁾ An attempt to apply quantum-transition theory in a treatment of an elementary chemical process of the type $AB + C \rightarrow A + BC$ has also been made by Golden [681, 682, 683]. His method has, however, been subjected to serious criticism (see, for example, the discussion by Golden and Peiser [683]). We should also mention Bauer's unsuccessful attempt [362] to calculate the probability of the process $AB + C \rightarrow A + B + C$ on the basis of perturbation theory.

parabola (curve A in Fig. 46). It was shown first that the probability of tunnelling through such a potential barrier differs little from the probability of penetrating a barrier closer to the actual shape [560] (curve B in Fig. 46) for which the potential-energy derivative is continuous throughout. For the probability of penetration by a particle of mass m , Bell obtained the approximate formula

$$G = \exp \left[-\frac{\pi a(2m)^{1/2}(\epsilon - W)}{\hbar \epsilon^{1/2}} \right] \quad (13.34)$$

where ϵ is the height of the barrier, W is the kinetic energy of the particle and $2a$ is the width of the base of the parabola.

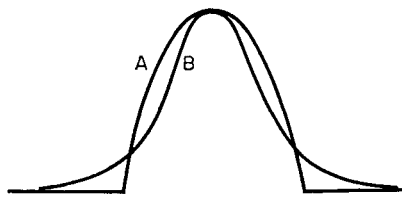


FIG. 46. Shapes of the potential barrier: A, parabolic (according to Bell [373a]), and B (according to Manning [560]).

Using this method it is not difficult to calculate the reaction rate constant, which is defined as the number of particles (representative mass points) crossing the barrier per unit time. Calculation gives

$$k = \frac{Z_0 \exp(-\epsilon/kT)}{1-x} - \frac{x}{1-x} Z_0 \exp(-\beta) \quad (13.35)$$

where

$$x = \frac{\hbar}{\pi a k T} \left(\frac{\epsilon}{2m} \right)^{1/2}, \quad \beta = \pi a \hbar^{-1} (2m\epsilon)^{1/2}.$$

At sufficiently high temperatures, when $x \ll 1$ and consequently

$$\exp(-\epsilon/kT) \gg \exp(-\beta)$$

the rate constant has the classical value

$$k = Z_0 \exp(-\epsilon/kT).$$

In the reverse case at low temperatures, when $x \gg 1$, the reaction is entirely determined by the tunnel effect and its rate constant is

$$k = Z_0 \exp[-\pi a(2m\epsilon)^{1/2} \hbar^{-1}]. \quad (13.36)$$

Figure 47 shows curves for the dependence of $\log k/Z_0$ on reciprocal temperature for two values of the activation energy and of the parameter a . The mass of the representative point is taken as equal to the mass of the hydrogen atom. The broken lines represent the behaviour of $\log k/Z_0$ obtained on the assumption that classical theory is valid down to low temperatures. As is seen from the figure, at high temperatures the tunnel effect makes practically no contribution to the reaction rate. At low temperatures, however, due to the tunnel effect, the rate constant is

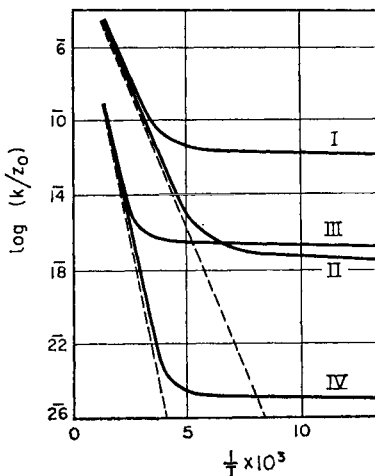


FIG. 47. Dependence of rate constant on temperature [373a],

$$m = 1.66 \times 10^{-24} \text{ g}$$

I	ε = 13 kcal	2a = 1 Å	III	ε = 26 kcal	2a = 1 Å
II	ε = 13 kcal	2a = 1.5 Å	IV	ε = 26 kcal	2a = 1.5 Å

several powers of ten higher than that given by the Arrhenius formula. It is therefore to be expected that at sufficiently low temperatures the tunnel effect may play a very important role, at least in the case of reactions involving hydrogen atoms or ions. With this condition, as we might expect on the basis of (13.36), the dependence of the rate on the mass of the reacting atoms should be very marked, the rate decreasing with increase in mass.⁽⁵⁴⁾

These conclusions are supported qualitatively by a series of observations. For instance it is known that, at low temperatures, isomerization of frozen radicals, which involves hydrogen-atom transfer, proceeds much more quickly than would be expected on the basis of the Arrhenius equation. On the other hand, investigation of protolytic reactions at normal temperatures [376] has shown quite convincingly that intermolecular

⁽⁵⁴⁾ See also [431a].

transfer of a proton under these conditions takes place over the potential barrier and not by quantum-mechanical "leakage". If the tunnel effect were playing a part in the reaction we should observe a deviation from the Arrhenius equation and a considerable decrease in the reaction rate when the proton is replaced by a deuteron. In fact, neither occurrence is observed.

As Wigner has shown [1289], at normal temperatures an approximate allowance for the influence of the tunnel effect on the reaction rate may be made by including in the transmission coefficient the factor

$$1 + \frac{1}{24} \left| \frac{\hbar v^*}{kT} \right|^2$$

where

$$v^* = \left(\frac{\partial^2 U}{\partial l^2} \right)^{1/2} / 2\pi\mu^{1/2}.$$

Here μ is the reduced mass of the activated complex corresponding to motion along the l coordinate of the reaction and the derivative $(\partial^2 U / \partial l^2)^*$ is taken at the maximum point. If the curvature of the potential-energy surface near the top of the barrier is slight, or if the temperature of the reacting system is high, the normalization factor is practically equal to unity. Under normal conditions, correction for the tunnel effect may be neglected.

Non-intersection of Potential Curves

As we have seen, each electron term of a system of atoms has its own corresponding potential energy surface. In order to study the mechanism of an elementary chemical reaction and to explain the possibility of non-adiabatic transitions, it is important to know whether (and in what circumstances) potential-energy surfaces may intersect, i.e. whether there is a configuration of the nuclei such that two different electronic states have the same energy.

To elucidate this problem, let us first consider a system of atoms in which only one interatomic distance, which we shall denote by X , varies [973]. We shall assume that for X infinite the system has two electronic states, which we shall denote by the figures 1 and 2, and their respective eigenfunctions by ψ_1 and ψ_2 . For example, in the case of two atoms state 1 may correspond to the ground state of the atoms (A, B), while 2 corresponds to a state in which one of the atoms (A, for instance) is excited, or in which an electron has passed from one atom to the other (for instance A^-, B^+). In the case of a system of three atoms (A, B, C), state 1 may be the state $AB(^1\Sigma) + C$ while 2 is the state $AB(^3\Sigma) + C$, where it is assumed that the distance A—B is fixed and the resultant spin is the same in both states.

Let $u(X, x)$ be the perturbation-energy operator; the perturbation may, for example, be the energy of the interaction of two parts of the system in question (x is the set of coordinates of the electrons). If the system could be in only one state, state 1 for example, for finite X the perturbation energy would be

$$\int \psi_1^* u \psi_1 dx = u_{11}(X). \quad (13.37)$$

In state 2 the perturbation energy would be

$$\int \psi_2^* u \psi_2 dx = u_{22}(X). \quad (13.38)$$

Figure 48 shows as examples the curves $u_{11}(X)$ (curve 1) and $u_{22}(X)$ (curve 2), it being assumed that when $X = \infty$, $u_{11} < u_{22}$. It is natural

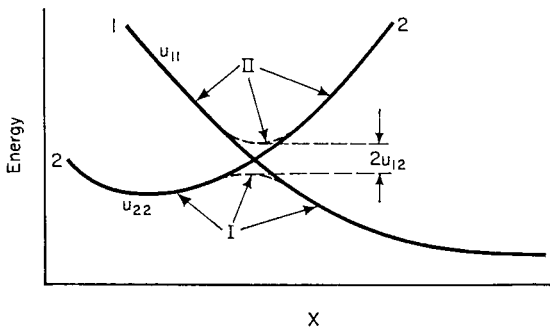


FIG. 48. Pseudo-intersection of potential curves 1 and 2. The actual potential-energy curves (I and II) in the region of pseudo-intersection are shown by broken lines.

that curves 1 and 2 may, generally speaking, intersect at a certain value of X , as shown in the figure. In practice, however, as soon as X becomes finite the functions ψ_1 and ψ_2 cease to be eigenfunctions of the system and may not, strictly speaking, be used in calculating the energy. This applies particularly to values of X near the point of intersection of curves 1 and 2, where degeneracy occurs. According to quantum mechanics, in such cases in order to calculate the perturbation energy we should use as an eigenfunction a linear combination $\psi = a\psi_1 + b\psi_2$ of ψ_1 and ψ_2 ; while ϵ should be determined from the equation

$$(H_0 + u)(a\psi_1 + b\psi_2) = (E_1 + \epsilon)(a\psi_1 + b\psi_2). \quad (13.39)$$

Here H_0 is the unperturbed-energy operator, the eigenfunctions of which are ψ_1 and ψ_2 , and E_1 is the unperturbed eigenvalue of the energy of state 1.

Considering that $H_0\psi_1 = E_1\psi_1$ and $H_0\psi_2 = E_2\psi_2$, ($E_1 < E_2$), we obtain as equations to determine a and b ⁽⁵⁵⁾

$$\left. \begin{aligned} (u_{11} - \epsilon)a + u_{12}b &= 0; \\ u_{21}a + (u'_{22} - \epsilon)b &= 0, \end{aligned} \right\} \quad (13.40)$$

where

$$u_{12} = u_{21} = \int \psi_1 \psi_2 \, dx, \quad u'_{22} = (E_2 - E_1) + u_{22};$$

u_{11} and u_{22} are determined by equations (13.36) and (13.37). From (13.39) we find two values for ϵ :

$$\epsilon_{I,II} = \frac{1}{2}(u_{11} + u'_{22}) \mp [\frac{1}{4}(u_{11} - u'_{22})^2 + u_{12}^2]^{1/2}. \quad (13.41)$$

The values of a and b corresponding to ϵ_I and ϵ_{II} are determined from equations (13.39). On the basis of the normalization and orthogonality conditions, the equations

$$a_I^2 + b_I^2 = 1, \quad a_{II}^2 + b_{II}^2 = 1, \quad a_I a_{II} + b_I b_{II} = 0, \quad (13.42)$$

should hold, which leaves only one of the four coefficients indeterminate.

It is immediately obvious from (13.41) that for the potential curves to intersect (or touch) two conditions must be satisfied simultaneously: $u_{11} = u_{22}$ and $u_{12} = 0$. According to our assumption u_{11} , u_{22} and u_{12} depend on only one parameter (X , the interatomic distance) and so these conditions will not be satisfied simultaneously and the potential curves will not intersect.

By using (13.41) it is not difficult to establish the general nature of the dependence of ϵ_I and ϵ_{II} on X . For sufficiently high values of X , when u_{11} , u_{22} and u_{12} are sufficiently small, $u_{11} - u'_{22} = (u_{11} - u_{22}) + (E_1 - E_2)$ is less than zero and $|u_{12}| \ll |E_1 - E_2|$. In accordance with (13.41) we find

$$\epsilon_I = u_{11}, \quad \epsilon_{II} = u'_{22}. \quad (13.43)$$

Substituting these values in (13.40) we obtain $b_I \approx 0$ and $a_{II} \approx 0$ and therefore $\psi_I \approx \psi_1$ and $\psi_{II} \approx \psi_2$.

At the point $X = X_0$, where the curves $u_{11}(X)$ and $u'_{22}(X)$ intersect, we have $u_{11} = u'_{22}$. If, to be specific, we now take $u_{12} < 0$, we find in accordance with (13.41)

$$\epsilon_I = u_{11} + u_{12}, \quad \epsilon_{II} = u_{11} - u_{12}. \quad (13.44)$$

⁽⁵⁵⁾ For finite X values the functions ψ_1 and ψ_2 are non-orthogonal in the general case. Taking qualitative results into consideration, however, we may assume that

$$\int \psi_1 \psi_2 \, dX = 0$$

for all values of X .

Thus, in accordance with what has been stated, at the point of intersection of curves u_{11} and u_{22} the actual energy values differ from each other and their difference is equal to $2u_{12}$. It follows from (13.40) and (13.42) that

$$\psi_I = 2^{-1/2}(\psi_1 + \psi_2), \quad \psi_{II} = 2^{-1/2}(\psi_1 - \psi_2).$$

When $X < X_0$, the difference $u_{11} - u'_{22}$ becomes positive; for sufficiently small values of X we may consider $u_{11} - u'_{22} \gg |u_{12}|$ and then, according to (13.41)

$$\epsilon_I \simeq u'_{22}, \quad \epsilon_{II} \simeq u_{11}.$$

It follows from (13.40) that

$$\psi_I \simeq \psi_2, \quad \psi_{II} \simeq \psi_1.$$

Thus the following picture is obtained. For large X values, the potential energy curve $\epsilon_I(X)$ of the ground state is practically the same as the curve 1 obtained as a zeroth approximation for (13.37). The smaller the X value and the stronger the interaction of the particles, the more do these curves diverge from one another. When $X < X_0$, the curve $\epsilon_I(X)$ begins to approximate to curve 2, obtained for the zeroth approximation for the excited state (13.38). On the other hand, curve $\epsilon_{II}(X)$, which is originally (for high X values) coincident with curve 2, deviates more and more from it as X decreases, until finally it practically merges with curve 1. The resulting (actual) curves $\epsilon_I(X)$ and $\epsilon_{II}(X)$ are shown in Fig. 48 by broken lines. They do not intersect anywhere and the higher the energy of interaction u_{12} , the greater is the minimum distance between them. In certain cases u_{12} may be very small but it is never zero. Thus if states 1 and 2 differ in their resultant spins, although to a first approximation $u_{12}=0$ (due to the orthogonality of the spin functions), in a higher approximation, when the magnetic interaction of the spins is taken into account, u_{12} will differ from zero and so the potential curves will not intersect.

Let us now assume that in this system two or more of the interatomic distances vary; we denote these by X_1, X_2, \dots [1215]. Here, as was the case for a single parameter, in order that the potential surfaces ϵ_I and ϵ_{II} should intersect it is necessary according to (13.41) that two conditions be met simultaneously: $u_{11} = u'_{22}$ and $u_{12} = 0$. Obviously, when there are two or more parameters, these conditions may be satisfied, and so at a certain point ϵ_I will equal ϵ_{II} . In the case of two-dimensional surfaces, this point will clearly be their point of contact; as may be shown (p. 220), near this point the surfaces will have approximately the shape of two cones with a common apex.

One simple case of potential-energy surfaces touching occurs in a system of three atoms (A, B, C). According to (10.2), the London equation for the ground and first excited states is of the form

$$\epsilon_{I,II} = A_1 + B_1 + C_1 \mp 2^{-1/2}[(\alpha_1 - \beta_1)^2 + (\beta_1 - \gamma_1)^2 + (\gamma_1 - \alpha_1)^2]^{1/2}. \quad (13.45)$$

If all three interatomic distances are variable the expression is an equation for a three-dimensional surface. When the distances between the atoms are such that $\alpha_1 - \beta_1 = \gamma_1$ then obviously $\epsilon_I = \epsilon_{II}$. This condition may be satisfied if the atoms are situated at the corners of a triangle.⁽⁵⁶⁾ If all three atoms are identical, the triangle will be equilateral. The potential surfaces will touch along the line for which $X_{AB} = X_{BC} = X_{AC}$.

If the two surfaces in question refer to different resultant spins, at least three independent parameters are needed for the surfaces to touch [1215]. This results from the fact that in this case u_{12} is a complex quantity, and therefore to vanish it must have zero real and imaginary parts.

Probability of Non-adiabatic Transitions

It has been stated above (§8) that in addition to the common adiabatic elementary chemical processes there are also non-adiabatic elementary reactions, in which transition from one potential surface to another occurs without the emission or absorption of energy. The fundamental problem of the theory of non-adiabatic processes is that of finding the probability of this type of transition as a function of the distance between the potential energy surfaces and the velocity of the nuclei. This problem has been solved by Landau [166] and by Zener [1330] for the case where only one coordinate (for example, X , the internuclear distance) varies in the course of the process.

As we have mentioned in §8, in quantum mechanics the probability of transition from one state (1) to another (2) due to the effect of a perturbation, u , is determined by a matrix element of type

$$u_{12} = \int \psi_1 u \psi_2 \, d\tau$$

[see (8.11) and (8.12a)]. It is possible to estimate this integral, under the condition that the motion of the system in question be quasi-classical (see §8). For the one-dimensional motion of a particle of mass μ this condition is equivalent to (8.33),

$$\mu \hbar p^{-3} d\epsilon/dX \ll 1, \quad (13.46)$$

where p is the momentum of the particle and ϵ its potential energy. Condition (13.46) means that a quasi-classical approximation is applicable when the gradient of the potential field is not too great and the momentum of relative motion of the nuclei is not too small. When this condition is satisfied, the probability χ of transition is proportional to the following

⁽⁵⁶⁾ Since the exchange integrals have a minimum value for a certain interatomic distance, the condition $\alpha_1 = \beta_1 = \gamma_1$ may also be satisfied with the atoms in line if they are close enough.

expression⁽⁵⁷⁾ (see [168], Chap. 7):

$$\chi \sim \exp \left[\frac{2\pi i}{h} \int (p_I - p_{II}) dX \right], \quad (13.47)$$

where

$$p_I = [2\mu(W - \epsilon_I)]^{1/2}, \quad p_{II} = [2\mu(W - \epsilon_{II})]^{1/2} \quad (13.48)$$

are the momenta of the representative mass point in the first and second states respectively (W is the total energy of the system). The integration in (13.47) may be confined to a region of close approach of the potential curves, where the transition from one state to another is most probable.⁽⁵⁸⁾ If the difference $\epsilon_I - \epsilon_{II}$ is sufficiently small in this region, it is possible to expand $p_I - p_{II}$ as a series in $\epsilon_I - \epsilon_{II}$ and confine ourselves to the linear term. Then

$$p_I - p_{II} = (\epsilon_I - \epsilon_{II}) dp/d\epsilon = -(\epsilon_I - \epsilon_{II})/v \quad (13.49)$$

since $\epsilon = W - p^2/2\mu$ and $d\epsilon/dp = -v$, where v is the relative velocity of the nuclei in this region. Equation (13.49) is valid if the quadratic term in the expansion is much less than the linear term. It can be shown that this condition is fulfilled if the smallest difference in energy of the potential curves is much less than the kinetic energy of the particle [according to (13.50) below, this means that $u_{12} \ll \frac{1}{2}\mu v^2$].⁽⁵⁹⁾

On the basis of (13.41) the distance between the potential curves may be written

$$\epsilon_{II} - \epsilon_I = [(u_{11} - u'_{22})^2 + 4u_{12}^2]^{1/2}. \quad (13.50)$$

This difference has a minimum at the point of intersection of the first approximation curves. Near this point, which corresponds to $X = X_0$, it is possible to expand u_{11} and u'_{22} in a series in $\eta = X - X_0$, and we may confine ourselves to the first term

$$u_{11} = F_1 \eta, \quad u'_{22} = F_2 \eta. \quad (13.51)$$

Let us substitute these expressions in (13.50) and introduce the notation $|u_{12}| = a$; on the basis of (13.49), the integral in (13.47) will then be

$$\begin{aligned} \frac{2\pi i}{h} \int (p_I - p_{II}) dX &= -\frac{2\pi i}{hv} \int (\epsilon_I - \epsilon_{II}) dX \\ &= \frac{2\pi i}{hv} \int [(F_1 - F_2)^2 \eta^2 + 4a^2]^{1/2} d\eta. \end{aligned} \quad (13.52)$$

⁽⁵⁷⁾ In the general case, different values W_I and W_{II} of the total energy, should appear in expressions (13.48). Since, however, we are concerned with a transition not accompanied by radiation, $W_I = W_{II}$.

⁽⁵⁸⁾ As London has shown [886], the probability of transition has a sharp maximum in this region, but is insignificantly small for other values of X .

⁽⁵⁹⁾ For high values of u_{12} the problem has not been solved, but the probability of non-adiabatic transition is then very small and plays no part in chemical kinetics.

The main contribution to this integral comes from the region of closest approach of the curves. Accordingly, we may determine the limiting values of η from the equation

$$(F_1 - F_2)^2 \eta^2 + 4a^2 = 0,$$

which gives

$$\eta_0 = \pm \frac{2ia}{|F_1 - F_2|}.$$

With the introduction of the new variable $\xi = i\eta$, expression (13.52) may be written

$$\frac{2\pi i}{h} \int (p_I - p_{II}) dX = \frac{2\pi}{hv} \int_{-\xi_0}^{\xi_0} [4a^2 - \xi^2(F_1 - F_2)]^{1/2} d\xi, \quad (13.53)$$

where

$$\xi_0 = \frac{2a}{|F_1 - F_2|}.$$

As the integrand in (13.53) is symmetrical about $\xi = 0$, we may replace (13.53) by

$$\frac{2\pi i}{h} \int (p_I - p_{II}) dx = - \frac{4\pi}{hv} |F_1 - F_2| \int_0^{\xi_0} (\xi_0^2 - \xi^2)^{1/2} d\xi = \frac{4\pi^2 a^2}{hv |F_1 - F_2|}.$$

Substituting this result in (13.47), we find that the probability of transition between the potential curves is proportional to the expression

$$\chi \approx \exp \left[- \frac{4\pi^2 a^2}{hv |F_1 - F_2|} \right]. \quad (13.54)$$

Zener [1330], using a different method of calculation, found that in this expression, the pre-exponential factor, which is indeterminate according to Landau, is equal to unity. Thus we may write finally

$$\chi = \exp \left[- \frac{4\pi^2 a^2}{hv |F_1 - F_2|} \right]. \quad (13.55)$$

As is apparent from this formula, the probability of non-adiabatic transition decreases very rapidly with increase in the least distance, $2a$, between the potential curves and with decrease in the relative velocity, v , of the nuclei. Thus, in accordance with §8, when the motion of the nuclei is very slow it is always possible to treat the process as adiabatic.

The probability that a system moving near the point of pseudo-intersection will remain on the same potential curve (see Fig. 23, p. 127) is, on the basis of (13.55), equal to

$$\rho = 1 - \chi = 1 - \exp \left[- \frac{4\pi^2 a^2}{h v |F_1 - F_2|} \right]. \quad (13.56)$$

When the distance between the lower and upper potential curves is sufficiently small, this expression may be expanded in a series. Confining ourselves to the first term, we find

$$\rho = \frac{4\pi^2 a^2}{h v |F_1 - F_2|}. \quad (13.57)$$

The probability of a system passing to another potential curve and remaining there is equal to $2\chi(1 - \chi)$.⁽⁶⁰⁾ This expression reaches its maximum of $\frac{1}{2}$ when $\chi = \frac{1}{2}$. If χ is close to unity, or alternatively much less than unity, however, this probability will be low.

Let us now consider the case of two independent parameters [1215]. We shall assume first of all that the representative point moves with a velocity v along the X coordinate, and describes the trajectory $Y = \text{const.}$; by changes in Y a family of such trajectories is obtained. At the point of intersection of the surfaces, $u_{11} = u_{22}'$ and $u_{12} = 0$, and we may therefore assume that near this point $a = a_0(Y - Y_0)$, where a_0 is a constant. With this condition, instead of (13.51) we may write $u_{11} = F_1\eta + F_1'\eta'$ and $u_{22}' = F_2\eta + F_2'\eta'$, where $\eta' = Y - Y_0$. It can be seen from these expressions that, as we have mentioned (p. 216), near the point of contact the surfaces take the form of two cones with a common apex. Substituting these expressions in (13.52), and integrating as before, we again obtain expression (13.54) with the sole difference that a should be replaced by $a_0\eta'$. Thus we find

$$\chi(\eta') = \exp \left[- \frac{4\pi^2 a_0^2 \eta'^2}{h v |F_1 - F_2|} \right]. \quad (13.58)$$

In order to find the total probability of transition near the point $\eta = \eta' = 0$, this expression should be integrated with respect to η' . Since $\chi(\eta')$ rapidly decreases with increase in η' , we may without significant error extend the integration from $-\infty$ to $+\infty$:

$$\begin{aligned} \bar{\chi} &= \int_{-\infty}^{+\infty} \chi(\eta') d\eta' = \int_{-\infty}^{+\infty} \exp \left[- \frac{4\pi^2 a_0^2 \eta'^2}{h v |F_1 - F_2|} \right] d\eta' \\ &= \left[\frac{h |F_1 - F_2| v}{4\pi a_0^2} \right]^{1/2}. \end{aligned} \quad (13.59)$$

(60) This formula contains the product of the probability (χ) of transition to the second curve and the probability $(1 - \chi)$ of the representative point remaining on this curve during the reverse motion. The factor 2 results from the fact that the system may approach the point of quasi-intersection from either side.

This expression has the dimensions of a length and may be interpreted as the mean width of the stream of representative points during their transition from one part of the double cone to the other. To obtain the probability of this transition properly we should find the relation of $\bar{\chi}$ to the width of the total stream of representative points in the direction X along the initial surface.

If allowance is made for the magnetic interaction of the electrons, the probability of non-adiabatic transition from one three-dimensional potential surface to another, accompanied by a change in the resultant angular momentum of the system, is expressed by the formula [1215]

$$\bar{\chi} = \frac{h|F_1 - F_2|\bar{v}}{4\pi a_0 b_0} \quad (13.60)$$

where a_0 and b_0 are the angular coefficients in the formula expressing the dependence (on the coordinates) of the real and imaginary parts of the matrix element u_{12} of the magnetic interaction of the electrons. By analogy with χ , the quantity $\bar{\chi}$ may be interpreted as the mean area of the cross-section of the stream of representative points during their transition from one three-dimensional surface to another.

Strictly speaking, the values of χ or ρ given above should be averaged over all possible velocities; but for an approximate estimate these formulae may be used with a mean velocity for v .

Effect of Non-adiabatic Transitions on the Reaction Rate

As we have already mentioned, when the probability of transition from one level to another is increased, the probability of the elementary process occurring adiabatically is decreased, i.e. the rate of the adiabatic reaction decreases. In the one-dimensional case in these conditions, the transmission coefficient κ should be written

$$\kappa = \rho \kappa_0, \quad (13.61)$$

where ρ is determined by expression (13.56) or by (13.57), while κ_0 is the transmission coefficient without allowance for non-adiabatic effects.

As we can see from (13.56), when the distance between the potential surfaces is increased, ρ rapidly approaches unity. For example, assuming for the purpose of evaluating ρ that $a = 0.1$ eV, $v \approx 10^5$ cm/sec and $|F_1 - F_2| \approx 1$ eV/Å, we find $\rho - 1 \approx 10^{-5}$. In this way when there is only one degree of freedom, the least distance between the potential curves must be very small to have a marked effect on the kinetics of the process.

A marked decrease in ρ is observed, for example, in processes accompanied by a change in the resultant spin of the system. In this case, the role of perturbation energy is played by the energy of magnetic interaction, i.e. spin-spin interaction or spin-orbital interaction. Since this energy is

small, of the order 10^{-3} to 10^{-5} eV, it is possible to use equation (13.57) to evaluate ρ ; then for the above values of v and $|F_1 - F_2|$, the probability of the system remaining on the same potential curve (with a change in multiplicity⁽⁶¹⁾) will be of the order 10^{-2} to 10^{-6} . The transmission coefficient will be of the same order. For example, calculations for the reactions below give the results

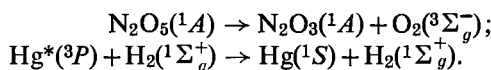
- (a) [901] $\text{C}_2\text{H}_4(^1B) \rightarrow \text{C}_2\text{H}_4(^3B) \rightarrow \text{C}_2\text{H}_4(^1B)$, $\kappa \sim 10^{-6}$;
- (b) [1272] $\text{O}(^3P) + \text{CO}(^1\Sigma) \rightarrow \text{CO}_2(^1\Sigma)$, $\kappa \sim 10^{-4}$;
- (c) [1172] $\text{N}_2\text{O}(^1\Sigma) \rightarrow \text{N}_2(^1\Sigma) + \text{O}(^3P)$, $\kappa \sim 10^{-4}$.

If the resultant spin is more than $\frac{1}{2}$ it may happen that although the values of the maximum total spin (corresponding to a parallel orientation of the resultant spins of the interacting atoms or molecules) differ in the initial and final states, the total spin quantum numbers of these states may include a pair (or several pairs) of identical numbers. Then, naturally, transition from the initial to the final state encounters no difficulties. Thus, for example, in the case of the process



the total spin quantum number of the system in the initial state may have two values, $\frac{3}{2}$ and $\frac{1}{2}$, while in the final state it may have one, $\frac{1}{2}$, and therefore this process is possible in spite of the change in multiplicity. If, however, the initial and final states of a system do not have the same total spin quantum number, transitions between such states should be of extremely low probability. This feature is known in the literature as the principle of conservation of multiplicity or Wigner's principle [1288]. This helps us, when analysing complex reactions, to ignore processes which proceed very slowly and play no part in the reaction as a whole, since other elementary processes, for which Wigner's principle is obeyed, prevail over them.

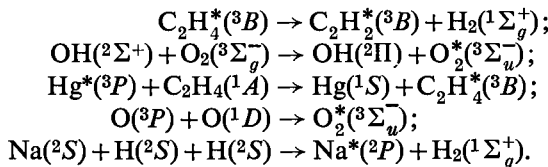
For example, the following processes cannot play any significant part in complex reactions, as their initial and final states do not have the same resultant spins:



On the other hand, the following processes may play a significant part in the appropriate reactions, either because there is no change in the resultant

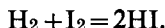
(61) Processes accompanied by a change in multiplicity are often called non-adiabatic. Strictly speaking, however, as the system remains on the *same* potential energy surface these processes are adiabatic. From this point of view, for example, reactions (a), (b) and (c) are adiabatic, although they are often called non-adiabatic. In contrast, the reaction $\text{O}(^1D) + \text{CO}(^1\Sigma^+) \rightarrow \text{CO}_2(^1\Sigma_g^+)$ is often considered to be adiabatic because the Wigner principle (see below) is obeyed, but in fact this reaction is non-adiabatic, as it is accompanied by transition from one potential curve to another (see [861]).

spin of the system or because there are identical resultant spin quantum numbers for the initial and final states:



As an example of a reaction in which a change in multiplicity seems to occur we may take the *cis-trans*-isomerization of ethylene derivatives. The slowest stage is rotation about the C=C double bond (one-dimensional case). This reaction follows two paths: (1) adiabatic, associated with a doubling of the multiplicity of the system during the course of reaction and having a low activation energy and a low pre-exponential factor (this path is the same as that of reaction (a) above), and (2) non-adiabatic, where transition from one potential curve to another occurs with conservation of multiplicity and the activation energy is large; here, owing to the small value of a , the probability of this type of transition is very close to unity (for a more detailed account see pp. 307-309).

We have mentioned (p. 160) that, according to molecular-orbital calculations the lowest state of the H_4 activated complex is the triplet, whereas the singlet state is an excited state. As the ground state of the initial molecules is a singlet, and transition between states of different multiplicities is of low probability, the presence of this triplet term has no effect on the mechanism of the reaction between H_2 molecules; as we have already remarked, the exchange reaction between two hydrogen molecules requires a very high activation energy and does not occur in practice. For this very reason, many other exchange reactions are chain reactions and have as intermediate stages reactions of molecules with atoms or radicals (for example, $\text{H}_2 + \text{Cl} \rightarrow \text{H} + \text{HCl}$ or $\text{Cl}_2 + \text{H} \rightarrow \text{Cl} + \text{ClH}$). It is known, however, that the reaction of hydrogen and iodine, for example, follows a molecular mechanism (at least at temperatures below 600°K):



There are two ways in which we may attempt to explain this: either by the fact that the energy of the singlet state of the H_2I_2 activated complex is so low that the molecular mechanism becomes of greater probability than a chain mechanism, or by the fact that in this reaction the probability of transition from the singlet to the triplet state is considerably higher than in other cases, and the reaction follows a path similar to path (1) for the isomerization reaction of ethylene derivatives with a relatively low activation energy (see above). In the latter case, in the regions of pseudo-intersection of the potential surfaces, adiabatic transitions occur in the

reaction, first from the singlet to the triplet state and then the reverse. Since the spin-orbital interaction energy increases rapidly with increase in atomic number of the element in question, a mechanism of this type should be more probable in the case of iodine than in the case of lighter elements.

An interesting example of a marked decrease in the probability of a reaction occurring adiabatically due to a small distance between potential curves is provided by the recombination of certain atoms which differ widely in electronegativity. In this case, the transmission coefficient κ for the adiabatic reaction decreases as a result of the fact that the overwhelming majority of collisions leads to transition of the system to the upper potential curve, corresponding to the homopolar state of the molecule. This process is considered in more detail in Chap. 4 (§14).

We might mention reactions of the $\text{H}_2 + \text{H} \rightarrow 3\text{H}$ type as an example of a non-adiabatic process for which our description must allow for several degrees of freedom. Dissociation of a hydrogen molecule on collision with an H atom may, generally speaking, take place either with transition of the system to the upper potential surface, corresponding to the same multiplicity, or without such a transition (adiabatically). According to (13.45), the difference in the energies of the ground state and the nearest excited state of a system of three H atoms is

$$\epsilon_I - \epsilon_{II} = -2^{1/2}[(\alpha_1 - \beta_1)^2 + (\beta_1 - \gamma_1)^2 + (\gamma_1 - \alpha_1)^2]^{1/2}.$$

In this case the potential surfaces ϵ_I and ϵ_{II} touch when

$$X_{AB} = X_{BC} = X_{AC}.$$

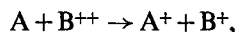
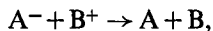
Consequently for this configuration there is a finite probability of non-adiabatic transition from the ground state I to the excited state II. When the distance between H_2 and H is large, state II corresponds to the triplet state of the hydrogen molecule and so a transition of this kind may lead to the decomposition of the transition complex H_3 into three H atoms, while the multiplicity of the system remains constant (equal to 2) throughout the whole process.

A quantitative evaluation of the probability of such a process has not been published, but on the basis of the above, it is clear that in order to calculate it we should proceed by generalizing formula (13.59).

As we have mentioned, the region in which non-adiabatic transition is possible is considerably increased in the case of two-dimensional surfaces, and even more so in the case of multidimensional surfaces, as compared with that in the one-dimensional case; and it is to be expected, therefore, that the resulting probability of this transition should also be much greater. This allows us to suppose that non-adiabatic transitions play an important part in the kinetics of some reactions during which more than

one parameter is changed, especially if reaction occurs at high temperatures. Such reactions include, for example, the oxidation of CO (in which a non-adiabatic transition is assumed to occur during formation of the excited CO₂ complex [687, 1272]), and the reaction of hydrogen with oxygen in flames [1135]. In order to establish that such transitions are possible, it is, of course, important to know the symmetry properties and the relative levels of the various terms of the system (see [687, 1135]).

Many examples of non-adiabatic transitions may be found in charge transfer processes in the gas phase, for example,



and so on [357, 519, 356, 900, 355]. Such processes are of interest from the point of view of the kinetics of reactions in electric discharge, the kinetics of radiation-induced reactions (Chap. 8), and also as preliminary models in constructing a theory of charge transfer in solution.

CHAPTER 4

BIMOLECULAR REACTIONS

BIMOLECULAR reactions form the most widespread class of chemical reactions. In particular, every simple reaction between two particles comprising one elementary act is bimolecular. Examples of these reactions are $H_2 + I_2 = 2HI$ and $NO_2 + CO = NO + CO_2$ and the reverse reactions $2HI = H_2 + I_2$ and $NO + CO_2 = NO_2 + CO$. In the case of complex chemical reactions the overwhelming majority of the elementary processes which together comprise the mechanism of the reactions are bimolecular also. Finally, bimolecular processes form the basic elementary steps in the mechanism of uni- and ter-molecular reactions (see Chap. 5).

As has been shown earlier (pp. 36 and 61), the overall law of a complex reaction is often expressed by an equation corresponding to a simple bimolecular reaction. In this case the effective rate constant usually represents a more or less intricate combination of the constants of the individual elementary processes which comprise the mechanism of the complex reaction. An example of this type of reaction is the combustion of moist carbon monoxide CO, where the kinetic law over a certain range of CO and oxygen concentration can be expressed by the simple equation:

$$(d/dt)[CO_2] = k[CO][H_2O].$$

In this case the quantity k , which formally corresponds to the "elementary process" $CO + H_2O = CO_2 + H_2$, does not in fact represent the rate constant of any elementary process in the complex mechanism of the induced combustion of CO, since $CO + H_2O = CO_2 + H_2$ is not itself an elementary process. In contrast with this, the constant k , which enters into the kinetic law

$$(d/dt)[CO_2] = k[CO][NO_2]$$

of the superficially analogous simple reaction $CO + NO_2 = CO_2 + NO$ mentioned above, does represent the true rate constant of the reaction. Obviously only in this and analogous cases can the elementary rate constant be obtained directly from the kinetic equation of the reaction. Determination of the rate constants of the elementary processes which enter into the mechanism of a complex reaction demands a detailed kinetic investigation of the reaction, i.e. a study of the kinetics of the conversion of the reactants and of the intermediate and final products. Such an investigation usually enables us (with certain simplifying assumptions) to

find the probable values of the rate constants for the separate elementary reactions. It frequently happens that one of the elementary processes in a complex reaction is the limiting step in the sense that the overall rate of the reaction is determined by the rate of this process, or is a multiple thereof. In this case the effective rate constant of the reaction equals (or is a multiple of) the rate constant of the corresponding (slowest) elementary process.

In this chapter we shall deal chiefly with simple bimolecular reactions and with bimolecular reactions which form the elementary steps of complex chemical reactions.

As the basic types of bimolecular reaction we shall examine addition ($A + B = AB$), metathetical or exchange ($A + BC = AB + C$) and double exchange ($AB + CD = AC + BD$) reactions.

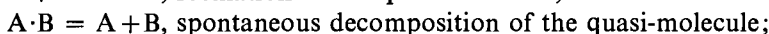
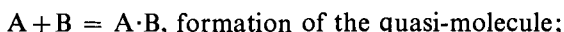
§14. Addition Reactions $A + B = AB$

Stabilization of the Quasi-molecule

To this class of bimolecular reactions belong the recombination of atoms and radicals, the addition of atoms or radicals to unsaturated molecules and the association of saturated molecules.

The bimolecular collision of two particles A and B in an addition does not constitute the whole mechanism of the reaction, since the completion of the process requires the *stabilization* of the *quasi-molecule* formed as a result of the collision between A and B; this quasi-molecule is rich in energy and therefore labile, irrespective of whether the particles A and B are atoms, radicals or saturated molecules. Stabilization involves the removal from the quasi-molecule of part of its energy, as a result of which it passes over into one of the physically stable quantum states of the product of the addition reaction—the molecule AB. This process can occur by *radiation* or by the *collision* of the quasi-molecule with some foreign molecule (*third body*), whose role consists in removing the surplus energy, thereby making the molecule AB stable.⁽¹⁾

From what has been said it is clear that an addition reaction is, generally speaking, a complex reaction consisting of several elementary steps. These steps are:



⁽¹⁾ We shall not consider here the heterogeneous process of stabilization of the quasi-molecule by collision with a wall, which thereby plays the part of a third body.

⁽²⁾ Here and in future the arrow denotes only the direction of the process as distinct from the equality sign which enters into the equation of the given process e.g. $A \cdot B + M = AB + M$.

Denoting the specific rates of these processes by k_1 , k'_1 and k_2 and assuming that the concentration of the quasi-molecule $A \cdot B$ is stationary, the steady-state condition

$$(d/dt)(A \cdot B) = k_1(A)(B) - (k'_1 + k_2)(A \cdot B) = 0$$

gives

$$(A \cdot B) = \frac{k_1}{k'_1 + k_2}(A)(B)$$

whence we find for the rate of formation of AB

$$(d/dt)(AB) = k_2(A \cdot B) = \frac{k_1 k_2}{k'_1 + k_2}(A)(B). \quad (14.1)$$

When the quasi-molecule is stabilized by radiation (*radiation stabilization*) the quantity k_2 , which enters into eq. (14.1), represents the frequency of the radiation process and can be equated with the inverse of the lifetime of the excited molecule ($k_2 = k = 1/\tau$). When stabilization occurs through the collision of the molecules (which we may call *collision stabilization*), the quantity k_2 is given by the number of effective (stabilizing) collisions experienced by the quasi-molecule in one second. Representing the concentration of stabilizing molecules by (M) , we find that $k_2 = k_2^0(M)$, where k_2^0 is the rate constant of the stabilizing process. If we admit the possibility of both mechanisms of stabilization and assume that $k_2 = k + k_2^0(M)$, we can rewrite eq. (14.1) as follows:

$$\frac{d(AB)}{dt} = k_1(A)(B) \left(1 + \frac{k'_1}{k + k_2^0(M)} \right)^{-1}. \quad (14.2)$$

As can be seen from this equation, the kinetic law will not usually correspond to a second order reaction, i.e. the reaction will not appear to be bimolecular (since M could be A or B).

It is easy to see, however, that at sufficiently high pressures, when the frequency of stabilizing collisions $k_2^0(M)$ considerably exceeds the frequency of decomposition of the quasi-molecule k'_1 , eq. (14.2) becomes the equation of a bimolecular reaction⁽³⁾

$$(d/dt)(AB) = k_1(A)(B). \quad (14.3)$$

A bimolecular law may also hold at low pressures (if radiation stabilization of the quasi-molecule is possible, i.e. if $k \neq 0$) when the condition $k_2^0(M) \ll k$ is fulfilled. In this case eq. (14.2) takes the form

$$\frac{d(AB)}{dt} = \frac{k_1 k}{k'_1 + k}(A)(B). \quad (14.4)$$

⁽³⁾ It will be noted that this equation corresponds to the rate of the elementary process of formation of the quasi-molecule $A \cdot B$; under the above conditions this process will be the limiting one.

As we shall see below, reactions, whose rate can be expressed by eq. (14.3) or (14.4) and where A and B are atoms or simple radicals, are very rare exceptions since in this case the condition $k \ll k_2^0(M) \ll k_1'$ most frequently obtains. As will readily be seen, eq. (14.2) then becomes

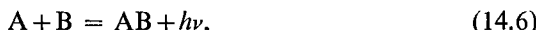
$$(d/dt)(AB) = (k_1 k_2^0/k_1')(A)(B)(M) \quad (14.5)$$

i.e. the reaction follows a *termolecular law*. Reactions of this class will be surveyed in Chap. 5.

Recombination of Atoms

The recombination of atoms is the simplest type of addition reaction. In this case the duration of the collision between the atoms A and B, a quantity τ' which is inversely proportional to the frequency of decomposition k_1 , is of the order of magnitude of the ratio of the mean diameter d of the atoms to their mean relative velocity v . Assuming $d = 10^{-8}$ cm and $v = 10^5$ cm/sec, we find that $\tau' = 10^{-13}$ sec and therefore $k_1' = 10^{13}$ sec $^{-1}$. Further, by assuming that the quasi-molecule A·B is stabilized by each collision A·B+M, we give the constant k_2^0 an order of magnitude equal to the constant of binary gas-kinetic collisions, i.e. the value 10^{-10} cm 3 molecules $^{-1}$ sec $^{-1}$. From the condition $k_2^0(M) \gg k_1$, which determines whether the bimolecular law holds (see above), it follows that $(M) \gg k_1'/k_2^0 = 10^{23}$ molecules/cm 3 . Consequently at normal temperatures the bimolecular law of atom recombination (with collision stabilization) will only be observed at a pressure of tens of thousands of atmospheres. Since the recombination of atoms has in every case been studied at considerably lower pressures (of the order of one atmosphere or lower), it is understandable that the reaction has always followed a termolecular law.

It is interesting to determine in what pressure range radiation and collision stabilization are equally effective, i.e. where the relation $k_2^0(M) \approx k$ is fulfilled. Remembering that stabilization of the quasi-molecule occurs by emission of the electronic excitation spectrum and adopting accordingly a value of k equal to 10^8 sec $^{-1}$, we obtain $(M) \approx k/k_2^0 = 10^{18}$ molecules/cm 3 , i.e. $p = 30$ mm Hg (at room temperature). So the recombination of atoms accompanied by the emission of light, i.e. the process



need not be such a rare phenomenon.

A clear case of this process was observed by Kondrat'ev and Leipunskii [153] on heating chlorine, bromine and iodine vapours to a temperature above 1000°C. The experiment showed that the emission spectrum of each of the halogens was the reverse of the absorption spectrum, in agreement with the fact that process (14.6) is the reverse of the photo-dissociation $AB + h\nu = A + B$. By determining the radiation intensity of the bromine

vapour and comparing the number of quanta emitted with the number of collisions between bromine atoms, Kondrat'ev and Leipunskii found that the probability of radiation stabilization of the bromine quasi-molecule (calculated for one collision) was of the order of 10^{-8} .

There is no doubt that the continuous emission spectra observed in various flames are in most cases connected with recombination processes, i.e. with the radiation stabilization of the quasi-molecules formed by the collision of atoms and radicals between themselves or with molecules present in the combustion zone; examples are the continuous spectra of flames containing halogens [1236, 892] or sulphur [144, 729, 657]. The continuous spectrum of the carbon monoxide flame may also be caused by one of the recombination processes $O + CO = CO_2 + h\nu$ [654] or $O + O = O_2 + h\nu$ ⁽⁴⁾ [781].

Of other experimental determinations of the probability of the radiation stabilization of molecules mention must be made of the results of Beutler and Polanyi [394] who, from a study of the reaction between sodium vapour and chlorine at low pressures, concluded that the probability of the recombination of atoms of Na and Cl must certainly be less than 10^{-4} .

The probability P of the radiation stabilization of molecules can also be determined theoretically. A rough value can be obtained by assuming that it is equal to the ratio of the duration of the collision of the particles, i.e. the lifetime of the quasi-molecule τ' , to the mean lifetime of the excited molecule τ ,

$$P = \tau'/\tau. \quad (14.7)$$

Bearing in mind that the recombination of atoms is accompanied by emission of the electronic spectrum, we can use the above mentioned values (p. 229) of the quantities τ' and $\tau (= 1/k)$, namely $\tau' = 10^{-13}$ sec and $\tau = 10^{-8}$ sec. Insertion of these values into eq. (14.7) gives P an order of magnitude of 10^{-5} .

It is easily seen that when the quasi-molecule is stabilized by the emission of *vibration quanta* (infrared spectrum) the probability of stabilization must be considerably less. In fact, since the mean lifetime τ of the vibrationally excited molecule is many orders greater than the lifetime of the electronically excited molecule, the value of P will be smaller by the same factor. In particular, when $\tau = 1$ sec and $\tau' = 10^{-13}$ sec, it follows from eq. (14.7) that $P = 10^{-13}$.

The value $\tau = 1$ sec cannot be considered too great since even for polar molecules τ has an order of magnitude not less than 10^{-2} to 10^{-3} sec.

⁽⁴⁾ Another theory of the production of a continuous spectrum by the carbon monoxide flame has been put forward by Knipe and Gordon [846], who consider that the appearance of this spectrum is connected with the decomposition of an excited molecule CO_3 formed by the recombination of an excited molecule of CO with a molecule of O_2 .

The probability of stabilization in this case can therefore hardly exceed 10^{-10} . This means that the rate of recombination of atoms accompanied by the emission of vibration quanta is negligibly small in comparison with the rate of recombination accompanied by the emission of the electronic spectrum.

An important point must be noted here. If we are concerned with the recombination of atoms which differ widely in their electronegativities then, because of the possibility of a non-adiabatic transition when the atoms collide, the system (the quasi-molecule A·B) may exist in an excited electronic state. Furthermore, if the optical transition from this state to the ground state of the molecule AB is not forbidden, then the molecule can be stabilized by emission of electronic energy. Let us examine, for example, the recombination of atoms of sodium and chlorine. When the distance between them is great, the difference in energy between the atomic (ground) and ionic states equals $I_{\text{Na}} - E_{\text{Cl}}$, where I is the ionization potential and E the electron affinity (see Fig. 49). But at short interatomic

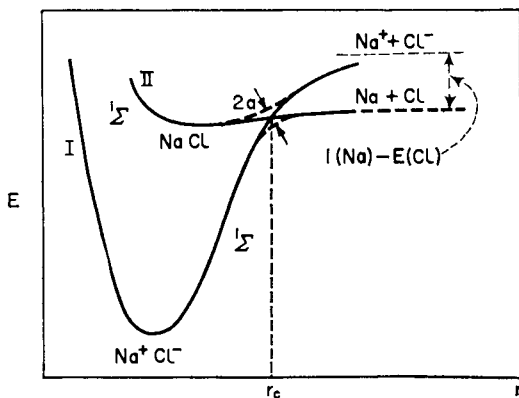


FIG. 49. Potential energy curves corresponding to the interaction of atoms and ions of sodium and chlorine (after Magee [899]).

distances the ionic state becomes the ground state since the former involves the greater attraction. Consequently the potential energy curves calculated to zero approximation intersect at a certain point (r_c). The true potential curves (broken lines in Fig. 49) are separated from each other by a certain amount $2a$. If this is small and if the system at large r is located on the lower curve, then there is a finite probability of the intermittent transition of the system onto the upper potential curve. It can be shown that a decreases as the distance of the point of pseudo-intersection of the potential curves from the equilibrium position increases. This dependence is caused by the fact that the exchange integral, which determines the magnitude of a , falls

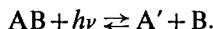
rapidly on interatomic separation. Therefore the probability of a non-adiabatic transition increases with r_c . Since curve II (Fig. 49) has very nearly the same height in the neighbourhood of the point of intersection as it has at an infinitely great interatomic distance, the point of intersection may be determined from the equation

$$I_{\text{Na}} - E_{\text{Cl}} = e^2/r_c.$$

Hence, the smaller the difference $I - E$, the larger r_c and the greater the probability of a non-adiabatic transition. According to the calculations of Magee (899) for sodium chloride $a = 219$ cal and the probability of a non-adiabatic transition is 0.07 (at 500°K) and so is comparatively small. For lithium fluoride, however, $a = 12$ cal and the probability is 0.992, i.e. practically every collision causes the attainment of the excited state of the molecule and hence the possibility of its stabilization by the radiation of its excitation energy.

If the electronic transition is forbidden, then the probability of the radiation stabilization of the quasi-molecule will be small. But since quantum restrictions are not absolutely rigid it may happen that the radiation of electron excitation energy is more probable than the radiation of vibration quanta, so that, in this case also, non-adiabatic transitions will increase the rate of formation of the molecule.

An accurate calculation of the magnitude of P for a diatomic molecule when stabilized by radiation of electron excitation energy has been made by Terenin and Prilezhayeva [265] using the principle of microscopic reversibility applied to processes of the type⁽⁵⁾



Denoting the absorption coefficient of light of frequency ν by k_ν , the intensity of the temperature radiation over the frequency interval between ν and $\nu + d\nu$ by $I_\nu d\nu$ and the number of molecules of absorbing gas in one cubic centimetre by n_{AB} , the rate of photo-dissociation over the above frequency interval, as determined by the number of quanta absorbed per second, will be

$$w = k_\nu I_\nu n_{AB} d\nu / h\nu.$$

As a result of this process w pairs (A + B) of atoms are produced every second per cm^3 ; the atoms of a pair have a relative velocity v determined by the condition $\frac{1}{2}\mu v^2 = h\nu - h\nu_0$, where μ is the reduced mass of the molecule AB and ν_0 the frequency of the long wavelength limit of continuous absorption, which is related to D , the dissociation energy of the

⁽⁵⁾ It is here generally assumed that one of the atoms appears in an excited state (A'). In addition, the assumption that one of the atoms is excited takes into account the fact that the products of photo-dissociation of a diatomic molecule are most frequently a normal and an excited atom.

molecule and E_A , the excitation energy of the atom A, by the equation $h\nu_0 = D + E_A$.

If microscopic reversibility holds true, the recombination of pairs of atoms with relative velocity between v and $v + dv$, accompanied by the emission of light of frequency ν , must produce w molecules per cm^3 every second. The number of molecules (w) formed in this way obviously equals the number of effective collisions and is expressed by the formula

$$w = q_v n'_A n_B (8\mu/\pi k T)^{1/2} \exp(-\mu v^2/2k T) v \, dv$$

where q_v is the effective cross-section and n'_A and n_B are the equilibrium numbers of the atoms A' and B per cm^3 . Equating the rates of the two processes and noting that $hd\nu = \mu v dv$, we obtain

$$k_v I_\nu n_{AB}/h\nu = q_v n'_A n_B h \mu^{-1} (8\mu/\pi k T)^{1/2} \exp(-\mu v^2/2k T).$$

Expressing I_ν in terms of ρ_ν , the density of black-body radiation and using Wien's equation for ρ_ν , we find

$$I_\nu = c \rho_\nu = 8\pi h \nu^3 c^{-2} \exp(-h\nu/k T).$$

Furthermore, from the law of mass action

$$n_A n_B / n_{AB} = K = f(T) \exp(-D/k T)$$

where

$$f(T) = (2\pi k \mu)^{3/2} s T^{1/2} (8\pi^2 I h k)^{-1}.$$

In the last expression s is a number which represents the symmetry of the molecule ($s = 1$ for a molecule composed of different atoms and $s = 2$ for a molecule with identical atoms), and $I = \mu r_0^2$ is the moment of inertia of the molecule (r_0 is the equilibrium distance). Finally, Boltzmann's law connects the number n'_A of excited atoms of A with the number n_A of normal atoms by the relation

$$n'_A / n_A = (g'/g) \exp(-E_A/k T)$$

where g' and g are the statistical weights of the excited and normal states of atom A. On inserting the above expressions for I_ν , $n_A n_B / n_{AB}$ and n'_A into the rate equations of the forward and reverse actions and noting that $h\nu = D + E_A + \frac{1}{2}\mu v^2$, we find

$$q_v/k_\nu = (8\pi^2/s)(g/g') (r_0/\lambda)^2 \quad (14.8)$$

where $\lambda = c/\nu$.

On turning to the experimentally observed dependence of the absorption coefficient k_ν on the frequency ν (or on the wavelength λ), which is usually a curve with a pronounced maximum (see, for example, Fig. 87), we see that the effective cross-section q_v must also have a maximum value at a definite relative velocity of the colliding atoms, fixed by the relation $\frac{1}{2}\mu v_{\max}^2 = h\nu_{\max} - h\nu_0$, where ν_{\max} is the frequency of the absorption

maximum. It must, however, be emphasized that this dependence of q_v on the relative velocities of the recombining atoms has meaning only in so far as we are interested in the probability of the formation of molecules in one particular vibration state. By calculations analogous to those described here, Kondrat'ev [124] showed that the effective cross-section for recombination leading to the formation of molecules in any vibration state is given by the same expression (14.8) as for q_v for the formation of non-vibrating molecules, which was the situation in the calculations of Terenin and Prilezhayeva. Moreover each type of newly formed molecule, which is characterized by a given vibration quantum number n , corresponds to a particular relative velocity of the recombining atoms, at which q_v and consequently the probability of recombination are a maximum; this velocity is determined by the condition

$$\frac{1}{2}\mu v_{\max}^2 = h\nu_{\max} - D - E_A + nh\omega$$

where ω is the frequency of the natural vibrations of the molecule (so that $nh\omega$ is an approximate expression for the vibration energy of a molecule in the n th vibration level). By replacing $\frac{1}{2}\mu v_{\max}^2$ in the above relation by its mean value kT at a given temperature T , we can find the vibration level n which will contain the majority of the molecules formed at this temperature:

$$nh\omega = D + E_A + kT - h\nu_{\max}.$$

This conclusion is based on the experimental fact (which also has a theoretical basis) that the maximum extinction coefficient in the region of the continuous spectrum is practically independent of the initial vibration state of the absorbing molecule. Hence, if we are not interested in the vibration state of the molecules formed by the recombination of atoms, we can consider the probability of their formation as independent of the relative velocity of the atoms (and therefore of the temperature of the gas) and calculate the effective cross-section from the equation

$$q = (8\pi^2 r_0^2/s)(g/g')(\kappa_v/\lambda^2)_{\max}. \quad (14.9)$$

The probability P of the formation of a molecule, calculated for one collision, is related to q by the expression

$$q = P\pi d^2(g_i/\sum g_i) \quad (14.10)$$

where g_i is the statistical weight of the electronic state to which the molecule AB is excited before its photochemical decomposition to A' + B; $\sum g_i$ is the sum of the statistical weights of all the electronic states of the molecule arising from a normal atom B and an excited atom A; and d is the mean gas-kinetic diameter of the atoms A' and B.

The need to introduce statistical weights is shown by the following considerations. At every collision between A' and B there is formed for a time of the order of the duration of the collision (10^{-13} sec) one of the

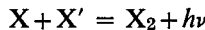
electronic states of the molecule AB arising from the electronic states of the colliding atoms. The frequency with which each such state is formed is proportional to its statistical weight; thus

$$Z_1 : Z_2 : Z_3 : \dots : Z_i : \dots = g_1 : g_2 : g_3 : \dots : g_i : \dots$$

where Z_i is the number of collisions per second leading to the i th electronic state of the molecule AB, and the total number of collisions experienced by a pair of atoms in one second is $Z = \Sigma Z_i$. It is easily seen that the fraction of collisions which are effective in the sense of producing the i th state is

$$Z_i/Z = Z_i / \sum Z_i = g_i / \sum g_i$$

Table 7 gives the values of q calculated by Terenin and Prilezhayeva for the process



($X = \text{Cl, Br, I}$). The table gives also the value of $g_i / \sum g_i$ calculated from spectroscopic data, the gas-kinetic cross-sections calculated on the assumption that the mean diameter of the normal and excited atoms of X equals the equilibrium interatomic distance in the excited molecule X_2 (Cl_2 2.26; Br_2 2.60; I_2 3.02 Å) and finally the probability P of the formation of the molecule by radiation stabilization, calculated from these data by means of eq. (14.10).

TABLE 7

The cross-section q and probability of formation P of the molecule X_2 by the recombination of atoms X' and X with radiation stabilization of the resultant quasi-molecule (after Terenin and Prilezhayeva [265])

X_2	Cl_2	Br_2	I_2
$q \times 10^{23} \text{ cm}^2$	0.6	1.4	7.6
$g_i / \sum g_i$	1/26	1/26	1/26
$\pi d^2 \times 10^{15} \text{ cm}^2$	1.61	2.13	2.86
$P \times 10^7$	1.0	1.7	6.9

From the data in this table it follows that for Cl_2 and Br_2 the probability P has the order of magnitude 10^{-7} while that for I_2 is 10^{-6} . This means that in the case of the halogens only one out of 10^7 – 10^6 collisions, which are favourable in the sense of producing an electronic state of the excited molecule X_2 which can combine with the normal state, leads to the formation of a molecule when the excess energy is lost as electronic radiation.⁽⁶⁾

⁽⁶⁾ As a supplement to these data it should be mentioned that according to Terenin and Prilezhayeva's calculation the probability of the process $\text{Na} + \text{I} = \text{NaI} + h\nu$ has an order of magnitude of 10^{-5} .

The good agreement between the values of P for bromine calculated by Terenin and Prilezhayeva (Table 7) and those found by Kondrat'ev and Leipunskii [153] from the thermal radiation intensity of bromine vapour (given on p. 230) must be emphasized, a difference of a factor of ten being fully admissible in this case because of the large error involved in measuring the radiation intensity; this is caused mainly by the difficulty of calculating the amount of reabsorption by bromine vapour, heated to 1500°K, of the radiation emitted on recombination. The discrepancy between the calculated and measured values of P may possibly be due to the complex nature of k_v (see [1003a]).

It follows from the table that the creation of a stable molecule from atoms, accompanied by the radiation of surplus energy, is a rather unlikely process. The weight and practical importance of this method of stabilizing the molecule are decreased even further by the circumstance, mentioned earlier, that in most cases, i.e. in adiabatic transitions, a condition for the recombination of atoms is that one of them should be excited. At ordinary temperatures and pressures, therefore, the chance of formation of a molecule accompanied by the radiation of light is insignificant compared with termolecular recombination. Judging by the widespread occurrence of continuous radiation in flames, however, radiation recombination obviously plays a considerable role in the radiation of flames.

Recombination of Radicals

If one or both of the recombining particles are radicals the rate is considerably increased compared with the rate of recombination of atoms. This is because polyatomic radicals possess many vibrational degrees of freedom, which can share the energy originally concentrated in the one degree of freedom corresponding to the coordinate of the relative motion of the colliding particles. This considerably increases the life of the quasi-molecule and consequently the probability of its stabilization both by radiation of part of the surplus energy and by collision with a third particle.

Let us consider the simple case of the recombination of the atom H with the diatomic radical CN, $H + CN \rightarrow HCN$. If the three atoms are arranged linearly at the moment of collision of H and CN, the energy of their relative motion will not, as in the collision of two atoms, be concentrated in the one bond H—C but be distributed between the two normal valence vibrations of the system (or quasi-molecule) H·CN.⁽⁷⁾

⁽⁷⁾ The ease of conversion of the energy of relative forward motion into vibrational energy in cases similar to those being examined is shown by experimental results on energy transfer during the collision of molecules (see Chap. 6). According to these results the probability of this energy conversion per collision is nearly unity when the colliding particles possess great energy. The quasi-molecule formed by the collision of two particles obviously satisfies this condition.

The probability of the reverse process, i.e. the dissociation of $\text{H}\cdot\text{CN}$ into $\text{H}+\text{CN}$, will be less than for a diatomic quasi-molecule because it requires the reconcentration of energy in the $\text{H}-\text{C}$ bond. In other words this bond will break only when the extension due to the combined action of the two valency vibrations of the quasi-molecule $\text{H}\cdot\text{CN}$ exceeds a certain critical value.

As shown by the approximate calculation of Kimball [831] based on classical mechanics, the probability of this occurrence falls rapidly with an increase in the number s of normal vibrations participating in the valence vibration of the new bond. The mean life τ of the quasi-molecule will therefore rise rapidly with increasing s .

Let us examine certain experimental results. The experimental rate constants k_3 of the termolecular reaction $\text{H}+\text{O}_2+\text{M} = \text{HO}_2+\text{M}$ vary with the nature of the third body (M) from values of the order of 10^{-33} to $10^{-32} \text{ cm}^6 \text{ molecules}^{-2} \text{ sec}^{-1}$. If we express the constant k_3 by the formula

$$k_3 = k_1 \tau' k_2^0 \quad (14.11)$$

[see eq. (14.5)], where k_1 and k_2^0 are the rates of formation and of collisional stabilization of the quasi-molecule $\text{H}\cdot\text{O}_2$ and $\tau' (= 1/k_1')$ denotes its lifetime, and if we assume that both formation and stabilization occur at each gas-kinetic collision of an atom of H with a molecule of O_2 , i.e. that the constants k_1 and k_2^0 have the order of magnitude $10^{-10} \text{ cm}^3 \text{ molecules}^{-1} \text{ sec}^{-1}$, we find that τ' is about 10^{-13} or 10^{-12} sec . A similar result was obtained by Rosen [1085] by a simplified quantum-mechanical calculation; he found that the mean life of the quasi-molecule $\text{H}\cdot\text{O}_2$ was of the order of 10^{-13} to 10^{-12} sec . There is good agreement therefore between the experimental and theoretical results.

An analogous calculation of the lifetime of the quasi-molecule $\text{H}\cdot\text{OH}$ from experimental values of the constant of the termolecular reaction $\text{H}+\text{OH}+\text{H}_2\text{O} = \text{H}_2\text{O}+\text{H}_2\text{O}$, namely $k_3 = 1.4 \times 10^{-31} \text{ cm}^6 \text{ molecules}^{-2} \text{ sec}^{-1}$, gives $\tau' = 1.4 \times 10^{-11} \text{ sec}$. From the experimental rate constants of the reaction $\text{OH}+\text{OH}+\text{M} = \text{H}_2\text{O}_2+\text{M}$, where $k_3 = 2 \times 10^{-30} \text{ cm}^6 \text{ molecule}^{-2} \text{ sec}^{-1}$ for $\text{M} = \text{He}$ and 4.5×10^{-30} for $\text{M} = \text{H}_2\text{O}$, we similarly obtain $\tau' = 2 \times 10^{-10}$ to $4.5 \times 10^{-10} \text{ sec}$.

From kinetic measurements of the photochemical decomposition of the simplest hydrocarbons and from the deuterium content of the products of the photochemical reaction when carried out in the presence of deuterium, Marcus [914] obtained the following values for the product $\tau' k_2^0$: $1.9 \times 10^{-19} \text{ cm}^3 \text{ molecules}^{-1}$ ($\text{CH}_2\text{D}\cdot\text{H}$), 3.1×10^{-19} ($\text{CHD}_2\cdot\text{H}$), 1.4×10^{-17} ($\text{CH}_3\cdot\text{CH}_3$)⁽⁸⁾ and 4.3×10^{-16} ($\text{CH}_3\cdot\text{C}_2\text{H}_5$). The values of the mean life of the quasi-molecules calculated from these data (assuming that $k_2^0 = 10^{-10} \text{ cm}^3$

⁽⁸⁾ The later and most accurate data of Kistiakowsky and Roberts [839] for the quasi-molecule $\text{CH}_3\cdot\text{CH}_3$ gave $\tau' k = 1.0 \times 10^{-17} \text{ cm}^3 \text{ molecules}^{-1}$.

molecules⁻¹ sec⁻¹) and the above-mentioned values of τ for $\text{H}\cdot\text{O}_2$, $\text{H}\cdot\text{OH}$ and $\text{HO}\cdot\text{OH}$ are given in Table 8. This table clearly shows how the mean life rises with the complexity of the molecule, as already indicated.

TABLE 8
The mean life of some quasi-molecules (experimental values)

Reaction					τ' , sec
$\text{H} + \text{O}_2 \rightarrow \text{HO}_2^*$	10^{-13} to 10^{-12}
$\text{H} + \text{OH} \rightarrow \text{H}_2\text{O}$	1.4×10^{-11}
$2\text{OH} \rightarrow \text{H}_2\text{O}_2$	2 to 4.5×10^{-10}
$\text{H} + \text{CH}_3 \rightarrow \text{CH}_4^{\dagger}$	2 to 3×10^{-9}
$\text{CH}_3 + \text{CH}_3 \rightarrow \text{C}_2\text{H}_6$	10^{-7}
$\text{CH}_3 + \text{C}_2\text{H}_5 \rightarrow \text{C}_3\text{H}_8$	4×10^{-6}

* According to [1013a] the life of $\text{H}\cdot\text{O}_2$ must exceed 10^{-7} sec.

† It can be assumed that the values of τ' for $\text{CH}_3\cdot\text{H}$, $\text{CH}_2\text{D}\cdot\text{H}$ and $\text{CHD}_2\cdot\text{H}$ have the same order of magnitude. This follows partly from the fact that Kistiakowsky and Roberts [839] obtained practically identical values of $\tau'k_2^0$ for $\text{CH}_3\cdot\text{CH}_3$ and $\text{CD}_3\cdot\text{CD}_3$.

Some of the figures in Table 8 agree closely with the values of τ' calculated by Kimball [831]. For the first three reactions Kimball found $\tau' = 1.1 \times 10^{-12}$, 2.7×10^{-12} and 3×10^{-10} sec., in good agreement with the experimental values. In other cases there is no such agreement. For the fourth and fifth reactions in Table 9, for example, Kimball found 3.2×10^{-12} and 2.4×10^{-12} sec, which are respectively three and five powers of ten less than the experimental values.

The discrepancy between experiment and theory is due to the very approximate nature of Kimball's method of calculation.⁽⁹⁾ Kassel [820] showed that the introduction of greater precision into Kimball's theory (remaining within the framework of classical mechanics) lowers Kimball's calculated values of τ' by a factor of

$$[\frac{1}{2}(s+1)]^{(s-1)/2},$$

where s is the number of normal vibrations of the quasi-molecule as used by Kimball. As is evident from this expression, the correction factor will

(9) Kimball's calculated values of τ' refer to 300°K (τ'_{300}). To obtain τ' at different temperatures he gives the formula

$$\tau'_T = \tau'_{300}(300/T)^{(s-1)/2}$$

Because of the gross approximations in Kimball's theory this formula can hardly be considered sufficiently accurate.

be particularly large for large s and equals 1.2, 2, 4 and 9 when $s = 2, 3, 4$ and 5.⁽¹⁰⁾ Both this fact and Kimball's choice of the values of s may account for the above-mentioned close agreement between the calculated and measured values of τ' for the first three reactions in Table 8. It should however be borne in mind that a substantial correction can also be introduced by allowing for the quantum characteristics of the system. In the opinion of Kassel [820] a quantum-mechanical theory might give a result substantially different from that obtained by classical treatment of this problem of the stabilization of quasi-molecules of varying structure.

Of great importance in connection with this problem is the number of degrees of freedom in the quasi-molecule which take part in energy transfer. This question was studied by Marcus [915] and his observations are relevant to our problem. He distinguishes between "active", "adiabatic" and "inactive" degrees of freedom. The first participate in the transfer of energy to the breaking bond without any limitations; the "adiabatic" degrees of freedom, which retain their quantum state during the reaction, contribute relatively little to the energy transfer, while the "inactive" degrees of freedom participate only when the quasi-molecule is in a transition state.

Directly connected with the number of normal vibrations (vibrational degrees of freedom) involved in energy transfer is the possibility of free rotation of the recombining radicals. Two limiting cases can be considered: the "loose" quasi-molecule where both radicals can rotate freely and the "rigid" quasi-molecule where the radicals have a completely fixed orientation relative to each other. In his analysis of this question Marcus [915] came to the conclusion that the experimental data were insufficient to resolve it. In the particular case of the recombination of methyl radicals⁽¹¹⁾ preference should, according to Marcus, be given to the "rigid" model of the quasi-molecule $\text{CH}_3 \cdot \text{CH}_3$. By applying the transition state method to the recombination of radicals and considering this process as the reverse of unimolecular decomposition Marcus further concluded that all the vibrational degrees of freedom could participate in intramolecular energy transfer and that the anharmonicity of the vibrations must play an important part in the exchange process.

Let us deal also with the temperature dependence of the rate of recombination of radicals. When the limiting step in the process is the formation of the quasi-molecule (by the collision of two radicals) the effect of temperature on recombination will be determined by the temperature dependence of the rate constant k_1 corresponding to this step. If we can assume that

⁽¹⁰⁾ Using this correction, which for the reaction $\text{H} + \text{C}_2\text{H}_5 \rightarrow \text{C}_2\text{H}_6$ ($s = 11$) equals $7^6 \approx 120,000$, Kassel found $\tau' = 2 \times 10^{-5}$ sec for the quasi-molecule $\text{H} \cdot \text{C}_2\text{H}_5$ instead of the value 2.1 sec obtained by Kimball.

⁽¹¹⁾ See however [839] p. 1642.

in the recombination of atoms the potential energy curve has no barrier⁽¹²⁾ and that the temperature dependence of the constant k_1 is expressed by a term $T^{1/2}$, we must, however, expect usually a more complex dependence of k_1 on temperature for the recombination of radicals (or of a radical and an atom). In particular, it is always possible that a potential energy barrier may exist because of a change in the bond angles during recombination or for other reasons (e.g. loss of conjugation) and the constant k_1 will therefore have an exponential (Arrhenius) temperature dependence, so that the possible presence of an activation energy cannot be excluded. Apart from this the large number of degrees of freedom leads one to expect a temperature dependence of the pre-exponential factor in the expression for k_1 more complex than a simple proportionality to $T^{1/2}$ (particularly for polyatomic radicals, see Chap. 3).

Turning now to the experimental results, it must be emphasized that the temperature dependence of the formation of the quasi-molecule (constant k_1) has not been studied at all since, in the almost complete absence of any quantitative investigation of the pressure dependence of the effective rate constant of recombination, it is usually impossible to establish whether the experimentally determined effective constant is identical with the elementary constant k_1 [cf. eq. (14.3)] or whether it is a complex quantity equal to $k_1^{-1}\tau'k_2^0(M)$ [cf. eq. (14.5)].

The greatest amount of work has been concerned with methyl radicals. According to the data of Kistiakowsky and Roberts [839], which appear to be more accurate than those of other workers, the effective constant for the recombination of CH_3 radicals at 180°C is given by the formula

$$k_{\text{eff}} = k_1/(1+4.6/p)$$

where p is the vapour pressure of acetone⁽¹³⁾ in mm Hg. It follows from this formula that, when the vapour pressure of acetone is a few cm Hg and consequently the second term in the denominator is sufficiently small compared to unity, k_{eff} almost coincides with k_1 . It can therefore be assumed that the constants for the recombination of CH_3 radicals measured by Gomer and Kistiakowsky [686], at an acetone vapour pressure of 50 mm Hg, represent the values of the constant k_1 . By combining their values of k_1 at 125°C ($0.75 \times 10^{-10} \text{ cm}^3 \text{ molecules}^{-1} \text{ sec}^{-1}$) and 175°C ($0.70 \times 10^{-10} \text{ cm}^3 \text{ molecules}^{-1} \text{ sec}^{-1}$) with values⁽¹⁴⁾ obtained using a different source

⁽¹²⁾ We are not here concerned with those relatively rare cases where the formation of the quasi-molecule by the recombination of either atoms or radicals is accompanied by the transition of the system to a new electronic state by surmounting a potential energy barrier. We also neglect the presence of any low barrier due to rotation.

⁽¹³⁾ In the experiments of Kistiakowsky and Roberts CH_3 radicals were obtained photochemically according to the scheme $(\text{CH}_3)_2\text{CO} + h\nu = 2\text{CH}_3 + \text{CO}$.

⁽¹⁴⁾ The data of Kistiakowsky and Roberts [839] for the constant k_1 at 165°C lead to the figure $0.9 \times 10^{-10} \text{ cm}^3 \text{ mole}^{-1} \text{ sec}^{-1}$.

of radicals (dimethylmercury CH_3HgCH_3) Gomer and Kistiakowsky found that the energy of activation for the formation of $\text{CH}_3\cdot\text{CH}_3$ from CH_3 radicals was⁽¹⁵⁾ $E = 0 \pm 0.7$ kcal. Ivin and Steacie [796] obtained for the activation energy in the formation of $\text{C}_2\text{H}_5\cdot\text{C}_2\text{H}_5$ from C_2H_5 radicals the result that⁽¹⁶⁾ $E < 0.7$ kcal. Similar low values of E (close to zero) have been established in other cases.⁽¹⁷⁾ It should also be pointed out that according to the measurements of Bryce and Ingold [462] the rate constant of the reaction $\text{CH}_3 + \text{NO} \rightarrow \text{CH}_3\text{NO}$ is 1.3×10^{11} and $1.4 \times 10^{11} \text{ cm}^3 \text{ mole}^{-1} \text{ sec}^{-1}$ at 480 and 900°C respectively. The activation energy is therefore practically zero in this case also. The low value of the rate constant (corresponding to a probability of 3×10^{-4} to 4×10^{-4} of the reaction occurring at each collision) in this case is probably to be connected with the low pressure (helium at 10 mm Hg) at which the experiments of Bryce and Ingold were carried out. The measured rate constant of the reaction is then obviously not the true constant k_1 . In contrast to radicals of simple structure, the activation energy for recombination of complex radicals is appreciable. For example, F. S. Dyachkovsky, N. N. Bubnov and A. E. Shilov, *Dokl. Akad. Nauk SSSR* 122, 629 (1958), find the activation energy for the process $(\text{C}_6\text{H}_5)_3\text{C} + (\text{C}_6\text{H}_5)_3\text{C} = (\text{C}_6\text{H}_5)_3\text{C} - \text{C}(\text{C}_6\text{H}_5)_3$ is 7 kcal.

Examination of the temperature dependence of the rate constant for the recombination of radicals observed at low pressures, where the termolecular reaction occurs, is outside the scope of this chapter. Let it simply be noted that in this case the variation with temperature of the rate constant can, generally speaking, be caused by the temperature dependence of either k_1 , τ' or k_2^0 . Assuming that the recombination of radicals (constant k_1) proceeded without activation energy ($E_1 = 0$), Benson [380] expressed the temperature dependence of the rate of recombination by a function T^{1-s} , where s is the number of internal "normal" coordinates determining the state of the active molecule during the reverse process of decomposition into radicals. The negative temperature coefficient resulting from this formula has in fact been observed in the recombination of CH_3 radicals in the low pressure region, where the limiting process is the collision stabilization of the quasi-molecule (see p. 228).

⁽¹⁵⁾ Ingold and Lossing [793] obtained a negative temperature coefficient for the constant of recombination of CH_3 radicals over the temperature range 161–814°C, corresponding to an activation energy of -2.2 ± 0.5 kcal. Later Ingold, Henderson and Lossing [791] obtained $E = -1.5$ kcal. These workers showed that their experimental recombination constant did in fact represent the quantity $k_1 k_2(M)_1/k$ [see eq. (14.5)] and its observed fall with temperature was in their opinion caused by the rise with temperature of the constant $_1$. See also Benson [380].

⁽¹⁶⁾ The quantity k_1 here equals $0.3 \times 10^{-10} \text{ cm molecules}^{-1} \text{ sec}^{-1}$. See also [1133b].

⁽¹⁷⁾ For literature see Steacie [1169] and also [1228], [774] and [338a].

It should be added that low activation energies (< 5 kcal) are also observed in the recombination of radicals in polymerization reactions and in oxidation and other reactions occurring in solution [1228].

Addition of Atoms and Radicals to Multiple or Conjugated Bonds

As in the recombination of atoms and radicals, reactions of this type obey a bimolecular law when at least one of the colliding particles (radical or molecule) has a sufficiently large number of vibrational degrees of freedom to impart a long life to the quasi-molecule. Table 9 gives the values of the activation energy and of the pre-exponential factor in the expression for the rate constant of certain reactions of the type being considered, the Arrhenius equation

$$k = A \exp(-E/RT)$$

being assumed for k . The constant A is expressed in the units $\text{cm}^3 \text{mole}^{-1} \text{sec}^{-1} = 6.02 \times 10^{23} \text{cm}^3 \text{molecules}^{-1} \text{sec}^{-1}$.

TABLE 9

Rate constants of some bimolecular reactions involving the addition of an atom or radical to an unsaturated molecule, with $k = A \exp(-E/RT) \text{cm}^3 \text{mole}^{-1} \text{sec}^{-1}$

Reaction			E kcal	$\log A$	Temperature Interval °C
$\text{H} + \text{C}_2\text{H}_2 \rightarrow \text{C}_2\text{H}_3$ [541]	.	.	1.8	11.3	2-99
$\text{H} + \text{C}_2\text{H}_4 \rightarrow \text{C}_2\text{H}_5$ [530, 950]	.	.	4.1*	13.5*	25-300
$\text{H} + \text{C}_2\text{H}_6 \rightarrow \text{C}_3\text{H}_7$ [530, 950]	.	.	5.0*	14.4*	25-300
$\text{CH}_3 + \text{C}_2\text{H}_4 \rightarrow \text{C}_3\text{H}_7$ [907]	.	.	$7 \pm 1.5 \dagger$	11.4	140-240
$\text{CH}_3 + \text{C}_3\text{H}_6 \rightarrow \text{C}_4\text{H}_9$ [907]	.	.	6‡	11.0	140-240
$\text{CH}_3 + \text{C}_4\text{H}_6 \rightarrow \text{C}_5\text{H}_9$ [907]	.	.	2.5	9.9	140-240
$\text{CH}_3 + \text{CH}_2\text{N}=\text{NCH}_3 \rightarrow (\text{CH}_3)_2\text{N}-\text{NCH}_3$ [809]	.	.	6.3	10.7§	24-190
$\text{CH}_3 + \text{O}_2 \rightarrow \text{CH}_3\text{O}_2$ [913]	.	.	0 ± 0.5	10.9§	25-200

* These figures are based on the assumption that the rate constant of the reaction $\text{D} + \text{H}_2 = \text{HD} + \text{H}$ can be expressed by the formula $k = 10^{13.4} \exp(-5000/RT) \text{cm}^3 \text{mole}^{-1} \text{sec}^{-1}$. Since this formula cannot be considered sufficiently exact (see below p. 257 and also [1228] p. 284), the values of E and A for the addition of H to olefins are not reliable.

† In the opinion of Steacie [1169] p. 584 this figure is too high and the real activation energy should be 3 ± 2 kcal. See however [440a].

‡ Steacie ([1169] p. 557) finds this too high and assumes as the more probable value $E = 1$ to 3 kcal.

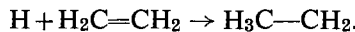
§ See also [1228] p. 298.

As can be seen from Table 9 the addition of an atom or radical to an unsaturated molecule at a double or triple bond involves a certain activation energy not present in recombination reactions, where the activation energy is small or zero (see above). The presence of a marked activation energy in the addition to a multiple bond is undoubtedly caused by a change in the valence state of the atoms involved in the multiple bond

(carbon and nitrogen in the case of the reactions listed in Table 9). Table 9 also draws attention to the relatively low values of the pre-exponential term (A) which in all but two cases is considerably smaller than $10^{-10} \text{ cm}^3 \text{ molecules}^{-1} \text{ sec}^{-1} \approx 10^{14} \text{ cm}^3 \text{ mole}^{-1} \text{ sec}^{-1}$, the value characteristic of a recombination reaction.

The peculiarities of the kinetics of addition to a multiple bond have a certain theoretical basis, for we are obviously concerned here with the addition of an atom or radical with the help of one of the π -electrons.

Let us examine the mechanism of addition of a univalent atom to a π -bond, e.g. the addition of a hydrogen atom to ethylene



Unlike metathetical reactions $\text{A} + \text{BC} = \text{AB} + \text{C}$, where the third atom recedes from the new bond and thereby creates the condition for the completion of the process, addition reactions require that all the atoms remain close together. If, then, during the approach of the H atom to the C_2H_4 molecule the latter does not alter its geometrical configuration or remains in its ground quantum state, the approaching particle will be repelled and the addition reaction will not take place (see Fig. 50 curve I).

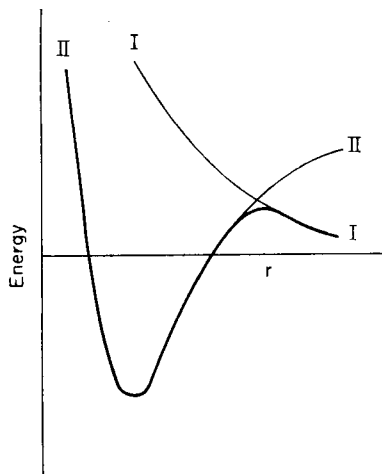


FIG. 50. Pseudo-intersection of potential energy curves of the singlet (I-I) and triplet (II-II) states of the system olefin + radical.

Addition to the double bond of ethylene can be accomplished in two ways. The first involves the transition of the π -electrons of ethylene from the singlet state corresponding to the curve of repulsion (curve I) to the triplet state characterized by a curve with a more or less pronounced

minimum (curve II). This transition occurs at the point of pseudo-intersection of curves I and II, so that the real change in energy as the particles C_2H_4 and H approach will be given by the curve shown as a thick line in Fig. 50. Since, however, the energy of spin-orbital interaction, which causes a splitting of the energy levels at the pseudo-intersection point, is usually small, then according to (13.21) the probability of the energy proceeding along the lower curve will be considerably less than unity. As was shown in §13 this means a considerable decrease in the transmission coefficient κ . We should therefore expect that in the mechanism under consideration, namely the addition of atoms or radicals to a double bond, the pre-exponential term in the Arrhenius equation would have a value several powers of ten less than that for metathetical reactions, where it often has a value of the order of 10^{13} to $10^{14} \text{ cm}^3 \text{ mole}^{-1} \text{ sec}^{-1}$ (see §15).

Another possible mechanism for addition to a double bond assumes *internal rotation* of the molecule about a line joining the two carbon atoms. Deflection of one CH_2 group in ethylene through 90° relative to the other obviously involves rupture of the π -bond, since in this configuration the axes of the p -orbitals of the carbon atoms are at right angles to each other and the corresponding exchange integral is zero. If this rotation occurred in an isolated molecule, it would require a large expenditure of energy, since it is known that in the unimolecular cis-trans isomerization of ethylene derivatives the energy of the activated complex, which has the indicated configuration, is about 40 to 60 kcal above the energy of the ground state (see Chap. 5, p. 308). The theoretical calculations of Mamotenko [179] lead to approximately the same result.

This rotation about the carbon-carbon bond in fact occurs simultaneously with the approach of an H atom, whose interaction with the nearest C atom lowers the energy of the system. The most energetically favourable configuration of the activated complex will obviously be that in which the H atom is situated on a line perpendicular to the $C=C$ bond and passing through one of the C atoms, thereby ensuring the maximum overlap of the p -electron orbitals of the latter with the orbital of the H atom (Fig. 51). If we replace the distance $C=C$ as the parameter determining the potential energy of the system by the angle ϕ between the axes of the p -orbitals of the carbon atoms (Fig. 51), then by considering this as a three-electron problem the activation energy for the addition of an atom to a double bond can be estimated using the London equation (10.2). Assuming that in the London equation α represents the exchange integral of the H—C bond, β the exchange integral of the $C=C$ π -bond dependent on the angle ϕ , and γ the exchange integral of the H and C atoms which are not directly bonded, it is easily shown that the simultaneous increase in the angle ϕ (causing a decrease in the integrals β and γ) and approach of the atom H (causing an increase in α) require considerably

less expenditure of energy than the rotation of the *p*-clouds through 90° in the isolated molecule (with the above definition of the integrals the energy of this rotation equals β). This means that the activation energy in the addition of an H atom to a double bond must be relatively small. It is also to be expected that in the second method of addition to a double bond the pre-exponential term in the expression for the rate constant of the reaction will not differ greatly in order of magnitude from Z , i.e. from the order $10^{14} \text{ cm}^3 \text{ mole}^{-1} \text{ sec}^{-1}$.

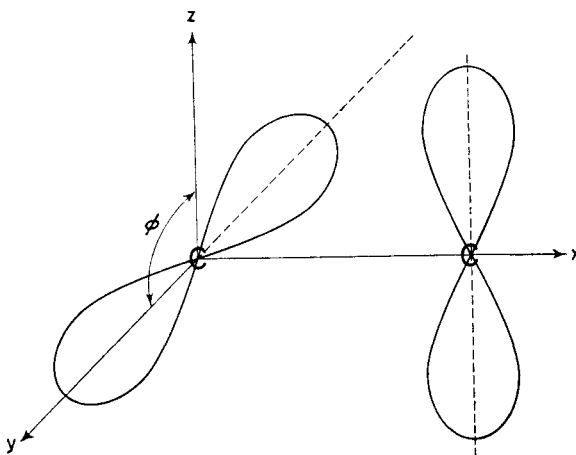


FIG. 51. Configuration of *p*-electron clouds in the activated complex in the addition of a radical to a double bond with rotation about the carbon–carbon bond of one part of the molecule through an angle ϕ relative to the other. In the diagram $\phi = 90^\circ$.

The experimental data seem to indicate that the addition of an H atom to an olefin or in general to any molecule with an isolated double bond proceeds in the majority of cases by the second method, namely rotation about the double bond. In Table 10 we list rate constants for the addition of an H atom to the isolated double bond of olefins and certain other compounds at 18°C and the corresponding collision efficiencies, i.e. the ratio of the rate constant k to the number Z of gas-kinetic collisions. The tabulated data show that for all olefins with the one exception of propylene⁽¹⁸⁾ the ratio k/Z is of the order of 10^{-3} . Assuming that this ratio equals $P \cdot \exp(-E/RT)$ (E is the activation energy of the reaction and $P = 10^{-x}$ is the probability factor) and noting that at 18°C the Arrhenius factor $\exp(-E/RT)$ can be written as $10^{-\frac{3}{4}E}$, we obtain $3 = x + \frac{3}{4}E$ or $E = 4 - \frac{4}{3}x$.

⁽¹⁸⁾ It is possible that because of the low pressure under experimental conditions the constant k for propylene is not the true constant of the bimolecular reaction producing the quasi-molecule $\text{C}_3\text{H}_6 \cdot \text{H}$. The low value of k in the case of C_2F_4 may also be due to the same cause.

TABLE 10

Rate constants and collision efficiencies for the addition of a H atom to the isolated double bond of olefins and derivatives at 18°C (after Allen, Melville and Robb [314])

Olefins and derivatives	$k \times 10^{-11} \text{ cm}^3 \text{ mole}^{-1} \text{ sec}^{-1}$	$k/Z \times 10^{-4}$
Ethylene $\text{H}_2\text{C}=\text{CH}_2$	5.1-7.5	7.6-11.4
Propylene $\text{H}_2\text{C}=\text{CHCH}_3$	1.6-1.8	1.7- 1.0
Isobutene $\text{H}_2\text{C}=\text{C}(\text{CH}_3)_2$	5.7	6.3
<i>trans</i> -But-2-ene $\text{CH}_3\text{CH}=\text{CHCH}_3$	6.3	5.5
<i>cis</i> -But-2-ene $\text{CH}_3\text{CH}=\text{CHCH}_3$	8.0	8.9
<i>cis</i> -n-Pent-2-ene $\text{H}_3\text{C}\cdot\text{HC}=\text{CH}\cdot\text{C}_2\text{H}_5$	5.8	4.6
Trimethylethylene $(\text{CH}_3)_2\text{C}=\text{CCH}_3\text{H}$	7.3	6.4
Tetramethylethylene $(\text{CH}_3)_2\text{C}=\text{C}(\text{CH}_3)_2$	4.8	4.2
2, 2, 3-Trimethylbutene $\text{H}_2\text{C}=\text{CCH}_3\cdot\text{C}_4\text{H}_9$	6.9	6.0
Methylmethacrylate $\text{H}_3\text{C}=\text{CCH}_3\cdot\text{COOCH}_3$	4.4	1.9
Tetrafluoroethylene $\text{F}_2\text{C}=\text{CF}_2$	0.6	0.3
Cyclohexene C_6H_8	8.0	7.9

Hence when $x > 0$ the activation energy of these reactions must satisfy the condition $E < 4 \text{ kcal}$ and the probability factor the condition $P > 10^{-3}$; in fact for $x = 1, 2, 3$ the activation energy $E \approx 3, 1, 0$ respectively. Assuming that P is of the order of 10^{-2} we find the activation energy to be 1 to 2 kcal.⁽¹⁹⁾

In the addition of atoms or radicals to isolated double bonds (as in many other types of reactions) there appears to be a linear relation between the energy of activation E and the heat of reaction Q (see Fig. 34). Since the energy of addition of an H atom to various olefins depends very little on the structure of the latter and varies within the limits 35-45 kcal, it is to be expected that the activation energy of the reaction $\text{H} + \text{olefin} \rightarrow \text{radical}$ will have similar values for the different olefins, not exceeding a few kilocalories. This conclusion is in full agreement with the above result.

Values of P for a number of reactions have been calculated theoretically by Stepukhovich and his coworkers [250] from the formula

$$P = \frac{n}{Z_0} \frac{kT}{h} \frac{Z^*}{Z_A Z_{BC}} \exp \left[\frac{1}{2} + T \frac{d}{dT} \left(\ln \frac{Z^*}{Z_A Z_{BC}} \right) \right] \quad (14.12)$$

obtained by the activated-complex method on the assumption that the transmission coefficient for these reactions is unity. Z_A , Z_{BC} and Z^* represent the partition functions of the H atoms, the olefin molecules and the activated transition complexes respectively, while n is the number of

⁽¹⁹⁾ The values of E and A for the reactions $\text{H} + \text{C}_2\text{H}_4$ and $\text{H} + \text{C}_3\text{H}_6$ listed in Table 9 cannot be considered sufficiently reliable (see note* under Table 9).

carbon atoms in the olefin molecule which are equivalent with respect to the addition of a H atom.⁽²⁰⁾ The values of P obtained by Stepukhovich and coworkers for the reaction of a H atom with ethylene, propylene and isobutylene are given in Table 11. Stepukhovich compares these with "experimental" values which he calculated from the data of Melville and Robb [530, 950] assuming that the activation energies equalled 2 kcal; these values are listed in the third column of Table 11. The fourth column

TABLE 11

Calculated and "experimental" values of the probability factor for the addition of a hydrogen atom to certain olefins

Reaction	$P \cdot 10^2$		
	Calculated [250]	From experimental data of [530, 950]	From experimental data of [314]
$H + C_2H_4 \rightarrow C_2H_5$	3.7	2.6	3.6-2.4
$H + C_3H_6 \rightarrow C_3H_7$	1.5	0.4*	0.3-0.5
$H + \text{iso-}C_4H_8 \rightarrow C_4H_9$	2.7	1.5	2.0

* Stepukhovich erroneously quoted the figure 1.2.

contains "experimental" values of k/Z_0 obtained in the same way from the more accurate data of Allen, Melville and Robb [314]. We see therefore that both methods of calculating the P factors give similar results, and we can conclude that in these reactions the probability factor must be about 0.01.

Where rotation about the π -bond is precluded because of the structure, as in molecules with a triple bond (acetylene C_2H_2 , hydrogen cyanide HCN, etc.) addition can proceed only by the first mechanism, namely by transition to the triplet state. Experimental confirmation of this conclusion in the case of addition to isolated (non-conjugated) multiple bonds is provided by data for the reaction $H + C_2H_2 \rightarrow C_2H_3$ (Table 9), which is characterized by a pre-exponential term of the order of $10^{11} \text{ cm}^3 \text{ mole}^{-1} \text{ sec}^{-1}$ which is unusually low for a hydrogen addition reaction. The P factor is 4×10^{-4} according to Dingle and Le Roy [541] and about 10^{-4} according to Melville and Robb [950]. The low value of P is in full accord with the supposition that this reaction must follow the first of the above two mechanisms. It is interesting to note that for this reaction Stepukhovich obtained $P = 0.5$. This wide discrepancy between the theoretical and experimental values is explained by the non-adiabatic character of the

⁽²⁰⁾ E.g. in ethylene C_2H_4 both carbon atoms are equivalent in this sense, while in propylene C_3H_6 one of the double-bonded carbon atoms is six times as reactive as the other with respect to the addition of a H atom (see [530, 950]).

reaction (first mechanism), corresponding to $\kappa \ll 1$ (as already mentioned, Stepukhovich took $\kappa = 1$ in his calculations).

It is to be expected that the addition of atoms and radicals to aromatic and conjugated molecules will proceed by this same mechanism, since rotation is precluded by the closed, conjugated ring. The correctness of this conclusion is shown by the following data. The collision efficiency in the reaction $\text{H} + \text{C}_6\text{H}_6 \rightarrow \text{C}_6\text{H}_7$ is 2×10^{-7} (at room temperature) according to Mund *et al.*, [961], while Allen, Melville and Robb [314] obtained the larger, though still small, value of 1.3×10^{-4} . The latter found the collision efficiency in the reaction $\text{H} + \text{C}_6\text{H}_5\text{CH}_3 \rightarrow \text{C}_7\text{H}_9$ to be 0.2×10^{-4} , while in $\text{H} + \text{CH}_3\text{C}_6\text{H}_4\text{CH}_3 \rightarrow \text{C}_8\text{H}_{11}$ and $\text{H} + \text{C}_3\text{H}_7\text{C}_6\text{H}_5 \rightarrow \text{C}_9\text{H}_{13}$ it was also less than 10^{-4} . We shall adduce one more argument in support of the non-adiabatic mechanism for the addition to aromatic compounds, which concerns liquid-phase reactions and the addition, not of an atom, but of a radical (CH_3). If we consider a series of aromatic compounds, we should

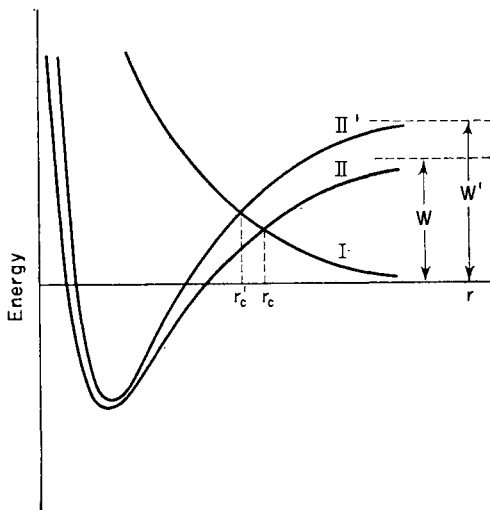


FIG. 52. Potential energy curves of the singlet and triplet states for two different values of the excitation energy to the triplet state.

expect that, to a first approximation, the greater the excitation energy of the triplet state W in the isolated molecule, the higher will be the point of pseudo-intersection of the potential energy curves of the singlet and triplet states (Fig. 52). Assuming then that the activation energy is approximately proportional to this excitation energy,

$$E \approx aW,$$

we should expect the logarithm of the rate constant for the addition of an

atom or radical to an aromatic molecule to be a linear function of W . This relation was in fact discovered by Szwarc [1201]. The relation he obtained is shown in Fig. 53; along the abscissa are plotted the excitation energies to the triplet state of a number of aromatic compounds, and along the ordinate the logarithm of the relative rates of addition of a methyl

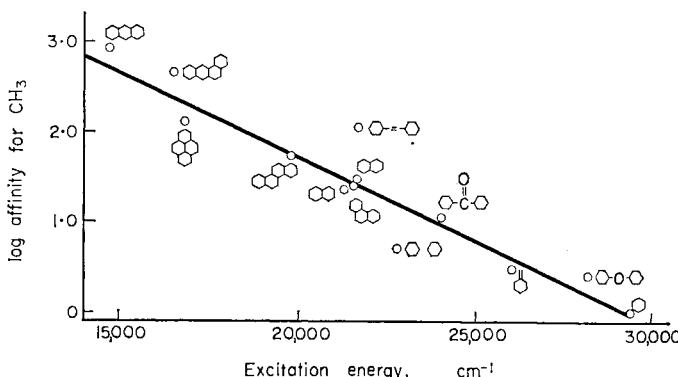


FIG. 53. Dependence of the relative rate of addition of methyl CH_3 on the excitation energy of the triplet state (after Szwarc [1201]).

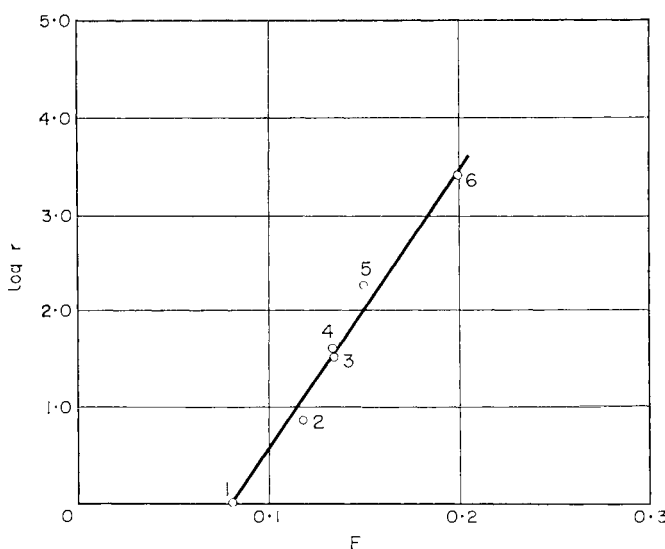


FIG. 54. The dependence of the logarithm of the relative rate of addition of methyl CH_3 on the free valence index of the most reactive carbon atom of various aromatic compounds (after Coulson [503]).

(1) benzene; (2) diphenyl; (3) naphthalene; (4) phenanthrene; (5) pyrene; (6) anthracene.

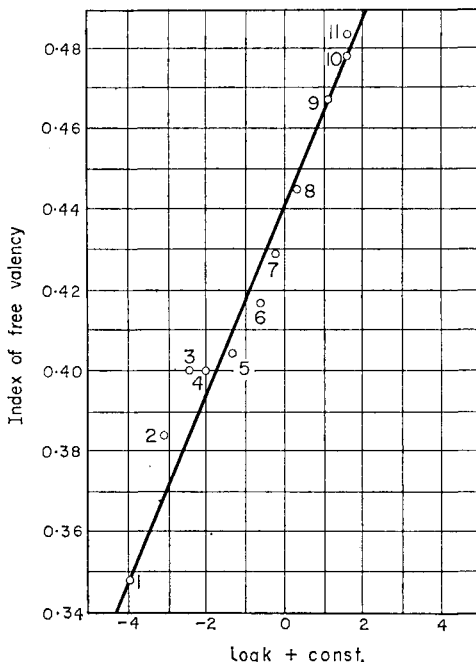


FIG. 55. Relation between the relative rate of addition of the radical CCl_3 to aromatic hydrocarbons and the free valence index (after Kooyman and Farenhorst [852]). (1) benzene; (2) diphenyl (2, 6, 2', 6'); (3) phenanthrene (1, 8, 9, 10); (4) naphthalene (1, 4, 5, 8); (5) chrysene (2, 8); (6) pyrene (3, 5, 8, 10); (7) stilbene (1, 1'); (8) 1, 2, 5, 6-dibenzanthracene (9, 10); (9) anthracene (9, 10); (10) naphthacene (5, 6, 11, 12); (11) 1, 2-benzanthracene (9). The positions of the carbon atoms with the highest valence index are shown in brackets.

radical [874]. The diagram shows that practically all the points lie fairly well on a straight line, in spite of the fact that the data refer to different types of compounds (hydrocarbons, nitrogenous heterocyclic bases, ketones and esters). A significant divergence is observed only in two cases: diphenyl $\text{C}_6\text{H}_5\text{C}_6\text{H}_5$ and stilbene $\text{C}_6\text{H}_5\text{CH}=\text{CHC}_6\text{H}_5$. A possible cause of the divergence in the latter case is that the rate data refer to the *trans* isomer, while the excitation energy to the triplet state was determined using the *cis* isomer.

It should be noted that the relative rate of addition of methyl to various aromatic molecules is closely connected with the free valence index⁽²¹⁾ of the most reactive carbon atom in the molecule (Fig. 54), as was shown by Coulson [503]. It has also been shown that the free valence index of the

⁽²¹⁾ The free valence index, introduced by Coulson [503], indicates the degree of unsaturation of a given atom in a conjugated chain. Coulson also suggested a method for calculating this quantity.

most reactive atoms in a series of hydrocarbons varies linearly with the logarithm of the relative rate of addition of the radical CCl_3 [852] (Fig. 55). Since, however, these reactions proceed in the liquid phase, a detailed examination of their characteristics is beyond the scope of this monograph.⁽²²⁾

The Association of Saturated Molecules

Association reactions of saturated molecules comprise various classes, of which we shall mention: the reactions between methylamines and boron trifluoride $(\text{CH}_3)_n\text{NH}_{3-n} + \text{BF}_3 = (\text{CH}_3)_n\text{NH}_{3-n}\text{BF}_3$; cyclization reactions, e.g. $2 \text{C}_2\text{F}_4 = \text{cyclo-C}_4\text{F}_8$ and the Diels-Alder reaction involving the formation of a cyclic compound by the interaction of two organic molecules of the diene type or of a diene and an aldehyde or olefin, e.g. C_4H_6 (butadiene) + C_2H_4 (ethylene) = C_6H_{10} (cyclohexene); the reaction between hydrogen halides and olefins, $\text{HX} + \text{C}_n\text{H}_{2n} = \text{C}_n\text{H}_{2n+1}\text{X}$, etc.

The first class of reactions with mono-, di- and trimethylamines CH_3NH_2 , $(\text{CH}_3)_2\text{NH}$ and $(\text{CH}_3)_3\text{N}$ was studied by Garvin and Kistiakowsky [648]. Their values for the rate constants of these very rapid bimolecular gaseous reactions are presented in Table 12.⁽²³⁾ From a comparison of the

TABLE 12

The rate constants of some bimolecular association reactions of saturated molecules, $k = A \exp(-E/RT) \text{ cm}^3 \text{ mole}^{-1} \text{ sec}^{-1}$

Reaction	$E \text{ kcal}$	$\log A$	Temperature °C
$\text{CH}_3\text{NH}_2 + \text{BF}_3 \rightarrow \text{CH}_3\text{NH}_2 : \text{BF}_3$ [648]	0	11.9	25
$(\text{CH}_3)_2\text{NH} + \text{BF}_3 \rightarrow (\text{CH}_3)_2\text{NH} : \text{BF}_3$ [648]*	0	13.5	25
$(\text{CH}_3)_3\text{N} + \text{BF}_3 \rightarrow (\text{CH}_3)_3\text{N} : \text{BF}_3$ [648]*	0	12.6	25
$\text{C}_2\text{F}_4 + \text{C}_2\text{F}_4 \rightarrow \text{cyclo-C}_4\text{F}_8$ [858, 335]	25.4	11.0	300-550
$\text{C}_2\text{F}_3\text{Cl} + \text{C}_2\text{F}_3\text{Cl} \rightarrow \text{cyclo-C}_4\text{F}_6\text{Cl}_2$ [858]	26.3	10.5	305-509
$\text{C}_2\text{F}_3\text{Cl} + \text{C}_2\text{F}_4 \rightarrow \text{cyclo-C}_4\text{F}_7\text{Cl}$ [858]	26.3	10.9	305-437
$\text{C}_4\text{H}_6 + \text{C}_2\text{H}_4 \rightarrow \text{cyclo-C}_6\text{H}_{10}$ [1092]	27.5	10.5	400-600
$\text{C}_4\text{H}_6 + \text{C}_4\text{H}_6 \rightarrow \text{cyclo-C}_8\text{H}_{12}$ [1092]	26.8	11.1	400-600

* See also [517a].

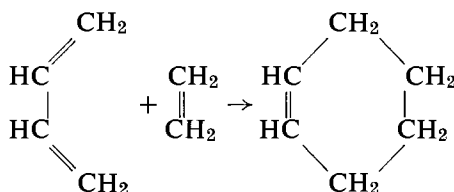
rate constants with the number of gas-kinetic collisions they concluded that the activation energy of these reactions was close to zero. It is interesting that dimethylamine is the most reactive of the three methylamines.

⁽²²⁾ For a survey of the literature see [460].

⁽²³⁾ See also [1228] p. 125 and [842].

The cyclization of fluorethylene was studied by Lacher, Tompkin and Park [858] and by Atkinson and Trenwith [335]. The former workers also studied two other analogous reactions. The activation energies and pre-exponential terms of these reactions are also given in Table 12.

The Diels–Alder reaction is a more complex type of cyclization. Table 12 contains the activation energies and pre-exponentials of the two simplest of the numerous reactions of this type which have been studied,⁽²⁴⁾ the reaction of butadiene with ethylene and of butadiene with butadiene. It is now accepted⁽²⁵⁾ that the Diels–Alder reaction takes place in one step through the direct interaction of the π -electrons according to the following scheme:⁽²⁶⁾



The activation energy of this type of reaction is usually 20–30 kcal (see Table 12). There has been very little theoretical work on the mechanism. Quantum-mechanical calculations have been made to estimate the relative reactivity of the various dienes in these reactions.

As shown by the data in Table 12, the pre-exponentials in the cyclization reactions are some ten to a thousand times smaller than those of the first three reactions. If we express A as the product PZ and remember that Z has an order of $10^{14} \text{ cm}^3 \text{ mole}^{-1} \text{ sec}^{-1}$, we find $P = 1$ to 0.01 for the first three reactions and $P = 10^{-4}$ for the cyclizations.

The bimolecular addition of hydrogen halides to olefins follows directly from the existence of the reverse reaction, namely the unimolecular decomposition of the halogenoalkyls according to the scheme $C_nH_{2n+1}X = C_nH_{2n} + HX$ [896, 698, 700]. From the activation energy and heat of this reaction one can calculate the activation energy of the bimolecular association to be 25–35 kcal.

§15. Metathetical or Transfer Reactions $A + BC = AB + C$, and Exchange (Double Transfer) Reactions $AB + CD = AC + BD$

These reactions, unlike addition reactions (§14), take place by one elementary step. This is because the excess energy liberated by the reaction is distributed between the products (AB and C) so that no stabilization is

⁽²⁴⁾ For literature see Trotman-Dickenson [1228] p. 131.

⁽²⁵⁾ See [385, 1226, 332, 333, 334, 536, 1270].

⁽²⁶⁾ The opinion has, however, been expressed that this reaction does not occur in one step and involves a radical mechanism. See, for example [644].

required. This class includes numerous reactions of atoms and radicals with various molecules, for example $H + C_2H_6 = H_2 + C_2H_5$ or $H + C_2H_6 = CH_4 + CH_3$, in particular isotopic exchange, e.g. $H + DCl = HCl + D$ or $I + CH_3I = ICH_3 + I$; reactions between radicals, e.g. $C_2H_5 + C_2H_5 = C_2H_6 + C_2H_4$ (disproportionation), or between radical-like molecules, e.g. $NO + NO = N_2O + O$, etc.

Reactions of Atoms with Molecules

The rate constants (activation energies E and pre-exponentials A) of some reactions of atoms with saturated molecules are presented in Table 13. The fourth column gives the heat effect of the corresponding reactions (proceeding from left to right), the figures -17 , -1.0 , 20.4 and -32.1 referring to $0^\circ K$ and the others to $25^\circ C$. As can be seen from the data in Table 13, the activation energy of the reactions when proceeding in the exothermic direction (sometimes called the "true activation energy") is in the majority of cases less than 5 kcal, this value being exceeded only in a few cases. There are also only a few cases where the pre-exponential has an order of magnitude less than $10^{13}-10^{14}$, whence it follows that in these reactions the P factor has, as a rule, a value of the order of 0.1 to 1 .

TABLE 13

*Rate constants of some reactions of atoms with saturated molecules,
 $k = A \exp(-E/RT) \text{ cm}^3 \text{ mole}^{-1} \text{ sec}^{-1}$*

Reaction	$\log A$	E kcal	Q kcal	Temperature $^\circ C$
$H + H_2 = H_2 + H^*$	13.7	7.5 ± 1	0	25-700
$H + CH_4 = H_2 + CH_3 \dagger$ [870] . .	10.5	6.6	1.7	99-163
$H + C_2H_6 = H_2 + C_2H_5$ [387] . .	12.5	6.8	6.4	80-163
$H + O_2 = HO + O$ [203] . .	14.1	18.8	-17	450-600
$Cl + H_2 = HCl + H$ [332] . .	13.9	5.5	-1.0	25-727
$Cl + CH_4 = HCl + CH_3$ [1049] . .	13.4	3.9	0.7	0-215
$Cl + C_2H_6 = HCl + C_2H_5$ [1049] . .	14.1	1.0‡	5.4	0-215
$Cl + NOCl = NO + Cl_2$ [469] . .	13.06	1.06	20.4	25-55
$Br + H_2 = HBr + H$ [420] . .	13.8	17.6**	-16.7	162-310
$Br + CH_4 = HBr + CH_3$ [841] . .	13.7	18.3	-15.0	210
$Br + C_2H_6 = HBr + C_2H_5$ [321] . .	—	13.9	-10.3	30-90
$O + NO = N + O_2$ [826] . .	12.9	40.5	-32.1	>1100
$K + HBr = KBr + H \dagger \dagger$ [1213] . .	—	3.4	5.3	—

* See Trotman-Dickenson [1228] pp. 171-173; see also Kassel [106] pp. 131-132 and [1241].

† Pritchard, Pyke and Trotman-Dickenson [1050] found $E = 9.0$ kcal and $\log A = 12.5$ for this reaction; see, however, [387a].

‡ See Trotman-Dickenson [1228] p. 188.

** See Trotman-Dickenson [1228] p. 191; see also [811].

†† According to the calculations of Taylor and Datz [1213] the P factor in this reaction is 0.1. Measurements were made using intersecting molecular beams of K and HBr with vapour temperatures of $540-840^\circ K$ (K) and $373-460^\circ K$ (HBr).

The reactions of atoms with saturated molecules have often been considered theoretically. The mechanism of these reactions was examined qualitatively in Chap. 3 §11. For a quantitative determination of the rate constant we may use eq. (12.55), which for reactions of the type $A + BC = AB + C$ (A , B and C being atoms) can be rewritten in the form [57]

$$k = \kappa \frac{g^*}{g_A g_{BC}} \left[\frac{m_A + m_B + m_C}{m_A(m_B + m_C)} \right]^{3/2} \frac{I^* \sigma_{BC}}{I_{BC} \sigma^*} \frac{h^2}{(2\pi)^{3/2} (kT)^{1/2}} \times \\ \times \frac{[1 - \exp(-hv_{BC}/kT)]}{\frac{3}{\Pi [1 - \exp(-hv^*/kT)]}} \exp(-E_0/RT). \quad (15.1)$$

The subscripts A , BC and \neq refer to the atom A , the molecule BC and the activated complex ABC respectively. Although an activation energy obtained by the use of a semi-empirical method (see Chap. 3 §10) cannot be considered strictly justifiable since the ratio of Coulomb and exchange integrals is chosen empirically, we shall in this case make use of the result of this type of calculation. It indicates how the rate constant of the elementary reaction could be calculated if the energy and other characteristics of the activated complex had been determined theoretically.

If we take the concrete example of the reaction $H + HD = H_2 + D$, which is one of the simplest transfer reactions, and assume that the activated complex $H \dots H \dots D$ has a linear structure and that the Coulomb integral comprises 20 per cent of the total bond energy, we find an activation energy $E_{C1} = 7.68$ kcal, neglecting the difference in zero point energy between the initial and activated states [57]. The activation energy at the absolute zero of temperature can be calculated from the expression

$$E_0 = E_{C1} + N_A \left(\frac{1}{2} \sum h\nu^* - \frac{1}{2} h\nu_{BC} \right) \quad (15.2)$$

where $\frac{1}{2} \sum h\nu^*$ is the sum of the zero-point energies of all the vibrational degrees of freedom of the activated complex (three components) and $\frac{1}{2} h\nu_{BC}$ is the zero-point energy of the initial molecule (HD). E_0 is now found to be 8.41 kcal (see below).

The moments of inertia of the initial molecule and of the activated complex are calculated from the equations

$$I_{BC} = [m_B m_C / (m_B + m_C)] (r_0)_{BC}^2;$$

$$I^* = M^{-1} [m_A (m_B + m_C) r_{AB}^2 + 2m_A m_B r_{AB} r_{BC} + m_C (m_A + m_B) r_{BC}^2],$$

where $M = m_A + m_B + m_C$, $(r_0)_{BC}$ is the equilibrium interatomic distance in the molecule BC ; r_{AB} and r_{BC} are the distances between the atoms $A \dots B$ and $B \dots C$ in the activated complex; the values of r_{AB} and r_{BC} may be found by calculating the potential energy surface of the system $A + B + C$ ($H + H + D$). The vibration frequencies of the activated complex

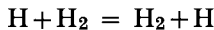
may also be obtained from the potential energy surface, namely the frequency ν_ϕ of the doubly degenerate deformation vibration and the frequency ν_s of the symmetrical vibration. The electronic statistical weights are calculated from the relation $g = 2J+1$: since the atom A is H, for which $J = \frac{1}{2}$, we find $g_A = 2$; similarly for the molecule BC ($J = 0$) and the complex ABC we find $g_{BC} = 1$ and $g^* = 2$.⁽²⁷⁾

A summary of all quantities necessary for the calculation of the rate constant k is given below [57]. The summary also includes values of the transmission coefficient κ for the reaction $H + HD = H_2 + D$.

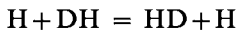
$m_A = m_B$	$1.67 \times 10^{-24} \text{ g}$	ν_{BC}	3825 cm^{-1}	g_A	2
m_C	$3.34 \times 10^{-24} \text{ g}$	$\frac{1}{2}N_A h\nu \neq \phi$	$0.88 (1.60) \text{ kcal}^*$	g_{BC}	1
$(r_0)_{BC}$	0.74 \AA	$\frac{1}{2}N_A h\nu \neq s$	$4.40 (3.91) \text{ kcal}$	g^*	2
r_{AB}	$1.35 \text{ \AA}^{(28)}$	$\frac{1}{2}N_A \sum h\nu \neq$	6.16 kcal	$\sigma_{BC} = \sigma^*$	1
r_{BC}	$0.75 \text{ \AA}^{(28)}$	$\frac{1}{2}N_A h\nu_{BC}$	5.38 kcal	$\kappa(300^\circ)$	0.192
I_{BC}	$0.61 \times 10^{-40} \text{ gcm}^2$	E_{C1}	$7.68 (5.98) \text{ kcal}$	$\kappa(600^\circ)$	0.332
I^*	$4.92 \times 10^{-40} \text{ gcm}^2$	E_0	8.41 kcal	$\kappa(1000^\circ)$	0.396

*See p. 257

The calculation of the quantity κ must be considered more fully. As already noted (p. 171), the probability of the return of the system to the initial state may become appreciable with the presence of a depression at the top of the barrier. If we neglect the repulsion caused by the contorted nature of the reaction path, the transmission coefficient for symmetrical reactions of the type

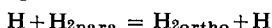


or



will be 0.5. In fact, if the system fell into this depression, the probability of the system escaping in either the forward or reverse direction will be equal because of the symmetry of the potential energy surface relative to the main diagonal. If the initial and final compounds are different ($H + HD = H_2 + D$), $\kappa \neq \frac{1}{2}$ because of the difference in zero point energy and moments of inertia. In this case the transmission coefficient can be calculated as follows.

(27) If we calculate the rate of *para-ortho* conversion of hydrogen



instead of $H + HD = H_2 + D$, we must introduce into eq. (15.1) the nuclear factor i , which equals $\frac{1}{2}$ for *para-ortho* conversion and $-\frac{1}{2}$ for the reverse reaction [57]. In addition, σ_{BC} and σ^* now equal 2, not 1.

(28) Since the use of a semi-empirical method leads to the presence of a slight depression near the top of the barrier on the potential energy surface (see Fig. 44), the activated complex corresponding to a side of this depression will have an asymmetric structure and r_{AB} will consequently not equal r_{BC} .

Let κ_1 and κ_2 be the transmission coefficients for the forward and reverse reactions respectively. Let us further assume that the direction of escape of the system from the depression is independent of its direction of entry. This means that $\kappa_1 + \kappa_2 = 1$. We now write the rate constants for the forward and reverse reactions in the form

$$k_1 = \kappa_1 G_1 \text{ and } k_2 = \kappa_2 G_2$$

where G_1 is the multiplier of κ in eq. (15.1) and G_2 the corresponding term in the expression for the rate constant of the reverse reaction. Then, by introducing the equation for the equilibrium constant

$$K = k_1/k_2 = \kappa_1 G_1/\kappa_2 G_2$$

and remembering that $\kappa_1 + \kappa_2 = 1$, we obtain

$$\kappa_1 = G_2 K / (G_1 + G_2 K) \text{ and } \kappa_2 = G_1 K / (G_2 + G_1 K) \quad (15.3)$$

Evaluating the equilibrium constant from the equation⁽²⁹⁾

$$K = \frac{Z_{H_2} Z_D}{Z_{HD} Z_H} \exp \left[- \frac{h\nu_{H_2} - h\nu_{HD}}{2kT} \right]$$

and G_1 from eq. (15.1) and G_2 from the analogous equation for the reverse reaction, we obtain the values of κ_1 and κ_2 from eq. (15.3). Values of κ_1 for three temperatures calculated in this way are included in the summary on the previous page.

TABLE 14

Experimental and calculated rate constants of reactions of hydrogen and deuterium at 1000°K (cm³ mole⁻¹ sec⁻¹)

Reaction	$k_{\text{calc}} \times 10^{-12}$		$k_{\text{exp}} \times 10^{-12}$	
	I	II	III	IV
$H + HD = H_2 + D$	0.45	0.39	0.37	0.95
$D + H_2 = HD + H$	1.2	1.03	0.98	2.5
$D + DH = D_2 + H$	0.50	0.44	0.40	0.79
$H + D_2 = HD + D$	0.74	0.67	0.61	1.2
$H + H_2 = H_2 + H$	1.5	—	—	2.2
$D + D_2 = D_2 + D$	0.76	—	—	1.1

The rate constants calculated as above of some reactions of hydrogen and deuterium are presented in column I of Table 14 [771].

Column II will be explained in the next paragraph. Column III lists

⁽²⁹⁾ For numerical values of the equilibrium constant at different temperatures see the tables of Zeise [1324], p. 187.

the experimental values of k [413] obtained by making allowance for the experimental inaccuracies contained in the old measurements [662, 597] (column IV). As can be seen from Table 14, the calculated and experimental values are in good agreement. But the theoretically determined temperature coefficient of the rate constant is too high, which can be seen from the fact that the rate constant of *ortho-para* hydrogen conversion measured at 283°K by Geib and Harteck [662] is three times greater [413, 1228] than the theoretical value.

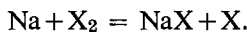
Farkas and Wigner [602] employed another semi-empirical method for determining rate constants. They suggested evaluating from kinetic data certain of the parameters defining the activated complex, e.g. E_{Cl} , v_{ϕ}^* and v_s^* , and hence calculating the rates of other reactions of hydrogen and deuterium. Since the temperature occurs in the expression for k (15.1) both in the term $\exp(-E_0/RT)$ and in the pre-exponential, the realization by this method of the correct temperature dependence of k over a wide range of T may be adduced in support of the argument that the above discrepancy is due to inaccuracies in calculating the potential energy surface and not to the approximate nature of the transition state method. If E_{Cl} , v_{ϕ}^* and v_s^* are calculated from the rate data of *ortho-para* hydrogen conversion at 1000°K, the values obtained are those listed in brackets in the summary on p. 255 [413]. The corresponding rate constants of some other reactions of hydrogen and deuterium at 1000°K are placed in column II of Table 14 [413]. As can be seen, the agreement with experiment is even better than when kinetic data are not used in the calculations. In addition, the theoretical rate constant of *ortho-para* hydrogen conversion at low temperatures now agrees well with the experimental data of Geib and Harteck [662], so that the correct temperature dependence of the rate constant has been obtained over a wide temperature range of about 700°.

It should also be noted that if we use the simple collision theory and insert into eq. (9.22) $\sigma = 2\pi d_0^2 = 6.3 \text{ \AA}^2$ ⁽³⁰⁾ and $P = 1$ when $E = 7.7 \text{ kcal}$ and $T = 1000^\circ\text{K}$, we find $k = 7.5 \times 10^{12} \text{ cm}^3 \text{ mole}^{-1} \text{ sec}^{-1}$ for *ortho-para* hydrogen conversion. As expected (p. 199), the simple collision theory leads to a satisfactory result in this reaction. This result is obviously possible only if the reaction proceeds adiabatically, which is in fact the case here.

Since the recombination of sodium and halogen atoms, which has been examined above (p. 231), sometimes shows a low transmission coefficient due to the non-adiabatic course of the reaction, the question arises whether an analogous hindrance occurs in the reaction of sodium (or other alkali

⁽³⁰⁾ In evaluating d_0 one may in this case proceed from the dimensions of the activated complex H_3 and assume $d_0 \approx 1 \text{ \AA}$.

metal) atoms with halogen molecules



As we have seen, the possibility of a non-adiabatic reaction arises because the difference in electronegativity between the metal and halogen atoms leads to a pseudo-intersection of the potential energy curves. An analogous intersection is observed in the reaction $\text{Na} + \text{X}_2$, but it is readily seen that the point of intersection now lies much closer to the final state, since the electron affinity of the molecule X_2 is considerably less than that of the atom X .⁽³¹⁾ Furthermore, since the splitting of the energy levels must be greater at small than at large values of r_c , the probability ρ of an adiabatic reaction will be greater between an atom and a molecule than between atoms. If, following Magee [899], we assume that

$$E_{\text{X}_2} = E_{\text{X}} - \frac{1}{2}D_{\text{X}_2}$$

(where D is the heat of dissociation of the X_2 molecule), the pseudo-intersection point of the potential energy curves for the reaction $\text{Na} + \text{Cl}_2$ will be at $r_c = 5.5 \text{ \AA}$, i.e. half the distance found for $\text{Na} + \text{Cl}$. With such a marked drop in r_c the distance between the true potential energy curves (2a) will clearly be great enough for us to be able to assume that $\rho = 1$.

Since the reactions of sodium with halogen atoms proceed without any activation energy (see p. 88), it is pertinent to ask what configuration of the system should be assumed for the activated complex. For systems with a pseudo-intersection of the potential energy curves but with no potential energy barrier the activated state may be taken to be near the point of intersection [899]. Calculation shows that a better agreement with experiment is attained by this method than by the usual calculation involving collision theory. The latter involves the assumption that the effective collision diameter for an atom with a molecule has its usual gas-kinetic value. The rate constants k for the reaction $\text{Na} + \text{X}_2 = \text{NaX} + \text{X}$ are then found to be approximately ten times less than the experimental values. If, however, the collision diameters are made equal to r_c , i.e. increased by a factor of about two, the values of k calculated from

$$k = r_c^2 [8\pi k T (m_{\text{Na}} + m_{\text{X}_2}) / m_{\text{Na}} m_{\text{X}_2}]^{1/2},$$

are found to agree well with experiment, as is clear from Table 15 (see [57] p. 310).

We have considered reactions of the type $\text{A} + \text{BC} = \text{AB} + \text{C}$ in which all three particles A , B and C were atoms and the transfer reaction consequently was one between an atom and a diatomic molecule. The picture

⁽³¹⁾ This follows directly from the equation

$$I_{\text{Na}} - E_{\text{X}_2} = e^2 / r_c.$$

The electron affinity of the chlorine molecule is $E \leq 32 \text{ kcal}$, while that of the chlorine atom is 87.3 kcal [1047].

TABLE 15

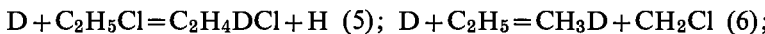
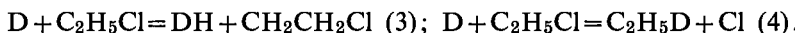
Calculated and experimental rate constants for the reaction
 $\text{Na} + \text{X}_2 = \text{NaX} + \text{X}$ ($\text{X} = \text{Cl}, \text{I}$) in $\text{cm}^3 \text{mole}^{-1} \text{sec}^{-1}$

Reaction	Calculated	Experimental
$\text{Na} + \text{Cl}_2$	4.5×10^{14}	4.1×10^{14}
$\text{Na} + \text{I}_2$	6.0×10^{14}	6.1×10^{14}

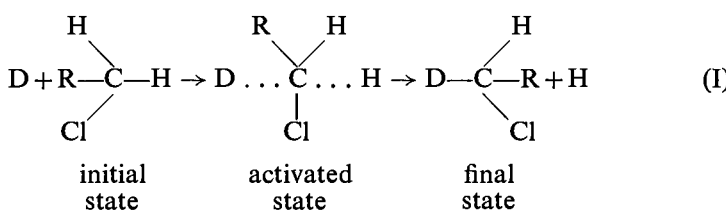
becomes more complex for the interaction of an atom and a polyatomic molecule, because the presence of a greater number of bonds in the polyatomic molecule leads to a greater number of possible paths for the reaction between the given pair of particles. For example, there are only two paths for the reaction between deuterium and a diatomic molecule, e.g. HCl ,



but the reaction of deuterium with a comparatively simple molecule such as $\text{C}_2\text{H}_5\text{Cl}$ can proceed in the following seven directions:

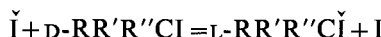


As regards the structure of the activated complex we can distinguish two possible modes of interaction of an atom with a molecule. The first mode, seen in reactions (1)–(3), involves the abstraction of an atom (Cl or H) from the molecule with the formation of a new saturated molecule (DCl or DH) and a radical, while the second involves the displacement of an atom or radical from the initial molecule. The second mode is seen in reactions (4)–(7), an atom (Cl or H) being displaced in the first two and a radical (CH_2Cl or CH_3) in the last two. If the displaced atom or radical is bonded directly to a tetrahedral carbon atom (as in the present example), the "displacement" reaction will be followed by *inversion*. Using this reaction when proceeding in the direction (5) as an example, the inversion mechanism can be schematically depicted as follows:



In the activated state all three particles, which are bonded to the carbon atom being attacked (H, Cl and R = CH₃), together with the carbon atom itself lie in a plane perpendicular to the line passing through the atoms D . . . C . . . H.

The possibility of this mechanism occurring in radical reactions was first put forward by Ogg and Polanyi [990] in connection with the inversion of optically active halogen derivatives of hydrocarbons in the gaseous phase.⁽³²⁾ According to their data, one of the steps in the inversion of t-butyl iodide RR'R''CI attended by racemization is the attack by an atom of iodine on the butyl iodide molecule, causing "Walden inversion"

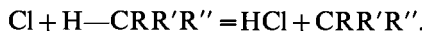


(D- and L- indicate that the first compound is the dextro- and the second the laevo-rotary stereoisomer). If the reaction proceeded via the free radical RR'R''C with all three carbon valencies in one plane, the final product would be optically inactive, a *racemic* mixture being obtained, i.e. a mixture of equal quantities of the dextro and laevo isomers.

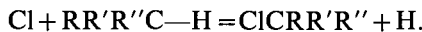
Examples are known of analogous reactions, which produce racemic mixtures and must therefore proceed via the corresponding radicals. The attack by chlorine atoms on 1-chloro-2-methylbutane



for example, leads to optically inactive 1,2-dichloro-2-methylbutane CH₂ClCCl(CH₃)CH₂CH₃, even though the latter contains an asymmetric carbon atom [459]. This is readily understood if the reaction is assumed to proceed through the stage



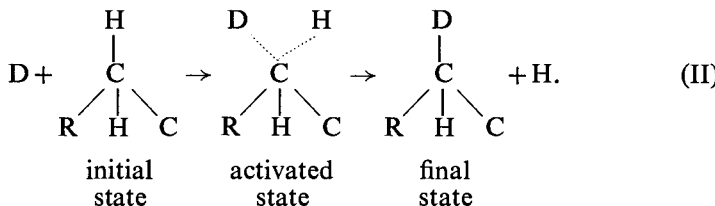
and not through



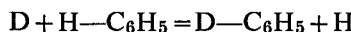
Leaving aside the radical mechanism, it should be borne in mind that inversion is apparently not the only possible mechanism for these displacement reactions. There is also the possibility that the molecule is

⁽³²⁾ The inversion mechanism of transfer reactions which proceed in conducting solutions by an ionic mechanism was discovered by Walden. Reactions of this type, which are observed with compounds possessing an asymmetric carbon atom, i.e. a carbon atom attached to four different groups, and which often occur with a change in sign of optical activity (dextro- and laevo-rotation of the plane of polarization), received the name of *Walden inversion*.

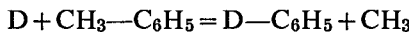
attacked from the side of the atom being displaced, as shown in the following scheme:



This mechanism is clearly possible for any of the reactions (4)–(7) on p. 259. In displacement reactions of the type

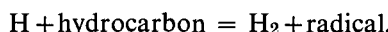


or



this must be considered the only possible mechanism, since the displaced atom or radical is not attached to a tetrahedral carbon atom.

The pre-exponential A in the Arrhenius equation for metathetical reactions of the “abstraction” type [reactions (1)–(3) on p. 259] can be calculated from the usual transition state equations. It often turns out that A is several powers of ten less than the corresponding number of collisions (Z_0). As was pointed out in §12 (p. 196 *et seq.*), this difference is quite natural, since the simple collision theory does not allow for the rotational degrees of freedom, and a change in their number during the transition to the activated state would have a great effect on the pre-exponential term. According to the calculations of Stepukhovich *et al.* [252, 249], the P factor for the abstraction of hydrogen,



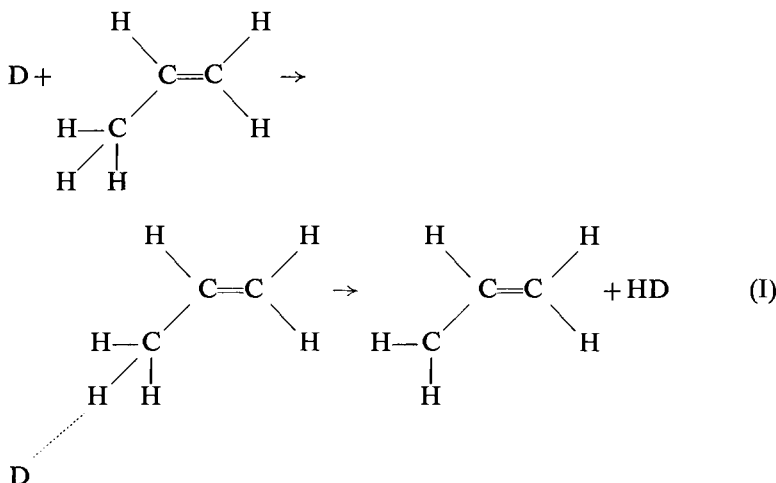
determined from eq. (12.73) of Chap. 3, has an order of magnitude between 10^{-2} and 10^{-3} . Experimental data, are in fact usually rather unreliable and often contradictory.⁽³³⁾ Berlie and Le Roy's [387] value $P = 5 \times 10^{-3}$ for $H + C_2H_6 = H_2 + C_2H_5$ may be considered sufficiently reliable. This or a similar order of magnitude for P in other reactions does not contradict the experimental data.⁽³⁴⁾ According to the results of numerous investigations, the activation energy of these reactions is usually a few kilocalories (up to 10 kcal).⁽³⁵⁾

⁽³³⁾ It is sufficient to point out that the P factors of different workers for the reaction $H + CH_4 = H_2 + CH_3$ vary within the limits 0.1 to 10^{-5} ; see Steacie [1169] p. 453.

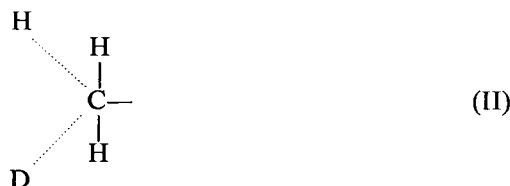
⁽³⁴⁾ See Steacie [1169] pp. 439, 440, 442, 453–456, 459, 460, 469, etc. It will be noted, however, that according to measurements made by Tikhomirova and Voevodskii [266] and recent data of N. I. Gorban and A. B. Nalbandyan [*Dokl. Akad. Nauk SSSR* 132, 1335 (1960)] the rate constant for the reaction $H + C_2H_6 = H_2 + C_2H_5$ is $8.3 \times 10^{-10} \exp(-13500/RT) \text{ cm}^3 \text{ molecules}^{-1} \text{ sec}^{-1}$.

⁽³⁵⁾ See Steacie [1169].

In both the pre-exponential term and the activation energy there is little difference between transfer reactions involving hydrogen atoms and unsaturated hydrocarbons (olefins) and their derivatives, which proceed by the "abstraction" mechanism, and the reactions of hydrogen atoms with saturated compounds.⁽³⁶⁾ It should be noted that in the olefins, beginning with propylene $\text{H}_3\text{C}-\text{CH}=\text{CH}_2$, the reaction proceeds by the abstraction of that hydrogen atom whose bond with carbon has the least energy. In the propylene molecule the lowest bond energy is shown by the hydrogen atoms attached to the tetrahedral carbon in the methyl group CH_3 . The scheme for the reaction $\text{D} + \text{C}_3\text{H}_6 = \text{HD} + \text{C}_3\text{H}_5$ can therefore be put as follows:



In this scheme the abstraction of a methyl hydrogen is depicted as the result of a direct attack by the deuterium atom, which is reacting with the propylene molecule. Another reaction scheme is also conceivable, in which the activated complex has, for example, the configuration



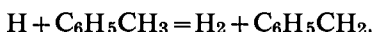
There is at present insufficient data to decide between these two schemes or to indicate the conditions under which one would prevail over the other. It is possible that the activated complex in scheme (I) is unstable and corresponds to the top of the potential energy barrier, while the complex

⁽³⁶⁾ See Steacie [1169] pp. 439, 442 and 518.

in scheme (II) corresponds to a slight energy minimum and therefore represents a relatively stable entity which subsequently decomposes. In the latter case the "abstraction" reaction has two stages: the union of the molecule and the attacking atom, followed by the decomposition of the activated complex (quasi-molecule) into the molecule HD and a radical. The different schemes (I and II) must obviously lead to different kinetic characteristics.

Transfer reactions of the "displacement" type have been studied kinetically even less than those of the "abstraction" type. From the available experimental data one can conclude that all particles react preferentially by abstraction, i.e. the rate constant for "abstraction" is greater than that for "displacement". In his analysis of the problem of the relative rates of reaction of a deuterium atom with a CH_4 molecule, for example, Steacie [1169] concluded that $\text{D} + \text{CH}_4 = \text{CH}_3\text{D} + \text{H}$ was slow compared to $\text{D} + \text{CH}_4 = \text{DH} + \text{CH}_3$. It should be noted that on the basis of theoretical calculations the slowness of the first reaction is sometimes connected with the inversion mechanism which is possible in this case. As the result of calculations based on spectroscopic data, Rice and Teller [1064] concluded that the negligibly small rate of this reaction (compared with that of abstraction) was due to a high activation energy, which in the case of $\text{R} + \text{C}_2\text{H}_6 = \text{RCH}_3 + \text{CH}_3$ they estimated to be 40 kcal.⁽³⁷⁾ Extending this conclusion to other systems, Trotman-Dickenson [1228, p. 238] considers that an inversion mechanism for transfer reactions between an atom or radical and a molecule is possible only when the bond being broken is considerably weaker than that being formed, neither bond being very strong.

As a second example let us take the "displacement" reaction $\text{H} + \text{C}_6\text{H}_5\text{CH}_3 = \text{C}_6\text{H}_6 + \text{CH}_3$, which was postulated by Szwarc [1198] as one of the elementary steps in his suggested mechanism for the thermal decomposition of toluene $\text{C}_6\text{H}_5\text{CH}_3$. Szwarc's experiments have recently been repeated by Steacie *et al.* [407]. Having discovered errors in Szwarc's analysis, they expressed doubts about the correctness of his conclusions, in particular about his proposed reaction mechanism. They also considered that the production of a large amount of hydrogen, but no methane, during the pyrolysis of dibenzyl $(\text{C}_6\text{H}_5\text{CH}_2)_2$ in the presence of toluene was inconsistent with the process $\text{H} + \text{C}_6\text{H}_5\text{CH}_3 = \text{C}_6\text{H}_6 + \text{CH}_3$. It should be added that, unlike the above "displacement" reaction, the following very fast "abstraction" reaction must be regarded as sufficiently reliably established:



⁽³⁷⁾ Using a very approximate semi-empirical method (due to Eyring) Gorin, Kauzmann, Walter and Eyring [691] found the activation energy of the reaction $\text{H} + \text{CH}_4 = \text{CH}_4 + \text{H}$ to be 37 kcal.

In concluding this section let us note the following fact. In all quantitative studies of elementary transfer reactions involving atoms, the pre-exponential term A in the expression for the rate constant

$$k = A \exp(-E/RT)$$

has an order of magnitude not greater than $10^{14} \text{ cm}^3 \text{ mole}^{-1} \text{ sec}^{-1}$ (see Table 13), whence it follows that $P \leq 1$. In sharp contrast to this are the data on transfer reactions obtained by van Artsdalén and his coworkers from a study of the reactions $\text{Br} + \text{C}_5\text{H}_{12} = \text{C}_5\text{H}_{11} + \text{HBr}$ [780] and $\text{Br} + \text{C}_4\text{H}_{10} = \text{C}_4\text{H}_9 + \text{HBr}$ [561]. For the first reaction they found $A = 10^{16.97}$ and for the second $A = 10^{17.57} \text{ cm}^3 \text{ mole}^{-1} \text{ sec}^{-1}$, i.e. values 10^3 to 10^4 times greater than the gas-kinetic value $Z_0 = 10^{14} \text{ cm}^3 \text{ mole}^{-1} \text{ sec}^{-1}$ and leading to a P factor of the order of 10^3 to 10^4 .

If these results were free of any incorrect interpretation of the experimental data, they would have to be interpreted as showing the inapplicability in the present case of the simple Arrhenius equation for the rate constant. But it does not appear possible at present to show why the equation is inapplicable in the case of these two reactions.⁽³⁸⁾

Reactions of Radicals with Molecules

All the transfer reactions which occur between atoms and molecules are clearly also possible between radicals and molecules. The rate constants of some of these reactions are listed in Table 16.

This table shows clearly the wide difference (of two to three powers of ten) in the pre-exponential term between the reactions of hydroxyl and those of the methyl and ethyl radicals (with similar activation energies). This difference is possibly connected with the change, mentioned on p. 261 above, in the number of rotational degrees of freedom during the transition of the system of colliding particles from the initial to the activated complex state.

Expressing the pre-exponential factor by the formula $A = PZ_0$ and assuming that Z_0 equals $10^{14} \text{ cm}^3 \text{ mole}^{-1} \text{ sec}^{-1}$, we find $P = 1$ to 0.1 for the reactions of hydroxyl and $P = 10^{-2}$ to 10^{-4} for the reactions of CH_3 and C_2H_5 .

Theoretical values of P for some of the reactions of the CH_3 radical listed in Table 16 have been calculated by Stepukhovich *et al.* [250, 253]. Their figures are compared in Table 17 with those obtained from measured values of A for corresponding mean diameters. As is seen from the table, the calculated values are close to the measured values. It should, however, be pointed out that an analogous calculation for the reactions of hydroxyl

⁽³⁸⁾ There are indications that the simple Arrhenius equation is also inapplicable in the thermal dissociation of molecules. A possible explanation of this fact is given in Chap. 5 (pp. 343 *et seq.*).

TABLE 16

Rate constants of some transfer reactions between radicals and molecules, $k = A \exp(-E/RT) \text{ cm}^3 \text{ mole}^{-1} \text{ sec}^{-1}$

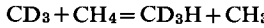
Reaction	$E \text{ kcal}$	$\log A$	Temperature °C
$\text{OH} + \text{H}_2 = \text{H}_2\text{O} + \text{H}^*$ [133]	10.0	14.15	600-1100
$\text{OH} + \text{CO} = \text{CO}_2 + \text{H}^\ddagger$ [11]	7.0	13.1	75-250
$\text{OH} + \text{C}_2\text{H}_6 = \text{H}_2\text{O} + \text{C}_2\text{H}_5$ [6]	5.5	14.1	75-250
$\text{CH}_3 + \text{D}_2 = \text{CH}_3\text{D} + \text{D}^\ddagger$ [903, 1284, 944]	11.7	12.0	130-420
$\text{CH}_3 + \text{CH}_4 = \text{CH}_4 + \text{CH}_3$ [943], [518a]	14.3	11.5	350-525
$\text{CH}_3 + \text{C}_2\text{H}_6 = \text{CH}_4 + \text{C}_2\text{H}_5$ [1229]	10.4**	11.33	25-340
$\text{CH}_3 + \text{n-C}_4\text{H}_{10} = \text{CH}_4 + \text{C}_4\text{H}_9$ [1229]	8.3	11.08	25-340
$\text{CH}_3 + \text{C}_2\text{H}_4 = \text{CH}_4 + \text{C}_2\text{H}_3$ [1230]	10.0	11.32	180-340
$\text{CH}_3 + \text{C}_3\text{H}_6 = \text{CH}_4 + \text{C}_3\text{H}_5$ [1230]	7.7	10.84	180-340
$\text{CH}_3 + \text{s-C}_4\text{H}_8 = \text{CH}_4 + \text{C}_4\text{H}_7$ [1230]	7.3	10.96	180-340
$\text{CH}_3 + \text{C}_5\text{H}_6 = \text{CH}_4 + \text{C}_5\text{H}_5$ [1231]	9.2	10.15	70-340
$\text{CH}_3 + \text{C}_6\text{H}_5\text{CH}_3 = \text{CH}_4 + \text{C}_6\text{H}_5\text{CH}_2$ [1231]	8.3	11.17	70-340
$\text{CH}_3 + \text{NH}_3 = \text{CH}_4 + \text{NH}_2$ [1231]	10.0	10.95	70-340
$\text{CH}_3 + \text{CH}_3\text{OH} = \text{CH}_4 + \text{CH}_2\text{OH}$ [1231]	8.2	10.74	70-340
$\text{C}_2\text{H}_5 + \text{C}_2\text{H}_5\text{CHO} = \text{C}_2\text{H}_6 + \text{C}_2\text{H}_5\text{CO}$ [1255]	7.6	11.37	122-156
$\text{CH}_3 + \text{CH}_3\text{COCOCH}_3 = \text{CH}_3\text{COCH}_3 + \text{CH}_3\text{CO}$ [406]	5.0	10.7	28-200

* Avramenko and Lorentso [11] found that, over the temperature range 105-215°C, $E = 10 \text{ kcal}$ and $\log A = 13.94$. Using their data Kondrat'ev found $E = 10 \text{ kcal}$ and $\log A = 14.14$.

† Using the data of Avramenko and Lorentso [11] Kondrat'ev found $E = 5.7 \text{ kcal}$ and $\log A = 12.46$.

‡ In calculating A in all the reactions of the methyl radical CH_3 the rate constant for the recombination of methyl radicals, $k = 5.3 \times 10^{13} \text{ cm}^3 \text{ mole}^{-1} \text{ sec}^{-1}$, obtained from the data of Kistiakowsky and Roberts [839], was used.

** The data of Wijnen [1292] for the activation energy of the reaction



lead to the figure 13 kcal (assuming that the probability factors of this reaction and of $\text{CD}_3 + \text{C}_2\text{H}_6 = \text{CD}_3\text{H} + \text{C}_2\text{H}_5$ are identical).

does not give a similar agreement with experiment. This question obviously needs further investigation.

The last reaction in Table 16 some workers [1228, p. 238] are inclined to consider as an example of a reaction occurring by an inversion mechanism. But since the carbon atoms in the $\text{CH}_3\text{COCOCH}_3$ molecule, which are attacked by the CH_3 radical, are not tetrahedral (carbonyl carbon atoms), this conclusion cannot be considered as consistent with the facts.

Table 18 gives the activation energy and pre-exponential term for some reactions of molecules with an odd number of electrons, i.e. radical-like

molecules. As can be seen from the table, the activation energies and pre-exponential terms of these reactions are with few exceptions close to those of the reactions of radicals (see Table 16). Exceptions are the reactions of

TABLE 17
Calculated and measured probability factors P for some reactions of the radical CH₃

Reaction	Collision diameter Å [1229]	P _{meas..}	P _{calc.}
CH ₃ + C ₂ H ₆ = CH ₄ + C ₂ H ₅ . . .	5.0	4.6 × 10 ⁻⁴	6.3 × 10 ⁻⁴
CH ₃ + n-C ₄ H ₁₀ = CH ₄ + C ₄ H ₉ . . .	5.8	2.1 × 10 ⁻⁴	4.1 × 10 ⁻⁴
CH ₃ + C ₂ H ₄ = CH + C ₂ H ₃ . . .	4.8	4.5 × 10 ⁻⁴	9.2 × 10 ⁻⁴
CH ₃ + C ₃ H ₈ = CH ₄ + C ₃ H ₅ . . .	5.4	1.2 × 10 ⁻⁴	1.4 × 10 ⁻⁴
CH ₃ + iso-C ₄ H ₈ = CH ₄ + C ₄ H ₇ . . .	5.8	1.5 × 10 ⁻⁴	1.3 × 10 ⁻⁴

TABLE 18
Rate constants of bimolecular reactions of molecules with an odd number of electrons

Reaction	E kcal	log A	Temperature range °C
NO + Cl ₂ = NOCl + Cl [334] . . .	20.3	12.6	250–320
NO + O ₃ = NO ₂ + O ₂ [805] . . .	2.5	11.9	–75–43
NO + NO ₂ Cl = NOCl + NO ₂ [629] . . .	6.9	11.9	0–70
NO + N ₂ O = NO ₂ + N ₂ [825] . . .	50.0	14.4	650–755
NO ₂ + CO = NO + CO ₂ [458, 804a] . . .	31.6	13.1	267–454
NO ₂ + F ₂ = NO ₂ F + F [1026] . . .	10.5	12.2	28–70
NO ₂ + O ₃ = NO ₃ + O ₂ [807] . . .	7.0	12.8	13–29
ClO ₂ + F ₂ = ClO ₂ F + F [338] . . .	8.5	10.6	–46––26

nitric oxide with Cl₂ and N₂O and of nitrogen peroxide with carbon monoxide, where the activation energies exceed 20 kcal. In the first case the large activation energy is caused by the endothermicity of the reaction.⁽³⁹⁾ In the case of the two other reactions the large activation energy (with positive heat effect) must be ascribed to the low reactivity of NO₂.

⁽³⁹⁾ The heat of this reaction is –20.4 kcal, whence it follows that the true energy of activation, i.e. the activation energy of the reaction proceeding in the exothermic direction, is zero.

The pre-exponential terms of the reactions listed in Table 18 (and of five other reactions) were calculated theoretically by Herschbach, Johnston, Pitzer and Powell [744]: (I) by a method analogous to that of Stepukhovich; (II) by using the assumption that the entropy of the activated complex is similar to that of the structurally analogous hydrocarbon; and (III) by using the collision theory. Table 19 gives a comparison of the calculated values of the logarithm of the pre-exponential divided by the transmission coefficient κ (by P in case III) with the experimental values.

TABLE 19

Comparison of the theoretical and experimental values of the pre-exponential factor in the Arrhenius equation for some bimolecular reactions [744]

Reaction	$\log A_{\text{exp}}$	$\log A/\kappa$ (I)	$\log A/\kappa$ (II)	$\log A/P$ (III)
$\text{NO} + \text{O}_3 \rightleftharpoons \text{NO}_2 + \text{O}_2$	11.9	11.6 ₅	11.8 ₃	13.6 ₇
$\text{NO}_2 + \text{O}_3 \rightleftharpoons \text{NO}_3 + \text{O}_2$	12.8	11.1 ₅	11.5 ₅	13.8
$\text{NO}_2 + \text{F}_2 \rightleftharpoons \text{NO}_2\text{F} + \text{F}$	12.2	11.1	11.6	13.7 ₇
$\text{NO}_2 + \text{CO} \rightleftharpoons \text{NO} + \text{CO}_2$	13.1	12.8	14.0	13.8 ₇
$2\text{NO}_2 \rightleftharpoons 2\text{NO} + \text{O}_2$	12.2 ₅	12.6 ₅	13.5 ₅	13.6 ₈
$\text{NO} + \text{NO}_2\text{Cl} \rightleftharpoons \text{NOCl} + \text{NO}_2$	11.9	11.9	—	13.8 ₅
$2\text{NOCl} \rightleftharpoons 2\text{NO} + \text{Cl}_2$	12.9 ₇	11.6 ₄	—	13.7 ₇
$\text{NOCl} + \text{Cl} \rightleftharpoons \text{NO} + \text{Cl}_2$	13.0 ₆	12.6 ₄	—	13.7 ₆
$\text{NO} + \text{Cl}_2 \rightleftharpoons \text{NOCl} + \text{Cl}$	12.6	12.0 ₈	—	13.9 ₇
$\text{F}_2 + \text{ClO}_2 \rightleftharpoons \text{FCIO}_2 + \text{F}$	10.5 ₄	10.9 ₁	—	13.6 ₇
$2\text{ClO} \rightleftharpoons \text{Cl}_2 + \text{O}_2$	10.7 ₈	10.0	—	13.4 ₁
$\text{COCl} + \text{Cl} \rightleftharpoons \text{CO} + \text{Cl}_2$	14.6	12.2 ₆	—	13.8 ₁

The table shows that the pre-exponentials calculated by the activated complex method (I and II) agree satisfactorily with the experimental values, from which we can conclude that the transmission coefficient for the majority of these reactions is close to unity. On the other hand, A/P is 10 to 1000 times greater than A_{exp} , which indicates a normal order of magnitude for the P factor of 10^{-1} to 10^{-3} . An exception is found in the last reaction, which Herschbach *et al.* [744] consider anomalous.

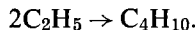
Transfer Reactions between Radicals or Radical-like Molecules

In the reaction between two radicals there is often observed, in addition to recombination, a competing transfer reaction, leading to the formation of two saturated molecules or of two new radicals. This is called the *process of disproportionation*. An example of disproportionation is the

bimolecular reaction between two ethyl C_2H_5 radicals resulting in the formation of ethane C_2H_6 and ethylene C_2H_4 ,



This reaction has a very low activation energy, requires no stabilizing collisions and therefore competes successfully with the recombination of ethyl radicals



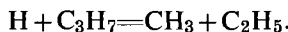
Assuming that the activation energy for the recombination of C_2H_5 is zero, the measurements of Ivin and Steacie [796] lead to an activation energy $E = 0.8$ kcal and a pre-exponential factor $A = 1.65 \times 10^{13} \text{ cm}^3 \text{ mole}^{-1} \text{ sec}^{-1}$ for disproportionation. Since, according to these workers, the rate constant for recombination is $1.57 \times 10^{18} \text{ cm}^3 \text{ mole}^{-1} \text{ sec}^{-1}$, we see that both processes have similar rates and that in both cases the P factor has an order of magnitude of $0.1(10^{13}/10^{14})$.⁽⁴⁰⁾ Let it be noted that this value of the rate constant for recombination is found only at sufficiently high pressures, where the limiting process is the formation of the quasi-molecule $C_2H_5 \cdot C_2H_5$ (see above, p. 228). At low pressures disproportionation must be the prevailing reaction of the two.

According to data available in the literature,⁽⁴¹⁾ the rate constants for disproportionation and recombination also have similar orders of magnitude in the case of the radicals $n\text{-}C_3H_7$, $\text{iso}\text{-}C_3H_7$, $n\text{-}C_4H_9$, $s\text{-}C_4H_9$, $t\text{-}C_4H_9$, etc.

As examples of disproportionation leading to the formation of two new radicals let us take the reactions



and



There appear to be sufficient experimental and theoretical grounds for supposing that these reactions play an important role in the overall reaction mechanism of systems containing H atoms and alkyl radicals (e.g. in photochemical reactions and reactions in an electric discharge).⁽⁴²⁾ These reactions may also be considered sufficiently rapid; it is possible that they have no activation energy and proceed with a probability P close to unity.

It should be added that, according to the data of Bagdasar'ian [20],

⁽⁴⁰⁾ Ivin and Steacie consider another possibility, namely that the activation energy for the recombination of ethyl radicals is 0.65 kcal and $A = 1.2 \times 10^{14} \text{ cm}^3 \text{ mole}^{-1} \text{ sec}^{-1}$. We now find $E = 1.45$ kcal and $A = 5.5 \times 10^{13} \text{ cm}^3 \text{ mole}^{-1} \text{ sec}^{-1}$ for the disproportionation reaction. For both reactions P is found to be of the order of 1.

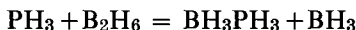
⁽⁴¹⁾ See Trotman-Dickenson [1228] p. 236; see also [1169, 774, 432a].

⁽⁴²⁾ See Steacie [1169] Chap. V, p. 35.

the disproportionation of radicals has a dominant and fundamental role in liquid-phase polymerizations.

Transfer reactions are also possible involving saturated molecules, but now the possibility of reaction is limited by the obvious condition that at least one of the reacting molecules must possess a multiple bond. The existence of these reactions is demonstrated, in particular, by the observation of the reverse reactions, the disproportionation of radicals, e.g. $2C_2H_5 = C_2H_6 + C_2H_4$ (see above). Because of their considerable activation energy,⁽⁴³⁾ apparently, such reactions have not been directly observed, although it has been postulated that they may enter into the mechanism of complex reactions involving hydrocarbons [46]. The existence of the reaction $RH + O_2 = R + HO_2$ [510], similar to the above mentioned type of reaction, $RH + C_2H_4 = R + C_2H_5$, has also been postulated.

There has recently been discovered the reaction



[461], which has a comparatively high velocity, as follows from its activation energy $E = 11.4$ kcal and pre-exponential $A = 3 \times 10^9 \text{ cm}^3 \text{ mole}^{-1} \text{ sec}^{-1}$ (over the temperature range -24 to 0°C). It should be noted that the possibility and relatively high rate of this reaction are due to the ease with which trivalent phosphorus becomes pentavalent, so that the phosphine molecule PH_3 must in a certain sense partake of the properties of a free radical (biradical). There are also indications that the ozone molecule O_3 can easily assume the biradical state [475].

Exchange Reactions $AB + CD = AC + BD$

The rate constants of practically all the gas-phase reactions of this type, which have been sufficiently well investigated, are presented in Table 20. In addition to proper exchange reactions, which are characterized by having the same number of molecules before and after the reaction, the table also includes a reaction (of $NOCl$) which leads to an increase in the number of molecules.

Table 20 clearly demonstrates the relatively large activation energy (true activation energy) of the reactions of hydrogen iodide, which is in full agreement with theoretical data about the reactions of saturated molecules (see above, p. 160). Note also the large pre-exponential terms in these reactions, corresponding to a probability factor close to unity, which must be connected with the large energy of the activated complex, facilitating the redistribution of the chemical bonds during the course of the reaction.

⁽⁴³⁾ From the heat of the reaction $C_2H_6 + C_2H_4 = 2C_2H_5$, which is -56.8 kcal, and the activation energy of the reverse reaction $E = 0.8$ kcal we obtain $E = 56.8 + 0.8 = 57.6$ kcal.

TABLE 20

Rate constants of exchange reactions of saturated molecules
(A , $\text{cm}^3 \text{mole}^{-1} \text{sec}^{-1}$)

Reaction	E kcal	Q kcal	$\log A$	Temperature range °C
$\text{H}_2 + \text{I}_2 \rightleftharpoons 2\text{HI}$ * [414]	39.0	2.2	14.1	283–508
$2\text{HI} \rightleftharpoons \text{H}_2 + \text{I}_2$ [414]	44.0†	— 2.2	13.9	283–508
$\text{HI} + \text{CH}_3\text{I} \rightleftharpoons \text{CH}_4 + \text{I}_2$ [986]	33.4	14.1	14.3	250–310
$\text{HI} + \text{C}_2\text{H}_5\text{I} \rightleftharpoons \text{C}_2\text{H}_6 + \text{I}_2$ [986]	29.8	13.7	13.7	250–310
$\text{HI} + n\text{-C}_3\text{H}_7\text{I} \rightleftharpoons \text{C}_3\text{H}_8 + \text{I}_2$ [986]	19.2	—	14.1	250–310
$\text{HI} + \text{H}_2 \rightleftharpoons \text{H}_2 + \text{HI}$ [1176]	44.0	0.0	13.7	420–480
$\text{O}_3 + \text{CH}_4 \rightleftharpoons \text{CH}_3\text{O} + \text{HO}_2$ ‡ [1113]	14.9	12.0	10.9	20–150
$\text{O}_3 + \text{C}_3\text{H}_8 \rightleftharpoons \text{C}_3\text{H}_7\text{O} + \text{HO}_2$ [1113]	12.1	17–22	9.5	20–150
$\text{O}_3 + n\text{-C}_4\text{H}_{10} \rightleftharpoons \text{C}_4\text{H}_9\text{O} + \text{HO}_2$ [1113]	11.1	19–24	8.9	20–150
$\text{O}_3 + \text{iso-C}_4\text{H}_{10} \rightleftharpoons \text{C}_4\text{H}_9\text{O} + \text{HO}_2$ [1113]	10.3	27.5	8.6	20–150
$\text{O}_3 + \text{C}_2\text{H}_2 \rightleftharpoons ?^{**}$ [476]	4.8	—	7.5	30–50
$2\text{NOCl} \rightleftharpoons 2\text{NO} + \text{Cl}_2$ [1257]	24.5††	— 16.5	13.0	150–250

* It has recently been shown [382] that at temperatures above 600°K a radical chain reaction (see Chap. 11) involving hydrogen and iodine molecules occurs in addition to the simple bimolecular reaction $\text{H}_2 + \text{I}_2 = 2\text{HI}$. Allowance for this reaction leads to a natural explanation of a number of anomalies observed in the reaction of iodine with hydrogen, as, for example, the large temperature coefficient of the activation energy of 21 cal/deg.

† That the difference in activation energy between the forward and reverse reactions ($44.0 - 39.0 = 5.0$ kcal) does not in this case equal the heat of reaction 2.2 kcal is explained by the superposition of a radical chain reaction (see previous note) on the simple bimolecular reaction, so that the experimental activation energies of the forward and reverse reactions differ somewhat from the values which would correspond to the pure bimolecular reactions $\text{H}_2 + \text{I}_2 = 2\text{HI}$ and $2\text{HI} = \text{I}_2 + \text{H}_2$. From this point of view the failure of the Arrhenius equation in the case of these two reactions over the temperature range 283–775°C [692] is also quite natural.

‡ Reactions of this type are also assumed by Cadle and Schadt [475] for olefins; the first step of the reaction, which has complicated kinetics (the order of the reaction changes with pressure, the consumption of olefin is two to three times greater than that of ozone, etc.,) is regarded as the transfer of an oxygen atom from ozone to olefin. It is also possible, however, that in the case of both paraffins and olefins the true mechanism of these reactions involves the preliminary decomposition of ozone into O_2 and O with subsequent reaction between the oxygen atom and the hydrocarbon. This same conclusion was reached by Nalbandian *et al.*, [108] from a study of the kinetics of the reaction between ozone and methane over the temperature range 100–400°C.

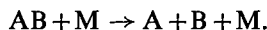
** Cadle and Schadt [475] explained the unusually low value of the pre-exponential in this reaction (as in the reactions of ozone with ethylene C_2H_4 and 1-hexene $\text{CH}_2 = \text{CHCH}_2\text{CH}_2\text{CH}_2\text{CH}_3$, which they also studied) as due to the process $\text{O}_3 + \text{M} = \text{MO} + \text{O}_2$ being, in their opinion, connected with a forbidden transition. A second explanation put forward by them was based on the assumption of an equilibrium between ozone and olefin on the one side and the complex formed by these molecules on the other.

†† According to the data of Ashmore and Chanmugam [332, 333, 334] a parallel, radical reaction involving chlorine atoms is superimposed on this reaction at 300°C, as on the reverse trimolecular reaction $2\text{NO} + \text{Cl}_2 \rightleftharpoons 2\text{NOCl}$.

§16. Bimolecular Dissociation Reactions

The decomposition of molecules appears as a second order reaction if the concentration of the necessary energy in the disrupting bond occurs more rapidly than energy transfer during collision. For polyatomic molecules these conditions are attained at adequately low pressures, where the course of the reaction is limited by the number of collisions in unit time. The decomposition of diatomic molecules always proceeds according to a bimolecular law (see §18).

As noted above (p. 136), the characteristic feature of bimolecular reactions of molecular decomposition is the breakdown of the Boltzmann distribution of the vibrational energy levels. This breakdown has the greatest effect on the rate of decomposition of diatomic molecules



Dissociation of Diatomic Molecules

If the vibrations of diatomic molecules followed the laws of classical mechanics, then dissociation could occur at every collision with a sufficiently fast molecule, since, according to classical mechanics, any amount of translational energy of the colliding molecule can be converted into vibrational energy of the second molecule and thereby cause its decomposition. In fact, there is in agreement with quantum mechanics an appreciable probability that the energy transferred during molecular collisions will be small compared to the dissociation energy D . The probability of the transfer of energy equal to one vibrational quantum (several hundred reciprocal centimeters or more) at ordinary temperatures is 10^{-2} to 10^{-5} per collision (§21), while the probability of a multiquantum exchange is much less. The direct transition of a molecule from one of the lower vibrational levels to the state of dissociation must, therefore, be practically excluded.⁽⁴⁴⁾

Actually the dissociation of a diatomic molecule is a multi-stage process, during which the molecule is excited to higher vibrational levels under the influence of collisions and eventually passes over into the region of continuous energy values, and so decomposes.

Calculation shows that the probability of this final transition is many times greater than that of vibrational excitation and approaches unity. Consequently, as is readily seen, the process of decomposition will lead to a depopulation of the upper vibrational levels compared to the equilibrium population (see p. 136), and the rate of decomposition will be the rate at which vibrationally excited molecules are “supplied” to the

⁽⁴⁴⁾ Note that Careri [480a, 480a'] developed a theory for the decomposition of diatomic molecules based on the possibility of just such a direct transition.

dissociation boundary, as long as this is the slowest step in the reaction.⁽⁴⁵⁾

Calculations on these lines of the rate constant of the decomposition of diatomic molecules have been carried out by Nikitin [214b]. The starting-point of these calculations is a system of kinetic equations describing the multi-stage process of excitation, de-activation and actual dissociation of the diatomic molecules. The assumption is made that a transition in the molecule on collision occurs only between neighbouring vibrational levels and that dissociation of the molecule is possible only from the last discrete vibrational level. If we assume that the Maxwell distribution of the colliding molecules is maintained, the principle of microscopic reversibility yields the following relation between the probability $P_{v,v-1}$ of the transition from level v to level $v-1$ for one collision and the probability of the reverse transition $P_{v-1,v}$:

$$P_{v-1,v} = \alpha_v P_{v,v-1},$$

$$\alpha_v = \exp\left(-\frac{E_{v,v-1}}{kT}\right).$$

Here $E_{v,v-1}$ denotes the difference in energy between the levels v and $v-1$. If we let $x_v(t)$ be the distribution function, i.e. the probability of the molecule being found in the v th level at the moment of time t , the system of kinetic equations can be written in the form:

$$\frac{dx_v}{dt} = Z_0[\alpha_v P_{v,v-1}x_{v-1} - (P_{v,v-1} + \alpha_{v+1}P_{v+1,v})x_v + P_{v+1,v}x_{v+1}] \quad (16.1)$$

with the condition $x_{-1} = x_{n+1} = 0$. The latter condition signifies that the vibrational spectrum of the molecule contains $n+1$ levels, the quantity $P_{n,n+1}\alpha_{n+1}$ representing the probability of transition from the last (n th) discrete level to the region of continuous energy.

The general solution of the system (16.1) has the form⁽⁴⁶⁾

$$x_k(t) = \sum_{j=0}^n A_k(\mu_j) \exp(-\mu_j t),$$

where μ_j are certain characteristic quantities. By using the general theory of local perturbation [171a] it can be shown [214b] that the quantity μ_0 represents the rate constant for the decomposition of a non-rotating

(45) Note in this connection the inadequacy of Rice's statement [1067, 1067a] that the rate of decomposition of molecules AB is determined by the rate of transition from the uppermost vibrational levels to the region with a continuous energy spectrum. Rice obviously neglected the disturbance of the equilibrium distribution in the levels near the dissociation boundary.

(46) The distribution function for a decomposing molecule can only be obtained in an explicit form by making the additional assumption that all the vibrational levels are equally spaced. See p. 135.

molecule AB. By the use of certain approximations μ_0 can be expressed in the form:

$$\mu_0 = Z_0 \frac{\hbar \alpha \bar{v}}{k T Z} \exp(-D/kT), \quad (16.2)$$

where Z is the vibrational partition function of the molecule AB, \bar{v} the mean velocity of the relative motion of the colliding particles, and α the reciprocal of the radius of action of the short-range ("exchange") forces (for the majority of molecules $1/\alpha$ equals 0.2 to 0.3 Å, cf. p. 353). In eq. (16.2) an approximate allowance has been made for the contribution of transitions between non-adjacent levels. The unknown rate constant k_d equals the quantity μ_0 averaged over the rotational states of the molecule AB. Allowance must be made for the distortion of the potential energy curve by rotation (cf. p. 189) and the true dissociation energy D is replaced by the effective value $D_{\text{eff}} = D - \lambda \epsilon_{\text{rot}}$, where ϵ_{rot} is the rotational energy of the molecule and the factor λ depends in a complex way on ϵ_{rot} , varying within the limits $0 < \lambda < 1$. The expression for k_d must also include the term g_{el} , equal to the number of stable electronic states in the molecule which lead to the ground state of its dissociation products. Thus

$$k_d = g_{\text{el}} \int_0^{\infty} \mu_0(D_{\text{eff}}) \exp(-\epsilon_{\text{rot}}/kT) \frac{d\epsilon_{\text{rot}}}{kT}. \quad (16.3)$$

Numerical calculation of D_{eff} for sufficiently heavy diatomic molecules (O_2 , Br_2 , I_2) and integration of (16.3) leads to the following result:

$$k_d = g_{\text{rot}} g_{\text{el}} \mu_0(D) = Z_0 g_{\text{rot}} g_{\text{el}} \frac{\hbar \alpha \bar{v}}{k T Z} \exp(-D/kT) \quad (16.4)$$

in which g_{rot} for the above mentioned molecules is from 5 to 10. Since no allowance has anywhere been made for the internal degrees of freedom of the molecule M, eq. (16.4) is applicable to the case of the collision of diatomic molecules AB with atoms. The calculation of k_d according to eq. (16.4) for the molecules Br_2 , I_2 and O_2 gives results agreeing satisfactorily with those of kinetic measurements of the rate constants for decomposition at high temperatures in a shock wave in an atmosphere of argon (Table 20a), satisfactory agreement being obtained at all temperatures for which there are experimental data (2000°–3000°K).

A number of workers [1067, 241] have remarked on the high value of the pre-exponential term in the equation for $k_d^{(0)}$ calculated from the equilibrium and the recombination rate constants, as compared with the number $Z_0 \simeq 10^{14}$ of gas-kinetic collisions. According to Willard⁽⁴⁷⁾, for

⁽⁴⁷⁾ Quoted by Palmer and Hornig [1004].

instance, the values of $k_d^{(0)}$ for the decomposition of bromine at 300°K are represented by

$$k_d^{(0)} = 10^{16} \exp(-D/kT). \quad (16.5)$$

This difference is explained, first, by the fact that dissociation involving the formation of a complex AM becomes important at low temperatures, decreasing the perturbation of the equilibrium distribution [O. K. Rice, *Monatsh. f. Chem.* **90**, 330 (1959); E. E. Nikitin, *Kinetika i Katalyz* (in Russian)]. Moreover, this difference is accounted for by factors such as the rotation of the dissociating molecule, the presence of certain stable electronic states and a slight increase in the diameter of the molecule due to vibrational excitation (see p. 190).

The Rate of Thermal Dissociation of Polyatomic Molecules

The equation (16.4) which we obtained above for the rate constant for the decomposition of diatomic molecules can be generalized for the case of the decomposition of polyatomic molecules.⁽⁴⁸⁾ Just as at low pressures the internal energy of AB will be fully redistributed over the vibrational degrees of freedom in the time between successive collisions between AB and M, so we can replace the real molecule with n degrees of freedom by a one-dimensional anharmonic oscillator, whose dissociation energy is determined by the strength of the disrupting bond, the statistical weight of the vibrational levels near the dissociation boundary being equal to $g_{vib} = (\bar{p} + n - 1)!/\bar{p}!(n - 1)!$, where $\bar{p} = D/\hbar\bar{v}$ is determined by the mean frequency \bar{v} of the decomposing molecule [106]. The constant of decomposition will now be determined by the equation

$$k_d = Z_0 g_{vib} g_{el} g_{rot} (\hbar\bar{v}/kT) \exp(-D/kT). \quad (16.6)$$

In contrast with the case of diatomic molecules, we must here assume $g_{vib} \approx 1$, since the centrifugal stretching of polyatomic molecules is small. Estimation shows that the term $\hbar\bar{v}g_{el}/kT$ for the usual conditions of decomposition of polyatomic molecules ($T \approx 500-1000^\circ\text{K}$) is roughly unity, so that eq. (16.6) agrees approximately with the equation of Kassel [106], whose derivation neglected both the breakdown of the Boltzmann distribution over the vibrational states and the increased statistical weight of g_{el} :

$$k_d = Z_0 \frac{(\bar{p} + n - 1)!}{\bar{p}!(n - 1)!} \exp(-D/kT). \quad (16.7)$$

It should be noted that the general equation (16.6) can be employed for the calculation of rate constants of decomposition of both poly- and di-atomic

⁽⁴⁸⁾ Nikitin, Sokolov, *J. Chem. Phys.* **31**, 1371 (1959); Nikitin, *Zh. Fiz. Khim.* **33**, 1893 (1959); *Dokl. Akad. Nauk., SSSR*, **129**, 157 (1959).

molecules, while eq. (16.7) refers only to the decomposition of polyatomic molecules. Since normally $\hbar\bar{\nu} \geq kT$, the quantization of the vibrations is important, and k_d cannot be determined from Kassel's formula [106] for a system of classical oscillators:

$$k_d = Z_0(D/kT)^{n-1}[(n-1)!]^{-1} \exp(-D/kT). \quad (16.8)$$

This equation (16.8) has in fact been used in a number of experiments (see, for example, [686b, 480a]), leading to a wide difference between the real and "effective" number of internal degrees of freedom. Thus, in applying Kassel's equation (16.8) to the experimental rate constants for the decomposition of N_2O_4 Cordes and Johnston [686b] found $n = 5$, while the number of vibrational degrees of freedom of N_2O_4 is 12.

TABLE 20a

Calculated and experimental values of the pre-exponential factor A/Z_0 for bimolecular decomposition of molecules

Reaction	Number of vibrational degrees of freedom n	Dissociation energy kcal/mole	Mean frequency	A/Z_0 exp.	A/Z_0 calc.
Br_2	1	45.5	325	6 [1004]	3
I_2	1	35	214	4 [444]	2
O_2	1	118	1580	3 [479b]	5
O_3	3	24	1000	50 [380a]	50
NO_2Cl	6	30	1000	6×10^2 [686b]	10^3
H_2O_2	6	45	2000	10^3 – 10^4 [643a]	3×10^3
N_2O_4	12	11	1000	1×10^3 [680a]	10^3
N_2H_4	12	60	2000	10^5 [676a]	10^5

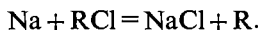
Table 20a gives the experimental values of the pre-exponential term A/Z_0 and those calculated from eq. (16.6) for a number of thermal decomposition reactions of polyatomic molecules with the corresponding references to experimental work. The values of the ratio A/Z_0 for polyatomic molecules correspond to the temperature range 400–1000°K. In connection with the decomposition of N_2H_4 it should be noted that Gilbert [676a] has recently analyzed the work of Szwarc [1201] and come to the conclusion that under the experimental conditions used by Szwarc hydrazine decomposes bimolecularly and not unimolecularly, as previously suggested. The agreement between the calculated and experimental values of k_d supports Gilbert's conclusion as to the kinetics of the decomposition of N_2H_4 .

§17. Dependence of the Rate of Transfer Reactions on the Structure of the Reacting Molecules

In the course of almost a century since Butlerov put forward his ideas on the connection between the chemical properties of compounds (their reactivity) and their structure, a huge amount of experimental material has been accumulated on a wide variety of compounds and classes of reactions, illustrating and confirming the correctness of Butlerov's ideas. Attempts at systematizing this material and giving a theoretical interpretation of the experimental laws were made by van't Hoff, Ostwald, J. J. Thomson, and Kossel on the basis of the theory of the structure of the atom, and later Pauling, Coulson and others on the basis of the quantum theory of the structure of atoms and molecules. As a result of these attempts ways were found leading to a partial theoretical elucidation of certain problems relating to the connection between the reactivity and chemical structure of compounds; but the problem as a whole is far from being solved. One of the greatest obstacles in the way of solving this problem is the lack of adequate data about reaction mechanisms, in particular the absence of sufficiently accurate and systematic quantitative data on the rates of individual elementary processes comprising the mechanism of a complex reaction.

Since our aim is not a detailed examination of the question of the relation between the structure and chemical properties of compounds, we shall only cite a few examples relating to transfer reactions. These examples will give some idea of the present state of the problem and the methods of treating certain of its aspects.

The most complete experimental data on the dependence of the rate of exchange on the structure of the molecule were obtained by Polanyi and his coworkers [732, 733, 1268] for the reactions of sodium atoms with chlorine derivatives of the hydrocarbons



These reactions have turned out to be extremely convenient for studying the influence of molecular structure on reactivity and can in a certain sense be considered as a model for the study of transfer reactions.

There have been only a few direct measurements of the activation energy of these reactions. But if we give the pre-exponential term in the Arrhenius equation a certain definite value, we can evaluate the activation energy if the rate constant is known at a certain temperature. Experiment shows that the pre-exponential terms for the identical reactions of homologous compounds (different R) differ very little amongst themselves; we can then, to a first approximation, adopt the same value of A for all the reactions of the type $\text{Na} + \text{RCl} = \text{NaCl} + \text{R}$. In the numerical data

listed below it is assumed that $A = Z = 5 \times 10^{14} \text{ cm}^3 \text{ mole}^{-1} \text{ sec}^{-1}$. In fact A is of the form PZ and since $P < 1$ the real value of the pre-exponential A is somewhat lower. But this does not affect the sequence of changes in E for a given series of reactions. In the table below the figures in the first rows represent the collision "efficiencies" (k is the rate constant of the reaction), here defined as the number of collisions necessary for one conversion. The figures in the third row denote the activation energies (in kcal) obtained by the above method, while those in the fourth denote the heat of the reaction (in kcal). Arrows indicate the direction of increase of reaction rates. The effect of the following structural features of the reacting molecules are examined:

1. Increase in the number of chlorine atoms attached to one carbon atom:

Z/k	10^4	9×10^2	1×10^2	25
RCI	$\text{CH}_3\text{Cl} \rightarrow \text{CH}_2\text{Cl}_2 \rightarrow \text{CHCl}_3 \rightarrow \text{CCl}_4$			
E	10.0	7.4	5.0	3.5
Q	14.5	19.5	24.5	29.6

2. Increase in the length of the carbon chain:

Z/k	10^4	7×10^3	4.4×10^3	3.3×10^3
RCI	$\text{CH}_3\text{Cl} \rightarrow \text{CH}_3\text{CH}_2\text{Cl} \rightarrow \text{CH}_3\text{CH}_2\text{CH}_2\text{Cl} \rightarrow \text{CH}_3\text{CH}_2\text{CH}_2\text{CH}_2\text{Cl}$			
E	10.0	9.4	9.2	8.6
Q	14.5	17.0	20.0	—

3. Increase in the number of methyl groups attached to the α carbon atom:

Z/k	7×10^3	3.3×10^3	1.5×10^3
RCI	$\text{CH}_3\text{CH}_2\text{Cl} \rightarrow (\text{CH}_3)_2\text{CHCl} \rightarrow (\text{CH}_3)_3\text{CCl}$		
E	9.4	8.6	7.8
Q	17.0	—	22.5

4. Effect of a double bond in the α -position:

Z/k	7×10^3	1.1×10^4
RCI	$\text{CH}_3\text{CH}_2\text{Cl} \leftarrow \text{CH}_2=\text{CHCl}$	
E	9.4	10.4
Q	17.0	11.0

5. Effect of a double bond in the β -position:

Z/k	4.4×10^3	2.5×10^2
RCI	$\text{CH}_3\text{CH}_2\text{CH}_2\text{Cl} \rightarrow \text{CH}_2=\text{CHCH}_2\text{Cl}$	
E	9.2	6.0
Q	20.0	39.5

6. Change of halogen atom:

Z/k	$> 10^6$	10^4	50	1
RX	$\text{CH}_3\text{F} \rightarrow \text{CH}_3\text{Cl} \rightarrow \text{CH}_3\text{Br} \rightarrow \text{CH}_3\text{I}$			
E	> 25	10.0	4.3	0
Q	~ 0	15.0	19.0	18.0

As is to be expected, the activation energy falls steadily with increase in the heat of reaction Q (see p. 161). Since Q represents the difference $D(\text{Na—Cl})—D(\text{R—Cl})$ of energy of breaking the respective bonds, an approximate treatment of the dependence of activation energy on the structure of these molecules may be based on an examination of the dependence of the energy of bond rupture on the structure of the molecule.

The opposite trends of the activation energy and the heat of reaction, are not maintained in the 6th (last) set of figures shown above. This might have been expected since during the course of reaction in this series the atoms which migrate to the sodium atom are *different*, although attached to the same radical (see §10).⁽⁴⁹⁾

The regularities observed in rows 1–5 may also be connected with certain other characteristics of the molecule. Eyring and coworkers [1155, 1156, 592] have suggested an approximate method for calculating the effective charge of atoms in halogen-substituted saturated hydrocarbons, starting from data on the dipole moments of the molecules CH_3X , the longitudinal polarizability of the bonds and the geometry of the molecules.⁽⁵⁰⁾ For the methane derivatives $\text{CH}_{4-n}\text{Cl}_n$ the effective charges (in units e) of the atoms C, H and Cl respectively were found to be, for $n = 1, 2, 3, 4$:

- | | |
|--------------------------|--------------------------|
| (1) 0·148, 0·019, -0·205 | (2) 0·232, 0·030, -0·146 |
| (3) 0·286, 0·037, -0·108 | (4) 0·324, —, -0·081 |

These effective atomic charges were calculated on the assumption that the dipole moment of the C—H bond in methane was zero (assumed values $\pm 0\cdot 3$ debyes also gave much the same results).

Let us consider exactly what constitutes the electronic mechanism of the elementary step



Since the chlorine atom of the Cl—R bond is negatively charged, while an electrically neutral radical R is formed as a result of the reaction, the centre of gravity of the bonding electron cloud is displaced in the direction $\text{Cl} \rightarrow \text{R}$ as R recedes from the chlorine atom. Simultaneously a displacement of the electron cloud of the Na atom occurs in the direction of the chlorine atom during the formation of the Na—Cl bond. It is to be expected, therefore, that the greater the effective negative charge e_{eff} of the chlorine

⁽⁴⁹⁾ It is not difficult to see that the activation energy changes in the same direction as the energy of rupture of the $\text{CH}_3\text{—X}$ bond, whose values are: $\text{CH}_3\text{—Cl}$ 80 kcal, $\text{CH}_3\text{—Br}$ 66 kcal and $\text{CH}_3\text{—I}$ 54 kcal. The situation is now as though the interaction of a sodium atom with atoms of different halogens has practically no effect on the height of the potential activation barrier, which in this series depends fundamentally only on the strength of the $\text{CH}_3\text{—X}$ bond.

⁽⁵⁰⁾ These workers obtained a satisfactory agreement between the calculated and experimental dipole moments of a number of halogen derivatives.

atom, the more difficult is redistribution of the electronic density and the higher the activation energy of the process. As is seen from Fig. 56, this rule is in fact observed for compounds of the same halogen. To determine the change in activation energy at constant effective charge, the varying ease of charge redistribution during the reaction must also be allowed for as a function of the polarizability of the α -bond C—X. Correspondingly, Smith and Eyring [1155] assumed that the activation energy was determined by the ratio of the effective charge of the halogen atom to the polarizability of the C—X bond. If the ratio e_{eff}/α is plotted along the ordinate and the free energy of activation along the abscissa, as in Fig. 56, all the

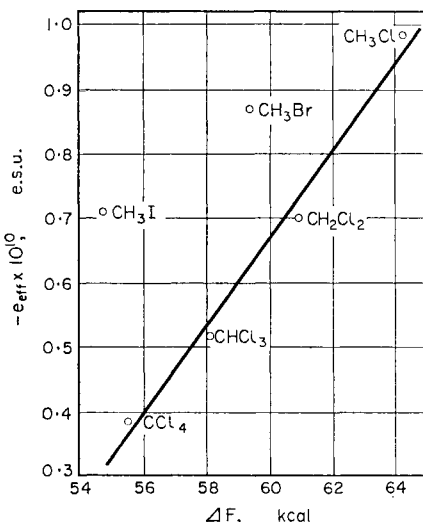


FIG. 56. The relation between the effective charge of the halogen atoms in halogenated methanes $\text{CH}_n\text{X}_{4-n}$ and the free energy of activation of the reactions of these compounds with sodium atoms (after Smith and Eyring [1155]).

points for halogenated methanes do in fact lie on a straight line (Fig. 57).⁽⁵¹⁾

Figure 58 shows the corresponding data for various halogen derivatives obtained by different workers, the abscissa giving the heats of activation ΔH_{eff} . The latter are obtained from ΔF_{eff} assuming that the entropy of activation is the same for all these reactions.⁽⁵²⁾ It should be noted that the deviation from a straight line is in general due to points drawn from the data of different authors using slightly different conditions; the data of any one worker have a much smaller scatter. Points corresponding to the halogen molecules X_2 do not obey the general rule, possibly because of the absence of residual charge on the X atoms.

⁽⁵¹⁾ The polarizability of the C—X bond is constant for compounds of the same halogen.

⁽⁵²⁾ ΔS_{eff} is taken to be equal to $0.101 \text{ cal. mole}^{-1} \text{ deg}^{-1}$.

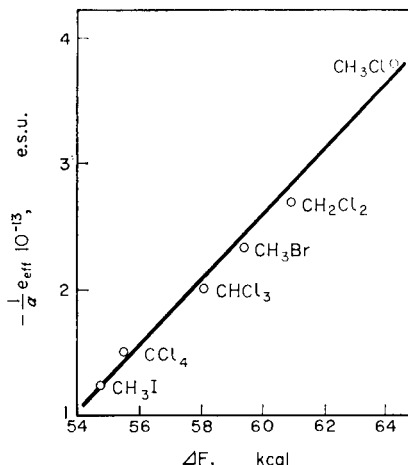


FIG. 57. The relation between the effective charge of the halogen atom, divided by the polarizability of the C—X bond, and the free energy of the reaction $\text{CH}_n\text{X}_{4-n}$ with sodium atoms (after Smith, Ree, Magee and Eyring [1156]).

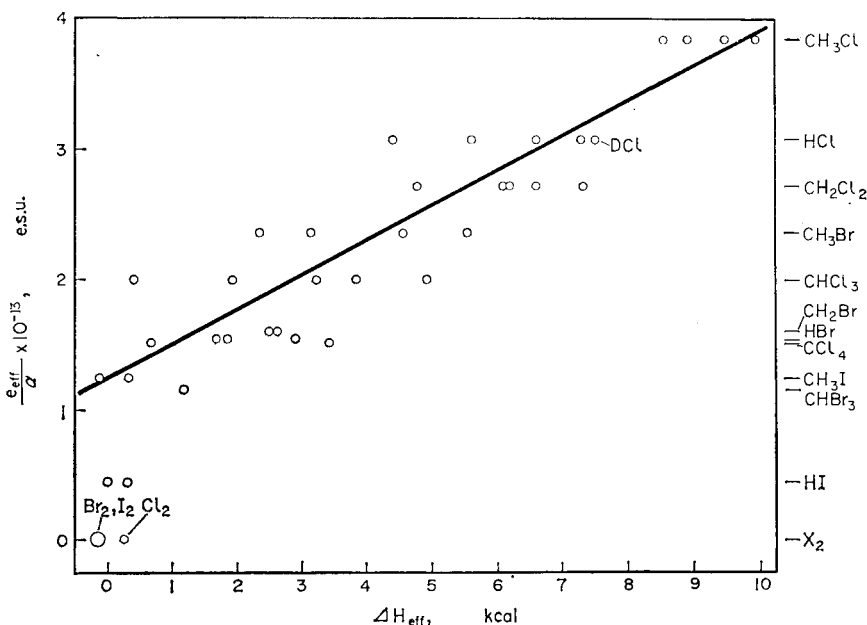


FIG. 58. The relation between the effective charge of the halogen atom, referred to the polarizability of the C—X bond, and the activation energy for the reactions of certain gases with sodium atoms (after Smith and Eyring [1155]). Points on the same level refer to the data of different workers.

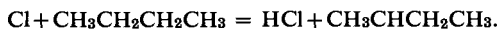
Proof of the existence of an increase of activation energy with e_{eff}/α for the halogenated derivatives of the homologues of methane is hampered by the lack of reliable experimental data on activation energies. The assumption made above that ΔS_{eff} has the same value for all RX molecules cannot be applied to the homologues of methane: at least this assumption does not lead to a linear relation between E and e_{eff}/α [1155].

The characteristic dependence of the rate of reaction on the structure of the molecule is also observed in a large number of other cases which have been studied. Here we shall examine some additional data relating to the reactions of chlorine atoms with aliphatic hydrocarbons and their chlorine derivatives. In n-butane $\text{CH}_3\text{CH}_2\text{CH}_2\text{CH}_3$, for example, the two middle (secondary) carbon atoms are most easily chlorinated, i.e. chlorine atoms most easily attack these carbon atoms.⁽⁵³⁾ The reaction of isopentane $(\text{CH}_3)_2\text{CHCH}_2\text{CH}_3$ with chlorine atoms involves principally the tertiary carbon atom. Even more reactive is t-butane $(\text{CH}_3)_3\text{CH}$, where also it is the tertiary carbon atom which is chlorinated. These tendencies, analogous to those observed in the reactions of sodium atoms with chlorides (see above), agree well with the energy required for abstracting a hydrogen atom from the corresponding molecules, e.g. $\text{CH}_3\text{CH}_2-\text{H}$ 98 kcal, $(\text{CH}_3)_2\text{CH}-\text{H}$ 89 kcal, $(\text{CH}_3)_3\text{C}-\text{H}$ 85 kcal.

The fall in the activation energy and energy of breaking the C—H (or C—X) bond with increasing number of methyl groups on the carbon atom can hardly be due to the effect of residual charges, as in the case of the chlorides, since there can be no appreciable electrical asymmetry of the bonds in saturated hydrocarbons. It should rather be compared with the difference in longitudinal polarizability of the C—C and C—H bonds [1155] (i.e. the polarizability in the direction of the line of the bond). As in the reactions of sodium atoms with chlorides, we may assume that the abstraction of a hydrogen atom, accompanied by the redistribution of the electrons of the C—H bond, proceeds more easily, the greater the longitudinal polarizability of the remaining bonds connecting the carbon atom with the neighbouring atoms. According to Denbigh [534] the longitudinal polarizability of the C—C bond, equal to $1.68 \times 10^{-24} \text{ cm}^3$, is more than twice as great as that of the C—H bond, which is $0.79 \times 10^{-24} \text{ cm}^3$. It becomes clear from these considerations why the activation energy and the energy of breaking the bond decrease with an increase in the number of carbon atoms directly joined to the relevant carbon atom.

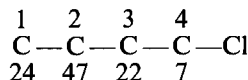
Slightly more complex are the tendencies shown in the reactions of chlorine with chlorinated aliphatic hydrocarbons.⁽⁵⁴⁾ Here, as in the previous

⁽⁵³⁾ The primary process appears to be

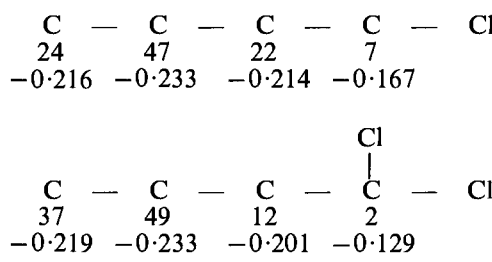


⁽⁵⁴⁾ For a survey of the relevant experimental data see [331].

case, the process consists of the transfer of a hydrogen atom to the chlorine atom. The relative ease of abstracting a hydrogen atom from different carbon atoms in butyl chloride is shown by the following figures (the upper figures show the numbering of the carbon atoms, the lower the relative frequency of attack by chlorine atoms):



To explain this sequence we have to consider two effects: the inductive effect, connected with the presence of a chlorine atom in the molecule, and the polarizability of the bonds. Since atoms 1 and 2 are sufficiently far removed from the chlorine atom, only the second effect is operative here; addition to the second carbon atom is facilitated by its participation in two C—C bonds, not only in one as for the first atom. The fourth carbon is the most strongly influenced by the chlorine atom, and therefore the main effect here is that of induction. One may suppose that the relative decrease in electron density at the hydrogen atoms in position 4 hinders their abstraction during interaction with chlorine atoms. In support of this hypothesis Smith and Eyring [1155] show that the effective charges of chlorine atoms introduced into chlorobutane in positions 1, 2, 3, 4 successively vary in the same direction as the figures given above for the relative reactivity of the carbon atoms. For mono- and di-chlorobutane the following results are obtained (the second row of figures denotes the effective charge of the chlorine in units of elementary charge):



The supposition that the activity of a hydrogen atom decreases under the influence of a halogen atom joined to the same carbon atom as the hydrogen agrees with the fact that the activity of the hydrogen atom in its reaction with chlorine is less in chlorinated methanes than in methane itself and falls with an increase in the number of chlorine atoms. According to the data presented on page 278 the effective positive charge of the hydrogen atoms increases in the same direction, i.e. with increase in the number of chlorine atoms attached to the carbon atom. See, further, [463a].

CHAPTER 5

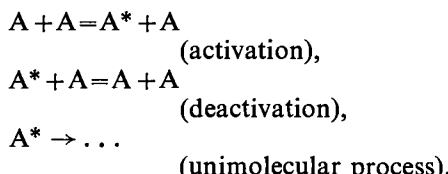
UNIMOLECULAR AND TERMOLECULAR REACTIONS

§18. Theory of Unimolecular Reactions

Rate of Reaction at High and Low Pressures

A unimolecular reaction is by definition a reaction taking place with the participation of one molecule. Decomposition, isomerization and inversion reactions may clearly be of this type. However in order for a reaction of this type to take place the molecule entering into it must have sufficient energy, namely the activation energy. If the reacting molecules do not obtain this energy from without (for example in the form of radiant energy), i.e. if the reaction is thermal (and not, for example, photochemical), the source of activation can only be *molecular collisions*.⁽¹⁾ It follows that activating molecular collisions are an essential stage in unimolecular reaction. We shall see later that this stage introduces complications into the course of a reaction, which make a unimolecular reaction law possible only at sufficiently high pressures.

From the above it follows that a unimolecular chemical reaction proceeds *in two stages*:⁽²⁾ the first stage is preliminary activation of molecules as a result of bimolecular collisions; the second stage is a strictly unimolecular reaction of the activated molecule. Instead of unimolecular conversion an active molecule may undergo *deactivating collisions* with other molecules which lead to the loss of a part of its energy, i.e. to the conversion of an active molecule into an inactive state. Consequently for a gas consisting of molecules of one sort (both active and inactive), with no admixtures, we must represent the mechanism of the unimolecular reaction as the sum of the processes:



⁽¹⁾ This idea was first put forward by Lindemann [880] (1922) who suggested that unimolecular decomposition takes place under the action of centrifugal force.

⁽²⁾ Here we are not considering secondary processes which may be observed in the case of unimolecular decomposition reactions and which take place after the process of unimolecular decomposition of a molecule of the initial substance.

Here A denotes a molecule of the substance converted and A^* denotes an active molecule of the same substance.⁽³⁾

The rate of formation of active molecules (the rate of activation) which are in a certain energy state characterized by an energy E_i may be expressed by the formula $Z_0 N N_i$, where

$$Z_0 = 4\sigma(RT/\pi M)^{1/2}, \quad (18.1)$$

σ is the effective collision cross-section, M the molecular weight; N is the concentration of inactive molecules and N_i is the equilibrium concentration of molecules having an energy E_i , so that according to the Maxwell–Boltzmann distribution

$$N_i = N(g_i \exp[-E_i/RT]) / (\sum_j g_j \exp[-E_j/RT]) \quad (18.2)$$

where g_i and g_j are statistical weights.

The rate of deactivation of active molecules is $Z_0 N n_i$ and the rate of their unimolecular conversion $k_i n_i$; here n_i is the concentration of active molecules of a given sort and k_i is the rate constant for their conversion. Considering the concentration of active molecules as stationary, then from the steady-state condition

$$dn_i/dt = Z_0 N N_i - Z_0 N n_i - k_i n_i = 0$$

we find

$$n_i = Z_0 N N_i / (Z_0 N + k_i).$$

Using this expression we obtain an equation for the specific rate of reaction, i.e. the rate of reaction per molecule:

$$k = -(1/N) dN/dt = \sum_i k_i Z_0 N_i / (Z_0 N + k_i). \quad (18.3)$$

In equation (18.3) the summation is taken over all possible energy states of the active molecule.

We shall consider first the two limiting cases: $k_i \ll Z_0 N$ (high concentrations or pressures) and $k_i \gg Z_0 N$ (low pressures). Neglecting k_i compared to $Z_0 N$, in the first case we may reformulate the expression (18.3) as

$$k = k_\infty = \sum_i k_i N_i / N, \quad (18.4)$$

or by (18.2) as

$$k_\infty = [\sum_i k_i g_i \exp(-E_i/RT)] / [\sum_j g_j \exp(-E_j/RT)]. \quad (18.5)$$

⁽³⁾ Here we mean by an *active* molecule a molecule with enough energy to have a non-zero chance of unimolecular conversion. Several authors also use the idea of an *activated molecule* which corresponds to the transition state or activated complex. Active and activated molecules may be denoted by the symbols A^* and A^{\neq} respectively.

In this way we see that at high pressures the specific reaction rate is constant (for constant temperature), i.e. the reaction follows a *unimolecular law*.

Leaving for the present the calculation of the constant k_∞ , we shall show that k_∞ varies with temperature approximately according to the Arrhenius equation. In fact, calculating the logarithmic derivative of the constant k_∞ (18.5)

$$\frac{d \ln k_\infty}{dT} = \frac{\sum_i (E_i/RT^2) k_i g_i \exp(-E_i/RT)}{\sum_i k_i g_i \exp(-E_i/RT)} - \frac{\sum_j (E_j/RT^2) g_j \exp(-E_j/RT)}{\sum_j g_j \exp(-E_j/RT)}$$

and noting that the first term in the expression obtained is the mean of the quantity E_i/RT^2 for active molecules (\bar{E}^*/RT^2) and the second term is the mean of this quantity for all molecules (\bar{E}/RT), we may write this expression in the form

$$(d/dt) \ln k_\infty = (\bar{E}^* - \bar{E})/RT^2 = E/RT^2, \quad (18.6)$$

where $E = \bar{E}^* - \bar{E}$ is the activation energy, according to its usual definition as the mean excess energy of the active molecules.⁽⁴⁾

In the second limiting case of very low pressures the quantity $Z_0 N$ may be neglected in comparison with k_i in formula (18.3) as $k_i \gg Z_0 N$ and we find (i denoting active states, j all states)

$$k = \sum_i Z_0 N_i = Z_0 N \left[\sum_i g_i \exp(-E_i/RT) \right] / \left[\sum_j g_j \exp(-E_j/RT) \right]. \quad (18.7)$$

We see that in this case the specific reaction rate is proportional to the concentration and hence follows a *bimolecular reaction law*

$$-dN/dt = \sum_i Z_0 N N_i = Z_0 N^2 \left[\sum_i g_i \exp(-E_i/RT) \right] / \left[\sum_j g_j \exp(-E_j/RT) \right]$$

This equation represents the over-all activation rate and shows that at low pressures the rate of the unimolecular reaction is determined by the rate of the activation stage which is the slower of the two consecutive stages; whereas at high pressures the slowest stage is that of the strictly unimolecular reaction whose rate is determined by the observed unimolecular reaction law.

⁽⁴⁾ In view of the fact that the quantities \bar{E}^* and \bar{E} , generally speaking, depend on temperature, here and earlier (p. 14) the Arrhenius equation holds only with the assumption that the temperature dependence is weak. One should expect that the constant k will obey the Arrhenius equation the more closely, the narrower the temperature range for which the temperature dependence of k is determined.

Hinshelwood's Theory

Both in the high-pressure case (18.4) and in the general case (18.3) it is necessary to use definite ideas about the quantities k_i in expressions (18.4) and (18.3) to calculate the specific reaction rate k . Hinshelwood's theory of unimolecular reactions [763] (1926) was the first theory based on Lindemann's conception of the activating (and deactivating) role of molecular collisions; it is assumed in this theory that the probabilities of unimolecular conversion of active molecules expressed by the quantities k_i do not depend on energy. In accordance with this assumption $k_i = \lambda = \text{const.}$, we may rewrite expression (18.3) in the form

$$k = (\lambda \sum_i N_i) / (N + \lambda / Z_0),$$

and hence, since $k_\infty = \lambda \Sigma (N_i / N)$ (18.4), we find

$$k = (k_\infty N) / (N + \lambda / Z_0). \quad (18.8)$$

The latter expression may also be presented in the following form. Substituting for the concentration N the pressure $p = (N / N_A)RT$ and introducing the notation

$$p_{1/2} = \lambda RT / Z_0 N_A, \quad (18.9)$$

we obtain from (18.8)

$$k_\infty / k = 1 + p_{1/2} / p. \quad (18.10)$$

In this way, according to Hinshelwood's theory, the inverse specific rate of the unimolecular reaction must be a linear function of the quantity $1/p$. It can be seen from formula (18.10) that the quantity $p_{1/2}$ is the pressure at which the specific reaction rate k is equal to half the maximum value (k_∞).

In accordance with the assumption that k_i is constant ($k_i = \lambda = \text{const.}$), in Hinshelwood's theory an active molecule is any molecule with an energy in excess of a certain critical value E_0 , independently of the nature of the distribution of energy between various internal degrees of freedom of the molecule. The fraction of molecules with an internal energy between E and $E + dE$ is, according to statistical calculation (the classical case—without taking into account quantization of energy), equal to [621]

$$(1/N)N(E) dE = [E^{(s/2-1)} \exp(-E/RT) dE] / [\Gamma(s/2)RT^{s/2}], \quad (18.11)$$

where s is the number of so-called square terms in the expression for the internal energy. In the case of a molecule containing n atoms

$$s = 2(3n - 6) + 3 \quad (18.12)$$

in accordance with the fact that each of the $3n - 6$ vibrational degrees of freedom corresponds to two square terms (one of which expresses the

kinetic energy and the second expresses the potential energy) and each of the three rotational degrees of freedom corresponds to one square term. $\Gamma(s/2)$ is the gamma-function. We note that, if $s/2$ is an integer,

$$\Gamma(s/2) = (s/2 - 1)!$$

Integrating equation (18.11) between the limits E_0 and ∞ , we obtain for the number of active molecules (according to Hinshelwood)

$$\begin{aligned} N_{\text{act}} &= [N/\Gamma(s/2)(RT)^{s/2}] \int_{E_0}^{\infty} E^{(s/2-1)} \exp(-E/RT) dE \\ &= N \exp(-E_0/RT) \times \\ &\quad \times [(E_0/RT)^{(s/2-1)}/\Gamma(s/2) + (E_0/RT)^{(s/2-2)}/\Gamma(s/2-1) + \dots + E_0/RT + 1] \end{aligned} \quad (18.13)$$

which for sufficiently high values of E_0/RT (for example when $E_0 > 10RT$) may be written in the approximate form

$$N_{\text{act}} = [N/\Gamma(s/2)](E_0/RT)^{(s/2-1)} \exp(-E_0/RT). \quad (18.13a)$$

Multiplying the quantity N_{act}/N by the probability of unimolecular conversion λ , we obtain the reaction rate constant

$$k_{\infty} = \lambda N_{\text{act}}/N. \quad (18.14)$$

It is not difficult to show that formula (18.14) is the classical analogue of formula (18.4) from which it may be obtained when $k_t = \lambda$, with the assumption that there is no quantization of the internal energy of the molecule.⁽⁵⁾

Calculating the logarithmic derivative of (18.14),

$$(d/dT) \ln k_{\infty} = [E_0 - (s/2 - 1)RT]/RT^2 = E_{\text{eff}}/RT^2, \quad (18.15)$$

we find for the effective activation energy E_{eff}

$$E_{\text{eff}} = E_0 - (s/2 - 1)RT.$$

Direct experimental checks were applied both to formulae (18.8) and (18.10), which give the specific rate of the unimolecular reaction as a function of pressure, and to the formula for the maximum value of the specific rate of the unimolecular reaction (k_{∞}) obtained from (18.13) and (18.14), and also formula (18.15) which expresses the temperature dependence of k_{∞} . The experimental check on the temperature dependence of k_{∞} showed that not all but only a half to two-thirds of the degrees of freedom of an active molecule normally take part in activation. This entirely natural result is also obtained from more precise theories. The pressure dependence

⁽⁵⁾ See, for example, Kassel [106]. Kassel uses s to denote the number of vibrational degrees of freedom of the molecule.

of the specific reaction rate derived from formulae (18.8) and (18.10) is only *qualitatively* supported by experiment. For example the pressure dependence of the specific rate of the decomposition of azomethane $\text{CH}_3\text{NNCH}_3 = \text{C}_2\text{H}_6 + \text{N}_2$ shown in Fig. 59 [1056] shows that, in accordance with formula (18.8), at sufficiently high pressures the specific rate approaches a constant (maximum) value ($k_\infty = 13.7 \times 10^{-5} \text{ sec}^{-1}$); at very low pressures it falls to zero. That in this case there is only qualitative agreement between the empirical dependence of the specific rate on pressure and that obtained from the theoretical formulae is clearly seen from Fig. 60, which shows the same data as Fig. 59 but with the coordinates $1/k$ and $1/p$. It can be seen in Fig. 60 that instead of a straight line corresponding to formula (18.10) a curve is obtained in practice. Such curves concavely inclined to the abscissa ($1/p$) are also observed in all other cases and hence Hinshelwood's theory is only a rough approximation to reality.

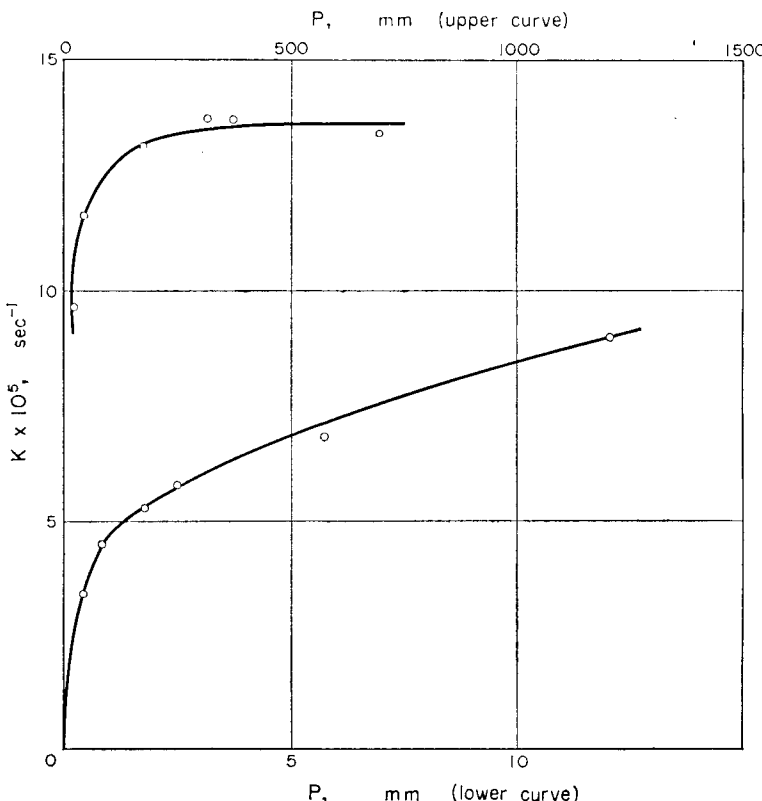


FIG. 59. The pressure dependence of the specific rate of the unimolecular decomposition of azomethane CH_3NNCH_3 at 290°C (according to Ramsperger [1056]).

The reason for the non-correspondence of this theory with experiment is the inaccuracy of its basic assumption that the rate constant (λ) for the unimolecular conversion of an active molecule is constant. In fact it is apparent from general considerations that the probability of a concentration of energy in the bonds broken during the unimolecular conversion (which is an essential condition for the conversion) must be the greater, the greater

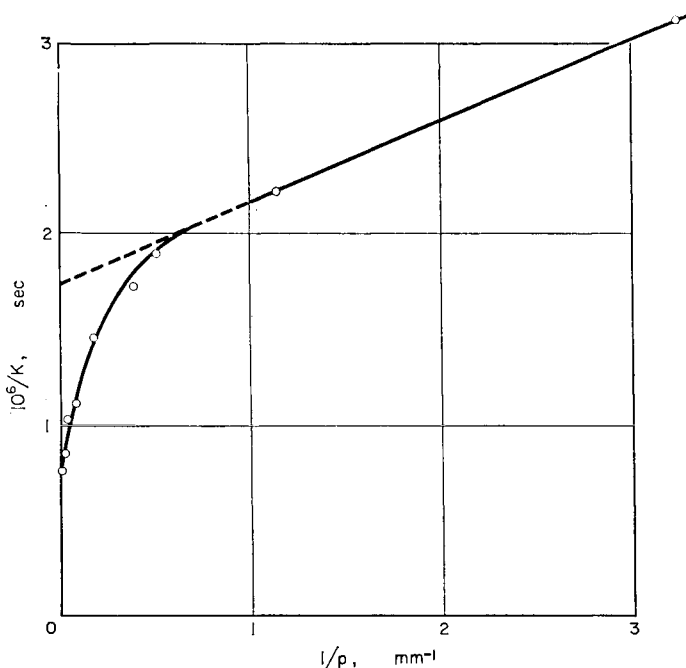


FIG. 60. Data from Fig. 59 plotted with coordinates $10^6/k$ sec, $1/p$ (mm Hg) $^{-1}$.

the supply of energy of the active molecule. The resulting dependence of the rate constant k_i on energy, expressed by the increase in k_i with increase in the energy supply E_i of the molecule, gives a simple physical explanation of the observed shape of the curves $1/k$ against $1/p$, i.e. the deviations of these curves from the straight-line relationship expressed by formula (18.10) are explained by the fact that with decreasing pressure an increasing part of the active molecules having an energy only slightly in excess of the activation energy E_0 become important in the reaction. Owing to the lowering of the probability of conversion k_i of such molecules, the effect is as if the part of the quantity k_∞ corresponding to them also decreased with

decreasing pressure, and as a result the dependence of $1/k$ on $1/p$ is also expressed by a curve similar to that shown in Fig. 60.

Such a relationship between $1/k$ and $1/p$ follows directly from formula (18.3). Actually, calculating the first and second derivatives of the quantity $1/k$ with respect to $1/p$, we find $d(1/k)/d(1/p) > 0$ and $d^2(1/k)/d(1/p)^2 < 0$, i.e. a monotonic increase of $1/k$ with $1/p$ and a curve with negative curvature for $1/k$ against $1/p$, in accordance with Fig. 60.

Attempts to construct a more precise theory for unimolecular reactions have been undertaken at various times by Rice and Ramsperger [1068] (1927-28), Kassel [187, 106] (1928-32), Landau [167] (1936), Slater [1143, 1144, 1145] (1939-53), Obreimov [215, 196] (1949) and others. In all these theories it is assumed that in the activation of a molecule only its vibrational degrees of freedom take part, i.e. that the activation energy of molecules takes the form of a vibrational energy. In its application to polyatomic molecules containing a large number of atoms, this assumption must be considered sufficiently well substantiated. Actually, since the number of vibrational degrees of freedom of a molecule containing n atoms is $3n - 6$, then even with a relatively small n the number of vibrational degrees of freedom may considerably exceed the number of rotational degrees of freedom which is always 3 or 2. For example in the azomethane case considered above, we have $n = 10$ which gives 24 vibrational degrees of freedom and in comparison the 3 rotational degrees of freedom may be ignored. However, in the decomposition of molecules with a small number of atoms the rotational energy may contribute to the energy of the active molecule. This contribution is apparently not large since for significant stretching of a polyatomic molecule under the influence of centrifugal force its rotational energy must be much greater than the vibrational energy. For this reason it is natural that in existing theories of unimolecular reactions the role of rotational energy is practically not considered.⁽⁶⁾

An important distinction between some later theories and Hinshelwood's theory is that according to these theories not every molecule is active which has an energy $E \geq E_0$, as is assumed in Hinshelwood's theory, but only a molecule in which a definite energy can be concentrated in the bond to be broken. In this way one of the main problems of a theory is the problem of calculating the probability of a concentration of the energy, which is distributed between many degrees of freedom of a molecule, in one degree of freedom. In the theory of Rice and Ramsperger and the similar theory of Kassel this problem is solved in the way described below.

⁽⁶⁾ Here one should only mention that in connection with determination of the configuration and number of vibrational degrees of freedom of an activated molecule it becomes necessary to consider the possibility of internal rotational degrees of freedom. See, for example, Rosenstock, Wallenstein, Wahrhaftig and Eyring [1086] and also Marcus [915, 914].

Kassel's theory

Hereafter we shall represent a molecule by the form adopted in Kassel's theory, i.e. as a system of harmonic oscillators; the coupling between the oscillators is sufficient to enable the energy of the molecule to be freely distributed between the various degrees of freedom, while at the same time the coupling is sufficiently weak to allow each oscillator to be considered as effectively independent (this allows the energy of a molecule to be represented as a sum of square terms corresponding to these oscillators). In Kassel's theory it is assumed that the number of oscillators is equal to the number of vibrational degrees of freedom f of the active molecule which participate in the activation, and the vibrational frequencies of all f oscillators are usually assumed all to have the same value ν .

According to probability theory the probability that, of a total energy $\epsilon = ih\nu$ shared by f oscillators, m quanta, i.e. the energy $\epsilon_0 = mh\nu$, is concentrated in one particular oscillator is

$$\frac{(i-m+f-1)!i!}{(i-m)!(i+f-1)!}.$$

In Kassel's theory the probability k_i of unimolecular conversion of an active molecule is actually assumed to be proportional to this probability, so that

$$k_i = A \frac{(i-m+f-1)!i!}{(i-m)!(i+f-1)!}, \quad (18.16)$$

where the proportionality factor A characterizes the rate of energy redistribution between the various oscillators. For sufficiently high i or, more precisely, in the limit when $i = \infty$, which corresponds to a transition to a system of classical (non-quantized) oscillators, formula (18.16) takes the form:

$$k = A(1-m/i)^{f-1} = A(1-E_0/E)^{f-1} \quad (18.17) \\ (E = N_A ih\nu, E_0 = N_A mh\nu).$$

On the basis of formula (18.16) and the earlier formulae (18.2) and (18.3) a general expression may be obtained for the specific rate of unimolecular reaction which must be accurate in so far as the model taken for the active molecule is admissible. We shall first calculate the maximum value for the specific reaction rate k_∞ (18.5). Substituting in this formula the statistical weight of the i th state which is expressed by the formula⁽⁷⁾

$$g_i = \frac{(i+f-1)!}{i!(f-1)!}, \quad (18.18)$$

⁽⁷⁾ See Kassel [106] pp. 34, 92 *et seq.*

and noting that the sum

$$\sum_j g_j \exp(-E_j/RT)$$

in the denominator of (18.5) in this case will be equal to

$$\begin{aligned} \sum_{j=0}^{\infty} g_j \exp(-\epsilon_j/kT) &= \sum_{j=0}^{\infty} \frac{(j+f-1)!}{j!(f-1)!} \exp(-jh\nu/kT) \\ &= 1 + f \exp(-h\nu/kT) + (1/2!)f(f+1) \exp(-2h\nu/kT) + \dots \\ &= [1 - \exp(-h\nu/kT)]^{-f}, \end{aligned}$$

and that the sum $\sum k_i g_i \exp(-E_i/RT)$ in the numerator may be reformulated using (18.16) and (18.18) (here $p = i - m$ and $E_0 = N_A \epsilon_0 = N_A m h\nu$) as

$$\begin{aligned} \sum_{i=m}^{\infty} k_i g_i \exp(-\epsilon_i/kT) &= A \sum_{i=m}^{\infty} \frac{(i-m+f-1)!}{(i-m)!(f-1)!} \exp(-ih\nu/kT) \\ &= A \exp(-E_0/RT) \sum_{p=0}^{\infty} \frac{(p+f-1)!}{p!(f-1)!} \exp(-ph\nu/kT) \\ &= A \exp(-E_0/RT) (1 - \exp[-h\nu/kT])^{-f}, \end{aligned}$$

we obtain

$$k_{\infty} = A \exp(-E_0/RT). \quad (18.19)$$

By the same method and using similar substitutions and simple transformations from (18.3), (18.2) and (18.19) we obtain an expression for the specific reaction rate in the general case

$$\begin{aligned} k &= k_{\infty} [1 - \exp(-h\nu/kT)]^f \times \\ &\times \sum_{p=0}^{\infty} \frac{[(p+f-1)!/p!(f-1)!] \exp(-ph\nu/kT)}{1 + (A/Z_0 N) [(p+f-1)!(p+m)!/p!(p+m+f-1)!]}. \end{aligned} \quad (18.20)$$

It is not difficult to obtain an expression for the specific reaction rate in the classical case (non-quantized oscillators) as well. In this case substituting in (18.3), instead of (18.16) and (18.2), the formulae (18.17) and (18.11) respectively, and replacing $s/2$ (Hinshelwood) by f (Kassel) and integrating between the limits $E = E_0$ and $E = \infty$, we have

$$k = \frac{A}{(f-1)!(RT)^f} \int_{E_0}^{\infty} \frac{(E-E_0)^{f-1} \exp(-E/RT) dE}{1 + (A/Z_0 N)(1-E_0/E)^{f-1}} \quad (18.21)$$

or introducing the notation

$$x = (E - E_0)/RT$$

$$k = \frac{A \exp(-E_0/RT)}{(f-1)!} \int_0^\infty \frac{x^{f-1} e^{-x} dx}{1 + (A/Z_0 N)[x/(E_0/RT + x)]^{f-1}} \quad (18.21a)$$

It is not difficult to see that in this case at high pressures, i.e. when $A/Z_0 N \ll 1$, since

$$\int_0^\infty x^{f-1} e^{-x} dx = f!$$

it follows from (18.21a) that, as in the previous case, $k_\infty = A \exp(-E_0/RT)$ (18.19), which permits us to rewrite expression (18.21a) in the form

$$k = \frac{k_\infty}{(f-1)!} \int_0^\infty \frac{x^{f-1} e^{-x} dx}{1 + (A/Z_0 N)[x/(E_0/RT + x)]^{f-1}}. \quad (18.21b)$$

At low pressures ($A/Z_0 N \gg 1$) (18.21a) gives

$$k = \frac{(E_0/RT)^{f-1}}{(f-1)!} \exp(-E_0/RT) Z_0 N \times \\ \times \left[1 + \frac{f-1}{E_0/RT} + \frac{(f-1)(f-2)}{(E_0/RT)^2} + \dots + \frac{(f-1)!}{(E_0/RT)^{f-1}} \right],$$

Thus, for sufficiently high E_0/RT ,

$$(d/dT) \ln k = [E_0 - (f-1)RT]/RT^2,$$

and consequently

$$E_{\text{eff}} = E_0 - (f-1)RT. \quad (18.23)$$

In this way we see that the values of the effective activation energies in the high-pressure region, where $E_{\text{eff}} = E_0$, and in the low-pressure region do not coincide. We note that by replacing $s/2$ in formula (18.15) by f this formula coincides with formula (18.23). Since, however, in Hinshelwood's theory the activation energy is the same in the high- and low-pressure regions, this theory and Kassel's theory give a different temperature dependence for the specific reaction rate.

The different temperature dependence of the specific reaction rate leads also to a different dependence of k on pressure. Actually, it follows from the lowering of the effective activation energy from E_0 to the value

expressed by formula (18.23) in the transition from the high- to the low-pressure region, that at low pressures unimolecular conversion is experienced by molecules with a lower mean energy compared with molecules which are converted at high pressures. And since, according to formula (18.17), the probability of conversion increases with increase in the energy of a molecule, then in the transition from low to high pressures a sharper increase in the specific reaction rate k should be observed than that obtained with the assumption that the probability of conversion of an active molecule is not dependent on its energy. Such an explanation was also given above (p. 289) for the observed curvature of the plot of $1/k$ against $1/p$, in contrast with the straight line obtained from Hinshelwood's theory, which assumes that the probability of unimolecular conversion is not dependent on the excess energy of the active molecule.

Landau's Theory

Landau's statistical treatment [167] of the unimolecular decomposition of complex molecules considers them as macroscopic systems. For the specific reaction rate of such molecules Landau obtains an expression of the form

$$k(E) = \frac{A \exp[(F_0 - E)/RT_0 + S(E)/R]}{\exp[\{S(E) - S(E - E_0)\}/R] + A/Z_0 N} \quad (18.24)$$

where E is the energy of the active molecule (per gram-molecule); F_0 is its free energy at thermal equilibrium (for a temperature T_0); $S(E)$ is the entropy of the molecule for uniform energy distribution and $S(E - E_0)$ is the entropy of the active molecule, i.e. of a molecule of whose energy a part E_0 (the activation energy) is concentrated in a certain small number of degrees of freedom; A is a quantity having dimensions sec^{-1} and of the order of a vibrational frequency.

From the form of formula (18.24), Landau comes to the conclusion that the main role in the decomposition (conversion) of molecules is played by active molecules with an energy corresponding to the maximum of the function $k(E)$. From the condition for the maximum it follows that at high pressures an important role in the reaction is played by molecules with an energy exceeding the activation energy by the mean energy \bar{E} of the molecules; whereas at low pressures molecules with energy near E_0 contribute most of the decompositions. Moreover, effective activation energies (heats of activation) are determined from the condition for the maximum of $k(E)$: $E_{\text{eff}} = E_0$ at high pressures and $E_{\text{eff}} = E_0 - \bar{E}$ at low pressures; these are the same values as those obtained from Kassel's theory. For the specific reaction rate at high pressures (k_∞) Landau obtains the expression

$$k_\infty = A \exp(-E_0/RT),$$

which is also the same as the corresponding expression (18.19) obtained from Kassel's theory.

“Equilibrium Theory” of Unimolecular Reactions

We have seen in Chap. 3 (pp. 189–191) that unimolecular reactions may also be considered using the statistical method of the transition state. In these reactions the transition state is the state of the activated molecule arising from bimolecular collision and the resulting transition of the active molecule into a critical transition state. Bearing in mind that there are active molecules of different energies the expression for the rate constant of a unimolecular reaction may be written as an integral

$$k = \int_0^{\infty} \kappa_{\epsilon} k_{\epsilon} K_{\epsilon} d\epsilon,$$

where k_{ϵ} is the transmission coefficient, k_{ϵ} the rate constant for passage of the active molecule to the critical transient state ($A^* \rightarrow A^*$) and K_{ϵ} is the equilibrium constant for the process $A + A \rightleftharpoons A_{\epsilon}^* + A$ [675].

The transmission coefficient κ_{ϵ} in these formulae may be written as the product of two factors: a factor γ representing the probability of the system penetrating the potential barrier and reaching the final state, and a factor a_{ϵ} which is a transmission coefficient determined by the non-equilibrium concentration of active molecules at low pressures. We should note that in adiabatic reactions the factor γ is close to unity and that only for non-adiabatic reactions may it be considerably less than unity.⁽⁸⁾

The factor a_{ϵ} is defined by the equation

$$a_{\epsilon} = \frac{Z_{\epsilon}^0 N}{Z_{\epsilon}^0 N + k_{\epsilon}}$$

(N is the concentration of the reacting gas and Z_{ϵ}^0 is the rate constant for the deactivation process). It can be seen from these two formulae that at sufficiently high pressures $a_{\epsilon} = 1$. The quantities Z_{ϵ}^0 in the formula and also the quantity κ_{ϵ} may be obtained in principle from an examination of the potential energy surfaces for each reaction [674].

To calculate k_{ϵ} and K_{ϵ} and consequently the rate constant k_{∞} for the unimolecular reaction at high pressures (correct to a κ -factor) it is necessary to select a definite model for the molecule. Thus if we follow Kassel (and also Rice and Ramsperger) and assume that the molecule in both the active state and also the activated complex state is a system of classical oscillators which are characterized by the vibrational frequencies

⁽⁸⁾ When there is tunnelling through the potential barrier the coefficient may be greater than unity.

ν_k and ν_k^{\neq} , respectively, and if f is the number of normal vibrations, then k_e and K_e may be expressed as [674, 675]:

$$k_e = \frac{\prod_k^f \nu_k}{\prod_k^{f-1} \nu_k^{\neq}} \left(\frac{\epsilon - \epsilon_0}{\epsilon} \right)^{f-1}$$

and

$$K_e = \frac{\epsilon^{f-1} \exp(-\epsilon/kT)}{(kT)^f \Gamma(f)}$$

where ϵ_0 is the minimum energy at which the reaction becomes possible (the activation energy). Substituting these expressions for k_e and K_e in the formula for the reaction rate constant at high pressures, namely

$$k_{\infty} = \int_0^{\infty} k_e K_e d\epsilon,$$

we obtain

$$k_{\infty} = \bar{\nu} \exp(-E_0/RT), \quad (18.25)$$

where

$$\bar{\nu} = \prod_k^f \nu_k / \prod_k^{f-1} \nu_k^{\neq} \quad (18.26)$$

and $E_0 = N_A \epsilon_0$. We see that formula (18.25) is identical with Kassel's (18.19) and with the formula obtained by Landau (p. 294); however, in contrast with these formulae, the pre-exponential factor $\bar{\nu}$ in (18.25) has an analytical expression (18.26) from which it may be calculated if the frequencies ν_k and ν_k^{\neq} are known from the assumed configuration of the active molecule and the activated transition state.⁽⁹⁾

Slater's Theory

Slater has shown that his theory, although based on essentially different grounds from those of Kassel's theory, nevertheless leads to results close to those obtained by Kassel. The basis of Slater's theory is the model of a molecule as a mechanical system of interconnected atoms which is capable of performing harmonic vibrations about an equilibrium configuration. The geometrical configuration of the molecule is described by generalized coordinates q_1, q_2, \dots, q_n , and it is assumed that its kinetic and potential energy may be expressed by the sum of the quadratic functions of the

(9) See also formulae (12.63) and (12.64), Chap. 3.

generalized velocities and coordinates respectively, namely

$$E_k = \frac{1}{2} \sum_1^n a_{rs} \dot{q}_r \dot{q}_s, \quad V = \frac{1}{2} \sum_1^n b_{rs} q_r q_s,$$

where n is the number of vibrational degrees of freedom. This permits us to describe the internal motion of a molecule as the sum of normal harmonic vibrations with frequencies $\nu_1, \nu_2, \dots, \nu_n$, energies $\epsilon_1, \epsilon_2, \dots, \epsilon_n$ and initial phases $\psi_1, \psi_2, \dots, \psi_n$. It is further assumed that the energies and phases change only as a result of collisions with other molecules. As we shall see, Slater's theory differs in this respect from Kassel's theory in which energy is continuously and spontaneously redistributed between individual oscillators. With these assumptions a certain coordinate q , which characterizes the internal motion of the molecule leading to its unimolecular conversion, may be expressed as

$$q = \sum_{i=1}^{n'} a_i \cos 2\pi(\nu_i t + \psi_i), \quad (18.27)$$

where n' is the number of normal vibrations taking part in the activation of the molecule and $a_i = \alpha_i \epsilon_i^{\frac{1}{2}}$ (the quantity α_i is called the amplitude factor). The time t is calculated from the moment of the last collision.

The active molecule becomes capable of unimolecular conversion when the coordinate q reaches a certain critical value q_0 . Thus in this theory the path of the reaction which corresponds to change in the coordinate q may be represented schematically by the curve shown in Fig. 61; the coordinate q is plotted along the abscissa and potential energy is plotted along the ordinate. Since the individual vibrations are independent,

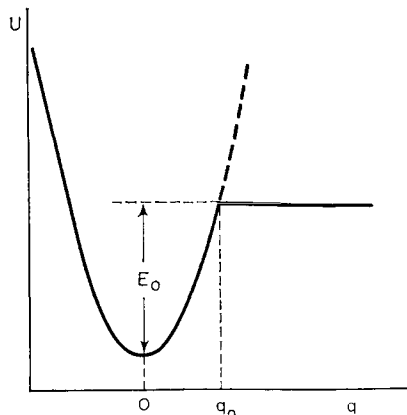


FIG. 61. The change in potential energy with the reaction coordinate q in Slater's model for the active molecule.

the quantity q (18.27) may reach a maximum, equal to $\sum |a_i|$, at a certain moment of time, and the condition determining the possibility of unimolecular conversion may be written

$$\sum |a_i| = \sum |\alpha_i| \epsilon_i^{1/2} \geq q_0. \quad (18.28)$$

If the values ϵ_{i0} of the normal vibration energies ϵ_i satisfy (18.28) while making the sum $\sum \epsilon_i$ a minimum, then the sum of these values (per mole) is the activation energy E_0 :

$$E_0 = N_A \sum \epsilon_{i0}. \quad (18.29)$$

When $E > E_0$ but condition (18.28) is not fulfilled, unimolecular conversion does not take place. Thus conditions (18.28) and (18.29) are not equivalent. However in order for conversion to take place in fact, these conditions must be fulfilled before the next collision occurs. Hence the probability of conversion must depend both on the properties of function (18.27) and on the frequency of molecular collisions. The task is therefore to calculate both these factors.

In Slater's theory the specific reaction rate is calculated by the following method.⁽¹⁰⁾ The rate of formation of active molecules (in cm^3), with energy $E = N_A \sum \epsilon_i$ distributed between the degrees of freedom so that in each degree of freedom the energy is between the limits ϵ_i and $\epsilon_i + d\epsilon_i$, may be expressed by the formula

$$Z_0 N^2 \prod_1^{n'} \exp(-\epsilon_i/kT) d\epsilon_i/kT = Z_0 N^2 \exp(-E/RT) \prod_1^{n'} d\epsilon_i/kT. \quad (18.30)$$

The rate of deactivation of these molecules is expressed by the formula

$$Z_0 N n^* \prod_1^{n'} d\epsilon_i \quad (18.31)$$

and the rate of their unimolecular conversion is

$$k^* n^* \prod_1^{n'} d\epsilon_i, \quad (18.32)$$

where n^* is the concentration of active molecules of the given type and k^* is the specific rate of their conversion. From the steady-state condition for the concentration of the active molecules, namely

$$Z_0 N^2 \exp(-E/RT) \prod_1^{n'} d\epsilon_i/kT - Z_0 N n^* \prod_1^{n'} d\epsilon_i - k^* n^* \prod_1^{n'} d\epsilon_i = 0$$

⁽¹⁰⁾ In Obreimov's theory [215], which is based on the same grounds as Slater's theory, only the problem of the decomposition of an active molecule, i.e. the unimolecular reaction at high pressures, is considered.

we find

$$n^* = \frac{N \exp(-E/RT)(kT)^{-n'}}{1 + k^*/Z_0 N} \quad (18.33)$$

and hence for the specific reaction rate we obtain

$$\begin{aligned} k &= -\frac{1}{N} \frac{dN}{dt} \\ &= \int \dots \int k^* n^* \prod_{i=1}^{n'} d\epsilon_i \\ &= \int \dots \int \frac{k^* \exp(-E/RT)}{1 + k^*/Z_0 N} \prod_{i=1}^{n'} (d\epsilon_i/kT). \end{aligned} \quad (18.34)$$

The integration is taken for all positive values of ϵ_i satisfying (18.28).

When k^* is a function only of the total energy E , as in Kassel's theory where $k^* = A(1 - E_0/E)^{f-1}$ (18.17), since

$$\int \dots \int_{E < N_A \sum \epsilon_i < E + dE} d\epsilon_1 \dots d\epsilon_f = \frac{1}{N_A^f} \frac{E^{f-1} dE}{(f-1)!},$$

Slater's formula (18.34) assumes the form

$$k = \frac{1}{(RT)^f (f-1)!} \int_0^{\infty} \frac{k^* E^{-1} \exp(-E/RT) dE}{1 + k^*/Z_0 N}. \quad (18.35)$$

It is not difficult to see that on substituting k^* (18.17) in it, formula (18.35) becomes identical with Kassel's formula (18.21).

For sufficiently high pressures when $k^*/Z_0 N \ll 1$, formula (18.34) may be rewritten

$$k = k_{\infty} = \int \dots \int k^* \exp(-E/RT) \prod_{i=1}^{n'} (d\epsilon_i/kT). \quad (18.36)$$

By substituting in this formula an accurate value of k^* (insofar as it is accurate to assume that the frequencies of the individual normal vibrations are incommensurable and that the general idea of a molecule as a system of harmonic oscillators is possible) Slater obtains the following expression for k_{∞} :

$$k_{\infty} = \nu \exp(-E_0/RT), \quad (18.37)$$

where ν is the "weighted" root mean square frequency of normal vibrations of the molecule,⁽¹¹⁾

$$\nu = (\sum \alpha_i^2 \nu_i^2 / \sum \alpha_i^2)^{1/2}. \quad (18.38)$$

Comparing (18.37) with formula (18.19) obtained from Kassel's theory, we conclude that the term A in Kassel's formula must be identical with the mean vibrational frequency of the active molecule.

The simplest form of (18.37) is obtained from (18.36) in the trivial case of a diatomic molecule, i.e. when $n' = 1$. Actually in this case k^* , which may be treated as a frequency of conversion or dissociation (Slater), will clearly be equal to the vibrational frequency ν when $E > E_0$ and equal to zero when $E < E_0$; hence moving $k^* = \nu$ outside the integral in expression (18.36) written in the form

$$k_\infty = (\nu / RT) \int_{E_0}^{\infty} \exp(-E/RT) dE$$

and carrying out the integration, we obtain (18.37). An analogous result is that for the frequently encountered unimolecular decomposition of a complex molecule dependent on the breaking of an isolated bond, the frequency expressed by the full formula (18.38) may be interpreted as the vibrational frequency of a certain diatomic molecule consisting of atoms with masses equal to the masses of the adjacent atoms of the complex molecule and with a dissociation energy equal to the energy of the broken isolated bond.

At low pressures, when $k^*/Z_0 N \gg 1$, we obtain from formula (18.34)

$$k = Z_0 N \Lambda \quad (18.39)$$

where

$$\Lambda = \int \dots \int \exp(-E/RT) \prod_1^{n'} (d\epsilon_i / kT). \quad (18.40)$$

Thus, as in the simple theory of Hinshelwood, the specific reaction rate at low pressures (or concentrations) is proportional to pressure (or concentration), i.e. the reaction follows a bimolecular law.

In Slater's theory the term Λ (18.40) is a function of the relative amplitude factors $\mu_i = \alpha_i / \alpha$ ($\alpha^2 = \sum \alpha_i^2$) the quantity $b = E_0 / RT$ and the number n' . Without giving the approximate formulae obtained by Slater we shall just indicate the results of his calculations in the particular case when all the μ_i are equal, i.e. all the amplitude factors α_i are equal, and $b = 40$;

⁽¹¹⁾ The frequency ν clearly must be less than the maximum of all the ν_i values and greater than the minimum.

for various n' the term Λ , multiplied by $\exp(E_0/RT) = 4 \times 10^{18}$, has the following values:

n'	=	1	5	9	13
$\Lambda \exp(E_0/RT)$	=	1	4×10^3	2×10^6	3.5×10^8

The effective activation energy is

$$E_{\text{eff}} = RT^2(d/dT) \ln k;$$

and from (18.39) it follows that

$$E_{\text{eff}} = E_0 - \frac{1}{2}(n' - 1)RT. \quad (18.41)$$

Comparing this formula with that obtained from Kassel's theory (18.23), we see that the formulae will be the same if we take $(n' - 1)/2 = f - 1$, i.e. $n' = 2f - 1$.

Finally, in the general case (intermediate pressures) the specific reaction rate, according to Slater, is expressed by the approximate equation

$$k = \nu \exp(-E_0/RT) J_{n'}(\vartheta) = k_\infty J_{n'}(\vartheta), \quad (18.42)$$

where

$$J_{n'}(\vartheta) = \frac{1}{\Gamma[\frac{1}{2}(n+1)]} \int_0^\infty \frac{x^{(n'-1)/2} e^{-x} dx}{1 + x^{(n'-1)/2}/\vartheta}; \quad (18.43)$$

$$\vartheta = (Z_0 N/\nu) f_{n'} b^{(n'-1)/2}; \quad (18.44)$$

$$f_{n'} = (4\pi)^{(n'-1)/2} \Gamma[\frac{1}{2}(n'+1)] \prod_1^{n'} \mu_i \quad (18.45)$$

$$(\nu^2 = \sum_1^{n'} \alpha_i^2 \nu_i^2 / \sum_1^{n'} \alpha_i^2, b = E_0/RT).$$

Slater used these formulae to calculate values of the pressure $p_{1/2}$, at which for various n' the specific reaction rate is equal to half the maximum (k_∞). Below are given values for $p_{1/2}$ (in mm Hg) calculated with the two assumptions: that $\mu_1 = \mu_2 = \dots = \mu_{n'}$, (α) and that $\mu_1 = 5\mu_{n'}$, with all the intermediate values of μ_i forming a geometric progression with μ_1 and $\mu_{n'}$, (β).

n'	3	5	7	9	11	13
(α)	9.6×10^4	4.4×10^3	330	34	4.6	0.74
(β)	2.9×10^5	1.8×10^4	2000	310	62	15

A definite temperature-dependence of the quantity $p_{1/2}$ is also obtained from the above formulae. It is apparent from formula (18.42) that the

ratio k/k_∞ for a given n' is a function of ϑ (18.44). Hence for a constant ratio $k/k_\infty = 1/2$ this quantity must be constant, i.e. in view of the fact that

$$Z_0 N \sim p T^{-1/2}$$

and

$$b^{(n-1)/2} \sim T^{-(n'-1)/2},$$

we obtain

$$p_{1/2} \sim T^{n'/2}.$$

Consequently, the higher the temperature of the experiment the greater is the pressure at which the specific reaction rate is half the maximum value (k_∞).

In the simple theory of Hinshelwood we had $p_{1/2} = \lambda k T / Z_0$ (18.9) and hence, since $\lambda = \text{const}$ and $Z_0 \sim T^{1/2}$, $p_{1/2} \sim T^{1/2}$.

Slater compared his general formula (18.42) for the specific reaction rate with the corresponding formula of Kassel and showed that both formulae lead to similar results if the quantity n' in (18.42) is taken as equal to $2f-1$. We have seen above that when $n' = 2f-1$, the values of the effective activation energy obtained in both theories are also identical. Since in both Slater's theory and in Kassel's theory n' and f denote the same quantity (the number of vibrational degrees of freedom of the active molecule) the reason for the non-correspondence of the numbers n' and f is not clear physically. In Slater's opinion a possible reason for this non-correspondence is that in Kassel's theory an activated molecule is defined as a molecule in which a critical energy E_0 is concentrated in one or several degrees of freedom whereas in Slater's theory the criterion of an activated molecule is a certain critical value of a *vibrational amplitude* which is expressed by the condition (18.28).

Slater [1146], on the basis of his theory, calculated the rate of isomerization of cyclopropane into propylene C_3H_6 and based his calculation on the assumption that the active state of the molecule arises from the proximity (as the result of vibrations) of one of the hydrogen atoms to a carbon atom in a neighbouring methylene group. The results of the calculation are in qualitative agreement with the experimental data obtained earlier by Chambers and Kistiakowsky [483]. In particular, the calculated value for the pre-exponential factor in formula (18.37) is $4 \times 10^{14} \text{ sec}^{-1}$ and the measured value is $15 \times 10^{14} \text{ sec}^{-1}$. For the further development of Slater's theory see his work [1147].

Recently Gill and Laidler [679a] have critically examined Slater's theory comparing it with Kassel's theory (applied to N_2O , H_2O_2 and others). In their opinion Slater's assumption, that the spontaneous redistribution of energy between the various degrees of freedom of the molecule is impossible, does not in some cases accord with the facts.

§19. Experimental Data

Experimental data for the most part are not sufficiently precise and are not always sufficiently reliable. On the other hand, all existing theories of unimolecular reactions also cannot lay claim to the required precision since at the basis of these theories there are assumptions which at best are only to be considered as very rough approximations to the facts. The assumption in Hinshelwood's theory is that the probability of unimolecular conversion does not depend on the energy of the active molecule; in all the other theories considered (save the statistical theory of Landau and the theory of Giddings and Eyring [675]) the assumption is that the vibrations of the active molecule are harmonic, i.e. the anharmonicity of these vibrations is disregarded. In the generally adopted form of Kassel's theory the rough approximation used is the assumption that the vibrational frequencies corresponding to all *f* oscillators are the same. The tacitly assumed retention of Maxwell-Boltzmann equilibrium in the reacting gas should be considered as an important deficiency of all the theories of unimolecular reactions.

For this reason at this stage one should talk only about a better or worse agreement between the experimental data and one or other of the existing theories and not about quantitative checking or a quantitative foundation of a theory.

Analysis of experimental data usually leads to a determination of a pressure region in which the specific reaction rate is independent of pressure i.e. to a determination of k_∞ ; this also leads to calculation of the activation energy from the temperature-dependence of k_∞ and finally to determination of the number of internal degrees of freedom taking part in the activation of the molecule from comparison of the observed temperature- or pressure-dependence of k with the dependence on these parameters obtained from one theory or another. On the basis of a survey of all the available experimental material it is possible to come to the following general conclusions with regard to these points.

The Pre-exponential Factor (A)

Representing the experimentally-determined k_∞ by formula (18.19)

$$k_\infty = A \exp(-E_0/RT)$$

and substituting in this formula the activation energy E_0 calculated from the temperature dependence we find the factor A . The values of A obtained in this way are in most cases about 10^{12} to 10^{14} sec⁻¹, i.e. of the same order as a vibrational frequency of a molecule, which is in agreement with formula (18.37). An idea of how often A is of this order is given by the following data which are taken mainly from Schumacher [1119] and

Szwarc [1200]. According to these data,⁽¹²⁾ the A factor is of the order of 10^4 in 1% of the reactions, 10^5 in 2%, 10^9 in 4%, 10^{10} in 9%, 10^{11} in 7%, 10^{12} in 12%, 10^{13} in 29%, 10^{14} in 19%, 10^{15} in 12%, 10^{16} in 3%, 10^{17} sec^{-1} in 1% (Fig. 66). In this way, the order 10^{12} to 10^{14} is observed in sixty cases out of a hundred, i.e. in the majority of cases.

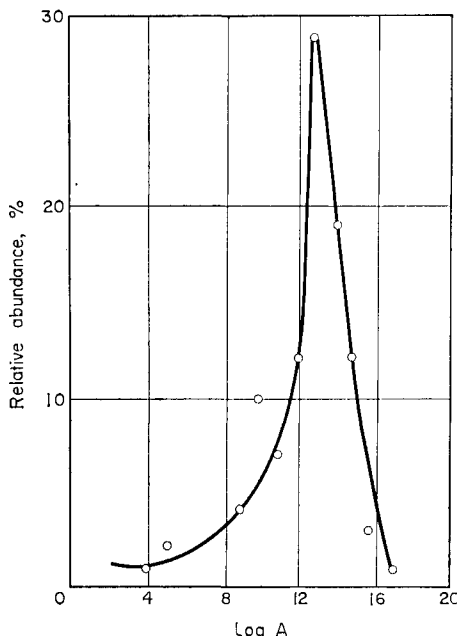
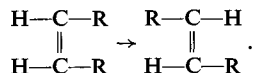


FIG. 62. The relative distribution of the pre-exponential factors A , occurring in the expression for the rate constant of unimolecular reactions $k = A \exp(-E/RT)$ according to their order of magnitude.

A value of the order of 10^{13} sec^{-1} for the pre-exponential factor is also obtained directly from formulae (18.25) and (18.37) by substituting in these formulae $\nu = \bar{\nu} = 10^{13} \text{ sec}^{-1}$, i.e. a mean frequency of an order of magnitude which is commonly observed. It should also be mentioned that

(12) Including reactions of thermal decomposition of both simple molecules, such as CH_3I , NO_2Cl , F_2O_2 , etc., and also the decomposition reactions of various complex organic substances, such as aldehydes, ketones, peroxides and others, and various reactions of isomeric conversion including *cis-trans*-conversion, i.e. conversion of the type



See also Patat [1009] and Trotman-Dickenson [1228] pp. 129-31.

formulae (18.25) and (18.37) are particular cases of the more general formula

$$k_\infty = \kappa k T h^{-1} (Z^*/Z) \exp(-E_0/RT), \quad (19.1)$$

which is obtained from formula (12.10). Assuming that in formula (19.1) the quantity Z^* is equal to $Z_{\text{trans}}^3 Z_{\text{rot}}^3 Z_{\text{vib}}^{3n-7}$, and the quantity Z is equal to $Z_{\text{trans}}^3 Z_{\text{rot}}^3 Z_{\text{vib}}^{3n-6}$, and noting that

$$Z_{\text{vib}} = \frac{\exp(-h\nu/2kT)}{1 - \exp(-h\nu/kT)},$$

we obtain for the pre-exponential factor in equation (19.1)

$$A = \frac{\kappa k T h^{-1} \exp(-2h\nu/2kT)}{1 - \exp(-h\nu/kT)} \text{ sec}^{-1}.$$

Substituting in this $T = 500^\circ\text{K}$, $\nu = 10^{13} \text{ sec}^{-1}$ and $\kappa = 1$, we obtain $A = 10^{13} \text{ sec}^{-1}$.

However this does not rule out the possibility that the partition functions of the activated complex are not of the same order as the corresponding partition functions of the inactive molecule. Since these quantities may differ either way (depending on the sign of the change in entropy of the molecule on its transition from the inactive to the active state), then it may be seen from formula (19.1) that values of A both greater and smaller than 10^{13} sec^{-1} are also possible. For example, in the study of the decomposition of azomethane it was found that $A \approx 10^{16}$. According to Glasstone, Laidler and Eyring [57], such a large value for the pre-exponential factor may be explained if it is assumed that during the activation of the azomethane molecule the entropy is increased by $10.8 \text{ cal. mole}^{-1} \text{ deg}^{-1}$.⁽¹³⁾

Other possible explanations have also been suggested to account for high pre-exponential factors A . One of the most frequently quoted explanations is based on formulae (18.13) and (18.14) which give for A

$$A = \frac{\lambda}{\Gamma(s/2)} (E_0/RT)^{s/2-1} \quad (19.3)$$

Arbitrarily assuming that λ is of the order of a vibrational frequency and noting that for sufficiently high values of s and E_0/RT the quantity

$$(E_0/RT)^{s/2-1}/\Gamma(s/2)$$

is large, then we conclude that A may be considerably greater than 10^{13} to 10^{14} sec^{-1} . Such an explanation is, however, scarcely probable, mainly

⁽¹³⁾ According to statistical mechanics, formula (19.1) may also be written

$$k_\infty = k T h^{-1} \exp[(E_0 - RT)/RT] \exp(\Delta S^*/R), \quad (19.2)$$

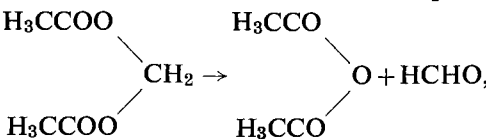
where ΔS^* is the change in entropy for the transition to the active state. Substituting in this formula $\Delta S^* = 10.8 \text{ cal mole}^{-1} \text{ deg}^{-1}$ and $T = 600^\circ\text{K}$, we obtain a value for the pre-exponential factor of $8 \times 10^{15} \text{ sec}^{-1}$, which is near 10^{16} sec^{-1} .

because of the inaccuracy of Hinshelwood's theory from which expression (19.3) is derived. We have seen that in more precise theories, which take into account the dependence of the probability of unimolecular conversion on the energy content of the active molecule, A is of the order of a molecular vibrational frequency. Moreover, the identification of λ with a vibrational frequency, with regard to formula (18.17) which is obtained from general statistical considerations, is equivalent to the statement that this quantity is equal to the maximum probability of conversion of a molecule with an infinitely large energy content, and this is not very probable.

Explanation of the causes of the considerable deviations of the pre-exponential factor A from the value 10^{12} to 10^{14} sec^{-1} is hindered also by the fact that the reaction mechanism is frequently not sufficiently clear. Thus the possibility is not ruled out that in some cases, and in particular in those reactions characterized by especially large values of A , the reaction actually follows a chain mechanism and the unimolecular law of the reaction is only apparent. Such a viewpoint was expressed by Semenov [239] who, from a survey of the mechanisms of a series of chain reactions, came to the conclusion that the overall kinetic law of a chain reaction very often corresponds to a unimolecular reaction law.

Some experimental facts may also be considered as an indication that this viewpoint is correct in certain cases. Especially it should be mentioned that a retardation is frequently observed when nitric oxide NO is added to certain decomposition reactions. A fairly prevalent view is that the action of the NO in these cases is based on coupling with the radicals first formed, i.e. the process $\text{R} + \text{NO} \rightarrow \text{RNO}$; as a result the secondary processes which follow a radical-chain mechanism accompanying the primary act of decomposition become impossible.⁽¹⁴⁾

Considerable doubts regarding the accuracy of the simple unimolecular mechanism arise from a consideration of the decomposition of methylene diacetate



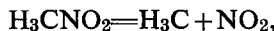
(14) It may be asserted with complete confidence that the assumed possibility of a secondary chain reaction does not hold for the reaction considered earlier of the decomposition of azomethane [1119], in spite of the fact that the actual mechanism of this reaction corresponds to the following scheme for the primary (unimolecular) act: $\text{CH}_3\text{NNCH}_3 = 2\text{CH}_3 + \text{N}_2$, i.e. a decomposition leading to the formation of two methyl CH_3 radicals.

The possibility is not excluded that the large A value (of the order of 10^{16} sec^{-1}) in this case is based on imprecision in the determination of the activation energy which was calculated from k_∞ values for only two temperatures. If it is assumed that the activation energy is equal to 45.5 kcal instead of 50 kcal, obtained in the above way, then the pre-exponential factor A takes on a normal value of the order of 10^{14} sec^{-1} .

The opinion has, however, been expressed that large values of A are characteristic of processes of decomposition into three particles [1268a].

which does not go to completion but reaches a definite equilibrium state; this is evidence of a parallel reverse reaction taking place [494].

It is also evident that there are many cases in which the decomposition follows two paths and consequently the measured reaction rate constant is a certain average value. For example, Hillenbrand and Kilpatrick [762] ascribe the large yield of formaldehyde HCHO which they obtained in the initial period of the decomposition of nitromethane H_3CNO_2 to the fact that along with simple breaking of the C—N bond, i.e. the process



there also takes place under their experimental conditions a process connected with the intramolecular rearrangement of the nitromethane which accompanies the decomposition yielding HCHO as one of its products.

TABLE 21

Kinetic data referring to isomeric cis-trans-conversions of ethylene derivatives (according to Glasstone, Laidler and Eyring [57])

Compound	Temperature °C	Pressure mm Hg	A, sec ⁻¹	<i>E</i> _{eff} , kcal
Maleic acid HC—COOH HC—COOH	140–150	Liquid phase	1.7×10^4	15.8
Dimethyl ester of maleic acid $\text{COOCH}_3\text{—CH}=\text{CH—COOCH}_3$	270–380	45–530	1.3×10^5	26.5
Dimethyl ester of methylmaleic acid $\text{COOCH}_3\text{—CH}_3\text{C}=\text{HC—COOCH}_3$	280–360	30–500	1.0×10^5	25.0
Methyl ester of cinnamic acid $\text{C}_6\text{H}_5\text{—CH=CH—COOCH}_3$	290–387	5–500	3.5×10^{10}	41.6
Nitrile of cinnamic acid $\text{C}_6\text{H}_5\text{—CH=CH—CN}$	308–378	20–450	4.0×10^{11}	46.0
Stilbene $\text{C}_6\text{H}_5\text{—CH=CH—C}_6\text{H}_5$	280–338	4–400	6.0×10^{12}	42.8
Monochlorstilbene $\text{C}_6\text{H}_5\text{—ClC=CH—C}_6\text{H}_5$	226–246	Liquid phase	1.4×10^{11}	37.0
Dichlorstilbene $\text{C}_6\text{H}_5\text{—CCl=CCl—C}_6\text{H}_5$	175–196	Liquid phase	9.9×10^{10}	34.1

It is apparently simpler to decide the cause of deviations of the pre-exponential factor from the normal value of 10^{12} to 10^{14} sec⁻¹ towards low values. When the deviations are large, it is doubtlessly connected with

the non-adiabatic character of the reactions; this was shown by Magee, Shand and Eyring [901] for the isomeric *cis-trans*-conversions of ethylene derivatives. The relevant data are shown in Table 21.

It is clear from Table 21 that these reactions fall into two groups: those characterized by a very low pre-exponential factor A (of the order of 10^4 to 10^5 sec $^{-1}$) and a relatively low activation energy, and those with A closer to 10^{13} sec $^{-1}$ and with a high activation energy⁽¹⁵⁾. Magee, Shand and Eyring [901] give the following interpretation of these data.

It has been shown above (§14, pp. 243-244) that the conversion of a molecule of an ethylene derivative from the *cis*- to the *trans*-isomer, which

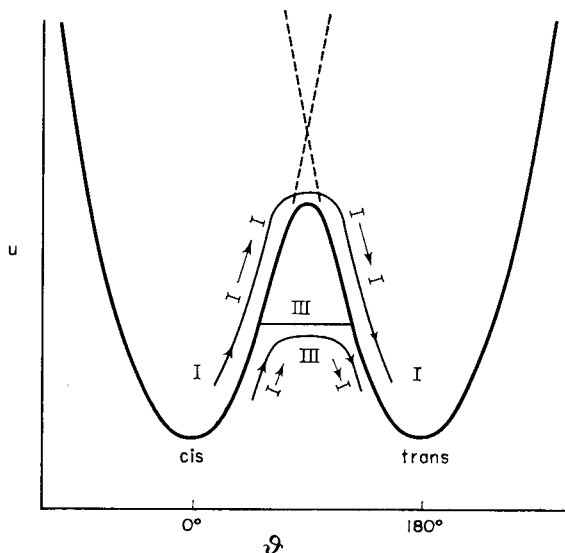


FIG. 63. The two reaction paths for the *cis-trans*-isomerization: without involving a multiplicity change (I \rightarrow I) and involving a change in multiplicity (I \rightarrow III \rightarrow I).

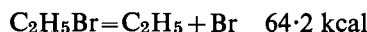
consists of rotating one part of the molecule 180° with respect to the other part about the C=C bond, is possible in two ways: (i) without involving a multiplicity change, i.e. the direct transition from the singlet ground state of the *cis*-isomer to another singlet state (the ground state of the *trans*-isomer), and (ii) involving a change in multiplicity, i.e. the transition to the intermediate triplet state which is nearest the main excited state of the substituted ethylene molecule (and also of ethylene itself). Both these reaction paths (I \rightarrow I and I \rightarrow III \rightarrow I) are shown in Fig. 63 in which θ ,

(15) To these data should be added the more recent kinetic data [550] for the *cis-trans*-isomerization of dideutero-ethylene DHC=CHD: 450 to 550°C , $p = 9$ mm Hg, $A = 10^{13}$ sec $^{-1}$, $E = 65$ kcal. See also Trotman-Dickenson [1228 p. 138, Table 3.9]. For the *cis-trans*-isomerization of HCIC=CCIH see [1051a].

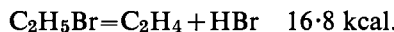
the angle of rotation, is plotted along the abscissa and the potential energy of the molecule along the ordinate. The reaction path $I \rightarrow I$ which is characterized by the higher potential barrier (large E_{eff}) and a larger transmission coefficient (large A) belongs to the second group of reactions shown in Table 21. The second path $I \rightarrow III \rightarrow I$ belongs to the group consisting of the first three reactions and their characteristic low A value is based on a low probability of intercombinations $I \rightarrow III$ and $III \rightarrow I$ (low transmission coefficient).

The Activation Energy of Unimolecular Reactions

According to formula (18.19) the activation energy for unimolecular conversion may be calculated from the temperature-dependence of the maximum specific reaction rate k_∞ . It follows from the vast amount of relevant experimental material that all unimolecular conversion processes may be divided into two classes depending on the relationship between the activation energy and the heat of reaction. One class includes processes with an activation energy different from their heat of reaction. This includes, in particular, *cis-trans*-isomerizations which have an activation energy of some tens of kilocalories per mole (see Table 21) with a heat of reaction of a few kilocalories per mole. A good example of this type of unimolecular reaction is the decomposition of nitrous oxide N_2O which follows the scheme $N_2O = N_2 + O$ and has an activation energy of about 60 kcal and a heat of 38.7 kcal. Another example is the decomposition reaction of ethyl bromide C_2H_5Br [293]; the activation energy of this reaction is 53.7 kcal and the heats of reaction for the two possible decomposition processes are:



and



Comparison of these thermal effects with the activation energy shows that the C_2H_5Br molecule decomposes into saturated molecules and not into radicals. A direct indication of the accuracy of this conclusion is given by the absence of radicals in the thermal decomposition zone of C_2H_5Br (at 506 to 614°C), which was directly established using the toluene method (see p. 79).

This class of reactions also includes the decomposition of the dichloropropanes $C_3H_6Cl = C_3H_5Cl + HCl$ [786] and also the decomposition of secondary propyl and butyl bromides $(CH_3)_2CHBr$ and $C_2H_5CH_3CHBr$, tertiary butyl bromide $(CH_3)_3CBr$ and cyclohexyl bromide $C_6H_{11}Br$ [698]. The molecular (and not radical) character of the decomposition of these bromides follows from the fact that in all these cases the activation energy

is less than the energy required to break the C—Br bond, and also from the absence of an inhibiting action by cyclohexene C_6H_{10} which would suppress the chain reaction which would arise if the initial molecule decomposed according to a radical mechanism.

However, there are cases in which the activation energy is less than the energy required to break one of the bonds and yet the molecule decomposes into radicals. For example, in the decomposition of the peroxide CH_3COOOH , the CH_3COO radical is unstable and decarboxylates simultaneously with the decomposition process of the initial peroxide according to the scheme



These decompositions have recently been surveyed theoretically [1201a].

The other class of unimolecular reactions consists of reactions with an activation energy equal to the heat of reaction (if we neglect the small rotational barrier due to change in the potential energy of the molecule as a result of its rotation, see above p. 190 *et seq.*). This class includes the thermal decomposition of many substances into free radicals. Table 22 shows some of the relevant data.

It is clear from Table 22 that within experimental error the activation energy and the corresponding bond dissociation energy are equal, so that the activation energy is equal to the heat of reaction, i.e. the "true" activation energy is zero. The radical nature of the decomposition in the examples of Table 22 was also established by using the toluene method. The equivalence of the activation energy and heat of reaction in reactions of this class makes it possible to measure directly the bond dissociation energy by determining the activation energy of the corresponding unimolecular decomposition reactions. This method has been used widely in thermochemistry.

Along with decomposition into monoradicals, cases of biradical decomposition of molecules fall to the same class, for example, the decomposition of ketene molecules (CH_2CO) into CO and the CH_2 biradical. In studying the thermal decomposition of $CHCl_3$ and $CDCl_3$ Shilov and Sabirova [(E. A. Shilov, R. D. Sabirova, *Dokl. Akad. Nauk SSSR* **114**, 1058 (1957)] have found recently that the decomposition of these molecules proceeds by the scheme $CHCl_3 = CCl_2 + HCl$. The rate constant of this process was found to be

$$k = 2.6 \times 10^{11} \exp(-47000/RT) \text{ sec}^{-1}.$$

The decomposition of alkyl nitrates $RONO$ (with R an alkyl radical) will also be considered here.⁽¹⁶⁾

⁽¹⁶⁾ And also peroxides, for example the decomposition of propionyl peroxide [1060].

TABLE 22

The activation energies for the thermal decomposition of various substances and the corresponding bond dissociation energies [1200].

Compound	E, kcal	Bond broken	Bond energy, kcal	The data from which the bond energy is calculated
Ethyl iodide	51.5	$\text{C}_2\text{H}_5-\text{I}$	50.2 ± 1	$\text{C}_2\text{H}_5-\text{H}$ bond energy and heats of formation.
Allyl chloride	59.3 [294]	$\text{C}_3\text{H}_5-\text{Cl}$	58 ± 2	Heats of formation.
Ethyl benzene	63 ± 1.5	$\text{C}_6\text{H}_5\text{CH}_2-\text{CH}_3$	62.3 ± 2.3	$\text{C}_6\text{H}_5\text{CH}_2-\text{H}$ and CH_3-H bond energies and heats of formation.
Benzyl bromide	50.5 ± 2	$\text{C}_6\text{H}_5\text{CH}_2-\text{Br}$	48.5 ± 4	$\text{C}_6\text{H}_5\text{CH}_2-\text{H}$ bond energy and a calorimetrically determined difference of the bond energies $\text{Br}-\text{CH}_2\text{C}_6\text{H}_5$ and $\text{H}-\text{CH}_2\text{C}_6\text{H}_5$.
Diacetyl	60	$\text{CH}_3\text{CO}-\text{COCH}_3$	58	$\text{C}_6\text{H}_5\text{CH}_2-\text{COCH}_3$ bond energy and heats of formation.
Propene	78	$\text{CH}_2\text{CHCH}_2-\text{H}$	77	Activation energy for the decomposition of 1-butene $\text{CH}_2\text{CHCH}_2\text{CH}_3$ and heats of formation.

The activation energies for the unimolecular decomposition of the simplest representatives of this class of compounds were determined by Steacie and his coworkers [1169]. The following values were obtained: 36.4 (CH_3ONO), 37.7 ($\text{C}_2\text{H}_5\text{ONO}$), 37.6 ($n\text{-C}_3\text{H}_7\text{ONO}$),⁽¹⁷⁾ 37.0 (iso- $\text{C}_3\text{H}_7\text{ONO}$) and 36.0 ($n\text{-C}_4\text{H}_9\text{ONO}$)⁽¹⁸⁾ kcal. In these cases the radical nature of the decomposition was not established directly, but the close agreement of the activation energies for all these compounds makes it extremely likely that the same bond, namely the O—NO bond, is broken in each case. For this reason the energy required to break this bond, i.e. the heat of the reaction $\text{RONO}=\text{RO}+\text{NO}$, is on average about 37 kcal.

It should be pointed out, however, that the reaction mechanism does not consist entirely of this process. Thus it can be seen from the composition of the thermal decomposition products of alkyl nitrites that this type of

⁽¹⁷⁾ 34.7 kcal according to the measurements of Nagiev and coworkers [197].

⁽¹⁸⁾ 36.2 kcal according to the measurements of Nagiev and coworkers [197].

initial stage of the reaction is followed by a series of processes in which RO radicals take part in addition to the initial nitrite and also, apparently, hydrogen atoms which are formed as a result of unimolecular decomposition of RO radicals into the corresponding aldehyde and an H atom. The occurrence of secondary processes following the primary process is a distinctive feature of decompositions proceeding by a radical mechanism.⁽²⁰⁾ Very often the complex nature of the overall reaction is evident from the overall law. For example, the kinetic reaction law for the thermal decomposition of di-iodo-ethane $C_2H_4I_2$ [325] and of secondary butyl iodide C_4H_9I [990] for a definite range of pressure and temperature is expressed by the equations

$$-(d/dt)(C_2H_4I_2) = k_1(C_2H_4I_2) + k_2(C_2H_4I_2)(I_2)^{1/2}$$

and

$$-(d/dt)(C_4H_9I) = k_1(C_4H_9I) + k_2(C_4H_9I)(I_2)^{1/2}$$

respectively. In these equations the first term expresses the rate of the strictly unimolecular process of decomposition of the iodide, i.e. the rate of the process $C_2H_4I_2 = C_2H_4I + I$ and of the process $C_4H_9I = C_4H_9 + I$, respectively; the second term expresses the rate of the secondary process of bimolecular interaction, with the initial iodide, of iodine atoms which are formed in the primary process and also in the dissociation of I_2 . In the decomposition of di-iodo-ethane the interaction of I atoms with $C_2H_4I_2$, corresponding to the second term, is a chain process (see Chap. 9). A more complex kinetic law has been established for the thermal decomposition of dimethyl ether CH_3OCH_3 in accordance with the more complex chain mechanism of this reaction [380].

An indication of a complex mechanism for a unimolecular reaction is the presence of a point of inflection on the $k-p$ curve which would not be observed with a simple reaction mechanism; the presence of this point of inflection has been established in several cases [1191, 808].

The characteristic sequence of energy changes in the two classes of unimolecular reactions is represented schematically in Fig. 64 (a and b). A modification of transition-state theory as applied to the second class of reactions (Fig. 64b) has been proposed by Szwarc [1200].

Rate of Reaction at Low Pressures

So far we have considered the results of investigations on unimolecular reactions at high pressures when the specific reaction rate has a constant value k_∞ . According to the above theories and experimental data, on lowering the pressure from a certain value p the specific reaction rate decreases and at low pressures is proportional to the pressure. The range of pressure

⁽²⁰⁾ Alkyl nitrites $RONO$ and also alkyl nitrates $RONO_2$ apparently decompose according to a chain mechanism; see, for example, [697].

in which the specific reaction rate is dependent on pressure is determined by the kinetic features of the reaction and the properties of the substance being converted. In accordance with the above theories (p. 301) the greater the number of degrees of freedom of the active molecule taking part in its activation, then, as a rule, the lower is the pressure range in which k is observed to be dependent on p . Hence the fewer the atoms in the molecule of the substance being converted, the higher is this pressure range.

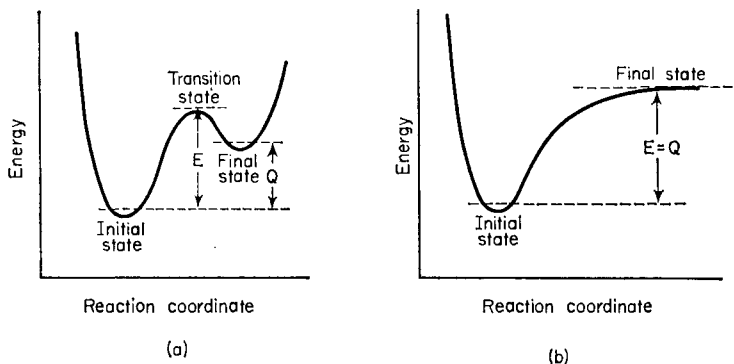


FIG. 64. The path of the unimolecular reaction when (a) $E > Q$, and (b) $E = Q$.

An extreme case of reaction with a constant specific rate (k_{∞}) region of very high pressure is the decomposition of nitrous oxide N_2O . Investigation of the kinetics of this reaction shows that the specific reaction rate is not constant even at as high a pressure as 40 atm. From detailed analysis of all the available experimental data on the thermal decomposition of nitrous oxide, H. S. Johnston [802] comes to the conclusion that the dependence of the specific rate of this reaction on pressure for the complete pressure range studied (14 mm Hg to 40 atm) may be described using a formula of the form of (18.21) with a number of oscillators $f=4$; however for this it is necessary to assume that the energy-dependence of the decomposition probability is somewhat different from the dependence expressed by formula (18.17).⁽²⁰⁾ Johnston comes to the conclusion, which is also supported by his later work [808, 803], that, in spite of the fact that some fifteen investigations have been devoted to the decomposition of nitrous oxide N_2O , further studies are required in order to complete the quantitative analysis of the kinetics of this reaction. However the mechanism

⁽²⁰⁾ Johnston does not give the analytical dependence of k on the energy of the active molecule but cites only the calculated values of k which correspond to energies in excess of the critical energy E_0 .

of this reaction should be considered to be sufficiently well established as the sum of the following elementary processes:⁽²¹⁾



In particular, it has been shown [634] by use of the method of labelled atoms (N^{15}) that the reaction mechanism, assumed earlier by Pease [1019], in which a basic role is played by the decomposition of an N_2O molecule into NO and an N atom, is incorrect.⁽²²⁾

The need for careful study of the kinetics of unimolecular reactions and for a cautious approach in interpreting experimental facts is particularly well illustrated by the decomposition of nitrogen pentoxide N_2O_5 . This reaction was the first known homogeneous unimolecular reaction, and has a series of anomalies which for a long time resisted theoretical interpretation. One of the anomalies is that the specific reaction rate is independent of N_2O_5 pressure down to pressures as low as about 0.1 mm Hg. Since the homogeneous character of this reaction was established (Daniels and E. H. Johnston [524]), more than twenty studies have been devoted to it and only relatively recently has the cause of its anomalous behaviour been discovered. Ogg [987] proposed a mechanism for the thermal decomposition of nitrogen pentoxide which begins with the unimolecular decomposition of N_2O_5 according to the scheme $\text{N}_2\text{O}_5 \rightarrow \text{NO}_3 + \text{NO}_2$ and is followed by a series of bimolecular processes (a similar mechanism was proposed by Smith and Daniels [1151] for the thermal decomposition of N_2O_5 in the presence of NO). This mechanism was supported by the later work of Mills and H. S. Johnston [953], indicating that the constant for the unimolecular decomposition at low pressures is only *apparent* and is

(21) The mechanism of this reaction does not consist entirely of these processes. For example, it is necessary to assume the presence of the process $\text{NO} + \text{O} \rightarrow \text{NO}_2$, with which is connected the yellow-green glow observed in the thermal decomposition of nitrous oxide [822]. However, this process and also process (4) seem to play only a secondary role in the mechanism of the reaction.

(22) An indirect indication that the primary chemical process here is the decomposition of the nitrous oxide molecule into N_2 and O is given by the kinetic data obtained from a study of the oxidation of gaseous sulphur dioxide SO_2 with nitrous oxide; here this process appears to play an important role [674].

The presence of the reverse reaction, i.e. the process $\text{N}_2 + \text{O} \rightarrow \text{N}_2\text{O}$, has recently been indicated. According to Harteck and Dondes [725] this reaction is the basis of the formation of nitrous oxide in a mixture of nitrogen and ozone at 295°C.

in fact the product of the equilibrium constant for



and the rate constant for the bimolecular process



this explains why the "rate constant" of the unimolecular decomposition of N_2O_5 remains unchanged at low pressures. Mills and Johnston showed that other anomalies of the thermal decomposition of N_2O_5 may also be explained on the basis of the assumed reaction mechanism. This reaction has received further study [804, 1299, 773, 821].

While the decomposition of relatively simple molecules, such as the triatomic molecule of nitrous oxide with its four vibrational degrees of freedom, has a pressure-dependent specific reaction rate up to 40 atm,⁽²³⁾ with an increase of the number of atoms in the molecule and with a corresponding increase in the number of vibrational degrees of freedom the pressure range in which the specific reaction rate does not depend on pressure is shifted further and further to the low-pressure side. Since the degree of participation of individual vibrational degrees of freedom in the activation of a molecule is determined by the structural characteristics of the molecule and its dynamics, a well-defined monotonic dependence of the number of degrees of freedom taking part in the activation on the number of atoms in the molecule (or on the total number of vibrational degrees of freedom of the molecule) should only be expected in a series of structurally similar molecules, especially in homologous series. The same might also be said with regard to the dependence of the position of the region, in which the specific reaction rate does not depend on pressure, on the number of atoms in the molecule. The corresponding data are given in Table 23.

In this table p represents the pressure below which the specific reaction rate becomes pressure-dependent; $p_{1/2}$ denotes the pressure at which the specific reaction rate is equal to half the maximum rate (k_∞); f denotes the number of oscillators or vibrational degrees of freedom taking part in the activation of the molecule calculated from the observed pressure-dependence of k using either formula (18.21) or (18.20). It is clear from Table 23 that in each homologous group the pressure p decreases regularly with increase in f , which increases with the total number of vibrational degrees of freedom of the molecule. We see that with the exception of fluorine dioxide F_2O_2 , in the activation of which all the vibrational degrees of freedom take part, only part of the total number of vibrational degrees of freedom is used in each case (in the case of $\text{C}_2\text{H}_5\text{I}$ —one half, and in the others—three-quarters

⁽²³⁾ The decomposition of F_2O (3 vibrational degrees of freedom) strictly follows a bimolecular law even at 800 mm Hg (250 to 270°C) [851].

TABLE 23

*The position of the region in which the specific rate of the unimolecular reaction is constant and the number of vibrational degrees of freedom taking part in the activation**

Compound	T°C	p mm Hg	$p_{1/2}$ mm Hg	f	$3n - 6$
F ₂ O ₂	-37.1	1000	10	6	6
CH ₃ I	300	50	25	7	9
C ₂ H ₅ I	300	10	11	9	18
CH ₃ ONO	211.2	50	—	12	15
C ₂ H ₅ ONO	221.5	10	—	19	24
n-C ₃ H ₇ ONO	210.5	0.5	—	26	33
CH ₃ NNCH ₃	290	300	5	18	24
CH ₃ NNC ₃ H ₇	285	30	—	32	42
C ₃ H ₇ NNC ₃ H ₇	290	1	—	46	60
CH ₃ N ₃	240	100	6	13	15
C ₂ H ₅ N ₃	239.6	20	0.5	14	24

* For literature see Schumacher [1119].

to four-fifths). The difference between $3n - 6$, the total number of vibrational degrees of freedom, and f for azo-compounds and alkyl nitrites is equal to the number of C—H bonds in the molecule of the appropriate compound. Kassel [106] noted that for azo-compounds this regularity is possibly explained by the fact that vibrations with the relatively high frequency corresponding to that of a C—H bond do not take part in activation (at the temperature of the experiments). Such an explanation is quite probable although it should be mentioned that in other cases shown in Table 23 this regularity is not observed. Another feature which was noted by Leermakers [867] is that f is close to three times the number of heavy atoms in a molecule of the substance being converted. Thus this feature ignores the participation of the vibrations of H atoms in activation. However this regularity and that noted by Kassel hold only in individual cases. Thus of the eleven substances shown in Table 23, only five (CH₃I, C₂H₅I, CH₃ONO, CH₃N₃ and C₂H₅N₃) satisfy the regularity noted by Leermakers.

It should be noted that the data of Table 23 for each homologous group are in qualitative agreement with the results of Slater's calculations shown on p. 301.

Influence of Admixtures

So far we have considered unimolecular reactions taking place in the absence of foreign admixtures. Since activation and deactivation by collision play a very important role in the course of a unimolecular reaction, the

action of admixtures should mainly be evident in these processes. Expressing the rates of activation and deactivation by collision with molecules of the admixture as $Z_x^0 N_x N_t$ and $Z_x^0 N_x n_t$ (N_x is the concentration of admixture), then from the steady-state condition we obtain the following expression for the concentration of active molecules (compare the similar formula on p. 284)

$$n_t = \frac{(Z^0 N + Z_x^0 N_x) N_t}{Z^0 N + Z_x^0 N_x + k_t},$$

from which we find the specific reaction rate k_x :

$$k_x = - \frac{1}{N} \frac{dN}{dt} = \frac{1}{N} \sum \frac{k_t N_t (Z^0 N + Z_x^0 N_x)}{Z^0 N + Z_x^0 N_x + k_t}. \quad (19.4)$$

Further, assuming the approximate applicability of Hinshelwood's theory (see p. 286 *et seq.*) and accordingly setting $k_t = \lambda = \text{const}$, we may rewrite expression (19.4) as

$$k_x = k_\infty \frac{Z^0 N + Z_x^0 N_x}{Z^0 N + Z_x^0 N_x + \lambda}, \quad (19.5)$$

where $k_\infty = \lambda \Sigma (N_t/N)$ (18.4), the specific reaction rate at sufficiently high concentrations of N and N_x (or the corresponding pressures), where $Z^0 N + Z_x^0 N_x \gg \lambda$. In this way the specific reaction rate tends to the limit k_∞ in the presence of an inert admixture, as in the absence of an admixture.

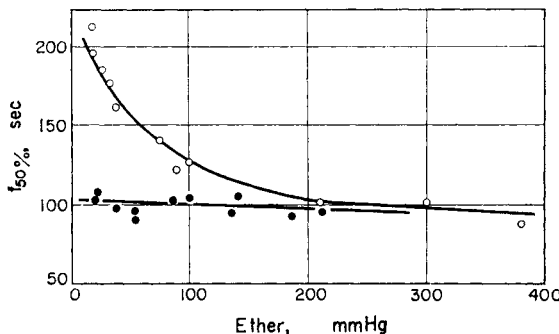


FIG. 65. The decomposition of ethyl ether $C_2H_5OC_2H_5$. The time for 50 per cent decomposition is shown as a function of ether vapour pressure; the circles refer to experiments without hydrogen and the dots refer to experiments with 400 mm Hg pressure of H_2 admixture (according to Hinshelwood and Staveley [765]).

We shall now consider cases when $Z^0 N = \lambda$ but owing to a considerable excess of admixture $Z_x^0 N_x \gg \lambda$. In the case when there is no admixture present, it is clear from formulae (19.5) and (18.8) that the specific reaction rate is equal to half the maximum rate, $k = k_\infty/2$. However it follows from (19.5) that in the presence of admixture $k_x = k_\infty$, i.e. the specific rate is

constant. As an illustration Fig. 65 shows data for the decomposition of ethyl ether [765]. It is clear from this figure that in the absence of hydrogen the time $t_{50\%}$ begins to increase markedly with lowering of the ether vapour pressure below approximately 200 mm Hg; in the presence of hydrogen admixture $t_{50\%}$ does not vary even at very low ether vapour pressures. The difference in the pressure-dependence of $t_{50\%}$ in these two cases is easily explained on the basis of formula (19.5).

By integrating the equation

$$-\frac{dN}{dt} = k_x N = k_\infty \frac{Z^0 N + Z_x^0 N_x}{Z^0 N + Z_x^0 N_x + \lambda} N$$

with the initial condition $N = N_0$ when $t = 0$, we find for the time of 50 per cent conversion ($N/N_0 = 1/2$)

$$t_{50\%} = \frac{1}{k_\infty} \left(\ln 2 + \frac{\lambda}{Z_x^0 N_0} \ln \frac{2Z_x^0 N_x + Z^0 N_0}{Z_x^0 N_x + Z^0 N_0} \right). \quad (19.6)$$

When $Z_x^0 N_x = 0$ this expression becomes

$$t_{50\%} = \frac{1}{k_\infty} \left(\ln 2 + \frac{\lambda}{Z^0 N_0} \right), \quad (19.7)$$

and hence when $Z^0 N_0$ is close to λ or considerably less than λ , $t_{50\%}$ deviates from the constant value of $(\ln 2)/k_\infty$ and increases (according to a hyperbolic law) on lowering the initial concentration N_0 (or the initial pressure). The curve of $t_{50\%}$ against p in Fig. 65 has precisely this form in the absence of hydrogen.

If it is assumed that when $Z_x^0 N_x \neq 0$, $Z_x^0 N_x \gg N_0 Z^0 \approx \lambda$, then we obtain from formula (19.6)

$$t_{50\%} = (\ln 2)/k_\infty, \quad (19.8)$$

i.e. $t_{50\%}$ is constant; and this is actually observed in the presence of hydrogen (Fig. 65).

It is interesting to note that a deuterium D_2 admixture has a much weaker action on the decomposition of ether than that of hydrogen H_2 ; thus the latter has a specific action in this reaction but the reason for this specificity is not clear.⁽²⁴⁾

(24) It should be mentioned that the thermal decomposition of dimethyl ether $(CH_3)_2O$ takes place at a rate proportional to the concentration of ether to the power 3/2, so that the reaction is not kinetically unimolecular. Study shows that this reaction has a fairly complex chain mechanism according to which the chains are initiated by the unimolecular process $CH_3OCH_3 \rightarrow CH_3 + CH_3O$ and are terminated as a result of the process $2CH_3 \rightarrow C_2H_6$ [380]. An accelerating action has been established for hydrogen and deuterium and is based on a process of "chain transmission"



which is practically identical for H_2 and D_2 .

According to reference [628a] the thermal decomposition of $(C_2H_5)_2O$ also follows a chain mechanism.

The efficiency of the activating and deactivating action of various gases may be calculated quantitatively. Let the specific reaction rate for a certain concentration of pure substance undergoing unimolecular conversion be

$$k = k_\infty \frac{Z^0 N}{Z^0 N + \lambda}.$$

Increasing the concentration of this substance by a quantity ΔN we obtain a specific rate

$$k + \Delta k = k_\infty \frac{Z^0 N + Z^0 \Delta N}{Z^0 N + Z^0 \Delta N + \lambda}.$$

However the same increase in the specific rate may be obtained by adding a foreign gas with a concentration determined by the condition

$$k_x = k + \Delta k = k_\infty \frac{Z^0 N + Z_x^0 N_x}{Z^0 N + Z_x^0 N_x + \lambda}.$$

We find from the two last formulae that $Z^0 \Delta N = Z_x^0 N_x$, or replacing concentrations by pressures, $Z^0 \Delta p = Z_x^0 p_x$. The ratio $\Delta p/p_x$ may also be used as a measure of the relative efficiency of a given admixture (with regard to pressure), namely

$$\gamma_p = \Delta p/p_x = Z_x^0/Z^0. \quad (19.9)$$

If we express Z^0 and Z_x^0 by the formulae

$$Z^0 = 2Pd^2(\pi RT/M)^{1/2}$$

and

$$Z_x^0 = P_x(d + d_x)^2 \left[\frac{\pi RT(M + M_x)}{2MM_x} \right]^{1/2}, \quad (19.10)$$

where P and P_x are the steric factors characterizing the efficiency of collisions, d and d_x are the molecular diameters, M and M_x are molecular weights, then we obtain from (19.9)

$$\gamma = P_x/P = 2\gamma_p \left(\frac{d}{d + d_x} \right)^2 \left(\frac{2M_x}{M + M_x} \right)^{1/2} \quad (19.11)$$

which may be called the relative efficiency per collision. To calculate γ using formula (19.11) from a relative efficiency with regard to pressure (γ_p), which is determined directly by experiment, it is necessary to know the gas-kinetic diameters of the molecules of the substance being converted and of the foreign admixture. However this calculation is based on the formulae from Hinshelwood's theory and assumes the approximate applicability of that theory. Examples of calculations of γ will be given in the following chapter.

Active Admixtures

Active admixtures are those which interact chemically with either the substance being converted or its decomposition products. Naturally the chemical action of active admixtures cannot be completely explained by a theory of strictly unimolecular reactions, and each particular case should be considered separately. In this connection we shall only mention that such admixtures may either be added deliberately or may be contaminants in the system.

Admixtures which interact directly with the initial substance superimpose on the unimolecular process of independent conversion of this substance another primary process, namely its bimolecular interaction with molecules or atoms of the admixture; this leads to a change in the kinetic law of the reaction and in particular may practically suppress the unimolecular reaction law. Admixtures which interact with the decomposition products of the initial substance may also change the kinetic reaction law, but only in those cases when the primary process of decomposition of the initial substance ceases to be the limiting process. Usually this process is the limiting one even in the presence of admixtures.

A particularly clear example of the action of active admixtures determining the kinetics of a reaction is the thermal decomposition of nitrous oxide in the presence of iodine and bromine. According to the measurements of Volmer and Bogdan [1256], in the presence of these substances the reaction satisfies the equation

$$-(d/dt)(N_2O) = k(N_2O)(X_2)^{1/2},$$

where (X_2) is the concentration of halogen; the reaction rate is on average 250 times greater than the decomposition rate of pure N_2O . It is interesting that the halogen is not consumed in this reaction, and its action must clearly be considered as purely catalytic. The products of both the catalytic reaction and the decomposition of pure N_2O are N_2 and O_2 .

The catalytic decomposition of nitrous oxide in the presence of bromine, chlorine and isopropyl iodide $(CH_3)_2CHI$ was studied earlier by Musgrave and Hinshelwood [965] and recently (in the presence of chlorine, bromine, iodine and ethyl iodide) by Kaufman, Gerri and Pascale [823]. The last-named authors measured the rate constants and activation energies for the bimolecular reactions of Cl, Br and I atoms with an N_2O molecule (see also [381]).

An example of the interaction of an admixture with decomposition products is the effect of nitric oxide on the unimolecular decomposition of ethers which has been studied by Hinshelwood and his coworkers. According to Hinshelwood and his coworkers [1168], nitric oxide, while not affecting the primary process of decomposition of the ether molecule,

interacts with the radicals formed in this process and as a result they are eliminated from the reaction (the nitric oxide is also consumed).⁽²⁵⁾ This explains the retardation of ether decomposition in the presence of NO, since the radicals formed in the ether decomposition are able to enter into a secondary reaction with the ether which leads to its decomposition.

Active admixtures may also arise as a result of the unimolecular reaction process itself; this takes place when the products of the primary decomposition of the molecules of the initial substances enter into chemical reaction with these molecules. A suitable example is the decomposition of di-iodoethane (p. 312) which has a rate determined both by the rate of the primary unimolecular decomposition of the $C_2H_4I_2$ molecule according to the scheme $C_2H_4I_2 = C_2H_4I + I$ and by the rate of the bimolecular interaction of $C_2H_4I_2$ molecules with iodine atoms $C_2H_4I_2 + I = C_2H_4I + I_2$. Here the iodine atoms are formed as a result of the primary decomposition of $C_2H_4I_2$ and also by thermal dissociation of iodine molecules.

In the foregoing example the decomposition product accelerates the reaction. An example of the inhibiting action of reaction products is the action of nitrogen dioxide NO_2 , formed in the unimolecular decomposition of nitric acid HNO_3 , on the rate of this reaction [806]. In this case the inhibiting action of NO_2 is apparently connected with the reaction $NO_2 + OH = HNO_3$, which is the reverse of the primary decomposition of the HNO_3 molecule.

§20. Termolecular Reactions

Known types of termolecular reactions in the gas phase are exchange reactions, in particular isotopic exchange reactions and reactions of recombination and addition to a multiple bond which follow a mechanism of collision stabilization (see §15). As in the case of bimolecular reactions, termolecular reactions may be considered from the standpoint of the gas-kinetic collision theory and from that of the activated complex method. The difference between termolecular exchange reactions and reactions of recombination and addition is that whereas in the first all *three* colliding particles form an activated reaction complex and take part in the chemical conversion (consisting of the redistribution of bonds or the redistribution

⁽²⁵⁾ Bryce and Ingold [462] have shown that the primary product of the interaction of CH_3 with NO is CH_3NO . They found that over the temperature range 480–900°C, for a pressure of 10 mm Hg, the mean efficiency of this reaction per binary collision is 3.9×10^{-4} to 3.4×10^{-4} . This does not exclude the possibility that the reaction actually takes place via ternary collisions.

It follows from the experiments of these authors that for sufficiently high contact times the reaction of CH_3 with NO yields a large number of other products along with CH_3NO . Thus it may be concluded that, depending on the experimental conditions, the action of NO is not always a simple coupling of radicals as was initially proposed by Hinshelwood. See also [1065].

of atoms and atomic groups), in recombination and addition reactions only *two* particles take part; the third particle serves to remove energy from the quasimolecule stabilized by it and does not change its chemical individuality as a result of the reaction. We shall begin our survey of termolecular reactions with exchange reactions.

Number of Ternary Collisions

On the basis of the gas-kinetic theory of binary collisions it is not difficult to find the number of ternary collisions in unit volume per unit time. The calculation may be carried out in the following way, according to Steiner [1177]. First it is necessary to find the number of unstable binary complexes formed in unit volume per unit time as the result of a collision of two molecules; then the number of collisions of these binary complexes with a third molecule is calculated (also per unit time).

We shall consider ternary collisions between the molecules A, B and C with masses m_A , m_B and m_C . We shall represent the number of binary collisions leading to the formation of binary complexes (quasi-molecules) A.B, B.C and A.C by $Z_{A,B}$, $Z_{B,C}$ and $Z_{A,C}$ respectively, so that $Z_{A,B} = Z_{A,B}^0 n_A n_B$ and so on, where, according to formula (9.15),

$$Z_{A,B}^0 = \sigma_{A,B} (8kT/\pi\mu_{A,B})^{1/2},$$

$\sigma_{A,B} = \pi(r_A + r_B)^2$ and $\mu_{AB} = M_A M_B / (M_A + M_B)$ (r_A and r_B are the molecular radii of A and B).

Let the mean lifetime of these complexes be $\tau_{A,B}$, $\tau_{B,C}$ and $\tau_{A,C}$ respectively. With the equilibrium condition for the complex A.B with concentration $n_{A,B}$, we have

$$(d/dt)n_{A,B} = Z_{A,B}^0 \tau_{A,B} n_A n_B - n_{A,B} / \tau_{A,B} = 0.$$

Corresponding equations hold for the complexes B.C and A.C. Thus from the conditions for equilibrium we obtain

$$n_{A,B} = Z_{A,B}^0 \tau_{A,B} n_A n_B,$$

$$n_{B,C} = Z_{B,C}^0 \tau_{B,C} n_B n_C,$$

and

$$n_{A,C} = Z_{A,C}^0 \tau_{A,C} n_A n_C.$$

The number of binary collisions of complexes of each type with a third molecule is

$$A \cdot B + C: Z_{A,B,C}^0 n_{A,B} n_C,$$

$$B \cdot C + A: Z_{B,C,A}^0 n_{B,C} n_A,$$

$$A \cdot C + B: Z_{A,C,B}^0 n_{A,C} n_B$$

per unit time. Here

$$Z_{A,B,C}^0 = \sigma_{A,B,C} \left(\frac{8kT}{\pi\mu_{A,B,C}} \right)^{1/2}.$$

$Z_{B,C,A}^0$ and $Z_{A,C,B}^0$ have similar expressions. The quantities $\sigma_{A,B,C}$ and $\mu_{A,B,C}$ and so on in these equations are $\sigma_{A,B,C} = \pi(r_{A,B} + r_C)^2$,

$$\mu_{A,B,C} = [(m_A + m_B)m_C / (m_A + m_B + m_C)]$$

and so on, where $r_{A,B}$ is the radius of the complex A.B. From these equations we have for the number of ternary collisions in unit volume per unit time

$$Z_3 = Z_{A,B,C}^0 n_A n_B n_C + Z_{B,C,A}^0 n_B n_C n_A + Z_{A,C,B}^0 n_A n_C n_B.$$

By substituting the equilibrium concentrations of the complexes A.B, B.C and A.C in this, we find

$$Z_3 = 8\pi k T \left(\frac{m_A + m_B + m_C}{m_A m_B m_C} \right)^{1/2} \{ (r_A + r_B)^2 (r_{A,B} + r_C)^2 \tau_{A,B} + (r_B + r_C)^2 (r_{B,C} + r_A)^2 \tau_{A,C} + (r_A + r_C)^2 (r_{A,C} + r_B)^2 \tau_{A,C} \} n_A n_B n_C. \quad (20.1)$$

Approximating $m_A = m_B = m_C = M/N_A$ (where M is the mean molecular weight), $\tau_{A,B} = \tau_{B,C} = \tau_{A,C} = \tau$, $r_A = r_B = r_C = \frac{1}{2}d$ and $r_{A,B} = r_{B,C} = r_{A,C} = d$ (d being the mean diameter) we obtain

$$Z_3 = Z_3^0 n_A n_B n_C \text{ where } Z_3^0 = 54\sqrt{3\pi R T M^{-1} \tau d^4}. \quad (20.2)$$

Z_3^0 is the quantity which occurs in the expression for the rate constant of ternary collisions, namely,

$$k_3 = P Z_3^0 \exp(-E/RT), \quad (20.3)$$

where E is the activation energy, and P the probability factor.

We shall determine the order of magnitude of Z_3^0 . In the simplest case of a monatomic molecule the mean life of the binary complex must be of the same order as the time spent by one particle close to another when they are moving freely, i.e. $\tau = d/v$, where v is the mean relative velocity of the two particles concerned. Setting $d = 3 \times 10^{-8}$ cm, $v = 5 \times 10^4$ cm sec⁻¹ and $M = 30$, we find from (20.3) that, when $T = 300^\circ\text{K}$, $Z_3^0 = 1.2 \times 10^{-31}$ cm⁶ molecule⁻² sec⁻¹ = 4.4×10^{16} cm⁶ mole⁻² sec⁻¹.

For the same values of d , M and T , according to (9.15) the appropriate value of Z^0 in the expression for the binary collision constant is

$$Z_2^0 = d^2 (8\pi R T / \frac{1}{2} M)^{1/2} = 1.8 \times 10^{-10} \text{ cm}^3 \text{ molecule}^{-1} \text{ sec}^{-1}.$$

We find from this that the ratio of the number of ternary to binary collisions is

$$Z_3/Z_2 = (Z_3^0 r^3) / (Z_2^0 n^2) = (2/3)n \times 10^{-21} = (2p/3kT) \times 10^{-21}, \quad (20.4)$$

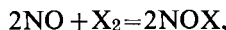
or

$$Z_3/Z_2 = 1.6 \times 10^{-2}p, \quad (20.4')$$

where p is the pressure in atmospheres ($T = 300^\circ\text{K}$).

This implies that atmospheric pressure and normal temperatures the number of ternary gas-kinetic collisions is about a hundred times smaller than the number of binary collisions. At low pressures this ratio is even smaller. However it should be borne in mind that the above value for the number of ternary gas-kinetic collisions is calculated with the assumption that τ is about 10^{-12} sec, which is characteristic of quasi-molecules formed from atoms or the simplest molecules. It has been shown in Chap. 4 (p. 238) that, by increasing the number of internal degrees of freedom according to the increase in the number of atoms in the molecule, the lifetime of a polyatomic quasi-molecule may be several powers of ten greater than 10^{-12} sec (see Table 7). It is clear that both Z_3 and the ratio of the numbers of ternary and binary collisions are thereby increased by a corresponding factor.

According to formula (20.3) the rate constant for the termolecular reaction may be obtained by multiplying Z_3^0 by the probability factor P and the Arrhenius factor $\exp(-E/RT)$. To find these factors we shall compare formula (20.3) with the experimental values for the rate constants of several termolecular reactions. The termolecular gas reactions which have been most adequately studied quantitatively are those involving nitric oxide, namely



where X_2 is a molecule of halogen or oxygen. These reactions, which have been studied by Trautz [1224] ($\text{X}=\text{Cl}$ and Br) and Bodenstein [417] ($\text{X}=\text{O}$) and others, are homogeneous gas reactions of third order. The experimental values for the reaction rate constant of $2\text{NO} + \text{Cl}_2 = 2\text{NOCl}$ ($Q^0 = 16.5$ kcal) over a temperature range 60 to 300°C may be written

$$k_3 = 10^{11.95} \exp(-7500/RT) \text{ cm}^6 \text{ mole}^{-2} \text{ sec}^{-1},$$

from which it follows that $PZ_3^0 = 10^{12} \text{ cm}^6 \text{ mole}^{-2} \text{ sec}^{-1}$. Substituting $Z_3^0 = 10^{16} \text{ cm}^6 \text{ mole}^{-2} \text{ sec}^{-1}$ (τ is about 10^{-12} sec), we find that P is about 10^{-4} . In contrast with this reaction, the reaction $2\text{NO} + \text{O}_2 = 2\text{NO}_2$ ($Q^0 = 25.6$ kcal) studied over the temperature range 193 to 390°C has zero activation energy.⁽²⁶⁾ From $k_3 = 7 \times 10^9 \text{ cm}^6 \text{ mole}^{-2} \text{ sec}^{-1}$ (at 300°K) when Z_3^0 is about $10^{16} \text{ cm}^6 \text{ mole}^{-2} \text{ sec}^{-1}$, we find that P is about 10^{-6} .⁽²⁷⁾

Such low values for the formal probability factor P in the expression for the reaction rate constant are not explicable in terms of collision theory.⁽²⁸⁾ As in the case of bimolecular reactions, this and other

⁽²⁶⁾ In this case the rate constant k_3 falls with rising temperature (by a factor of about ten for a temperature increase from 80 to 400°K).

⁽²⁷⁾ The reaction $2\text{NO} + \text{Br}_2 = 2\text{NOBr}$ has been insufficiently studied quantitatively [1225].

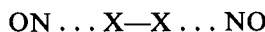
⁽²⁸⁾ Since 10^{-12} sec is apparently the lower limit of τ (see Table 8, p. 238), even lower values for the probability factor P should be expected in these termolecular reactions.

peculiarities of the kinetic rate constant may be satisfactorily explained by using activated complex theory. In each particular case it is necessary to begin with a definite configuration for the complex. We shall use this method to consider some termolecular reactions.

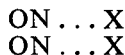
Reactions Involving a Termolecular Acyclic Complex

The above reactions of nitric oxide belong to this type. Since these reactions are of the third order, it is implied that the activated complex involved contains three molecules. The entropy of the system is lowered considerably owing to the loss of six rotational degrees of freedom and therefore reactions of this type are generally slower than bimolecular elementary reactions with the same activation energy. We have already seen (p. 200) that this is the main cause of the low pre-exponential factor in the expression for the rate constant.

Without special calculation it is usually impossible to say what configuration of the termolecular complex is favoured by energy considerations. Generally speaking, a linear configuration may be assumed, for example



or a rectangular configuration



or a configuration intermediate between them. In favour of the linear configuration is the fact that here the mutual repulsion of NO molecules is lowest. However in the reaction with oxygen $2\text{NO} + \text{O}_2 = 2\text{NO}_2$ an argument in favour of the rectangular model is that here a considerable overlap of the π -electron cloud of the O_2 molecule and the valence-electron cloud of each of the NO molecules is possible. In neither of these cases has the activated complex a cyclic configuration.

Assuming that the activated complex has a rectangular configuration, the reaction rate constant may be expressed by the equation [669]

$$k_3 = A \frac{(8\pi^2/h^4\sigma^4)(8\pi^3ABC)^{1/2}(8\pi^2 I_D k T)^{1/2} \prod_{i=1}^{10} [1 - \exp(-hv_i^*/kT)]^{-1}}{\prod_{i=1}^3 (2\pi m_i k T/h^3)^{3/2} \prod_{i=1}^3 (8\pi^2 I_{ik} k T/h^2\sigma_i) \prod_{i=1}^3 [1 - \exp(-hv_i/kT)]^{-1}} \times \exp(-E_0/RT) \quad (20.5)$$

where

$$A = (kT/h)(g^*/g)(2\pi m^* k T/h^3)^{3/2} (kT)^{3/2}.$$

The subscript i refers to the initial molecule. Here it is understood that one of the vibrations of the activated complex is actually an internal rotation

about the O—O axis. Accordingly, one of the vibrational partition functions has been replaced by the rotational partition function

$$(8\pi^2 I_D k T / h^2)^{1/2},$$

where I_D is the moment of inertia relative to this axis. To determine the activation energy from experimental data, we isolate the factors involving temperature in (20.5). After taking logarithms we obtain

$$\ln k + 3 \ln T - \ln \prod_{i=1}^7 (1 - \exp[-h\nu_i^*/kT])^{-1} = a - b/T, \quad (20.6)$$

where a and b are constants and $b = E_0/R$. The number of vibrational partition functions is here reduced to seven, as the three partition functions in the denominator of (20.5) contain frequencies which are close to the corresponding frequencies in the partition functions in the numerator. We may take for the remaining seven vibrational frequencies the value known for the N_2O_4 molecule.⁽²⁹⁾ Plotting the left-hand side of (20.6) as a function of $1/T$ gives a straight line of practically zero slope [669]. Hence for the reaction $2NO + O_2 = 2NO_2$, $E_0 = 0$. This is not surprising since the NO molecule is actually a radical and the O_2 molecule is a bi-radical. Substituting the appropriate values for the parameters in (20.5) gives the results shown in Table 24.

TABLE 24

*Calculated and measured values for the rate constant of the reaction
 $2NO + O_2 = 2NO_2$ (according to Gershinowitz and Eyring [669])*

$T^{\circ}\text{K}$	$k \times 10^{-9} \text{ cm}^6 \text{ mole}^{-2} \text{ sec}^{-1}$	
	calculated	measured [417, 440]
80	86.0	41.8
143	16.2	20.2
228	5.3	10.1
300	3.3	7.1
413	2.2	4.0
564	2.0	2.8
613	2.1	2.8
662	2.0	2.9

If we take into account the approximate nature of both the calculation and the experimental data, the correspondence obtained between the calculated and measured values should be recognized as completely satisfactory. A similar result is obtained for the reaction of nitric oxide with

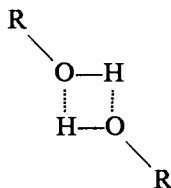
(29) These frequencies are: 283, 380, 500, 600, 752, 813 and 813 cm^{-1} [1195].

chlorine, but in this case the activation energy is $E_0 = 4.8$ kcal assuming an activated complex with a rectangular configuration [669].⁽³⁰⁾

The close correspondence of the calculated and measured values for the rate constants of these reactions clearly solves the problem of the size of the probability factor P in the approximate expression for the rate constant of a termolecular reaction (20.3) as obtained from collision theory.

Reactions Involving a Termolecular Cyclic Complex

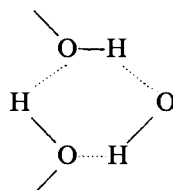
Certain substances in the gas phase form molecular complexes (polymers) of variable composition which are in equilibrium with the molecules of monomer. In particular this refers to substances which are capable of forming hydrogen bonds, for example, carboxylic acids, alcohols, hydrogen fluoride, etc. It is natural that some of these aggregates may be cyclic [1275]. The number of molecules in a cyclic aggregate may vary. The formation of over-large complexes is, however, improbable since this involves the loss of many rotational degrees of freedom, and consequently a considerable decrease in entropy. On the other hand the formation of complexes with less than three molecules is not favoured by energy considerations. Actually, in a dimer, for example of an alcohol, the angles



between the bonds should be about 90° and therefore much less than the angle between the O—H bond and the direction of the axis of the unshared electron pair cloud of the O-atom which is responsible for the formation of the hydrogen bond (this angle is usually 105 to 120°). The optimum configuration for forming a hydrogen bond is a linear arrangement of the three atoms O—H . . . O. In practice the angle O—H . . . O apparently may be decreased to 120 to 140° . For example, in the formation of the intramolecular hydrogen bond in salicylic acid $\text{OHC}_6\text{H}_4\text{COOH}$ the O—H . . . O angle is about 140° . Moreover, for normal distances of O—H and H . . . O in the dimeric cyclic complex, the distance between O atoms is about 2.0 Å; this is considerably less than the sum of the

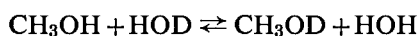
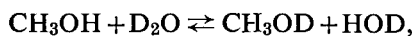
⁽³⁰⁾ Assuming that the rate constant for the reaction $2\text{NO} + \text{Cl}_2 = 2\text{NOCl}$ is inversely proportional to T^3 , as is the rate constant for the reaction $2\text{NO} + \text{O}_2 = 2\text{NO}_2$ (20.5), it is not difficult to show that E_0 and the effective activation energy in (20.3) have the approximate relation $E - E_0 = RT \ln BT^3$, where B is a constant. From this equation, for the temperature range 333 to 566°K we find $E = E_0 + 2.6 = 4.8 + 2.6 = 7.4$ kcal which is a value practically identical with that on p. 324 (7.5 kcal).

van der Waals' radii of the oxygen atoms (2.8 \AA). This means a marked repulsion between the O atoms. In ternary cyclic complexes, whose role was first noted by Shilov [296, 297], for example in the complex



the sizes of the angles and distances between O atoms are more favourable (the O . . . O distance is 2.4 \AA) but still do not reach the optimum value.

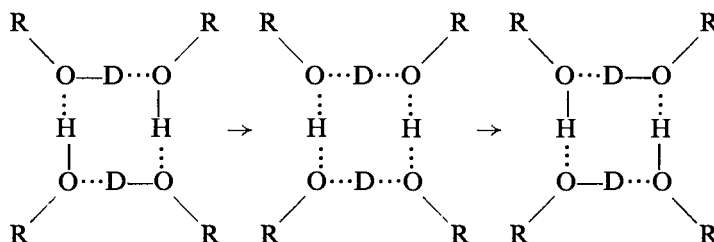
It is natural to expect that, in similar cyclic complexes in the gas phase, *exchange reactions* of hydrogen atoms may take place. This was first put forward by Kwart, Kuhn and Bannister [857] on the basis of the results of their studies on isotopic exchange of hydrogen in the liquid and gas phases of an alcohol and water.⁽³¹⁾ They found from infra-red spectra that in the reactions



and



equilibrium is established very rapidly so that the half-period of the reaction⁽³²⁾ is less than 20 sec. Since in the gas phase an ionic exchange mechanism (which is usual in solutions) is excluded, these authors conclude that the isotopic exchange occurs in the cyclic complex, where the reaction does not involve formation of free ions. They consider possible the following scheme in which the complex contains four molecules:⁽³³⁾



(31) It should however be mentioned that under the conditions of these experiments we must not exclude a catalytic effect of the walls and of mercury vapour [98].

(32) The time in which is established a distribution of isotopes corresponding to 50 per cent of the equilibrium distribution.

(33) In fact the angles between the bonds are probably somewhat different from those shown in this scheme and are approximately 135° .

The elementary act of the reaction apparently consists of the simultaneous transfer of the hydrogen and deuterium nuclei from the oxygen atoms, to which they were covalently bonded in the initial state, to the oxygen atoms with which initially they were only hydrogen-bonded. Here the reaction coordinate is the normal coordinate of the complex corresponding to the completely symmetrical vibration of H and D atoms. The transfer of these nuclei from one equilibrium position to another is naturally an adiabatic process and is accompanied by a corresponding redistribution of electron density.

The hydrogen bond is to a considerable extent dependent on donor-acceptor interaction of an H atom, possessing a certain effective positive charge, with an unshared electron pair of a neighbouring molecule. On this basis the following mechanism for hydrogen exchange has been proposed [247]. First we assume that the complex consists only of two molecules, for example the molecules RA—H and BR', linked by a hydrogen bond, RA—H . . . BR'. In such a complex the hydrogen may be transferred from RAH to BR' only as a proton, since a neutral H atom will always be repelled by the unshared pair of the B atom involved in the formation of the hydrogen bridge. The transfer of a proton from one molecule to another implies the formation of two ions RA⁻ and (HBR')⁺. In the gas phase this process is strongly endothermic. In the ion (HBR')⁺ the bond ^{+H} : B is a typical donor-acceptor bond and therefore it is natural to regard the formation of a hydrogen bond as always the first step in proton transfer. With transfer to the B atom the proton penetrates more deeply into the deformed electron cloud of the unshared pair of the B atom and this signifies a strengthening of the H . . . B donor-acceptor bond. The stronger this bond in the transition state, the lower is the activation energy for the proton transfer. If the complex has a cyclic configuration the fundamental mechanism remains the same. The difference is that, in the ring, ions are not formed at any stage in the proton transfer, as their transfer is accompanied by a simultaneous distortion of the electron density. In such a mechanism the activation energy for the process is considerably lowered and therefore it may also take place in the gas phase.

The formation of an equilibrium molecular complex does not in itself influence the rate of isotopic exchange of hydrogen since, as we have seen above, the reaction rate constant depends only on the initial (monomeric) and transition states. However, it might be maintained that the stronger the hydrogen bond, the lower is the activation energy for the proton transfer, as the nature of the H . . . B interaction in both the initial state and in the transition complex is fundamentally the same. Thus the study of the properties of a complex with a hydrogen bond makes it possible to determine the relative rates of hydrogen exchange in suitable (cyclic) systems.

Using the transition-state method it is not difficult to calculate the pre-exponential factor in the Arrhenius equation for the rate of hydrogen exchange in a termolecular complex. We shall use as an example hydrogen exchange between water molecules.

According to §12, the rate constant in this case is

$$k_3 = B \times$$

$$\frac{(8\pi^2/h^3\sigma^*)(8\pi^3A^*B^*C^*)^{1/2}(kT)^{3/2}\prod_{i=1}^{20}(1-\exp[-hv^*/kT])^{-1}\exp(-E_0/RT)}{\{(2\pi mkT/h^2)^{3/2}(8\pi^2/h^3\sigma)(8\pi^3ABC)^{1/2}(kT)^{3/2}\prod_{i=1}^3(1-\exp[-hv/kT])^{-1}\}^3}, \quad (20.7)$$

where

$$B = (kT/h)(2\pi m^*kT/h^2)^{3/2}.$$

Since the activated complex $(H_2O)_3$ contains nine atoms, it has twenty vibrational degrees of freedom. Using the following values for the quantities in (20.7):

$$A = 10^{-40}, B = 2 \times 10^{-40}, C = 3 \times 10^{-40} \text{ g.cm}^2;$$

$$A^* = B^* = 2 \times 10^{-38}, C^* = 10^{-38} \text{ g.cm}^2;$$

$$\sigma = 2, \sigma^* = 3; T = 300^\circ\text{K}$$

we find

$$k_3 = 1.4 \times 10^{10} \prod_{i=1}^{11} (1 - \exp[-hv^*/kT])^{-1} \exp(-E_0/RT) \text{ cm}^6 \text{ mole}^{-2} \text{ sec}^{-1}$$

Here it has been considered that the vibrational frequencies in the initial molecules and the nine activated complex frequencies corresponding to them are sufficiently high for the relevant partition functions to be close to unity. The remaining eleven frequencies of the activated complex, generally speaking, may be high or low. In the first limiting case when we may reckon $hv^* \gg kT$, we find

$$k_3 = 1.4 \times 10^{10} \exp(-E_0/RT) \text{ cm}^6 \text{ mole}^{-2} \text{ sec}^{-1};$$

in the second limiting case when $hv^* \ll kT$, we obtain

$$k_3 = 1.4 \times 10^{10} \prod_{i=1}^{11} (kT/hv^*) \exp(-E_0/RT) \text{ cm}^6 \text{ mole}^{-2} \text{ sec}^{-1}.$$

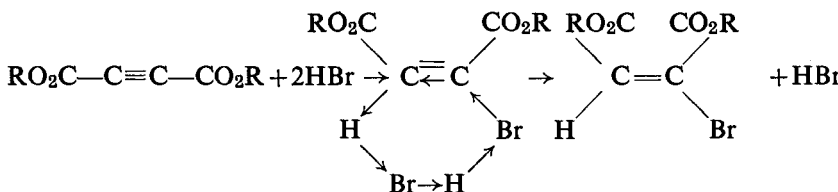
We note that low frequencies are more probable than high frequencies in a molecular complex in which the molecules are bound by any intermolecular forces. In order to calculate k_3 in this case we assume that on average $v^* = 50 \text{ cm}^{-1}$. Then we obtain

$$k_3 = 10^{17} \exp(-E_0/RT) \text{ cm}^6 \text{ mole}^{-2} \text{ sec}^{-1}.$$

Unfortunately Kwart, Kuhn and Bannister [857] do not indicate the pressure at which they conducted their experiments on isotopic exchange

in the gas phase. If it is assumed that the pressure was atmospheric, then we may conclude from their data that the rate constant for the exchange is about $10^8 \text{ cm}^6 \text{ mole}^{-2} \text{ sec}^{-1}$. In order to give such a rate of exchange the activation energy in the first case ($h\nu^* \gg kT$) should be about 3 kcal and in the second case ($h\nu^* \ll kT$) about 12 kcal. The actual value for the activation energy probably lies between these values.

It is entirely probable that certain other gas-phase reactions which are usually assumed to have a more or less complex mechanism with many steps actually involve a termolecular cyclic complex. This may be inferred from the fact that a series of organic reactions in solution, formerly thought to be ionic, also take place in inert media (hexane, benzene and others) which exclude the formation of ions. Some of these reactions have been shown to be termolecular. According to Shilov [296, 297], these reactions occur in a cyclic complex of three molecules and, as in the above example of hydrogen exchange, the reaction follows a donor-acceptor mechanism in which the electron pairs are not split and only the appropriate distortions of the electron clouds take place. For example, the addition of hydrogen bromide HBr to the triple bond of an acetylene dicarboxy-ester $\text{RO}_2\text{C}-\text{C}\equiv\text{C}-\text{CO}_2\text{R}$ (in hexane and in other media) is second-order with regard to HBr and, according to Shilov [242], takes place in the following way:

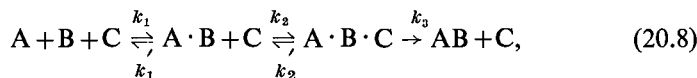


Here the arrows in the intermediate complex show the direction of the electron displacements. Since in similar reactions ions are not formed and the solvent does not play a specific role, it might be expected that reactions of this type may also take place in the gas phase. Experimental indications of such a mechanism for gas reactions are still lacking.

Recombination and Addition to a Multiple Bond

We have seen in Chap. 4 that at sufficiently high pressures reactions of this type follow a bimolecular law. The condition for a reaction to be bimolecular is that the (pressure-dependent) frequency of molecular collisions stabilizing the quasi-molecule should be much greater than the reciprocal of the lifetime of the quasi-molecule. With the opposite relation between the magnitudes of the collision frequency and the lifetime of the quasi-molecule the reaction follows a termolecular law.

In contrast with the above termolecular reactions, in reactions of recombination and addition the third molecule (third particle) remains unchanged and takes part only in the steps of formation of the intermediate complex or of relatively unstable intermediate compounds. In the usual way the termolecular recombination $A + B + C \rightarrow AB + C$ may be represented by the scheme



in which $A \cdot B$ and $A \cdot B \cdot C$ indicate intermediate complexes (quasi-molecules) and k_1, k_1', k_2 , etc. are the rate constants for the corresponding processes.⁽³⁴⁾ We have noted earlier (p. 322) that in similar reactions an important function of the third particle (C) is to remove excess energy from the quasi-molecule $A \cdot B$, which leads to its stabilization.

Table 25 shows experimental values for the rate constant of ternary collision corresponding to the recombination of atoms



($M = C$, the third particle), i.e. the constant $k_3 = k$ in the rate equation for recombination

$$-(d/dt)(A) = k(M)(A)^2.$$

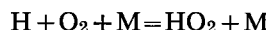
This table includes data for the recombination of atomic hydrogen, nitrogen, bromine; and also for the recombination of hydroxyl,



of hydroxyl with atomic hydrogen,



and for addition reactions of oxygen,



and



The recombination of iodine atoms has been studied in most detail; the experimental data for this reaction are shown in Table 26. The values of k obtained by various authors for the same third partner (M) in collision differ considerably and these differences exceed experimental error [489]. The main reason for the differences when $M = He, Ne, Ar, Kr$ and Xe , according to Norrish and coworkers [489], is neglect of the action of the iodine molecule as a third particle. These authors showed that the measured

⁽³⁴⁾ Here, for simplicity we shall not consider the formation of the quasi-molecules $B \cdot C$ and $A \cdot C$ (see p. 322 *et seq.*).

TABLE 25

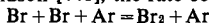
Constants for the recombination of atoms during ternary collision
 $A + A + M = A_2 + M$, (in $\text{cm}^6 \text{molecule}^{-2} \text{sec}^{-1} \times 10^{32}$)

M \ A	H [1178]	N [1052]	Br [1052]	OH [128] 20°C	O + O ₂ [834] 77.5°C	O + OH [128] 20°C	H + O ₂ [203] 500°C
	25°C						
He	—	0.2†††	0.76 (0.07)* [761]	200	(0.13)	—	—
Ar	—†	1.7 [729a]	1.3	—	(0.22)	—	—
	—	—	(0.03)	—	—	—	—
	—	—	1.38 [1189]	—	—	—	—
	—	—	0.19† [443]	—	—	—	—
H ₂	8.8 [318]	—	2.2	—	—	—	0.31
	6.1	—	(0.11) [761]	—	—	—	(1) [1294]
	9.4 [601]	—	—	—	—	—	—
N ₂	—†	1.7 [729a]	2.5	—	(0.28)	—	0.13
	—	1.5†††	—	—	—	—	—
	—	3**	(0.21) [761]	—	—	—	(0.25-0.35)
O ₂	—	—	3.2	—	(1.00)††	—	0.11
	—	—	—	—	—	—	1.5 [498]†† (0.38)
CO	—	—	(1.50) [761]	—	(0.62)	—	—
Br ₂	—	—	(1.00) [761]	—	—	—	—
HCl	—	—	(1.31) [761]	—	—	—	—
HBr	—	—	(0.75) [761]	—	—	—	—
CO ₂	—	—	5.4	—	(0.80)	—	0.45*** (0.90)
H ₂ O	6††† [1003']	—	—	450	—	14 150*** [1003']	1.53
CH ₄	—	—	3.6	—	—	—	—

* Measured at 490°K.

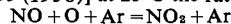
† According to Farkas and Sachsse [601], the efficiencies of H₂, Ar and N₂ in the process H + H + M = H₂ + M are of the same order of magnitude.

‡ According to Britton and Davidson [441], the rate constants for the reaction



and Br + Br + Br₂ = Br₂ + Br₂ at 1500°K are 0.09×10^{-32} and $(0.09 \text{ to } 0.19) \times 10^{-32} \text{ cm}^6 \text{ molecule}^{-2} \text{ sec}^{-1}$ respectively. See also [1004] [E. K. Gill, K. J. Laidler, *Canad. Chem. J.* 36, 79 (1958)].

** See also [T. Wentink, Jr., J. O. Sullivan, K. L. Wray, *J. Chem. Phys.* 29, 231 (1958)] and [R. Kelly, C. A. Winkler, *Canad. Chem. J.* 37, 62 (1959)]. According to [P. Harteck, R. R. Reeves, G. Manella, *J. Chem. Phys.* 29, 1333 (1958)] at 25°C the rate constant for the process



is $k = 7.6 \times 10^{-32}$. In [H. F. Ford, N. Endow, *J. Chem. Phys.* 27, 1156 (1957)] $k = 5 \times 10^{-32}$ is given for the process NO + O + N₂ = NO₂ + N₂.

†† According to [380a], at 300°K, $k = 2 \times 10^{-34} \text{ cm}^6 \text{ molecule}^{-2} \text{ sec}^{-1}$. See also [940, 826a].

††† Measured at 0°C. In sharp contradiction with this and the other values for the rate constant of the reaction H + O₂ + M = HO₂ + M in Table 25 is the value obtained by Farkas and Sachsse [601]; it is less than the values shown here by one and a half to two powers of ten. It was suggested that this discrepancy results from the existence of two forms of the HO₂ radical differing in the stability of the H—O₂ bond [47].

*** According to Danby and Hinselwood's data [523], the efficiencies of N₂O and CO₂ as third particles in the reaction H + O₂ + M are the same.

†††† [J. T. Herron, J. L. Franklin, P. Bradt, V. H. Dibeler, *J. Chem. Phys.* 29, 230 (1958); 30, 959 (1959)].

††††† 1380°C. As the temperature falls the constants slightly increase.

TABLE 26

Constants for the recombination of iodine atoms during ternary collision at 25°C (in $\text{cm}^6 \text{molecule}^{-2} \text{sec}^{-1}$)

M \ A	Britton and coworkers [442]	Norrish or coworkers		Marshall and coworkers		Rabinowitch and coworkers [1052]	Rollefson and Eyring [1082]	Russell and Simons [1096]
		[489]	[490]	[533]	[917]			
He . . .	0.10*	0.67	1.73	—	—	1.8	—	0.94
Ne . . .	—	0.92	1.86	—	—	—	—	1.00
Ar . . .	1.21	1.84	2.42	2.3	2.3	3.6	2.5	2.00
	0.25†	—	—	—	—	—	—	—
Kr . . .	—	2.25	3.41	—	—	—	—	—
Xe . . .	—	2.99	3.44	—	—	—	—	—
H_2 . . .	—	—	—	—	—	4.0	—	2.63
N_2 . . .	0.39†	—	—	—	—	6.6	—	2.49
O_2 . . .	0.29†	—	—	—	—	10.5	—	3.69
I_2 . . .	720	470**	—	—	—	—	—	—
CO_2 . . .	0.51‡	—	—	—	—	18	—	7.44
H_2O . . .	—	—	—	—	—	—	—	27.4
CH_4 . . .	—	—	—	—	—	12	—	4.9
CH_2Cl_2 . . .	—	—	—	—	—	—	—	26.3
CCl_4 . . .	—	—	—	—	—	—	—	28.0
CH_3OH . . .	—	—	—	—	—	—	—	35.8
C_2H_4 . . .	—	—	—	—	—	—	—	9.45
C_2F_4 . . .	—	—	—	—	—	—	—	11.6
CH_3NO_2 . . .	—	—	—	—	—	—	—	103
$\text{C}_2\text{H}_5\text{Cl}$. . .	—	—	—	—	—	—	—	26.3
$\text{C}_2\text{H}_5\text{Br}$. . .	—	—	—	—	—	—	—	44.2
$\text{C}_2\text{H}_5\text{I}$. . .	—	—	—	—	—	—	—	138
$(\text{CH}_3)_2\text{O}$. . .	—	—	—	—	—	—	—	34.1
C_3H_6 cyclopropane	—	—	—	—	—	—	—	21.8
C_3H_8 . . .	—	—	—	—	—	—	—	16.8
C_6H_6 . . .	—	—	—	—	100	—	—	48.0
Trifluorobenzene	—	—	—	—	—	—	—	48.4
$\text{C}_6\text{H}_5\text{CH}_3$. . .	—	—	—	—	—	—	—	116
$\text{C}_6\text{H}_4(\text{CH}_3)_2$. . .	—	—	—	—	—	—	—	183
$\text{C}_6\text{H}_3(\text{CH}_3)_2$. . .	—	—	—	—	—	—	—	224
C_5H_{12} . . .	—	—	—	36	—	—	—	—
$(\text{CH}_3)_4\text{C}$. . .	—	—	—	32	—	—	—	25.9
C_6H_{12} . . .	—	—	—	—	—	—	—	30.0

* Measured at 1400°K.

† Measured at 1300°K.

‡ Measured at 1120°K.

** See also [463b].

constant for the recombination (under experimental conditions with inert gases) is actually

$$k_{\text{measured}} = k_M + \frac{(I_2)}{(M)} k_{I_2}$$

where k_M is the rate constant for the process $\text{I} + \text{I} + \text{M} = \text{I}_2 + \text{M}$ and k_{I_2} for the process $\text{I} + \text{I} + \text{I}_2 = \text{I}_2 + \text{I}_2$. The values for k_M obtained by Norrish and coworkers allowing for the participation of an I_2 molecule in the

recombination of iodine atoms should be considered the most reliable of all the values shown in Table 26 for k_M when $M = \text{He, Ne, Ar, Kr and Xe}$. Russell and Simons [1096] obtained the closest figures to these values and therefore it might be assumed that their measured constants for the recombination of iodine atoms with a great variety of M (Table 26) are the correct ones.

It is clear from Table 26 that Rabinowitsch and coworkers [1052] obtained values of k for the recombination of iodine atoms two to three times greater than those obtained from the data of Norrish and coworkers [489]. It might be assumed therefore that the values of k for the recombination of bromine atoms are also somewhat high, though not, perhaps, to the same degree. In any case the k values for this reaction shown in Table 25 must be of the right order of magnitude⁽³⁵⁾ as also must be the k values obtained by Rabinowitsch and coworkers for the recombination of iodine atoms. Rabinowitsch [1052] compared these data with his constants, calculated from gas-kinetic data, for the recombination of iodine and bromine atoms⁽³⁶⁾ and determined the efficiency of ternary collisions for all the substances he studied. According to these calculations, when $M = \text{N}_2, \text{O}_2, \text{CO}_2$ or CH_4 each gas-kinetic encounter of three particles $X + X + M$ ($X = \text{Br, I}$) leads to recombination and hence P , the probability (efficiency) of removing energy from the quasi-molecule $X \cdot X$, is close to unity. When $M = \text{He}$ or H_2 , the quantity P is about 0.1 and when $M = \text{Ar}$ it is 0.2 to 0.3. In the reaction $\text{I} + \text{I} + \text{C}_6\text{H}_6 = \text{I}_2 + \text{C}_6\text{H}_6$, $P = 4$, a value greater than unity. Rabinowitsch connects this with the formation of a relatively stable $\text{C}_6\text{H}_6\text{I}$ complex which leads to a considerable increase in the probability of the reaction. The formation of such "chemical" complexes also appears to take place in the recombination reactions of iodine in the presence of various other molecules, especially in the reaction $\text{I} + \text{I} + \text{I}_2 = \text{I}_2 + \text{I}_2$ (see below, p. 341 *et seq.*) where the I_3 complex must play an important role [489]. The marked stability of this complex was predicted theoretically by Rollefson and Eyring [1082]. See also D. L. Bunker, N. Davidson, *J. Amer. Chem. Soc.* **80**, 5090 (1958).

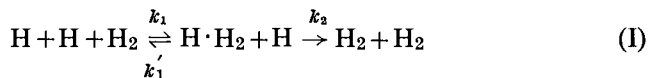
The large values of the recombination constant observed for the recombination $\text{OH} + \text{OH}$ may be explained by the high stability of the quasi-molecule $\text{OH} \cdot \text{OH}$; this is in accordance with its long lifetime of 2×10^{-10} to 4.5×10^{-10} sec according to the data of Table 7.

⁽³⁵⁾ The relative values for k shown in brackets are on average twenty times less than the values obtained by Wood and Rabinowitsch. Multiplying these relative values by twenty, we find for $M = \text{CO, Br}_2, \text{HCl}$ and HBr that $k = 30, 20, 26$ and $15 \times 10^{-32} \text{ cm}^6 \text{ molecule}^{-2} \text{ sec}^{-1}$ respectively.

⁽³⁶⁾ The basis of these calculations is that the duration of collision of two particles is determined by twice the time taken by them to describe a path equal to the difference between the mean diameter calculated without Sutherland's correction and the diameter calculated with this correction.

According to Willbourn and Hinshelwood [1294], and also Voevodskii and Nalbandyan [203], values of P close to unity are also obtained in the addition of an H atom to an O_2 molecule when the third particle M is a diatomic molecule. When $M = CO_2$ or H_2O , P is greater than unity.⁽³⁷⁾

Finally it is not difficult to see that the efficiency of collisions in the reaction $H + H + H_2 \rightleftharpoons H \cdot H_2 + H \rightarrow H_2 + H_2$ is also close to unity. Actually, expressing the mechanism of this reaction by the simplified scheme



and assuming that in the formula for the rate constant of ternary collision $k = k_1 \tau' k_2$ (see p. 229) the quantities k_1 , k_2 and $\tau' (= 1/k_1')$ are: $k_1 = k_2 = 3 \times 10^{-10} \text{ cm}^6 \text{ molecule}^{-2} \text{ sec}^{-1}$ (the mean collision diameter $d = 2 \times 10^{-8} \text{ cm}$) and $\tau' = 10^{-13} \text{ sec}$, we obtain $k = 0.9 \times 10^{-32} \text{ cm}^6 \text{ molecule}^{-2} \text{ sec}^{-1}$. The experimental value is 3×10^{-32} to $5 \times 10^{-32} \text{ cm}^6 \text{ molecule}^{-2} \text{ sec}^{-1}$.⁽³⁸⁾

It follows from the data in Tables 25 and 26 for the recombination of iodine and bromine atoms at room temperature and also at a temperature above $1000^\circ K$ that the rate constant for the recombination *decreases* with increase in temperature.⁽³⁹⁾ However the data available at present are not sufficiently precise to determine the exact temperature-dependence of k . It is possible that this dependence is expressed by the Arrhenius equation; however we should not exclude the possibility that k varies as T^{-n} [444, 442].

The experimental data in Tables 25 and 26 were considered above on the basis of simple collision theory. We have seen that for the most part these data are in accordance with the assumption that the effective cross sections of molecular collisions, corresponding to the individual elementary steps of the reaction, are close to the gas-kinetic cross sections. We might also use the transition-state method to calculate the rate constant for the termolecular reaction $A + B + C \rightleftharpoons AB + C$. This method was first applied to this problem by Eyring, Gershinowitz and Sun [587] and Wigner [1290]. See also D. W. Jepson, J. O. Hirschfelder, *J. Chem. Phys.* **30**, 1032 (1959).

⁽³⁷⁾ According to Walsh [1262], the large efficiencies of CO_2 and H_2O in this reaction are explained by the fact that these molecules possess frequencies close to the vibrational frequencies of the HO_2 radical; Walsh ascribes to this radical frequencies corresponding to hydroxyl and the oxygen molecule.

⁽³⁸⁾ This constant is the constant k_{H_2} in the equation $(d/dt)(H_2) = k_{H_2}(M)(H)^2$, whereas the constants shown in Table 25 are those in the equation

$$-(dH/dt) = k_H(M)(H)^2.$$

It is not difficult to see that $k_{H_2} = \frac{1}{2} k_H$.

⁽³⁹⁾ We should add that, according to the measurements of Russell and Simons [1096], the recombination constant for iodine atoms with various third bodies M is decreased by 2 to 3 times on increasing the temperature from 20 to $127^\circ C$.

In the simplest case let the particles A, B and C represent hydrogen atoms. We shall consider at first that on collision all three atoms are on a straight line. The potential energy surface shown in Fig. 40 (p. 172) corresponds to this case. We have already seen (§11) that for an AB molecule to be formed as the result of ternary collision, it is necessary that there be a redistribution of the initial translational energy of the three atoms so that the energy corresponding to the vibrational degree of freedom of the AB molecule formed is less than its dissociation energy. In general, therefore, not every collision leads to reaction.

We shall assume that the representative point corresponding to the system $H + H + H$ is moving on the right of the main diagonal (see Fig. 40, the half-surface x_1, y_1) and the energy of the representative point is greater than the dissociation energy D . If the representative point does not cross the main diagonal, reaction does not take place, since the vibrational energy, corresponding to movement along y_1 , is not converted into translational energy, corresponding to movement along x_1 . The latter circumstance depends on the nature of the potential surface (Fig. 40) according to which the energy on each side of the main diagonal may be written as the sum of two terms; the first term depends only on x_1 (or x_2) and the other term only on y_1 (or y_2). An exception is the relatively small part of the potential surface for which $\epsilon < 45$ kcal where the energy contours are not parallel with the x_1 coordinate. However, for the most part, the representative points do cross the main diagonal in the region $\epsilon < 45$ kcal and here the above considerations hold.

To calculate the rate of the reaction $A + B + C = AB + C$ it is necessary to find the number of representative points crossing the diagonal line in unit time and satisfying the condition that, after crossing, their vibrational energy corresponding to the y_2 coordinate is less than D .⁽⁴⁰⁾ This number, by analogy with formula (12.1) Chap. 3, may be written

$$v^* dn_z/dl$$

where dn_z is the concentration of representative points on the line of the pass in the range dl , which satisfy the above condition; the range dl is taken along the coordinate perpendicular to the main diagonal. In order to simplify the calculations we shall take instead of the actual velocity v^* , as in (12.1), the mean velocity \bar{v}^* of the representative points when they cross the main diagonal.

There is no transmission coefficient in the foregoing expression as we are assuming that dn_z includes only those systems which reach the final state. In order to satisfy this condition we isolate from the partition function dZ_z the factors corresponding to two degrees of freedom, for

⁽⁴⁰⁾ Strictly speaking, the rotation of the molecule AB should be allowed for, but as a rule it may be neglected.

example x_1 and y_1 , and the transfer of energy between these degrees of freedom determines whether reaction occurs. We shall call the momenta corresponding to these degrees of freedom p_{x_1} and p_{y_1} . It is convenient to introduce new coordinates l and η instead of x_1 and y_1 ; l (the "reaction coordinate") is perpendicular to the main diagonal and η is coincident with the main diagonal. The potential energy V close to this line may be considered as a function $V(\eta)$ of η only. In this way the rate of the reaction considered is given by the equation

$$w = n_A n_B n_C \frac{Z_z \bar{v}^*}{Z_A Z_B Z_C} \frac{1}{dl} \int d\eta \int \frac{dp_{x_1}}{h} \int \frac{dp_{y_1}}{h} \exp \left[-\frac{p_{x_1}^2 + p_{y_1}^2}{2\mu k T} + \frac{V(\eta)}{k T} \right] dl, \quad (20.9)$$

where $\mu = (m_A + m_B) m_C / (m_A + m_B + m_C) = \frac{2}{3}m$ ($m = m_A = m_B = m_C$). The integration limits are chosen so that only those representative points which lead to reaction are considered. The partition function Z_z takes into account translational and rotational motion of the linear activated complex and also its deformation vibration.

The calculation of the integrals (20.9), starting from the energy of the separated atoms, gives [587]

$$w = n_A n_B n_C \frac{Z_z \bar{v}^*}{Z_A Z_B Z_C} \frac{2\mu k T}{h^2} 1.64 \times 10^{-8}. \quad (20.9a)$$

Substituting in this the corresponding partition functions and

$$\bar{v}^* = (k T / 2\pi m^*)^{1/2},$$

where m^* is the effective mass corresponding to the coordinate l , we find for the reaction rate constant

$$k = \left(\frac{g^*}{g_A g_B g_C} \right) \frac{(8\pi^2 I^* k T / \sigma^* h^2) \prod_{i=1}^2 (1 - \exp[-h\nu_i^*/k T])^{-1}}{(2\pi m k T / h^2)^{9/2}} \times \left(\frac{2\pi m^* k T}{h^2} \right)^{3/2} \left(\frac{2\pi k T}{h^2} \right) \left(\frac{k T}{2\pi m^*} \right)^{1/2} (1.64 \times 10^{-8}), \quad (20.10)$$

where g^* , g_A , g_B and g_C are the statistical weights of the activated complex and the initial atoms, respectively. In the activated complex ($\text{H}\cdot\text{H}\cdot\text{H}$) the resultant angular momentum is $S = \frac{1}{2}$ and consequently $g^* = 2S+1 = 2$; in the initial state of the system ($\text{H}+\text{H}+\text{H}$), $S = 1/2$ for each of the atoms and therefore the quantity $g_A g_B g_C = (2S+1)^3 = 8$. In this way we find $g^*/(g_A g_B g_C) = \frac{1}{4}$.

When $h\nu \ll kT$, the vibrational partition functions give in the denominator the factor ν^{*2} , where ν^* is the frequency of deformation vibrations of the activated complex. Moreover the rate constant k is proportional to $m^{*-1/2}$

and this is supported by the data of Amdur [316] who studied the isotope effect in the recombination of hydrogen and deuterium. This shows us that the frequency ν^* is small. In accordance with this, assuming that $\nu^* \approx 100 \text{ cm}^{-1}$, we find from (20.10) at 300°K , $k = 0.86 \times 10^{-32} \text{ cm}^6 \text{ molecule}^{-2} \text{ sec}^{-1} = 3.1 \times 10^{15} \text{ cm}^6 \text{ mole}^{-2} \text{ sec}^{-1}$.

This value, however, should be considered as rather low since we have taken into account only a linear configuration for the colliding atoms and in fact the reaction $\text{A} + \text{B} + \text{C} = \text{AB} + \text{C}$ is also possible with an activated complex of triangular structure. An estimate [587] has shown that when other possible configurations of the complex are taken into account, the result may be increased by not more than 2 to 3 times. In this way it should be considered that the theoretical value for the rate constant of the reaction $\text{H} + \text{H} + \text{H} = \text{H}_2 + \text{H}$ must be about $10^{16} \text{ cm}^6 \text{ mole}^{-2} \text{ sec}^{-1}$.

Precise experimental values of k are not known. Moreover, there is a marked divergence between the estimates of this quantity by different authors. Thus, according to Steiner [1178], the rate constant for the reaction $\text{H} + \text{H} + \text{H} = \text{H}_2 + \text{H}$ must be at least ten times less than the rate constant for the reaction $\text{H} + \text{H} + \text{H}_2 = \text{H}_2 + \text{H}_2$, whereas Smallwood [1149] finds that, on the contrary, the constant for the latter reaction is more than fifty times less than the constant for the first reaction. The rate constant for the reaction $\text{H} + \text{H} + \text{H} = \text{H}_2 + \text{H}$ is $k = \frac{1}{2} \times 1.7 (\pm 0.3) \times 10^{16} \text{ cm}^6 \text{ mole}^{-2} \text{ sec}^{-1}$, according to Smallwood. Amdur [316], like Smallwood, assumes that the efficiency of H atoms as third particles is at least ten times greater than the efficiency of H_2 molecules and gives the following values for k : $(2.05 \pm 0.07) \times 10^{16} \text{ cm}^6 \text{ mole}^{-2} \text{ sec}^{-1}$ for $\text{H} + \text{H} + \text{H} = \text{H}_2 + \text{H}$, and $(1.51 \pm 0.05) \times 10^{16} \text{ cm}^6 \text{ mole}^{-2} \text{ sec}^{-1}$ for $\text{D} + \text{D} + \text{D} = \text{D}_2 + \text{D}$. Moreover, according to the data of Steiner [1178] and the data of the earlier work of Amdur and Robinson [318] (see Table 25), the rate constant for the reaction $\text{H} + \text{H} + \text{H}_2 = \text{H}_2 + \text{H}_2$ is 1.1×10^{16} (Steiner) and 1.6×10^{16} (Amdur and Robinson) $\text{cm}^6 \text{ mole}^{-2} \text{ sec}^{-1}$. In more recent work Amdur [317] also finds that the rate constant for the reaction $\text{H} + \text{H} + \text{H}_2 = \text{H}_2 + \text{H}_2$ is 0.9×10^{16} to 1.2×10^{16} and the rate constant for the reaction $\text{H} + \text{H} + \text{H} = \text{H}_2 + \text{H}$ is 0.0×10^{16} to $3.1 \times 10^{16} \text{ cm}^6 \text{ mole}^{-2} \text{ sec}^{-1}$. We have seen above that collision theory gives a value about $10^{16} \text{ cm}^6 \text{ mole}^{-2} \text{ sec}^{-1}$ for the rate constant of the reaction $\text{H} + \text{H} + \text{H}_2 = \text{H}_2 + \text{H}_2$.

The method indicated here for calculating the rate of recombination of H atoms may be used also for other atoms and, in general, for other systems. It should be mentioned that in the case studied, the complex has only one degree of freedom to act as a reservoir of excess energy. If there are more such degrees of freedom, for example, as in the recombination of radicals or in the addition of an atom or radical to a molecule, the rate of reaction is accordingly increased for the same activation energy.

It was shown in §11 that by substituting for one of the H atoms an atom

of helium or another inert gas, the probability of recombination is decreased and this is connected mainly with the lack of chemical interaction with this atom and, accordingly, with the decrease in the probability of the redistribution of energy stabilizing the quasi-molecule $A \cdot B$.⁽⁴¹⁾

Wigner [1290] calculated the rate of recombination of atoms by ternary collision also in the case in which the potential-energy surface of the three atoms has no barrier, as for example in the recombination of two atoms in the presence of an atom of an inert gas. At the same time, the method he proposed takes into account automatically all possible orientations of the atoms when they come together. Wigner used the formula he obtained to calculate the rate constant for the recombination of atoms of iodine, bromine and chlorine in the presence of atoms of He and Ar, and also H_2 and N_2 . In contrast with the above example of the recombination of hydrogen atoms, the ratio of the statistical weights g^*/g_0 of the "activated complex"⁽⁴²⁾ and of the initial particles in these cases is equal to 1/16, as the ground state of the halogen atoms is ${}^2P_{3/2}$ and hence

$$g_0 = g_x g_x = (2J+1)^2 = 16,$$

and in the "activated state" the system $X \cdot X \cdot M$ has zero angular momentum and consequently $g^* = 1$. However, in calculating the reaction rate it should also be taken into account that the formation of a halogen molecule may take place not only during ternary collision, when it appears in the ground state, but also during collisions which result in a stable excited state (i.e. collisions for which the potential curve has a minimum). Then the resulting rate of recombination will be equal to the sum of the rates of formation of molecules in each of these states. The influence of excited levels may be taken into account if the recombination constant, obtained allowing only for the ground state, is multiplied by the over-all statistical weight of all the stable states of the X_2 molecule. For iodine this number is equal to five.

In Table 27, Wigner's calculated values for the recombination constants of iodine and bromine atoms are compared with the experimental values obtained by Rabinowitsch (see Tables 25 and 26). It can be seen that in every case the theoretical value is larger than the experimental value. This was to be expected, as in Wigner's calculation not all degrees of freedom of the system are taken into account, and consequently, as in the normal activated complex method, the values obtained for the rate constant are high (see §12).

Returning to the problem of the mechanism of termolecular reactions

(41) The replacement of an H atom by an He atom influences the reaction rate through the change in form of the potential energy V in the integral (20.9).

(42) In the absence of a potential barrier the activated complex is considered as a system of atoms in close proximity.

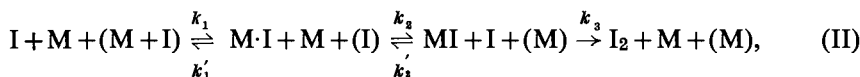
TABLE 27

Calculated and measured values of the rate constants for the recombination of iodine and bromine atoms

Third body	$k \times 10^{32} \text{ cm}^6 \text{ molecule}^{-2} \text{ sec}^{-1}$			
	Iodine		Bromine	
	calculated	measured	calculated	measured
He	6.1	1.8	4.25	0.76
Ar	7.7	3.8	5.4	1.3
H ₂	6.4	4.0	4.5	2.2
N ₂	8.1	6.6	5.9	2.5

of the type considered, then as we have already seen (p. 335) in connection with the exceptionally large (about $10^{-30} \text{ cm}^6 \text{ molecule}^{-2} \text{ sec}^{-1}$) recombination constants for iodine atoms when $M = C_6H_6$, I₂, etc., the mechanism of recombination (or of addition) is apparently not always the simple formation of a quasi-molecule with subsequent stabilization of the reaction-product molecule. We have pointed out that in these cases the formation of relatively stable molecules of the type C₆H₆I or I₃ is very likely.

For example, in contrast with the usual mechanism of termolecular recombination of atoms (as considered on p. 336 for the recombination of H atoms), we may assume the following scheme (as applied to the recombination of iodine atoms):



where M·I represents the usual quasi-molecule; MI represents the physically stable molecule and k_1 , k'_1 , k_2 , etc., are rate constants. Considering the concentrations of M·I and MI particles as stationary, from the steady state conditions

$$d(M \cdot I)/dt = 0$$

and

$$d(MI)/dt = 0$$

we find for the rate of recombination

$$w_r = \frac{k_1 k_2 k_3 (I)^2 (M)^2}{k'_1 k'_2 (M) + k'_1 k_3 (I) + k_2 k_3 (M)(I)} = k_r (I)^2 (M), \quad (20.11)$$

where k_r is the effective recombination constant

$$k_r = \frac{k_1 k_2 k_3(M)}{k'_1 k'_2(M) + k'_1 k_3(I) + k_2 k_3(M)(I)}. \quad (20.12)$$

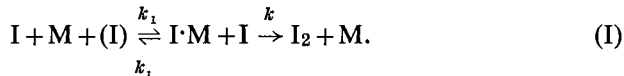
Since $k_3(I)$ is small, k_r may be written in the following simpler form with a high degree of accuracy:

$$k_r = \frac{k_1 k_2 k_3}{k'_1 k'_2} = k_r \text{ (II).}$$

In this way we obtain the usual termolecular reaction law

$$-\frac{1}{2} d(I)/dt = d(I_2)/dt = k_r(I)^2(M)$$

($k_r = \text{const}$), as in the usual recombination mechanism (the scheme on p. 336). However, with an identical over-all reaction law, the mechanism (II) shown on page 341 differs with regard to the rate constant k_r from the usual mechanism, which in this case may be represented by the scheme



Actually, since the concentration of $I \cdot M$ quasi-molecules is low in comparison with the concentration of M (for similar k_1 and k), in this case we have

$$k_r = k_1 k / k'_1 = k_r \text{ (I).}$$

Noting that the equilibrium constant for $I + I \rightleftharpoons I_2$ is

$$K = \frac{(I)^2_{\text{equilib}}}{(I_2)_{\text{equilib}}} = \frac{k'_1 k'_2 k'_3}{k_1 k_2 k_3} = \frac{k'_1 k'}{k_1 k},$$

where k'_3 and k' are the rate constants for the processes $I_2 + M = MI + I$ and $I_2 + M = M \cdot I + I$ respectively, we may write the expressions for the reaction rate constants corresponding to mechanisms (I) and (II) as

$$k_r \text{ (I)} = k' / K \quad \text{and} \quad k_r \text{ (II)} = k'_3 / K.$$

Substituting for the constants k'_3 and k' , which are equal to

$$k'_3 = A \exp(-E'_3/RT) \quad \text{and} \quad k' = A \exp(-E'/RT),$$

we find that

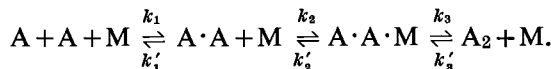
$$\frac{k_r \text{ (II)}}{k_r \text{ (I)}} = \frac{k'_3}{k'} = \exp[(E' - E'_3)/(RT)], \quad (20.13)$$

and hence, since $E' > E'_3$ ⁽⁴³⁾ we obtain $k_r \text{ (I)} < k_r \text{ (II)}$. Consequently

⁽⁴³⁾ The difference $E' - E'_3$ may be considered as close to the bond energy of $M - I$ in the MI molecule.

mechanism (II) leads to a higher value for the recombination constant; so the possibility is not excluded that some of the above cases of high values for this constant are connected with the appropriate reactions taking place according to mechanism (II). We have already seen that this mechanism is possible with regard to the reaction $I + I + C_6H_6 = I_2 + C_6H_6$; this was first postulated by Rabinowitsch [1052] who proposed the existence of a stable C_6H_6I radical. Later Rabinowitsch's idea was developed by Rice [1067].

Rice also studied at the same time the reverse reaction—the dissociation of a molecule into its appropriate parts—which is of importance with regard to the mechanism of recombination. Actually, both these reactions—recombination and dissociation—may be considered on the basis of a *single* mechanism. Consider for example, the reaction $A + A \rightarrow A_2$ and its reverse reaction, $A_2 \rightarrow A + A$; then assuming the first of the above two mechanisms to be correct, the single mechanism for these reactions may be represented by



In this scheme, which is somewhat different from the above scheme (I), the intermediate complex $A \cdot A \cdot M$ is introduced as well as the complex $A \cdot A$.

The general scheme shown in the case of the recombination of A particles is written



and in the case of the dissociation of the A_2 molecule it is written



Considering the concentrations of $A \cdot A$ and $A \cdot A \cdot M$ quasi-molecules to be stationary, we may express the rates of both reactions by the general equations:

$$w_r = \frac{k_1 k_2 \alpha}{k'_1 + k_2 \alpha(M)} (A)^2 (M) = k_r (A)^2 (M) \quad (20.14)$$

and

$$w_d = \frac{k'_1 (1 - \alpha) k'_3}{k_1 + k_2 \alpha(M)} (A_2) (M) = k_d (A_2) (M), \quad (20.15)$$

where $\alpha = k_3 / (k'_2 + k_3)$,

$$k_r = \frac{k_1 k_2 \alpha}{k'_1 + k_2 \alpha(M)} \quad \text{and} \quad k_d = \frac{k'_1 (1 - \alpha) k'_3}{k'_1 + k_2 \alpha(M)}. \quad (20.16)$$

The expressions for the effective constants k_r and k_d may be simplified according to the reaction conditions. Thus, in the low-pressure region when

the concentration of M molecules is low (and also the concentration of A and A₂) and $k'_1 \gg k_{2\alpha}(M)$, we have

$$k_r = \frac{k_1 \alpha k_2}{k'_1} \quad \text{and} \quad k_d = (1 - \alpha) k'_3 \quad (20.17)$$

(cf. above p. 229). On the other hand, at high pressures, that is when $k'_1 \ll k_{2\alpha}(M)$, the effective constants are

$$k_r = k_1/(M) \quad \text{and} \quad k_d = \frac{k'_1 k'_2 k'_3}{k_2 k_3(M)} = K k_1/(M).$$

Accordingly the rates of recombination and dissociation are in this case

$$w_r = k_1(A)^2 \quad \text{and} \quad w_d = \frac{k'_1 k'_2 k'_3}{k_2 k_3} (A_2) = K k_1 (A_2). \quad (20.18)$$

It can be seen from these formulae that at sufficiently high pressures the recombination reaction follows a bimolecular law and the dissociation reaction follows a unimolecular law.

Keeping in mind the expression for the equilibrium constant

$$K = (k'_1 k'_2 k'_3) / (k_1 k_2 k_3)$$

and the above expression for the quantity α , we obtain from (20.16)

$$k_d = K k_r. \quad (20.19)$$

This general relation between the rate constants of the forward and reverse reactions in the equilibrium state naturally does not depend on the mechanism assumed. In particular it holds for mechanism (II).

Using the relation (20.19), the equilibrium rate constant k_d may be calculated if k_r and the equilibrium constant K are known. From measurements of k_r for the reactions I + I + M = I₂ + M and Br + Br + M = Br₂ + M, which were carried out by Rabinowitsch and coworkers [1052], and from the tabulated values for the equilibrium constants for iodine and bromine Rice [1067] showed that if k_d is expressed, using the collision-theory formula, as

$$k_d = A \exp(-D/RT), \quad (20.20)$$

where

$$A = 2 d^2 (2\pi k T / \mu)^{1/2},$$

then relation (20.19) is satisfied in this case only with values of the effective collision diameter d greater than the gas-kinetic diameter by a factor of about ten.

Later and more precise data lead to the same result. For example, from the constants for the recombination I + I + Ar = I₂ + Ar measured by Norrish and coworkers [489] shown in Table 26 and from the equilibrium

constant for $I + I \rightleftharpoons I_2$, which is 3.80×10^{-26} mole/cm³ (at 300°K), we find $k_d = 1.3 \times 10^{-10}$ cm³ mole⁻¹ sec⁻¹. Substituting in formula (20.20) this value of k_d , the heat of dissociation of iodine (35,500 kcal), and T = 300°K, we find $A = 10^{16}$ cm³ mole⁻¹ sec⁻¹, i.e. a quantity 100 times larger than the gas-kinetic collision number which is about 10^{14} cm³ mole⁻¹ sec⁻¹.⁽⁴⁴⁾ An explanation of this discrepancy was given in §16.

Even earlier Rice [1067] put forward another explanation which, in essence, is the replacement of the usual reaction mechanism (mechanism I) by mechanism II which assumes the formation of relatively stable MX complexes (of type C₆H₆I or I₃) in the course of the reaction. According to the foregoing (p. 342), in this case the rate constant for the dissociation is expressed by the formula

$$k_d \text{ (II)} = k'_3 = A \exp(-E'_3/RT), \quad (20.21)$$

where E'_3 represents the activation energy for the process $I_2 + M = MI + I$. Assuming the bond energy of M—I to be small, we can consider the activation energy (E_3) for the reverse process $I + MI = I_2 + M$ to be close to zero, and hence we obtain $E'_3 = D_{I_2} - D_{MI}$, where D_{MI} is the dissociation energy of the M—I bond.

It is not difficult to see that if mechanism II is assumed to be correct, i.e. if the possibility of formation of these complexes is assumed, many deviations from formulae (20.19) and (20.20) can be explained simply. For example, in the above reaction $I + I + Ar = I_2 + Ar$ (p. 344) by substituting in formula (20.21) $k_d = 10^{-10}$ and $A = 10^{14}$ cm³ mole⁻¹ sec⁻¹, we find $E_3 = 33.0$ kcal; hence the bond energy Ar—I = $35.5 - 33.0 = 2.5$ kcal. This value is close to the bond energy in van der Waals molecules and is therefore entirely probable.

A similar calculation using the values in Table 26 for the recombination constants of $I + I + C_6H_6 = I_2 + C_6H_6$ and $I + I + I_2 = I_2 + I_2$ gives $D_{C_6H_6-I} = 4.5$ kcal and $D_{I_2-I} = 6.0$ kcal respectively. See also [1188a and 463c] and D. L. Bunker, N. Davidson, *J. Amer. Chem. Soc.* **80**, 5090 (1958). For the reaction $H + H + H_2 = H_2 + H_2$ we find $k_d = 4 \times 10^{16}$ cm³ mole⁻¹ sec⁻¹ and $D_{H_2-H} = 3.5$ kcal. It is important, however, to note that the reaction $H + H + H = H_2 + H$ clearly cannot follow the second mechanism.

One method of checking the accuracy of the dissociation mechanism would perhaps be a direct measurement of the activation energy of the dissociation process.

⁽⁴⁴⁾ See also [444].

CHAPTER 6

ENERGY CONVERSION DURING MOLECULAR COLLISIONS

IN view of the fact that an active molecule, which is a molecule with an increased amount of energy, obtains its excess energy as the result of collisions with other molecules, energy conversion during molecular collisions plays an exceptionally important role in the kinetics of chemical reactions. Energy conversion is also the basis of *thermal relaxation* of gases, i.e. the basis of those processes which determine the equilibrium distribution of energy between molecules in a system disturbed from the equilibrium state by rapid change in temperature or by chemical reaction and so on.⁽¹⁾ Moreover, since activation energy is predominantly a vibrational energy and also owing to the specific nature of processes connected with transformation of vibrational energy during molecular collisions (see below), the processes of conversion of vibrational energy or processes connected with the transformation of various forms of energy into vibrational energy are particularly important. For this reason we must pay particular attention to the problem of vibrational energy transformations during molecular collisions. However, we must first consider briefly the transformation of translational and rotational energy.

§21. Transformation of Translational and Rotational Energy

Conversion of Translational Energy into Translational and Internal Energy

We shall consider first the interconversion of translational energy. The transfer of energy of translational motion during molecular collisions without change in the form of the energy takes place in accordance with the laws governing the collisions of elastic spheres. It follows from these laws that in the simplest case of *direct impact* of a rapidly-moving particle of mass m_1 on a stationary particle of mass m_2 , the fraction $\Delta K/K$ of energy transferred to the stationary particle on impact is

$$\frac{\Delta K}{K} = \frac{4m_1m_2}{(m_1+m_2)^2}. \quad (21.1)$$

Thus the amount of energy transferred depends on the masses of the colliding particles. The most favourable case for energy transfer occurs

⁽¹⁾ The thermal relaxation of gases has been considered from the point of view of energy transfer during molecular collisions by Shuler [1095, 957, 1137], Brout [457] and others. For literature, see [1136].

when the masses of both particles are the same. With direct impact and equal masses, $\Delta K/K = 1$ and hence in this case the fast particle transfers all its energy to the stationary particle. If, on the other hand, m_1 and m_2 differ considerably, the amount of energy transferred is small. Actually when $m_1 \ll m_2$, we obtain from formula (21.1) $\Delta K/K = 4m_1/m_2 \ll 1$, and when $m_1 \gg m_2$, $\Delta K/K = 4m_2/m_1 \ll 1$.

The amount of energy transferred in an oblique impact is naturally less than that transferred in a direct impact. On average it is

$$\frac{\overline{\Delta K}}{K} = \frac{2m_1m_2}{(m_1+m_2)^2}, \quad (21.2)$$

i.e. half the energy transferred by direct impact.

Owing to the large difference between the mass of an electron and the mass of any molecule, an electron may undergo a large number of collisions with gas molecules without marked loss of energy, as is in fact observed. When electrons are passed through a gas, the molecules of which may only collide elastically with electrons of a given velocity, then the velocity of the electrons is practically unchanged. On the other hand, fast molecules, arising in the gas by some means, very quickly lose their energy during collisions with other molecules, especially with molecules of the same sort. For this reason the relaxation time of translational energy of molecules, i.e. the time in which statistical equilibrium (corresponding to Maxwellian distribution of molecular velocities) is established in a monoatomic gas, is equal or close to the mean interval between two consecutive molecular collisions (4×10^{-10} sec in air at normal temperatures and pressures).

When considering the process of transfer of energy of translational motion during collision of molecules treated as elastic spheres, detailed

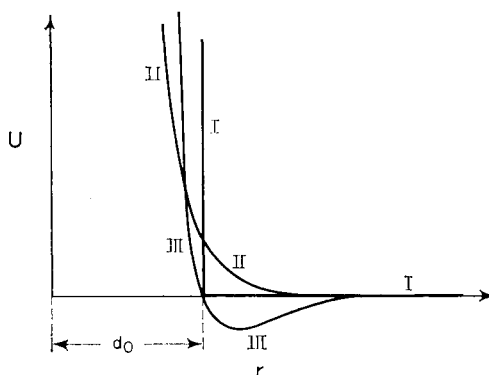


FIG. 66. Potential energy curves for colliding particles.

assumptions are not usually made about the mechanism of impact. According to this treatment the potential energy of a system of two colliding particles is the function of the distance r between their centres, illustrated by Fig. 66 (curve I). For distances greater than d_0 , the distance between the centres of the particles at the moment of impact, there is no interaction between the particles; consequently the potential energy is zero. At the moment of impact repulsive forces arise and the potential energy sharply increases. In fact the repulsive forces do not increase discontinuously but gradually, since actual molecules are not solid spheres but electrical systems and their force fields do not have sharp boundaries. However, the increase in the repulsive forces usually takes place very rapidly corresponding to the actual curves for the potential energy of colliding particles (curves II and III).

Whereas during elastic collision of solid spheres the quantity d_0 is defined precisely, during the collisions of atoms or molecules such a strictly defined quantity does not exist. The values of d determined experimentally using formulae from the kinetic theory of gases are certain mean values which characterize the distances at which there is a considerable change in the velocities of the colliding molecules when they come together.

When there are forces of attraction between gas molecules (curve III, Fig. 66) the quantity d is a certain definite function of temperature. If $V(r)$ is the potential of the attractive forces with r the distance between the centres of the molecules, and u and u_0 are the relative velocities of the molecules at a distance r and at infinity respectively, then from the law of the conservation of energy we may write

$$\frac{1}{2}\mu u^2 = \frac{1}{2}\mu u_0^2 + V(r),$$

where $\mu = m_1 m_2 / (m_1 + m_2)$ is the reduced mass. Writing u^2 as the sum of two components, one parallel with the radius-vector and the other perpendicular to it,

$$u^2 = \dot{r}^2 + r^2\dot{\phi}^2$$

(a dot denotes a differentiation with respect to time) and noting that according to the law of the conservation of angular momentum $r^2\dot{\phi} = u_0 d$, where d is the impact parameter (the minimum distance between the centres of the molecules at the moment of their closest proximity in the absence of attractive forces between them), we may write the equation of conservation of energy in the form

$$\frac{1}{2}\mu \dot{r}^2 + \frac{1}{2}\mu u_0^2 d^2/r^2 = \frac{1}{2}\mu u_0^2 + V(r).$$

If at the position of closest proximity (in the presence of attractive forces),

$r_{\min} = d_0$, then since $\dot{r} = 0$ here, we obtain from the foregoing expression

$$\frac{d^2}{d_0^2} = 1 + \frac{V(d_0)}{\frac{1}{2}\mu u_0^2}$$

or, as the mean value u_0^2 is proportional to the temperature T , taking $2V(d_0)/\mu u_0^2 = C/T$, we find

$$d = d_0(1 + C/T)^{1/2}. \quad (21.3)$$

It follows from formula (21.3) that the mean collision diameter tends to d_0 when $T \rightarrow \infty$.

Experiments show that the constant C (Sutherland's constant) is 50 to 300°K for various gases. Thus, in the presence of attractive forces the mean collision diameter of molecules is a decreasing function of temperature.

As in the interchange of translational energy, the amount of translational energy converted into *internal* energy of the colliding molecules is a function of their masses (more precisely, of the ratio of the masses). By internal energy we mean the rotational and vibrational energy of molecules or the energy of their electronic excitation. Owing to the conservation of motion of the centre of gravity of the system, the conversion of translational energy into internal energy is limited to the energy of *relative* translational motion. Thus, writing the initial energy of the colliding particles as the sum of this energy of relative motion and the energy of motion of the mass centre of the system (cf. p. 142)

$$K = \frac{1}{2}m_1c_1^2 + \frac{1}{2}m_2c_2^2 = \frac{1}{2}\mu u^2 + \frac{1}{2}(m_1 + m_2)C^2$$

(c_1 and c_2 are the velocities of the particles; C is the velocity of the centre of gravity) we obtain the following condition which limits the amount of energy converted into internal energy E of the system (in the case of direct impact the equality sign holds):

$$\beta = E/K \leq \frac{\frac{1}{2}\mu u^2}{\frac{1}{2}m_1c_1^2 + \frac{1}{2}m_2c_2^2} = \frac{(c_1 - c_2)^2 m_1 m_2 / (m_1 + m_2)}{m_1 c_1^2 + m_2 c_2^2}. \quad (21.4)$$

In the case of most practical interest when a fast particle collides with a slow one and when $c_2 = 0$, expression (21.4) becomes

$$\beta \leq \frac{m_2}{m_1 + m_2}. \quad (21.5)$$

Consequently, in the most favourable case, when all the kinetic energy of relative motion is converted into internal energy (direct impact),

$$\beta = \frac{m_2}{m_1 + m_2}. \quad (21.5a)$$

It follows from (21.5) that the larger the mass m_2 of the slow particle compared with the mass m_1 of the fast particle, the larger is the part of the

latter's energy which may be converted into internal energy. In the limit, when m_1 may be neglected in comparison with m_2 , for example in the collision of a fast electron with a molecule (since $m_1/m_2 = m_{\text{el}}/m_{\text{mole}} = 1/1840M < 1/1840$, where M is the molecular weight), we obtain $\beta = 1$, i.e. practically all the energy of the fast particle may be converted into internal energy of the slow molecule. The measurement of excitation and ionization potentials of atoms and molecules in the electron impact method is based on this fact.

Conversion of Translational and Rotational Energy

We shall now consider the conversion of translational energy into rotational energy of the colliding molecules. When rotation is excited the relative translational momentum (which is not zero for oblique impact) is partially, or in the most favourable case completely, converted into angular momentum. The results obtained by applying the conservation laws to the excitation of rotation, within the limits of classical mechanics, i.e. neglecting quantization of rotational motion, were analysed in detail by Beutler and Rabinowitsch [391] and by Oldenberg [992].

The process of conversion of translational energy into rotational energy may be made clear by considering the process as similar to the impact of elastic spheres. This method does not require additional assumptions regarding the impact mechanism.



FIG. 67. Transformation of rotational energy during molecular collision.
Mechanical model.

Representing the molecule as a system of two interconnected solid spheres, it is easy to see that when particle A (Fig. 67a) strikes an atom of the molecule M perpendicular to the axis of the molecule, the molecule begins to rotate. The amount of translational energy converted into rotational energy will depend (as in the case of elastic impact) on the ratio of the masses of the colliding particle and the atom undergoing collision. If these masses are identical the conversion of energy will be greatest; on the other hand, when the masses differ greatly the conversion will be small. In this way, for example, in the collision of an electron with a molecule the amount of its energy that may be converted into rotational energy of the molecule is very small from this mechanical point of view. The reverse process of conversion of rotational energy into translational energy (Fig. 67b) must be quite similar.

Assuming that a similar mechanical treatment is valid for the interconversion of translational energy as for its conversion into rotational energy, the considerable efficiency of simple mechanical impact would lead to the conclusion that the probability for translational-rotational conversion (and vice versa) in collisions of molecules with other molecules or atoms is of the same order of magnitude as translational interconversion.

A large probability of conversion of translational energy into rotational energy during gas-kinetic molecular collision is also evident from the following general considerations. Considering the collision of a molecule M and an atom A, we conclude that the probability of excitation of rotational levels of M on account of the energy of the relative translational motion of A and M will be small while the duration of collision τ is large in comparison with the period of rotation, i.e. if $\tau\nu \gg 1$, where ν is the frequency of rotation. In view of the fact that the duration of collision must be a quantity of order d/u (d is the distance between particles M and A at the moment of impact and u is the velocity of their relative motion), the foregoing inequality may be rewritten

$$d\nu/u \gg 1. \quad (21.6)$$

Multiplying numerator and denominator by $2\pi I = 2\pi\mu r_0^2$, where I is the moment of inertia of the molecule M, μ is its reduced mass and r_0 is the equilibrium distance between its constituent atoms (which is about the same as d), and noting that the angular momentum $2\nu I$ of the rotating molecules is of the order of h , we may further rewrite (21.6) in the form

$$\lambda/2\pi r_0 \gg 1, \quad (21.7)$$

where $\lambda = h/\mu u$, the de Broglie wave length. Since the opposite inequality, i.e. $\lambda \ll r_0$, usually holds (with the exception of the lightest molecules at low temperatures), it follows that the condition for low probability of conversion of translational energy into rotational energy (21.7) is fulfilled only in rare cases, i.e. that the probability of excitation of rotational levels during molecular collision on account of translational energy is large.

As we shall see below, this conclusion does not always correspond to reality, especially if we compare the probability of exchange of translational and rotational energy with the probability of transfer of translational energy (without change in form of energy), since frequently the probability of excitation of rotational levels is one power of ten, and in certain cases several powers of ten, less than the probability of interchange of translational energy. We may conclude from this that a simple mechanical treatment of the exchange process of translational and rotational energy must be of limited applicability. The reason for this is the quantum nature of the rotational motion of molecules.

The conversion of translational into internal energy (and vice versa)

during molecular collision has been considered by a series of authors using quantum-mechanical methods. The main difficulty in theoretical treatment is the absence of an expression for the potential energy of the interaction of colliding particles which is at the same time both precise and sufficiently simple. For this reason more or less crude approximations must be used.

In the absence of chemical interaction the potential energy of two atoms a distance X apart may be expressed approximately by the following formula due to Lennard-Jones [869]

$$U = U_{\min} \left[\left(\frac{X_0}{X} \right)^{12} - 2 \left(\frac{X_0}{X} \right)^6 \right], \quad (21.8)$$

where U_{\min} and X_0 are respectively the energy of interaction and the distance between the atoms at the potential-energy minimum. This expression includes both attraction at large distances and repulsion at short distances. Landau and Teller [169] have shown that the attractive forces acting at large distances do not directly affect the probability of conversion of translational energy into internal (here vibrational) energy. Therefore, as a rule, we may limit ourselves to a consideration of only the repulsive forces which may be represented by an exponential function

$$U = C \exp(-\alpha X) \quad (21.9)$$

more conveniently than by a power function as in (21.8). Here the quantity α^{-1} may be considered as an effective radius of the influence of the repulsive forces. In practice this radius is considerably less than the interatomic distance in the molecule [1126]. Therefore formula (21.9) may also be used in the case of collision of two molecules (which do not have a very high kinetic energy) by taking into account the interaction of only those atoms (in each molecule) which are nearest.

We shall consider the interaction of two diatomic molecules. When the molecules lie on a straight line at the moment of collision their energy will be the energy of interaction of two atoms. Instead of the quantity X it is more convenient in this case to introduce the distance r between the centres of gravity of the molecules. If s and s' are the distances between the atoms in each molecule, we may write

$$X = r - \lambda s - \lambda s',$$

where λ and λ' are constants depending on the ratio of the masses of the atoms in each molecule. Substituting this expression in (21.9) we may rewrite it in the form

$$U = U_0 \exp[-\alpha(r-r_0)] \exp[+\lambda(s-s_0)] \exp[+\lambda'(s'-s'_0)]. \quad (21.10)$$

Here U_0 is the energy of interaction of the molecules when $s = s_0$, $s' = s'_0$ and $r = r_0$ and s_0 and s'_0 are the equilibrium bond lengths of

A—B and A'—B', r_0 is the least distance between atoms A and A' on collision of the molecules, which is determined by the condition

$$U_0(r_0, s_0, s'_0) = \frac{1}{2}\mu u_0^2$$

(u_0 is the initial velocity of the relative motion of the molecules before collision, μ is their reduced mass). According to this condition r_0 depends on the initial velocity of the particles and consequently on temperature.

If the stretching of the bonds $s—s_0$ and $s'—s'_0$ is small then (21.10) may be written

$$U = U_0 \exp[-\alpha(r-r_0)][1+\lambda(s-s_0)][1+\lambda'(s'-s'_0)]. \quad (21.11)$$

The parameter α in this formula satisfies the relation $1/\alpha = 0.2$ to 0.3 \AA for a large number of gases [1125].

For a non-linear configuration of the colliding molecules, it is necessary to introduce a dependence of U on orientation as well as on the variables r and s . In the simplest case of the collision of a symmetric diatomic molecule with an atom, it is possible to express the energy of interaction on the basis of (21.9), as (see Fig. 68)

$$U = C[\exp(-\alpha X_1) + \exp(-\alpha X_2)]. \quad (21.12)$$

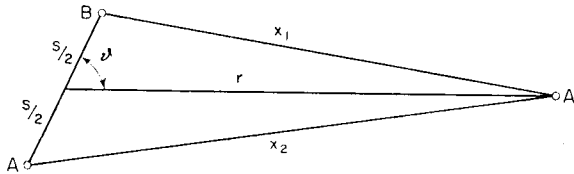


FIG. 68. Coordinates of an AB molecule colliding with an A' atom. s is the interatomic distance in the AB molecule.

The distances X_1 and X_2 are clearly related to r and s by the equations

$$X_1 = (r^2 + \frac{1}{4}s^2 - rs \cos \vartheta)^{1/2}, \quad (21.13a)$$

$$X_2 = (r^2 + \frac{1}{4}s^2 + rs \cos \vartheta)^{1/2}, \quad (21.13b)$$

where ϑ is the angle between the axis of the molecule and the direction of the line joining the atom and the centre of gravity of the molecule. If the relative velocity of the atom and molecule is not very large we may assume $s/r < 1$, and expand expressions (21.13) into a series in powers of s/r . Limiting ourselves to the first term of the series and substituting the results in (21.12) we find

$$U = U_0 \exp(-\alpha r)[\exp(c \cdot \cos \vartheta) + \exp(-c \cdot \cos \vartheta)] \quad (21.14)$$

where $c = \frac{1}{2}\alpha s$. Expanding (21.14), we find

$$U = U_0(1 + b^2 \cos^2 \vartheta) \exp(-\alpha r). \quad (21.15)$$

Here the quantity b^2 may be regarded as a measure of the deviation of the interaction potential from spherical symmetry.

An expression of the form of (21.15) was used by Zener [1331] to calculate the probability of conversion of translational into rotational energy during the collision of a rigid symmetric diatomic molecule with an atom. The calculations were made using a method, subsequently known as the method of distorted waves (see above, p. 205 *et seq.*), assuming that the rotation occurs in one plane. Zener found that exchange of translational and rotational energy takes place as a rule with great ease.

Somewhat later Roy and Rose [1094] used a quantum-mechanical calculation to show that the effective cross section corresponding to the conversion of rotational energy into translational energy⁽²⁾ during collision of two hydrogen molecules must be greater than 10^{-18} cm^2 ; hence the probability P (calculated per collision) for this process is found to be greater than 10^{-3} , which is in good agreement with experiment (see below). The same problem was solved by Brout [456] using expression (21.15); in this study of the collision of the molecules the angle ϑ for each of them was introduced (see Fig. 68); the terms in $\cos^2\vartheta$ were expressed as spherical harmonics which considerably simplifies the calculations. From Brout's calculation it follows that the probability of conversion of two rotational quanta into energy of translational motion during the collision of an H_2 molecule in the rotational level $J = 2$ (*para*-hydrogen), or of a molecule in the level $J = 3$ (*ortho*-hydrogen), with another hydrogen molecule is, respectively, $P_{2,0} = 3.04 \times 10^{-3}$ and $P_{3,1} = 2.96 \times 10^{-3}$, i.e. on average 3.0×10^{-3} (at room temperature). These calculations are in agreement with the most precise of the known experimental values for P obtained by Zartmann [1323] from measurements of the dispersion of sound in hydrogen, namely $P = 3.3 \times 10^{-3}$.

Similar values for P are obtained from measurements of the absorption of sound in hydrogen [1239] and also from measurements of relaxation time in hydrogen using the shock-tube method [815, 706]. See also [1187, 1240]. In contrast with Brout's calculation, Beckerle's calculation [368] starting from function (21.14) and a simplified model of collision gives values for P which differ by one to one and a half powers of ten from the measured values. In Beckerle's opinion this discrepancy results from the simplified nature of his chosen model.

Brout [455] also calculated the probability of conversion of rotational into translational energy during molecular collision for other diatomic molecules. To represent P for heavy molecules (with molecular weight greater than 20) he obtained the approximate formula:

$$P = \frac{1}{2}(r_0/d_0)^2, \quad (21.16)$$

(2) Below (p. 355) it will be shown that the probabilities of conversion of translational energy into rotational energy and vice versa are of the same order of magnitude.

where r_0 is the equilibrium distance between the atoms in the molecule and d_0 is the mean gas-kinetic diameter. Substituting in formula (21.16) $r_0 = 1.2 \text{ \AA}$ and $d_0 = 3.6 \text{ \AA}$ for O_2 , and $r_0 = 1.1 \text{ \AA}$ and $d_0 = 3.8 \text{ \AA}$ for N_2 , Brout obtains for these gases $P_{\text{O}_2} = 0.057$ (i.e. each 17th collision is effective) and $P_{\text{N}_2} = 0.043$ (each 23rd collision effective). These P values are in good agreement with those measured by a variety of methods. Thus measurement of the dispersion of ultrasonic waves in oxygen at room temperature gives $P = 0.033$ [1217]. This method [1332] and also the shock-tube method [706] give $P = 0.14$ for nitrogen, and measurements of the relaxation in a shock-wave front give $P = 0.05$ [699].⁽³⁾ Thus the values of P for nitrogen and oxygen are some ten times greater than for hydrogen and are of the order of 0.1.⁽⁴⁾ See also H. J. Bauer, H. O. Kneser and E. Sittig, *J. Chem. Phys.* **30**, 1119 (1959).

Near to room temperature the probability of conversion of translational into rotational energy is of the same order of magnitude as the probability of conversion of rotational into translational energy. Actually, it follows from the principle of detailed balancing, that

$$P_{J \rightarrow J'} n(J) = P_{J' \rightarrow J} n(J') n,$$

where $n(J)$ and $n(J')$ are the equilibrium numbers of molecules in rotational levels J and J' , and n is the total number of molecules. Substituting in this formula

$$n(J) = \frac{2J+1}{Z} \exp[-E(J)/kT] n$$

and

$$n(J') = \frac{2J'+1}{Z} \exp[-E(J')/kT] n$$

(E is the rotational energy and Z is the rotational partition function). we obtain

$$P_{J' \rightarrow J} / P_{J \rightarrow J'} = \frac{2J+1}{2J'+1} \exp[-\Delta E(J)/kT], \quad (21.17)$$

where $\Delta E(J) = E(J) - E(J')$.

Assuming that in the conversion of rotational energy into translation energy and vice versa one rotational quantum is involved, i.e. $J' = J - 1$, and that the quantum number J corresponds to the most probable rotational

⁽³⁾ See also [700]. Measurements of relaxation in a shock-wave front in hydrogen [700] give $P < 7 \times 10^{-3}$ and this is in agreement with the above value, $P = 3 \times 10^{-3}$.

⁽⁴⁾ In sharp contrast with these data are the data obtained by Parker and coworkers [1007] from measurements of the absorption of ultrasonic waves in N_2 and O_2 ; they found $P \approx 0.5$ for these gases. It should also be mentioned that the formula $\tau_{\text{rot}} = 1/ZP$ (τ_{rot} is the rotational relaxation time) used in experimental determination of P should not be considered to be convincingly established. This relationship should be considered the more reliable the greater the magnitude of the rotational quanta.

level for this temperature, so that

$$E(J) = kT,$$

we find

$$\frac{P_{J' \rightarrow J}}{P_{J \rightarrow J'}} = \frac{2J+1}{2J-1} \exp\left(-\frac{2}{J+1}\right). \quad (21.18)$$

Since near to room temperature the most probable values of J for molecules such as N_2 or O_2 are 10 or 11, it is not difficult to show from formula (21.18) that in this case $P_{J' \rightarrow J}$ is practically equal to $P_{J \rightarrow J'}$.

For hydrogen, which has $J' = J - 2$, a similar calculation gives $P_{0 \rightarrow 2} = 2P_{2 \rightarrow 0}$, i.e. the $P_{J' \rightarrow J}$ and $P_{J \rightarrow J'}$ values are again similar.

Comparing the probabilities for the transference of translational energy and the conversion of translational into rotational energy (and vice versa) we see that whereas the transference of translational energy occurs as the result of a few collisions, tens of collisions are necessary for the conversion of translational into rotational energy. Owing to the quantal nature of the rotational motion of molecules (as taken into account in quantum-mechanical calculation of the probability of exchange of rotational and translational energy during molecular collision), the simple mechanical treatment of the exchange process, which leads to similar probabilities for the conversion of translational and rotational energy into translational energy, is inadequate, generally speaking, and must be considered as a crude approximation which becomes less valid the larger the size of the rotational quanta exchanged. The decisive role of the quantal nature of rotational motion here is indicated by the fact that the greatest difference between the probabilities of these two exchange processes is observed for hydrogen which has the greatest size of rotational quanta:⁽⁵⁾ the transition from the level $K = 2$ to $K = 0$ and from $K = 3$ to $K = 1$ corresponds to a decrease in rotational energy of H_2 of 1.03 and 1.72 kcal respectively, whereas transition from the level $K = 11$ to $K = 10$ (see above) corresponds to a decrease in the energy of the N_2 and O_2 molecules of only 0.12 and 0.09 kcal respectively.⁽⁶⁾

According to Brout [455] the simplicity of his formula (21.16), and in particular the absence of a dependence of the probability of exchange of

(5) On the basis of a non-equilibrium distribution of rotational energy in the spectrum of excited hydroxyl OH , which is emitted by the inner cone of a methane-air flame, Brodia [446] concludes that the probability of conversion of rotational energy of excited hydroxyl into translational energy must be less than 10^{-4} . However, because there is water present in the flame zone and it has a strong quenching action [127] we consider Brodia's conclusion incorrect. In later work [451] Brodia gives $P = 0.007$ for the upper limit of the probability of conversion of rotational energy of excited hydroxyl into translational energy (under electric discharge conditions).

(6) We may assume that the probability of exchange of rotational and translational energy of N_2 and O_2 molecules in the $K = 1$ level, which corresponds to an energy of 0.01 kcal, is of the order of unity.

molecular translational and rotational energy (for molecular weights greater than 20) on temperature or on the mass of the colliding molecules may be explained in the following way. With increase in temperature the most probable value of J increases (see above), and consequently the gap between rotational levels (which is proportional to the number J) increases. This leads to a decrease in the probability of energy exchange. However, this effect is compensated by increase in the probability of exchange due to increase in the kinetic energy of the colliding molecules with rise in temperature. With regard to the lack of dependence of the probability of energy exchange on the mass of the molecules, the decrease in probability of exchange with increase in the molecular masses [1331, 1328] is compensated by the fact that the gap between rotational levels, and consequently the size of the rotational quantum exchanged, decreases so that, as we have seen above, the probability of exchange increases.

A certain hindrance to exchange of rotational and translational energy is also observed in polyatomic gases. Thus, Keller [828] notes that in gaseous ammonia and in nitrogen the ratio of his measured absorption coefficient for ultrasonic waves to the square of the frequency is somewhat higher than the classical value. Keller interprets this fact as an indication of hindrance to relaxation of rotational energy. See also [828a].

Spectroscopic Method of Studying Energy Conversion Processes in Molecular Collisions

The study of emission spectra of molecules undergoing collisions with foreign molecules is of considerable interest in relation to the experimental study of exchange processes of translational and rotational (and also vibrational) energy. The optical method of exciting spectra (fluorescence) is particularly convenient. Thus, at sufficiently low pressures, when the mean time between consecutive molecular collisions is much greater than the mean lifetime of the excited molecule (and also at sufficiently low temperatures), it is possible to obtain by optical excitation molecules in a definite vibrational (v') and rotational (J') level; consequently in the absence of collisions the fluorescence spectrum contains lines corresponding to transitions from these excited levels (v' and J'). An example of such a spectrum, which is called a *resonance* spectrum, is the fluorescence spectrum of iodine vapour shown in Fig. 69 (upper spectrum) [1320]. This spectrum, obtained by exciting I_2 molecules with the green line of mercury at $5460\cdot6$ Å, is a Deslandres v -series corresponding to transitions from the initially excited vibrational level $v' = 26$ to the levels of the ground state of the molecule, $v = 1, 2, 3, 4, 5, \dots$. Each band in this series consists of only two lines (doublet), corresponding to the transitions $J' = 34$ (the initially excited rotational level) $\rightarrow J = J' \pm 1$ (35 and 33).

When collisions do occur, if the excited molecule is capable of giving up

or obtaining vibrational and rotational quanta, new lines (as well as the doublets) appear which correspond to transitions from the changed excited levels ($v' \pm \Delta v'$ and $J' \pm \Delta J'$, where $\Delta v'$ and $\Delta J'$ are the numbers of vibrational and rotational quanta obtained or lost by the molecule). In this way, from observations of fluorescence spectra when collisions do occur it is possible to draw conclusions about the transfer of energy in these collisions. The above-mentioned character of the change in the fluorescence spectrum of iodine vapour in the presence of a foreign gas (helium) is shown by the middle spectrum of Fig. 69. The fluorescence spectrum of iodine vapour excited by white light is shown in the lower spectrum of Fig. 69.

By measuring the ratios of the intensities of lines appearing in the fluorescence spectrum when collisions occur, to the intensity of the initially excited lines, the probability of energy conversion during molecular collision may be determined if the number of collisions is known. In the case of collisions of an excited molecule with atoms, only conversion of vibrational and rotational energy into translational energy (and the reverse) is possible; in the case of collisions with molecules, conversion into rotational and into vibrational energy is also possible.

This method was used to investigate the transfer of energy for the molecules I_2 , S_2 [1318, 1315, 1320], Se_2 , Te_2 [1083] during their collision with molecules of different foreign gases, but the transfer of rotational energy has been studied only for I_2 [625, 1320]. It has been established that, in agreement with theory, a considerable number of rotational quanta may be given up on each collision⁽⁷⁾ (the number is always even since in the iodine molecule, which consists of identical atoms, even and odd rotational levels are in different symmetry classes and transitions between them are forbidden both in the absorption and emission of light and during collisions). Quantitative estimates show that the probability of conversion of rotational energy into translational energy (and the reverse) is large; the effective cross section is of the order of the gas-kinetic cross section. Owing to the small size of the rotational quanta of the excited iodine molecule (0.165 J cal)⁽⁸⁾ this result is quite natural, since in this case the quantal nature of rotational energy must play a relatively small role. It has also been shown that the probability of transfer of rotational energy in the collision of excited I_2 molecules with N_2 molecules is greater than in collision with H_2 molecules or He atoms. If we assume

⁽⁷⁾ From Fermi's calculations [608] it follows that during the exchange of translational and rotational energy the excitation of any number of rotational quanta may be observed.

⁽⁸⁾ As previously, by size of the rotational quantum we mean the difference in energy between two adjacent rotational levels. As in the I_2 molecule only even levels are combined with even and odd with odd, here the quantity of energy exchanged must be $0.165(2J-1)$, i.e. about twice the size of the quantum corresponding to J .

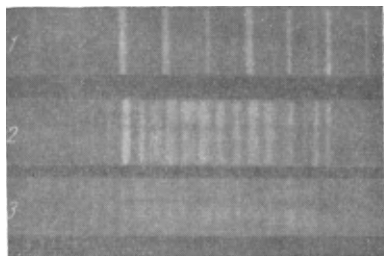


FIG. 69. The fluorescence spectrum of iodine vapour (according to Wood and Franck [1318]). (1) The fluorescence of iodine vapour with monochromatic excitation; two resonance series are observed (the weaker is excited by the yellow line of mercury); (2) the fluorescence spectrum with the same excitation but in the presence of He (2 mm Hg); (3) the fluorescence spectrum with excitation by white light.

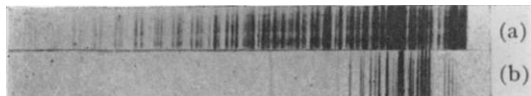
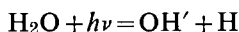


FIG. 70. The hydroxyl OH band at 3064 \AA in the discharge spectrum of water vapour (a), and of water vapour with helium present (b). According to Oldenberg [993, 994].

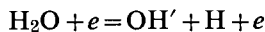
that a mechanical treatment of the process of inelastic collision is possible, then this result may be explained by using the theory of impact of elastic spheres, according to which the probability of translational-rotational conversion and of rotational-translational conversion is larger, the lower the difference in the masses of the colliding particles.

On the basis of these ideas Beutler and Rabinowitsch [391], and also Oldenberg [992], attempted to explain anomalies in the distribution of intensity observed in the spectrum of HgH. According to these authors, the anomalies may be explained by assuming that the HgH molecule loses its rotational energy relatively slowly on collision with nitrogen molecules, and this follows from the considerable difference in mass of an H atom (rotation of an HgH molecule is in effect the rotation of an H atom round the heavy atom of Hg) and an N₂ molecule (see Fig. 67b; in this case A represents a nitrogen molecule which is struck by the H atom rotating in the HgH molecule). The rotational quantum of HgH in the ground state is 0.031J kcal and in the excited state is 0.038J kcal. At room temperature the most probable value of *J* is 5 and so the most probable quantity of energy exchanged will be 0.15 to 0.20 kcal; this is not small enough for the energy exchange on collision of HgH and N₂ molecules to be considered as a simple mechanical process. For this reason we think it more correct in this case to ascribe the slowness of exchange of energy to the largeness of the amounts converted, without invoking a mechanical treatment of the process. If the mean gas-kinetic diameter of HgH and N₂ molecules is 4 Å (the distance between Hg and H atoms in the HgH molecule is 1.74 Å) then from formula (21.16) we find *P* = 0.1.

Let us take another example. A rich rotational structure is observed in the fluorescence spectrum of hydroxyl excited by exposing water vapour to Schumann ultraviolet radiation and also in the discharge spectrum of water vapour, i.e. in the excitation of OH in the processes



(optical excitation) and



(excitation by electron impact). Calculation on the assumption that the rotational energy in the excited OH molecules is distributed according to Boltzmann's law shows that the "rotational temperature" of hydroxyl is about 10,000°. It can be shown that the high "rotational temperature" in this case is a consequence of the excited OH molecules formed in the dissociation of H₂O and occupying high rotational levels [127]. The hydroxyl OH' band at 3064 Å which Oldenberg [996] obtained in the discharge spectrum of water vapour is shown in Fig. 70a. Figure 70b shows the same band obtained by Oldenberg by discharge in water vapour with helium present (helium pressure 20 mm Hg). In the latter case the

“rotational temperature” of the band is 670°K. Such a sharp difference in the intensity distribution between rotational lines in the OH band results from conversion of rotational energy of the OH' molecules into translational energy on collisions with He atoms.⁽⁹⁾ Calculation of the probability of energy conversion in this case gives for the cross section of effective collisions a quantity of the order of the gas-kinetic cross section.⁽¹⁰⁾

We shall not dwell here on other experimental methods for studying energy exchange during molecular collisions. Some of these methods (for example, the method of dispersion and absorption of sound) will be considered below in connection with vibrational energy conversions. Descriptions of other methods may be found in the scientific literature: here we particularly have in mind the shock-tube method [815] and shock-wave method [505, 699, 700].

In conclusion we should note that recently, in an investigation of the dispersion of ultrasonic waves in methyl alcohol CH_3OH vapour, an indication was obtained that there is an effect resulting from internal rotation of the CH_3OH molecule (about the C—O axis) [570]. The probability P for exchange of rotational and translational energy, deduced from a measured relaxation time of 2.27×10^{-9} sec, is about 0.04.

§22. Transformation of Vibrational Energy

The Conversion of Translational into Vibrational Energy and Vice Versa

Turning to the study of the interconversion of translational and vibrational energy, we shall begin with a mechanical picture of this process as shown in Fig. 71a. Whereas for translational-rotational energy transfer the most profitable direction of impact is perpendicular to the axis of the molecule (Fig. 67a), for the excitation of vibrations the most profitable impact is along the axis of the molecule (Fig. 71a). The amount of energy converted in this case must also depend on the mass-ratio of the colliding particles. For the reverse process of vibrational-translational energy transfer (Fig. 71b) it must be realized that energy conversion from the vibrational phase may only take place when most of the vibrational energy is in the form of kinetic energy, i.e. during only part of the vibrational period [997].

The transition-state method also gives a clear picture of energy conversion. It was shown earlier (§11) that this method may be used to solve the

⁽⁹⁾ A similar effect was detected by Terenin and Neuimin [214] in the fluorescence spectrum of hydroxyl.

⁽¹⁰⁾ This result is in sharp contrast with Broida and Kane's calculation of the probability for energy exchange on collision of an excited hydroxyl molecule with a helium atom [451]. Since in Lyman's experiments [894] an equilibrium distribution of rotational energy in the spectrum of hydroxyl is not reached even with a helium pressure of 50 cm Hg, they conclude that P must be less than 10^{-4} in this case. As shown above (p. 356), the reason for the low P values must lie in the neglect of the quenching action of H_2O .

problem of the form of the activation energy and of the energy of the reaction products in the simplest case of chemical interaction of an atom with a diatomic molecule. A similar method may be applied to the problem of energy conversions of colliding particles not undergoing chemical change. If the energy of the particles is not sufficient to surmount the potential-energy barrier, collision does not lead to reaction but may result in energy conversion. A possible case of energy exchange is shown in

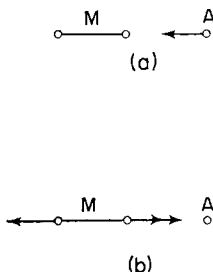


FIG. 71. Conversion of vibrational and translational energy during molecular collision. Mechanical model.

Fig. 36 (p. 169). Here the dotted line with arrows represents the trajectory of the representative point, and as the initial part of the trajectory (the close approach of the particles) is parallel to the corresponding coordinate axis, it shows that the initial energy of the system is in the form of translational energy. According to the potential-energy surface of the system, corresponding to Fig. 36, the representative point after closest approach of the particles moves with a zigzag trajectory and hence the collision has converted a certain amount of the initial energy into vibrational energy of the molecule taking part in the collision. If the colliding molecule has some vibrational energy the reverse case to that in Fig. 36 is possible (with the motion of the representative point opposite to the sense represented by the arrow).

The above ideas clearly show the possibility of translational-vibrational energy conversion (and vice versa) but do not give any indication how probable it is. Theoretical and experimental studies of this type of energy conversion show that its probability is different for molecules with low and high energies. We shall consider first energy-exchange processes for the collision of molecules with low energy. In particular, these processes include vibrational-translational energy conversion during the collision of a molecule having one vibrational quantum ($v = 1$) with a non-vibrating ($v = 0$) molecule or with an atom. For quantitative estimation of the probability of this process we may use the condition of low probability of the energy conversion (21.6) where v is a vibrational frequency in this case.

Substituting in (21.6) $v = 3 \times 10^{13} \text{ sec}^{-1}$ (1000 cm^{-1}), $d = 3 \times 10^{-8} \text{ cm}$ and $u = 3 \times 10^4 \text{ cm/sec}$ (the reduced mass of the colliding molecules is about $20m_H$, where m_H is the mass of an H atom) as for room temperature, we obtain

$$vd/u = 30 \gg 1,$$

and hence, in contrast with rotational-translational energy conversion (p. 351), vibrational-translational energy conversion is a *process of low probability*.

For energy exchange during gas-kinetic collisions of molecules (21.6) may be rewritten in the following form. Introducing the vibrational amplitude⁽¹¹⁾

$$a \approx (\hbar/\pi\nu\mu)^{1/2}$$

(μ is the reduced mass of the vibrating molecule) and taking

$$\frac{1}{2}\mu'u^2 = kT$$

(μ' is the reduced mass of the colliding molecules), we obtain from (21.6)

$$\frac{d}{2\pi a} \left(\frac{\mu' h\nu}{\mu kT} \right)^{1/2} \gg 1. \quad (22.1)$$

The inequality (22.1) is to be preferred to (21.6) since the temperature-dependence of the probability criterion is shown in a clear form.

An approximate quantitative solution for the probability of vibrational-translational energy conversion during molecular collision was given by Zener [1328, 1331] for energy exchange between a nitrogen molecule in the first vibrational level ($v = 1$) and a helium atom. Zener used the function (21.11) with $s' = s_0 = 0$, in accordance with the conditions of the problem. Using the method of distorted waves (see p. 205 *et seq.*) the probability of transition of an A'B' molecule from the vibrational state with quantum number v to the state with quantum number $v+1$ for the one-dimensional case (all three atoms lying on a straight line) is determined by the formula [cf. (13.24)]:

$$P_{v \rightarrow v+1} = \frac{m^2}{h^4} \left| \int_0^\infty dr \int ds U(r, s) \chi_p(r) \chi_{p'}^*(r) \psi_v(s) \psi_{v+1}(s) \right|^2 \quad (22.2)$$

where $m = m_A(m_{A'} + m_{B'})/(m_A + m_{A'} + m_{B'})$. If the vibrations of an isolated molecule may be considered as harmonic then ψ_v and ψ_{v+1} in equation (22.2) will be eigenfunctions of a harmonic oscillator. The functions $\chi_p(r)$ and $\chi_{p'}(r)$ correspond to incident and scattered waves

⁽¹¹⁾ This expression is obtained by equating the energy of a classical vibrator $E = \frac{1}{2}(2\pi\nu)^2\mu a^2$ to the quantity $h\nu$.

respectively and must be determined from equations similar to (13.22) and (13.23), Chap. 3. Since in (21.11) $\lambda(s-s_0) \ll 1$, in these equations the matrix elements for the potential energy may be taken as

$$U_{v,v} \approx U_{v+1,v+1} \approx U_0 \exp[-\alpha(r-r_0)].$$

Accordingly the functions χ_p and $\chi_{p'}$ are determined from the equations

$$\left[\frac{\hbar^2}{2m} \frac{d^2}{dr^2} + \frac{p^2}{2m} - U_0 \exp[-\alpha(r-r_0)] \right] \chi_p(r) = 0 \quad (22.3)$$

and

$$\left[\frac{\hbar^2}{2m} \frac{d^2}{dr^2} + \frac{p'^2}{2m} - U_0 \exp[-\alpha(r-r_0)] \right] \chi_{p'}(r) = 0, \quad (22.4)$$

where p and p' are the momenta of the system before and after collision. Using the χ functions calculated from these equations and the eigenfunctions of a harmonic oscillator, Zener obtained the following expression for the probability of transition from the vibrational state $v+1$ to the state v :

$$P_{v+1 \rightarrow v} = \frac{\pi^2 m U_0}{16m^*} \frac{v+1}{E_{v+1} - E_v} \left(\frac{p}{p'} \right)^{\sqrt{(4mU_0/\alpha^2)}}, \quad (22.5)$$

where $m^* = m_A \cdot m_B / (m_A + m_B)$; E_v and E_{v+1} are the energies of the $A'B'$ molecule in the v th and $(v+1)$ th vibrational states respectively. Hence, according to Zener, the probability $P_{1 \rightarrow 0}$ of the process

$$N_{2(v=1)} + He = N_{2(v=0)} + He,$$

is 6×10^{-8} (at room temperature).⁽¹²⁾

Zener also calculated the probability of transfer of a vibrational quantum on collision of one nitrogen molecule with another without conversion into other forms of energy, i.e. the probability of the process

$$N_{2(v=1)} + N_{2(v=0)} = N_{2(v=0)} + N_{2(v=1)},$$

which he estimated to be about 10^{-5} . Zener showed that the probability of this process decreases sharply with deviation from energy resonance, i.e. when passing from identical molecules to molecules with different vibrational quanta. Thus, according to his calculations, a deviation from resonance of 0.01 eV (0.23 kcal) leads to a fifty-fold decrease in the transfer probability for a vibrational quantum. It may be concluded from this that in the absence of resonance the probability of transfer of a vibrational quantum and the probability of its conversion into translational energy should not differ widely.

⁽¹²⁾ In making this calculation, Zener assumed that $\alpha = 2.14$, $(p/p')^2 = 1/8$, $mU_0 = 58$ and $m^*(E_1 - E_0) = 274$.

Certain authors have developed further the quantum-mechanical theory of conversion processes of vibrational (and also rotational) energy during molecular collision. Schwartz, Slawsky and Herzfeld [1126] have proposed a generalization of Zener's calculations for the collision of two rigid molecules using a one-dimensional model. On the basis of the function (21.11) and using the method of distorted waves they calculated the probability for transition from the first vibrational level to the zeroth level ($P_{1,0}$) for pure gases and binary mixtures; these values differ from the experimental probabilities by a factor of ten. However, the averaging of the cross-section on the basis of a three-dimensional and not a one-dimensional distribution of velocities made the calculation self-contradictory. If the appropriate corrections are introduced, as Schwartz and Herzfeld showed [1125], better agreement with the experimental data may be obtained using the one-dimensional model. Moreover it has been shown by successive averaging that the one-dimensional treatment of the vibrational deactivation of molecules gives approximately the same result as that obtained by a three-dimensional treatment.

Zener's method was first extended to "three-dimensional" collision by Castellan and Hulbert [481] and later by Curtiss and Adler [514] and Schwartz and Herzfeld [1125]. The latter authors used three dynamic variables r , θ and s , in the calculation with the three-dimensional model, but assumed that the energy of interaction is not a function of the angle θ and that the molecules remain in one plane throughout. Schwartz and Herzfeld defined the angle θ as the angle between the line joining the centres of gravity of the molecules in their arbitrary configuration and the line connecting these centres at the closest approach of the molecules.

Table 28 shows values calculated by Schwartz and Herzfeld and measured values for $P_{1,0}$ the probability of conversion of one vibrational quantum into translational energy (calculated per collision), i.e. the probability of a process similar to one shown on p. 363 (the energy exchange on collision of a nitrogen molecule with a helium atom). It can be seen from this table that in the first four cases the calculations give the right order for $P_{1,0}$. Oxygen and nitrogen are exceptions, but the large difference between calculated and measured values of $P_{1,0}$ (two powers of ten) in the case of nitrogen must clearly be attributed to the fact that here the measured value was obtained for nitrogen containing 0.05 per cent water. The divergence of theory and experiment in the case of oxygen must apparently be attributed to inaccuracy in the theoretical value [430a]. According to the latest measurements [406b], at 288°K, $P_{1,0}$ is 4×10^{-8} , in agreement with Table 28. See also H. S. Glick and W. H. Wurster, *J. Chem. Phys.* 27, 1224 (1957) and M. Salkoff and E. Bauer, *J. Chem. Phys.* 30, 1614 (1959).

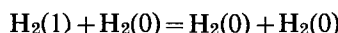
TABLE 28

Calculated and measured values for $P_{1 \rightarrow 0}$ the probability of conversion of a vibrational quantum into translational energy during molecular collision (according to Schwartz and Herzfeld [1125])

Colliding molecules	$T^{\circ}\text{K}$	$P_{1 \rightarrow 0}$	
		Calculated	Measured
$\text{CO}_2 + \text{CO}_2$	288	1.1×10^{-5}	2.0×10^{-5}
$\text{CO}_2 + \text{H}_2$	288	5.7×10^{-3}	2.0×10^{-3}
$\text{Cl}_2 + \text{Cl}_2$	288	0.9×10^{-5}	3.0×10^{-5}
$\text{Cl}_2 + \text{N}_2$	288	3.7×10^{-5}	2.3×10^{-5}
$\text{O}_2 + \text{O}_2$	288	2.3×10^{-9}	4.6×10^{-8}
$\text{N}_2 + \text{N}_2$	600	1.7×10^{-10}	3.0×10^{-8}
$\text{O}_2 + \text{N}_2$	288	2.0×10^{-8}	—
$\text{N}_2 + \text{H}_2$	600	10^{-5}	—

Tanczos [1209] has applied the method of Schwartz, Slawsky and Herzfeld [1126] to polyatomic molecules. He calculated relaxation times [see formula (22.17)], among other constants, corresponding to vibrational-energy exchange for CH_4 , CH_3Cl , CH_2Cl_2 , CHCl_3 and CCl_4 ; in the case of CH_4 and CH_3Cl satisfactory agreement was obtained between calculated and measured values (for example, for methane CH_4 the calculated relaxation time is 2.86×10^{-6} sec and the measured value is 1.3×10^{-6} sec). In the remaining three cases calculated and measured values differ by a factor of about ten. It is essential to note that as well as the simple process of dispersion of one vibrational quantum, i.e. the conversion of one quantum into translational energy of the colliding molecules, Tanczos also considered the more complex process of the simultaneous change of the vibrational state of both colliding molecules involving two or three quanta in the exchange. He found that it is necessary to allow for exchange of three quanta in the case of CH_2Cl_2 , CHCl_3 and CCl_4 . For the increase of probability for vibrational energy exchange due to participation of two and more quanta see also B. H. Mahan, *J. Chem. Phys.* **62**, 100 (1958).

The calculation of the probability of conversion of a vibrational quantum of the H_2 molecule into translational energy on its collision with an H atom is also interesting. According to Bauer's calculations [362, 363], in this case $P_{1 \rightarrow 0}$ is 10^{-3} to 10^{-4} . Bauer based his calculations on the method he developed for the calculation of the probability of inelastic collision of molecules, using potential functions which, in contrast with (21.11), have a minimum.⁽¹³⁾ The $P_{1 \rightarrow 0}$ value corresponding to process



⁽¹³⁾ These functions were proposed by Evett and Margenau [583].

was calculated by M. Salkoff and E. Bauer, *J. Chem. Phys.* **29**, 26 (1958) for various energies of colliding molecules. It follows from these calculations that for $T = 1130^\circ\text{K}$ $P_{1,0} = 10^{-4}$ (the relaxation time being $\tau = 4 \times 10^{-6}$ sec). This value is probably considerably too high.

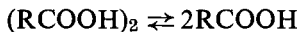
Among other studies of the quantum-mechanical treatment of the process of inelastic collision of molecules [1206, 1207, 1208, 795, 513, 328], we should mention that of Aroeste [328] who used a Born approximation to calculate the probability of excitation for each of the three normal vibrations of the F_2O molecule during its collision with an Ne atom. He found that the lower the frequency of the excited vibrational quantum the more easily is it excited. We should also mention the work of Kerner [829], who also used a Born approximation to calculate the angular distribution in inelastic dispersion of symmetrical diatomic molecules during their collision with other similar molecules (the excitation of vibration and rotation).

Experimental Studies of Vibrational-Energy Conversion. Dispersion and Absorption of Ultrasonic Waves

We shall consider first, studies of the dispersion and absorption of sound in relation to vibrational and translational energy exchange. It follows from Einstein's theory of the propagation of sound in polyatomic gases that at sufficiently high sound frequencies, when the relaxation time is greater than the period of acoustic vibrations, the gas deviates from the equilibrium state on the passage of sound [566]. This causes sound dispersion, which is expressed as a dependence of the sound propagation velocity on the sound frequency, and an anomalous absorption of sound by the gas which differs from normal (classical) absorption both in size, being greater than the classical value by 10 to 100 times, and in a different dependence of the absorption coefficient on the frequency of the sound.

Dispersion and absorption of sound, explicable in terms of a final relaxation time, are also observed in gases in which chemical reaction is possible, leading to the establishment of equilibrium, for example, the equilibrium $\text{X}_2 \rightleftharpoons 2\text{X}$ in a dissociating gas. It has been shown that by measuring the velocity and absorption coefficient of sound, the rate constant and heat of a chemical reaction may be determined. Thus Richards and Reid [1071] studied the dispersion of sound in N_2O_4 and measured the dissociation rate of this gas, i.e. the rate of the reaction $\text{N}_2\text{O}_4 \rightarrow 2\text{NO}_2$. Later this method was proposed for study of the kinetics of fast reactions [521] and of reactions in solution. The method has since been used to study the kinetics of the association of acetic CH_3COOH and propionic $\text{C}_2\text{H}_5\text{COOH}$ acids in the liquid phase, and to determine the rate constant

and activation energy for dissociation processes of the dimer $(RCOOH)_2$ and the heat of reaction corresponding to the equilibrium



[628]. It is also possible to calculate rate constants (and certain other constants) for processes of formation and decomposition of molecular complexes in gases on the basis of acoustic measurements [157]. The literature relating to the study of kinetics and chemical equilibria using acoustic measurements may be found in the articles of Tabuchi [1204] and Damköhler [521].

Here we are interested only in gases whose thermal equilibrium is completely determined by the distribution of energy between various degrees of freedom of molecules of fixed composition. Since experiment and theory show unambiguously that translational-energy exchange between molecules occurs as a result of a few gas-kinetic collisions, and that interchange of rotational and translational energy also occurs (with few exceptions, for example, H_2) as a result of a small number of collisions, it follows that persistence of non-equilibrium states of the gases considered may be ascribed only to delay in the exchange of molecular vibrational energy, i.e. to a hindrance of vibrational-translational and vibrational-rotational energy interconversion.⁽¹⁴⁾ The idea of a hindrance to conversion of vibrational energy into other forms of energy during molecular collision was first suggested by Herzfeld and Rice [755] and is a basis of their theory of the dispersion and absorption of sound, which will now be described.

If τ is the mean or "relaxation" time required to excite vibrational degrees of freedom of a molecule by means of translational energy during molecular collision, and C_{vib} is the molecular heat capacity corresponding to vibrational degrees of freedom, we may take

$$C_{vib}^{(t)} = C_{vib}[1 - \exp(-t/\tau)] \quad (22.6)$$

where $C_{vib}^{(t)}$ is the vibrational heat capacity (for incomplete excitation), at a time t after fast particles appear in a given volume element of gas. A time equal to the half-period of the vibrations is available for complete excitation of the vibrational heat capacity. If this time, i.e. the time for adiabatic compression of the gas, is greater than τ , as is observed at *low* sound frequencies (ω), then $C_{vib}^{(t)}$ will not differ much from C_{vib} , the fully-excited vibrational heat capacity. In this case, in Laplace's formula for the velocity c of sound at pressure p and density ρ , namely

$$c = \sqrt{(yp/\rho)}$$

⁽¹⁴⁾ See Richards' review [1070], where uses of the method of ultrasonic dispersion and absorption in various fields are also examined.

($\gamma = C_p/C_v$, the ratio of heat capacities C_p at constant pressure and C_v at constant volume) we write $C_v = C = C_a + C_{\text{vib}}$, where C_a is the heat capacity of the gas at constant volume after deduction of the vibrational heat capacity. This gives (as $C_p = C_v + R$) for the velocity c_0 of sound

$$c_0 = \left[\frac{p}{\rho} \left(1 + \frac{R}{C_a + C_{\text{vib}}} \right) \right]^{1/2}. \quad (22.7)$$

At high frequencies, when the half-period of vibrations is less than τ , the heat capacity $C_{\text{vib}}^{(t)}$ will be practically zero, i.e. all the energy contained in the given element of gas will be in the form of translational and rotational energy; then c_∞ the velocity of sound has the limiting form

$$c_\infty = [(p/\rho)(1 + R/C_a)]^{1/2}. \quad (22.8)$$

This corresponds also to the case of "adiabatic" expansion of a gas.

The quantities c_0 and c_∞ , (22.7) and (22.8), represent two asymptotes to the dispersion curve corresponding to the general expression for the velocity of sound, which is obtained as a result of solving the wave equation describing the propagation of sound and has the form

$$c = \left\{ \frac{p}{\rho} \left[1 + R \frac{(C + R) + (C_a + R)\tau^2\omega^2}{C(C + R) + C_a(C_a + R)\tau^2\omega^2} \right] \right\}^{1/2}. \quad (22.9)$$

It is not difficult to see that in the two limiting cases when $\omega = 0$ and when $\omega = \infty$, this formula gives (22.7) and (22.8) respectively. The curve of c against ω corresponding to formula (22.9) is S-shaped. If c^2 is plotted as ordinate and $\ln \omega$ as abscissa, then with these coordinates the point of inflection of the S-shaped curve occurs when the frequency $\omega = \bar{\omega}$, where

$$\bar{\omega} = \frac{1}{\tau} \left[\frac{C(C + R)}{C_a(C_a + R)} \right]^{1/2}. \quad (22.10)$$

Substituting this value of $\bar{\omega}$ in formula (22.9), we obtain the corresponding value

$$\bar{c}^2 = \frac{p}{\rho} \left(1 + R \frac{C + C_a}{2CC_a} \right) = \frac{c_0^2 + c_\infty^2}{2}. \quad (22.11)$$

In this way we see that the point of inflection of the dispersion curve (with coordinates c^2 , $\ln \omega$) lies midway between the asymptotes, and that the curve is symmetrical with respect to both asymptotes (c_0 and c_∞).

The solution of the wave equation also leads to an expression for the sound absorption coefficient μ in the well-known formula

$$I = I_0 \exp(-\mu x),$$

where I is the intensity of sound in a plane wave at a distance x (in wave lengths) from the source of sound; I_0 is the intensity when $x = 0$. The parameter μ is

$$\mu = \frac{2\pi R C_{\text{vib}} \tau \omega}{C(C+R) + C_a(C_a+R)\tau^2 \omega^2}. \quad (22.12)$$

It follows from this that the maximum value of the absorption coefficient is

$$\mu_{\text{max}} = \frac{\pi R C_{\text{vib}}}{C(C+R)} \left[\frac{C(C+R)}{C_a(C_a+R)} \right]^{1/2}. \quad (22.13)$$

The absorption maximum corresponds to the value $\omega = \bar{\omega}$ as in (22.10), so that the position of the absorption maximum coincides with the point of inflection of the dispersion curve. It may be concluded from this that both absorption and dispersion of sound arise from the same cause—a hindrance to vibrational-energy conversion during molecular collisions of the gas which is characterized by the quantity τ . This quantity is unambiguously related to the probability of this energy conversion and may be calculated from the frequency $\bar{\omega}$, which is found from the position of the point of inflection on the dispersion curve or from the position of the absorption maximum.

Let n be the number of vibrating molecules in unit volume, N_0 the total number of molecules in unit volume, $Z_{0 \rightarrow 1}^0$ the frequency of molecular collisions (per molecule) leading to excitation of one quantum of vibrational energy of the molecule by means of the translational energy of the relative motion of the colliding molecules, and $Z_{1 \rightarrow 0}^0$ the frequency of collisions corresponding to the reverse process. Then we may write⁽¹⁵⁾

$$dn/dt = Z_{0 \rightarrow 1}^0 N_0 (N_0 - n) - Z_{1 \rightarrow 0}^0 N_0 n. \quad (22.14)$$

Integrating this equation, we obtain

$$n = N [1 - \exp\{-N_0 t (Z_{0 \rightarrow 1}^0 + Z_{1 \rightarrow 0}^0)\}] \quad (22.14a)$$

(N represents the equilibrium concentration of vibrating molecules) and hence from the obvious relation

$$n/N = C_{\text{vib}}^{(t)} / C_{\text{vib}},$$

⁽¹⁵⁾ At the temperatures of almost all investigations carried out on the dispersion and absorption of sound there can be excitation of only one vibrational quantum. For this reason the processes of energy exchange under consideration are processes connected with the conversion of *one* quantum; this lets us in our subsequent calculation confine ourselves to a consideration of the interaction of only two vibrational states of the molecule ($v = 0$ and $v = 1$). The general case for any number of states has been treated in various papers. For literature see Brout [457].

and from equation (22.6), we find

$$\tau = 1/[N_0(Z_{0 \rightarrow 1}^0 + Z_{1 \rightarrow 0}^0)]. \quad (22.15)$$

The quantities $Z_{0 \rightarrow 1}^0$ and $Z_{1 \rightarrow 0}^0$ are interrelated; for, from the equilibrium condition $dn/dt = 0$, we have

$$\frac{Z_{0 \rightarrow 1}^0}{Z_{1 \rightarrow 0}^0} = \frac{N}{N_0 - N} = \frac{g_1}{g_2} \exp(-h\nu_{\text{vib}}/kT). \quad (22.16)$$

Here g_1 and g_0 are statistical weights of the vibrating and non-vibrating molecules (usually $g_1 = g_0$) and ν_{vib} is the frequency of natural vibrations of the molecule.

Since at these temperatures the quantity $h\nu_{\text{vib}}$ is generally several times larger than kT , we may, to a first approximation, neglect $Z_{0 \rightarrow 1}^0$ in comparison with $Z_{1 \rightarrow 0}^0$ and write equation (22.15) more simply

$$\tau = 1/(Z_{1 \rightarrow 0}^0 N_0). \quad (22.17)$$

If $Z_{1 \rightarrow 0}^0$ is expressed in the form (19.10), namely

$$Z_{1 \rightarrow 0}^0 = P_{1 \rightarrow 0} 2d^2(\pi RT/M)^{1/2}, \quad (22.18)$$

the factor $P_{1 \rightarrow 0}$ may be defined as the probability of conversion of one vibrational-energy quantum into energy of translational (or rotational) motion (calculated per collision). The reciprocal $1/P_{1 \rightarrow 0}$ is, therefore, the average number of collisions which the vibrating molecule must suffer before its vibrational energy is converted into translational energy. Consequently, measurement of τ enables us to find the probability $P_{1 \rightarrow 0}$ and, on the basis of (22.16), to find $P_{0 \rightarrow 1}$ the probability of vibrational excitation since the ratio $Z_{0 \rightarrow 1}^0/Z_{1 \rightarrow 0}^0$ may be replaced by $P_{0 \rightarrow 1}/P_{1 \rightarrow 0}$. The results of such measurements for various gases are shown in Table 29.

The third column of Table 29 shows the vibrational frequencies of the corresponding molecules (the lowest frequencies in the case of triatomic and more complex molecules). The dependence of the probability P on the size of the vibrational quantum is clearly indicated in the table: in similar molecules (O_2 and Cl_2 , CO_2 , COS and CS_2 , CH_4 and its halogen derivatives) *the probability P increases with decreasing vibrational frequency*. A similar regularity has been established in other cases [863, 615]. For this purpose, the frequency in Table 29 characterizing the size of the most easily converted vibrational quantum is taken to be the lowest frequency of each polyatomic molecule.

From the dependence of P on the frequency of the quantum converted, it would be expected that in tri- and polyatomic molecules, which have

TABLE 29

*The probability of excitation ($P_{0 \rightarrow 1}$) and loss ($P_{1 \rightarrow 0}$) of a vibrational quantum during collision of molecules of the same gas**

Gas	$T, ^\circ\text{C}$	ν, cm^{-1}	$P_{1 \rightarrow 0}$	$P_{0 \rightarrow 1}$	Method of investigation
O_2	15	1556	$4\text{--}6 \times 10^{-8}$	$2\cdot3 \times 10^{-11}$	Ultrasonic absorption and dispersion [847].
Cl_2	15	557	$2\cdot9 \times 10^{-5}$	$1\cdot9 \times 10^{-6}$	Ultrasonic dispersion [574].
I_2	—	213	$(3\cdot0 \times 10^{-4})$	—	Electric discharge [558]†
NO^\ddagger	20	1878	$3\cdot7 \times 10^{-4}$	$3\cdot7 \times 10^{-8}$	Ultrasonic absorption ††
CO_2	15	668	$2\cdot1 \times 10^{-5}$	$1\cdot6 \times 10^{-6}$	Ultrasonic dispersion [574].
COS	15	525	$1\cdot0 \times 10^{-4}$	$1\cdot0 \times 10^{-5}$	Ultrasonic dispersion [1103].
CS_2	30	397	$5\cdot2 \times 10^{-4}$	$1\cdot6 \times 10^{-4}$,
N_2O^{**}	20	589	$1\cdot8 \times 10^{-4}$	$1\cdot9 \times 10^{-5}$	Ultrasonic ".
SO_2	20	525	$1\cdot0 \times 10^{-3}$	$7\cdot6 \times 10^{-5}$	Ultrasonic absorption.
CH_4	30	1306	$2\cdot1 \times 10^{-4}$	$4\cdot6 \times 10^{-7}$	Ultrasonic dispersion [1132].
CH_3Cl	30	732	$1\cdot2 \times 10^{-3}$	$3\cdot9 \times 10^{-5}$,
CH_2Cl_2	30	704	$2\cdot1 \times 10^{-3}$	$7\cdot9 \times 10^{-5}$	"
CH_2Cl_2	30	283	$3\cdot2 \times 10^{-2}$	$8\cdot5 \times 10^{-3}$	"
CHCl_3	30	260	$9\cdot1 \times 10^{-3}$	$2\cdot7 \times 10^{-3}$	"
CCl_4	30	218	$8\cdot1 \times 10^{-3}$	$3\cdot0 \times 10^{-3}$	"
C_2H_4	15	810	$4\cdot0 \times 10^{-4}$	$7\cdot4 \times 10^{-6}$	Ultrasonic dispersion [935].

* Similar data are given in references [1088, 614] and elsewhere. See also reviews [844, 934a].

† The method used in reference [558] is based on the fact that when an electric discharge is passed through iodine vapour a non-equilibrium concentration of I_2 molecules in the first vibrational level ($v = 1$) is observed. Absorption-spectrum measurement of the concentration of these molecules, at various times after the discharge has ceased, makes it possible to determine the thermal relaxation time and consequently the quantity $P_{1 \rightarrow 0}$ for the iodine molecules.

White [1281] used a similar method to obtain CN radicals in the $v = 1$ state in the presence of argon. Detection (by their absorption spectrum) of these radicals, in the presence of a quantity of argon such that during the lifetime (3×10^{-3} sec) of CN in the $v = 1$ state they undergo about 10^4 collisions with argon atoms, is a clear indication that in this case $P_{1 \rightarrow 0}$ must be less than 10^{-4} . The frequency corresponding to the first vibrational quantum of CN is $2042\cdot4 \text{ cm}^{-1}$.

‡ Robben [F. Robben, *J. Chem. Phys.*, **31**, 420 (1959)] has obtained the value $P_{1 \rightarrow 0} = 8 \times 10^{-4}$ as a result of investigating the vibrational relaxation in a shock tube at 500°K .

** According to [855], $P_{1 \rightarrow 0} = 1\cdot3_8 \times 10^{-4}$.

†† H. J. Bauer, H. O. Kneser and E. J. Sittig, *J. Chem. Phys.*, **30**, 1119 (1959).

several vibrational degrees of freedom corresponding to different frequencies, vibrational-energy exchange would be characterized by a corresponding number of P values and of relaxation times τ . Although the data in Table 29 (see also [320]) contradict this conclusion, its general validity can scarcely be doubted, since more detailed analysis of the available experimental data enables us to consider this contradiction as superficial and based on the inadequacy and low precision of these data.

Actually, in earlier papers on the processes of vibrational-translational energy conversion [575, 855] an identical relaxation time was found for both valence and deformation vibrations of triatomic molecules, including the CO_2 molecule for which P was found to be 2×10^{-5} (see Table 29). However in the more recent work of Pielmeier [1028] there are indications that two ultrasonic absorption maxima are present (according to the experimental data of Fricke [631], see Fig. 72): the main maximum is at

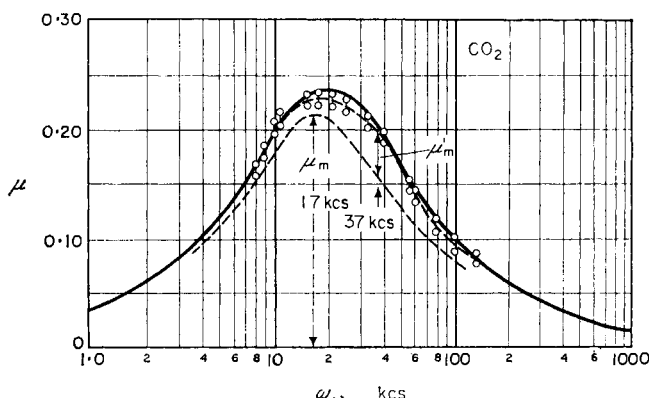


FIG. 72. Ultrasonic absorption in dry carbon dioxide (according to Pielmeier [1028]). The symmetrical broken curve with a maximum at 17 kc and the curve with a maximum at 37 kc give an over-all absorption curve which is in better agreement with the measured values for the absorption coefficient μ than is the simple symmetrical curve with one maximum (the continuous curve).

a frequency of 17 kilocycles per second and the other maximum (five times weaker) is at 37 kilocycles per second (at atmospheric pressure). According to Pielmeier the two relaxation times he detected correspond to a deformation and a valence vibration of the CO_2 molecule (at frequencies 668 and 1345 cm^{-1}).⁽¹⁶⁾ Two relaxation times have recently been found for SO_2 also [536b, 863a].

Different vibrational-excitation probabilities in a triatomic molecule for different vibrational degrees of freedom are also obtained from a

(16) These times correspond to $P = 2 \times 10^{-5}$ and 4.4×10^{-5} .

quantum-mechanical calculation of translational and vibrational-energy exchange during collision of F_2O molecules [328]. For CH_2Cl_2 , CHCl_3 and CCl_4 molecules, calculation [1209] gives two different relaxation times, i.e. two values for the probability of vibrational-energy conversion. In the case of CH_2Cl_2 , as will now be indicated, this result has received experimental support.

These data refer to experiments at 30°C and at this temperature the nine frequencies of the natural vibrations of the CH_2Cl_2 molecule—283, 704, 737, 899, 1155, 1266, 1429, 2984 and 3048 cm^{-1} —correspond to the respective vibrational heat capacities (at constant volume): 0.8626, 0.4246, 0.3937, 0.2623, 0.1263, 0.0894, 0.0529, 0.0001 and 0.0001 (in R units). Comparison of these heat capacities with the vibrational heat capacities 2.21, 0.86 and 0.00 calculated from measured values for the ultrasonic velocity c_0 , $c_{\infty 1}$ and $c_{\infty 2}$, referring to the two dispersion regions c_0 to $c_{\infty 1}$ and $c_{\infty 1}$ to $c_{\infty 2}$ in accordance with the two different values of P established for CH_2Cl_2 (see Table 29) shows that whereas in the low-frequency region the energy exchange involves almost all (seven out of nine) the vibrational degrees of freedom, in the ultrasonic high-frequency region only the lowest frequency (283 cm^{-1}) is involved. It is possible that the exceptional position of this frequency results from its relatively low value (the frequency 283 cm^{-1} is 2.5 times lower than the frequency closest to it, 704 cm^{-1}) which is unlike any frequencies in methane or in its other derivatives. Thus, the vibrational heat capacity of CCl_4 is $6.1188R$ at 30°C and is distributed between the nine degrees of freedom of this molecule in the following way: two degrees of freedom, corresponding to the two-fold degenerate vibration with frequency 218 cm^{-1} , have $1.8306R$; two three-fold degenerate vibrations with frequencies 305 and 775 cm^{-1} have heat capacities of $2.5263R$ and $1.0797R$ respectively and the one single vibration with frequency 460 cm^{-1} has $0.6822R$. It follows from these data that at 30°C all the vibrational degrees of freedom of CCl_4 play a comparable part in the heat capacity of CCl_4 and consequently they take part in the energy exchange during collisions of CCl_4 molecules. This does not exclude the possibility that owing to the similarity of the frequencies (adjacent frequencies differ by a factor of ~ 1.5), the ultrasonic dispersion regions corresponding to the excitation of the individual vibrations blend into one region.

Another explanation for the absence of several ultrasonic dispersion regions in CCl_4 and in similar cases is given by Lambert and Rowlinson [863], who suggest that in these cases vibrations corresponding to different natural frequencies have *the same probability* of being excited (or converted into other forms of energy) during molecular collision. According to these authors the same probabilities of excitation of different vibrations of a molecule indicate that in polyatomic molecules on collision the relative translational energy brings about primarily an excitation of vibration

corresponding to the most easily excited lowest frequency, and then this vibration energy is rapidly (with a very short relaxation time) passed to other vibrational degrees of freedom. The ease of intramolecular vibrational-energy exchange is accounted for by a strong coupling between the individual vibrations in the molecule [1088]. According to Schäfer [1103] several values for the relaxation time are observed when some but not all of the vibrations of the molecule are coupled.

Alexander and Lambert [313] have also detected three ultrasonic dispersion regions (and their corresponding absorption regions) in acetaldehyde vapour CH_3CHO ; this indicates that there are here three different P values (Fig. 73). The measured values of the quantity $\beta = 1/ZP$ (Z is

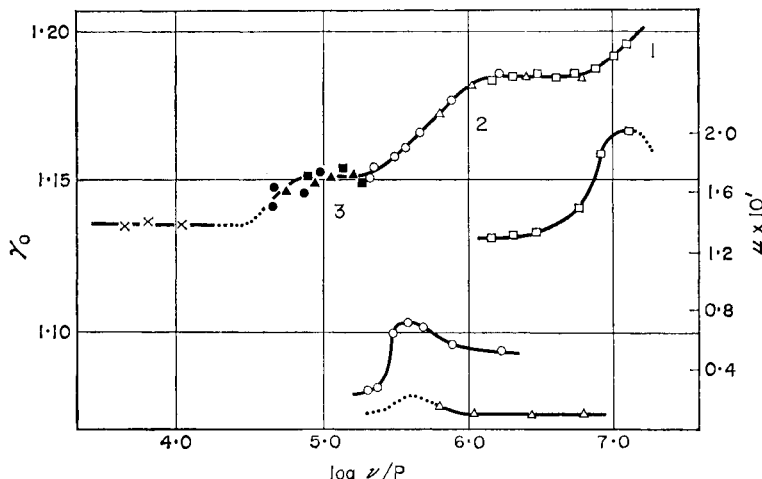


FIG. 73. Three ultrasonic dispersion regions in acetaldehyde CH_3CHO vapour—upper curve. The lower curves are for ultrasonic absorption (according to Alexander and Lambert [313]).

the total number of collisions of the vibrationally-excited molecule with other molecules in 1 cm^3 during 1 sec), with the assumption $h\nu_{\text{vib}} \gg kT$ (at room temperature), are equal to 1.3×10^{-8} , 4.6×10^{-7} and 3.7×10^{-6} sec respectively. In this way the probabilities of vibrational-energy conversion corresponding to different vibrational states have a total relative range of nearly 300 to 1 in this case. Alexander and Lambert relate the three different values of P to the three different types of bond in the CH_3CHO molecule: C—C, C—H and C=O.

It follows from the data of Table 29 that there is a distinct tendency for the probability of energy exchange to increase with the number of atoms in the molecule; this must be mainly a result of the increase in the number of vibrational degrees of freedom (which is $3N - 6$, where N is the number of atoms in the molecule).

Finally, from the data of Table 29 it follows that near room temperature $P_{1 \rightarrow 0}$, the probability of conversion of the energy of one vibrational quantum into translational energy, lies between 10^{-2} and 10^{-8} . From the above-mentioned dependence of P on the frequency of the quantum converted it should be expected that for molecules such as N_2 , CO , HCl and H_2 with particularly large natural vibrational frequencies ($\nu_{\text{N}_2} = 2330.7$, $\nu_{\text{CO}} = 2142.1$, $\nu_{\text{HCl}} = 2885.6$ and $\nu_{\text{H}_2} = 4154.7 \text{ cm}^{-1}$) $P_{1 \rightarrow 0}$, the probability of conversion of the energy of a quantum into translation energy, will be considerably less than 10^{-8} . It has already been noted that the experimental value of this quantity for nitrogen (Table 28, p. 365), which is 3×10^{-8} at 600°K , was obtained for moist nitrogen and therefore must be high. The theoretical value of $P_{1 \rightarrow 0}$ for nitrogen, according to the calculations of Schwartz and Herzfeld [1125], is 1.7×10^{-10} at 600°K and must be less than 10^{-12} at room temperature. Moreover, according to the calculations of de Wette and Slawsky [1279], the maximum values of $P_{1 \rightarrow 0}$ for CO and HCl (calculated for collinear collisions of the molecules, which corresponds to their maximum interaction), during collision with the lighter and the heavier atom of the vibrating molecule are respectively 6.1×10^{-9} and 3.4×10^{-9} (CO) and 5.2×10^{-9} and 5.7×10^{-12} (HCl). A considerably lower value for $P_{1 \rightarrow 0}$ would be expected for H_2 . Recently the vibrational relaxation time of CO has been measured at high temperatures [1301a, 700a]. Similar data have also been obtained for N_2 and O_2 [406a, 892a].

Certain authors have suggested that ternary collisions are important in connection with the low probability of vibrational-energy conversion in these processes. Thus, Walker [1258] proposed that the vibrational excitation of COS in its mixture with argon or nitrogen, in the experimental conditions of Eucken and Aybar [572], is due to the ternary collisions



However, since it has subsequently been shown [1259] that ternary collisions do not play a part in vibrational excitation of the N_2O molecule (which has a structure similar to that of COS) by collision with atoms of He , Ar , and also N_2 , Walker's conclusion seems doubtful.

The available experimental data on energy exchange in collisions of molecules in the electronic ground state do not adequately solve the problem of the probability of simultaneous conversion of two or more vibrational quanta. However, judging by the results obtained from study of energy exchange during collision of electronically-excited molecules (see below), the probability for conversion of several quanta must be *less* than the probability for conversion of one quantum. We should add that the probabilities $P_{1 \rightarrow 0}$ and $P_{2 \rightarrow 1}$, i.e. the probabilities for the processes

$M^*(v=1) + M = M(v=0) + M$ and $M^*(v=2) + M = M^*(v=1) + M$, must be of the same order of magnitude, since otherwise the dispersion region would be observed to be wider for a series of gases. This conclusion also follows from a theoretical consideration of the conversion of a vibrational quantum.

So far we have considered a pure gas. In a mixture of two gases A and B, the quantity τ is a certain over-all quantity which characterizes a mixture of given composition. However, it is not difficult to relate this quantity to the constants τ_{AA} and τ_{AB} which are determined by the probabilities for energy exchange in collisions of molecules A and A, and A and B (it is assumed that B+B molecular collisions do not affect the establishment of equilibrium). By relating these quantities to the pressure p of the mixture, and by denoting the partial pressures of the A and B components by p_A and p_B respectively, the total number of effective collisions suffered by the vibrating molecule A in one second, which is equal to $1/\tau$, may be written as the total of the number of collisions with A molecules and with B molecules, i.e.

$$\tau^{-1} = (p_A/p)/\tau_{AA} + (p_B/p)/\tau_{AB},$$

or, denoting the ratio p_B/p by b ,

$$\tau^{-1} = (1-b)/\tau_{AA} + b/\tau_{AB}. \quad (22.19)$$

In this way, knowing τ_{AA} (from measurements in the pure gas) and b , we may calculate from (22.19) the quantity τ_{AB} (τ is measured directly) and consequently the probability $P_{1 \rightarrow 0}$ of exchange of energy during collision of A and B molecules, which is related to τ_{AB} by equations similar to (22.17) and (22.18). Some of the data obtained by this method are shown in Table 30.

It is seen from Table 30 that there is a vast difference in the efficiencies of collisions of molecules, which indicates a well-defined specificity in the energy-exchange processes recalling the specificity of chemical interaction. This specificity forces us to reject any attempt at treating the energy-exchange process during molecular collision as a simple mechanical process. In particular, comparison of the efficiencies of collisions of $Cl_2 + CO$ and $Cl_2 + N_2$ satisfies us of this; in spite of the closeness of the masses of the atoms C, N and O and the similarity of other properties of carbon monoxide and nitrogen, collisions of CO molecules are about 200 times more efficient than collisions of N_2 molecules. Another example is the fact that during conversion of the vibrational energy of ethylene, D_2 is eight times less effective than H_2 , whereas the simple difference in the masses on substitution of H_2 by D_2 should only have given a decrease of less than two-fold in the efficiency of collisions (see also [713]). According to Richards [1069] the observed eight-fold difference is explained by the

TABLE 30

The mean number of collisions, $1/P_{1 \rightarrow 0}$, of vibrating molecules of oxygen, chlorine, carbon dioxide, nitrous oxide and ethylene with various molecules, leading to loss of one (the first) vibrational quantum at $20^\circ C$

X \ A	O ₂ [850]	Cl ₂ [574]	CO ₂ [574]	N ₂ O [574]	C ₂ H ₄ [1072]
He	165,000	900	1700 2600 [855]	1700 1000 [855]	— 2500
Ar	—	~32,000	47,000	—	—
H ₂	20,000	780	480 300 [855]	630	250
D ₂	—	—	—	440	2000
N ₂	100,000	43,000	35,000 [190]	—	5000 * [935]
O ₂	500,000	—	—	—	
CO	7700	230	230 [190]	3600	—
NO	—	—	260 [190]	—	—
Cl ₂	—	34,000	—	—	—
HCl	—	120	130	—	—
CO ₂	25,000	—	47,000 51,300 [190] 50,000 [855]	~5000	—
N ₂ O	—	—	—	5600 7500 [855]	—
H ₂ O	416?	—	40 60 [190] 105 [855]	60 105 [855]	85 [935]
H ₂ S	4160	—	—	—	—
O ₃	33,000?	—	—	—	—
NH ₃	385	—	—	450	—
C ₂ H ₂	1200	—	—	—	—
CH ₄	—	190	2400	840	—
CHCl ₃	7700?	—	—	—	—
CCl ₄	4160	—	—	—	—
C ₂ H ₄	—	—	—	—	2500 [935]
C ₂ H ₅ OH	118	—	—	—	—
C ₃ H ₈	—	—	—	—	2500
C ₆ H ₆	400	—	—	—	—

* Air.

fact that in the case of hydrogen preferential conversion of the vibrational energy of C₂H₄ into rotational energy of H₂ takes place.⁽¹⁷⁾

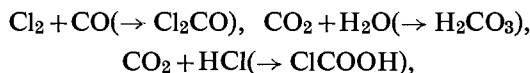
It may be concluded from the data of Tables 29 and 30 that when the colliding molecules have a dipole moment the probability of energy

⁽¹⁷⁾ A similar explanation for the different effects of H₂O and D₂O on the thermal relaxation of CO₂ in the presence of heavy and light water vapour has been shown to be incorrect [1133].

exchange is increased. The ease of energy exchange in the case of SO_2 in comparison with CO_2 , and also the high efficiency of collisions of the polar HCl and H_2O , lead to the same conclusion. However, the idea of a simple electrostatic interaction of the colliding particles is certainly not sufficient to explain the observed exchange of energy. This becomes clear if we compare the efficiencies of collisions of $\text{Cl}_2 + \text{CH}_4$ and $\text{Cl}_2 + \text{HCl}$ (see Table 30), as these are close in spite of the sharp difference in the polar properties of the CH_4 and HCl molecules; or if we compare the efficiencies of the collisions $\text{O}_2 + \text{H}_2\text{O}$, $\text{O}_2 + \text{NH}_3$ and $\text{O}_2 + \text{C}_6\text{H}_6$ which are identical, although the dipole moment of the C_6H_6 molecule is zero in contrast with the polar molecules H_2O and NH_3 .

In the last example, however, the possibility is not excluded that the high efficiency of H_2O , NH_3 and C_6H_6 is due to a *resonance effect*, the presence of which may be considered as established in the case of H_2O . Actually, according to Boudart [430a], the presence of a resonance effect in the conversion of a vibrating molecule of oxygen $\text{O}_2^*(v=1)$ into a non-vibrating molecule $\text{O}_2(v=0)$ in the presence of water may be seen as follows. In experiments with H_2O and D_2O it was established that the rate of the relaxation process increases in proportion to $(\text{H}_2\text{O})^2$ and to the first degree of (D_2O) concentration. This difference results from a high rate for the process $\text{O}_2^* + \text{H}_2\text{O} \rightarrow \text{O}_2 + \text{H}_2\text{O}^*$ which has a resonance character (the vibrational quanta of O_2 , $\nu = 1556 \text{ cm}^{-1}$ and of H_2O , $\nu_3 = 1595 \text{ cm}^{-1}$, differ only by 40 cm^{-1}), and consequently the subsequent slower process $\text{H}_2\text{O}^* + \text{H}_2\text{O} \rightarrow \text{H}_2\text{O} + \text{H}_2\text{O}$ is the limiting one. Resonance does not take place in the case of D_2O , where the frequencies of O_2 and D_2O ($\nu_2 = 1178 \text{ cm}^{-1}$) differ by about 400 cm^{-1} . Therefore, here the limiting process is $\text{O}_2^* + \text{D}_2\text{O} \rightarrow \text{O}_2 + \text{D}_2\text{O}^*$ with a rate proportional to (D_2O) .

We should also mention the idea of Franck and Eucken [623] that the physical process of energy exchange in a system of colliding particles should be considered as the start of a *chemical* process of molecular conversion. Therefore energy exchange should take place with particular ease in those cases where, in principle, the colliding particles are capable of reacting with each other. Such, for example, are the cases



etc., where a high efficiency for the collisions is actually observed (see Table 30). Figure 74, taken from Eucken and Becker's article [573], is a graphic illustration of Franck and Eucken's ideas (see also [572]).

It follows from these ideas that all factors favourable to chemical interaction of the colliding particles should assist the exchange of energy. These factors include electrostatic interaction of polar molecules, formation

of hydrogen bonds and also the effect of the number of atoms in the system of colliding molecules. The role of the last factor is that increasing the number of atoms increases the lifetime of the quasi-molecule formed by the colliding molecules and therefore increases their contact time, which assists the exchange of energy in the system, as this is in essence a redistribution of the internal energy of the quasi-molecule (see also [935]).

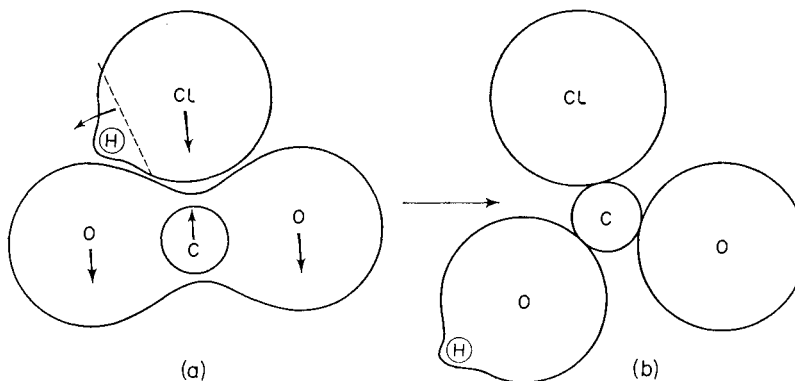


FIG. 74. The movement of atoms during collision of chemically-interacting molecules (according to Eucken and Becker [573]).

The viewpoint expounded here on energy-exchange processes was proposed earlier in another form during an examination of energy conversion in molecular collisions on the basis of the theory of absolute reaction rates (pp. 170-1), in which the initial stage in the energy-exchange process, and the initial stage of the chemical process, are described by the same trajectory of the representative point.⁽¹⁸⁾

An attempt to allow for the specific interaction of the colliding molecules in a quantum-mechanical treatment of the vibrational-energy exchange process was made by Widom and Bauer [1285] who used the method of calculation proposed earlier by Zener [1328]. With the assumption that the translational motion of the colliding particles may be treated as a purely classical motion in which the relative coordinates of the particles are considered as depending on a time parameter (and not as dynamic variables), they expressed the potential energy U for the interaction of the particles just as a function of the time t . Moreover for approximate calculations time-dependent perturbation theory may be used. According to this theory, the probability of the transition of a system from a state with

⁽¹⁸⁾ Gershinowitz also considered the energy-exchange process from this point of view [668]. See also Glasstone, Laidler and Eyring [57, p. 115].

energy E_0 to a state with energy E_n is [see (8.12)]

$$P_{0 \rightarrow n} = \hbar^{-2} \left| \int_{-\infty}^{+\infty} U_{0n}(t) \exp(it\Delta E/\hbar) dt \right|^2 \quad (22.20)$$

where $\Delta E = E_0 - E_n$ and

$$U_{0n} = \int \Psi_0 U \Psi_n^* d\tau.$$

Here Ψ_0 and Ψ_n are the wave functions for the initial and final states of the excited molecule. Since U depends on the relative coordinates, which are functions of time, U_{0n} is also dependent on t .

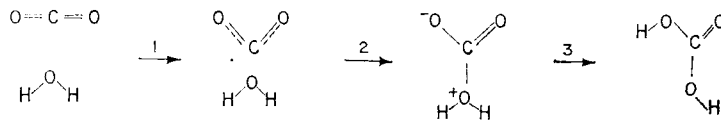


FIG. 75. Collision of H_2O and CO_2 molecules. A deformation of the CO_2 molecule, connected with the exchange of energy, takes place in stage 1; this stage is also the initial stage of the chemical process which in subsequent stages (2 and 3) is completed by the formation of the H_2CO_3 molecule [1285].

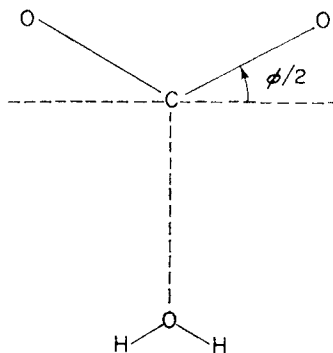


FIG. 76. Configuration of the complex $\text{H}_2\text{O} \cdot \text{CO}_2$ on collision of H_2O and CO_2 molecules [1285].

Widom and Bauer calculated the dependence of the potential energy U on the coordinates, for the system $\text{CO}_2 + \text{H}_2\text{O}$. They started from the assumption that during collisions the predominant orientation of the molecules is such that the C atom interacts directly with the O atom of the water molecule, so that on close approach of the water molecule the CO_2 molecule is deformed (Fig. 75, cf. Fig. 74). It is clear that in this case the energy of interaction will depend not only on the distance r between

C and O atoms but also on the angle φ between the initial bond axis O=C=O when $r = \infty$ and the direction of each of the bonds in the deformed CO₂ molecule on collision (Fig. 76).

Postulating a dependence $U(r, \varphi)$ which represents their assumed model, Widom and Bauer calculate r and φ as functions of t and, substituting these expressions in (22.20), they obtain a value for the cross section of inelastic collisions of CO₂+H₂O correct to within a factor of ten. An important defect of this calculation is the assumption that the energy of interaction of CO₂ and H₂O molecules has too deep a minimum, corresponding to an energy $\epsilon = 8$ kcal. However, Schwartz and Herzfeld [1125] have shown that consideration of the specific interaction of molecules does not require the assumption of such a strong molecular attraction since in their method the quantity ϵ appears in the expression for P in the index of an exponential $\exp(\epsilon/kT)$ and not as a multiplying factor as in Widom and Bauer's method. Nikitin [214b] has shown that if a more precise form of potential curve is used for the molecular interaction, this additional factor will have the form $\exp(\lambda\epsilon/kT)$, where $\lambda > 1$.

Temperature Dependence of the Probability of Vibrational-energy Conversion

Considering the energy-transfer process as the initial stage of a chemical process, we must expect in energy-transfer processes features characteristic of a chemical process. In particular, it might be supposed that the probability of energy transfer should increase with temperature, in accordance with the fact that energy-transfer processes should be connected with an *activation energy*, like chemical reactions. The increase in $P_{1 \rightarrow 0}$ with temperature has actually been detected in certain cases by Eucken and coworkers [574, 575] who studied the dispersion of sound in chlorine, carbon dioxide and nitrous oxide and in mixtures of these gases with other gases at different temperatures (see also [855]). Some of their results are shown in Table 31. In Fig. 77 the corresponding values of $\log P_{1 \rightarrow 0}$ are shown as functions of the inverse temperature. It is seen from Table 31 and Fig. 77 that in each case, save that of CO₂+H₂O, $P_{1 \rightarrow 0}$ increases with temperature. In two cases (N₂O+N₂O and CO₂+CO₂) this increase obeys the Arrhenius equation

$$P_{1 \rightarrow 0} = A \exp(-B/T) \quad (22.21)$$

quite satisfactorily. The slopes of the plots of $\log P_{1 \rightarrow 0}$ against $1/T$ give for the "activation energies" the values 1.3 kcal (N₂O) and 2.0 kcal (CO₂). In the remaining cases (with the exception of CO₂+H₂O), according to Eucken and Nümann [575], the quantity $P_{1 \rightarrow 0}$ may be expressed approximately by the formula

$$P_{1 \rightarrow 0} = A T^n \exp(-B/T). \quad (22.22)$$

TABLE 31

The temperature dependence of the mean number of collisions, $1/P_{1 \rightarrow 0}$

$A + X$ $t, {}^{\circ}\text{C}$	$\text{Cl}_2 + \text{Cl}_2$	$\text{Cl}_2 + \text{CO}$	$\text{N}_2\text{O} + \text{N}_2\text{O}$	$\text{N}_2\text{O} + \text{H}_2$	$\text{CO}_2 + \text{CO}_2$	$\text{CO}_2 + \text{H}_2\text{O}$
-32	60,000	390	—	—	—	—
-30	—	—	—	750	—	—
18	34,000	230	—	—	—	—
20	—	—	7500	650	57,000	105
74	18,000	130	—	—	—	—
100	—	—	4500	460	29,000	65
142.5	9000	80	—	—	—	—
195	—	—	—	290	—	—
200	—	—	3300	—	17,000	102
300	—	—	2500	—	10,000	150
400	—	—	2100	—	8000	250

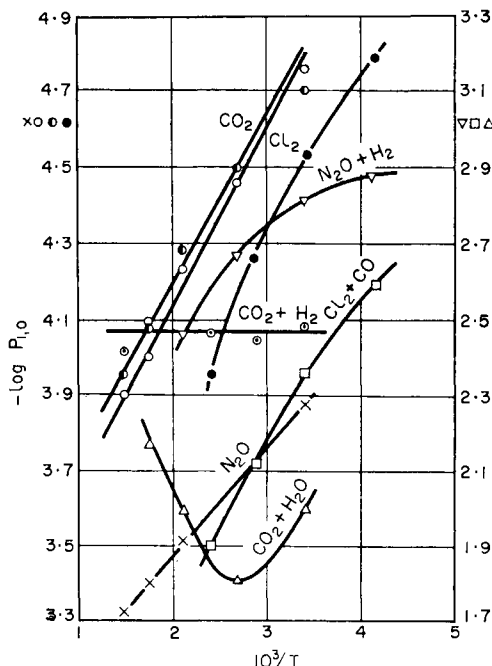
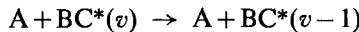


FIG. 77. The temperature dependence of the probability for conversion of a vibrational quantum into translational energy during molecular collision.

The temperature dependence of the probability of vibrational-translational energy conversion (and the probability of the reverse process) may also be obtained theoretically (see Jackson and Mott [798], Schwartz and Herzfeld [1125], and also Mott and Massey [193]). Thus, considering the inelastic collision of an atom A with a molecule BC and assuming that the interaction energy of these particles is⁽¹⁹⁾

$$V(r) = C \exp[-(r - \lambda s_0)/a] \quad (22.23)$$

Jackson and Mott [798] and also Zener [1331] and Devonshire [535] found that the probability for the process



is proportional to the vibrational energy of the BC molecule, $v\nu_{vib}$, and consequently to the vibrational quantum number v . The calculations of these authors show, moreover, that the probability of conversion of more than one quantum is considerably smaller than the probability of conversion of one quantum. Thus, the probability for the transition $v \rightarrow v-2$ is a hundred times less than the probability for the transition $v \rightarrow v-1$ (see also [328]). At normal temperatures the dependence of $P_{v,v\pm 1}$ on frequency may be written [798]

$$P_{v,v\pm 1} \sim v_{vib} [v + \frac{1}{2} \pm \frac{1}{2}] \exp(-4\pi^2 a v_{vib}/u). \quad (22.24)$$

This relationship is correct while $4\pi^2 a v_{vib}/u$ is considerably greater than unity, i.e. at not too high temperatures.

Assuming the Maxwell-Boltzmann distribution law, we find that the mean value of the exponential is⁽²⁰⁾

$$\frac{\int_0^\infty \exp(-4\pi^2 a v_{vib}/u) \exp(-\mu u^2/2kT) u^3 du}{\int_0^\infty \exp(-\mu u^2/2kT) u^3 du}. \quad (22.25)$$

⁽¹⁹⁾ Here it is assumed that at the moment of impact all three atoms are on a straight line, A...B—C, and consequently interaction between the extreme atoms A and C is neglected. Cf. formula (21.10). In (22.23) r is the distance between the nucleus of atom A and the centre of gravity of the molecule BC; s_0 is the distance between B and C atoms in the molecule BC; $\lambda = m_C/(m_B + m_C)$, where m_B and m_C are the masses of atoms B and C; a is the radius of influence of the forces of interaction of particles A and BC, which is of an order of magnitude 10^{-8} cm.

⁽²⁰⁾ Here the mean relative velocity $u = \frac{1}{2}(u_v - u_{v\pm 1})$ is identified with the velocity u_v before impact, which is quite permissible within the limits of accuracy of the calculation. Actually, calculating the ratio $(u_v - u_{v\pm 1})/(u_v + u_{v\pm 1})$, we may satisfy ourselves that under gas-kinetic conditions it is considerably less than unity and hence $u_v \approx u_{v\pm 1} \approx u$.

It is seen from this expression that the probability of energy exchange should be determined mainly by those relative velocities u which are close to u_0 , namely the velocity at which the index of the exponent in the numerator of the integrand

$$\frac{4\pi^2 a \nu_{\text{vib}}}{u} + \frac{\mu u^2}{2kT}$$

has a minimum. From the condition for a minimum, namely

$$u_0 = (4\pi^2 a \nu_{\text{vib}} k T / \mu)^{1/3},$$

we obtain by substituting this in the exponent

$$P_{v,v-1} \sim \exp \{ -3(2\pi^4 a^2 \nu_{\text{vib}}^2 \mu / k T)^{1/3} \}. \quad (22.26)$$

This form of dependence of the probability of conversion of a vibrational quantum was also obtained by Landau and Teller [169].

According to formula (22.26), the temperature dependence of P is expressed not by the Arrhenius equation but by a law in which $\ln P$ is a linear function of $T^{-1/3}$. By way of experimental support for (22.26) Massey and Burhop [924] quote certain data on the temperature dependence of $1/P$ for N_2O and CO_2 obtained by Eucken and coworkers. However it should be pointed out that these and other data on N_2O and CO_2 (in particular, more recent data of Eucken and Nümann [575] obtained over a temperature range of 380°) also satisfy the Arrhenius equation within experimental error, as is evident from Fig. 77. Therefore it must be considered an open question as to which law expresses the temperature dependence of P ; here we need better precision of both experimental data and theoretical calculations. It should be added that the calculations of Herzfeld and coworkers [1126, 1125], from which values of P for different temperatures may be obtained [1025], do not give the analytical expression for the dependence of P on temperature. From the results of these authors it follows that at high temperatures the dependence of P on T is stronger than at low temperatures, and that its character is approximately expressed by (22.21). We should also add that existing calculations do not explain the peculiar temperature dependence of P which has been established experimentally for certain mixtures including $\text{CO}_2 + \text{H}_2\text{O}$ and $\text{N}_2\text{O} + \text{H}_2$ (see Fig. 77). In the range of ν_{vib} values for which $4\pi^2 a \nu_{\text{vib}} / u \gg 1$, the probability $P_{v,v\pm 1}$ decreases with increasing frequency, as in formula (22.26).

It is possible to use the method of potential-energy curves, which has been successfully used to describe chemical processes, to describe and illustrate graphically processes of vibrational-energy conversion during molecular collision. Curves of such a type are shown in simplified form (in reality they are the trajectories of the representative point on the potential-energy surfaces) in Fig. 78; the lower curve corresponds to the interaction

of two non-vibrating molecules and the upper curve corresponds to interaction of a non-vibrating molecule and a vibrationally-excited molecule (here van der Waals forces are not taken into account). Since the forces of repulsion between two non-vibrating molecules are stronger than the forces of repulsion between a vibrating molecule and a non-vibrating molecule, the upper curve should rise less steeply; therefore the curves may intersect. Moreover since the probability of transition from the upper to the lower curve, corresponding to the process $M^*(v=1) + M(v=0) = 2M(v=0)$, should be important only when the curves are sufficiently close together, the energy of the colliding molecules should exceed a certain minimum value a (as is seen from Fig. 78), which clearly has the significance of an activation energy.

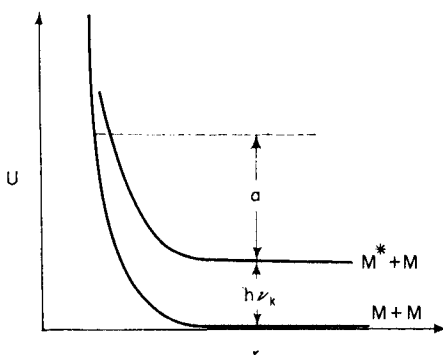
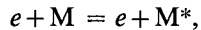


FIG. 78. Potential-energy curves corresponding to the interaction of two non-vibrating molecules (lower curve) and the interaction of a non-vibrating molecule with a vibrationally-excited molecule (upper curve).

At present the inadequacy of the experimental material does not allow us to say to what extent this idea of the nature of the temperature dependence of the energy-exchange probability is generally valid. However, these ideas are certainly of some value as a working hypothesis. In particular, on the basis of Fig. 78 it is possible to give a qualitative explanation of the peculiar temperature-dependence of $P_{1,0}$ which has been established for $\text{CO}_2 + \text{H}_2\text{O}$ (see Fig. 77). A possible explanation of this is that, with the increase in the relative velocity of the colliding molecules with increasing temperature, the duration of their interaction decreases, i.e. the lifetime of the quasi-molecule formed by them, decreases, which leads to a decrease in the energy-exchange probability. A similar effect is apparently observed in fluorescence quenching, which is connected with the conversion of energy of electronic excitation into other forms of energy which occurs on collision of electronically-excited atoms and molecules with other (unexcited) molecules [140].

Dissipation of Vibrational Energy under Electrical Discharge Conditions

We shall now consider the results of studies of the dissipation of the vibrational energy of molecules in an electric discharge. Terenin and coworkers [264, 62, 63] have shown that, under discharge conditions, vibrationally-excited molecules are formed as a result of collisions with slow electrons. With increasing gas pressure the intensity of the infrared bands⁽²¹⁾ tends to a certain limiting (maximum) value which may be explained as the result of "quenching", i.e. conversion of vibrational energy into translational and rotational energy on molecular collision. Accordingly, assuming that the following processes take place in the discharge zone:



we find that the intensity of the stationary glow (which is determined by the condition $dn^*/dt = 0$, where n^* is the concentration of vibrationally-excited molecules M^*) is expressed by

$$I = An^* = AkJn/(A + PZn),$$

where A is the probability of radiation, k is a quantity proportional to the cross section of vibrational excitation on electron impact, J is the current and n is the concentration of molecules in the discharge zone. It follows from this expression that the limiting (maximum) value for the intensity, which is determined by the condition $n \gg A/PZ$ (sufficiently high pressures), is

$$I_\infty = AkJ/PZ.$$

Substituting I_∞ in the expression for I we find

$$I_\infty/I = 1 + A/PZn. \quad (22.27)$$

At the basis of the deduction of formula (22.27), which was first obtained by Terenin and Neuimin [264], is the assumption that k (i.e. the cross section of vibrational excitation) does not depend on the gas pressure; and this holds only at sufficiently low pressures when the mean velocity of the electrons is constant. Using data obtained by Coblenz [492] from the glow discharge of CO and CO₂ at low pressures (0.25 to 5 mm Hg), Terenin and Neuimin showed that the data satisfy (22.27) quite well. They obtained $P = 1 \times 10^{-5}$ for CO from the known value $A = 50 \text{ sec}^{-1}$ for the probability of conversion (dissipation) of one vibrational quantum of

⁽²¹⁾ Here we are considering the radiation of one quantum, corresponding to one of the fundamental frequencies, since overtones and combined frequencies have low intensity in the discharge spectrum due to the low probability of radiation of these frequencies.

CO (fundamental frequency 2142 cm^{-1}) into translational or rotational energy on its collision with another CO molecule. Taking A for CO_2 as 100 sec^{-1} they found that the probability of dissipation of a vibrational quantum (in CO_2) corresponding to asymmetric vibrations of the CO_2 molecule (fundamental frequency 2349 cm^{-1}) is $P = 4 \times 10^{-6}$.

It should be mentioned that these figures differ considerably from the figures obtained later by Dodonova [62] using the same method: for $\text{CO}^* + \text{CO}$ she found 0.4×10^{-6} (instead of 1×10^{-5}) and for $\text{CO}_2^* + \text{CO}_2$, 5×10^{-5} (instead of 4×10^{-6}).

The $P_{1 \rightarrow 0}$ values obtained in an electric discharge using Terenin and Neuimin's method are apparently not comparable with data obtained using other methods. In fact, owing to the sharp and not always monotonic temperature dependence of the probability of energy exchange during molecular collisions (see Table 31), it is necessary to know the temperature of the gas in the discharge zone. However, since the temperature was not measured in Terenin and Neuimin's experiments or in Dodonova's experiments⁽²²⁾ their calculated values for $P_{1 \rightarrow 0}$ must not be compared with data obtained by various other authors for definite temperatures. Moreover, since the electric discharge in these experiments was very powerful, we cannot state for certain that in these experiments product molecules, yielded by chemical conversion under the action of the discharge, did not also take part in the energy-exchange processes in addition to molecules of the initial substances. Finally, the basic assumption in Terenin and Neuimin's method of a constant energy for the electrons exciting vibrational levels of the molecules can only be correct for a narrow pressure range in the low-pressure region and therefore $P_{1 \rightarrow 0}$ values obtained at high pressures may contain an unconsidered error connected with change in the energy spectrum of the electrons.

Terenin and Neuimin also studied the effect of various gases, which do not radiate in the infrared region, on the intensity of CO and CO_2 bands in the discharge spectrum. Their calculated probabilities $P_{1 \rightarrow 0}$ for the dissipation of vibrational energy of CO and CO_2 molecules during collision with various molecules and atoms (N_2 , H_2 , O_2 , He and Ar) and also of vibrating nitrogen molecules with N_2 , CO and CO_2 are between 10^{-5} and 10^{-6} . These data are quite different from the data obtained using other methods as shown in Tables 29 and 30, and this should be attributed to the reasons mentioned above.⁽²³⁾ These same reasons seem to explain

⁽²²⁾ According to the latest measurements of Dodonova [63] the temperature of the gas (CO or CO_2) in the discharge under her experimental conditions reaches 2000°C .

⁽²³⁾ Terenin and Neuimin's measured probability for the dissipation of a vibrational quantum during collision of a vibrating nitrogen molecule and a non-vibrating nitrogen molecule, $P_{1 \rightarrow 0} = 3 \times 10^{-6}$, is identical with that calculated by Schwartz and Herzfeld [1125] for 2000°K , which is similar to the temperature of the discharge measured by Dodonova [see note (22)].

the above-mentioned difference in the data of Terenin and Neuimin and Dodonova.

Owing to the complex and uncertain conditions in an electric discharge in these experiments the considerable difference (two powers of ten) between Dodonova's measured value (5×10^{-5}) for the probability of dissipation of a vibrational quantum of CO_2 , corresponding to valence (asymmetric) vibrations, and her approximate value (0.4×10^{-6}) obtained for a quantum corresponding to deformation vibrations of CO_2 , must be regarded as requiring careful checking. According to Pielmeier (p. 372), the study of ultrasonic dispersion and absorption in CO_2 for valence (symmetric) and deformation vibrations of the CO_2 molecule gives probabilities for the dissipation of a vibrational quantum which differ only by a factor of about two.

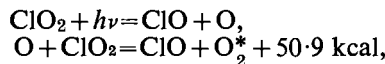
According to Terenin and Neuimin's calculation, the probability of transfer of a vibrational quantum on molecular collision (without its conversion into other forms of energy) is of the same order of magnitude as the probability of dissipation of the quantum.

An electric discharge was also used by Dwyer [558] to obtain vibrationally-excited molecules in the ground electronic state and to study vibrational-energy dissipation processes in collisions. From the absorption spectrum of iodine Dwyer established that the concentration of iodine molecules in the first vibrational state is considerably increased (relative to the equilibrium concentration) when an electric discharge of short duration is passed through iodine vapour. He obtained the absorption spectrum at different times after the discharge and found that to convert a vibrational quantum of the I_2 molecule into other forms of energy several thousand collisions with other iodine molecules are required. This qualitative result is in good agreement with the fact that the probability of conversion of a vibrational quantum increases with decrease in the size of the quantum (see above p. 370 and p. 384). In fact, since the frequency of natural vibrations of the I_2 molecule (213.2 cm^{-1}) is almost three times less than the vibrational frequency of the Cl_2 molecule (556.9 cm^{-1}), a considerable decrease in $1/P$ should be expected on passing from chlorine ($1/P = 34,000$, see Table 30) to iodine, and this is in accordance with Dwyer's measurements.

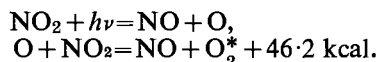
A very promising method for studying energy-exchange processes has recently been proposed by Norrish and coworkers [884]. In a study of the absorption spectrum of the gas formed as a result of short exposure of ClO_2 , and also of NO_2 , in the presence of large quantities of nitrogen, to a powerful light source (flash photolysis, see p. 424), these authors detected intense bands of molecular oxygen connected with transition from the 4, 5, 6, 7 and 8th vibrational levels; these are not observed in normal conditions owing to the insignificant concentration of O_2 molecules in

states with high v (the energy of a vibrationally-excited O_2 molecule in the $v = 8$ state is 34 kcal).⁽²⁴⁾ Analysis of the experimental conditions leads to the conclusion that vibrationally-excited oxygen molecules O_2^* are formed as a result of the following processes:

photolysis of ClO_2 :



photolysis of NO_2 :



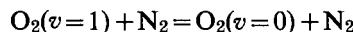
Norrish and coworkers measured the intensity of the absorption bands of oxygen corresponding to $v = 6$ at different times after the exposure of mixtures of ClO_2 and NO_2 with nitrogen, and also in the presence of CO_2 and Ar, and showed that these data may be used to calculate the efficiency of conversion of a vibrational quantum of the O_2 molecule (the level $v = 6$ corresponds to the frequency 1440 cm^{-1} for the quantum) on collision with other molecules. Preliminary data obtained by these authors for $(1/P)$ are shown in Table 32.

TABLE 32

The mean number of collisions $1/P_{6 \rightarrow 5}$ of a vibrationally-excited oxygen molecule in the $v = 6$ level with various molecules resulting in loss of one vibrational quantum (the transition $6 \rightarrow 5$), at 20°C (according to Norrish and coworkers [884])

Deactivating substance	$1/P_{6 \rightarrow 5}$	Deactivating substance	$1/P_{6 \rightarrow 5}$
Ar	$>10^7$	ClO_2	~ 2000
N_2	$>10^7$	CO_2	7000
ClO	2000	NO_2	<500

The data for N_2 in this table may be compared with similar data on the conversion of a vibrational quantum of an O_2 molecule in the first vibrational level, i.e. the quantity $1/P_{1 \rightarrow 0}$ (see Table 30). It is seen from Tables 28 and 30 that there is a sharp difference between the calculated and measured values of $1/P_{1 \rightarrow 0}$ for the process



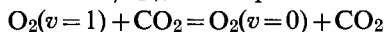
⁽²⁴⁾ Excitation of high vibrational levels ($v \leq 10$) has also been detected for hydroxyl produced in the reaction $\text{H} + \text{O}_3 = \text{OH} + \text{O}_2$ ([853a] and D. Garvin, *J. Amer. Chem. Soc.*, **81**, 3173 (1959), and for HCl produced in the reaction $\text{H} + \text{Cl}_2 = \text{HCl} + \text{Cl}$ [480c].

which apparently must be largely attributed to errors in measurement. The theoretical value 5×10^7 of $1/P_{1,0}$ [1125] should therefore be considered as closer to reality. Since, according to (22.24), P should be proportional to v we find from this value for $P_{1,0}$ that

$$1/P_{6,5} = 1/6P_{1,0} \approx 10^7,$$

a value close to that obtained by Norrish and coworkers for the lower limit of $1/P_{6,5}$.

The experimental value for $1/P_{1,0}$ in the process



is 25,000 according to the data of Table 30 and therefore

$$1/P_{6,5} = \frac{1}{6} 25,000 = 4000,$$

which is also in good agreement with the value shown in Table 32.

According to the measurements of Norrish and his coworkers, NO_2 has the largest deactivating effect (see Table 32). In the opinion of these authors the reason for this is both strong interaction of the unpaired electrons of the O_2 molecule with the unpaired electron of NO_2 and also the similarity of the vibrational frequency of the O_2 molecule (1440 cm^{-1}) and the vibrational frequencies of NO_2 (1320 and 1621 cm^{-1}). The value of this method is that at present it is the only experimental method for studying energy-exchange processes during the collision of molecules occupying high vibrational levels, such as occur in the flames of high-temperature combustion reactions, which are an extremely important class of chemical reaction.

Conversion of the Vibrational Energy of Electronically-excited Molecules

One experimental method for studying vibrational-energy transfer by electronically-excited molecules is based on the study of the fluorescence spectra for various pressures of the fluorescing gas or in the presence of foreign gases. We have shown above (p. 357) that in the presence of foreign gases, besides the resonance series $v' \rightarrow v$, new Deslandres series $v' \pm \Delta v' \rightarrow v$ appear in the fluorescence spectrum of iodine vapour. (These new series, namely $25, 24 \rightarrow v$ and $27, 28 \rightarrow v$ are seen in Fig. 69.) Similar changes in fluorescence spectra have been found for other gases. Intensity measurements of the different series in these spectra for various pressures enable us to calculate the probability P of conversion of the vibrational energy of an excited molecule into other forms of energy during molecular collision. Values for P found in this way are shown in Table 33.

It should be mentioned that the data in this table have a relatively low precision. The main cause of error is the low precision in determining the intensities of the different series in emission spectra, and also the mean lifetime of the excited molecule (which must be known in order to calculate P) is not always known with sufficient precision. Thus, in the opinion of Rabinowitsch [1052], the high values of P found by Rössler [1089] for the

TABLE 33

The probability of transfer of vibrational energy of electronically-excited molecules

Colliding particles	Magnitude of the quantum transferred cal/mole	P	Reference
I ₂ ' + He	255	0.5 8.3	[123] [1089]
I ₂ ' + Ne	255	10.5	[1089]
I ₂ ' + Ar	255	13.8	[1089]
I ₂ ' + Kr	255	16.6	[1089]
I ₂ ' + Xe	255	24.0	[1089]
I ₂ ' + H ₂	255	25.0	[70]
"	510	18.0	[70]
I ₂ ' + N ₂	255	130.0	[70]
"	510	35.0	[70]
S ₂ ' + He	1200	0.05 0.86	[123] [557]
S ₂ ' + Ne	1200	0.77	[557]
S ₂ ' + Ar	1200	0.58	[557]
S ₂ ' + Kr	1200	0.56	[557]
S ₂ ' + Xe	1200	0.80	[557]
NO' + Ar	3500	1.0 *	[145]
NO' + He	6670	0.02	[109]
NO' + Ne	6670	0.07	[109]
NO' + Ar	6670	0.05	[109]
NO' + H ₂	6670	0.01	[109]
NO' + N ₂	6670	0.07	[109]
NO' + CO	6670	0.6	[109]
NO' + NO	6670	8.0	[109]
NO' + CO ₂	6670	4.0	[109]
NO' + H ₂ O	6670	10.0	[109]
NO' + CH ₄	6670	0.05	[109]
NO' + C ₂ H ₄	6670	3.0	[109]
NO' + C ₂ H ₅ OH	6670	5.0	[109]
NO' + C ₆ H ₁₄ (hexane)	6670	0.3	[109]
NO' + C ₆ H ₁₂ (cyclohexane)	6670	0.7	[109]
CN' + Ar	6090	0.002	[311]
CN' + N ₂	6090	0.02	[311]
SO ₂ ' + SO ₂	1080	4.3 43.0	[889] [123]
HCHO' + HCHO	3380	1.0	[123]
C ₆ H ₆ ' + C ₆ H ₆	—	14.5	[123]

* The data from reference [145] show that the probability of conversion of a vibrational quantum during collision with an NO molecule is nearly unity in this case.

transfer of energy during collisions of an excited iodine molecule with inert-gas atoms must be attributed to the fact that Rössler assumed the mean lifetime τ of the iodine molecule to be 10^{-8} sec [788]. Rabinowitsch shows that, when $\tau = 10^{-7}$ sec and the gas-kinetic diameters are taken without Sutherland's correction, the values of P obtained from Rössler's data are less than one. Rabinowitsch's observation clearly applies equally to the results of El'yashevich [70]. Stevens [B. Stevens, *Canad. J. Chem.* 37, 831 (1959)] adopts the value of $\tau = 1.6 \times 10^{-6}$ for the lifetime of an excited iodine molecule. By means of this figure he obtains the following values of the probability P of translational energy transfer: 0.02 (H_2), 0.05 (D_2), 0.10 (He and Ne), and 0.07 (Ar and O_2).

However, in spite of the inaccuracy in P values, data from experimental study of vibrational-energy exchange during collision of excited molecules with various molecules and atoms give a definite idea of the probability of these energy-exchange processes.

We should first point out that, with electronic excitation, energy-exchange processes during molecular collisions have a high probability; in many cases the effective cross section of the exchange is much greater than the gas-kinetic cross section ($P > 1$). A relatively high probability for conversion of the vibrational energy of excited molecules also follows from the equality of "rotational" and "vibrational" temperatures measured by the intensity distribution of the atmospheric O_2 bands (the transition $^1\Sigma_g^+ - ^3\Sigma_g^-$) in the discharge spectrum and afterglow spectrum of oxygen [433]. Since under experimental conditions the excited O_2 ($^1\Sigma_g^+$) molecules formed by recombination of O atoms should have up to 3.5 eV excess vibrational energy, the low "vibrational" temperature of these molecules must be considered as an indication of the relative ease of conversion of their vibrational energy on collision with other O_2 molecules. The vibrational frequency of an O_2 molecule ($^1\Sigma_g^+$) is 1405 cm^{-1} . Comparison of the data of Table 33 with Tables 29-32 shows that the probability of energy exchange increases considerably with excitation of the molecule.⁽²⁵⁾

In addition to the data of Table 33, we should mention that the intensity distribution in the emission bands of H_2 varies with increasing pressure in such a way that the bands connected with transitions from high vibrational levels weaken whereas at the same time new rotational lines appear in the zeroth band which correspond to high rotational levels (high J) of the hydrogen molecule [1074, 1152]. With a trace of helium the distribution of

(25) According to Rössler [1089], the probability of conversion (dissipation) of rotational energy of excited iodine molecules during their collision with inert-gas atoms is of the same order of magnitude as the probability of dissipation of vibrational energy (see Table 33). According to Durand [557], P_{vib} and P_{rot} are of the same order of magnitude for excited sulphur molecules.

the rotational energy of H_2 becomes normal. According to Oldenberg [993, 994], this effect results from collisions of excited H_2 molecules, and consequently the vibrational energy of excited molecules in high vibrational levels is partially converted into the translational energy of relative motion of the colliding molecules and partially into rotational energy of the H_2 molecules themselves, which is the reason for the appearance of new rotational lines. Insofar as it is possible to judge from these data, the transfer of vibrational energy by excited molecules is a very probable process in this case also.

This conclusion is supported by Smith's data [1152] on the position of the maximum in the continuous emission spectrum of hydrogen. It is known [1301] that this spectrum is emitted during transition of an excited H_2 molecule in the stable low triplet state $^3\Sigma_g^+$ to the unstable state $^3\Sigma_u^+$. Smith found that in the presence of helium or neon the maximum of the continuous hydrogen spectrum is displaced to the long wavelength side; this is explained by the transition of excited H_2 molecules in high vibrational levels to the level $v=0$ as a result of collisions with inert-gas atoms. According to Smith a helium pressure of 20 mm Hg is sufficient for a vibrating H_2 molecule to pass to the zeroth vibrational state. Since for a pressure of 20 mm Hg the time between two consecutive collisions of an excited H_2 molecule with an He atom is close to the mean lifetime (about 10^{-8} sec) of the excited molecule, it follows from these data that P is about 1.

Investigations on the effect of a nitrogen admixture on the intensity distribution in the fluorescence spectrum of HgH also show a high probability for conversion of the vibrational energy of an excited molecule into rotational energy of the molecule [1075, 395, 924]. See also [1164a].

Returning to the data of Table 33, we note that they show the well-known specificity of the energy-exchange process with respect to the nature of the colliding particles, which is similar to that observed for collision of non-excited molecules; they show also the absence of any kind of definite dependence of the probability P on the mass of the molecules.⁽²⁶⁾ In this way data for excited molecules also clearly force us to reject a simple mechanical treatment of the energy-exchange process during molecular collision.

It also follows from these data that predominantly only *one* quantum, and less frequently two (as in the case of iodine), is converted with significant probability into translational (or rotational) energy on molecular collision (see also [1089]). The simultaneous conversion of many quanta is practically never observed.

⁽²⁶⁾ In spite of the low precision of the data of Table 33, it seems possible to conclude from them that P decreases with increase of the quantum converted, just as in the case of non-excited molecules (see p. 370).

The above conclusions on the process of energy exchange of excited molecules is supported in the main by new data obtained using the so-called stabilized fluorescence method; this method is based on the discovery by Neporent [212] that the fluorescence of aromatic compounds becomes stronger as a result of vibrational deactivation during collisions of excited molecules with other molecules. Neporent found that the intensity of fluorescence of beta-naphthylamine $C_{10}H_7NH_2$ for excitation by different wave lengths is increased in the presence of He, H_2 , N_2 , CO_2 , NH_3 , $CHCl_3$ and $n-C_5H_{12}$.⁽²⁷⁾ Later a similar effect was found in the presence of deuterium and SF_6 by Boudart and Dubois [431, 1182]. See also [31].

The basis of this effect apparently consists in an excited molecule with a certain vibrational energy (distributed between various vibrational degrees of freedom), on collision with other molecules or atoms, passing to lower vibrational levels and thus becoming more stable as regards spontaneous non-optical transition to another electronic state. This leads to an increase in the mean lifetime of the excited molecule and consequently to an increase in the relative yield of fluorescence [212].

Measurements of the intensity of fluorescence for different pressures of the foreign gas enable us to determine the mean amount of vibrational energy E which is lost by the excited molecule on collision with a molecule of the foreign gas. Values for E (in cal) obtained in this way for various gases and with varying degrees of vibrational excitation in the fluorescing beta-naphthylamine molecules are shown in Table 34. This table also contains in the last column values for the "coefficient of accommodation" α , which characterizes the efficiency of the corresponding gas in removing vibrational energy from the excited naphthylamine molecule and is a measure of the probability of energy transfer during molecular collision. Here $\alpha = 0$ corresponds to an absence of energy transfer (high relaxation times) and $\alpha = 1$ corresponds to an equilibrium distribution of vibrational energy between all the molecules (low relaxation times).

From the data of Table 34 it is seen that on average the amount of energy transferred to a C_5H_{12} molecule per collision is 18 times greater than the amount of energy transferred to an He atom with an identical accommodation coefficient. Hence it follows that the efficiency of energy exchange depends strongly on the degree of complexity of the colliding molecules. Moreover, it follows from the fact that the amounts of energy transferred by a naphthylamine molecule to an H_2 molecule and an He atom (when $\alpha_{H_2} = 0.1$ and $\alpha_{He} = 0.2$) are identical, that internal degrees of freedom of the H_2 molecule do not take part in the energy exchange [1182]. Finally from the fact that the mean amount of energy transferred by a naphthylamine molecule to a molecule colliding with it is about the

⁽²⁷⁾ This effect does not occur in the presence of O_2 , which quenches the fluorescence of beta-naphthylamine according to Neporent.

TABLE 34

Transfer of vibrational energy during collision of excited beta-naphthylamine molecules with molecules of various gases

(according to the data of Neporent [212] and Boudart and Dubois [431])

Gas	$T, ^\circ\text{C}$	Vibrational energy, cal/mole	E cal/mole	α
He	150	24,200	200	0.2
H ₂	150	24,200	200	0.1
	150	29,200	200	0.1
D ₂	186	29,200	140	—
N ₂	150	24,200	545	0.3
CO ₂	150	24,200	1570	0.5
	150	29,200	1715	0.3
NH ₃	150	24,200	2720	0.9
	150	29,200	3060	0.8
	190	24,200	2520	0.8
	190	29,200	2860	0.7
CHCl ₃	150	24,200	2860	0.5
	150	29,200	3550	0.5
SF ₆	186	29,200	1630	0.5
C ₅ H ₁₂	150	24,200	3660	0.2
	150	29,200	4830	0.2
	190	24,200	3550	0.2
	190	29,200	4150	0.2

same as, or some ten times smaller than, a vibrational quantum, it may be concluded that the probability for energy transfer in this case must be of the order of 1 or 0.1.

Energy Conversion in Unimolecular Reactions

Studies of unimolecular reactions also give valuable information on processes of energy transfer. We have seen in the previous section that in the kinetics of unimolecular reactions an important role is played by the processes of activation and deactivation of molecules on binary collision (a bimolecular process); these processes consist of, respectively, the gain or loss by the active molecules of part of their energy, mainly in the form of vibrational energy. Experimental determination of an intermediate pressure region, i.e. a region in which the unimolecular reaction law changes to a bimolecular law, and direct measurement of the rate of activation enable us to estimate the order of magnitude of the probability of energy transfer in the process of chemical activation or deactivation taking place during collisions of identical or different molecules.

We shall consider relative values γ for the probabilities of activation and deactivation determined from experimental data using equation (19.11).

Table 35 shows data on the efficiencies of various substances in the process of activation and deactivation as obtained by various authors. It is seen that the efficiencies of different gases differ among themselves by at most a factor of 17.⁽²⁸⁾ The reasons for the difference between the data of Tables 29 to 32 and Table 35 will be examined at the end of this section (p. 401 *et seq.*).

TABLE 35
Relative efficiencies γ for activation and deactivation (calculated per collision) during unimolecular conversions of various substances

Activating or deactivating substance	F ₂ O [851] (250°C)	N ₂ O [1256] (653°C)	F ₂ O ₂ [640] (-37.1°C)	NO ₂ Cl [1121] (100°C)	N ₂ O ₅ (+ NO) [1298] (50.5°C)	CH ₃ NNCH ₃ [1138] (310°C)
H ₂	—	—	—	0.06	—	—
D ₂	—	—	—	—	—	0.37
He	0.40	0.66	0.07	—	0.0650	0.07
Ne	—	0.47	—	—	0.0855	—
Ar	0.82	0.20	0.40	—	0.154	—
Kr	—	(0.18)	—	—	0.208	—
Xe	—	0.16	—	—	0.189	—
N ₂	1.01	0.24	0.21	0.15	0.228	0.21
O ₂	1.13	0.23	1.20	0.22	—	0.37
F ₂	1.13	—	0.33	—	—	—
Cl ₂	—	—	—	0.18	—	—
NO	—	—	—	—	0.300	—
CO	—	—	—	0.20	—	0.13
CO ₂	—	1.32	0.45	0.18	0.387	0.25
H ₂ O	—	1.50	—	—	—	0.46
N ₂ O	—	1.00	—	—	—	—
NO ₂	—	—	—	0.50	—	—
F ₂ O	1.00	—	—	—	—	—
F ₂ O ₂	—	—	1.00	—	—	—
NO ₂ Cl	—	—	—	1.00	—	—
CH ₄	—	—	—	—	—	0.20
CCl ₄	—	—	—	—	0.673	—
SiF ₄	0.88	—	—	—	—	—
SF ₆	—	—	—	—	0.443	—
CH ₃ NNCH ₃	—	—	—	—	—	1.00
N ₂ O ₅	—	—	—	—	1.000	—

Absolute values for the probabilities of activation and deactivation in unimolecular reactions may be calculated in the following way. We have seen (p. 285) that in the low-pressure region the specific reaction rate is

(28) It has been noted [1051] that energy exchange in the unimolecular decompositions of cyclopropane C₃H₆ and cyclobutane C₄H₈ during collision of these molecules with molecules of complex structure takes place more readily than during collision with molecules of monatomic and diatomic gases. This feature is also observed to some extent in the data of Table 35.

equal to the rate of activation. Expressing the number of molecules with energy greater than the activation energy E_0 by the classical formula (18.13a), i.e. assuming

$$\sum_i N_i = \frac{N}{(f-1)!} (E_0/RT)^{f-1} \exp(-E_0/RT) \quad (22.28)$$

(here the number s of square terms is replaced by $2f$, where f is the number of vibrational degrees of freedom involved in the activation) and substituting this number in formula (18.7) along with

$$Z_0 = 2Pd^2(\pi RT/M)^{1/2} \quad (19.10)$$

(here P is the probability for deactivation), we find that the specific reaction rate is

$$k = 2Pd^2(\pi RT/M)^{1/2} \frac{N}{(f-1)!} (E_0/RT)^{f-1} \exp(-E_0/RT). \quad (22.29)$$

Using this formula we may calculate P (per collision) on the basis of a measured value for the specific reaction rate at a corresponding temperature and pressure, and also the probability for activation which may be defined as

$$P_{act} = \frac{P}{(f-1)!} (E_0/RT)^{f-1} \exp(-E_0/RT). \quad (22.30)$$

It is seen from (22.29) that to calculate the probability P for deactivation it is necessary to know (as well as k) d the diameter of the molecule, E_0 the activation energy and f the number of degrees of freedom of the active molecule which are involved in activation. To calculate the probability of activation it is sufficient to know k and d , as is clear from the formula

$$k = 2P_{act}d^2(\pi RT/M)^{1/2} N, \quad (22.31)$$

which is obtained from (22.29) and (22.30).

We shall calculate as an example the probabilities P of deactivation of the molecules N_2O and F_2O . From Johnston's data [802] for N_2O we find that k/N at 888°K is $2.3 \times 10^{-23} \text{ cm molecule}^{-1} \text{ sec}^{-1}$. Substituting this figure in (22.29) along with $d = 3.2 \times 10^{-8} \text{ cm}$, $E_0 = 59,200 \text{ kcal}$ and $T = 888^\circ\text{K}$, we obtain

$$P = \frac{62(f-1)!}{33^{f-1}},$$

from which we find for $f = 2, 3$ or 4 that $P = 2, 1/9$ or $1/100$ respectively. Since the best agreement between calculated values and specific rates measured at different pressures is obtained when $f = 4$ according to

Johnston (cf. p. 313), the most probable value for P in this case of N_2O should be taken as 1/100. From the measured constant for the bimolecular activation of F_2O molecules colliding with one another [851], namely $k/N = 2.3 \times 10^{-23} \text{ cm}^3 \text{ molecule}^{-1} \text{ sec}^{-1}$ ($T = 523^\circ\text{K}$, $d = 3.2 \times 10^{-8} \text{ cm}$ and $E_0 = 40.6 \text{ kcal}$) we obtain for $f = 2, 3$ or 4 that $P = 15, 0.75$ or 0.06 respectively. Of these three values, the figure $0.75 \approx 1$, which corresponds to the maximum number of vibrational degrees of freedom of the F_2O molecule, should be considered as the true value for the probability of deactivation of active F_2O molecules. According to Schumacher's data [1119], results of similar calculations on the probability of deactivation of the other simple molecules F_2O_2 and NO_2Cl are given by the figures: F_2O_2 , $P \approx 1$, $f = 6$ and NO_2Cl , $P > 1/10$, $f = 4$. It is seen from these figures that the probability of deactivation of an active molecule with simple structure, with the exception of N_2O (see below), is *about unity*. It follows from the fact that the relative efficiencies for more complex molecules (see Table 35) are of the same order of magnitude as the relative efficiencies for simple molecules, that the probabilities of deactivation of complex molecules are also *about unity*.

The mean lifetime of an active molecule is also of some interest; this is defined as the reciprocal of the mean probability for unimolecular conversion,

$$\tau = 1/\lambda.$$

The quantity τ may be obtained from formulae (18.13a) and (18.14) as

$$\tau = N_{\text{act}}/k_\infty N = \frac{\exp(-E_0/RT)(E_0/RT)^{f-1}}{k_\infty(f-1)!}. \quad (22.32)$$

Thus in order to calculate τ , we must know k_∞ , f and E_0 .

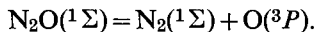
We shall compare the values of τ for the triatomic molecules F_2O and N_2O . Since the decomposition of F_2O follows a bimolecular law

$$-d(\text{F}_2\text{O})/dt = k(\text{F}_2\text{O})^2,$$

up to the maximum pressure of 800 mm Hg at which it has been studied (250 to 280°C), it must be expected that in this case τ will be small. Assuming that τ is 100 times smaller than the mean time interval between two collisions, which for this temperature and pressure is $0.7 \times 10^{-9} \text{ sec}$, we find $\tau_{\text{F}_2\text{O}} = 10^{-11} \text{ sec}$. Substitution of this figure in the formula (22.32) for the pre-exponential factor in the expression for k_∞ gives $A = 7 \times 10^{13} \text{ sec}^{-1}$; this may be considered an additional indication that the order of magnitude for the mean lifetime of an active F_2O molecule is correct (see Fig. 62). On the other hand, by using in (22.32) the known values of k_∞ ($\approx 10^{-3} \text{ sec}^{-1}$), f ($= 4$) and E_0 ($= 60,000 \text{ cal/mole}$), we obtain

$$\tau_{\text{N}_2\text{O}} = 10^{-8} \text{ sec.}$$

Such a large difference in the value of τ for F_2O and N_2O , which contain the same number of atoms, is clearly not fortuitous and must be a result of the fact that whereas the decomposition of the F_2O molecule is an adiabatic process ($\text{F}_2\text{O} = \text{FO} + \text{F}$), the decomposition of N_2O violates the law of conservation of spin, as is clear from its decomposition scheme



Since, according to Wigner [1020, 1288, 585], non-adiabatic processes occur with a probability a thousand times smaller than the probability of adiabatic processes, the above difference in the values $\tau_{\text{F}_2\text{O}} = 10^{-11}$ sec and $\tau_{\text{N}_2\text{O}} = 10^{-8}$ sec is naturally attributed to this effect [764].⁽²⁹⁾

Values of τ calculated from (22.32) for more complex molecules are about 10^{-9} to 10^{-10} sec (instead of 10^{-11} sec); this must be attributed to the increase in the number f of degrees of freedom involved in activation on passing from simple to complex molecules.

Stabilization of Molecules During Ternary Collisions

According to the theory of termolecular reactions (see Chap. 5), the process of stabilization during ternary collision of a quasi-molecule, which is unstable with regard to decomposition, consists of the removal of a part of its energy by a stabilizing third particle. Since the deactivation of molecules in unimolecular decompositions is also a removal of energy from an active molecule (capable of spontaneous decomposition) by collision with a deactivating molecule, there must be a close parallelism between the relative efficiencies, and accordingly the probabilities, of both processes. In particular, it is expected that the efficiencies of ternary collisions will be close to unity (since the efficiencies of the processes of deactivation of active molecules are close to unity, see p. 398), so that a molecule must be formed on nearly *every* gas-kinetic collision of three particles.

For ternary collisions corresponding to the recombination of atoms



(M is the third particle), the corresponding rate constants k in the recombination equation

$$-d(\text{A})/dt = k(\text{M})(\text{A})^2,$$

are a measure of the relative efficiency of the molecules of the substance M with respect to stabilization of the quasi-molecule $\text{A}\cdot\text{A}$. These constants are shown in Table 25 (p. 333).

⁽²⁹⁾ See also [1172]. We should add that the low probability for the intercombination transition in the N_2O molecule is also observed in the low light absorption by nitrous oxide in the long wave-length region of the spectrum of N_2O vapour, corresponding to the decomposition of N_2O into N_2 and O in the ground states [984].

Considering this table on the basis of collision theory, we come to the conclusion (see p. 336) that the effective cross sections of the bimolecular processes of formation and stabilization of quasi-molecules (for example, the processes $A + A = A \cdot A$ and $A \cdot A + M = A_2 + M$) are approximately the same as the gas-kinetic cross sections. This result may clearly be considered as support for the above conclusion that the efficiency of ternary collisions is close to unity.

In addition to what has been said in Chap. 5 about the efficiency of ternary collisions, we should mention that the data for various M in the reaction $I + I + M = I_2 + M$, which has been studied in most detail, show that k , which for the inert gases and gases such as H_2 , N_2 and O_2 is about $1 \times 10^{-32} \text{ cm}^6 \text{ molecule}^{-2} \text{ sec}^{-1}$, is tens or hundreds of times larger for more complex substances. According to Russell and Simons' ideas [1096],

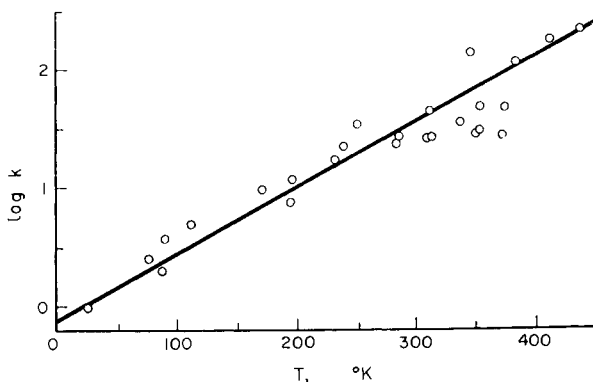


FIG. 79. The relationship between the rate constant of termolecular recombination of iodine atoms $I + I + M = I_2 + M$ and the boiling point of substance M (according to Russell and Simons [1096]).

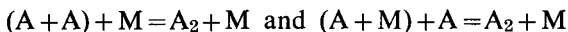
the efficiency of a substance involved in the reaction as a third particle (M) must be determined by the disturbing field this particle produces on the quasi-molecule $A \cdot A$ ($I \cdot I$). Assuming that this field is based mainly on van der Waals forces and taking the boiling point of the substance as a measure of this field, Russell and Simons show that the smoothed-out dependence of the logarithm of k on boiling point of M is nearly linear (Fig. 79).⁽³⁰⁾ They conclude from this relationship that a hypothesis of a specific chemical action of M particles is not necessary to explain the quite different effect of M particles of different structure.

(30) Within the limits of accuracy of this approximate relationship the point corresponding to iodine (see Table 26), with boiling point 457°K , also lies on the straight line in Fig. 79.

Russell and Simons show that a dependence similar to that expressed by the straight line in Fig. 79 is also obtained when the critical temperature or ionization potential of M is taken as a measure of its efficiency.

This conclusion is in sharp contrast with the ideas of Franck and Eucken [623], according to which the forces of chemical interaction between the colliding particles play an important role in energy-exchange processes during molecular collisions. It should be kept in mind however that van der Waals forces must play a relatively more important role when there are high effective cross sections, which are characteristic of termolecular reactions and distinguish them from energy-exchange processes in collisions of molecules in low degrees of excitation. The low specificity of interaction for high efficiencies was mentioned earlier in connection with energy-exchange in unimolecular reactions (see pp. 396-8). It would be expected that chemical forces would be less masked by van der Waals forces in the case of the simplest molecules, which do not have such large effective diameters. Thus the possibility is not excluded that the effect of chemical forces may explain the efficiency of carbon monoxide, which is nearly ten times higher than that of nitrogen in the recombination of Br atoms, $\text{Br} + \text{Br} + \text{M} = \text{Br}_2 + \text{M}$ (see Table 25). In view of the similar boiling points of CO and N₂ (83 and 77°K) this difference in the efficiencies of the gases is not explained by Russell and Simons' ideas, whereas from Franck and Eucken's point of view the relatively high efficiency of CO is explained by the ease of energy exchange in the Br·Br·CO complex, which corresponds to an unstable state of the bromophosgene molecule Br₂CO.

We should also keep in mind the possibility that high efficiencies of M may be connected with two concurrent mechanisms of the termolecular reaction, namely



(see §20). In this case, it is very probable that interaction between A and M particles in the quasi-molecule A·M results to a considerable extent from chemical forces.

Probability of Vibrational Energy Conversion in Strongly Vibrating Molecules and in Molecules Possessing One Vibrational Quantum

From the data of Tables 35, 25 and 26 and the corresponding probabilities of energy transfer during molecular collisions it follows that, in accordance with theoretical ideas on deactivation processes in unimolecular reactions, and on stabilization of quasi-molecules during ternary collisions, the probabilities of these processes are similar and do not differ greatly from unity (calculated per collision) in contrast with the probability for conversion of one vibrational quantum into translational energy, which is usually much less than unity and rarely reaches 0·01 (see Table 30).

The reason for this difference, according to Patat and Bartholomé [1012], is that in sound absorption and dispersion the exchange of energy

is actually conversion of a vibrational quantum into translational or rotational energy (or the reverse), whereas deactivation of molecules in unimolecular reactions or in recombination processes is the transfer of one or more vibrational quanta to the deactivating molecule or third particle without conversion into other forms of energy. Assuming that the probability for the latter process, i.e. the transfer of vibrational energy from some molecules to others without its conversion into other forms, in contrast with the probability for conversion of vibrational energy into translational or rotational energy, is close to unity, Patat and Bartholomé actually attribute the low efficiency of molecular collisions in sound absorption and dispersion to the difference in these probabilities. This point of view has been supported by Eucken and Nümann [575]. In their ultrasonic experiments they found the same excitability for both valence and deformation vibrations of the N_2O and CO_2 molecules (see above) and connected this with the ease of establishing equilibrium distribution of energy between both vibrational forms, since they postulated a high probability for vibrational-energy transfer during molecular collision (without conversion into other forms of energy).

It is not difficult to see, however, that Patat and Bartholomé's hypothesis clearly contradicts the experimental data and the theory of inelastic collisions. In fact, it is seen from Tables 35, 25 and 26 that the efficiency of monatomic gases with regard to deactivation of active molecules or stabilization of quasi-molecules is at most ten times smaller than the efficiency of diatomic and some polyatomic gases, and in certain cases it is even somewhat greater than the efficiency of the latter. Since, however, when the deactivating particle is an atom, the transfer of a vibrational quantum without its conversion into translational energy is excluded, the high efficiency of atoms (compared with the efficiency of molecules) is completely inexplicable on the basis of Patat and Bartholomé's hypothesis. We should add that on this basis there is also no explanation for the higher efficiency of hydrogen and carbon monoxide compared with chlorine (by about 40 and 150 times, see Table 30) observed in the dispersion of sound in mixtures of these gases with chlorine, or for the higher activity of the same gases compared with oxygen (by 25 and 65 times, see Table 30); since the size of the vibrational quantum of H_2 (11.85 kcal) and of CO (6.13 kcal) is *larger* than that of chlorine (1.60 kcal) and of oxygen (4.64 kcal), both H_2 and CO in mixtures with chlorine and with oxygen should behave as monatomic gases with regard to vibrational-energy exchange.

As we have shown on p. 363, according to Zener's calculations the probability of transfer of a vibrational quantum during molecular collision without its conversion into energy of relative translational motion is sharply decreased with departure from resonance, so that with a difference in vibrational frequencies of the colliding molecules it tends to approach

the probability of conversion of vibrational energy into translational energy. Consequently Patau and Bartholomé's hypothesis also contradicts the results of these theoretical calculations.⁽³¹⁾

We may also look for the cause of the high probability of deactivation of active molecules in unimolecular reactions, or the probability of stabilization of quasi-molecules, in the *high degree of excitation* of active molecules or quasi-molecules compared with molecules possessing only one vibrational quantum. It is natural to assume that strongly vibrating molecules exchange energy more readily. An argument in favour of this is the fact that according to the theory of conversion of a vibrational quantum during molecular collisions, the probability of conversion of one vibrational quantum into translational or rotational energy is proportional to the vibrational quantum number, as may be seen from (22.24). It follows from this formula that a strongly vibrating molecule in the v th vibrational level should be deactivated (losing one vibrational quantum) v times more readily than a molecule possessing one vibrational quantum. However, it is not difficult to see that it is impossible to explain on the basis of (22.24) the high quantitative difference in the probabilities for energy exchange in unimolecular reactions or recombination processes and in sound dispersion or absorption. Actually, calculating as an example the maximum (limiting) vibrational quantum number for the Cl_2 molecule using the formula $v_{\text{max}} = 1/(2x)$ we find (since the anharmonicity coefficient $x = 0.007$) $v_{\text{max}} = 70$; therefore we may conclude that the probability of the recombination process $\text{Cl} + \text{Cl} + \text{M} \rightarrow \text{Cl}_2 + \text{M}$ should be seventy times greater than $P_{1,0}$, the probability of conversion of one vibrational quantum of the Cl_2 molecule in the vibrational level $v = 1$ on collision with an M particle. When M is an N_2 molecule, we find from Table 30 that the probability for the process $\text{Cl} + \text{Cl} + \text{N}_2 \rightarrow \text{Cl}_2 + \text{N}_2$ is $70/43,000 \approx 0.002$, i.e. a figure at least two powers of ten less than the actual value for the probability of recombination.⁽³²⁾ A similarly large discrepancy is also obtained when $\text{M} = \text{Ar}$ or Cl_2 (0.002 instead of 1).⁽³³⁾ An even greater discrepancy is obtained for the recombination of oxygen atoms, which has a probability which should be close to the probability for recombination of other atoms and consequently should be of the order of unity, whereas calculation on

⁽³¹⁾ Similar values for the probability of dissipation and the probability of transfer of a vibrational quantum were obtained by Terenin and Neuimin (see p. 387).

⁽³²⁾ The probability of recombination of chlorine atoms is not known. However, it must be assumed that it is close to the probability for recombination of bromine and iodine atoms. When $\text{M} = \text{N}_2$ the figure for iodine is close to unity (see p. 335), according to Rabinowitsch [1052].

⁽³³⁾ It is interesting to note that in the recombination of chlorine atoms, when $\text{M} = \text{CH}_4$ calculation gives $P = 0.8$, i.e. a figure of the order of unity, as was obtained by Rabinowitsch for CH_4 . When $\text{M} = \text{CO}$ or HCl the values of P obtained are also of the order of unity (0.6 and 1.2). For He and H_2 , P is found to be 0.16 and 0.18 respectively, i.e. figures of the same order as those of Rabinowitsch (0.1) [1052].

the basis of the data of Table 30 (in the case of O_2 also, the constant x is equal to 0.007) for the probability of recombination when $M = O_2$, He, N_2 or H_2 gives 0.00014, 0.00043, 0.0007 or 0.0035 respectively.

The unsuitability of a formula of type (22.24) in explaining high probabilities of energy exchange during collisions of strongly vibrating molecules with other molecules or atoms must apparently be attributed to the fact that one of the basic assumptions in deducing this formula was that the vibrations are harmonic. In fact, as vibrations are excited, i.e. as the vibrational quantum number increases, the vibrational frequency becomes lower and lower, and as a result the probability of energy exchange increases, since in the limit when the vibrational frequency tends to zero (or to a very low value) the vibrational-energy conversion process should approximate to a translational-energy exchange process. Consequently in the limit the probability of conversion of a quantum into translational energy may reach unity, which is characteristic of the transfer of translational energy. Physically this may be explained by the idea that as the vibrations slow down the difference between the periodic vibrational motion and the aperiodic translational motion becomes more and more indistinct.

In comparing the probabilities of deactivation in unimolecular reactions with the probabilities of conversion of a vibrational quantum in sound dispersion and absorption, we must also consider the temperature dependence of the probability of energy transfer. As we have seen (p. 382, Fig. 77), in certain cases this dependence may be approximately expressed by the Arrhenius equation or a similar law, and may be used to calculate the probability of energy transfer at the required temperature. For example, calculating the probability of conversion of one (the first) vibrational quantum of the N_2O molecule from the data of Table 31 at a temperature of $888^\circ K$, i.e. a temperature suitable for the unimolecular decomposition of nitrous oxide, we find $1/P_{1,0} = 1650$, i.e. $P_{1,0} = 0.0006$. Comparing this figure with the probability (0.01) we calculated earlier (p. 398) for the deactivation of an active N_2O molecule at the same temperature, we see that the extrapolated value is 16.5 times less than that found from the measured deactivation rate. However, since an active N_2O molecule has an energy of at least 59.2 kcal/mole and consequently is in high vibrational levels, it must be taken that the extrapolated probability is much too low. A correction for the high excitation of the active molecule may be made in the following manner. Since all four vibrational degrees of freedom of the N_2O molecule take part in its activation and taking the mean value of its three fundamental frequencies to be 1175 cm^{-1} , or the size of the corresponding vibrational quantum to be 3.35 kcal, we obtain an approximate value for the maximum vibrational quantum number by dividing the activation energy 59.2 kcal/mole by the energy of the average quantum,

which gives $v_{\max} = 17.5$. Moreover, assuming that deactivation of an active N_2O molecule consists of its losing one vibrational quantum, we find the probability for deactivation to be $0.0006 \times 17.5 \approx 0.01$, which is in complete agreement with the figure calculated from the rate of deactivation during unimolecular decomposition of N_2O .

The ideas underlying these calculations, however, have the important defect that they do not allow for the above-noted specificity, which is characteristic of energy-exchange processes during collisions of molecules and which still awaits explanation. The possibility is not excluded that here, and in conversions of one vibrational quantum, a definite role, perhaps sometimes decisive, is played by chemical factors (in the sense of Franck and Eucken's concepts [623]) in addition to physical factors (see p. 378). In particular, during recombination processes the chemical factor may be important for the mean lifetime of the quasi-molecule, which may give rise to the specificity in the action of different gases in these processes.

The problem of the main causes of the specificity in the action of a given gas in energy-exchange processes during molecular collisions is made difficult by the fact that the mechanism of most reactions has been inadequately studied so far. For example, Small and Ubbelohde [1148] show that if the existence of energy chains is assumed (see below, p. 568) in the oxidation of acetaldehyde, then the inhibiting action of hydrogen they found in this reaction may be explained by the deactivation of active molecules as a result of vibrational-energy transfer to the H_2 molecules colliding with them.

CHAPTER 7

PHOTOCHEMICAL REACTIONS

§23. Photochemical Activation of Molecules

Lambert-Beer law

In photochemical reactions, i.e. reactions taking place under the action of light, the chief source of activation of molecules of the reacting substance is light energy. Naturally only the light absorbed by the substance in question is photochemically active. If we regard the absorption of light as the interaction of photons with molecules of the absorbing substance, and take as a measure of the intensity of light of a given wave length λ the number of corresponding photons I_λ , then the weakening of light in an absorbing layer of thickness x may be expressed by the equation

$$-dI_\lambda = \mu_\lambda^0 I_\lambda d(cx), \quad (23.1)$$

where μ_λ^0 is a proportionality factor, dependent on the wave length and on the nature of the absorbing substance, called the *specific absorption coefficient*; c is the concentration of the absorbing substance. Integrating expression (23.1) we obtain

$$I_\lambda = I_\lambda^0 \exp(-\mu_\lambda^0 cx). \quad (23.2)$$

Here I_λ^0 is the intensity of incident light and I_λ is the intensity of light passing through the layer of absorbing substance of thickness x .

For a constant concentration of absorbing substance c , expression (23.1) may be reformulated as

$$-(\partial I_\lambda / \partial x)_c = \mu_{\lambda c} I_\lambda, \quad (23.3)$$

where

$$\mu_{\lambda c} = \mu_\lambda^0 c. \quad (23.4)$$

Formula (23.3) expresses *Lambert's law* according to which the amount of light absorbed when $c = \text{const.}$ is determined by the thickness of the absorbing layer.

When the thickness of the absorbing layer x is constant, it follows from (23.1) that

$$-(\partial I_\lambda / \partial c)_x = \mu_{\lambda x} I_\lambda, \quad (23.5)$$

where

$$\mu_{\lambda x} = \mu_\lambda^0 x. \quad (23.6)$$

Formula (23.5) expresses *Beer's law*, according to which for $x = \text{const.}$ the amount of light absorbed is determined by the concentration of the absorbing substance.

Formula (23.1) or its integrated form (23.2) thus expresses the general law for the absorption of light and is called the *Lambert-Beer law*.

From formula (23.2) it is possible to determine the amount of light absorbed in a layer of thickness x by using the equation

$$\delta I_\lambda = (I_\lambda^0 - I_\lambda) / I_\lambda^0 = 1 - \exp(-\mu_\lambda^0 cx). \quad (23.7)$$

For weak absorption (low concentration or a low absorption coefficient) or for a sufficiently small x , formula (23.7) may be expressed in the form

$$\delta I_\lambda = \mu_\lambda^0 cx. \quad (23.8)$$

In this case the amount of light absorbed is *proportional to the concentration of the absorbing substance*. For strong absorption the exponential term in expression (23.7) becomes insignificantly small compared with unity, and δI_λ is practically equal to one. This means practically complete absorption of light in a layer of thickness x .

It is obvious from formula (23.7), independently of the individual values of c and x , that when cx is constant the amount of absorbed light δI_λ must also be constant.

The formula (23.2) clearly holds as long as the absorption coefficient μ_λ^0 is independent of c and x ; this, however, is not always the case. Thus there are deviations from the Lambert-Beer law.

One of the usual reasons for the breakdown of this law lies in the change in *composition* of the absorbing substance when its concentration is changed. For example, with increase in pressure the equilibrium between NO_2 and N_2O_4 is displaced to the N_2O_4 side; as a result of the difference in the absorption coefficients of both gases the absorption coefficient of the mixture changes (approaching the absorption coefficient of N_2O_4). Similar changes in absorption coefficients, resulting from the changing composition of the absorbing substance due to displacement of the equilibrium, are often observed in solutions of electrolytes due to the difference in the absorption coefficients of the undissociated substance and its dissociation products (ions).

In the case of line absorption (the spectra of atoms and the band spectra of molecules) one reason for the breakdown of the Lambert-Beer law is the large value for the absorption coefficient in the centre of the line; this leads to practically complete absorption of light in the section of the line near to its centre even for small thicknesses of the absorbing layer. Deviation from the absorption law is in fact an indication of the change in the amount of absorption taking place in this section with change in the

concentration of the absorbing substance (as a result of broadening of the absorption lines) or with change in thickness of the absorbing layer.

Increase in light absorption resulting from broadening of the spectral lines is very important for quantitative determination of the efficiency of the photochemical action of light, which is expressed as the so-called quantum yield (see §26). When determining the efficiency of light it is necessary to study this effect under various conditions of temperature and pressure.

Deviations from the Lambert-Beer law are particularly large in the region of induced predissociation (see below); here an increase in the concentration or a simple increase in pressure by the addition of any foreign gas with constant concentration of the absorbing gas leads to anomalously large broadening of the absorption lines. The reason for anomalous broadening of the spectral lines in this case is that, in contrast with the usual collision or Doppler broadening, the area of the line (i.e. the magnitude of the integral

$$\int \mu_\nu^0 d\nu,$$

which determines the probability of the quantum transition) does not remain constant (allowing for the complete absorption of light in the centre of the line, mentioned above), but increases with increase in pressure. Thus the ultimate reason for this increase in absorption is an increase in

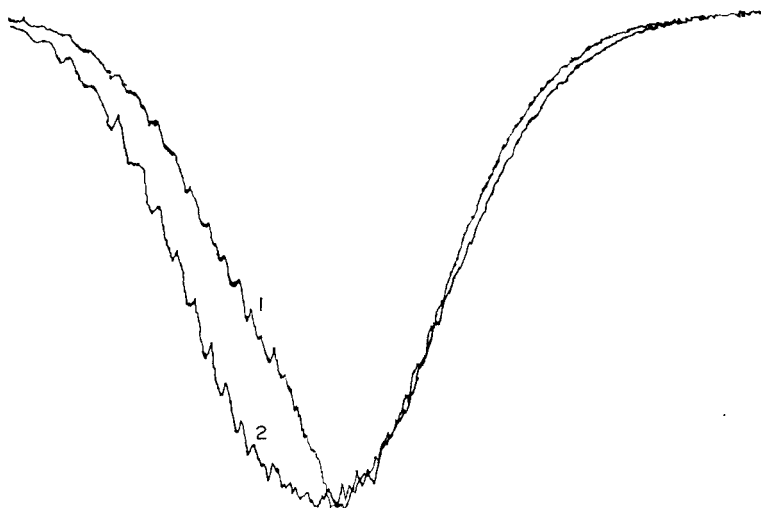


FIG. 80. Microphotograms of the absorption spectra (1) of bromine vapour and (2) of bromine in the presence of nitrogen (according to Avramenko and Kondrat'ev [8, 126]).

the probability of optical transition (as a result of the removal or weakening of prohibition of transition by the absorption of light by a molecule at the moment of its collision with another molecule.) An illustration of this effect is shown in Fig. 80, which is a microphotogram of the absorption spectrum of bromine vapour in the visible region (curve 1) and of bromine vapour for the same values of c_{Br_2} and x but in the presence of nitrogen (curve 2). The structure of the absorption spectrum of bromine vapour is such that to the left of the minimum of the curves in Fig. 80 the spectrum has a banded structure and to the right of the minimum the spectrum is continuous. The figure shows that addition of nitrogen has practically no effect on the intensity of the bromine absorption in the continuous spectral region and causes a sharp intensification of the absorption in the discrete spectral region. As a result a clear violation of the Lambert-Beer law is observed, in the inconstancy of δI_λ with constant $c_{Br_2} \cdot x$.

Breakdown of the absorption law as a result of increase in the probability of quantum transition due to the weakening of forbidden transitions during the collision of molecules is also possible for continuous or diffuse spectra. Such a case has recently been established for the continuous spectrum of oxygen [864].

However, in the case of gases, violations of the light absorption law are relatively rare and deviations from the law are usually not large. Thus one should regard violations of the absorption law as exceptions rather than the rule. Thus within certain limits the Lambert-Beer law and all formulae derived from it may be considered sufficiently accurate.

The Primary Photochemical Process

From the point of view of the mechanism of a photochemical reaction the essential problem is the result of the primary effect of light on a molecule of the absorbing substance. Depending on the frequency of the light and the structural characteristics of the light-absorbing molecules, the result of photochemical activation (light absorption) may be *excitation*, *ionization* or *dissociation* of the molecule. In a large number of cases, particularly when considering gases and vapours, *the nature of the primary photochemical process can be established from the structure of the absorption spectrum*.

This problem is most simply solved in the case of the *continuous absorption spectra* of gases: in this case the absence of rotation-vibration structure is a sure indication of the instability of the excited state of the molecule, i.e. an indication that light absorption leads to immediate *dissociation* of the molecule. We shall consider the origin and properties of continuous absorption spectra using the spectra of diatomic molecules as examples.

Here continuous absorption spectra arise in two situations: when the

upper (excited) state of a molecule is completely unstable and is characterized by a potential curve of repulsion or when, as a result of light absorption, the molecule appears in an unstable region of the upper curve (Fig. 81, Cl_2), i.e. in a region where the molecule's store of internal energy exceeds its dissociation energy. Examples of the first situation are shown by the spectra of the hydrogen halides HF , HCl , HBr and HI , by the spectrum of F_2 and also clearly in the spectra of a large number of halide salts; examples of the second situation are shown by the spectra of Cl_2 , Br_2 and I_2 , by the spectra of O_2 and S_2 etc.

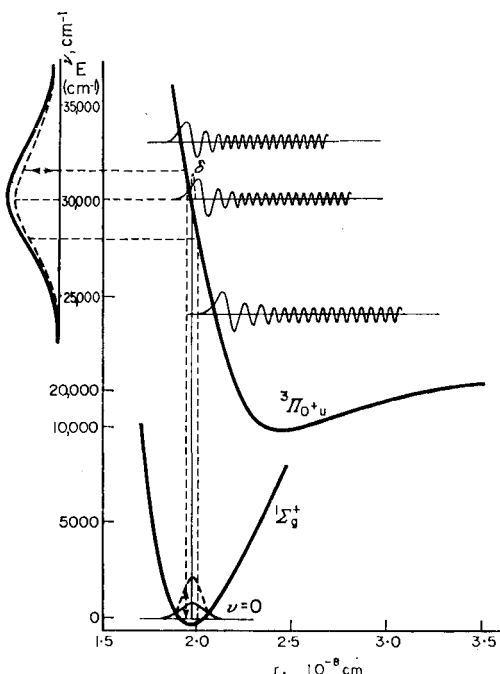


FIG. 81. Potential curves and eigenfunctions of the Cl_2 molecule in the ground state ($^2\Sigma_g^+$), $v = 0$ and in an excited state (the unstable part of the curve), (according to Gibson, Rice and Bayliss [673]). To the left is shown the intensity distribution in the continuous absorption spectrum of Cl_2 .

The intensity distribution in an absorption spectrum is determined by the quantity

$$v \left| \int \psi'_{v'} \psi_v dr \right|^2, \quad (23.9)$$

where $\psi'_{v'}$ and ψ_v are the vibrational wave functions of the upper and lower (ground) states of the molecule (i.e. functions of the distance r)

between the atoms). The dependence of ψ on r in stable states of a molecule for various values of the vibrational quantum number is shown by the dotted line in Fig. 82 [501]. The dependence of the wave functions in an unstable state on r is shown in Fig. 81 (for various energies). In this diagram the wave function in the ground state of a molecule is given only

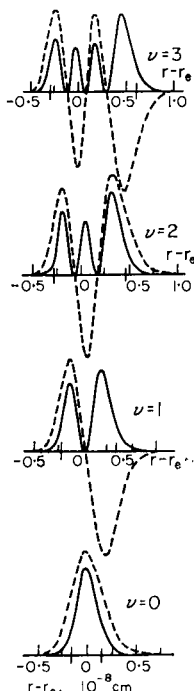


FIG. 82. Eigenfunctions (dotted curves) and distribution of density of probability (continuous curves) of an anharmonic oscillator for $v = 0, 1, 2$ and 3 .

for $v = 0$. At low temperatures, when very nearly all of the molecules are in the zero vibrational state, this is the appropriate wave function to use in (23.9). Calculation of the intensity distribution for the continuous absorption spectrum gives in this case an almost symmetrical (bell-shaped) curve with a maximum. Such a curve, calculated for the Cl_2 molecule, is shown in Fig. 81 (upper left). This curve is seen to be in good agreement with the experimental curve.

In the absorption spectrum of chlorine the main part of the intensity is in the continuous portion while the discrete bands adjoining the continuous spectrum on the long wave length side are of a very low intensity. This intensity distribution is a result of the weak overlapping of the wave

functions of the lower state of the Cl_2 molecule with the wave functions corresponding to the discrete vibrational levels of the upper state; the weak overlap is due to the comparatively large difference in the equilibrium distances between the atoms in the two states ($r_0 = 1.983$ and $r'_0 = 2.42 \text{ \AA}$). With decrease of the $r'_0 - r_0$ term the intensity maximum shifts to the banded side of the spectrum, as is immediately obvious from Fig. 81.

In polyatomic molecules quantum states are characterized not by potential curves but by potential surfaces, and an optical transition is a transition of a molecule from one potential surface to another. Unstable states correspond to potential surfaces with energies greater than the energy of the dissociation products of the molecule; optical transitions to such surfaces give rise to the continuous absorption spectra. Thus also in the case of polyatomic molecules the continuous absorption spectra characterize photodissociation of the molecule.

The problem of the chemical nature and energy state of the photodissociation products of the molecule is considerably more difficult. Even in the simplest case of diatomic molecules further investigation is necessary of this problem, which is important from the point of view of the kinetics and mechanism of photochemical reaction. This would require a determination of the quantum nature and origin of the excited state of a molecule. In individual cases, however, it is sufficient to know the dissociation energy of the molecule to find out the energy levels of the dissociation products. For example, from the fact that the long wave limit of the continuous absorption spectra of hydrogen halides (HX) corresponds to an energy E which satisfies the condition $D < E < D+A$, where A is the lowest excitation energy of the dissociation products (of atom X), it follows that during absorption in the quartz ultra-violet region the HX molecules dissociate into *unexcited* atoms [686a]. In the same way it follows from the position of the boundary between the continuous and discrete parts of the absorption spectra of O_2 and S_2 molecules that these molecules dissociate into normal and excited atoms by the absorption of light in the continuous spectral region.

The excited atoms generated are in a metastable state and cannot be detected by the emission of light. However in similar cases the excited states of the products of the photodissociation are not metastable; in these cases study of the fluorescence spectrum permits us to establish definitely the character of the dissociation process and the energy state of the dissociation products. The optical method for studying photodissociation, which was developed by Terenin [260], is based on this principle. Data obtained by this method are shown in Table 36.⁽¹⁾

⁽¹⁾ A survey of the large amount of experimental material relating to the photodissociation of vapours of salts of type MX , MX_2 , MX_3 and MX_4 is given in Terenin's book: *The Photochemistry of Salt Vapours*, Moscow-Leningrad, GTTI, 1934.

TABLE 36

Excitation of fluorescence during the photodissociation of molecules [263]

Process	Effective wave length Å	Fluorescing particle
$\text{H}_2\text{O}_2 + h\nu = \text{OH}' + \text{OH}$	2025–2138	$\text{OH}'(^2\Sigma)$ [1237]
$\text{I}_2 + h\nu = \text{I}' + \text{I}$	<1470	$\text{I}'(^3s^2P_{3/2})$
$\text{H}_2\text{O} + h\nu = \text{OH}' + \text{H}$	<1370	}
$\text{CH}_3\text{OH} + h\nu = \text{OH}' + \text{CH}_3$	<1560	
$\text{C}_2\text{H}_5\text{OH} + h\nu = \text{OH}' + \text{C}_2\text{H}_5$	<1560	$\text{OH}'(^2\Sigma)$
$\text{HCOOH} + h\nu = \text{OH}' + \text{HCO}$	<1560	
$\text{HCOOH} + h\nu = \text{HCO}' + \text{OH}$	<1560	HCO'
$\text{CH}_3\text{COOH} + h\nu = \text{OH}' + \text{CH}_3\text{CO}$	<1560	
$\text{CH}_3\text{CN} + h\nu = \text{CN}' + \text{CH}_3$	<1580	$\text{CN}'(^2\Sigma)$
$\text{NH}_3 + h\nu = \text{NH}_2' + \text{H}$	<1640	
$\text{N}_2\text{H}_4 + h\nu = \text{NH}_2' + \text{NH}_2$	<1580	}

TABLE 37

*Photodissociation products established from absorption spectra**

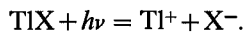
Process	Effective wave length, Å	Absorbing particle	Reference
$\text{I}_2 + h\nu = \text{I} + \text{I}'$	<5000	$\text{I}(^2P_{3/2}), \text{I}'(^2P_{1/2})$	[1233]
$\text{CS}_2 + h\nu = \text{CS} + \text{S}'$	<2000	CS	[155]
$\text{HCN} + h\nu = \text{H} + \text{CN}$	1450–2000	CN	[968]
$\text{H}_2\text{S} + h\nu = \text{H} + \text{HS}$	2000	SH	[1054, 1036]
$\text{D}_2\text{S} + h\nu = \text{D} + \text{DS}$	"	SD	
$\text{H}_2\text{CO} + h\nu = \text{H} + \text{HCO}$	"	HCO	[1055, 751]
$\text{CH}_3\text{CHO} + h\nu = \text{CH}_3 + \text{HCO}$	"	HCO	
$\text{C}_2\text{H}_5\text{CHO} + h\nu = \text{C}_2\text{H}_5 + \text{HCO}$	"	HCO	
$\text{C}_2\text{H}_3\text{CHO} + h\nu = \text{C}_2\text{H}_3 + \text{HCO}$	"	HCO	
$(\text{HCO})_2 + h\nu = \text{HCO} + \text{HCO}$	"	HCO	
$\text{CH}_3\text{CDO} + h\nu = \text{CH}_3 + \text{DCO}$	"	DCO	
$\text{NH}_3 + h\nu = \text{H} + \text{NH}_2$	"	NH ₂	[752]
$\text{ND}_3 + h\nu = \text{D} + \text{ND}_2$	"	ND ₂	
$\text{N}^{15}\text{H}_3 + h\nu = \text{H} + \text{N}^{15}\text{H}_2$	"	N ¹⁵ H ₂	
$\text{Hg}(\text{CH}_3)_2 + h\nu = \text{HgCH}_3 + \text{CH}_3$	"	CH ₃	
$\text{Hg}(\text{CD}_3)_2 + h\nu = \text{HgCD}_3 + \text{CD}_3$	"	CD ₃	[754]
$\text{CH}_3\text{I} + h\nu = \text{I} + \text{CH}_3$	"	CH ₃	
$\text{CH}_3\text{Br} + h\nu = \text{Br} + \text{CH}_3$	"	CH ₃	
$\text{CH}_3\text{CHO} + h\nu = \text{HCO} + \text{CH}_3$	"	CH ₃	
$(\text{CH}_3)_2\text{CO} + h\nu = \text{CH}_3\text{CO} + \text{CH}_3$	"	CH ₃	
$(\text{CH}_3)_2\text{N}_2 + h\nu = \text{CH}_3 + \text{N}_2 + \text{CH}_3$	"	CH ₃	

* With the exception of the first two lines of this table, all the data were obtained by the flash photolysis method (see p. 424). For this reason it is impossible to regard as completely reliable the schemes for the primary photochemical acts given in column 1.

In certain cases the nature of the photodissociation products of molecules has been established on the basis of the absorption spectra of the product free atoms and radicals. The relevant data are shown in Table 37. Suitable electronic levels, ensuring the applicability of the absorption method in identifying the photodissociation products of a molecule, occur in fact extremely rarely, so that the optical absorption method can be used only in rare individual cases.

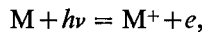
Recently, using a paramagnetic resonance method [794], various radicals have been detected which are formed during the exposure of a series of substances to ultraviolet light. In particular, during the exposure of hydrogen peroxide H_2O_2 the hydroxyl radical was detected, from which it follows that the photochemical decomposition of H_2O_2 takes place according to the scheme $\text{H}_2\text{O}_2 + h\nu = 2\text{OH}$. We have already noted this in connection with the problem of detecting free atoms and radicals arising during thermal reactions.

It should be noted that in addition to the photodissociation of molecules into neutral particles (one of which is excited), Terenin and Popov [261] observed cases of photoionization consisting of the decomposition of a molecule into oppositely charged ions. This type of photoionization was detected during the exposure of halide salts of univalent thallium TlCl , TlBr , TlI , which decompose according to the scheme



For the three salts the effective wave lengths corresponding to maximum absorption are ≤ 1850 , 2000 and 2125 Å respectively.

It should also be noted that photoionization consisting of the detachment of an electron from a molecule, i.e. the process

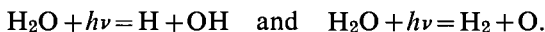


is a particular case of the photoelectric effect, but in ordinary photochemical reactions it apparently does not play a particularly important part since the ionization potential of molecules is usually 10 eV and higher which corresponds to a wave length ($\lambda \leq 1200$ Å) in the vacuum region of the spectrum which is rather difficult to attain experimentally.

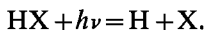
Photoionization processes play an important part in photochemical reactions taking place under the action of short wave radiation and especially under the action of X- and gamma-rays (see Chap. 8).

While the photodissociation processes in which the products of the splitting of the molecule are excited or ionized particles can comparatively easily be interpreted from the point of view of the chemical nature of these particles, the photodissociation of molecules into unexcited neutral particles presents great difficulties in this regard. Even in the case of a substance as simple as water vapour it is not reliably known into what

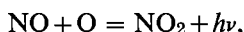
kind of particles an H_2O molecule dissociates when exposed to light in the 2000 Å region. In this spectral region dissociation is energetically possible according to the schemes



On the grounds that the absorption band of water lying in this region has small width ($7.6 - 6.7 = 0.9$ eV) and a relatively sharply defined red limit which corresponds to an energy considerably in excess of the dissociation energy of the H_2O molecules into H and OH , Neuimin and Terenin [214, 263] consider dissociation into $\text{H}_2 + \text{O}$ to be the more probable. On the other hand from geometrical considerations of the H_2O molecule and also on the grounds that the electronic shells of hydroxyl OH and the halogen atoms X are similar in structure, the more probable of the schemes shown seems to be the first, i.e. the process $\text{H}_2\text{O} + h\nu = \text{H} + \text{OH}$, similar to the photodissociation process of hydrogen halide molecules,



A well known argument in favour of this scheme is provided by the experimental data of Rodebush and Wahl [1078] who, carrying out a Stern-Gerlach experiment, did not detect oxygen atoms in the gas arising from the electrodeless electrical discharge in water vapour, nor did they find even molecular oxygen (which could have been formed as a result of atomic recombination) in the discharge zone (see also Rollefson and Burton [1081] §6-7). In contrast with this,⁽²⁾ from the yield of CO_2 formed by introducing carbon monoxide into a stream of the gas produced by discharge in water vapour (using a discharge tube of the usual type with aluminium electrodes), and also from observations of the air afterglow arising during the introduction of nitric oxide into this stream and based on the process [653, 654, 50, 104]

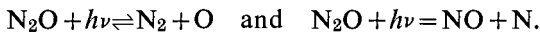


Avramenko [3] came to the conclusion that the atomic oxygen formed in the discharge should have a concentration exceeding that of the hydroxyl concentration by a factor of at least ten. Thus one should recognize there is no unambiguous experimental demonstration of the accuracy of either scheme for the process of the photodissociation of the H_2O molecule in the region of the long wave absorption bands ($\lambda = 2000$ Å); this is in contrast with the process $\text{H}_2\text{O} + h\nu = \text{OH}' + \text{H}$, which takes place during

⁽²⁾ This contradiction apparently results from a difference in pressure of the water vapour and conditions of discharge in the experiments of the authors mentioned. From a mass-spectrometric analysis of the gas from discharge in water vapour Lavrovskaya Skurat and Tal'roze [165] found that the concentration of O atoms in this gas at a water vapour pressure of 3 mm of mercury is considerable; it diminishes rapidly when the water vapour pressure is lowered.

the exposure of water vapour to light of wave length less than 1400 Å; this scheme has been unambiguously established by Neuimin and Terenin [263, 214] (see also [487]).

A similar case is the photodissociation of nitrous oxide which may proceed according to the schemes



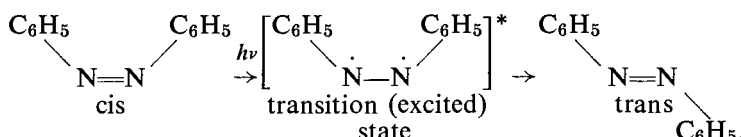
Indirect considerations indicate the greater probability of the former scheme [1325].

With an increase in the number of atoms in a molecule the number of possible types of decomposition increases, and an experimental explanation of the true nature of the dissociation products becomes especially difficult.

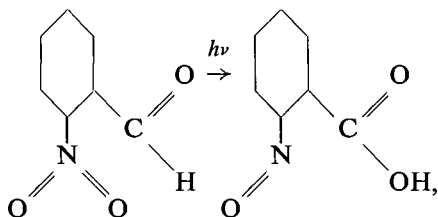
While the continuous absorption spectra of gases give evidence regarding the photochemical dissociation of molecules, spectra with distinct line-banded structure indicate that the primary photochemical process can produce excited molecules which are thus initial centres of reaction. But, cases in which the initial centre of reaction is an excited molecule are apparently extremely rare in reactions of *simple molecules*, and at present it is possible to quote only a very limited number of examples of this kind of reaction.

There are however, a large number of photochemical reactions involving *complex molecules* (especially molecules of aromatic compounds, for example the molecules of a large number of dyes); here the initial centres of reaction certainly are excited molecules. This clearly follows from the fact that in many cases (referring to dyes) photochemical changes take place as the result of absorption of visible light whose energy is usually insufficient to break the intramolecular bonds.

Isomeric changes of complex compounds in particular belong to the class of reactions taking place through the electronically excited molecules primarily generated [262]. Thus, according to current ideas, stereo-isomeric *cis-trans*-conversions under the action of light (photostereo-isomerization) takes place in such a way that, as a result of light absorption a *cis*-compound molecule passes into an excited state; from this state it may return to its initial state with the emission of light (fluorescence), or else by partial conversion of electronic excitation energy into torsional vibrations round the axis of the molecule, making possible the reversal of one of its parts in relation to the other, it may pass to a new state, viz. the *trans*-form. As an example the *cis-trans*-conversion of azobenzene may be represented by the following scheme:



Another example of the conversion of a complex molecule taking place via an excited state (under the action of violet or ultraviolet light) is given by the tautomeric conversion of *ortho*-nitrobenzaldehyde into *ortho*-nitrobenzoic acid



which occurs both in the gas phase and also in solutions and in the solid state; when the reaction takes place in the gas phase approximately one aldehyde molecule is converted for each quantum of light absorbed.

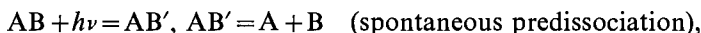
Many *photo-addition* reactions also take place via the excited states of the reacting molecules; among these are reactions of dimerization, condensation and addition of oxygen. An example of photodimerization is the conversion of anthracene into dianthracene which is observed when concentrated anthracene solutions are exposed to light exciting fluorescence (Terenin [262]).

Particularly numerous are the addition reactions of oxygen to excited molecules of aromatic compounds which result in the formation (i) of relatively unstable "moloxides" MO₂, which decompose readily when the oxygen is pumped off (into M+O₂), and also (ii) of stable oxidation products such as aldehydes and acids. An example of these reactions is given by the discoloration reactions of dyes. According to Terenin [262], an important part in the addition reactions of oxygen and molecules of other substances is played by the metastable states of the biradical, i.e. the states of an excited molecule possessing two valency electrons as well as a supply of electron excitation energy. For this reason the ability of molecules in a biradical state to add other molecules is particularly high [861, 1039a].

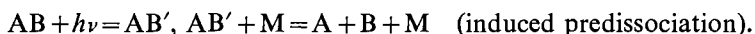
As a result of *predissociation*, which consists either of the spontaneous dissociation of the excited molecule or of its dissociation through collision, it is very often not the excited molecules but their dissociation products which are the initial centres of photochemical reactions taking place in the discrete spectral region. Predissociation as the spontaneous decomposition of an excited molecule is observed when transition to an unstable state is not connected with the violation of a selection rule. However even in the case of forbidden transitions predissociational decomposition may be possible because of external factors which remove the quantum

prohibition. In this case the predissociation is called *induced* predissociation. Up to the present time the cases of predissociation detected by direct experiments are predissociation induced by a magnetic field (I_2) and by molecular collisions (I_2 , Br_2 , N_2 , NO , S_2 , Se_2 , Te_2). From the point of view of the mechanism of photochemical reactions, predissociation induced by molecular collisions (pressure) is of the greatest interest.

The predissociational decomposition of molecules (spontaneous or induced) is clearly the most frequently encountered case of a primary photochemical act, characteristic of photochemical reactions in the discrete absorption spectral region [1081]. In addition to the structure of the spectrum, which is not always sufficiently well known, evidence of the wide occurrence of predissociational decomposition is given by data on the interrelation between the centre of excitation of the molecule and the broken bonds. For example, in aldehydes, ketones and carboxylic acids the excitation centre is the group $>CO$ common to all these compounds; this follows from the position of their long wave length spectrum. The bonds broken during the photochemical decomposition of the molecule here may be bonds with the C-atom of this group as well as bonds in other groups, as follows from analysis of the photochemical decomposition products of aldehydes, ketones and acids. The breaking of bonds not subjected to the direct action of light is obviously possible only when an *excited* molecule is first created during the light absorption, and then this molecule decomposes as the result of a subsequent redistribution of energy, either spontaneously (spontaneous predissociation) or because of a collision (induced predissociation). Accordingly, photochemical dissociation in the discrete absorption spectral region should be regarded as the result of the processes.



or of the processes



Analysis of extensive experimental material relating to the photolysis of compounds of various classes leads to the conclusion that in fact both photolysis schemes occur [1081].

The first of the schemes shown may be illustrated by the predissociational decomposition of an excited aniline molecule $C_6H_5NH_2$ [211, 1183]. Experiments show that excited aniline molecules, formed during the exposure of aniline vapour to light of wave length 2878 Å, are not capable of spontaneous decomposition and lose their excitation energy by radiation (fluorescence). Aniline molecules excited by the action of light of wave length less than 2800 Å partly fluoresce and partly dissociate (apparently according to the scheme $C_6H_5NH_2 = C_6H_5 + NH_2$

since one of the photodissociation products of aniline in the region $\lambda = 2800$ to 2500 Å is hydrazine N_2H_4 so that the probability of dissociation increases with a decrease in wave length of the exciting light. Table 38 shows values for the lifetime of excited aniline molecules; this is given by the formula

$$\tau = 1/(f+d), \quad (23.10)$$

where f is the probability (mathematical expectation) of radiation and d is the probability of dissociation. The table also shows dissociation probabilities for various wave lengths, i.e. for various excitation states of the $C_6H_5NH_2$ molecule. It can be seen from this table that the probability of dissociation increases with increase in excitation energy of the aniline molecule.

TABLE 38

Lifetime τ and probability of dissociation d of excited aniline molecules at 1.6 mm Hg and 70°C
(according to Stevens [1183])

$\lambda, \text{Å}$	2878	2791	2670	2598	2529
$d \cdot 10^{-7} \text{ sec}^{-1}$	0.0	1.2	10.4	19.1	50.4
$\tau \cdot 10^9 \text{ sec}$	7.87	6.45	4.03	3.05	1.55
$T_{\text{vib}} \text{ } ^\circ\text{C}$	—	410.0	470.0	508.0	547.0

It should be added that according to Stevens [1183] the quantity d may be expressed by the formula

$$d = 3.6 \times 10^{13} \exp(-12,000)/RT_{\text{vib}}, \quad (23.11)$$

where T_{vib} is the vibrational temperature which is given by the formula [431]

$$T_{\text{vib}} = T + h(\nu_{\text{excit}} - \nu_0)/C_{\text{vib}}. \quad (23.12)$$

Here ν_{excit} is the frequency corresponding to the excitation energy of the aniline molecule; ν_0 is a constant equal to $34,034 \text{ cm}^{-1}$ (see [38]); C_{vib} is the molar vibrational heat capacity of the excited aniline molecule and T is the temperature (343°K).

The values of the vibrational temperature T_{vib} for various excitation states of $C_6H_5NH_2$ are shown in the fourth line of Table 38. Figure 83 shows $\log d$ as a function of $1/T_{\text{vib}}$; it can be seen that in accordance with formula (23.11) this relationship is expressed by a straight line.

Returning to the problem of the chemical nature of the photodissociation products of a light-activated complex molecule (in the predissociation

and continuous light absorption regions), we find from numerous experiments that these products may equally well be saturated molecules or free radicals [1081]. Analysis of photolysis products and study of the influence of various factors (wave length, pressure of the foreign gases etc.) on the reaction rate and on the composition of the products show that the same molecule is often capable of decomposing both into saturated molecules and into radicals.

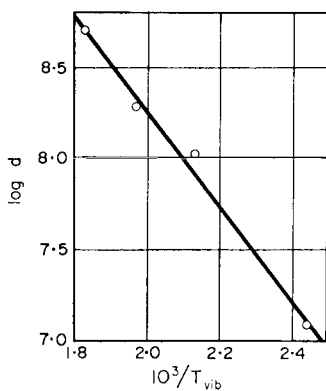
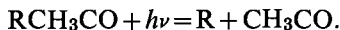


FIG. 83. The dissociation constant for the electronically excited molecule of aniline $\text{C}_6\text{H}_5\text{NH}_2$ as a function of the inverse "vibrational" temperature (according to Stevens [1183]).

Rather than linger on a detailed inspection of the vast amount of experimental material relating to this problem, we shall limit ourselves to illustrating the various possible types of the photodissociation of molecules with a few examples. Owing to the existence of a series of physico-chemical experimental methods for the detection of free atoms and radicals the data obtained by these methods are the most reliable. We have already quoted (pp. 413-4 above) certain results obtained using the spectroscopic method for detecting and identifying the atoms and radicals formed during the primary photochemical act. Using the method of para-ortho conversion of hydrogen, West [1276] established the radical character of the photolysis of methyl iodide CH_3I . Using this method and also the mirror method it has been shown that alkyl radicals are formed during the photolysis of ketones [1016]. These radicals were detected by Pearson and his coworkers [1017] during the photolysis of the following ketones: $(\text{CH}_3)_2\text{CO}$, $\text{CH}_3\text{C}_2\text{H}_5\text{CO}$, $(\text{C}_2\text{H}_5)_2\text{CO}$, $\text{CH}_3\text{C}_3\text{H}_7\text{CO}$, $\text{CH}_3\text{isoC}_3\text{H}_7\text{CO}$, $(\text{C}_3\text{H}_7)_2\text{CO}$, $(\text{iso C}_3\text{H}_7)_2\text{CO}$, $\text{CH}_3\text{C}_4\text{H}_9\text{CO}$, $(s\text{-C}_4\text{H}_9)_2\text{CO}$, $(t\text{-C}_4\text{H}_9)_2\text{CO}$. Investigations of the photolysis of methylketones RCH_3CO show that decomposition of the ketone molecule into radicals is the main photolytic

process;⁽³⁾ the products of this decomposition are an alkyl radical R and an acetyl radical CH_3CO ,

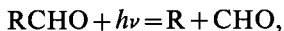


It has been established that during the decomposition of acetone the radicals CH_3 and CH_3CO are formed in approximate equal quantities (see Rollefson and Burton [1081], p. 235–236; also see [985]). We should add that at temperatures higher than 60°C acetyl is apparently unstable and decomposes into $\text{CH}_3 + \text{CO}$.⁽⁴⁾ This conclusion follows from the fact that at temperatures higher than 60°C the acetone photolysis products do not include diacetyl ($\text{CH}_3\text{CO})_2$, the formation of which is connected with the recombination process of acetyl radicals, $2(\text{CH}_3\text{CO}) = (\text{CH}_3\text{CO})_2$. Besides this there is evidence that in the discrete absorption region acetone decomposes according to the scheme

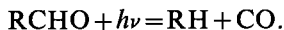


It is assumed that this process takes place according to an induced pre-dissociation mechanism (see Rollefson and Burton [1081, §8]).

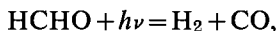
Photolytic decomposition into saturated molecules is found to be clearly possible in the case of other classes of compounds also. Thus one may assume that as well as the decomposition into radicals



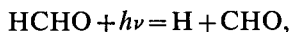
aldehydes may also decompose according to the scheme



Besides the data quoted by Rollefson and Burton [1081, §8, p. 72] the occurrence of both types of aldehyde decomposition is shown by Schoen's work [1112] on the photochemical decomposition of formaldehyde HCHO. According to Schoen's data in the region of wave lengths $\lambda > 3650 \text{ \AA}$ the photolysis of HCHO takes place according to the scheme



but in the short wave length region there is also the parallel process

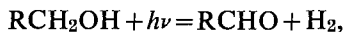


the latter having a higher rate; for wave length $\lambda = 3650 \text{ \AA}$ the rate of decomposition of the HCHO molecule into radicals exceeds the rate of

⁽³⁾ It is known that thermal decomposition of acetone also follows mainly a radical mechanism; this permits the use of the pyrolysis of acetone to obtain free methyl radicals.

⁽⁴⁾ According to the measurements of Szwarc and Taylor [1202] the energy of breaking the bond $\text{H}_3\text{C}—\text{COCH}_3$ is 72 kcal; therefore the energy of decomposition of the acetyl radical into CH_3 and CO is 16 kcal. Assuming unimolecular decomposition and taking the rate constant for this reaction as $k = 10^{13} \exp(-16,000/RT) \text{ sec}^{-1}$, we obtain the lifetime of the CH_3CO radical at 60° as $\tau = 1/300 \text{ sec}$; see [479a], however.

decomposition into saturated molecules by at least a factor of 5. A weighty argument in favour of the assumption that decomposition of alcohols RCH_2OH goes according to the scheme



is the fact that during the photolysis of methyl alcohol CH_3OH no free radicals were detected using the method of the para-ortho conversion of hydrogen [1010].

In concluding this short survey of the nature of primary photochemical processes we should note that in reactions in the liquid phase (in general, in a condensed phase), determination of the nature of the primary photochemical act is made more difficult by the fact that the absorption spectra of condensed substances are practically always diffuse. The reason for this diffuseness is the action of the molecular field (the Stark effect) leading to splitting and broadening of the levels. For this reason spectral structure alone may not serve as a criterion as to whether excitation or dissociation of a molecule takes place during light absorption. This problem may be solved with a greater or lesser degree of reliability on the basis of data on the absorption spectrum of the given substance in the gas phase, when the interaction between molecules in the condensed phase is not great, i.e. when the heat of vaporization or the heat of solution is small. In these cases the spectrum of the liquid does not differ by much from the spectrum of the gas in its general characteristics. The spectra of the liquid and gas forms of benzene, the liquid and gas forms of bromine etc. are examples of this. In all such cases one may assume that the primary photochemical act is identical in both the gas and liquid phases. When the interaction between molecules is large and consequently the spectrum of the liquid differs strongly from the spectrum of the gas, the problem of the nature of the primary photochemical act during photochemical reaction in the liquid phase requires special investigation.

§24. Secondary Processes during Photochemical Reactions

Secondary Processes in the Case of Atoms and Radicals

If as a result of the primary photochemical process valence-unsaturated free atoms and radicals are formed, then following the primary process there are secondary processes of their interaction or their reaction with other molecules. These processes may be of two types: processes causing the development or extension of the reaction and processes leading to the termination of the reaction. Examples of the first type are the process $\text{O} + \text{NO}_2 = \text{NO} + \text{O}_2$ following the primary process $\text{NO}_2 + h\nu = \text{NO} + \text{O}$ in the photochemical decomposition of nitrogen dioxide, or the process

$\text{Cl} + \text{H}_2 = \text{HCl} + \text{H}$ following the process $\text{Cl}_2 + h\nu = \text{Cl} + \text{Cl}$, in the photosynthesis of hydrogen chloride from hydrogen and chlorine. Processes of termination of a reaction may consist of the interaction of atoms (radicals) with molecules of reaction products or with molecules of an additive, for example the process $\text{O} + \text{NO} \rightarrow \text{NO}_2$ in the decomposition of NO_2 or the process $\text{Cl} + \text{O}_2 \rightarrow \text{ClO}_2$ in the formation of HCl (in the presence of oxygen as an inhibitor); also the interaction of atoms with the wall of the reaction vessel (adsorption, heterogeneous breaking of the reaction) or the interaction of atoms with one another (recombination), for example $\text{O} + \text{O} \rightarrow \text{O}_2$ or $\text{Cl} + \text{Cl} \rightarrow \text{Cl}_2$.

The nature of the reaction-terminating processes may often be established from the experimentally determined dependence of the photochemical reaction rate on the light intensity. Actually, when the primary photochemical process is the only source of atoms, the condition for their steady-state concentrations may be expressed in the form

$$\frac{dn}{dt} = \Delta I - \sum_i a_i n - bn - cn^2 = 0. \quad (24.1)$$

Here ΔI is the number of quanta absorbed in 1 second; $\sum_i a_i n$ is the overall rate of all the processes of interaction of atoms with molecules of any sort; bn is the rate of the heterogeneous termination of the reaction and cn^2 is the recombination rate.

The quantity ΔI , equal to $\delta I \cdot I^0$ (23.7), is proportional to the light intensity I^0 . Therefore when recombination of atoms does not play a significant part in the balance, i.e. when the term cn^2 in equation (24.1) is negligible, the stationary concentration of atoms and consequently the rate of reaction, which is equal to

$$w = n/\tau_p \quad (24.2)$$

($1/\tau_p$ is the frequency of the reaction process), is directly proportional to the light intensity. On the other hand, when the main terminating process is the recombination of atoms in which the rate of recombination is considerably greater than the overall rate of all other atomic processes, it is possible to neglect the middle terms in equation (24.1). A consequence of this is that the stationary concentration of atoms and the stationary reaction rate will be proportional to the square root of the light intensity. Recombination reaction-breaking must play a particularly large part when there are large concentrations of atoms. In the general case when all the components of equation (24.1) are comparable with one another, the expression of the reaction rate as a function of light intensity is more complex: over a not very wide intensity range this expression may clearly be represented approximately by a power law with an index between 1 and 1/2.

Free atoms and radicals originate as primary active centres of a photochemical reaction when the reaction is controlled by the flash photolysis method developed by Porter and Norrish [1037, 982]. In this method the light source is provided by a pulse spark discharge in hydrogen (or in any other gas) with a very large discharge energy (up to 10,000 joules) and with a pulse duration of some tenths of a millisecond to several milliseconds. During exposure of the gas, which is at a pressure of several millimetres or centimetres of mercury and is capable of absorbing the light emitted by the source, practically complete dissociation of the gas into atoms and radicals is possible. For example, Porter observed the disappearance of the absorption spectrum for molecular chlorine, thus showing the complete dissociation of Cl_2 molecules into atoms. This is shown also by the rise in pressure (from 10 to 20 mm of mercury) observed at the moment of exposure without a substantial rise in temperature. Porter also observed the glow from the recombination of chlorine atoms, i.e. the glow connected with the process $\text{Cl}({}^2P_{3/2}) + \text{Cl}({}^2P_{1/2}) = \text{Cl}_2 + h\nu$, which is the reverse process of the photochemical dissociation of Cl_2 .⁽⁵⁾ During the exposure of carbon disulphide CS_2 vapour the radical CS was detected by its absorption spectrum. Similarly the radical ClO , formed during the exposure of a mixture of chlorine and oxygen, was detected by its absorption spectrum. We give below a series of radicals which were detected by their absorption spectra during explosion of various gas mixtures by exposure to an intermittent light source.

Mixture	Radicals
H_2, O_2	OH [979, 980]
$\text{C}_2\text{H}_4, \text{NO}_2$	CN, NH [979, 980]
$\text{C}_2\text{H}_2, \text{O}_2, \text{NO}_2$	$\text{CN}, \text{NH}, \text{CH}, \text{C}_2, \text{C}_3(?)$ [981]

Because of the large concentration of radicals (which are the primary reactive centres) appearing during flash photolysis, the secondary chemical processes in these reactions are mainly processes taking place between free radicals. This feature of the chemical mechanism of these reactions is shown particularly in the striking difference between the products of these reactions and those of ordinary photochemical reactions [977, 849].

Secondary Processes involving Excited Molecules

Let us consider cases in which excited molecules are generated as a result of the primary photochemical process. We find that their further fate depends on the processes in which they take part.

In the general case these processes are: light emission by an excited molecule (fluorescence), energy loss by collision with another molecule

⁽⁵⁾ Here $\text{Cl}({}^2P_{3/2})$ represents the normal chlorine atom and $\text{Cl}({}^2P_{1/2})$ is the metastable atom possessing electronic excitation energy corresponding to the difference of the terms ${}^2P_{1/2} - {}^2P_{3/2} = 881 \text{ cm}^{-1}$, i.e. 2.5 kcal/g. atom.

(quenching of fluorescence), spontaneous or induced predissociational decomposition of a molecule (if the light absorption comes into the predissociation region) and lastly, the interaction of an excited molecule with other molecules, leading to reaction.

If the molecules absorbing light are in a homogeneous medium, all the above processes may be regarded as homogeneous. Since the mean life time of an excited molecule is more than 10^{-8} sec only in rare cases, while the mean velocity of a molecule is of the order 10^4 – 10^5 cm/sec (at not very high temperatures), the distance of the excited molecule from its place of excitation (up to the time of emission of its energy) does not on average exceed 10^{-4} – 10^{-3} cm. Therefore the place of excitation of a molecule and the place where one of the possible secondary processes occurs may be regarded as practically identical. Consequently, during the excitation of molecules in a homogeneous medium, heterogeneous secondary processes (such as processes on the walls of the reaction vessel in which excited molecules take part) are practically excluded.

Denoting the concentration of excited molecules by n' and the frequency of the secondary processes by ν_f , ν_q , ν_p and ν_r , we find

$$\frac{dn'}{dt} = \Delta I - (\nu_f + \nu_q + \nu_p + \nu_r)n'. \quad (24.3)$$

Here $\nu_f = 1/\tau_f$ is the frequency of fluorescence (τ_f is the mean life time of an excited molecule); $\nu_q = k_q p$ is the frequency of quenching of the fluorescence (k_q is the constant of quenching and p is the pressure or concentration); $\nu_p = k_p + k'_p p$ is the frequency of the predissociational decomposition (the first term is the rate constant for spontaneous decomposition and the second term for induced decomposition); $\nu_r = k_r c$ is the frequency of reaction of excited molecules (k_r is the reaction rate constant, c is the concentration of reagent).

If predissociational decomposition is absent or unimportant, the reaction rate will be determined by the quantity ν_r , or more precisely by the quantity $\nu_r n'$, i.e. by the rate of interaction of excited molecules with molecules of reagent. In the absence of tertiary or further processes the rate of the over-all reaction will be $w = \nu_r n'$ (24.2). In this case we can find the rate of the stationary reaction; for the condition $dn'/dt = 0$ gives

$$n' = \Delta I / (\nu_f + \nu_q + \nu_r)$$

so that

$$w = \frac{\nu_r}{\nu_f + \nu_q + \nu_r} \Delta I. \quad (24.4)$$

As is obvious from this formula, the reaction rate in this case cannot exceed the molecular excitation rate ΔI , and is determined by the presence

of the deactivating processes, namely fluorescence and quenching of fluorescence.

The reaction mechanism is considerably complicated when predissociational decomposition plays an important part. This is particularly so when, as a result of predissociation, chemically unsaturated particles are formed which appear in the photochemical reaction zone so that tertiary and other processes follow. When predissociational decomposition predominates, the overall reaction rate is determined mainly by the interaction of predissociation products and not that of excited molecules, and the situation is close to the one considered at the beginning of this section. However, it differs in that the reaction rate depends to a large degree on the condition of the medium, which determines the relative role of the deactivation processes.

Fluorescence. Metastable Molecules

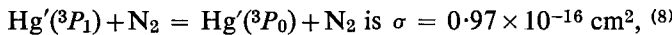
Let us consider in more detail the quantities ν . It has already been noted that the frequency of fluorescence ν_f is of the order 10^8 sec^{-1} . This value of ν_f holds for most gases. In a series of cases, however, both for gases and particularly for solutions, ν_f is observed to be of the order 10^9 sec^{-1} [191, 262]. The shortening of the mean life time of an excited atom in the liquid state is determined by the action of surrounding molecules. However, for gases and liquids alike, cases are possible in which the frequency may be considerably less than 10^8 sec^{-1} . Such cases are possible when the excited state is metastable, i.e. when the optical transition of a molecule from an excited state to the normal state (or generally to a lower-lying state) has small probability. The reverse transition, i.e. that of a normal molecule to a metastable state, is also of low probability; therefore the immediate optical excitation of metastable levels takes place with a probability significantly lower than that of the excitation of allowed transitions. An example of such excitation is that of the atmospheric bands of the oxygen molecule connected with the metastable state ${}^1\Sigma_g^+$.⁽⁶⁾ Apparently the commonest cases of excitation of metastable states (especially in a condensed phase) will be those in which, as a result of light absorption, transition takes place to a normal excited state and then the molecule goes over to a metastable state either in an optical way, i.e. emitting or absorbing light, or as a result of collisions.

In the latter case the transition of an optically active excited molecule into a metastable state is one example of fluorescence quenching; this is usually a transition to another (optically inactive) electronic state (see below) upon collision of the excited molecule with another molecule. In the case considered this state is a metastable state of the excited molecule.

⁽⁶⁾ The lifetime of this state is 7 sec. [434] and therefore the frequency of fluorescence is of the order of 10^{-1} sec^{-1} .

It should be noted that fluorescence quenching which transfers a molecule into a metastable state will obviously only be a feature of the deactivation of the excited molecule when the metastable level is considerably lower than the level originally excited, so that transition to a metastable state is connected with the loss by the excited molecule of a large part of its excitation energy. When the metastable level is situated near the original level, deactivation of the molecule need not necessarily be a result of fluorescence quenching. On the contrary, in these cases the fluorescence quenching, which brings the molecule into a metastable state, leads to an increase in the life time of the molecule due to the large value of τ_f in this state; this leads to an increase in the relative probability of its entering into reaction.

An example of such a process is the fluorescence quenching of mercury atoms, which has been well studied. During absorption of the resonance line of mercury ($\lambda = 2536.5 \text{ \AA}$) by mercury vapour the initial excited state Hg'^3P_1 of mercury atoms arises, the mean life time of which is $1.55 \times 10^{-7} \text{ sec}$ [454, 453]; after this time the excited atoms return to the ground state 1S_0 , emitting monochromatic light of wave length 2536.5 \AA . However, during its life time the excited atom may experience quenching collisions, as a result of which it may go over either to the ground state 1S_0 or to the metastable state 3P_0 ,⁽⁷⁾ which is 0.218 eV from the primary excited state. Study of the quenching of the resonance fluorescence of mercury by nitrogen shows that the second of these processes is considerably more probable than the first. Thus, according to Samson [1100], the effective cross section for the process



while the cross section for the process



The occurrence of the transition to the metastable state 3P_0 during fluorescence quenching of mercury by nitrogen (and also by other gases and vapours) is immediately obvious from observations on the absorption by mercury vapour of the line 4046.6 \AA during excitation of the resonance glow of mercury (2536.5 \AA) in the presence of nitrogen, carbon monoxide or water vapour [649, 650, 845, 1034]. Since absorption of the line 4046.6 \AA is connected with the transition $6s6p^3P_0 \rightarrow 6s7s^3S_1$, the detection of this

⁽⁷⁾ The mean life-time of the metastable state 3P_0 of the mercury atom is estimated to be 10^{-3} sec [1034].

⁽⁸⁾ According to the more recent measurements of Matland [925], σ increases with temperature and is $0.6 \times 10^{-16} \text{ cm}^2$ at 325°K and $1.1 \times 10^{-16} \text{ cm}^2$ at 525°K .

⁽⁹⁾ According to [925], the effective cross sections for the processes

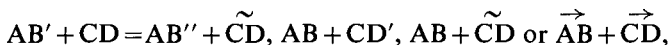
$\text{Hg}'^3P_0 + \text{N}_2 = \text{Hg}'^3P_1 + \text{N}_2$ and $\text{Hg}'^3P_0 + \text{N}_2 = \text{Hg}^1S_0 + \text{N}_2$
are $\sigma = 0.21 \times 10^{-16} \text{ cm}^2$ and $\sigma < 0.000006 \times 10^{-16} \text{ cm}^2$.

line in the absorption spectrum of mercury vapour shows that it goes over to the metastable state 3P_0 when the excited atoms 3P_1 first generated collide with molecules of the admixtures mentioned. The emergence of a metastable level under these conditions is also clearly indicated by the observations of Wood and Gaviola [1319] who found that in the presence of small quantities of nitrogen or water vapour the fluorescence spectrum of mercury contains the weak ("forbidden") line 2655.7 Å, connected with the transition $6s6p {}^3P_0 \rightarrow 6s6s {}^1S_0$, as well as the line 2536.6 Å.

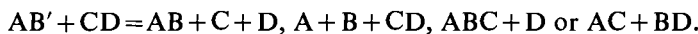
Since the difference in the energies of excited mercury atoms found in the states 3P_1 (112 kcal/g atom) and 3P_0 (107 kcal/g atom) is low, they must be practically identical in chemical activity. However, because of the long life of the metastable atoms, their chemical action in practice is greater than that of atoms in the 3P_1 state; this has been established for a series of photochemical reactions. For example, Meyer [952] found that the addition of nitrogen leads to an increase in the reaction rate in a system containing hydrogen and mercury vapour (the interaction of hydrogen with metallic oxides).

Quenching of Fluorescence

Quenching of fluorescence consists of the weakening of the intensity of fluorescence in the presence of foreign admixtures or during increase in pressure (or concentration) of the fluorescent substance itself. Considering the quenching of fluorescence of an excited atom or molecule as a transition of the system—the excited particle plus the quenching molecule—from a certain initial quantum state to another state, we may treat from a common viewpoint both the physical processes of transfer and transformation of energy in the system, and also those chemical changes which often follow the quenching of fluorescence. Among such physical types are processes which may be represented schematically in the forms



where the prime or two primes denote an electronically excited molecule, the tilde denotes a vibrationally excited molecule and the arrow denotes a molecule possessing excess energy of translational motion. The chemical processes in the system $AB' + CD$ may be represented schematically as



From this point of view all these processes represent transitions of the system from one potential surface, corresponding to the initial state of the system, to different surfaces according to whatever final state of the system results from the quenching of the fluorescence.

Data referring to some of the above mentioned processes are set out in Table 39; this gives possible schemes for the mechanism of quenching

of the fluorescence of mercury (3P_1) by various substances and also experimental values of σ , the effective cross sections of fluorescence-quenching which are a measure of the probability of quenching processes.

Some remarks are necessary on the data in Table 39. In investigations of the quenching of the mercury resonance fluorescence by hydrogen it is usually accepted that the second of the processes indicated in the table is the main one; this also explains the sensitizing action of mercury in photochemical reactions in which hydrogen participates. An indication of high probability of the first process, consisting of the transition of an excited mercury atom to a metastable state, was found by Darwent and Hurtubise [527], who detected the metastable Hg atoms which are formed during exposure of mercury vapour in the presence of hydrogen; these atoms were detected by the electronic emission they caused in metallic nickel [951]. According to these authors the cross sections for both processes shown in Table 39 are almost the same.

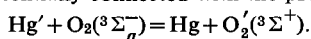
The most exhaustively studied mechanism is that of the quenching of the fluorescence of mercury by nitrogen, which undoubtedly consists of the transition of a mercury atom to a metastable state, with simultaneous transition of a nitrogen molecule to the vibrational state⁽¹⁰⁾ $v = 1$. The most accurate values for the cross section of this process were obtained by Matland [926], who found $\sigma = 0.5 \times 10^{-16} \text{ cm}^2$ at 325°K and $1.0 \times 10^{-16} \text{ cm}^2$ at 525°K . The figure $6 \times 10^{-16} \text{ cm}^2$ cited by Bates [355] must be considered erroneous.

The mechanism of the quenching action of oxygen is not completely clear. In recently published work based on indirect evidence obtained from a study of the effect of various gases on the ozone yield in the photochemical sensitization of the reaction $3\text{O}_2 \rightarrow 2\text{O}_3$ by mercury, Volman [1253] came to the conclusion that in the quenching process the mercury atom goes over to the ground state and the O_2 molecule to the vibrationally excited fundamental (${}^3\Sigma_g^-$) or singlet state. Still earlier Volman [1252] had shown that the process $\text{Hg}' + \text{O}_2 = \text{HgO} + \text{O}$ does not take place. We may add that in the presence of oxygen, metastable atoms of mercury are not detected [527]; this may be regarded as an indication that the process $\text{Hg}' + \text{O}_2 \xrightarrow{\text{---}} \text{Hg}'' + \text{O}_2$ is absent or has low probability.^(10a)

The mechanism of the quenching action of carbon monoxide and nitric oxide apparently consists of the transition of a mercury atom to a

⁽¹⁰⁾ This fact was established by the work of Wood [1317], Klumb and Pringsheim [845] and Samson [1100]. See also [926] and [383].

^(10a) After Gill and Laidler [*Canad. J. Chem.*, **36**, 79 (1958)] the quenching of mercury fluorescence by oxygen is essentially connected with the process



However, this conclusion cannot be considered as fully justified [Volman, Gill and Laidler, *J. Chem. Phys.*, **30**, 589 (1959)].

TABLE 39*

Quenching of the resonance fluorescence of mercury by various gases

Gas	Suggested quenching process	$\sigma \times 10^{16} \text{ cm}^2$
H ₂	Hg' + H ₂ = Hg'' + H ₂	27.0 [1327], 18.8 [578]
H ₂	Hg' + H ₂ = Hg + 2H	
D ₂	Hg' + D ₂ = ?	26.6 [578]
N ₂	Hg' + N ₂ = Hg'' + \tilde{N}_2	0.86 [1327]
O ₂	Hg' + O ₂ = Hg + \tilde{O}_2	62.5 [1327], 70.0 [998]
CO	Hg' + CO = Hg'' + C \tilde{O}	18.3 [1327]
NO	Hg' + NO = Hg'' + $\tilde{N}O$	111.0 [1327]
H ₂ O	Hg' + H ₂ O = Hg'' + H ₂ O	4.5 [1327], 3.1 [578]
H ₂ O	Hg' + H ₂ O = HgH + OH	
CO ₂	Hg' + CO ₂ = Hg + $\tilde{C}O_2$?	11.1 [1327]
NH ₃	Hg' + NH ₃ = ?	13.2 [1327], 10.4 [578]
CH ₄	Hg' + CH ₄ = Hg'' + C \tilde{H}_4	0.26 [1327], 0.18 [358]
CH ₄	Hg' + CH ₄ = Hg + CH ₃ + H	
C ₂ H ₆	Hg' + C ₂ H ₆ = Hg'' + C ₂ \tilde{H}_6	0.35 [525]
C ₂ H ₆	Hg' + C ₂ H ₆ = Hg + C ₂ H ₅ + H	
C ₃ H ₈	Hg' + C ₃ H ₈ = Hg'' + C ₃ \tilde{H}_8	4.1 [525]
C ₃ H ₈	Hg' + C ₃ H ₈ = Hg + C ₃ H ₇ + H	
n-C ₄ H ₁₀	Hg' + C ₄ H ₁₀ = Hg'' + C ₄ \tilde{H}_{10}	9.4 [525]
n-C ₄ H ₁₀	Hg' + C ₄ H ₁₀ = Hg + C ₄ H ₉ + H	
C ₆ H ₆	Hg' + C ₆ H ₆ = Hg + C ₆ H ₅ + H?	188.0 [1327], 132.0 [358]

* The table consists of data from the book of Mitchell and Zemansky [191] and more recent data. Hg' represents an excited mercury atom in the state 3P_1 ; Hg'' in the metastable state 3P_0 and Hg in the ground state (1S_0).

metastable state and of CO and NO molecules to the vibrational state $v = 1$. One of the arguments supporting this conclusion is the regular increase in quenching cross section along the series of diatomic molecules N₂, CO and NO, along with the decrease in the difference between the energy lost by the mercury atom $^3P_1 - ^3P_0 = 0.218 \text{ eV}$ and the energy of the vibrational quantum of these molecules [191]:

Molecule	N ₂	CO	NO
Difference in energy, eV	0.070	0.047	0.013
Cross section, Å ²	0.86	18.3	111

This increase is evidence of the effect of energy resonance, which is also possible on theoretical grounds.

The first of the two mechanisms shown in Table 39 for the quenching of the fluorescence of mercury by water vapour agrees with the established efficiency of water molecules in the conversion of excited mercury atoms

to the metastable state [1317, 845, 1100]; the second mechanism takes into account the photochemical decomposition of water sensitized by mercury [1129].

The mechanism of the quenching action of CO_2 and NH_3 has not been established. The absence of metastable mercury atoms during the exposure of mercury vapour in the presence of CO_2 [527] requires one to consider the process $\text{Hg}' + \text{CO}_2 = \text{Hg}'' + \tilde{\text{CO}}_2$ as being of low probability.

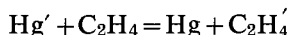
The data of Table 39 for the three members of the normal paraffin series (from C_2H_6 to C_4H_{10}) are part of a large amount of data obtained by Darwent [525] from a study of the quenching action of hydrocarbons of various structures. From an analysis of these data Darwent came to the conclusion that the quenching action of the hydrocarbon molecule is determined by the *number and type* of C—H bonds (primary, secondary and tertiary C—H bonds), the greatest efficiency belonging to tertiary bonds, the least efficiency to primary. The dependence of the quenching action on the number of C—H bonds is evidence that the interaction of an excited mercury atom with a molecule of a saturated hydrocarbon leads to breaking of one of the C—H bonds of the molecule. This conclusion also follows from experimental data on the photochemical decomposition of hydrocarbons [1169, 531]. Cvetanović [516] considers that the actual mechanism of the quenching process corresponds to the scheme $\text{Hg}' + \text{RH} = \text{HgH} + \text{R}$, in which the hydride HgH formed in the primary quenching process decomposes into Hg and H atoms or, reacting with the radical R , gives an energy-rich molecule RH (the latter in its turn is stabilized and changes into the original hydrocarbon or decomposes into two radicals⁽¹¹⁾). A direct indication of the existence of a quenching process ($\text{Hg}' + \text{RH} = \text{Hg}'' + \tilde{\text{RH}}$) taking place simultaneously with the above process and leading to metastable mercury atoms is given by the detection of these atoms during exposure of Hg vapour in the presence of a hydrocarbon [526]. According to [516], in the case of normal butane the probabilities of the processes $\text{Hg}' + \text{RH} = \text{Hg}'' + \text{RH}$ and $\text{Hg}' + \text{RH} = \text{HgH} + \text{R}$ (see Table 39) are in the ratio 3 to 4.⁽¹²⁾

Darwent and his coworkers [527] have studied the quenching of the fluorescence of mercury by a large number of halides and other derivatives of the hydrocarbons, and also the quenching action of a large number of unsaturated compounds [528]. From the regularities established in the experiments with saturated compounds we may deduce that the cross-

⁽¹¹⁾ The relatively low yield of hydrogen during the photochemical decomposition of hydrocarbons is a result of the reactions of HgH and R , according to Cvetanović.

⁽¹²⁾ It follows from the data of Cvetanović that the ratio of the cross sections (probabilities) of the processes $\text{Hg}' + \text{N}_2\text{O} = \text{Hg}'' + \text{N}_2\text{O}$ and $\text{Hg}' + \text{N}_2\text{O} = \text{Hg} + \text{N}_2 + \text{O}$ is equal to 1 : 4.

section of quenching, which is an over-all value corresponding to both mechanisms of the process (the transitions ${}^3P_1 \rightarrow {}^1S_0$ and ${}^3P_1 \rightarrow {}^3P_0$), increases on substituting for a carbon atom a group containing an atom of oxygen, nitrogen, sulphur or mercury; the same effect is also observed on substituting for an atom of hydrogen an atom of chlorine, bromine or iodine, whereas replacement of hydrogen by an atom of fluorine decreases the cross section of quenching. A series of regularities has also been established for unsaturated compounds. In connection with the mechanism of the quenching of the fluorescence of mercury by unsaturated hydrocarbons we note that, according to the available data [862, 478], (in contrast with the effect of saturated compounds) along with the photodissociation, for example the process $Hg' + C_2H_4 = Hg + H + C_2H_3$ another process



also takes place, which results in the formation of an electronically excited molecule. Of the two processes indicated here, for quenching by ethylene C_2H_4 the second process takes place about 100 times faster than the first at $25^\circ C$.

Theory of Quenching of Fluorescence

Denoting the frequencies of the relevant quenching processes by ν_i , we have in a stationary state

$$dn'/dt = \Delta I - (\sum \nu_i + \nu_f)n' = 0$$

(n' is the steady-state concentration of excited particles), from which we find that the intensity of fluorescence is

$$I = \nu_f n' = \nu_f \Delta I / (\nu_f + \sum \nu_i).$$

It is not difficult to see that in the absence of quenching the intensity of fluorescence I_0 is equal to the quantity ΔI , i.e. the number of quanta emitted is equal to the number of quanta absorbed. If we assume ΔI equal to I_0 and introduce quenching constants k_i which are related to the frequencies of quenching ν_i by

$$k_i = \nu_i / p,$$

where p is the pressure of the quenching gas, and if we neglect the quenching action of the fluorescent gas itself (which is permissible for sufficiently small pressures of the gas), then we may put the previous expression for the intensity of fluorescence in the form

$$I_p = I_0 / (1 + \tau_f \sum k_i p). \quad (24.5)$$

An expression of this type was first obtained by Stern and Volmer [1180]. Recently it has been established that low pressure of the fluorescent gas is not the only condition for the validity of the Stern–Volmer formula

[191]. In particular it has been shown that at large pressures of the quenching gas, as a result of *impact broadening* of the absorption line of the fluorescent substance, its absorption coefficient is changed (cf. p. 409), so that the quantity $I_0 = \Delta I$ becomes a function of the pressure of the absorbing gas. Consequently for the Stern–Volmer formula to be valid both the pressure of the fluorescent substance and the pressure of the quenching gas must be sufficiently small.

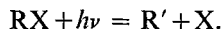
It has already been suggested that change of light absorption with change in pressure (and also with change in temperature) has a substantial influence on the course of a photochemical reaction (p. 408). Underestimation of the role of this factor often leads to inaccurate conclusions about the kinetics of photochemical reactions and also to erroneous inferences of the quenching action of these or other gases. Thus, allowing for the change in light absorption resulting from the impact broadening of the absorption lines, it has been shown [191] that quenching of the resonance fluorescence of mercury by helium and argon (detected by Stuart [1190]) and the quenching of the resonance fluorescence of sodium by a mixture of helium and neon (observed by Mannkopff [910, 604]) are a result of change in the absorption of the exciting light, and consequently have nothing in common with true fluorescence quenching.

Further, it has been shown [191] that besides the effect of broadening of the absorption lines it is necessary to allow for *diffusion of radiation* in the fluorescent gas, both as regards absorption of the emitted (resonance) radiation from the fluorescent substance and also the reverse process. Allowance for the diffusion of radiation (based on the theory developed by Milne [954]) leads to a complex relationship between the intensity of fluorescence and the pressure of the quenching gas (although this relation can, at low densities of the absorbing gas, be reduced to the Stern–Volmer formula). Values for the cross-sections of quenching of the resonance fluorescence of mercury shown in Table 39 were calculated allowing for diffusion of the radiation, and are free from errors connected with impact broadening, since the pressures for which these data were obtained do not give rise to appreciable broadening of the lines of resonance absorption of mercury [191].

Allowance for the diffusion of radiation and the broadening of the absorption lines is particularly necessary when studying resonance fluorescence, i.e. fluorescence excited by the resonance lines of the given substance (such as the line $\lambda = 2536.5 \text{ \AA}$ for mercury and the *D*-line for sodium). In these cases the simple Stern–Volmer formula does not indicate any change of intensity of the fluorescence with change in pressure of the quenching gas over a wide pressure range.

The Stern–Volmer formula is sufficiently accurate in other cases however. Of these, there is in particular the quenching of the fluorescence

of atoms and molecules formed during optical dissociation of various substances, i.e. as a result of the process



Typical curves (straight lines) for the quenching are shown in Fig. 84 for quenching of the *D*-fluorescence of sodium, formed during the optical dissociation of NaI vapour (by exposure to a cadmium spark) by iodine vapour, carbon dioxide, hydrogen and argon [1300, 265] (see also [720]).

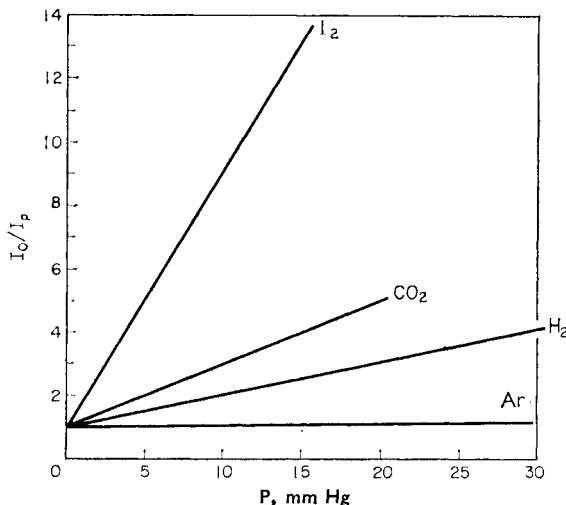


FIG. 84. Quenching of the fluorescence of sodium by iodine vapour, carbon dioxide, hydrogen and argon (according to various authors, see Mitchell and Zemansky [191]).

It follows from the Stern–Volmer formula that the quantity I_0/I_p must be a linear function of the pressure of the quenching gas, namely

$$I_0/I_p = 1 + \tau_f \sum k_i p; \quad (24.6)$$

and this is in agreement with Fig. 84. From the slope of the straight line (24.6) the quantity $\tau_f \sum k_i$ is found, from which the effective cross-section of quenching for the given gas may be calculated if the mean life τ_f of the excited atom is known. In those cases where the quenching of the fluorescence is connected with several parallel processes, the effective cross-section calculated is the over-all cross-section (see Table 39). In the case where one of the possible quenching mechanisms predominates, the measured cross-section is the cross-section for this process. The latter case should be most frequently observed since any similarity of cross-sections (even to an order of magnitude) of the different processes is quite improbable.

From the data of Fig. 84 the effective cross-section of quenching of the fluorescence of sodium by the given gas can be calculated by the following method. The mean effective wave length 2232 Å in the cadmium spark spectrum corresponds to an energy $N_A h\nu_0 = 127$ kcal/mole. After the subtraction of the dissociation energy of the NaI molecule, namely $D_{\text{NaI}} = 72$ kcal/mole, and the excitation energy of the sodium atom, $N_A A_{\text{Na}} = 48$ kcal/g atom, there remains 7 kcal. This energy is distributed between the Na' and I atoms so that the sodium atom receives an amount (determined by the conservation of energy and momentum)

$$K_{\text{Na}} = (M_{\text{I}}/M_{\text{Na}})[(N_A h\nu_0 - D_{\text{NaI}} - N_A A_{\text{Na}})/(M_{\text{Na}} + M_{\text{I}})]$$

(M = atomic weight), which comes to 6 kcal/g atom. This energy is several times bigger than the mean translational energy of thermal motion of the molecules at the temperature of the experiments (550°C). Thus as an approximation we may consider the quenching molecules to be stationary [265], and the rate constant for the process of quenching may be calculated according to the formula

$$k = \sum_i k_i = \sigma n v_{\text{Na}}, \quad (24.7)$$

where σ is the effective cross-section of quenching of fluorescence; n is the number of molecules of quenching gas in 1 cm³, and v_{Na} is the velocity of the excited sodium atoms.

From the data of Fig. 84 the following values were calculated for the effective cross section of quenching (for $\tau_f = 1.6 \times 10^{-8}$ sec.):

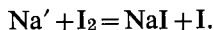
$$335 \times 10^{-16} \text{ cm}^2 (\text{I}_2), \quad 75 \times 10^{-16} \text{ cm}^2 (\text{CO}_2), \quad 25 \times 10^{-16} \text{ cm}^2 (\text{H}_2), \\ 25 \times 10^{-16} \text{ cm}^2 (\text{Ar}).$$

The sum of the effective radii of the sodium atom and the appropriate quenching molecule calculated from these σ values may be compared with the sum of the gas-kinetic radii of these particles:

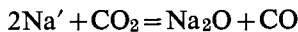
Quenching particle	I_2	CO_2	H_2	Ar
(Sum or radii) _{quenching}	10.3 Å	4.5 Å	2.7 Å	0.9 Å
(Sum of radii) _{gas-kinetics}	3.6 Å	3.0 Å	2.6 Å	2.8 Å

From this comparison it follows that the cross-section of quenching of fluorescence of sodium by iodine vapour is some ten times the gas-kinetic cross-section. Since the rate constant for the reaction of a sodium atom (unexcited) with an iodine molecule, i.e. the rate constant for the process $\text{Na} + \text{I}_2 = \text{NaI} + \text{I}$, is also some ten times greater than the constant calculated assuming that each gas-kinetic collision of Na and I_2 leads to

reaction (see p. 89), then the quenching of the fluorescence of sodium by iodine must surely be connected with the chemical process



It is also possible to ascribe the greater efficiency of quenching of the fluorescence of sodium by carbon dioxide to the chemical interaction of an excited sodium atom with a CO_2 molecule. This assumption does not contradict the thermochemical data, from which it follows that the process



has a positive thermal effect, which is 8 to 13 kcal/mole. However, it is not possible to explain the greater efficiency of quenching of the fluorescence of sodium by hydrogen in terms of the chemical interaction of an excited sodium atom with a molecule of hydrogen, since the process $\text{Na}' + \text{H}_2 = \text{NaH} + \text{H}$ is endothermic (the thermal effect is -8 kcal/mole). In the latter case, apparently, the quenching of the fluorescence should be connected with the process of converting the electronic excitation energy of the sodium atom into vibrational energy of the H_2 molecule, i.e. the process $\text{Na}' + \text{H}_2 = \text{Na} + \tilde{\text{H}}_2$. It is extremely probable that the quenching of the fluorescence of Na by carbon dioxide takes place by a fundamentally similar mechanism. The comparatively small cross-section

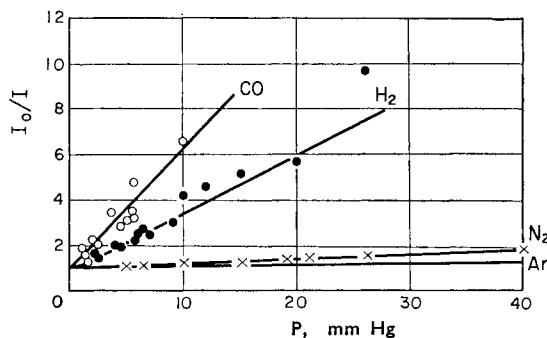


FIG. 85. Quenching of the fluorescence of hydroxyl by carbon monoxide, hydrogen, nitrogen and argon (according to Neuimin and Terenin [214, 263]).

of quenching of the fluorescence of sodium by argon (several times smaller than the gas-kinetic cross section) may be ascribed to the low probability of conversion of the electronic excitation energy into energy of translational motion.

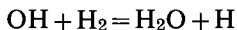
Figure 85 shows the results of Neuimin and Terenin [214 and 263] on the quenching of the fluorescence of hydroxyl (obtained during the photo-dissociation of H_2O) by carbon monoxide, hydrogen, nitrogen and argon.

In spite of the considerable scattering, the experimental points lie satisfactorily on the straight lines corresponding to the Stern-Volmer formula. From the slope of these lines and the life of excited hydroxyl, which is of the order of 10^{-6} sec., we obtain the following values for the cross-sections of quenching:

$$1.6 \times 10^{-16} \text{ cm}^2 (\text{CO}), 0.3 \times 10^{-16} \text{ cm}^2 (\text{H}_2), 0.06 \times 10^{-16} \text{ cm}^2 (\text{N}_2), \\ 0.03 \times 10^{-16} \text{ cm}^2 (\text{Ar}).$$

We note that these cross-sections are considerably less than the cross-sections of quenching of the fluorescence of sodium (e.g. the cross-section of quenching of hydroxyl by hydrogen is about 1/100 of the cross-section of quenching of sodium). This difference may evidently be ascribed to the difference in the temperatures of the experiments, since the data for sodium were obtained at 550°C and the data for hydroxyl at room temperature. We assume the presence in this case of a definite potential barrier separating the initial and final states of the system. From this point of view, which treats the process of quenching as a transition of the system from one potential surface to another, the presence of such a barrier (and the "activation energy" corresponding to it) is quite possible both in the case of the chemical mechanism of the quenching of fluorescence and in the case of the physical process of transfer or transformation of energy.

Regarding the actual mechanism of quenching of fluorescence of hydroxyl, in the case of CO and H₂ it is possible to talk about the chemical mechanism, since close study of the processes of chemical interaction of unexcited hydroxyl with CO and H₂ shows that they are sufficiently fast. For example, from the known rate constant for the process



(see p. 611) it is possible to obtain a measured value for the cross-section of quenching of the fluorescence of hydroxyl by hydrogen ($0.3 \times 10^{-16} \text{ cm}^2$) if we assume that the activation energy for the process $\text{OH}' + \text{H}_2 = \text{H}_2\text{O} + \text{H}$ is 1.8 kcal/mole, which is quite reasonable. The chemical mechanism of quenching is also possible in the case of quenching of the fluorescence of hydroxyl by nitrogen since the process $\text{OH}' + \text{N}_2 = \text{NO} + \text{NH}$ is also exothermic. However, to decide whether the chemical mechanism predominates (both in the case of nitrogen and also in the case of CO and H₂) or whether the physical mechanism predominates is not possible at the moment.

Neuimin and Terenin [263, 214] are of the opinion that basically the mechanism of quenching of fluorescence of hydroxyl lies in the conversion of electronic excitation energy into vibrational energy of the molecules of CO, H₂ and N₂. They find confirmation of this point of view in the fact

that carbon monoxide has the highest quenching action of these three gases and the energy of one of its vibrational levels ($v = 17$) is closest to the excitation energy of hydroxyl (corresponding to *energy resonance* between electronic excitation energy and vibrational energy).

Indications of this sort of resonance have also been obtained in other cases. Mitchell and Zemansky [191] connect the large cross-section of quenching of fluorescence of mercury by nitric oxide $\text{NO}(111 \times 10^{-16} \text{ cm}^2)$ with the fact that the value of the vibrational quantum of the NO molecule (0.233 eV) is nearest to the transferable energy of electronic excitation corresponding to the difference in the levels $^3P_1 - ^3P_0$ of the mercury atom (0.218 eV). The resonance effect may also be used to explain the fact that O_2 and NO molecules, which have vibrational levels ($v = 12$ and $v = 10$, respectively) nearest to the excitation level of the sodium atom, most strongly quench the fluorescence of the sodium atom during the photodissociation of NaI under the action of a zinc spark [138]. However, there are data which contradict the idea that energy resonance is important in fluorescence quenching processes. Thus, according to Prilezhaeva [219], in contrast with oxygen, hydrogen scarcely quenches the fluorescence of thallium vapour, whereas the vibrational levels of both these gases give rise to equally sharp resonance with the excitation level of the thallium atom. Similarly the cross section of quenching of fluorescence of mercury

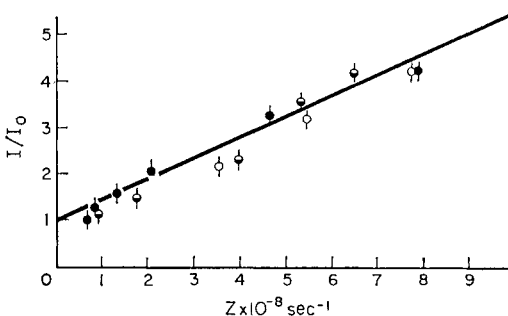


FIG. 86. Quenching of the fluorescence of beta-naphthylamine $\beta\text{-C}_{10}\text{H}_7\text{NH}_2$ by oxygen and nitric oxide (according to Dubois [552]). Temperature 150°C, beta-naphthylamine pressure 1.2 mm Hg, wave length 3660 Å.

by carbon dioxide is some ten times less than the cross-section of quenching by nitric oxide, despite the close resonance between the energy of a vibrational quantum of CO_2 and NO molecules and the difference in energy of the levels $^3P_1 - ^3P_0$ of the mercury atom.

In connection with this Kondrat'ev and Ziskin [138] expressed the opinion that the efficiency of quenching of fluorescence is determined by the forces of the chemical interaction of the excited and quenching particles;

a measure of this is given by the heat effect of the chemical reaction possible between these particles. Kondrat'ev and Ziskin, using the quenching of the fluorescence of sodium as an example, showed that there is a positive relation between the quenching action of various gases and the heat effect of the corresponding chemical processes. Extending this point of view to other systems shows, however, that this relation is apparently limited to similar systems (for example to diatomic molecules); it follows from this that one of the factors determining the quenching efficiency is the *configuration* of the complex formed by the excited and quenching particles. It is clear that in the mechanism of quenching the various factors which control the process need further theoretical and experimental investigations in spite of the large amount of work already carried out in this field.

Finally, as an example of the quenching of the fluorescence of a complex substance, Fig. 86 shows data for quenching of the fluorescence of beta-naphthylamine vapour $C_{10}H_7NH_2$ by oxygen and nitric oxide [552]. It is clear from this diagram that the quenching of fluorescence in this case, as in the case of atoms and the simpler molecules, follows the Stern-Volmer formula.

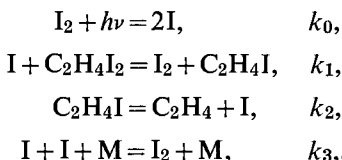
§25. Photochemical Sensitization

The transfer or redistribution of energy during collisions of molecules is the basis of *photochemical sensitization*. Many substances, such as hydrogen and aliphatic and other hydrocarbons, absorb light in the far ultraviolet spectral region which is difficult to study; this makes it difficult to carry out photochemical reactions with these substances. However, mixing with a foreign substance—a *sensitizer*—which absorbs light in a more accessible spectral region, and using the possibility of transfer of excitation energy of the sensitizer to reagent molecules, makes it possible to carry out photochemical reactions of substances which do not absorb in this spectral region. Photochemical sensitization is widely used in photography where, by introducing the appropriate sensitizer into an emulsion, it may be made light-sensitive in those regions of the spectrum in which it would not normally be sensitive. The basic reagent of a photographic emulsion is silver chloride or bromide. The selectivity of light absorption by these salts makes the photoemulsion sensitive only to a definite part of the spectrum corresponding to a comparatively short wave length. Addition to the emulsion of a sensitizer, which is usually an organic dye, permits broadening of the region of sensitivity on the longer wave length side (approximately to 15,000 Å). Leaving aside the question of the mechanism of photographic sensitization (which has not yet received an unambiguous interpretation because of the complexity of the course of

the photochemical process in the emulsion and also because of the lack of theoretical and experimental investigations of this process) we return to a consideration of photochemical sensitization in gas reactions.

Photosensitization by Halogens

In a sensitized photochemical reaction the light acts directly on a molecule (or atom) of the sensitizer. The primary photochemical process can be either the decomposition of a molecule of the sensitizer into its component atoms, or its excitation. An example of a process taking place by the first course is the photochemical decomposition of ethylene iodide in the presence of iodine. This reaction has been studied by several authors (see reference [1081]); all the experimental data lead to the following reaction mechanism:



According to this mechanism the rate of decomposition of $\text{C}_2\text{H}_4\text{I}_2$ is

$$w = k_1(\text{C}_2\text{H}_4\text{I}_2)(\text{I}).$$

This expression, from the steady state conditions

$$\frac{d(\text{C}_2\text{H}_4\text{I})}{dt} = k_1(\text{C}_2\text{H}_4\text{I}_2)(\text{I}) - k_2(\text{C}_2\text{H}_4\text{I}) = 0$$

and

$$\frac{d(\text{I})}{dt} = 2\Delta I - k_1(\text{C}_2\text{H}_4\text{I}_2)(\text{I}) + k_2(\text{C}_2\text{H}_4\text{I}) - 2k_3(\text{M})(\text{I})^2 = 0$$

can be reformulated as

$$w = k_1 k_3^{-1/2} (\text{M})^{-1/2} (\text{C}_2\text{H}_4\text{I}_2) (\Delta I)^{1/2};$$

this is identical with the experimentally established kinetic equation of the reaction. We note that the quantity ΔI is proportional to the light intensity I_0 , whence $w \sim I_0^{1/2}$ in accordance with the fact that the process terminating the reaction is the recombination of atoms in the gas (see p. 423).

Both iodine and the other halogens are quite widely used as sensitizers in various photochemical reactions. This is explained by the ease of activating halogens which results from the fact that their absorption spectra are in the visible or near ultraviolet region. The light absorption coefficients of iodine, bromine and chlorine vapour⁽¹³⁾ are shown as a function

⁽¹³⁾ The absorption maximum for fluorine comes at a wave length about 2900 Å. The maximum absorption coefficient is approximately equal to 0.2 cm^{-1} .

of wave length in Fig. 87 [30] (see also [1181]), in which the arrows indicate the boundary between the discrete and continuous parts of the spectrum (the band convergence limit), corresponding to the following wave lengths: 4995 Å (I_2), 5107 Å (Br_2) and 4785 Å (Cl_2). During the absorption of wave lengths shorter than these limiting wave lengths, the X_2 molecules decompose into atoms, $X_2 + h\nu = X'(^2P_{1/2}) + X(^2P_{3/2})$, which must thus be considered as primary centres of the sensitized photochemical reaction.

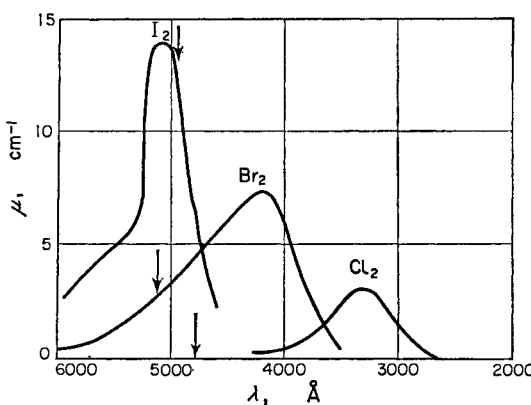
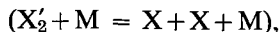


FIG. 87. Absorption coefficient of iodine, bromine and chlorine vapour in the visible and quartz ultraviolet spectral regions.

In the long wave length region, excited X_2 molecules are formed initially; these can return to their initial ground state with emission of light (fluorescence), splitting into atoms on collision with other molecules



or can enter into chemical reaction. Chemical reactions of excited halogen molecules have not been established with certainty although certain authors have postulated such a mechanism.⁽¹⁴⁾ Induced predissociation has been studied in sufficient detail, and takes place with great ease (as the cross-sections here are increased relative to the gas-kinetic cross-sections). It is extremely likely that an excited halogen molecule, entering into reaction undergoes induced predissociation which should be considered as the first (initial) stage [810]. For this reason it may be considered that in practically every case the primary active centres of photochemical reactions sensitized by halogens are halogen atoms.

⁽¹⁴⁾ For example, Bodenstein and Kistiakowsky [419] assumed that the primary active centres of the photochemical decomposition of chlorine monoxide Cl_2O which is sensitized by chlorine are excited Cl_2 or Cl_2O molecules entering into reaction with Cl_2O and Cl_2 molecules respectively.

The photochemical decomposition of $C_2H_4I_2$ sensitized by iodine vapour has been considered above and serves as a characteristic example. According to the measurements of Schumacher and Stieger [1122] the rate of this reaction during exposure to light of wave length 4358 Å, i.e. in the continuous absorption spectral region for iodine vapour, is four times greater than the rate observed during exposure to light of wave length 5461 and 5770–90 Å in the discrete (banded) absorption region. From this it is possible to conclude that part of the excited iodine molecules, which arise in the latter case, dissipate their energy (by fluorescence and conversion of electronic excitation energy into thermal energy) leading to a lowering of the rate of reaction. However, Dickinson and Nies [537] showed that there was a systematic error in the work of Schumacher and Stieger, in that their calculation did not take into account the substantial difference in the rate of dissociation of an I_2 molecule (and consequently in the rate of reaction) on passing from the continuous absorption region (4358 Å) to the banded absorption region. This reminds us of the conclusion reached earlier that halogen atoms are primary active centres of the photochemical reactions in which they participate.

The accuracy of this conclusion has been further confirmed by spectroscopic data. It was shown [1058] that in the region 5107–6800 Å, i.e. in the discrete absorption region for bromine vapour, along with the transition $^1\Sigma_g^+ - ^3\Pi_{0u}^+$ (which is connected with the formation of stable excited bromine molecules and consequently with the discrete character of the absorption spectrum) the transition $^1\Sigma_g^+ - ^3\Pi_{1u}$ is observed, which leads to dissociation of the bromine molecule into *unexcited* atoms. For a source of light with a continuous spectrum (such as is usual in photochemical experiments with halogens), light absorption in the spectral region indicated must lead mainly to the emergence of the state $^3\Pi_{1u}$, i.e. to the dissociation of the bromine molecules. Accordingly in the region of wave lengths 4800–6800 Å the efficiency of the action of light in the photochemical bromination of ethylene $Br_2 + C_2H_4 = C_2H_4Br_2$ is independent of wave length [840]. It is interesting that light of wave length 7150 Å is also absorbed by bromine molecules but leads to the emergence of stable vibrational levels of the $^3\Pi_{1u}$ state and is photochemically inactive.⁽¹⁵⁾

In connection with photochemical sensitization by halogens one should note that apparently only in the case of iodine are reactions possible in which the sensitizer is not consumed, as in fact happens in the above example of the decomposition of ethylene iodide. In the case of bromine and chlorine, whose atoms possess large chemical activity compared with iodine atoms, transformation of a definite quantity of the sensitizer is observed to be irreversible under the experimental conditions in

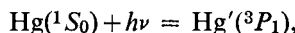
⁽¹⁵⁾ The wave length 7150 Å corresponds to an energy of 39.7 kcal, which is less than the heat of dissociation of the bromine molecule (45.4 kcal).

practically every reaction studied. For example, considerable quantities of Cl_2O_4 are formed in the photochemical decomposition of ozone sensitized by chlorine [474].

It has recently been shown [1254] that, as a result of photochemical activation of O_2 molecules in the discrete absorption region (1849.6 Å), O atoms are formed as primary active centres; in the continuous absorption region also there is a similarity to the halogen case.

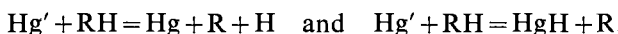
Photosensitization by Mercury

Mercury vapour is very often used as a sensitizer; it is one in which *excited* atoms are initially formed. During the exposure of a mixture of reacting substances, containing a small quantity of mercury vapour, to light from a quartz mercury arc, excited atoms of mercury $\text{Hg}'(^3P_1)$ are formed,



with an excitation energy of 112 kcal. Conversion of the excitation energy of a mercury atom into *chemical* energy of a molecule (or molecules) of the reacting substances is the actual origin of a strictly chemical reaction. For best use of the excitation energy the efficiency of this collision should be sufficiently large, otherwise the energy will be radiated (fluorescence) or converted to heat (as a result of fluorescence quenching). The probability of energy dissipation is particularly great at low pressures. Actually the number of gas-kinetic collisions is approximately equal to $Z = 10^7 p$, where p is the pressure (in mm Hg), so that at a pressure of 1 mm Hg an excited atom of mercury experiences on an average not more than one collision in its lifetime (1.55×10^{-7} sec.); for this reason for $p < 1$ mm Hg one would expect a large probability of fluorescence and a small probability of photochemical activation.⁽¹⁶⁾

A particularly large amount of work has been devoted to study of the mercury-sensitized photochemical reactions of substances containing hydrogen (H_2 , hydrocarbons etc.), especially decomposition and oxidation reactions. In these reactions the secondary process of interaction of an excited mercury atom with a reagent molecule can take place in *two ways* corresponding to the schemes:

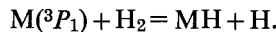


Both ways are energetically possible, since the excitation energy of the mercury atom $\text{Hg}'(^3P)$ is in every case greater than the energy required to

⁽¹⁶⁾ We have seen earlier (p. 427) that quenching the fluorescence of an excited mercury atom $\text{Hg}'(^3P_1)$ during collision with foreign molecules may result in its transition to the metastable state 3P_0 , which leads to an increased probability of photochemical activation (as a result of the long lifetime of the metastable atoms).

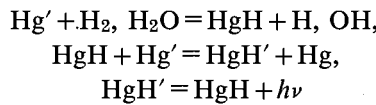
break the bond of the H atom in the molecule, which does not exceed 103 kcal (with the exception of the H_2O molecule whose decomposition to hydroxyl and an H atom takes place with the expenditure of about 118 kcal). The possibility of the *first way* is apparent from the case of the decomposition of hydrogen [479] which is sensitized by xenon (the excitation energy of the xenon atom is 193 kcal, 1469 Å); in this reaction the hydride cannot be formed and consequently the first way, which is followed by the secondary process, is the only one possible.⁽¹⁷⁾

The *second way* is realized in a pure form in the decomposition of H_2 which is sensitized by cadmium and zinc [378]. In view of the fact that the excitation energies of atoms of Cd and Zn are 87 and 92 kcal respectively, the decomposition of the H_2 molecule into two atoms on its collision with an excited atom of cadmium or zinc is energetically impossible; the appearance of hydrogen atoms during the irradiation of hydrogen, containing an admixture of the vapour of one of these metals, by the resonance line of the metal is explained by the process



Since the energy of formation of the hydride molecule from the metal atom and an H atom is equal to 15.6 and 19.5 kcal for Cd and Zn respectively, the heat effect for this process will be

$87 + 15.6 - 103.2 = -0.6$ kcal (Cd) and $92 + 19.5 - 103.2 = +8.3$ kcal (Zn), so that the process is energetically possible in both cases. Direct evidence of the possibility of this process is given by the observations of Wood and Gaviola [651] on the emission spectra of hydrides MH during irradiation of hydrogen or water vapour containing an admixture of the appropriate metal vapour by the resonance line of the latter. According to Beutler and Rabinowitsch [395] the mechanism of excitation of the HgH spectrum under the experimental conditions of Gaviola and Wood is the sum of the following processes:

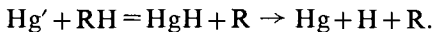


We note that owing to the comparatively large heat effect (16.3 kcal) of the process $\text{Hg}' + \text{H}_2 = \text{HgH} + \text{H}$ and the comparatively small dissociation energy (8.5 kcal) of the HgH molecule, the HgH molecule formed in this process has a large probability of decomposition. For this reason it may

(17) Recently a similar process has been established by Groth and Oldenberg [708] for the system Kr' (excitation energy 10.0 eV) + N_2 . They found that the dissociation of nitrogen molecules in the presence of excited krypton atoms is a result of the transition of the N_2 molecule into an unstable electronically excited state, which leads to its decomposition to normal atoms.

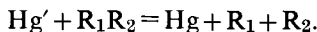
be considered that both possible ways for the secondary process of the mercury-sensitized dissociation of hydrogen lead, eventually, to decomposition of the H_2 molecule into two free atoms. It is possible that the large effective cross-section of quenching of fluorescence of mercury by hydrogen, which is practically equal to the gas-kinetic cross-section (see Table 39), should be considered as evidence of a large probability for the mercury-sensitized dissociation of H_2 .

In the photodissociation of hydrocarbons and other hydrogen-containing substances, the secondary process may obviously be expressed by the scheme

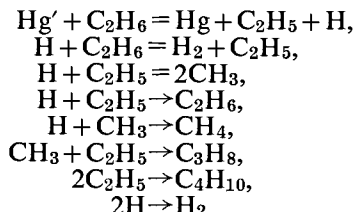


The H atoms and R radicals formed in this are the active centres which ensure the further development of the reaction.

This scheme is not, however, the only one possible. For example, mass-spectrometric investigation of the mercury-sensitized photochemical decomposition of acetone vapour CH_3COCH_3 shows that in this case CH_3 radicals and CH_3CO radicals are formed in large quantities, and there is a complete absence of acetonyl radicals CH_3COCH_2 , which must be formed if the process is to go according to the above scheme. Therefore it should be concluded that in the photolysis of acetone the secondary process is $Hg' + CH_3COCH_3 = Hg + CH_3 + CH_3CO$; in the general case this process can be represented by the scheme

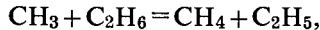


As an example of the large number of mercury-sensitized photochemical decompositions of hydrocarbons we may take the decomposition of ethane, which has been studied by several authors (see Steacie [1169, Chap. V, p. 35]). The composition of the products of this reaction and its kinetics for temperatures close to room temperature is apparently described most accurately by the mechanism:



This mechanism in its basic features holds good also for higher temperatures (up to $475^\circ C$). There is reason to consider that at these

temperatures, along with the above-mentioned processes, a part must be played by the process



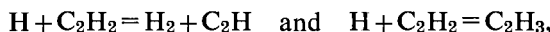
and also by the process



Among the individual features of this mechanism we may note the following. According to Steacie and Darwent (see Steacie [1169, Chap. V, p. 35]), it is possible to explain the observed dependence of the yield of hydrogen and methane on pressure if it is assumed that each of the reactions between H and C_2H_5 takes place in two stages: $\text{H} + \text{C}_2\text{H}_5 \rightarrow \text{C}_2\text{H}_6^*$ and correspondingly $\text{C}_2\text{H}_6^* \rightarrow 2\text{CH}_3$ and $\text{C}_2\text{H}_6^* + \text{M} \rightarrow \text{C}_2\text{H}_6 + \text{M}$. The activation energy of the process $\text{H} + \text{C}_2\text{H}_6 \rightarrow \text{H}_2 + \text{C}_2\text{H}_5$ is 6.8 kcal/mole (see p. 253), of the process $\text{CH}_3 + \text{C}_2\text{H}_6 \rightarrow \text{C}_2\text{H}_4 + \text{C}_2\text{H}_5$ is 10.4 (see Steacie [1169, Chap. VII, p. 81]) and of the process $\text{C}_2\text{H}_5 \rightarrow \text{C}_2\text{H}_4 + \text{H}$ about 40 kcal/mole (see Steacie [1169, Chap. V, p. 35]). The activation energy of the recombination processes is equal or close to zero.

According to the above reaction mechanism, the role of the photochemical sensitization is restricted to the creation of initial centres (mainly H atoms); as a result, the basic features of the mechanism should hold for any other means of generating initial active centres (for example, in an electric discharge), if other conditions are not changed in carrying out the reaction. Here it should be kept in view that different concentrations of these initial active centres often result from different methods of generation. This leads to changes in the relationships between individual elementary processes which make up the reaction mechanism, and hence to changes in the relationship and even in the composition of the reaction products.

A clear example of this is the reaction of acetylene C_2H_2 with atomic hydrogen which has been studied by Le Roy and Steacie [871] both by obtaining H atoms in an electric discharge and also by a photochemical method, namely mercury sensitization. In the first case, when the concentration of H atoms is large, only their catalytic recombination was observed and the concentration of acetylene remained practically constant. In the opinion of these authors the radicals C_2H and C_2H_3 , which are formed in the primary processes⁽¹⁸⁾



⁽¹⁸⁾ Spectroscopic investigations of the reaction show, however, that at least part of the acetylene undergoes more profound changes in the course of the reaction, since the reaction is accompanied by a considerable heat evolution and by a bright glow whose spectrum contains CH and C_2 bands [1269, 428].

under these experimental conditions (large H concentrations) preferentially react according to the scheme

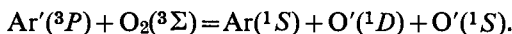


When the H atoms are formed photochemically, and their concentration is low, the C_2H and C_2H_3 radicals react according to the scheme



Le Roy and Steacie consider that the ethane and butane observed in the reaction products are formed as the result of disproportionation and recombination of C_2H_5 radicals. Whether or not the proposed reaction mechanism is reliable, the sharp difference in composition of the products in the two cases studied is a well established fact which is also supported by other data (see Steacie [1169, Chap. VI, p. 5]).

Without lingering on other examples of mercury-sensitized photochemical decompositions of hydrocarbons⁽¹⁹⁾ and other compounds, we shall go on to consider the interaction of excited mercury atoms with an O_2 molecule, which is of importance in connection with the use of mercury sensitization in photochemical oxidation reactions. As an example of one of the possible types of interaction of an excited mercury atom with an O_2 molecule we shall consider the process $\text{Hg}' + \text{O}_2 = \text{Hg} + \text{O} + \text{O}$. Study of the electric discharge spectrum in a mixture of $\text{O}_2 + \text{Ar}$ leads to the conclusion that the dissociation of the O_2 molecule on collision with excited Ar atoms probably corresponds to the scheme [945, 107]



This process can be treated as the transition of an O_2 molecule to an unstable state at the expense of the excitation energy of an Ar atom (equal to 265 kcal). This unstable state is formed from the 1D and 1S states of the O atom with subsequent dissociation of the molecule into two atoms. (The states 1D and 1S correspond to energies of 45 and 96 kcal, the heat of dissociation of an O_2 molecule is 118.0 kcal; consequently the energy loss is $118 + 45 + 96 = 259 < 265$ kcal.)

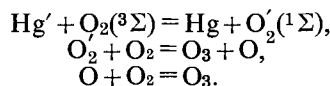
When mercury is used as a sensitizer for the photochemical decomposition of oxygen (detected by ozone formation), it is difficult to interpret the secondary process (which is rapid) because the energy of excitation of the sensitizing atom (112 kcal) is less than the heat of dissociation of the O_2 molecule (118.0 kcal). By analogy with the process $\text{Hg}' + \text{H}_2 = \text{HgH} + \text{H}$, and also taking into account the formation of HgO during the exposure

⁽¹⁹⁾ A large number of examples of these reactions is given in Steacie's book [1169]. According to Laidler and Shuler [862], during interaction of an excited mercury atom and a molecule of an unsaturated compound, the triplet (biradical) state of the latter may arise.

of oxygen containing an admixture of mercury vapour to the resonance line of the latter, it is natural to represent the interaction of the excited Hg atom with an O₂ molecule as the chemical process Hg' + O₂ = HgO + O.

The same conclusion about the mechanism of the interaction of an excited mercury atom with a molecule of oxygen was drawn by Leipunskii and Zagulin [170] from study of the mercury-sensitized photochemical formation of ozone (see also Darwent [526]). However, certain facts lead one to suppose that the oxide of mercury HgO is formed during the secondary interaction of an ozone molecule with a normal mercury atom, namely O₃ + Hg = gHO + O₂, and not as a result of the process preceding the formation of the ozone (see also [1252]). The most convincing evidence for the absence or low probability of direct formation of oxygen atoms during the interaction of an excited mercury atom with an O₂ molecule (the process Hg' + O₂ = HgO + O) is given by the experimental results of Fok and Nalbandyan [274] on the mercury-sensitized photochemical oxidation of propane (see below). These authors found that for partial replacement of oxygen by nitrogen in the initial mixture, which contained 50 per cent propane C₃H₈ and 50 per cent oxygen, the rate of formation of the isopropyl hydroperoxide (CH₃)₂CHO₂H, which is the only reaction product at room temperature, is practically unchanged for a change in the concentration of oxygen from 50 to 0.75 per cent. This constancy of the reaction rate would not obtain if the primary active centres were O atoms.

The result obtained by Fok and Nalbandyan makes the mechanism for formation of ozone proposed by Dickinson and Sherill [538] extremely likely. According to this mechanism, during the interaction of an excited mercury atom with a molecule of O₂ an excited molecule of oxygen is formed (cf. p. 429) which reacting with an unexcited O₂ molecule gives a molecule of ozone and an atom of O. According to Dickinson and Sherill the mechanism of this reaction may be represented by the sum of the following processes:⁽²⁰⁾

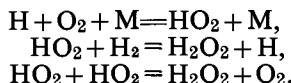


Mercury-sensitized photochemical oxidations have been studied by many authors, for example the oxidation of hydrogen, methane, ethane, and propane. In connection with the first of these we note that according to Bates and Salley [360] the main product at room temperature (14°C) is hydrogen peroxide H₂O₂ which forms more than 85 per cent of the reaction products.⁽²¹⁾ This result confirms the conclusion, mentioned above,

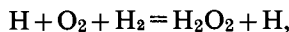
⁽²⁰⁾ This does not exclude the possibility that in this case the excited molecule of oxygen is a vibrationally excited molecule in the electronic ground state [1253].

⁽²¹⁾ From this Bates and Salley concluded that H₂O₂ is the only primary product of the reaction.

that oxygen atoms are not primary products of the interaction of an excited mercury atom and an O_2 molecule, since in this case the main reaction product must be water. Proceeding from the assumption that hydrogen atoms are first formed from the interaction of an excited mercury atom with H_2 , Bates [359] suggested the reaction mechanism:

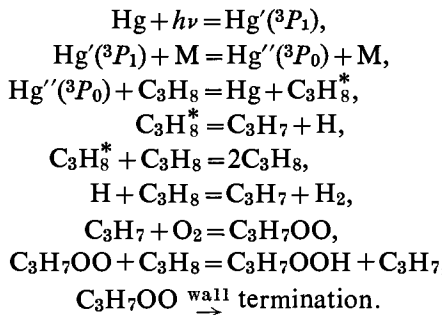


However, since the second of these processes has a negative heat of reaction (-15 kcal/mole) and consequently is associated with a considerable activation energy, Bates' mechanism may have significance only at high temperatures. It is possible that the formation of hydrogen peroxide at room temperature occurs as a result of the termolecular process



which explains the observed high yields in H_2O_2 (see Rollefson and Burton [1081, §10, p. 32]). The heat effect of this process is 31.8 kcal/mole.

The photochemical oxidation of hydrocarbons has been studied in most detail by Fok and Nalbandyan [274]. We shall consider in rather more detail the oxidation of propane which was mentioned earlier. Proceeding from the fact that the reaction rate is independent of oxygen content in a mixture of the type $\frac{1}{2}C_3H_8 + (\frac{1}{2} - x)O_2 + xN_2$, Fok and Nalbandyan relate the primary activation to the splitting of the propane molecule into an H atom and a C_3H_7 radical. For reaction at room temperature they propose a mechanism which satisfies all the kinetic features and results of this reaction, and which may be written in the following somewhat simplified form:



From this mechanism, using the steady state method, the following expression is obtained for the reaction rate, i.e. for the rate of formation

of isopropyl hydroperoxide, which is practically the only reaction product at temperatures near to room temperature:

$$\frac{d(C_3H_7OOH)}{dt} = 2\Delta I A \frac{(C_3H_8)}{1 + B(C_3H_8)},$$

where ΔI is the number of absorbed quanta, A and B are constants in terms of the rate constants of the individual elementary processes which make up the reaction mechanism. Fok and Nalbandyan show that the expression they obtain for the reaction rate is in quantitative agreement with the experimental data.

With increase from room temperature to 300°C the products of the photochemical oxidation of propane contain acetaldehyde CH_3CHO , formaldehyde $HCHO$, carbon monoxide CO and acetone CH_3COCH_3 . The order in which these products appear is clear from Fig. 88 which

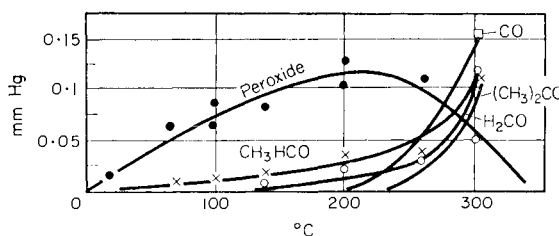


FIG. 88. Yield of products of the photochemical oxidation of propane as a function of temperature for a contact time of 30 sec (according to Fok and Nalbandyan [274]).

shows the quantities of the various products (in mm Hg) formed in a circulating mixture of propane and oxygen for a contact time of 30 sec and various temperatures. It is clear from Fig. 88 that with increase of temperature the aldehyde is formed after the hydroperoxide; at 200°C carbon monoxide appears in the reaction products, and at still higher temperatures acetone appears. Fok and Nalbandyan show that the kinetic curves of the peroxide and aldehydes at various temperatures follow parallel paths, and so they conclude that these products are formed in *independent* and *parallel* ways. In accordance with the mechanism of low temperature oxidation of propane, the peroxide is formed during the interaction of the peroxide radical C_3H_7OO with a propane molecule, and the aldehydes are formed as a result of the decomposition of this radical into an aldehyde molecule and the corresponding alkoxy radical (CH_3O or C_2H_5O). Acetone is formed as a result of the decomposition of isopropyl hydroperoxide into CH_3COCH_3 and H_2O . Finally, the carbon monoxide is formed, in accordance with ideas on the mechanism of the thermal oxidation of hydrocarbons, by further oxidation of the aldehydes

(and other products of incomplete oxidation—peroxides, alcohols, acids etc.). The kinetic studies of Fok and Nalbandyan support this conclusion, and it follows that at 200–300°C the kinetic curves of the peroxides and aldehydes, in contrast to that of carbon monoxide, display saturation (and apparently a further falling off), indicating the *intermediate character* of these products. According to Fok and Nalbandyan the very same difference in the course of the kinetic curves of aldehydes and carbon monoxide is observed in the case of the photochemical oxidations of ethane C_2H_6 and methane CH_4 .

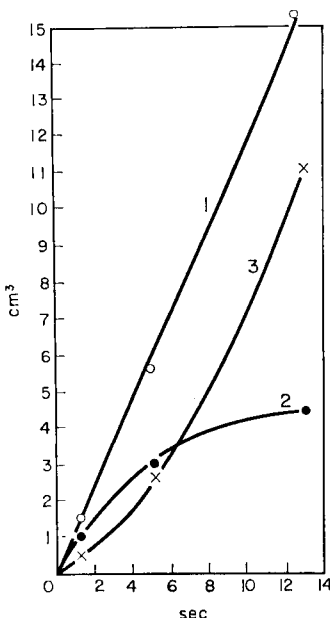


FIG. 89. Kinetic curves of the consumption of methane (1), the formation of formaldehyde (2), and the formation of carbon monoxide (3) during the photochemical oxidation of CH_4 at 400°C (according to Fok and Nalbandyan [274]).

Figure 89 shows the kinetic curves for the consumption of methane and the curves for the formation of formaldehyde and carbon monoxide (at 400°C) to illustrate the data obtained by these authors.

The intermediate nature of the formaldehyde in the thermal oxidation of methane, and the formation of carbon monoxide in this reaction only via formaldehyde oxidation, were established using the kinetic tracer method (see above p. 49) and also by means of the usual kinetic method [563]. In the latter case hydrogen peroxide H_2O_2 was detected as a second

intermediate substance besides H_2CO . The kinetic curves of both intermediates are shown in Fig. 90, which also shows the curve of change in pressure of the methane–oxygen mixture in the course of the reaction. We note that the position of the maxima of both kinetic curves coincides with the point of inflection of the pressure-change curve, i.e. with the maximum rate of reaction, as measured by the change in pressure of the mixture (cf. Fig. 6, p. 23). Detection of considerable quantities of H_2O_2 during the oxidation of H_2CO [182] leads one to suppose that the formation of formaldehyde precedes, at least in part, the formation of hydrogen peroxide. This is also borne out by the fact that at the start of the reaction the rate of formation of H_2CO exceeds the rate of formation of H_2O_2 (see Fig. 90).⁽²²⁾

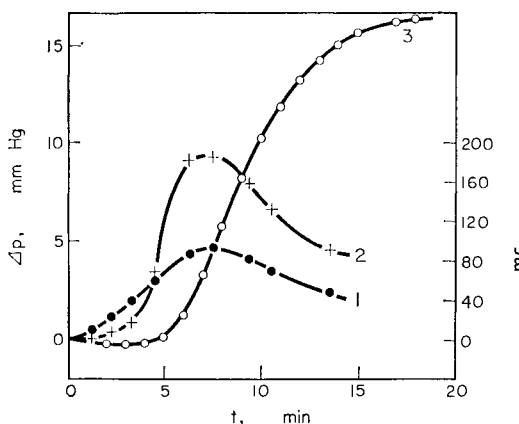


FIG. 90. Kinetic curves of the formation of formaldehyde H_2CO (1) and hydrogen peroxide H_2O_2 (2) during the thermal oxidation of methane at 460°C (according to Egerton *et al.* [563]). Composition of the mixture: 33% CH_4 + 67% O_2 . Curve 3 shows the change in pressure of the mixture in the course of the reaction.

§26. Quantum Yield of Photochemical Reactions

The Basic Photochemical Law

According to the Stark–Einstein photochemical law [1167] (1908–12), the number of primary acts in a photochemical reaction must be equal to the number of light quanta absorbed. Denoting the number of primary acts by ΔN^* , the total quantity of absorbed light energy by ΔI , and the quantum by $h\nu$, this law may be represented by the formula

$$\Delta N^* = \Delta I/h\nu. \quad (26.1)$$

⁽²²⁾ Also supporting this conclusion, according to the data of Markevich [182], is the fact that in the oxidation of formaldehyde the hydrogen peroxide, which is a primary oxidation product, is formed amounting to 30 per cent of the formaldehyde oxidized.

Often the magnitude of ΔN^* is identified with the number of reacting molecules ΔN . However, it follows from the foregoing (§24) that such an identification is permissible only in those rare, very simple cases when the mechanism of the photochemical reaction consists of the one primary process. In most cases, owing to secondary processes taking place, the number of molecules reacting does not coincide with the number of primary photochemical acts. In the general case it is possible to characterize the efficiency of the photochemical action of light by a certain quantity

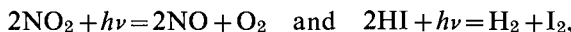
$$\eta = \Delta N / \Delta N^*. \quad (26.2)$$

This quantity is called the *quantum yield* and is the number of molecules reacting per quantum absorbed.

Measurements of the quantum yield of various reactions give values lying in a very wide range. Thus according to Bodenstein [415] who measured the quantum yield of a large number of reactions, the values of η range from 0.002 for the decoloration reactions of certain dyes to 10^6 for the reaction of chlorine with hydrogen and for the bromination of toluene. Quantum yields for several reactions are shown in Table 40.

One of the reasons for the frequently observed low quantum yields ($\eta < 1$) is *deactivation* of the primary active centres of the photochemical reaction. When these centres are excited molecules, deactivation consists of the transfer of excitation energy during a collision of an excited molecule with other molecules, or the radiation of this energy (fluorescence). When the active centres are free atoms or radicals—the photodissociation products of the original molecules—deactivation is brought about by the recombination of these centres. In a series of cases the low quantum yield of the photochemical reaction results from the occurrence of the *reverse* reaction which also is photochemical. The occurrence of the reverse reaction is also indicated by the kinetic law for the over-all reaction, in particular by the fact that the rate of the latter becomes zero for concentrations of the reacting substances differing from the thermodynamic equilibrium values.

A quantum yield of 2 is often met and is observed when, as a result of the primary photoactivation process (which consists of the dissociation of the molecule which absorbed the light) one or two simple secondary processes follow. For example, there are reactions such as



whose mechanisms are a combination of the following processes:

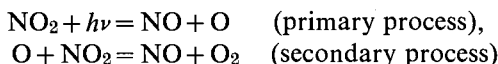
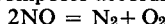


TABLE 40
Quantum yields of certain reactions

Reaction	Effective wave length, Å	Quantum yield
$2\text{NH}_3 = \text{N}_2 + 3\text{H}_2$	2100	0.25*
Decomposition of nitric oxide NO^\dagger	1860–1990	0.75
$\text{COBr}_2 = \text{CO} + \text{Br}_2$	<3200	1.0
$\text{H}_2\text{S} = \text{H}_2 + \text{S}$	2080	1.0 [620]†
$\text{H}_3\text{CN}\text{NCH}_3 = \text{N}_2 + \text{C}_2\text{H}_6$	2900–3900	1.0 [809]**
$2\text{HI} = \text{H}_2 + \text{I}_2$	2070–2820	2.0
Decomposition of acetaldehyde CH_3CHO	3130	2.0
$2\text{NO}_2 = 2\text{NO} + \text{O}_2$	<4000	2.0
Decomposition of nitrous oxide N_2O	1900	3.9
Polymerization of acetylene C_2H_2	2150	9.2
$\text{C}_2\text{H}_4\text{I}_2 = \text{C}_2\text{H}_4 + \text{I}_2$	4360	25††
$\text{CO} + \text{Cl}_2 = \text{COCl}_2$	4000–4360	1000
$\text{H}_2 + \text{Cl}_2 = 2\text{HCl}$	4000–4360	10 ⁵

* It was found when conducting the reaction in a stream of gas under the action of light of 1849 Å that the quantum yield for the decomposition of NH_3 in this case is about twice the quantum yield under static conditions [936].

† According to the data of McDonald [937], on exposure of nitric oxide NO in the region $\lambda = 1900$ Å, 90 per cent decomposes according to the over-all formula



and 10 per cent according to the equation $3\text{NO} = \text{N}_2\text{O} + \text{NO}_2$. Kondrat'ev [125] has shown that on exposure of nitric oxide to a mercury arc ($\lambda = 1849$ Å) the reaction takes place in two stages. In the first of these the overall pressure falls to three-quarters of the initial NO pressure, corresponding to the gross equation $4\text{NO} = 2\text{NO}_2 + \text{N}_2$ and in the second stage the overall pressure slowly increases, corresponding to the equation $2\text{NO}_2 = \text{N}_2 + 2\text{O}_2$ (this result is not inconsistent with the formation of small quantities, 5 per cent, of N_2O).

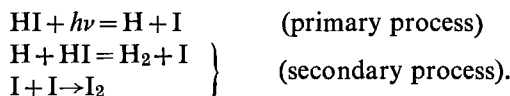
In contrast with the above data, Moore, Wulf and Badger [958] find that during the exposure of nitric oxide to light of wave lengths 2144 and 2265 Å the final reaction product is N_2O_3 (overall equation $6\text{NO} = 2\text{N}_2\text{O}_3 + \text{N}_2$). The possibility is not excluded that this discrepancy is connected with the different nature of the primary photochemical act during exposure of NO to light of different wave lengths.

‡ See also Rollefson and Burton [1081, pp. 178–80].

** In the temperature range studied (24–190°C) the quantum yield is dependent on temperature.

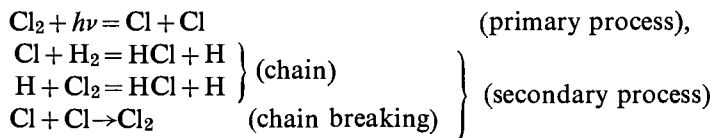
†† According to the data of Schumacher and Wiig [1123] on the decomposition of $\text{C}_2\text{H}_4\text{I}_2$ dissolved in carbon tetrachloride CCl_4 .

and



Finally a quantum yield of $\eta > 2$ is evidence of a *chain mechanism* for the reaction, i.e. one or any number of alternate secondary processes

following the primary process and leading to regeneration of active centres (see Chap. 9). The simplest example of a photochemical chain reaction is the reaction between chlorine and hydrogen, which follows the mechanism



Dependence of Quantum Yield on Wave Length

Since light of various wave lengths may have different effects on the absorbing molecule, change of wave length usually changes the quantum yield and consequently the rate of the photochemical reaction. To illustrate this we shall consider several different photochemical reactions. For example, according to Hertel's measurements [745], in passing from the region of continuous absorption ($\lambda < 4780 \text{ \AA}$) to that of discrete absorption, the quantum yield of hydrogen chloride during the photochemical formation of HCl from H₂ and Cl₂ decreases by a factor of seven. Hertel explains this decrease in quantum yield by the unreactivity of the excited chlorine molecules which must be decomposed into atoms for the reaction to be possible (see also Rollefson and Burton [1081, §11, p. 34]).

A characteristic example of the dependence of quantum yield on wave length is given by the photochemical decomposition of nitrogen dioxide NO₂. Fluorescence is observed in the long wave length region in this case and its intensity decreases with decrease in wave length.⁽²³⁾ For $\lambda \leq 4100 \text{ \AA}$ there is no fluorescence. Parallel to the weakening of fluorescence the quantum yield of the NO₂ decomposition increases from zero in the long wave length region to the value $\eta = 2$ in the short wave length region. Thus, when the absorption coefficients in the spectral region close to 4360 and 3600 \AA are identical, then in the first, longer wave length region, excitation of the NO₂ molecule takes place, the quantum yield being zero; in the second, photodissociation takes place with the maximum quantum yield of 2 in the complete absence of fluorescence (see p. 454). We note that, in contrast with the above cases of the molecules of Cl₂, Br₂ and I₂, there is no continuous absorption region in the absorption spectrum of NO₂. However in the NO₂ spectrum close to 4100 \AA there is a predissociation limit. The occurrence of a predissociation region also determines the photochemical decomposition of NO₂ molecules in the short wave length spectral region and leads to the value $\eta = 2$.

⁽²³⁾ The relation between the intensity of fluorescence of NO₂ and the wave length is apparently expressed by a complex law, since there are grounds for assuming that the different electronic states of the NO₂ molecule are excited by different wave lengths [970].

It is clear from these examples that this observed dependence of quantum yield on wave length is always connected with a change in the character of the absorption spectrum (a transition from the discrete to the predissociation region). When the wave lengths studied are in a spectral region of one definite character, the dependence of quantum yield on wave length is either absent or weak. One example is the decomposition of hydrogen iodide $2\text{HI} = \text{H}_2 + \text{I}_2$ where a change in wave length of the photochemically active light from 2820 to 2070 Å, i.e. through 750 Å, scarcely affects the quantum yield [1266]:

Wave length, Å	2820	2530	2070
Quantum yield	2.09 ± 0.13	2.08 ± 0.07	1.97 ± 0.08

These wave lengths lie in the continuous absorption region for HI, which ranges from 3200 to 2000 Å.

§27. Temperature Coefficient and Mechanism of Photochemical Reactions

Temperature Coefficient

The rate of photochemical reactions depends to a greater or less degree on temperature, and only in a comparatively few cases is the temperature coefficient of a photochemical reaction unity. Below we give the temperature coefficients of several reactions (according to Kistiakowsky [835]); here the temperature coefficient is the ratio of the reaction rates at two temperatures differing by 10° [cf. formula (2.12) p. 15].

TABLE 41

The temperature coefficient of photochemical gas reactions [835]

Reaction	Temperature coefficient	Temperature range, °C	Light source
$\text{Cl}_2 + \text{SO}_2 = \text{SO}_2\text{Cl}_2$	0.88	291–372	Mercury arc
$2\text{HI} = \text{H}_2 + \text{I}_2$	1.00	150–175	Mercury arc, quartz
$2\text{NOCl} = 2\text{NO} + \text{Cl}_2$	1.00	0–78	Incandescent lamp, glass
$3\text{O}_2 = 2\text{O}_3$	1.00	–180–18	<2000 Å
$2\text{O}_3 = 3\text{O}_2$	1.0 (at low concentrations)	0–20	5800–6500
$2\text{Cl}_2\text{O} = 2\text{Cl}_2 + \text{O}_2$	1.09	10–40	Mercury arc, glass
$2\text{O}_3 + \text{Cl}_2 = 3\text{O}_2 + \text{Cl}_2$	1.17	16–25	Mercury arc, glass
$\text{Cl}_2 + \text{H}_2 = 2\text{HCl}$	1.21	11–60	Sunlight
$\text{H}_2 + \text{Br}_2 = 2\text{HBr}$	1.48	160–218	Incandescent lamp, glass

The temperature coefficient of photochemical reactions may be determined by the temperature dependence of both the primary act, as a result of which the active centres of the reaction are formed, and the secondary processes. One would expect a temperature dependence when the reaction

takes place in the spectral region near the boundary of the discrete and continuous absorption spectra or near the predissociation limit. Actually owing to the increase (with temperature) in the number of molecules at higher vibrational levels, wave lengths which at low temperatures are in the discrete part of the absorption spectrum can appear in the continuous absorption region or the predissociation region when the temperature is increased. The result of this is that the efficiency increases at these wave lengths. A clear illustration of this shift of the limit of photochemically active light is given by the shift in the limit of predissociation to the long wave length side on increasing the temperature, as was established by Henri [743]. Such cases are comparatively rare among the photochemical reactions studied, and the temperature course of the reaction in the overwhelming majority of cases is linked with the temperature dependence of the secondary processes.

Table 41 includes an example of a reaction whose temperature coefficient is less than unity. Since it is difficult to propose a reaction mechanism which would lead to a decrease in the rate of the primary or secondary processes with increase in temperature, it is most natural to ascribe a temperature coefficient less than unity to the occurrence of the reverse reaction which accelerates with increase in temperature more quickly than the forward reaction. Another possible reason for a temperature coefficient less than unity may be a change in direction of the reaction with increase in temperature.

Examples of Reactions with a Temperature Coefficient of Unity

In certain cases the reaction rate is observed to be independent of temperature; this is expressed by a temperature coefficient of unity, and indicates the simplicity of the reaction mechanism. Returning to one of the reactions studied in most detail, the decomposition of hydrogen iodide shown on p. 454, we find for the rates in the stationary reaction

$$w = -d(HI)/dt = 2d(H_2)/dt = 2d(I_2)/dt. \quad (24)$$

Further, introducing the rate constants k and k' for the secondary processes, we have

$$-d(HI)/dt = \Delta I + k(HI)(H), \quad d(H_2)/dt = k(HI)(H)$$

and

$$d(I_2)/dt = k'(I)^2,$$

(24) These equations are identical with the steady state condition introduced earlier, which equates the rate of change of concentration of the intermediate substance to zero. In fact, writing the following kinetic equations for the two intermediate substances, H and I, taking part in this reaction

$$d(H)/dt = \Delta I - k(HI)(H) \quad \text{and} \quad d(I)/dt = \Delta I + k(HI)(H) - 2k'(I)^2$$

we obtain

$$d(H)/dt = 0 \quad \text{and} \quad d(I)/dt = 0,$$

i.e. the usual steady state conditions.

where ΔI denotes the number of quanta absorbed of photochemically active light. [According to (23.7) $\Delta I = \delta I \cdot I^\circ \sim I^\circ$]. Using these formulae we find from the expression for the reaction rate

$$k(\text{HI})(\text{H}) = k'(\text{I})^2 = \Delta I,$$

and consequently,

$$w = -d(\text{HI})/dt = 2\Delta I.$$

Since the photochemically active light in this case comes in the continuous absorption region, then the quantity ΔI also is independent of temperature; hence the temperature coefficient of this reaction is observed experimentally to be unity. In accordance with experiment, we obtain from the previous equation that the quantum yield of the reaction is

$$\eta = w/\Delta I = 2.$$

The relations are even simpler in the case of the decomposition of nitrosyl chloride, for which the mechanism is clearly identical with that shown on p. 454 for the decomposition of nitrogen dioxide (it is only necessary to substitute Cl for O). In this case the rate in the stationary reaction is

$$w = -d(\text{NOCl})/dt = d(\text{NO})/dt = 2d(\text{Cl}_2)/dt;$$

hence it follows that

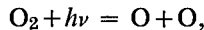
$$k(\text{NOCl})(\text{Cl}) = \Delta I,$$

which gives

$$w = 2\Delta I \quad \text{and} \quad \eta = 2 \quad (\text{and also } d(\text{Cl})/dt = 0).$$

As follows from the equations $w = 2\Delta I$, the rate of the photochemical reaction in both the cases considered is *proportional* to the intensity of light I° .

A simple mechanism may also be assumed in the formation and decomposition reactions of ozone. Regarding the first of these reactions, the primary photochemical act is here undoubtedly the splitting of the oxygen molecule into atoms,



and the formation of ozone is connected with the secondary process



From this mechanism, as in the previous cases, the rate in the stationary reaction is

$$w = d(\text{O}_3)/dt = -\frac{2}{3}d(\text{O}_2)/dt;$$

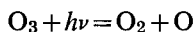
hence, since

$$d(\text{O}_3)/dt = k'(\text{O}_2)(\text{O}) \quad \text{and} \quad -d(\text{O}_2)/dt = \Delta I + k'(\text{O}_2)(\text{O})$$

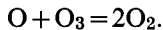
we obtain

$$w = d(\text{O}_3)/dt = 2\Delta I \quad \text{and} \quad \eta = 2 \quad (\text{and also } d(\text{O})/dt = 0).$$

The mechanism of the photochemical decomposition of ozone in the spectral region shown in Table 41 seems to be in its general features a sum of two processes:



and



It follows from this mechanism, as in the previous case, that for the stationary reaction

$$w = -d(\text{O}_3)/dt = \frac{2}{3}d(\text{O}_2)/dt = 2\Delta I, \quad \eta = 2 \quad \text{and} \quad d(\text{O})/dt = 0.$$

The mechanism of the photochemical decomposition of ozone in the ultraviolet spectral region is more complex; its quantum yield in this region exceeds 4 according to the measurements of Heidt [738]. According to Heidt's mechanism for this reaction, metastable oxygen molecules play a substantial role.

Formation of HBr from H₂ and Br₂

As an example of a reaction whose temperature coefficient considerably exceeds unity, we shall consider the reaction $\text{H}_2 + \text{Br}_2 = 2\text{HBr}$ which has been studied in detail by Bodenstein and other authors (for references, see Rollefson and Burton [1081, §11-2]). According to the data of these authors, the over-all reaction rate is expressed by the formula

$$w = d(\text{HBr})/dt = k(\text{H}_2)(\Delta I)^{1/2}p^{-1/2}[1 + k'(\text{HBr})/(\text{Br}_2)]^{-1}, \quad (27.1)$$

where k is temperature dependent and k' practically remains constant over the temperature range studied. According to Bodenstein and Jung [418] $k' = 0.12$. In formula (27.1) p denotes the total pressure.

The mechanism set out below for the photosynthesis of hydrogen bromide was proposed by various authors [1081]. This mechanism consists of the following elementary processes:

- (0) $\text{Br}_2 + h\nu = \text{Br} + \text{Br}, \quad k_0,$
- (1) $\text{Br} + \text{H}_2 = \text{HBr} + \text{H} - 16.7 \text{ kcal}, \quad k_1,$
- (2) $\text{H} + \text{Br}_2 = \text{HBr} + \text{Br} + 41.1 \text{ kcal}, \quad k_2,$
- (3) $\text{H} + \text{HBr} = \text{H}_2 + \text{Br} + 16.7 \text{ kcal}, \quad k_3,$
- (4) $\text{Br} + \text{HBr} = \text{Br}_2 + \text{H} - 41.1 \text{ kcal}, \quad k_4,$
- (5) $\text{Br} + \text{Br} + \text{M} = \text{Br}_2 + \text{M}, \quad k_5,$
- (6) $\text{H} + \text{H} + \text{M} = \text{H}_2 + \text{M}, \quad k_6.$

Rejecting process 4 as strongly endothermic and 6 as of low probability as a result of the low concentration of H atoms, and writing the following equations for the rate in the stationary reaction:

$$w = d(\text{HBr})/dt = -2d(\text{H}_2)/dt = -2d(\text{Br}_2)/dt,$$

we obtain the following relation between the rates of the individual elementary reactions:

$$k_1(\text{H}_2)(\text{Br}) = k_2(\text{Br}_2)(\text{H}) + k_3(\text{HBr})(\text{H}),$$

$$\Delta I = k_5 p(\text{Br})^2.$$

It is not difficult to see that the first of these relations leads to the steady state condition $d(\text{H})/dt = 0$ and the second (allowing for the first) leads to the condition $d(\text{Br})/dt = 0$. The stationary concentrations of bromine and hydrogen atoms are given by the equations

$$(\text{Br}) = (\Delta I/k_5 p)^{1/2}$$

and

$$(\text{H}) = \frac{k_1(\text{H}_2)(\text{Br})}{k_2(\text{Br}_2) + k_3(\text{HBr})}.$$

Substituting these values of (Br) and (H) in the expression for the rate of reaction, we obtain

$$w = d(\text{HBr})/dt = \frac{2k_1(\text{H}_2)(\text{Br})}{1 + (k_3/k_2)(\text{HBr})/(\text{Br}_2)}$$

$$= \frac{2k_1 k_5^{-1/2} p^{-1/2} (\Delta I)^{1/2} (\text{H}_2)}{1 + (k_3/k_2)(\text{HBr})/(\text{Br}_2)}. \quad (27.2)$$

Comparing expressions (27.1) and (27.2) we see that the theoretical expression (27.2) obtained from the reaction mechanism coincides completely with the empirical expression (27.1). This agreement is a weighty argument in favour of regarding the above reaction mechanism as the actual mechanism of the photosynthesis of hydrogen bromide. Comparing expressions (27.1) and (27.2) we obtain

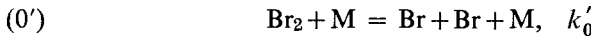
$$k = 2k_1 k_5^{-1/2} \quad \text{and} \quad k' = k_3/k_2.$$

As we have already noted, the quantity k' has the constant value 0.12 (over the temperature range 160–218°C). Hence it may be concluded that processes 2 and 3 have very similar activation energies, which is indeed very probable. Further, since k_5 is practically temperature independent, the temperature coefficient of the reaction under investigation must be determined by the temperature dependence of k_1 . Substituting in the expression for the temperature coefficient

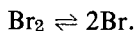
$$(k_1)_{T+5}/(k_1)_{T-5} = \exp \left[\frac{10E_1}{R(T+5)(T-5)} \right]$$

its empirical value of 1.48 and the value $T = 462^\circ\text{K}$ of the mean temperature we find that the activation energy of process (1) is $E_1 = 16.5 \text{ kcal}$, so that it is practically identical with the heat of this process (16.7 kcal).

The mechanism of the thermal reaction of bromine with hydrogen differs from the above mechanism for the photochemical reaction only in that the primary active reaction centres—the bromine atoms—are supplied in the thermal reaction by thermal motion. For this reason instead of the process (0); we have in this case the process



(it is assumed that the bromine atoms are generated in the gas phase). Moreover, just as one of the steady state conditions for the photochemical reaction is that the rate of thermal decomposition of bromine molecules should equal the rate of recombination of bromine atoms, the similar steady state condition for the thermal reaction is that the rates of the processes (0') and (5) should be equal, i.e. this condition is the equilibrium condition



Substituting the equilibrium concentration of bromine atoms

$$\text{Br} = [K(\text{Br}_2)]^{1/2}$$

in the expression for the rate of reaction, we obtain

$$\begin{aligned} w_{\text{therm}} &= \frac{d(\text{HBr})}{dt} = \frac{2k_1(\text{H}_2)(\text{Br})}{1 + (k_3/k_2)(\text{HBr})(\text{Br}_2)} \\ &= \frac{2k_1 K^{1/2}(\text{Br}_2)^{1/2}(\text{H}_2)}{1 + (k_3/k_2)(\text{HBr})/(\text{Br}_2)}. \end{aligned} \quad (27.3)$$

Comparing the rates of the photochemical and thermal reactions of bromine with hydrogen, (27.2) and (27.3), we find

$$w_{\text{photochem}}/w_{\text{therm}} = [\Delta I/k_5 p K(\text{Br}_2)]^{1/2}.$$

In this way, by measuring the rate of both reactions at the same temperature and pressure, it is possible to find the value of k_5 , since all the remaining quantities in this relation can be measured directly. Having determined k_5 in this way, it is then possible to find k_1 from measurements of the rate of reaction at different temperatures using (27.2) or (27.3). From the data of Bodenstein and Lütkemeyer [420] we obtain for this constant:

$$k_1 = 5.63 \times 10^{-12} T^{1/2} \exp(-17,640/RT) \text{ cm}^3 \text{ sec}^{-1}.$$

Comparing the activation energy of process (1) with its heat effect (16.7 kcal) we see that the "true" activation energy is only about 1 kcal.

The relatively large endothermic effect of process (1), which is the main secondary process of the photochemical reaction, and the large activation energy resulting from this are the reason for the slowness of this process; this is expressed by the fact that the quantum yield is of the order 0.001 over the temperature range 160–218°C.

It is easy to see that with the simultaneous action of temperature and light the concentration of bromine atoms must be larger than their equilibrium concentration (at a given temperature). The stationary concentration of bromine atoms in this case is given by the equation

$$(Br) = [K(Br_2) + \Delta I/k_5 p]^{1/2},$$

which can also be written in the form

$$(Br)^2 = (Br)_{\text{equilibrium}}^2 + \Delta I/k_5 p.$$

It follows from this expression that the larger the value of ΔI the more the stationary concentration of bromine atoms exceeds their equilibrium concentration. In particular, at sufficiently low temperature and sufficiently large ΔI , the equilibrium concentration of atoms may be insignificantly small compared with the quantity $(\Delta I/k_5 p)^{1/2}$ and this specifies the possibility of the purely photochemical reaction taking place, i.e. a reaction in which the primary active centres (bromine atoms) are mainly generated by light.

If the concentration of bromine atoms, which are the primary active centres of the reaction, exceeds the equilibrium concentration only during exposure of the reacting mixture to photochemically active light, and if with decrease in the amount of light energy absorbed it approaches the equilibrium concentration, then the stationary concentration of hydrogen atoms considerably exceeds that equilibrium concentration even in the thermal reaction when the concentration of Br atoms is the equilibrium concentration. Actually, from the foregoing, the stationary concentration of H atoms is

$$(H) = k_1(H_2)(Br)/[k_2(Br_2) + k_3(HBr)].$$

In view of the fact that $k_2/k_3 \approx 10$ (see p. 460), up to the time when the Br_2 concentration becomes comparable with the concentration of the reaction product HBr , we may reckon the second term in the denominator of the previous expression to be small in comparison with the first term and so may represent the expression by

$$(H) = (k_1/k_2)(Br)(H_2)/(Br_2),$$

or, because the concentrations of H and Br atoms are small compared with the concentrations of H_2 and Br_2 , for a stoichiometric mixture when $(H_2) = (Br_2)$, by

$$(H) = (k_1/k_2)(Br).$$

Calculating the ratio of the constants⁽²⁵⁾ (see foot of p. 463)

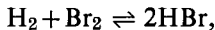
$$\frac{k_1}{k_2} = \frac{k_1 k_3}{k_3 k_2} \approx \frac{1}{10k_3} = \frac{1 (HBr)_{\text{equilibrium}} (H)_{\text{equilibrium}}}{10 (H_2)_{\text{equilibrium}} (Br)_{\text{equilibrium}}} = \frac{1}{10K' (Br)_{\text{equilibrium}}},$$

we obtain $(H)/(H)_{\text{equilibrium}} = (Br)/10K' (Br)_{\text{equilibrium}}$.

Hence, since $(\text{Br})/(\text{Br})_{\text{equilib}} \geq 1$ and $10K' \ll 1$ (at temperatures lower than 2000°) it follows that $(\text{H})/(\text{H})_{\text{equilib}} \gg 1$, i.e. $(\text{H})_{\text{stat}} \gg (\text{H})_{\text{equilib}}$.

The Limit of a Photochemical Reaction

It follows from formula (27.2) that the rate of the photochemical reaction vanishes, i.e. the reaction stops, when all the hydrogen or all the bromine has been consumed, i.e. when the initial substances have been completely converted to the reaction product HBr. This limit of the reaction corresponds to the equilibrium



shifted to the HBr side owing to the fact that the reaction is exothermic. This fact is shown in the low value for the equilibrium constant K' .

The coincidence of the reaction limit with its equilibrium, which is inevitable for thermal reactions, is not always observed with photochemical reactions.⁽²⁶⁾ Usually the limit of the reaction does not coincide with the equilibrium in photochemical reactions when the light acts in different ways in the forward and reverse reactions. We shall consider such a case in the same reaction of bromine with hydrogen.

Figure 87 shows the absorption spectrum of bromine vapour.⁽²⁷⁾ From this diagram it is clear that in the wave length region lower than about 3500 \AA , bromine vapour does not absorb light. On the other hand the light absorption by hydrogen bromide HBr only begins at 3260 \AA [531], extending from this "red" limit⁽²⁸⁾ to the short wavelength region, the absorption coefficient μ increasing very slowly with decrease in wavelength and scarcely reaching the value 0.03 cm^{-1} (at a pressure of 1 atm) at 2000 \AA . Thus while the absorption of bromine vapour takes place in the visible and near ultraviolet spectral region, the absorption of hydrogen bromide lies in the far ultraviolet, mainly outside the quartz spectral

⁽²⁵⁾ K' is the equilibrium constant for $\text{H}_2 + \text{Br}_2 \rightleftharpoons 2\text{HBr}$,

$$K' = [(\text{H}_2)_{\text{equilib}}(\text{Br}_2)_{\text{equilib}}]^{1/2}/(\text{HBr})_{\text{equilib}}.$$

At 400 , 800 , 1200 and 1600°K the quantity K' has the values 6.9×10^{-8} , 1.6×10^{-4} , 2.2×10^{-8} and 0.85×10^{-2} .

⁽²⁶⁾ Below (Chap. 9) it will be seen that the non-coincidence of the limit of the reaction with its equilibrium is a property of a certain class of thermal reactions also (branched-chain reactions).

⁽²⁷⁾ In this figure the plot along the ordinate axis is the index of absorption related to 1 cm of absorbing layer (at a pressure of 1 atm), i.e. the quantity

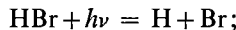
$$\mu = (1/x) \log(I_0/I)$$

(x is the thickness of the absorbing layer in cm) and the plot along the abscissa axis is the wave length in \AA .

⁽²⁸⁾ This limit corresponds to an energy of 87.7 kcal which is close to the heat of dissociation of hydrogen bromide (86.5 kcal). Thus the observed "red" limit of the absorption of HBr is practically the natural limit for the dissociation (into normal H and Br) of this substance.

region.⁽²⁹⁾ Consequently, light in the first of these regions acts only on the bromine (as was taken into account in the above mechanism for the photosynthesis of hydrogen bromide), while light in the short wavelength region acts only on HBr. When using a light source with wavelengths belonging to both regions of the spectrum, activation of both bromine and hydrogen bromide takes place.

Taking this into account, we shall include in the mechanism for the photosynthesis of hydrogen bromide HBr the process



we shall also consider the process $\text{Br} + \text{HBr} = \text{Br}_2 + \text{H}$ (4). Denoting the amounts of light absorbed by the bromine and hydrogen bromide by ΔI_1 and ΔI_2 , respectively, we find for the stationary reaction

- (a) $-\Delta I_2 + k_2(\text{Br}_2)(\text{H}) + k_3(\text{HBr})(\text{H}) = k_1(\text{H}_2)(\text{Br}) + k_4(\text{HBr})(\text{Br})$,
 (b) $k_5 p(\text{Br})^2 = \Delta I_1 + \Delta I_2$.

Using these relations we obtain for the rate in the stationary reaction

$$w = d(\text{HBr})/dt = 2[k_1(\text{H}_2)(\text{Br}) - k_3(\text{HBr})(\text{H})].$$

Equating the rate of reaction to zero we find

$$(c) \quad k_1(\text{H}_2)(\text{Br}) = k_3(\text{HBr})(\text{H}).$$

Solving (a), (b) and (c) we obtain

$$\frac{(\text{H}_2)(\text{Br}_2)}{(\text{HBr})^2} = K'^2 \left[1 + \frac{(k_5 p)^{1/2}}{k_4} \frac{\Delta I_2}{(\text{HBr})(\Delta I_1 + \Delta I_2)^{1/2}} \right], \quad (27.4)$$

where K' is the equilibrium constant for $\text{H}_2 + \text{Br}_2 \rightleftharpoons 2\text{HBr}$. In a stoichiometric mixture $(\text{H}_2) = (\text{Br}_2)$ and $(\text{H}_2)_{\text{equilb}} = (\text{Br}_2)_{\text{equilb}}$ and the expression (27.4) can be put more simply as

$$\frac{(\text{Br}_2)}{(\text{HBr})} = \frac{(\text{Br}_2)_{\text{equilb}}}{(\text{HBr})_{\text{equilb}}} \left[1 + \frac{(k_5 p)^{1/2}}{k_4} \frac{\Delta I_2}{(\text{HBr})(\Delta I_1 + \Delta I_2)^{1/2}} \right]^{1/2}. \quad (27.5)$$

This expression determines the ratio of the concentrations of initial substance (Br_2) and product (HBr) when the reaction ceases, i.e. the extent of conversion in the photochemical reaction.

It follows from (27.5) that in the absence of hydrogen bromide activation, i.e. in the absence of the reverse photochemical reaction, since $\Delta I_2 = 0$,

$$(\text{Br}_2)/(\text{HBr}) = (\text{Br}_2)_{\text{equilb}}/(\text{HBr})_{\text{equilb}},$$

i.e. the limit of the photochemical reaction is thermodynamic equilibrium. This is the reaction limit we obtained earlier in discussing the particular

⁽²⁹⁾ The short wavelength limit of the transparency region of fused quartz for 1 mm thickness corresponds to a wavelength of about 2000 Å.

case when the photochemical reverse reaction did not take place. In the more general case, when the forward and reverse photochemical reactions take place simultaneously, i.e. when $\Delta I_2 \neq 0$ (as also ΔI_1), the ratio between the initial substance (Br_2) and the product (HBr) at the end of the reaction may be entirely different from the equilibrium ratio. Moreover, since $K' \ll 1$, the cases in which the concentrations of bromine and hydrogen bromide are comparable, or $(\text{Br}_2) \gg (\text{HBr})$, occur when the second term in the main square root in formula (27.5) is considerably greater than unity, i.e. when

$$\frac{(k_5 p)^{1/2}}{k_4} \frac{\Delta I_2}{(\text{HBr})(\Delta I_1 + \Delta I_2)^{1/2}} \gg 1.$$

Using the relation (b), this inequality can be written

$$\Delta I_2 \gg k_4(\text{HBr})(\text{Br}),$$

from which it follows that the reaction limit, when the concentrations of the initial and final substances differ considerably from the equilibrium concentrations, is encountered when the number of bromine atoms formed per second from the photochemical dissociation of hydrogen bromide exceeds by a large amount the number of atoms entering into reaction (4).

TABLE 42

Degree of decomposition of hydrogen halides HX (as percentages) in the photochemical stationary states obtained by exposing the gas to light of different spectral ranges [493]

Wave length, Å	Degree of decomposition, %		
	HCl	HBr	HI
>2000	0.42	100	92
>2500	0.0	80	100
>3000	0.0	0	100

From the dependence of the reaction limit on the ratio of the quantities ΔI_1 and ΔI_2 it follows that this limit must be displaced if there is a change in the spectral composition of the photochemically active light. To illustrate this, Table 42 shows the data of Coehn and Stuckardt [493] relating to the photochemical decomposition of HCl , HBr and HI .

Coehn and Stuckardt also showed that the same equilibrium concentrations are obtained starting from the equimolecular mixture $\text{H}_2 + \text{X}_2$.

The displacement of the limit of the photochemical reaction with wave length may be seen particularly clearly from the data for HBr. In this case there is complete decomposition of HBr when it is exposed to light of short wavelength, but in the long wavelength region decomposition does not take place at all.

CHAPTER 8

CHEMICAL REACTIONS IN ELECTRICAL DISCHARGE

§28. Activation in Electrical Discharge

Excitation of Atoms and Molecules by Electron Impact. The Excitation Function.

In reactions taking place in electric discharge the role of photons, which are the activating factor in photochemical reactions, is played by fast electrons and to a much lesser extent by ions. The activating role of fast electrons is that on collision of an electron with a molecule, the conversion of the energy of the electron results in the appearance of an excited or ionized molecule, or the molecule dissociates into neutral or ionized fragments (atoms, radicals, ions). In every case (save processes leading to formation of negative ions, which are discussed later), we are concerned with conversions of the kinetic energy of the electron into internal energy of the molecule. According to the theory of collision of elastic spheres (see p. 349), for the transfer of an energy E to the molecule on direct impact it is sufficient that K , the energy of the electron, be not less than E . The probability of energy transfer, i.e. the probability of activation by electron impact, which is usually characterized by the size of the corresponding effective cross-section, is a function (*the excitation function or ionization function*) of K , the energy of the electron, and also depends on the structure of the molecule.

We shall consider first the process of *excitation* of a molecule by electron impact. Here we may consider together both the strict process of excitation, resulting in the appearance of an excited molecule, and the process of dissociation of a molecule, since the latter may be treated as excitation of an unstable state of the molecule (which leads to its decomposition into fragments).

Two types of excitation function are observed; suitable examples are the excitation functions for the mercury lines $\lambda = 2655 \text{ \AA}$, $4^1D_2 - 2^3P_1$, and $\lambda = 2653 \text{ \AA}$, $4^3D_1 - 2^3P_1$, shown in Fig. 91 [1104]. The former is a function which increases relatively slowly from the excitation energy (E) for the level 4^1D_2 and reaches a maximum at a value of several times greater than E ; the excitation function corresponding to the line at $\lambda = 2653 \text{ \AA}$ rapidly increases over 2 to 3 eV to a maximum and equally rapidly decreases to a certain low value.

The first function corresponds to the case in which the initial and final states of the excited particle (an Hg atom) have the same multiplicity (the transition $1^1S_0 \rightarrow 4^1D_2$) and the second to the case in which the particle changes its total spin on excitation (the transition $1^1S_0 \rightarrow 4^3D_1$).

From the point of view of molecular activation by electron impact the latter case should be the more important. Indeed, when excited molecules arise as a result of electron impact, a change in multiplicity usually implies that the excited state is metastable, and consequently the excited molecule has a relatively long life: the probability of such a molecule entering into chemical reaction will be higher than for a normal excited molecule, which rapidly loses its excitation energy as fluorescence (this difference, however, disappears at high pressures where the probability of fluorescence becomes negligibly small). When electron impact leads to the dissociation of the molecule the dissociation process which takes place with change in multiplicity is also of main interest, since frequently the ground state of valence-saturated molecules is a singlet state and the unstable state is a triplet.

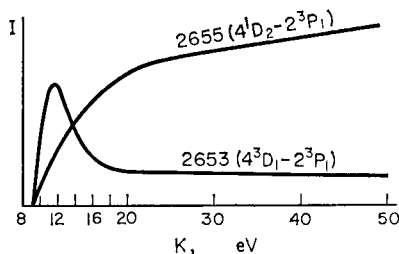


FIG. 91. Excitation functions for the mercury lines $\lambda = 2655 \text{ \AA}$, $4^1D_2 - 2^3P_1$, and $\lambda = 2653 \text{ \AA}$, $4^3D_1 - 2^3P_1$, on electron impact (according to Schaffernicht [1104]). The graphs show the dependence of the intensity I of the lines on the energy of the electrons.

The absolute probability of excitation, namely the ratio of the number of effective collisions of an electron with a molecule to the total number of collisions, is equal to the ratio of effective and gas-kinetic cross-sections:

$$P = \sigma_{\text{eff}}/\sigma; \quad (28.1)$$

experiment shows that P may range in different cases from very low values to about unity. Certain measured values for P referring to the maximum of the excitation function are shown in Table 43.

It is seen from these data that the probability of excitation of atomic levels (at the maximum) for forbidden transitions is of the order of 0.01 for helium and of the order of 0.1 for mercury. The probability of excitation for non-forbidden transitions at the maximum of the excitation function is about unity. The connection between the probability of excitation by electron impact and the probability of optical transition, which

TABLE 43

*Probabilities of excitation of various atoms on electron impact
(calculated for one gas-kinetic collision of an electron with the
atom) at the maximum of the excitation function*

Atom	Level	E , eV	K_{\max} , eV	P	Transition
He	$1s\ 2s\ ^1P$	20.6	21	0.008	Forbidden [902]
	$1s\ 2p\ ^3P$	19.7	20	0.015	Forbidden [902]
	$2p\ ^5\ 3s\ ^3P$	16.6	22	0.0095	Forbidden [270]
Ne	$3p\ ^2P$	2.12	7.0	4	Allowed [491]
Hg	$6s\ 6p\ ^3P_1$	4.86	6.5	0.17	Forbidden *[439]
	$6s\ 6p\ ^1P$	6.67	15	0.43	Allowed [326]
	$6s\ 7s\ ^3S$	7.69	9.3	0.065	Forbidden [719]
	$6s\ 6d\ ^1D$	8.80	15	0.2	Forbidden [326]

* It follows from the data of [326] that $K_{\max} = 7$ eV, $P = 0.42$.

determines the degree of strictness of the quantum prohibition, also follows from the quantum-mechanical calculation of the excitation cross-section of atoms for the impact of fast particles.

Figure 92 shows functions for excitation by electron impact for a series of helium levels as calculated by Massey and Mohr [924a]. In the same figure the dotted line shows the observed excitation functions; the theoretical and experimental curves are made to coincide when $K = 200$ eV. It is seen that the theoretical curves give the shape of the excitation functions satisfactorily, especially in the case of the S -terms (see also [693]). We should note the narrower maxima in the case of forbidden transitions. There is agreement of calculated and measured excitation functions in other cases also; the theory gives not only the correct dependence of the excitation function on electron energies, but also gives an order of magnitude for the absolute excitation cross-sections which agrees with the observed order. For example,⁽¹⁾ for the maximum cross-section of excitation of the $6s6p^3P_1$, $6s6p^1P_1$ and $6s7s^3S_1$ levels of the mercury atom Yavorskii [308, 309] obtained by a theoretical method 2.7, 12.2 and 1.4 cm^{-1} , whereas the measured values are 6.0, 15.0 and 2.3 cm^{-1} respectively. Moreover, the probabilities of excitation of the $6s6p^1P_1$, $6s6p^3P_2$, $6s6p^3P_1$ and $6s6p^3P_0$ levels of the mercury atom on bombardment with 10 eV electrons according to Penney's calculations [1023] should be in the

⁽¹⁾ The cross section measured in cm^{-1} units is strictly a cross section σ (in cm^2) multiplied by the number of molecules in 1 cm^3 of gas at 0°C and with a pressure of 1 mm Hg, namely $n_1 = 3.53 \times 10^{16} \text{ cm}^{-3}$. In this way the quantity σn_1 gives the number of acts of excitation effected by the electron in a 1 cm path in the gas with a pressure of 1 mm Hg and for a corresponding energy of the electron.

ratios $7.0 : 3.5 : 1.9 : 0.4$, whereas the measured relative probabilities for excitation of the first three levels are $6.6, 3.5$ and 2.26 . From the data of Table 43, which were obtained by various authors, the measured ratio of probabilities for excitation of 1P_1 and 3P_1 levels at the maxima of the excitation functions (15 and 7 eV) is 2.5 instead of the calculated 4.5 .⁽²⁾

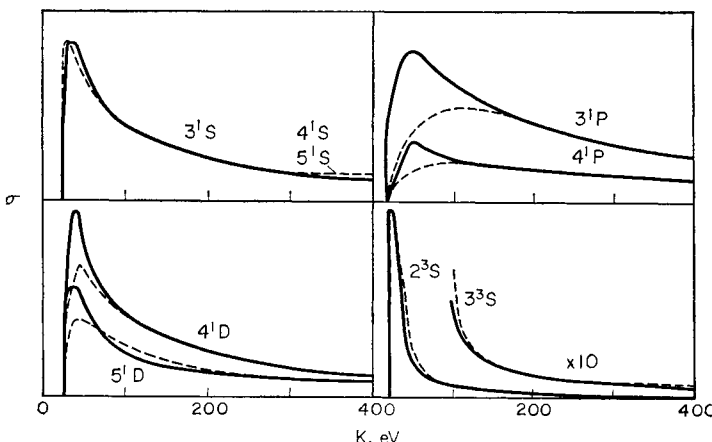


FIG. 92. Functions for excitation by electron impact of various helium levels (according to the calculations of Massey and Mohr [924a]). The dotted lines are the measured functions for excitation of corresponding helium levels. The theoretical and experimental curves are made to coincide when $K = 200$ eV.

The theory of interaction of particles on their collision gives a connection, also observed experimentally, between the probability of excitation on electron impact and the probability of the corresponding optical transition. Calculating the cross section σ_{ij} for excitation by electron impact of the quantum transition $i \rightarrow j$ using the Born approximation, we may write σ_{ij} as a series, each term of which is proportional to the square of the matrix element [193]

$$|q_{ij}^s|^2 = \left| \int \Psi_i q^s \Psi_j^* d\tau \right|^2 \quad (28.2)$$

(q is a coordinate, Ψ_i and Ψ_j are the wave functions of the excited atom corresponding to its initial and final states), determining the probability (intensity) for the optical transition $j \rightarrow i$ with dipole radiation ($s = 1$), quadrupole ($s = 2$) and so on. For non-forbidden optical transitions ($s = 1$) we may neglect all terms in the expression for σ_{ij} save the first,

⁽²⁾ Recently Jefferies [800] calculated the cross sections for excitation of $4p^2P_{1/2}$ and $4p^2P_{3/2}$ levels of the Ca^+ ion for four-volt electrons; he obtained $6.6 \pi a_0^2$ and $9.9 \pi a_0^2$, where a_0 is the radius of the one-quantum Bohr orbit of the H atom.

and consequently the cross-section for excitation will be proportional to the quantity

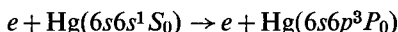
$$|q_{ij}|^2 = \left| \int \Psi_i q \Psi_j^* d\tau \right|^2, \quad (28.2a)$$

i.e. to the square of the matrix element corresponding to dipole radiation. If a given optical transition is forbidden and consequently $|q_{ij}|^2$ is zero, the cross-section for excitation on electron impact will be determined by the matrix element corresponding to quadrupole radiation. It follows from this calculation that the probability of excitation of a given level by electron impact should be proportional to the probability of the corresponding optical transition.

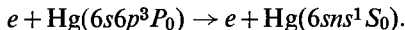
Owing to the approximate nature of this calculation it should not be expected that this relationship will be strictly obeyed, particularly when the energy of the electrons is small. However, in so far as it is possible to judge from the available experimental data, which are still very limited and not always sufficiently precise, there is apparently a definite parallelism between the probability of excitation by electron impact and the probability of the corresponding optical transition. The theory also gives a qualitatively accurate idea of the shape of the excitation functions of allowed and forbidden transitions in the high-energy region. Thus, according to the calculations, the effective excitation cross-section in the first case should decrease with increase in the electron velocity v according to a $1/v^2$ law (cf. formula (13.18)), and in the second case should decrease as $\ln v/v^2$; thus, the cross-section for excitation of a non-forbidden transition should decrease with increase in energy of the electron *more slowly* than the excitation of a forbidden transition. This is in fact what happens (see, for example, Fig. 91).

It is not uncommon for the excitation function to have two maxima instead of one. Excitation functions of this type are shown in Fig. 93. Kagan and Zakharova [99], who measured the excitation cross-section for the mercury lines shown in this figure, drew attention to the fact that excitation functions with two maxima are observed when the excitation cross-section for the corresponding levels is small. Thus they obtained, for the excitation cross-sections of $6s6p^1P_1 - 6s8s^1S_0$, $6s6p^1P_1 - 6s9s^1S_0$ and $6s6p^3P_1 - 6s7s^1S_0$ lines (Fig. 93) at the maximum of the excitation function, values within the range 1×10^{-2} to $5 \times 10^{-2} \text{ cm}^{-1}$. These values correspond to an excitation probability of P of the order 10^{-4} to 10^{-3} which is considerably smaller than the excitation probability for other mercury lines. Such a low probability for excitation of $6sns^1S_0$ levels corresponds to a negligibly small probability for transitions $6s6s^1S_0$ (the ground state of the mercury atom) to $6sns^1S_0$, which results from a double prohibition ($\Delta L = 0$ and $J = 0 \rightarrow J = 0$). These data lead to the conclusion that the presence of two maxima in the excitation function of the lines

considered (and of similar lines) is connected with so-called *cascade* or *step-wise excitation* of the corresponding atomic levels, i.e. with excitation of the atom by consecutive impacts of fast electrons, for example



and



The probability of step-wise excitation should be particularly high when there are metastable states (in this example the 3P_0 state) which arise in the individual stages of the excitation. The shape of excitation functions for

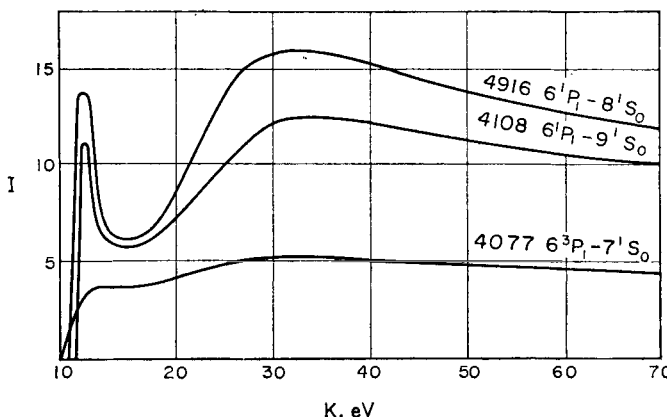
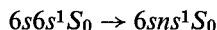


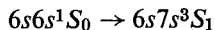
FIG. 93. Excitation functions of a mercury atom for electron impact; two maxima are displayed (according to Kagan and Zakharova [99]).

levels of different multiplicity leads us to think that the narrow maximum for the excitation functions in Fig. 93 corresponds to step-wise excitation of the ns^1S_0 levels and the wide maximum at high electron energies corresponds to direct excitation of these levels, i.e. the direct transition



on electron impact (see also [281]).

In addition to what has been said about the connection between the probability of excitation by electron impact and the probability of optical transition, we should mention that, according to the data of Fabrikant, Butaeva and Tsirg [269], the excitation cross-section for the non-forbidden transition $6s6p^3P_0 \rightarrow 6s7s^3S_1$ of the mercury atom during electron impact is 12.5 cm^{-1} ($P = 0.36$) at the maximum of the excitation function, whereas the excitation cross-section for the forbidden transition



is 1.4 cm^{-1} ($P = 0.04$) which is about ten times smaller. It must be assumed that when metastable mercury atoms are present in significant concentration, step-wise excitation of the $6s7s^3S_1$ level of the Hg atom via a metastable state of the atom will play an appreciable role as well as direct excitation.⁽³⁾ See also [223a, 281a].

Data on the *excitation of molecules* by electron impact are even more limited. We conclude from the data available that excitation of molecules by electron impact does not differ in principle from excitation of atoms (in that the excitation cross-section depends on electron energy in the sense of absolute cross-sectional values). The dissociation of molecules,

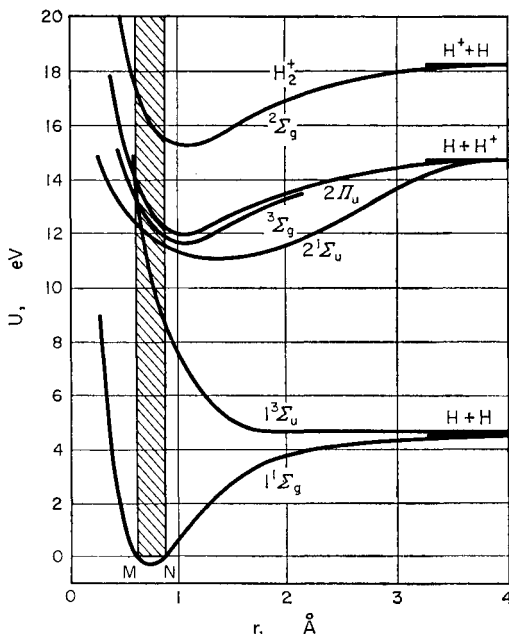


FIG. 94. Quantum transitions in the H_2 molecule which are most probable from the point of view of the Franck-Condon principle.

which is frequently observed during electron impact, may be considered as a particular case of excitation since here we are dealing with a quantum transition of the molecule into another electron state just as in normal

⁽³⁾ The possibility is not excluded that this is the reason for the somewhat unusual shape of the excitation function for the mercury line $\lambda = 5461 \text{ Å}$ ($6s7s^3S_1 \rightarrow 6s6p^3P_2$) which is reflected in the sharp fall of the effective cross section from the maximum (at 9.3 eV) and in the slow decrease with further increase in the energy of the electrons (between 19 and 60 eV the cross section decreases only one and a half times) [719].

excitation. We shall consider as an example the fact that according to Ramien's measurements [1053] the probability of excitation of the unstable state $^3\Sigma_u^+$ of the hydrogen molecule, i.e. the probability of the process $e + H_2(^1\Sigma_g^+) \rightarrow e + H_2(^3\Sigma_u^+) \rightarrow e + H + H$, on bombardment with 11.7 eV electrons (this energy is close to that corresponding to the most probable transition from the point of view of the Franck-Condon principle, see Fig. 94) is 0.06 [714, 1185]. This value practically coincides with the maximum probability of excitation of a mercury atom in the case of the intercombination transition $^1S \rightarrow ^3S$, which is of the same type as the transition $^1\Sigma \rightarrow ^3\Sigma$ in the H_2 molecule (see Table 43). The maximum probability for the dissociation of H_2 is assessed as $P \approx 0.1$ [924] from Poole's data [1035]. We may conclude from measurements for different electron energies that the excitation function of the $^3\Sigma_u^+$ level has a maximum close to the threshold of excitation at 8.8 eV [924], i.e. it is a function of a type characteristic of intercombination transitions.⁽⁴⁾

Ionization of Atoms and Molecules by Electron Impact

There have been a very large number of studies on the ionization of atoms and molecules by electron impact. These studies show that the ionization function, like the excitation function, increases from zero at an

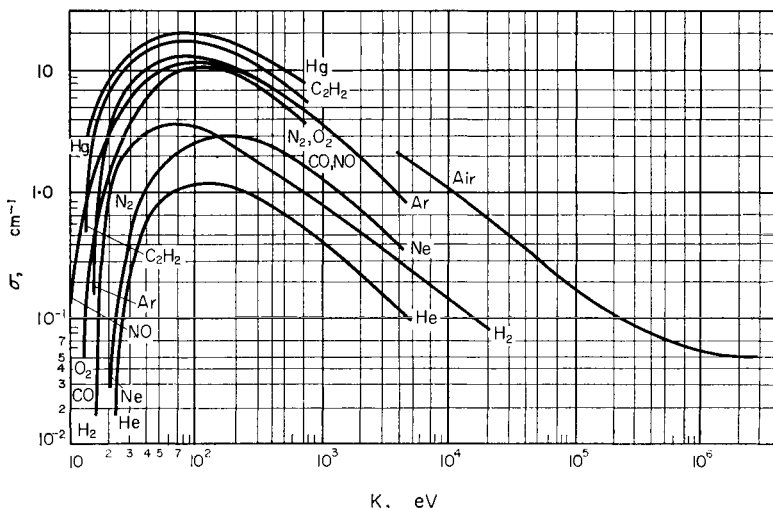


FIG. 95. Ionization functions of various gases for electron impact.

energy of the ionizing electrons corresponding to the ionization threshold, i.e. at $K_{\min} = I$ (the ionization potential); it reaches a maximum for energies of some tens to a hundred eV (less frequently up to 200

⁽⁴⁾ A theory for the process of dissociation of the H_2^+ ion on electron impact has recently been given by Kerner [830] (using a Born approximation).

eV) and then falls. Typical curves for the dependence of the ionization cross-section on electron energy (the ionization function) for various monatomic and polyatomic gases using the data of various authors (for literature see [59]) are shown in Fig. 95. In connection with this diagram we should note the following important point: the usual method of measuring an ionization function is by measuring the number of ion pairs (of positive and negative charges) formed in a 1 cm path traced out by an ionizing electron of a given initial velocity; consequently at high electron energies, owing to the superposition on the first (single) ionization of repeated and also multiple ionization, i.e. ionization with the formation of multiply-charged ions and ionization by secondary electrons, a certain overall value is measured which only conditionally may be called the "overall" ionization cross-section. When the electrons have high energies this "overall" cross-section may differ considerably from the true ionization cross-section, which corresponds to a single act of collision of an electron with an atom. An idea of the effect of multiple ionization on the shape of the

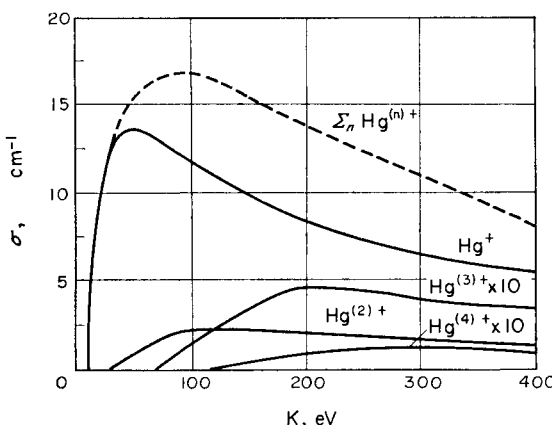


FIG. 96. Cross sections for single and multiple ionization of mercury by electron impact (according to Bleakney [408]).

ionization function is given by Fig. 96 which shows functions of one- (Hg^+), two- (Hg^{2+}), three- (Hg^{3+}) and four-fold (Hg^{4+}) ionization of the mercury atom and also the overall curve (dotted line) representing the change in the "overall" ionization cross-section with electron energy [408]. We see that the superposition of multiple on single ionization, as well as the increase in ionization cross-section when the energies of the electrons are large, leads to a considerable displacement of the maximum of the ionization function. Repeated ionization and ionization by secondary electrons clearly give an effect in the same direction, i.e. in the direction of increasing cross-section and of displacement of the maximum. Therefore

the curves of Fig. 95 give only approximately the ionization functions corresponding to a single act of ionization. However it is certain that superposition of different single ionization acts does not change the order of magnitude of the cross-section corresponding to the basic (predominating) process.

Study of the ionization function of different atoms close to the ionization threshold using electrons with approximately the same energy shows the complex structure of this function, which results from the excitation of different levels of the ions formed. For example, the irregularities in the ionization functions for zinc, cadmium and mercury atoms, which are observed for the first few volts after the ionization threshold, are connected with the auto-ionization of the excited atoms (the Auger effect) resulting from excitation of inner electrons [757]. The breaks in the ionization function curves for Ne^{2+} , Ar^{2+} , Kr^{2+} and Xe^{2+} (the processes $e + \text{Ne} = \text{Ne}^{2+} + 3e$, etc.) are interpreted as the result of superposition of linear components which are the ionization functions corresponding to the ground (3P) and excited (1D and 1S) states of the ions indicated [760]. The rectilinear path of the ionization function for the first few volts after the ionization threshold for the singlet state of the ion formed is seen clearly in the case of the ionization function of helium corresponding to the process $e + \text{He} = \text{He}^+ + 2e$, which is strictly linear for a whole eight volts.

The problem of changes in the ionization function near the ionization threshold has also been considered on the basis of the quantum-mechanical theory of collisions. Thus, Bates, Fundaminsky, Leech and Massey [353] have used the Born approximation and shown that the ionization cross-section near the threshold increases in proportion to the excess energy of the ionizing electron, i.e. in proportion to the quantity $K - I$, where K is the energy of the electron and I is the ionization potential. Similarly Geltman [665], also using the Born approximation, obtained the same linear dependence on $K - I$ for the ionization cross-section of H and He atoms (formation of singly-charged ions). According to Geltman (see also [784]), in contrast to singly-charged ions, the cross-section for the process $e + \text{He} = 3e + \text{He}^{2+}$ is proportional to the square of $K - I$ and in the general case of formation of an ion with charge n it is proportional to $(K - I)^n$. However it should be mentioned that according to Wannier's calculations [1264], which involve a statistical method allowing for the fact that the ionization is a process involving three particles, the cross-section for ionization of atoms is proportional to $(K - I)^{1.127}$, and only in the case of ionization of charged particles does the dependence of the ionization cross section on $K - I$ approximate to a direct proportionality.

When the energy of the ionizing electrons is increased, the differences in the ionization cross-sections of different atoms and molecules resulting

from their structures and energy characteristics become progressively smoothed out, and when the electrons have sufficiently high energies the ionization cross-sections are determined mainly by the number of electrons in the ionized particle. Thus when the energy of the electrons is greater than 5 keV the ionization cross-sections of different diatomic and polyatomic gases divided by the number of electrons in the molecule differ by no more than 30 per cent for a difference in the cross-sections themselves by a factor as high as 13 (see [59], p.158). The ratio of the ionization cross-section to the number of electrons is also observed to be constant for the inert gas atoms; however when passing from atoms to molecules this ratio is increased several fold (approximately threefold). In this way it follows from these data that for high electron velocities the probability of ionization of a molecule, like the probability of ionization of an inert gas atom, is proportional to the number of electrons in the ionized particle.

This result has also been established by Otvos and Stevenson [1003] for the ionization of various molecules by beta-rays of C^{14} (0.15 MeV), and of a mixture of Sr^{90} and Y^{90} isotopes (0.61 and 2.35 MeV). At the same time they show that the scatter of the points (up to 30 per cent), about the straight-line plot of cross-section against number of electrons in the molecule, is to a considerable extent removed if a straight line is plotted for each class of compounds (hydrocarbons in this case). It follows from this that in practice even when the ionizing electrons have very high energies the structural characteristics of the molecules still have a noticeable effect on the ionization cross-section.

Otvos and Stevenson show, moreover, that the relative ionization cross-sections measured for electrons with about 75 eV energy are in fairly close agreement with the sum of the relative ionization cross-sections of the atoms composing the molecule. A similar relation also holds for the ionization of molecules by beta-particles; the relative ionization cross-sections measured by the number of ions formed as a result of the impact of one beta-particle, are proportional to the relative cross-sections calculated from the ionization cross-sections of the atoms in the molecule.

Table 44 shows the probabilities of ionization of various atoms and molecules at the maximum of the ionization function, which are determined as the ratio of σ the ionization cross-section to the gas-kinetic cross-section. It is seen from the table that with rare exceptions the probability of ionization has a value between 0.2 and 0.5.

The theory of ionization on impact of a fast particle does not differ in principle from the theory of excitation. The only difference is that the final state of the ionized atom or molecule corresponds here to a continuous energy spectrum which is allowed for by the appropriate wave functions. The ionization functions for H and He atoms and the H_2 molecule have been calculated with the most precision. In Figs. 97 and 98 we compare

TABLE 44
*Probability of ionization of atoms and molecules at the maximum
of the ionization function*
(using data of various authors [924, 624])

Atom or molecule	Ion	I^* , eV	K_{\max} , eV	$\sigma \cdot 10^{16} \text{ cm}^2$	P
He	He^+	24.5	110	0.35	0.12
	He^{2+}	75	300	0.0015	0.0005
Ne	Ne^+	21.5	150	0.78	0.19
	Ne^{2+}	63.0	250	0.045	0.01
Ar	Ar^+	15.7	50	3.21	0.52
	Ar^{2+}	44.0	115	0.31	0.05
Hg	Hg^+	10.4	50	5.85	0.57
	Hg^{2+}	29.1	115	0.90	0.09
	Hg^{3+}	71	210	0.20	0.02
H_2	H_2^+	15.6	70	1.01	0.25
	$\text{H}^+ + \text{H}$	28	110	0.004	0.001
N_2	N_2^+	15.8	110	2.87	0.38
O_2	O_2^+	12.5	120	2.91	0.44
	$\text{O}^+ + \text{O}^-$	18.9	~40	0.0022	0.0003
NO	NO^+	9.5	110	3.25	0.49
CO	CO^+	14.1	100	3.07	0.38
HCl	—	13.8	125	4.90	0.74
CO_2	—	14.4	140	—	0.45
C_2H_2	C_2H_2^+	11.6	80	5.00	0.6
CH_4	—	14.5	80	—	0.28

* In the case of molecules I is the so-called vertical ionization potential corresponding to a Franck-Condon transition (see Fig. 94).

calculated curves [924a] and measured curves for the energy dependence of ionization cross-sections of He (Fig. 97)[1154] and of H_2 (Fig. 98)[1212]. Similar curves for neon and mercury are shown in Figs. 99 (Ne) and 100 (Hg). In these figures the upper curves are again the theoretical curves for the dependence of the ionization cross section on K/I (K is the energy of the electrons, I is the ionization potential) [353] and the lower curves represent experimental values [408, 983].

An important difference between the ionization of molecules and the ionization of atoms by electron impact is that, along with the formation of singly-charged or multiply-charged parent ions, the ionization of molecules may involve their splitting into some charged and uncharged fragments—atoms and radicals. For example, on bombarding CH_4 molecules with electrons of about 60 eV the ion-fragments CH_3^+ , CH_2^+ , CH^+ , C^+ and H^+ are observed as well as the parent ion CH_4^+ .

The nature and composition of the ionization products are established by using mass-spectrometric analysis of the ion beam formed by electron

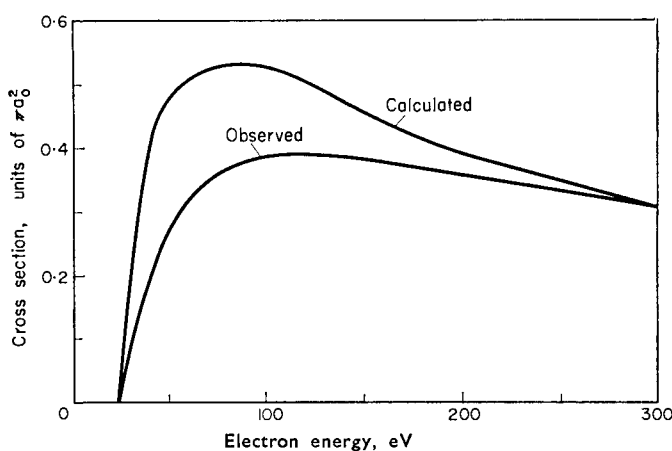


FIG. 97. Theoretical and experimental ionization functions for electron impact in the case of helium (according to Massey and Mohr [924a]).

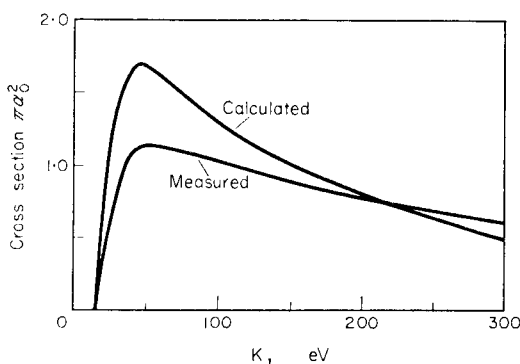


FIG. 98. Theoretical and experimental ionization functions for electron impact in the case of an H_2 molecule (according to Massey and Mohr [924a]).

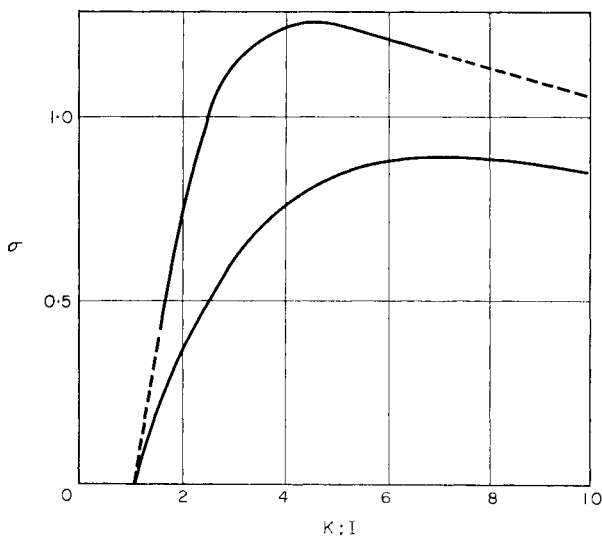


FIG. 99. Theoretical and experimental ionization functions for electron impact in the case of neon.

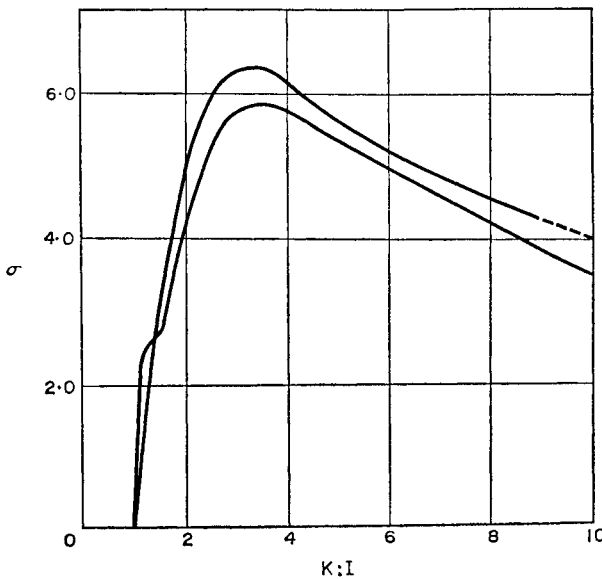


FIG. 100. Theoretical and experimental ionization functions for electron impact in the case of mercury.

bombardment of the gas. Figure 101 shows the mass spectrum of ions obtained in CH_4 (line 17 corresponds to the isotopic ion $\text{C}^{13}\text{H}_4^+$).

The mass spectrum is particularly complex in the case of ionization of a polyatomic gas, and consequently there is a large variety of types of decomposition of a complex molecule during electron impact. All types of decomposition are in effect observed which are energetically possible

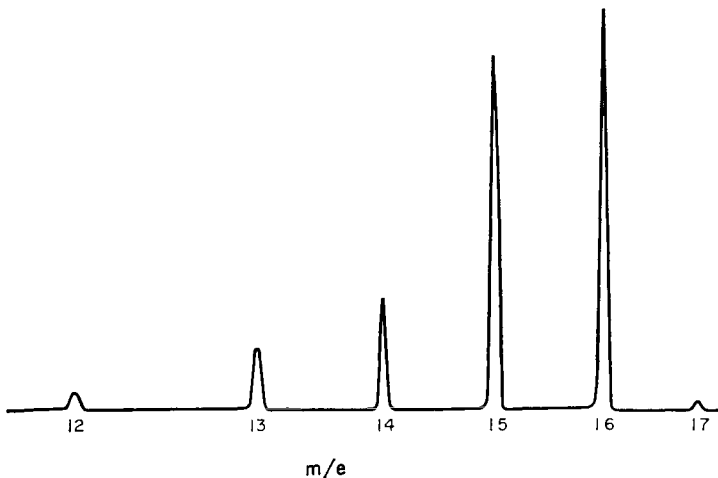


FIG. 101. The mass spectrum of ions obtained by bombarding methane CH_4 with 60 eV electrons.

for a given energy of the ionizing electrons. However, the probabilities of different decomposition paths are not identical, and roughly speaking obey the two following empirical principles:

(1) dissociative ionization plays a greater role in comparison with ionization without dissociation, the weaker the appropriate bonds;

(2) other conditions being equal, ions with lower free energy predominate in the mass spectrum.

The first principle is clearly demonstrated by the mass spectra of C_6H_6 benzene, C_8H_{18} n-octane and its isomer $(\text{CH}_3)_3\text{C}(\text{CH}_2)_3\text{CH}_3$ 2,2-dimethylhexane, which are shown in Table 45. It can be seen that on electron bombardment of such a stable molecule as benzene far fewer ion-fragments are formed than on bombardment of normal, and especially isomeric, octane.

To illustrate the second principle Fig. 102 shows a section of the mass spectrum of paraffin oil (which is a mixture of liquid hydrocarbons of the paraffin series, i.e. hydrocarbons with structure $\text{C}_n\text{H}_{2n+2}$). In this spectrum there is a peculiar clear alternation of intensities. Ions with odd masses, having an odd number of electrons, are ion radicals. From a thermodynamical point of view they are less stable than their neighbouring ions

TABLE 45

*Composition of the main products of ionization of C₆H₆ benzene, C₈H₁₈ n-octane and (CH₃)₃C(CH₂)₃CH₃ 2,2-dimethylhexane by impact of 70 eV electrons**

M	Benzene [1077]	M	n-Octane [412]	2,2-Dimethylhexane [412]
78	100	114	6.9	0.01
77	18.4	112	0.02	0.01
76	5.13	99	0.1	5.1
75	0.02	85	30.0	36.1
74	3.79	84	6.0	7.6
73	0.63	71	23.5	47.0
63	1.55	70	12.2	17.1
62	0.17	69	1.3	3.5
61	0.16	57	34.2	40.7
53	0.27	56	18.1	5.3
52	17.5	55	10.2	11.9
51	14.7	43	100	100
50	12.0	42	15.8	3.7
49	0.84	41	38.9	29.4
40	0.08	29	34.5	22.8
39.5	0.08	—	—	—
39	11.3	27	26.2	29.8
38.5	0.13	—	—	—
38	3.81	15	2.2	3.0
37.5	0.42	—	—	—
37	2.30	—	—	—
36	0.50	—	—	—
28	0.17	—	—	—
27	0.56	—	—	—
26	0.46	—	—	—

* The line intensities are given as percentages of the intensity of the strongest line of the mass spectrum.

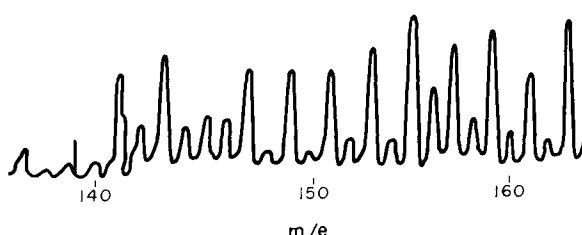


FIG. 102. The mass spectrum of ions formed by bombarding paraffin oil with 60 eV electrons.

with even numbers of electrons which, in accordance with principle 2, correspond to the more intense lines. This alternation of intensities in the mass spectra of hydrocarbons, which is particularly clear in the case of hydrocarbons with long chains, was first noted by Conrad [496].

The tendency to form the most stable ion-fragments is so great that they are formed even when rearrangement of bonds is necessary in the course of the process. For example, on electron bombardment of isobutane $(\text{CH}_3)_2\text{CHCH}_3$, among other ions there are formed C_2H_5^+ ions which cannot be obtained by simple bond-breaking.

Excitation of Molecular Vibration and Rotation by Electron Impact

Excitation of molecular vibration and rotation by electron impact is also possible as well as electronic excitation, dissociation or ionization of the molecule. The processes considered however are quite unimportant in the activation of molecules in an electric discharge, as may be surmised from the available experimental and theoretical data. Actually it follows from these data that only one vibrational quantum is at all likely to be excited on electron impact. The probability of excitation of a single quantum by impact of 5.2 eV electrons according to Harries [724] is in the case of N_2 , 1/110 and in the case of CO , 1/30; according to Ramien [1053] in the case of H_2 with 3.5 to 7.0 eV electrons it is 0.03 to 0.02. Crompton and Sutton [508] found for $K = 2$ eV that the excitation of a vibrational quantum of N_2 occurs on every twelfth electron impact. According to Haas [711a] when $K = 2$ eV the cross-section has a maximum and many vibrational quanta are excited for one impact; he connects this with formation of the short-lived N_2^- ion. According to the theory of collision of elastic spheres, as a result of the unfavourable mass ratio the amount of kinetic energy of the electron converted into vibrational (and rotational) energy of the molecule is negligibly small; for this reason from the point of view of this theory excitation of molecular vibrations and rotation should not take place on electron impact (considering slow electrons). The observed excitation of vibrations indicates the inapplicability of a simple mechanical model to this process. Franck [624, 922] proposed a mechanism for excitation of vibrations of a molecule on electron impact with the basic idea that on close approach of the electron to the molecule the internal field of the molecule is distorted and thus changes the interaction of atoms in the molecule, as a result of which its vibrational state may change.

A quantum-mechanical calculation of the cross-section for excitation of vibrations in the hydrogen molecule on electron impact, considering coulombic interaction of the exciting electron with the electrons and nuclei of the H_2 molecule, has been carried out by Ta-You-Wu [1203] (see also [480b]). The function he calculated for the excitation of a vibrational quantum of H_2 is shown in Fig. 103. It is seen from this figure that the

excitation cross section for electrons with an energy of the order of a few electron-volts is about $0.5 \times 10^{-18} \text{ cm}^2$, i.e. the probability P is about 0.001. This value is ten times smaller than that measured by Ramien [1053] (see above); however, in view of the fact that the calculation contains simplifying assumptions, the agreement of the calculated and measured cross sections should be considered satisfactory.

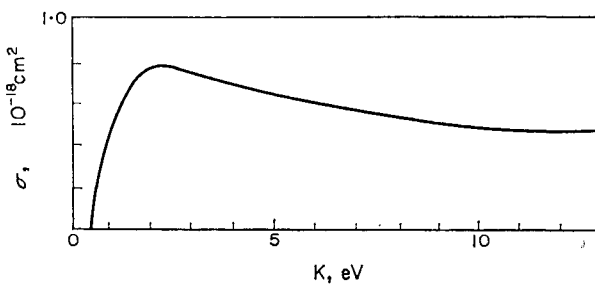


FIG. 103. The theoretical function for the excitation of a vibrational quantum of the H_2 molecule ($E = 0.515 \text{ eV}$, $\nu = 4155 \text{ cm}^{-1}$) by electron impact (according to Ta-You-Wu [1203]).

Ta-You-Wu also calculated the dependence of the cross-section for excitation of optically-active molecular vibrations on the energy of the exciting electrons. The excitation function he obtained for $E = 0.1 \text{ eV}$ ($\nu \approx 800 \text{ cm}^{-1}$) is shown in Fig. 104 (the cross-section is in arbitrary units);

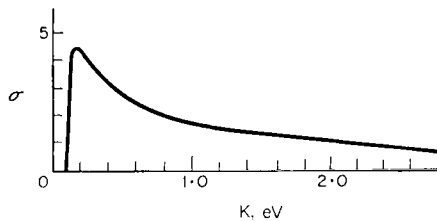


FIG. 104. The theoretical function for the excitation of a quantum of optically active molecular vibrations ($E = 0.1 \text{ eV}$, $\nu = 800 \text{ cm}^{-1}$) by electron impact (according to Ta-You-Wu [1203]). The σ -axis scale is arbitrary.

this shows that the cross-section increases rapidly with decrease in the energy of the electrons (from a few electron-volts). The increase in the probability of excitation of vibrations with decrease in electron energy also follows from Penning's calculations [1024]. A dependence of the probability of excitation of vibrations of the CO_2 molecule on electron energy similar to that calculated by Ta-You-Wu was apparently obtained by Dodonova [63], who measured the intensity of radiation of the CO_2 band $\lambda = 4.65 \mu$, which is excited in electric discharge, at various pressures

and current strengths. We should add that according to Ta-You-Wu's estimate, the results of his calculations are in satisfactory agreement with the experimental data of Harries [724] (see above) relating to the excitation of a vibrational quantum of the CO molecule.

With regard to excitation of molecular rotation, in so far as it is possible to judge from the distribution of intensity in bands of electronic spectra excited in an electric discharge, the rotational energy of molecules changes only slightly on the impact of a fast electron. However, when the electron energy is less than 1 eV the probability of exciting rotation becomes considerable, as is clear from experimental studies on the retardation of electrons in various gases [924, 737, 508, 322]. In particular, it follows from these experiments that while in the case of helium, neon and argon, the mean energy loss on collision of an electron with a gas atom corresponds to $2m_eK/m$ (see p. 347) in accordance with the theory of elastic impact, the losses in molecular gases are much greater than this quantity. Theoretical data also yield this result. Thus Massey [921] calculated the cross-section for excitation of rotation of a polar molecule by electron impact and found that the energy loss of the electrons in this case is much greater than the losses in elastic collisions. According to Morse's calculations [959] energy losses of the electrons on collision with non-polar molecules composed of identical atoms should be of the order of elastic losses; however as a result of more precise calculations Gerjuoy and Stein [666] showed that in this case the amount of energy transferred is much greater than that calculated from the theory of elastic impact. In the case of nitrogen the two quantities differ by a full power of ten. Stein, Gerjuoy and Holstein [1174] found that when the electron energy is large compared with the distance between rotational levels the cross section for excitation of rotation of the nitrogen molecule should be about 10^{-17} cm^2 (P about 10^{-2}). For the H_2 molecule Gerjuoy and Stein's calculations [667] give poorer agreement than for N_2 between the calculated and measured values for the loss in energy of the electron on collision with a molecule (see also [480b]). The calculated losses are low compared with those obtained experimentally. It follows from the above that the probability of exciting rotation by electron impact should be close to the probability of exciting vibrations, and owing to the smallness of the amounts of energy transferred, rotational and vibrational excitation of molecules by electron impact should be considered of low importance in the chemical activation of molecules.

Owing to the low efficiency of direct excitation of molecular vibrations and rotation by electron impact, we must assume that, even if vibrationally or rotationally excited particles play a part in electric-discharge reactions, they are formed by indirect (secondary) means. For example, a molecule in a high vibrational level (but in the ground electronic state) may be obtained by electronic excitation of the non-vibrating molecule and a

subsequent optical transition to the ground electronic state, as shown in Fig. 105.

Moreover, a vibrationally or rotationally excited particle may appear as a result of dissociation of a molecule on electron impact. A clear example of rotational excitation during molecular dissociation is that of hydroxyl formed in the process $e + H_2O = H + OH + e$. On the basis of the laws of conservation it may be shown [145] that in this case the rotational energy of OH may reach very high values which are much greater than the mean

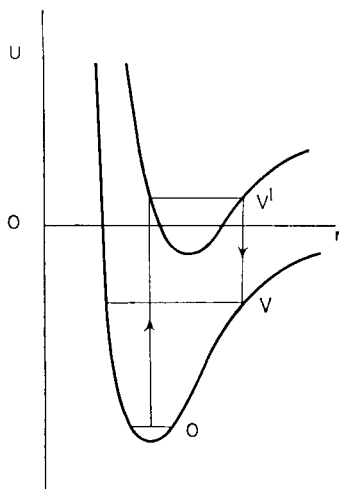


FIG. 105. Production of a vibrationally-excited molecule by electronic excitation on impact of a fast electron.

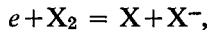
values corresponding to equilibrium. In accordance with this, measurements of "rotational temperature" of excited OH⁽⁵⁾ formed in electric discharge in water vapour (at low pressures) give for T_{rot} a value of the order 10,000°. There are also indications that vibrationally-excited particles may arise as a result of charge transfer [734, 881] (see p. 509), and also as a result of secondary processes of chemical interaction of the positive ions formed by electron bombardment of neutral molecules. This conclusion is strongly supported by the data of Frankevich [279, 256a] who studied secondary processes of the type $H_2O^+ + H_2O = H_3O^+ + OH$. Finally it may be supposed that vibrationally- and rotationally-excited molecules are also formed during collisions with fast ions.

Formation of Negative Ions on Electron Impact

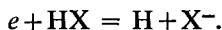
Since many atoms and radicals possess an electron affinity, there is another specific activating effect of electron impact. This is most evident

(5) It is interesting to note that such high "rotational" temperatures do not arise in the excitation of hydroxyl by positive hydrogen rays [778].

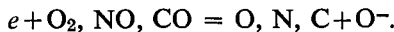
in the case of the halogens whose atoms have a particularly high electron affinity, greater than the dissociation energy of the halogen molecule. Detection of negative atomic ions in the vapour of iodine [775, 462a, 642c, 405a] and bromine [409] during the passage of slow electrons shows that the formation of ions should in this case be connected with the process



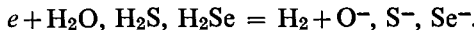
where $X = I$, Br (and also very probably Cl). A similar process has been found in the case of various halogen compounds, for example for HX ($X = Cl$, Br and I), where dissociation is observed according to the scheme⁽⁶⁾ [974, 711, 621a, 642d]



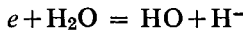
Moreover, negative atomic ions have also been detected in oxygen [890, 714, 924], nitric oxide [924] carbon monoxide [924], water vapour [909], hydrogen sulphide H_2S , hydrogen selenide H_2Se [971], etc., with electron energies of $K \geq 3.0 \pm 0.4$ eV (O_2), $\geq 3.2 \pm 0.5$ eV (NO), $\geq 9.5 \pm 0.1$ eV (CO), ≥ 5.4 eV (H_2O), $\geq 2.9 \pm 0.3$ (H_2S), and $K \geq 2.3 \pm 0.3$ eV (H_2Se) respectively. In O_2 , NO and CO the process follows the scheme



In water vapour, H_2S and H_2Se decomposition processes have been established in accordance with the scheme

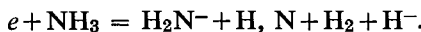


In addition, the process



has been observed in water vapour. It is interesting that in this case the hydroxyl ion HO^- has not been detected [909] and according to Laidler [860] this is connected with the high excitation energy of the electronic state of the ion molecule H_2O^- , which on dissociation gives $H + HO^-$.

In ammonia, H_2N^- and H^- ions have been detected and their appearance is apparently connected with the processes [909]



Measurements of the yield of atomic ions enable us to calculate the cross-section or probability P of the corresponding process (calculated for one collision of an electron with a molecule). These measurements show that the size of P depends on the nature of the dissociating molecule

⁽⁶⁾ The cross-section for this process has a maximum close to 0.77 (HCl), 0.21 (HBr), 0.05 (HI) eV and in each case the process is initiated at an electron energy almost exactly in agreement with $D_{HX} - Ex$ (D is the heat of dissociation, E the electron affinity). For an electron energy in excess of 13 eV the process $e + HX = H^+ + X^- + e$ is observed [711].

and the energy of the electrons. In many of the cases studied P increases with electron energy and at a certain value (usually of the order of some electron-volts) it reaches a maximum and then decreases with further increase in energy. In the case of oxygen two such maxima were found at electron energies of about 7 and 14 eV, and were attributed to dissociation processes of the molecule corresponding to different states of excitation of the oxygen atom, $e + O_2 = O + O^-$ and $e + O_2 = O' + O^-$. One of these maxima is shown in Fig. 106, in which electron energy is plotted as the abscissa and the ion current for the O^- ion is plotted as the ordinate. The probability of splitting of the oxygen molecule into $O + O^-$ corresponding to this maximum is $P = 1.2 \times 10^{-8}$ (see also [507]). The maximum at 14 eV (not shown in Fig. 106) corresponds to the probability 2.0×10^{-5} which is 60 times lower.⁽⁷⁾

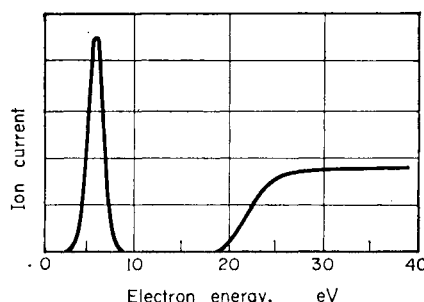


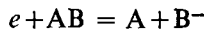
FIG. 106. The yield of O^- ions on bombarding O_2 molecules with electrons of various energies (according to Massey and Burhop [924]).

In contrast with these cases, in iodine and hydrogen iodide (and also in CCl_4 , CF_3I , CCl_2F_2) the atomic halide ion X^- may be formed when the energy of the electrons is very small. Accordingly the maximum of the ion-yield curve occurs when the energy is not greater than some tenths of an electron-volt. Thus, the cross-section of the process $e + HI = H + I^-$ has a maximum value at 0.05 eV [642d] and the cross-section of the process $e + I_2 = I + I^-$ at 0.34 eV [642c]. The maximum value of the cross-section for the latter process is $3.2 \times 10^{-15} \text{ cm}^2$, i.e. $P \approx 1$ [405a]. The cross-sections for the processes $e + CCl_4 = CCl_3 + Cl^-$ and $e + CF_3I = CF_3 + I^-$ are $1.3 \times 10^{-16} \text{ cm}^2$ and $7.8 \times 10^{-17} \text{ cm}^2$ respectively [35a]. In this way the probabilities of splitting of a molecule by an electron to form a negative ion are of the order 10^{-3} to 1.

The characteristic dependence on electron energy of the probability of dissociation of a molecule, with simultaneous formation of a negative atomic or radical ion, is explained on the basis of potential-energy curves of the

(7) The O^- ions formed when the electron energy is greater than 20 eV (Fig. 106) appear as a result of the process $e + O_2 = e + O^+ + O^-$.

type shown in Fig. 107. In this figure the AB curves are the potential-energy curves of the AB molecules and the AB⁻ curves are those of the ions AB⁻. The decomposition of the AB molecule according to the scheme



may be considered as its transition under the action of the electron into the ionic state AB⁻, with subsequent dissociation of the latter into A + B⁻ [777]. It does not matter whether the ionic state AB⁻ is unstable for any distance between A and B⁻ or whether it corresponds to a potential-energy curve with a minimum (the dotted curve in Fig. 107). If the AB → AB⁻ transition takes place from the zeroth vibrational state of the AB molecule (as is the case for not too high temperatures) then the most probable (maximum) cross-section of the process will correspond to an electron energy determined by the vertical (or energy-coordinate) distance of the AB⁻ curve from the minimum of the AB curve (this is indicated by the heavy arrow in Figs. 107a and 107b). In accordance with the type of wave function of the zeroth vibrational state (see Fig. 81, p. 410) the region of the AB → AB⁻ transition is shown by the shaded zone in Figs. 107a and 107b; the low-energy side is indicated by the short arrow and the high-energy side by the long arrow. This region actually corresponds to the left-hand curve for the yield of O⁻ ions in Fig. 106. It follows from Fig. 107 that the form of

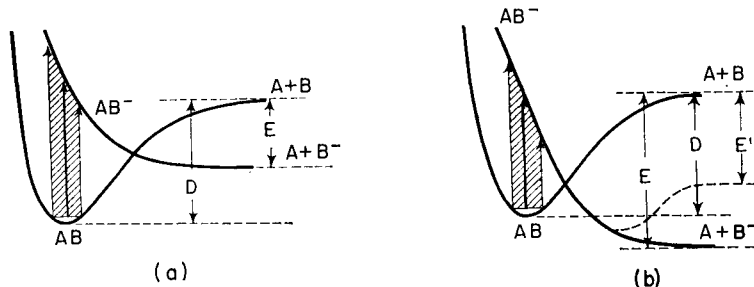


FIG. 107. Explanation of the process $e + AB = A + B^-$ using potential energy curves. (a) when the electron affinity (E_B) of the B atom is less than the heat of dissociation (D_{AB}) of the AB molecule; (b) when $E_B > D_{AB}$. The dotted curve in Fig. 107b corresponds to a stable state of the AB⁻ ion molecule (in this case $E_B < D_{AB}$).

this curve should not depend on the ratio of the heat of dissociation (D_{AB}) of the AB molecule to the electron affinity (E_B) of the B atom (radical), i.e. on whether $D_{AB} > E_B$ (Fig. 107a) or $D_{AB} < E_B$ (Fig. 107b). We should just mention that in the second case there is a higher probability that the curve AB⁻ will cross the curve AB near the minimum: in this case the process will obviously be energetically possible even for thermal electrons, and the maximum probability for the process will occur when

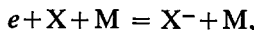
the electron energy is equal or close to zero. With increase in energy the probability of the process must decrease. Such a case is clearly realized in the interaction of I_2 and HI molecules with thermal electrons.

The following processes illustrate the formation of negative ions with simultaneous splitting of the molecule. Hickam and Fox [758, 759] observed in SF_6 , in addition to formation of the SF_6^- ion, formation of the SF_5^- ion as a result of the process $e + SF_6 = SF_5^- + F$.⁽⁸⁾ Both ions are formed with greatest probability when the electron energy is less than 0.1 eV.⁽⁹⁾ Dukel'skii and coworkers [64] observed negative molecular ions in the vapour of salts of group one and two metals, in sulphur vapour and so on [68] (see also [546, 536a, 757a]). With 80 eV electrons, in addition to S_8^- , all the remaining negative ions: S_7^- , S_6^- , S_5^- , S_4^- , S_3^- , S_2^- , S^- , have been detected in sulphur.

We have seen that, as a result of the dissociation of a molecule on its interaction with an electron, cases of electron capture by the molecule without its decomposition (SF_6^-) are also observed. We should add that Biondi [402] has observed the formation of negative molecular ions O_2^- of oxygen on capture of thermal electrons ($K = 0.04$ eV) by O_2 molecules. Comparison of his measured cross section $\sigma = 1.2 \times 10^{-22} \text{ cm}^2$ ($P = 2 \times 10^{-7}$) with that calculated for the process of radiation capture of an electron [923] shows that O_2^- is formed according to the scheme $e + O_2 = O_2^- + h\nu$.

The probability of radiation capture is low, and consequently to explain the frequently observed high yields of negative molecular ions (see footnote⁽⁹⁾) we normally use a mechanism of resonance capture, which occurs when the electron energy is equal to the energy for excitation (vibrational or electronic) of the resulting molecular ion. From resonance-capture theory [410] a value is obtained for the cross section of formation of a negative ion which is some powers of ten larger than the cross section for radiation capture in the absence of resonance.

At sufficiently high pressures an important role in the formation of negative ions may be played by a "termolecular" mechanism



similar to the scheme for the recombination of atoms or radicals (see §20). A confirmation of this mechanism is provided by the linear dependence of the ion current ratio, $i_{O_2^-}/i_{O^-}$, on pressure of O_2 in the case of electron capture by molecular oxygen (process $e + O_2 + O_2 = O_2^- + O_2$) [E. E. Muschlitz, *J. Appl. Phys.*, **28**, 1414, (1957)]. The possibility of a

⁽⁸⁾ When the electron energy is high F_2^- and F^- are formed in addition to SF_6^- and SF_5^- [312].

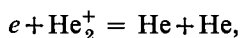
⁽⁹⁾ The maximum cross section for electron capture of the SF_6 molecule is 10^{-22} cm^2 [759]. See also [35a].

“termolecular” or recombination mechanism is clear from the existence of the reverse process, namely the splitting off of an electron from a negative ion which collides with a neutral molecule or atom (see below, p. 504, and also [963]). To realize the process $e + X + M = X^- + M$ it may be assumed that, as in the recombination of atoms (cf. p. 336), practically all ternary collisions are effective [228].

Negative ions may be yielded in secondary processes also. For instance OH^- ions in water vapour are apparently formed as a result of proton transfer in the process $\text{H}^- + \text{H}_2\text{O} = \text{H}_2 + \text{OH}^-$. The cross-section for this process is about 10^{-17} cm^2 (E. E. Muschlitz, *loc. cit.*).

We must now consider the process of recombination of an electron and an ion. Owing to the low probability of radiation capture, i.e. of the process $e + A^+ = A + h\nu$ [351], it would be expected that, as in negative-ion formation, an important role would be played by a mechanism of ternary collision $e + A^+ + M = A + M$.

The probability of recombination should also be especially high for the recombination of an electron and a molecular ion when the neutral molecule formed may split into atoms or atomic groups: $e + AB^+ = A + B$. The possibility of such a recombination mechanism was directly indicated by Rogers and Biondi [1079] in the case of the process



with which is associated an unusually large cross-section for the electron-ion recombination observed under discharge in helium. In view of the fact that one of the He atoms produced during the recombination of an electron and the He^+ ion is in an excited state, and the excess energy is distributed equally between both He atoms in the form of translational energy, it is possible to detect these fast atoms by the Doppler broadening of the spectral line emitted by one of them [405]. Indeed Rogers and Biondi showed that the helium line 5876 \AA in the after-glow spectrum is greatly broadened. It was found from the Doppler width of this line that the kinetic energy of the He atom is about 0.1 eV ; this is in agreement with the figure required for each He atom produced as a result of the suggested process of *dissociative recombination*.

Faire, Fundingsland and Aden [595] measured the recombination coefficient α of thermal electrons with molecular ions of nitrogen and obtained a value of the order of $10^{-6} \text{ cm}^3 \text{ sec}^{-1}$ (see also [461a]). Substituting in the formula

$$\alpha = \sigma v \quad (28.3)$$

the values $\alpha = 10^{-6} \text{ cm sec}^{-1}$ and the velocity of thermal electrons $v = 2 \times 10^7 \text{ cm/sec}^{-1}$, we find that the cross-section for dissociative recombination, i.e. the cross-section for the process $e + \text{N}_2^+ = \text{N} + \text{N}$, is

$\sigma = 5 \times 10^{-14} \text{ cm}^2$. This figure corresponds to a probability $P = 100$, i.e. an effective radius which is ten times the gas-kinetic radius.

We should add that Zelikoff and Aschenbrand [1326] connect the dissociative recombination $e + \text{NO}^+ = \text{N} + \text{O}$ with the photochemical dissociation (which they have observed) of the nitric oxide on exposure to light of 1236 Å, which has the primary effect of ionizing the NO molecule: $\text{NO} + h\nu = \text{NO}^+ + e$. See also [364a].

Since the probability of radiation recombination is low, ion recombination occurs either by a three-body collision $\text{A}^+ + \text{B}^- + \text{M} = \text{AB} + \text{M}$, or by ion neutralization $\text{A}^+ + \text{B}^- = \text{A} + \text{B}$. Thus according to P. F. Knewstubb and T. M. Sugden, *Trans. Faraday Soc.*, **54**, 372, (1958) the recombination of ions of alkali elements and of hydroxyl ions in flame follows the scheme Na^+ , $\text{Li}^+ + \text{OH}^- = \text{Na}$, $\text{Li} + \text{OH}$, with a recombination coefficient of $\alpha = 0.5 \times 10^{-8} \text{ cm}^3 \text{ molecule}^{-1} \text{ sec}^{-1}$.

§29. Activation by Bombardment with Fast Ions and Atoms

Excitation of Atoms and Molecules by Collisions with Fast Ions and Atoms

Turning to the excitation and ionization of atoms and molecules by impact of fast ions and also of fast neutral atoms (usually obtained by charge transfer in collisions of ions with gas molecules or with a solid surface), it should be noted that these processes have as yet been inadequately studied experimentally. According to the data available, when the energy K of the ions is close to

$$K_{\min} = \frac{m + m_i}{m} E \quad (29.1)$$

(m_i is the mass of the ion; m the mass of the atom or molecule suffering impact, E the excitation energy or ionization potential), and often even when it is several times greater than this quantity, then the probability of excitation or ionization by impact of an ion is negligibly small.

For example, according to Kirschtein's measurements [833], the mercury resonance line 2537 Å with excitation energy 4.87 eV is observed when mercury vapour is bombarded with Na^+ ions with energy $K \geq 35 \text{ eV}$,⁽¹⁰⁾ i.e. when the energy is 6.5 times larger than

$$K_{\min} = 4.87(200 + 23)/200 = 5.43 \text{ eV.}$$

According to Kirschtein's data, when $K = 50 \text{ eV}$ only one in 100,000 collisions of Na^+ and Hg leads to excitation of the mercury atom. A large difference is observed between the minimum "excitation energy" and K_{\min} in other cases also. For example, on the collision of fast Li^+ , K^+ and Cs^+ ions with helium atoms, the excitation of lines both of helium and

⁽¹⁰⁾ According to Appleyard's measurements $K > 100 \text{ eV}$ [323].

of these ions was observed by Maurer [930]. Thus in the case of $\text{Cs}^+ + \text{He}$ the helium line 5876 Å with excitation energy 23.0 eV appears when the energy of the caesium ions is about 1000 eV, and the Cs^+ ion lines with similar electronic excitation energy (in particular, the line $\lambda = 4603.2 \text{ \AA}$) appear when the energy of the ions is 7000 eV. In the first case the minimum "excitation energy" is only 30 per cent greater than K_{\min} , which in this case is 790 eV, but for the Cs^+ lines this excitation energy is approximately ten times greater than K_{\min} .⁽¹¹⁾

There are also indications that, in contrast with excitation by ion impacts, in excitation by neutral particles the minimum excitation energy may be practically identical with K_{\min} . Thus according to Maurer's data [929] the excitation of the triplet lines of helium by impact of fast He atoms is observed when the latter have energy equal to or greater than 80 eV. Owing to the intercombination prohibition, the excitation of these lines is possible only with simultaneous excitation of the triplet levels of both colliding atoms, and consequently K_{\min} in this case should be equal to twice the sum of the excitation energies of the triplet lines (23.0 eV) and the lowest triplet level $1s2s^3S_1$ of the He atom (19.8 eV), i.e. $2 \times (23.0 + 19.8) = 85$ eV, which is close to the observed minimum excitation energy (≈ 80 eV).

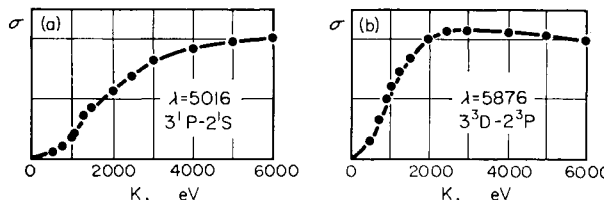


FIG. 108. Excitation functions of the singlet 5016 Å (a) and the triplet 5876 Å (b) helium lines for impact of He atoms (according to Maurer [929]).

The cross-section for excitation by impact of a fast ion or atom increases with the energy of the exciting particle. The character of the excitation function on ion impact may be seen from Fig. 108 [929] which shows the excitation functions for the helium lines 5016 Å, $1s3p^1P - 1s2s^1S$ (Fig. 108a), and 5876 Å, $1s3d^3D - 1s2p^3P$ (Fig. 108b), by impact of fast helium atoms. For comparison Figs. 109a and b show the excitation functions for the same lines for electron impact [1218]. It is seen from these figures that in both cases the excitation cross-section passes through a

⁽¹¹⁾ It should however be mentioned that for very long exposure times Maurer has observed the Cs^+ line 4003.8 Å at 2000 eV, i.e. when the energy of the Cs^+ ions is only three times greater than the quantity K_{\min} . This observation indicates that there is no well-defined threshold for excitation of atoms by ionic impact.

maximum; however, for excitation by electron impact the maximum occurs when the energies of the electrons are 100 eV (5016 Å) and 30 eV (5876 Å) but for excitation by impact of a fast He atom it occurs when the energy of the atom has values > 6000 eV and 2500 to 3000 eV respectively. With such a large difference in the energies of the electrons and the helium atoms at the maximum of the excitation function, the corresponding velocities of these particles are of similar orders of magnitude. In fact,

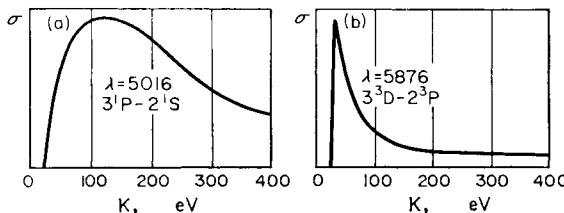


FIG. 109. Excitation functions of the singlet 5016 Å (a) and the triplet 5876 Å (b) helium lines for impact of an electron (according to Thieme [1218]).

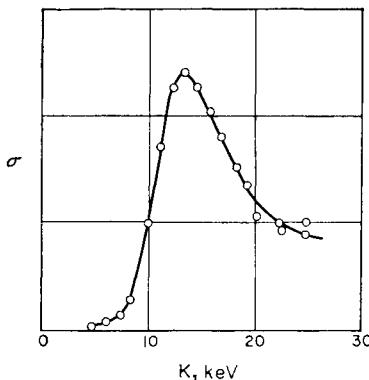


FIG. 110. Excitation function of the caesium ion Cs^+ line 3959.5 Å on collision of Cs^+ with a helium atom (according to Maurer [930]).

for the singlet line we have $v_e = 5.9 \times 10^8$ cm/sec and $v_{\text{He}} > 0.5 \times 10^8$ cm/sec, which differ by a factor of about ten; the same difference occurs for the triplet line, where $v_e = 3.2 \times 10^8$ cm/sec and $v_{\text{He}} = 0.4 \times 10^8$ cm/sec. A somewhat higher difference in velocities at the maximum of the excitation function is observed during the excitation of the Cs^+ ion lines by collisions of fast Cs^+ ions with helium atoms. According to Maurer's measurements [930] the maximum of the excitation function of the different lines occurs between 13.5 and 20.0 keV. Figure 110 shows the excitation function of the Cs^+ line 3959.5 Å, which is typical of this case. From the energy of the Cs^+ ions at the maximum we obtain the velocity of the

ions as 1.4×10^7 cm/sec. This value is more than ten times less than the corresponding electron velocity, which cannot be less than 2.8×10^8 cm/sec (corresponding to an electron energy of 23 eV).

Moreover, according to the measurements of Döpel [547], whose results are shown in Fig. 111, the maxima of the excitation functions of the helium singlet and triplet lines, on bombardment of helium by hydrogen atoms, occur when the velocities of the H atoms are greater than 3×10^8 cm/sec and are close to the velocities, 3.5×10^8 and 6.0×10^8 cm/sec, of the electrons corresponding to the maxima of the excitation functions of these lines for electron impact; thus the cross-sections for excitation of both lines by electron impact and H-atom impact are similar for similar particle velocities. A similar result was obtained by Hanle [718] for the

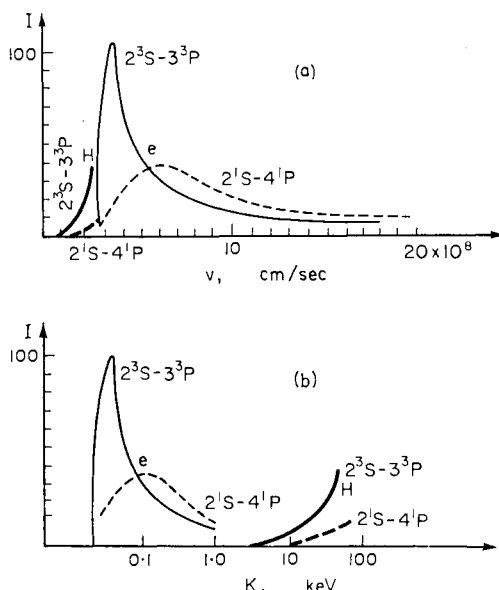


FIG. 111. Excitation functions for the helium singlet and triplet lines in the case of protons (H) and electrons (e) according to Döpel [547]. Velocity (a) and energy (b) of the exciting particles are plotted along the abscissa axis.

excitation of argon by H and D atoms. Figure 112a and b shows excitation functions for the argon line 4259 Å, in the case of impact by H and D atoms and by an electron, as a function of the energy (Fig. 112a) and velocity (Fig. 112b) of these particles (the ordinate scale is different for different particles). It is seen from Fig. 112b that the velocities of the different particles at the maxima of the corresponding excitation functions are very similar: 1.7×10^8 cm/sec for D atoms, 2.0×10^8 cm/sec for H atoms and

2.8×10^8 cm/sec for electrons. We should also mention that according to the measurements of Horie and Otsuka [778] the velocity of canal rays in hydrogen (calculated for H atoms or ions) at the maximum excitation of hydroxyl HO by impact of these particles is greater than 0.9×10^8

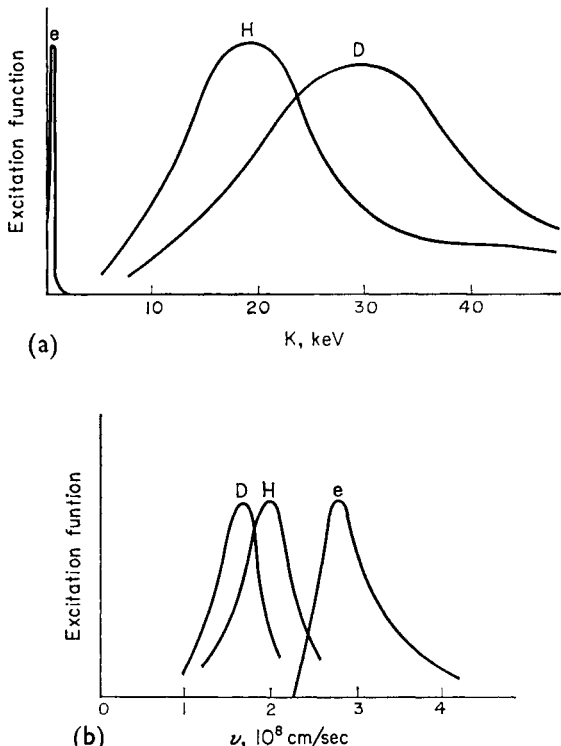


FIG. 112. Excitation of the argon line 4259 Å by impact of H and D atoms and of an electron (according to Hanle [718]).

cm/sec, whereas the electron velocity is 2.65×10^8 cm/sec. Owing to charge transfers (see below) at low energies of the electrons, protons and He^+ the spectra excited by them are considerably different; this does not occur at high energies [596a].

Ionization of Atoms and Molecules by Collisions with Fast Ions and Atoms

An energy dependence of the effective cross-section similar to that established in the excitation of gases by impact of heavy particles is also observed in the ionization of atoms and molecules by these particles. Here the minimum "ionization energy" is also usually much greater than K_{\min} (29.1). Thus the ionization of inert gases on their bombardment

with ions Li^+ , Na^+ , K^+ , Rb^+ and Cs^+ of the alkali metals becomes measurable only when the energy of the ions is 100 to 400 eV (the ionization potential being of the order of 10 to 20 eV) [369, 1247, 956a]. Comparison of these observed "critical ionization potentials" with the K_{\min} values calculated from formula (29.1) shows that the measured values are several times (from 2 to 20 times) larger than the corresponding K_{\min} values. With an increase in energy of the ions, the probability of ionization increases rapidly (see below). The same effect is observed for ionization of the inert gases by their own ions [1090]: the start of noticeable ionization of He, Ne and Ar is established when the energy of the ions is about 100 eV, i.e. when the energy is also several times larger than K_{\min} , which in this case is twice the ionization potential (since $m_i = m$). Typical curves for the dependence of the effective cross-section σ_i for ionization on the energy of the ions (the ionization function) are shown in Fig. 113 [1090].

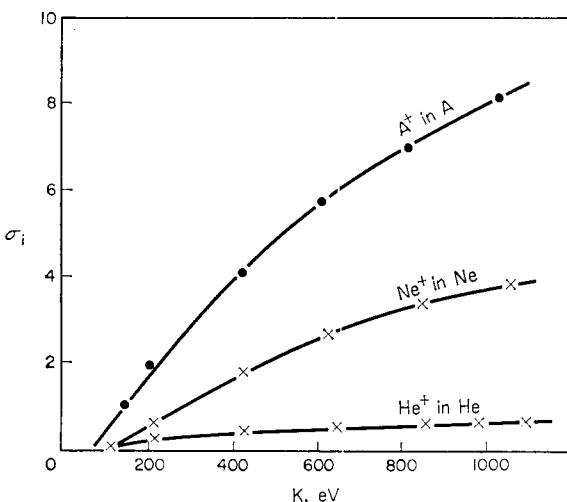


FIG. 113. Functions for the ionization of inert gases by their own ions (according to Rostagni [1090]).

Besides the ionization of inert gases by ion impacts, ionization by impacts of fast neutral atoms of these gases has been studied. In contrast with the case of ions, the minimum ionization energy observed on bombardment of the inert gases with their atoms is much closer to that calculated from formula (29.1). Thus, Varney [1247] studied the ionization of neon, argon, krypton and xenon by fast atoms of these gases and obtained for the energy at the start of perceptible ionization values which are on average only one and a half times greater than twice the ionization potentials of the corresponding gases. However, by using more sensitive

methods Horton and Millest [785] observed the start of ionization in helium when the energy of the fast He atoms was about 50 eV, which is almost exactly twice the ionization potential of helium ($2 \times 24.5 = 49$ eV), whereas Varney did not obtain marked ionization in helium even when the energy of the atoms was 400 eV (see, however [1248]); consequently it must be assumed that the actual minimum energies for ionization by impact of fast atoms in the case of Ne, Ar, Kr and Xe should be closer to twice the ionization potentials of the corresponding gases.

The ionization of inert-gas atoms by fast atoms of another gas has also been studied. It may be concluded from the available experimental data that the probability of ionization of an atom by impact of an atom of another sort is *less* than the probability of ionization of the gas by its own fast atoms. For example, Wayland's measurements [1271] show that the minimum energy for ionization by impacts of fast argon atoms in Ne, Kr and Xe is on average approximately three times greater than that calculated from formula (29.1). According to the measurements of this author for ionization in Ar (by Ar atoms), the minimum energy observed is only one and a half times greater than that calculated from (29.1).

Studies on the ionization of gases by impacts of ions or neutral atoms show the following type of dependence of the probable cross-section of ionization on the energy of the ionizing particles. Marked ionization is observed at an energy which is usually considerably greater than the minimum energy K_{\min} (29.1) at which the process would become possible according to conservation laws. With increase in energy of the ionizing particle, the ionization cross-section increases and becomes approximately equal to the cross-section for ionization by electron impact, i.e. some tenths of the gas-kinetic cross-section. It follows from data obtained from the study of the ionization of various gases by fast ions and atoms, and also from theoretical studies of ionization by impact of heavy particles (see below), that at a certain energy the ionization cross-section reaches a *maximum* and then decreases smoothly. In certain cases the maximum of the ionization cross-section corresponds to a velocity of the ionizing particle which is *close* to the velocity of the electron at the maximum of the ionization function of the gas for electron impact. As an example Fig. 114 [307] shows the cross sections for ionization of air by alpha-particles (curve α), by protons (curve p) and by electrons (e). Here the velocity of the ionizing particle is the abscissa, and the ordinate is the ionization cross-section σ (in cm^2) multiplied by the number $n_1 = 3.53 \times 10^{16} \text{ cm}^{-3}$ (see p. 469). It is seen from Fig. 114 that the maximum cross-sections for ionization of air by impact of an alpha-particle and of a proton correspond to similar velocities of these particles which are of the same order of magnitude (10^9 cm/sec) as the optimum electron velocity. It may be concluded from

this that the efficiency of ionization in the case considered is determined not by the energy but by the *velocity* of the ionizing particle. We should note the large difference in the energies corresponding to the maximum ionization cross-sections; the maximum cross-section for ionization by electrons corresponds to an electron energy of about 100 eV but the corresponding energies of the protons and alpha-particles are 1.3×10^6 and 1.8×10^6 eV. It also follows from Fig. 114 that in this case the maximum cross-section for electrons is 0.4, for protons 1.5, and for alpha-particles 3.5, times the gas-kinetic cross-section.

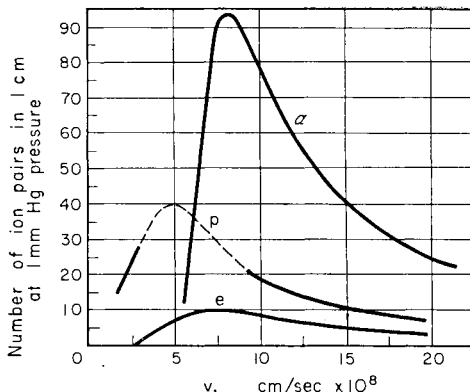


FIG. 114. Functions for the ionization of air by alpha-particles (α), by protons (p) and by electrons (e) (according to Engel and Steenbeck [307]).

This conclusion, that the efficiency of ionization is determined by the velocity (not the energy) of the ionizing particle and consequently does not depend appreciably on the mass of the particle, apparently refers only to ionization by elementary particles (and by H atoms) and cannot be extended to all other ions and atoms. The following data in particular support this. Studying ionization in argon and nitrogen by impacts of fast atoms of Ar and N respectively, Berry, Varney and Newberry [389] found that in the first case the maximum of the ionization function occurs when the energy of the Ar atoms is less than 900 eV and in the second case when the energy of the N atoms is about 2500 eV. These data show that the velocities of the Ar and N atoms at the maximum of the ionization function are $< 0.7 \times 10^7$ cm/sec (Ar) and 1.8×10^7 cm/sec (N) which differ by more than a factor of ten from the electron velocity of 4.2×10^8 cm/sec at $K_{\max} = 50$ eV. In just the same way, according to Frische's data [641], the maximum cross-section for ionization of argon by K^+ ions corresponds to an ion velocity of 1.4×10^7 cm/sec ($K = 4$ keV) which differs by more than a factor of ten from the electron velocity at the maximum of the corresponding ionization function for argon, 7.3×10^8 cm

sec^{-1} ($K_e = 150 \text{ eV}$). The maximum cross-section for ionization by electrons (10.3 cm^{-1}) is close to the maximum cross-section for ionization by K^+ ions (8.5 cm^{-1}). Similar maximum cross-sections for ionization are also observed in the ionization of neon by impact of a K^+ ion (2.5 cm^{-1}) and by impact of an electron (3.2 cm^{-1}).

Comparing these data with those given earlier on excitation by impact of fast ions and atoms we may conclude that the maximum of the function of excitation or ionization by impact of an alpha-particle, a proton or an atom H or D occurs when the velocity of the bombarding particle is close to the electron velocity corresponding to the maximum of the function of excitation or ionization by impact of an electron. As the electron shell of the bombarding particle becomes complicated the difference between the velocity of this particle and the velocity of the electron at the maximum of the corresponding functions of excitation and ionization becomes more and more marked, and the more complicated the electron shell of the bombarding particle the lower is the velocity of this particle compared with the electron velocity. Thus in the case of He the two velocities differ by no more than a factor of ten but in the case of N and Ar atoms and Cs^+ ions this difference is already greater than a factor of ten. This conclusion was drawn from very limited experimental material which is not sufficient to determine how general it is. However, it should be considered certain that both the position of the maximum of the excitation or ionization function and also the absolute probability of the corresponding process are determined with an accuracy of up to one to one and a half powers of ten by the *velocity* and not by the energy of the bombarding particle.

Mechanism of Excitation and Ionization by the Impact of Fast Ions and Atoms

The quantitative theory of inelastic collision of a fast ion with an atom or of an atom with an atom has as yet been inadequately developed. The problem of inelastic collision of an electron with an atom reduces to the problem of an atom with many electrons, but the problem of excitation or ionization of an atom by impact of an ion or neutral atom is in essence the problem of a diatomic molecule, with all the difficulties inherent in the calculations of this problem. Thus although the mechanism of inelastic collisions is quite clear qualitatively, the quantitative theory of this process is as imperfect as the theory of diatomic molecules.

We shall explain the basic features of the mechanism of inelastic collision by using as an example the excitation and ionization of a helium atom by the collision of two He atoms or of an He atom and an Li^+ ion. On the close approach of two He atoms or of an atom and an ion, two of the four $1s$ electrons of the system go over to the two-quantum state, since Pauli's principle must be satisfied, and consequently different states of the He_2 molecule or HeLi^+ ion arise, corresponding to the electronic configurations:

$1s^22s^2$, $1s^22s2p$ or $1s^22p^2$. Each of these states corresponds to a definite potential-energy curve, according to which the potential energy of the system changes with change in the inter-nuclear distance. A similar system of potential curves is obtained on the close approach of an excited or ionized helium atom and an atom (or Li^+ ion) in the ground electronic state. When the nuclei come near enough (in this example due to the energy of relative translational motion of the atoms or of the atom and the ion) the potential curves of one system may *intersect* the curves of another system (or approach sufficiently *close*) so that there is *energy resonance* of the corresponding states of the system. In the region of energy resonance, i.e. in the region of intersection (or close approach) of the potential curves of the different systems corresponding to the states $\text{He} + \text{He}(\text{Li}^+)$, $\text{He}' + \text{He}(\text{Li}^+)$ or $\text{He}^+ + \text{He}(\text{Li}^+)$, the Auger effect allows the system to pass from the initial state $\text{He} + \text{He}(\text{Li}^+)$ to the state $\text{He}' + \text{He}(\text{Li}^+)$ or to the state $\text{He}^+ + \text{He}(\text{Li}^+)$ (in the last case with the simultaneous loss of an electron) which is its final state.

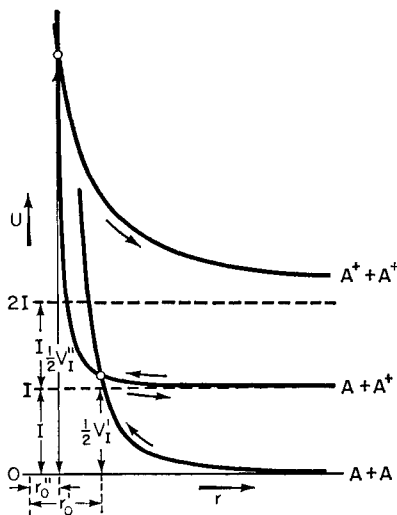


FIG. 115. Interpretation of the process of ionization of an A atom by impact of a fast A atom or A^+ ion (according to Weizel and Beeck [1274]).

In accordance with the mechanism described for inelastic collision the process of ionization on impact of a fast atom or ion may be depicted by using the potential curves in Fig. 115 [1274]. On the close approach of two A atoms the potential energy of the system increases according to the $\text{A} + \text{A}$ curve. At a certain distance r_0 the mutual potential energy of the A atoms becomes equal to the potential energy of the ion-atom system

(curve $A + A^+$). At the point of intersection (or close approach) of the two curves the system may pass from the state $A + A$ to the state $A + A^+$, with ionization of one of the atoms. Since the point of intersection must be close to the level $A + A^+$ (I), it follows that the measured minimum ionization energy will be close to the quantity determined by (29.1), i.e. equal to or only slightly greater than twice the ionization potential of the atom. As we have seen this actually takes place.

The ionization of an atom by an ion in Fig. 115 corresponds to the rise in the $A + A^+$ curve. However, owing to polarization interaction of the atom A with the ion A^+ this curve initially (at high r) scarcely departs from the asymptote $U = I$ and consequently its intersection with the hyperbolic curve $A^+ + A^+$ must occur at relatively low r (r_0''), i.e. at high energy. Therefore the corresponding minimum energy of ionization should be much greater than $2I$, which has also been established experimentally (for the ionization of inert gases by ions of the alkali metals and their own ions).⁽¹²⁾

It has already been noted that an accurate solution of the problem of inelastic collision of heavy particles reduces to solving the corresponding quantum-mechanical problem for a diatomic molecule, i.e. to solving an appropriate wave equation. An approximate solution of this problem was given by Massey and Smith [924b] for the proton–helium system. The calculation of these authors shows that the excitation cross-section becomes appreciable only when the energy of the bombarding proton is greater than a certain value which they conditionally call the “activation energy”. A similar result was obtained somewhat earlier by London [886] for the general case of the excitation of an atom or molecule by the impact of a fast ion.⁽¹³⁾

The solution of the problem of inelastic collision with a Born approximation shows that the effective cross-section of the process is appreciable only when the quantity $(k - k_{ij})r_0$, (where k and k_{ij} are the wave numbers before and after collision and r_0 is the minimum distance between the colliding particles and is approximately equal to the sum of their radii) is small in comparison with unity, i.e. $(k - k_{ij})^2 r_0^2 \ll 1$. If the kinetic energy of relative motion of the fast particle before collision is K' ($= \frac{1}{2}\mu v^2$, where μ is the reduced mass, v the velocity of the fast particle before impact) and the energy transferred to the excited (or ionized) particle is $\Delta E = E_j - E_i$, the wave numbers are

$$k = 2\pi/\lambda = (2\mu K')^{1/2}/\hbar$$

⁽¹²⁾ It might be attempted to use similar curves to give a qualitative explanation of the regularities established for the process of excitation by impact of an atom or ion; but as potential curves for neutral atoms are largely arbitrary, such an attempt is hardly reliable.

⁽¹³⁾ Bates and Griffing [354] have calculated functions for excitation and ionization of hydrogen atoms by impact of a proton and an H atom.

and

$$k_{ij} = 2\pi/\lambda_{ij} = [2\mu(K' - \Delta E)]^{1/2}/\hbar$$

(λ and λ_{ij} are the corresponding de Broglie wave lengths). Moreover, taking the energy K' to be large compared with ΔE , we may determine the difference $k - k_{ij}$ as approximately

$$k - k_{ij} = (\mu/2K')^{1/2}(\Delta E/\hbar)$$

so that

$$(k - k_{ij})^2 r_0^2 = \mu(\Delta E)^2 r_0^2 / 2\hbar^2 K' \ll 1.$$

We find from this inequality the limiting value for the energy K_{lim} of the bombarding particle (m is the mass of the particle) and the corresponding limiting velocity v_{lim} , namely

$$K_{lim} = \frac{1}{2}mv_{lim}^2 = m(\Delta E)^2 r_0^2 / 2\hbar^2 \quad (29.2)$$

and

$$v_{lim} = \Delta E r_0 / \hbar. \quad (29.3)$$

It follows from equations (29.2) and (29.3) that the limiting velocity of the bombarding particle does not depend on its mass or, in other words, particles of different mass but with the same velocity should have the same or a similar efficiency for exciting a given quantum transition (ΔE). This conclusion is in agreement with that reached earlier (p. 500) on the basis of the available experimental data, namely that the efficiency of impact is determined not by the energy of the bombarding particle but by its velocity.

It also follows from equation (29.2) that on excitation of a given level by particles with different masses but otherwise identical (for example, H and D atoms), then when the quantity $(\Delta E)^2 r_0^2$ remains constant, the lighter particle should have the higher efficiency. Accordingly the initial intensity of excitation of the argon line 4259 Å and the helium line 3888 Å in Hanle's experiments [718] on the excitation of these lines by impact of H atoms is approximately twice as much as for excitation by D atoms. In the same way, owing to the fact that the limiting energy is proportional to $(\Delta E)^2$, it must be expected that the collision partner whose excitation energy is the lower will be the more readily excited. Comparison with a large number of experimental data shows that this conclusion is supported in most cases [931]. For example, on bombarding helium with H and D atoms the helium lines become marked only when the energy of the fast particles is greater than 2 keV, whereas the lines of the more readily excited hydrogen have a high intensity even when the energy is below 500 eV. On bombarding helium with ions of lithium and sodium, the He lines are observed when the energy of the ions is below 1 keV, and the lines of Li^+ and Na^+ are observed only when the energy of the ions is more than 20 keV. The foregoing conclusion, however, is not borne out in the case where both

collision partners have an identical or similar excitation energy and consequently on the basis of (29.2) it might be expected that they would be excited with equal probability. As we have shown earlier (p. 493) on bombardment of helium with caesium ions the He lines with excitation energy close to the excitation energy of the Cs^+ lines are excited much more readily than the Cs^+ lines.

Comparison of formulae (29.2) and (29.3) with experimental data shows therefore that in most cases there is qualitative agreement between theory and experiment. We should add that according to London's calculations [886], and also the similar calculations of Stueckelberg [1192], the maximum cross-section for excitation on impact of a fast particle must be similar to the gas-kinetic cross-section. As we have seen, this result is also supported in the main by experiment.

It also follows from Stueckelberg's calculations that the cross-section for ionization by impact of a low-energy ion must be proportional to the quantity $(K - K_0)^{3/2}/K$, where K is the energy of the ion and K_0 is the energy corresponding to the point of intersection of the initial and final potential curves. Stueckelberg showed that this result is in good agreement with the experimental data of Nordmeyer [976] on the ionization of argon by impact of K^+ ions. For this case K_0 is 55 eV when $K_{\min} = 31$ eV, i.e. it is 1.8 times larger than K_{\min} .

In the same way as the collision of a fast positive ion or atom with an atom or molecule of a gas causes the ionization of the bombarded or bombarding particle with the splitting-off of an electron, so also a negative ion colliding with a particle may lose an electron and become neutral. This process may be of great interest for the kinetics of chemical reactions in electric discharge, since negative ions are usually negatively charged atoms (halide ions) or radicals (the ions HO^- , NH_2^- , etc.) and as a result of electron loss are converted into chemically active neutral atoms and radicals.

The process of splitting off an electron on collision of fast negative ions with molecules of different substances (neutralization) has been studied by Dukel'skii and coworkers [65, 66] for the cases of Na^- ions in helium and argon, K^- in helium, halide ions in all the inert gases, Te^- and Sb^- ions in helium and neon, etc., with ion energies from 300 to 2000 eV. It was shown that, in each case the cross-section for neutralization increases with the energy of the ion, and far from the ionization threshold it is from some cm^{-1} up to some tens of cm^{-1} . Measurements of the cross-section for neutralization of Na^- , K^- , O^- , Cl^- , HO^- and O_2^- ions in oxygen for ions of energy 720 eV gave a quantity of the order of 100 cm^{-1} .

The neutralization process was studied by Hasted [735, 736] for H^- on its collision with inert-gas atoms and by Simons and coworkers [963] for H^- on collisions with H_2 molecules. In the latter case it was found that

with decrease in energy of the H^- ion (from 400 eV) the cross-section of the process $H^- + H_2 = H + e + H_2$ decreases and is 1 cm^{-1} ($P = 0.02$), at $K_{H^-} = 7 \text{ eV}$, and is practically zero when K_{H^-} lies between 5 and 0 eV.

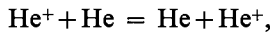
A theoretical calculation of the probability of neutralization of H^- ions on collision with He atoms has been carried out by Sida [1139] for ions with energy of about 20 keV. In agreement with experiment [735, 736], the calculated cross-section for the process $H^- + He = H + e + He$ increases with increase in energy of the ion.

There are also indications that atoms and molecules may be ionized by impact of negative ions. Thus according to Hasted's experiments [735, 736], H^- ions are capable of ionizing argon atoms (the process $H^- + Ar = Ar^+ + e + H^-$). Simons and coworkers [963] indicate that the process $H^- + H_2 = H^- + H_2^+ + e$ or the process $H^- + H_2 = H^- + H + H^+ + e$ is possible. According to the measurements of these authors, when the energy of the H^- ions is about 400 eV the cross-section for the process of ionization of hydrogen is 0.1 cm^{-1} .

Charge (Electron) Transfer Processes

From the point of view of chemical activation in electric discharge it is also extremely interesting to consider charge (electron) transfer processes, as a result of which new ions, radicals or atoms may be produced from some of the ions.

Studies on charge transfer make it necessary to distinguish between *symmetrical* processes between ions and atoms of the same gas, for example



and *asymmetrical* processes, for example



As far as it is possible to judge from the experimental results of Hasted [734] and Potter [1040] on charge exchange of the ions He^+ in helium, Ne^+ in neon and Ar^+ in argon and also from the data of Dillon *et al.* [539] on Kr^+ in krypton, Xe^+ in xenon and Hg^+ in mercury, then in accordance with their resonance character these processes take place for any energy of the colliding ion and atom and have a maximum probability when the energy is zero (or close to zero). Hasted's data in Fig. 116 show that when the energy of the ions is about 10 eV the effective cross-section of the process $He^+ + He = He + He^+$ is 40 cm^{-1} and when the energy is increased from 10 to 900 eV the cross-section decreases by approximately one half. Such a drop in cross-section also occurs for argon. At 10 eV the cross-section of the process $Ar^+ + Ar = Ar + Ar^+$ is 140 cm^{-1} . Figure 117 shows the theoretical cross-sections for symmetrical transfer in helium, $He^+ + He = He + He^+$ (in 10^{-16} cm^2 units), calculated by Gurnee and Magee [709a] (the continuous curve) and the experimental data of various authors [900] (points).

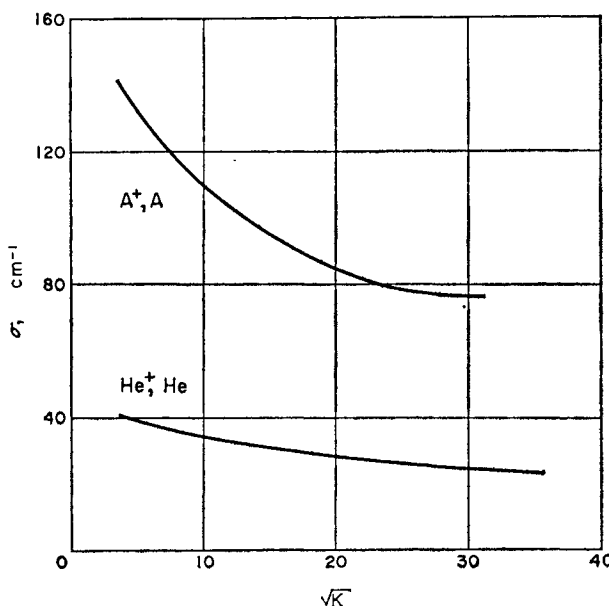


FIG. 116. Cross-sections for symmetrical charge transfer in helium and argon as functions of ion velocity (according to Hasted [734]).

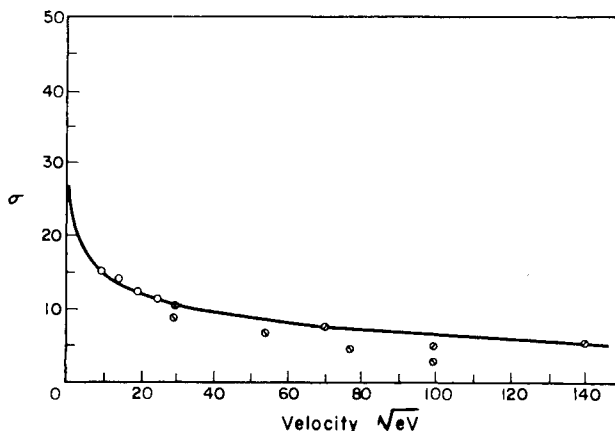


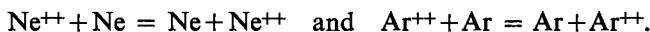
FIG. 117. Cross-section for symmetrical charge transfer in helium (in 10^{-16} cm^2 units) $\text{He}^+ + \text{He} \rightarrow \text{He} + \text{He}^+$; theoretical curve obtained by Gurnee and Magee [709a], points are the experimental data of various authors (according to Magee [900]).

A similar dependence of the cross-section for symmetrical charge transfer on ion energy is also observed for molecular ions. Thus according to Wolf's measurements [1309] the cross-section for the process $H_2^+ + H_2 = H_2 + H_2^+$ over the range of energy studied (64 to 1024 eV) increases with decrease in energy of the H_2^+ ions and at 64 eV is 31 cm^{-1} . This result is in agreement with the data obtained by Simons and co-workers [1140] who also detected a small increase in the transfer cross-section with decrease in H_2^+ energy, and for an energy of 4 eV obtained the cross-section 35.1 cm^{-1} . Similar results were recently obtained by Dillon *et al.* [539] for O_2 , NO , N_2 , CO and Cl_2 (and also for H_2). These last authors found that the transfer cross-section is the greater the smaller the difference between the interatomic distance in the molecule (X_2) and in the ion (X_2^+).

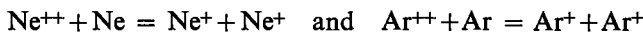
We should add that Dukel'skii and Zandberg [65] have also observed symmetrical charge transfer for the negative ion O_2^- in oxygen. For an ion energy of 720 eV they obtained 70 cm^{-1} for the cross-section. They compare this figure with the cross-section measured by them for symmetrical transfer in O_2^+ with the same ion energy, which is 175 cm^{-1} . It follows from these data that the transfer cross-section of O_2^+ is several times greater than that for O_2^- . However see [539].

Calculated cross-sections for charge transfer $H^+ + H = H + H^+$ (T. J. M. Boyd and A. Dalgarno, *Proc. Phys. Soc.*, **72**, 694, 1958) for an H atom in the ground and excited states, at a proton energy of several eV, are $4.4 \times 10^{-15} \text{ cm}^2$ and $4.4 \times 10^{-14} \text{ cm}^2$, respectively. Increase in the transfer cross-section with increasing excitation of the H atom is due to stronger interaction between the proton and excited atom.

In addition to symmetrical charge transfer connected with the transfer of one electron, cases are also observed of symmetrical transfer when two electrons are transferred from the atom to the ion. Such cases have been studied especially by Wolf [1308] in the cases of doubly-charged neon and argon ions,



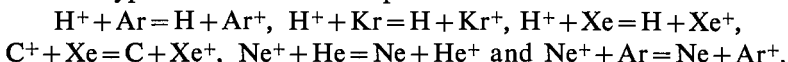
For an ion energy of 400 eV Wolf obtained the following effective transfer cross-sections: 11 cm^{-1} for neon and 35 cm^{-1} for argon. The asymmetrical transfer cross-sections of Ne^{2+} and Ar^{2+} ions, i.e. the cross-sections of the processes



for the same ion energy (400 eV) are much less and are $\frac{1}{2} \text{ cm}^{-1}$ for neon and 1 cm^{-1} for argon [327].

In all the cases studied of *asymmetrical transfer* the cross-section increases with increase in energy of the ion and at a certain energy reaches

a maximum and then decreases with further increase in energy. Figure 118 shows typical curves for the processes



It is seen from this figure that the maximum cross-sections for asymmetrical transfer also reach high values and differ little from the cross-sections for symmetrical transfer. Thus for the process $\text{H}^+ + \text{Kr} = \text{H} + \text{Kr}^+$ we have

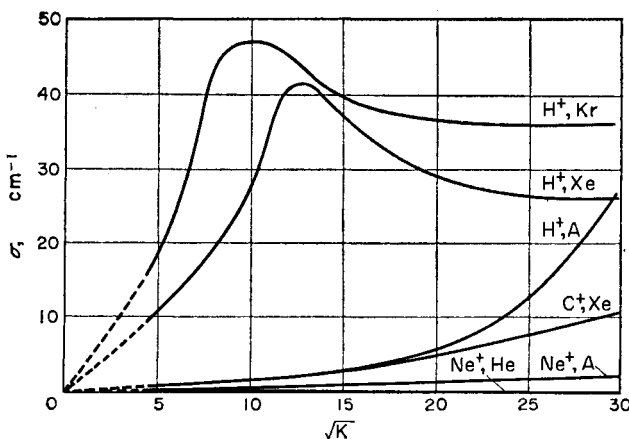


FIG. 118. Cross-sections for asymmetrical charge transfer as functions of ion velocity (according to Hasted [734]).

$\sigma_{\max} = 48 \text{ cm}^{-2}$ and for the process $\text{H}^+ + \text{Xe} = \text{H} + \text{Xe}^+$ we have $\sigma_{\max} = 42 \text{ cm}^{-2}$. Moreover it follows from Fig. 118 that the maximum cross-sections for the other processes shown by curves in the figure correspond to energies greater than 900 eV.⁽¹⁴⁾

Analysis of the available experimental data on charge transfer in atomic ions shows that the position of the maximum of the effective transfer cross-section is mainly determined by the difference in ionization potentials of the atoms taking part in the transfer and by the mass of the fast ion in the transfer reaction. This feature may be given a theoretical basis. Assuming that the limiting energy of the bombarding particle (ion) expressed by formula (29.2) is the same as that corresponding to the maximum probability for electron transfer, and also that the order of magnitude of r_0 varies little on passing from one ion-atom pair to another, it might be expected that the quantity $\sqrt{K_{\max}}$ (K_{\max} is the energy of the ion at the maximum transfer cross-section) will vary like the quantity $[\Delta I]\sqrt{m}$, where ΔI is the difference in the ionization potentials. Table 46 which

⁽¹⁴⁾ Dukel'skii and Zandberg [65] have observed asymmetrical charge transfer of the negative ions Na^- , K^- , O^- , Cl^- and HO^- in oxygen.

summarizes the data of Hasted [734] and other authors [924] shows that the expected correlation between K_{\max} and $|\Delta I|/\sqrt{m}$ does occur (see also [678 and 671a]). However see [678a].

TABLE 46

Relation between the energy of the ion at the maximum charge-transfer cross-section, the mass of the ion, and the difference in ionization potentials of the particles taking part in the exchange

Ion	Atom	ΔI , eV	$ \Delta I /\sqrt{m}$	$\sqrt{K_{\max}}$
H^+	K	- 0.41	0.41	10
H^+	Xe	+ 1.45	1.45	13
D^+	Xe	+ 1.45	2.05	20
H^+	Ar	- 2.16	2.16	29-34
C^+	Xe	- 0.86	2.98	40-55
D^+	Ar	- 2.16	3.06	50
H^+ [827]	He	-10.94	10.94	164
Ne^+	He	- 3.00	13.55	very high*
Ne^+	Ar	+ 5.78	26.0	very high*
K^+ [641]	Ar	-15.69	98.1	2000†

* The precise value of $\sqrt{K_{\max}}$ is not known, but is very high.

† In this line data for the process of ionization by ion impact, i.e. the process $K^+ + Ar = K^+ + Ar^+ + e$, are given for comparison. In this case ΔI is equal to the ionization potential of argon.

In contrast with the examples shown in Table 46, in the processes $O^+ + Ar = O + Ar^+$, $N^+ + Ar = N + Ar^+$ and also the process $O^+ + N_2 = O + N_2^+$ there is a different dependence of effective cross-section on ion energy, namely a more rapid increase in cross-section with energy of the ion (see also [353]). According to Hasted this "anomaly" may be connected with the presence of the metastable O^+ and N^+ ions. See also S. N. Ghosh, W. F. Sheridan, *J. Chem. Phys.* **27**, 1436 (1957) and G. G. Meisels, *J. Chem. Phys.*, **31**, 284 (1959). For charge transfer involving molecules Hasted assumes also that vibrational and rotational energy is involved in the energy exchange, resulting in a decrease in $|\Delta I|$ and consequently in an increase in the probability of transfer (see also [881]). Dissociation of molecules is also possible [671].

The dependence of the cross-section for the process $O^+ + N_2 = O + N_2^+$ ($\Delta I = -1.96$ eV) on K , the energy of the O^+ ion, is shown in Fig. 119. It is seen from this figure that for the minimum energy in the 6 to 900 keV range, $K = 6$ eV, the cross-section is 10 cm^{-2} . In contrast with this case the cross-section for the processes $Li^+, K^+ + H_2 = Li, K + H_2^+$ ($\Delta I = -10.01$ and -11.05 eV) is very small and in the energy range 200 to 1100 eV it is

on average 0.45 and 0.31 cm^{-1} respectively [1308] (see also [932] $\text{Na}^+ + \text{He} = \text{Na} + \text{He}^+$). The cross-section for the process $\text{Al}^+ + \text{H}_2 = \text{Al} + \text{H}_2^+$ ($\Delta I = -9.45 \text{ eV}$) reaches its maximum value of 4 cm^{-1} when $K = 9 \text{ keV}$ [1134].

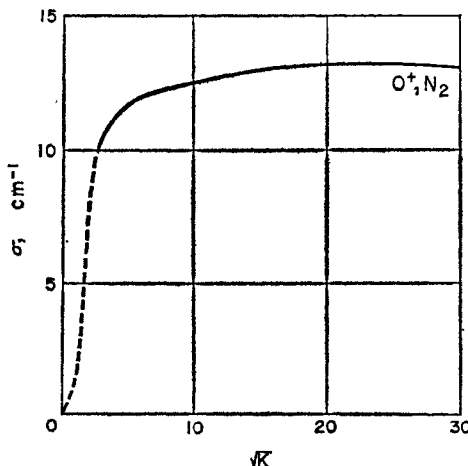


FIG. 119. Cross-section for the process $\text{O}^+ + \text{N}_2 = \text{O} + \text{N}_2^+$ as a function of the velocity of O^+ ions (according to Hasted [734])

We should mention further [1306] that the cross-section for the process $\text{N}_2^+ + \text{H}_2 = \text{N}_2 + \text{H}_2^+$ ($\Delta I = +0.14 \text{ eV}$) in the energy range 36 – 1000 eV increases from 16 cm^{-1} at 36 eV and reaches a maximum of 66 cm^{-1} at 200 eV . In the same temperature range the cross-section for the reverse process: ($\Delta I = -0.14 \text{ eV}$) increases from 20 cm^{-1} at 36 eV to 26 cm^{-1} at 1000 eV , passing through a rather low maximum. From these and other available data we may conclude that charge transfer involving molecules has in most cases the same qualitative features (Table 46) as for atomic ions.⁽¹⁵⁾ It has already been mentioned that an exception here is the case $\text{O}^+ + \text{N}_2 = \text{O} + \text{N}_2^+$.⁽¹⁶⁾

The charge-transfer processes for H^+ and H_2^+ ions in water vapour, and also for H^+ , H_2^+ and H_3^+ ions in hydrocarbons, should be mentioned. These cases should apparently be considered to be anomalous, if the correctness of their interpretation is confirmed. Thus Simons and co-workers [1141] have found a sharp increase in the cross-sections of the

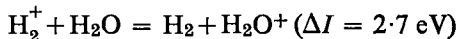
⁽¹⁵⁾ See also [1307] (charge transfer in the systems $\text{H}_2^+ + \text{Ar}$ and $\text{D}_2^+ + \text{Ar}$). For the theory of charge transfer in these and similar cases see [709a].

⁽¹⁶⁾ This does not exclude the possibility that the reason for the anomaly in this case is chemical interaction between the O^+ and N_2 : $\text{O}^+ + \text{N}_2 = \text{NO}^+ + \text{N}$ [1041].

processes



and



on decrease in the energy of the ions (in the first case the cross-section has a shallow minimum) and at 3 eV the cross-section of the first process reaches 122.8 cm^{-1} and that of the second reaches 229.7 cm^{-1} .

A similar behaviour of charge-transfer cross-section of hydrogen ions has also been established in the case of hydrocarbons by Muschlitz and Simons [964]. For example, in methane and ethane the transfer cross-section of a proton rapidly increases with decrease in proton energy and tends towards the values 170 to 200 cm^{-1} (CH_4) and 200 cm^{-1} (C_2H_6). In the opinion of these authors the high cross-sections they observed result from the fact that the energy change in the transfer process is close to zero owing to the participation of vibrational and rotational energy, and the consequence is a higher probability of transfer (see p. 509). However, both the unusually high values and also the behaviour of the cross-sections give rise to doubts of the accuracy of attributing these cross-sections to the transfer processes we have described. In the work of Simons and coworkers the occurrence of charge transfer was established by the appearance of slow ions, and consequently the possibility is not excluded that at low ion energies processes of transfer of a proton or H atom may have high probability, in accordance with mass-spectrometric data (see below, p. 517).

The strong dependence of charge-transfer probability on ΔI is also made evident by other data. For example, according to the data of Sherwin [1134] when the energy of B^+ ions is 6 to 24 keV the cross-section for the process $\text{B}^+ + \text{He} = \text{B} + \text{He}^+$, for which $\Delta I = -16.28 \text{ eV}$, is too small to measure; the cross-section for the process $\text{B}^{2+} + \text{He} = \text{B}^+ + \text{He}^+$, for which $\Delta I = +0.54 \text{ eV}$, is 6 to 11 cm^{-1} over the same energy range.

Moreover, according to Trittelwitz [1227] when the energy of the helium ions is $K = 4000 \text{ eV}$ the cross-section for the process



which takes place with an energy change of -20.04 eV , is 0.01 cm^{-1} whereas the cross-section for the process [1308]



for which $\Delta I = 3.0 \text{ eV}$, is 10 cm^{-1} for the same helium ion energy.

In addition to processes considered above, cases are also known where the sign of the charge of the ions changes on their collision with various particles. Thus, Dukel'skii and Fedorenko [69] have observed the conversion of I^- into I^+ ions during diffusion of the negative ions with energy 5 and 10 keV in neon, argon and krypton. The conversion of fast positive

ions into negative ions, for example Br^+ into Br^- ions, has also been observed [158, 159]. Negative ions are formed as a result of electron capture when a positive ion passes close to a metallic surface and also when positive ions collide with molecules [273a].

Dissociation of Molecules by the Impact of Fast Ions

When a molecule goes into an unstable electronic state on collision with a fast atom or ion, the result of the collision will be dissociation of the molecule into fragments (atoms, radicals or ions). Molecular dissociation into neutral particles by the impact of fast atoms or ions has not been studied systematically and must be considered as practically unexplored. Here we shall just mention the work of Leipunskii and Shekhter who studied the effect of the fast ions Li^+ , Na^+ and K^+ on hydrogen [171] and the effect of K^+ ions on nitrogen [289]. These authors observed a pressure drop in the pure gases when the ion energy was greater than a limiting value peculiar to each type of ion, and they connected this with the adsorption of atoms, formed by dissociation of H_2 or N_2 molecules as a result of ion impact, on the glass walls which were cooled with liquid air. The limiting ion energies measured were: 80 (Li^+), 160 (Na^+) and 260 (K^+) eV. The quantity E calculated from these values using formula (29.1) is close to the excitation energy of the H_2 molecule⁽¹⁷⁾ (for Na^+ and K^+ ions, where the measurements are more reliable) and consequently these authors conclude that ion impact in hydrogen gives rise to excited H_2 molecules which then dissociate into atoms. In nitrogen the limiting energy of potassium ions at which the pressure drop is first observed is 20 to 30 eV and on the basis of (29.1) $E = 8$ to 12 eV, which is close both to the excitation energy and to the heat of dissociation of the N_2 molecule.⁽¹⁸⁾

However, a series of difficulties arise from the hypothesis of excitation of the H_2 molecule by ion impact with subsequent dissociation. Actually since the minimum energy for dissociation of an H_2 molecule into normal and excited atoms, namely 14.6 eV, is greater than the energy which the Na^+ or K^+ ion can communicate to the H_2 molecule (12.8 and 12.7 eV), only dissociation into two normal H atoms is possible. However, since this process may take place only as a result of excitation of the ${}^3\Sigma_u$ level (see Fig. 94), i.e. as a result of the forbidden transition ${}^1\Sigma_g \rightarrow {}^3\Sigma_u$, its probability must be low. Meanwhile according to Shekhter's estimate

⁽¹⁷⁾ The E values calculated are: 12.8 eV for Na^+ ions, 12.7 eV for K^+ ions and 17.8 eV for Li^+ ions. The first two values are close to the vertical excitation potentials of the levels ${}^3\Sigma_u^+$ (10 eV), ${}^1\Sigma_u^+$ (12 eV), ${}^3\Sigma_g^+$ (12.5 eV) and ${}^1\Pi_u$ (13 eV).

⁽¹⁸⁾ In nitrogen the levels with an excitation energy close to 8 to 12 eV are ${}^3\Sigma_u^+$ (6.1 eV), ${}^3\Pi_g$ (7.3 eV), ${}^1\Pi_u$ (8.5 eV) and ${}^3\Pi_u$ (11.0 eV). $D_{\text{N}_2} = 9.76$ eV.

there is approximately one dissociating H_2 molecule for each ion impact. Consequently excitation of H_2 must be considered to be excluded. The ionization of an H_2 molecule by ion impact, or the formation of an H_2^+ ion as a result of charge transfer, is also of low probability. In fact, according to the measurements of Frische [641], ionization of hydrogen by K^+ ions becomes appreciable only when the energy of the ions is greater than 1600 eV. The cross-section for the transfer process $K^+ + H_2 = K + H_2^+$, according to Wolf [1308], does not exceed 0.3 cm^{-1} for 200 to 1100 eV K^+ ions, i.e. it is at least 100 times smaller than the gas-kinetic cross-section. For this reason the nature of the activation of hydrogen by ion impact in Leipunskii and Shekhter's experiments must be considered to be open to question. The possibility is not ruled out that the hydrogen pressure drop observed by these authors was a result of some secondary processes.

Similar difficulties arise in the activation of nitrogen by K^+ ion impact, although here the hypothesis regarding the excitation, dissociation or charge transfer is not as improbable as in the hydrogen case, since according to Shekhter's calculations there is only one dissociating N_2 molecule for a hundred K^+ ion impacts.

Shekhter and coworkers [195] have also studied the synthesis of ammonia by bombarding an H_2 and N_2 mixture with Li^+ , Na^+ , K^+ and Cs^+ ions. According to their data the formation of ammonia becomes appreciable at the following minimum values for the energy of the ions: 26 ± 2 eV (Li^+), 38 ± 2 eV (Na^+), 45 ± 5 eV (K^+) and 127 ± 1 eV (Cs^+). Using formula (29·1) to calculate the upper limit for the energy transferred on impact we find 21, 21, 19 and 22 eV respectively. In the opinion of these authors the primary act of activation in this case is the formation of an ionized nitrogen molecule (ionization potential 15·6 eV). This conclusion is supported by mass-spectroscopic data, according to which an N_2H^+ ion is formed as the primary product of the interaction of hydrogen and nitrogen during electron bombardment of a mixture of H_2 and N_2 (see below, p. 533 [39]).

Thus the possibility of a gas molecule dissociating by fast ion impact is not substantiated experimentally for these energies of the alkali-element ions. However, the dissociation of molecular ions on collision with gas molecules is a well-established fact for sufficiently high ion energy. It may be concluded from this that the dissociation of molecules by fast ion impact requires considerably higher ion energies than those used in the experiments of Shekhter and his coworkers.

The decomposition of ions is most frequently observed when the gas pressure in the analyser of a mass spectrometer is increased, and it is detected by the appearance in the mass spectrum of peaks corresponding to ions with apparently non-integral (fractional) masses. If it is assumed that the ion velocity before and after decomposition remains the same then

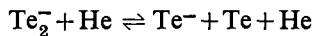
the apparent mass M^* is determined by the formula

$$M^* = M^2/M_0 \quad (29.4)$$

(M is the mass of the new ion appearing in the decomposition, M_0 is the mass of the ion before decomposition.) The fact that the mass M^* is fractional actually follows from this formula.

Thus Kupriyanov [158] has observed fractional peaks in the mass spectra of many substances (CO, CO₂, C₂H₂, C₂H₄, CH₄, CCl₄, CH₃Cl, CH₂Cl₂, etc.). He showed that the relative intensity of these peaks increases approximately proportionally to the gas pressure, which is an indication of the role of collisions in the formation process of the new ions. In different cases for an ion energy of 2500 eV the cross-sections of dissociation lie in the range 0.15 to 5 cm⁻¹ and decrease with decrease in ion energy, tending to zero at a threshold energy of 300 to 800 eV. It has also been established that the dissociation cross-section is a function of the energy of the electrons in the ionization chamber of the mass spectrometer; consequently we may conclude that in the dissociation of the primary ion its excitation state is extremely important [243]. This influence of electron energy on dissociation of the ion was also established by Kolotyrkin [118]; he found that with an electron energy of 100 to 60 eV the cross-section of the process CH⁺+CH₄=C⁺+H+CH₄ is 28 to 21 cm⁻¹ and increases a hundredfold on decreasing the electron energy to 25 eV.

Dukel'skii and Zandberg [67] also observed the dissociation of various negative ions on collision with helium and argon atoms. In their experiments the energy of the ions was 300 to 950 eV. A dissociation threshold was observed for helium. For example, the process



has a threshold at about 300 eV and according to (29.1) this corresponds to a threshold energy of relative motion of the Te₂⁻ ion and the He atom of $E=4.6$ eV. Dukel'skii and Zandberg consider this figure to be the upper limit for the energy of dissociation of the Te₂⁻ ion into Te⁻ and Te.

Along with dissociation yielding ions of the same charge sign as that of primary ions, oppositely charged ions are also often observed in ion-molecular collisions. See, for example, V. M. Dukel'skii and N. V. Fedorenko, *J. Exp. Theor. Phys.* **29**, 473, (1955), [159], C. E. Melton, *J. Chem. Phys.*, **28**, 359, (1958).

Study of the excitation and ionization of molecules by ion impact leads to the conclusion that these impacts are of relatively low efficiency when the energies of the ions are those usual in electric discharge (tens of electron-volts). But at these energies the cross-section for excitation or ionization by electron impact is close to the maximum; consequently it must be

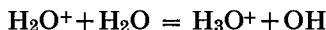
considered that, in molecular activation in electric discharge, ion impacts play only a secondary role and *the main activating factor is the fast electron impact.*

Electron impacts give rise in the discharge zone to different types of active particles: excited molecules and atoms,⁽¹⁹⁾ free radicals formed as a result of molecular dissociation, and ions. The role of excited atoms and molecules in chemical reactions is evident from photochemical data, especially from the phenomenon of photochemical sensitization. Atoms and free radicals are the normal active centres of chemical reactions. As a rule most ions in an electric discharge in simple gases are singly-charged molecular ions such as H_2^+ , N_2^+ , O_2^+ and the like, i.e. ions which have an unpaired electron and are therefore radical *ions*. Electric charge should impart to ions a particularly high chemical activity (see below, p. 518).

As an example of the particularly high chemical activity of an ion (however, in this case not a molecular but an atomic ion) we shall consider the reaction of the O^+ ion with a nitrogen molecule, $O^+ + N_2 = NO^+ + N$, which was observed by Potter [1041] in a mass-spectroscopic investigation of ions in air. According to his data the rate constant for this reaction at $400^{\circ}K$ is $1.0 \times 10^{-8} \text{ cm}^3 \text{ sec}^{-1}$; this is some ten times greater than that calculated from the number of gas-kinetic collisions. It may be concluded from this that the activation energy of this reaction, which has a positive heat effect of 25.3 kcal, should be zero. It is interesting to compare this reaction with the similar reaction between a neutral O atom and an N_2 molecule, $O + N_2 = NO + N$, which has an activation energy of 68 kcal⁽²⁰⁾ according to Zel'dovich [79].

Processes Connected with Proton or H Atom Transfer

The high activity of ions is particularly evident in the readiness with which they enter into chemical reaction with different molecules. Thus the molecular ion H_2O^+ readily reacts with water molecules, and this is detected by the appearance of a secondary product—the hydroxonium ion, H_3O^+ , in relative concentrations (H_3O^+ concentrations referred to H_2O^+ concentration) which increase in proportion to the water-vapour pressure in the chamber of the mass spectrometer (Fig. 120, curve 3) [256]. This reaction proceeds according to the scheme



⁽¹⁹⁾ In addition to the usual excited particles of short life there also arise metastable particles (see for example [619]), which should play a particularly important role in the chemical processes in the discharge zone.

⁽²⁰⁾ This figure cannot be precise since it is less than the negative heat of the reaction considered (75 kcal at $0^{\circ}K$).

and does not require an activation energy. As a result a "valence-saturated" ion H_3O^+ and a radical are formed.⁽²¹⁾

Figure 120 also shows the ratios of the number of propyl ions C_3H_7^+ , formed by bombarding propylene C_3H_6 with electrons, to the number of primary C_3H_6^+ ions (curve 1), and of the number of CH_5^+ ions to the number of primary CH_4^+ ions formed in methane (curve 2) as a function of the pressure of propylene and methane, respectively. It is seen from this figure that the straight lines obtained do not pass through the coordinate origin;

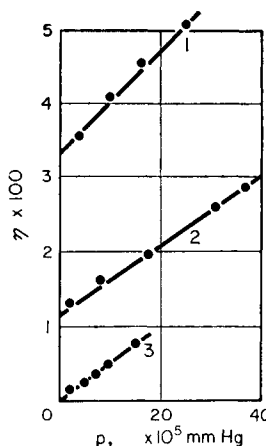
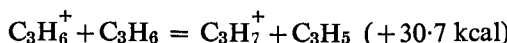


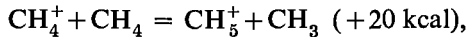
FIG. 120. The dependence of the yield η of the ions H_3O^+ (3), C_3H_7^+ (1) and CH_5^+ (2), formed in the ionization chamber of a mass spectrometer, on the pressure of H_2O , C_3H_6 and CH_4 respectively (according to Tal'roze and Lyubimova [256]).

this results from the presence of C^{13} isotopes in natural propylene and methane. In fact the intercepts on the ordinate axis correspond almost exactly to the relative content of isotopic molecules $\text{C}^{13}\text{C}^{12}_2\text{H}_6$ in natural propylene, 3.3 per cent, and the relative content of C^{13}H_4 molecules in natural methane, 1.1 per cent. In this way, by introducing a correction for the isotopic composition of carbon, we find in these cases also a proportionality to the pressure of the appropriate gas and consequently the observed "heavy" ions, similar to the hydroxonium ions, are formed as a result of the processes



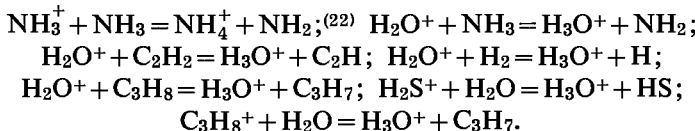
(21) It follows from the ease of reaction between the H_2O^+ ion and an H_2O molecule that the reaction has a positive heat effect, i.e. that the bond between the proton and the water molecule in the H_3O^+ ion must be stronger than the bond between the proton and hydroxyl in the H_2O^+ ion. From the ionization potential of the water molecule, which is 12.7 eV, we obtain 6.1 eV for the heat effect of the process $\text{H}^+ + \text{OH} = \text{H}_2\text{O}^+$ and consequently the energy of proton abstraction from the H_3O^+ ion must be more than 6.1 eV; similarly, for the energy of the process $\text{H} + \text{H}_2\text{O}^+ = \text{H}_3\text{O}^+$ we obtain a figure more than 5.2 eV. According to Tal'roze and Frankevich's measurements [257] the energy of proton abstraction from the H_3O^+ ion (the proton affinity of water) is 7.33 ± 0.15 eV.

and



i.e. processes of disproportionation connected with transfer of a proton or an H atom.

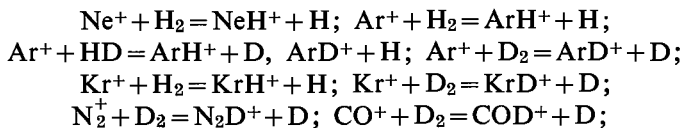
Tal'roze and Frankevich [257] also established the following similar processes:



Although the first of these processes, like the three illustrated above, may involve either proton transfer or H atom transfer, so that we do not know which of these transfers actually takes place, the remaining processes give an unambiguous answer to this problem. Thus all processes with H_2O^+ ions clearly involve a transfer of an H atom to the H_2O^+ ion⁽²³⁾ and the last two processes, which involve H_2O molecules, result in a transfer of a proton to an H_2O molecule. Thus both transfers are observed. See, for example [257].

The occurrence of these processes in the ionization chamber of a mass spectrometer for pressures of the order 10^{-5} to 10^{-4} mm Hg and with practically zero velocities of the colliding particles is evidence that their probability must be close to unity. This conclusion is also supported by the fact that Tal'roze and his coworkers failed to detect the endothermic process $\text{C}_2\text{H}_4^+ + \text{C}_2\text{H}_4 = \text{C}_2\text{H}_5^+ + \text{C}_2\text{H}_3 - 0.35 \text{ eV}$, whereas the similar exothermic processes for propylene C_3H_6 and isobutylene C_4H_8 were easily detected [256, 257].

The readiness of transfer of both an H atom and a proton is also evident from the data of Stevenson and Schissler [1186, 1111] (see also [710] and F. W. Lampe and F. H. Field, *J. Amer. Chem. Soc.*, **79**, 4244, (1957)). Stevenson and Schissler give the results of measurements of the rate constants for reactions involving H and D atom transfer:



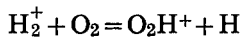
⁽²²⁾ It has recently been suggested that this process may play a part in the radiolysis of gaseous ammonia [1322]. See also [1115a].

⁽²³⁾ The possibility of H atom transfer was established earlier [39] for the reactions $\text{N}_2^+ + \text{H}_2 = \text{N}_2\text{H}^+ + \text{H}$ and $\text{CO}^+ + \text{H}_2 = \text{COH}^+ + \text{H}$ by showing that the appearance potentials for N_2H^+ and COH^+ ions are the same as those for N_2^+ and CO^+ ions respectively.

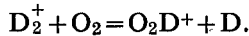
the reactions



and also reactions involving proton and deuteron transfer



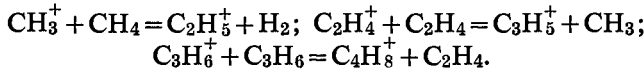
and



The rate constants they measured for these reactions vary from 0.3 to $11.1 \times 10^{-9} \text{ cm}^3 \text{ molecule}^{-1} \text{ sec}^{-2}$, and it follows that the reactions listed take place on practically every collision of an ion with a molecule.⁽²⁴⁾ See also [609], [1186'], [F. W. Lampe, F. H. Field and J. L. Franklin, *J. Amer. Chem. Soc.*, **79**, 6132 (1957)].

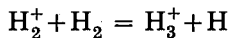
In this respect processes connected with H(D) atom or proton (deuteron) transfer are in sharp contrast with the processes of charge transfer for low ion energy which have a high probability only in the case of symmetrical transfer (see Table 46).

In addition to processes connected with transfer of an H atom or a proton, Schissler and Stevenson [1111] discovered and investigated the more complex processes of formation and breaking of C—C bonds. In particular the following processes are of this type:



According to their measurements these processes, like the processes of transfer of an H atom or a proton, often take place with an increased cross-section (compared with the gas-kinetic cross-section). A distinctive feature of these processes is the increase in cross-section (or rate constant) on decreasing the energy of the ions involved. It is very important to note that the first of the above processes, the process $\text{CH}_3^+ + \text{CH}_4 = \text{C}_2\text{H}_5^+ + \text{H}_2$, with cross-section $165 \times 10^{-18} \text{ cm}^2$ for a CH^+ ion energy $K = 0.1 \text{ eV}$, i.e. much greater than the gas-kinetic cross-section, does not involve a radical ion, like most of the studied interaction processes of ions with molecules, but a "valence-less" ion, CH_3^+ . It must be concluded from the high rate of this process that the main cause of the high chemical activity of ions is the presence of an electric charge. Other conditions being equal, ion radicals and "valence-less" ions seem to react at the same rates.

The high probability of processes connected with H atom or proton transfer may also be supported by a calculation of the rate constant for the reaction



⁽²⁴⁾ The role of processes of this type in radiolytic reactions has been pointed out by Meisels, Hamill and Williams [948] and also by Tal'roze [256a].

using the activated complex method (assuming that the interaction of H_2^+ and H_2 is based on polarization of the H_2 molecule in the field of the H_2^+ ion [589]). In accordance with mass-spectrometric data it is found from this calculation that the rate constant is $k = 10^{-9} \text{ cm}^3 \text{ sec}^{-1}$ (the transmission coefficient is taken as $\frac{1}{2}$), which is close to that calculated from the formula

$$k = 2d^2(2\pi RT/M)^{1/2},$$

from which $k = 0.4 \times 10^{-9} \text{ cm}^3 \text{ sec}^{-1}$ for a gas-kinetic diameter $d = 2.3 \times 10^{-8} \text{ cm}$ and $T = 290^\circ\text{K}$. See further G. Gioumonsis, D. P. Stevenson, *J. Chem. Phys.*, **29**, 294 (1958).

As was mentioned there are also many cases of ions dissociating on collision with molecules; in this the excitation of ions plays an important role [948b, 948a], [G. G. Meisels, *J. Chem. Phys.*, **31**, 284 (1959)]. For the excitation of ions see [642b, 642a, 948c, 1085a].

§30. Types of Electrical Discharge

Silent Discharge. Spark Discharge

The effect of an electric discharge on chemical substances depends on the nature of the discharge, which is determined in the first instance by the potential difference, the pressure in the discharge zone, and the current density. We may distinguish three basic types of electric discharge: silent, glow and arc discharge. Figure 121 shows schematically the regions of existence of these basic types of discharge. Here the ratio of the pressure

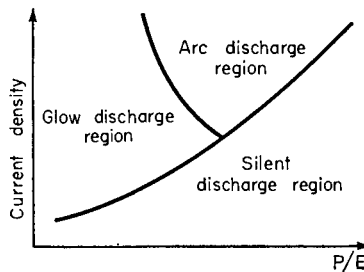


FIG. 121. The regions of existence of the basic types of electric discharge. The ratio of gas pressure to electric field strength is plotted along the abscissa axis.

in the discharge zone to the electric field strength is plotted along the abscissa axis and the discharge-current density along the ordinate axis. One type of discharge turns into another on varying these parameters. *Silent discharge*, usually observed for pressure close to atmospheric pressure and for relatively high potential differences between the electrodes, is a self-contained discharge resulting from the conductivity of the gas due to

its residual ionization. Accordingly silent discharge is characterized by a low current density and the absence of space charge effects related to it.

With the increase in potential difference the current density increases and at a certain potential difference a particular type of silent discharge called *corona discharge* appears. Corona discharge is particularly readily started in the case of a non-homogeneous electric field, for example that arising from a highly-curved surface of one or both electrodes. In this case, in the region where the field is least homogeneous, i.e. close to the electrode with a small radius of curvature, a glowing layer is observed, the so-called corona layer or *corona*. Impact ionization of the gas takes place in the corona and accounts for the self-contained nature of the corona discharge; it does not occur in the discharge region outside the corona (the outer region of the corona discharge). When only one electrode has a corona only ions of one sign fall into the outer discharge region and its conductivity is unipolar. The intensity of the current in the corona discharge is determined by the potential difference of the electrodes. Estimation of the energy of the positive ions in the corona gives a figure about 100 eV [1110].

When the current intensity is sufficiently high the corona discharge turns into a *spark discharge*. A characteristic feature of the latter is its discontinuity even when the discharge is supplied by a constant voltage. The reason for the discontinuity of a spark discharge is that after its appearance the resistance of the discharge gap falls sharply and consequently there is a redistribution of potential which leads to a decrease in the potential difference between the electrodes, which becomes insufficient to support discharge. The discharge is quenched; but after the discharge has stopped, the voltage between the electrodes begins to increase again, and this leads to the appearance of a spark discharge when the voltage reaches a value sufficient for breakdown of the discharge gap (the disruptive voltage). This process is then periodically repeated.

When a capacity is included in parallel with the discharge gap, the time interval between two consecutive sparks is increased. In addition the intensity of the spark, in particular the discharge-current density, also increases. Such a discharge is called a *condensed spark discharge*.

Owing to the high pressures and low temperatures, silent and corona discharges particularly favour the occurrence of chemical reactions of polymerization or, in general, processes in which the reaction products have high molecular weight compared with the initial substances. The simplest reaction of this type is the formation of ozone. The technical method of producing ozone is based on the use of a silent discharge taking place in special discharge tubes—ozonizers. One of the most frequently used types of ozonizer is the Siemens tube shown in Fig. 122. Usually this consists of two coaxial glass tubes which are sealed one within the other and have each one conducting surface: one surrounds the wide

tube and the other is inside the narrow tube. To these surfaces is connected a high (alternating) voltage sufficient to support silent discharge in the gap between the tubes. By passing oxygen (or air) through this gap ozone is obtained in the exit gas.

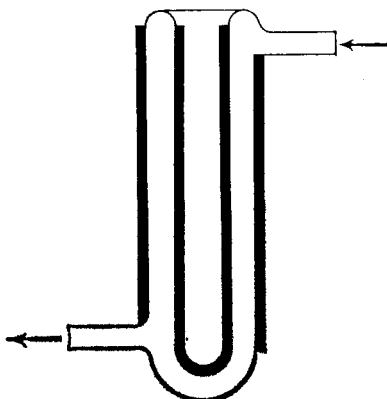


FIG. 122. Siemens ozonizer.

Owing to the high voltage and high current density in the condensed spark channel this type of discharge is particularly suitable for carrying out extensive dissociation of molecules requiring large amounts of energy. For example, condensed discharge gives particularly high yields of atomic nitrogen as a result of dissociation of N_2 molecules which are among the most stable molecules.

Glow Discharge

This is usually observed at pressures of some centimetres of mercury and below, although under definite conditions, in particular by cooling the cathode, this type of discharge may be obtained at atmospheric pressure. A peculiar distribution of luminescence in the gap between the electrodes is characteristic of glow discharge; this reflects the corresponding potential distribution. A typical illustration of the distribution of luminescence and potential in glow discharge is shown in Fig. 123. This distribution results from the following discharge mechanism. By impacts of fast ions electrons are freed from the cathode, and are accelerated in the strong field close to the cathode (the cathode potential drop). This field results from an electrical double layer formed by the negative charge of the cathode and the space charge of the positive ions. The accelerated electrons become capable of exciting gas molecules on collision. As a result there appears a glow in the form of a fine sheath (the cathode glow) separated from the cathode by a dark layer (the Aston dark space) and passing into

a weakly-glowing layer (the cathode dark space). The Aston dark space, the cathode glow and the cathode dark space occupy the region of the cathode potential fall, which is usually 300 V [1173]. This region is adjacent to the region of negative or glow luminescence which has a high luminosity. It is assumed that in this region there is recombination of positive

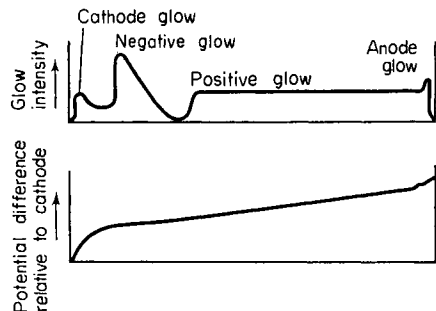


FIG. 123. Distribution of glow and potential in glow discharge.

ions and electrons and also excitation of gas molecules, and this gives rise to the high luminosity of negative glow. In the spectrum of the latter the predominant bands are those belonging to ionized molecules (for example, N_2^+ , CO^+ , O_2^+ bands, etc.) and this is evidence of the high energy of the bombarding electrons.

Of the three possible mechanisms for recombination of positive ions and electrons



and



the most significant under discharge conditions appears to be (3) (see p. 491). In fact, calculation of the rate constant for the radiation recombination (1) gives a figure of the order $10^{-12} \text{ cm}^3 \text{ sec}^{-1}$ [351] which is 3 to 6 powers of ten less than the experimental values. For pressures near atmospheric the ternary collision process (2) may have a much higher probability (compared with that of the radiation recombination) and when $p = 1 \text{ atm}$. its rate constant is estimated as about $10^{-10} \text{ cm}^3 \text{ sec}^{-1}$.⁽²⁵⁾ However, since the pressure in a discharge is often much less than atmospheric and the concentration of molecular ions is considerable [784] process (3) must predominate [401]. According to Richardson's measurements [1072] the rate constant for this process in the case $e + \text{Xe}_2^+ = \text{Xe} + \text{Xe}'$ is about $10^{-6} \text{ cm}^3 \text{ sec}^{-1}$.

(25) The cross-section of the reverse process in the case of $\text{He}' + \text{Ar} = \text{He} + \text{Ar}^+ + e$ is $1 \times 10^{-15} \text{ cm}^2$ and for the process $\text{Ne}' + \text{Ar} = \text{Ne} + \text{Ar}^+ + e$ is $3 \times 10^{-16} \text{ cm}^2$ [400].

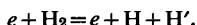
In the negative glow region the potential gradient decreases sharply, sometimes becoming negative; this is a result of the diffusion of slow electrons, which leave the ions behind owing to a high diffusion coefficient. The absence of fast electrons at the edge of the negative glow region follows both from the occurrence of a potential gradient minimum and from the fact that after the negative glow there is a dark space (the Faraday dark space), in which the electrons have such a low energy that they cannot excite the gas molecules. In the Faraday dark space the potential gradient increases continuously, and as a result the electrons gradually accumulate energy, and on passing into the positive glow region adjacent to the Faraday space are again capable of exciting a gas glow. The length of the positive glow column is determined exclusively by the length of the tube, in contrast with the extents of the region of the cathode potential fall, the negative glow and the Faraday dark space, which are dependent on the gas pressure in the discharge tube. A positive glow column of any length may be obtained by increasing the separation of the electrodes. In the positive glow, which extends practically up to the anode, the potential gradient is constant and is usually a few volts per mm or per cm. In the positive-glow spectrum the predominant bands are those of neutral molecules. Figure 124 shows the glow-discharge spectrum in hydrogen (in the presence of mercury vapour), taken in such a way that the transition region from Faraday dark space to the positive glow was projected on to the spectrograph slit [611]. The isolated lines in this figure are the green mercury line at 5461 Å (on the right, excitation potential 7.7 V), the yellow mercury lines at 5790 and 5770 Å (excitation potential 8.8 V) and the H_{α} hydrogen line at 6563 Å (on the left, excitation potential 12.0 V); the other lines belong mainly to the line spectrum of H_2 . It is seen from Fig. 124 that with penetration into the positive-glow region (from top to bottom) the electrons are able to excite increasingly less-excitable spectra.⁽²⁶⁾ This is clear evidence that in the Faraday dark space the electrons have small energy, as we have already noted.

The positive glow is usually a uniform column of glowing gas. However, at definite pressures and current densities the positive column decomposes into separate *layers* or *strata* separated by dark intervals of equal size.

⁽²⁶⁾ In contrast with the mercury lines Fig. 124 which have constant intensity along their length, the H_{α} line which appears at a potential of 12.0 V according to Finkelnburg, Lau and Reichenheim [611] is sharply intensified at 16.3 V. From the fact that the difference $16.3 - 12.0 = 4.3$ V is almost exactly equal to the dissociation energy of the H_2 molecule, the conclusion is reached by these authors that at 12.0 and 16.3 V excitation of the H_{α} line takes place as a result of the processes



and



The distance between strata increases with decrease in pressure. When strata are present (striated discharge) the potential distribution in the positive column has a periodic character, and the potential drop in each stratum is the same all along the whole column. At high current densities and low pressures this potential drop is often equal to the ionization potential or excitation potential of the gas. The temperature distribution in striated discharge is also of a periodic character. The reason for the periodicity of striated discharge is that in the region of the strata the electrons lose their energy as a result of inelastic collisions with gas molecules and accumulate it afresh in the intervals between strata.

The temperature of the positive glow (or the mean temperature in the striated discharge region) is usually a few hundred degrees centigrade [143]. In the region of the cathode potential drop (close to the cathode) the temperature is higher than that in the positive column.

The gas in the positive column of glow discharge, in arc discharge at high pressures and in certain other forms of discharge (and also in the incandescent atmosphere of stars) is in a particular state called the *plasma* state. The characteristics of this state are a high degree of ionization of gas, reaching 100% in the limiting cases, and a mean electrical density almost exactly equal to zero, i.e. the mean concentrations of electrons and ions are equal. The mutual attraction of electrons and ions, and also polarization interaction (attraction) of free charges and neutral molecules (for incomplete ionization of the gas) result in the plasma being a unique system of interacting particles and possessing specific properties (the plasma state is, in a certain sense, similar to the metallic state of matter).

Plasma may be either isothermal or non-isothermal. In *isothermal* plasma the electrons and ions are in thermodynamic equilibrium. Such is the state of plasma formed at high gas temperatures, for example in the atmosphere of stars, and also in an electric arc at high pressures and in the channel of spark discharge.⁽²⁷⁾ In a *non-isothermal* plasma, since energy exchange is difficult in collisions of electrons with molecules and ions, the mean energy of the electrons is much larger than the mean energy of the ions or gas molecules. Assuming a Maxwellian distribution of electron velocities we may speak about their temperature (*electronic temperature*). The difference in energy of the electrons and the ions is such that when the gas (i.e. molecules and ions) in the positive column of glow discharge has a temperature of the order of a few hundreds of degrees centigrade, the

(27) An electric arc has in fact been described which burns in argon or nitrogen at atmospheric pressure and a current of 500 amps. It was shown that in such an arc thermodynamic equilibrium is established between electrons, atoms and ions and the temperature reaches 30,000° [610]. An experimental method of establishing the presence or absence of thermodynamic equilibrium in an arc consists by using an oscillograph to measure the field strength and intensity of the spectral lines; by this method temperature excitation may be distinguished from excitation by the electric field [1303].

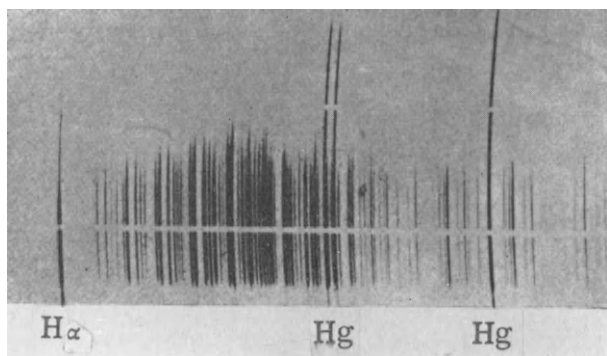
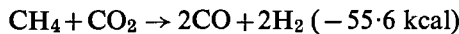
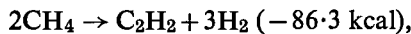


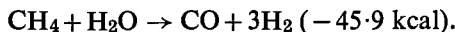
FIG. 124. Glow-discharge spectrum in hydrogen (in the presence of mercury vapour) (according to Finkelnburg, Lau and Reichenheim [611]).

electronic temperature is of the order of thousands and even tens of thousands of degrees or higher.⁽²⁸⁾

In the positive column of the usual type of glow discharge we have the following conditions: as a rule, low pressure (usually about 0.1 to 100 mm Hg), a moderate gas temperature (of the order of a few hundreds of degrees) and a high "electronic temperature". These conditions are similar to those for photochemical reactions, where the role of fast electrons is played by photochemically active light quanta. By reason of their moderate energy fast electrons correspond rather to quanta of hard radiation (the far ultraviolet). For this reason glow discharge should favour endothermic reactions, i.e. chemical reactions in which the main role is played by processes of decomposition of molecules, as for example,



and



Investigations of reactions of this type show that the reacting system comes to a certain limiting state which is characterized by the concentrations of initial substances and reaction products being considerably different from the equilibrium concentrations, as in endothermic photochemical reactions or in reactions for which the reverse, also photochemical, reaction takes place simultaneously with the forward reaction (see p. 465).

Chemical reactions take place more rapidly near the cathode, i.e. in the region of the cathode potential drop, than in the positive column; this is accounted for by the high electron velocities and higher temperature in the former region of the glow discharge. However, because the cathode drop region is small, and the extent of the positive column is practically unlimited, the overall rate of reaction taking place in the column may be much greater than the rate of reaction close to the cathode. For this reason it is in practice more expedient to conduct reactions mainly in the positive column.

Free atoms, radicals and ions are the most effective chemically active centres in the electric-discharge zone. Since adsorption and recombination of atoms and radicals as well as ions occurs most readily at metallic electrodes, these cause a substantial decrease in the concentration of these particles. In this respect *high-frequency electrodeless discharge* has many advantages; here, owing to the absence of solid surfaces favouring atom recombination and ion discharge, the degree of dissociation of the gas,

⁽²⁸⁾ Thus the electronic temperature of pulsed electrodeless discharge at 1000 to 15 μ Hg pressure has been measured as 10^6 degrees for an apparently Maxwellian distribution of electron energy [430].

and therefore the concentration of atoms, is especially high. High concentrations of atoms may be detected by the afterglow (the glow after cessation of discharge) frequently observed in electrodeless discharge, which is a result of the homogeneous (volume) recombination of atoms being slow (the source of the afterglow is the energy liberated during the recombination of atoms).

One type of electrodeless discharge is *microwave discharge*, which has a particularly high activating effect. Thus, according to the measurements of McCarthy [934], in microwave discharge at a frequency of 2450 megacycles/sec and pressures in the range 16 to 200 mm Hg the yield of atoms in hydrogen is 1.00 g atom, in oxygen 0.80 and nitrogen 0.58 g atom/kW hr.⁽²⁹⁾ These yields are approximately ten times greater than the yields of atoms and radicals obtained in low-frequency discharges or in direct-current discharge (at the same pressures and field strengths). An important property of microwave discharge is that, although it is initiated at low pressure (5 to 30 mm Hg), it may burn like a glow discharge even on a subsequent increase of the pressure to an atmosphere or higher.

Arc Discharge

With increase in current the temperature of the electrodes increases and the glow discharge is gradually transformed into *arc discharge*. Owing to intense evaporation of metal from incandescent electrodes the predominant lines in an arc-discharge spectrum are those of the electrode metal, which have a relatively low intensity in a glow-discharge spectrum.

The potential difference between the electrodes decreases simultaneously with the increase in current. In a stationary arc this potential difference is usually only a few tens of volts (a potential difference of a few hundreds or thousands of volts is required to maintain glow discharge). High current density and low voltage are the main characteristics of a direct-current electric arc. Arcs may burn at both low and high pressures. An example of a low-pressure arc is the mercury arc burning between metallic electrodes (especially mercury electrodes) in an atmosphere of mercury vapour; an example of an arc burning at atmospheric pressure is the normal carbon arc or an arc with metallic electrodes. Arcs are also used that burn at pressures much higher than atmospheric. Owing to the low voltage, electrons have relatively low velocities in arc discharge. Therefore in an arc spectrum the predominant lines and bands are those belonging to neutral atoms and molecules. In connection with this, spectra emitted by neutral particles are often called *arc spectra* in contrast with *spark spectra* which predominate in electric-spark radiation and are emitted by ions.

⁽²⁹⁾ These yields correspond to an energy consumption of 37.4, 46.8 and 64.5 eV per H, O and N atom respectively (the "theoretical" consumption calculated as half the heat of dissociation of the corresponding molecule is in these cases 2.24, 2.56 and 4.88 eV respectively).

Usually we are concerned with incandescent cathode arcs with a temperature of a few thousands of degrees. The hottest part of the cathode is the cathode spot. Strong emission of electrons (thermionic electrons) by the cathode is one of the conditions for the occurrence of an electric arc. However, there are also arcs with cold electrodes (for example, the mercury arc). In this case the arc discharge is maintained by auto-electronic emission of the cathode as a result of electrons tunnelling through the potential barrier formed by the electrical double layer at the surface of the cathode. The possibility is not ruled out that the source of the electric charges in an arc with cold electrodes burning at high pressure is thermal ionisation of the hot gas near the cathode.

The state of the gas in arc discharge usually corresponds to that of an isothermal plasma. Owing to the high temperature of the gas and the high "electronic temperature", which reaches a few thousand degrees,⁽³⁰⁾ the high current density and frequently the high pressure, the predominant chemical processes in an arc are those characteristic of high temperatures and especially high-temperature cracking processes and endothermic processes.

A special type of arc discharge is the so-called torch discharge discovered by Zilitinkevich [93] in 1928. Torch discharge is "kindled" at an electrode supplied by a sufficiently powerful high-frequency generator (frequency 1 to 1000 megacycles) and has the shape of the flame of a gas burner. In contrast with the other (corona) type of one-electrode discharge, torch discharge appears at the unusually low voltages of a few hundreds or thousands of volts. When a conductor is introduced into a torch it becomes a second electrode and the torch discharge is transformed into a normal high-frequency arc.

According to the measurements of Mochalov [194, 254] the electronic temperature of a torch discharge is much higher than the temperature of the gas. Therefore the plasma in a discharge of this type is non-isothermal.

§31. Chemical Reactions in Electrical Discharge and Yields of These Reactions

The great variety of types and forms of electric discharge and the possibility of chemical activation of substances over a wide range of pressures and temperatures make it possible to carry out chemical conversions successfully under the action of electric discharge. However, it should be

⁽³⁰⁾ For example, Burhorn [465] measured the temperature of the gas in an iron electrode arc by the Doppler shift of the spectral lines, and the electronic temperature by the absolute intensity of the continuous spectrum of the arc; he found that the two temperatures were identical and equal to 6300°K. He concluded from this that thermodynamic equilibrium is established in the arc. See also [561a].

mentioned that in spite of the vast amount of work on a variety of chemical reactions, the electric-discharge method of carrying out chemical reactions has not yet received wide practical application, since in most cases it is uneconomic and unable to compete with other chemical-technological methods. Nevertheless all our available experience in conducting chemical reactions in various types of electric discharge leads to the conclusion that more detailed study of the kinetics and mechanism of reactions in discharge should reveal reaction conditions giving better yields of valuable products than has been possible up till now.

In this section we shall consider some typical reactions taking place in electric discharge, in order to explain their micro- and macroscopic properties, and to establish the factors determining the yield of reaction products and the rate and direction of the reaction.

Ozone Production

The production of ozone in a silent discharge (ozonizer) is practically the only industrial method of synthesizing this substance, which has a variety of practical applications. Depending on the ozone content of the air from the ozonizer the yield of ozone (for one type of ozonizer) is from 30 to 50 g/kW hr; this corresponds to an energy of 60 to 36 eV per molecule of ozone [1267]. As the formation of an ozone molecule from molecular oxygen requires an energy input of 34.5 kcal, i.e. 1.5 eV, the theoretical yield of ozone should be 1200 g/kW hr, i.e. a figure 40 to 20 times greater than that obtained in practice. One of the reasons for such a large difference between practical and theoretical yields of ozone is undoubtedly that a large part of the ozone in the ozonizer is decomposed by the action of electrons. That the reverse process of ozone decomposition occurs is evident from many data, in particular from the above-noted dependence of ozone yield on its percentage content in the ozonized air, namely the increase in yield with decrease in percentage content (since, with decrease in percentage content of ozone, its decomposition becomes less probable).

From general considerations it may be concluded that the occurrence of forward and reverse reactions is a distinguishing feature of all reactions conducted in an electric discharge, and they will be reversible save when special reaction conditions (for example, freezing out reaction products) are in force. In fact the discharge zone always contains electrons sufficiently fast to be capable of activating both the initial and final substances, i.e. to be capable of exciting both the forward and the reverse reaction. And whereas by changing the spectral composition of the active radiation in photochemical reactions it is possible to force the reaction into either the forward or the reverse direction, in reactions carried out in electric discharge such a control of the ratio of forward and reverse reaction rates is not practically feasible. (For example, by exposing a mixture of oxygen

and ozone to light of short wavelength, which is absorbed by oxygen and not by ozone, we may obtain a high percentage of ozone in the mixture; by exposing this mixture to visible light, which is absorbed only by the ozone molecules, complete decomposition of the ozone may be attained.) For this reason the reverse reaction here will always be important, and the yield of product will always be less than the theoretically possible yield.

In addition to the occurrence of the reverse reaction, the discrepancy noted above between the observed and theoretical yields of ozone may be partially due to the following circumstance. The electron-impact activation of oxygen molecules, which precedes the formation of ozone, theoretically may consist of their excitation, dissociation or ionization. As the discharge zone contains electrons of different velocities and there is also a different relationship between the probability (cross-section) of each of the activation processes and the energy of the bombarding electron, it might be assumed that the activation of oxygen in a discharge is connected to some extent with each of these processes. When the activation of oxygen consists of excitation of O_2 molecules then, since the heat of the endothermic process $2O_2 = O_3 + O$ is 4.0 eV (93.1 kcal), this process may be energetically possible only when the excitation energy of an O_2 molecule is greater than 4.0 eV. The lowest excited state of an oxygen molecule which satisfies this condition is the metastable state ${}^3\Sigma_u^+$ with an excitation energy of 4.6 eV. This figure is the lowest possible for the energy of the bombarding electrons in order for ozone formation to be theoretically possible as a result of electron bombardment of O_2 molecules (the dissociation of an O_2 molecule is associated with an energy consumption of 5.1 eV and ionization is associated with an energy consumption of 12.1 eV). However, since the probability of excitation (and also the probability of ionization) by electron impact is zero when the energy of the bombarding electron is equal to the excitation energy, and becomes significant only when the electron energy K exceeds by some amount K_{\min} the excitation energy, the "effective" electron energy K_{eff} must be a corresponding amount greater than 4.6 eV.

From the point of view of the Franck-Condon principle, the most probable transition from the ground state of the O_2 molecule to the metastable state, ${}^3\Sigma_g^- \rightarrow {}^3\Sigma_u^+$, corresponds to an energy of about 7 eV, which exceeds the heat of dissociation (5.1 eV) of the O_2 molecule by a relatively small amount (Fig. 125). This is a weighty argument in favour of the activation of oxygen consisting in the *dissociation* of O_2 molecules. Since the transition of an O_2 molecule to the state ${}^3\Sigma_u^-$ also leads to its dissociation, and this transition, in contrast with ${}^3\Sigma_g^- \rightarrow {}^3\Sigma_u^+$, is not forbidden and consequently should be more probable, we should possibly consider it more likely that the activation of O_2 molecules in silent discharge is connected with the transition ${}^3\Sigma_g^- \rightarrow {}^3\Sigma_u^-$. Moreover, from the point of view of the Franck-Condon principle the most probable transition to the state ${}^3\Sigma_u^-$

corresponds to an energy of about 8 eV and consequently K_{eff} should be considered to be not less than 8 eV. It follows from this that the theoretical yield of ozone under these conditions should be less than the thermodynamic yield in the ratio $\frac{1}{2}8 : 1.5 = 8/3$,⁽³¹⁾ i.e. the theoretical yield should be equal to $1200/(8/3) = 450$ g/kW hr. The experimental yields differ from this figure by approximately 10 times. If it is assumed that the activation of oxygen in silent discharge consists in ionization of O_2 molecules and each O_2^+ ion gives two ozone molecules, then the theoretical yield is about 300 g of ozone per kW hr.

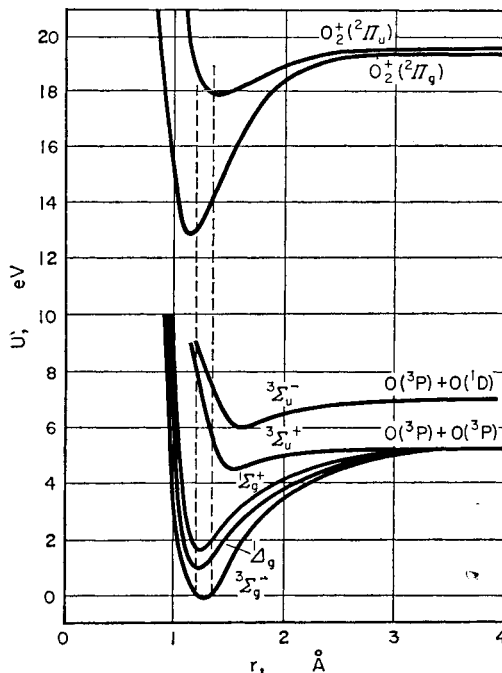


FIG. 125. Energy levels of O_2 and O_2^+ and the energy of the most probable transitions from the ground state of the oxygen molecule (from the point of view of the Franck-Condon principle).

The greatest yield of ozone has been obtained in the synthesis of ozone in glow discharge [437]. In this case the maximum yield is 150 g/kW hr and corresponds to one ozone molecule per 11.9 eV. This yield is about the same as the theoretical yield calculated above (one O_3 molecule/4 eV) and hence it may be concluded that the K_{eff} value at the basis of this calculation is also near to the actual value. A yield of 150 g/kW hr is successfully obtained only at low pressures and when the discharge tube is cooled

⁽³¹⁾ Here the factor $\frac{1}{2}$ allows for the fact that in the dissociation of an O_2 molecule two oxygen atoms are formed and each may give a molecule of ozone.

with liquid air: ozone is frozen out at the cold walls and the low pressure favours its fast diffusion to the walls. In this way the reverse reaction of ozone decomposition is eliminated or reduced to a minimum; the high ozone yield observed under these conditions should also be attributed to this, and is obtained exclusively in the positive column of the glow discharge. In the region of the cathode potential drop, especially in the negative glow region, ozone is not formed; and it has been shown by special experiments that the reason for this lies in rapid decomposition of the ozone. It follows that in the negative-glow region the rate of the reverse reaction is higher than the rate of the forward reaction.

Attempts to produce ozone by bombarding oxygen with electrons of a given velocity (corresponding to an energy of some tens of electron-volts) gave very low yields, undoubtedly connected with the very low pressures (about 1 mm Hg) required by these experiments [1265]. In fact, since the formation of ozone is most probably a termolecular process



the probability of the process at low pressure must be very low.

Synthesis of Ammonia from Nitrogen and Hydrogen

In contrast with ozone synthesis, the synthesis of ammonia is an exothermic reaction ($\frac{1}{2}N_2 + \frac{3}{2}H_2 \rightarrow NH_3 + 11.0 \text{ kcal}$). However, since activation is necessary, this reaction is also associated with an energy input; this applies equally to the thermal reaction and the reaction carried out in an electric discharge. Much work has been devoted to the latter reaction in discharges of various types [290]. It has been shown that a definite limit of reaction is established depending on the type of discharge and the reaction conditions. Thus it has been found that in spark discharge the reaction limit corresponds to 3 per cent ammonia, in corona discharge the limiting concentration of ammonia in a stoichiometric mixture is 4.1 per cent and in glow discharge it is about 6 per cent. Moreover, in electrodeless discharge the limiting concentration of ammonia reaches 36 per cent and in glow discharge when the ammonia is frozen out with liquid air it reaches 98 per cent. These data are evidence of the occurrence of the reverse reaction of NH_3 decomposition parallel with the forward reaction of synthesis. The yield of ammonia is usually a few grams per kilowatt-hour, and on changing the conditions and type of discharge varies from some tenths of a gram to about ten grams. The highest yield (8.2 g/kW hr) has apparently been obtained in silent discharge, and must be attributed to the higher pressure. The yield of ammonia obtained from bombardment of a mixture of nitrogen and hydrogen with electrons of a given energy has also been measured. Thus, for 25 eV electrons there is one molecule of NH_3 per five electrons, and this corresponds to a yield of

5.1 g/kW hr. We should mention also that a different chemical effect has been established in the various parts of the discharge when the reaction is carried out in a glow discharge. To illustrate this Fig. 126 shows the distribution of ammonia along the discharge tube (according to Brewer and Westhaver [436]). It is seen from this figure that the maximum quantity of ammonia is obtained in the negative-glow zone where, according to these measurements, the yield is 5.4 times greater than in the positive column. It is interesting to note that in the synthesis of ozone the reverse is observed (cf. p. 531).

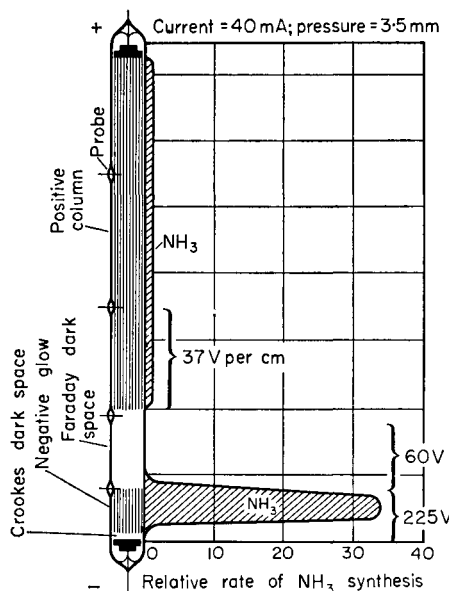


FIG. 126. Distribution of the yield of ammonia along the discharge tube for the synthesis of ammonia from nitrogen and hydrogen in a glow discharge (according to Brewer and Westhaver [436]).

The yields of ammonia by synthesis in an electric discharge are still very far from the industrial yield obtained in the usual synthesis (a catalytic reaction at high pressure) of 1 kg/kW hr, i.e. about 100 times greater than the best yields in the electric-discharge method. It is seen from this that at present the synthesis of ammonia in electric discharge has no technical importance.

In spite of the large amount of work on the synthesis of ammonia in electric discharge, the mechanism of the reaction has received little study so far. From data on the synthesis of ammonia by bombarding a mixture of nitrogen and hydrogen with electrons of a given energy, it follows that the minimum electron energy required for formation of ammonia is

17 eV. As this figure is close to the ionization potential (15.65 eV) of the nitrogen molecule, most investigators assume that the primary active centres in the synthesis of ammonia are nitrogen ion molecules N_2^+ .⁽³²⁾ These ions must react readily with hydrogen. It may be concluded from mass-spectrometric study of this reaction that the primary product of this interaction is N_2H^+ ions, apparently formed as a result of the process $N_2^+ + H_2 = N_2H^+ + H$ [39]. Further processes, which lead finally to ammonia formation, apparently take place at the walls of the discharge tube; this is supported by the facts that (i) many authors have observed a sharp dependence of NH_3 yield on the state of the walls, (ii) in experiments with electrodeless discharge the NH_3 yield has been found to be proportional to the surface area of the discharge tube, and (iii) the yield increases on placing glass wool in the tube. In the reaction in a glow discharge the reaction rate has been found to be proportional to the discharge-current strength, and this supports the idea that further conversions of the N_2H^+ ion do not involve other ions or active particles. However, it should not be assumed that N_2^+ ion radicals are the only type of active particles in the synthesis of ammonia in electric discharge. Formation of ammonia in the interaction of active nitrogen and hydrogen shows that nitrogen atoms also are capable of initiating this reaction. It is interesting to note that in the synthesis of ammonia in active nitrogen, i.e. in the absence of ions, a sharp dependence of NH_3 yield on the state and nature of the walls is again observed. The problems of the mechanism of the synthesis of ammonia in electric discharge consist in explaining the nature of the active centres of the reaction and also the role of the walls, and in establishing the nature of the chemical processes taking place at the walls.

From an analysis of the kinetic conditions for reactions in glow discharge and from data on the synthesis of ammonia and other reactions compiled by various authors, Shekhter [292] showed that heterogeneous processes involving atoms and radicals and taking place at the walls of the discharge tube must play a large part in the mechanism of chemical reactions in glow discharge. Shekhter comes to the general conclusion that the chemical reactions taking place in electric discharge have a *homogeneous-heterogeneous* character.

Production of Acetylene from Methane

The synthesis of acetylene from methane (and also from a mixture of gases containing methane) is one example of organic synthesis in electric discharge carried out in practice on a large scale and successfully competing with the usual carbide method of acetylene production. Various

⁽³²⁾ The formation of oxides of nitrogen during the bombardment of a mixture of nitrogen and oxygen with electrons of different velocities is also observed only when the electron energy is 17 eV or higher. It may be concluded from this that in this reaction also the nitrogen ion molecules N_2^+ are the primary active centres.

types of electric discharge have been used to produce acetylene from methane. However, since the first studies showed that the yield of acetylene in silent discharge is negligibly small, further attempts to carry out this reaction with a C_2H_2 yield of practical interest have been concentrated mainly on glow and arc discharge.

A large number of papers have been devoted to study of acetylene synthesis in glow and arc discharge, and we should mention especially the work of Peters and coworkers, Koller, Bozhko, Eremin and coworkers and Kobozev and coworkers (for literature see [16]). The work of Russian investigators has shown conclusively the practical possibility of using the electric-discharge method to synthesize acetylene on an industrial scale and the ability of this method to compete with the carbide method.

As a result of these studies it has been established that under the most favourable conditions (optimum pressure, gas composition, rate of flow, etc.) it is possible to obtain up to 10–20 per cent acetylene in the final gas and almost complete conversion of the initial methane into acetylene (or other valuable products).

The best acetylene yields attained are 120 g/kW hr. From the heat effect of the process $2CH_4 = C_2H_2 + 3H_2$, namely -86.3 kcal per mole C_2H_2 , the thermodynamic yield obtained is 259 g/kW hr. Consequently, the maximum yields attained are 46 per cent of the thermodynamic yield. The acetylene yield in the carbide process (from calcium carbide) is 105 to 90 g/kW hr, i.e. 40–35 per cent of the thermodynamic yield. An electric-discharge method using a type of arc discharge has received the most extensive practical application.⁽³³⁾

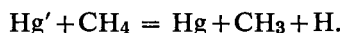
The mechanism of conversion of methane into acetylene in an electric discharge has not yet been adequately studied. At 1500–2000°K, the usual temperatures of arc discharge, thermodynamic equilibrium in methane or its mixtures with hydrogen corresponds to complete decomposition of the acetylene into carbon and hydrogen, and consequently, from the fact that it is possible to produce considerable yields of acetylene on the action of an electric discharge in methane, we conclude that the conversion in an arc takes place in two stages. The first stage corresponds to the reaction $2CH_4 = C_2H_2 + 3H_2$ and the second to the reaction $C_2H_2 = 2C + H_2$. An argument supporting the occurrence of these two main reaction stages may be found in the fact that the energy yield of acetylene (yield in grams per kW hr) increases on increase in the velocity of the gas; it follows from this that parallel with the formation of acetylene from methane there

⁽³³⁾ As an idea of the scale of the industrial use of this method we should mention that, according to the data available, the annual production of one German factory in 1942 was 58,000 tons of acetylene. In this factory a high-voltage arc was used at a mean temperature of 1600°K and the flow-rate of the gas through the arc was 1000 m/sec. which corresponds to a reaction time of about 1/1000 sec. The energy yield of acetylene was 93 g/kW hr.

occurs acetylene decomposition in the discharge zone; this decomposition plays the smaller part, the shorter the time spent by the acetylene in the discharge zone, i.e. the higher the gas velocity. The idea has also been put forward that the increase in the yield of acetylene (per methane decomposed) observed on diluting the methane with hydrogen is connected with a shift of the equilibrium $C_2H_2 \rightleftharpoons 2C + H_2$ to the acetylene side, i.e. with a retardation of the second reaction stage.

One of the main problems in the mechanism of conversion of methane in an electric discharge concerns the nature of the active centres of the reaction. In view of the facts that the discharge spectrum in methane contains intense bands of CH and at high discharge current densities C_2 bands are also observed, Fischer and Peters [612] (and subsequently other authors) suggest that both CH radicals and C_2 radicals take part in the formation of C_2H_2 , and that one of the methods of acetylene formation in the discharge zone is connected with hydrogenation of the C_2 radicals by atomic hydrogen, which also is detected spectroscopically [723].

General considerations arising from the high chemical activity of free atoms and radicals (especially at relatively high discharge temperatures), and also experimental data, show that these particles play an active role in chemical reactions in electric discharge. For example, according to the observations of Kobozev, Vasil'ev and Gol'braikh [111], with mercury vapour present in the glow discharge zone in methane the yield of unsaturated hydrocarbons is considerably increased; the concentration of these decomposition products of methane increases in proportion to the content of mercury vapour in the gas. In view of the well-known sensitizing effect of mercury in photochemical reactions (see p. 443) it is natural to assume that in this case also the effect of the mercury consists in splitting the molecules into free radicals as a result of collisions with excited mercury atoms, for example



Owing to the favourable properties of the excitation function of the Hg atom which are reflected in the high value of the maximum excitation cross-section and in the position of the maximum at relatively low electron energy (see Table 43), excitation of mercury atoms in the discharge zone is very probable.

Direct indications of the presence of free CH_3 radicals in the discharge zone in methane are provided spectroscopically and also by Willey's experiments [1295], in which he detected dimethyl zinc $Zn(CH_3)_2$ after passing the gas from discharge in methane through a hollow zinc electrode, which indicates that there are CH_3 radicals in the discharge zone.

Developing the idea of a radical mechanism in the conversion of methane in electric discharge, Peters and Wagner [612] attribute the main

role in this reaction to hydrogen atoms. To a considerable extent they used the results of Bonhoeffer and Harteck, who studied the interaction of H atoms and various hydrocarbons. In particular it was shown that H atoms dehydrogenate ethane and ethylene, converting them into acetylene which the H atoms scarcely affect. In this way a special stability must be attributed to acetylene, and this explains the possibility of almost complete conversion of methane into acetylene under certain conditions. On the basis of these data Peters and Wagner conclude that at low current densities acetylene is formed mainly as a result of the dehydrogenating action of H atoms, which convert methane and CH_3 radicals into CH_2 and then into C_2H_4 and C_2H_2 . At high discharge densities, according to Peters and Wagner, acetylene is formed predominantly as a result of the recombination of CH radicals and the hydrogenation of C_2 radicals.

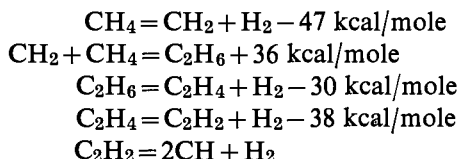
These ideas, which lead to the conclusion that the first of the above two macroscopic reaction stages (namely the conversion of methane into acetylene) has a complex (multistage) character, are supported both by the analytical data of Peters and Wagner themselves and by the data of other authors. Thus from a study of the kinetics of the process and the composition of the products of the conversion of methane in a silent discharge, St. Auney [1165] concludes that the primary reaction product is ethane C_2H_6 which as a result of subsequent dehydrogenation is converted into ethylene C_2H_4 , acetylene C_2H_2 and the products of their polymerization. Formation of ethane in the first stage of the synthesis of acetylene from methane (in high-frequency spark discharge) was also observed by Amemiya [319]. The primary character of C_2H_6 is evident from the observed increase in its yield on increasing the flow-rate.⁽³⁴⁾

Ethane, which is a primary product of the decomposition of methane, is rapidly decomposed in the discharge zone, and is therefore usually present in the reaction products in only negligible amounts; consequently the ethylene obtained from it (or parallel with it) commonly accompanies the acetylene. Thus Peters and Wagner always obtained a small quantity of ethylene in a glow discharge in a mixture of two parts of methane and one part of hydrogen, when suitable reaction conditions were chosen, in addition to acetylene which is the main reaction product under these conditions. In the same way, in factory production (to which we have referred earlier, p. 534) about 1 m^3 of ethylene is obtained for each 10 m^3 of acetylene. We should add that under certain reaction conditions it is possible to convert methane quantitatively into ethylene and hydrogen in a glow discharge [438].

It may be noted that there are definite features of similarity between

⁽³⁴⁾ Increase in the volume flow-rate from 100 to 200 ml/min gave an increase in the yield of ethane from 3.4 to 9.2 volume % for a practically constant yield of acetylene (28.6 to 29.6 volume %).

the above mechanism for the reaction in electric discharge and the mechanism of thermal decomposition of methane, with regard to the step-wise nature of the conversion of methane into acetylene. Kassel [818] showed that all the kinetic features of the pyrolysis of methane may be explained on the basis of the following reaction mechanism:



The following facts also are in favour of this mechanism. Storch [1188] studied the decomposition of methane at a carbon filament, and found that under certain conditions up to 95 per cent of the methane is converted into ethane C_2H_6 . It may be concluded from this that ethane is the primary product of the conversion of methane. Moreover, Belchettz [371] passed hot methane over a tellurium mirror and as a result of the interaction of the substances formed with bromine and iodine compounds, CH_2Br_2 and CH_2I_2 were observed; he concluded from this that hot methane contains CH_2 methylene radicals. Study of the decomposition of methane on hot platinum also leads to this conclusion, i.e. that CH_2 radicals are formed as the primary product in the thermal decomposition of methane [372].⁽³⁵⁾

The detection of dimethyl tellurium $(\text{CH}_3)_2\text{Te}$ on passing hot methane over a tellurium mirror shows that the gas also contains CH_3 radicals [1062]. In Kassel's opinion [819], however, these radicals do not play an important role in methane conversions.

In the above mechanism for the pyrolysis of methane (Kassel) the decomposition of CH_4 , C_2H_6 , C_2H_4 and C_2H_2 molecules follows a unimolecular law in which the source of activation is the thermal energy of the molecules. Under discharge conditions, when the electronic and molecular temperatures are different, an important (if not dominating) role in the activation of the molecules should be played by electron impacts. Extending Kassel's mechanism to the discharge reaction, we conclude that the first of the above reaction stages (conversion of methane into acetylene) has a complex (multistage) character. Another difference in the mechanism of the two reactions is clearly connected with the CH_3 radicals and H atoms; according to Kassel these do not play an important part in the pyrolysis reaction, but under discharge conditions they may be important in the development of the reaction owing to the high activating effect of the discharge.

⁽³⁵⁾ However, the possibility is not ruled out that methylene CH_2 is formed as a result of the process $\text{CH}_3 + \text{CH}_3 = \text{CH}_2 + \text{CH}_4$, with a heat of 6 kcal.

Burton and Magee [471] (1955) have put forward a new point of view regarding the nature and mechanism of chemical activation in discharge. According to these authors an important role in the chemical activation process should be played by *slow electrons* ($K=0.5$ to 4 eV) which are present in the discharge zone in considerable quantities. In their opinion the role of these electrons consists in the consecutive (step-wise) excitation of different electron levels of the molecules and radicals in the discharge zone, so that active particles are formed with different degrees of activation, in particular particles with energy much greater than the energy of the slow electrons and which cannot be excited on a single collision with a slow electron. Applying these ideas to the formation of acetylene from methane in an electric discharge, Burton and Magee postulate a formal reaction mechanism in which an important role is played not only by H atoms and CH and CH_3 radicals but also by CH_2 radicals which are in different degrees of excitation and so are capable of different conversions. From this mechanism they derive a kinetic reaction law (with the rate of formation of acetylene proportional to the concentration of methane and to the square root of the discharge-current strength) identical with the law established empirically by Wiener and Burton [1287] for the stationary reaction on passing a stream of methane through a discharge. The agreement between theoretical and empirical reaction laws should not of course be considered as proof of the accuracy of the mechanism postulated by Burton and Magee.⁽³⁶⁾ However it is certain that under some conditions slow electrons do play an important role in the process of chemical activation.

In all the mechanisms proposed recently for the formation of acetylene from methane in an electric discharge, an important part is played by chains. The likelihood of a chain mechanism for discharge reactions follows both from theoretical considerations of the fact that there are different types of free atoms and radicals in the discharge zone which have high chemical activity under high-temperature discharge conditions, and also from the experimental facts, which are most simply explained on the basis of chain mechanisms. For example, a study of the products of electrocracking of various organic vapours in silent discharge shows that their composition is very similar to that of the products of thermal cracking (pyrolysis) of these substances. As an illustration Table 47 shows the results of analysing the products of cracking of acetone vapour in silent discharge, and the pyrolysis products.

A similar agreement between the composition of the products of electrical and thermal cracking is also observed in other cases. We should

⁽³⁶⁾ It should be mentioned that the related mechanism proposed by Wiener and Burton, which does not allow for the possibility of slow electrons taking part in the activation processes, apparently does not give the reaction rate observed.

TABLE 47

Composition of the products of electrocracking in silent discharge and products of the pyrolysis of acetone vapour (in %) [912]

Product	Electrocracking	Pyrolysis
CO ₂	0·6	0·6
CO	42·1	36·0
C ₂ H ₄	2·9	3·3
C ₂ H ₆	30·0	21·8
H ₂	24·4	38·3

mention that a similar product composition is obtained for the decomposition of benzene vapour in a silent discharge, in pyrolysis and in the photochemical reaction when sensitized by mercury. In view of the different natures of the primary active centres in these three reactions, a similar product composition would be expected only when they are formed for the most part as a result of secondary processes; this can take place only in chain reaction mechanisms.

The ideas expounded above regarding the radical mechanism of the conversion of methane in an electronic discharge are mainly based on data from chemical analysis of the composition of the reaction products, on kinetic data and on data from spectroscopic studies of discharge in methane.

Spectral analysis, however, detects by no means all the variety of active particles, atoms, ions and radicals which are formed in the discharge zone, as only a negligible part of these particles have spectra accessible to observation. The mass-spectrometric method is much more effective in this respect. Mass-spectrometric analysis of the ions formed in the electric-discharge zone in methane provides evidence of the presence both of ions such as H⁺, C⁺, CH⁺, CH₂⁺, CH₃⁺ and CH₄⁺ which are products of the direct decomposition of methane, and also ions such as C₂⁺, C₂H⁺, C₂H₂⁺, C₂H₃⁺, C₂H₄⁺, C₂H₅⁺, C₂H₆⁺, C₃⁺, C₃H⁺, C₃H₂⁺, C₃H₃⁺, C₃H₄⁺, C₃H₅⁺ and C₃H₆⁺, which are formed either as a result of secondary processes or as a result of dissociation and ionization of products of the synthesis. In addition to ions in the discharge zone there should also be a variety of neutral active particles, free atoms and radicals, formed both by dissociation of molecules and molecular ions under the action of electron impact and also as a result of the processes of charge exchange and neutralization of ions.

This variety of ionized and neutral active particles should be regarded as characteristic of discharges observed at low pressures and having a

relatively high electronic temperature. These discharge conditions apparently correspond most closely to Eisenhut and Conrad's picture [567] of the chemical processes occurring in the zone of this type of discharge. By delivering the ions from the discharge zone in methane (and also in ethane, ethylene and acetylene) as a beam of canal rays and carrying out a mass analysis of the ions (using the parabola method of J. J. Thomson) these authors detected not only ions of group C₁, i.e. the ions C⁺, CH⁺, CH₂⁺, CH₃⁺ and CH₄⁺, which have a high intensity under the experimental conditions, but also ions of groups C₂ and C₃. They conclude from this that in the discharge zone, in addition to the formation of ions from the decomposition of the initial substance (in this case, methane), processes of synthesis take place as a result of which substances of groups C₂ and C₃ are formed from the fragmentary ions and radicals which are products of the primary decomposition of methane.⁽³⁷⁾ We should note that Eisenhut and Conrad do not rule out the possibility of the processes of synthesis taking place at the walls of the discharge tube.

The ideas of these authors and the above ideas on the radical (and in certain cases chain) mechanism of the conversion of methane in an electric discharge should not be regarded as mutually exclusive. Actually, the state of the gas in an electric-discharge zone, generally speaking, is that of a non-isothermal plasma,⁽³⁸⁾ which even in the case of a substance as simple in composition as methane is composed of a variety of ions and radicals which interact chemically with one another. The efficiency of this interaction, the nature of the chemical processes, and consequently the composition of the reaction products, are determined by the initial composition of the gas and its pressure, the time of the discharge action, its power, the electronic and molecular temperatures of the discharge zone and other factors.

At sufficiently high pressures and the high molecular temperature which is characteristic of discharge at these pressures, a dominating role should be played by the interaction of atoms and radicals—the products of limited primary "electrolysis"—with molecules of the initial and intermediate substances, i.e. the reaction should follow a more or less distinct radical mechanism. At low pressures (low molecular and high electronic temperatures), predominant among the ions and radicals should be products of extensive decomposition, the recombination of which (in the volume or at the walls of the discharge tube) should be a predominant stage in the reaction mechanism.

⁽³⁷⁾ It should be mentioned that studies on photochemical reactions taking place during flash photolysis (see Chap. 6, p. 424) also lead to similar views regarding the synthesis of reaction products from atoms and radicals.

⁽³⁸⁾ The thermodynamic non-equilibrium of the process of electrocracking of methane, in particular, was established by Frish and Kagan on the basis of spectroscopic studies of the discharge [282].

We should mention in concluding this section that the dual character of chemical processes in electric discharge, as reflected in the parallel occurrence of reactions of decomposition and synthesis, is to some extent specific for all hydrocarbons (and also compounds of other classes) in so far as it is possible to establish this from the composition of the reaction products and also the composition of the ions using a mass spectrometer. Here we should just mention the following feature: in an electric discharge the products of the conversion of relatively heavy hydrocarbons, and of other compounds involving a large number of carbon atoms, consist predominantly of substances with a smaller number of C atoms, so that the main process is decomposition (cracking); but the effect of an electric discharge on light compounds, especially at high pressures and low temperatures, is that a considerable part of the reaction products is composed of condensation products, i.e. substances containing a higher number of C atoms relative to the initial substances. For example, subjecting ethane at a pressure of 672 mm Hg and a temperature of 23.2°C to a silent discharge for some hours, Lind [879] found that 136.8 cm³ of C₂H₆ gives: 84.30 cm³ H₂, 32.20 cm³ CH₄, 0.76 cm³ C₂H₆, 21.60 cm³ C₃H₈, 6.76 cm³ C₄H₁₀, 3.39 cm³ C₅H₁₂ and also a certain amount of liquid condensation products. Analysis of the liquid obtained showed that it is a complex mixture of heavy hydrocarbons; the light fraction of this mixture mainly consists of octanes C₈H₁₈ and octylenes C₈H₁₆. Similar liquid products are obtained from the action of a silent discharge on methane, ethane, propane, butane and ethylene.⁽³⁹⁾

§32. Chemical Reactions Taking Place under the Action of Penetrating Radiations (Radiation-induced Chemical Reactions)

The basic types of penetrating (radioactive) radiations of natural origin are alpha-, beta- and gamma-radiation. With rare exceptions, such as when the radioactive preparation contains *one* radioactive element emitting radiation of one type, natural radioactive substances are usually a mixture of an initial element and the products of its conversions and emit all three types of radiation. For example, radium in equilibrium with the products of its decay emits six groups of alpha-particles (with energy in the range 4.879 to 7.829 MeV) and five groups of beta-particles (with maximum energy in the range 3.15 to 0.0255 MeV). In beta-decay gamma-rays are emitted in addition to beta-particles.

Activating action of alpha-particles

The action of fast alpha-particles on molecules of an exposed substance comprises ionization, excitation or dissociation of this substance. The ions

⁽³⁹⁾ For details of the individual reactions and literature, see Andreev's book [16] and also the review article by Thomas, Egloff and Morrell [1219].

or neutral radicals and atoms arising must be considered as primary active centres of the reactions taking place under the action of alpha-particles. Electrons (so-called delta-rays) appearing simultaneously with the ions have an energy which is sufficient to ionize, excite or dissociate molecules of the exposed substance and are therefore also a source of its chemical activation.

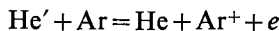
By ionizing and exciting molecules in their path, alpha-particles gradually lose energy and this leads to their slowing down. Therefore an alpha-particle having a certain initial energy $K_\alpha = K_0$ traverses only a certain finite path in the medium; this *path length* depends on the energy K_0 and the properties of the medium which are characterized by a so-called stopping power. The denser the medium and the higher the number of electrons in the molecules, the greater is the stopping power of the medium and the shorter the path length. For a given medium the following approximate relationship obtains between R the path length and the initial energy of the alpha-particles:

$$R = R_1 K_0^{3/2}, \quad (32.1)$$

where R_1 is a constant depending on the properties of the medium and numerically equal to the path length of an alpha-particle with energy $K_\alpha = 1$ MeV. The path length in air at atmospheric pressure and room temperature for alpha-particles of Ra ($K_\alpha = 4.879$ MeV) is 3.21 cm, of Rn ($K_\alpha = 5.589$ MeV) is 3.91 cm and of RaC' ($K_\alpha = 7.829$ MeV) is 6.60 cm, and so on.

In its path in a given medium an alpha-particle of a given initial energy forms a definite number of ion pairs (an ion plus an electron). Thus, alpha-particles of radium in air form 1.47×10^5 ion pairs per alpha-particle, of Rn 1.67×10^5 ion pairs and of RaC' 2.37×10^5 ion pairs, and so on. Dividing the energy of an alpha-particle by the number of ion pairs formed by it we obtain the mean energy spent in ionizing one molecule of the air as about 33 eV. This figure is approximately twice as large as the ionization potential of the nitrogen molecule (15.65 eV) and almost three times as large as the ionization potential of the oxygen molecule (12.70 eV). An explanation of this discrepancy is that the figure 33 eV also includes losses connected with the acceleration of electrons liberated from a molecule, with the abstraction not only of the most weakly but also of more firmly bound electrons, and with excitation and dissociation of gas molecules. The fact that excited particles as well as ions are formed when alpha-particles are passed through a gas is particularly clear from the following data [709]. Studies on the ionization of helium and neon by alpha-particles from polonium show [801] that on average for one ion pair in helium 41.3 eV is expended, and in neon 36.3 eV. Addition of 0.13 per cent argon to helium leads to a lowering of the energy expended in creating

an ion pair to 29.7 eV; in just the same way 0.12 per cent argon in neon gives 26.1 eV instead of 36.3 eV. The increase in the number of ion pairs per alpha-particle which is observed on addition of argon is explained by the fact that the excited atoms of He and Ne formed simultaneously with the ions He^+ and Ne^+ are capable of ionizing argon atoms whose ionization potential (15.75 eV) is less than the excitation energy of He atoms (19.82 eV or higher) and Ne atoms (16.62 eV or higher). We should add that direct measurements of the cross-sections for the processes



and



give $9.7 \times 10^{-17} \text{ cm}^2$ and $2.6 \times 10^{-16} \text{ cm}^2$ respectively, i.e. values only some ten times smaller than the gas-kinetic cross-sections [403].

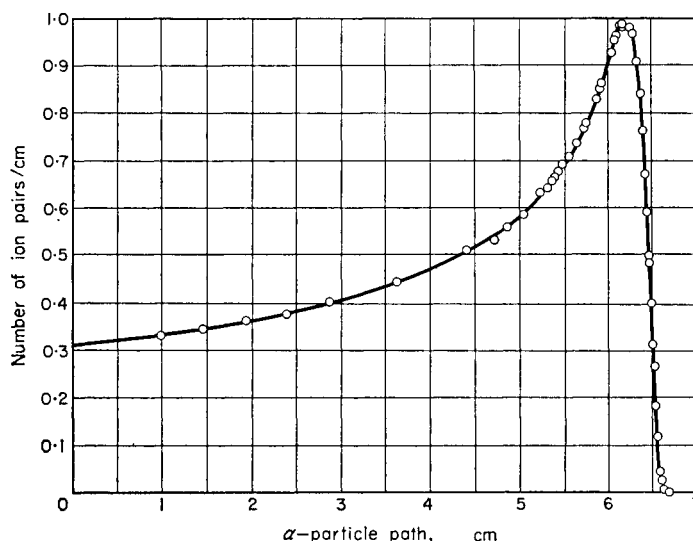


FIG. 127. Change in ionizing capacity of alpha-particles from RaC along the length of their path in air (according to Henderson [742]).

The ionizing capacity of an alpha-particle, which is measured by the number of ion pairs formed in unit path length, is not constant over the whole path length. The number of ion pairs formed in 1 cm of the path is small at the beginning of the path where the alpha-particle energy is a maximum, and increases with slowing-down of the alpha-particle, reaching a maximum at the end of the path (Fig. 127).

It is not difficult to see that this dependence of the ionizing capacity of alpha-particles is a direct reflection of the ionization function shown in

Fig. 114. In fact, if the distance traversed by the alpha-particle from the beginning of its path is x , we find from formula (32.1)

$$R - x = R_1 K^{3/2} = R(K/K_0)^{3/2},$$

or, since $K_0 = \frac{1}{2}mu_0^2$ and $K = \frac{1}{2}mu^2$ (m is the mass of an alpha-particle, u_0 is its initial velocity and u the velocity at the point x),

$$(R - x)/R = (u/u_0)^3$$

and consequently,

$$u = u_0(1 - x/R)^{1/3}. \quad (32.2)$$

The monotonic relationship between u and x expressed by this formula actually indicates the possibility of transition from the relationship $\sigma = \sigma(u)$ shown in Fig. 114 (p. 499) to a dependence of the ionizing capacity of the alpha-particle, which is proportional to $u\sigma(u)$, on the distance x ; this is of the form $u(x)\sigma[u(x)]$ and is shown in Fig. 127.

The number of ion pairs formed by the alpha-particles is determined by the initial energy of the alpha-particles, and is usually taken as a measure of their effect on a substance. The nature of this effect depends relatively weakly on alpha-particle energy. For this reason it may be assumed that the chemical effect of artificially produced alpha-particles ("helions") obtained by accelerating helium ions using an electric field should at all energies be the same as the effect of natural alpha-particles.

Beta-radiation

Interaction with beta-particles, as with alpha-particles, leads mainly to ionization and excitation of molecules. However, owing to the lower probability of activation on collision of a beta-particle with a molecule compared with that of an alpha-particle (see Fig. 114, p. 499), the activating effect of beta-radiation in one centimetre of the beta-particle path is much less than the effect of alpha-radiation. Accordingly the path length of beta-particles is much greater than the path length of alpha-particles. Thus, the path length in air of beta-particles from RaC ($K_\beta = 3.15$ MeV) is 3 m, i.e. it is two powers of ten greater than the path length of alpha-particles (we should note that the path in lead of these beta-particles is less than 2 mm).

The ionizing (exciting) capacity of fast beta-particles ($K > 100$ eV), like the ionizing capacity of alpha-particles, decreases with increase in their energy; this follows from the dependence of the cross-section for ionization by electron impact on electron energy (Fig. 114) and is also seen from Table 48, which shows data for the dependence of the path (R) of beta-particles in air and the number (ν) of ion pairs, formed by a beta-particle in 1 cm of the path in air, on particle energy.

TABLE 48

Ionizing capacity of beta-particles (according to M. Curie [162])

K, keV	R, cm	ν
0.15	—	7700
2.6	0.04	2100
10.5	0.23	1000
24.7	1.0	400
46.6	3.4	250
79.1	7.3	180
127.8	17.9	130
204.7	37.5	95
341	83	70
662	217	50
1127	437	45
3114	1300	41

It is seen from this table that the ionizing capacity of beta-particles (electrons) tends to a certain constant value when their energy is increased. It may be concluded from this that the chemical effect of artificially-obtained fast beta-particles on a substance for an electron energy of about 1 MeV will be little different from the effect of natural beta-rays both quantitatively and as regards the nature of the effect. The advantage of exposure to artificial beta-particles is that it is possible to obtain much higher densities in electron flux than those possible with natural beta-particles.

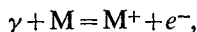
A very important source of artificial beta-particles, apart from their production by means of electron acceleration (an electron tube), is provided by beta-active isotopes of various elements which may be obtained as a result of nuclear reactions. We shall mention in particular the strontium isotopes Sr^{89}_{38} and Sr^{90}_{38} which are rare kinds of beta-active isotopes not emitting gamma-rays. The beta-particles of strontium 89 have a maximum energy of 1.50 MeV; its half life is 55 days. The half life of strontium 90 is several years.

The chemical effect of beta-particles in gases is relatively small, due to their long path length. However, in liquid and solid material, where the path of beta-particles is much less (by three powers of ten), their chemical effect on the substance may be quite considerable.

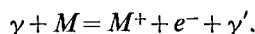
Gamma-radiation

Gamma-rays have an even greater path length. The hardest gamma-quanta have a path length of several hundred metres in air (the path length

in lead is of the order of several tens of centimetres). Ionization by gamma-rays is based on either the photoelectric effect



or Compton scattering of the gamma-quanta



The mean number of ion pairs formed by one gamma-photon in 1 cm is shown in Fig. 128 as a function of the hardness of the gamma-rays. Fast photoelectrons or Compton electrons in their turn are able to ionize molecules of the medium. It has already been shown that secondary ionization takes place on the action of electrons liberated from molecules by alpha- and beta-particles. However, since the energy of photo-electrons and Compton electrons is large, secondary ionization and excitation under the action of these electrons are the main source of the chemical activation of a substance by gamma-rays.

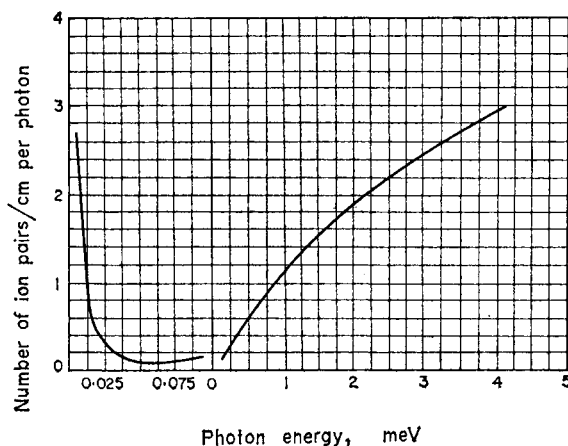


FIG. 128. Mean number of ion pairs formed by one photon in 1 cm of the path in air (according to Fluharty [613]).

As beta- and gamma-rays are absorbed differently, their effect on matter is different. In fact, to reduce the energy of a 1 MeV beam of gamma- or X-rays by half requires a water depth of 12 cm, while electrons of the same energy may penetrate water only to a depth not greater than 0.5 cm. For this reason, when the layer of substance to be exposed is not very thick, exposure to gamma-rays can be carried out uniformly throughout the substance even in the case of liquids; this is not always possible with exposure to electrons.

At the present time, compared with natural sources of gamma-radiation (preparations of naturally radioactive elements), artificial sources, i.e. various radioactive isotopes, are much more powerful and more easily accessible. The cobalt isotope Co_{27}^{60} has been most widely used and is formed from common cobalt Co_{27}^{59} in a nuclear reactor by slow-neutron capture by the nuclei. Cobalt 60 emits 1.3 MeV gamma-rays and has a half life of 5.25 yr. As an indication of the power of cobalt sources of gamma-radiation we should mention that, whereas the activity of a natural source comprising 1 g of pure radium is 1 curie,⁽⁴⁰⁾ the activity of cobalt 60 in present use is measured in hundreds, thousands and tens of thousands of curies.

The continuous X-radiation arising from the retardation of electrons in the Coulombic field of nuclei (*Bremsstrahlung*), which is observed when fast electrons are passed through matter, is also used as a source of artificial gamma-radiation. It has been established that electrons with 10 MeV energy emit about 50 per cent of their energy in the form of Bremsstrahlung and the amount of energy radiated increases with electron energy. In contrast with gamma-radiation which is usually monochromatic, consisting of photons of one frequency (or, in the general case, of several discrete frequencies), Bremsstrahlung has a continuous spectrum ranging from $\nu = 0$ to $\nu = K_{\max}/h$, where K_{\max} is the maximum electron energy. The number of photons emitted in a given (narrow) energy range is approximately inversely proportional to the mean energy of the range. The normal Roentgen apparatus may be used to obtain Bremsstrahlung of moderate hardness, and also characteristic X-rays.

Neutrons

Neutron radiation is also of interest for radiation-induced chemical reactions. The only practical neutron source which is sufficiently powerful to produce measurable yields of products of chemical conversion is an atomic reactor which generates neutrons by fission of a suitable "nuclear fuel" (uranium or plutonium). The spectrum of neutrons from fission of uranium 235 is shown in Fig. 129 [507a]; it is seen from this that these neutrons have a fairly wide range of energy, but since there is a marked maximum a considerable part of the neutrons has an energy of about 0.7 MeV. The path length in air of such neutrons is about 200 m. The neutrons gradually lose their energy by colliding with molecules and become *thermal* neutrons, i.e. neutrons having thermal velocities. In light substances the slowing-down of neutrons results mainly from elastic collisions. In accordance with the laws governing collisions of elastic spheres the most effective collisions, with regard to the slowing-down, are those with

⁽⁴⁰⁾ One gram of pure radium undergoes 3.66×10^{18} decompositions per second. This number of decompositions corresponds to one curie.

hydrogen nuclei which differ very little in mass from a neutron. A neutron loses on average half its energy on colliding with an H atom. For this reason 25 such collisions are sufficient to convert a 1 MeV neutron into a thermal neutron.

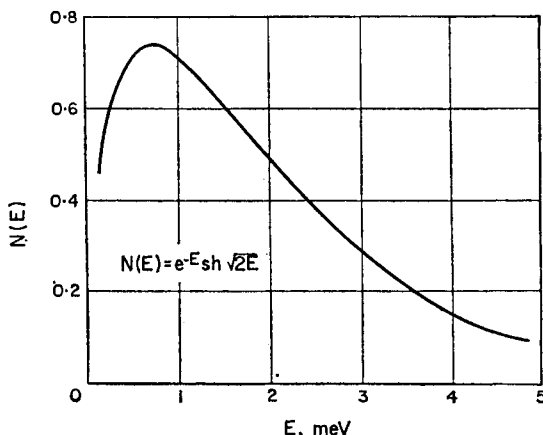


FIG. 129. Spectrum of neutrons from fission of uranium 235.

Recoil atoms, i.e. atoms which have received part of the energy of a neutron as a result of elastic collision, are consequently capable of ionizing, exciting or dissociating molecules of the substance; this is one of the causes of chemical activation of substances on their exposure to fast neutrons.

It should be mentioned that when the neutron energy is sufficiently high, the recoil atoms are themselves partially ionized by losing electrons. In this case the energy of a neutron is expended not only on accelerating a recoil atom but also (mainly) on ionizing (and exciting) it.

Thermal neutrons are captured with high probability by the nuclei of many elements. This results in the formation of a nucleus of a new, heavier isotope of the element. The energy liberated is usually 6 to 8 MeV and is radiated as a gamma-photon.⁽⁴¹⁾ Here an important exception is the formation of deuterium $n_0^1 + H_1^1 = D_1^2$ with an energy effect of 2.22 MeV. As a gamma-photon with energy E_γ has momentum E_γ/c (c is the velocity of light), an atom formed as a result of neutron capture by a nucleus must receive the same momentum. It follows from this that the energy of a recoil atom is

$$K_A = E_\gamma^2 / 2c^2 m_A, \quad (32.3)$$

where m_A is the mass of the nucleus. Replacing m_A by the atomic weight

(41) Consequently neutron-capture reactions are represented by the symbol (n, γ) .

A, we obtain from (32.3)

$$K_A = E_\gamma^2/1862A \text{ MeV.} \quad (32.3a)$$

Substituting in equation (32.3a) $E_\gamma = 2.22 \text{ MeV}$ and $A = 2$, we find that the energy of a deuteron formed as a result of neutron capture by a proton is $K_A = 1320 \text{ eV}$. This energy is much greater than the bond energy in the hydrogen molecule which is 4.5 eV . For this reason a newly-formed deuterium atom does not remain in the molecule and, as it has a large supply of energy, it must be not merely an active particle but also a particle capable of activating molecules colliding with it.

Hot particles

Recoil atoms with sufficiently high energy, which are consequently called "hot atoms", are obtained as a result of neutron capture by practically all nuclei. Hot atoms are also obtained as a result of other nuclear reactions, for example in the $(n, 2n)$ reaction, which results in formation of a lighter isotope of the element, e.g. $n + \text{Cu}^{63} = \text{Cu}^{62} + 2n$, and in the (γ, n) reaction, which is the reverse of neutron capture.⁽⁴²⁾

It is not difficult to see that hot atoms may also be formed as a result of beta-decay of nuclei. In this case it follows from the law of the conservation of momentum that the maximum energy of recoil atoms is

$$K_A = E_\beta/1839A, \quad (32.4)$$

where E_β is the maximum beta-particle energy. From this formula, when $E_\beta = 1 \text{ MeV}$ and $A = 10$, the energy K_A of the hot atoms is 54 eV . In the particular case of the C^{14} carbon isotope, as $(E_\beta)_{\text{max}}$ here is only 0.154 MeV , the energy of the hot N^{14} atom formed from C^{14} by beta-decay is only 6 eV . As this figure is only a little larger than the bond energy of the atoms in the molecule, being at the same time the maximum energy of translational motion of the hot atom, it might be expected that only a small number of such atoms could be liberated from the molecules. Also a study of the distribution of activity in a system initially containing ethane $\text{H}_3\text{C}^{14}\text{C}^{14}\text{H}_3$ (doubly labelled with C^{14}), showed that only 47 per cent of the ethane molecules in which a carbon atom underwent beta-decay remain in an undecomposed form, i.e. as methylamine $\text{H}_3\text{C}^{14}\text{NH}_2$ [1311]. It follows from this that during beta-decay of nuclei there is another source of energy which enables chemical bonds to be broken. Detailed study of the beta-decay process of C^{14} shows that in this case the source is the change in energy of the electron shell which results from the increase in nuclear charge on

⁽⁴²⁾ Schuler [1115] studied the chemical activity of hot iodine atoms obtained in the reactions $\text{I}^{127}(d, p) \text{I}^{128}$, $\text{I}^{127}(n, 2n) \text{I}^{126}$ and $\text{I}^{127}(\gamma, n) \text{I}^{128}$; their activity is identical with that of iodine atoms obtained in the reaction $\text{I}^{127}(n, \gamma) \text{I}^{128}$. He concludes from this that the energy of a hot atom has only a small effect on its chemical activity. See, however, [1116].

beta-decay, and which becomes considerable (~ 45 eV [1131]) when this process is non-adiabatic. The experimental result for the beta-decay of ethane is also apparently supported by theoretical calculation [1314].

The high chemical activity of hot atoms is reflected in their ability to replace other atoms or atomic groups in various compounds. For example, detection of radioactive CH_2I_2 when CH_3I is exposed to neutrons, or of radioactive CH_3I and $\text{C}_2\text{H}_5\text{I}$ when a solution of iodine in ethyl alcohol is exposed,⁽⁴³⁾ is evidence that hot iodine atoms are able to replace H atoms, OH and CH_2OH radicals and so on. It has been established [280, 60, 58] that the degree of conversion of CH_3I into CH_2I_2 is temperature-independent in the temperature range -195 to 15°C . It follows from this that in this case the reaction cannot be represented by the scheme



which is the usual scheme for the chemical metathetic reaction. The possibility is not ruled out that part of the energy of the hot atom is transferred to other parts of the molecule at the moment of its departure, and consequently the molecule undergoes more extensive splitting, decomposing for example into CH_2 , H and I. The formation of CH_2I_2 may be connected with the process $\text{CH}_2 + 2\text{CH}_3\text{I} = \text{CH}_2\text{I}_2 + \text{C}_2\text{H}_6$.

We should note that CH_2I_2 is also formed in the photolysis of CH_3I (in the presence of silver). In this case the formation of CH_2I_2 is attributed by West and Schlessinger [1277] to the processes $\text{CH}_3 + \text{CH}_3\text{I} = \text{CH}_4 + \text{CH}_2\text{I}$ and $\text{CH}_2\text{I} + \text{I} = \text{CH}_2\text{I}_2$, which apparently have a heterogeneous character and a considerable activation energy [1098]. However, it must be pointed out that these results are disputed by Schultz and Taylor [1118] who found that the rate of formation of methane when methyl iodide CH_3I is exposed to the line 2537 \AA is temperature-independent in the temperature range 40 to 100°C (see also [1161]). They conclude from this that under their experimental conditions hot CH_3 radicals are formed and interact with CH_3I , according to the scheme $\text{CH}_3 + \text{CH}_3\text{I} = \text{CH}_4 + \text{CH}_2\text{I}$, with zero activation energy. Assuming that an excited iodine atom (excitation energy 22 kcal) is formed in the photolysis of CH_3I , Schultz and Taylor obtain from the energy absorbed (112 kcal) and the bond energy of $\text{H}_3\text{C—I}$ (54 kcal) and the law of conservation of momentum that the energy of the hot CH_3 radical is 32 kcal. In the opinion of Martin and Noyes [919] the hypothesis of the formation of hot CH_3 radicals in the photolysis of CH_3I ,

⁽⁴³⁾ In this case the hot atoms are atoms of the beta-active iodine isotope I^{128}_{53} which is formed on neutron capture by iodine 127. The energy radiated in this process is 7.26 MeV and hence, from formula (32.3), the energy of an iodine 128 atom is 220 eV. Iodine 128 has a half life of 25 min and a relatively complex beta-spectrum, comprising several groups of beta-particles.

and also of $\text{Hg}(\text{CH}_3)_2$, is supported by their investigations of the reaction of CH_3 and O_2 .⁽⁴⁴⁾ See also [787, 716].

In the above estimation of the energy of a hot CH_3 radical it was assumed that it differs from a normal ("cold") radical by having an excess of energy of translational motion. This assumption may be correct in certain cases. Thus, there is scarcely any other explanation for the two-fold increase, detected by Kondrat'ev and coworkers [142], in the amount of HI oxidized when the wave length of the photochemically active light is decreased (corresponding to an increase from $K_{\text{H}} = 11.5$ kcal to $K_{\text{H}} = 21.5$ kcal in the kinetic energy of the H atom initially formed).⁽⁴⁵⁾ However, owing to the ease of translational-energy exchange during collisions of atoms and molecules (see §21), it would be expected that hot atoms and radicals may be fast particles only in exceptional cases when the mass ratio of the colliding particles hinders energy exchange (as is the case in the system $\text{H} + \text{HI} + \text{O}_2$). In other cases hot atoms and radicals are, apparently, electronically-excited (especially metastable) particles, or possibly vibrationally-excited radicals. As there are few experimental facts, the question of the nature of hot particles in photochemical reactions is still unsettled.

As hot particles detected in radiation-chemical reactions have relatively high energy, it is very probable that they are electronically excited metastable particles and possibly also ionized particles. For example, Levey and Willard [873] studied the reaction of hot iodine atoms formed in the process $\text{I}^{127}(n, \gamma)\text{I}^{128}$ with methane CH_4 , $\text{I} + \text{CH}_4 = \text{CH}_3\text{I} + \text{H} - 49.4$ kcal, and found that adding the inert gases He, Ar and Xe decreases the yield of CH_3I , but not to such a degree as would have been the case if the hot atoms were fast iodine atoms. Moreover, these authors found that, of all the foreign gases they studied, the greatest inhibiting action belongs to those gases with ionization potentials less than the ionization potential of the iodine atom, i.e. to I_2 , CH_3I , $\text{C}_2\text{H}_5\text{I}$, $\text{C}_3\text{H}_7\text{I}$ and NO . It is possible that this fact should be considered as an indication that in this case the hot iodine atoms are I^+ ions (which may be in metastable states).

In favour of the idea that hot atoms and radicals are ionized particles is the high chemical activity of ions (see above, p. 515 *et seq.*); it is possible that the cases observed of temperature-independent radiation-induced chemical reactions should be considered as reactions of ions.

The reactions of hot particles, discovered by Szillard and Chalmers [1197], have found practical application in the chemical separation of various isotopes, in the synthesis of labelled substances with high specific activity, and also in neutron dosimetry.

⁽⁴⁴⁾ This hypothesis was first put forward by Williams and Ogg [1297].

⁽⁴⁵⁾ The occurrence of "hot" H atoms is also supported by the experiments of Williams and Ogg [1296] and Schwarz, Williams and Hamill [1127].

Ionic Yields of Radiation-Chemical Reactions

Quantitative studies of chemical reactions taking place under the action of radioactive radiation show that *ionic yields* of reactions, which are measured by the number of molecules reacted divided by the number of ion pairs formed, may have a variety of values for different reactions, in the same way as quantum yields. The ionic yields for some reactions are shown in Table 49.

TABLE 49

Ionic yields of radiation-chemical reactions

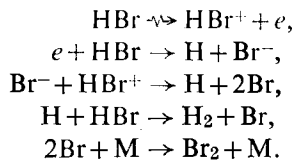
		Gas phase			
Reaction		Radiation	Ionic yield	Temperature, °C	
$2\text{H}_2 + \text{O}_2 = 2\text{H}_2\text{O}$.	α	3.4—4.0	—75—+25	
$2\text{CO} + \text{O}_2 = 2\text{CO}_2$.	α	3.9—4.4	—	
$\text{CO} + \text{Cl}_2 = \text{COCl}_2$.	α	8.5×10^4	—	
Polymerization of C_2H_2	.	α	20	—	
$\text{H}_2 + \text{I}_2 = 2\text{HI}$.	α	6	—	
$\text{H}_2 + \text{Br}_2 = 2\text{HBr}$.	α	2	—	
$2\text{HBr} = \text{H}_2 + \text{Br}_2$.	α	3	—	
$\text{H}_2 + \text{Cl}_2 = 2\text{HCl}$.	α	5×10^5	25	
$2\text{NH}_3 = \text{N}_2 + 3\text{H}_2$.	α	0.80	18	
" "	.	α	1.58	108	
" "	.	α	2.33	220	
" "	.	α	2.55	315	
Condensed phase					
$\text{H}_2\text{O} \rightarrow \text{H}_2 + \text{O}_2 + \text{H}_2\text{O}_2$.	α	0.86—1.05	—	
$2\text{HBr} = \text{H}_2 + \text{Br}_2$.	α	2.6	—	
Ice $\rightarrow \text{H}_2 + \text{O}_2$.	α	0.05	—	
$\text{H}_2\text{O} \rightarrow \text{H}_2\text{O}_2$.	β, γ	0.2—0.5	—	
Decomposition of $\text{C}_2\text{H}_5\text{OH}$.	β, γ	0.2	—	
" " $(\text{C}_2\text{H}_5)_2\text{O}$.	β, γ	3	—	
" " CHCl_3	.	β, γ	0.1	—	
" " $(\text{CH}_3)_2\text{CO}$.	β, γ	2—8	—	

It is seen from this table that for certain reactions the ionic yield is less than unity. One reason for low ionic yields, as in the case of photochemical reactions, may be the occurrence of the reverse reaction.

However, the main reason for low yields in radiation-chemical reactions is apparently the occurrence of deactivation processes, namely recombinations of the initially formed ion pair (an ion plus an electron) or recombinations of radicals.

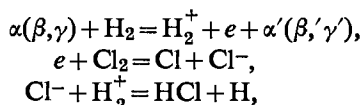
For many simple systems we may take as a standard ionic yield that of four molecules reacting for each ion pair (similar to a quantum yield of two).

which is characteristic of many photochemical reactions). An ionic yield of 4, for instance, is obtained from the following mechanism for the decomposition of hydrogen bromide HBr, proposed by Eyring, Hirschfelder and Taylor [590] for the reaction effected by alpha-particles:

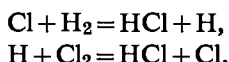


It is natural to attribute the somewhat lower ionic yield (3, Table 49) actually observed in this case to the occurrence of deactivation processes (for example, $e + \text{HBr}^+ \rightarrow \text{HBr}$ or $\text{H} + \text{H} \rightarrow \text{H}_2$). It is interesting that the ionic yield for the decomposition of HBr under the effect of X-rays is 4.6, i.e. is greater than 4 [1333]. The decomposition of excited molecules, which are formed to a certain extent in parallel with ion pairs, must be considered as responsible for this increase [1333]. The absence of the effect (or the lesser effect) of deactivation processes in the reaction excited by X-rays must be attributed to the lower ionizing capacity of the latter, and consequently to the lower density of active particles; here, therefore, the recombination processes are less probable than in the case of the reaction effected by bombarding HBr with alpha-particles.

Ionic yields much greater than 4 are evidence that the reaction has a chain character. A typical example, as in the case of photochemical reactions, is the reaction of chlorine with hydrogen. It is seen from Table 49 that the ionic yield of this reaction is of the same order as the quantum yield (10⁶). The similarity of ionic and quantum yields of hydrogen chloride is evidence that the mechanisms of the radiation-chemical and photochemical reactions are the same, in particular that the active chain-carrying centres (H and Cl atoms) leading to reaction are the same. These centres may be formed as a result of a primary process of dissociation of an H₂ or Cl₂ molecule on the action of an alpha- or beta-particle, and also as a result of subsequent conversions of the ions initially formed. In this case the following processes are possible:



followed by the normal chain reaction



and so on.

An interesting example of a chain reaction is the decomposition of chloroform CHCl_3 in an oxygen atmosphere under the action of gamma-rays (Co^{60}) which has been studied by Schulte, Suttle and Wilhelm [1117]. According to their data the reaction proceeds in two stages, and the main product of the first stage is the peroxide CCl_3OOH with a rate of formation independent of oxygen concentration. In the second stage of the reaction the peroxide disappears and in its place appear phosgene COCl_2 , HCl , CCl_4 , CO , CO_2 and other products. It is important to note the similarity to the thermal chain oxidation of hydrocarbons near room temperature which takes place in stages (the peroxide is formed predominantly in the first stage, see p. 627). This may be considered as an indication that there are similar features in the chain mechanism of the secondary processes in the two reactions.

TABLE 50

Ionic yields of radiation-chemical reactions and quantum yields of the corresponding photochemical reactions (according to Dainton [518])

Reaction	Radiation-chemical reaction		Photochemical reaction	
	Radiation	Ionic yield	Wave length Å	Quantum yield
Decomposition of NH_3	Alpha-particles Electrons	1.37 1.20	2144	1
Decomposition of HI	Alpha-particles X-rays	6 8	2000–2800	2
Decomposition of N_2O	Alpha-particles Electrons	4.4 3.9	1850–2000	1.3
Decomposition of H_2S	Alpha-particles	2.7	2080	1.0
Decomposition of CO	„ „	2	1295	1.0
Polymerization of $(\text{CN})_2$	„ „	7.4	2150	3.0
Oxidation of CO	„ „	6.6	1295, 1470	0.4

In Table 50 ionic yields of various radiation-chemical reactions excited by alpha-particles, electrons or X-rays are compared with one another and with the quantum yields of the corresponding photochemical reactions. It is seen from these data that the ionic yields of the same reaction caused by different penetrating radiations do not differ considerably. It may be

concluded from this that all three types of radiation have qualitatively the same activating effect. This fact is naturally explained when it is considered that the action of both alpha-particles and also beta-particles and gamma-quanta consists in the ionization or excitation of a molecule (see above).

TABLE 51

Products of the decomposition of methyl alcohol by Co^{60} gamma-rays and by 28 MeV helium ions (according to McDonell and Gordon [938]). The yields of the various products are expressed as the number of molecules per 100 eV)

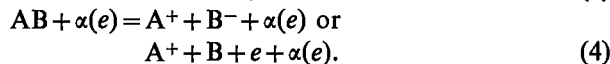
Product	Molecular yield per 100 eV	
	Gamma-rays	Helium ions
H_2	4.0 ± 0.3	3.46 ± 0.05
CO	0.16 ± 0.02	0.23 ± 0.01
CH_4	0.24 ± 0.06	0.36 ± 0.01
HCHO	1.3 ± 0.1	1.67 ± 0.05
$\text{HOH}_2\text{CCH}_2\text{OH}$ (ethyleneglycol)	3.0 ± 0.2	1.74 ± 0.04

This conclusion is also supported by the data of Table 51. In this table the yields of various products of the decomposition of methyl alcohol CH_3OH under action of Co^{60} gamma-rays are compared with yields of the same products obtained by decomposition of CH_3OH with helium ions of energy 28 MeV. The table shows that, in spite of the sharp difference between such activating radiations as gamma-rays and helium ions, the yields of individual products of the decomposition of CH_3OH do not differ considerably;⁽⁴⁶⁾ this would scarcely be possible if the mechanisms of the two reactions were very different.

Moreover the comparison of ionic yields with quantum yields of the corresponding reactions shown in Table 50 shows that in practically every case the quantum yield is lower than the ionic yield. The main cause of this difference is undoubtedly that not only ions are formed under the action of ionizing radiations but also excited molecules, which are one form of chemically active particle under radiation-chemical reaction conditions. In other words, the ionic yield does not completely characterize the activating effect of a penetrating radiation.

⁽⁴⁶⁾ The greatest difference in relative yields of ethyleneglycol and formaldehyde, $3.0 : 1.3$ (gamma-rays) and $1.74 : 1.67$ (helium ions), is explained according to McDonell and Gordon [938] by the relatively important role of recombination processes in the case of helium ions (cf. above), and accordingly the lower probability of the process $\text{H} + \text{CH}_3\text{OH} = \text{H}_2 + \text{CH}_2\text{OH}$, which leads to a lowering in the yield of ethyleneglycol formed as a result of the recombination of CH_2OH radicals.

Essex [571] considered different mechanisms for the primary (initiating) reaction in the case of the decomposition of NH_3 and N_2O and certain other reactions taking place under the action of alpha- and beta-particles. He considers the following mechanisms most probable for the model reaction $\text{AB} = \text{A} + \text{B}$:



By measuring the yield of reaction products when the radiation-chemical reaction is conducted in electric fields of different voltages (at low radiation intensities) and at different pressures, Essex estimated the relative role of each of the four initiation mechanisms for the various reactions he studied. Thus, for the decomposition of N_2O on the action of Ra alpha-particles (at a pressure of 105.7 mm Hg) he finds that of the overall ionic yield (yield per ion pair) of 2.47 N_2O molecules decomposed, 0.0, 0.43, 1.39 and 0.41 come from mechanisms (1), (2), (3) and (4) respectively and 0.24 from unknown mechanisms. According to Essex the main role in the formation of H and Cl atoms in the reaction of chlorine with hydrogen is played by mechanism (1) and a smaller role by mechanisms (2) and (4).⁽⁴⁷⁾

Primary active centres may apparently be formed as a result of the direct action of radioactive radiation on any molecule, whether it be a molecule of the reacting substance, of a reaction product or of an admixture, as indicated by measurement of the ionic yield of certain reactions in the presence of various inert gases. The results of such measurements are shown in Table 52. It is seen from these data that the ionic yield varies little in the presence of an inert gas. However, by diluting the reacting substances with an inert gas some part of the radiation energy is expended in ionizing molecules of this gas. In this case the observed small change in ionic yield may be explained by the activity of inert gas ions being not very much lower than that of the ions of the reacting substances, or by a high probability of charge transfer processes. These two explanations seem to be not without foundation. In fact, the high activity of singly-charged ions of all the substances studied would be expected because of their electric charge; the high probability of charge transfer, which results in the conversion of a molecule of the reacting substance into an ion radical on its collision with an ion of the inert admixture, would be expected since the ionization potentials of admixtures in all the reactions shown in Table

⁽⁴⁷⁾ The mechanism of formation of active centres (ions and radicals) in the radiolysis of water vapour has been considered by Laidler [860]. For the mechanism of other radiation-chemical reactions see, for example, [219a].

52 are higher than those of the reacting substances. This is evident from the following comparison of ionization potentials: the ionization potentials of the reacting substances are 11.41 eV (C_2H_2), 12.1 eV (O_2), 14.0 eV (CO), 10.2 eV (NH_3); the ionization potentials of admixtures are 15.65 eV (N_2), 24.45 eV (He), 21.47 eV (Ne), 15.69 eV (Ar), 13.94 eV (Kr), 12.08 eV (Xe), 15.37 eV (H_2), 13.79 eV (CO_2).

TABLE 52

Ionic yields of reactions taking place on the action of alpha-particles in the presence of inert admixtures at 25°C

Reaction	With no admixture	Ionic yield (number of molecules per ion pair)							
		Admixture							
		N_2	He	Ne	Ar	Kr	Xe	H_2	CO_2
Polymerization of C_2H_2	19.8	18.5	19.7	19.2	18.2	19.6	18.0	19.6	16.4
$2H_2 + O_2 = 2H_2O$	5.1	5.4	—	4.6	3.6	—	—	—	—
$2CO + O_2 = 2CO_2$	6.5	—	—	—	3.9	—	—	—	—
Decomposition of NH_3	1.0	—	—	1.0	—	—	—	—	—
Decomposition of HBr [1333]	4.6	—	—	—	4.7	4.0	4.7-5.2	—	—

Thus in most cases the charge transfer process is exo-energetic and consequently very probable (owing to the possibility of electronic or vibrational excitation of the molecular ion formed) (see p. 509).

In addition, certain effects observed when radiation-induced reactions are carried out in mixtures of two or more substances must also be attributed to the high probability of conversion of active centres resulting from charge transfer. Thus, it has been known for some time that the composition of the products of radiolysis of a binary mixture is quite different from the composition obtained when the components of the mixture are exposed separately and results for individual products are subsequently added up. The reason for this difference is that charge transfer to the component with the higher ionization potential from the more easily ionized component is rapid, and consequently there is a peculiar *screening* effect of the latter. The effect is that the substance with the higher ionization potential undergoes in the presence of the second substance considerably less conversion than would have been expected from its content in the mixture. Such an effect is detected, for instance, in the radiolysis of a mixture of benzene C_6H_6 and cyclohexane C_6H_{12} under the action of 540 keV electrons [908]. Since the ionization potential of benzene is 9.2 eV and that of cyclohexane is 9.9 eV, in this case a marked

screening effect of benzene would be expected. This screening effect is reflected, for example, in the fact that the yield of ethylene C_2H_4 is 0.17 molecules per 100 eV in pure cyclohexane vapour but is zero in a mixture of $0.45 C_6H_{12} + 0.55 C_6H_6$. Benzene also greatly influences the yield of hydrogen, which in pure cyclohexane vapour is 1.4 molecules per 100 eV but in the mixture of $0.45 C_6H_{12} + 0.55 C_6H_6$ is only 0.2 molecules per 100 eV (see also [879a]).

However, it must be noted that in the latter case the decreased yield apparently results not only from the charge transfer process but also from the interaction of hydrogen atoms with C_6H_6 molecules, which leads to H addition according to the scheme $H + C_6H_6 = C_6H_7$ competing with the formation of molecular hydrogen, $H + C_6H_{12} = H_2 + C_6H_{11}$.

In certain cases the effect of admixtures on the yield of products of radiation-induced reactions may be purely chemical. An interesting example of such a chemical effect is the decomposition of CO_2 on the action of radiation from radon or from a nuclear reactor, which has been studied by Harteck and Dondes [726]. These authors showed that an admixture of nitrogen dioxide NO_2 in such a small amount as 0.5 per cent completely suppresses the reverse reaction and increases the yield of $CO + \frac{1}{2}O_2$ to $G = 9$ to 10,⁽⁴⁸⁾ whereas in the absence of NO_2 only 0.1 per cent of the initially dissociated CO_2 is decomposed. According to the mechanism proposed by Harteck and Dondes for the radiolysis of CO_2 in the presence of NO_2 , the effect of the NO_2 is that it interacts with O and C atoms formed as a result of the initial dissociation of CO_2 molecules by the action of ionizing radiation; thus, $O + NO_2 = NO + O_2$ and $C + NO_2 = NO + CO$ ($2NO + O_2 = 2NO_2$). In this way, removing C and O atoms suppresses the reverse reaction of CO_2 formation (and also the products of polymerization, C_nO_m), which leads to higher yields of $CO + \frac{1}{2}O_2$. Harteck and Dondes also propose a mechanism for the decomposition of CO_2 in the absence of NO_2 , on the basis of which they give a quantitative explanation of Lind's classic experiments on the radiolytic oxidation and decomposition of CO. These data clearly illustrate the large role of secondary, purely chemical radical and radical-chain processes in the mechanism of the radiation-induced reaction. These processes also play an important role in the mechanism proposed by Harteck and Dondes [727] for the formation of NO_2 and N_2O (the fixation of nitrogen) by the action of ionizing radiation from an atomic reactor on a mixture of nitrogen and oxygen.

The above example of the radiolysis of a mixture of benzene and cyclohexane shows clearly the influence of structural properties of the compounds irradiated (in this case the presence or absence of an aromatic bond) on the nature of the reaction, and consequently on the composition of the

⁽⁴⁸⁾ Here the yield is measured in terms of G (the *energy yield*), which is expressed as the number of molecules of reaction product per 100 eV of energy absorbed.

radiolysis products. The connection between the nature of the radiolytic reaction and the structure of the compounds irradiated is also shown by other examples. Thus, study of products from radiolysis of various (the simplest) alkyl iodides by electrons or X-rays shows that C—I bonds are broken much more readily than C—C bonds; this is in accordance with the relative stability of the bonds. Gevantman and Williams [670] irradiated gaseous alkyl iodides in the presence of small quantities of molecular iodine containing the radioactive I^{131} isotope and, by measuring the activity of the reaction products formed by interaction of the primary products of the radiolysis with elementary iodine, determined the distribution of activity between the various iodides so formed (as percentages of the total activity). Their results are shown in Table 53.

TABLE 53

Distribution of activity in products from radiolysis of various alkyl iodides in the presence of radioactive iodine

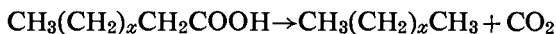
Initial iodide	Radiation	Activity of reaction products					
		CH ₃ I	C ₂ H ₅ I	n-C ₃ H ₇ I	iso-C ₃ H ₇ I	n-C ₄ H ₉ I	CH ₂ I ₂
CH ₃ I	Electrons	82	5	—	—	—	13
C ₂ H ₅ I	2 MeV X-rays	27	55	6	—	3	9
C ₂ H ₅ I	50 keV X-rays	34	66	0	—	0	0
n-C ₃ H ₇ I	" "	15	6	56	11	6	6
n-C ₄ H ₉ I	" "	10	7	2	2	71	8

It is seen from this table that in the radiolysis of CH₃I the radical CH₃ is formed with the highest probability; in the radiolysis of C₂H₅I the radical C₂H₅, of n-C₃H₇I the radical n-C₃H₇ and of n-C₄H₉I the radical n-C₄H₉ is formed with the highest probability; it is concluded from this that rupture of the C—I bond occurs the most readily.

According to measurements by the same authors of the radiolysis of alkanes (RH, R = alkyl) in the presence of iodine, the iodide of the initial R radical is not formed preferentially (except in the case of methane radiolysis). For example, in the radiolysis of normal butane n-C₄H₁₀ the following are formed in almost equal quantities: CH₃I (14.5%), C₂H₅I (13%), n-C₃H₇I (15.5%) and n-C₄H₉I (11.5%). It is interesting that in the radiolysis of normal pentane CH₃(CH₂)₃CH₃ the iodides CH₃I and C₂H₅I have 24 and 30 per cent, respectively, of the activity, whereas in the radiolysis of neopentane C(CH₃)₄ they have 80 and 4 per cent.

A peculiar effect of structural properties is observed during radiolysis

of fatty acids using alpha-particles. Here a predominant reaction is that of decarboxylation



whose yield decreases linearly with the increase in the number of carbon atoms in the initial acid molecule (from $x+3 = 2$ to $x+3 = 22$). The decreased yield of this reaction when the carbon chain is lengthened is undoubtedly connected with alpha-particle energy losses in activating the chain, so that the activation is not transmitted to the carboxyl group of the acid molecule and therefore does not lead to elimination of CO_2 . Here, then, we have an effect which is the reverse of that observed in the examples of Table 52, where activation of the admixture is equivalent to activation of the reacting substances themselves.

Further examples of the effect of the structural properties of organic compounds on their radiation-induced chemical reactions may be found in the review by Collinson and Swallow [495].

CHAPTER 9

CHAIN REACTIONS

§33. Simple Chain Reactions

Two Types of Complex Reactions: Non-chain and Chain Reactions

We may distinguish between simple and complex chemical reactions (see p. 4): a simple reaction takes place *in one elementary act* and its chemical equation is *identical* with its stoichiometric equation, whereas a complex reaction is a *combination* of consecutive or parallel elementary processes or acts. Therefore a complex chemical reaction always has a more or less *complex mechanism* which is the sum of the individual simple *elementary processes*. Only in rare cases does the chemical equation of a complex reaction coincide with its stoichiometric equation (see above, p. 61).

The formation of *intermediate substances*, which are usually more reactive than the initial substances, is characteristic of complex chemical reactions.

It is necessary to distinguish *two types* of complex reactions. The first of these may be represented by the scheme shown in Fig. 130. In this scheme A represents an active particle (a molecule, atom or radical), X an intermediate substance and C a reaction product. The figures 0, 1, 2, 3 and 4 denote the individual elementary processes thus: (0) the activation process, (1) the reaction of the active molecule leading to formation of the intermediate substance X, (2) the deactivation process, (3) the reaction of substance X resulting in formation of the reaction product C and (4) a process leading to disappearance of the intermediate substance but without formation of the reaction product. If the rate of activation is W_0 and the probabilities of the remaining four elementary processes are represented by w_i ($i = 1, 2, 3, 4$), we may express the rate W of the complex reaction by the formula:

$$W = d(C)/dt = W_0 w_1 w_3. \quad (33.1)$$

Here (C) denotes the concentration of the reaction product.

The probabilities w_1 and w_3 in (33.1) may be written

$$w_1 = v_1/(v_1 + v_2), \quad w_3 = v_3/(v_3 + v_4) \quad (33.2)$$

(by definition $w_2 = 1 - w_1$ and $w_4 = 1 - w_3$). The quantities v_1, v_2, v_3 and v_4 are the *frequencies* of the appropriate processes, i.e. the number of acts of

interaction of one particle (A or X) per second. Each of the v_i may be expressed as the product of the rate constant of the appropriate elementary process and the concentration of the molecules reacting with the given molecule (A or X).

Substituting (33.2) in (33.1) we obtain

$$W = W_0 \frac{v_1 v_3}{(v_1 + v_2)(v_3 + v_4)} = W_0 \frac{1}{1 + (v_2 v_3 + v_1 v_4 + v_2 v_4)/v_1 v_3} < W_0. \quad (33.3)$$

Consequently the rate of a complex reaction of this type must always be less than the rate of the activation process. Only in the limit when $w_1 = 1$ (i.e. $v_2 = 0$ so that deactivation does not occur), and $w_3 = 1$ (i.e. $v_4 = 0$ so that interaction of the intermediate substance always gives the reaction product), does the rate W of reaction equal the rate W_0 of activation.

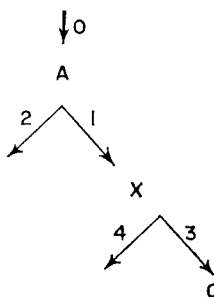


FIG. 130. Scheme of a complex reaction in which the active molecules A enter into reaction [path (1)] and form the intermediate substance X which in the course of the reaction is converted into the final reaction product C [by path (3)] or reacts without forming C [path (4)]; (0) the activation path, (2) path for deactivation of the active A molecules.

The expression (33.1) for the rate of reaction may also be obtained by integrating the kinetic equations of the reaction. When the reaction corresponds to the scheme in Fig. 130 these equations have the form

$$\left. \begin{aligned} d(A)/dt &= W_0 - (v_1 + v_2)(A) \\ d(X)/dt &= v_1(A) - (v_3 + v_4)(X) \\ d(C)/dt &= v_3(X). \end{aligned} \right\} \quad (33.4)$$

Integrating the first two equations under the assumption that the frequencies v are constant (this assumption is a rough approximation and is permissible only for the initial period of the reaction when the concentrations of the initial substances have changed but little), with the initial conditions that $(A) = 0$ and $(X) = 0$ when $t = 0$, we find

$$(A) = \frac{W_0}{v_1 + v_2} \{1 - \exp[-(v_1 + v_2)t]\}$$

and

$$(X) = W_0 w_1 \frac{(v_1 + v_2)\{1 - \exp[-(v_3 + v_4)t]\} - (v_3 + v_4)\{1 - \exp[-(v_1 + v_2)t]\}}{[(v_1 + v_2) - (v_3 + v_4)](v_3 + v_4)}. \quad (33.5)$$

In this case the rate of reaction is $W = v_3(X)$. Substituting in this expression the value found for (X) , we obtain for the reaction rate:

$$W = W_0 w_1 w_3 \frac{(v_1 + v_2)\{1 - \exp[-(v_3 + v_4)t]\} - (v_3 + v_4)\{1 - \exp[-(v_1 + v_2)t]\}}{(v_1 + v_2) - (v_3 + v_4)}. \quad (33.6)$$

According to (33.6) the rate of reaction is zero when $t = 0$. Expanding the exponential factors in series and limiting ourselves to the first three terms we obtain from (33.6)

$$W = \frac{1}{2} W_0 v_1 v_3 t^2. \quad (33.7)$$

Expression (33.7) is correct for times satisfying the conditions

$$t \ll (v_1 + v_2)^{-1}, (v_3 + v_4)^{-1},$$

i.e. for times much less than $\tau_A = (v_1 + v_2)^{-1}$ the lifetime of the active molecule A, and $\tau_X = (v_3 + v_4)^{-1}$ the lifetime of the intermediate substance X.

When the opposite relationship between t and τ_A and τ_X holds, i.e. for sufficiently large t satisfying the conditions $t \gg \tau_A, \tau_X$, the exponential factors in (33.6) become negligibly small and this expression takes the form of (33.1), i.e. $W = W_0 w_1 w_3$. Expression (33.1) may also be obtained directly from equations (33.4) assuming the concentrations (A) and (X) to be stationary. In fact, from the steady-state conditions

$$d(A)/dt = 0 \quad \text{and} \quad d(X)/dt = 0$$

we find

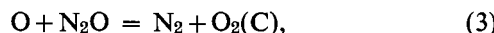
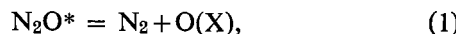
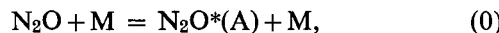
$$(A)_{st} = W_0(v_1 + v_2) \quad \text{and} \quad (X)_{st} = v_1/(v_3 + v_4)$$

$$(A)_{st} = W_0 w_1/(v_3 + v_4). \quad (33.8)$$

Substituting $(X)_{st}$ in the expression for the reaction rate $W = v_3(X)_{st}$ we obtain (33.1). Thus the probability treatment of reactions given at the beginning of this section may be used only when the reaction is *stationary* (steady). The expression for the reaction obtained in this way gives the rate in the stationary reaction.

An example of a complex reaction of this type is the thermal decomposition of nitrous oxide, the mechanism of which is the sum of the following

five processes (including the process of activation of N_2O molecules):



Here M stands for any particle capable of activating or deactivating a nitrous oxide molecule (in contrast with the formal scheme in Fig. 130, process (4) also leads to formation of a reaction product, O_2).

If the rate of activation of N_2O molecules is W_0 , then by introducing the probabilities w_i of the elementary processes, we find that the rate in the stationary reaction is

$$W = \frac{d(\text{O}_2)}{dt} = W_0 w_1 (w_3 + \frac{1}{2}w_4),$$

or, since $w_3 + w_4 = 1$,

$$W = \frac{1}{2} W_0 w_1 (1 + w_3).$$

Moreover, expressing the probabilities w_1 and w_3 in terms of the corresponding frequencies

$$w_1 = v_1/(v_1 + v_2) = k_1/[k_1 + k_2(\text{M})]$$

$$w_3 = v_3/(v_3 + v_4) = k_3(\text{N}_2\text{O})/[k_3(\text{N}_2\text{O}) + k_4]$$

since $W_0 = k_0(\text{M})(\text{N}_2\text{O})$, we have

$$W = \frac{d(\text{O}_2)}{dt} = \frac{k_0(\text{M})(\text{N}_2\text{O})k_1[k_3(\text{N}_2\text{O}) + \frac{1}{2}k_4]}{[k_1 + k_2(\text{M})][k_3(\text{N}_2\text{O}) + k_4]},$$

and hence $W < W_0$. In the limit, at sufficiently low (M) and (N_2O) the rate of the stationary reaction may become equal to $\frac{1}{2}W_0$ and only becomes equal to W_0 when process 4 does not take place ($k_4 = 0$). At higher pressures, for example pressures at which the reaction follows a unimolecular law and $k_2(\text{M}) \gg k_1$ and $k_3(\text{N}_2\text{O}) \gg k_4$, the rate of the stationary reaction

$$W = (k_0 k_1 / k_2)(\text{N}_2\text{O}) = k_1 W_0 / k_2(\text{M}),$$

in view of the first of these inequalities, is much less than the rate of activation W_0 .

The second type of complex reaction is shown schematically in Fig. 131. Reactions of this type differ from the previous type in that here an active molecule A is formed simultaneously with the molecule C of reaction product. Consequently, simultaneously with the generation of active molecules due to heat or some other external factor (for example, radiant energy), active molecules are also formed in reactions of this type by the

reaction itself, resulting in continuous *regeneration* of active molecules: the reaction supplies new active particles to replace those which have entered into reaction. A reaction, beginning with one active particle by repeating the same cycle or link so that a new active particle is generated each time, does not cease until the link sequence is broken by destruction of the active molecule. Such reactions are called *chain reactions*. A characteristic property of chain reactions is the periodic regeneration of active particles.

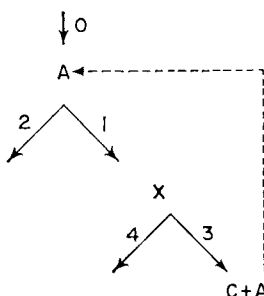


FIG. 131. Scheme of a chain reaction. In this complex reaction there are two sources of active A molecules: thermal or external (for example, photochemical) activation—path 0 and the reaction itself—paths 1 and 3—leading to the regeneration of active molecules.

By allowing for the two sources of active molecules—the effect of the factor⁽¹⁾ supplying active molecules at a rate W_0 and the chemical reaction itself supplying active molecules at the same rate as that of formation of the reaction product, i.e. at the reaction rate W —we may express the rate in the stationary chain reaction by the equation

$$W = W_0 w_1 w_3 + W w_1 w_3,$$

from which we find

$$W = \frac{W_0}{(1/w_1 w_3) - 1} = W_0 \nu. \quad (33.9)$$

The quantity

$$\nu = \frac{1}{(1/w_1 w_3) - 1} = \frac{w_1 w_3}{1 - w_1 w_3} \quad (33.10)$$

is called the *chain length*. It is apparent from expression (33.9) that the chain length is equal to the ratio of the rate of reaction, W , to the rate of thermal generation of active molecules, W_0 , i.e. ν is equal to the number of molecules of reaction product formed per active molecule formed by the action of heat.

⁽¹⁾ In future for simplicity we shall just consider heat, i.e. the thermal generation of active centres (particles).

Expressing the product w_1w_3 in terms of the corresponding frequencies,

$$w_1w_3 = \frac{v_1v_3}{(v_1 + v_2)(v_3 + v_4)},$$

it is not difficult to see that, when the frequency v_1 is much greater than v_2 and v_3 much greater than v_4 , this quantity is quite close to unity, i.e. the chain is quite long. When $w_1w_3 = 1$ the chain length $\nu = \infty$. Experiments show that the chain length is sometimes of the order of 10^5 to 10^6 .

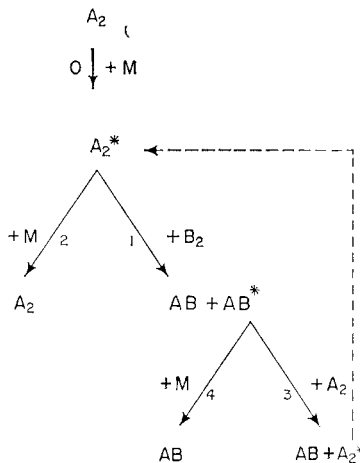
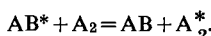


FIG. 132. Scheme of an energy chain. The regeneration of active A_2^* molecules takes place as a result of energy transfer from the reaction product AB^* to molecules of initial substance on collision



On the basis of the ideas of van't Hoff and Arrhenius regarding the possibility and frequent occurrence of bimolecular reactions between chemically-saturated molecules, several authors have suggested that the active molecules in chain reactions are also chemically-saturated molecules rich in energy as is the case, for example, in unimolecular reactions (see the foregoing example). According to these ideas, as put forward by Bodenstein [416], Christiansen and Kramers [488] and others, active molecules formed on account of the reaction result from energy transfer to molecules of the initial substances from molecules of the reaction products; this is shown schematically in Fig. 132 for the reaction $A_2 + B_2 = 2AB$. Here the process 0 represents the primary activation of a molecule A_2 of initial substance on its collision with an M molecule (thermal activation). The active molecule A_2^* either interacts chemically with a molecule B_2 of the second initial substance, (process 1), or is deactivated by colliding with an M molecule (process 2). The reaction-product molecules AB^* formed in

process 1 initially have an increased energy consisting of the energy of the A_2^* and B_2 molecules and the heat liberated by the exothermic reaction 1. Moreover, it may be assumed that this energy may be transferred by the AB^* molecule to an A_2 molecule colliding with it, so that A_2 is activated (process 3); alternatively by colliding with an M molecule AB^* may lose its energy (process 4). By writing the expression for the reaction rate allowing for the possibility of A_2 molecules being activated as a result of the reaction,

$$W = d(AB)/dt = 2W_0w_1 + Ww_1w_3,$$

we find

$$W = 2w_1W_0/(1 - w_1w_3) = W_0\nu,$$

where

$$\nu = 2w_1/(1 - w_1w_3).$$

It is seen from the expression obtained for the rate in the stationary reaction that the assumption regarding active molecules as molecules having an increased energy formally leads to the result we obtained earlier, namely that long (in the limit, infinite) chain lengths are possible. However, in order for this to occur it is necessary that the probabilities w_1 and w_3 should be quite close to unity; but on the basis of all the known experimental data on energy transfer during molecular collisions and on rates of elementary chemical processes this is very unlikely. In fact the experimental rate constants of various bimolecular processes show that as a rule these processes have a steric factor of about 0.1 to 0.01, i.e. that only one in 10 or even one in 100 collisions of active molecules is effective. An active molecule which undergoes this number of collisions has a good chance of being deactivated; and this apparently takes place in practice. This is quite to be expected, since from general considerations it may be concluded that a chemical process, which is always connected with a rearrangement of the reacting system, must be less probable than the simpler physical process of energy redistribution which leads to molecular deactivation. An experimental indication of the correctness of this conclusion is that the rate of unimolecular decomposition at pressures high enough for the requisite rate of molecular activation is much less than the rate of deactivation. Therefore the chance of the probability w_1 of process 1 being unity must be considered to be small.

It is even less probable that w_3 should be nearly unity. In this case the competing processes are the transfer of a large amount of energy from the AB^* molecule to an A_2 molecule colliding with it, and deactivation, i.e. dissipation of energy by collision of the AB^* molecule with an M molecule. But, as we have seen earlier (p. 383), during molecular collisions energy is transferred between molecules only in small amounts. Consequently,

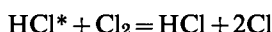
deactivation of an AB^* molecule must be considered much more probable than process 3.

Chains involving active molecules, which are energy-rich chemically-saturated molecules, are called *energy chains*. Above we have given some general considerations, based on experimental data, which indicate a low probability for energy chains. However, the most weighty argument against the widespread occurrence and even the possibility of pure energy chains is the fact that scarcely any chain reaction studied has supported the hypothesis of energy chains.

In fact, only in the one case of the photochemical decomposition of ozone are there grounds for considering that the chain mechanism involves energy-rich molecules of oxygen as well as oxygen atoms (see below, p. 572). However, since this reaction involves *two types* of active centres, the chains here are not pure energy chains but should be called *mixed chains*.⁽²⁾ It should also be mentioned that the energy-rich active molecules of oxygen in this reaction are apparently electronically excited metastable molecules. As it is very probable that hot particles are also metastable particles (see p. 551) the possibility is not ruled out that reactions involving hot particles follow a mixed chain mechanism.

Shuler [1136] has recently taken up the question of energy chains in connection with the fast chemical reactions occurring in high-temperature flames. However, it seems that here we must also think of mixed radical-energy chains, as it is scarcely possible to assume that at high temperatures free atoms and radicals lose their role as active centres of chain reactions.

In flame conditions it is very probable that there are mixed chains of the type postulated by Semenov in his theory of so-called branched-chain reactions (see below) as applied to the formation of hydrogen chloride HCl from hydrogen and chlorine [932]. Assuming that the energy liberated in the elementary process $H + Cl_2 = HCl + Cl + 45.5$ kcal is initially concentrated mainly in the reaction-product molecule HCl^* —this assumption was confirmed later [J. K. Cashion and J. C. Polanyi, *J. Chem. Phys.*, **29**, 455 (1958); **30**, 1097 (1959)]—and that, owing to the high temperature of the flame, the concentration of chlorine molecules with energy much greater than the mean thermal energy is sufficient for the process



to compete successfully with the process of energy dissipation on collision of HCl^* with other molecules (see above), we obtain an additional source of chlorine atoms which is “cheaper” than the usual thermal dissociation of Cl_2 molecules. Indeed, the dissociation process requires an expenditure of 57.2 kcal, whereas the formation of the same two chlorine atoms as a

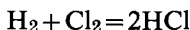
⁽²⁾ This mechanism is apparently also followed by the isotopic exchange reaction of oxygen ($O^{16}O^{16} + O^{18}O^{18} = 2O^{16}O^{18}$) which is catalysed by ozone [991].

result of the process $\text{HCl}^* + \text{Cl}_2 = \text{HCl} + 2\text{Cl}$ requires only 11.7 kcal in the limit, i.e. when the entire heat of the reaction $\text{H} + \text{Cl}_2 = \text{HCl} + \text{Cl}$ is used. The part played by the energy in a mixed chain reaction must obviously be especially great when the reacting chemical system is far from equilibrium, as would be expected in the case of hot flames.

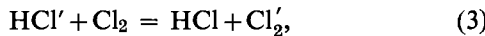
Experimental studies of the mechanism of chain reactions show that the active molecules or active centres in chain reactions are chemically unsaturated fragments of molecules—*free atoms and radicals*. The leading role of active centres of this type is shown by kinetic investigations of various chain reactions, by direct detection of free atoms and radicals in the reaction zone, and also by many experiments on the effect of atoms and radicals on the rate of chemical reactions. The high chemical activity of free atoms and radicals is also a cause of the high rate and wide occurrence of chain reactions. Chains carried by free atoms or radicals are called *chemical or radical chains*.

Reaction of Chlorine with Hydrogen

An example of a radical-chain reaction is the photochemical (and also thermal) formation of hydrogen chloride HCl from hydrogen and chlorine which we considered earlier. In 1913 Bodenstein [415] measured the “quantum yields” of twenty-two reactions, including the reaction

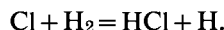


for which he obtained 10^6 . This factor itself indicated the chain character of the reaction. Bodenstein first suggested that the chains are connected with electrons formed, as he thought, as a result of photo-ionization of chlorine molecules. This assumption was not supported experimentally, however. Also lacking experimental support is his suggestion (1916) [416] that the mechanism of the photosynthesis of hydrogen chloride is based on energy chains and consists of the following processes (the prime denotes an electronically excited active molecule):



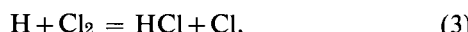
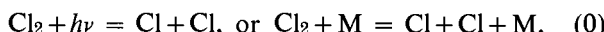
(In the reaction mechanism proposed by Bodenstein there is another process allowing for the inhibiting effect of oxygen which has been experimentally established.) It is not difficult to see that this mechanism corresponds precisely to that shown in Fig. 132 for a reaction involving energy chains.

The currently accepted mechanism for the reaction of hydrogen and chlorine, which has been substantiated quantitatively by many experiments, is based on Nernst's suggestion (1918) [969] that the primary active centres of the photochemical reaction are chlorine atoms resulting from photochemical splitting of Cl_2 molecules (in the thermal reaction the chlorine atoms are formed by thermal dissociation of the molecules) and reacting with hydrogen molecules according to the scheme

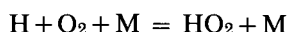


The hydrogen atoms formed react in their turn with chlorine molecules, $\text{H} + \text{Cl}_2 = \text{HCl} + \text{Cl}$, thus regenerating chlorine atoms and making propagation of the reaction chain possible. Thus the reaction of chlorine and hydrogen involves two active centres, namely Cl and H atoms.

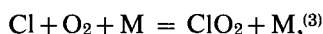
In the radical-chain mechanism for the photochemical and thermal reactions of chlorine and hydrogen the most important elementary processes are:



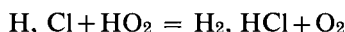
Here we have not considered the recombination of H atoms (i.e. the processes $\text{H} + \text{H} + \text{M} = \text{H}_2 + \text{M}$ and $\text{H} + \text{Cl} + \text{M} = \text{HCl} + \text{M}$) which, as the H atoms have relatively low concentration due to their high activity, does not play an important role and in practice cannot compete with the fast processes (3) and (4). The inhibiting effect of various foreign admixtures (negative catalysts such as O_2 , ClO_2 , NCl_3 , NH_3 , see [1081, pp. 307–10]) leads to the conclusion that the reaction mechanism must include processes connected with interaction of H atoms (and also Cl atoms) with admixture molecules and causing chain breaking. In the case of inhibition by molecular oxygen these processes are apparently the following [422, 854]:



and



followed by the processes



⁽³⁾ Porter and Wright [1039] found that under their experimental conditions chlorine atoms disappear forty-six times faster as a result of interaction with O_2 than as a result of recombination (when oxygen is replaced by nitrogen).

and



A clear case of the inhibiting effect of an admixture (which is frequently uncontrollable) is the occurrence of the so-called *induction period* of a photochemical reaction. As early as 1801 it was noted [509] that the reaction of chlorine with hydrogen (and also with hydrocarbons) is not immediate: the rate of reaction becomes appreciable only after a certain interval of time. Subsequent investigations showed that the duration of this interval, which is called the induction period [464], depends on the way the mixture was prepared and on other factors (for example, on preliminary exposure to light). The inhibiting effect of oxygen discovered by Bunsen and Roscoe is very important in explaining the nature of the induction period in this reaction.⁽⁴⁾ Later it was shown that the presence of foreign admixtures in the reacting mixture is the main factor determining the duration of the initial time lag or induction period of the reaction. In the presence of admixtures the primary active centres (Cl atoms) react mainly with admixture molecules and consequently in practice the chains cannot develop so that the reaction rate is immeasurably small. Only at the end of the induction period when most of the admixture has been used up do the chains begin to play an appreciable role, resulting in a measurable reaction rate.

Taking process 2 as the sum of the processes leading to chain termination by destruction of Cl atoms and introducing process 4 as the sum of processes connected with destruction of H atoms, then the generalized reaction mechanism for the initial period when the concentration of reaction product is still small may be represented by a scheme practically identical with the formal scheme of Fig. 131. Introducing the probabilities of the relevant processes and denoting the rate of the photochemical or thermal generation of chlorine atoms by W_0 , then on the basis of this scheme the rate in the stationary reaction will be represented by the equation

$$W = d(\text{HCl})/dt = 2W_0w_1(1+w_3) + Ww_1w_3,$$

whence

$$W = \frac{2W_0}{[(1+w_1)/w_1(1+w_3)]-1} = W_0\nu,$$

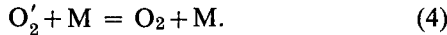
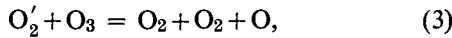
where

$$\nu = \frac{2}{[(1+w_1)/w_1(1+w_3)]-1}.$$

⁽⁴⁾ Bunsen and Roscoe [464] found that an admixture of 0.5% oxygen in a mixture of chlorine and hydrogen leads to a ten-fold decrease in the reaction rate.

As we shall see, the chain length, and consequently the reaction rate, tends to ∞ when w_1 and w_3 tend to unity. For this to occur it is necessary that processes 1 and 3, leading to extension of the reaction, should be much more probable than the processes connected with chain breaking.

Let us consider another example of a chain reaction. According to the data of Schumacher [1120], which have subsequently been supported by several authors [739], the chain reaction for the photochemical decomposition of ozone⁽⁵⁾ follows the mechanism:



Here O_2' denotes an excited oxygen molecule. Since the heat of process (1) is 93.2 kcal it may be assumed that this process results in the formation of metastable O_2' molecules in the state ${}^1\Sigma_g^+$ with an excitation energy of 37.2 kcal. The interaction of these molecules with ozone molecules is an exothermic process (3) with a heat effect of 13.0 kcal.

According to the above mechanism for ozone decomposition, this reaction, like the formation of hydrogen chloride from chlorine and hydrogen considered above, involves two active centres. In contrast with the latter reaction, however, ozone decomposition involves (as we have already noted) active centres of *different types*: O atoms and electronically excited (metastable) O_2' molecules. No other reliable examples of mixed chain reactions are known.

The chain reactions considered in this section are called *simple chain reactions*. From the point of view of their mechanism simple chain reactions are distinguished by the property that there is *not more than one* newly created (regenerated) active centre for each one disappearing in each link of the chain in these reactions.

§34. Formal Kinetics of Chain Reactions

To explain the general features of the course of chemical chain reactions we shall consider a simplified reaction model as shown by the scheme in Fig. 133. Here the process (0), as before, represents the thermal generation of active A centres, process (1) the sum of elementary processes leading to formation of the reaction product C and ϵ active A centres, and process (2) the sum of processes connected with disappearance of the active centre,

⁽⁵⁾ Schumacher's assumption that the energy chains account for the thermal decomposition of ozone as well is apparently erroneous [380a].

i.e. with chain termination. To have general validity it must be taken that the number ϵ , i.e. the mean number of active centres formed in one link of the chain may have values other than unity; $\epsilon = 1$ corresponds to a simple chain reaction.

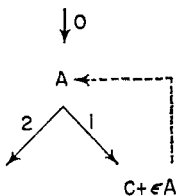


FIG. 133. Simplified scheme of a chain reaction involving one active centre. (0) Thermal (or external) generation of active centres A; (1) the sum of processes leading to formation of the reaction product C and ϵ active A centres; (2) the sum of processes leading to chain breaking.

Mean Chain Length

Introducing W_0 the rate of thermal generation of active centres (thermal generation of chains) and $w_1 = \alpha$ the probability of the reaction following path 1, which we shall call the *probability of chain propagation* after Semenov [232], then from the scheme in Fig. 133 the rate of the stationary reaction may be expressed by the equation

$$W = W_0\alpha + \epsilon W\alpha,$$

i.e.

$$W = d(C)/dt = W_0\alpha/(1 - \epsilon\alpha) = W_0\nu, \quad (34.1)$$

$$\nu = \alpha/(1 - \epsilon\alpha). \quad (34.2)$$

It is not difficult to see that in the case of simple chain reactions ($\epsilon = 1$) the chain length ν is the *mean number of links* per primary active centre, i.e. the *mean chain length*. In fact, the probability of the chain containing s links is clearly equal to

$$p_s = \alpha^s(1 - \alpha). \quad (34.3)$$

Here the quantity $1 - \alpha$ (which Semenov denoted by β) is the probability of chain breaking. From the foregoing formula we find the mean number of links of the chain is

$$\begin{aligned} \bar{\nu} &= \sum_{s=1}^{\infty} sp_s = \sum_{s=1}^{\infty} s\alpha^s(1 - \alpha) = (1 - \alpha)(\alpha + 2\alpha^2 + 3\alpha^3 + \dots) \\ &= \alpha/(1 - \alpha) = (1/\beta) - 1 = \nu. \end{aligned} \quad (34.4)$$

We shall show that short chains are the most probable. Taking the logarithm of the quantity $p_s = \alpha^s(1 - \alpha)$ and then differentiating $\ln p_s$

with respect to s we obtain $(d/ds) \ln p_s = \ln \alpha < 0$ (since $\alpha < 1$). Consequently the larger s the number of chain links, the smaller is p_s . By choosing a definite probability α of chain propagation, i.e. by choosing a definite

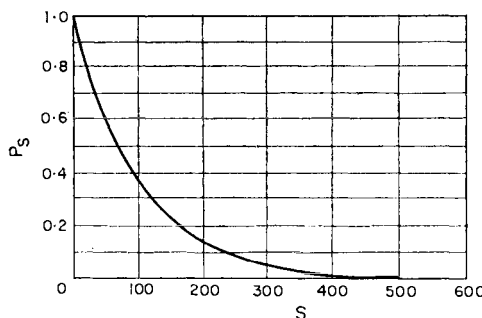


FIG. 134. Probability of the chain containing s links for $\alpha = 0.99$ and $\bar{v} = 100$ (according to Semenov [232]).

mean chain length \bar{v} , we may calculate p_s for different s from formula (34.3). Results of this calculation for $\bar{v} = 100$, i.e. $\alpha = 0.99$, are shown in Fig. 134 (according to Semenov [232]).

Development of Chains with Time

Writing the kinetic equations for n the concentration of active centres A and for the concentration of reaction product (C)

$$dn/dt = W_0 - (v_1 + v_2)n + \epsilon v_1 n = W_0 - (v_1 + v_2)(1 - \epsilon \alpha)n \quad (34.5)$$

and

$$W = d(C)/dt = v_1 n. \quad (34.6)$$

we may analyse the development of chains with time.

We shall consider first the case when $v_1 = 0$, i.e. when there is no reaction. In this case the differential equation for the concentration of active centres has the form

$$dn/dt = W_0 - v_2 n. \quad (34.7)$$

Integrating this equation with the initial condition $n = n_0$ when $t = 0$ we obtain

$$n = (W_0/v_2)(1 - \exp[-v_2 t]) + n_0 \exp(-v_2 t). \quad (34.8)$$

When $t \gg 1/v_2 = \tau_2$ (the lifetime of the active centre) the exponential factors disappear and the concentration of active centres becomes equal to the stationary concentration $n_{st} = W_0/v_2$, which is also obtained from the condition that $dn/dt = 0$. When activation results from thermal energy $n_{st} = n_{\text{equilib.}}$

Returning to the case when reaction does occur ($v_1 \neq 0$) we shall first consider the simple reaction ($\epsilon = 0$). In this case the differential equation for n has the form

$$\frac{dn}{dt} = W_0 - (v_1 + v_2)n, \quad (34.9)$$

and for the concentration of active centres we obtain

$$n = [W_0/(v_1 + v_2)][1 - \exp\{-(v_1 + v_2)t\}] + n_0 \exp\{-(v_1 + v_2)t\}.$$

For times much greater than the lifetime of the active centre, which is $(v_1 + v_2)^{-1} = \tau_0$ in this case, the stationary concentration $n_{st} = W_0/(v_1 + v_2)$ is *less* than the stationary concentration obtained in the absence of reaction. This decrease in the concentration of active centres results from their being consumed in the reaction. The rate of the stationary reaction is $W = v_1 n_{st} = W_0 v_1 / (v_1 + v_2) = W_0 \alpha$ (see 34.6).

When $\epsilon > 0$ the reaction becomes a chain reaction. Here we shall consider only the cases when $\epsilon \alpha < 1$. In this case integration of (34.5) yields

$$n = \frac{W_0}{(v_1 + v_2)(1 - \epsilon \alpha)} \{1 - \exp[-(v_1 + v_2)(1 - \epsilon \alpha)t]\} + n_0 \exp[-(v_1 + v_2)(1 - \epsilon \alpha)t]. \quad (34.10)$$

When t is much greater than the lifetime of the active centre, namely

$$(v_1 + v_2)^{-1}(1 - \epsilon \alpha)^{-1} = \tau,$$

this expression gives the stationary concentration of active centres, namely

$$n_{st}^{(r)} = W_0 / (v_1 + v_2)(1 - \epsilon \alpha).$$

Dividing this quantity by the stationary concentration in the absence of reaction, $n_{st} = W_0 / v_2$, and noting that $v_2 / (v_1 + v_2) = 1 - \alpha$, we find

$$n_{st}^{(r)} / n_{st} = (1 - \alpha) / (1 - \epsilon \alpha). \quad (34.11)$$

It follows from this expression that the occurrence of reaction leads to decrease or increase in the stationary concentration of active centres according as $\epsilon < 1$ or $\epsilon > 1$. When $\epsilon < 1$ the number of active centres consumed in reaction is greater than the number regenerated by the chain reaction and their stationary concentration is lowered in the presence of reaction. When $\epsilon > 1$ the opposite occurs.

Neglecting n_0 , the initial concentration of active centres, and introducing $\tau = 1 / (v_1 + v_2)(1 - \epsilon \alpha)$, the lifetime of the active centre, into (34.10), we obtain for the rate of reaction in this case

$$\begin{aligned} W &= v_1 n = [W_0 \alpha / (1 - \epsilon \alpha)][1 - \exp(-t/\tau)] \\ &= W_0 \nu [1 - \exp(-t/\tau)], \end{aligned} \quad (34.12)$$

where $\nu = \alpha / (1 - \epsilon \alpha)$, the mean chain length. Figure 135 shows graphically

the development of a chain reaction of this type with time. When the time is sufficiently great ($t \gg \tau$), the reaction becomes stationary. The rate in the stationary reaction is $W_{st} = v_1 n_{st} = W_0 v$. It is not difficult to see that the stationary rate of a chain reaction is greater than the rate of the non-chain reaction, $W = W_0 \alpha$.

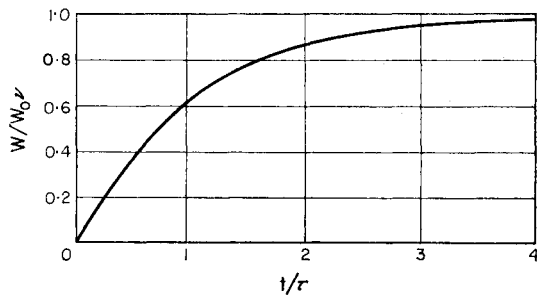


FIG. 135. Development of a chain reaction with time when $\epsilon\alpha < 1$.

Multiplying $\tau = 1/(v_1 + v_2)(1 - \epsilon\alpha)$ by v_1 and $1/v_1$ and noting that $1/v_1$ is τ_1 , the *time of development of one chain link*, since $v_1/(v_1 + v_2) = \alpha$ we obtain $\tau = v\tau_1$. Consequently, the lifetime τ of the active centre is equal to the time of development of one chain link multiplied by the number

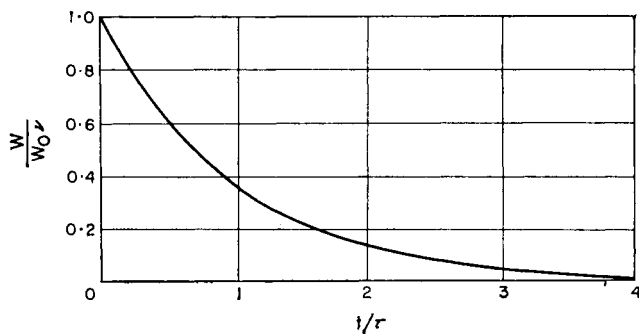


FIG. 136. Termination of a chain reaction as a result of active centres no longer being generated.

of links, i.e. the lifetime τ of the active centre is equal to the total lifetime of all the active centres involved in development of one chain and is the sum of the individual lifetimes τ_1 .

We shall also consider the attenuation of the reaction when active centres are no longer generated. In this case, since $W_0 = 0$, the differential

equation for n the concentration of active centres may be written in the form

$$\frac{dn}{dt} = -(v_1 + v_2)(1 - \epsilon\alpha)n = -n/\tau. \quad (34.13)$$

Integrating (34.13) with the condition that $n = n_{st} = W_0\tau$ when $t = 0$ we obtain

$$n = W_0\tau \exp(-t/\tau),$$

and hence the rate of reaction W is

$$W = v_1n = W_0v_1\tau \exp(-t/\tau) = W_0v \exp(-t/\tau). \quad (34.14)$$

Figure 136 shows graphically the dependence of the reaction rate as expressed by (34.14).

The cases when $\epsilon\alpha \geq 1$ will be considered in §37.

§35. Chain Initiation

Thermal Generation of Active Centres in the Gas Phase

It has already been shown that chemical chain reactions involve free atoms and radicals. Therefore the formation of active centres of this type is a necessary condition for the occurrence of chain reactions. Here we shall consider only thermal reactions and leave aside photochemical reactions and reactions induced by ionizing radiation and fast electrons. In contrast with these reactions the mechanism of formation of radicals and atoms in thermal reactions is far from being clear in every case. At any temperature a certain quantity of free atoms and radicals is always present in a gas as a result of thermal (equilibrium) dissociation of the gas. At temperatures below 1000°K, however, their concentration and rate of formation by simple molecular collision



(R and R' are radicals, M is any particle) are not always sufficient for a chain reaction to have a measurable rate.

It is usually considered that thermal equilibrium is established practically instantaneously, and in all kinetic calculations the initial concentration of active centres is assumed to be equal to their equilibrium concentration at the given temperature and concentrations of reacting substances. This, however, is by no means always the case in practice. We shall examine the rate of establishing dissociation equilibrium in the homogeneous gas phase.

We shall consider first the case when reaction does not occur. In this case, in a gas containing X_2 molecules capable of dissociating into X atoms, and inert-gas molecules, the following two processes take place: the dissociation process $X_2 + M \rightleftharpoons 2X + M$ and the reverse process of

recombination of atoms $2X + M \rightleftharpoons X_2 + M$. For simplicity we shall consider the efficiency of each of these processes to be independent of the nature of M which may be a molecule of any substance present in the gas ($M = X_2$, X or a molecule of the inert admixture). If the rate constants of the forward and reverse reactions are k and k' respectively, then representing concentrations by partial pressures we find

$$\frac{dp_X}{dt} = -2\frac{dp_{X_2}}{dt} = 2kp_{X_2} - 2k'p(p_X)^2.$$

In view of the fact that p_X is small compared with p_{X_2} , we may consider p_{X_2} to be constant and equal to the initial (and also equilibrium) pressure of X_2 ; the total pressure p in this case may also be considered to be constant. Introducing the constant for the equilibrium $X_2 \rightleftharpoons 2X$, namely

$$K = (p_X)_{\text{equilibrium}}^2 / p_{X_2} = k/k'$$

and denoting the quantity $4pk'(Kp_{X_2})^{1/2}$ by $1/\tau$, we may write the last equation in the form

$$\frac{d\xi}{dt} = (1 - \xi^2)/2\tau,$$

where $\xi = p_X/(p_X)_{\text{equilibrium}}$. Integrating this equation (reckoning $p_X = 0$ when $t = 0$) we obtain

$$\xi = p_X/(p_X)_{\text{equilibrium}} = [1 - \exp(-t/\tau)]/[1 + \exp(-t/\tau)]. \quad (35.2)$$

Substituting in this formula $t = \tau$, we obtain

$$\xi_\tau = (e - 1)/(e + 1) = 0.46 \approx \frac{1}{2}.$$

Therefore τ is the time in which the partial pressure of the atoms becomes approximately half the equilibrium value. Taking $1/\tau$ as a measure of the rate of establishing equilibrium let us calculate its value for various temperatures in the case of the equilibria $H_2 \rightleftharpoons 2H$ and $Cl_2 \rightleftharpoons 2Cl$. In both cases we shall take $p = p_{X_2} = 1$ atm. The recombination constant of H atoms in the rate expression for the recombination $2H + H_2 \rightleftharpoons 2H_2$ is 3×10^{-32} sec $^{-1}$. The recombination constant of chlorine atoms is about 10^{-31} sec $^{-1}$. Substituting the values for these constants in the expression for $1/\tau$, we obtain

$$1/\tau_H = 6 \times 10^{12} (K_H)^{1/2} / T^2 \text{ sec}^{-1}$$

and

$$1/\tau_{Cl} = 2 \times 10^{13} (K_{Cl})^{1/2} / T^2 \text{ sec}^{-1},$$

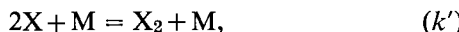
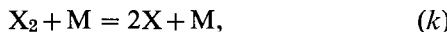
where K is the appropriate equilibrium constant. The $1/\tau$ values calculated from these formulae are shown in Table 54. It is clear from this table that in the case of hydrogen even when $T = 1000^\circ\text{K}$, $1/\tau$ is still relatively small. In the case of the more easily dissociated chlorine the rate of establishing equilibrium is much greater.

TABLE 54

Rate of the homogeneous reactions establishing the dissociation equilibria of hydrogen and chlorine at various temperatures

T° K	$H_2 \rightleftharpoons 2H$		$Cl_2 \rightleftharpoons 2Cl$	
	K, atm	$1/\tau, sec^{-1}$	K, atm	$1/\tau, sec^{-1}$
600	3.9×10^{-33}	10^{-9}	4.7×10^{-16}	1.2
800	1.3×10^{-23}	3.4×10^{-5}	1.0×10^{-10}	310
1000	7.4×10^{-18}	1.6×10^{-2}	1.7×10^{-7}	8200

We shall now return to an examination of the establishment of dissociation equilibrium in a reacting mixture. We shall consider that a simple chain reaction takes place in the mixture (see above, p. 573). A good example is the reaction $Cl_2 + H_2 = 2HCl$ (or the reaction $Br_2 + H_2 = 2HBr$) whose mechanism in the initial period (until the reaction product accumulates in appreciable quantities) is the sum of the four processes:



Here, as earlier, we shall neglect thermal generation of H atoms, i.e. the process $H_2 + M = 2H + M$, as the rate of this process is negligibly small compared with the rate of the process $X + H_2 = HX + X$; in just the same way we shall consider the process $H + X_2 = HX + X$ as the predominant process leading to removal of H atoms. The following kinetic equations result from this reaction mechanism:

$$dp_X/dt = 2kp p_{X_2} - 2k'p p_X^2 - k_1 p_{H_2} p_X + k_2 p_{X_2} p_H$$

and

$$dp_H/dt = k_1 p_{H_2} p_X - k_2 p_{X_2} p_H$$

and by addition we obtain

$$dp_X/dt + dp_H/dt = 2kp p_{X_2} - 2k'p p_X^2.$$

Since H atoms have high activity it may be taken that in the initial period of the reaction before the stationary state has been reached dp_H/dt will be negligibly small compared with dp_X/dt and consequently the last equation may be written

$$dp_X/dt = 2kp p_{X_2} - 2k'p(p_X)^2$$

(in any case in the initial period of the reaction, since $dp_H/dt > 0$, dpx/dt cannot be greater than $2kpp_{X_2} - 2k'p(p_X)^2$). Comparing this expression with that on p. 574 for the rate of change of concentration of atoms in the absence of reaction, we see that the two expressions are identical. It follows from this that the occurrence of a simple chain reaction *does not accelerate* the attainment of equilibrium and does not lead to a value of p_X greater than the equilibrium value.

In contrast with halogen atoms, the concentration of hydrogen atoms, formed practically exclusively as a result of reaction, may be much greater than the equilibrium concentration. Thus, assuming the reaction has reached a steady state, i.e. that the two steady-state conditions $dp_H/dt = 0$ and $dpx/dt = 0$ are fulfilled, and taking p_{H_2} and p_{X_2} to be approximately the same, we find that $p_H = (k_1/k_2)(p_X)_{\text{equilb}}$. On the other hand, we have

$$(p_H)_{\text{equilb}} \approx (K_H/K_X)^{1/2}(p_X)_{\text{equilb}}.$$

From these last two relations, therefore, we obtain

$$\frac{p_H}{(p_H)_{\text{equilb}}} \approx \frac{k_1}{k_2} \left(\frac{K_X}{K_H} \right)^{1/2},$$

and hence, as the rate constant k_1 is close to k_2 (for the reaction of chlorine and hydrogen) and the equilibrium constant K_X is several powers of ten larger than K_H , $p_H/(p_H)_{\text{equilb}} \gg 1$.

The reason for the slow attainment of thermal equilibrium in pure gases or in their mixtures with inert admixtures is that the process of dissociation of a molecule on its collision with another molecule is difficult. However, there are many cases known where various active admixtures and solid surfaces have a catalytic effect on the rate of chain reactions, i.e. on the rate of formation of active centres—free atoms and radicals. These data force us to assume that, in the process of formation of radicals, simple energy exchange during molecular collision plays only a secondary role compared with chemical interaction.

Formation of radicals by simple thermal dissociation of molecules according to scheme (35.1) may play an important role only at relatively high temperatures, for example flame temperatures. Near room temperature, or even at a few hundred degrees Centigrade, this process is important only in the case of compounds of relatively low stability such as ozone, certain peroxides, nitrites and nitrates, azocompounds, etc. In particular, the well-known catalytic effect of peroxides is usually connected with the ease of their dissociation into radicals of type RO as a result of the relatively low stability of the O—O bond.⁽⁶⁾ However, the fact that even at

⁽⁶⁾ The energy required to break the O—O bond in alkyl peroxides, i.e. in peroxides of structure RO—OR, where R is an alkyl radical, is 32 to 37 kcal [695]. The energy required for hydrogen peroxide decomposition into two hydroxyl radicals is 48 kcal.

175°C hydrogen peroxide decomposes only at solid surfaces [149] raises doubts with regard to the reliability of assuming that the decomposition of peroxides is homogeneous—at least near room temperature. The possibility is not ruled out that, like the decomposition of hydrogen peroxide, the decomposition of other peroxides is a heterogeneous catalytic process.⁽⁷⁾ The data of various authors on the effect of the solvent on the kinetics of decomposition of peroxides also show that the mechanism is complex. For example, according to the data of Stannet and Mesrobian [1166], tertiary hydroperoxides, *tert*-ROOH, decompose with different rates in different solvents. These data show that in the thermal dissociation of peroxides, as in other radical-formation processes, *chemical factors* play an important role.

Generation of Active Centres in the Gas Phase as a Result of Chemical Interaction

In its most general form chemical interaction leading to formation of radicals may be represented by the elementary processes:

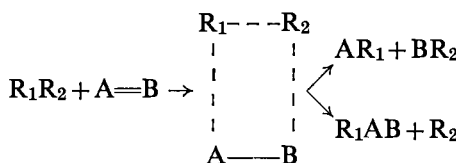


and



where R_1 and R_2 are radicals; R_0 is an inactive radical or molecule having the properties of a radical; M , M_1 and M_2 are saturated molecules.

It must be assumed that process (35.3) is realized most frequently when one of the interacting molecules contains multiple (double) bonds, as for example do the oxygen molecule $O=O$, an olefin $RHC=CH_2$, an aldehyde $RHC=O$, and so on. Representing such a molecule by the symbol $A=B$ and the molecule interacting with it by R_1R_2 , the process of formation of radicals may be represented by one of the following schemes:



The formation of chains in oxyhydrogen gas is apparently connected with the first of these processes. In this case the process is expressed by the scheme $H_2 + O_2 = 2OH$ and its heat is only -19 kcal so that it is the least endothermic of all the possible bimolecular homogeneous processes of radical (or atom) formation in the H_2 and O_2 mixture.⁽⁸⁾ However, the

⁽⁷⁾ See also [251]. In the oxidation of methane CH_4 formation of peroxides at high temperatures has been established [955]. This is evidence of their stability.

⁽⁸⁾ In fact this process takes place at the walls of the reaction vessel owing to the high activation energy (see p. 610).

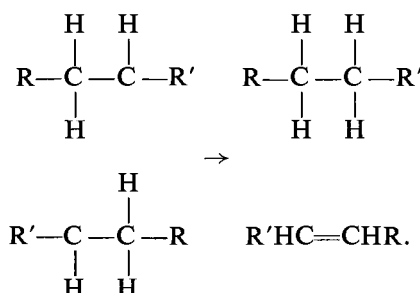
mechanism expressed by the process



should be considered a more general mechanism of radical formation involving oxygen. The activation energy of this process apparently differs little from its heat effect, which is estimated as 40 to 50 kcal. Therefore the rate of process (35.5) must be much greater than the rate of any process connected with simple dissociation of the molecule, which usually requires an energy of 80 kcal or higher.⁽⁹⁾

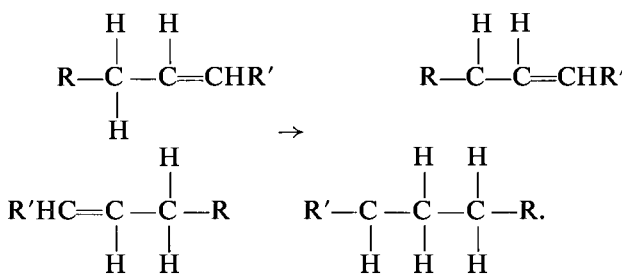
The initiating role of oxygen becomes obvious when we compare the temperature conditions for pyrolysis and slow oxidation of the same compounds. Indeed, whereas pyrolytic reactions have a measurable rate only at temperatures of 500°C and higher, oxidation reactions take place readily, as a rule, as low as 300°C. We might also mention the catalytic effect of oxygen in cracking processes where addition of oxygen considerably accelerates the process. A similar catalytic effect of oxygen is observed in the processes of hydrocarbon oxidation. Thus, Chernyak and Shtern [286] show that in mixtures of propane and oxygen, even with excess oxygen, pyrolysis more and more dominates the oxidation with increasing temperature⁽¹⁰⁾ [foot of p. 583]. Therefore it is natural that even small additions of oxygen may abruptly accelerate the cracking process.

In chain reactions not involving oxygen, however, a process similar to (35.5) may also be important as a source of homogeneous initiation of radicals. In particular the possibility is not ruled out that radical formation in thermal polymerization of pure substances is based on such processes. Studies of the kinetics and mechanism of thermal polymerization lead to the conclusion [20] that here chain breaking most frequently occurs as a result of disproportionation processes, which may be represented by the general scheme:

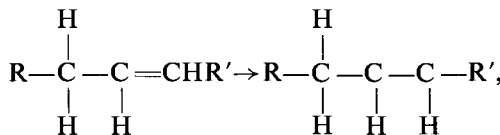


⁽⁹⁾ On the basis that the effective activation energy of formaldehyde H₂CO oxidation at relatively low temperatures (300 to 370°C) is 21 kcal, whereas the heat of the reaction H₂CO + O₂ = HCO + HO₂ is about 55 kcal (actually it is ~ 32 kcal), Norrish *et al.* [337] suggest that chain initiation in a mixture of H₂CO and O₂ is connected with the practically thermoneutral process H₂CO + O₂ = HCOOH + O - 0.2 kcal. The objection raised by Norrish is apparently based on some misunderstanding, as the effective activation energy must not necessarily be equal to the activation energy of the initiating process.

Here the disappearance of two radicals leading to the breaking of two chains is caused by the transfer of an H atom from one radical to the other. The activation energy of disproportionation processes is low, only a few kilocalories, and indicates the ease of this process. It would be expected, therefore, that the reverse transfer of an H atom from one molecule to another, i.e. formation of two radicals on molecular interaction, must have high probability and the activation energy of this process should be close to the heat of the reaction and approximately equal to the difference in C=C and C—C bond energies (≈ 60 kcal). For example, radical formation in thermal polymerization of a pure ethylenic hydrocarbon may be represented by the scheme:



The following process evidently competes with the above process:



and leads to formation of a biradical.

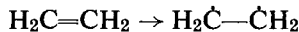
The problem as to which of these processes (which we shall call the bimolecular and unimolecular processes) predominates may be solved by comparing their rates. Expressing the rates of these processes by formulae $w_2 = k_2(M)^2$ and $w_1 = k_1(M)$ respectively, where k_1 and k_2 are the rate constants and $k_1 = A_1 \exp(-E_1/RT)$, $k_2 = A_2 \exp(-E_2/RT)$, we find

$$w_2/w_1 = (A_2/A_1) \exp[-(E_2 - E_1)/RT](M).$$

As we have already mentioned, the activation energy E_2 of the bimolecular process is approximately estimated as 60 kcal. We still have no sufficiently definite data on E_1 , the activation energy for formation of the biradical; this energy must be equal to the difference in energy between

⁽¹⁰⁾ The predominance of cracking products over oxidation products in the high-temperature oxidation ($T > 400^\circ\text{C}$) and the preferential formation of such products as aldehydes, alcohols, acids and peroxides in the low-temperature reaction ($T = 250-400^\circ\text{C}$) is also observed for other hydrocarbons (when the number of C atoms is 3 or more) and is a well-established fact. See, for example, [848].

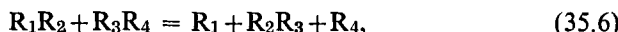
the triplet level nearest to the ground level and the ground level, which is the singlet level of the olefin molecule: $E_1 = E_{\text{trip}} - E_{\text{sing}}$. From spectroscopic data for unsaturated compounds (absorption and phosphorescence spectra) and also from theoretical calculations of $E_{\text{trip}} - E_{\text{sing}}$ for olefins the E_1 values are from 40 to 80 kcal.⁽¹¹⁾ Thermochemical data on the energy of the transition of the ethylene C_2H_4 molecule to the biradical state, i.e. the energy for the process



give 60 kcal [241, 137a]. This figure is in good agreement with both the foregoing data and the activation energy directly measured for *cis-trans* isomerization of dideutero-ethylene $\text{DHC}=\text{CHD}$ which takes place via the biradical state $\text{DHC}-\dot{\text{C}}\text{HD}$.⁽¹²⁾

As thermochemical calculation of the excitation energy of the biradical state of an olefin is in essence calculation of the difference in $\text{C}=\text{C}$ and $\text{C}-\text{C}$ bond energies, the close agreement of E_2 , the activation energy of the bimolecular process estimated earlier, and E_1 is not fortuitous. Assuming $E_2 = E_1$ (= 60 kcal) we obtain $w_2/w_1 = (A_2/A_1)(M)$. Substituting in this, $A_1 = 10^{13} \text{ sec}^{-1}$, $A_2 = 10^{-12} \text{ cm}^3 \text{ molecule}^{-1} \text{ sec}^{-1}$ and $(M) = 10^{19} \text{ molecule/cm}^3$, we obtain $w_2/w_1 = 10^{-6}$, i.e. $w_1 \gg w_2$. In this way calculation shows that thermal excitation of the triplet levels of olefin molecules must play an important role in the mechanism of homogeneous formation of active centres using olefins.⁽¹³⁾

Semenov [241] discussed a mechanism for the formation of two monoradicals on bimolecular collision of saturated molecules, corresponding to the scheme



where R_1 , R_2 , R_3 and R_4 are monoradicals. On the basis of the fact that interaction of a radical and a molecule (for example the process $\text{R}_1 + \text{R}_2\text{R}_3 = \text{R}_1\text{R}_2 + \text{R}_3$) has a relatively low activation energy and assuming that when the molecule is attacked simultaneously by two radicals [the opposite process to (35.6)] the activation energy should be even less, Semenov concludes that the activation energy of process (35.6) will be close to zero if the process is exothermic, and in absolute value close to its heat if the process involves consumption of energy.

(11) In aromatic compounds $E_{\text{trip}} - E_{\text{ground}}$ is 84 (benzene) to 29 kcal [940, 1201].

(12) The activation energy of the *cis-trans* isomerization of dideutero-ethylene is 65 kcal [550].

(13) According to Zimakov [94], biradical formation is the basis of the mechanism of the radical reactions in thermal decomposition of ethylene oxide $(\text{CH}_2)_2\text{O}$ and of the reactions of ethylene oxide with various organic compounds at temperatures higher than 400°C.

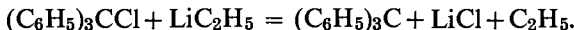
The activation energy of the endothermic process may be calculated from the equation

$$E = D_{R_1-R_2} + D_{R_3-R_4} - D_{R_2-R_3}, \quad (35.7)$$

where D is the energy to break the appropriate bonds (the heat of dissociation). It is seen from formula (35.7) that the mechanism considered for the generation of active centres is important only when the heat of dissociation of the newly-formed R_2R_3 molecule is greater than the largest heat of dissociation of the initial molecules. Actually in this case since $D_{R_2-R_3} > D_{R_1-R_2}$ we have $E < D_{R_3-R_4}$, i.e. the heat of activation of process (35.6) will be less than the heat of dissociation of the least stable molecule, and process (35.6) may be energetically profitable.

To establish the possibility of process (35.6), Shilov, D'yachkovskii and Bubnov [69a] studied the reaction of lithium ethyl LiC_2H_5 and triphenylchloromethane $(\text{C}_6\text{H}_5)_3\text{CCl}$ in a hydrocarbon solvent, in which the first step, when it follows scheme (35.6), must be exothermic.⁽¹⁴⁾

Using the spin resonance method it has been established that $(\text{C}_6\text{H}_5)_3\text{C}$ radicals are actually formed in this system and in the first moments of the reaction their concentration is several times greater than the equilibrium concentration (corresponding to the dissociation of hexaphenylethane $(\text{C}_6\text{H}_5)_3\text{C}-\text{C}(\text{C}_6\text{H}_5)_3$ which is the product of recombination of $(\text{C}_6\text{H}_5)_3\text{C}$ radicals). This is a definite indication of the primary character of the formation of radicals according to the scheme



Kinetic data lead to the conclusion that radical formation has a very low activation energy, not greater than 4 to 5 kcal. Consequently for suitable conditions reaction between saturated molecules according to (35.6) may occur without a significant activation barrier.⁽¹⁵⁾

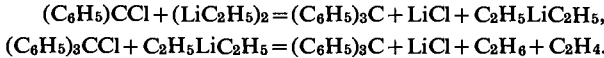
We shall give further consideration to process (35.4). An example of

⁽¹⁴⁾ Actually, according to the data of Szwarc and coworkers [1128a], the energy required to break the C—Cl bond in the $(\text{C}_6\text{H}_5)_3\text{CCl}$ molecule is 48 kcal. The heat of dissociation of the LiCl molecule is 118 kcal. In this way we obtain

$$Q = 118 - 48 - D(\text{Li}-\text{C}_2\text{H}_5)$$

for the heat of the reaction in question. If we take for $D(\text{Li}-\text{C}_2\text{H}_5)$ the geometric mean of the heats of dissociation of Li_2 and $\text{H}_5\text{C}_2-\text{C}_2\text{H}_5$ which is 46 kcal, then for Q we find $Q = 70 - 46 = 24$ kcal.

⁽¹⁵⁾ The actual mechanism of this reaction is apparently somewhat more complex than that shown above. Having unsuccessfully attempted to detect ethyl radicals by the products of their interaction with the solvent, and also butane, Shilov and co-workers [69a] conclude that formation of $(\text{C}_6\text{H}_5)_3\text{C}$ radicals takes place according to the following scheme in their experimental conditions:



molecules having to some extent the properties of radicals is given by the oxides of nitrogen NO and NO_2 . In particular, the possibility is not ruled out that the catalytic effect of the oxides of nitrogen in the slow oxidation of hydrocarbons is in part based on the process



i.e. a process of type (35.4). The bond energy of the H atom in the HNO_2 nitrous acid molecule is 43 kcal and thus there is an energy gain compared with the simple decomposition of the RH molecule into R and H, so that R radicals are formed with greater ease in the presence of NO_2 . See, for example, [271a].

Chain Initiation at the Wall

The initiating action of surfaces plays a very large part in the kinetics of chain reactions. The possibility of radical formation at a surface with subsequent release into the volume of the vessel was first clearly demonstrated by the experiments of Polyakov [217] who showed that hydrogen activated by palladium has all the properties of atomic hydrogen and in particular may initiate a chain reaction of oxidation. In just the same way, Neiman and Popov [208] have shown by using the kinetic tracer method that active centres formed as a result of the heterogeneous reaction on a silver catalyst may give rise to a homogeneous chain reaction in the volume of the gas at a temperature lower than that of the catalyst.

The initiating action of surfaces, which act as the catalyst, was also shown conclusively in the experiments of Bogoyavlenskaya and Koval'skii [29] and of Markevich [181]. By measuring the temperature distribution along the radius of a cylindrical reaction vessel when a catalytic reaction is taking place (the catalyst is deposited either on a thin rod placed along the axis of the reaction vessel or directly on the inner surface of the vessel), these authors found that in certain reactions ($\text{H}_2 + \text{O}_2$, $\text{CH}_4 + \text{O}_2$, $\text{C}_2\text{H}_6 + \text{O}_2$ and others) the greater part of the heat is liberated in the volume of the reaction vessel. Hence the conclusion is inevitable that the role of a heterogeneous catalyst in these reactions is no more than the formation of active centres which are then liberated from the surface of the catalyst into the volume of the vessel and excite the homogenous chain reaction.

We may also explain the mechanism of radical formation at solid surfaces from a chemical viewpoint. The predominating role of chemical factors in the surface catalytic process is clear from the exceptional specificity of these processes. Considering the activating action of a surface as the result of the chemical interaction of the activated substance with the catalyst, it is easy to see that radical formation at the surface should be thermodynamically more advantageous than the simple dissociation of

the molecule into radicals. In fact, representing the process of heterogeneous catalytic formation of a radical by the equation



(K is the catalyst, R'K is the product of chemisorption of the R' radical), we see that process (35.8) gives an energy gain (equal to the amount of energy liberated in the formation of the exothermic compound R'K)⁽¹⁶⁾ compared with the process $RR' = R + R'$. Process (35.8) is similar in its chemical nature to the homogeneous catalytic process of type (35.3). The possibility of process (35.8) follows directly from the occurrence of the reverse process of chain breaking at the wall, which is considered in the following section (see also [43a]).

§36. Chain Breaking

Chain Breaking in the Gas Phase

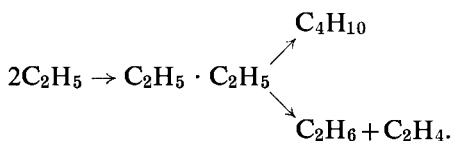
Chain breaking is connected with the destruction of the active centres of reaction—free atoms and radicals, i.e. with chemical processes which involve atoms and radicals but do not lead to their regeneration. These processes may take place both in the volume and at the surface (at the walls of the reaction vessel or on solid or liquid particles if present in the reaction zone). At sufficiently high concentrations of active particles, and in the absence of competing processes, chain breaking in the volume is *recombination* of free atoms and radicals. Here the recombination of simple particles (atoms or simple radicals) is a ternary collision process



which is the converse of process (35.1). The rate of this process is proportional to the square of the concentration of active centres (*quadratic chain breaking*) and to the over-all pressure. The recombination of polyatomic radicals is usually a bimolecular process since as a result of the energy of radical interaction being redistributed among many degrees of freedom, the quasi-molecule formed in the radical recombination acquires a protracted stability and always has the possibility of transferring its excess energy to a molecule colliding with it or to the wall. In addition the increased energy of the quasi-molecule may sometimes lead to disproportionation, so that two stable molecules are formed. For example, two ethyl C_2H_5 radicals form the quasi-molecule $C_2H_5 \cdot C_2H_5$ which as a result of subsequent stabilization is either converted into a molecule of butane C_4H_{10} or as a result of disproportionation decomposes into an

⁽¹⁶⁾ Some idea of the energy of the bond between the radical and the solid catalyst is given by the heat of adsorption of atoms on metals. Thus, according to the measurements of Buben and Shekhter [35], the heat of adsorption of the nitrogen atom on nickel is 55 ± 2 kcal. The heat of adsorption of H atoms on tungsten is 73.7 kcal according to Roberts [1076] (see also Shekhter [291]).

ethane molecule C_2H_6 and an ethylene molecule C_2H_4 :

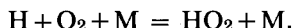


We should note that in quadratic chain breaking *two* chains are always broken. Semenov calls such a process a negative interaction of chains.

When reaction is retarded by admixtures or substances with which atoms and radicals form saturated compounds or radicals of low chemical activity, the rate of chain breaking is directly proportional to the concentration of active particles (*linear chain breaking*). Like the process of recombination, in the case of atoms and simple radicals linear chain breaking is a process of ternary collision: for example,

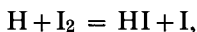


or



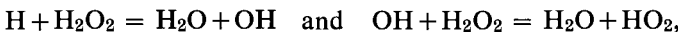
The rate of these processes is proportional to the overall pressure and to the partial pressure of the molecules (CO and O_2) interacting with the atom. In the first of these examples a divalent atom disappears and a saturated molecule is formed; in the second example an active H atom is replaced by an HO_2 radical of low activity.

Linear chain breaking frequently follows a bimolecular law. For example, the inhibiting effect of iodine vapour in the hydrogen combustion reaction is associated with the bimolecular process



as a result of which an extremely active H atom is replaced by an I atom of very low activity; therefore interaction of an H atom with an iodine molecule is in fact a chain breaking process [203].

A peculiar chain breaking in the hydrogen combustion reaction is observed in the presence of hydrogen peroxide. Here the retarding effect of H_2O_2 must apparently be associated with the processes



as a result of which active H and OH particles are replaced by the less active OH and HO_2 respectively. Note that the retarding effect of hydrogen peroxide is determined by the square of its concentration [620b].

Chain Breaking at the Wall. Diffusion and Kinetic Region of the Reaction

In addition to spatial chain breaking we must consider chain breaking at the walls of the reaction vessel. Chain breaking at the walls becomes

predominant at low pressures. The mechanism of this type of chain breaking is clearly adsorption of active centres (atoms or radicals) with the subsequent recombination of two atoms, one adsorbed and one from the gas phase.⁽¹⁷⁾

Considering chain breaking at the wall as a heterogeneous reaction of active centres, we shall treat the rate of this reaction as the rate of chain breaking. Since the reaction is of first order with respect to the active centres its rate may be represented by the formula

$$W = kn', \quad (36.2)$$

where k is the reaction rate constant and n' the concentration of active centres near the surface (of the wall). At sufficiently high pressures the active centres are supplied to the surface by the diffusion current

$$q = -D(dn/dx),$$

where D is the diffusion coefficient and dn/dx the concentration gradient of the active centres along the normal to the surface. By introducing a certain "reduced film" of thickness Δ the concentration gradient will be represented by the approximate form $-dn/dx = (n - n')/\Delta$, where n is the concentration of active centres in the gas phase; then according to Frank-Kamenetskii [278] the current q may be written as

$$q = \beta(n - n'). \quad (36.3)$$

The quantity β in this formula is equal to D/Δ and is called the *diffusion rate constant* (by analogy with k the reaction rate constant).

Equating (in the case of a stationary process) the rate of reaction of active centres at the surface to the rate of their delivery by diffusion, i.e. to q , we find

$$W = kn' = \beta(n - n'),$$

and hence

$$n' = \beta n/(k + \beta). \quad (36.4)$$

Substituting (36.4) in (36.2) we obtain

$$W = k\beta n/(k + \beta) = k^*n, \quad (36.5)$$

where the effective rate constant is

$$k^* = k\beta/(k + \beta) \quad \text{or} \quad 1/k^* = 1/k + 1/\beta. \quad (36.6)$$

On the basis of equation (36.6) the quantities $1/k$ and $1/\beta$ may be called the diffusion and kinetic resistances.

⁽¹⁷⁾ This mechanism follows from the data of Lavrovskaya and Voevodskii [163] on the adsorption of H atoms and also from the data of Buben and Shekhter [35]. See also Müffling [960]. According to Müffling, the decrease in the lifetime of the adsorbed atom at high temperatures causes quadratic chain breaking to begin to predominate over linear breaking there.

We shall consider the following two limiting cases obtained from the general formula (36.5):

(1) The reaction rate constant k is much greater than the diffusion rate constant β , $k \gg \beta$. In this case $k^* = \beta$ and

$$W = \beta n, \quad (36.7)$$

i.e. the rate of reaction is determined by the rate of diffusion. For this reason the reaction is said to take place in the *diffusion region*. It follows from formula (36.4) that in the diffusion region

$$n' = \beta n/k \ll n,$$

i.e. the concentration (n') of active centres at the surface is much less than their concentration (n) in the gas phase, which is a consequence of the high rate of the chemical process.

(2) In the second limiting case the rate of the chemical process is small compared with the rate of diffusion, $k \ll \beta$, so that we have $k^* = k$ and

$$W = kn, \quad (36.8)$$

i.e. the overall rate of reaction is determined by the rate of the chemical process itself. In this case the reaction is said to take place in the *kinetic region*. In the kinetic region the concentration of active centres at the surface is practically equal to their concentration in the gas phase, as follows from (36.4).

Rate of the Steady Chain Reaction [232]

The kinetics of a chemical chain reaction, its rate and the mean chain length, are naturally directly related to the reaction conditions, and in the first instance are connected with the conditions of chain initiation and breaking. Here we shall consider the rate of the steady reaction, confining ourselves to the case when the chains are initiated homogeneously but are terminated both homogeneously and at the surface. In this we shall assume that homogeneous chain breaking follows a linear law and the reaction takes place in the diffusion region. In this case (the one-dimensional problem for a flat reaction vessel) the following differential equation holds for a simple chain reaction (steady reaction):

$$D(d^2n/dx^2) - gn + W_0 = 0. \quad (36.9)$$

The first term in this equation determines the change in active-centre concentration owing to diffusion, the second term determines the rate of homogeneous chain breaking, i.e. the number of active centres destroyed in 1 cm^3 per sec, and the third term determines the rate of the thermal (or "external") generation of active centres, i.e. the number of active centres formed per second in 1 cm^3 . Since in a simple chain reaction, for each active centre entering into reaction a new centre is formed by the reaction

itself (the regeneration of active centres) it is natural that equation (36.9) does not contain terms expressing the rates at which the active centres enter into reaction and at which they are formed as a result of reaction.

The solution of (36.9), for the case with the limiting condition for the diffusion region that the concentration of active centres at the surface of the reaction vessel be zero, has the form,

$$n = \frac{W_0}{g} \left\{ 1 - \frac{\cosh[(g/D)^{1/2}(x - \frac{1}{2}d)]}{\cosh[(g/4D)^{1/2}d]} \right\}, \quad (36.10)$$

where d is the distance between the walls of the reaction vessel. The total number of active centres in the volume of the reaction vessel will be equal to

$$N = S \int_0^d n(x) dx = \frac{W_0 S d}{g} \left\{ 1 - \frac{\tanh[(g/4D)^{1/2}d]}{(g/4D)^{1/2}d} \right\}$$

(S is the area of the vessel). Dividing the number N by the mean time of development of one chain link τ_1 , we obtain the rate of reaction $W = N/\tau_1$, which may also be taken as equal to $W_0 \nu d S$. From these expressions we find the mean chain length ν

$$\nu = \frac{1}{g\tau_1} \left\{ 1 - \frac{\tanh[(g/4D)^{1/2}d]}{(g/4D)^{1/2}d} \right\}. \quad (36.11)$$

From the general expression (36.11) referring to the case when the chains are broken both homogeneously and at the walls it is not difficult to obtain the particular expressions corresponding to the case when the chains are preferentially terminated homogeneously and to the case when the chains are preferentially terminated at the walls. In the first case the coefficient g has a high value and the quantity

$$\{\tanh[(g/4D)^{1/2}d]\}/\{(g/4D)^{1/2}d\}$$

may be taken as equal to zero; then

$$\nu = 1/g\tau_1. \quad (36.12)$$

This expression was obtained earlier in a somewhat different form. Actually since $1/g$ is τ , the lifetime of the active centre, it is easy to see that (36.12) is identical with the formula

$$\nu = \tau/\tau_1, \quad (36.13)$$

obtained on p. 576.

When the chains are terminated preferentially at the walls the coefficient g must be small. In this case we may expand the quantity

$$\{\tanh[(g/4D)^{1/2}d]\}/\{(g/4D)^{1/2}d\}$$

into a series in

$$d(g/4D)^{1/2}.$$

Confining ourselves to the first two terms of the expansion, namely

$$1 - \frac{1}{3}(g/4D)d^2,$$

we obtain

$$\nu = d^2/(12\tau_1 D). \quad (36.14)$$

Introducing the efficiency coefficient q of active-centre collisions leading to propagation of the chain, namely

$$q = Z/Z^* \quad (36.15)$$

(Z is the total and Z^* the effective number of collisions), we obtain

$$\tau_1 = 1/Z^* = q/Z,$$

or since $Z = c/\lambda$ (c is the mean molecular velocity and λ the mean path length) $\tau_1 = q\lambda/c$. Moreover, since $D = \frac{1}{3}c\lambda$, $3\tau_1 D = q\lambda^2$. Substituting this expression in formula (36.14) we obtain

$$\nu = (1/4q)(d/\lambda)^2. \quad (36.16)$$

Similar formulae are also obtained for cylindrical and spherical vessels:

$$\text{cylindrical vessel } \nu = (1/10q)(d/\lambda)^2, \quad (36.17)$$

$$\text{spherical vessel } \nu = (1/20q)(d/\lambda)^2. \quad (36.18)$$

The decrease in chain length when passing from the flat vessel to a cylindrical or spherical vessel is explained by the fact that with corresponding sizes of vessel (the distance between walls of the flat vessel equal to the diameter of the cylindrical and spherical vessels) the walls of the cylindrical vessel are more accessible to the active centres diffusing to them than the walls of the flat vessel, and the walls of the spherical vessel are more accessible than those of the cylindrical vessel.

§37. Branching Chains

Branched Chain Length

We have considered earlier (p. 575) certain features of chain reactions characterized by the formation of *more than one* new active centre on average for each centre disappearing in one chain link, i.e. reactions in which $\epsilon > 1$. In such reactions the condition $\epsilon\alpha \geq 1$ (see §34) may be

fulfilled. Reactions of this type are called *branched chain reactions*. According to Semenov [232], who discovered branched reactions and developed their theory, an important quantity characterizing a branched chain reaction is δ , the *probability of branching* in one chain link, defined by

$$\delta = \epsilon - 1. \quad (37.1)$$

We represent a simple chain reaction conventionally as a zigzag line (Fig. 137a) with one segment for each chain link so that the number of segments is equal to the number of links, i.e. to the chain length ν . As $\delta > 0$ a branched chain reaction must be represented by a branched zigzag line (Fig. 137b), because from time to time *branches* are formed in the individual chain links, i.e. two chains start to develop instead of one. In the limiting case when $\delta = 1$ branching occurs *in each* chain link. Such chains are called *completely branched chains* (Fig. 137c).

Substituting $\epsilon = 1 + \delta$ in formula (34.2) which expresses the chain length of the reaction corresponding to the scheme shown in Fig. 133 and noting that $1 - \alpha = \beta$, we obtain

$$\nu_{\text{branch}} = \alpha/(\beta - \delta\alpha),$$

or, since the length ν of a simple chain is, according to (34.4),

$$\nu = \alpha/(1 - \alpha) = \alpha/\beta,$$

we have

$$\nu_{\text{branch}} = \nu/(1 - \delta\nu). \quad (37.2)$$

The quantity $\delta\nu$ in this formula may be called the probability of branching for the complete length of the simple chain (as opposed to the probability of branching in one chain link, δ). We see that even when only one branch is formed in the whole chain the length ν_{branch} of the branched chain becomes infinite, i.e. explosion occurs.

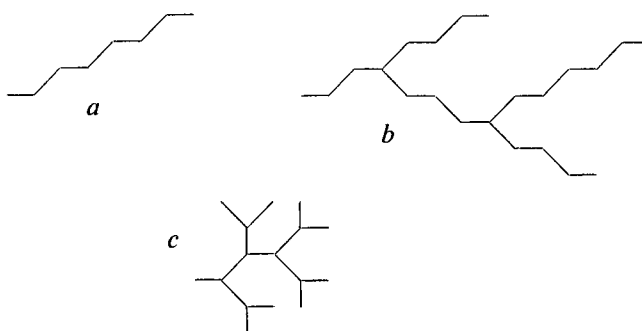


FIG. 137. Scheme of a simple chain (1), a branched chain (b) and a continuously branched chain (c).

Limiting Phenomena. Ignition Peninsula

A characteristic property of branched chain reactions is the occurrence of limiting phenomena comprising a sharp change in reaction rate on varying slightly a parameter such as pressure, temperature or mixture composition. Study of one such limiting phenomenon, the ignition limits of phosphorus vapour, led in fact to the discovery of branched chain reactions [284]. The essence of this effect is that at a definite pressure of phosphorus vapour there are two oxygen pressure limits—*the upper and lower limits* p_2 and p_1 —between which lies the *ignition region* of phosphorus and outside which, i.e. when $p > p_2$ or $p < p_1$, phosphorus vapour does not ignite. The ignition region of phosphorus vapour (according to Koval'skii [112]) is shown in Fig. 138.

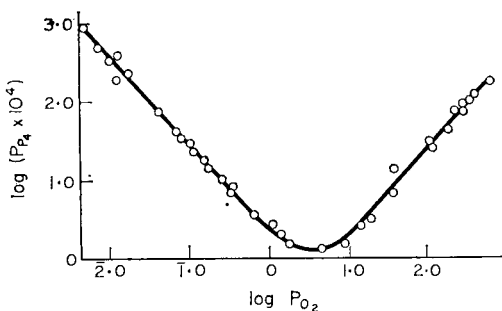


FIG. 138. Ignition region of phosphorus vapour (according to Koval'skii [112]).

Actually, as a result of detailed quantitative study of the upper and lower ignition limits of phosphorus vapour which had been carried out by Khariton and Val'ta (1926) [284], Semenov (1927) [230] and Koval'skii (1929) [113], Semenov formulated the fundamentals of the theory of branched chain reactions, in the light of which the occurrence of limits was given its first theoretical explanation.

According to Semenov's theory, the occurrence of ignition limits is a direct consequence of the kinetics and mechanism of a branched chain reaction. We have seen above (p. 573) that when $\epsilon\alpha < 1$ (simple chain reaction) the reaction rate tends towards the constant value

$$W = W_0\alpha/(1-\epsilon\alpha)$$

(the rate in the stationary reaction). In the case of a branched chain reaction ($\epsilon\alpha \geq 1$) the expression for the reaction rate, (34.12), takes the form

$$W = W_0\alpha[\exp(\varphi t) - 1]/(\epsilon\alpha - 1), \quad (37.3)$$

where

$$\varphi = (v_1 + v_2)(\epsilon\alpha - 1). \quad (37.4)$$

For sufficiently large t ($t \gg 1/\varphi$) expression (37.3) may be written in the form

$$W = W_0\alpha \exp(\varphi t)/(\epsilon\alpha - 1). \quad (37.5)$$

The law expressed by (37.5), established theoretically by Semenov, has been confirmed in a vast number of experiments on many different chemical reactions. The exponential increase of reaction rate with time (the autocatalytic *acceleration* of the reaction) resulting from this law is a characteristic feature of branched chain reactions.

Increasing according to $\exp(\varphi t)$, the rate of the branched chain reaction after a certain time interval (generally speaking not large) may become so large that the reaction takes on the character of an explosion.⁽¹⁸⁾ This takes place, however, only when the quantity φ (37.4) is positive ($\epsilon\alpha > 1$) not only at the initial moment of time but throughout the reaction. Change in sign of φ in the process of the reaction may be connected with change in the relationship between the rates of the processes of branching and chain breaking. Setting $\epsilon = 1 + \delta$ in the expression (37.4) for φ and noting that $\alpha = v_1/(v_1 + v_2)$ and $\beta = 1 - \alpha = v_2/(v_1 + v_2)$, we obtain

$$\varphi = \delta v_1 - v_2. \quad (37.6)$$

The frequency of the process leading to branching, i.e. the quantity δv_1 is proportional to the concentration of one of the initial substances; therefore in an isothermal process this quantity must decrease with time, i.e. as the reacting substances are consumed. The frequency of processes leading to chain breaking, v_2 , either does not change or varies as a result of the accumulation of substances formed in the course of the reaction. In particular, substances favouring chain breaking may appear in the course of reaction. For example, in the hydrogen combustion reaction the probability of homogeneous chain breaking increases as water is formed, since water molecules are more effective partners in the ternary collisions leading to homogeneous chain breaking than the hydrogen or oxygen molecules in the process $\text{H} + \text{O}_2 + \text{H}_2\text{O} = \text{H}_2\text{O} + \text{HO}_2$ (see p. 613). In this and similar cases v_2 increases with time. As a result of decrease in δv_1 , or decrease in δv_1 simultaneously with increase in v_2 , the quantity φ decreases in the course of the reaction, and this leads to retardation of the increase in reaction rate or even to its decrease after a certain time (when φ changes sign from plus to minus). In the latter case explosion clearly does not occur. Semenov called this phenomenon a *degenerate explosion*.

⁽¹⁸⁾ Thus according to the measurements of Norrish and Porter [980], oxy-hydrogen gas $2\text{H}_2 + \text{O}_2$ explodes 10^{-4} sec after the start of exposure to a powerful source of light.

Figure 139 shows a series of curves expressing the time dependence of the rate of a branched chain reaction. In the figure curves 1 and 2 show the time dependence of the reaction rate when auto-acceleration of the reaction leads to explosion. Curve 1 corresponds to a higher temperature (or a higher pressure). Curves 3 and 4 in this figure correspond to even lower

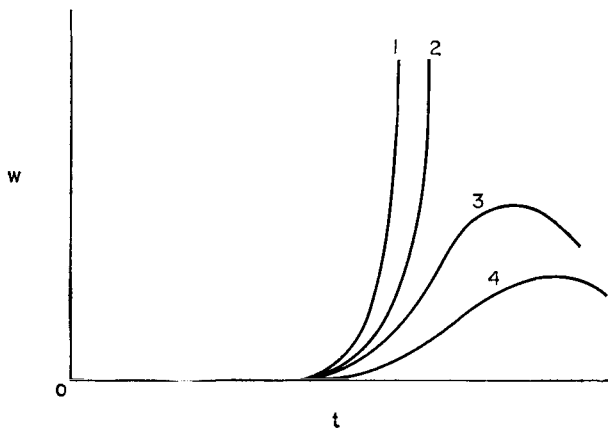


FIG. 139. Auto-acceleration of a branched chain reaction. 1 and 2—auto-acceleration leading to explosion; 3 and 4—owing to the slow increase in reaction rate explosion does not occur (a degenerate explosion).

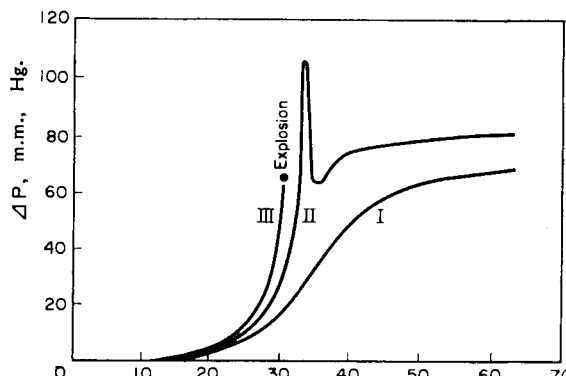


FIG. 140. Kinetic curves expressing the time dependence of pressure change (Δp) in a mixture of methane and oxygen $2\text{CH}_4 + \text{O}_2$ at 535°C and a pressure of 1 atm [1243]: I—slow reaction, II—slow reaction with cool-flame flashes (the peak on the curve); III—explosion. Curves I, II and III were obtained for somewhat different compositions of the mixture. [The abscissa is time in seconds].

temperatures (or pressures) and show the behaviour of the reaction rate in the case of degenerate explosion. In this case the rate of reaction reaches a certain final maximum and then begins to fall.

Figure 140 shows kinetic curves expressing the time dependence of pressure change (Δp) in a mixture of methane and oxygen $2\text{CH}_4 + \text{O}_2$ at 535°C and a pressure of 1 atm obtained by Vanpée and Grard [1243]. Here curves I and II correspond to the slow reaction (degenerate explosion); the peak on curve II is due to cool-flame flashes (see p. 691). Curve III corresponds to the slow reaction ending in explosion.⁽¹⁹⁾

It should be noted that, in the course of the reaction, transition to the explosive regime is usually favoured by *heating up*, which may occur even at a relatively low reaction rate, leading to an acceleration of the reaction which usually ends in *thermal explosion* (see §40).

Since according to the above when $\epsilon\alpha < 1$ we have a relatively slow stationary reaction and when $\epsilon\alpha > 1$ a rapid spontaneously accelerating reaction resulting in explosion, the condition for transition from the stationary to the non-stationary regime, i.e. the condition for a limit (or limits) of ignition, may be formulated as

$$\epsilon\alpha = 1. \quad (37.7)$$

Substituting $\epsilon = 1 + \delta$ in this formula we obtain

$$\delta\alpha = \beta, \quad (37.8)$$

or since $\alpha = v_1/(v_1 + v_2)$ and $\beta = v_2/(v_1 + v_2)$,

$$\delta v_1 = v_2. \quad (37.9)$$

Assuming

$$v_1 = ap \quad \text{and} \quad v_2 = bp^2 + b'$$

(in the expression for v_2 the first term corresponds to homogeneous chain breaking following a ternary collision mechanism, the second term corresponds to chain breaking at the walls, with the kinetic region in mind), we reduce (37.9) to the quadratic equation

$$p^2 - (\delta a/b)p + (b'/b) = 0.$$

Solving this equation we obtain the following values for the pressures p_1 and p_2 at the lower and upper ignition limits:

$$p_1 = \delta a/2b - (\delta^2 a^2/4b^2 - b'/b)^{1/2} \quad (37.10)$$

and

$$p_2 = \delta a/2b + (\delta^2 a^2/4b^2 - b'/b)^{1/2}. \quad (37.11)$$

Approximate values of the pressures at the lower and upper ignition limits may be obtained by considering that, near the lower ignition limit,

⁽¹⁹⁾ For the cool-flame spectrum of methane see [656a].

chain breaking at the walls predominates (the term bp^2 is small compared with the b' term), while near the upper limit the chains are preferentially terminated homogeneously ($bp^2 \gg b'$). In this way we obtain

$$p_1 \approx b'/\delta a \quad (37.12)$$

and

$$p_2 \approx \delta a/b. \quad (37.13)$$

When $p_2 \gg p_1$ we have $\delta a/b \gg b'/\delta a$, or $\delta^2 a^2/b^2 \gg b'/b$, which allows us to expand (37.10) and (37.11) into series; we then obtain

$$p_1 = b'/\delta a - \dots \approx b'/\delta a$$

and

$$p_2 = \delta a/b - b'/\delta a + \dots \approx \delta a/b,$$

i.e. expressions identical with (37.12) and (37.13). According to (37.10) and (37.11)

$$p_1 + p_2 = \delta a/b \quad (37.14)$$

The quantities p_1 and p_2 should have a definite temperature dependence. Thus, as the constant a , which may be called the rate constant of chain propagation, increases with temperature like the probability of branching δ , and the constant b , which is proportional to the rate constant of the termolecular process, is only weakly dependent on temperature like the

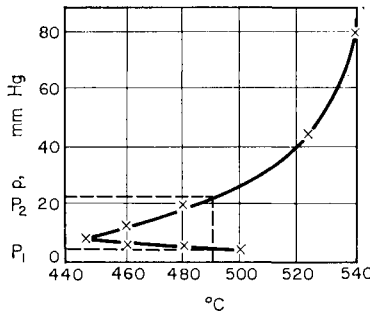


FIG. 141. "Ignition peninsula" of a stoichiometric hydrogen-oxygen mixture [75]. p_1 —pressure at the lower limit, p_2 —pressure at the upper ignition limit.

rate constant b' of chain breaking at the walls, the quantity $p_1 \approx b'/\delta a$ must decrease and $p_2 \approx \delta a/b$ increase with increase in temperature. Consequently with decrease in temperature p_1 and p_2 must come closer and closer together and at a temperature determined by the condition $\delta^2 a^2/b^2 = b'/b$, have identical values

$$p_M = p_1 = p_2 = \frac{1}{2}\delta a/b. \quad (37.15)$$

This temperature dependence of p_1 and p_2 is shown in Fig. 141 for the case of the hydrogen combustion reaction and is taken from the article

by Kopp, Koval'skii, Zagulin and Semenov [75]; this article and those of Zagulin [74] and Hinshelwood and Thompson [1221a] are the pioneer investigations in the field of branched chain reactions. These results, along with the investigations mentioned earlier on the ignition limits of phosphorus vapour, formed the basis of Semenov's chain theory. An ignition region confined by a curve similar to that in Fig. 141 is often called an ignition peninsula. The "cape" of the ignition peninsula lies at $p = p_M$ (37.15).

The above formulae for p_1 and p_2 refer to the case when chain breaking at the walls takes place in the kinetic region. When this process takes place in the diffusion region, instead of b' we have in v_2 a term b'_0/p , and for determination of the pressure at the upper and lower ignition limits instead of the quadratic equation a cubic equation is obtained, namely

$$p^3 - (\delta a/b)p^2 + (b'_0/b) = 0.$$

From this expression we obtain the following approximate values of p_1 and p_2 :

$$p_1 \approx (b'_0/\delta a)^{1/2}, \quad (37.16)$$

$$p_2 \approx \delta a/b. \quad (37.17)$$

It is also not difficult to show that the third root of the cubic equation has a negative value. Indeed, from the relation $p_1 p_2 p_3 = -b'_0/b$, as $p_1 > 0$ and $p_2 > 0$, it follows that $p_3 < 0$. The root p_3 being negative has no physical significance.

Temperature Dependence of the Rate of Chain Reactions

The formal scheme of branched chain reactions (Fig. 133) also gives an unusual temperature dependence for the rate of this type of reaction. We have seen above that the temperature dependence of simple chemical reactions is expressed by the Arrhenius equation

$$W = Z \exp(-E/RT).$$

It can be shown that the rate of a simple chain reaction may also obey this equation. In fact, for a thermal reaction the quantity W_0 in the expression for the rate of the stationary reaction

$$W = W_0 \nu,$$

may be taken as equal to $W_0 = Z_0 \exp(-E_0/RT)$. Moreover, substituting $v_1 = a_1 \exp(-E_1/RT)$ and $v_2 = a_2 \exp(-E_2/RT)$ in the chain length expression $\nu = \alpha/\beta = v_1/v_2$, we obtain

$$\nu = \nu_0 \exp[-(E_1 - E_2)/RT],$$

where $\nu_0 = a_1/a_2$. The temperature dependence of the chain length ν expressed by this formula is also found experimentally; the difference

$E_1 - E_2$ is positive, or close to zero. In this way, from the foregoing expressions for W_0 and ν we obtain for the rate of the simple chain reaction

$$W = Z_0 \nu_0 \exp[-(E_0 + E_1 - E_2)/RT] = Z_0 \nu_0 \exp(-E/RT)$$

($E = E_0 + E_1 - E_2$). It is seen from this formula that in this case the temperature dependence of the reaction rate is expressed by the Arrhenius equation as in the case of a simple reaction.

In contrast with these two cases a different temperature dependence of reaction rate would be expected for a branched chain reaction. Actually, using the values obtained earlier for W_0 and ν , the quantities occurring in the expression for the rate of the stationary branched chain reaction,

$$W = W_0 \nu / (1 - \delta \nu),$$

and taking δ the probability of branching as

$$\delta = \delta_0 \exp(-\Delta/RT),$$

we obtain

$$W = \frac{Z_0 \nu_0 \exp(-E/RT)}{1 - \delta_0 \nu_0 \exp[-(\Delta + E_1 - E_2)/RT]}.$$

This equation is different from the Arrhenius equation (an "anti-Arrhenius" temperature dependence of the reaction rate).

Sometimes there are attempts in theoretical treatments of experimental data to represent the temperature dependence of a branched chain reaction

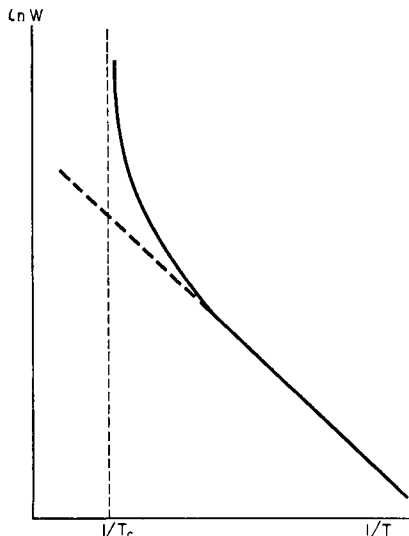


FIG. 142. Temperature dependence of the rate of a branched chain reaction.

by using the Arrhenius equation. These attempts usually show that the Arrhenius equation may be applied only over a relatively narrow range of temperature. Over a wide range of temperature the "apparent" or "effective" activation energy E^* in the "empirical" expression for the reaction rate

$$W = Z \exp(-E^*/RT),$$

is a function of temperature. Thus instead of the usual straight line plot of $\ln W$ against $1/T$, we obtain in this case a curve corresponding to the formula $\ln W = -E^*(T)/RT + \text{const.}$ Such a curve is shown in Fig. 142. Comparing the "empirical" formula for the reaction rate with the theoretical formula obtained earlier shows that E^* increases with temperature. Moreover the reaction rate also increases and at a certain temperature T_c —the critical temperature of the explosion—becomes infinite. The condition for explosion is that the denominator in the expression for W be zero, i.e. that

$$\delta_0 v_0 \exp[-(\Delta + E_1 - E_2)/RT] = 1. \quad (37.18)$$

This expression also determines the critical temperature of the explosion.

Interaction of Chains. Degenerate Branching

Here we shall consider the *interaction of chains*, a problem forming part of Semenov's theory of branched chain reactions. Earlier (p. 588) we came across examples of the negative interaction of chains, where as a result of radical recombination or disproportionation processes two chains are terminated simultaneously. Semenov also shows that the *positive* interaction of chains is possible and in his opinion may take place when the energy of two exothermic links of two chains developing in parallel is sufficient for the generation of a new additional reaction centre, so that three active centres are formed instead of two. As a possible example of this type of chain interaction, Semenov cites the reaction of chlorine with hydrogen. If it is assumed that the energy liberated in the most exothermic link, $\text{H} + \text{Cl}_2 = \text{HCl}^* + \text{Cl} + 45.0 \text{ kcal}$, is concentrated mainly in the HCl^* molecule, and that the probability of additional activation due to this energy is not vanishingly small, then in addition to the main elementary processes in the reaction mechanism we must assume that the rare process $2\text{HCl}^* + \text{Cl}_2 = 2\text{HCl} + 2\text{Cl}$ is responsible for the additional activation.

In its experimental aspect the positive interaction of chains has so far received little study, so that at present there are few experimental data which may be interpreted with complete reliability as the positive interaction of chains. The first experimental indication of the existence of positive chain interaction was given by Voronkov and Semenov [49], who studied flame propagation in carbon disulphide containing small amounts

of oxygen. Another indication of the occurrence of positive chain interaction is found in the work of Nalbandyan [199] who attributed the shift of the upper ignition limit, that he detected in the photochemical reaction of hydrogen and oxygen, to the process $\text{HO}_2 + \text{HO}_2 = \text{H}_2\text{O} + \text{O}_2 + \text{O}$; this is an infrequent process and results in the replacement of two inactive HO_2 radicals, formed during homogeneous chain breaking, by a very active oxygen atom.

In its essentials Semenov's idea [232] regarding *degenerate branching* is close to the idea of positive chain interaction. His idea arose from the necessity of explaining the kinetics of many slow reactions, having the characteristic properties of branched-chain reactions, on the basis of chain theory. In particular these reactions obey the $\exp(\varphi t)$ law but are distinguished by an unusually slow development of the chain. According to Semenov [232] "the main chain in such cases develops with the usual velocity (i.e. very rapidly) and is not accompanied by branching in the usual sense of this term as we see it." However, "as a result of the reaction in this primary chain a relatively stable *intermediate* product and not the final one is formed. This intermediate product accumulating in the original gas will then react independently and slowly, leading to the final product. Sometimes, however, at the cost of the energy of this secondary reaction, centres are created which are again able to start the chain of the primary reaction." Semenov calls these secondary chains "degenerate branches".

Such reactions following a chain mechanism with degenerate branching include the reactions of slow oxidation of various classes of organic substances (in particular, hydrocarbons).

We shall now consider the kinetics of chain reactions when chains interact. Substituting $\epsilon = 1 + \delta$ in equation (34.5) we obtain

$$\frac{dn}{dt} = W_0 + \delta v_1 n - v_2 n. \quad (37.19)$$

If propagation (branching) of a chain is first order with respect to n (the concentration of active centres), and the rate of chain breaking is proportional to the square of the concentration of active centres (negative interaction of chains) we should put $v_2 = v_2^0 n$ in equation (37.19), so that

$$\frac{dn}{dt} = W_0 + \delta v_1 n - v_2^0 n^2. \quad (37.20)$$

The solution of (37.20) with the limiting condition that $n = 0$ when $t = 0$ yields

$$n = \frac{2W_0[1 - \exp(-\gamma t)]}{\gamma[1 + \exp(-\gamma t)] - \delta v_1[1 - \exp(-\gamma t)]}, \quad (37.21)$$

where

$$\gamma = (\delta^2 v_1^2 + 4W_0 v_2^0)^{1/2}.$$

It is not difficult to see that in the initial period of the reaction ($t \ll 1/\gamma$) expression (37.21) may be written simply:

$$n = W_0 t, \quad (37.22)$$

and the initial rate of reaction is expressed by the equation

$$W = W_0 v_1 t.$$

After a sufficiently long time ($t \gg 1/\gamma$) the concentration of active centres becomes stationary:

$$n_{\text{stat}} = (\delta v_1 / 2v_2^0) [1 + (1 + 4W_0 v_2^0 / \delta^2 v_1^2)^{1/2}] \quad (37.23)$$

The rate of the steady reaction is

$$W = (\delta v_1^2 / 2v_2^0) [1 + (1 + 4W_0 v_2^0 / \delta^2 v_1^2)^{1/2}]. \quad (37.24)$$

As we see, in this case the rate of reaction never goes to infinity; consequently in this case there is no non-stationary regime. The cause of this is quadratic chain breaking.

We should also note the following case. As follows from (34.5), if the concentration of active centres is zero at the start of the reaction, the reaction may begin only if active centres are generated thermally or externally, i.e. if $W_0 \neq 0$. However, having started, the reaction continues even when the external generation of active centres ceases, due to the generation of active centres by the reaction itself. The concentration of active centres reaches the stationary value

$$n_{\text{stat}} = \delta v_1 / v_2^0;$$

the rate of the steady reaction is

$$W = \delta v_1^2 / v_2^0.$$

This case is closely similar to that of the transition of a non-selfsustained electric discharge to a self-sustained discharge; in both cases the process is started by an external factor (the external generation of active centres, the ionizing effect of an external agent) and continues even when the latter is removed, due to the generation of active particles (radicals and electrons) by the process itself. The basis of this analogy is the similarity of the mechanisms and kinetics of the two processes. In fact, the branching process in the electric discharge is the ionization of molecules by impact of a fast electron or ion (impact ionization), as a result of which one new electron and one new ion appear, i.e. two new "active centres". The rate of this branching process, like the rate of the chemical branching process in the case considered, is directly proportional to the concentration of active (ionizing) particles. The process analogous to termination of chemical chains is the recombination of ions and electrons in the electric discharge, i.e. a quadratic process similar to quadratic chain breaking.

A result which is superficially similar to the foregoing is obtained when chain branching follows a quadratic law (positive interaction of chains) and the chain breaking is proportional to n , although this case is scarcely met in practice. In this case we have $v_1 = v_1^0 n$ and equation (37.19) may be written

$$dn/dt = W_0 + \delta v_1^0 n^2 - v_2 n.$$

The solution of this equation with the initial condition that $n = 0$ when $t = 0$ yields for the concentration of active centres

$$n = \frac{2W_0[1 - \exp(-\gamma t)]}{\gamma[1 + \exp(-\gamma t)] + v_2[1 - \exp(-\gamma t)]} \quad (37.25)$$

$[\gamma = v_2(1 - 4W_0\delta v_1^0/v_2^2)^{1/2}]$ which is similar to expression (37.21). Like (37.21), expression (37.25) takes the form of (37.22) at sufficiently small t . For large t this expression, like (37.21), is constant:

$$n = (v_2/2\delta v_1^0)[1 - (1 - 4W_0\delta v_1^0/v_2^2)^{1/2}]. \quad (37.26)$$

However, in contrast with the constant value of (37.23), which is obtained from (37.21) and corresponds to the stationary concentration of active centres, (37.26) expresses the stationary concentration of active centres only when $4W_0\delta v_1^0/v_2^2 < 1$. When this condition is not obeyed, i.e. when $4W_0\delta v_1^0/v_2^2 > 1$, the quantity n becomes imaginary and hence in this case the stationary regime is not possible.

Moreover, in contrast with the case considered earlier, where W_0 tends to zero, the stationary concentration of active centres in the case of quadratic branching also tends to zero, i.e. the stationary reaction is impossible when there is no external generation of active centres.

Finally, we consider the case where both chain branching and breaking follow a quadratic law, i.e. where the kinetic equation has the form

$$dn/dt = W_0 + (\delta v_1^0 - v_2^0)n^2.$$

The solution of this equation when $\delta v_1^0 - v_2^0 > 0$ gives for the concentration of active centres:

$$n = [W_0/(\delta v_1^0 - v_2^0)]^{1/2} \tan\{[W_0(\delta v_1^0 - v_2^0)]^{1/2}t\}, \quad (37.27)$$

and hence a stationary regime is not possible in this case. When

$$\delta v_1^0 - v_2^0 < 0$$

the solution of the kinetic equation has the form

$$n = \left[\frac{W_0}{v_2^0 - \delta v_1^0} \right]^{1/2} \frac{1 - \exp\{-2\sqrt{[W_0(v_2^0 - \delta v_1^0)]}t\}}{1 + \exp\{-2\sqrt{[W_0(v_2^0 - \delta v_1^0)]}t\}}. \quad (37.28)$$

In this case after an adequate reaction time a stationary concentration of active centres is established, namely

$$n_{\text{stat}} = \sqrt{[W_0/(v_2^0 - \delta v_1^0)]}. \quad (37.29)$$

It is apparent from (37.29) that when $\delta v_1 = v_2$ the concentration of active centres, and consequently the rate of reaction, becomes infinite. Therefore $\delta v_1^0 = v_2^0$ expresses the condition for explosion. We should emphasize that, like the cases considered earlier (p. 601), the condition for explosion does not involve the quantity W_0 , i.e. when this condition is fulfilled the explosion is independent of W_0 . The time of onset of the explosion is, however, markedly dependent on the value of W_0 : the higher the rate W_0 of generation of active centres the sooner the rate of reaction reaches a value at which the explosive régime sets in.

§38. Macroscopic Stages in Chain Reactions

Earlier (in §3) we considered the effect of foreign admixtures on the course of chemical reactions (homogeneous catalysis). The effect of admixtures, both accelerating (positive catalysis) and retarding (negative catalysis) reaction, is particularly large in the case of chain reactions. In most cases the accelerating effect consists in making chain initiation easier, or in causing branching, which does not take place or is of low probability in the absence of admixtures. Such is the effect of different types of initiating admixtures, which usually represent a substance readily decomposing into free atoms or radicals. In the case of branched chain reactions the effect of such admixtures leads to broadening of the ignition region, as for example is observed when small quantities of nitrogen dioxide NO_2 are added to a detonating mixture: according to the data of Nalbandyan [200] the addition of 0.008 per cent NO_2 raises the upper explosion limit by approximately twofold (in the temperature range 440 to 475°C); addition of 0.24 per cent NO_2 leads to a decrease in the ignition temperature of 100° (from 470 to 370°C when the pressure of the mixture is about 20 mm Hg).

Retarding effects of admixtures on chain reactions apparently lead in most cases to chain breaking as a result of destruction of active centres: the length of the chain consequently may decrease so much that the reaction loses its chain character. As an example of this mechanism we shall consider the inhibiting effect of oxygen on the reaction of chlorine with hydrogen [24]. Thus, data in favour of this mechanism were obtained by Markevich [181] in a study of the effect of nitrogen and oxygen on the rate of formation of HCl . It was shown that in contrast with the nitrogen admixture, oxygen markedly decreases the reaction rate; this is explained by chain breaking as a result of the reaction of H and Cl atoms with

oxygen molecules. Apparently this is also the mechanism of the effect of nitrogen trichloride NCl_3 on the reaction of hydrogen with chlorine, for which it is one of the most active inhibitors. According to Griffith and Norrish [705], insignificant quantities of NCl_3 decrease the quantum yield of HCl from some tens of thousands to two, i.e. the reaction becomes a non-chain reaction.

In a series of studies by Hinshelwood and coworkers (see [1119]) on the thermal decomposition of paraffins and ethers a similar mechanism is assumed for the effect of NO . With increase in NO content the reaction rate decreases to a limiting value which, in the opinion of the authors, is the rate of the non-chain molecular (and not radical) reaction which takes place in parallel with the chain process (which occurs in the absence of NO). On the other hand, in references [1257a], [216a] and [1065] referring to paraffin cracking in the presence of deuterated molecules, which are capable of exchanging deuterium atoms with radicals of the chain, it was shown that exchange in the products at a similar extent of reaction does not depend on the inhibitor admixture. Thus there are doubts as to the accuracy of the main hypothesis of Hinshelwood concerning the non-radical character of the inhibitor reaction. Poltorak and Voevodskii suggested that the effect of NO in thermal decomposition reactions is related to the decrease in the rate of the heterogeneous initiation of chains in these systems [44a]. In this way the effect of inhibitors may consist of suppression of chain initiation, in addition to chain breaking.

Detailed study of the effect of inhibitors shows that frequently their retarding action is displayed only when the inhibitor is added to the *initial mixture*. Addition of the inhibitor to a mixture already reacting does not markedly affect the reaction rate. For example, Emanuel' [305] found that adding sulphur vapour (0.5 to 1 mm Hg) to a mixture of hydrogen sulphide and oxygen completely stops the H_2S oxidation, although the same amount of sulphur added to a reacting mixture (after the maximum rate of reaction has been reached) does not affect the course of the reaction. Still earlier, Frost and coworkers [61] showed that addition of propylene C_3H_6 to the original ethane C_2H_6 markedly retards the thermal decomposition of ethane, and practically does not affect the rate of decomposition when added to ethane in the process of conversion. Another example is the oxidation of propane in the presence of hydrogen bromide HBr , which yields acetone CH_3COCH_3 as the main product. It was shown by Maizus and Emanuel' [177] that when acetone is added to the original mixture there is a retarding effect on the reaction. Figure 143 shows these authors' kinetic curves for the formation of acetone at 200°C in a mixture containing propane (80 mm Hg), oxygen (80 mm Hg), HBr (17 mm Hg) and various amounts of acetone (from 0 to 100 mm Hg). According to these data, an increase in the amount of acetone added is paralleled by a decrease in acetone yield; when sufficient

acetone is added (75 mm Hg and larger amounts) the reaction is completely stopped.

To explain this and similar facts Emanuel' suggested the occurrence of two (or more) *macroscopic reaction stages*, with the inhibitor (in the last example, acetone) affecting only the first, initiating stage of the reaction. In this stage, as a result of interaction of the catalyst (in the last example, HBr) with the initial substances, an active intermediate substance is formed which is the initiator of the chain process forming the reaction product and taking place in subsequent stages of the reaction. Here the extent of

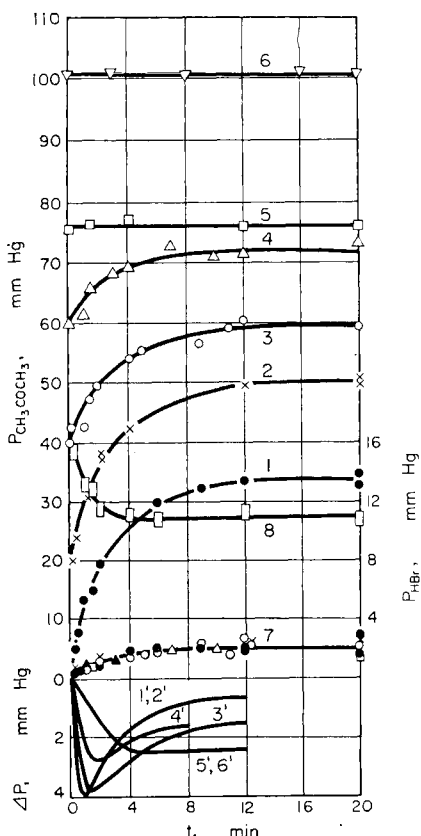


FIG. 143. Kinetic curves for formation of acetone in a mixture of propane C_3H_8 (80 mm Hg) + hydrogen bromide HBr (17 mm Hg) + acetone ($P_{C_2H_5COCH_3}$ mm Hg) with oxygen. Acetone pressure: (1) 0 mm; (2) 20 mm; (3) 40 mm; (4) 60 mm; (5) — 75 mm (limiting concentration); (6) 100 mm; (7) kinetic curve for the formation of acids under the conditions of experiments (1) to (6); (8) kinetics of propane consumption in experiments (1) to (6); (1') to (6') kinetic curves with respect to pressure change [experiments (1) to (6)] (according to Emanuel' [177]).

conversion is determined by the amount of intermediate substance formed. When an inhibitor is added to the original mixture, then owing to retardation of the initial reaction stage, the amount of active intermediate substance decreases to a greater extent the larger the amount of inhibitor added; parallel with the decrease in concentration of the active substance the extent of conversion decreases. For a limiting (or higher) concentration of inhibitor the initiating stage of the reaction is completely suppressed and the active substance is not formed, so that the end product of the reaction is not formed either (i.e. the extent of conversion is zero).

The idea of the occurrence of an initiating stage in homogeneous catalytic reactions followed by stages leading to the end product of the reaction is supported by the experiments of Emanuel' and coworkers [175] who used Koval'skii's method (see p. 45) to measure the heating up of the reacting mixture in the course of reaction. The heating curve of a mixture of propane, oxygen and HBr at 220°C is shown in Fig. 144, in which

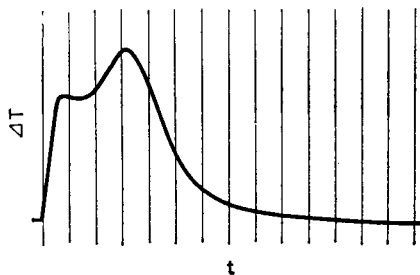


FIG. 144. Photo-registration of heating in a reacting mixture of C_3H_8 , O_2 and HBr at 200°C. The vertical lines are spaced at 30 sec time intervals. The second heating maximum is 4.9° (according to Maizus, Markevich and Emanuel' [175]).

time is plotted along the abscissa axis and the amount of heating along the ordinate axis. It is apparent from this curve that in the course of the reaction there are two heating maxima; the first (the left-hand) maximum is attributed by the authors to the evolution of heat in the initiating macroscopic reaction stage and the second maximum to evolution of heat in subsequent stages. Similar curves with two maxima have also been obtained in the case of oxidation of ethane in the presence of HBr [299] and for the oxidation of propane which is catalysed by oxides of nitrogen [178].

The idea of macroscopic stages in chain reactions requires a chemical basis. This means that for each definite reaction we must establish the chemical nature of the active intermediates which are formed in the first, initiating, stage and also the character and mechanism of the processes leading to the formation of the active substances. The fruitfulness of this idea of macroscopic stages is already obvious, however. For instance, in

the opinion of Emanuel' the occurrence of an initial stage determining the extent of conversion (see above) should be directly related to the existence of limits to the conversion in a given system; these limits are shown by the cessation of reaction long before the initial substances have been completely consumed, and have nothing in common with the limits which are fixed by the chemical equilibrium in the system. For example, in the above example of propane oxidation the thermodynamic limit is the complete conversion of propane into acetone, whereas in its final state the system contains both unconsumed propane and oxygen, in larger amounts the larger the amount of inhibitor (acetone) added to the original mixture (see above). Another example is that mentioned earlier (p. 18) regarding the oxidation of acetaldehyde; at a definite stage of this reaction oxygen ceases to take part in the reaction although it is present in the system. This and similar facts must clearly be attributed to chemical changes in the system (in the case of homogeneous catalytic reactions the changes are determined by processes in the initiating stage), as a result of which either the system undergoes transition to a new state characterized by a new set of processes, or chemical conversion ceases. A common case of a reaction ceasing long before thermodynamic equilibrium has been reached occurs in the branched-chain reactions in the combustion of various gases where, after a definite amount of the original fuel has been burned up, the system undergoes transition to a state in which processes of chain breaking predominate over branching processes and the reaction ceases (is extinguished), although both fuel and oxygen are present in the system in amounts much greater than their equilibrium concentrations. Apparently it must be considered that limiting phenomena, which have been established for slow oxidation reactions and are shown by the reaction ceasing completely at a definite extent of conversion or by its transition from one macroscopic reaction stage to another, are also determined by the ratios of the rates of the individual elementary processes; these ratios reach limiting (critical) values at definite stages of chemical conversion in the system.

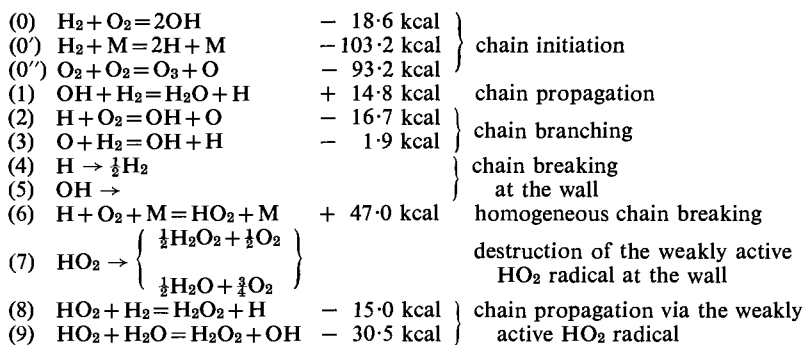
§39. The Combustion of Hydrogen as a Model Reaction

Mechanism of the Reaction

We have already shown that the combustion of hydrogen is a reaction the experimental study of which has given essential material on which the theory of branched-chain reactions is based. The mechanism of the hydrogen combustion reaction has now been studied in great detail; in the large number of studies devoted to this reaction the work of Russian chemists occupies a prominent position [203, 151, 877]. Moreover, it has been shown that the main features of the mechanism of this reaction are

also characteristic of the combustion reactions of other gases. For this reason the combustion of hydrogen should be considered as a model reaction representing to some extent combustion reactions in general. This justifies the more detailed examination of the hydrogen combustion reaction given in this section.

The following elementary processes should be considered at present as those most precisely representing the actual mechanism of hydrogen combustion:



According to this mechanism, H and O atoms and OH and HO_2 radicals are the active centres of the hydrogen combustion reaction. The HO_2 radical, however, is of low activity and consequently plays only a secondary role (see below) as an active centre propagating the chain. All four active centres H, O, OH and HO_2 have been directly detected [616, 617, 790] in the combustion zone of hydrogen; the measured concentrations of H atoms [150, 151] and OH radicals [139, 133] were found to be hundreds and thousands of times greater than their equilibrium concentrations, i.e. the concentrations if all the substances in the flame were in thermal equilibrium.

Let us consider the individual elementary processes in this reaction mechanism. At the present time it is not known with complete reliability which of the three possible chain-initiation processes given above occurs in practice. According to Semenov [237], the main role here must be played by process (0) as it is much more favourable energetically than the other two processes. The activation energy of this process is 45 kcal according to Semenov. It is not reliably known whether the chain-initiating processes take place homogeneously or heterogeneously. The slow rate at which the dissociation equilibrium is established without involving a surface (see pp. 578-80) and also the marked effect of the nature of the surface on the hydrogen flame tend to support the heterogeneous mechanism of chain initiation. A convincing argument in favour of heterogeneous initiation of chains in the hydrogen combustion reaction is given by the recent work of

Patrick and Robb [1013] who found that coating the walls of the reaction vessel with potassium chloride KCl retards only the thermal⁽²⁰⁾ and not the photochemical reaction of H₂ and O₂. It follows from this that the retarding effect of KCl in this case does not consist in chain breaking but in suppressing chain initiation at the surface.

Processes (1) and (2) have been studied quite adequately. The rate constant of process (1) has been calculated from the experimental data of Avramenko [1] on parallel measurements of the rate of combustion of hydrogen and the concentration of hydroxyl in the flame (for mixtures of different composition) and shown to be [134]

$$k_1 = 2 \cdot 3 \times 10^{-10} \exp(-10,000/RT) \text{ cm}^3 \text{ molecule}^{-1} \text{ sec}^{-1}.$$

Analysis of data obtained by various authors and referring to the upper (second) ignition limit of hydrogen showed that the rate constant of process (2) is [203]

$$k_2 = 2 \cdot 1 \times 10^{-10} \exp(-18,800/RT) \text{ cm}^3 \text{ molecule}^{-1} \text{ sec}^{-1}.$$

It should be mentioned that according to [104a] the pre-exponential factor of k_2 is $0 \cdot 9 \times 10^{-10} \text{ cm}^3 \text{ molecule}^{-1} \text{ sec}^{-1}$ and the activation energy is 15,100 cal. As follows from V. V. Azatyan, V. V. Voevodskii and A. B. Nalbandyan, *Dokl. Akad. Nauk*, **132**, 864 (1960), $A = 1 \cdot 65 \times 10^{-10} \text{ cm}^3 \text{ molecule}^{-1} \text{ sec}^{-1}$, and $E = 16 \cdot 3$ kcal [V. V. Voevodskii and V. N. Kondrat'ev, *Determination of rate constants for elementary steps in branched chain reactions*; in *Progress in Reaction Kinetics*, Pergamon Press, 1960 p. 41]. See also G. L. Schott and J. L. Kinsey, *J. Chem. Phys.*, **29**, 1177 (1958).

The rate constant for process (3) is

$$k_3 = 1 \cdot 5 \times 10^{-10} \exp(-12,100/RT) \text{ cm}^3 \text{ molecule}^{-1} \text{ sec}^{-1}$$

[V. V. Azatyan, V. V. Voevodskii and A. B. Nalbandyan, *loc. cit.*].

The rates of (4), (5) and (7), the chain breaking processes at the wall, are determined in different ways depending on whether the heterogeneous process of breaking takes place in the kinetic or the diffusion region (cf. p. 590). If $\epsilon d/\lambda < 1$ (ϵ is the probability of an atom or radical "sticking" on its collision with the wall, d is the diameter of the reaction vessel and λ the mean free path of the given centre) breaking takes place in the kinetic region. In this case the rate constant of chain breaking at the wall is

$$k_4 = B\epsilon v/d, \quad (39.1)$$

where B is a constant equal to 1 for a cylindrical vessel and 3/2 for a spherical vessel; v is the mean thermal velocity of the active centre.

⁽²⁰⁾ Still earlier Pease [1018] found that washing the reaction vessel with a potassium chloride solution decreases the rate of the thermal reaction of hydrogen with oxygen by approximately 2000-fold.

If $\epsilon d/\lambda \gg 1$ the process takes place in the diffusion region and the rate constant in this case is determined by the equation

$$k_4 = AD/d^2. \quad (39.2)$$

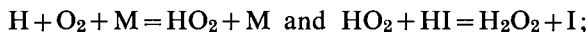
Here D is the diffusion coefficient; A is a constant equal to 23.2 for a cylindrical vessel and 39.3 for a spherical vessel.

Direct measurements of ϵ for H atoms show that this quantity depends on the nature of the surface and has values over a wide range: from 1 for platinum, graphite and certain other substances to 10^{-5} for freshly fused glass or for glass rinsed with certain substances (for example, potassium tetraborate $K_2B_4O_7$) [203].

Chain breaking at the wall by OH radicals "sticking" is important only in poor mixtures of H_2 and O_2 , i.e. at low concentrations of hydrogen, when the concentration of hydroxyl in the flame is relatively high. For this reason and owing also to the difficulty of obtaining sufficiently high concentrations of hydroxyl in pure form the quantity ϵ for OH has been studied in much less detail than ϵ for H. The most reliable data have been obtained by Nalbandyan and Voevodskii [203] from a kinetic analysis of the dependence of the lower (first) ignition limit of hydrogen on the composition of the hydrogen–oxygen mixture. It follows from these data that ϵ_{OH} for various types of glass is about 10^{-3} to 10^{-2} .

There has also been little study of ϵ for the HO_2 radical. It may be concluded from kinetic data that for pure, freshly fused vessels ϵ_{HO_2} is small and is about 10^{-5} , and for vessels rinsed with various salts (KCl , $K_2B_4O_7$) ϵ_{HO_2} is large and this leads to rapid destruction of HO_2 radicals at the wall.

Homogeneous chain breaking involving a ternary collision process was introduced as a hypothetical process to explain the second ignition limit. The reality of this process was indicated by many subsequent experiments. Here we shall mention the work of Cook and Bates [498] who showed that the kinetic features of the photochemical formation of H_2O_2 in the $HI + O_2$ system are in good agreement with the mechanism of this reaction consisting of the elementary processes



the work of Foner and Hudson [616, 617] shows that the HO_2 radicals they detected mass-spectrometrically (see also [790]) are formed as a result of the termolecular process $H + O_2 + M \rightleftharpoons HO_2 + M$.

From kinetic data on the second ignition limit (and also on the "cape" of the ignition peninsula) it was found that the rate constant of process (6) for a stoichiometric mixture is

$$k_6 = 2.4 \times 10^{-33} \text{ cm}^6 \text{ molecule}^{-2} \text{ sec}^{-1}.$$

This value is obtained assuming that k_6 does not depend on temperature. In fact a weak temperature dependence is observed and k_6 apparently decreases with increasing temperature (see p. 336).

The constant k_6 depends on gas composition according to the equation:

$$k_6 = (1/p)[k_6^{(H_2)}p_{H_2} + k_6^{(O_2)}p_{O_2} + k_6^{(H_2O)}p_{H_2O} + k_6^{(X)}p_X]$$

where p_{H_2} , p_{O_2} and p_{H_2O} are the partial pressures of hydrogen, oxygen and water vapour; p_X is the partial pressure of a possible inert admixture and p the total pressure.

The values of k_6 for O_2 , N_2 , CO_2 and H_2O , referred to $k_6^{(H_2)}$, are [203]:

H_2	O_2	N_2	CO_2	H_2O
1.00	0.35	0.43	1.43	5.0

Finally, the chain propagation processes involving HO_2 radicals are important in the so-called slow oxidation of hydrogen which occurs above the upper (second) ignition limit, i.e. at relatively high pressures; here, owing to retardation of the diffusion of HO_2 radicals to the walls, processes of interaction of these radicals in the gas phase leading to chain propagation begin to compete with the processes of their destruction at the wall. The formation of hydrogen peroxide in the gas phase is directly indicated by the results of analysing the slow oxidation reaction products. It follows from this analysis that when the reaction is carried out so that the products are rapidly withdrawn from the reaction zone (quenching), up to 85 per cent H_2O_2 is detected in the reaction products [133] (see Fig. 5, p. 21). Formation of hydrogen peroxide under these conditions may be associated with both processes (8) and (9). That these processes are possible is clear from the high probability of the corresponding reverse processes. Thus it is known that the rate of reaction of H atoms with hydrogen peroxide is high, and this may be connected with the process $H + H_2O_2 = H_2 + HO_2$, i.e. a process the reverse of (8) [660]; it has also been established that hydroxyl rapidly disappears in the presence of hydrogen peroxide and this is undoubtedly connected with the process $OH + H_2O_2 = H_2O + HO_2$, which is the reverse of (9) [643]. From analysis of the reaction kinetics of slow oxidation of hydrogen, Voevodskii and Talrose [V. V. Voevodskii and V. L. Talrose *J. phys. Chem. Moscow*, **22**, 1192 (1948)] found that the rate constant of process (8) is

$$k_8 = 3 \times 10^{-12} \exp(-24,000/RT) \text{ cm}^3 \text{ molecule}^{-1} \text{ sec}^{-1}.$$

The rate constant of process (9) is [V. N. Kondrat'ev, *Dokl. Akad. Nauk*, **137**, 120 (1961)]

$$k_9 = 3 \times 10^{-11} \exp(-30,000/RT) \text{ cm}^3 \text{ molecule}^{-1} \text{ sec}^{-1}.$$

Let us now consider first a reaction occurring near or inside the ignition peninsula, i.e. under conditions such that chain propagation involving HO₂ radicals does not play an appreciable part and the formation of this radical in fact characterizes chain termination. Under these conditions the rates of processes (8) and (9) will be considered to be zero.

Kinetics of the Reaction at Low Pressures

As the reaction involves three active centres (H, O and OH) its scheme is much more complex than that of the branched chain reaction shown in Fig. 133 (p. 573) which involves only one active centre. In future we shall consider that thermal initiation of chains is associated with process (0). In addition, for simplicity we shall assume that the rate of process (5) is zero.

If the concentrations of OH, H and O are n_1 , n_2 and n_3 respectively, and the frequencies of processes (1), (2), (3), etc., are v_1 , v_2 , v_3 , ..., we may write the kinetic equations

$$\begin{aligned} \frac{dn_1}{dt} &= 2W_0 - v_1n_1 + v_2n_2 + v_3n_3, \\ \frac{dn_2}{dt} &= v_1n_1 - (v_2 + v_4 + v_6)n_2 + v_3n_3, \\ \frac{dn_3}{dt} &= v_2n_2 - v_3n_3. \end{aligned}$$

Taking the frequencies v_i to be approximately constant, which is permissible in the initial period of the reaction when the concentrations of initial substances still differ little from the original concentrations, the above kinetic equations constitute a system of linear differential equations. The solutions of this system may be written

$$n_i = n_i^0 + A_i \exp(\lambda_1 t) + B_i \exp(\lambda_2 t) + C_i \exp(\lambda_3 t), \quad i = 1, 2, 3. \quad (39.3)$$

Calculating the derivatives dn_i/dt and substituting them together with the n_i values in the kinetic equations, and equating coefficients of similar exponential terms [$\exp(\lambda t)$] we obtain algebraic equations from which we find the parameters n_i^0 , $\lambda_{1,2,3}$, A_i , B_i and C_i .

In this way the n_i^0 quantities are found to be

$$n_1^0 = \frac{2(v_4 + v_6)W_0}{v_1(v_4 + v_6 - 2v_2)}; \quad n_2^0 = \frac{2W_0}{v_4 + v_6 - 2v_2}; \quad n_3^0 = \frac{2v_2W_0}{v_3(v_4 + v_6 - 2v_2)}. \quad (39.4)$$

It is not difficult to see that the quantities n_i^0 are solutions of the steady problem, i.e. solutions of the system of algebraic equations

$$\begin{aligned} \frac{dn_1}{dt} &= 0, \\ \frac{dn_2}{dt} &= 0, \\ \frac{dn_3}{dt} &= 0. \end{aligned}$$

Moreover, the quantities λ_1 , λ_2 , and λ_3 are the roots of the cubic equation

$$\lambda^3 + (v_1 + v_2 + v_3 + v_4 + v_6)\lambda^2 + [v_1v_3 + (v_1 + v_3)(v_4 + v_6)]\lambda - v_1v_3(2v_2 - v_4 - v_6) = 0.$$

Without solving this equation it is not difficult to satisfy oneself that in a developing reaction, i.e. for a non-stationary regime, two roots out of the three are *negative* and in their absolute size are *larger* than the positive root. Actually, in this case the probability of chain propagation (via H atoms) $\alpha_H = v_2/(v_2 + v_4 + v_6)$ (which is also the probability of branching) should be greater than the probability of chain breaking, namely

$$\beta_H = (v_4 + v_6)/(v_2 + v_4 + v_6);$$

thus the factor $2v_2 - v_4 - v_6$ in the last term of the cubic equation has a positive sign. From the property of cubic equations that the last term taken with the opposite sign is equal to the product of the roots of the equation, it follows that $\lambda_1\lambda_2\lambda_3 > 0$, and hence either all three roots are positive or one is positive and two are negative. It is easy to see that the latter case holds in practice: it is evident from another property of cubic equations as expressed by the relation

$$\lambda_1 + \lambda_2 + \lambda_3 = -(v_1 + v_2 + v_3 + v_4 + v_6) < 0,$$

that the sum of the negative roots must be greater in magnitude than the positive root.

Approximate values for the roots of the above cubic equation may be obtained in the following way. From values for the constants k_1 , k_2 and k_3 given on p. 611 it follows that, for temperatures $T \leq 1000^\circ\text{K}$, frequencies v_1 and v_3 must be greater than v_2 by at least a factor of ten. Moreover, since we have $2v_2 - v_4 - v_6 > 0$ (see above) we find the following relationship between these five frequencies in the cubic equation:

$$v_1, v_3 \gg v_2 > v_4 + v_6.$$

Allowing for this relationship we may write the cubic equation in the approximate form

$$\lambda^3 + (v_1 + v_3)\lambda^2 + v_1v_3\lambda - v_1v_3(2v_2 - v_4 - v_6) = 0,$$

and hence the following approximate values for the roots are obtained: $\lambda_1 \approx -v_1$, $\lambda_2 \approx 2v_2 - v_4 - v_6$ and $\lambda_3 \approx -v_3$. Since $\lambda_1 < 0$ and $\lambda_3 < 0$, when $t \gg 1/|\lambda_1|$, $1/|\lambda_3|$ the second and fourth terms in (39.3) vanish and the concentration of active centres may be expressed by the simpler equations

$$n_t = n_t^0 + B_t \exp(\lambda t), \quad (39.5)$$

where $\lambda = \lambda_2$.

Finally, the ratios of quantities A_1 , A_2 and A_3 , etc., are

$$A_1 : A_2 : A_3 = \frac{v_2(2v_3 + \lambda_1)}{(v_1 + \lambda_1)(v_3 + \lambda_1)} : 1 : \frac{v_2}{v_3 + \lambda_1},$$

$$B_1 : B_2 : B_3 = \frac{v_2(2v_3 + \lambda_2)}{(v_1 + \lambda_2)(v_3 + \lambda_2)} : 1 : \frac{v_2}{v_3 + \lambda_2},$$

$$C_1 : C_2 : C_3 = \frac{v_2(2v_3 + \lambda_3)}{(v_1 + \lambda_3)(v_3 + \lambda_3)} : 1 : \frac{v_2}{v_3 + \lambda_3}.$$

Only the ratios of the B_i quantities are of interest with regard to (39.5). Substituting in these ratios $\lambda_2 = 2v_2 - v_4 - v_6$, and remembering that $v_1, v_3 \gg \lambda_2$ we may write the ratios in the approximate form:

$$B_1 : B_2 : B_3 = 2v_2/v_1 : 1 : v_2/v_3.$$

It is apparent from this that $B_2 \gg B_1, B_3$ and hence

$$dn_2/dt \gg dn_1/dt, dn_3/dt.$$

In view of this inequality we may reckon dn_1/dt and dn_3/dt to be approximately zero (compared with dn_2/dt). We should note that equating the time derivatives of the concentrations of the most active intermediate substances OH and O to zero is an expression of Semenov's method of partially stationary concentrations as applied to this case. Adding dn_1/dt , dn_2/dt and dn_3/dt (p. 614), we have then

$$dn_1/dt + dn_2/dt + dn_3/dt = 2W_0 + v_2n_2 + v_3n_3 - (v_4 + v_6)n_2 \approx dn_2/dt$$

or as $v_2n_2 = v_3n_3$ from $dn_3/dt \approx 0$,

$$dn_2/dt \approx 2W_0 + (2v_2 - v_4 - v_6)n_2. \quad (39.6)$$

It is not difficult to see that equation (39.6) is substantially the same as (37.19), which we obtained earlier for the simplified mechanism of a branched chain reaction involving one active centre. In fact, the first term $2W_0$ in (39.6) corresponds to the first term W_0 in (37.19): both terms express the rate of thermal generation of active centres [the factor 2 in (39.6) corresponds to our assumption that in the reaction of hydrogen with oxygen two active centres (OH radicals) are formed simultaneously in one elementary act (0)]. Moreover, the quantity $2v_2n_2$ in (39.6) corresponds to the second term $\delta v_1 n$ in (37.19): both these quantities express the rate of chain branching; the factor 2 in (39.6) expresses the fact that in the hydrogen combustion reaction there are two branching processes, (2) and (3), with overall rate $v_2n_2 + v_3n_3 = 2v_2n_2$. Finally, the quantity $(v_4 + v_6)n_2$ in (39.6) and the quantity v_2n in (37.19) express the rate of chain breaking. This correspondence between equations (39.6) and (37.19) shows that it is possible to reduce formally (approximately) the kinetics of a complex

chemical reaction involving several active centres to the kinetics of a simpler reaction involving *one* active centre. Mathematically this reduction corresponds to the possibility of replacing a system of differential equations by one differential equation and a corresponding number of algebraic equations. The possibility of this replacement is based on the fact that the various active centres participating in the reaction nearly always have different activities, and this in its turn makes it possible to use the method of partially stationary concentrations, which reduces the number of kinetic differential equations.

The conditions under which it is possible to reduce formally the problem involving several active centres to that involving one centre has recently been analysed in detail by Sayasov [228].

Upper and Lower Ignition Limits

The mechanism for the hydrogen combustion reaction shown on p. 610 gives a quantitative explanation of all the macroscopic properties of the reaction. We shall consider first the problem of ignition limits, the occurrence of which, as was shown above, is one of the main features of reactions following a branched chain mechanism.

Integrating equation (39.6) we find

$$n_2 = [C \exp(\varphi t) - 2W_0]/\varphi, \quad (39.7)$$

where $\varphi = (2v_2 - v_4 - v_6)$ and C is the constant of integration, which we need not determine here. When $\varphi > 0$ (a non-stationary regime of the reaction) we may neglect the quantity $2W_0$ in (39.7) for sufficiently high values of t , and this gives

$$n_2 = (C/\varphi) \exp(\varphi t), \quad (39.8)$$

i.e. Semenov's kinetic law, according to which the concentration of active centres (and consequently the reaction rate) in the case of a non-stationary branched chain reaction increases with time according to an exponential law (see p. 595). When $\varphi < 0$ expression (39.7) may be written

$$n_2 = [2W_0 - C \exp(-|\varphi|t)]/|\varphi|. \quad (39.9)$$

It is apparent from this equation that for large t the concentration n_2 of active centres becomes constant and equal to

$$n_2 = 2W_0/|\varphi|, \quad (39.10)$$

which is the stationary concentration of active centres, $(n_2)_{\text{stat}}$. The steady-state condition $dn_2/dt = 0$ also yields (39.10).

It follows from the above that transition from the stationary to the non-stationary regime of the reaction corresponds to change in sign of the

quantity φ in the kinetic equation. In this way, the critical condition for this transition may be written as an equation

$$\varphi = 2v_2 - v_4 - v_6 = 0. \quad (39.11)$$

The v_i quantities in this expression have the values: $v_2 = k_2 p_{O_2}$, $v_4 = k_4$ (kinetic region) or k_4^0/p (diffusion region) and $v_6 = k_6 p p_{O_2}$, where p_{O_2} is the partial pressure of oxygen and p the overall pressure. Assuming that $p_{O_2} = \alpha p$ (α is a quantity determined by the composition of the mixture) and substituting the v_i quantities in (39.11), we obtain the following equation for the pressures at the limits of ignition in the case of the kinetic region:

$$p^2 - 2ap + b^2 = 0, \quad (39.12)$$

and in the case of the diffusion region the equation

$$p^3 - 2ap^2 + b_0^2 = 0. \quad (39.13)$$

Here $a = k_2/k_6$, $b^2 = k_4/\alpha k_6$ and $b_0^2 = k_4^0/\alpha k_6$.

Let us consider the first of these cases (the kinetic region). Solving the quadratic equation (39.12) we find for the pressures at the lower and upper ignition limits:

$$p_1 = a - \sqrt{(a^2 - b^2)} \quad \text{and} \quad p_2 = a + \sqrt{(a^2 - b^2)}. \quad (39.14)$$

It is apparent from (39.14) that the sum $p_1 + p_2 = 2a$. Since for pressures sufficiently remote from the "cape" of the ignition peninsula p_2 is much larger than p_1 , we may obtain this result by considering that b^2 in formulae (39.14) is small compared with a^2 . In this case p_1 and p_2 are given by the approximate formulae:

$$p_1 \approx b^2/2a \quad \text{and} \quad p_2 \approx 2a - b^2/2a \approx 2a. \quad (39.15)$$

As k_6 , the termolecular collision constant, is independent or only weakly dependent on temperature and as the activation energy of chain breaking at the wall is in any case less than that of the branching process (2) (as follows from direct experimental study of destruction of atoms and radicals at various surfaces), the temperature dependence of p_1 and p_2 may be expressed approximately by the formulae:

$$p_1 = a_1 \exp(E_1/RT) \quad \text{and} \quad p_2 = a_2 \exp(-E_2/RT), \quad (39.16)$$

where $E_1 = E_2 - E_4$ (E_2 and E_4 are the activation energies of processes 2 and 4 respectively). It follows from (39.16) that p_1 decreases, whereas p_2 increases, with increase in temperature; this gives rise to the peculiar shape of the ignition peninsula (see Fig. 141, p. 598).

The cubic equation (39.13) for the diffusion region also gives two ignition limits, as the third root of the equation is negative and consequently has no physical significance. Actually, at high pressures, i.e. at the upper

ignition limit, we may neglect the quantity b_0^2 in formula (39.13) and this gives the approximate value

$$p_2 = 2a. \quad (39.17)$$

At the lower limit, on the other hand, p^3 must be small. Neglecting this quantity we obtain from (39.13)

$$p_1 = b_0(2a)^{-1/2}. \quad (39.18)$$

As we have already shown, the third root of equation (39.13) is negative. Actually from the relation $p_1 p_2 p_3 = -b_0 < 0$ it follows that $p_3 < 0$.

From (39.17) and (39.18) we obtain the following approximate formulae the temperature dependence of p_1 and p_2 :

$$p_1 = a_1 \exp(E_2/2RT) \quad \text{and} \quad p_2 = a_2 \exp(-E_2/RT). \quad (39.19)$$

The temperature dependence of p_1 and p_2 in this reaction has been the object of an all-round detailed study by Semenov's school. This study has been of great importance in providing quantitative confirmation and an experimental basis for the chemical reaction mechanism. In particular, the first, and most reliable, value for the rate constant of process (2) was obtained by Voevodskii [41] on the basis of a study of the temperature dependence of the upper ignition limit of hydrogen.

Induction Period

One of the characteristic properties of the hydrogen combustion reaction, and also of other branched chain reactions, is the occurrence of an *induction period*. Koval'skii has carried out the most detailed study of the induction period in the hydrogen combustion reaction by investigating the rate of reaction inside the ignition peninsula [113]. The significance of an induction period in branched chain reactions has been explained by Semenov on the basis of the general mechanism of these reactions.

In the hydrogen combustion reaction and similar reactions the induction period shows itself by the absence of any appreciable pressure change during a more or less lengthy time interval. After this time interval—the induction period—the pressure begins to change markedly. In this way, a false impression is created that reaction does not occur in the induction period. In fact, according to the theory of branched chain reactions, reaction starts at the very moment when the mixture is admitted to the reaction vessel, but in the initial period it has an immeasurably low rate. The reaction rate increases according to the $\exp(\varphi t)$ law and becomes measurable, using given experimental methods, at a certain time τ . Hence we see that the induction period is a quantity depending essentially on the sensitivity of the method of measuring the reaction rate and therefore does

not have the significance of a constant characteristic of the reaction. We shall show below how the induction period varies with a change in sensitivity of the method of measurement, and with a change of method of following the reaction.

It follows from this that for a given method of measuring the rate of reaction and for constant sensitivity of the method, the induction period must be the shorter, the higher the reaction rate, i.e. the higher the temperature or the higher the pressure of the reacting gas (if the reaction rate increases with pressure). This conclusion is supported by a large number of experiments. To illustrate the dependence of τ on reaction rate we give in Fig. 145 Koval'skii's data on measurements of the rate of combustion of a stoichiometric mixture of hydrogen and oxygen at constant temperature (485°C) but with different initial pressures (from 8.2 to 5.8 mm Hg). It is seen from this figure that with a pressure increase from 5.8 to 8.2 mm Hg the induction period is reduced from 0.2 to 0.05 sec.

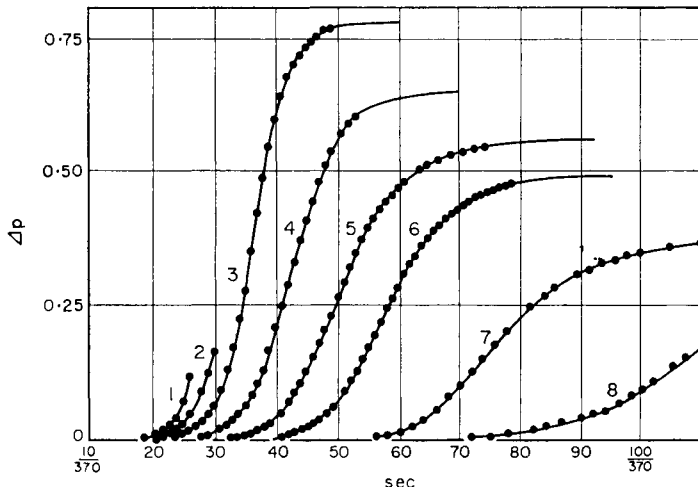


FIG. 145. Kinetic curves for the combustion of a stoichiometric mixture of hydrogen and oxygen at $T = 485^{\circ}\text{C}$ and initial pressures: (1) 8.2 mm Hg (2) 7.8; (3) 7.4; (4) 7.1; (5) 6.8; (6) 6.4; (7) 6.1; (8) 5.8 mm Hg (according to the data of Koval'skii [113]).

On the basis of the simplified mechanism we assumed for the combustion of hydrogen, the rate of change of the total pressure is found as the sum of the rates of change of the partial pressures of H_2 , O_2 , H_2O , H , OH and O :⁽²¹⁾

⁽²¹⁾ $W'_0 = kT W_0$, $v' = kT v_t$.

$$\begin{aligned}
 \frac{dp_{H_2}}{dt} &= -W'_0 - v'_1 n_1 - v'_3 n_3 + \frac{1}{2} v'_4 n_2, \\
 \frac{dp_{O_2}}{dt} &= -W'_0 - v'_2 n_2 + \frac{3}{4} v'_6 n_2 - v'_6 n_2, \\
 \frac{dp_{H_2O}}{dt} &= v'_1 n_1 + \frac{1}{2} v'_6 n_2, \\
 \frac{dp_H}{dt} &= v'_1 n_1 - v'_2 n_2 + v'_3 n_3 - v'_4 n_2 - v'_6 n_2, \\
 \frac{dp_{OH}}{dt} &= 2W'_0 - v'_1 n_1 + v'_2 n_2 + v'_3 n_3, \\
 \frac{dp_O}{dt} &= v'_2 n_2 - v'_3 n_3, \\
 \hline
 \frac{dp}{dt} &= -\frac{1}{2}(v'_4 + \frac{3}{2} v'_6) n_2. \tag{39.20}
 \end{aligned}$$

In this way, to calculate the pressure in the initial period of the reaction we must know the time dependence of n_2 , for which we may use formula (39.7). It is true that doubts arise here regarding the applicability of this formula in describing the process in the initial period of induction, since it was obtained by integrating equation (39.6) assuming that the concentrations of OH radicals and O atoms (see p. 616) are quasi-stationary, which at the very start of the reaction should not be the case. It may be shown, however, that formula (39.7) is a fairly good approximation.

In fact, solving the system of differential equations for H, OH and O (p. 614) we obtain for n_2 (the concentration of H atoms):

$$\begin{aligned}
 n_2 &= \frac{2W_0}{\varphi} \left[\frac{\lambda_2 \lambda_3 (v_3 + \lambda_1)}{v_3 (\lambda_1 - \lambda_2) (\lambda_1 - \lambda_3)} \exp(\lambda_1 t) + \right. \\
 &\quad \left. + \frac{\lambda_1 \lambda_3 (v_3 + \lambda_2)}{v_3 (\lambda_2 - \lambda_1) (\lambda_2 - \lambda_3)} \exp(\lambda_2 t) + \frac{\lambda_1 \lambda_2 (v_3 + \lambda_3)}{v_3 (\lambda_3 - \lambda_1) (\lambda_3 - \lambda_2)} \exp(\lambda_3 t) \right].
 \end{aligned}$$

Substituting in this formula the approximate values of λ_1 , λ_2 and λ_3 ($\lambda_1 = -v_1$, $\lambda_2 = \varphi$, $\lambda_3 = -v_3$) obtained earlier (p. 615) and allowing for the fact that in their absolute value λ_1 and λ_3 are at least ten times greater than λ_2 , we obtain from the last formula

$$n_2 = [2W_0/\varphi][\exp(\varphi t) - 1], \tag{39.21}$$

i.e. a formula identical with (39.7) if in the latter $C = 2W_0$ (which is equivalent to assuming that in the initial moment of time the concentration of H atoms is zero).

Substituting (39.21) in (39.20) and integrating this equation between limits 0 and t , we find

$$\Delta p = p_0 - p = A[\exp(\varphi t) - (1 + \varphi t)], \tag{39.22}$$

where p_0 is the initial pressure of the hydrogen–oxygen mixture and $A = (W_0/\varphi^2)(v_4 + \frac{3}{2}v_6)$. The $\Delta p/A$ values calculated from (39.22) are shown as a function of φt in Fig. 146. Here three curves are plotted using scales (along the ordinate axis) which differ from each other by 100 and

10,000 times. Since changing the scale corresponds to changing the sensitivity of the method of measurement, the curves in Fig. 146 give a standard for the dependence of the measured induction period τ of the reaction on the sensitivity of the method of measuring its rate. It is apparent from the figure that for a certain sensitivity, assumed to be 1 (the right-hand curve), the induction period is about 10 in φt units. When the sensitivity of the method is increased by 100 (the middle curve) and by 10,000 times (the

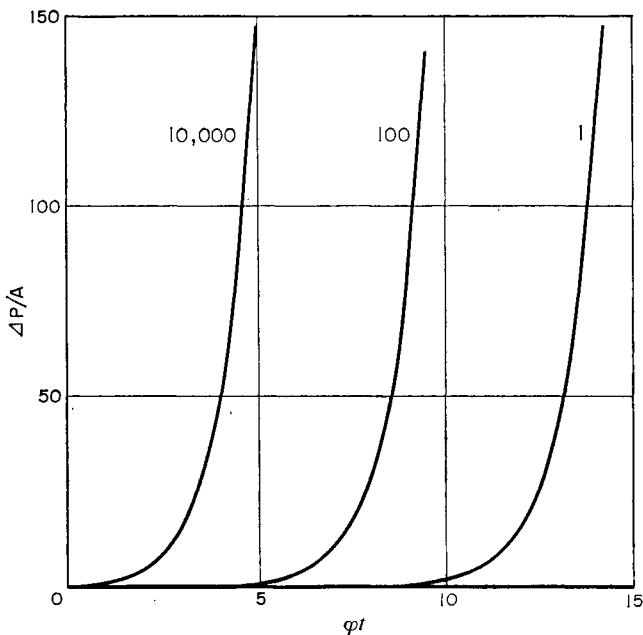


FIG. 146. Induction period in the hydrogen combustion reaction for various sensitivities of the method of measuring pressure.

left-hand curve) the induction period decreases to 5 and 1 φt unit respectively. The scale of $\Delta p/A$ determines the minimum measurable value of $\Delta p/(\Delta p)_{\min}$, for a given sensitivity of the method of measurement. Substituting this value in formula (39.22) and neglecting (as is almost always allowable) $1+\varphi t$ compared with $\exp(\varphi t)$, we obtain for the induction period τ :

$$\tau = (1/\varphi) \ln(\Delta p_{\min}/A). \quad (39.23)$$

The accuracy of (39.23) for the hydrogen combustion reaction was demonstrated experimentally by Koval'skii by showing that at the start of the reaction, when the burn-up of initial substances is still small, $\ln \Delta p$ is a linear function of time (see Fig. 152). Various authors have established

experimentally a formula of type (39.23) for a large number of other reactions. Moreover, on the basis of theoretical analysis of Koval'skii's data on measurements of Δp as a function of time, Semenov [237] calculated the activation energy of process (2) and found a value which has since been confirmed.

Reaction Kinetics Taking Account of Fuel Consumption. Overall Law of the Reaction

So far we have considered the frequencies v_i of the elementary processes to be constant, so that the mathematical kinetic problem has consisted of solving a system of differential equations with constant coefficients. Such a simplification of the problem is possible as long as we confine our study of the reaction to its initial stage, when the concentration of initial substances remains substantially the same. For an appreciable extent of reaction, however, it is clear that we must allow for the change in concentrations of all substances in the reaction zone; the problem then involves differential equations with variable coefficients, which are insoluble in the general case. Using the method of quasi-stationary concentrations, however, we may frequently reduce the problem to a system of two equations which is relatively simple to solve in certain cases. Using this solution we obtain definite ratios of the concentrations of active centres to the concentrations of initial substances; this enables us to express the rate of reaction by the concentration of initial substance. In this way the *overall law of the reaction* is obtained.

We shall consider as an example the hydrogen combustion reaction at a pressure so high that chain termination at the walls may be neglected. Let us replace formally the sum of processes (6) and (7) by the process $H + O_2 = \frac{1}{2}H_2O + \frac{3}{4}O_2$; and if the effective rate constant of this process is k , when $d(O)/dt = 0$ and $d(OH)/dt = 0$ we obtain

$$\begin{aligned} d(H)/dt &= 2W_0 + (2k_2 - k)(O_2)(H), \\ d(O_2)/dt &= -W_0 - (k_2 + \frac{1}{4}k)(O_2)(H). \end{aligned}$$

When the reaction is inside the ignition peninsula we have $2k_2 - k > 0$. Therefore, starting from a certain time t_x when the concentration of H atoms is sufficiently high, we may neglect the first term (W_0) in each of the foregoing equations, so that

$$\begin{aligned} d(H)/dt &= (2k_2 - k)(O_2)(H), \\ -d(O_2)/dt &= (k_2 + \frac{1}{4}k)(O_2)(H). \end{aligned}$$

Dividing one of these equations by the other and integrating we find

$$(O_2)_x - (O_2) = C[(H) - (H)_x],$$

where $C = (k_2 + \frac{1}{4}k)/(2k_2 - k)$, and $(O_2)_x$ and $(H)_x$ are the concentrations

of O_2 and H at the time t_x . Substituting the expression thus obtained for (H) in the differential equation for (O_2) and taking the oxygen loss as a measure of the reaction rate, we obtain

$$W = -d(O_2)/dt = (2k_2 - k)[C(H)_x + (O_2)_x - (O_2)](O_2).$$

Introducing the following notation: $(O_2)/(O_2)_x = 1 - \eta$, $(2k_2 - k)(O_2)_x = K$ and $C(H)_x/(O_2)_x = \eta_0$, we may rewrite the last equation

$$d\eta/dt = K(\eta_0 + \eta)(1 - \eta). \quad (39.24)$$

Expression (39.24) is formally identical with the usual expression for the rate of an autocatalytic reaction catalysed by an end product of the reaction (see p. 40). As in the case of an autocatalytic reaction, for sufficiently high values of η , i.e. for a sufficiently great extent of conversion, we may consider η_0 to be small compared with η ; in this case expression (39.24) becomes

$$d\eta/dt = K\eta(1 - \eta). \quad (39.25)$$

The correspondence of the overall law of the branched chain reaction with the law of the autocatalytic reaction in the general case was analysed by Semenov, who also established the limits of this correspondence [236].

Third Ignition Limit

We shall now consider the *third ignition limit* of the stoichiometric mixture of hydrogen and oxygen. On passing beyond the second ignition limit (p_2) to the high-pressure side, the rate of reaction decreases sharply owing to the predominance of chain breaking over branching. However, as the pressure is increased the reaction rate passes through a minimum and then increases again. The cause of this increase in reaction rate when the pressure is sufficiently high is the hindrance to HO_2 radicals diffusing to the wall, so that processes (8) and (9) (p. 610) leading to chain propagation begin to compete more successfully with this process. For a certain pressure of the mixture the absolute rate of the reaction may be so high that the heat liberated cannot be removed in time and the temperature of the mixture starts to increase. The increase in temperature gives rise to an even larger increase in the rate of reaction. As a result of this auto-acceleration in the reaction a thermal explosion occurs. This is the origin of the third ignition limit (p_3) of hydrogen as shown in Fig. 147 by the upper broken line. All the available experimental data show that the third ignition limit is of thermal type in practically every case studied.

However, it was shown by Voevodskii and Nalbandyan [203] theoretically and confirmed experimentally by Voevodskii and Poltorak [47] that in certain special cases the third ignition limit may also be of chain type. This happens, for example, during ignition of a stoichiometric mixture of

hydrogen and oxygen in vessels treated with potassium chloride; this treatment favours destruction of radicals at the walls and leads to a retardation of the reaction.

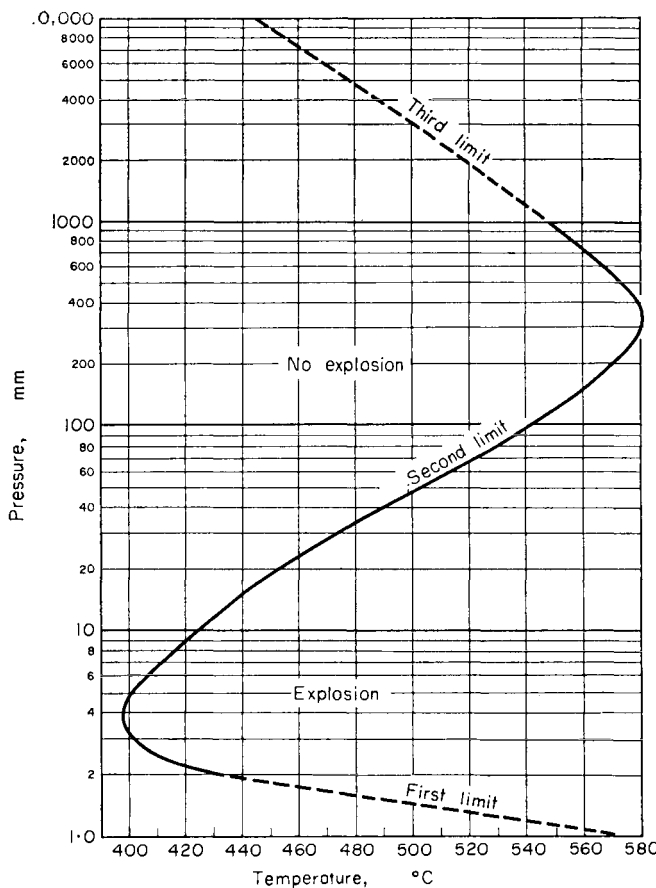


FIG. 147. Ignition limits for a stoichiometric mixture of hydrogen and oxygen in a spherical vessel of diameter 7.4 cm coated with KCl. The first and third limits are partially extrapolated (broken line) (according to Lewis and von Elbe [174]).

Voevodskii and Nalbandyan showed that the above reaction mechanism (p. 610) correctly describes the course and properties of the reaction of hydrogen and oxygen not only inside but also outside the ignition peninsula. In particular, this mechanism gives a quantitatively correct description of the slow oxidation of hydrogen between the second and third ignition limits and shows that chain ignition is possible at the third limit. This is possible when processes (8) and (9) are included in the reaction mechanism.

The rate of slow oxidation may be obtained from the quasi-steady state conditions

$$d(OH)/dt = 0, \quad d(H)/dt = 0, \quad d(O)/dt = 0 \text{ and } d(HO_2)/dt = 0.$$

We obtain from these conditions, assuming that at high pressures process (4), i.e. chain breaking at the walls (as a result of adsorption of H atoms), is not important, the following expression for the overall rate of reaction:

$$W = \frac{dp_{H_2O}}{dt} + \frac{dp_{H_2O_2}}{dt} \\ = 2W'_0 \frac{\frac{3}{2} + (k_8p_{H_2} + k_9p_{H_2O})/k_7}{1 - (2k_2/k_6p)[1 + (k_8p_{H_2} + k_9p_{H_2O})/k_7]}. \quad (39.26)$$

If the original mixture does not contain water vapour then the rate in the initial period of the reaction may be represented by the equation

$$W = \frac{2W'_0(\frac{3}{2} + k_8p_{H_2}/k_7)}{1 - (2k_2/k_6p)(1 + k_8p_{H_2}/k_7)}. \quad (39.27)$$

It is seen from these expressions that a stationary reaction can be assumed until the denominator in the relevant formula is greater than zero, i.e. until the quantity

$$(2k_2/k_6p)[1 + (k_8p_{H_2} + k_9p_{H_2O})/k_7]$$

or

$$(2k_2/k_6p)(1 + k_8p_{H_2}/k_7)$$

is less than unity. With increase in pressure (here we must bear in mind that at high pressures the slow oxidation takes place in the diffusion region, whence $k_7 = k_7^0/p$), these quantities increase and at a certain time may be equal to unity. At this moment the reaction rate becomes infinite, i.e. a chain explosion occurs. Therefore, the condition for transition to an explosion in this case may be written

$$(2k_2/k_6p)[1 + (k_8p_{H_2} + k_9p_{H_2O})(p/k_7^0)] = 1 \quad (39.28)$$

or

$$(2k_2/k_6p)(1 + k_8p_{H_2}/k_7^0) = 1. \quad (39.29)$$

For simplicity we take the latter expression (for $p_{H_2O} = 0$), and write

$$k_2/k_6 = a, \quad (k_8/k_7^0)(1 - \alpha) = c,$$

where $\alpha = 1 - p_{H_2}/p$ (p is the over-all pressure of hydrogen and oxygen) is determined by the composition of the mixture. This gives the equation

$$p^2 - p/2(ac) + (1/c) = 0, \quad (39.30)$$

the roots of which are the pressures at the second (p_2) and third (p_3) ignition limits of the stoichiometric mixture of hydrogen and oxygen.

According to this equation, $p_2 + p_3 = 1/2ac$; therefore, since $p_3 \gg p_2$, we obtain approximately for the pressure at the third ignition limit:

$$p_3 = 1/2ac = k_6 k_7^0 / 2k_2 k_8 (1 - \alpha). \quad (39.31)$$

Moreover, we have $p_2 p_3 = 1/c$, and hence

$$p_2 = 2a = 2k_2/k_6. \quad (39.32)$$

As is to be expected, (39.32) is identical with (39.17) which was obtained by neglecting chain breaking at the walls due to adsorption of H atoms.

The Mechanism of Oxidation and Combustion of Hydrocarbons

In conclusion we shall deal with the mechanism of the oxidation and combustion reactions of organic substances (for example hydrocarbons); these are in practice a very important class of oxidation reactions. Their mechanism has been studied in much less detail than the mechanism of oxidation and combustion of hydrogen, but points of similarity can be seen.

In fact, studies using spectroscopic methods have shown that hydroxyl and oxygen atoms are present in the hot flames of hydrocarbons. Therefore the following elementary processes must occur in these flames:



and



similar to processes (1) and (3) which are characteristic of the hydrogen flame. The probable source of O atoms in hot hydrocarbon flames is the process



similar to the process



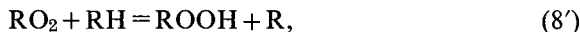
The difference between processes (2) and (2') is that the first of these processes has a relatively low activation energy (16 kcal) whereas the second must have an activation energy not less than 25 kcal owing to its high endothermicity (about 25 kcal). Thus process (2') must be much slower than process (2), and for this reason may act as the main branching process only at a fairly high flame temperature. For this reason the process⁽²²⁾



similar to process (6), should compete with process (2') more successfully. According to W. C. Sleppy and J. G. Calvert, *J. Amer. Chem. Soc.*, **81**,

⁽²²⁾ Where R=CH₃, Marcotte and Noyes [913] replace process (6') by the process CH₃+O₂→HCO+H₂O, which does not appear very probable.

769 (1959), process (6'), like (6), is a termolecular one and its rate constant is of the order $10^{-31} \text{ cm}^6 \text{ molecule}^{-2} \text{ sec}^{-1}$. [See also P. L. Hanst and J. G. Calvert, *J. Phys. Chem.*, **63**, 71 (1959).] An indirect indication of the formation of an RO_2 peroxide radical during oxidation and combustion of hydrocarbons is that the hydroperoxide ROOH is detected in oxidation of hydrocarbons and also in relatively low-temperature hot flames of hydrocarbons near the concentration limits of ignition. The hydroperoxide is formed as a result of the process



similar to process (8), in which hydrogen peroxide is formed and is detected in the products of slow oxidation of hydrogen.

As we see, all the main processes in the mechanism of the combustion and slow oxidation of hydrogen have their analogues in the probable mechanism of the corresponding hydrocarbon reactions. Hydrocarbon reactions, however, have their own peculiarities which are based mainly on the following two factors: first, the different ratio of the rates of the individual elementary processes mentioned above, and second, the greater complexity of the molecular structure of the hydrocarbon compared with that of hydrogen; this second factor is connected with the greater variety of elementary processes, of substances taking part in them, and of reaction products. Consequently, the mechanism of hydrocarbon reactions is much more complex than the mechanism of the analogous reactions of hydrogen. In particular, it has been shown [286] that, besides oxidation processes, thermal decomposition (cracking) processes play an important part in the mechanism of hydrocarbon oxidation, making it much more complex.

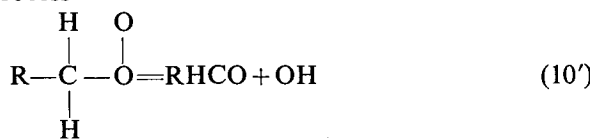
The low rate of the branching process (2') noted above means that even at relatively high temperatures and pressures the main role is played by process (6') and the reaction develops according to the simple chain mechanism



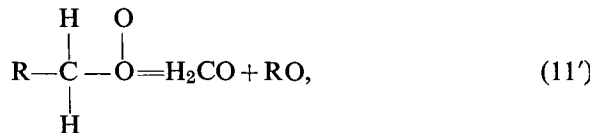
with branching from time to time (degenerate branching, see above, p. 602).⁽²³⁾ Moreover, the peroxide radical ROO or RCH_2OO is capable of unimolecular decomposition, i.e. of the process competing with process

⁽²³⁾ As the peroxide accumulates, a large part of it seems to decompose at the walls of the reaction vessel (cf. p. 581). From time to time peroxide decomposition takes place in the gas phase with rupture of the O—O bond and this leads to degenerate branching (see below).

(8'). For instance, the process

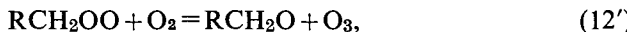


is probable, as is the similar process



resulting in the formation of an aldehyde—a substance more reactive than the initial hydrocarbon RCH_3 —and an OH or RO radical propagating the reaction chain.

It is also supposed that the peroxide radical interacts with oxygen yielding an alcohol radical and an ozone molecule [721]



i.e. an active radical and an active reagent.⁽²⁴⁾ The formation of alcohols from interaction of ozonized oxygen and hydrocarbons near room temperature gives a basis for assuming that the direct reaction of hydrocarbons with ozone is possible [1113], for example $\text{RH} + \text{O}_3 = \text{RO} + \text{HO}_2$.⁽²⁵⁾ At high temperatures, however, it seems to be more probable that ozone decomposes into $\text{O}_2 + \text{O}$ [108] with subsequent interaction of the O atom and an RH molecule.

At present there are no reliable data for the elementary processes on which the degenerate branching mechanism is based. Norrish and co-workers [337] (see p. 582) consider that chain initiation in formaldehyde H_2CO oxidation is connected with interaction of H_2CO and O_2 , resulting in the formation of HCOOH and O atoms. (In their opinion CO and H and HO_2 radicals are formed as a result of this interaction at sufficiently high temperatures.) These authors also associate the degenerate branching observed during hydrocarbon oxidation with these processes.

New data have been obtained recently, showing the effect of formaldehyde in branched oxidation of hydrocarbons. Karmilova, Enikolopyan and Nalbandyan [L. V. Karmilova, N. S. Enikolopyan and A. B. Nalbandyan, *J. Phys. Chem., Moscow*, **31**, 851 (1957)] have found that after a certain time τ , methane oxidation (stream with $p = 220\text{--}760$ mm Hg, $T = 420\text{--}720^\circ\text{C}$) is no longer autocatalytic and proceeds at a constant rate; at

⁽²⁴⁾ According to [1112a], reaction (12') is the basis of degenerate branching in the oxidation of hydrocarbons.

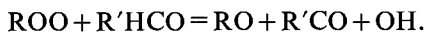
⁽²⁵⁾ The heat of this exothermic process is 11.5, 17 and 21–22 kcal for the oxidation of CH_4 , C_2H_6 and C_3H_8 respectively.

time τ the concentration of formaldehyde formed in methane oxidation becomes stationary. Addition of formaldehyde to the initial mixture in concentrations equal to the steady-state values completely suppresses the autocatalytic part of the reaction, and the oxidation rate is then constant from the very start of the reaction. From this and the overall reaction kinetics the authors conclude that formaldehyde is the only substance responsible for the degenerate branching they connect with the process $\text{HCHO} + \text{O}_2 = \text{HCO} + \text{HO}_2$. Bell and Tipper [K. M. Bell and C. F. H. Tipper, *Trans. Faraday Soc.*, **53**, 982 (1957)] suggest that the same process accounts for degenerate branching in the slow oxidation of methyl alcohol.

The role of peroxides in the gas-phase degenerate branching remains unsettled. Whereas degenerate branching in liquid-phase oxidation may be connected with the decomposition of peroxides or with interaction between the latter and other molecules (cf. p. 581), there are no reasons yet for applying this concept to the gas phase. For instance, the possibility is not excluded that at temperatures corresponding to appreciable decomposition of peroxides the latter do not form at all, due to decomposition of peroxide radicals.

According to a paper in 1950 [46], branching may arise as a result of the process $\text{CH}_3 + \text{O}_2 = \text{H}_2\text{CO} + \text{OH}$ (or a similar process) which is the sum of type (6') and (10'). As this process is highly exothermic (51 kcal) the energy liberated may from time to time be in the form of electronic excitation of the formaldehyde molecule H_2CO . Since the excited state of H_2CO is clearly a triplet state the molecule may be considered as a biradical $\text{H}_2\text{C}-\text{O}$. The interaction of the latter with a molecule of the initial hydrocarbon gives two monoradicals: $\text{H}_2\text{C}-\text{O} + \text{RH} = \text{H}_3\text{CO} + \text{R}$ or $\text{H}_2\text{COH} + \text{R}$. According to the data of Gaydon and Moore [656], when small quantities of CH_4 are added to a rich mixture of CO and O_2 the spectrum of the so-called pre-flame glow is found to contain excited formaldehyde bands, whereas when H_2CO is added (instead of CH_4) these bands are not present. Gaydon and Moore conclude that under these conditions (a rich oxygen mixture of CO containing small amounts of methane) formaldehyde is formed in an *excited* state (see also [652]). In their opinion this process is connected with O atoms or ozone taking part in the reaction.

According to another point of view [45], the degenerate branching may result from interaction of one of the radicals formed in the course of the reaction with one of the intermediate substances, for example interaction of a peroxide radical with an aldehyde molecule, resulting in the formation of three new radicals. The process may be written



Voevodskii and Vedeneev [45] estimate the heat of this process as -10 kcal.

At present we have just as little information on the mechanism of so-called *cool flames* (see §42) which appear in definite regions of temperature and pressure during oxidation of hydrocarbons and certain other organic substances. A cool flame is characterized by an increase in temperature⁽²⁶⁾ and the occurrence of a glow whose spectrum consists of bands of electronically excited formaldehyde H_2CO . By carrying out the reaction in a closed vessel, several successive cool flames are observed in the oxidation of certain hydrocarbons; these flames are detected by the appearance of a glow and by pressure jumps due to the temperature increase. For example, in the oxidation of propylene $\text{H}_3\text{C}-\text{CH}=\text{CH}_2$ three cool flames are observed. The pressure jumps connected with these flames stand out clearly on the curve of Δp against t (time) shown in Fig. 148,

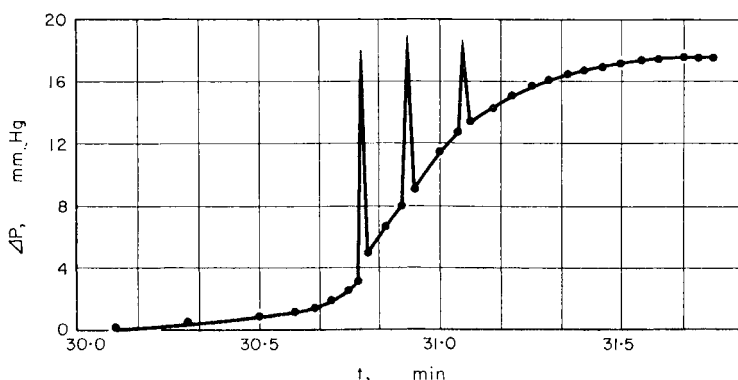


FIG. 148. Kinetics of the pressure change in the slow oxidation of propylene by oxygen at 300°C and an initial pressure of the mixture of $\text{C}_3\text{H}_6 + \text{O}_2$ of 320 mm Hg (according to Shtern and Polyak [300]). The three peaks on the smooth Δp vs. t curve correspond to three consecutive cool flames.

taken from the work of Shtern and Polyak [300]. It is seen from this figure that cool-flame processes superimposed on the slow oxidation reaction disturb the smooth path of this reaction for a short time interval. We conclude from this that a cool flame is a secondary phenomenon arising in the process of development of slow oxidation [300]. Norrish [848] suggests that the cause of the cool-flame phenomenon is the thermal instability of slow low-temperature oxidation reactions.

The possibility is not ruled out that cool flames are connected with "branching flashes" which are rapidly extinguished owing to the disappearance of substances accumulating in the reaction zone up to the

⁽²⁶⁾ The temperature of a cool flame differs by 100 to 200° from the temperature of the reaction zone in slow oxidation taking place at a similar pressure and mixture composition.

appearance of the cool flame. In the opinion of Neiman [205] and other authors, these substances include peroxides which decompose into radicals when they have reached a certain critical concentration. Other authors, however, consider that the substances giving rise to degenerate branching and the cool flames associated with it [568] are aldehydes. For example, it has been shown by the experiments of Polyak and Shtern [301] that in the oxidation of propylene the degenerate branching must be connected with acetaldehyde CH_3HCO . In these experiments synthetic mixtures are used similar in composition to partially reacted mixtures of propylene C_3H_6 and oxygen; the method used consists of interrupting the reaction at a definite time and keeping the reacting mixture in an intermediate vessel at room temperature until all labile intermediate substances such as peroxides have been destroyed.

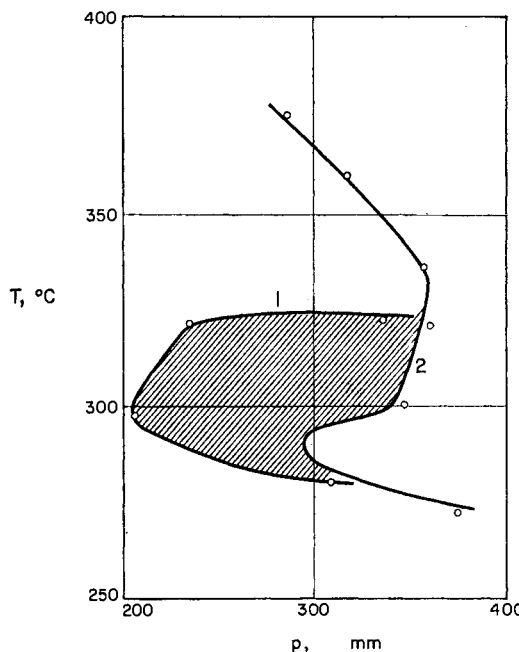


FIG. 149. Region of hot and cool flames (hatched) in a propylene-oxygen mixture ($\text{C}_3\text{H}_6 : \text{O}_2 = 1$) (according to Shtern and Polyak [300]).

As a result of suppressing the branched-chain oxidation of hydrocarbons by the degenerately-branched slow oxidation reactions there is no ignition peninsula. At a sufficiently high pressure or temperature the rate of oxidation becomes so great that the heat liberated by the reaction does not have time to escape, the temperature of the reaction zone increases and an explosion occurs, which is undoubtedly of thermal character in this case.

In a pressure-temperature diagram the explosion (ignition) region is separated from the slow-oxidation region by a curve whose smooth path is in many cases disturbed by the occurrence of a cool flame region. As a typical example Fig. 149 shows the curves [300] bounding the hot and cool flame regions (hatched) and the slow (flameless) oxidation region of propylene. The curves bounding the different regions of the reaction are usually plotted on a T - p diagram.

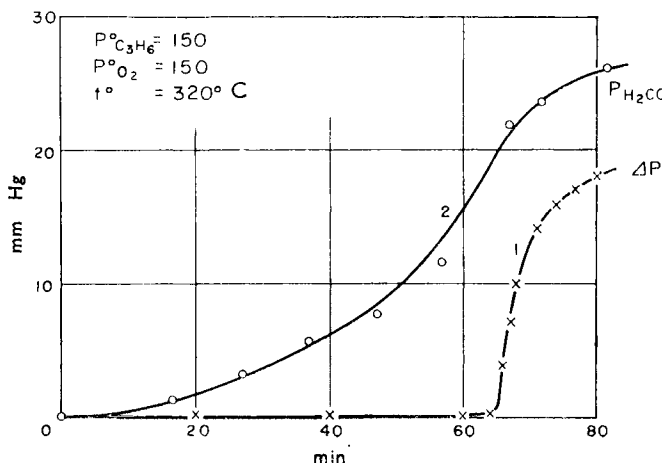


FIG. 150. Pressure change (1) and formaldehyde yield (2) at different times in propylene oxidation (according to Karmilova and Kondrat'ev).

Returning to the curve in Fig. 148, we see that in that case an appreciable pressure change is observed only after 30 min. It may be concluded from this that the induction period, τ , is 30 min. The dependence of τ on experimental method is seen very clearly if instead of the pressure change (Δp) we choose as the measure of the reaction rate the yield of formaldehyde. Using such a method to register the reaction development in the oxidation of propylene, the induction period is found to be zero, as formaldehyde formation is observed as soon as the reacting mixture is admitted to the reaction vessel. As an illustration we show in Fig. 150 one of the pressure-change curves obtained by Karmilova and Kondrat'ev alongside a parallel formaldehyde-yield curve (obtained from the absorption spectrum of formaldehyde) for propylene oxidation.

CHAPTER 10

COMBUSTION PROCESSES

§40. Spontaneous Combustion

Chain Explosion

When a fuel mixture is admitted to a closed vessel heated to a certain temperature T , the mixture rapidly comes to this temperature. The time of heating is proportional to the pressure of the mixture and at atmospheric pressure is about 0.1 sec. In the heated mixture a chemical reaction occurs, the course of which is determined by the temperature, pressure and composition of the mixture. When the values of these parameters are such that the state of the fuel mixture corresponds to a point outside the ignition peninsula (see p. 598) on the p vs. T diagram, a slow stationary reaction will occur in the mixture. The experiments of Hinshelwood and coworkers [766], who studied the slow combustion of hydrogen in oxygen, show that near the upper ignition limit, i.e. at pressures only slightly exceeding the pressure at the upper limit, p_2 , and also below the lower ignition limit, i.e. when $p < p_1$, this reaction occurs at the wall of the reaction vessel (a catalytic reaction). With increase in pressure (from p_2) a slow homogeneous reaction occurs parallel with this reaction, and its rate rapidly increases with pressure, being proportional to the cube of the partial pressure of hydrogen and directly proportional to the partial pressure of oxygen. Later more detailed studies of the kinetics of this reaction have shown that it follows a chain mechanism (with non-branched chains) [203].

When the state of the fuel mixture corresponds to the ignition region, the stationary reaction will not be possible: in this case a self-accelerating chain reaction occurs in the mixture, leading to explosion at sufficiently high pressures and temperatures. At low values of p and T (lying inside the ignition peninsula), however, explosion does not occur, and after reaching a certain maximum rate the reaction slowly dies away (degenerate explosion).

Semenov [231, 232] first showed that in chemical systems where a branched chain reaction is possible, the self-accelerating reaction leading to explosion may develop at *constant* temperature for low p and T . In these cases we are concerned with *chain ignition* or *chain (isothermal) explosion*. That an isothermal chain ignition is experimentally possible was first established by Koval'skii [113] for hydrogen combustion. Figure 145 (p. 620) shows Koval'skii's kinetic curves expressing the dependence

of the pressure drop Δp , associated with combustion in the mixture $2\text{H}_2 + \text{O}_2$, on the time t since the mixture was admitted to a quartz vessel at 485°C . It is seen from this figure that at relatively low pressures ($p_0 = 8.2$ to 5.8 mm Hg) and temperature the reaction is characterized by a fairly long induction period (about 0.05 sec when $p_0 = 8.2$ mm Hg and about 0.20 sec when $p_0 = 5.8$ mm Hg). According to chain theory, throughout the induction period and later (until the maximum rate is reached) a self-accelerating branched-chain reaction develops in the mixture but becomes measurable (for the method used to measure the rate of reaction) only after the induction period (see p. 622).

In Koval'skii's experiments the rate of change of pressure was used as a measure of the reaction rate

$$W = -dp/dt = d(\Delta p)/dt.$$

Accordingly the rate of reaction is obtained by graphical differentiation of the kinetic curves expressing the time-dependence of the pressure of the

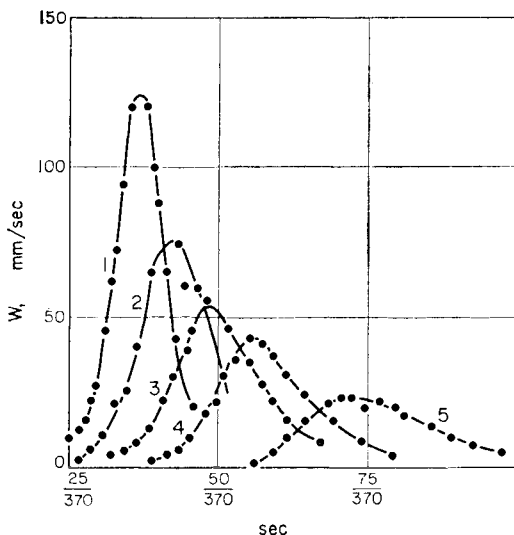


FIG. 151. Reaction rate of $2\text{H}_2 + \text{O}_2 = 2\text{H}_2\text{O}$ at 485°C and initial pressures of: (1) 7.4 mm Hg; (2) 7.1 mm Hg; (3) 6.8 mm Hg; (4) 6.4 mm Hg and (5) 6.1 mm Hg, calculated from the data of Fig. 145 (according to Semenov [232]).

reacting mixture. The reaction-rate curves obtained in this way for various initial pressures of the stoichiometric hydrogen–oxygen mixture are shown in Fig. 151. These curves clearly correspond to degenerate explosion (a measurable maximum rate of reaction). Explosion in the usual sense occurred in Koval'skii's experiments only when the initial pressure

$p_0 = 8.2$ mm Hg and possibly when $p_0 = 7.8$ mm Hg, insofar as it is possible to judge from Fig. 145. The isothermal character of the explosion (ignition) in these experiments results from the low reaction rate at the pressures and temperature of the experiments. One of the most convincing indications that the reaction is isothermal is the existence of a linear dependence of $\ln \Delta p$ on the time t of the reaction (for the initial stages of the reaction), as follows from Semenov's expression for the rate of an isothermal branched-chain reaction (see p. 595). As an illustration Fig. 152 shows the straight lines obtained by plotting $\ln \Delta p = \varphi t + \text{const.}$ using kinetic curves similar to those shown in Fig. 145.

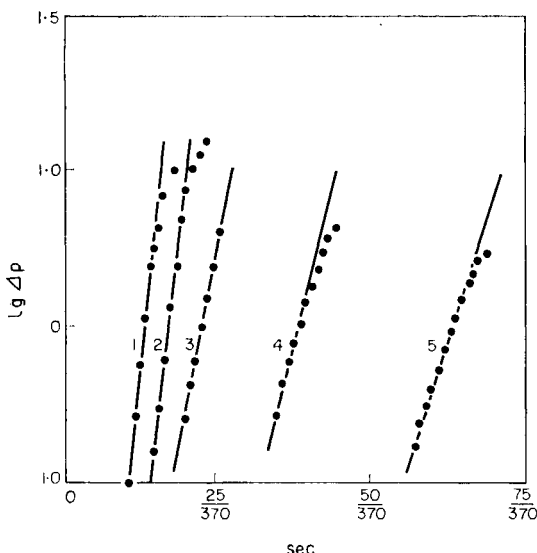


FIG. 152. The linear dependence of $\log \Delta p$ on time t showing Semenov's law for an isothermal branched-chain reaction (according to Semenov [232]). (1) 560°C , $p_0 = 5.7$ mm Hg; (2) 520°C , $p_0 = 5.8$ mm Hg; (3) 485°C , $p_0 = 8.2$ mm Hg; (4) 485°C , $p_0 = 6.8$ mm Hg; (5) 485°C , $p_0 = 6.1$ mm Hg.

In this example the cause of explosion is accumulation of active reaction centres as a result of the branched-chain mechanism; this accumulation leads to rapid increase in the rate of reaction (when $t > \tau_{\text{Ind}}$) up to a scarcely measurable value, i.e. to self-ignition of the fuel mixture. Purely isothermal explosion is, however, quite rare. In fact, only in a few cases does the ignition region extend to such low pressures and temperatures as in the case of the hydrogen–oxygen mixture. In most cases ignition occurs at pressures of tens and hundreds of millimetres of mercury and fairly high temperatures; and owing to the high absolute rate of reaction the amount

of heat liberated by the reaction may be very large. When heat is liberated rapidly it may not escape fast enough, and consequently the temperature of the reaction zone, and therefore the rate of reaction, will progressively increase so that the reaction ends in explosion. The explosion in these cases is called a *thermal explosion*.

Thermal Explosion

It was proposed as early as last century [37] that the increase in temperature due to the rate of heat production predominating over the rate of removal of heat may be the cause of the initial acceleration of the reaction leading to explosion. At the beginning of the twentieth century Nernst [596] suggested that the condition for self-ignition of a gas is that the heat removed be equal to the heat produced at the ignition temperature; but only at the end of the nineteen-twenties was a detailed quantitative theory of thermal explosion given by Semenov [231].

In the case of a homogeneous gas reaction, the rate of heat production (i.e. the amount of heat liberated in 1 cm³ of the reaction zone per sec) may be taken as

$$\Phi_+ = Qw, \quad (40.1)$$

where Q is the molar heat of the reaction (in kcal per g. molecule) and w is the rate of reaction (in moles per cm³ per sec).

In Semenov's theory it is assumed that Φ_- , the rate of removal of heat, is proportional to the temperature difference $T - T_0$, where T is the temperature of the reaction zone and T_0 is the wall temperature of the reaction vessel, and may be taken as equal to

$$\Phi_- = (\alpha S/V)(T - T_0), \quad (40.2)$$

where α is the heat-transfer coefficient and S and V are the surface area and volume of the reaction vessel.

Assuming that there is an Arrhenius (or approximately Arrhenius) dependence of reaction on temperature, the rate of heat production as a function of temperature T may be shown graphically as an exponential curve. Curves (1, 2 and 3) in Fig. 153 for different initial pressures of the fuel mixture are of this type. In this figure, the straight line 4 intersecting the temperature axis at $T = T_0$ represents the heat removed.

Let us consider the course of reaction in relation to the conditions determining the temperature change of the reaction zone during the reaction. If these conditions are such that the rate of heat production corresponds to curve 1, then when $t = 0$ (the time when the mixture is admitted to the reaction vessel) the rate of heat production will be greater than the rate of removal of heat and the temperature of the reaction zone will increase. The corresponding increase in Φ_+ and Φ_- will follow curves

1 and 4. Where these curves intersect ($T = T_1$) the rate of heat production is equal to the rate of heat removal. Since $\Phi_+ < \Phi_-$ when $T > T_1$, then as the temperature T_1 has been reached there is no further increase in temperature, and the reaction will proceed steadily at this temperature.

We shall now consider the course of the reaction when the rate of heat production follows curve 3. (These conditions may be achieved by an appropriate increase in the initial pressure of the fuel mixture, for example.)

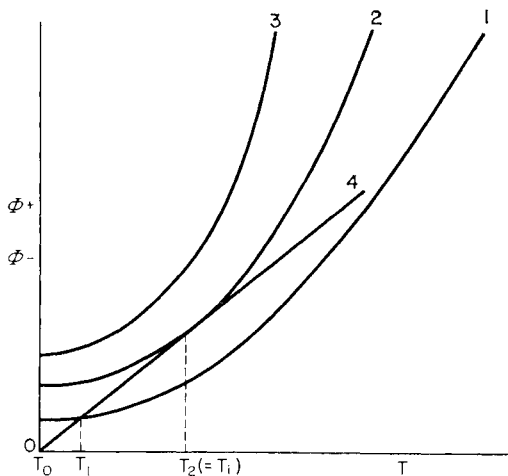


FIG. 153. Thermal explosion. The straight line passing through the origin shows the temperature dependence of the amount of heat removed; curves 1, 2 and 3 show the temperature dependence of the amount of heat liberated by the reaction (which is proportional to the rate of reaction). Curves 1 and 2 refer to a stationary reaction (the heat removed is less than or equal to the heat produced), curve 3 refers to the reaction leading to explosion.

In this case the Φ_+ and Φ_- curves do not intersect and the rate of heat production is always greater than the rate of heat removal, so that a steady reaction is not possible: as a result of progressive increase in temperature the reaction continuously accelerates and thermal explosion occurs.

The boundary between the two limiting cases considered, the slow steady reaction and the self-accelerating reaction ending in explosion, is determined by the conditions for the heat production (curve 2) and heat removal curves touching each other. These conditions are also the *explosion conditions* as expressed by equating the rates of heat production and removal:

$$\Phi_+(T_2) = \Phi_-(T_2) \text{ i.e. } Qw(T_2) = (\alpha S/V)(T_2 - T_0) \quad (40.3)$$

and equating the derivatives of Φ_+ and Φ_- with respect to T

$$(\mathrm{d}\Phi_+/\mathrm{d}T)_{T_2} = (\mathrm{d}\Phi_-/\mathrm{d}T)_{T_2} \text{ or } Q(\mathrm{d}w/\mathrm{d}T)_{T_2} = \alpha S/V. \quad (40.4)$$

The temperature T_2 corresponding to the point of contact of curves 2 and 4 is the *ignition temperature* T_i of the mixture, and the pressure p_2 corresponding to curve 2 is the *minimum explosion pressure* (at the ignition temperature T_2 or at the initial temperature T_0). These critical parameters of thermal ignition, T_2 and p_2 , may be calculated from conditions (40.3) or (40.4) if the dependence of w , the rate of reaction on pressure and temperature, is known.

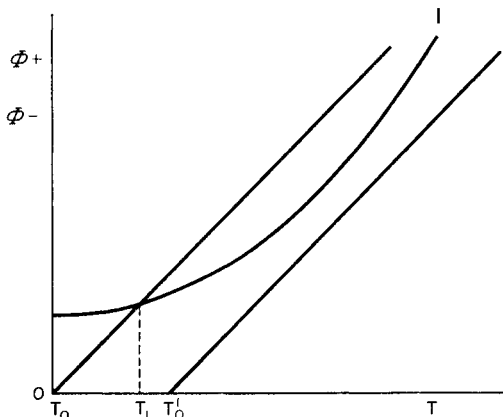


FIG. 154. Thermal explosion. Increase in wall temperature of the reaction vessel, displacing the heat removal curve to the right, shifts the reaction from the stationary regime region to the explosion region (the heat removal is less than the heat production). (1) heat production curve.

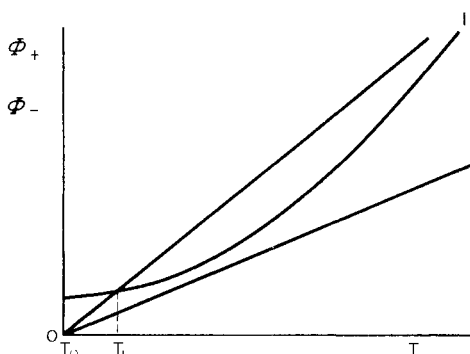


FIG. 155. Thermal explosion. Decrease in heat removal shifts the reaction from the stationary regime region to the explosion region. (1) heat production curve.

In the experimental conditions corresponding to Fig. 153 (with the temperature T_0 of the walls of the reaction vessel constant), a transition from the stationary regime to explosion occurs as a result of increase in the initial pressure of the mixture, which leads to an increase in the reaction rate and consequently in the rate of heat production Φ_+ . The same effect may be produced by increasing the wall temperature ($T_0 \rightarrow T'_0$) as is evident from Fig. 154, and also (in principle) by decreasing the heat-transfer coefficient, i.e. changing the slope of the straight line Φ_- vs. T (Fig. 155).

At the start of many complex chain reactions, when the consumption of initial substances is not yet large, the dependence of reaction rate on temperature and pressure p of the reacting mixture may be expressed by a simple formula of type

$$w = kp^n \exp(-E/RT), \quad (40.5)$$

where k is a constant, depending usually on the composition of the mixture; n is a small integer or fraction determining the effective order of the reaction; E is a quantity having the significance of an effective activation energy.

Using formula (40.5) for the rate of reaction and substituting w and dw/dT , calculated from (40.5), in the expression

$$w(T_2) = (T_2 - T_0)(dw/dT)_{T_2},$$

which is obtained from (40.3) and (40.4), we obtain the following quadratic equation for the ignition temperature:

$$T_2^2 - (E/R)T_2 + ET_0/R = 0.$$

The lower of the two roots of this equation represents the required ignition temperature, namely

$$T_2 = (\frac{1}{2}E/R)[1 - \sqrt{1 - 4RT_0/E}]. \quad (40.6)$$

Often E is more than 20,000 cal and $T_0 < 1000^\circ\text{K}$ and consequently $4RT_0/E < 0.4$, so that without introducing substantial errors we may expand the expression inside the root sign, and confining ourselves to the first three terms of the series, we obtain the approximation

$$T_2 = T_0 + RT_0^2/E. \quad (40.7)$$

The quantity $\theta = T_2 - T_0 = RT_0^2/E$ clearly represents the *pre-explosion heating* of the mixture. Substituting $E > 20,000$ cal and $T_0 < 1000^\circ$ in this expression, we find that in this case the pre-explosion heating is less than 100° .

It is not difficult to see that, within the limits of accuracy of this calculation, increasing the temperature from T_0 to the ignition temperature T_2 , i.e. by θ , leads to an increase in the reaction rate (40.5) by a factor e . In

fact, substituting $T = T_2$ (40.7) in (40.5) and carrying out the following rearrangements (which are permissible since $\theta = RT_0^2/E$ is small compared with T_0):

$$\exp(-E/RT_2) = \exp\left(\frac{-E/RT_0}{1+RT_0/E}\right) \approx \exp[-(E/RT_0)(1-RT_0/E)] = e \cdot \exp(-E/RT_0)$$

we obtain $w_2/w_0 = e$, where

$$w_2 = kp^n \exp(-E/RT_2)$$

and

$$w_0 = kp^n \exp(-E/RT_0).$$

Because of this property of $\theta = RT_0^2/E$, it is called the "characteristic temperature range".

From the explosion conditions (40.3) and (40.4) we may also calculate the pressure p_2 of the explosion. In accordance with the above approximation, substituting $w_2 = ew_0$ and $T_2 - T_0 = RT_0^2/E$ in (40.3) we obtain after rearrangement

$$\ln(p_2^{n/2}/T_0) = A/T_0 + B, \quad (40.8)$$

where $A = \frac{1}{2}E/R$ and $B = \frac{1}{2}\ln(\alpha SR/QekVE)$. When $n = 2$ expression (40.8) becomes

$$\ln(p_2/T_0) = A/T_0 + B. \quad (40.8a)$$

A formula of this type may also be obtained when $n \neq 2$ if we use the approximate relationship:⁽¹⁾

$$T = T_{\text{mean}} \exp\{(T - T_{\text{mean}})/T\}. \quad (40.9)$$

⁽¹⁾ This relationship is obtained as follows. The possibility of representing the function $f(T) = T$ by an exponential function of the Arrhenius type $\varphi(T) = b \exp(-a/RT)$ is naturally limited to a temperature range near the point of contact (T_{mean}) of the line $f(T)$ and the curve $\varphi(T)$. At the point of contact both the f and φ functions themselves and their first derivatives must be exactly equal, i.e.

$T_{\text{mean}} = b \exp(-a/RT_{\text{mean}})$, or $\ln T_{\text{mean}} = \ln b - a/RT_{\text{mean}}$ and $1/T_{\text{mean}} = a/RT_{\text{mean}}^2$, and hence $a = RT_{\text{mean}}$ and $b = eT_{\text{mean}}$. Substituting these values of a and b in $T = \varphi(T)$, which is approximately true also when $T \neq T_{\text{mean}}$ (in a certain temperature range), we obtain the relationship (40.9). An idea of the degree of accuracy of this relationship is given by the following figures. Characterizing a given temperature range by the quantity $\Delta T/T_{\text{mean}} = T/T_{\text{mean}} - 1$ and the deviation of T , calculated according to (40.9), from the actual temperature by $\delta T/T_{\text{mean}}$ where $\delta T = T - \varphi(T)$, we obtain on the basis of (40.9) for different values of $\Delta T/T_{\text{mean}}$:

$\Delta T/T_{\text{mean}}$	0.1	0.2	0.3	0.4	0.5
$\delta T/T_{\text{mean}}$	0.005	0.02	0.04	0.07	0.10

In this way we see that even when $\Delta T = T - T_{\text{mean}} = \frac{1}{2}T_{\text{mean}}$ the error is only 10% and when $\Delta T = 0.1T_{\text{mean}}$ it is only 0.5%. Errors similar to these calculated values are also obtained when $\Delta T < 0$ [84].

Here T_{mean} is the temperature corresponding to the middle of the temperature range studied. Rewriting the expression $p_2^{n/2}/T_0$ in the form $(p_2/T_0)^{n/2}T^{n/2-1}$, or on the basis of (40.9) in the form

$$(p_2/T_0)^{n/2}(T_0)_{\text{mean}}^{n/2-1} \exp[(\frac{1}{2}n-1)(T_0 - (T_0)_{\text{mean}})/T_0]$$

and substituting this in (40.8), we obtain after rearrangement

$$\ln(p_2/T_0) = A'/T_0 + B', \quad (40.8b)$$

where

$$A' = [E - R(2-n)(T_0)_{\text{mean}}]/nR$$

and

$$B' = (1/n) \ln[\alpha SR(eT_0)_{\text{mean}}^{2-n}/QekVE]$$

We should note that the quantity $E' \equiv E - R(2-n)(T_0)_{\text{mean}}$, determining the temperature dependence of p_2/T_0 , is not very sensitive to n . Actually, it is not difficult to see that when $(T_0)_{\text{mean}} = 500^\circ\text{K}$, E' differs from E by only 1 kcal and when $(T_0)_{\text{mean}} = 1000^\circ\text{K}$ they differ by 2 kcal (when $n = 1$ or 3). Naturally $E' = E$ when $n = 2$.

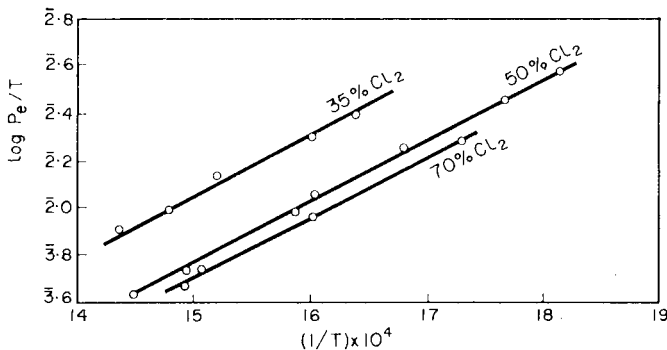


FIG. 156. Dependence of the minimum explosion pressure (p_e) on the temperature (T_0) for H_2 and Cl_2 mixtures of various compositions (according to Zagulin [74]).

A relationship of the type (40.8b) between p_2 and T_0 has been established empirically in a large number of cases. As an example let us take the reaction $\text{H}_2 + \text{Cl}_2 = 2\text{HCl}$, which is a simple chain reaction (see p. 569). The dependence of the minimum explosion pressure p_e ($= p_2$) on the temperature of the reaction vessel T ($= T_0$) has been established by Zagulin [74] for H_2 and Cl_2 mixtures of various compositions, and is shown in Fig. 156; it is apparent from this figure that in this case the experimental

relationship corresponds to (40.8).⁽²⁾ Zagulin also studied the minimum pressure as a function of mixture composition (when $T_0 = \text{const.}$). This dependence is shown for $T_0 = 625^\circ\text{K}$ in Fig. 157. It is seen from this figure that the minimum explosion pressure is near $p_{\text{Cl}_2} = \frac{2}{3}p$ and $p_{\text{H}_2} = \frac{1}{3}p$ (p is the over-all pressure of the H_2 and Cl_2 mixture).

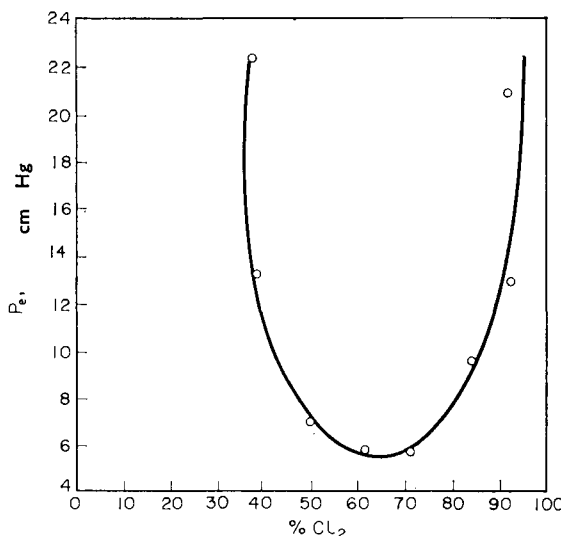


FIG. 157. Dependence of the minimum explosion pressure (p_e) on composition of the hydrogen-chlorine mixture at 625°K (according to Zagulin [74]).

It should be pointed out, however, that a formula of practically the same type as (40.8b) is obtained for the dependence of pressure on ignition temperature in the case of chain explosions as well. Actually, the constants in the approximate formulae (37.12) and (39.31) expressing the relation between p and T at the first and third ignition limits are a function of temperature as expressed by the Arrhenius equation, so that we obtain from these formulae

$$p_1 = A_1/T + B_1 \quad \text{and} \quad p_3 = A_3/T + B_3. \quad (40.10)$$

It follows, therefore, that the experimental dependence of pressure on temperature at the ignition limits does not allow us to decide whether we have a thermal or a chain explosion.

⁽²⁾ However, it does not follow from this that the effective order of the reaction $n = 2$ since, as noted above, p_2/T_0 is not very sensitive to n and the measurements of p_2 and T_0 are not sufficiently precise, so that formula (40.8) may apply here with $n \neq 2$.

The solution of this problem has been possible only as a result of a more precise development of the theory of thermal explosion and a comparison of theoretical yields with the most precise experimental data. A more precise theory of thermal explosion has been given by Frank-Kamenetskii [275].

An important deficiency in Semenov's theory as expounded above is the assumption that the temperature of the gas is constant throughout the reaction vessel. This assumption corresponds to the case where intensive convection occurs in the gas during the pre-explosion period to equalize the temperature; this, however, does not usually take place. In most practical cases it is necessary to allow for inequalities of temperature in the gas; this has been done in Frank-Kamenetskii's theory. In his stationary theory of thermal ignition there are the following simplifying assumptions: that the pre-explosion heating-up is not large compared with the wall temperature of the reaction vessel; that the thermal conductivity of the walls is infinitely great and that the reaction rate is an Arrhenius function of temperature.

Using expression (40.5) for the reaction rate and relating the heat removal to the thermal conductivity of the gas, i.e. putting Φ equal to $\lambda\Delta T$, where λ is the coefficient of thermal conductivity and ΔT the Laplace operator, we find that in the stationary state

$$\Delta T + (Q/\lambda)kp^n \exp(-E/RT) = 0. \quad (40.11)$$

Equation (40.11) was solved by Frank-Kamenetskii for vessels of various shapes, and his results have been compared with a series of experimental data. Without dwelling on the method of solution we shall merely mention some of the results arising from a comparison of this theory with Semenov's theory and also with experimental data. First of all it was shown by Frank-Kamenetskii that his expression for the critical ignition pressure agrees with the expression (40.8) obtained from Semenov's theory, correctly to within a numerical factor which results from the fact that the heat-transfer coefficient in Semenov's theory is indeterminate. Comparison of the results of the two theories shows that this factor depends on the coefficient of thermal conductivity of the gas and the cross section of the reaction vessel (for vessels of various shapes). Moreover, according to Frank-Kamenetskii, the maximum pre-explosion heating $T_e - T_0$ is equal to $1.20RT_0^2/E$ in the case of a plane parallel vessel, $1.37 RT_0^2/E$ for a cylindrical vessel and $1.60RT_0^2/E$ for a spherical vessel, whereas according to Semenov's theory $T_e - T_0 = RT_0^2/E$.

A comparison of theoretical results and experimental data has been carried out by Frank-Kamenetskii and other authors and shows that in most cases there is quantitative agreement. Thus, in the case of a series of reactions (azomethane decomposition $(\text{CH}_3)_2\text{N}_2 \rightleftharpoons \text{C}_2\text{H}_6 + \text{N}_2$, methyl

nitrate decomposition $2\text{CH}_3\text{ONO}_2 = \text{CH}_3\text{OH} + \text{CH}_2\text{O} + 2\text{NO}_2$, hydrogen sulphide oxidation $2\text{H}_2\text{S} + 3\text{O}_2 = 2\text{H}_2\text{O} + 2\text{SO}_2$ and so on) the calculated ignition temperatures for various pressures are practically identical with measured values. Moreover, Frank-Kamenetskii predicted the then unknown thermal explosion in the decomposition of nitrous oxide ($2\text{N}_2\text{O} = 2\text{N}_2 + \text{O}_2$) which has actually been observed by Zel'dovich and Yakovlev [92], and their measured values of the critical explosion temperature were in good agreement with those calculated, as is seen from Table 55.

TABLE 55

*Comparison of calculated and measured values of the critical explosion temperature in the decomposition of nitrous oxide
(according to Frank-Kamenetskii [278])*

p , mm Hg	Explosion temperature, °K	
	Calculated	Measured
170	1255	1285
330	1175	1195
590	1110	1100

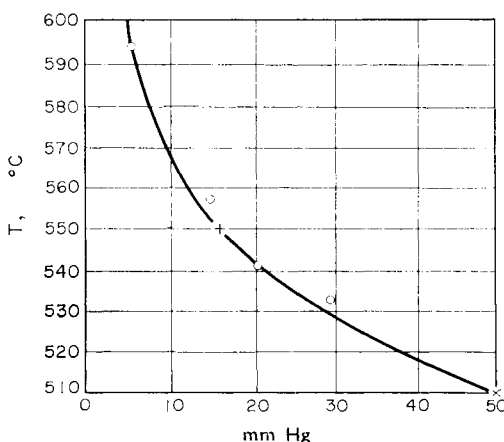


FIG. 158. Dependence of the ignition temperature at the third ignition limit of the $2\text{H}_2/\text{O}_2$ mixture on diameter of the reaction vessel according to Frank-Kamenetskii (circles are Ziskin's data, the erect cross is a result obtained by Pease and the diagonal cross is a result obtained by Frank-Kamenetskii).

We have already mentioned that the more precise theory of thermal explosion enables us to decide in each particular case whether the explosion is of chain (chemical) or thermal nature. For instance, the theory gives a definite relation between explosion temperature and diameter of the reaction vessel which may be checked experimentally. Thus Frank-Kamenetskii examined the third ignition limit of the $2\text{H}_2/\text{O}_2$ mixture and showed that it is of thermal type; this has been established in other cases also. Figure 158 shows the results of this comparison; here the full line is Frank-Kamenetskii's theoretical curve [278], the circles are Ziskin's experimental results [95] and the erect cross is a result obtained by Pease [1018]. All the data refer to the $2\text{H}_2/\text{O}_2$ mixture at 1 atm.

Ignition of a Gas Mixture by a Heated Surface

Let us now consider the problem of the ignition of gas mixtures by a heated surface; this problem is closely related to that of self-ignition. We shall take the case of a parallel-sided vessel bounded by two plane surfaces, a hot surface at temperature T_h and a cold surface at T_0 , separated by a distance d . We shall also assume that heat is transferred from the hot to the cold surface through the gas only by thermal conduction (without convection).

As the rate of reaction is markedly temperature-dependent (we shall use (40.5) to express the reaction rate), the reaction will occur mainly near the hot surface. For this reason the heat liberated by the reaction results in the temperature gradient near the hot surface being smaller.

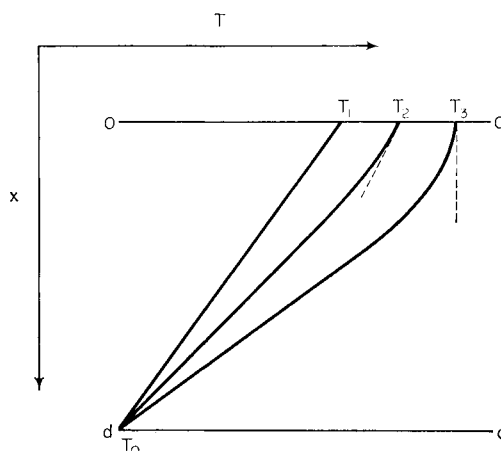


FIG. 159. Temperature gradient between hot ($x = 0$) and cold ($x = d$) plane-parallel surfaces when the temperature of the cold surface is T_0 and for various temperatures of the hot surface; an exothermic reaction takes place in the volume between the two surfaces.

Moreover, the higher the rate of reaction, i.e. the higher the temperature of the igniting surface, the smaller must be the temperature gradient near this surface (Fig. 159). In the limit when the temperature of the layer of gas next to the hot surface is equal to the temperature of the surface, i.e. when the following condition holds near the surface,

$$(dT/dx)_{x=0} = 0, \quad (40.12)$$

then the hot surface will not lose heat. According to Zel'dovich, condition (40.12) is also the condition for the ignition of a gas mixture by a hot surface. The temperature at which this condition is fulfilled is the *ignition temperature*.

The temperature distribution in a plane parallel vessel is determined by the equation

$$\lambda d^2T/dx^2 + F(T) = 0, \quad (40.13)$$

where λ is the coefficient of thermal conductivity and $F(T)$ is the rate of production of heat by the reaction, namely

$$F(T) = Qw = F_0 \exp(-E/RT). \quad (40.14)$$

As the gas temperature near the hot surface, where the main reaction occurs, scarcely differs from the surface temperature T_h , the quantity $F(T)$ may be represented by the approximations:

$$\begin{aligned} F(T) &= F_0 \exp(-E/RT) \\ &= F_0 \exp\{-(E/RT_h)/[1 - (T_h - T)/T_h]\} \\ &\approx F_0 \exp\{(E/RT_h)[1 + (T_h - T)/T_h]\} \\ &\approx F(T_h) \exp\{-(E/RT_h^2)(T_h - T)\}. \end{aligned} \quad (40.15)$$

In this case equation (40.13) becomes

$$\lambda d^2T/dx^2 + F(T_h) \exp\{-(E/RT_h^2)(T_h - T)\} = 0. \quad (40.16)$$

Solving this equation with the condition that

$$T_{(x=0)} = T_h$$

and

$$(dT/dx)_{x=0} = 0$$

(the condition for ignition), we obtain

$$\frac{dT}{dx} = \sqrt{\left\{ \frac{2F(T_h)RT_h^2}{\lambda E} \left[1 - \exp\left(-\frac{E(T_h - T)}{RT_h^2}\right) \right] \right\}}. \quad (40.17)$$

According to formula (40.17), the temperature gradient, which is zero near the hot surface, increases with distance from the surface and becomes practically constant and equal to

$$dT/dx = \sqrt{2F(T_h)RT_h^2/\lambda E} \quad (40.18)$$

at a certain distance (which is small compared with d). This constant gradient may be taken as approximately equal to $(T_h - T_0)/d$ and hence

$$d = (1 - T_0/T_h)[\lambda E/2RF(T_h)]^{1/2}, \quad (40.19)$$

which is equivalent to the ignition condition (40.12). One of the ignition parameters (T_h , p , d , etc.) may be determined from (40.19) if the remaining parameters are known.

The expression of most practical interest is that of the condition for ignition by a wire placed along the axis of a cylinder with temperature T_0 ; this has the form

$$r \ln(R/r) = (1 - T_0/T_h)[\lambda E/2RF(T_h)]^{1/2}, \quad (40.20)$$

where r and R are the radii of the wire and cylinder respectively.

Two-stage Self-ignition

The combustion of hydrocarbons and certain other fuels (alcohols, aldehydes, etc.) often occurs in two stages: a cool-flame combustion stage and a hot-flame stage. Accordingly the self-ignition of such fuel mixtures has a two-stage character: when the mixture is admitted to a hot vessel a cool flame appears (or several successive cool flames) after a certain time interval τ_1 as a result of the initial acceleration, and after a time

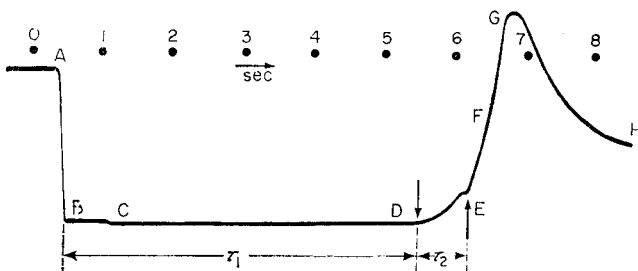


FIG. 160. Induction periods of the cool (τ_1) and hot (τ_2) flames of a pentane-air mixture when $\alpha = 0.6$, $p_0 = 3.9$ atm and $T = 309^\circ\text{C}$ (according to Neiman [205]).

interval τ_2 the flame becomes a normal hot flame. The quantities τ_1 and τ_2 are called the induction periods of the cool and hot flames and τ_2 is always much less than τ_1 . The relationship between these quantities is apparent from Fig. 160 which illustrates the kinetics of the pressure change during combustion of a pentane-air mixture; the mixture was admitted at $t = 0$ to a vessel heated to 309°C . It is seen from the figure that under these conditions $\tau_1 = 5.5$ sec and $\tau_2 < 1$ sec.

In a large number of papers by Neiman and coworkers (see for example [205]) and by other authors it has been shown that the cool-flame induction

period varies exponentially with temperature:

$$\tau_1 = A \exp(B/T), \quad (40.21)$$

where A is a diminishing function of pressure and B a positive constant.

The theoretical temperature dependence of the induction period is readily obtained for completely branched chains. Actually, in this case Semenov's formula (37.5) for the reaction rate may be rewritten

$$W = W_0 e^{\varphi t} \quad (40.22)$$

since $\epsilon = 2$ and $\alpha \approx 1$; φ takes on a value $\varphi \approx v_1$, where v_1 is the frequency of the branching process. When $t = \tau_1$ the rate of reaction has a certain constant value W^0 (determined by the sensitivity of the experimental techniques) so that, since

$W_0 = W_0^0 \exp(-E_0/RT)$ and $v_1 = v_1^0 \exp(-E_1/RT)$, we have

$$\tau_1 = (1/v_1^0) \{ \ln(W_0/W_0^0) + E_0/RT \} \exp(E_1/RT) = A \exp(E_1/RT), \quad (40.23)$$

an expression practically identical with (40.21).

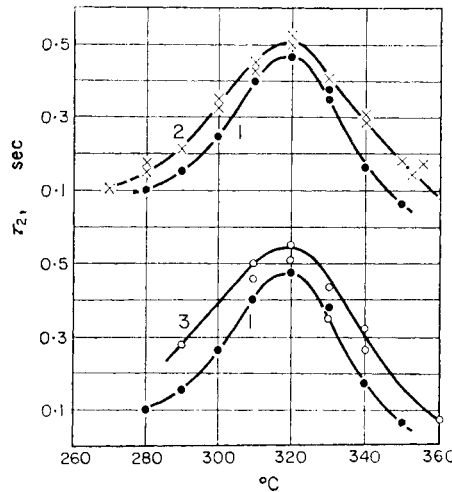


FIG. 161. Temperature dependence of the induction period of a hot flame for the mixtures: (1) $\text{C}_4\text{H}_{10} + \text{O}_2$; (2) $\text{C}_4\text{H}_{10} + \text{O}_2 + \text{H}_2$; (3) $\text{C}_4\text{H}_{10} + \text{O}_2 + \text{CO}_2$ (according to Aivazov and Neiman [13, 205]).

The theoretical calculation of τ_1 in terms of T for reactions following a degenerately branching chain mechanism is made difficult by our inadequate knowledge of these mechanisms—especially of branching. The experimentally observed exponential dependence of τ_1 on T (40.21), which is apparently universal in character, suggests that here also the theoretical dependence will be close to that resulting from the simple law of Semenov.

The temperature dependence of τ_2 , the induction period of the hot flame, is more complex, as far as may be judged from the experiments of Aivazov, Neiman and Khanova [13, 205]. The dependence of τ_2 on T that they obtained for the mixtures (1) $\text{C}_4\text{H}_{10} + \text{O}_2$, (2) $\text{C}_4\text{H}_{10} + \text{O}_2 + \text{H}_2$ and (3) $\text{C}_4\text{H}_{10} + \text{O}_2 + \text{CO}_2$ is shown in Fig. 161, from which it is seen that in contrast with τ_1 , which varies monotonically with temperature, τ_2 has a maximum at a certain temperature (320°C). In Neiman's opinion [205], this dependence of τ_2 is explained by the fact that the increase in the rate of chemical processes with temperature leads to a natural reduction of the induction period, as observed to the right of the maximum; with decrease in temperature from that corresponding to the maximum τ_2 , peroxides formed in the cool flame accelerate the oxidation of the hydrocarbon, and this effect increases with decreasing temperature, resulting in a decrease in τ_2 .

Adiabatic Explosion

The conditions of heat removal have a substantial effect on the course of combustion in the pre-explosion period, but from the time of the onset of explosion (ignition), heat removal ceases to play an important part in the heat balance of the system owing to the high rate of reaction, and hence the course of the reaction becomes approximately adiabatic.

When the heat liberated by the reaction is used mainly in the self-heating of the mixture, i.e. when the heat balance of the adiabatic process may be expressed fairly reliably by the equation

$$C_v dT = -Q dc, \quad (40.24)$$

the temperature of the fuel mixture is proportional to the rate of reaction. In (40.24) Q represents the molar efficiency of the fuel, i.e. the amount of heat liberated when one mole is burned, c is the fuel concentration (in moles per unit volume) when the temperature of the burning mixture is T , and C_v is the heat capacity (at constant volume) of the mixture per unit volume. The heat balance equation is written in its integral form:

$$\int_{T_0}^T C_v dT = Q(c_0 - c), \quad (40.24a)$$

where c_0 is the initial concentration of fuel.

Introducing the maximum temperature T_{\max} , corresponding to complete combustion in adiabatic conditions and defined by

$$\int_{T_0}^{T_{\max}} C_v dT = Qc_0, \quad (40.25)$$

we find from (40.24a) and (40.25) that

$$c = (1/Q) \int_T^{T_{\max}} C_v dT = (\bar{C}_v/Q)(T_{\max} - T), \quad (40.26)$$

where \bar{C}_v is the mean heat capacity of the mixture.

Moreover, expressing the rate of reaction by the formula

$$w = k_0 c^n \exp(-E/RT), \quad (40.5a)$$

which is similar to (40.5), we find

$$dT/dt = -(Q/C_v)dc/dt = (Q/C_v)w = k_0(Q/C_v)c^n \exp(-E/RT), \quad (40.27)$$

or, using (40.26) and for simplicity taking $C_v = \bar{C}_v$,

$$dT/dt = k_0(C_v/Q)^{n-1}(T_{\max} - T)^n \exp(-E/RT). \quad (40.27a)$$

Solving equation (40.27a) enables us to find the time dependence of temperature and concentration (40.26) when the reaction is adiabatic.⁽³⁾ We shall give below the solution of this equation for $n = 1$.⁽⁴⁾ In this case equation (40.27a) is

$$dT/dt = k_0(T_{\max} - T) \exp(-E/RT). \quad (40.27b)$$

This last equation is solved graphically for $E = 20,000$ cal, $T_0 = 800^\circ\text{K}$ and $T_{\max} = 2000^\circ\text{K}$ in Fig. 162, where the gas temperature T and the relative concentration c/c_0 are given as a function of $t' = k_0 t$. Figure 162 also shows the reaction-rate curve (w in arbitrary units). It is seen from this figure that in the course of a long time interval (the induction period) the gas temperature increases relatively slowly, and only after this time does the temperature begin to increase rapidly simultaneously with rapid consumption of the reacting substances. The reaction rate reaches a maximum when the gas temperature reaches 1700°K , i.e. a temperature which is 85 per cent of the maximum. Calculations show that with an increase in the effective activation energy E the maximum rate of combustion is displaced to the high-temperature side. Thus, for the same $T_0 = 800^\circ\text{K}$ and $T_{\max} = 2000^\circ\text{K}$ but $E = 40,000$ cal, the maximum rate is obtained when $T = 1800^\circ\text{K}$ (90 per cent of the maximum temperature). The induction period is even greater compared with the reaction period. If we take as a conditional measure of the reaction period the time in which the rate of

⁽³⁾ Equation (40.26) is solved by numerical integration. Such calculations have been made by Todes [267] for various values of the parameters E/R , n and T_{\max}/T_0 . Results of approximate calculations are given by Zel'dovich and Voevodskii [84].

⁽⁴⁾ Such is the case for example when one of the components of the fuel mixture is in large excess.

reaction changes from 5 per cent of w_{\max} to w_{\max} , and as a measure of the induction period the time for the reaction rate to reach $w = 0.05w_{\max}$, then we find that in the first of the above cases ($E = 20,000$ cal) the ratio

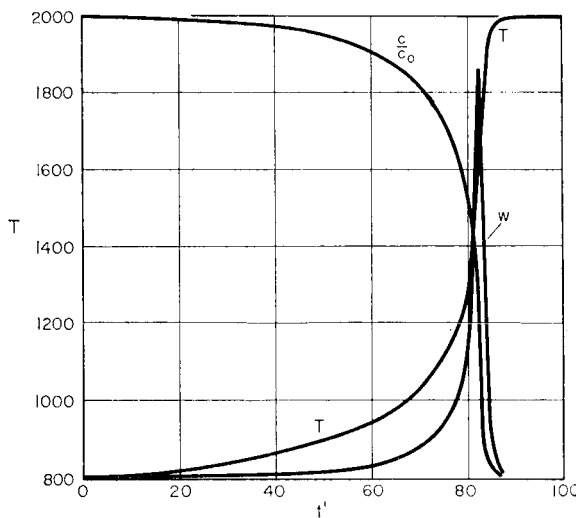


FIG. 162. The variation of temperature, concentration and reaction rate as a function of time in an adiabatic reaction; $E = 20$ kcal, $T_{\max} = 2000^{\circ}\text{K}$ and $T_0 = 800^{\circ}\text{K}$.

of reaction period to induction period is 0.2 and in the second case ($E = 40,000$ cal) it is 0.0003.

Allowance for Incomplete Combustion

It should be pointed out, however, that the foregoing calculation cannot pretend to great accuracy in rendering precisely all the details of thermal explosion. The reason for this lies not only in the scheme assumed when describing the explosion process, and expressed by the approximate nature of the kinetic law of the reaction (40.5a), but also in certain other substantial simplifications. One of these is the assumption of complete combustion of the gas, which gives the formula (40.25) used in the above calculation. In fact, the reaction ceases when chemical equilibrium is reached at a certain temperature T'_{\max} which may be much less than T_{\max} calculated from formula (40.25). As an example, let us consider the explosion of a stoichiometric mixture of carbon monoxide and oxygen.

According to (40.25), the amount of heat liberated when one mole of CO is burnt completely ($Q = 66,767$ cal) is equal to the difference in the

molar heat contents of the carbon dioxide

$$Q = \int_0^{T_{\max}} C_v dT - \int_0^{T_0} C_v dT$$

(here C_v is the molecular heat capacity of CO_2 at constant volume). From the heat content of CO_2 at 800°K (6107 cal), we find that the heat content at the maximum explosion temperature T_{\max} is equal to

$$\int_0^{T_{\max}} C_v dT = 66,767 + 6,107 = 72,874 \text{ cal}$$

on the basis of the above formula. Hence, taking the heat capacity of CO_2 as 13 cal/mole degree, we obtain the maximum explosion temperature as $T_{\max} = 5600^\circ\text{K}$.⁽⁵⁾

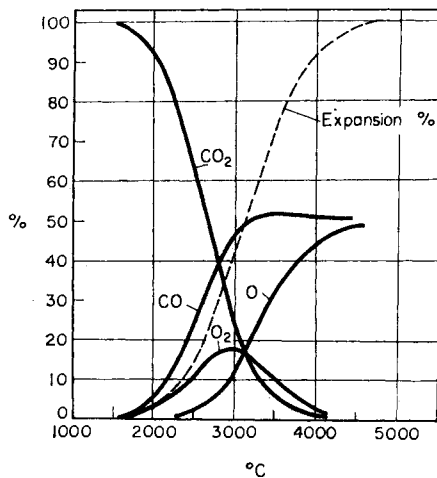


FIG. 163. Equilibrium composition of the gas obtained from thermal dissociation of CO_2 at different temperatures (according to Fehling and Leser [272]).

The unreality of this result is clear from the fact that at as high a temperature as 5600° carbon dioxide should be completely dissociated into CO and O; this follows from Fig. 163, which shows the temperature

⁽⁵⁾ $C_v = 13$ cal/mole degree is the *maximum* heat capacity of CO_2 . Actually, the linear CO_2 molecule has three translational, two rotational and four vibrational degrees of freedom, so that $C_v = \frac{1}{2}R \times (3 + 2 + 2 \cdot 4) = 13$ cal/mole degree. Consequently, the value of T_{\max} calculated from formula (40.25) should be even greater than the value obtained above.

dependence of the composition of the mixture of gases obtained from thermal dissociation of CO_2 . Allowance for incomplete conversion of CO into CO_2 is therefore a necessary condition for finding the correct value of the maximum explosion temperature of the CO and O_2 mixture.

Owing to incomplete conversion, the gas at T'_{\max} , the maximum explosion temperature, consists of the four components CO , O_2 , O and CO_2 . The concentrations of these components may be calculated for a given temperature by solving the following four equations: two equations expressing the constant composition of the mixture,

$$c_{\text{CO}}^0 = c_{\text{CO}} + c_{\text{CO}_2},$$

$$c_{\text{O}_2}^0 = c_{\text{O}_2} + c_{\text{CO}_2} + \frac{1}{2}c_{\text{O}} + \frac{1}{2}c_{\text{CO}}$$

(the index 0 denotes initial concentrations of CO and O_2), and two equations for the equilibrium constants of $\text{CO} + \text{O} \rightleftharpoons \text{CO}_2$ and $\text{O}_2 \rightleftharpoons 2\text{O}$,

$$K = c_{\text{CO}} c_{\text{O}} / c_{\text{CO}_2},$$

$$K_0 = c_{\text{O}}^2 / c_{\text{O}_2}.$$

The concentrations of CO , O_2 , O and CO_2 calculated in this way for various temperatures are shown in Fig. 163 (as percentages of the initial concentration of CO_2).

Allowing for incomplete conversion the heat balance equation for the system has the form (for a stoichiometric mixture of CO and O_2 when $c_{\text{CO}}^0 = 1$)

$$Q' = \sum c_i \int_{T_0}^{T_{\max}} C_v^{(i)} dT = c_{\text{CO}} \int_{T_0}^{T_{\max}} C_v^{(\text{CO})} dT + c_{\text{O}_2} \int_{T_0}^{T_{\max}} C_v^{(\text{CO}_2)} dT +$$

$$+ c_{\text{O}} \int_{T_0}^{T_{\max}} C_v^{(\text{O})} dT + c_{\text{CO}_2} \int_{T_0}^{T_{\max}} C_v^{(\text{CO}_2)} dT.$$

Here Q' is the amount of heat liberated during conversion of one mole of CO and half a mole of O_2 to c_{CO} moles of CO , c_{O_2} moles of O_2 , c_{O} moles of O and c_{CO_2} moles of CO_2 ($c_{\text{CO}_2} \times Q'$) minus the heat of formation of c_{CO_2} moles of CO_2 ($c_{\text{CO}_2} \times Q$) minus the heat of formation of c_{O} moles of atomic oxygen ($c_{\text{O}} \times \frac{1}{2}D_{\text{O}_2}$) (D_{O_2} is the heat of dissociation of oxygen), i.e.

$$Q' = c_{\text{CO}_2} Q - \frac{1}{2} c_{\text{O}} D_{\text{O}_2}.$$

Using values from the tables for the heat contents of CO , O_2 , O and CO_2 and knowing the values of Q and D_{O_2} ($= 118,000$ cal), we

find from the above formulae that the maximum explosion temperature $T_{\max} = 2880^{\circ}\text{K}$. Therefore, the actual temperature of adiabatic explosion of a stoichiometric CO/O_2 mixture, T'_{\max} , is approximately half the T_{\max} calculated earlier for complete conversion of $\text{CO} + \frac{1}{2}\text{O}_2$ into CO_2 . The temperature $T_{\max} = 2880^{\circ}\text{K}$ obtained here is close to the temperature directly measured for the oxygen flame of carbon monoxide (2730°K) for a stoichiometric mixture.⁽⁶⁾

When the maximum explosion temperature T'_{\max} has been reached and the chemical equilibrium corresponding to this temperature attained, the gas starts to cool due to the removal of heat (heat transfer to the cold walls of the reactor or radiation of heat by the hot gas). Parallel with the decrease in temperature there is a corresponding shift of the equilibrium; at a certain temperature, however, the chemical processes are so slow that the reaction leading to equilibrium practically stops, the mixture is "quenched" and further cooling of the mixture occurs at constant composition of the mixture. Therefore the composition of the combustion products corresponds to the chemical equilibrium at the quenching temperature, and may differ considerably from that for complete combustion. In other words, the percentage burn-up during explosion of a fuel mixture in a closed vessel should always be less than 100.⁽⁷⁾

This picture of an explosion dying out corresponds most closely to a reaction following a simple chain mechanism. In the case of a branched chain reaction the final stage of the attenuation of the explosion is characterized by a set of non-equilibrium processes, which stop at a certain pressure and temperature when the rate of branching ceases to predominate over the rate of chain breaking. In this case the composition of the combustion products is determined by suitable limiting conditions and will differ from the composition corresponding to the chemical equilibrium at the temperature when the reaction stops.

We should add that a special apparatus developed by Khariton, Ryabinin and coworkers [227] is of considerable interest with regard to study of chemical (and also physical) processes taking place under the conditions of adiabatic compression. This apparatus enables us to carry out chemical reactions at the high temperatures (thousands of degrees) which develop during rapid adiabatic compression of gas mixtures, when maximum pressures of thousands of atmospheres (up to 10,000 atm) are reached [227]. Rapid expansion of a compressed mixture ensures rapid quenching of the gas, with a composition corresponding to the maximum

⁽⁶⁾ A direct comparison of the maximum explosion temperature in a closed vessel and the flame temperature has no significance, as in the first case combustion occurs at constant volume and in the second case at constant pressure. It might be maintained, however, that, other conditions being equal, the flame temperature should be somewhat lower than the temperature of the explosion (since $C_p > C_v$).

⁽⁷⁾ Here, of course, we are considering a mixture containing sufficient oxygen.

pressure and temperature. Without describing the principles of this apparatus and its construction, which are explained in Ryabinin's article [227], we shall merely give some data obtained using this apparatus and illustrating its possibilities.

Figure 164 shows the analytically measured yields of nitric oxide as a function of the maximum pressure of compression for two mixtures of nitrogen and oxygen (in the presence of 5.5 per cent methane CH_4 , added to

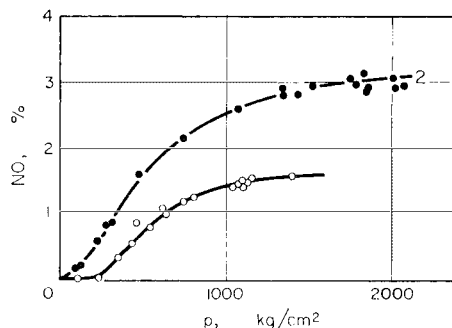


FIG. 164. Yields of nitric oxide NO as a function of the maximum pressure of compression for two mixtures of nitrogen and oxygen (in the presence of 5.5% CH_4 , according to Ryabinin, Markevich and Tamm [225]): (1) 24.2% O_2 + 70.3% N_2 ; (2) 52.7% O_2 + 41.8% N_2 .

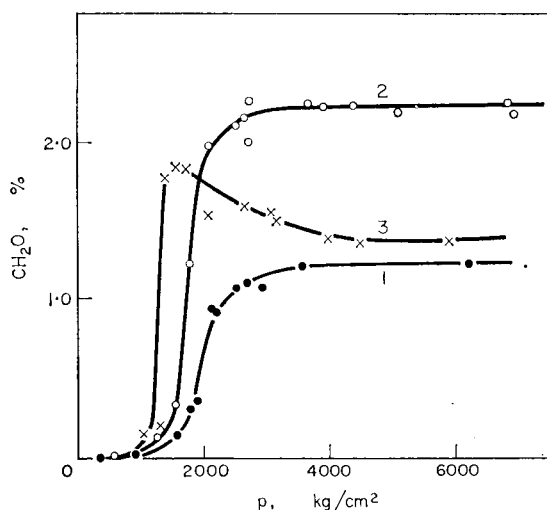


FIG. 165. Formaldehyde H_2CO yields during adiabatic compression of rich mixtures of methane and oxygen (according to Ryabinin, Markevich and Tamm [226]): (1) 6%, (2) 9%, (3) 12% O_2 .

increase the temperature using the heat liberated in its combustion) [225]. From these yields and their ratios corresponding to the law of mass action, it follows that the concentration of nitric oxide formed in these conditions is close to the equilibrium value at the maximum compression temperature. It may be concluded, therefore, that with these experimental conditions the reaction reaches equilibrium although the compression time is extremely small (about 5×10^{-4} sec); this is associated with the high temperature, which reaches a maximum of 2800°K.

Figure 165 shows the yields of formaldehyde H_2CO formed during adiabatic compression of rich mixtures of methane and oxygen [226]. With an oxygen content less than 12 per cent, the yield of formaldehyde increases with the oxygen content of the mixture. However, even with 12 per cent oxygen a sharp decrease in the yield of H_2CO is observed at a pressure of about 1500 atm; this is a result of the start of further oxidation. With a higher content of oxygen (> 15 per cent) a flash is observed at the start of compression. In this case the yield of formaldehyde is practically zero. These results must clearly be interpreted using a two-stage mechanism for the ignition of the gas during adiabatic compression [154].

§41. Flames Burning Without Preliminary Mixing of the Gases

The energy liberated in the course of an exothermic chemical reaction frequently takes the form of radiant energy, so that the reaction is accompanied by the emission of light—a flame. Calling a flame any glow whose source is a chemical reaction. We have a very large variety of flames, beginning with flames which burn near room temperature and have spectra with an intensity distribution indicating non-equilibrium radiation, and ending with flames with spectra close to the spectra of the thermodynamic-equilibrium temperature glow of the gases heated to the appropriate temperatures. We shall consider below different types of flame with regard to both their physico-chemical nature and the chemical mechanism of the combustion reactions.

Flames usually fall into two classes: those burning without preliminary mixing of the reacting substances, and those burning in previously prepared mixtures. The first class includes *diffusion flames* in which the gases are mixed by molecular diffusion (*laminar diffusion flames*) and also by diffusion accompanied by a turbulent (eddy) motion (*turbulent diffusion flames*).⁽⁸⁾ Also in this class are the so-called *highly-rarefied flames* in which feeding and mixing of the reacting substances takes place either by diffusion or, when the mean free path of the molecules is greater than the diameter of the reaction vessel, that is when the pressure in the combustion zone is very low, by a mechanism of Knudsen molecular flow.

⁽⁸⁾ Combustion may be turbulent in previously prepared mixtures also.

Highly Rarefied Flames

We shall begin our survey of the various flames with highly rarefied flames which are observed, for instance, during interaction of vapours of the alkali metals with halogens or certain other substances and are distinguished by the very simple chemical mechanism of the reactions in them. As we have already noted (p. 84), these flames burn at very low pressures, usually 0.001 to 0.01 mm Hg, and also at relatively low temperatures, 200 to 300°C.

In one method for producing highly rarefied flames which has been used by various authors to study the reactions of sodium and potassium vapours with chlorine, bromine and iodine vapours, $HgCl_2$, $HgBr_2$, HgI_2 and certain other substances, the reacting substances are admitted as two opposing vapour streams. A modification of this method consists of admitting the substance reacting with the alkali metal through a nozzle at the centre of the reaction tube (against the vapour stream of the alkali metal).

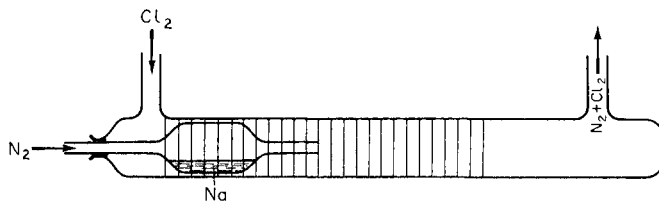


FIG. 166. Production of a highly-rarefied flame during the interaction of sodium vapour and chlorine (according to Polanyi and Schay [1032])

Another method for producing highly rarefied flames is by feeding the vapours of the two reacting substances into the reaction zone in parallel streams, as is shown in Fig. 166.⁽⁹⁾

The fact that the excitation spectra of highly rarefied flames is very probably connected with the heats of definite elementary chemical processes (see pp. 85-87) shows the non-equilibrium nature of the radiation (chemiluminescence). A direct indication of this is given by measurement of the absolute yield of light, i.e. the number of quanta of radiant energy per reaction-product molecule. Thus, according to the measurements of Bogdandy and Polanyi [424], when the pressure of sodium vapour is 0.01 mm Hg, about 35 per cent of the energy liberated in the $Na + Cl_2$ reaction is radiated as the *D*-lines of sodium. Such a large yield of light shows that in this reaction the radiation is very far from being equilibrium

⁽⁹⁾ This figure is taken from the article by Polanyi and Schay [1032] who studied the effect of nitrogen on the luminosity of various flames; the figure refers to the $Na + Cl_2$ flame burning in a stream of circulating nitrogen.

radiation. Indeed, it follows from the magnitude of the light yield that the number of quanta of *D*-radiation emitted in this case is as much as one third of the number of NaCl molecules formed. With sodium vapour and chlorine pressures of the order of 0.01 mm Hg the number of NaCl molecules formed is about 10^{19} molecule/cm³ sec, and hence the number of excited sodium atoms in 1 cm³ of the reaction zone (obtained by multiplication of this last number by the mean lifetime of the excited sodium atom, $\tau = 1.5 \times 10^{-8}$ sec) is about 10^{11} atoms. The equilibrium concentration of excited sodium atoms (excitation energy 48.0 kcal) is found from the formula

$$n' = n \exp(-48,000/RT),$$

where n' and n are the concentrations of excited and non-excited atoms respectively. With a sodium vapour pressure of 0.01 mm Hg and a temperature of 250°C it follows from this formula that $n' = 4 \times 10^{-4}$ atoms /cm³, i.e. one excited atom per 2.5 l. Comparing the two values found for the concentration of excited atoms (10^{11} and 4×10^{-4}) we see that in this case the actual concentration exceeds the equilibrium concentration by a factor of more than 10^{14} .

In spite of the relatively simple chemical mechanism of reactions in highly rarefied flames, an accurate account of these flames encounters great difficulties due to inadequate knowledge of the gas-kinetic and chemical parameters characterizing the reactions. Actually, assuming the following mechanism (see p. 87) for the M + X₂ reaction (this allows for interaction of M and X atoms at the surface of the reaction tube which was not taken into account earlier):



(k_1 , k_2 and k_3 are the rate constants of the corresponding processes), we obtain the following initial kinetic equations for the Knudsen pressure region (where the mean free path of the molecules is greater than the tube diameter) [394]:⁽¹⁰⁾

$$\frac{\partial p_M}{\partial t} = -k_1 p_{MPX_2} + k_2 p_{M_2} p_X - k_3 p_{MPX} + \frac{1}{S} \frac{\partial}{\partial x} \left(\frac{1}{K_M} \frac{\partial p_M}{\partial x} \right),$$

$$\frac{\partial p_{X_2}}{\partial t} = -k_1 p_{MPX_2} + \frac{1}{S} \frac{\partial}{\partial x} \left(\frac{1}{K_{X_2}} \frac{\partial p_{X_2}}{\partial x} \right),$$

⁽¹⁰⁾ These calculations refer to the one-dimensional case. A theory of spherical diffusion flames has been given by Garvin and Kistiakowsky [648] and Smith [1150]. See also [647].

$$\begin{aligned}\frac{\partial p_{M_2}}{\partial t} &= -k_2 p_{M_2} p_X + \frac{1}{S} \frac{\partial}{\partial x} \left(\frac{1}{K_{M_2}} \frac{\partial p_{M_2}}{\partial x} \right), \\ \frac{\partial p_X}{\partial t} &= k_1 p_M p_{X_2} - k_2 p_{M_2} p_X - k_3 p_M p_X + \frac{1}{S} \frac{\partial}{\partial x} \left(\frac{1}{K_X} \frac{\partial p_X}{\partial x} \right), \\ \frac{\partial p_{MX}}{\partial t} &= k_1 p_M p_{X_2} + k_2 p_{M_2} p_X + k_3 p_M p_X + \frac{1}{S} \frac{\partial}{\partial x} \left(\frac{1}{K_{MX}} \frac{\partial p_{MX}}{\partial x} \right) = \\ &= w + \frac{1}{S} \frac{\partial}{\partial x} \left(\frac{1}{K_{MX}} \frac{\partial p_{MX}}{\partial x} \right),\end{aligned}$$

where $w = k_1 p_M p_{X_2} + k_2 p_{M_2} p_X + k_3 p_M p_X$ is the rate of reaction in the section of the reaction tube defined by the coordinate x ; S is the cross-section of the tube and K_M , K_{X_2} , K_{M_2} , K_X and K_{MX} are constants characterizing the resistance of the tube to molecular flow of the gas. For a tube of diameter d the constants K are expressed by the formula:

$$K = (6/d^3) \sqrt{(MRT/2\pi)} \quad (41.1)$$

where M is the molecular weight of the given substance.

For the steady reaction we shall consider that

$$\partial p_M / \partial t = \partial p_{X_2} / \partial t = \partial p_{M_2} / \partial t = \partial p_X / \partial t = 0.$$

In this case we find from the kinetic equations of the reaction that

$$w = \frac{1}{S} \frac{d}{dx} \left(\frac{1}{K_M} \frac{dp_M}{dx} + 2 \frac{1}{K_{M_2}} \frac{dp_{M_2}}{dx} \right) = \frac{1}{S} \frac{d}{dx} \left(\frac{1}{K_X} \frac{dp_X}{dx} + 2 \frac{1}{K_{X_2}} \frac{dp_{X_2}}{dx} \right),$$

and hence in this case the reaction rate is determined by the rate of the reacting substances arriving in the reaction zone.

Integrating these last equations we find for the overall rate of reaction

$$\begin{aligned}W &= S \int_0^\infty k_1 p_M p_{X_2} dx + S \int_0^\infty k_2 p_{M_2} p_X dx + S \int_0^\infty k_3 p_M p_X dx = \\ &= - \frac{1}{K_M} \left(\frac{dp_M}{dx} \right)_0^\infty - \frac{2}{K_{M_2}} \left(\frac{dp_{M_2}}{dx} \right)_0^\infty = 2 \frac{1}{K_{X_2}} \left(\frac{dp_{X_2}}{dx} \right)_0^\infty \\ \text{or, since} \quad &\int_0^\infty k_1 p_M p_{X_2} dx = \int_0^\infty k_2 p_{M_2} p_X dx + \int_0^\infty k_3 p_M p_X dx,\end{aligned}$$

we have

$$W = 2S \int_0^\infty k_1 p_M p_{X_2} dx. \quad (41.2)$$

Here variation of x from 0 to ∞ corresponds to movement through the reaction zone from the sodium side to the halogen side.

All the above kinetic equations, and expressions for w and W derived from them, are also valid for the diffusion region, i.e. for diffusion flames. In this case the quantities K should be taken as equal to $K = 1/DS$, where D is the appropriate diffusion coefficient. The transition from the region of molecular flow to the diffusion region occurs at pressures of about 0.01 mm Hg. The highly rarefied flames burning at pressures of 0.01 to 0.1 mm Hg (for instance, flames burning in the presence of nitrogen as mentioned above), which have been obtained by various workers, are in essence diffusion flames. At pressures near 0.1 mm Hg, when the mean free path is about 1 mm, the flame is concentrated near the nozzle (when one of the reacting substances is fed into the reaction zone through a nozzle) and is similar in form to high-temperature diffusion flames.

Using equation (41.2) we may calculate the rate constant k_1 from the measured overall reaction rate W if the distribution of sodium and halogen along the reaction tube is known. Apparently we may obtain a realistic distribution if we simplify the initial kinetic equations by making the approximations now to be described.

In the conditions of the experiments the partial pressure of Na_2 is at least 100 times less than that of Na and consequently we may neglect $k_2 p_{\text{M}_2} p_{\text{X}}$ compared with the sum $k_1 p_{\text{M}} p_{\text{X}_2} + k_3 p_{\text{M}} p_{\text{X}}$. Introducing this simplification and also substituting the approximation $k_1 p_{\text{M}} p_{\text{X}_2} = k_3 p_{\text{M}} p_{\text{X}}$ for the mean of $k_1 p_{\text{M}} p_{\text{X}_2}$ and $k_3 p_{\text{M}} p_{\text{X}}$, and assuming that K_{M} and K_{X_2} are constant, we have

$$\frac{1}{K_{\text{M}}} \frac{d^2 p_{\text{M}}}{dx^2} = 2S k_1 p_{\text{M}} p_{\text{X}_2} = S w,$$

$$\frac{1}{K_{\text{X}_2}} \frac{d^2 p_{\text{X}_2}}{dx^2} = S k_1 p_{\text{M}} p_{\text{X}_2} = \frac{1}{2} S w.$$

On the basis of these equations, which cannot be integrated analytically, the partial pressures of alkali-metal vapour and halogen as functions of the x -coordinate are obtained by using a graphical double integration of the experimental $w(x)$ curve:

$$p_{\text{M}}(x) = SK_{\text{M}} \int dx \int w dx \quad \text{and} \quad p_{\text{X}_2}(x) = \frac{1}{2} SK_{\text{X}_2} \int dx \int w dx.$$

The values of p_{Na} and p_{Cl_2} calculated in this way, and also the reaction rate $U = w(x)S = 2k_1 p_{\text{Na}} p_{\text{Cl}_2} S$ (in arbitrary units) are shown in Fig. 167. In this we have used the ratio derived from equation (41.1):

$$K_{\text{Cl}_2}/K_{\text{Na}} = \sqrt{(M_{\text{Cl}_2}/M_{\text{Na}})} = \sqrt{(71/23)} = 1.8.$$

The position of the maximum reaction rate has been taken as the origin of coordinates ($x = 0$). Beutler and Polanyi [394] used a graphical integration of the above system of differential equations, and obtained

$$k_1 = 27/(b^3 2 S_w K_{\text{Na}} K_{\text{Cl}_2}), \quad (41.3)$$

where b is the half-width of the reaction zone. From this formula, using measured values of K_{Na} and K_{X_2} , the following values of k_1 have been obtained: $4 \times 10^{14} \text{ cm}^3 \text{ mole}^{-1} \text{ sec}^{-1}$ (for the reaction of sodium and chlorine) and $6 \times 10^{14} \text{ cm}^3 \text{ mole}^{-1} \text{ sec}^{-1}$ (for the reaction of sodium and iodine).⁽¹¹⁾

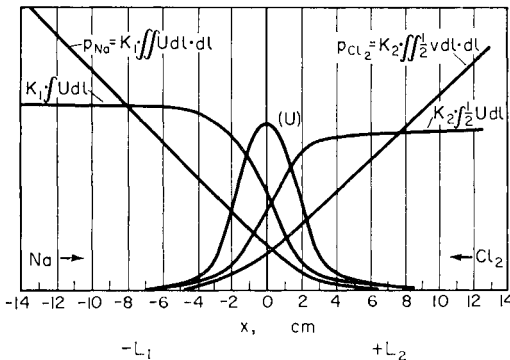


FIG. 167. Vapour pressures of sodium and chlorine and the rate of the reaction $2\text{Na} + \text{Cl}_2 = 2\text{NaCl}$ at different distances (x) along the reaction tube (according to Beutler and Polanyi [394]).

As a result of more detailed study of the $\text{M} + \text{X}_2$ flames and also the $\text{M} + \text{HgX}_2$ flames it has been shown, moreover, that all the experimental features such as the distribution of reaction product and glow along the reaction zone, the dependence of zone width and light yield on the partial pressure of the metal and on temperature, may be obtained by using the kinetic equations for the chemical mechanism of these reactions [1030].

The Cool Flame of Carbon Disulphide

An example of a flame which is intermediate between highly rarefied flames of the diffusion type ($p \geq 0.01 \text{ mm Hg}$) and hot diffusion flames is the carbon disulphide flame burning in an atmosphere of oxygen. In Kondrat'ev's experiments [130, 129] the carbon disulphide flame was produced in an electrically-heated quartz tube to which the oxygen was admitted through a side arm (cf. chlorine feed in Fig. 166) and the carbon disulphide vapour through a fine nozzle (cf. $\text{Na} + \text{N}_2$ feed in Fig. 166).

⁽¹¹⁾ The corresponding values of k_1 , calculated assuming that each gas-kinetic collision leads to reaction, are 0.6×10^{14} and $0.5 \times 10^{14} \text{ cm}^3 \text{ mole}^{-1} \text{ sec}^{-1}$, i.e. a factor of ten less than the measured values.

The flame temperature was about 300°C, the pressure in the combustion zone varied from 2 to 16 mm Hg and the ratio $p_{\text{CS}_2}/p_{\text{O}_2}$ from 1.5 to 0.013 in different experiments.

Although the carbon disulphide flame was obtained at pressures exceeding those characteristic of highly rarefied flames by some powers of ten, the extent of the combustion zone of carbon disulphide at these pressures is comparable with the extent of highly rarefied flames, of the order of a few centimetres. As we shall see, this is connected with the relatively high inertia of the CS_2 combustion reaction. Like the zone of highly rarefied flames, the CS_2 flame zone at these pressures uniformly fills the complete cross section of the reaction tube but unlike highly rarefied flames extends only to one side of the nozzle.

The dependence of the length (l) of the CS_2 combustion zone on pressure (p) is approximately $l \propto p = \text{const}$. This result may be obtained in the following way. Using the known relationship $x^2 = 2Dt$ between the mean square diffusion length x^2 , the diffusion time t , and the coefficient of diffusion D , we may write

$$l^2 = 2D\tau, \quad (41.4)$$

where τ is the mean lifetime of the leading active centre of the reaction, i.e. the active centre whose interaction is the limiting step of the combustion reaction. We represent τ and D by the formulae

$$\tau^{-1} = k_0 p \exp(-E/RT) \quad (41.5)$$

and

$$D = \frac{1}{3}u\lambda,$$

where k_0 is the pre-exponential factor in the rate constant expression, p is the mean pressure of the substance involved in the reaction, E is the activation energy of the active-centre reaction, u is the mean thermal velocity of the molecules and λ is the mean free path. In addition, we use the usual expression for k_0 ,

$$k_0 = \alpha \epsilon \sigma u,$$

where ϵ is the steric factor, σ is the gas-kinetic collision cross section and $\alpha = 10^{19} T^{-1}$ is a factor which we introduce so that in subsequent formulae the pressures may be expressed in millimetres of mercury. We also represent the diffusion coefficient by the formula

$$D = u/3\alpha\sigma P$$

(since $\lambda = 1/\alpha\sigma P$), where P is the total pressure in the combustion zone and we assume that $p = P/2$. We may now finally write (41.4) in the form

$$lP = \frac{2 \exp(E/2RT)}{\alpha\sigma\sqrt{3\epsilon}} \quad (41.6)$$

or, putting $\sigma = 3 \times 10^{-15} \text{ cm}^2$, in the form⁽¹²⁾

$$lP = \frac{2}{3} 10^{-4} [T/\sqrt{(3\epsilon)}] \exp(E/2RT). \quad (41.6a)$$

The sole assumption on which the deduction of equations (41.6) is based is that there is a leading elementary chemical process corresponding to the limiting step of the reaction. With few exceptions it seems that this is the case, so that (41.6) should be considered as one of the basic relations characterizing diffusion flames.⁽¹³⁾

The product of combustion zone width and pressure is found to be constant also for flames burning in premixed gases. As an example Fig. 168

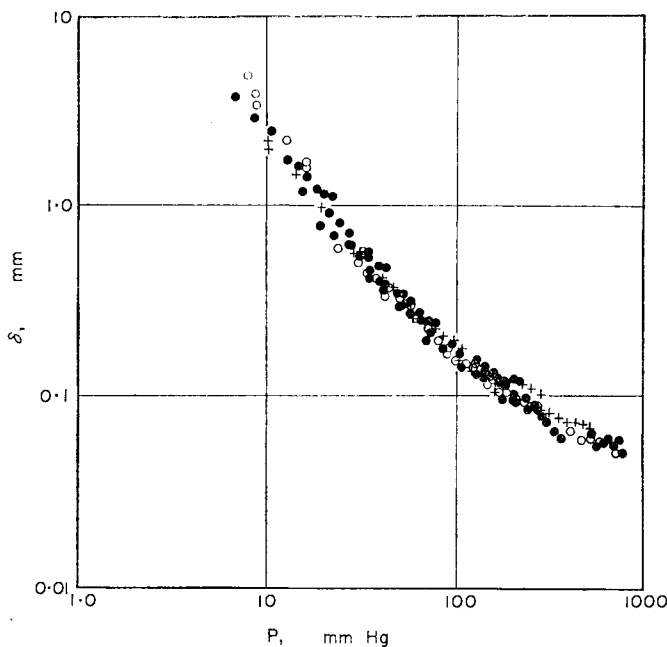


FIG. 168. Thickness δ of the luminous zone of oxyacetylene flames for various ratios of C_2H_2 and O_2 (as a function of P the pressure of the mixture) (according to Wolfhardt [1312]). (●) $30 \text{ cm}^3 \text{ O}_2$ and $12 \text{ cm}^3 \text{ C}_2\text{H}_2$; (+) $75 \text{ cm}^3 \text{ O}_2$ and $6 \text{ cm}^3 \text{ C}_2\text{H}_2$; (○) $3.75 \text{ cm}^3 \text{ O}_2$ and $1.5 \text{ cm}^3 \text{ C}_2\text{H}_2$.

(12) Equation (41.6) may also be written as

$$l = [2/\sqrt{(3\epsilon)}]\lambda \exp(E/2RT), \quad \text{or} \quad lP = [2/\sqrt{(3\epsilon)}]\lambda_1 \exp(E/2RT), \quad (41.6b)$$

where $\lambda_1 = \lambda P$, the free path at a pressure of 1 mm Hg. It is seen from this last equation that when $E = 0$ the length l of the flame zone and of the free path λ should be similar in order of magnitude (cf. p. 89).

(13) The relation (41.6) should also be applicable to highly-rarefied flames in the pressure region where these may be considered as diffusion flames, i.e. when $P \geq 0.01 \text{ mm Hg}$. Thus, putting $E = 0$, $\epsilon = 10$ (see p. 663) and $P = 0.01 \text{ mm Hg}$, we find $l = 1 \text{ cm}$, a value of the same order as that obtained experimentally for this pressure.

shows the thickness of the luminous zone of oxyacetylene flames (in mm) as a function of pressure (in mm Hg) for various mixtures of C_2H_2 and O_2 [1312]. It is apparent from this figure that the luminous zone thickness δ decreases with increase in p the pressure, and the product $p\delta$ remains approximately constant. See also [676].

We shall use (41.6) to calculate the activation energy of the leading process in the combustion of CS_2 . It follows from experiment that at a temperature of about $600^{\circ}K$ and a pressure of $p = 10$ mm Hg the length of the flame zone is about 5 cm. Substituting these values of T , p and l in (41.6) and putting $\epsilon = 0.1$, we find $E = 15.5$ kcal. We shall see below that this value for the activation energy is supported by data from spectroscopic investigations of the reaction of the CS radical with oxygen.

Study of the emission and absorption spectra of the CS_2 flame shows that in addition to the initial substance CS_2 and one of the reaction products, SO_2 , the flame zone contains S_2 and CS particles, which are detected both by emission spectra of the flame and by absorption spectra of cold gas taken from the reaction zone. It is important to note that S_2 , CS and S_2O_2 are observed in absorption only in the case of rich mixtures, for instance when the mixture composition $p_{O_2}/p_{CS_2} < 2.5$. Special experiments show that neither S_2 nor CS appears in the flame zone as a result of thermal dissociation of CS_2 , as the observed concentrations of these substances are very much greater than those calculated from the equilibrium $2CS_2 \rightleftharpoons S_2 + 2CS$. For example, in one of the experiments (total pressure 3 mm Hg, temperature about $600^{\circ}K$) the measured mean value of the partial pressure of CS radicals is 10^{-2} mm Hg, whereas that calculated from the equilibrium is 10^{-11} mm Hg. The same ratio is found for the actual and equilibrium partial pressures of diatomic sulphur vapour. It follows from this that CS and S_2 are formed chemically and not thermally. See also [967].

Measurements of the absolute light-yield show that the cool-flame radiation of carbon disulphide is also non-equilibrium. It follows from these measurements that the maximum light-yield (the number of quanta emitted per CS_2 molecule reacting), observed for a gas composition $p_{O_2}^0/p_{CS_2}^0 \approx 6$, is 0.024, i.e. one quantum per 40 CS_2 molecules. This figure corresponds to the emission of 10^{15} to 10^{16} quanta in one second, whereas the equilibrium figure (at $600^{\circ}K$) of quanta emitted (4000 \AA) is 2. Therefore the radiation accompanying the low-temperature oxidation of carbon disulphide, like the radiation of highly-rarefied flames, is pure chemiluminescence. We should add that the non-equilibrium character of the radiation from the CS_2 flame is also clear from the negative temperature coefficient of the light yield; it has been established that on increasing the temperature by 70° (from $290^{\circ}C$) the light-yield undergoes a two-fold decrease.

In addition to S_2 , CS and SO bands, the emission spectrum of the CS_2 flame is found to have a continuous background stretching from 4700 to 3000 Å which is particularly intense when $p_{O_2}^0/p_{CS_2}^0 > 2.5$, when the flame has a bright blue-violet colour (close to the colour of the sulphur and H_2S flames); this is accounted for by the continuous emission spectrum. When $p_{O_2}^0/p_{CS_2}^0 < 2.5$ the flame is green; intense bands of S_2 predominate in the green flame spectrum of the carbon disulphide flame.

The continuous spectrum of the blue-violet flame indicates that this spectrum is based on recombination processes. It follows from the short-wave limit of the continuous spectrum, which corresponds to an energy of about 100 kcal, that at least one of the reactants in these processes must be a free atom or radical. The nature of the latter, however, has not yet been reliably established, although it is very probable that it is a sulphur atom or an SO radical.

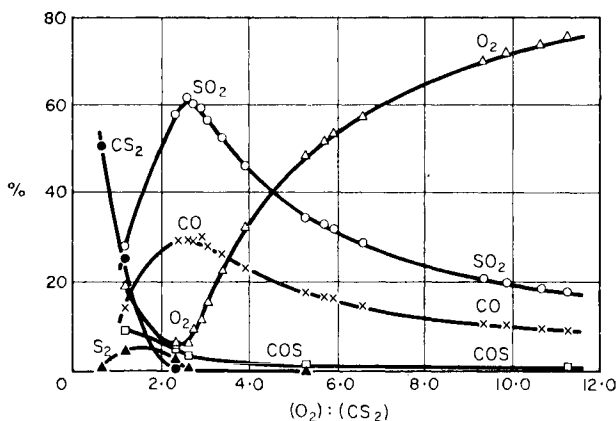
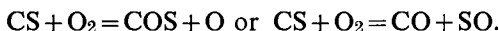


FIG. 169. Composition of the products of combustion of carbon disulphide CS_2 vapour for different ratios of CS_2 and O_2 (according to Kondrat'ev [130]).

Analysis of the products of the combustion of carbon disulphide in oxygen (see Fig. 169) show that there is an abrupt change in product composition when passing from a rich mixture ($p_{O_2}^0/p_{CS_2}^0 < 2.5$) to a weak one ($p_{O_2}^0/p_{CS_2}^0 > 2.5$). Thus, in the rich gas the reaction products contain elemental sulphur along with the SO_2 , CO and COS, but the sulphur disappears on using weak mixtures. Studies show that the sulphur is removed from the flame zone as sulphur monoxide S_2O_2 , which decomposes into elemental sulphur and SO_2 on heating the condensate collected (using liquid air) to room temperature. It is seen from Fig. 169 that the maximum amount of sulphur (calculated as S_2) is about 5 per cent by volume. A small amount of CS is also removed from the combustion zone

in the rich gas; when $p_{O_2}^0/p_{CS_2}^0 = 1.79$ the concentration of CS is about 0.5 per cent by volume. It is also apparent from Fig. 169 that the presence of considerable amounts of residual CS_2 and oxygen is characteristic of the rich gas. The main products of combustion of CS_2 in excess oxygen are SO_2 and CO and also a small amount of COS.

These facts, however, like the above spectroscopic and other data are not sufficient to explain the chemical mechanism of the combustion of carbon disulphide. For instance, the nature of the leading elementary process determining the overall reaction rate is at present an open question. Here we may only suggest that the reaction of the CS radical with an O_2 molecule is the leading process. The basis for this assumption is that the activation energy ($E = 15.5$ kcal) calculated above (p. 665) agrees with the activation energy of the reaction of CS and O_2 , which is about 15 kcal according to Kondrat'ev's calculations [131]. On the basis that this reaction is first order with respect to the concentration of CS it may be proposed that it follows one of the two schemes:



Hot Diffusion Flames

In the examples of diffusion flames considered above, owing to the low absolute reaction rate resulting from the low pressures and temperatures, practically all the heat liberated in the combustion zone is lost to the walls of the reaction vessel, and the flame temperature differs by only a small amount from the wall temperature.⁽¹⁴⁾ With an increase in pressure of the reacting gases or an increase in temperature of the reaction vessel, the rate of reaction increases and, since the thermal conductivity of the gas in the flame zone is practically independent of pressure and scarcely varies with temperature, the flame temperature increases, and with increase in the reaction rate exceeds the wall temperature of the reaction vessel by more and more. An increase in temperature also tends to reduce the dimensions

⁽¹⁴⁾ The amount of heating up may be estimated from the simple formula appropriate to a planar problem:

$$WQ/N_A = \lambda S \Delta T / \Delta x,$$

where W is the total (overall) rate of reaction; Q is the heat of the reaction; N_A is Avagadro's number; λ is the coefficient of thermal conductivity equal to $\lambda = \rho C D$ (ρ is density, C the molecular heat capacity and D the diffusion coefficient); $\Delta T / \Delta x$ is the mean temperature gradient; S is the surface area of the reaction tube for the length equal to the length of the flame. Considering the flame of carbon disulphide and using the previous formula with $\lambda = MCu/3\sigma N_A$, i.e.

$$\Delta T / \Delta x = 3Q\sigma W/CSMu$$

(M is the mean molecular weight, u the mean thermal velocity of the molecules, σ the gas-kinetic cross section), then for the measured reaction rate $W = 10^{18}$ mole/sec, $Q = 191,000$ cal/mole, $C = 5$ cal/mole degree, $S = 25$ cm^2 , $M = 30$, $\sigma = 3 \times 10^{-15}$ cm^2 and $u = 10^5$ cm/sec , we find that $\Delta T / \Delta x = 5^\circ/cm$. Consequently, in this flame the heating up is no more than a few degrees.

of the combustion zone [cf. formula (41.6)], so that the rate of heat removal decreases. At near-atmospheric pressures we have normal hot flames with temperatures of 2000 to 3000°K.

Examples of hot diffusion flames are given by the flame of any fuel gas (CO, CH₄, etc.) burning in air (or in oxygen) when the gas is fed through a fine tube (nozzle) into atmospheric air (oxygen). The simplest model of such a flame is the flame produced using two coaxial tubes, as is shown in Fig. 170. The fuel gas is fed through the narrow (inner) tube with a velocity

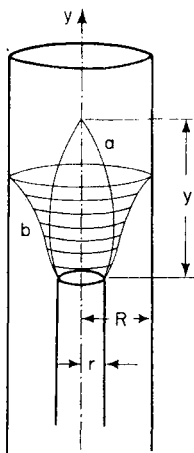


FIG. 170. Hot diffusion flames (according to Burke and Schumann [466]): (a) flame with excess oxygen (lean mixtures); (b) with excess fuel (rich mixtures).

u and air or oxygen is fed through the wide (outer) tube with the same velocity. With excess oxygen the flame tapers upwards (a) and with excess fuel the upper part of the cone of the flame is broadened (b). The dimensions and shape of the flame may be found from the diffusion equation

$$\frac{\partial c}{\partial z} = \frac{D}{u} \left(\frac{\partial^2 c}{\partial r^2} + \frac{1}{r} \frac{\partial c}{\partial r} \right) \quad (41.7)$$

(c is the concentration of the fuel gas, z the distance from the nozzle, D the diffusion coefficient, u the linear feed velocity of the gas and r the distance from the axis of the flame), which is obtained by using certain simplifying assumptions in the overall kinetic equation

$$\frac{\partial c}{\partial t} = -w - \frac{\partial u c}{\partial z} + \frac{\partial}{\partial x} D \frac{\partial c}{\partial x} + \frac{\partial}{\partial y} D \frac{\partial c}{\partial y} + \frac{\partial}{\partial z} D \frac{\partial c}{\partial z}. \quad (41.8)$$

For if we assume that the gas velocity u and the diffusion coefficient D are constant (in fact these quantities vary with temperature and gas composition), neglecting diffusion along the axis of the flame, i.e. assuming $(\partial/\partial z)(D\partial c/\partial z) = 0$, and representing the combustion zone (the flame front) as an infinitesimally thin layer (which forms a surface around the gas issuing from the nozzle), so that w is practically zero throughout the volume, we obtain for the stationary case ($\partial c/\partial t = 0$) the equation

$$u \frac{\partial c}{\partial z} = D \left(\frac{\partial^2 c}{\partial x^2} + \frac{\partial^2 c}{\partial y^2} \right),$$

or, considering a cylindrical flame and using cylindrical coordinates (r, z) we obtain equation (41.7).

This equation was first used by Burke and Schumann [466], and gives the distribution of fuel concentration at any point near the flame front. Determination of the dimensions and shape of the front requires an additional assumption about the concentration of fuel in the combustion zone. Burke and Schumann based their calculations on the assumption that the fuel and oxygen are in stoichiometric proportions in the flame front. In subsequent theories it is assumed that the fuel concentration in the flame front is zero; this is more consistent and physically more justifiable.

Burke and Schumann and other authors have checked experimentally the conclusions, drawn from an approximate solution of the diffusion equation, about the dependence of the shape of the front and flame height on the composition of the gases entering the combustion zone, on the gas-feed rate and on the diameters of the inner and outer tubes; in spite of errors introduced by the above assumptions, good agreement is obtained between theory and experiment.

This is explained by the high fuel-concentration gradients near the flame front, where its width is slight so that any definition of the flame front scarcely affects its calculated shape. In addition Frank-Kamenetskii [277] showed that many of Burke and Schumann's results, obtained by solving analytically the diffusion equation, may be derived solely from dimensional considerations.

Thus, introducing the dimensionless coordinates

$$r' = r/R \quad \text{and} \quad z' = Dz/uR^2$$

(R is the radius of the outer tube) we may write equation (41.7) in the form

$$\frac{\partial c}{\partial z'} = \frac{\partial^2 c}{\partial r'^2} + \frac{1}{r'} \frac{\partial c}{\partial r'}, \quad (41.9)$$

which contains no parameters. Moreover, the boundary conditions $r = 0$, $r = R$ and $r = L$ (L is the radius of the inner tube), give $r' = 0$, $r' = 1$

and $r' = L/R$, so that the solution of (41.9) contains only one dimensionless parameter L/R ; consequently,

$$c/c_0 = f(r', z', L/R) = f(r/R, Dz/uR^2, L/R) \quad (41.10)$$

(c_0 is the initial concentration of fuel).

Defining the flame front as the geometric location of the points at which the fuel concentration is zero, we obtain the following equation for the shape of the front:

$$f(r/R, Dz/uR^2, L/R) = 0. \quad (41.11)$$

This equation shows in particular that the flame height z_0 , which is equal to the z coordinate when $r = 0$ with an excess of oxygen, and when $r = R$ with an excess of fuel, should be proportional to uR^2/D when L/R is constant (i.e. when geometric similarity is maintained).

This rule is supported by Burke and Schumann's experiments and was also obtained by Jost [97] on the basis of the following simple considerations. Consider a flame burning in excess oxygen; from the approximate equation

$$R^2 = 2Dt$$

we may find the time t in which the oxygen diffusing to the flame axis reaches a depth R equal to the diameter of the inner tube, i.e. reaches the flame axis. On the other hand, this time may be put approximately (to the extent that we may consider the gas velocity constant) equal to

$$t = z_0/u.$$

Eliminating t from the two equations, we obtain the required expression

$$z_0 = uR^2/2D. \quad (41.12)$$

A study of the distribution of fuel and oxygen at various cross sections of the diffusion flame perpendicular to the flame axis indicates the situation shown schematically in Fig. 171. It is apparent that oxygen is completely absent in the volume confined by the flame front (broken line) and that the fuel is absent outside the confines of this volume (see also [551]). This picture, however, is often complicated by different types of side processes. Most often the complication arises as a result of the occurrence of turbulence in the gas streams; this is observed when the gas velocities are sufficiently high or when external factors disturb the laminar flow of the gas.⁽¹⁵⁾ Flames in which mixing of gases occurs predominantly by a convection mechanism are called *turbulent flames*. Turbulent flames include practically all commercial flames, for instance furnace flames.

⁽¹⁵⁾ For the effect of turbulence on the rate of combustion see, for example, Karlovitz [815a].

The structure of a diffusion flame is no less frequently complicated by the cracking of the fuel in the preheating zone (the volume confined by the flame front) which leads to formation of soot particles. An example of such a flame is that shown in Fig. 172 [346]. In this the true diffusion

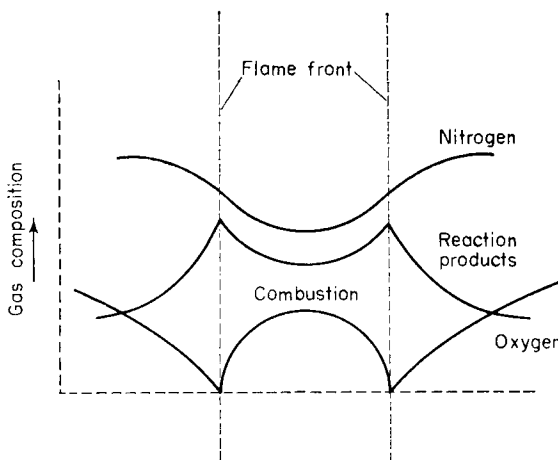


FIG. 171. Distribution scheme for fuel and oxygen in a diffusion flame.

flame is in the shape of a cylindrical zone (the thin vertical lines in the figure) and it does not end in the usual cone but in a luminous zone where the combustion of solid carbon particles takes place; these carbon particles are formed in the dark preheating zone below the luminous zone. The combustion of the carbon particles obeys different laws from those governing the combustion of gases with a diffusion mechanism of mixing. In luminous flames, therefore, the rules of the simple theory of diffusion flames do not hold.

Another example of a diffusion flame which is also complicated by soot formation is the flame of an ordinary candle. The structure of this flame is clear from Fig. 173 which also shows the temperature distribution both in the candle flame itself and close to it. In III, the dark preheating zone at 600–1000°C, cracking⁽¹⁶⁾ of the fuel vaporized from the wick II occurs and leads to the formation of soot particles. These particles are burnt in the luminous zone V of the flame which has a temperature of 1200°C. The main reaction occurs in zones IV and VI which are the zones of the true diffusion flame.

Let us consider the chemical mechanism of soot formation in flames. In early work the appearance of soot particles was usually connected with

⁽¹⁶⁾ Mass-spectrometric analysis of the primary products of hydrocarbon cracking in the case of a paraffin candle shows that these products are mainly unsaturated hydrocarbons [1157].

formation of C_2 radicals which were detected by their emission spectrum; this spectrum is particularly intense in the case of rich mixtures. As a result of work in recent years, however, this point of view has been abandoned [1169, 1008, 981]. In this respect the work of Norrish, Porter and Thrush [981] has been especially persuasive; they showed that there is no

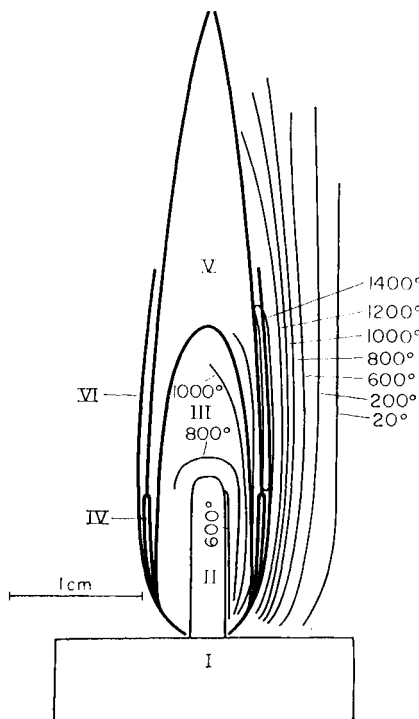
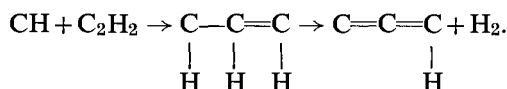


FIG. 173. Candle flame (according to Gaydon and Wolfhard [658]).
 I. Candle; II. Wick; III. Dark zone; IV. C_2 and CH radical zone; V. Luminous zone; VI. Main reaction zone.

parallelism between soot formation and C_2 radical concentration (as determined from their absorption spectra) in the explosion of an acetylene-oxygen mixture. In Porter's opinion [1038], the mechanism of soot formation in flames is based on simultaneous processes of polymerization and dehydrogenation, for example:



Behrens [370] suggests that the process $CO + H = C + OH$ is the main elementary process in the mechanism of soot formation. This mechanism is also considered in references [330, 1105, 606a]. (See also the work of

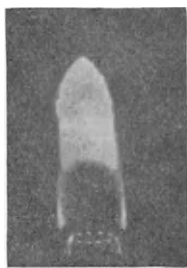


FIG. 172. The luminous diffusion flame of a rich mixture of fuel with air (according to Barr and Mullins [346]).

Gaydon and Fairbairn [655] in which the mechanism of soot formation in electric discharge in C_2H_2 and CO is examined.)

Diffusion flames also include the case of liquid droplet combustion, for instance combustion in a Diesel engine. According to current ideas regarding droplet combustion, each drop in the cylinder of the engine is surrounded by a layer of gaseous fuel evaporating from the drop as a result of the heat supplied from the combustion zone. The fuel diffuses from this layer, which is the preheating zone, into the combustion zone counter to the oxygen diffusing from the space outside. We should add that these conditions are also similar to those in combustion of liquid and solid explosives. It has been shown by Belyaev [26] that here the heat from the combustion zone results in evaporation (sublimation) of the explosive into the dark preheating zone; above this zone is the combustion zone fed by fuel and oxygen diffusing counter to each other from the preheating zone and the surrounding space respectively.

This presentation of the mechanism of droplet combustion is apparently applicable only to sufficiently large drops. In the case of drops less than a few hundredths of a millimetre in size the situation changes, since these may evaporate before reaching the combustion region. In this case the fuel mist, which is a mixture of fine droplets in air, reaches the combustion region as a homogeneous mixture of fuel vapour and air. In this way the combustion characteristics of such a mist must be close to those of previously prepared gas mixtures; this is supported by observations on the combustion of finely dispersed mists.

§42. Flames Burning in Previously Prepared Mixtures

Rarefied Flames

In this short survey of the properties of flames burning after previous mixing of the fuel with air or oxygen we shall first be concerned with so-called *rarefied flames*, i.e. flames burning below atmospheric pressure. These are exemplified by the oxygen flames of hydrogen and carbon monoxide, which have been especially well studied; these flames appear when a mixture of the fuel gas and oxygen is passed through a quartz tube heated to 500 to 600°C. When the velocity of the gas mixture is constant, a stationary luminous flame zone is established in the tube and is orange for the H_2 -O₂ mixture and dark blue for the CO-O₂ mixture. The orange colour of the oxy-hydrogen flame is based mainly on the sodium *D*-lines which are the satellite of many flames and are particularly marked in the flame spectrum of hydrogen due to its low luminosity,⁽¹⁷⁾ and on

⁽¹⁷⁾ Measurements of the absolute light yield in the hydrogen flame spectrum show that one excited hydroxyl appears for approximately every 100,000 water molecules formed. In the spectrum of the considerably more luminous carbon monoxide-oxygen flame, one excited molecule appears for approximately every 100 carbon dioxide molecules formed [133].

the weak bands of hydroxyl and water. The maximum intensity in the hydrogen flame spectrum occurs at the hydroxyl bands in the ultraviolet region, which have most of the electronic radiation of this flame.

The intensity of rarefied hydrogen flames is considerably greater than that of the thermal radiation at the temperature of these flames. For example, a flame burning when the pressure of the H_2-O_2 mixture is a few millimetres of mercury and the temperature $1000^{\circ}K$ emits about 10^{14} quanta/sec. The intensity of the equilibrium radiation in these conditions does not exceed 10^3 quanta/sec. Therefore the radiation of rarefied hydrogen flames is pure chemiluminescence. Measurements of the intensity of rarefied carbon monoxide flames lead to a similar conclusion, as the difference between the flame and equilibrium intensities is as large as in the case of hydrogen. Thus the rarefied $2CO+O_2$ flame burning at a pressure of 100 mm Hg and a temperature of $1400^{\circ}K$ emits about 10^{15} quanta/sec. The equilibrium radiation in these conditions (calculated for excited O_2 molecules with an excitation energy of 140,000 cal and a mean life-time of 10^{-8} sec) is about 10^5 quanta/sec [133]. In the flame spectrum of carbon monoxide the following have been identified: O_2 bands (the Schumann-Runge system and atmospheric bands), bands attributed to the CO_2 molecule [658, 1261], and a continuous radiation which is relatively quite intense at high pressure and temperature and must be attributed to recombination processes [450].

It should be mentioned, however, that according to Knipe and Gordon [846] the radiation of the continuous flame spectrum of CO may be connected with the dissociation of excited CO_3 molecules which are formed on the collision of electronically-excited CO molecules in the $^3\Pi$ state with oxygen molecules: $CO' + O_2 \rightarrow CO_3'$. The presence of excited molecules of CO ($^3\Pi$) in the combustion zone of CO, according to Knipe and Gordon, follows from the fact that in the explosion of a dry $CO-O_2$ mixture there are observed absorption bands which they attribute to the transition $^3\Pi \rightarrow ^3\Pi_t$ in the CO molecule. The absence of a continuous emission spectrum of atomic CO flames [450], i.e. flames appearing when CO reacts with atomic oxygen, and also of $CO+O_3$ flames [76], is clearly difficult to reconcile with a dissociation (and not recombination) mechanism for the emission of this spectrum.

The non-equilibrium character of rarefied-flame radiation is also shown in the quenching of chemiluminescence which is shown by a decrease in the light yield when the pressure of the burning gases is increased or foreign (inert) gases are admitted to the flame zone. Water has a particularly large quenching action, which is connected with the high probability of transformation of electronic excitation energy into other forms of energy on collision of an excited molecule with a water molecule. In rarefied hydrogen flames the quenching effect of water vapour is shown

by the displacement of the maximum glow to the side of low water-vapour content, as shown in Fig. 174. These data, which were obtained by Skalov,

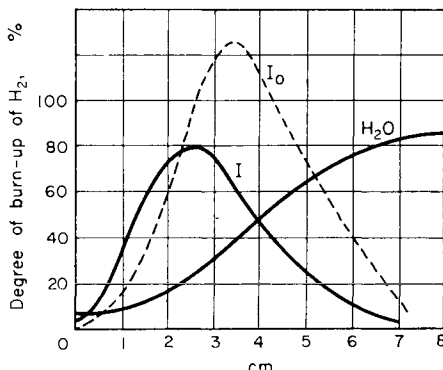


FIG. 174. Degree of burn-up of hydrogen, and flame intensity, at different points along the combustion zone for the $\text{H}_2 + \text{O}_2$ mixture at 20 mm Hg (according to the data of Skalov). The flame-intensity curves are given in arbitrary units.

refer to an equimolar $\text{H}_2\text{--O}_2$ mixture burning at a pressure of 20 mm Hg. In Fig. 174 the H_2O curve represents the percentage conversion of H_2 into H_2O measured by withdrawing gas samples from different points along the reaction tube (the abscissa axis), and the curve I represents the intensity of the flame measured photometrically. The probable cause of the displacement of the intensity maximum relative to the reaction rate maximum (the point of inflection of the H_2O curve), which is shown clearly in Fig. 174, is the quenching effect of water. This is seen from the fact that when allowance is made for quenching, the flame-intensity (broken curve I_0) and reaction-rate (the point of inflection of the H_2O curve) maxima practically coincide.⁽¹⁸⁾ A similar situation is observed for other compositions of the hydrogen-oxygen mixture.

Figure 175 shows the dependence of the relative light yield (i) in the carbon monoxide flame on the pressure of the added water vapour [146]. The experimental points lie (with some scatter) on a line constructed according to the formula

$$1/i = 1 + 2.5p_{\text{H}_2\text{O}}$$

⁽¹⁸⁾ Owing to the strong quenching action of water vapour, the glow intensity corrected for the quenching effect is obtained by simply multiplying I by γ (the degree of burn-up). Actually, in this case ($k\rho_{\text{H}_2\text{O}} \gg 1$) the formula

$$I = I_0/(1 + k\rho_{\text{H}_2\text{O}})$$

takes the form $I = I_0/k\rho_{\text{H}_2\text{O}}$ [143] and hence, since $\rho_{\text{H}_2\text{O}} = \gamma p/2$, $I_0 \sim \gamma I$.

According to the data of Broida and Carrington [448], excited hydroxyl loses electronic excitation energy on every gas-kinetic collision in the flame.

We may conclude from this fact, which is characteristic of fluorescence quenching (see p. 428), that in this case the action of water vapour should be interpreted as chemiluminescence quenching. It has also been established that CO, O₂ and N₂ have a quenching action in the carbon monoxide flame although it is weaker than that of water vapour.

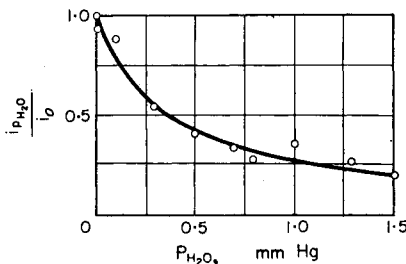


FIG. 175. The relative light yield in the carbon monoxide-oxygen flame with different amounts of water vapour in the mixture (according to Kondrat'eva and Kondrat'ev [146]).

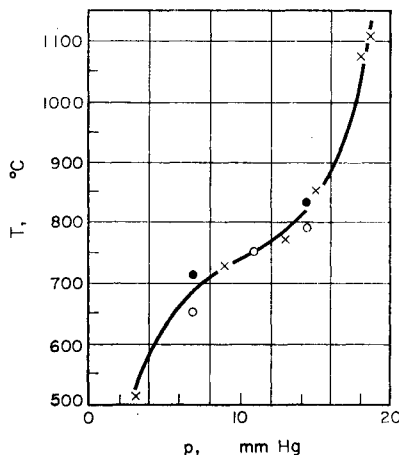


FIG. 176. Flame temperature of a stoichiometric hydrogen-oxygen mixture at different pressures (according to Kondrat'ev [143]).

The ignition temperatures of oxygen mixtures with hydrogen and carbon monoxide are relatively high, so that the absolute rates of combustion of these gases are quite large even near the lower ignition limit. For this reason the heating-up of the burning gas (the difference in temperature of the flame and of the walls of the reaction vessel) is appreciable even at relatively low pressures. To illustrate this Fig. 176 shows the flame temperature of a stoichiometric hydrogen-oxygen mixture measured at different pressures [143]. It is seen from the curve shown that a pressure increase of

1 mm in the pressure range studied (3 to 19 mm Hg) leads to an increase in flame temperature of 40° on average. At a pressure of 20 mm Hg the flame temperature is 1400°K . Figure 177 provides another illustration,

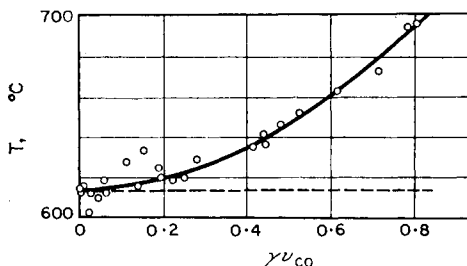


FIG. 177. Dependence of heating-up of the flame zone on the combustion rate of a $2\text{CO} + \text{O}_2$ mixture (according to Kondrat'eva and Kondrat'ev [152]).

showing the dependence of the temperature of a rarefied carbon monoxide ($2\text{CO} + \text{O}_2$) flame on the product of v_{CO} , the volumetric velocity of the gas mixture, and γ , the degree of burn-up, which is taken as a measure of the combustion rate [152]. It is evident from this figure that the reaction rate is directly proportional (within the limits of scatter of the points) to the difference in temperature of the flame and of the walls of the reaction vessel (near 600°C). This indicates that in the temperature range studied the conditions of heat liberation are constant.

The excited particles of OH in the hydrogen flame, and O_2 , CO_2 , OH, etc. in the carbon monoxide flame, are present in the combustion zone in concentrations much greater than their equilibrium values at the flame temperature. In addition, various methods show that these flames also contain unexcited active particles—free atoms and radicals—in concentrations much greater than their equilibrium concentrations. It follows from this that the chemical reaction itself is the source of these particles as well as of excited molecules. The hydrogen flame and the carbon monoxide flame have been found to contain hydroxyl, H atoms and O atoms. Calculations of the rates of the processes $\text{OH} + \text{H}_2 = \text{H}_2\text{O} + \text{H}$ and $\text{OH} + \text{CO} = \text{CO}_2 + \text{H}$, from the directly measured concentrations of hydroxyl in the flame zones and the known rate constants of these processes, show that their rates are close to the overall rates of the corresponding reactions. Consequently these processes predominate in the combustion of hydrogen and carbon monoxide; this also follows from the chemical mechanism.

In accordance with the combustion mechanism of hydrogen, measurements give very high concentrations (up to 10 to 15% of the total pressure)

of H atoms in hydrogen flames. In rarefied carbon monoxide and acetylene flames, the partial pressures of atomic hydrogen are much lower and usually do not exceed some tenths of a per cent of the total pressure; in these flames, however, they are much greater than their equilibrium values.

Measurements of the overall rate of chemical conversion in rarefied flames show a marked dependence of the extent of conversion on the ratio of the combustion-zone pressure p and the pressure p_1 at the lower ignition limit, i.e. on the amount of penetration into the ignition peninsula (from the low-pressure side). Figure 178 shows data obtained for rarefied hydrogen flames, which in this respect have been studied in great detail [150].

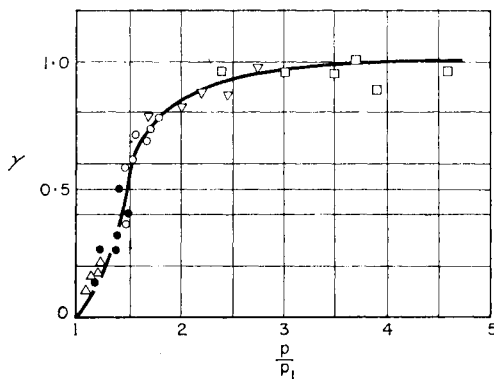


FIG. 178. Dependence of extent of hydrogen conversion into water on p/p_1 for hydrogen-oxygen mixtures of different compositions:
 $\alpha = 2p_{O_2}^{0.0}/p = \frac{1}{2}(\Delta)$; 1(\bullet); 2(\circ); 4(∇); and 8 (\square)
 (according to Kondrat'eva and Kondrat'ev [150]).

Here the different points correspond to the degree of conversion γ ($\gamma = 1$ corresponds to complete conversion) in the combustion of mixtures of different compositions. We should note that the degree of conversion for identical values of p/p_1 does not depend on α , and also the fact that practically complete conversion ($\gamma = 1$) takes place only when the penetration into the ignition peninsula corresponds to the pressure p being several times larger than p_1 .

Measurements of the rate of reaction in rarefied carbon monoxide flames reveal that the degree of conversion of CO into CO_2 (for low degrees of conversion, thus ruling out appreciable heating-up of the gas) is directly proportional to the moisture content of the $CO-O_2$ mixture [133]; these measurements also show that the reaction stops practically completely when moisture is removed from the zone of a reaction already in progress [132]. These data show that the water vapour acts as an homogeneous catalyst in the mechanism of carbon monoxide combustion.

Hot Flames

When the fuel mixture is at a pressure near atmospheric (or higher than atmospheric) the flame temperature reaches 2000 to 3000°K owing to the high absolute rate of reaction, and we have ordinary hot flames with their characteristic structure (the *flame-front* structure).⁽¹⁹⁾ A hot flame may have a different structure depending on the combustion conditions. The simplest structure belongs to flames burning without access to external air. Such are the flames which burn in tubes, for instance, the flame obtained when a fuel mixture is fed through a narrow short tube into a tube of larger diameter which is connected to the external air only in its upper part. In this case the flame has two zones: a zone of preheating of the gas mixture and a combustion zone (the internal flame). Figure 179 shows the

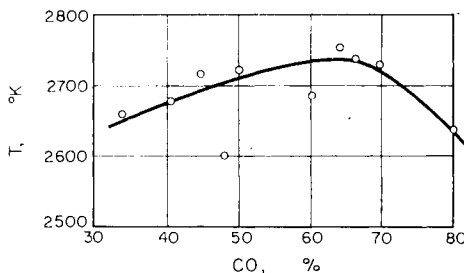


FIG. 179. Temperature of carbon monoxide-oxygen flames burning without access to air for different compositions of the CO-O₂ mixture (according to Karmilova and Kondrat'ev [104]).

dependence of the temperature of the carbon monoxide-oxygen flame obtained in this way on the CO content in the mixture [104]. The concentration of atomic oxygen in this flame has been estimated using a method based on measuring the intensity of the yellow-green glow appearing when small amounts of nitric oxide are added to the fuel mixture, due to the process $\text{NO} + \text{O} = \text{NO}_2 + h\nu$ [1077a, 653, 654, 50]. The partial pressures of O atoms for this flame were found to be close to the equilibrium values [104].⁽²⁰⁾

⁽¹⁹⁾ Flames with much higher temperatures are also known (*extra-hot flames*). Thus, the temperature of the hydrogen-fluorine flame at atmospheric pressure is 4300°K [1299]. The temperature of the C₂N₂-O₂ flame containing argon ($p_{\text{Ar}} = 6.8$ atm) reaches 5050°K owing to suppression of dissociation products of the combustion [497].

⁽²⁰⁾ Similar investigations of the distribution of oxygen atoms in hydrogen-air flames have been carried out by James and Sugden [799] who found that the intensity of the yellow-green glow is proportional to the equilibrium concentration of O atoms calculated from measurements of temperature and composition of the gas. From the distribution they found for the glow intensity these authors conclude that directly above the inner flame (cone) the O-atom concentration exceeds the equilibrium concentration, but rapidly reaches equilibrium on moving away from the cone.

Flames of this type also include the inner flame produced in the Teclu-Smithells-Ingle flame-separator. This separator is similar in construction to the burner mentioned above consisting of two concentric tubes, as is shown in Fig. 180 [712]. The outer cone (the outer flame) produced using this separator for incomplete combustion of the gas in the inner cone, where combustion occurs without access to the external air, is a diffusion flame in which the oxygen of the atmosphere allows combustion of the initial fuel unburnt in the inner flame and also of the combustible products of chemical conversion of the fuel.

An idea of the extent of chemical conversion in the inner flame is given by an analysis of the interconal gases. On combustion of mixtures of air with various hydrocarbons or other fuel gases, the samples of the interconal gas contain not only end-products of the combustion (H_2O and CO_2 in the case of hydrocarbons) and nitrogen but also large quantities of the products of incomplete oxidation, which are capable of further chemical conversion. For example, Smithells and Ingle [1159] obtained an interconal gas of the following composition during combustion of ethylene C_2H_4 in air: 60.0% N_2 , 15.6% CO , 9.5% H_2O , 9.4% H_2 , 3.6% CO_2 and 1.3% of other compounds containing oxygen. The absence of oxygen in the interconal gases shows that all the oxygen of the initial mixture is consumed in the inner flame. Consequently, the main cause of incomplete chemical conversion in the inner flame is the lack of oxygen. As we have noted above, combustion in the outer flame is maintained by the oxygen of the surrounding air.

Quantitative analysis of the interconal gas similar to the above gives quantities of CO , CO_2 , H_2 and H_2O close to those corresponding to equilibrium at the temperature of the flame. Thus, Table 56 gives data

TABLE 56
Water-gas equilibrium in the inner cone of a domestic gas flame
(according to Haber and Richardt [712]).

T°, K	K_T	K_A	$CO_2, \%$
1780	3.88	3.80	0
1643	3.33	3.26	10.8
1528	2.71	2.66	13.6

obtained by Haber and Richardt [712] for a domestic gas-air flame (the averages from five, two and four experiments respectively are given in the table). The first column of the table shows the maximum temperature (T)

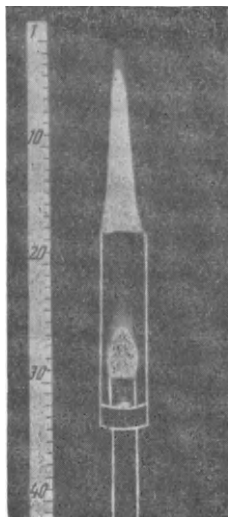


FIG. 180. Separated flames of domestic gas (the inner and outer cones of the flame) (according to Haber and Richardt [712]).

of the inner flame cone; the second column, the water-gas equilibrium constant (K_T),



calculated for the maximum temperature; the third column gives the equilibrium constant (K_A) found from analysis of the interconal gas for CO, CO₂, H₂ and H₂O; and the fourth column, the content of CO₂ (%) added to the initial gas mixture (this causes a lowering of the flame temperature and a corresponding shift of the water-gas equilibrium).

It is seen from Table 56 that K_T and K_A are practically the same. The difference in their values (on average 0.07) corresponds to a temperature difference of only 20°, which is within the limits of accuracy of the measurements.

On the basis of these data Haber and Richardt conclude that the chemical equilibrium, which is established in the hot flame (in contrast with rarefied flames), is practically unchanged when the gases are removed from the combustion zone and quenched at a temperature close to the maximum flame temperature. These authors compare the results of their experiments on flames with different maximum temperatures, and suggest that the possible cause of the chemical reaction outside the combustion zone being slow (as reflected in the absence of a marked displacement of the water-gas equilibrium) is the absence of oxygen in the interconal gas.

As the combustion zone contains active particles (free atoms and radicals), quenching of the gas at such high temperatures as 1500°K and above (see Table 56) and with such a relatively low rate of flame propagation (see below) should be considered to be improbable. For this reason the experimental results of Haber and Richardt on quenching of the mixture must be considered not sufficiently precise. More recent experiments show that in conditions similar to those of Haber and Richardt's experiments quenching occurs at a temperature of about 1000°K.

The character of the chemical processes occurring in the inner and outer flames of hydrocarbons is reflected in the spectra of these flames (cf. cyanogen flame, p. 70). Thus, in the inner-flame spectrum C₂ bands are observed in the green region, CH bands in the violet region, relatively weak bands of HCO in the near ultraviolet and OH bands also in the ultraviolet region. The C₂ bands are particularly intense in rich mixtures. On increasing the oxygen content of the mixture, these bands become weaker; this leads to a change in colour of the inner flame, on impoverishment of the mixture, from blue-green (in the case of rich mixtures) to blue-violet due to the predominating intensity of the CH bands. In this way, the ratio of the intensities of C₂ and CH bands may be considered as a measure of the extent of oxidation in hydrocarbon combustion reactions. This conclusion also follows from measurements of the relative intensities of C₂

and CH bands in rarefied oxygen–acetylene flames for different mixtures of C_2H_2 and O_2 . The results of these measurements, which were carried out by Avramenko [2], are shown in Fig. 181. In the figure I_{C_2}/I_{CH} (the ratio of intensities of the C_2 and CH bands) is plotted as ordinate and the content of acetylene in its mixture with oxygen is plotted as abscissa. It is apparent that the relative intensity of C_2 bands increases sharply when the

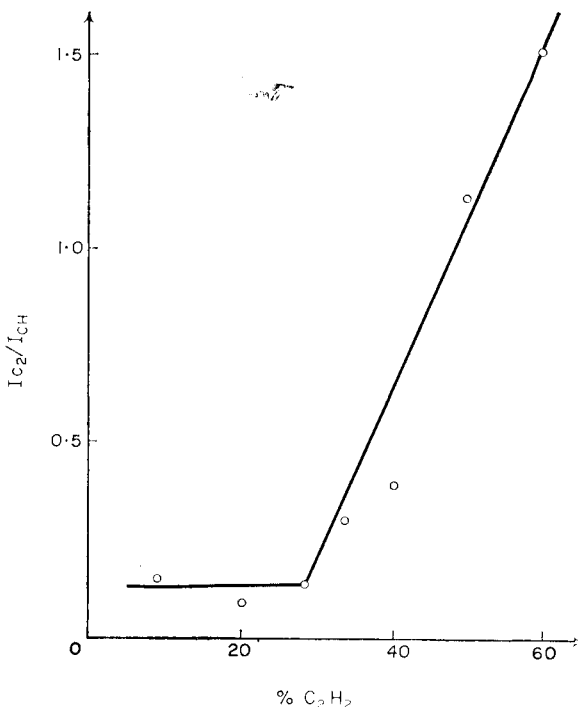


FIG. 181. Relative intensity of C_2 and CH bands in rarefied oxygen acetylene flames for different mixtures of C_2H_2 and O_2 (according to the data of Avramenko [2]).

acetylene content becomes greater than 30 per cent, i.e. when the mixture becomes richer than the stoichiometric mixture, which corresponds to 28.6 per cent acetylene. Avramenko analysed the combustion products of acetylene, and found complete conversion into water and carbon dioxide in poor acetylene–oxygen mixtures up to the stoichiometric mixture, and products of incomplete combustion of acetylene in rich mixtures. A high intensity of the green bands of C_2 has been established in other flames during the combustion of rich mixtures.

The outer-flame spectrum of hydrocarbons shows light blue and is identical with the flame spectrum of moist carbon monoxide mixtures (see

p. 674). It follows that the main chemical process occurring in the outer flame of hydrocarbons is oxidation of CO (and also of H₂).⁽²¹⁾

Valuable information regarding the chemical processes taking place in the inner and outer flames is given by studies of the spectra of these flames when nitric oxide is added to the gas mixture. As we have mentioned above, the resulting yellow-green glow which is based on the process



is an indicator of atomic oxygen. This glow is particularly intense in the carbon monoxide flame, indicating a high concentration of O atoms in the CO combustion zone. This is also in agreement with the fact that, when NO is added to a mixture of CH₄ or other hydrocarbons with air, the NO₂ glow appears almost entirely in the outer flame and hence the oxidation of CO is predominantly in this flame. In earlier stages of the oxidation process O atoms are formed only in insignificant concentrations in the inner flame. It is interesting to note that in the combustion of C₄H₁₀ and CO mixtures with oxygen the NO₂ glow is also observed in the inner flame; in this case CO oxidation accompanied by the formation of high concentrations of oxygen atoms takes place parallel with the early stages of oxidation of the butane in the inner flame [653, 654, 50].

One of the commonest types of flame obtained by the combustion of previously prepared mixtures is that of a Bunsen burner. In this burner the mixture of fuel gas and air entering through special orifices in the lower part of the burner burns in the inner cone of the flame.⁽²²⁾ However, since the content of oxygen in the initial mixture never (under the conditions of a Bunsen burner) reaches a value sufficient for complete combustion, the product of the reaction in the inner cone of the Bunsen flame is a gas capable of further oxidation, which takes place in the outer cone. The latter is an ordinary diffusion flame in which the oxygen diffusing from the surrounding air allows complete combustion of the gas from the inner cone. Therefore the only difference between the ordinary Bunsen flame and the separated flames treated above is that in the Bunsen flame there is no interconal gap so that the inner and outer cones are in direct contact with each other.⁽²³⁾ It is interesting that as early as 1873 Blochmann [411] showed by analysis of gas samples from the inner part of a Bunsen

⁽²¹⁾ For the spectra of hydrocarbon flames see also [50, 783, 664].

⁽²²⁾ Mass-spectrometric analysis of the gas from the dark space between the burner orifice and the inner cone shows that a preflame reaction takes place in this space (the preheating zone) with an appreciable rate and leads to a substantial change in the composition of the gas [473].

⁽²³⁾ In weakly-luminous poor flames of acetylene and ethylene a dark zone is observed between the inner and outer cones, which must clearly be identical with the interconal zone of separated flames. The nature of this dark zone, however, has not yet been adequately explained [658].

flame that the gas does not contain oxygen but consists of CO, CO₂, H₂, H₂O, N₂ and CH₄. The first four gases are found in amounts close to those corresponding to the water-gas equilibrium at the temperature of the flame (cf. p. 680).

Thermodynamic Equilibrium in Flames

The above facts are usually taken as an indication that there is thermodynamic equilibrium in hot flames, i.e. that the concentration of active particles (free atoms and radicals) in hot flames is the equilibrium concentration. The fact noted above (p. 679) that the measured concentration of O atoms in a hot carbon monoxide flame is identical with their equilibrium concentration at the temperature of the flame might also be considered as an indication that this conclusion is correct. We shall now consider some relevant data.

Wolfhard and Parker [1313] have measured the temperatures of various flames (using the sodium-line reversal method or the absorption spectrum of hydroxyl). Table 57 shows the results of their measurements and for comparison the theoretical temperatures calculated for thermodynamic

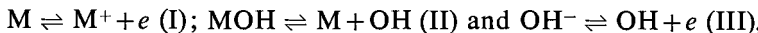
TABLE 57
Calculated and measured temperatures of various flames
according to Wolfhard and Parker [1313])

Mixture	Combustion temperature, °K	
	Calculated	Measured
H ₂ + $\frac{1}{2}$ O ₂	2810	—
H ₂ + NO	2840	2820
H ₂ + $\frac{1}{2}$ NO ₂	2660	1550
NH ₃ + $\frac{3}{4}$ O ₂	2560	—
NH ₃ + $\frac{5}{6}$ NO	2675	2640
C ₂ H ₂ + $\frac{5}{2}$ O ₂	3055	—
C ₂ H ₂ + 5NO	3090	3095
C ₂ H ₂ + 7NO	2855	—
C ₂ H ₆ + 7NO	—	2865

equilibrium. Agreement of the calculated and measured values shows that there is equilibrium in the flame. The non-correspondence of the calculated and measured temperatures in combustion of the H₂ + $\frac{1}{2}$ NO₂ mixture (as also for CO + NO₂) is explained by incomplete combustion.

Sugden [1193] has determined the concentration of hydroxyl in the hydrogen-air flame from measurement of ionization in the flame containing

alkali metals, using a microwave spectroscopic method. This method is based on the assumption that the following equilibria occur:



from which it follows that

$$(e)^2 = \frac{(K_I)(K_{II})(K_{III})(M)_0}{[K_{II} + (OH)][K_{III} + (OH)]},$$

where K_I , K_{II} and K_{III} are the appropriate equilibrium constants; (e) , $(M)_0$ and (OH) are the concentrations of electrons, of the metal added to flame, and of hydroxyl respectively. We may determine the hydroxyl concentration in the flame using this formula, by measuring the concentration of electrons from the absorption of radio waves, and the flame temperature from the known values of K_I , K_{II} and K_{III} for the given temperature. The values of (OH) obtained in this way are given in Table 58; here the first column shows the temperatures measured using the sodium *D*-line reversal method, the second column the equilibrium concentrations of OH calculated for each temperature from the composition of the initial gas, and the third column the measured concentrations (in atmospheres) of hydroxyl for the corresponding temperatures.

TABLE 58

Calculated thermodynamic-equilibrium and measured concentrations of hydroxyl in hydrogen-air flames
(according to Sugden [1193]).

$T, ^\circ\text{K}$	Hydroxyl concentration, atm	
	Calculated	Measured
2150	5.6×10^{-4}	4.0×10^{-4}
2109	3.4×10^{-4}	2.1×10^{-4}
2063	2.1×10^{-4}	1.7×10^{-4}
2010	1.2×10^{-4}	9.6×10^{-5}
1965	7.3×10^{-5}	6.3×10^{-5}
1907	3.7×10^{-5}	3.6×10^{-5}
1855	2.1×10^{-5}	2.3×10^{-5}

It is seen from Table 58 that the measured hydroxyl concentrations agree well with the calculated equilibrium values. It may be concluded, therefore, that the concentration of hydroxyl in hydrogen-air flames is the equilibrium concentration.

Spectroscopic data lead to a similar conclusion. For example, according to the data of Broida [445], the concentration of OH in methane-air flames

is 3×10^{-5} atm at the maximum temperature of the flame, and this is close to the equilibrium concentration. Similarly Penner and Björnerud [1022] conclude that their calculated hydroxyl concentrations in the $\text{C}_2\text{H}_2 + 2\cdot5\text{O}_2$ flame, and the flame of the same mixture diluted by adding 60 per cent argon, are of the same order of magnitude as the theoretical equilibrium concentrations.

Another argument in favour of the existence of equilibrium in hot flames is perhaps given by the results of measurements of the intensity of radiation and the temperature of these flames. The intensity of radiation from rarefied flames is much greater than the intensity of the equilibrium radiation at the temperature of the flame and indicates practically pure chemiluminescence, whereas the intensity of hot flames is usually much the same as the intensity of the equilibrium radiation. The equilibrium character of the radiation from certain hot flames follows from the intensity distribution in the spectra of these flames, and in particular from the close correspondence of the "rotational" temperature, i.e. the temperature calculated from the intensity distribution in the bands of the electronic emission spectrum of the flame, and the actual flame temperature. Such, for example, are the flames of hydrogen and carbon monoxide, and also the oxygen flames of methyl alcohol, formaldehyde and formic acid, in which the "rotational" temperature of hydroxyl is close to the flame temperature. The temperature measured using a method such as the spectrum-line reversal method, which is based on the assumption that the excited atoms in the flame zone are in equilibrium concentrations, is frequently close to the maximum temperature corresponding to chemical equilibrium in the flame [658]; this is seen, for instance, from the data of Table 57.

There are also indications of equilibrium ionization in flames. For example, Jost and Wagner [813] found that in cool flames of ether and oxygen at about 400°K the concentration of ions corresponds to less than one ion per 10^{14} reacting ether molecules, which is not more than 2×10^4 ions/cm³. They conclude from this that in this case the ionization is of a purely thermal (equilibrium) nature. In their opinion, the strong ionization which is observed in certain hot flames results from the emission of electrons by soot particles.

Along with the facts indicating the existence of chemical equilibrium in flames, however, there are facts which may be considered as indications that equilibrium does not exist. For example, the flames of certain organic substances frequently show "rotational" temperatures of hydroxyl much greater than the actual temperature of the flame. For example, the maximum temperature of the oxy-acetylene flame is about 3400°K , whereas the hydroxyl "rotational" temperature at one atmosphere is 5400°K (at a pressure of 1.5 mm Hg the "rotational" temperature is 8750°K), and the

“rotational” temperature of C_2 is $4880^{\circ}K$ [658]. Similarly, according to Broida’s data [445, 452], the hydroxyl “rotational” temperature in methane-air mixtures, for methane-air ratios of 5·6–10·8 per cent, is $3250^{\circ}K$, which is 1100° larger than the maximum equilibrium temperature. In Broida’s opinion, the anomalous intensity distribution in the emission spectrum of hydroxyl (which leads to an increased “rotational” temperature) is evidence that excited OH radicals with higher rotational energy are formed in the course of the chemical reaction.⁽²⁴⁾

Considerable deviations from equilibrium are also indicated by anomalous ionization in flames [658], i.e. ionization greater than the equilibrium ionization (see below). Finally, there are data showing that atoms and radicals are present in hot flames in concentrations much greater than their equilibrium concentrations. For example, according to the calculations of Hirschfelder, Curtiss and Campbell [769], the concentration of oxygen atoms in the O_3 ozone decomposition flame is some ten thousand times greater than their equilibrium concentration for the conditions of this flame. In the same way, according to Kascan’s measurements [W. E. Kascan, *Comb. and Flame*, 2, 229, 286 (1958); 3, 49 (1959)] the hydroxyl concentration near the combustion zone in hydrogen-air flames exceeds the equilibrium concentration of OH at maximum flame temperature by factors of hundreds or thousands. The concentrations of atomic hydrogen and oxygen (as well as those of OH) in H_2 -air, H_2 -CO-air, C_2H_4 -air flames, as measured by Kascan, are considerably higher than equilibrium concentrations of these active centres. It may also be noted that Fenimore and Jones [604b, 604c] find O and H atom concentrations in combustion zones of H_2 -air and H_2 -CO-air exceed equilibrium concentrations by factors of hundreds or thousands. See also [463b], [J. R. King, *J. Chem. Phys.*, 31, 855 (1959)], [1136].

The discrepancy in the experimental data on equilibria in flames, and the sometimes very considerable deviations from equilibrium, are apparently due to the fact that the data, which were obtained by different authors using different methods, refer to flames with different structures of the *front*, or to different parts of the flame front. Thus, it is certain that, owing to the very small width of the combustion zone (reaction zone)

⁽²⁴⁾ From the intensity distribution in the emission spectrum of the acetylene-atomic oxygen flame (the O atoms were produced in an electrodeless radio-frequency electric discharge) Ferguson and Broida [607] found that in this flame the excited hydroxyl has two rotational temperatures: an anomalously high temperature of $12,000^{\circ}K$, and a temperature of $1900^{\circ}K$ identical with the actual temperature of the flame. Hence it may be concluded that there are two different mechanisms of excited-hydroxyl formation under the conditions of this flame.

We should mention that two quite different rotational temperatures of excited hydroxyl are also observed in the discharge spectrum of water vapour. Thus, the data of Lyman [894, 895] give temperatures of 580 and $16,500^{\circ}K$ [143]; Broida and Kane [451] found 800 and $15,000^{\circ}K$.

and the relatively great extent of the zone of hot burnt gases at the maximum (equilibrium) temperature, the above data on measurement of the concentration of oxygen atoms in the CO flame (p. 679) or on measurement of the concentration of hydroxyl in hydrogen, methane-air or acetylene-air flames (p. 685), refer essentially to the concentration of active particles in the latter zone, i.e. in the burnt gas. It is natural that here the measured concentration of active particles should be equal or close to the equilibrium concentration. These measurements clearly show that the concentration of O atoms or OH radicals in the *reaction zone* is not well determined. This is apparently often the case with measurements of the intensity of radiation from the flame, which give the total intensity of the reaction zone and the burnt-gas zone; this intensity, owing to the relatively insignificant volume of the reaction zone, is mainly that of the radiation from the hot-gas zone, where there is thermodynamic equilibrium (see, for example [449]).

However, direct measurements of the distribution of intensity in the spectra of different parts of the flame front and also measurements of ionization in the reaction zone and its adjacent zones in the flame front clearly show that *equilibrium is not attained in the reaction zone*. For example, Broida's experiments [448] showed that although the intensity distribution in the OH spectrum emitted by the hot gases above the reaction zone of the acetylene-oxygen flame corresponds to the temperature of the burnt gases, intensity measurements of the OH spectrum emitted by the reaction zone give a "rotational" temperature which is a few hundred degrees higher than the maximum ("adiabatic") temperature of the flame.

The non-equilibrium nature of the radiation from the reaction zone is also indicated by the fact that in many flames iron particles glow brighter in the reaction zone than in the adjacent parts of the flame [1313].

The most convincing indications that equilibrium is lacking in the reaction zone of the flame front are given by studies of ionization in flames. Thus, Aravin, E. S. Semenov and Sokolik [19] have studied the nature of ionization in hydrogen-air and propane-air flames by measuring the ionization current during propagation of a spherical flame front in a constant-volume bomb. Simultaneous registration of the flame track made it possible to determine precisely the time when the flame front passed through the electrode gap providing a measurement of the current. The pressure was also measured at various times corresponding to the appropriate points of the current oscillogram using optical membrane recorders. The current and pressure curves are shown in Fig. 182, from which it is seen that the ionization current has a sharp maximum, corresponding to the time when the flame front passes through the electrode gap, and a smooth maximum, corresponding to the time when the maximum pressure is reached as a result of combustion of the initial mixture, accompanied by an increase in temperature (due to compression of the

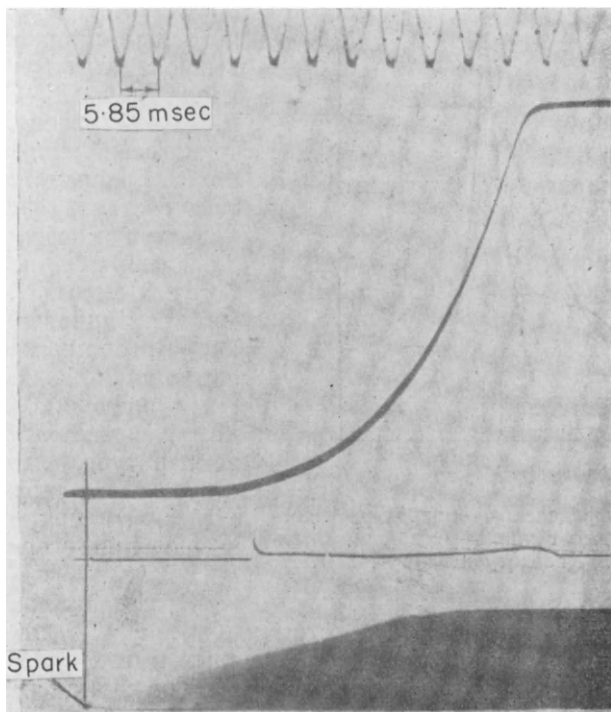


FIG. 182. Ion-current and pressure curves during propagation of a spherical flame front in a propane-air mixture in a constant-volume bomb (according to Aravin [19]).

gas). The sharp decrease in current after the flame front has passed through the electrode gap, in spite of the gas behind the flame front being at the maximum temperature, is a clear indication that ionization in the reaction zone is of a *non-thermal* nature. This is also supported by a comparison of the measured maximum current and the equilibrium current calculated using the Saha equation:⁽²⁵⁾ according to Aravin and E. S. Semenov, the measured current is a factor of 10^2 to 10^3 greater than the equilibrium current for approximately stoichiometric mixtures, the factor being 10^7 for very poor or very rich mixtures.⁽²⁶⁾ The ionization current corresponding to the second maximum is close to the equilibrium value calculated from the maximum pressure and temperature; this indicates its thermal (equilibrium) nature. (In these calculations I is taken as 12.5 eV.)

Calcote and King [477] obtained a similar result to the above for flat propane-air flames. Figure 183 shows one of the curves obtained by them

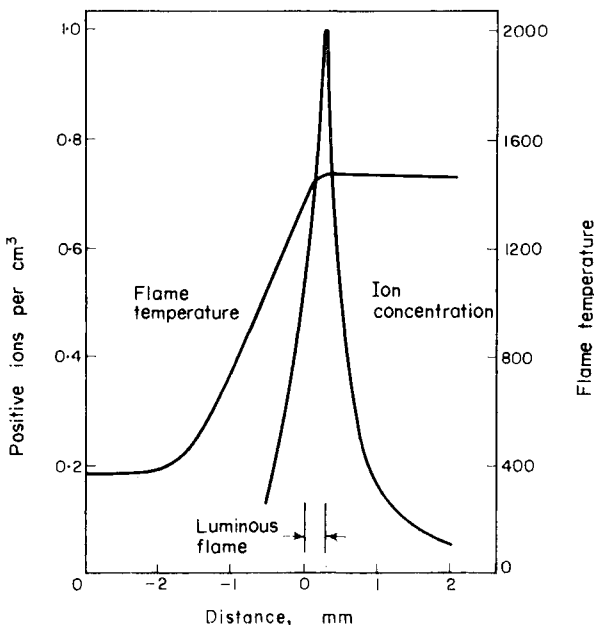


FIG. 183. Distribution of temperature and ion concentration in the propane-air flame (according to Calcote and King [477]).

⁽²⁵⁾ The Saha equation [1099] which is obtained from thermodynamics relates the constant of the ionization equilibrium $A \rightleftharpoons A^+ + e$, $K = (A^+)(e)/(A)$, to the absolute temperature; thus

$$\log K = -5050I/T + \frac{5}{2}\log T - 6.50,$$

where I is the ionization potential in electron-volts.

⁽²⁶⁾ As the determination of the measured current did not allow for space charge its values should be considered rather high.

for the dependence of the measured concentration of ions on distance from the luminous flame zone (the reaction zone) together with a curve giving the temperature distribution in the flame front. We see that in this case the shape of the ion-concentration curve is similar to the shape of the left-hand part of the curve in Fig. 182 and the concentration maximum occurs in the luminous zone, which is about 0.25 mm wide here. The sharp fall in the ion-concentration curve to the burnt gas (maximum temperature) side is also evidence that in neither case does the appearance of ions (i.e. of a current) result from thermal ionization of an admixture or of nitric oxide (with the relatively low ionization potential of 9.2 eV) formed in the flame. In poor propane-air mixtures the thermodynamic equilibrium concentration of NO^+ ions is less than one ion per cm^3 , whereas the measured concentration is of the order 10^9 per cm^3 . Kinbara and Nakamura [832] also found that the concentration of ions in the reaction zone is greater than that in the burnt-gas zone in the case of a Bunsen flame. According to these authors, ionization in hydrocarbon flames is of non-thermal origin and the formation of ions is connected with the presence of excited C_2 molecules in the reaction zone.⁽²⁷⁾

Thus there is no doubt that the thermodynamic equilibrium is not attained in the combustion zone (both with regard to radiation and ionization and also concentration of active particles) (see also [928, 452a]). The only question here is the extent of departure from equilibrium. One of the main causes of this departure is disturbance of the Maxwell-Boltzmann distribution, due to the high rate of the chemical conversions in flames (a short reaction time compared with the thermal relaxation time). Under definite reaction conditions this cause can play a very important part. At present, however, we do not know how often such conditions are realized. Departures from equilibrium in flames are considered in Shuler's article [1136].

We should mention an interesting idea of Behrens [370] who shows that stable substances may be in equilibrium with each other for non-equilibrium concentrations of radicals if the concentration ratio of the latter is equal to the equilibrium ratio, for example,



See also W. E. Kascan, *Comb. and Flame*, **2**, 229, 286 (1958); **3**, 49 (1959).

Cool Flames

In concluding this section we shall briefly consider cool flames (see above, pp. 631-3) which are observed under definite conditions in the

⁽²⁷⁾ According to Ferguson [606], formation of the excited C_2 radicals in hydrocarbon flames occurs mainly by interaction of particles containing one C atom (for example, as a result of the reaction $2\text{CH} = \text{C}_2 + \text{H}_2$). See also [747, 655].

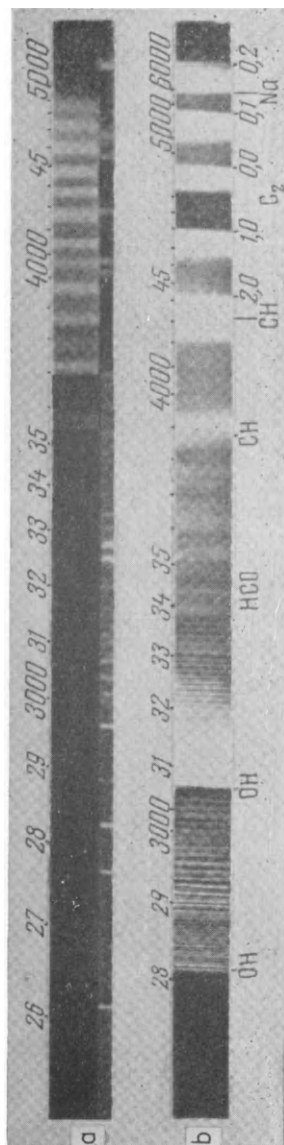


FIG. 184. Spectra of a cool (a) and a hot (b) ether $C_2H_5OC_2H_5$ flame (according to Gaydon [653, 654]).

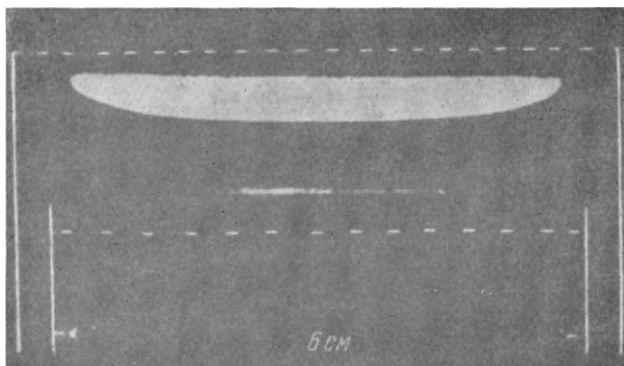


FIG. 185. The cool (lower) and hot (upper) flames observed simultaneously in a rich ether-air mixture (according to Thabet [1216]). The broken lines show the burner rim and the stabilizing grid.

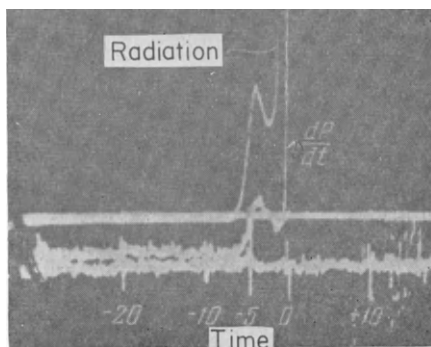


FIG. 186. Time sequence of the cool-flame stage and the hot-flame stage during ignition of a heptane-air mixture, illustrating the two-stage character of the ignition process (according to Levedahl [872]).

combustion of hydrocarbons and organic compounds of other classes. Cool flames appear at temperatures of 200 to 300°C in both static and flow conditions, and may be detected by a characteristic pale-blue glow and a temperature rise of 100 to 200°. The spectra of all the cool flames studied are identical and consist solely of H₂CO formaldehyde bands [120, 653, 654, 50]; these spectra are quite different from those of hot flames of the same substances, as may be seen from Fig. 184 [653, 654, 50] in which the spectra of a cool (a) and a hot (b) ether flame are shown. The hot flame spectrum contains bands of OH, CH and HCO (the last are called hydrocarbon-flame bands); the H₂CO bands in the cool-flame spectrum are not present in the hot-flame spectrum.

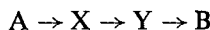
It has been proposed that most of the formaldehyde formed in a cool flame is initially in the form of excited H₂CO molecules [652, 656]. The following schemes of formation of excited formaldehyde molecules (with excitation energy of about 80 kcal) have been suggested by various authors: RCH₂O + OH = ROH + H₂CO + 75.3 kcal (when R = CH₃, Walsh [1250]), RCH₂O + R' = RR' + H₂CO + 70.9 kcal (when R = R' = CH₃, Damköhler and Eggersglüss [522]), CH₃ + HO₂ = H₂O + H₂CO + 122.1 kcal (von Elbe [568]) and CH₃HCO + O = 2H₂CO + 75.2 kcal (Norrish [978]). Owing to the high excitation energy of H₂CO molecules, the participation of two radicals (or a molecule and a biradical) in the excitation process is quite natural. The first three of the above schemes are apparently the most probable, and from an energy viewpoint von Elbe's scheme is favoured. We consider Norrish's scheme less probable, as it can scarcely be doubted that there are no O atoms in cool flames.

In a *p-T* diagram a cool flame corresponds to a clearly defined region, as is seen for instance in Fig. 149 (p. 632), which gives the ignition diagram of a propylene-oxygen mixture (the cool-flame region is hatched). For temperatures and pressures outside the combustion region an oxidation reaction (slow oxidation) takes place in the mixture, forming (in addition to water and carbon dioxide) products of incomplete oxidation—carbon monoxide, alcohols, aldehydes, acids and peroxides, and also cracking products (hydrocarbons and hydrogen). The slow oxidation reaction manifests itself outwardly by an increase in pressure, which becomes measurable at the end of the induction period. When the reaction occurs inside the cool-flame region, sharp peaks are superimposed on the smooth rise in pressure at definite times; these result from the temperature increase when the cool flame flashes. Three such peaks (corresponding to three consecutive cool flames of propylene) are seen in the pressure-rise curve in Fig. 148 (p. 631).

The occurrence of consecutive cool flames shows the *periodicity* of chemical processes which is particularly characteristic of cool-flame combustion. Cases are known where the number of consecutive cool flames reaches 7

or 8; and Gervart and Frank-Kamenetskii [52] have observed cool-flame flashes in the form of a long periodic process during continuous addition of a fuel mixture (a mixture of petrol with air or oxygen) in a so-called turbulent reactor where the fresh gas is completely mixed with the reacting mixture. That a chemical process may be periodic due to purely kinetic factors was first shown by Lotka [888] and has been studied in detail by Frank-Kamenetskii [276, 278] with respect to cool-flame combustion and two-stage ignition. According to Frank-Kamenetskii's proposal, which is based on Neiman's idea [205] that a cool-flame flash arises as a result of the accumulation of peroxides in critical concentrations, the oxidation of hydrocarbons is autocatalytic and involves two intermediate substances formed consecutively, one of which is an aldehyde and the other an organic peroxide.

In this way, representing these substances by X and Y, we obtain from the general reaction scheme



the following system of kinetic equations:

$$\begin{aligned} dx/dt &= k_1 ax - k_2 xy, \\ dy/dt &= k_2 xy - k_3 ay, \end{aligned}$$

where k_1 , k_2 and k_3 are the rate constants of the corresponding reactions and a , x and y are the concentrations of A (the initial substance), X and Y. Let us introduce the deviations $\epsilon_x = x - X$ and $\epsilon_y = y - Y$ of x and y from the stationary values of X and Y, determined by the stationary conditions

$$dx/dt = 0 \quad \text{and} \quad dy/dt = 0.$$

If these deviations are small we may rewrite the foregoing system of equations as

$$\begin{aligned} d\epsilon_x/dt &= -ak_3\epsilon_y, \\ d\epsilon_y/dt &= ak_1\epsilon_x, \end{aligned}$$

or

$$d^2\epsilon/dt^2 = -a^2k_1k_3\epsilon,$$

where $\epsilon = \epsilon_x$ or ϵ_y . The last equation is the usual equation of harmonic vibrations with frequency

$$\nu = (a/2\pi)\sqrt{(k_1k_3)}.$$

We shall not give a detailed analysis of the dependence of this frequency on concentration of the initial substance and on temperature (the latter is included in the constants k_1 and k_2) because of the simplified character of the reaction mechanism at the basis of the calculations, which only very

approximately represents the actual reaction mechanism.⁽²⁸⁾ Quantitative studies of a similar dependence for a reaction scheme closer to the actual mechanism and allowing for temperature variations may serve as an effective method of studying the mechanism of cool-flame oxidation of hydrocarbons.

An example of such an investigation (although not sufficiently complete) is the work of Gray [694], who observed periodic cool flames in a mixture of ethane C_2H_6 and oxygen in a flow system. From analysis of the reaction products he constructs a chain-reaction scheme involving C_2H_5 , HO_2 (formed by $C_2H_5 + O_2 = C_2H_4 + HO_2 + 7 \text{ kcal}$) and OH radicals (formed by decomposition of hydrogen peroxide H_2O_2 , giving rise to branching).

On the basis of Frank-Kamenetskii's theory a periodic solution is obtained for the concentrations of C_2H_5 and HO_2 radicals from the assumed reaction mechanism; this is used by the author to explain the periodic cool flames he observed. See also [891] and N. S. Enikolopyan, V. Ya. Shtern and S. S. Polyak, *J. Phys. Chem., Moscow*, **32**, 2224 (1958).

A hot flame appears in a mixture whose pressure and temperature correspond to the ignition region enclosed by the continuous curve in Fig. 149 (p. 632). The appearance of the hot flame is very often preceded by a cool-flame combustion stage which is detected by its characteristic glow. In stationary flames the cool-flame stage is sometimes observed simultaneously with the hot-flame stage, separate from it in space. Such is the case, for example, in the combustion of rich ether-air mixtures. Figure 185 [1216] shows a thin cool flame situated directly above the burner rim (the lower broken line) and a bright hot flame (with a stabilizing grid above it) above the cool flame. As the fuel moves upwards with a certain velocity the cool-flame stage should be considered as preceding the hot-flame stage in time. This time sequence of the two stages is shown clearly in Fig. 186 for the self-ignition of a weak heptane-air mixture in an engine [872].

It is seen from Figs. 185 and 186 (and also from Fig. 148 for the cool-flame region) that the transition to the hot flame is preceded by extinction of the cool flame (in Fig. 148 the transition is from one cool flame to another). In von Elbe's opinion [568], the retardation of the reaction at the end of the cool-flame stage and the subsequent acceleration leading to the hot ignition are based on the following processes. The easily-decomposed active peroxides formed in the course of the reaction are gradually replaced by more stable peroxides. As the hydrocarbon is oxidized, higher aldehydes are replaced by formaldehyde $HCHO$ and consequently the relatively stable performic acid $HCOOOH$ or hydrogen

⁽²⁸⁾ For instance, the autocatalytic reaction law taken here represents only to a certain extent the branched-chain character of the cool-flame oxidation of hydrocarbons [12, 205, 1043].

peroxide H_2O_2 (formed from HCOOOH by losing CO) begin to predominate in the peroxides. Owing to the great stability of the $\text{O}-\text{O}$ bond in the H_2O_2 molecule, the probability of chain branching is decreased, and this leads to retardation of the reaction. However, following this the formaldehyde HCHO and the remaining higher aldehydes are rapidly oxidized, and consequently active radicals are formed which accumulate in the system and lead to explosion (the hot flame).

Independently of the accuracy of these ideas regarding the mechanism of the chemical processes preceding the hot flame, it must be assumed that the cool-flame stage taking place before ignition of the fuel mixture plays a substantial part in the ignition process. This part consists of preparing the mixture for self-ignition by forming relatively easily oxidized products of the cool-flame combustion. These ideas are the basis of the theory of two-stage ignition, which was first formulated by Neiman [205] and applied to combustion processes in an engine by Sokolik [246] and has received wide application in subsequent years.⁽²⁹⁾ Cases are also known where the cool flame itself is a two-stage process. See, for example, [546a].

§43. Flame Propagation

Normal Rate of Combustion

A flame arising in a fuel mixture is capable of propagation towards the unburnt gas. In practical conditions we meet with flames propagating in a closed volume of initially stationary gas, and flames burning in a gas stream entering the combustion zone with a definite velocity. An example of a flame propagating in a closed volume is that formed in a tube or spherical flask containing a fuel mixture which is ignited by a hot wire or an electric spark. An example of a flame propagating in a gas stream is given by any stationary flame burning in a tube when a fuel mixture is passed through it (with a definite constant velocity) or a Bunsen burner flame. For both propagation in a closed vessel and combustion in a gas stream the flame is characterized by a certain rate of propagation which is always a relative rate, i.e. the rate of propagation of the flame front relative to the unburnt gas.

The main quantitative characteristic of a flame is its so-called *normal, or fundamental rate of combustion*, which is the relative velocity, or rate of displacement, of the flame front normal to the surface of the front and is given by the formula

$$u_0 = dz/dt \quad (43.1)$$

(z is the distance along the normal). It follows from this definition of the normal rate that only in the case of an ideally-plane front will the normal rate coincide with the mean rate of combustion.

⁽²⁹⁾ See, for example, *Proceedings of Symposia on Combustion* (III to VI).

The normal rate is a function of the chemical and thermodynamic properties of the fuel mixture and may be measured in each individual case.⁽³⁰⁾ One experimental method of determining the normal rate of combustion is that first applied to the Bunsen flame by Mikhel'son [192]. In this method, considering u_0 to be constant (Gouy [688]) and representing the surface area of the flame front (its inner cone) by S , it is assumed that

$$u_0 S = \bar{u} S_0, \quad (43.2)$$

where \bar{u} is the mean flow rate of the fresh gas mixture and S_0 is the cross-sectional area of the mouth of the Bunsen burner. Assuming that the flame front is strictly conical in shape, we obtain $S_0 = S \sin \vartheta$, where ϑ is the half angle of the cone. In this way we obtain

$$u_0 = \bar{u} \sin \vartheta, \quad (43.3)$$

from which we may find u_0 after measuring \bar{u} and ϑ .⁽³¹⁾

We shall not concern ourselves here as to how accurate formula (43.3) is. This problem is considered in detail in the scientific literature on the theory of the Bunsen burner.⁽³²⁾ We should just mention that in the strict theory (43.3) is replaced by

$$u_0 = u(r) \sin \vartheta(r),$$

where $u(r)$ is the velocity of fresh gas at a distance r from the axis of the burner and ϑ is the angle between $u(r)$ and the tangent to the front. It is also important to note that in the strict theory it is necessary to allow for conditions at the rim of the burner orifice, where the normal combustion rate u_0 tends to zero owing to the removal of heat.

We shall consider another experimental method of determining u_0 , which was proposed by Stevens [1184] and consists of introducing a fuel mixture into a soap bubble (which may be considered as a constant pressure bomb) and igniting it centrally with an electric spark. The propagating flame is photographed on moving film through a narrow slit, thus allowing measurement of the diameter of the spherical flame front at different times. The image of the flame on the film is in the form of an isosceles triangle the apex of which corresponds to the moment of ignition of the mixture. If we know the rate of motion v of the film and have measured α , the angle at the apex of the triangle, then from the formula $u = v \tan(\frac{1}{2}\alpha)$ we find the rate of propagation of the flame, which is the

⁽³⁰⁾ For a review of the various methods of measuring the rate of combustion see, for example, Linnett's article [883]. See also van Tiggelen and Vaerman [1244].

⁽³¹⁾ Usually instead of measuring the angle ϑ , the height $h = r_0 \cot \vartheta$ of the flame cone is measured (r_0 is the radius of the burner aperture). When the shape of the front differs considerably from that of a cone, u_0 is determined with greater accuracy from (43.2) by photographing the flame cone and measuring its surface area S .

⁽³²⁾ See Jost [97, pp. 88–100]. For more recent work see Fristrom [642].

rate at which the burnt gas leaves the combustion zone. The latter rate is related to the normal rate u_0 of the flame by

$$u_0 \rho_0 = u \rho, \quad (43.4)$$

which expresses the condition that the gas flow be hydrodynamically continuous. In (43.4) ρ_0 is the density of the unburnt gas and ρ that of the burnt gas; ρ_0 is clearly inversely proportional to the initial volume of the bubble, i.e. to r_0^3 (r_0 is the radius of the soap bubble before ignition of the gas), and ρ to the volume of the bubble at the moment of complete burn-up of the mixture, i.e. to r^3 . Consequently,

$$u_0 = (r_0/r)^3 u,$$

and hence we may find the normal rate u_0 having measured u , r_0 and r .

Measurements of the normal rate show that it may be a few centimetres to a few metres per second depending on the properties of the fuel mixture. An example of one of the slowest-burning mixtures is given by a mixture of 6 per cent methane and 94 per cent air which has a normal rate of combustion of 5 cm/sec. One of the fastest-burning mixtures is a mixture of 75 per cent H_2 and 25 per cent O_2 which has a normal rate of combustion of about 10 m/sec.⁽³³⁾

The effect of various factors on the normal rate of combustion of gas mixtures has been frequently studied. All the work leads to the conclusion that the main factor governing the rate of flame propagation in gas mixtures is the *chemical reaction of combustion* which acts as the source of thermal and chemical energy maintaining combustion and securing the propagation of the flame. The idea of the basic role played by the chemical reaction and its kinetics in the mechanism of flame propagation was first proposed by Payman and Wheeler [1015] (1929); on this basis they gave a qualitative explanation of the experimental dependence of flame velocity on the composition of the fuel mixture. The effect of gas composition on flame velocity, in the opinion of these authors, is in changing the rate of the combustion reaction and changing the temperature of the flame by changing the concentrations of the reacting substances. For example, Fig. 187 shows the dependence of flame velocity in oxygen–nitrogen–methane mixtures on mixture composition; it is seen that the flame velocity sharply decreases on addition of methane or oxygen above their stoichiometric proportions (corresponding to $CH_4 + 2O_2$) or on addition of nitrogen. In the opinion of Payman and Wheeler, the effect of an excess concentration of reacting substances, or of nitrogen, is primarily in decreasing the rate of reaction by lowering the temperature of the flame; this lowering is especially large

⁽³³⁾ The velocity of a normal flame in mixtures of H_2 with F_2 is ten times greater than the flame velocity in mixtures of H_2 and O_2 [706a]. Aliev, Rozlovskii and Shaulov [15] found $u_0 = 15.7$ m/sec in the mixture $C_2H_2 + 2O_2$.

when methane is added owing to its high heat capacity (compared with those of O_2 and N_2). The markedly weaker effect of oxygen compared with that of nitrogen, although it has practically the same heat capacity, is explained by the fact that along with the temperature decrease and the associated decrease in reaction rate, the excess concentration of oxygen, which takes part in the reaction, gives rise to a reverse effect, i.e. to a relative increase in the reaction rate.

It has been suggested that the effect of the composition of the fuel mixture (and also of other factors) on flame velocity is primarily an effect on the flame temperature and consequently on the rate of the combustion reaction. Thus, from the fact that increasing the flame temperature by

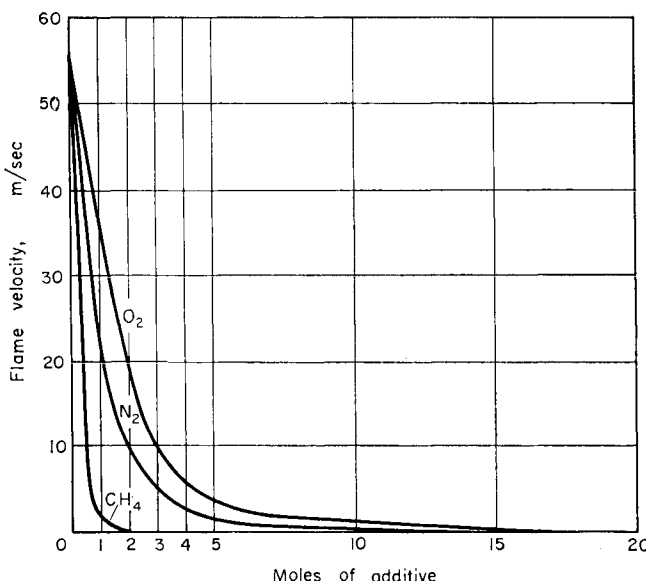


FIG. 187. Decrease in rate of turbulent combustion of a methane-oxygen mixture on addition of nitrogen, and also on addition of methane or oxygen above their stoichiometric proportions (according to Payman and Wheeler [1015]). The maximum rate of flame propagation (55 m/sec) corresponds to the stoichiometric mixture $CH_4 + 2O_2$.

adding oxygen to a methane-air mixture gives rise to the same increase in flame velocity as increasing the temperature (by the same amount) by preheating the gas mixture [347], it is concluded that the effect of preheating on the normal rate of combustion consists solely in increasing the temperature of the flame. The effect on the temperature of the flame may also be used to explain the following case, in which preheating the gas

mixture does not accelerate but retards the reaction. Dugger *et al.* [556] found that in combustion of propane-air mixtures the pre-flame reaction (which becomes appreciable above 867°K) leads to a decrease in the flame velocity. The authors attribute this effect to dilution of the mixture by carbon dioxide and water vapour, which are formed in the pre-flame reaction; consequently the flame temperature is lowered and this leads to a decrease in the reaction rate.

This viewpoint is, however, incorrect since in practice changing the mixture composition, and preheating, primarily affect the chemical reaction of combustion, which is the main factor on which the very existence of the flame depends. In the final analysis the course of the chemical reaction (under definite physico-chemical conditions) unambiguously determines the flame temperature which, therefore, may be considered as the factor governing the reaction rate only in a formal manner owing to its mathematical functional dependence.

The effect of temperature on the rate of the combustion reaction, and consequently on the flame velocity, results from the marked temperature dependence of the reaction rate as expressed by the Arrhenius equation. The increase in flame temperature, which is especially marked when passing from air to oxygen mixtures, leads to an increase in the rate of the chemical processes in the combustion zone and also to an increase in the

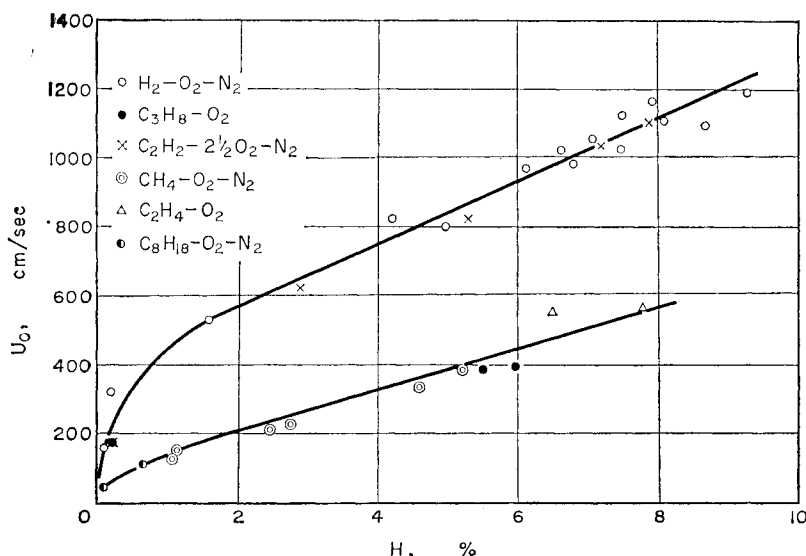


FIG. 188. Normal rate of combustion of various mixtures as a function of the equilibrium concentration of hydrogen atoms in the burnt-gas zone (according to Gaydon and Wolfhard [658]).

equilibrium concentrations of free atoms and radicals in the burnt gas.⁽³⁴⁾ In the opinion of some authors (Bartholomé, Pease and others) this increase in the rate of reaction (flame velocity) is greatly dependent on the diffusion of these active centres into the combustion zone, and in this respect hydrogen atoms should be the most efficient as their rate of diffusion is greatest.

In the opinion of these authors, an indication of the accuracy of this concept is given by the experimental dependence of flame velocity on the equilibrium concentration of H atoms, as shown by the increase in flame velocity parallel with H atom concentration. An example of such a dependence is given by the data for various mixtures shown in Fig. 188 (see Gaydon and Wolfhard [658, p. 93]).

Similarity of Temperature and Concentration Fields

We have already shown that the frequently observed sharp dependence of the velocity u_0 of flame propagation on combustion temperature T_c is evidence that the rate of the chemical reaction in the combustion zone is the main factor determining u_0 . Accordingly studies on flame propagation, for instance measurements of the normal rate of combustion, make it possible in principle to study chemical reactions occurring at such high temperatures as those of ordinary hot flames, 1500 to 3000°K. The application of this method starts from the functional dependence of u_0 on the rate of the chemical reaction in the combustion zone. This dependence may be established by considering the chemical processes and the transfer processes (heat transfer and diffusion) taking place together in the flame. The relevant equations are:

(1) the heat-transfer (conductivity) equation which, for the one-dimensional case and a stationary flame (assuming that there is no heat transfer by radiation or to the walls), may be written⁽³⁵⁾

$$\frac{d}{dx} \left(\lambda \frac{dT}{dx} \right) + c_p \rho u \frac{dT}{dx} + Qw = 0 \quad (43.5)$$

or, since

$$\rho u = \rho_0 u_0, \quad (43.4)$$

$$\frac{d}{dx} \left(\lambda \frac{dT}{dx} \right) + \rho_0 u_0 c_p \frac{dT}{dx} + Qw = 0, \quad (43.6)$$

⁽³⁴⁾ The concentration of atoms and radicals in the burnt gas is also dependent to a large extent on the pressure of the gas, and increase in pressure leads to a lowering of the degree of dissociation. Thus, Conway, Smith, Liddell and Grosse [497], as we have noted earlier, obtained a cyanogen–oxygen flame (using a stoichiometric mixture in a chamber filled with argon) at a pressure of 6.8 atm and a calculated temperature of 5050°. Such a high flame temperature is evidence that dissociation of the combustion products is considerably reduced.

⁽³⁵⁾ See, for example, Frank-Kamenetskii [278].

where λ is the coefficient of thermal conductivity, c_p is the specific heat of the gas at constant pressure, ρ is the density of the gas in the flame zone (at a temperature T), ρ_0 is the density of the unburnt gas (at the initial temperature T_0), u_0 is the normal flame velocity (the velocity of the flame relative to the unburnt gas), Qw is the rate of heat liberation by the reaction (w is the rate of reaction in unit volume of the combustion zone, Q is the heat of reaction);

(2) the diffusion equations which, when thermal diffusion, i.e. diffusion resulting from a temperature gradient, is neglected, may be written

$$\frac{d}{dx} \left(\frac{D_i}{kT} \frac{dp_i}{dx} \right) + \frac{d}{dx} \left(\frac{up_i}{kT} \right) - w_i = 0, \quad (43.7)$$

where p_i is the partial pressure, D_i is the diffusion coefficient and w_i is the rate of chemical conversion of the i th substance;

(3) the kinetic equations of the reaction, which express the rate of conversion of the various substances as a function of concentration and temperature, and are determined by the chemical reaction mechanism.

For a constant overall pressure, $p = \rho RT/M = \rho_0 RT_0/M_0$. Moreover, if we may consider M , the mean molecular weight of the gas in the flame, as not very different from M_0 , the mean molecular weight of the initial mixture, then

$$\rho T = \rho_0 T_0 \quad \text{and} \quad u T_0 = u_0 T. \quad (43.8)$$

In this case, by simple rearrangement the diffusion equations (43.7) may be written more conveniently as

$$\frac{d}{dx} \left(D_i \rho \frac{d(n_i/\rho)}{dx} \right) + \rho_0 u_0 \frac{d(n_i/\rho)}{dx} - w_i = 0, \quad (43.9)$$

where $n_i = \rho_i/kT$ is the concentration of the i th substance, expressed as the number of molecules per cm^3 .

When this substance is an initial substance or a reaction product the corresponding w_i clearly represents the rate w of the overall reaction. Moreover, if the following conditions hold:

$$-dn_{\text{initial}}/dt = dn_{\text{product}}/dt = w \quad \text{and} \quad dn_{\text{intermediate}}/dt = 0,$$

(which are characteristic of a steady reaction occurring under the same conditions, see p. 24), we have a linear relation between (n_{initial}) the concentration of initial substances and (n_{product}) the concentration of reaction products, like that between ($n_{\text{intermediate}}$) the concentration of any one of the intermediate substances and (n_{initial}) or (n_{product}). In this case, if the diffusion coefficients of the various substances are similar and may be taken as equal to a mean value D , all the diffusion equations reduce to *one equation* for one initial substance or one reaction product.

Considering such a case and ignoring for the present the analytical expression of the w_t functions, i.e. considering a problem irrespective of any definite chemical reaction, we note one important feature of equations (43.6) and (43.9). It was first shown by Lewis and von Elbe [876] for the ozone-decomposition flame and by Zel'dovich and Frank-Kamenetskii [89, 90] for the general case, that under certain conditions these equations may be written in the same form. For this (after Zel'dovich and Frank-Kamenetskii) we replace the temperature T by the dimensionless variable

$$\theta = (T - T_0) / T_c - T_0$$

(T_0 is the initial temperature of the gas mixture and T_c the maximum flame temperature which is equal to the temperature of the burnt gases) and replace n/ρ by the dimensionless quantity

$$\alpha = \frac{n/\rho - n_0/\rho_0}{n_c/\rho_c - n_0/\rho_0} = \frac{n^{(0)} - n_0}{n_c^{(0)} - n_0}$$

(n_0 is the original concentration of initial substance or reaction product at T_0 , n_c is the final concentration at T_c , $n_c^{(0)}$ is the final concentration at T_0 , where $n_c^{(0)} = n_c T_c / T_0$, and n is the concentration at T , $n^{(0)} = nT / T_0$). Also we assume that c_p is constant and equal to the mean specific heat over the temperature range T_c to T_0 .⁽³⁶⁾ We may then write equations (43.6) and (43.9) as

$$\frac{d}{dx} \left(\lambda \frac{d\theta}{dx} \right) + u_0 \rho_0 c_p \frac{d\theta}{dx} + \frac{Q_w}{T_c - T_0} = 0 \quad (43.10)$$

and

$$\frac{d}{dx} \left(D c_p \frac{d\alpha}{dx} \right) + u_0 \rho_0 c_p \frac{d\alpha}{dx} - \frac{\rho_0 c_p w}{n_c^{(0)} - n_0} = 0. \quad (43.11)$$

It is not difficult to see that the last term in (43.10) is equal to the last term in (43.11). Actually, the relationship obtained by equating these terms

$$(-n_c^{(0)} + n_0)Q = c_p \rho_0 (T_c - T_0) \quad (43.12)$$

expresses the fact that the heat liberated by the reaction is completely consumed in the heating-up of the gas. Moreover, since in this case the

⁽³⁶⁾ The problem is also soluble when the specific heat is variable. In this case, however, instead of the temperature we must use the heat content

$$H = \int_0^T c_p dT.$$

See Semenov [233] and Zel'dovich [82].

mass of the molecules which diffuse according to (43.9), i.e. the mass of the molecules of the initial substances or reaction products, may be considered as close to the mean mass of the heat-conducting molecules, the diffusion coefficient term may be equated to the coefficient of thermal conductivity:

$$D\rho c_p = \lambda. \quad (43.13)$$

In this case the heat transfer equation (43.10) and the diffusion equation (43.11) are identifiable.

It follows from the fact that these equations are identical that the temperature field, i.e. the temperature considered as a function of the x -coordinate, $T = T(x)$, and the concentration field, $n = n(x)$, are identical or similar. According to the foregoing, this similarity holds good for initial substances and reaction products, and also for intermediate substances in so far as their concentrations may be expressed in terms of the concentration of initial substances or reaction products. As equations (43.6) and (43.9) are identifiable, $\theta = \alpha$, i.e.

$$(T - T_0)/(T_c - T_0) = (n^{(0)} - n_0)/(n_c^{(0)} - n_0), \quad (43.14)$$

which may be considered as the *condition for similarity* of temperature and concentration fields. In this way by solving the heat-transfer equation for $T(x)$ we automatically obtain the concentration $n^{(0)}$ at any point in the flame zone. In other words, when the condition for similarity holds, the problem reduces to solving *one* equation (the heat-transfer equation or the identical diffusion equation) instead of a system of two or more equations.

It is not difficult to see that, on the basis of (43.12) and (43.8), equation (43.14) may be rewritten

$$(Qn + \rho c_p T)/\rho = (Qn_0 + \rho_0 c_p T_0)/\rho_0,$$

or

$$(Qn + \rho c_p T)V = (Qn_0 + \rho_0 c_p T_0)V_0 = \text{constant} \quad (43.15)$$

(V and V_0 are the specific volumes of the gas). Hence the sum of the chemical (QnV) and thermal ($\rho_0 c_p TV$) energies of unit mass of a gas is constant. The postulate expressed by (43.15) that the sum of thermal and chemical energies of a gas is constant in any layer between the initial mixture and the burnt gas was proposed by Lewis and von Elbe [876] and used by them as a basis for their theory of flame propagation in the decomposition of ozone (see below, pp. 706-8). This postulate is equivalent to the postulate that the temperature and concentration fields are similar, and should hold to the same extent as the condition for similarity of the fields holds.

In this case, because ignition of the fresh mixture mainly results from heat transfer to the unburnt gas from the combustion zone, flame propagation here is often called *thermal propagation*.

First Theories of the Thermal Propagation of Flames

In the first theories of thermal propagation of flames one of the main parameters governing the normal rate is the ignition temperature T_i . Taking as a basis the heat-transfer equation (43.6) and dividing the flame zone into two parts—the preheating zone stretching from $x = +\infty$ to $x = 0$ (Fig. 189) and the combustion zone together with the adjacent

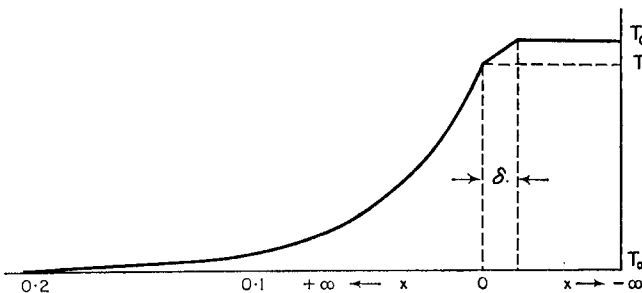


FIG. 189. Preheating zone ($\infty > x \geq 0$), the combustion zone ($0 \geq x \geq -\delta$) and the burnt-gas zone ($-\delta \geq x > -\infty$).

burnt-gas zone, stretching from $x = 0$ to $x = -\infty$ —we have in the first zone $w = 0$, and consequently

$$\frac{d}{dx} \left(\lambda \frac{dT}{dx} \right) + u_0 \rho_0 \bar{c}_p \frac{dT}{dx} = 0. \quad (43.16)$$

By solving this equation with the boundary conditions $dT/dx = 0$ and $T = T_0$ when $x = +\infty$ and $T = T_i$ when $x = 0$, we obtain

$$\lambda dT/dx = -u_0 \rho_0 \bar{c}_p (T - T_0) \quad (43.17)$$

and

$$T = T_0 + (T_i - T_0) \exp(-u_0 \rho_0 \bar{c}_p x / \lambda). \quad (43.18)$$

It follows from (43.18) that the temperature rises exponentially in the preheating zone. Considering the temperature gradient in the combustion zone to be approximately constant (which is equivalent to assuming that the reaction rate w is constant) and introducing δ as the effective width of the combustion zone⁽³⁷⁾ (see Fig. 189), we have

$$-(dT/dx)_{x=0} = (T_c - T_i)/\delta.$$

Substituting this quantity in (43.17) we find

$$u_0 = (\bar{\lambda}/\rho_0 \bar{c}_p)(1/\delta)(T_c - T_i)/(T_i - T_0). \quad (43.19)$$

⁽³⁷⁾ The conception of the width of the flame zone was first introduced by Mikhelson [192].

This expression is close to the formula

$$u_0 = (\lambda/c)[(T_c - T_i)/(T_i - T_0)]f(T_c, T_i),$$

which was obtained by Mallard and Le Chatelier [906] (1883) from ideas similar to those from which formula (43.19) is deduced.⁽³⁸⁾

Mallard and Le Chatelier's work was the first attempt to construct a thermal theory of flame propagation. The thermal theory has been developed since in the direction of increasing the preciseness of Mallard and Le Chatelier's ideas by allowing formally for the rate of the chemical reaction.

By introducing the reaction rate w explicitly in the formula (43.19) for the normal rate of combustion we may throw it into a somewhat different form. Thus, assuming that diffusion plays only a subordinate role in supplying fresh gas to the combustion zone, the condition that the flow of gas be continuous may be expressed by the equation:

$$u_0 n_0 = \bar{w} \delta \quad (43.20)$$

(n_0 is the original concentration of one of the initial substances, \bar{w} is the mean rate of reaction). Hence for the effective width of the combustion zone we find $\delta = u_0 n_0 / \bar{w}$; substituting this in formula (43.19) we have

$$u_0 = \sqrt{\left[\frac{\bar{\lambda}}{\bar{c}_p \rho_0 n_0} \frac{T_c - T_i}{T_i - T_0} \bar{w} \right]}. \quad (43.21)$$

Formulae of this type (or close to this type) have been obtained by Jouguet (1913), Crussard (1914), Nusselt (1915), Daniell (1930) and others.

An important deficiency in all these formulae is that they contain the ignition temperature T_i as having the significance of a physical constant, which it does not have in reality.

It is not difficult to see that the quantity T_i in the formula for u_0 in no way corresponds to the self-ignition temperature as measured under normal (static) conditions. This is especially clear from the fact that according to the data of many authors the normal rate of combustion of hydrocarbons is relatively independent of the hydrocarbons' individual properties which do, however, have a considerable effect on the self-ignition temperature. Thus, Bartholomé and Sachsse [349] have shown that changes in the octane number⁽³⁹⁾ of the fuel within a very wide range (from 0 for normal heptane $n\text{-C}_7\text{H}_{16}$ to 102 for tryptane) scarcely affect u_0 .

⁽³⁸⁾ Even earlier (1875) a similar expression was obtained by Mallard [904]. Mallard and Le Chatelier's $\lambda(T_c - T_i)$ is the heat flow from the combustion zone to the preheating zone; c is the mean specific heat of 1 cm³ of the gas (in the temperature range $T_c - T_0$). Consequently $f = 1/\delta$.

⁽³⁹⁾ The octane number characterizes the capacity of a fuel-air mixture for ignition when heated to 500 to 600°C by adiabatic compression, and is defined as the percentage content of iso-octane $iso\text{-C}_8\text{H}_{18}$ (octane number 100) in a mixture with normal heptane (octane number 0), the mixture having the same antiknock characteristics as the given fuel.

According to Bartholomé and Sachsse the normal rate of combustion is also practically independent of the various active additives which have a considerable effect on the self-ignition of fuel mixtures. It follows from this that the mechanisms of self-ignition and of ignition from the flame front are different. Moreover, it follows from Bartholomé's data [347] on combustion of a rich methane-oxygen mixture (63 per cent CH_4 + 37 per cent O_2) that the normal rate of combustion is relatively little affected by preheating the gas mixture. Thus, preheating the mixture by 1000° increases u_0 from 30 to 80 cm/sec, i.e. less than three-fold. Bartholomé concludes from this that the processes occurring in the mixture below 1000°C do not have a decisive effect on the normal rate.

The non-correspondence of the self-ignition temperature and T_i is also evident from the following considerations. The self-ignition temperature corresponds to an induction period rarely less than some tenths of a second in the case of air mixtures at a pressure of 1 atm.⁽⁴⁰⁾ The time of preheating fresh gas in flames is short (owing to the high rate of flame propagation) and consequently the induction period measured by this time should be some powers of ten less than the τ_{ind} obtained under static conditions. Using the relationship

$$\tau_{\text{ind}} \sim \exp(E/RT_i) \quad (43.22)$$

which has a satisfactory experimental basis and relates the induction period and ignition temperature, we may estimate the change in ignition temperature for a known change in induction period. Thus, for $E/T_i = 20$ ($E = 20,000$ cal, $T_i = 1000^\circ\text{K}$) it follows from (43.22) that a hundredfold decrease in the induction period corresponds to a twofold increase in the ignition temperature.

It follows from this calculation (which is in complete agreement with experiment) that the ignition temperature corresponding to the boundary between the preheating and combustion zones is much greater than that obtained from static measurements. Therefore the ignition temperature in (43.18) and (43.21) must be considered only as a parameter, i.e. as a pre-determined quantity having a purely descriptive significance.⁽⁴¹⁾

⁽⁴⁰⁾ For example, according to the measurements of Prettre [1042], the ignition temperatures of a carbon monoxide-air mixture (CO content 32.4 per cent, 658 to 675°C), correspond to induction periods in the range 4 to 0.5 sec.

⁽⁴¹⁾ Zel'dovich and Semenov [87] attempted to use (43.22) to estimate the ignition temperature in flame conditions. By introducing the reaction time τ , defined as $\tau = \delta/u_0$, we may write on the basis of (43.20)

$$\tau = \delta/u_0 = n_0/\bar{w}, \quad (43.23)$$

or $\bar{w} = n_0/\tau$. Substituting this quantity in (43.21) we obtain

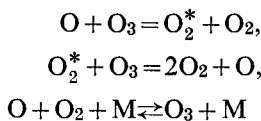
$$u_0 = \sqrt{\left[\frac{\lambda}{c_p \rho_0 \tau} \frac{T_c - T_i}{T_i - T_0} \right]}. \quad (43.24)$$

continued on page 706

In the subsequent development of the thermal theory of flame propagation the ignition temperature is either completely excluded from the discussion or is used as a subsidiary factor not appearing in the final formulae. A great step forward in the theory of flame propagation was the introduction of data from chemical kinetics by replacing the mean reaction rate (or a similar quantity) with a quantity which is a definite function of the concentration and temperature variables.

Theory of Lewis and von Elbe

The first step in this direction was made by Lewis and von Elbe [876] (1934) by solving approximately the problem of flame propagation for the explosive decomposition of ozone. On the basis of the reaction mechanism



and assuming that under flame conditions ozone and atomic oxygen are in equilibrium, Lewis and von Elbe obtain for the reaction rate

$$w = -d(\text{O}_3)/dt = 2k(\text{O})(\text{O}_3)$$

(k is the rate constant of the first of the above processes) and the formula

$$w = 2k_0 K \frac{[(\text{O}_2)_c T_c - (\text{O}_2)T]^2 (\text{O}_2)}{T^2 [K + (\text{O}_2)]^2} \exp(-E/RT),$$

by assuming the equilibrium $\text{O} + \text{O}_2 \rightleftharpoons \text{O}_3$ and using the obvious equality

$$(\text{O}) + (\text{O}_2) + (\text{O}_3) = (T_c/T)(\text{O}_2)_c.$$

Here K is the equilibrium constant $(\text{O})(\text{O}_2)/(\text{O}_3)$, and the subscript c refers to the burnt-gas zone (the maximum temperature). The possibility of representing the reaction rate as a function of temperature and concentration of *only one* substance (for example, of molecular oxygen as above), which is based on the assumption that atomic oxygen is in equilibrium

continued from page 705

Taking the quantity τ as the induction period τ_{ind} , Zel'dovich and Semenov used (43.22) to obtain the following expression for the ignition temperature T_i corresponding to the maximum flame velocity assuming that $T_0^2 \ll T_c^2 \ll (E/R)^2$:

$$T_i = T_c - RT_c^2/E. \quad (43.25)$$

It follows from this expression that when $(E/R)^2 \gg T_c^2$ the quantity T_i should be close to T_c , the maximum temperature of the flame (also see below, p. 715).

Calculation of T_i from the more accurate formula $\tau = \delta/\bar{u}$, where \bar{u} is the velocity of the gas at the temperature $T = \frac{1}{2}(T_c + T_i)$, gives values practically identical with those calculated from formula (43.25).

concentration, reduces the problem to solving a system of two simultaneous equations—the heat-transfer equation and the diffusion equation for this substance. To overcome difficulties in the solution, Lewis and von Elbe introduce the postulate mentioned earlier that the sum of thermal and chemical energies per unit mass of the gas is constant; this reduces the problem to the integration of only one equation. As a result it is possible to calculate $T = T(x)$ and, accordingly, (O_2) , (O) and (O_3) as a function of the distance x , and also $w = w(x)$ and $w = w(T)$.

The normal rate of flame propagation in ozone is determined by the formula

$$u_0 = 2 \sqrt{\left[\frac{D}{3(O_3)_0(T_c - T_0)} \int_{T_0}^{T_c} w dT \right]}.$$

Substituting $w = w(T)$ we may find by graphical integration the values of u_0 corresponding to known experimental conditions (initial temperature, composition of the ozone–oxygen mixture). The values calculated by Lewis and von Elbe [876] and by Frank-Kamenetskii⁽⁴²⁾ are compared with the experimental values of u_0 measured by Lewis and von Elbe [875] in Table 59. The last two columns of the table contain values of u_0 calculated by von

TABLE 59

Calculated and measured rates of flame propagation in the explosive decomposition of ozone (in cm/sec)

P , mm Hg	$(O_2)_0/(O_3)_0$	T_0 , °K	T_c , °K	u_0 , cm/sec			
				Measured	Calculated		
					Lewis and von Elbe	Frank-Kamenetskii	von Kármán and Penner
624	3.054	300	1239	55	253	145	84
2560	3.054	427	1343	158	451	258	—
595	1.016	302	1922	160	333	257	—
3760	1.016	468	2044	747	664	513	225

Kármán and Penner [816] for a reaction mechanism different from that assumed by Lewis and von Elbe (p. 706), namely a mechanism based on the hypothesis that the concentration of O atoms in the flame front is stationary, the rates of processes $O_3 + M = O + O_2 + M$ and $O + O_3 = 2O_2$

⁽⁴²⁾ The foregoing formula which was obtained by Frank-Kamenetskii [277] is somewhat different from the analogous formula obtained by Lewis and von Elbe from less precise calculations.

being equal. The figure in the penultimate column of Table 59 was calculated by von Kármán and Penner from the thermal theory, i.e. the theory based on the assumption that the sum of thermal and chemical energies of the gas is constant; this according to the calculations of these authors, gives the upper limit of the rate of flame propagation. The figures in the last column of the table were obtained from more precise calculations, not limited by the condition that the sum of the thermal and chemical energies of the gas in the flame front should be constant. It is seen from Table 59 that the results of these calculations give the best agreement with the experimental data; this should clearly be attributed to the greater precision of the calculations and the closer correspondence of the assumed reaction mechanism with the true mechanism.⁽⁴³⁾ We should note that the maximum concentration of oxygen atoms calculated by von Kármán and Penner for temperatures near T_c is 10^5 times greater than the equilibrium concentration.

The theory of Lewis and von Elbe was only the first attempt to replace the formal ideas of previous thermal theories of flame propagation by definite physical concepts based on contemporary chemical reaction kinetics. The decomposition of ozone with its simple kinetics was chosen to test the theory; for this particular reaction it was shown that in principle a new kinetic approach to the problem of flame propagation is possible. Subsequent development of flame-propagation theory has shown the great efficiency and fruitfulness of this kinetic approach in combustion theory.

Theory of Zel'dovich and Frank-Kamenetskii [90, 84, 233]

The basis of this theory is the idea that the combustion reaction mainly takes place at a temperature close to the maximum combustion temperature T_c . This idea is based on the high temperature coefficient of most combustion reactions and the short time the particles (molecules, atoms, radicals) are in the flame zone due to its small width. By expressing the temperature dependence of the reaction rate by the Arrhenius equation

$$w = w_0 \exp(-E/RT),$$

which is correct for a more or less wide temperature range, we obtain for a large number of combustion reactions values of E (the effective activation energy) which are usually between 20 and 80 kcal.⁽⁴⁴⁾ Taking $E = 50$ kcal,

⁽⁴³⁾ In the opinion of Frank-Kamenetskii [277], the unsatisfactory agreement of calculated and measured values of the normal rate results from the fact that the thermal theory holds only when there is a strong temperature dependence of the reaction rate, i.e. for sufficiently high activation energies, which is not so in this case ($E = 6000$ cal).

⁽⁴⁴⁾ Effective activation energies of combustion reactions have recently been determined by Fenn and Calcote [605] for a large number of organic substances. These values lie in the range 20 to 30 kcal.

the mean of this range, we find from the Arrhenius equation that when the temperature is lowered from 2000 to 1500°K the rate of reaction decreases by about 60 times, from 1500 to 1000°K by 5000 times and from 1000 to 500°K by 10¹¹ times.

To estimate the time the particles are in the flame we shall calculate the mean time τ_0 that the particles take to pass through the preheating zone.⁽⁴⁵⁾ We shall take as the zone width the distance $\Delta x = \delta_0$ in which there is a decrease by a factor e in the heating-up from the maximum value of $T_i - T_0$ for the preheating zone. On the basis of formula (43.18) the zone width δ_0 defined in this way is

$$\delta_0 = \bar{\lambda} / \bar{c}_p \rho_0 u_0. \quad (43.26)$$

Substituting $\lambda = D \bar{c}_p \bar{\rho}$, we find that since $D \sim T^{3/2}$ and $\rho \sim T^{-1}$

$$\delta_0 = (D_0 / u_0) \sqrt{(T / T_0)}, \quad (43.27)$$

where D_0 is the diffusion coefficient at the temperature T_0 and T is the mean temperature of the zone. For particles with molecular weight about 20 the diffusion coefficient D_0 is 0.1 to 0.2 cm²/sec at atmospheric pressure. Taking $u_0 = 100$ cm/sec and $T/T_0 = 3$ to 10 we find that δ_0 is 10⁻³ to 10⁻² cm. The time spent in the zone of width δ_0 is

$$\tau_0 = \delta / \bar{u}, \quad (43.28)$$

where \bar{u} is the mean velocity of the gas, related to the normal rate of combustion by $\bar{u} \bar{\rho} = u_0 \rho_0$ or $\bar{u} = u_0 \bar{T} / T_0$. Substituting this in (43.27) we obtain from (43.28)

$$\tau_0 = (D_0 / u_0^2) \sqrt{(T_0 / \bar{T})}. \quad (43.29)$$

Hence when $D_0 = 0.1$ to 0.2 cm²/sec, $u_0 = 100$ cm/sec and $\bar{T} / T_0 = 3$ to 10, the time τ_0 is of the order 10⁻⁵ sec.⁽⁴⁶⁾

We shall show that the time (τ) the particles are in the combustion zone must be less than this figure. In fact by using the same process as that for τ_0 above to estimate τ , we find for the width of the combustion zone (using formula (43.19))

$$\delta = \frac{\bar{\lambda}}{\bar{c}_p \rho_0 u_0} \frac{T_c - T_i}{T_i - T_0},$$

or, considering (43.26),

$$\delta = \delta_0 (T_c - T_i) / (T_i - T_0). \quad (43.30)$$

⁽⁴⁵⁾ As we shall see below, the time the particles are in the combustion zone is less than τ_0 .

⁽⁴⁶⁾ In the flame 9.7 per cent CH₄ + air, with a velocity of the order 10 cm/sec, Dixon-Lewis and Wilson's measurements [543] give $\tau_0 = 10^{-3}$ sec, which is in good agreement with formula (43.29).

Substituting $T_c - T_i$, which is of the order RT_c^2/E according to Zel'dovich and Semenov's calculations (see p. 706), in this formula we find, since $T_c \gg T_0$, the width of the combustion zone is

$$\delta = \delta_0 RT_c/E. \quad (43.31)$$

Estimating $E = 50,000$ cal (as above) and $T_c = 2500^\circ\text{K}$ we obtain $\delta = 0.1\delta_0$. Moreover expressing the time τ by the formula

$$\tau = \delta/u, \quad (43.32)$$

which is similar to (43.29), and assuming $u \simeq \bar{u}$, we find

$$\tau = (\delta/\delta_0)\tau_0,$$

i.e. it is approximately ten times smaller than τ_0 . Therefore the time the particles spend in the flame may be considered as close to the order of magnitude of the time τ_0 as calculated above.

Let us compare this time with the reaction time τ_{reaction} which we may obtain from the expression

$$\tau_{\text{reaction}} = 1/kn,$$

where k is the reaction rate constant of the chain carrier and n is the concentration of one of the initial substances reacting with it. Writing k in the usual form

$$k = k_0 \exp(-E/RT) = 5 \times 10^{-10} \exp(-E/RT) \text{ cm}^3/\text{molecule sec},$$

and taking the concentration n to be 2×10^{18} molecules/cm³, we find

$$\tau_{\text{reaction}} = 10^{-9} \exp(-E/RT).$$

Substituting in this $E = 50,000$ cal at $T = 1000^\circ\text{K}$, we find $\tau_{\text{reaction}} = 100$ sec, i.e. it is much longer than τ_0 , the time the particles spend in the pre-heating zone (when $E = 30,000$ cal and $T = 1000^\circ\text{K}$, $\tau_{\text{reaction}} = 10^{-2}$ sec); a τ_{reaction} commensurate with the time τ is only obtained when $T \approx 2700^\circ\text{K}$. In this way the foregoing calculation supports the basic assumption of Zel'dovich and Frank-Kamenetskii's theory that the combustion reaction takes place at a temperature close to T_c .

This assumption is also accordant with certain experimental facts. Bartholomé [348] calculated, from the temperature dependence of the induction period of ignition in a $\text{CH}_4 + 2\text{O}_2 + 8\text{N}_2$ mixture, the rate of increase in temperature due to reaction $(dT/dt)_{\text{chem}}$, and compared this with the rate due to heat transfer $(dT/dt)_{\text{heat}}$. He found that up to a temperature of 2100°K , which is close to the maximum combustion temperature (2228°K) of this mixture, $(dT/dt)_{\text{chem}}$ is greater than $(dT/dt)_{\text{heat}}$ and only when $T > 2100^\circ\text{K}$ is the position reversed. Consequently, combustion mainly takes place in the temperature region $T > 2100^\circ$, i.e. when $T_c - T$ (the temperature in the combustion zone) $\ll T_c$.

This result is also supported by data of Dixon-Lewis and Wilson [543] who determined the rate of heat liberation as a function of distance from the front of a methane-air flame burning at atmospheric pressure; they found that the liberation of heat, which indicates that an exothermic reaction is in process, becomes appreciable only at a temperature of about 1200°K and rapidly increases as it approaches the maximum flame temperature of 2150°K.

Investigations of the *structure of the flame front* have been considerably advanced in recent years as a result of development of methods of so-called *flat flames*, which are obtained when gas mixtures are passed through a matrix containing a large number of fine holes.⁽⁴⁷⁾ By using a

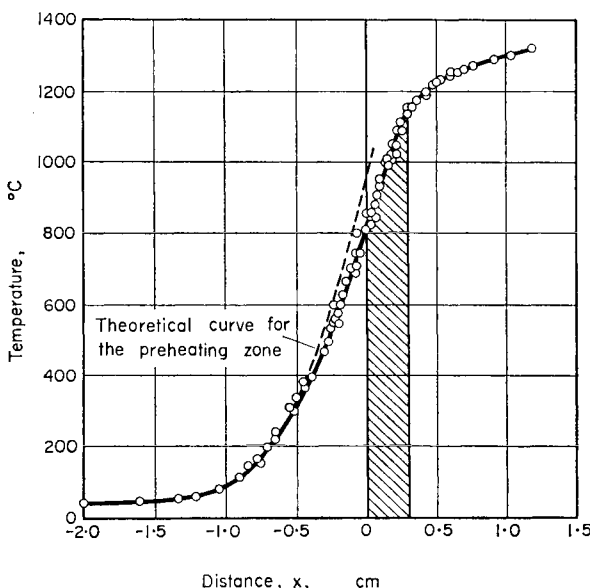


FIG. 190. Temperature of the propane-air flame measured using a platinum-platinum-rhodium thermocouple (with a ceramic coating) at different distances (x , cm) from the start of the luminous zone (according to Friedman and Burke [637]).

flat flame at low pressure (some tens of millimetres of mercury) or with mixture compositions close to those corresponding to the concentration limits, a combustion zone is obtained which is sufficiently wide (a few millimetres and wider) for reliable measurements to be carried out on the concentration distribution of the individual components of the gas mixture, and on the temperature distribution, as characteristics of the structure of the flame front. As an illustration Fig. 190 shows Friedman and Burke's

⁽⁴⁷⁾ This matrix is usually a porous bronze disc.

direct measurements [637] of the temperature of a weak propane-air flame burning at a pressure of 45 mm Hg at different distances from the luminous zone (the hatched region in Fig. 190). Using numerical differentiation of the $T(x)$ curve Friedman and Burke calculated the first two terms of the heat-transfer equation (43.5) for various x , and thus found values of the heat-liberation function Q_w for the corresponding values of x , i.e. the distribution of the rate of the chemical reaction in the flame front. A heat-liberation curve obtained in this way is shown in Fig. 191. It can be seen from this figure that the reaction rate has a sharp maximum for the luminous zone of the flame front at the section corresponding to a temperature of 1100°C , which is only 230° from the maximum temperature of this flame (the adiabatic temperature of the flame is 1332°C). See also [635].

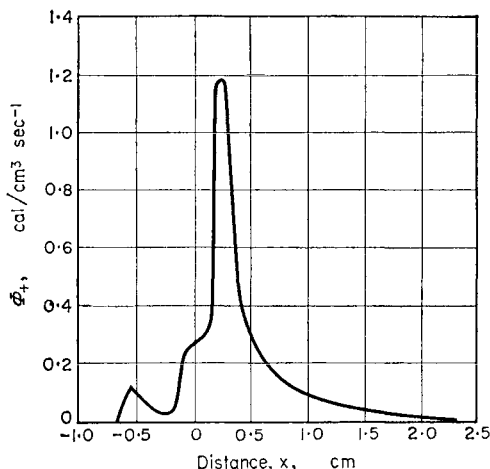


FIG. 191. Rate of heat liberation (in $\text{cal}/\text{cm}^3 \text{ sec}$) at different distances x (in cm) from the start of the luminous zone ($x = 0$) of the propane-air flame (according to Friedman and Burke [637]).

We should note that according to Fig. 191 only 55 per cent of all the energy of the reaction is liberated before the boundary of the luminous zone on the burnt-gas side (the boundary is 0.29 cm from the start of the zone). In the opinion of Friedman and Burke, this is based on the fact that propane oxidation under rarefied-flame conditions occurs in two stages: in the first stage, which is accompanied by a bright glow and is localized mainly in the luminous zone of the flame, propane C_3H_8 is oxidized to CO according to $\text{C}_3\text{H}_8 + \frac{7}{2}\text{O}_2 = 3\text{CO} + 4\text{H}_2\text{O}$ (I) and in the second stage, which corresponds to the over-all equation $3\text{CO} + \frac{3}{2}\text{O}_2 = 3\text{CO}_2$ (II), CO is oxidized to CO_2 . This conclusion is supported by the work of Friedman and Cyphers [638] who measured the distribution of various gases in the flame front. For instance, they showed that hydrocarbons are completely absent

in the gas behind the luminous zone, and the ratio of (CO) to (H₂) does not correspond to the water-gas equilibrium (see also [336]). Further support for the correctness of this conclusion is given by the following calculation: the heat liberated in stages (I) and (II) is found by calculation to be 285.6 and 203.0 kcal respectively (calculated for the indicated overall reactions); so that the proportion of heat liberated in the first stage of the reaction is equal to $(285.6 \times 100)/(285.6 + 203.0) = 58.5$ per cent, which is in close agreement with the measured value of 55 per cent.⁽⁴⁸⁾

A clear example of localization of a reaction zone in the front of a propane-air flame (as shown by a glow and an increased concentration of ions) near the maximum temperature zone is also given by Fig. 183 (p. 689).

In the theory of Zel'dovich and Frank-Kamenetskii the conditions for a combustion reaction to take place at a temperature near the maximum temperature of combustion is written as an inequality:

$$RT_c^2/E \ll T_c - T_0,$$

where E is the effective activation energy of the reaction.

When the temperature in the combustion zone is close to the maximum temperature T_c , we may consider that all the heat liberated by the reaction is lost from the combustion zone by heat transfer, i.e. we may neglect the heat consumed in the heating-up of the gas in the combustion zone. This assumption enables us to ignore the middle term in equation (43.5) and consequently to write it

$$\frac{d}{dx} \left(\lambda \frac{dT}{dx} \right) + Q_w = 0. \quad (43.33)$$

Integrating (43.33) with the boundary condition that $dT/dx = 0$ when $T = T_c$, we obtain

$$\lambda dT/dx = \sqrt{[2Q \int_T^{T_c} \lambda_w dT]}.$$

⁽⁴⁸⁾ A flame front with a complex structure, due to complex chemical kinetics, is apparently quite a frequent occurrence. For example, by measuring the temperature distribution in the front of the flat flame of methyl nitrite CH₃ONO decomposition, and simultaneously analyzing the gas in various sections of the flame, Arden and Powling [324] concluded that there are two reaction zones: a practically isothermal zone in which the methyl nitrite decomposes thermoneutrally into methyl alcohol CH₃OH, formaldehyde HCHO and nitric oxide, and an exothermic reaction zone in which the main products are CO, H₂O, H₂, NO and N₂. Considerable amounts (up to 40 per cent) of NO are reduced to elementary nitrogen in this reaction; in the opinion of Arden and Powling this is connected with the interaction of NO and the CH₃O alkoxyl radical.

Another example of a flame with two separate reaction zones is given by a mixture of hydrogen with nitrous oxide N₂O and nitric oxide NO, which has been studied spectroscopically by Wolfhard and Parker [1313]. In this case the two reaction zones are connected with the fact that the reactions H₂ + N₂O and H₂ + NO occur in different temperature ranges. See also [966, 715].

Now equating the amount of chemical energy liberated per second with the heat flowing into the unburnt mixture,

$$u_0 n_0 Q = \lambda_i (dT/dx)_i$$

(n_0 is the concentration of fuel in the fresh mixture, and the subscript i refers to the boundary between the combustion zone and the preheating zone), we obtain for the normal rate of combustion:

$$u_0 = \sqrt{[(2/Qn_0^2) \int_{T_i}^{T_c} \lambda w dT]} \quad (43.34)$$

The reaction rate is markedly temperature-dependent and therefore we may replace the lower integration limit T_i by 0 without committing a large error. Thus (43.34) may be rewritten

$$u_0 = \sqrt{[(2/Qn_0^2) \int_0^{T_c} \lambda w dT]} \quad (43.35)$$

For convenience in integration, however, we shall start from (43.34).

Taking w_0 in the expression for the reaction rate

$$w = w_0 \exp(-E/RT)$$

to be constant (this corresponds to a reaction of order zero) and replacing the coefficient of thermal conductivity λ by its mean value over the temperature range $T_c - T_i$, we isolate the temperature-dependent part of the integral in (43.34) as

$$I = \int_{T_i}^{T_c} \exp(-E/RT) dT$$

Moreover, introducing the new variable $\theta = T_c - T \ll T_c$ and integrating, we obtain approximately

$$\begin{aligned} I &= \exp(-E/RT_c) \int_0^{\theta_i} \exp(-\theta E/RT_c^2) d\theta \\ &= (RT_c^2/E) \exp(-E/RT_c) [1 - \exp(-\theta_i E/RT_c^2)] \end{aligned}$$

where $\theta_i = T_c - T_i$.

In the theory of Zel'dovich and Frank-Kamenetskii θ_i is taken as equal to RT_c^2/E and is, therefore, the characteristic "temperature range" for the combustion zone, i.e. it is the temperature difference which corresponds to an e-fold decrease in the rate of reaction. This definition of θ_i yields for the ignition temperature

$$T_i = T_c - RT_c^2/E, \quad (43.36)$$

which gives the correct order of magnitude for the drop in temperature in the combustion zone.

When $\exp(-\theta_i E/RT_c^2)$ is sufficiently small, we obtain for the integral I :⁽⁴⁹⁾

$$I = (RT_c^2/E) \exp(-E/RT_c).$$

Substituting this in formula (43.34) we find

$$u_0 = \sqrt{[(2\bar{\lambda}/Qn_0^2)(RT_c^2/E)w_0 \exp(-E/RT_c)]}. \quad (43.37)$$

Comparing (43.37) and (43.21) and noting that $Qn_0 = c_p \rho_0 (T_c - T_0)$ or, considering the assumption made in deducing (43.37) that the heating of the gas in the combustion zone is negligibly small (see p. 713), that

$$Qn_0 = c_p \rho_0 (T_i - T_0),$$

then if we take $w = w_0 \exp(-E/RT_c)$ we obtain $T_i = T_c - 2RT_c^2/E$. As we have seen, the error in calculating the normal flame velocity from (43.34), and consequently from (43.21), is about 7 per cent in this case.

As $w_0 = \text{const.}$, formula (43.37) refers to a reaction of order zero. If, however, the reaction rate depends on the concentration of one of the reacting substances then it is not difficult to obtain an expression for the normal rate of combustion in this case also provided the condition for similarity of temperature and concentration fields is fulfilled. Thus, for reactions of first and second order, with reaction rates

$$w = k_0 n \exp(-E/RT) \quad \text{and} \quad w = k_0 n^2 \exp(-E/RT)$$

respectively, the theory of Zel'dovich and Frank-Kamenetskii gives the formulae:⁽⁵⁰⁾

$$u_0 = \sqrt{[(2\bar{\lambda}c_p k_0 / \rho_0 L^2)(T_0/T_c)(RT_c^2/E)^2 \exp(-E/RT_c)]} \quad (43.38)$$

and

$$u_0 = \sqrt{[4\bar{\lambda}c_p^2 k_0 n_0 / \rho_0 L^3](T_0/T_c)^2 (RT_c^2/E)^3 \exp(-E/RT_c)]}. \quad (43.39)$$

⁽⁴⁹⁾ Here the error in calculating the flame velocity u_0 (43.34) is 20 per cent when $\theta_i = RT_c^2/E$, 7 per cent when $\theta_i = 2RT_c^2/E$ and 2.5 per cent when $\theta_i = 3RT_c^2/E$.

⁽⁵⁰⁾ See [233]. In these formulae the quantity L represents the heat of combustion of 1 g of the initial mixture (this includes any inert gas in the mixture).

The theory of Zel'dovich and Frank-Kamenetskii has been developed ([87], [233], [82]) to cover the case where the reaction involves a change in the number of molecules, and also the case where the coefficient of thermal conductivity is not equal to the diffusion coefficient term, i.e. when (43.13) does not hold. In these cases we obtain

$$u_0 = \sqrt{[(2\lambda_e c_p k_0 / \rho_0 L^2)(T_0 / T_c)(A/B)(N_0 / N_c)(RT_c^2 / E)^2 \exp(-E/RT_c)]} \quad (43.40)$$

for the unimolecular reaction and

$$u_0 = \sqrt{[(2\lambda_e k_0 n_0 / \rho_0 L^3)(T_0 / T_c)^2(A/B)^2(N_0 / N_c)^2(RT_c^2 / E)^3 \exp(-E/RT_c)]} \quad (43.41)$$

for the bimolecular reaction, instead of formulae (43.38) and (43.39). Here $A/B = \lambda c_p / D\rho$ and N_0 / N_c is the ratio of the number of molecules in the initial mixture and in the reaction products. Moreover, Semenov [233] has shown that in bimolecular reactions the formulae are only applicable when $RT_c/E \leq 0.1$. In the case of unimolecular reactions there is no similar restriction in practice.

Zel'dovich and Frank-Kamenetskii's theory has been repeatedly tested by experiment. One of the first attempts to test the theory was made by Belyaev [26, 27] in the case of nitroglycol $C_2H_4(ONO_2)_2$ combustion.⁽⁵¹⁾ Still earlier this author had shown [25] (see p. 673) that all volatile explosives burn in the gas phase, i.e. that their combustion is preceded by evaporation (see also [1102]): consequently the theory is also applicable to the combustion of liquid and solid explosives. It is known from experiment [17] that the mass rate of nitroglycol combustion, i.e. the quantity $v_M = \rho_0 u_0$, is proportional to the external pressure and hence the normal flame velocity u_0 does not depend on pressure. Moreover, according to formulae (43.40) and (43.41), u_0 is inversely proportional to $p^{1/2}$ in unimolecular reactions and does not depend on pressure in bimolecular reactions (since $p^{1/2} \rho_0 \sim n_0 \sim q$) and it may therefore be concluded that, as u_0 is pressure independent, the combustion of nitroglycol is a second-order reaction.

Apin [26, 27] has shown, however, that the decomposition of nitroglycol vapour at low temperatures follows the law

$$w = k_0 n \exp(-35,000/RT),$$

i.e. the reaction is first-order.

According to Belyaev this contradiction is resolved by the fact that Apin's result is not directly applicable to the combustion of nitroglycol, since at high temperatures the reaction rate is so high that the loss of the active centres entering into the reaction is not made up by the activation process; the latter becomes in this way the limiting process. Consequently

⁽⁵¹⁾ The term "combustion" here refers to any chemical reaction (in this case, a decomposition reaction) accompanied by a flame.

the kinetic law of the reaction, which is unimolecular at low temperatures, becomes bimolecular at high temperatures.⁽⁵²⁾ This law may be written in the form [233]

$$w = k_0 n \sum n_i \exp(-E/RT_c)$$

(n is the number of molecules of nitroglycol and $\sum n_i$ is the total number of molecules in 1 cm³ of the combustion zone) or, since

$$p = n_0 k T_0 = \sum n_i k T_c,$$

$$w = k_0 n_0 (T_0/T_c) n \exp(-E/RT).$$

Therefore we must replace k_0 in (43.40) by $k_0 n_0 T_0/T_c$; assuming $A = B$, this gives

$$u_0 = \sqrt{[(2\lambda_c c_{p,c} k_0 n_0 / \rho_0 L^2) (T_0/T_c)^2 (N_0/N_c) (RT_c^2/E)^2 \exp(-E/RT_c)]}. \quad (43.42)$$

Since $\rho_0 = M n_0 / N_A$ (where M is the molecular weight of nitroglycol), it follows from this formula that the normal rate of combustion does not depend on pressure; this is in agreement with experiment.

According to Apin's analysis, the products of low-temperature decomposition of nitroglycol C₂H₄(ONO₂)₂ and consequently the products of the inner-cone combustion (i.e. not involving external air), which determines the flame velocity, are NO, CO, H₂O, CO₂ and H₂. We may therefore conclude that two parallel reactions occur in the nitroglycol flame:



and



Belyaev has calculated the heat of reaction L ($= 460$ cal/g) and the maximum flame temperature T_c ($= 1650^\circ\text{K}$ when $T_0 = 293^\circ\text{K}$) from analysis of the composition of the products, using heat capacities from tables. Moreover, from the stoichiometric equations of the reactions $N_0/N_c = 1/6$. Belyaev used these data and also $E = 35,000$ cal, and obtained for the mass rate of nitroglycol combustion from Zel'dovich and Frank-Kamenetskii's formula a value close to the measured value of

$$v_M = 4.5 \times 10^{-2} \text{ g/cm}^3 \text{ sec}$$

(the corresponding value of u_0 is 7 cm/sec) [233].

In independent experiments Belyaev measured the mass rates of nitroglycol combustion for different initial temperatures in the range 20 to 200°C. By calculating the maximum combustion temperature T_c for each

⁽⁵²⁾ The possibility of transition from first to second order at high temperatures due to a more rapid increase with temperature of the probability of unimolecular decomposition compared with the probability of molecular activation has recently been surveyed by Shuler [1136].

of these temperatures (the corresponding values of T_c are between 1650 and 1870°K), Belyaev found from the temperature dependence of the combustion rate an effective activation energy of $E_{eff} = 36,000$ to $37,000$ cal, i.e. a figure practically identical with that of 35,000 cal obtained by Apin for quite different reaction conditions.

In the subsequent years different authors have made numerous attempts to explain experimental flame-propagation data on the basis of the theory of Zel'dovich and Frank-Kamenetskii. The advantage of this particular thermal theory of flame propagation is that it allows us to represent u_0 by a simple formula of type (43.40) or (43.41) relating the rate of flame propagation to the rate of the chemical combustion reaction. Examination of the results of using formulae of this type to calculate rates of flame propagation in various types of reaction shows that in most cases the calculated and measured values of u_0 are in satisfactory qualitative, and frequently quantitative, agreement. An important difficulty in testing experimentally Zel'dovich and Frank-Kamenetskii's theory and the thermal theory in its general form is the inadequacy of our knowledge regarding the kinetics and mechanism of chemical combustion reactions. This has led to the formulation of a kinetic approach as helpful in the development of combustion theory.

Theoretical studies of flame propagation, for instance those of Hirschfelder and coworkers,⁽⁵³⁾ von Kármán, Spalding and others, show that the thermal theory and likewise the so-called diffusion theory of flame propagation (see below) are of a limited applicability which is determined by the postulates on which these theories are based. These studies show that the most consistent approach in the development of combustion theory should be based on solving the system of the diffusion and heat-transfer equations without being restricted to the condition for similarity of temperature and concentration fields, or the condition that the concentrations of intermediate substances be stationary, although in certain particular cases these conditions, which greatly simplify the calculations, may be used successfully.

Further Development in the Theory of Flame Propagation

The characteristic features of recent developments in flame-propagation theory can be shown most clearly by considering data on individual flames. We shall take as an example the flame of the explosive decomposition of hydrazine N_2H_4 . Murray and Hall [962] attempted to calculate the normal rate of this flame using the theory of Zel'dovich and Frank-Kamenetskii and the kinetics of the reaction. According to the measurements of Szwarc [1199], for the temperature range 620 to 780°C and a

⁽⁵³⁾ In these investigations electronic computers were used for the first time to solve flame-propagation problems.

pressure of a few millimetres of mercury, the decomposition of hydrazine vapour obeys a unimolecular law with a rate constant

$$k = 4 \times 10^{12} \exp(-60,000/RT) \text{ sec}^{-1}.$$

Assuming that the limiting reaction stage in the combustion zone is the unimolecular process



and calculating the normal flame velocity from Zel'dovich and Frank-Kamenetskii's formula for a unimolecular reaction

$$u_0 = \sqrt{\left[\frac{2\lambda_c k_0}{\rho_0 L(T_c - T_0)} \left(\frac{RT_c^2}{E} \right)^2 \exp(-E/RT_c) \right]},$$

Murray and Hall find $u_0 = 111 \text{ cm/sec}$, instead of the measured value of 200 cm/sec , for $T_0 = 423^\circ\text{K}$, $T_c = 1930^\circ\text{K}$ and the density of the hydrazine vapour $\rho_0 = 9.25 \times 10^{-4} \text{ g/cm}^3$ (ρ_0 is calculated as the density of an ideal gas). Allowing for the imprecise value of λ_c (which they found as $0.0067 \text{ cal/cm degree sec}$) and also for the fact that the rate constant used was found for much lower pressures and temperatures (see above) than those at which the normal flame velocity was measured, Murray and Hall reckon that the agreement between their calculated value and the measured value of u_0 is quite good.

By using the more precise formula (43.40), which differs from the above formula of Zel'dovich and Frank-Kamenetskii by a factor

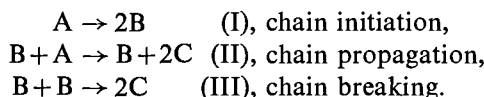
$$(T_0 A N_0 / T_c B N_c)^{1/2},$$

however, we obtain worse agreement with experiment. For, according to Murray and Hall's measurements, the decomposition of hydrazine in the flame follows the over-all equation $2\text{N}_2\text{H}_4 = 2\text{NH}_3 + \text{N}_2 + \text{H}_2$ and therefore we have $N_0/N_c = \frac{1}{2}$. If $A = B$ then we find for the factor by which Murray and Hall's figure of 111 cm/sec must be multiplied $\sqrt{[1/2 \cdot 423/1930]} = \frac{1}{3}$ and consequently $u_0 = 37 \text{ cm/sec}$ (instead of the measured value of 200 cm/sec).

Hirschfelder and coworkers [768] and von Kármán and Penner [816] have also obtained values close to this figure (28 to 40 cm/sec compared with 37 cm/sec), by solving the problem of flame propagation in hydrazine vapour without introducing the restriction, imposed by the condition characteristic of thermal theory, that the temperature and concentration fields of N_2H_4 be similar. Von Kármán and Penner attribute the disagreement between the calculated and measured values of the rate of flame propagation in hydrazine to the fact that in this case the kinetics of the overall reaction do not correspond to a simple process of unimolecular decomposition of the hydrazine molecule (see also [696]).

In order to test the accuracy of the assumption, basic in the foregoing calculations, that the limiting stage of the explosive decomposition of hydrazine is $\text{N}_2\text{H}_4 = 2\text{NH}_2$, Adams and Stocks [311] studied the effect of pressure and temperature on the rate of propagation of explosion in mixtures of hydrazine vapour and H_2O . Experiments at various pressures in effect supported the unimolecular reaction law, but the activation energy calculated from the temperature dependence of the explosion propagation rate was much less than the value of 60,000 cal corresponding to the process $\text{N}_2\text{H}_4 = 2\text{NH}_2$. Adams and Stocks suggest that hydrazine decomposition follows a chain mechanism in which H atoms and N_2H_3 radicals play an important part.

An attempt to allow for the (simple) chain character of the mechanism of such reactions as the decomposition of hydrazine was made by Spalding [1162] on the basis of the simplified scheme:



Here A is the initial substance (in the case of hydrazine decomposition, N_2H_4), B is an active intermediate (NH_2 or H) and C is the reaction product (N_2 , H_2 or NH_3). If the concentrations of A and B are n_A and n_B and the rate constants of processes (I), (II) and (III) are

$$k_1 = Z_1 \exp(-E_1/RT), \quad k_2 = Z_2 \exp(-E_2/RT)$$

and

$$k_3 = Z_3 (E_3 = 0)$$

respectively, we obtain the kinetic equations:

$$-\frac{dn_A}{dt} = w_A = Z_1 n_A \exp(-E_1/RT) + Z_2 n_A n_B \exp(-E_2/RT)$$

and

$$\frac{dn_B}{dt} = w_B = 2Z_1 n_A \exp(-E_1/RT) - 2Z_3 n_B^2.$$

In an investigation of whether the concentration of the active intermediate substance B is stationary, Spalding concludes that the steady-state assumption (expressed by the condition $\frac{dn_B}{dt} = w_B = 0$) may be correct only when the concentration of B radicals in the flame zone is very small due to their high recombination rate.⁽⁵⁴⁾ Reckoning that at moderate pressures the chain-breaking reaction (III) involving ternary collisions has a low rate in comparison with process (I), Spalding considers the steady-state condition $\frac{dn_B}{dt} = 0$ to be inapplicable in this case. Neglecting the second term in the expression for w_B and the first term in the expression

⁽⁵⁴⁾ Spalding also shows that the steady-state assumption regarding the concentration of the intermediate substance should lead, generally speaking, to an overestimate of the calculated rate of flame propagation.

for w_A (since the activation energy E_2 of the radical reaction (II) must be small compared with E_1), Spalding starts from the simplified kinetic equations:

$$w_A = Z_2 n_A n_B \exp(-E_2/RT)$$

and

$$w_B = 2Z_1 n_A \exp(-E_1/RT).$$

He uses these expressions for w_A and w_B in solving the three basic differential equations, the heat-transfer equation and two diffusion equations:

$$\begin{aligned} c_p \frac{\partial T}{\partial t} &= \frac{\partial}{\partial \psi} \left(\lambda \rho \frac{\partial T}{\partial \psi} \right) + \frac{Q w'_A}{\rho}, \\ \frac{\partial m_A}{\partial t} &= \frac{\partial}{\partial \psi} \left(D_A \rho^2 \frac{\partial m_A}{\partial \psi} \right) - \frac{w'_A}{\rho}, \\ \frac{\partial m_B}{\partial t} &= \frac{\partial}{\partial \psi} \left(D_B \rho^2 \frac{\partial m_B}{\partial \psi} \right) + \frac{w'_B}{\rho}. \end{aligned}$$

In these equations m_A and m_B are the numbers of grams of substances A and B in 1 gram of gas and are related to the concentrations of these substances, n_A and n_B , by

$$m_A = M_A n_A / N_A \rho \quad \text{and} \quad m_B = M_B n_B / N_A \rho$$

(M_A and M_B are the molecular weights of A and B and N_A is Avogadro's number). Also

$$w'_A = N_A w_A / M_A \quad \text{and} \quad w'_B = N_B w_B / M_B$$

and

$$\partial \psi = -\rho \partial x.$$

Assuming that the diffusion coefficients D_A and D_B are identical ($D_A = D_B = D$), replacing the specific heat c_p by its mean value, assuming in addition that $\lambda = D c_p \rho$ (here λ , D , c_p and ρ refer to the initial gas) and introducing the function

$$r \equiv (T - T_0) / (T_c - T_0) = (m_{A0} - m_A) / (m_{A0}),$$

i.e. in effect using the condition for similarity of temperature and concentration fields (43.14), Spalding reduces the three foregoing equations to two:

$$\partial r / \partial t = (\lambda_0 \rho_0 / c_p) (\partial^2 r / \partial \psi^2) + w'_A / m_{A0} \rho$$

and

$$\partial m_B / \partial t = (\lambda_0 \rho_0 / c_p) (\partial^2 m_B / \partial \psi^2) + w'_B / \rho.$$

By solving this system of equations using the method of finite differences, Spalding obtains by dimensional analysis the two following equations

for the normal rate of combustion:

$$\rho_0 u_0 = \text{const} \sqrt{[(\lambda_0 \rho_0 / c_p) \rho_0 Z_A (m_{B_{\max}} / M_B) \exp(-E_2 / RT_c)]}$$

and

$$\rho_0 u_0 = \text{const} \sqrt{[(\lambda_0 \rho_0 / c_p) Z_B (m_{A_0} / M_A) (M_B / m_{B_{\max}}) \exp(-E_1 / RT_c)]}.$$

Here $Z_A = N_A^3 Z_2 / M_A^2$ and $Z_B = 2N_A^2 Z_1 / M_B^2$. The quantity $m_{B_{\max}}$ is a characteristic concentration of radicals. Eliminating this quantity by multiplying the two foregoing equations, we find

$$u_0 = \text{const} [(\lambda_0^2 \rho_0 / c_p^2 \rho_0^2) Z_A Z_B (m_{A_0} / M_A) \exp\{-(E_1 + E_2) / RT_c\}]^{1/4}.$$

It can be seen from this expression that the effective activation energy of flame propagation, $E_{\text{eff}} = \frac{1}{4}(E_1 + E_2)$ is (since E_2 is much lower than E_1) essentially smaller than the activation energy $E_{\text{eff}} = \frac{1}{2}E_1$ obtained by assuming a single-stage reaction mechanism. This result is in qualitative agreement with the data of Adams and Stocks (see p. 720) on the hydrazine flame. Spalding also indicates the possibility of obtaining quantitative agreement. Taking $E_1 + E_2$ as equal to 73 kcal and using a graphical calculation method, he obtains for the hottest and coolest flames of hydrazine $u = 190$ cm/sec and $u_0 = 12$ cm/sec respectively, where the experimental values are 185 and 10 cm/sec. See also [715a].

We should note that Spalding also considered the general case of flame propagation for a combustion reaction proceeding by a branched-chain mechanism. In this case Spalding concludes that the flame velocity should be some ten times greater than in the case of a simple chain reaction.

The system of initial equations taken by Spalding [1162] for the simplified chain-reaction scheme was recently solved by Lovachev [171b], who obtained simple approximate formulae to determine the rate of flame propagation. These formulae show that the flame-propagation rate is pressure dependent, as is observed experimentally.

Lovachev [171c] also found solutions for non-branched chain reactions involving two active centres. Good agreement was obtained between the experimental and theoretical absolute values of the flame-propagation rates in chlorine-hydrogen flames.

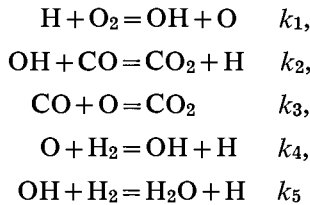
Lovachev has also obtained solutions for the rates of flame propagation in systems with degenerate branching, and for hydrogen flame taken as an example of a branched chain reaction [L. A. Lovachev, *Dokl. Akad. Nauk SSSR*, **123**, 501 (1958); **128**, 995 (1959)]. In the latter case the rate constant for the branching process $H + O_2 = OH + O$ was obtained from the measured rate of flame propagation and was in good agreement with the results of other authors.

The first calculations on flame propagation in the case of a reaction known to follow a branched-chain mechanism were carried out by

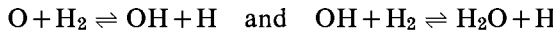
Zel'dovich and Semenov [87]; they calculated the normal rate of combustion of moist air and oxygen mixtures of carbon monoxide using the thermal theory of Zel'dovich and Frank-Kamenetskii and data on the kinetics and mechanism of CO combustion. This study was a great step forward in the use of chemical kinetics in combustion theory. Zel'dovich and Semenov found by analysing experimental data on flame propagation in CO mixtures that the rate of the carbon monoxide combustion reaction can be expressed by the formula

$$w = k_0 \exp(-25,000/RT)(H_2O)(CO).$$

On the other hand, they obtained a formula close to this on the basis of the following mechanism for the combustion of moist carbon monoxide:



(k_1 , k_2 , k_3 , k_4 , and k_5 are the rate constants of the corresponding processes) by assuming the occurrence of the equilibria



for stationary concentrations of H, O and OH, i.e. for the conditions $d(H)/dt = 0$, $d(O)/dt = 0$ and $d(OH)/dt = 0$. The theoretical formula obtained may be written in the form:

$$w = (2k_2^2/k_3 K_4 K_5)(T_0/T_c)(H_2O)_0(CO),$$

where K_4 and K_5 are the equilibrium constants

$$K_4 = k'_4/k_4 = (O)(H_2)/(OH)(H)$$

and

$$K_5 = k_5/k'_5 = (H_2O)(H)/(OH)(H_2)$$

(the primes indicate the rate constants of the reverse processes). In accordance with the assumed reaction mechanism water is not consumed in the reaction and its concentration (H_2O) in the combustion zone should be related to the initial concentration ($H_2O)_0$ thus:

$$(H_2O) = (T_0/T_c)(H_2O)_0.$$

Bearing this in mind, and comparing the theoretical and experimental formulae for the rate of reaction, we find

$$k = k_0 \exp(-25,000/RT) = 2k_2^2/(k_3 K_4 K_5). \quad (43.43)$$

It can be shown that the temperature dependence of k expressed by (43.43) does not contradict the experimentally known values of the activation energies of reactions (2) and (3) and the heats of reactions (4) and (5). Actually, according to calculations based on the measurements of Avramenko and Kolesnikova (Lorentso) [11], the activation energy of process $\text{OH} + \text{CO} = \text{CO}_2 + \text{H}$ (2) is 6 kcal. The temperature coefficient of $K_4 K_5$ is determined by the heat of the process $2\text{OH} = \text{H}_2\text{O} + \text{O}$ which is 16 kcal. Finally, the activation energy of the process $\text{CO} + \text{O} = \text{CO}_2$ (3) must be considered to be very small. We find from these data that the effective activation energy of the overall reaction satisfies

$$E \leq (2 \times 6) + 16 + 0 = 28 \text{ kcal},$$

a figure resembling the empirical value of Zel'dovich and Semenov.

Moreover it may be shown that formula (43.43) also gives the correct order of magnitude of the absolute value of k if it is assumed that the process $\text{CO} + \text{O} \rightarrow \text{CO}_2$ follows a bimolecular law.⁽⁵⁵⁾ Thus, if we assume the rate constant of this process is $10^{-3}Z$ (Z is the collision number),⁽⁵⁶⁾ and if we calculate k_2 for 2000°K from the formula

$$k_2 = 2.3 \times 10^{-13} T^{1/2} \exp(-5700/RT) \text{ cm}^3 \text{ molecule}^{-1} \text{ sec}^{-1}$$

obtained from the data of Avramenko and Kolesnikova (Lorentso) [11] (so that $k_2 = 2.4 \times 10^{-12}$) and use values from the tables for $K_4 K_5$ at 2000°K we obtain $k = 14.6 \times 10^{-22}/Z$. By equating this figure to the empirical value ($2.8 \times 10^{-3}Z$) of the effective rate constant for 2000°K obtained by Zel'dovich and Semenov, we find that the collision number $Z = 7.2 \times 10^{-11} \text{ cm}^3/\text{sec}$; the gas-kinetic value is $6 \times 10^{-10} \text{ cm}^3/\text{sec}$.

It is not difficult to find an expression for the normal rate of combustion from the reaction rate law so obtained. Considering the case where CO and O_2 are in stoichiometric proportions in the initial mixture or where there is an excess of oxygen, and using expression (43.14) for carbon monoxide with

$$n_0 = (\text{CO})_0, \quad n^{(0)} = (T/T_0)(\text{CO}) \approx T_c/T_0(\text{CO})$$

and

$$n_c^{(0)} = (T_c/T_0)(\text{CO})_c = 0$$

(55) In the mechanism of low-pressure combustion of carbon monoxide it is assumed that the formation of CO_2 from CO and O follows a termolecular law ($\text{CO} + \text{O} + \text{M} = \text{CO}_2 + \text{M}$). This law gives, however, an incorrect pressure dependence of flame velocity; this obliged Zel'dovich and Semenov to assume a bimolecular law for the usual flames. In other words, it is assumed that under these conditions the limiting stage of the process is not stabilization ($\text{CO} \cdot \text{O} + \text{M} = \text{CO}_2 + \text{M}$) but formation of the quasimolecule $\text{CO} \cdot \text{O}$ ($\text{CO} + \text{O} = \text{CO} \cdot \text{O}$).

(56) According to Wigner, the probability of a non-adiabatic process, such as $\text{CO} + \text{O} \rightarrow \text{CO}_2$, should be approximately 2000 times less than that of adiabatic processes; this accounts for the 10^{-3} factor.

(complete burn-up), we find

$$(\text{CO}) = (\text{CO})_0 (T_0/T_c) (T_c - T)/(T_c - T_0).$$

Substituting this expression in the formula for the reaction rate and integrating approximately, we obtain

$$\int_0^{T_c} w \, dT = k_0 \left(\frac{T_0}{T_c} \right)^2 \left(\frac{RT_c^2}{E} \right)^2 \frac{(\text{H}_2\text{O})_0 (\text{CO})_0}{T_c - T_0} \exp(-E/RT_c)$$

and in addition, since the concentration n_0 in (43.35) is equal to $(\text{CO})_0$ in this case, we find from this formula

$$u_0 = \sqrt{\left[\frac{2\bar{\lambda}k_0}{Q(T_c - T_0)} \left(\frac{T_0}{T_c} \right)^2 \left(\frac{RT_c^2}{E} \right) \frac{(\text{H}_2\text{O})_0}{(\text{CO})_0} \exp(-E/RT_c) \right]}. \quad (43.44)$$

A similar formula is obtained when the initial mixture contains an excess of carbon monoxide.

Formula (43.44) shows primarily that for constant water content in the fuel mixture the normal flame velocity should not depend on pressure and should be inversely proportional to $\sqrt{(\text{CO})_0}$ at constant $(\text{H}_2\text{O})_0$. Supporting this conclusion, that u_0 does not depend on pressure, Zel'dovich and Semenov cite the data of Ubbelohde and Koelliker [1235] on CO-air mixtures with constant water content. Studies in recent years clearly support this result since various authors have found that the rate of CO combustion is only weakly pressure-dependent⁽⁵⁷⁾ or is entirely independent of pressure [639]. The small increase in the normal rate with pressure of the mixture (approximately as $p^{1/4}$) observed in earlier work on CO-O₂ stoichiometric mixtures is explained, according to Zel'dovich and Semenov, by strong dissociation of the gas in these flames due to their high temperatures, up to 3000°K. (The flame temperature of mixtures with air is about 2000°K.)

Zel'dovich and Semenov used their formulae for the normal flame velocity to calculate values of u_0 for CO-air mixtures of various compositions.⁽⁵⁸⁾ The calculated values (for a constant water content of 2.3 per cent) are compared in Fig. 192 (the broken line) with experimental data obtained by various authors, represented by various types of points. It is seen from the figure that the calculated values of u_0 are quite close to the

⁽⁵⁷⁾ This dependence is expressed by a p^n proportionality where $n = 0.06$ to -0.17 (according to the data of various authors).

⁽⁵⁸⁾ In these calculations, as the rate constants of the individual processes in the mechanism of CO combustion (which are required to determine the gas composition in the flame zone) were not known with sufficient accuracy when this work was carried out, Zel'dovich and Semenov used a method in which each constant k for a given temperature was represented as the product of a mean collision number Z and a definite number N . It can be shown that the constants obtained are similar in order of magnitude to the actual values determined later.

measured values. The theoretical curve also gives accurately the position of the rate maximum occurring between 40 and 50 per cent of CO.

Barskii and Zel'dovich [22] attempted to solve the reverse problem, i.e. to obtain the kinetic law of the reaction of CO with oxygen by using data on the rate of flame propagation in mixtures of CO and O₂. For rich mixtures these authors confirmed the dependence of the reaction rate on CO and H₂O concentrations established earlier (and the fact that it is independent of O₂ concentration), but they concluded that the temperature dependence of the effective rate constant does not follow the Arrhenius equation (E_{eff} is not a constant). A similar result was also obtained by Karzhavina [102] who studied the preflame reaction of CO oxidation at high temperatures (up to 1500°C). It should be mentioned, however, that

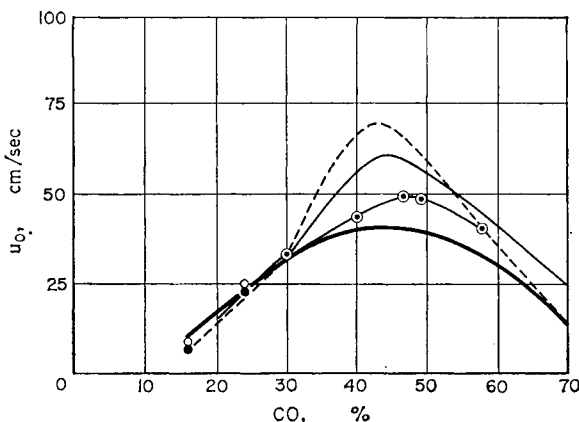


FIG. 192. Calculated and measured combustion rates of CO-air mixtures of various compositions (according to Zel'dovich and Semenov [87]).
 — calculated, $E = 25,000$; - - - calculated, $E = 35,000$ (without allowing for dissociation) — experimental, Passauer; ○ experimental, Khitrin; ● experimental, Barskii; ○ experimental, Barskii (for 2.3 per cent H₂O).

from analysing the experimental data of Barskii and Zel'dovich and Karzhavina, Rozlovskii [224] concludes that these data require correction, and consequently the conclusion that they contradict the data of Zel'dovich and Semenov is premature.

Apparently more serious grounds for doubting that the chemical mechanism assumed by Zel'dovich and for Semenov CO combustion accurately reflects the reaction kinetics are given by the experiments of Barskii and Zel'dovich on lean mixtures of CO and O₂ for which they obtained a kinetic law corresponding to $w \sim p_{\text{CO}}v/(p_{\text{H}_2\text{O}})$. This result was supported by Friedman and Cyphers [639], who measured the propagation rate of combustion in mixtures of CO, O₂, N₂ and H₂O of various

compositions (using the flat-flame method). Figure 193⁽⁵⁹⁾ shows the relation obtained by these authors between the square of the normal flame velocity and the quantity $(CO)_0(H_2O)_0^{1/2}$, for a pressure of 60 mm Hg and a constant combustion temperature $T = 2010^\circ\text{K}$ (maintained by varying the nitrogen content of the mixture). It follows from this figure that

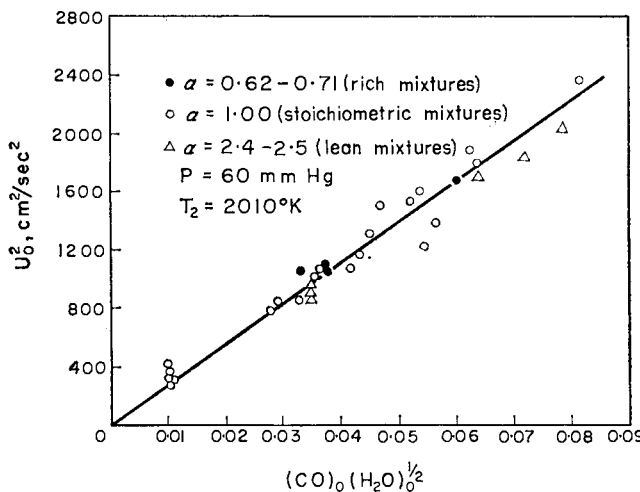


FIG. 193. Dependence of the flame velocity of carbon monoxide on CO and H₂O contents in the initial mixture (according to Friedman and Cyphers [639]).

under the conditions of Friedman and Cyphers' experiments the proportionality of the reaction rate to $(CO)_0(H_2O)_0^{1/2}$ is obeyed fairly well for both lean and rich mixtures.⁽⁶⁰⁾ It is important to note that by using all the known data from measurements of the CO flame velocity at various temperatures, Friedman and Cyphers obtain for the effective activation energy, defined as

$$E_{\text{eff}} = -[d/d(1/T_c)][u_0^2(CO)_0^{-1}(H_2O)_0^{-1/2}], \quad (43.45)$$

the value $E_{\text{eff}} = 20$ kcal for the temperature range $T_c = 1550$ to 3200°K . See, however, [604a]. See also [1270a].

It is clear from this that in order to solve finally the question of the applicability of thermal theory to carbon monoxide flames, it is necessary

⁽⁵⁹⁾ Here α characterizes the ratio CO/2O₂ in the mixture; for the stoichiometric mixture $\alpha = 1$, for a rich mixture $\alpha < 1$ and for a lean mixture $\alpha > 1$.

⁽⁶⁰⁾ The proportionality of the reaction rate to $(H_2O)_0^{1/2}$ must clearly be considered as an indication that an important role in the mechanism of CO combustion is played by chain breaking as a result of the recombination of active centres (cf. p. 588).

to develop further quantitative studies on the kinetics and mechanism of the CO combustion reaction (obtaining more precise values of the rate constants of CO and O recombination) and to make more precise measurements of the normal rate of CO combustion over a wide range of reaction conditions. It is also necessary to make a detailed analysis of the limits of applicability of the condition for similarity of temperature and concentration fields in the case of branched-chain reactions.

Diffusion Propagation of Flames

The chemical and physical processes occurring in many (for instance, air) flames are such that the accuracy of the basic assumptions of thermal theory as applied to these flames cannot be doubted; however there are flames to which this theory is known to be inapplicable. Fulfilment of the condition for similarity of temperature and concentration fields should be considered as the most general criterion for the applicability of the thermal theory of flame propagation. All the conditions formulated by various authors to determine the possibility of a thermal mechanism of flame propagation may be reduced in the final analysis to this criterion. For example, Bartholomé [347, 348, 1097] assumes that a thermal mechanism is not followed in hot flames (above 2500°K), where the high degree of dissociation results in a considerable part of the energy liberated by the reaction being in the form of chemical energy of free atoms and radicals, which diffuse from the combustion zone into the fresh mixture ahead of the heat flow; this is the main cause of flame propagation. Bartholomé starts from the fact that the rate of flame propagation in air mixtures (which burn at temperatures below 2400°K) is usually 30 to 70 cm/sec whereas the combustion rates of oxygen mixtures ($T_c = 2700^{\circ}\text{K}$) are 400 to 1200 cm/sec. At the temperature of an oxygen flame the gas is considerably dissociated, and therefore it is natural to suggest that there is a connection between u_0 and a high concentration of atoms and radicals—which are the dissociation products of the hot gas. According to Bartholomé, the basis of the mechanism of propagation of such flames is the diffusion of atoms (mainly hydrogen atoms) into the cool mixture; he suggests that the main role of the atoms consists in their recombination, which is accompanied by the liberation of large amounts of heat, in this way contributing to heat transfer from the hot to the cool gas.⁽⁶¹⁾

Bartholomé sees in the monotonic dependence of flame propagation rate on the equilibrium concentration of H atoms in the flame, which he observed in certain hot flames (oxygen flames of H_2 , C_2H_2 , C_2H_4 , CH_4 , C_3H_8 and also the $\text{H}_2\text{--C}_2\text{N}_2$ flame), an indication that flame propagation

⁽⁶¹⁾ The important role of H-atom diffusion in flame propagation is also assumed in Manson's theory [911].

of this type is connected with the diffusion of H atoms. This dependence was established earlier by Tanford and Pease [1211] for mixtures of CO, O₂, N₂ and H₂O of various compositions; these authors also showed that there is not a similar dependence of flame velocity on the concentration of O atoms and OH radicals. Critical examination of this dependence, however, shows (Gaydon and Wolfhard [658]) that, at least in the case of hydrocarbon flames, this dependence cannot be explained unambiguously as an indication of the basic role of H-atom diffusion in flame propagation. Moreover, Gaydon and Wolfhard have compared the flame velocity in oxygen mixtures of C₂H₂ and C₂H₄ of various compositions with the calculated values of H-atom concentrations in these flames, and have shown that the monotonic relation between u_0 and (H) does not occur here. Similarly Pickering and Linnett [1027] found that with gradual replacement of nitrogen by oxygen in the mixture 9% C₂H₄ + 19.1% O₂ + 71.9% N₂ the normal rate of combustion increases continuously (approaching a constant value which is established for 80 per cent O₂ in the mixture), whereas the concentration of H atoms initially increases, reaches a maximum at 25 per cent O₂ and then decreases with further increase in the percentage content of O₂. Gaydon and Wolfhard have analysed these and other results and conclude that only in the case of carbon monoxide flames and possibly hydrogen flames should it be considered established that u_0 is directly dependent on (H). That the CO flame propagation rate is directly dependent on H-atom concentration appears directly from the mechanism of CO combustion (see above, p. 723), according to which the rate of combustion is proportional to the concentration of water vapour, as Zel'dovich and Semenov's approximate calculation shows that (H) \sim (H₂O)₀.

In my opinion one of the most convincing arguments in favour of diffusion propagation of flames is given by the work of Stephens, Scott, Golden and Faunce [1179] on the hydrogen-air diffusion flame. They found that when small amounts of oxygen are added to the stream of hydrogen, a second combustion zone appears inside the main zone of the diffusion flame, apparently corresponding to the inner cone of a Bunsen flame, being a flame in premixed H₂ and O₂ (a very rich mixture). Measurements of temperature along the flame axis showed that the temperature of this "inner cone" is 150 to 160°C. These authors conclude from this that combustion in this "cone" is maintained by diffusion of active centres from the zone of the main diffusion flame.

From studies of the conditions for excitation of C₂, CH and HCO radicals in the so-called preflame glow of propane-oxygen and propane-air mixtures, Gaydon and Moore [656] also conclude that radical diffusion is important in flame propagation.

When flame propagation is mainly determined by diffusion, this alone is a sufficient indication that the condition for similarity of temperature

and concentration fields is not fulfilled.⁽⁶²⁾ The failure of this condition would be expected when the rate of diffusion of active centres is large compared with the mean rate of diffusion of particles in the flame; this occurs, for example, when the active centres are H atoms.⁽⁶³⁾ For this reason a diffusion mechanism of flame propagation is especially probable in such flames. In each individual case, however, it is necessary to consider the features of the combustion mechanism in order to decide correctly the flame-propagation mechanism.

Let us consider as an example the combustion reactions of hydrogen and carbon monoxide and the reaction of chlorine with hydrogen. The first of these follows a continuously-branched chain mechanism (see p. 593) in which the chain carriers are H atoms. As the reaction is autocatalytic in character the H-atom concentration may be markedly greater than the equilibrium concentration at the temperature of the flame and consequently diffusion of H atoms into the fresh mixture should play an important part in its ignition. It would be expected, therefore, that propagation of the hydrogen flame should possess features which are characteristic of the diffusion mechanism. This conclusion also follows from the fact that only 10 per cent of the total energy is liberated in the development stage of the branched-chain mechanism of hydrogen combustion, as is clear from the equation of the reaction



In contrast with hydrogen combustion, carbon monoxide combustion has a much less autocatalytic character, the cause of which is that the reaction goes only in the presence of water vapour, whose content in the mixture limits the concentration of active centres of the reaction, namely O and H atoms and OH radicals. For this reason the rate of reaction in the flame zone rapidly reaches a stationary value determined by temperature and by the near-equilibrium concentrations (for this temperature) of substances throughout the combustion zone, which ensures a fairly precise fulfilment of the condition for similarity of temperature and concentration fields.

In the same way, it may be concluded from the fact that in the hydrogen-chlorine flame, where the reaction follows the simple-chain mechanism of Nernst (see p. 570 *et seq.*), all the heat is liberated in the development

(62) Diffusion also plays an important part in the thermal mechanism of flame propagation, as heat transfer by thermal conduction and the diffusion propagation of the reacting substances take place in parallel, due to the similarity of the fields. Here, however, diffusion is just an attendant factor and not the cause of flame propagation as in the case of the diffusion mechanism.

(63) In flames containing appreciable concentrations of atomic or molecular hydrogen the condition for similarity of the fields is more restrictive, because here it is not always permissible to neglect thermal diffusion.

stage of the reaction in accordance with the equation



that in this case there is no basis for thinking that hydrogen-atom diffusion is important in propagation of the flame.

Diffusion Propagation of Flames under Isothermal Conditions

When the conditions for similarity of temperature and concentration fields and for stationary concentrations of intermediate substances are not fulfilled then the calculation of the normal flame velocity, even when the reaction mechanism is known, involves major difficulties connected with the need for solving adequately a complex system of differential equations. Only in the limiting case of isothermal flame propagation, due to a pure diffusion mechanism, is the problem again simplified; in its simplest form it reduces to solving one diffusion equation.⁽⁶⁴⁾ The

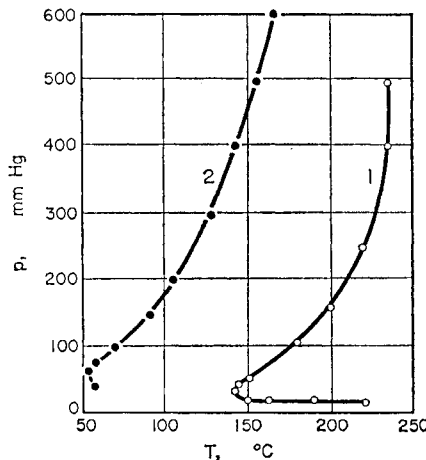


FIG. 194. (1) Self-ignition region, (2) flame-propagation region in the mixture 0.03 per cent CS_2 + 99.97 per cent air (according to Voronkov and Semenov [49]).

only case of flame propagation at a constant temperature (which is practically identical with that of the reaction-tube wall) has been observed and studied by Voronkov and Semenov [49] using a very lean mixture of carbon disulphide CS_2 and air (0.03 per cent CS_2). In this case the small amount of heat liberated by the reaction (the adiabatic self-heating of this mixture is 15°) ensures that the reaction is isothermal; all the heat liberated is supplied to the walls and the reaction goes at the wall

⁽⁶⁴⁾ Boys and Corner [432] consider the other extreme case, entirely neglecting diffusion. See, however, Corner [502].

temperature of the reaction tube. Figure 194 shows Voronkov and Semenov's measured self-ignition region (curve 1) and flame-propagation region (curve 2) for this mixture. It is apparent that under the experimental conditions of these authors the flame is propagated at temperatures of 50 to 150°C, which are about 100° below the self-ignition temperature of the mixture at the same pressures. It follows that in this case the thermal factor scarcely plays any role whatever, and the flame is propagated solely by diffusion of active centres.

The diffusion theory of flame propagation in isothermal conditions has been treated by Zel'dovich and Frank-Kamenetskii [89, 278]. At constant pressure and temperature equations (43.7) may be rewritten

$$D_i \frac{d^2 n_i}{dx^2} + u_0 \frac{dn_i}{dx} + w_i = 0. \quad (43.46)$$

Let us introduce the dimensionless concentration

$$c = (n - n_0)/(n_c - n_0)$$

(the index i will be omitted) and the dimensionless coordinate

$$\xi = x/(\tau D)^{1/2},$$

where τ is the characteristic reaction time in the rate expression

$$w = \tau^{-1} f(n) = (n_c - n_0) \tau^{-1} \varphi(c).$$

Let us also write $y = -dc/d\xi$; then equation (43.46) may be written

$$y \frac{dy}{dc} - \mu y + \varphi(c) = 0, \quad (43.47)$$

where μ is the dimensionless velocity of the flame,

$$\mu = u_0(\tau/D)^{1/2}. \quad (43.48)$$

Equation (43.47) has the boundary conditions that

$$y = 0 \text{ when } c = 0 \text{ and } c = 1,$$

corresponding to the conditions

$$\frac{dn}{dx} = 0 \text{ when } n = n_0 \text{ and } n = n_c.$$

Zel'dovich and Frank-Kamenetskii showed that one of the simplest forms of the function $\varphi(c)$ which has a simple analytical solution corresponds to second-order autocatalysis (quadratic branching of chains) accompanied by the parallel first-order reaction of consumption of the active substance (where the order of the reaction is determined with respect to the active substance). In fact, taking one of the simplest functions satisfying the above boundary conditions, namely

$$y = c(1 - c),$$

we find from (43.47)

$$\varphi(c) = 2c^2(1 - c) - (1 - \mu)c(1 - c),$$

or

$$\frac{dc}{dt} = 2\tau^{-1}c^2(1 - c) - \tau^{-1}(1 - \mu)c(1 - c). \quad (43.49)$$

Voronkov and Semenov obtain the kinetic law of the CS_2 combustion reaction corresponding to (43.49) by postulating the following reaction mechanism. They consider that development of the main reaction involves two alternating active centres, and suggest that one of these centres reacts with the initial substance, forming simultaneously a second active centre and an intermediate substance also able to give active centres in the course of further conversion. The authors suppose that these active centres are formed by the bimolecular (quadratic) interaction of molecules of the intermediate substance; the latter may also give the reaction product as well as interacting with the initial substance. It is also assumed that as the intermediate substance is of relatively low chemical activity, an appreciable amount of fuel (carbon disulphide) is changed into this substance in the first stage of the reaction, and is converted into the reaction product only in a subsequent second stage.⁽⁶⁵⁾ In this case, if the ratio of the concentration of intermediate substance to the initial CS_2 concentration is ζ , we may approximately take $\zeta = 1 - (\text{CS}_2)/(\text{CS}_2)_0 = 1 - \eta$. On the basis of the assumed reaction mechanism and the above assumptions, Voronkov and Semenov obtain the kinetic equation

$$\frac{d\zeta}{dt} = a + f\zeta^2(1 - \zeta) - g\zeta(1 - \zeta), \quad (43.50)$$

which differs from (43.49) by the presence of a term (a) independent of ζ , allowing for the rate of thermal generation of the intermediate substance.⁽⁶⁶⁾

Comparing (43.50) and (43.49) we obtain $f = 2/\tau$ and $g/f = \frac{1}{2}(1 - \mu)$, and hence

$$\mu = 1 - 2g/f,$$

or, on the basis of (43.48),

$$u_0 = (1 - 2g/f)\sqrt{(\frac{1}{2}Df)}. \quad (43.51)$$

The quantities f and g in formulae (43.50) and (43.51) are functions of pressure and temperature (for a given mixture composition). From the relation $4af = g^2$ determining the self-ignition limits (see above, p. 604), Voronkov and Semenov obtain for the dependence of f and g on the pressure p of the mixture:

$$f = Ap^2/(B + cp^2) \quad \text{and} \quad g = g_0p.$$

⁽⁶⁵⁾ The occurrence of chemical chain reactions which take place in a similar way is apparently not rare. For example, Pavlov, Semenov and Emanuel' [216] found that in the initial stage of the oxidation of hydrogen sulphide H_2S , up to 20 per cent H_2S is converted into the intermediate sulphur monoxide S_2O_2 .

⁽⁶⁶⁾ The problem of flame propagation in isothermal conditions has also been solved by Franze, Jost and Lesemann [627] for a somewhat different reaction mechanism.

Using these formulae and the equation $a = a_0 p$, the lower and upper limits (P_1 and P_2 respectively) of self-ignition may be obtained from the self-ignition condition and are approximately expressed (when $P_1 \ll P_2$) by the formulae

$$P_1 = g_0^2 B / 4a_0 A \quad \text{and} \quad P_2 = 4a_0 A / g_0^2 C.$$

Taking the rate of flame propagation as zero we obtain from (43.51) the condition $f = 2g$, determining the flame-propagation boundaries. By substituting the above values of f and g , we find from the quadratic equation so obtained that the lower and upper limits (p_1 and p_2 respectively) of flame propagation are approximately (when $p_1 \ll p_2$) $p_1 = 2g_0 B / A$ and $p_2 = A / 2g_0 C$.

Calculating the ratios of the lower and upper limits of self-ignition to those of flame propagation we obtain $P_1/p_1 = g_0/8a_0$ and $P_2/p_2 = 8a_0/g_0$; hence, as $a_0 \ll g_0$ (a low rate of thermal formation of the intermediate substance), $p_1 \ll P_1$ and $p_2 \gg P_2$, i.e. the flame-propagation region is much wider than the self-ignition region; this is in agreement with experiment (see Fig. 194).

Expressing g/f and f in terms of p_1 and p_2 , the flame propagation rate is determined by Voronkov and Semenov using the equation

$$u_0 = k\alpha^{-1/2}(1-\alpha), \quad (43.52)$$

where k is a function of temperature and mixture composition, and⁽⁶⁷⁾

$$\alpha = p_1/p - p/p_2.$$

Voronkov and Semenov found that their theoretical formulae for the flame velocity give a quantitative description of the experimental data for different temperatures, pressures, mixture compositions, reaction-tube diameters and conditions of the tube walls (glass and silvered tubes). Therefore the possibility of a pure diffusion mechanism of flame propagation should be considered as experimentally proven.

In this case the success of the theory is to a considerable extent due to the constant temperature in the combustion zone, which greatly simplifies the mathematical treatment.

Calculations of flame velocity from the kinetics of the combustion reaction are especially complicated in the case of diffusion flame propagation in non-isothermal conditions. For this reason all attempts so far to solve this problem have been rather unsatisfactory and have to some extent a

⁽⁶⁷⁾ This expression is obtained for the kinetic region of the reaction, i.e. for the case when chain breaking at the walls of the reaction tube does not depend on pressure. In Voronkov and Semenov's experiments this was the case when glass tubes were used. When silvered tubes were used the reaction went over to the diffusion region, for which the rate formula for flame propagation has the same form but with

$$\alpha = (p_1/p)^2 + p/p_2.$$

purely qualitative or formal mathematical character. One of the attempts is the diffusion theory of flame propagation developed by Tanford and Pease [1210, 1211]. We shall give below a short exposition of this theory in a form somewhat different from that expounded by the authors themselves.

The Theory of Tanford and Pease

The idea at the basis of the theory of Tanford and Pease is that there is thermodynamic equilibrium in the hot gas at the maximum combustion temperature T_c behind the flame front. Here the free atoms and radicals (the active centres of the reaction) present in equilibrium concentrations diffuse into the combustion zone, where their concentration is *greater* than their equilibrium concentration corresponding to the temperature of the appropriate part of the combustion zone. Accordingly the chemical processes in the combustion zone which involve these active centres decrease their concentration, which then approaches the equilibrium value.

On this basis we shall take the quantity w_i in the diffusion equation of a given active centre, as expressed by (43.7), as equal to

$$w_i = -n_i \sum k_j^{(i)} n_j$$

where $k_j^{(i)}$ is the rate constant for interaction of the active centre with the appropriate molecules present in the combustion zone in concentration n_j . Replacing $\sum k_j^{(i)} n_j$ multiplied by kT by a mean value constant throughout the combustion zone, we obtain $w_i = -A_i p_i$, where

$$A_i = kT \sum k_j^{(i)} n_j. \quad (68)$$

Substituting w_i in equation (43.7) we obtain

$$\frac{d}{dx} \left(\frac{D_i}{kT} \frac{dp_i}{dt} \right) + \frac{d}{dx} \left(\frac{up_i}{kT} \right) - A_i p_i = 0. \quad (43.53)$$

Moreover, assuming that the pressure $p = \rho RT/M$ and the mean molecular weight M of the gas in the combustion zone are approximately constant, it is easy to see that D_i/T and u/T are approximately constant. Actually, as $D_i \sim T^{1/2} n^{-1}$ and $p = nkT$, we obtain $D_i/T \sim T^{1/2} p^{-1}$ and consequently, owing to the relatively small change in $T^{1/2}$ in the flame zone, we may consider D_i/T as approximately constant. In the same

⁽⁶⁸⁾ The assumption that A_i is approximately constant has substance in that the chemical conversions of these particular active centres are mainly connected with their destruction. As a rule, the rate constants of these processes have a small temperature coefficient and should therefore decrease by a relatively small amount with decrease in temperature, i.e. with distance from the flame front. The concentration of substances, mainly initial substances, with which the active centres react increases with distance from the flame front, and this distribution of n_j compensates to some extent for the change in the constants $k_j^{(i)}$.

way, as $u\rho = u_0\rho_0$ and $\rho \sim p/T$ (since $M = \text{const.}$), we have $u/T \simeq \text{const.}$ In this way, allowing for the fact that D_i/T and u/T are approximately constant, we may write (43.53) in the form:

$$\frac{d^2p_i}{dx^2} + \alpha \frac{dp_i}{dx} - \beta p_i = 0, \quad (43.54)$$

where $\alpha = u/D_i$ and $\beta = kT A_i/D_i$.

By solving (43.54) with the boundary conditions $p_i = p_{ic}$ when $x = 0$ and $p_i = 0$ and $dp_i/dx = 0$ when $x = \infty$, we find

$$p_i = p_{ic} \exp(-\gamma x), \quad (43.55)$$

where

$$\begin{aligned} \gamma &= \frac{1}{2}\alpha[1 + (1 + 4\beta/\alpha^2)^{1/2}] = (u/2D_i)[1 + (1 + 4kT D_i A_i/u^2)^{1/2}] = u B_i/D_i \\ B_i &= \frac{1}{2}[1 + (1 + 4kT D_i A_i/u^2)^{1/2}]. \end{aligned}$$

It is assumed in the theory of Tanford and Pease that the temperature of the combustion zone is constant and equal to the mean value T_m , which is a definite fraction of the maximum combustion temperature T_c . Accordingly all the temperature-dependent quantities, D_i , u , ..., are taken at this mean temperature, as D_{im} , u_m , With this assumption the expression for the concentration of active centres is

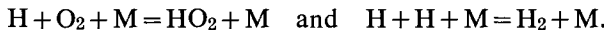
$$n_i = n_{ic} \exp[-B_i u_m x/D_{im}], \quad (43.56)$$

where

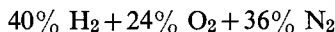
$$B_i = \frac{1}{2}[1 + (1 - 4A'_i D_{im}/u_m^2)^{1/2}], \quad A'_i = -kT A_i;$$

this differs little from the expression (43.55).

Tanford used formula (43.56) to calculate the concentration of H atoms at different points of the combustion zone of moist carbon monoxide and hydrogen, assuming that in the combustion zone, (the temperature of which, T_m , is $0.7T_c$) the H atoms in both reactions take part in the processes



The distribution of temperature in the combustion zone was calculated from the heat-transfer equation assuming that w differs from zero only when $x = 0$. It is found in Tanford's calculations that the concentration of H atoms scarcely varies within the flame zone; for a mixture containing 60 per cent CO and about 40 per cent O_2 the partial pressure of atomic hydrogen decreases from 2.4×10^{-3} to 2.1×10^{-3} atm on passing from a point of the zone at 2630°K to a point at 630°K ; for a mixture of



the partial pressure decreases from 1.32×10^{-2} to 1.07×10^{-2} atm on passing from 2390°K to 500°K . With increasing distance from the flame

front the partial pressure of the diffusing hydrogen differs increasingly from the equilibrium pressure at the temperature of the combustion zone. The results of these calculations, however, are questionable, as the assumptions made seem quite arbitrary and improbable.

It is assumed in Tanford and Pease's theory that the reaction products are formed in the combustion zone by interaction of the active centres, diffusing from the region of thermodynamic equilibrium, with molecules of the initial substances.⁽⁶⁹⁾ If c is the fuel concentration in the flame, then by considering only the interaction of active centres with fuel molecules in order to simplify the calculations, we find that the overall rate of the combustion reaction is

$$w = \sum k_i n_i c,$$

where k_i is the rate constant of the interaction of active centres of the i th sort with the fuel. The total amount of reaction product formed in the flame is clearly equal to

$$\int_0^\infty w dx.$$

In the case of complete combustion this quantity may be taken as equal to $\mu p u_0 / k T_0$, where μ is the mole fraction of fuel (when the proportion of fuel is less than stoichiometric) or oxygen (when there is insufficient O_2) in the initial mixture. Equating these expressions we find

$$\int_0^\infty \sum k_i n_i c dx = \mu p u_0 / k T_0.$$

By substituting in this $n_i = p_i / kT = (p_{ic} / kT) \exp(-\gamma x)$ and replacing the concentration c of the initial fuel by its mean value and the constants k_i , D_i and u by their values when $T = T_c$, we obtain after integration

$$\sum (k_{ic} p_{ic} c D_{ic} / T_c u_c B_i) = \mu u_0 p / T_0,$$

or, as⁽⁷⁰⁾ $D_{ic} \approx D_{i0} (T_c / T_0)^2$ and $u_c = u_0 (T_c / T_0)$,

$$u_0 = \sqrt{[\sum (k_{ic} \pi_{ic} c D_{i0} / Q B_i)]}, \quad (43.57)$$

where $\pi_{ic} = p_{ic} / p$ is the relative partial pressure of the corresponding active centre in the zone of thermodynamic equilibrium.

Tanford and Pease use formula (43.57) to calculate the rate of flame propagation in CO , O_2 , N_2 and H_2 , O_2 , N_2 mixtures assuming that in both

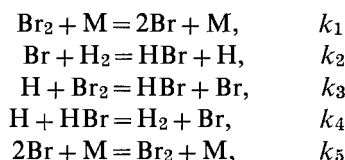
⁽⁶⁹⁾ These processes may partially coincide with the processes considered above, leading to destruction of the active centres.

⁽⁷⁰⁾ The temperature dependence of the diffusion coefficient in a non-uniform gas is apparently better represented by the formula $D \sim T^2$ than by $D \sim T^{3/2}$ [485].

cases the rate of the overall reaction is determined by reactions involving H atoms and hydroxyl (here we are considering the reaction of H atoms with oxygen and of OH with CO and H₂). The rate constants of these reactions are taken as identical ($k_H = k_{OH} = k$) and the diffusion coefficient of H equal to that of OH; the mean concentration of fuel (or oxygen) is assumed to be equal to 0.7 of the maximum concentration. The constant term for each reaction is introduced in formula (43.57). This term was obtained by extrapolating to zero (H) and (OH) concentrations the curves expressing the dependence of the experimental normal flame velocities on the concentrations of H atoms and OH, calculated for the maximum combustion temperature; finally, the value of the constant k is chosen so that the calculated values of u_0 correspond most closely to the measured values. In this way Tanford and Pease are able to calculate normal flame velocities in oxygen–nitrogen–carbon monoxide and oxygen–nitrogen–hydrogen mixtures for a wide range of mixture compositions; the mean deviation of the calculated from the measured values of u_0 is about 10 per cent. It is apparent from the foregoing, however, that in this case we may hardly talk about comparing theoretical and experimental values, owing to the large number of simplifying assumptions made and the fact that the theoretical formula contains two parameters taken directly from experiment (a constant additive term and rate constant); at best this formula should be considered as semi-empirical. Therefore all Tanford and Pease's conclusions regarding the mechanism of CO and H₂ flame propagation, based on agreement between calculated and experimental values of the normal flame velocity, should be considered as insufficiently substantiated.

Cooley and Anderson [500] made a more consistent attempt to calculate the normal rate of combustion by using a formula of type (43.57) for flames in hydrogen–bromine mixtures. Flame propagation in these mixtures was first observed by Kokochashvili [117] who noted that the condition for similarity of temperature and concentration fields did not obtain, so that the flame velocity could not be calculated on the basis of the Zel'dovich and Frank-Kamenetskii theory. As there is a large difference between the diffusion coefficients of bromine and hydrogen, it is natural to assume that in this case diffusion should play an important part in propagating the flame.

On the basis of the following reaction mechanism:



it would be expected that diffusion of both H and Br atoms would play a part in propagating the flame. After calculating the equilibrium concentrations of H and Br, their diffusion coefficients and the rate constants of their interaction with Br_2 , HBr and H_2 molecules⁽⁷¹⁾ at the maximum flame temperature, however, Cooley and Anderson conclude that, in spite of the fact that the equilibrium concentration of H atoms is much less than that of Br, the H atoms play the main role in propagating the flame.⁽⁷²⁾ According to Cooley and Anderson, this is clear from the data of Table 60. The first column of the table shows the percentage of bromine in the initial mixture, the second column the maximum flame temperature (T_c) for the different mixtures (when $T_0 = 50^\circ\text{C}$), the third column the relative partial pressures of H and Br atoms corresponding to equilibrium at T_c ,

TABLE 60

Relative efficiencies of H and Br atoms in diffusion propagation of a flame in hydrogen–bromine mixtures

Br ₂ content, %	T_c , °K	$\pi_i = (p_i/p)$		D_i , cm ² /sec		k_i , cm ³ /sec		$k_i\pi_i D_i \times 10^{15}$	
		H	Br	H	Br	H	Br	H	Br
30	1230	6.4×10^{-6}	5.8×10^{-3}	1.03	0.13	3.1×10^{-10}	1.1×10^{-15}	2.04	0.00083
40	1495	1.8×10^{-5}	1.2×10^{-2}	0.97	0.11	4.7×10^{-10}	2.1×10^{-14}	8.20	0.028
50	1660	8.4×10^{-6}	2.5×10^{-2}	0.93	0.10	5.7×10^{-10}	7.1×10^{-14}	4.45	0.177

the fourth column diffusion coefficients, the fifth column the rate constants k_i of the atom reactions, equal to the sum of k_3 and k_4 in the case of H atoms and to k_2 in the case of Br, and the last column the product $k_i\pi_i D_i$ which, according to (43.57) characterizes the degree of efficiency of the atoms in diffusion propagation of the flame.

⁽⁷¹⁾ Cooley and Anderson use the following values for the rate constants: $k_1 = 1.19 \times 10^{-11}T \exp(-45,230/RT)$ cm³/sec, $k_2 = 1.34 \times 10^{-13}T \exp(-17,700/RT)$ cm³/sec, $k_3 = 4.31 \times 10^{-13}T \exp(-1100/RT)$ cm³/sec, $k_4 = 5.12 \times 10^{-14}T \exp(-1100/RT)$ cm³/sec and $k_5 = 1.57 \times 10^{-32}$ cm³/sec.

⁽⁷²⁾ This conclusion contradicts the results of calculation on the basis of numerical integration of the heat-transfer and diffusion equations, from which it follows that in this case the flame velocity is extremely sensitive to change in the concentration of bromine atoms [480]. These calculations also show that the steady-state condition does not hold for the bromine-atom concentration. A similar conclusion follows from study of the temperature dependence of the induction period for hydrogen combustion in bromine [1029a]. It should, however, be noted that, also by calculation, Gilbert and Altman [677] come to the opposite conclusion, that the steady-state condition does hold satisfactorily. On the basis of this conclusion they assert that flame-propagation theories based on the assumption that H or Br atoms have a leading role are physically inadmissible.

The leading role of H atoms in diffusion propagation of flame in hydrogen-bromine mixtures is also seen from the following data of Cooley and Anderson. Flame-velocity measurements in mixtures of various compositions show that when $T_0 = 50^\circ\text{C}$ the maximum velocity occurs for about 40% Br_2 in the mixture. It is apparent from Table 60 that the maximum value of the product $k_{\text{H}}\pi_{\text{H}}D_{\text{H}}$ also corresponds to this bromine content, whereas the maximum product $k_{\text{Br}}\pi_{\text{Br}}D_{\text{Br}}$ occurs for 50% Br_2 . Moreover, measurements of u_0 for a mixture of the same composition but different initial temperatures (Fig. 195), and consequently for various T_c ,

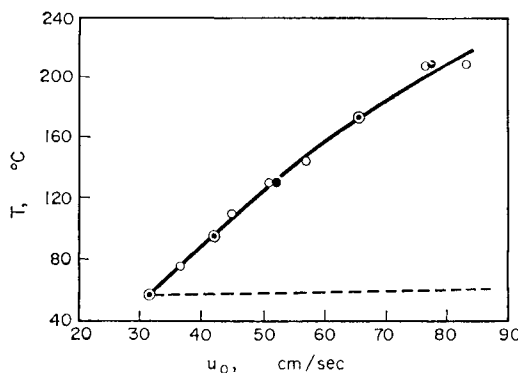


FIG. 195. Flame-propagation rate in a hydrogen-bromine mixture for various values of T_0 (according to Cooley and Anderson [500]). The points are the measured values of the normal rate of combustion; the circles are the calculated values of u_0 for $E = 1200$ cal; the broken line shows the calculated values of u_0 for $E = 17,700$ cal.

give a temperature dependence of k in (43.57) corresponding to an activation energy $E = 1200$ cal, which is practically identical with the activation energy of the processes $\text{H} + \text{Br}_2 = \text{HBr} + \text{Br}$ and $\text{H} + \text{HBr} = \text{H}_2 + \text{Br}$ ($E = 1100$ cal). If the leading role were played by bromine atoms, the temperature coefficient of k would correspond to the activation energy of the process $\text{Br} + \text{H}_2 = \text{HBr} + \text{H}$, $E = 17,700$ cal, which would give a much greater increase in u_0 with temperature (the broken line in Fig. 195) than is the case in practice. Finally, the leading role of H atoms, according to Cooley and Anderson, is also evident from the close correspondence of the calculated and measured values of u_0 shown in Fig. 195. We should note that, in contrast with the CO and H_2 cases considered above, in this case the temperature coefficient of the flame velocity is small and therefore the error arising as a result of replacing the rate constant k_{H} by its maximum value corresponding to the temperature T_c is not so large. For this reason the use of formula (43.57), which is obtained as a result of such a replacement, is better substantiated for hydrogen-bromine flames.

In the case of thermal flame propagation the temperature coefficient of the rate should correspond to an effective activation energy of about 40 kcal, as is noted by Cooley and Anderson. Actually, in this case the rate in the stationary reaction is determined by the equation

$$w = \frac{d(HBr)}{dt} = 2 \frac{k_2 k_3 (Br_2) (H_2)}{k_3 (Br_2) + k_4 (HBr)} \sqrt{\left[\frac{k_1}{k_5} (Br_2) \right]},$$

so that we find $E_{\text{eff}} = 40.3$ kcal, using the above values of the activation energies of the corresponding processes.

It is necessary to point out that such a sharp difference between the results of applying thermal and diffusion theories to the flame-propagation process is rarely encountered. In most cases the results of calculating the normal rate of flame propagation on the basis of different theories are fairly close, and it is practically impossible to decide which theory most closely represents the processes occurring in the flame. We have shown above that the rate of flame propagation in carbon monoxide-air mixtures is accurately described by the Zel'dovich and Frank-Kamenetskii theory, and according to Tanford and Pease [1211] it may also be described

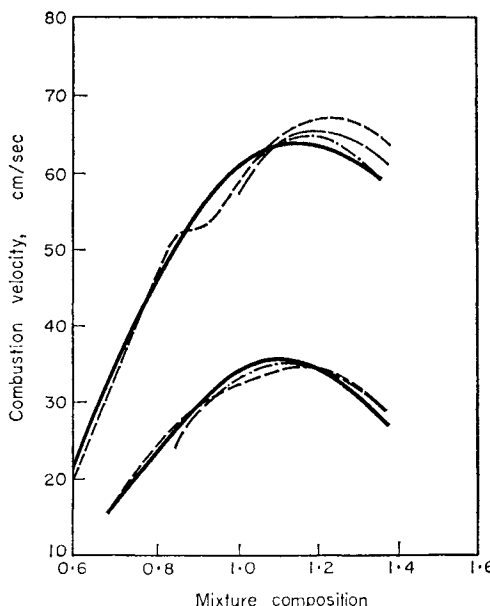


FIG. 196. Theoretical and experimental values of the normal rate of combustion of ethylene-air and pentane-air mixtures of various compositions (according to Dugger and Simon [555]). The fuel/oxygen ratio in the stoichiometric mixture is taken as unity;
 — experiment, - - - Semenov, - - - - Tanford and Pease
 - - - - Manson.

satisfactorily by their pure diffusion theory. In the same way, Dugger [554] compared the normal rates of combustion of ethylene-air and propane-air mixtures, which he measured for various initial temperatures (T_0), with those calculated according to the Zel'dovich and Frank-Kamenetskii theory and according to the Tanford and Pease theory, and found that in the first case diffusion theory gives somewhat better agreement and in the second case thermal theory; both theories give the dependence of u_0 on T_0 quite satisfactorily.

A clear illustration of the practical impossibility of preferring any theory on the basis solely of comparison of the calculated normal rate of combustion with measured values is given in Fig. 196. This figure shows measured values of the flame-propagation rates in ethylene-air and pentane-air mixtures of various compositions compared with values calculated by Dugger and Simon [555] using different theories. It is apparent from the figure that the rates of combustion calculated on the basis of the Zel'dovich and Frank-Kamenetskii theory (which Dugger and Simon call the Semenov theory), on the basis of the diffusion theory of Tanford and Pease and on the basis of the phenomenological theory of Manson [911], agree equally well with the measured values of u_0 .

It is impossible to solve unambiguously the problem of the flame-propagation mechanism in most cases, as the theoretical calculations are not sufficiently precise—frequently due to incomplete knowledge of the chemical mechanism of the reaction and the necessity for making simplifying assumptions in order to obtain a mathematical solution to the problem. Some approximate theories of flame propagation have recently been surveyed and compared by Spalding [1163a]. See also Ya. B. Zel'dovich and G. I. Barenblat, *Comb. and Flame*, 3, 61 (1959) and G. Klein, *Phil. Trans. Roy. Soc. A249*, 389 (1957).

Theory of van Tiggelen

Let us now turn to the flame-propagation theory developed by van Tiggelen [1245]. In accordance with Semenov's theory of branched-chain reactions (see p. 593), van Tiggelen assumes that the rate of a chain reaction in the flame is determined by the relationship between the probabilities of chain branching and chain breaking. According to van Tiggelen's theory, the normal rate of combustion is determined by the equation

$$u_0 = (4T_0/\pi)\sqrt{[2R(\delta - \beta)/3MT]}, \quad (43.58)$$

where δ and β are the respective probabilities of chain branching and chain breaking (for one link of the chain), M is the mean molecular weight of the active centres of the combustion reaction and T is the mean temperature of the reaction zone taken as $T = T_0 + \frac{3}{4}(T_c - T_0)$.

Assuming that, far from the ignition limits, the probability of chain breaking is small compared with that of chain branching, formula (43.58) may be written more simply

$$u_0 = (4T_0/\pi)(2R/3M)^{1/2}(\delta/T)^{1/2} = K(\delta/T)^{1/2}. \quad (43.59)$$

Van Tiggelen used formula (43.59) to calculate the rates of flame propagation in H_2 , O_2 and N_2 mixtures of various compositions. Assuming that the leading radicals in the chain are H and HO_2 , and that all processes involving these radicals are bimolecular and characterized by rate constants with identical pre-exponential factors, van Tiggelen obtains for δ :

$$\delta = \frac{(O_2)}{p} \frac{(H_2)}{p} \frac{(H_2)}{(H_2) + (O_2)} \exp\left(-\frac{17,000}{RT}\right).$$

The u_0 values calculated from this expression are on average one and a half times greater than the measured values.

Van Tiggelen also used the measured values of the rate of flame propagation in mixtures of NH_3 , O_2 and N_2 to calculate the activation energy of the branching process from (43.59), and found that in this case it is about 50 kcal. The author connects this high value of E with the fact that a flame is propagated in NH_3 -air mixtures only when the mixtures are enriched with oxygen.

Recently van Wonterghem and van Tiggelen [1246] made a similar attempt to determine the activation energy of the branching process in the acetylene combustion reaction. They assumed that δ , the probability of branching, is determined by the equation

$$\delta = f(C_2H_2, O_2) \exp(-E/RT),$$

where E is the activation energy and $f(C_2H_2, O_2)$ is a function characterizing the dependence of δ on the concentrations of C_2H_2 and O_2 . Using measurements of the combustion rate u_0 at various temperatures T , obtained by varying the composition of the mixture by dilution with nitrogen, van Wonterghem and van Tiggelen find from the slope of the $\log u_0$ vs $1/T$ graphs that $E = 30$ to 34 kcal. As the value of E obtained is close to that ($E = 30$ kcal) found from the temperature dependence of the intensity of hydroxyl radiation in acetylene flames, so, by assuming that this radiation is pure chemiluminescence, van Wonterghem and van Tiggelen conclude that hydroxyl formation in the flame is connected with the branching process.

We should add that ideas similar to those of van Tiggelen were also put forward in a qualitative form by Spalding [1162], who concluded that in branched-chain reactions the reaction rate should be determined by the rate of the branching process, because of its leading role, and that the

reaction mechanism in the simplest case should be identical with that of a simple one-stage reaction.

All the theories of normal flame propagation considered above and other modifications not treated here⁽⁷³⁾ refer to cases in which turbulence of the gas flow does not play an appreciable role. Turbulent combustion was first theoretically considered by Damköhler [520]⁽⁷⁴⁾ who also made reliable experimental studies of the effect of turbulence on a Bunsen flame for Reynolds numbers up to 17,000. We shall not consider turbulent combustion in detail, as a large number of articles has been devoted to its study; we shall just mention that, according to Damköhler [520], the acceleration of the flame observed in a turbulent gas results from two factors: (1) increase in the rate of heat transfer and gas feed in the flame front during small-scale turbulence, i.e. when the dimensions of the heterogeneities caused by the gas turbulence are small compared with the width of the front, and (2) change in the shape of the flame front during large-scale turbulence, when the dimensions of the heterogeneities are larger than the width of the front. Theoretical examination of turbulent combustion shows that the flame velocity in turbulent combustion is definitely related to the flame velocity in laminar flow; different authors have obtained different analytical expressions for this relation depending on the assumptions made [520, 303, 1128]. The expressions, however, do not give satisfactory agreement with the experimental data [815a]. This is evidence of the inadequacy of the theory of turbulent combustion.

Extremely important from the point of view of combustion reaction kinetics is the effect of gas turbulence on the occurrence of chemical processes in flames; this very important problem, however, also awaits theoretical treatment.

Among the numerous experimental studies of turbulent combustion we should mention the work of Gaydon and Wolfhard [659] who made a comparative study of the spectra of laminar and turbulent flames. They reached the conclusion that gas turbulence does not introduce substantial changes in the flame radiation or in the mechanism of the combustion reaction.

Another very important problem requiring study is that of the applicability of the Maxwell-Boltzmann distribution law, and the Arrhenius equation expressing the temperature dependence of the reaction rate, under flame conditions. This problem, which was raised by Wolfhard and

⁽⁷³⁾ A review of normal combustion theories is given in the article of Evans [582]. For later theoretical studies see [588, 1293, 1084, 636, 769, 1163].

⁽⁷⁴⁾ See also Shchelkin [303], Frank-Kamenetskii [278], Zel'dovich and Frank-Kamenetskii [88], Gaydon and Wolfhard [658], articles in *Symposium (international) on Combustion*, IV, 1953; V, 1956; VI, 1957; see also articles in *Selected Combustion Problems*, Pergamon Press, AGARD, London, 1954 and *Combustion Processes*, Princeton, 1956.

Gaydon [658] (see also Shuler [1136]), arises in connection with the idea that the high rates of chemical reactions in flames may prevent there being a Maxwell-Boltzmann distribution of energy between the gas molecules.⁽⁷⁵⁾ These authors find support for this idea in separate observations on the anomalies in the intensities of spectra and ionization in flames, finding an explanation on the basis of the hypothesis of a disturbed distribution law and also in the fact that in many cases (partly because of diffusion) the activation energy calculated from the rate of flame propagation is less than the activation energy of the slow combustion reaction. On the basis of these data Wolfhard and Gaydon conclude that in the case of fast reactions, such as those in flames, either the Arrhenius equation must not be used or the activation energy in this equation must be understood as a quantity having a different significance from the activation energy of slow reactions.⁽⁷⁶⁾ The grounds for this conclusion, however, appear to me to be very precarious, and the problem in general has not been studied sufficiently to make such far-reaching conclusions possible. The actual position corresponds rather to the reverse picture, for experimental checks of the theoretical conclusions based on the Arrhenius equation and concerning flame propagation indicate that this equation is obeyed quite strictly.

Limits of Flame Propagation

We have seen that varying the composition of the fuel mixture changes the rate of flame propagation. For a certain optimum mixture composition the combustion rate is a maximum, and decreases on both the poor and rich mixture sides. At certain limiting compositions in both poor and rich mixtures the flame is not propagated, i.e. the velocity u_0 of flame propagation in these mixtures is equal to zero. These limiting compositions, which are expressed in terms of fuel content of the mixture or the corresponding quantity α , characterize the so-called *concentration limits of flame propagation*. Experiment shows that, on passing beyond a concentration limit, flame propagation stops at a certain value of u_0 .

It is natural to connect the occurrence of flame propagation limits with the phenomenon of ignition limits by transferring the concepts of gas ignition in static conditions to ignition of the fresh mixture in the conditions of a propagating combustion front. For instance, we may seek a correspondence between the mechanism of gas ignition in a flame front and

⁽⁷⁵⁾ Still earlier, on the basis of the fact that the calculated specific heats of N_2 and O_2 during explosion of H_2 , O_2 and N_2 mixtures are rather low, Wohl and Magat [1304] concluded that the duration of the explosion is not sufficient to excite the vibrational degrees of freedom of the N_2 and O_2 molecules.

⁽⁷⁶⁾ Gaydon and Wolfhard [658] consider from this point of view that the formal mathematical theory of flame propagation developed by Bechert [366] is a great step forward. In this theory the activation energy is a parameter chosen to make the calculated flame velocity close to the measured value.

chain or thermal ignition occurring under certain conditions. According to theory (see p. 634 *et seq.*) the condition for chain ignition is that the rate of chain branching be greater than that of chain breaking. The condition for thermal ignition is that the rate of heat production be greater than that of heat removal (see p. 637 *et seq.*). It would be expected that, like chain ignition, gas ignition in flame conditions proceeding by a pure chain mechanism should be a very rare occurrence, especially if the temperature variation in the flame front is considered. It is quite natural, therefore, that a pure chain mechanism of ignition should have been observed so far only in the single case of isothermal flame propagation in very poor mixtures of carbon disulphide vapour and air (see p. 731 *et seq.*). In all other cases studied, including the cases where the diffusion mechanism of flame propagation is quite probable and diffusion of active centres into the fresh mixture (ending in chemical reactions) plays an appreciable part in igniting the gas and consequently in propagating the flame, the thermal factor plays an important part in the self-acceleration of the chemical reaction in the flame front as a result of the liberation of heat by the reaction itself and also as a result of heat supplied from the hot flame zone. In this way the ignition of fresh mixtures in a flame front and the corresponding critical phenomena of flame propagation should have points in common with thermal ignition of a gas under static conditions. For instance, removal of heat from the flame zone should play a definite role as regards the limits of flame propagation. Direct experimental indications of the accuracy of this conclusion are given by many observations of the dependence of the rate of flame propagation in tubes on tube diameter, and the existence of a certain *critical minimum diameter* below which flame propagation becomes impossible. When the tube diameter is equal to or less than the critical value, loss of heat to the walls is obviously so great that combustion cannot take place in this particular mixture.

The occurrence of concentration limits of flame propagation, which are independent of tube diameter and are also observed for combustion in the absence of walls (for example, combustion in spherical vessels with ignition at the centre), is evidence, moreover, that the heat losses are not always determined by heat elimination at the walls, and that it is necessary to consider other forms of heat removal as well (for example, the radiation of a hot gas).

The connection between flame-propagation limits and heat losses was first shown clearly by Taffanel [1205] who suggested that there is always a certain minimum chemical reaction rate necessary to maintain combustion in given conditions of heat removal. When the reaction rate becomes less than the minimum critical rate, flame propagation becomes impossible. The quantitative thermal theory of flame-propagation limits based on these ideas has been developed by Zel'dovich [77] (see also [78, 84, 240]).

It is assumed in Zel'dovich's theory that heat losses may be connected with heat removal to the walls of the tube and towards the cooled burnt gases both by thermal conduction and by radiation. In the *absence* of heat losses we have on the basis of formula (43.12)⁽⁷⁷⁾

$$q = c_p \rho_0 (T_c - T_0), \quad (43.12a)$$

where q is the amount of heat liberated when 1 cm³ of gas is burned ($q = n_0 Q$). Representing by Φ the heat losses per second for 1 cm³ of the flame zone by emission to the outer space, we find that the amount of heat lost each second by 1 cm² of the surface of the flame front is $\delta_0 \Phi$ (δ_0 is the width of the flame zone), or, by reference to (43.26), $\kappa \Phi / u'_0$ (κ , the coefficient of thermal diffusivity, equals $\lambda / c_p \rho_0$). Zel'dovich showed that the heat losses to the burnt-gas side should be equal to the losses by heat transfer to the outer space, i.e. equal to $\kappa \Phi / u'_0$. In this way, the heat balance equation when heat losses occur will have the form

$$q u'_0 = c_p \rho_0 u'_0 (T'_c - T_0) + 2 \kappa \Phi / u'_0. \quad (43.60)$$

Here T'_c is the maximum temperature of the flame when losses cannot be neglected.

By solving simultaneously (43.12a) and (43.60) we find

$$T_c - T'_c = 2 \kappa \Phi / c_p \rho_0 u'^2_0 = A / u'^2_0. \quad (43.61)$$

As would be expected, heat losses lower the maximum temperature of the flame and the decrease in T_c is the greater, the lower the flame velocity.

On the basis of the Zel'dovich and Frank-Kamenetskii thermal theory of flame propagation the temperature dependence of flame velocity may be expressed as

$$u_0 \sim \exp(-E/2RT_c),$$

and, accordingly

$$u'_0 \sim \exp(-E/2RT'_c),$$

or

$$u'_0 = u_0 \exp[-E(T_c - T'_c)/2RT_c T'_c]. \quad (43.62)$$

Substituting in this equation the difference $T_c - T'_c$ from formula (43.61) and introducing the notation

$$AE/RT_c T'_c = a u_0^2 \quad \text{and} \quad (u_0/u'_0)^2 = \xi,$$

we may rewrite (43.62)

$$\xi = \exp(a\xi). \quad (43.63)$$

⁽⁷⁷⁾ Here we assume $n_C^{(0)} = 0$ (complete combustion).

It is not difficult to see that equation (43.63) has real solutions only for definite values of the parameter α which are equal to or less than a certain critical value

$$\alpha_{\text{critical}} = 1/e.$$

At this critical value of α the quantity ξ becomes equal to e , so that the only real solution of (43.63) is obtained when $\alpha = 1/e$, i.e.

$$\xi = \exp(\xi/e).$$

It follows from the condition $\xi = e$, that

$$u'_0 = u_0 e^{-1/2}. \quad (43.64)$$

This value of u'_0 is the minimum value of the flame velocity, corresponding to the propagation limits. In accordance with experiment, therefore, the minimum value of u'_0 is not zero.

In addition, substituting $u_0/u'_0 = e^{1/2}$ in (43.62), we obtain the minimum value of T'_c corresponding to the flame-propagation limit, namely

$$T'_c = T_c / (1 + RT_c/E), \quad (43.65)$$

or, when $(RT_c/E)^2 \ll 1$,

$$T'_c = T_c - RT_c^2/E. \quad (43.65a)$$

By comparing (43.65a) with formula (43.25) obtained by Zel'dovich and Semenov, we see that the two formulae differ only in that the first contains T'_c and the second T_i .⁽⁷⁸⁾ It might be possible to explain this result by saying that flame propagation becomes impossible as soon as heat losses lower the maximum temperature T'_c of the flame below the minimum value T_i for which the mixture may be ignited in the given conditions. This explanation, however, contradicts the fact of the discontinuity in flame velocity near the limits of propagation. Thus the equality $T'_c = T_i$ obtained from (43.65) and (43.25) must be considered as a rough approximation, based on the approximate character of the formulae in the thermal theory of Zel'dovich and Frank-Kamenetskii.

The theory of Zel'dovich also gives a simple explanation of the occurrence of a critical diameter for flame propagation in fairly narrow tubes. By expressing the amount of heat lost by unit volume of gas per second as

$$\Phi = \alpha(T'_c - T_0)S/V$$

and noting that for cylindrical tubes the coefficient α of heat transfer is

⁽⁷⁸⁾ We have already noted (p. 704) that the ignition temperature T_i is a parameter here and has nothing in common with the self-ignition temperature measured in static conditions.

equal to $8\lambda/d$ (d is the tube diameter) and the surface to volume ratio $S/V = 4/d$, we may write

$$\Phi = (32\lambda/d^2)(T'_e - T_0).$$

Equating Φ to its value at the limit of flame propagation as obtained from (43.61) and using (43.65a), we find for the critical diameter

$$d_{\text{critical}} = (8\kappa/u'_0)(E/RT_0)^{1/2}. \quad (43.66)$$

The main cause of heat losses in flame propagation in tubes of small diameter is heat loss to the walls of the tube, but in tubes of large diameter heat losses by radiation become predominant. According to Zel'dovich's calculations [84] for the carbon monoxide flame, when the tube diameter is greater than 5 cm, heat losses by radiation (considering the infrared radiation of the flame) exceed those by thermal conduction. This result is in agreement with the fact that increasing the tube diameter facilitates flame propagation only up to a diameter of about 5 cm. Further support for the accuracy of Zel'dovich's conclusion regarding the connection between the limits of flame propagation and radiation⁽⁷⁹⁾ may be seen in the close correspondence between his calculated concentration limits of flame propagation and the measured values in CO-air mixtures [78]. Thus, the calculated values are 10 to 13.5 per cent for the lower limit and 81 to 87.5 per cent for the upper limit; the experimental values are 12.5 to 13.6 per cent and 70 to 85 per cent respectively.

It must be noted, however, that the theory of Zel'dovich has not been systematically checked experimentally, and comparison of the results of calculation with experimental data has been fragmentary and mostly qualitative. Thus the individual aspects of the theory require a much wider experimental basis. It is also necessary to investigate the limits of applicability of the theory in its simple form, as based on the thermal flame-propagation theory of Zel'dovich and Frank-Kamenetskii.

In the same way as thermal ignition of an explosive mixture may be prevented in two ways, either by increasing the removal of heat or by decreasing the reaction rate by varying the composition of the mixture or adding inhibitors, so also the probability of flame propagation may be lowered by increasing heat losses or by affecting the combustion reaction. In Zel'dovich's theory these two methods of influencing flame propagation are directly evident from formula (43.61), from which it follows that the maximum temperature T'_e of the flame may be lowered by increasing Φ or by decreasing u'_0 , i.e. the combustion velocity.

When considering heat losses (Φ) above, we were concerned with heat loss to the surrounding space and to the cooled burnt gas. It should be

⁽⁷⁹⁾ The connection between flame-propagation limits and radiation was apparently first indicated by Alekseev [14] for the acetylene flame.

added that, in the presence of inert dust, heat is also consumed in heating dust particles, leading to a lowering of the temperature and consequently to a retardation of the flame (see, for example, [545, 933]). When the concentration of dust in the gas is sufficient the flame cannot propagate. The retarding action of dust consists mainly of this and is widely used in practice; the possibility is not ruled out, however, that in addition to heat loss when dust is present, heterogeneous chain breaking by adsorption of active particles on the surface of dust particles also takes place [234, 544]. Such a direct effect of dust on a reaction would be expected when the dust consists of substances (metals and certain oxides) with a particularly high capacity of absorption of free atoms and radicals. Inert gases have a similar action: increase in heat consumption as a result of heating the inert gas added to the fuel mixture leads to a lowering of the flame temperature, and consequently to retardation or extinction of the flame.

In contrast with inert gases, which have a perceptible effect only when they are present in amounts which appreciably change the specific heat of the mixture, certain substances (for example, halogen derivatives in the case of hydrocarbon combustion) strongly affect the flame velocity in concentrations as low as fractions of a per cent. As such small admixtures do not appreciably change the specific heat or thermal conductivity of the mixture, it is natural to connect their action with a direct effect on the course of the reaction. Thus, in the opinion of certain authors [646, 377], the inhibiting effect of halogen derivatives in the case of methane and other hydrocarbon flames consists in decreasing the concentration of active centres (predominantly H atoms); this decrease is apparently connected with the reaction $H + RX = RH + X$ or $HX + R$, which is equivalent to a chain-breaking reaction since it results in very active H atoms being replaced by the much less active R or X. Zel'dovich [78] cites an interesting case of the effect of dilution on combustion rate: by comparing literature data on flame-propagation limits in mixtures of methane, oxygen and nitrogen, he shows that addition of excess methane to a stoichiometric methane-air mixture has a much stronger retarding effect than addition of nitrogen. Thus, 5.9 per cent CH_4 has the same effect as 32.6 per cent N_2 , i.e. the effect of methane is five times greater than the effect of nitrogen, although the specific heat of methane in the corresponding temperature range does not exceed the specific heat of nitrogen by more than a factor of two. In the opinion of Zel'dovich, the strong effect of methane is explained by the fact that it enters into endothermic reaction with combustion products, for example $CH_4 + CO_2 = 2CO + 2H_2 - 55.5 \text{ kcal}$; this leads to a more pronounced lowering of temperature than the addition of an inert diluent.

Near the flame-propagation limits, phenomena are observed which indicate that the combustion process becomes relatively unstable as the

limits are approached. These phenomena are illustrated by the dependence of the concentration limits of flame propagation in vertical tubes on the direction of propagation (the flame is propagated within a narrower concentration range from top to bottom than from bottom to top, i.e. the former is more difficult [1280]), by distortions or instability of the continuous plane front of the flame [116], and so on; the phenomena are most clearly shown in mixtures of gases which differ considerably in molecular weight. This suggests a connection between these phenomena and the difference in diffusion coefficients of the individual components of the mixture. A qualitative explanation of the phenomena at the limits has been given from this point of view by Goldmann [684], Zel'dovich [78], Jost [812] and others (see [658, pp. 34 to 37]). Layzer [865] has examined quantitatively the instability of flames near the propagation limits. See also [1163b].

§44. Detonation

In concluding this chapter we shall consider briefly the detonation propagation of a flame in gas mixtures. The occurrence of detonation in gases was discovered in 1881 by Mallard and Le Chatelier [905] and independently by Berthelot and Vieille [390]; the phenomenon is of great practical importance as it is necessary to suppress detonation in view of its destructive action. Detonation of dust-air mixtures in coal mines is a particularly striking case of this. Catastrophic explosions in mines stimulated interest in flame propagation and led to the discovery of detonation and its subsequent extensive study. Detonation of gas and dust-like mixtures in various industrial conditions belongs to the same category as detonation in an internal combustion engine, which leads to rapid deterioration and destruction of the engine. Here we shall consider detonation not from a practical point of view but only with regard to the chemistry and kinetics of combustion processes in a detonation wave.

According to current ideas, detonation occurs under the action of shock waves or as a result of the self-acceleration of a flame (when combustion propagates in tubes). Self-acceleration of a flame gives rise to a compression wave (shock wave) in which self-ignition of the mixture occurs due to the high temperature and pressure [302, 81, 80, 85]. The shock wave generated in detonation is therefore accompanied by a combustion wave; the two waves together form a *detonation wave* and are propagated in the gas with a certain velocity (the detonation velocity) which is much greater than the normal velocity of the flame and is usually 2 to 5 km/sec.

The basis of the detonation theory developed by Chapman [484], Mikhelson [192] and Jouguet [814] (see also Becker [367]) is the hydrodynamic theory of shock waves in a chemically inert gas developed earlier

by Riemann (1860), Rankine (1870) and Hugoniot (1887, 1889). On the basis of the hydrodynamic equation for continuity of a gas flow (the mass-conservation law),

$$u_0 \rho_0 = u \rho, \quad (44.1)$$

or

$$u_0/v_0 = u/v, \quad (44.1')$$

where u is the velocity, ρ is the density and v the specific volume of the gas ($v = 1/\rho$, the subscript 0 refers to the cold gas at the initial temperature T_0), and law of conservation of momentum

$$u_0^2/v_0 + p_0 = u^2/v + p \quad (44.2)$$

(p is the pressure), we find by simple rearrangements that

$$u_0 = v_0 \sqrt{\left(\frac{p - p_0}{v_0 - v}\right)} \quad \text{and} \quad u = v \sqrt{\left(\frac{p - p_0}{v_0 - v}\right)}.$$

Defining the velocity of a shock wave as the velocity of the wave front relative to the cold gas and using a prime to denote quantities referring to the gas in the wave front, we have for the rate of propagation of shock waves

$$D = u_0 = v_0 \sqrt{[(p' - p_0)/(v_0 - v')].} \quad (44.3)$$

Accordingly the velocity of the hot gas relative to the cold gas is

$$w = u_0 - u' = \sqrt{[(p' - p_0)(v_0 - v')],} \quad (44.4)$$

Note that when $p' - p_0 \ll p_0$ and $v_0 - v' \ll v_0$, then

$$(p' - p_0)/(v_0 - v') = -\Delta p/\Delta v \simeq -dp/dv,$$

and as the process is adiabatic for infinitesimal changes in p and v , we obtain

$$-\Delta p/\Delta v = \gamma p/v \quad (\gamma = c_p/c_v)$$

and, consequently

$$D = (\gamma p v)^{1/2}. \quad (44.5)$$

This formula is the well-known Laplace formula for the velocity of sound. In this way, for small changes in p and v the rate of propagation of shock waves should be close to the velocity of sound.

The state of the gas in a shock wave is determined by equations (44.1) and (44.2), which express the laws of mass and momentum conservation, and also by the law of conservation of energy

$$E_0 + \frac{1}{2} u_0^2 + p_0 v_0 = E + \frac{1}{2} u^2 + p v, \quad (44.6)$$

where E is the internal energy of unit mass of the gas. Equation (44.6) may be rewritten using (44.1) and (44.2) in the form

$$E - E_0 = \frac{1}{2}(p + p_0)(v_0 - v), \quad (44.7)$$

or, since

$$E - E_0 = \int_{T_0}^T c_v dT = \bar{c}_v(T - T_0),$$

in the form

$$\bar{c}_v(T - T_0) = \frac{1}{2}(p + p_0)(v_0 - v). \quad (44.8)$$

Equation (44.7) is called *Hugoniot's equation* and when p and p_0 and, accordingly, v and v_0 differ by little, it becomes in the limit Poisson's equation

$$dE = -p dv,$$

which corresponds to an isentropic (adiabatic) process.

Conditions in a shock wave, generally speaking, are therefore not isentropic and they become less and less isentropic the greater the difference between the pressures and specific volumes of the cold and heated gas. The reason that shock-wave processes are not isentropic lies in their irreversibility, which results from a finite rate of change of the state of the gas. One of the consequences of the processes being non-isentropic is that the gas in a shock wave is heated much more strongly than during isentropic compression. A direct cause of additional heating-up consists in the rapid compression of the gas by an outgoing stream of hot gases.

When a chemical reaction taking place in the combustion wave is accompanied by a shock wave, change in internal energy of the gas results not only from the energy of compression, $\frac{1}{2}(p + p_0)(v_0 - v)$, but also from chemical energy liberated by the reaction. If the energy liberated during conversion of 1 g of a substance is L , then in this case we obtain

$$E - E_0 = \int_{T_0}^T c_v dT = \frac{1}{2}(p + p_0)(v_0 - v) + L \quad (44.9)$$

instead of equations (44.7) and (44.8).

The velocity of a shock wave is expressed by formula (44.3), which is obtained from the general conservation laws; this formula contains only quantities which are characteristic of the initial and final states of the gas and consequently it is clearly valid also when the shock wave is accompanied by a combustion wave propagated with the same velocity. In other

words, the formula expressing the velocity of a detonation wave should be similar to formula (44.3). The difference between the two formulae is just that the final state of the gas in a shock wave is determined by p' and v' , corresponding to the temperature T' obtained from (44.8), whereas the final state (which is the state of the combustion products) of the gas in a detonation wave is determined by p_c and v_c , corresponding to the maximum temperature T (the detonation temperature) of the detonation wave obtained from (44.9). Thus the detonation velocity is determined by the equation

$$D = u_0 = v_0 \sqrt{[(p_c - p_0)/(v_0 - v_c)]}. \quad (44.10)$$

The equations (44.10) and (44.9), obtained from the laws of conservation of mass, momentum and energy, and the ideal-gas equation of state $pv = rT$ (where $r = R/M$, R is the gas constant and M the mean molecular

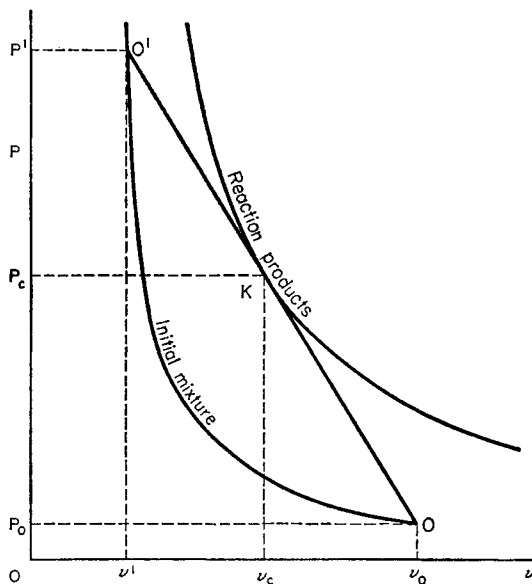


FIG. 197. Hugoniot's curves of an initial mixture and its reaction products.

weight of the mixture), are not sufficient to determine the detonation velocity D , however, as these equations contain four unknowns p_c , v_c , T_c and D . The missing fourth equation may be obtained, according to Chapman, from the condition for the minimum detonation velocity as determined by the tangent to Hugoniot's curve passing through the point p_0, v_0 (Fig. 197) corresponding to the initial state of the gas. This minimum detonation velocity corresponds, from many points of view,⁽⁸⁰⁾ to

(80) See Zel'dovich [78, §4], Jost [97, p. 194 *et seq.*, p. 226 *et seq.*] and also [553].

the only possible stationary regime (for given p_0 and v_0) of the detonation wave. By calculating from (44.9) the quantity $-dp/dv$, which is equal to the slope of the tangent to Hugoniot's curve, and using the Clapeyron equation we find

$$\tan \alpha = -\frac{dp}{dv} = \frac{(p-p_0)+\gamma(p+p_0)}{(v+v_0)-\gamma(v_0-v)}$$

($\gamma = c_p/c_v$). Equating this quantity to the slope of the indicated straight line,

$$\tan \alpha = (p-p_0)/(v_0-v),$$

we obtain after simple rearrangement (taking $p = p_c$, $v = v_c$ and $\gamma = \gamma_c$)⁽⁸¹⁾

$$(p_c-p_0)/(v_0-v_c) = \gamma_c p_c/v_c. \quad (44.11)$$

Introducing the compression $\epsilon = v_0/v_c$ and eliminating p_c and p_0 using equations $p_c v_c = r_c T_c$ and $p_0 v_0 = r_0 T_0$ ($r_c = R/M_c$, $r_0 = R/M_0$) from (44.10), (44.9) and (44.11), we may rewrite these equations

$$D = \epsilon(\gamma_c r_c T_c)^{1/2}, \quad (44.12)$$

$$\int_{T_0}^{T_c} c_v dT = L + \frac{1}{2}(\epsilon-1)(r_c T_c + r_0 T_0/\epsilon) \quad (44.13)$$

and

$$\gamma_c \epsilon^2 - (\gamma_c + 1)\epsilon + r_0 T_0/r_c T_c = 0. \quad (44.14)$$

The three unknowns D , ϵ and T_c may be calculated from these three equations. As c_p/c_v is temperature dependent, $\gamma_c = \gamma_c(T_c)$, these calculations are not simply solved as a system of three algebraic equations but by a method of successive approximation. The calculations are also complicated by the need to allow for dissociation of the combustion products, which becomes particularly important at high temperatures.⁽⁸²⁾

To illustrate this, Table 61 shows the maximum pressures and temperatures (p_c and T_c) in a detonation wave and detonation velocities for

⁽⁸¹⁾ It is seen from this relation that the required tangent to Hugoniot's curve is also a tangent to Poisson's (at p_c , v_c), whose slope is expressed by $-dp/dv = \gamma p/v$. Therefore the condition for the minimum detonation velocity is sometimes formulated as the condition that the indicated straight line touches Poisson's curve, or as the condition that Poisson's and Hugoniot's curves touch.

⁽⁸²⁾ The sharp dependence of detonation velocity on the degree of dissociation of the combustion products forms the basis of a method of determining heats of dissociation by measuring the detonation velocity. Thus, Zel'dovich [78] showed that the observed detonation velocity in mixtures of dicyanogen C_2N_2 with oxygen is only compatible with a heat of dissociation of CO greater than 210 kcal. Later Kistiakowsky and Zinman [843] found that the detonation velocities measured in acetylene-oxygen mixtures coincide with those calculated only if the heat of dissociation of CO is 256 kcal (the most precise value of the heat of dissociation of CO as obtained by various methods).

In the same way Toennies and Greene [1222] determined the heat of dissociation of nitrogen by measuring the velocity of shock waves.

various mixtures of H_2 , O_2 and N_2 calculated by Lewis and Friauf [878] from the experimental data of Dixon [542] and Payman and Walls [1014]. The table also gives the contents of hydroxyl and atomic hydrogen

TABLE 61

Detonation velocities, maximum pressure and maximum temperature and contents of hydroxyl and atomic hydrogen in the burnt gas, during detonation of mixtures of hydrogen, oxygen and nitrogen for $p_0 = 1$ atm and $T_0 = 291^\circ K$ (according to Lewis and Friauf [878])

Mixture	p_c , atm	T_c , $^\circ K$	(OH), %	(H), %	D , m/sec	
					calculated	measured
$2H_2 + O_2$	18.05	3583	25.3	6.9	2806	2819
$2H_2 + O_2 + 1O_2$	17.4	3390	28.5	1.8	2302	2314
$2H_2 + O_2 + 3O_2$	15.3	2970	13.5	0.2	1925	1922
$2H_2 + O_2 + 5O_2$	14.13	2620	6.3	0.07	1732	1700
$2H_2 + O_2 + 1N_2$	17.37	3367	14.7	3.3	2378	2407
$2H_2 + O_2 + 3N_2$	15.63	3003	5.5	0.9	2033	2055
$2H_2 + O_2 + 5N_2$	14.39	2685	2.1	0.2	1850	1822
$2H_2 + O_2 + 2H_2$	17.25	3314	5.9	6.5	3354	3273
$2H_2 + O_2 + 4H_2$	15.97	2976	1.2	3.0	3627	3527
$2H_2 + O_2 + 6H_2$	14.18	2650	0.3	1.1	3749	3532

in the burnt gas, corresponding to the equilibria $H_2O \rightleftharpoons \frac{1}{2}H_2 + OH$ and $H_2 \rightleftharpoons 2H$.

Table 61 is noteworthy for the close correspondence of the calculated and measured values of the detonation velocity: for all cases save the last three the difference between the calculated and measured values of D does not exceed 2 per cent, and is less than 1 per cent on average. This correspondence may be considered as an indication that the basic postulate of the hydrodynamic theory of detonation is accurate; this postulate is that the rate of the chemical reaction is sufficiently rapid for thermodynamic equilibrium to be established in the detonation-wave front. The last three cases are characterized by a particularly high detonation velocity, and the differences between the calculated and measured values of D are 2.5, 2.8 and 6.1 per cent. One of the probable causes of this difference as considered by Jost [97, p. 200] is an insufficiently high rate of chemical reaction, so that the reaction in the detonation wave is not completed and the actual detonation velocity is lower than that calculated assuming that the reaction goes to completion. This means that at high detonation velocities the chemical reaction becomes the limiting factor. This limiting action of a chemical reaction is shown in the occurrence of detonation limits, which confine detonation propagation of a flame within a definite range of fuel concentration in its

mixtures with air or oxygen. The slow rate of chemical reaction outside this region explains the failure of mixtures of corresponding composition to detonate.⁽⁸³⁾ As an example Fig. 198 shows the detonation limits for propane-oxygen mixtures [435]. It is seen from the figure that mixtures containing not less than 3·1 per cent and not more than 37 per cent propane are capable of detonation.

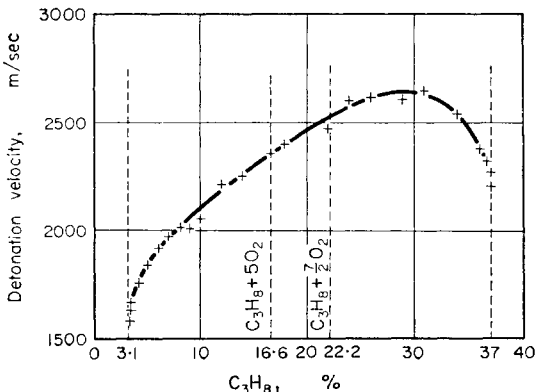


FIG. 198. Concentration limits of detonation in propane-oxygen mixtures (according to Breton [435]).

The detonation limits of oxygen-hydrogen mixtures correspond to a hydrogen content of not less than 15 per cent (lower limit) and not more than 90 per cent (upper limit). The fact that the greatest difference (6·1 per cent) between the calculated detonation velocity in oxygen-hydrogen mixtures and the measured value is observed for the 8H₂ + O₂ mixture, which is close to the limiting composition (9H₂ + O₂), is a weighty argument in favour of the accuracy of Jost's viewpoint.⁽⁸⁴⁾

⁽⁸³⁾ In the propagation of a detonation wave, heat and gas-dynamic losses are also important [85]; this is clear from the experimentally observed broadening of the concentration limits of detonation on replacing narrow by wide tubes. A particularly clear example is given by detonation in methane-air mixtures. Kogarko and coworkers [115] have studied these mixtures and established that in tubes of 305 mm diameter stationary propagation of a detonation wave is possible within the limits 6·3 to 13·5 per cent methane in the mixture, whereas in tubes of small diameter detonation of methane-air mixtures is known to be impossible.

⁽⁸⁴⁾ Jost also discusses the suggestion that the difference between calculated and measured detonation velocities may be connected with the difficulty of exchanging translational and vibrational energy during molecular collisions (see §22) and the resulting disturbance of the Maxwell-Boltzmann distribution of molecular energy. Calculations of detonation velocity, assuming that equilibrium is established when in fact this is not so, lead to differences between the calculated and measured values of *D*. Considering, however, that the calculated and measured values of *D* coincide in very many cases of rapidly-reacting mixtures, Jost concludes that there is also a quite rapid distribution of energy among the various degrees of freedom in detonation-wave conditions.

Table 61 is also noteworthy for the high values of T_c , the maximum temperature of detonation; these values are much higher than the maximum temperatures of normal combustion. Thus for a stoichiometric $2\text{H}_2 + \text{O}_2$ mixture T_c is 3583°K , whereas the maximum temperature of normal combustion in the same mixture is 3083°K , according to Gaydon and Wolfhard [658] (in this case flame-temperature measurements using the sodium-line reversal method give 2760°K). A particularly large difference between the maximum temperature in a detonation wave and the maximum flame temperature during normal combustion is observed for a $\text{C}_2\text{N}_2 + \text{O}_2$ mixture. In this case Mikhelson and Zel'dovich [78] estimate the detonation temperature to be higher than 6000°K and, according to Gaydon and Wolfhard's calculations [658], the temperature of normal combustion is 4850°K . It has already been noted (p. 753) that the cause of the stronger heating-up of the gas in the detonation wave is compression of the gas by a stream of outgoing hot gases.

In addition, it is seen from Table 61 that there is a high degree of dissociation of the gases in a detonation wave, and hence it is necessary to allow for this effect in calculating the detonation velocity, as was mentioned above (p. 755). It is apparent from the table that the difference in velocities and temperatures of detonation when oxygen is replaced by an equivalent amount of nitrogen must arise mainly from the difference in the degree of dissociation of the mixtures. The amount of water which gives hydroxyl on dissociation according to the scheme $\text{H}_2\text{O} + \frac{1}{2}\text{O}_2 \rightarrow 2\text{OH}$ (and hence $p_{\text{OH}}^2/p_{\text{H}_2\text{O}} \sim \sqrt{p_{\text{O}_2}}$) increases with increase in the oxygen content of the mixture, as is actually observed (see Table 61).⁽⁸⁵⁾ As a result of the additional absorption of energy consumed in increasing dissociation, the temperature of detonation is lowered with excess oxygen and leads to a decrease in the detonation velocity.

A similar picture is observed in the detonation of C_2N_2 , O_2 and N_2 mixtures, where the increase in velocity and temperature of detonation when oxygen is replaced by nitrogen is explained by a decrease in the degree of dissociation of oxygen taking place. Thus, according to Zel'dovich's calculations [78], the detonation velocity increases from 2135 to 2265 m/sec⁽⁸⁶⁾ and the detonation temperature from 4095 to 4395°K , on passing from a $\text{C}_2\text{N}_2 + 3\text{O}_2$ mixture to a $\text{C}_2\text{N}_2 + \text{O}_2 + 2\text{N}_2$ mixture. Dixon, who discovered the increase in detonation velocity on replacing oxygen by nitrogen, interpreted this effect as an indication that carbon monoxide is not oxidized to carbon dioxide in the detonation wave. Zel'dovich has shown that this conclusion is in error.

⁽⁸⁵⁾ The simultaneous decrease in the content of water, which gives atomic hydrogen on dissociation, follows from the relation $p_{\text{H}_2}/p_{\text{H}_2\text{O}} \sim 1/\sqrt{p_{\text{O}_2}}$ from the corresponding scheme $\text{H}_2\text{O} \rightleftharpoons 2\text{H} + \frac{1}{2}\text{O}_2$.

⁽⁸⁶⁾ The measured detonation velocities are 2110 m/sec for the first mixture (Dixon) and for the second mixture 2166 m/sec (Dixon) and 2230 m/sec (Campbell) [78].

In connection with Table 61 we should also note the relatively high maximum pressures in a detonation wave. In spite of this, however, the degree of compression of the gas in a detonation wave is not high owing to the high temperature, and is close to 2.⁽⁸⁷⁾

In considering Table 61 we have followed Jost and concluded that it is necessary to compare the detonation velocity and the chemical reaction rate in a detonation wave particularly in the case of mixtures with composition close to the limiting composition, where the insufficiently high rate of the combustion reaction becomes the limiting factor. Other authors have also indicated a connection between detonation velocity and the rate and mechanism of chemical reactions. To select just one example, Fig. 199

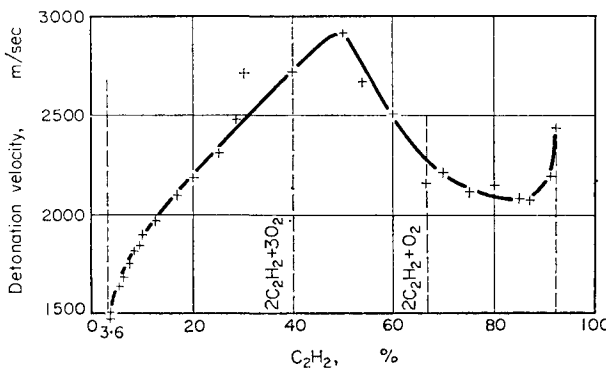


FIG. 199. Detonation velocity of acetylene–oxygen mixtures of various compositions (according to Breton [435]).

shows the dependence of the detonation velocity of acetylene–oxygen mixtures on the acetylene content of the mixture, as obtained by Breton [435]. It is seen from this figure that starting from the lower limit at 3.6 per cent C₂H₂, the detonation velocity increases, reaches a maximum at 50 per cent and then decreases, passing through a minimum at about 85 per cent C₂H₂ and sharply increasing to the upper detonation limit at about 92 to 93 per cent C₂H₂. According to Breton and Laffitte (see Jost [97, pp. 210, 211]), this unusual shape of the detonation-limit curve is based on two different chemical reactions: the combustion of acetylene which predominates at low acetylene concentrations, and the explosive cracking of acetylene, which is the main reaction at high C₂H₂ concentrations and is stimulated by acetylene combustion.

⁽⁸⁷⁾ The degree of compression may be estimated using the formula

$$\epsilon = v_0/v_c = p_c M_c T_0 / p_0 M_0 T_c,$$

where M_0 and M_c are the mean molecular weights of the gas in the initial mixture and combustion products respectively. For a stoichiometric mixture $M_0 = 12$ and $M_c \approx 18$ and hence $\epsilon = 2.2$ (as $p_c = 18.05$ atm, $p_0 = 1$ atm, $T_c = 3583^\circ\text{K}$ and $T_0 = 291^\circ\text{K}$).

The connection between detonation and the combustion on which it is based has been most clearly discussed by Zel'dovich [78] who also resolved it most satisfactorily (see also [548, 972], [J. O. Hirschfelder and Ch. F. Curtiss, *J. Chem. Phys.*, **28**, 1130, 1147 (1958)] and [R. E. Duff, *J. Chem. Phys.*, **28**, 1193 (1958)]). Zel'dovich first clearly formulated a direct connection between the mechanism of detonation propagation of a flame and the combustion reaction. The starting point here is the suggestion of various authors that the mechanism of detonation propagation consists in the transmission of pressure from layer to layer, leading to ignition of the gas. Zel'dovich and Shlyapintokh [91] have given direct experimental evidence that a gas may be ignited when it is compressed by a shock wave (produced in the fuel mixture by a bullet travelling with supersonic velocity).⁽⁸⁸⁾ On the hypotheses that the change in state of the gas in a shock wave takes place in the free path length of the molecules, i.e. that the width of the shock-wave front is equal to the path length λ (of order 10^{-5} cm), that the rate of propagation of detonation has an order of magnitude similar to the molecular velocity at the detonation temperature⁽⁸⁹⁾ and that any chemical reaction requires a considerable number of collisions, Zel'dovich concludes that the gas in the shock-wave front has the same composition as the initial mixture. This means that the point p' , v' , which corresponds to the state of the gas in the shock-wave front, lies on the same Hugoniot curve as the point p_0 , v_0 , which corresponds to the initial mixture (the points O' and O in Fig. 197) and that the equation of this curve is expressed by formula (44.8).

In the front of a shock wave (or in its immediate vicinity) ignition of the compressed gas occurs and, owing to the high rate of propagation of the shock wave, diffusion and thermal conduction are not important.⁽⁹⁰⁾ Consequently the mixture enters into reaction undiluted by reaction products and containing no active centres which were formed in adjacent layers of the gas that had entered into reaction previously. For this reason, ignition of a fuel mixture in a shock wave should correspond more closely to self-ignition of a gas in static conditions than to ignition during normal combustion (where heat transfer by thermal conduction and diffusion of active centres play the main role in flame propagation). It follows from these ideas that the aptitude of a mixture for detonation

⁽⁸⁸⁾ Subsequently various authors have shown that an explosive mixture may be ignited by a shock wave generated by bursting a diaphragm. We should add that Gaydon and Fairbairn [593] initiated a comparative study of flame and detonation-wave spectra and spectra excited in a fuel mixture by a shock wave. The first results of these experiments are promising from the point of view of establishing the mechanism of formation of free radicals at high temperatures.

⁽⁸⁹⁾ The mean velocity of molecules of a substance of molecular weight 30 is 3 km/sec at 3000°K. The detonation velocity is usually 2 to 5 km/sec.

⁽⁹⁰⁾ Cook, Keyes and Filler [499] dispute this.

propagation should be determined by the induction period of the ignition of the mixture at the temperature T' of the shock-wave front. Qualitative experimental evidence of the accuracy of these ideas is given by the data of Sokolik [244], Rivin and others [223] on the effect of small concentrations of active admixtures. These data show in particular that active admixtures broaden equally the concentration limits both of detonation (without affecting the detonation velocity, however) and of self-ignition of the same mixtures in static conditions; they also accelerate the self-ignition.

One of the most convincing experimental indications of the accuracy of the idea that ignition of a fuel mixture by a shock wave is a purely thermal effect is given by the results of Steinberg and Kaskan [1175], involving measurements of the self-ignition temperature, and ignition temperature in a shock wave, in a hydrogen with oxygen mixture and a propane with air mixture. Thus, for the $2\text{H}_2 + \text{O}_2$ mixture they obtained a self-ignition temperature of 760 to 740°K (at 5 to 7.5 atm pressure) and an ignition temperature in a shock wave of 800°K . The ignition temperature of this mixture for adiabatic compression is 820 to 800°K according to the results of various authors.

In a mixture ignited by compression in a shock wave, a chemical reaction of combustion develops and is propagated at a constant rate. This constant rate leads to a linear law for the change of state of the gas (from equation (44.10)), as proposed by Mikhelson [192]. This change of state in Fig. 197 (p. 754) corresponds to a transition of the gas along the line $O'KO$, from the state represented by the point O' identical in composition with the state of the initial mixture (O), to the state of the reaction products which is represented by the point $p_c, v_c (K)$, i.e. transition from the original Hugoniot curve (initial mixture) to the reaction-product curve. Note that the equation of the latter is expressed by formula (44.9).

The transition of the gas from the state corresponding to the point O' , at which the combustion reaction begins, to the state corresponding to the point K , at which the reaction finishes, is completed in a certain time interval comparable with the induction period of self-ignition, or with an initial period of auto-acceleration, which is the slowest macroscopic stage of the reaction. During this time (the reaction time τ) each molecule of the initial substances on average undergoes the ν collisions which are necessary for reaction to occur.⁽⁹¹⁾ Therefore the width of the detonation wave, δ_D , is ν times larger than the width of the shock wave (equal to λ , the mean path length of the molecules in the gas). Hence the width of the detonation wave is 1 to 10 mm when $\lambda = 10^{-5}$ cm and $\nu = 10^4$ to 10^5 .

⁽⁹¹⁾ According to Gilkerson and Davidson's estimate [679], in the case of a detonation wave initiated by a shock wave in a mixture of $\text{H}_2 + \text{O}_2$ at a pressure of 0.035 atm ν is between 1000 and 4000. See also Th. Just and H. G. Wagner, *Z. Phys. Chem.*, **13**, 241 (1957); G. B. Kistiakowsky, F. D. Talbut, *J. Chem. Phys.*, **30**, 577 (1959).

The picture arising from Zel'dovich's theory gives the distribution of temperature, pressure, density and concentration of initial and final substances in a detonation wave as shown in Fig. 200. The point O' in each of the four diagrams of this figure corresponds to the point O' in Fig. 197. The points K in the two figures also correspond. The distance between O' and K (along the abscissa axis) is equal to the width of the detonation wave.

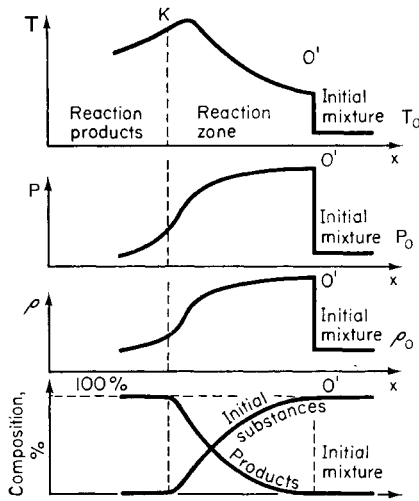


FIG. 200. Distribution of temperature, pressure, density and concentration of the initial substances and reaction products in a detonation wave (according to Zel'dovich [78]).

It is necessary to elucidate two peculiarities of the diagrams in Fig. 200. The first is there is a peak of temperature in the detonation wave, i.e. there is a section of the detonation wave with temperature higher than the temperature T of the burnt gases (the detonation temperature). The attainment of the peak temperature before reaction is complete is explained by the fact that the last portion of heat liberated is accompanied by considerable expansion of the gas, and this leads to a lowering of the temperature (by 100 to 200°). The second peculiarity is the pressure drop in the detonation wave (falling from a maximum value in the shock-wave front). This pressure drop (with parallel increase in temperature) is also a result of the gas expanding due to the heat liberated by the reaction.

In an elementary exposition of the theory of detonation limits due to Zel'dovich, the above-mentioned limiting role of the chemical reaction, which determines the limits of detonation propagation of combustion, is allowed for by the equation:

$$D = D_T - a\tau, \quad (44.15)$$

where D_T is the theoretical detonation velocity calculated for infinitely fast reaction (reaction time $\tau = 0$), and α is a coefficient characterizing losses during propagation of the detonation wave (the losses result from the hydraulic resistance of the tube and from turbulent heat exchange).⁽⁹²⁾ The reaction time τ is mainly determined by the temperature T' of the shock wave and may be expressed as

$$\tau = b \exp(E/RT'), \quad (44.16)$$

where E is the activation energy of the reaction and b is a quantity depending on the composition of the mixture and the reaction mechanism. In addition to (44.15) and (44.16) a third equation may be obtained from (44.10) and (44.9), and may be written in the approximate form, when $p \gg p_0$, $v_0 \gg v$ and $T \gg T_0$ ($L = 0$):

$$cT' = D^2, \quad (44.17)$$

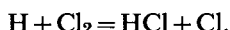
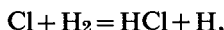
where $c = 2c_v$. The three equations (44.15), (44.16) and (44.17) are the basis of Zel'dovich's elementary theory of detonation limits.

From an analysis of this system of equations Zel'dovich concludes that there is a real solution only when the parameters in the equations satisfy the inequality

$$2e(abRD_T/cE) \exp(cE/RD_T^2) \leq 1,$$

which is therefore the condition for detonation limits. In addition Zel'dovich shows that inside the detonation region the actual detonation velocity D should be close to the theoretical value (D_T), as when D and D_T differ by only 10 to 15 per cent a limit is reached for the stationary detonation regime.

In the case of two reactions—hydrogen with chlorine and hydrogen with oxygen—Zel'dovich [78] shows how the mechanism of the reaction is reflected in the detonation velocity of the mixture. The first of these reactions follows a simple-chain mechanism in which, owing to the high temperature of the detonation wave, the main role is played by alternating processes of a Nernst chain



These equations together give $\text{H}_2 + \text{Cl}_2 \rightarrow 2\text{HCl}$, so that the reaction of hydrogen chloride formation may reach equilibrium for any concentration of Cl and H active centres. As the activation energy of the above processes is much less than that of the process $\text{Cl}_2 \rightarrow 2\text{Cl}$ (which is equal to 57.2 kcal,

⁽⁹²⁾ The losses accounted for by cooling of the gas as a result of light emission become appreciable at sufficiently high temperatures. See, for example W. Roth, *J. Chem. Phys.*, **31**, 844 (1959).

the heat of dissociation of Cl_2 molecules), the concentration of active centres will not vary substantially during the reaction time. Therefore the number of particles remains practically constant in the hydrogen-chlorine reaction, and it may be concluded that the detonation velocity of the $\text{H}_2 + \text{Cl}_2$ mixture will not depend on pressure. As is seen from the data of Table 62, this conclusion is supported by experiment: for an increase in the initial pressure of the mixture from $p_0 = 200$ mm Hg to $p_0 = 760$ mm Hg, the detonation velocity varies by only 0.7 per cent. The fact that the measured values of D are somewhat larger than the calculated values (especially when $p_0 = 200$ mm Hg) is attributed by Zel'dovich to a considerable part of the reaction occurring with a concentration of chlorine atoms less than that corresponding to the dissociation equilibrium $\text{Cl}_2 \rightleftharpoons 2\text{Cl}$,⁽⁹³⁾ so that the true detonation temperature is higher than the temperature T calculated for the equilibrium process and, consequently, the true detonation velocity is higher than that calculated for the equilibrium temperature.

TABLE 62

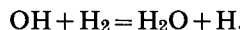
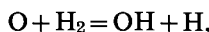
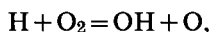
Detonation velocity in $\text{H}_2 + \text{Cl}_2$ and $2\text{H}_2 + \text{O}_2$ mixtures for various initial pressures

(according to Zel'dovich [78])

$$\Delta\% = \frac{D_{760} - D_{200}}{D_{760}} \cdot 100\%$$

Mixture	p_0 , mm Hg	Calculated		Measured			
		D , m/sec	$\Delta\%$	Dixon		[245]	
				D , m/sec	$\Delta\%$	D , m/sec	$\Delta\%$
$\text{H}_2 + \text{Cl}_2$	200	1680	2.3	—	—	1729	0.7
$\text{H}_2 + \text{Cl}_2$	760	1720	—	—	—	1741	—
$2\text{H}_2 + \text{O}_2$	200	2760	2.5	2627	6.9	2685	7.1
$2\text{H}_2 + \text{O}_2$	760	2820	—	2821	—	2835	—

In contrast with the hydrogen-chlorine reaction, the reaction of hydrogen with oxygen follows a branched-chain mechanism. The main elementary processes occurring in the detonation wave are



⁽⁹³⁾ According to the calculations of Zel'dovich, the equilibrium state of the mixture for an initial pressure of chlorine and hydrogen of one atmosphere is characterized by the following values of temperature, pressure and concentrations of the components of the mixture: $T_e = 3130^\circ\text{K}$, $p_e = 21$ atm, HCl 80.1 per cent, H_2 5.8 per cent; Cl_2 0.2 per cent; H 1.4 per cent; Cl 12.5 per cent.

which together give $2\text{H}_2 + \text{O}_2 = \text{H}_2\text{O} + \text{OH} + \text{H}$. Hence the formation of water in the course of the reaction is accompanied by a parallel formation of active centres, which should have very considerable concentrations in the first stage of the reaction. In the final stage of the reaction these radicals recombine, liberating large amounts of energy. Therefore, in contrast with the previous reaction, the temperature reaches its maximum value at the end of the reaction and, as recombination of the radicals occurs on ternary collision, increasing the pressure of the mixture should lead to increase in the detonation velocity. Actually, according to Table 62, increasing the pressure from 200 mm Hg to 1 atm gives an increase in detonation velocity of 7 per cent. Zel'dovich explains the discrepancy between the calculated and measured values of D at low pressure by a large reaction time τ , leading to high losses and accordingly to a lower "true" detonation velocity compared with the measured value (cf. formula (44.15)).

It follows from the account given in this section that the velocity of detonation-flame propagation and the chemistry and kinetics of processes in a detonation wave are closely linked; this is very clearly shown by the dependence of detonation velocity on the features of the chemical mechanism of the combustion reactions, and is most clearly shown near the detonation limits. In addition, it is clear from the data considered that study of detonation provides fresh opportunities for studying chemical conversions at high temperatures,⁽⁹⁴⁾ particularly as outlined in Zel'dovich's work. That these opportunities are not confined to detonation of gas mixtures but may be extended to detonation of liquid and solid substances is also important. Actually, according to Belyaev's theory, the combustion of explosive substances takes place in the gas phase as the result of evaporation or sublimation of the fuel mixture (in the case of secondary explosive substances which are characterized by a relatively high volatility) or as the result of decomposition of a condensed phase (in the case of initiating substances). The fact that combustion of liquid and solid explosives takes place in the gas phase explains in particular the pressure dependence of combustion rates (expressed by a linear law or by a direct proportionality between combustion rate and pressure) established by Andreev [17] and other authors (see p. 716).

⁽⁹⁴⁾ See, for example, the work of Kistiakowsky and coworkers [838].

REFERENCES*

1. L. I. AVRAMENKO, *Acta Phys.-Chim. URSS*, **17**, 197 (1942).
2. L. I. AVRAMENKO, *J. Phys. Chem., Moscow*, **18**, 207 (1944).
3. L. I. AVRAMENKO, *J. Phys. Chem., Moscow*, **21**, 1135 (1947); **23**, 790 (1949).
4. L. I. AVRAMENKO, *J. Phys. Chem., Moscow*, **20**, 1299 (1946).
5. L. I. AVRAMENKO and R. V. KOLESNIKOVA (LORENTSO), in *Problems of Chemical Kinetics, Catalysis and Reactivity* (*Sb. Voprosy Khimicheskoi Kinetiki, Kataliza i Reaktsionnoi Sposobnosti*), p. 7, Acad. Sci. U.S.S.R., Moscow (1955).
6. L. I. AVRAMENKO and R. V. KOLESNIKOVA (LORENTSO), *Dokl. Akad. Nauk SSSR*, **67**, 867 (1949).
7. L. I. AVRAMENKO and R. V. KOLESNIKOVA (LORENTSO), *Dokl. Akad. Nauk SSSR*, **92**, 349 (1953).
8. L. I. AVRAMENKO and V. N. KONDRAT'EV, *J. Exp. Theor. Phys.*, **7**, 249 (1937).
9. L. I. AVRAMENKO and V. N. KONDRAT'EV, *J. Exp. Theor. Phys.*, **7**, 842 (1937).
10. L. I. AVRAMENKO and R. V. LORENTSO, Ref. 6.
11. L. I. AVRAMENKO and R. V. LORENTSO, *J. Phys. Chem., Moscow*, **24**, 207 (1950).
12. B. V. AIVAZOV and M. B. NEIMAN, *Acta Phys.-Chim. URSS*, **4**, 575 (1936).
13. B. V. AIVAZOV, M. B. NEIMAN and I. I. KHANOVA, *Izv. Akad. Nauk. (Otd. Khim. N.)*, 307 (1938); *Acta Phys-Chim. URSS*, **10**, 765 (1938).
14. D. V. ALEKSEEV, *Izv. Ped. in-ta im. Shchelaputina*, **4**, (1915).
15. A. A. ALIYEV, A. I. ROZLOVSKII and YU. KH. SHAULOV, *Dokl. Akad. Nauk SSSR*, **99**, 559 (1954).
16. D. N. ANDREEV, *Organic Synthesis in Electrical Discharges* (*Organicheskii Sintez v Elektricheskikh Zaryadakh*), Acad. Sci. U.S.S.R., Moscow-Leningrad (1953).
17. K. K. ANDREEV, in *Articles on the Theory of Explosives* (*Sb. Statei Po Teorii Vzryvchayk Veshchestv*), p. 39, Oborongiz (1940).
18. I. N. ANTONOVA, V. A. KUZ'MIN, R. I. MOSHKINA, A. B. NALBANDYAN, M. B. NEIMAN and G. I. FEKLISOV, *Izv. Akad. Nauk. (Otd. Khim. N.)*, 789 (1955).
19. G. S. ARAVIN, Thesis, Inst. Chem. Phys., Acad. Sci. U.S.S.R., Moscow (1951).
20. KH. S. BAGDASAR'YAN, Thesis, Karpov Physico-Chem. Inst., Moscow (1950).
21. KH. S. BAGDASAR'YAN, *J. Phys. Chem., Moscow*, **23**, 1375 (1949).
22. G. A. BARSKII and YA. B. ZEL'DOVICH, *J. Phys. Chem., Moscow*, **25**, 523 (1951).
23. I. F. BAKHAREVA, *Dokl. Akad. Nauk SSSR*, **102**, 1151 (1955).
24. K. C. BAILEY, *Retardation of Chemical Reactions*, Chap. 24, Edward Arnold London (1937).
25. A. F. BELYAEV, *J. Phys. Chem. Moscow*, **12**, 94 (1938).
26. A. F. BELYAEV, Thesis, Inst. Chem. Phys., Acad. Sci. U.S.S.R., Moscow (1946); also in *Articles on the Theory of Explosives* (*Sb. Statei Po Teorii Vzryvchayk Veshchestv*), p. 21, Oborongiz (1940).
27. A. F. BELYAEV, *J. Phys. Chem., Moscow*, **14**, 1009 (1940).
28. D. I. BLOKHINTSEV, *Elements of Quantum Mechanics* (*Osnovy Kvantovoi Mekhaniki*), Gostekhiteoretizdat, Moscow-Leningrad (1949).
29. M. L. BOGOYAVLEN'SKAYA and A. A. KOVAL'SKII, *J. Phys. Chem., Moscow*, **20**, 1325 (1946).

*References 1-310 (which are in Cyrillic alphabetical order) are to Russian authors (using various languages) and to books which have been translated into Russian. These book references are here generally to the original non-Russian editions.

30. K. F. BONHOEFFER and P. HARTECK, *Grundlagen der Photochemie*, Verlag Theodor Steinkopff, Dresden and Leipzig (1933).
31. N. A. BORISEVICH, *Dokl. Akad. Nauk SSSR*, **99**, 695 (1954).
32. S. E. BRESLER and G. V. SAMSONOV, *Usp. Khim.*, **24**, 985 (1955).
33. A. I. BRODSKII and I. I. KUKHTENKO, *Dokl. Akad. Nauk SSSR*, **279** (1950); *J. Phys. Chem., Moscow*, **25**, 920 (1951).
34. A. I. BRODSKII, G. P. MIKLUKHIN, I. I. KUKHTENKO and I. P. GRAGEROV, *Dokl. Akad. Nauk SSSR*, **57**, 463 (1947); A. I. BRODSKII, Chemistry of Isotopes (*Khimiya Izotopov*), pp. 240-2, 257-9, Acad. Sci. U.S.S.R., Moscow (1952).
35. N. YA. BUBEN and A. B. SHEKHTER, *Acta Phys.-Chim. URSS*, **10**, 371 (1939).
- 35a. N. S. BUCHEL'NIKOVA, Summary of thesis, Moscow (1958); *Usp. Phys. Nauk* **65**, 351 (1958).
36. L. A. WEINSTEIN and B. M. YAVORSKII, *Dokl. Akad. Nauk SSSR*, **89**, 813 (1953).
37. J. H. VAN'T HOFF, *Studies in Chemical Dynamics*, Williams and Norgate, London (1896).
38. A. T. VARTAN'YAN, *Izv. Akad. Nauk (Phys.)*, No. 3, 341 (1938).
39. V. N. VASIL'EV, Diploma paper, Leningrad Polytech. Inst. (1938).
40. R. F. VASIL'EV, Summary of Thesis, Inst. Chem. Phys., Acad. Sci. U.S.S.R., Moscow (1955).
41. V. V. VOEVODSKII, Thesis, Inst. Chem. Phys., Acad. Sci. U.S.S.R., Moscow (1944).
42. V. V. VOEVODSKII, *J. Phys. Chem., Moscow*, **20**, 1285 (1946).
43. V. V. VOEVODSKII, in *Problems of Organic Reaction Mechanisms (Problemy Mekhanizma Organicheskikh Reaktsii)*. Trud. Kiev. soveshch., p. 58, Kiev (1953).
- 43a. V. V. VOEVODSKII, *Dokl. Akad. Nauk SSSR*, **90**, 815 (1953).
44. V. V. VOEVODSKII, *Dokl. Akad. Nauk SSSR*, **94**, 909 (1954).
- 44a. V. V. VOEVODSKII, *Thesis* (1954); V. A. POLTORAK, *Thesis* (1953).
45. V. V. VOEVODSKII and V. I. VEDENEV, *Dokl. Akad. Nauk SSSR*, **106**, 679 (1956).
46. V. V. VOEVODSKII and V. N. KONDRAT'EV, *Usp. Khim.* **19**, 673 (1950).
47. V. V. VOEVODSKII and V. A. POLTORAK, *J. Phys. Chem. Moscow*, **24**, 299 (1950).
48. M. V. VOL'KENSHTEIN, M. A. YEL'YASHEVICH and B. I. STEPANOV, *Molecular Vibrations (Kolebaniya Molekul)*, vols. 1 and 2, Moscow-Leningrad (1949).
49. V. G. VORONOV and N. N. SEMENOV, *J. Phys. Chem. Moscow*, **13**, 1695 (1939).
50. A. G. GAYDON, *Spectroscopy and Combustion Theory*, Chapman and Hall, London (1948).
51. J. HEYROVSKY, *Polarographie*, Springer-Verlag, Vienna (1941).
52. YU G. GERVART and D. A. FRANK-KAMENETSKII, *Izv. Akad. Nauk (Otd. Khim. N.)*, No. 4, 210 (1942).
53. G. HERZBERG, *Infrared and Raman Spectra of Polyatomic Molecules*, New York (1946).
54. G. HERZBERG, *Molecular Spectra and Molecular Structure, I Diatomic Molecules*, New York (1939).
55. C. N. HINSHELWOOD, *Kinetics of Chemical Change in Gaseous Systems*, Oxford (1926).
56. S. GLASSTONE, *Theoretical Chemistry*, New York (1946).
57. S. GLASSTONE, K. LAIDLER and H. EYRING, *The Theory of Rate Processes*, McGraw-Hill, New York (1941).
58. S. GOLDHABER and J. E. WILLARD, *J. Amer. Chem. Soc.* **74**, 318 (1952).
59. V. L. GRANOVSII, *Electric Current in Gas (Elektricheskii Tok v Gaze)*, Gostekhretodzdat, Moscow-Leningrad (1952).
60. J. H. GREEN, *Rev. Pure Appl. Chem.*, **1**, 235 (1951).
61. A. I. DINTSES, D. A. KVYATKOVSKII, A. D. STEPUKHOVICH and A. V. FROST, *J. Gen. Chem., Moscow*, **7**, 1754 (1937).
62. N. YA. DODONOVA, Thesis, Leningrad Univ. (1953); *Dokl. Akad. Nauk SSSR*, **98**, 753 (1954).
63. N. YA. DODONOVA, *Dokl. Akad. Nauk SSSR*, **98**, 933 (1954).
64. V. M. DUKEL'SKII, E. YA. ZANDBERG and N. I. IONOV, *J. Exp. Theor. Phys.*, **20**, 877 (1950); V. M. DUKEL'SKII and E. YA. ZANDBERG, *Dokl. Akad. Nauk SSSR*, **86**, 263 (1952).

65. V. M. DUKEL'SKII and E. YA. ZANDBERG, *Dokl. Akad. Nauk SSSR*, **82**, 33 (1952).
66. V. M. DUKEL'SKII and E. YA. ZANDBERG, *J. Exp. Theor. Phys.*, **21**, 1270 (1951); **24**, 339 (1953); F. YU. BYDIN, Summary of Thesis, Leningrad Inst. Phys. and Tech. (1955); F. YU. BYDIN and V. M. DUKEL'SKII, *J. Exp. Theor. Phys.*, **31**, 569 (1956).
67. V. M. DUKEL'SKII and E. YA. ZANDBERG, *Dokl. Akad. Nauk SSSR*, **99**, 947 (1954).
68. V. M. DUKEL'SKII and N. I. IONOV, *Dokl. Akad. Nauk SSSR*, **81**, 767 (1951).
69. V. M. DUKEL'SKII and N. V. FEDORENKO, *J. Tech. Phys., Moscow*, **25**, 2193 (1955).
- 69a. F. S. D'YACHKOVSKII, N. N. BUBNOV and A. E. SHILOV, *Dokl. Akad. Nauk SSSR*, **123**, 870 (1958).
70. M. A. YEL'YASHEVICH, *Phys. Z. Sow.*, **1**, 510 (1932).
71. N. S. YENIKOLOPYAN, L. V. KARMILOVA, A. B. NALBANDYAN and N. N. SEMENOV, *J. Phys. Chem., Moscow*, **34**, 1176 (1960).
- 71a. N. S. YENIKOLOPYAN and G. P. KONAREVA, *Izv. Akad. Nauk. (Otd. Khim. N.)*, No. 3, 719 (1960).
72. A. A. ZHUKHOVITSKII, O. V. ZOLOTAREVA, V. A. SOKOLOV and N. M. TURKEL'TAUB, *Dokl. Akad. Nauk SSSR*, **77**, 435 (1951).
73. A. A. ZHUKHOVITSKII and N. M. TURKEL'TAUB, *Usp. Khim.*, **25**, 859 (1956).
74. A. V. ZAGULIN, *Z. phys. Chem.*, B **1**, 275 (1928).
75. A. V. ZAGULIN, A. A. KOVAL'SKII, D. I. KOPP and N. N. SEMENOV, *J. Phys. Chem. Moscow*, **1**, 263 (1930); *Z. phys. Chem.*, B **6**, 307 (1930).
76. M. ZATSIORSKII, V. KONDRAT'EV and S. SOLNYSHKOVA, *J. Phys. Chem., Moscow*, **14**, 1521 (1940).
77. YA. B. ZEL'DOVICH, *J. Exp. Theor. Phys.*, **11**, 159 (1941).
78. YA. B. ZEL'DOVICH, *Theory of Combustion and Detonation of Gases (Teoriya Gorenija i Detonatsii Gazov)*, Acad. Sci. U.S.S.R., Moscow-Leningrad (1944).
79. YA. B. ZEL'DOVICH, *Dokl. Akad. Nauk SSSR*, **51**, 213 (1946).
80. YA. B. ZEL'DOVICH, *Shock-wave Theory and an Introduction to Gas Dynamics (Teoriya Udarnykh Voln i Vvedeniye v Gazodinamiku)*, Acad. Sci. U.S.S.R., Moscow-Leningrad (1946).
81. YA. B. ZEL'DOVICH, *J. Tech. Phys., Moscow*, **17**, 3 (1947).
82. YA. B. ZEL'DOVICH, *J. Phys. Chem. Moscow*, **22**, 27 (1948).
83. YA. B. ZEL'DOVICH, *Acta Phys.-Chim. URSS*, **21**, 577 (1946).
84. YA. B. ZEL'DOVICH and V. V. VOEVODSKII, *Thermal Explosion and Flame Propagation in Gases (Teplovoi Vzryv i Rasprostraneniye Plameni v Gazakh)*, p. 103 Moscow Mech. Inst., (1947).
85. YA. B. ZEL'DOVICH and A. S. KOMPANEETS, *Theory of Detonation*, New York, Academic Press (1961); *Teoriya Detonatsii*, Gostekhizdat, Moscow (1955).
86. YA. B. ZEL'DOVICH, P. YA. SADOVNIKOV and D. A. FRANK-KAMENETSKII, *Oxidation of Nitrogen during Combustion (Oksisljeniye Azota pri Gorenii)*, Acad. Sci. U.S.S.R., Moscow-Leningrad (1947).
87. YA. B. ZEL'DOVICH and N. N. SEMENOV, *J. Exp. Theor. Phys.*, **10**, 1116, 1427 (1940).
88. YA. B. ZEL'DOVICH and D. A. FRANK-KAMENETSKII, *Turbulent and Heterogeneous Combustion (Turbulentoje i Geterogennoye Gorenije)*, Moscow Mech. Inst. (1947).
89. YA. B. ZEL'DOVICH and D. A. FRANK-KAMENETSKII, *Dokl. Akad. Nauk SSSR*, **19**, 693 (1938).
90. YA. B. ZEL'DOVICH and D. A. FRANK-KAMENETSKII, *J. Phys. Chem. Moscow*, **12**, 100 (1938).
91. YA. B. ZEL'DOVICH and V. YA. SHLYAPINTOKH, *Dokl. Akad. Nauk SSSR*, **65**, 871 (1949).
92. YA. B. ZEL'DOVICH and V. I. YAKOVLEV, *Dokl. Akad. Nauk SSSR*, **19**, 699 (1938).
93. S. I. ZILITINKEVICH, *Telegr. i Telefon. Bez Provodov*, **9**, 652 (1928).
94. P. V. ZIMAKOV, *J. Phys. Chem. Moscow*, **29**, 76 (1955).

95. M. S. ZISKIN, *Dokl. Akad. Nauk SSSR*, **34**, 279 (1942).
96. D. D. IVANENKO, V. V. RACHINSKII, T. B. GAPON and YE. N. GAPON, *Dokl. Akad. Nauk SSSR*, **60**, 1189 (1948).
97. W. JOST, *Explosion and Combustion Processes in Gases*, McGraw-Hill, New York (1946).
98. M. I. KABACHNIK, *Zh. Khim. Ukr.*, **22**, 64 (1956).
99. YU. M. KAGAN and V. M. ZAKHAROVA, *J. Exp. Theor. Phys.*, **18**, 52 (1948).
100. R. A. KALINENKO and V. V. VOEVODSKII, *J. Phys. Chem. Moscow*, **30**, 537 (1956).
101. S. N. KAMENSKAYA and S. S. MEDVEDEV, *Acta Phys.-Chim. URSS*, **15**, 565 (1940).
102. N. A. KARZHAVINA, *J. Phys. Chem. Moscow*, **19**, 551 (1945).
103. L. V. KARMILOVA, Thesis, Inst. of Chem. Phys., Acad. Sci. U.S.S.R., Moscow (1954).
104. L. V. KARMILOVA and V. N. KONDRAT'EV, *J. Phys. Chem., Moscow*, **25**, 312 (1951).
- 104a. L. V. KARMILOVA, A. B. NALBANDYAN and N. N. SEMENOV, *J. Phys. Chem., Moscow*, **32**, 1193 (1958).
105. A. V. KARYAKIN and V. A. NIKITIN, *Izv. Akad. Nauk (Phys.)*, **17**, 636 (1935).
106. L. S. KASSEL, *Kinetics of Homogeneous Gas Reactions*, Chemical Catalog Co., New York (1932).
107. B. KIZIL'BASH and V. N. KONDRAT'EV, *Zh. Russk. Phys.-Khim. Ob-va. (Phys.)*, **62**, 523 (1931).
108. N. A. KLEIMENOV, I. N. ANTONOVA, A. M. MARKEVICH and A. B. NALBANDYAN, *J. Phys. Chem., Moscow*, **30**, 794 (1956).
109. A. V. KLEINBERG and A. N. TERENIN, *Dokl. Akad. Nauk SSSR*, **101**, 445 (1955); A. V. KLEINBERG, Summary of Thesis, Leningrad Univ. (1954).
110. H. O. KNEZER, *Z. Phys.*, **87**, 717 (1928).
111. N. I. KOB佐EV, S. S. VASIL'EV and E. YE. GOL'BRAIKH, *Dokl. Akad. Nauk SSSR*, **2**, 236 (1935).
112. A. A. KOVAL'SKII, *Z. phys. Chem.*, **B 4**, 288 (1929).
113. A. A. KOVAL'SKII, *Phys. Z. Sow.*, **4**, 723 (1933).
114. D. G. KNORRE, Z. K. MAIZUS and N. M. EMANUEL', *Dokl. Akad. Nauk SSSR*, **112**, 457 (1957).
115. S. M. KOGARKO, Thesis, Inst. of Chem. Phys., Acad. Sci. U.S.S.R., Moscow (1952).
116. V. I. KOKOCHASHVILI, Thesis, Inst. of Chem. Phys., Acad. Sci. U.S.S.R., Moscow (1942).
117. V. I. KOKOCHASHVILI, *J. Phys. Chem., Moscow*, **25**, 444 (1951).
118. V. M. KOLOTYRKIN, Summary of Thesis, Karpov Physico-chem. Inst., Moscow (1954); M. V. TIKHOMIROV, V. M. KOLOTYRKIN and N. N. TUNITSKII, *Dokl. Akad. Nauk SSSR*, **101**, 903 (1955).
119. V. N. KONDRAT'EV, *Zh. Russk. Phys.-khim. Ob-va. (Phys.)*, **60**, 229 (1928).
120. V. N. KONDRAT'EV, *Z. Phys.*, **63**, 322 (1950).
121. V. N. KONDRAT'EV, *Phys. Z. Sow.*, **4**, 57 (1933).
122. V. N. KONDRAT'EV, *J. Phys. Chem., Moscow*, **4**, 783 (1933).
123. V. N. KONDRAT'EV, *Usp. Phys. Nauk* **14**, 982 (1934).
124. V. N. KONDRAT'EV, *J. Exp. Theor. Phys.*, **5**, 250 (1935).
125. V. N. KONDRAT'EV, *J. Phys. Chem., Moscow*, **7**, 192 (1936).
126. V. N. KONDRAT'EV, *J. Exp. Theor. Phys.*, **7**, 256 (1937).
127. V. N. KONDRAT'EV, *Usp. Khim.*, **8**, 195 (1939).
128. V. N. KONDRAT'EV, *J. Phys. Chem., Moscow*, **13**, 880 (1939).
129. V. N. KONDRAT'EV, *J. Phys. Chem., Moscow*, **131**, 260 (1939).
130. V. N. KONDRAT'EV, *J. Phys. Chem., Moscow*, **14**, 281, 287 (1940); *Acta Phys.-Chim. URSS*, **12**, 637 (1940).
131. V. N. KONDRAT'EV, *Izv. Akad. Nauk (Otd. Khim. N.)* 501 (1940).
132. V. N. KONDRAT'EV, *J. Phys. Chem., Moscow*, **18**, 110 (1944).
133. V. N. KONDRAT'EV, *Spectroscopic Study of Chemical Gas Reactions (Spektroskopicheskoye Izuchenie Khimicheskikh Gazovykh Reaktsii)*. Acad. Sci. U.S.S.R., Moscow-Leningrad (1944).

134. V. N. KONDRAT'EV, *Dokl. Akad. Nauk SSSR*, **44**, 21 (1944).
135. V. N. KONDRAT'EV, *J. Phys. Chem., Moscow*, **18**, 110 (1944); YE KONDRAT'EV and V. KONDRAT'EV, *J. Phys. Chem., Moscow*, **21**, 669 (1947).
136. V. N. KONDRAT'EV, *Dokl. Akad. Nauk SSSR*, **49**, 38 (1945).
137. V. N. KONDRAT'EV, *Vopr. Istor. Yestestvoznan. i Tekh.*, No. 2, 9 (1956).
- 137a. V. N. KONDRAT'EV, *Usp. Khim.*, **26**, 861 (1957).
- 137b. V. N. KONDRAT'EV, in *Seventh Symposium on Combustion*, p. 41. Butterworth, London (1958).
138. V. N. KONDRAT'EV and M. S. ZISKIN, *Phys. Z. Sow.*, **8**, 644 (1935).
139. V. N. KONDRAT'EV and M. S. ZISKIN, *J. Phys. Chem., Moscow*, **9**, 542 (1937); *Acta Phys.-Chim. URSS*, **6**, 307 (1937).
140. V. N. KONDRAT'EV and M. S. ZISKIN, *J. Exp. Theor. Phys.*, **6**, 110 (1936).
141. V. N. KONDRAT'EV and M. S. ZISKIN, *J. Exp. Theor. Phys.*, **6**, 1083 (1936).
142. V. KONDRAT'EV, H. KONDRAT'EVA and A. LAURIS, *J. Phys. Chem., Moscow*, **5**, 1411 (1934).
143. V. KONDRAT'EV, *Free Hydroxyl (Svobodnyi Gidroksil)*, p. 58, Gonti, Moscow (1939).
144. V. N. KONDRAT'EV, *J. Phys. Chem., Moscow*, **14**, 281 (1940).
145. H. KONDRAT'EVA and V. KONDRAT'EV, *J. Exp. Theor. Phys.*, **5**, 797 (1935).
146. H. I. KONDRAT'EVA and V. N. KONDRAT'EV, *J. Phys. Chem., Moscow*, **11**, 331 (1938).
147. H. I. KONDRAT'EVA and V. N. KONDRAT'EV, *J. Phys. Chem., Moscow*, **13**, 1053 (1939).
148. H. I. KONDRAT'EVA and V. N. KONDRAT'EV, *J. Phys. Chem., Moscow*, **14**, 1 (1940).
149. H. I. KONDRAT'EVA and V. N. KONDRAT'EV, *J. Phys. Chem., Moscow*, **19**, 178 (1945).
150. H. I. KONDRAT'EVA and V. N. KONDRAT'EV, *Dokl. Akad. Nauk SSSR*, **51**, 607 (1946); *Acta Phys.-Chim. URSS*, **21**, 1, 629 (1946).
151. H. I. KONDRAT'EVA and V. N. KONDRAT'EV, *J. Phys. Chem., Moscow*, **20**, 1239 (1946).
152. H. I. KONDRAT'EVA and V. N. KONDRAT'EV, *J. Phys. Chem., Moscow*, **21**, 769 (1947); V. N. KONDRAT'EV, L. V. KARMILOVA and YE. I. KONDRAT'EVA, *J. Phys. Chem., Moscow*, **22**, 561 (1948).
153. V. N. KONDRAT'EV and A. I. LEIPUNSKII, *J. Phys. Chem., Moscow*, **1**, 327 (1930); V. N. KONDRAT'EV, *J. Phys. Chem., Moscow*, **3**, 383 (1932).
154. V. N. KONDRAT'EV, A. M. MARKEVICH, YU. N. RYABININ and I. I. TAMM, in *Sixth Symposium on Combustion*, p. 821. Reinhold New York, (1957).
155. V. N. KONDRAT'EV and A. V. YAKOVLEVA, *J. Exp. Theor. Phys.*, **10**, 1038 (1940).
156. D. P. KONOVALOV, *Z. phys. Chem.*, **1**, 62 (1887).
157. B. B. KUDRYAVTSEV, *J. Phys. Chem., Moscow*, **27**, 1693 (1953).
158. S. YE. KUPRIYANOV, Summary of thesis, Karpov Physico-chem. Inst., Moscow (1955).
159. S. YE. KUPRIYANOV and V. K. POTAPOV, *Dokl. Akad. Nauk SSSR*, **103**, 449 (1955).
160. D. N. KURSANOV and V. V. VOEVODSKII, *Usp. Khim.*, **23**, 641 (1954).
161. M. YA. KUSHNEREV and A. B. SHEKHTER, *Dokl. Akad. Nauk SSSR*, **32**, 560 (1941).
162. M. CURIE, *Radioactivité*, Hermann, Paris (1935).
163. G. K. LAVROVSKAYA, and V. V. VOEVODSKII, *J. Phys. Chem., Moscow*, **26**, 1164 (1952).
164. G. K. LAVROVSKAYA, R. YE. MARDALEISHVILI and V. V. VOEVODSKII in *Problems of Chemical Kinetics, Catalysis and Reactivity (Sb. Voprosy Khimicheskoi Kinetiki, Kataliza i Reaktsionnoi Sposobnosti)*, p. 40, Acad. Sci. U.S.S.R., Moscow (1955).
165. G. K. LAVROVSKAYA, V. YE. SKURAT, V. L. TAL'ROZE and G. D. TANTSYREV, *Dokl. Akad. Nauk SSSR*, **117**, 641 (1957).
166. L. D. LANDAU, *Phys. Z. Sow.*, **1**, 88 (1932); **2**, 46 (1932).

167. L. D. LANDAU, *Phys. Z. Sow.*, **10**, 67 (1936).
168. L. D. LANDAU, E. M. LIFSHITZ, *Kvantovaya Mekhanika*. Moscow-Leningrad, Gostekhizdat (1948); English translation published as "Quantum Mechanics", Addison Wesley/Pergamon Press (1959).
169. L. D. LANDAU and E. TELLER, *Phys. Z. Sow.*, **10**, 34 (1936).
170. A. I. LEIPUNSKII and A. V. ZAGULIN, *Z. phys. Chem.*, B **1**, 362 (1928).
171. A. I. LEIPUNSKII and A. B. SHEKHTER, *Z. Phys.*, **59**, 857 (1930).
- 171a. E. M. LIFSHITZ, *J. Exp. Theor. Phys.*, **17**, 1017 (1947).
- 171b. L. A. LOVACHEV, *Dokl. Akad. Nauk SSSR*, **120**, 1287 (1958); **123**, 501 (1958).
- 171c. L. A. LOVACHEV, *Dokl. Akad. Nauk SSSR*, **124**, 1271 (1959); **125**, 129 (1959).
172. A. F. LUKOVNIKOV and M. B. NEIMAN, *Dokl. Akad. Nauk SSSR*, **91**, 581 (1953).
173. A. F. LUKOVNIKOV and M. B. NEIMAN, *J. Phys. Chem., Moscow*, **29**, 1410 (1955).
174. B. LEWIS and G. VON ELBE, *Combustion, Flames and Explosions of Gases*, 2nd Ed. Academic Press, New York (1951).
175. Z. K. MAIZUS, A. M. MARKEVICH and N. M. EMANUEL', *Dokl. Akad. Nauk SSSR*, **89**, 1049 (1953).
176. Z. K. MAIZUS, and N. M. EMANUEL', *Izv. Akad. Nauk. (Otd. Khim. N.)*, No. 2, 182 (1948).
177. Z. K. MAIZUS and N. M. EMANUEL', *Dokl. Akad. Nauk SSSR*, **87**, 241, 437, 801 (1952); N. M. EMANUEL', in *Problems of Chemical Kinetics, Catalysis and Reactivity* (sb. *Voprosy Khimicheskoi Kinetiki, Kataliza i Reaktsionnoi Sposobnosti*), p. 117, Acad. Sci. U.S.S.R., Moscow (1955); *Uch. Zap. Mosk. gos. Univ.*, No. 174, 101 (1955).
178. Z. K. MAIZUS and N. M. EMANUEL', *Dokl. Akad. Nauk SSSR*, **95**, 1009 (1954).
179. M. F. MAMOTENKO, in *Collected Papers on Physical Chemistry* (*Sbornik Rabot po Fizicheskoi Khimii*), p. 1, Acad. Sci. U.S.S.R., Moscow (1947).
180. R. YE. MARDALEISHVILI, G. K. LAVROVSKAYA and V. V. VOEVODSKII, *J. Phys. Chem., Moscow*, **28**, 2195 (1954).
181. A. M. MARKEVICH, *J. Phys. Chem., Moscow*, **22**, 941 (1948).
182. A. M. MARKEVICH and L. F. FILIPPOVA, *J. Phys. Chem., Moscow*, **21**, 2649 (1947).
183. A. M. MARKEVICH, Ref. 181.
184. A. M. MARKEVICH, *J. Phys. Chem., Moscow*, **30**, 735 (1956).
185. S. S. MEDVEDEV, O. M. KORITSKAYA and YE. ALEKSEYEV, *J. Phys. Chem., Moscow*, **16**, 391 (1943).
186. N. I. MEDVEDEVA and YE. S. TORSUEVA, *Trud. Komiss. po Analit. Khim. (Trans. Commission on Analyt. Chem.)*, Acad. Sci. U.S.S.R., **6**, 88 (1955).
187. E. A. MOELWYN-HUGHES, *The Kinetics of Reactions in Solution*, 2nd. Ed., Oxford (1947).
188. D. I. MENDELEEV, *Zh. Russk. Phys.-Khim. Ob.-va.*, (Otd. 1) **18**, 8 (1886).
189. N. MENSHTUKIN, *Ber. deutsch. chem. Ges.*, **15**, 2512 (1882).
- 189a. H. S. W. MASSEY and E. H. S. BURHOP, *Electronic and Ionic Impact Phenomena*, Oxford (1952).
190. I. M. METTER, *Phys. Z. Sow.*, **12**, 233 (1937).
191. A. C. G. MITCHELL and M. W. ZEMANSKY, *Resonance Radiation and Excited Atoms*, Chap. 4, Cambridge (1934).
192. V. A. MIKHEL'SON, Collected Works, vol. 1, (*Novyi Agronom*), Moscow (1930); *Ann. Phys. Lpz.*, **37**, 1 (1889).
193. N. F. MOTT and H. S. W. MASSEY, *The Theory of Atomic Collisions*, 2nd Ed., Oxford (1949).
194. K. N. MOCHALOV, *Dokl. Akad. Nauk SSSR*, **96**, 553 (1954).
195. I. V. MOCHAN, S. Z. ROGINSKII, F. FEDOROV and A. B. SHEKHTER, *Dokl. Akad. Nauk SSSR*, **2**, 365 (1934).
196. Ch. K. MUKHTAROV, Thesis, Moscow Inst. of Phys. and Engng. (1956).
197. M. F. NAGIYEV, Z. G. PETROVA and A. I. SULTANOVA, *Dokl. Akad. Nauk SSSR*, **109**, 573 (1956).
198. A. B. NALBANDYAN, *Acta Phys.-Chim. URSS*, **1**, 305 (1934).

199. A. B. NALBANDYAN, Thesis, Inst. of Chem. Phys., Acad. Sci. U.S.S.R., Moscow, **20**, 1259 (1946).
200. A. B. NALBANDYAN, *J. Phys. Chem., Moscow*, **20**, 1283 (1946).
201. A. B. NALBANDYAN, *J. Phys. Chem., Moscow*, **19**, 210 (1945).
202. A. B. NALBANDYAN, *Dokl. Akad. Nauk SSSR*, **60**, 607 (1948); *J. Phys. Chem., Moscow*, **22**, 1443 (1948).
203. A. B. NALBANDYAN and V. V. VOEVODSKII, *Mechanism of the Oxidation and Combustion of Hydrogen* (*Mekhanizm Okisleniya i Goreniya Vodoroda*), Acad. Sci. U.S.S.R., Moscow-Leningrad (1949).
204. A. B. NALBANDYAN and S. M. SHUBINA, *J. Phys. Chem., Moscow*, **20**, 1249 (1946).
205. M. B. NEIMAN, *Acta Phys.-Chim. URSS*, **9**, 527 (1938).
206. M. B. NEIMAN, A. A. DOBRINSKAYA, and V. I. GNYUBKIN, *The Mechanism of the Formation of the Cool Flame of Butane* (*Mekhanizm Obrazovaniya Kholodnogo Plameni Butana*), Zelinskii Univ., Moscow, (1940).
207. M. B. NEIMAN, A. F. LUKOVNIKOV, and G. I. FEKLISOV, in *Problems of Chemical Kinetics, Catalysis and Reactivity* (*Sb. Voprosy Khimicheskoi Kinetiki, Kataliza i Reaktsionnoi Sposobnosti*), p. 184, Acad. Sci. U.S.S.R., Moscow (1955).
208. M. B. NEIMAN and E. I. POPOV, *C.R. Acad. Sci., Paris*, **245**, 1234 (1957).
209. M. B. NEIMAN, A. F. LUKOVNIKOV and G. I. FEKLISOV, *Zh. Obshch. Khim.*, **25**, 1317 (1955).
210. M. B. NEIMAN and G. I. FEKLISOV, *Dokl. Akad. Nauk SSSR*, **91**, 1137 (1953); M. B. NEIMAN, *J. Phys. Chem., Moscow*, **28**, 1235 (1954).
211. B. S. NEPORENT, *J. Phys. Chem., Moscow*, **13**, 965 (1939).
212. B. S. NEPORENT, *J. Phys. Chem., Moscow*, **21**, 1111 (1947); **24**, 1219 (1950).
213. G. G. NEUIMIN and B. N. POPOV, *Z. phys. Chem., B* **27**, 15 (1934).
214. G. G. NEUIMIN and A. N. TERENIN, *Izv. Akad. Nauk (Phys.)*, No. 4, 529 (1936).
- 214a. E. E. NIKITIN, *Dokl. Akad. Nauk SSSR*, **116**, 584 (1957). (trans. *Soviet Phys. Dokl.*, **2**, 453 (1957)).
- 214b. E. E. NIKITIN, *Dokl. Akad. Nauk SSSR*, **119**, 526 (1958).
- 214c. E. E. NIKITIN and N. D. SOKOLOV, *J. Chem. Phys.*, **31**, 1371 (1959).
- 214d. E. E. NIKITIN and N. D. SOKOLOV, *Dokl. Akad. Nauk SSSR*, **124**, 366 (1959).
215. I. V. OBREIMOV, *J. Exp. Theor. Phys.*, **19**, 396 (1949).
216. D. S. PAVLOV, N. N. SEMENOV and N. M. EMANUEL', *Izv. Akad. Nauk (Otd. Khim. N.)*, 98 (1942).
- 216a. V. A. POLTORAK and V. V. VOEVODSKII, *Dokl. Akad. Nauk SSSR*, **91**, 589 (1953).
217. M. V. POLYAKOV, *Naturwissenschaften*, **15**, 539 (1927).
218. M. V. POLYAKOV, in *Problems of Chemical Kinetics, Catalysis and Reactivity* (*Sb. Voprosy Khimicheskoi Kinetiki, Kataliza i Reaktsionnoi Sposobnosti*), p. 368, Acad. Sci. U.S.S.R., Moscow (1955).
219. N. A. PRILEZHAEVA, *J. Phys. Chem., Moscow*, **5**, 1239 (1934).
- 219a. S. YA. PSHEZHETSKII and M. T. DMITRIEV, *Usp. Khim.*, **26**, 725 (1957).
220. G. A. RAZUVAEV, in *Problems of Chemical Kinetics, Catalysis and Reactivity* (*Sb. Voprosy Khimicheskoi Kinetiki, Kataliza i Reaktsionnoi Sposobnosti*), p. 790, Acad. Sci. U.S.S.R., Moscow (1955).
221. G. A. RAZUVAEV, G. P. PETUKHOV, A. F. REKASHEVA and G. P. MIKLUKHIN, *Dokl. Akad. Nauk SSSR*, **90**, 569 (1953); G. P. MIKLUKHIN and A. F. REKASHEVA, in *Problems of Chemical Kinetics, Catalysis and Reactivity* (*Sb. Voprosy Khimicheskoi Kinetiki, Kataliza i Reaktsionnoi Sposobnosti*), p. 24, Acad. Sci. U.S.S.R., Moscow (1955).
222. F. O. RICE and K. K. RICE, *The Aliphatic Free Radicals*, Johns Hopkins Press, Baltimore (1935).
223. M. A. RIVIN, A. S. SOKOLIK, *J. Phys. Chem., Moscow*, **7**, 571 (1936); **8**, 767 (1936); **10**, 692 (1937); M. A. RIVIN, R. BRESKER and A. S. SOKOLIK *J. Phys. Chem., Moscow*, **10**, 688 (1937).
- 223a. K. I. ROZGACHEV and V. A. FABRIKANT, *Dokl. Akad. Nauk SSSR*, **114**, 528 (1957).

224. A. I. ROZLOVSKII, Summary of thesis, Karpov Inst. of Phys. Chem., Moscow, (1956).
225. YU. N. RYABININ, A. M. MARKEVICH and I. I. TAMM, *Dokl. Akad. Nauk SSSR*, **112**, 283 (1957).
226. YU. N. RYABININ, A. M. MARKEVICH, and I. I. TAMM *J. Phys. Chem., Moscow*, **32**, 2242 (1958).
227. YU. N. RYABININ, *J. Exp. Theor. Phys.*, **23**, 461 (1952); see also V. G. KLYAZER Thesis, Inst. of Chem. Phys., Acad. Sci. U.S.S.R., Moscow, (1939); YU. B. KHARITON, N. M. REINOV and V. G. KLYAZER in *Scientific Research Work by the Chemistry Institutes and Laboratories of the Acad. Sci. U.S.S.R. for 1940* (*Sb. Nauchno-Issledovatel'skiye Raboty Khimicheskikh Institutov i Laboratori Akad. nauk SSSR za 1940*), p. 121 (1940).
228. YU. S. SAYASOV, *Dokl. Akad. Nauk SSSR*, **113**, 548 (1957); *Ann der Phys.*, **6**, 1 (1960).
- 228a. YU. S. SAYASOV and A. B. VASIL'eva, *J. Phys. Chem., Moscow*, **29**, 802 (1955).
229. M. F. SEDOVA and N. M. EMANUEL', *Izv. Akad. Nauk (Otd. Khim. N.)* No. 6, 658 (1956).
230. N. N. SEMENOV, *Z. Phys.*, **46**, 109 (1927).
231. N. N. SEMENOV, *Z. Phys.*, **48**, 571 (1928).
232. N. N. SEMENOV, *Tsepnyye Reaktsii*. Goskhimtekhizdat, Leningrad (1934); *Chemical Kinetics and Gas Reactions*, Oxford (1935).
233. N. N. SEMENOV, *Usp. Phys. Nauk*, **24**, 433 (1940).
234. N. N. SEMENOV, *Acta Phys.-Chim. URSS*, **18**, 93 (1943).
235. N. N. SEMENOV, *J. Phys. Chem., Moscow*, **17**, 187 (1943).
236. N. N. SEMENOV, *Dokl. Akad. Nauk SSSR*, **43**, 360 (1944).
237. N. N. SEMENOV, *Acta Phys.-Chim. URSS*, **20**, 291 (1945).
238. N. N. SEMENOV, *Usp. Khim.*, **20**, 673 (1951).
239. N. N. SEMENOV, *Usp. Khim.*, **21**, 641 (1952).
240. N. N. SEMENOV, *Izv. Akad. Nauk SSSR, Otdel Tekh. Nauk*, No. 5, 708 (1953).
241. N. N. SEMENOV, *O Nekotorykh Problemakh Khimicheskoi Kinetiki i Reakstionnoi Sposobnosti*. Acad. Sci. U.S.S.R., Moscow (1954); English translation *Some Problems of Chemical Kinetics and Reactivity*, Pergamon Press (1959).
242. I. V. SMIRNOV-ZAMKOV and E. A. SHILOV, *Dokl. Akad. Nauk SSSR*, **67**, 671 (1949).
243. R. M. SMIRNOVA, Thesis, Karpov Inst. of Phys. Chem., Moscow (1954).
244. A. S. SOKOLIK, *Usp. Khim.*, **7**, 976 (1938).
245. A. S. SOKOLIK and K. I. SHCHELKIN, *J. Phys. Chem., Moscow*, **5**, 1459 (1934).
246. A. S. SOKOLIK, S. A. YANTOVSKII, *Acta Phys.-Chim. URSS*, **19**, 329 (1944); *J. Phys. Chem., Moscow*, **20**, 13 (1946); A. S. SOKOLIK, M. YA. GEN and S. A. YANTOVSKII, *J. Phys. Chem., Moscow*, **21**, 1263 (1947).
247. N. D. SOKOLOV, *Usp. Phys. Nauk*, **57**, 205 (1955); *Zh. Khim. Ukr.*, **22**, 19 (1956).
248. N. D. SOKOLOV, *Dokl. Akad. Nauk SSSR*, **112**, 710 (1957).
249. A. D. STEPUKHOVICH, *Dokl. Akad. Nauk SSSR*, **92**, 127 (1953).
250. A. D. STEPUKHOVICH, *Usp. Khim.*, **25**, 263 (1956).
251. A. D. STEPUKHOVICH and V. V. TATARINTSEV, *Dokl. Akad. Nauk SSSR*, **99**, 1049 (1954).
252. A. D. STEPUKHOVICH and L. M. TIMONIN, *J. Phys. Chem., Moscow*, **26**, 145 (1952).
253. A. D. STEPUKHOVICH and YE. I. ETINGOF, *Dokl. Akad. Nauk SSSR*, **99**, 815 (1954).
254. A. L. STOLOV, Thesis, Kazan Univ. (1956).
255. H. A. STUART, *Die Struktur des freien Moleküls*, Springer-Verlag, Berlin (1952).
- 255a. R. B. TAGIROV, *J. Phys. Chem., Moscow*, **30**, 949 (1956).
- 255b. R. B. TAGIROV and I. P. SHEVCHUK, *Dokl. Akad. Nauk SSSR*, **116**, 797 (1957).
256. V. L. TAL'ROZE, Thesis, Inst. of Chem. Phys., Acad. Sci. U.S.S.R., Moscow (1952); V. L. TAL'ROZE, A. K. LYUBIMOVA, *Dokl. Akad. Nauk SSSR*, **86**, 909 (1952).
- 256a. V. L. TAL'ROZE, *Proc. 1st All-Union Conf. on Radiation Chem. (Trud. 1-ogo vsesoyuz. Soveshch. po Radiats. Khim.)*, p. 13, Acad. Sci. U.S.S.R., Moscow (1958).
257. V. L. TAL'ROZE and YE. L. FRANKEVICH, *Dokl. Akad. Nauk SSSR*, **111**, 376 (1956).
258. M. I. TEMKIN, *J. Phys. Chem., Moscow*, **14**, 1054 (1940).

259. M. I. TEMKIN, "The Activated Complex" Appendix 1 to N. N. SEMENOV, *O Nekotorykh Problemakh Khimicheskoi Kinetiki i Reaktsionnoi Sposobnosti*, Acad. Sci. U.S.S.R., Moscow (1954). English trans. as Ref. 241 above.
260. A. N. TERENIN, *Z. phys.*, **37**, 98 (1926); *Naturwissenschaften*, **15**, 73 (1927); *Z. phys.*, **44**, 713 (1927); *Trud. GOI* (Trans. State Optical Inst.), No. 40 (1928); *The Photochemistry of the Vapours of Salts (Fotokhimiya Parov Solei)*, Gostekhretzdat, Moscow-Leningrad (1934).
261. A. N. TERENIN, *Phys. Rev.*, **36**, 147 (1930); A. N. TERENIN and B. POPOV, *Z. Phys.*, **75**, 338 (1932); *Phys. Z. Sow.*, **2**, 299 (1932).
262. A. N. TERENIN, *The Photochemistry of Dyes and Allied Organic Compounds (Fotokhimiya Krasitelei i Rodstvennykh Organicheskikh Soyedinenii)*, Acad. Sci. U.S.S.R., Moscow-Leningrad (1947).
263. A. N. TERENIN and G. G. NEUIMIN, *Nature*, **134**, 255 (1934).
264. A. N. TERENIN and G. G. NEUIMIN, *Acta Phys.-Chim. URSS*, **16**, 257 (1942).
265. A. N. TERENIN and N. A. PRILEZHAEVA, *Phys. Z. Sow.*, **2**, 337 (1932).
266. N. N. TIKHOMIROVA and V. V. VOEVODSKII, *Dokl. Akad. Nauk SSSR*, **79**, 993 (1951); *Canad. Nat. Res. Council*, TT-260 (1951).
267. O. M. TODES, *J. Phys. Chem., Moscow*, **13**, 868 (1939); O. M. TODES and P. V. MELENT'EV, *J. Phys. Chem., Moscow*, **13**, 1594 (1939); *ibid.* **14**, 1026 (1940).
268. V. I. URIZKO and M. V. POLYAKOV, *Dokl. Akad. Nauk Ukr. SSR*, 397 (1953); *Dokl. Akad. Nauk SSSR*, **95**, 1239 (1954).
269. V. A. FABRIKANT, F. A. BUTAEVA and I. TSIRG, *J. Exp. Theor. Phys.*, **8**, 35 (1938).
270. V. A. FABRIKANT and K. PANEVKA, *Dokl. Akad. Nauk SSSR*, **20**, 441 (1938).
271. R. H. FOWLER and E. A. GUGGENHEIM, *Statistical Thermodynamics*, Ch. XII, Cambridge (1940).
- 271a. T. V. FEDOROVA, A. P. BALLOD, A. V. TOPCHIYEV and V. YA. SHTERN, *Dokl. Akad. Nauk SSSR*, **123**, 860 (1958).
272. H. FEHLING and T. LESER, *Third Symposium on Combustion*, p. 634, Williams and Wilkins, Baltimore (1949).
273. E. FERMI, *Molecole e cristalli*, Bologna, Nicola Zanichelli (1934).
- 273a. A. M. FOGEL' and L. I. KRUPNIN, *J. Exp. Theor. Phys.*, **21**, 209 (1955).
274. N. V. FOK and A. B. NALBANDYAN, in *Problems of Chemical Kinetics, Catalysis and Reactivity* (Sb. *Voprosy Khimicheskoi Kinetiki, Kataliza i Reaktsionnoi Sposobnosti*), p. 219, Acad. Sci. U.S.S.R., Moscow (1955).
275. D. A. FRANK-KAMENETSKII, *J. Chem. Phys. Moscow*, **13**, 738 (1939); *Acta Phys.-Chim. URSS*, **10**, 365 (1939); **16**, 357 (1942); **20**, 729 (1945).
276. D. A. FRANK-KAMENETSKII, *Dokl. Akad. Nauk SSSR*, **25**, 672 (1939); *J. Phys. Chem., Moscow*, **14**, 30 (1940).
277. D. A. FRANK-KAMENETSKII, Editorial addendum to Russian trans. of B. LEWIS and G. VON ELBE: *Combustion, Flames and Explosions of Gases*, p. 286, For. Lit. Publ. House, Moscow (1948). See (174).
278. D. A. FRANK-KAMENETSKII, *Diffuziya i Teploperedacha v Khimicheskoi Kinetike*. Acad. Sci. U.S.S.R., Moscow-Leningrad (1947); English translation published as *Diffusion and Heat Exchange in Chemical Kinetics*, Princeton Univ. (1955).
279. YE. L. FRANKEVICH, Thesis, Inst. of Chem. Phys., Acad. Sci. U.S.S.R., Moscow (1957).
280. G. FRIEDLANDER and J. W. KENNEDY, *Introduction to Radiochemistry* (1949). Revised and republished as "Nuclear and Radiochemistry", New York, Wiley and London, Chapman and Hall (1955).
281. S. E. FRISH and I. P. ZAPESOCHNYI, *Dokl. Akad. Nauk SSSR*, **95**, 971 (1954).
- 281a. S. E. FRISH and I. P. ZAPESOCHNYI, *Izv. Akad. Nauk (Phys.)*, **19**, 5 (1955).
282. S. E. FRISH and YU. M. KAGAN, *Izv. Akad. Nauk (Phys.)*, **9**, 238 (1945).
283. N. A. FUKS, *Usp. Khim.*, **25**, 845 (1956).
284. YU. B. KHARITON and Z. F. VAL'TA, *Z. Phys.*, **39**, 547 (1926).
285. A. M. CHAIKIN, Summary of thesis, Moscow Univ. (1955).
286. N. YA. CHERNYAK and V. YA. SHTERN, *Dokl. Akad. Nauk SSSR*, **78**, 91 (1951).
287. N. M. CHIRKOV, *Acta Phys.-Chim. URSS*, **6**, 915 (1937).

REFERENCES

288. F. I. SHEMYAKIN, D. S. MITSLOVSKII and D. V. ROMANOV, in *Chromatographic Analysis* (*Sb. Khromatograficheskii Analiz*), Goskhimizdat, Moscow (1955).
289. A. B. SHEKHTER, *Z. Phys.*, **75**, 671 (1932); N. N. SEMENOV and A. B. SHEKHTER, *Nature*, **126**, 436 (1930).
290. A. B. SHEKHTER, *Chemical Reactions in Electric Discharge* (*Khimicheskiye Reaktsii v Elektricheskem Razryade*), Onti, Leningrad-Moscow (1935).
291. A. B. SHEKHTER, *Acta Phys.-Chim. URSS*, **10**, 379 (1939).
292. A. B. SHEKHTER, *Izv. Akad. Nauk (Otd. Khim. N.)* No. 4, 493 (1940).
293. A. E. SHILOV, Thesis, Inst. of Chem. Phys., Acad. Sci. U.S.S.R., Moscow (1955).
294. A. E. SHILOV, *Dokl. Akad. Nauk SSSR*, **98**, 601 (1954).
295. E. A. SHILOV, in *Problems of the Mechanism of Organic Reactions* (*Sb. Voprosy Mekhanizma Organicheskikh Reaktsii*), p. 7, Kiev (1953).
296. E. A. SHILOV, *Dokl. Akad. Nauk SSSR*, **18**, 643 (1938); **30**, 219 (1941).
297. E. A. SHILOV, in *Problems of Chemical Kinetics, Catalysis and Reactivity* (*Sb. Voprosy Khimicheskoi Kinetiki, Kataliza i Reaktsionnoi Sposobnosti*), p. 749, Acad. Sci. U.S.S.R., Moscow (1955).
298. N. A. SHILOV, *Conjugated Reactions of Oxidation* (*O Sopryazhennykh Reaktsiyakh Okisleniya*), Moscow (1905).
299. V. YA. SHTERN, in *Problems of Chemical Kinetics, Catalysis and Reactivity* (*Sb. Voprosy Khimicheskoi Kinetiki, Kataliza i Reaktsionnoi Sposobnosti*), p. 197, Acad. Sci. U.S.S.R., Moscow (1955).
300. V. YA. SHTERN and S. S. POLYAK, *Dokl. Akad. Nauk SSSR*, **65**, 311 (1949); S. S. POLYAK, V. YA. SHTERN, *J. Phys. Chem., Moscow*, **27**, 341 (1953).
301. V. YA. SHTERN and S. S. POLYAK, *Dokl. Akad. Nauk SSSR*, **66**, 235 (1949); V. YA. SHTERN and S. S. POLYAK, *J. Phys. Chem., Moscow*, **27**, 631 (1953).
302. K. I. SHCHELKIN, *Dokl. Akad. Nauk SSSR*, **23**, 636 (1939).
303. K. I. SHCHELKIN, *J. Tech. Phys., Moscow*, **13**, 520 (1943).
304. H. EYRING, J. WALTER and G. KIMBALL, *Quantum Chemistry*, New York, Wiley; and London, Chapman and Hall (1944).
305. N. M. EMANUEL', *J. Phys. Chem., Moscow*, **14**, 863 (1940).
306. N. M. EMANUEL', *Dokl. Akad. Nauk SSSR*, **95**, 603 (1954); in *Problems of Chemical Kinetics, Catalysis and Reactivity* (*Sb. Voprosy Khimicheskoi Kinetiki, Kataliza i Reaktsionnoi Sposobnosti*), p. 117, Acad. Sci. U.S.S.R., Moscow (1955).
307. A. VON ENGEL and M. STEENBECK, *Elektrische Gasentladungen, ihre Physik und Technik*, Vol. I, Springer, Berlin (1933).
308. B. M. YAVORSKII, *Izv. Akad. Nauk (Phys.)*, **9**, 233 (1945).
309. B. M. YAVORSKII, *Dokl. Akad. Nauk SSSR*, **48**, 185 (1945); **51**, 267 (1946).
310. A. V. YAKOVLEVA, *Acta Phys.-Chim. URSS*, **1**, 296 (1934).
- 310a. J. ADAM, S. DU SOLEIL and P. GOLDFINGER, *Bull. Soc. Chim. Belg.*, **65**, 942 (1956).
311. G. K. ADAMS and G. W. STOCKS, *Fourth Symposium on Combustion*, p. 239, Baltimore, (1953).
312. A. J. AHEARN and N. B. HANNAY, *J. Chem. Phys.*, **21**, 119 (1953).
313. E. A. ALEXANDER and J. D. LAMBERT, *Proc. Roy. Soc., A* **179**, 499 (1942).
314. P. E. M. ALLEN, H. W. MELVILLE and J. C. ROBB, *Proc. Roy. Soc., A* **218**, 311 (1953).
315. H. N. ALYEY and F. HABER, *Z. phys. Chem.*, **B 10**, 193 (1930).
316. I. AMDUR, *J. Amer. Chem. Soc.*, **57**, 856 (1935).
317. I. AMDUR, *J. Amer. Chem. Soc.*, **60**, 2347 (1938).
318. I. AMDUR and A. L. ROBINSON, *J. Amer. Chem. Soc.*, **55**, 1395 (1933).
319. T. AMEMIYA, *J. Soc. Chem. Ind. Japan*, **41**, 11, Suppl. bind. 371-B (1938).
320. R. AMME and S. LEGVOLD, *J. Chem. Phys.*, **26**, 514 (1957).
321. H. C. ANDERSON and E. R. VAN ARTSDALEN, *J. Chem. Phys.*, **12**, 479 (1944).
- 321a. J. M. ANDERSON, *Proc. Phys. Soc., A* **70**, 887 (1957).
- 321b. J. M. ANDERSON, A. V. KAVADAS and R. M. MCKAY, *Proc. Phys. Soc., A* **70**, 877 (1957).
322. J. M. ANDERSON and L. GOLDSTEIN, *Phys. Rev.*, **102**, 388 (1956).
323. E. T. S. APPLEYARD, *Proc. Roy. Soc., A* **128**, 330 (1930).

324. E. A. ARDEN and J. POWLING, *Sixth Symposium on Combustion*. p. 177, N.Y., (1957).
325. L. B. ARNOLD JR. and G. B. KISTIAKOWSKY, *J. Chem. Phys.*, **1**, 166 (1933).
326. F. L. ARNOT and G. O. BAINES, *Proc. Roy. Soc., A* **151**, 256 (1935).
327. F. L. ARNOT and W. D. HART, *Proc. Roy. Soc., A* **171**, 383 (1939).
328. H. AROESTE, *J. Chem. Phys.*, **21**, 870 (1953).
329. S. ARRHENIUS, *Z. phys. Chem.*, **4**, 226 (1889).
330. J. R. ARTHUR and D. H. NAPIER, *Fifth Symposium on Combustion*. p. 303, N.Y., (1955).
331. A. B. ASH and H. C. BROWN, *Record Chem. Progress*, **9**, 81 (1948).
332. P. G. ASHMORE and J. CHANMUGAM, *Trans. Faraday Soc.*, **49**, 254 (1953).
333. P. G. ASHMORE and J. CHANMUGAM, *Trans. Faraday Soc.*, **49**, 265 (1953).
334. P. G. ASHMORE and J. CHANMUGAM, *Trans. Faraday Soc.*, **49**, 270 (1953).
335. B. ATKINSON and A. B. TRENWITH, *J. Chem. Soc.*, 2082 (1953).
336. W. H. AVERY, *Fifth Symposium on Combustion*. p. 86, N.Y. (1955).
337. D. W. E. ALEXANDER and R. G. W. NORRISH, *Nature*, **160**, 537 (1947); R. G. W. NORRISH, *Nature*, **162**, 367 (1948); A. J. HARDING and R. G. W. NORRISH, *Nature*, **163**, 797 (1949).
338. P. J. AYMONINO, J. E. SICRE and H. J. SCHUMACHER, *J. Chem. Phys.*, **22**, 756 (1954).
- 338a. P. B. AYSCOUGH, *J. Chem. Phys.*, **24**, 944 (1956).
339. P. B. AYSCOUGH and E. W. R. STEACIE, *Canad. J. Chem.*, **34**, 103 (1956).
340. R. A. BACK, M. MENZIES and C. A. WINKLER, *Canad. J. Chem.*, **32**, 399 (1954).
341. R. A. BACK and C. A. WINKLER, *Canad. J. Chem.*, **32**, 718 (1954).
342. A. BAEYER, *Ann. Chem. Pharm.*, **103**, 178 (1857).
343. H. C. BAILEY and R. G. W. NORRISH, *Proc. Roy. Soc., A* **212**, 311 (1952).
- 343a. E. J. BAIR, J. T. LUND and P. C. CROSS, *J. Chem. Phys.*, **24**, 961 (1956).
344. R. R. BALDWIN, N. S. CORNEY and R. F. SIMMONS, *Fifth Symposium on Combustion*, p. 502, N.Y. (1955).
345. R. S. BARKER, R. L. SNOW and H. EYRING, *J. Chem. Phys.*, **23**, 1686 (1955).
346. J. BARR and B. P. MULLINS, *Fuel*, **28**, 181, 225 (1949); J. BARR, *Fuel*, **28**, 200 (1949); B. P. MULLINS, *Fuel*, **28**, 205 (1949).
347. E. BARTHOLOMÉ, *Naturwissenschaften*, **36**, 171 (1949).
348. E. BARTHOLOMÉ, *Naturwissenschaften*, **36**, 206 (1949).
349. E. BARTHOLOMÉ and H. SACHSSE, *Z. Elektrochem.*, **53**, 326 (1949).
350. M. R. BARUSCH, H. W. CRANDALL, J. Q. PAYNE and J. R. THOMAS, *Industr. Engng. Chem. (Industr.)*, **43**, 2764 (1951); M. R. BARUSCH, J. T. NEU, J. Q. PAYNE and J. R. THOMAS, *Industr. Engng. Chem. (Industr.)*, **43**, 2766 (1951).
351. D. R. BATES, *Phys. Rev.*, **77**, 718 (1950).
352. D. R. BATES, *Proc. Phys. Soc., A* **68**, 344 (1955).
353. D. R. BATES, A. FUNDAMINSKY, J. W. LEECH and H. S. W. MASSEY, *Phil. Trans. Roy. Soc.*, **243**, 117 (1950); D. R. BATES, A. FUNDAMINSKY and H. S. W. MASSEY, *Phil. Trans. Roy. Soc.*, **243**, 93 (1950).
354. D. R. BATES and G. GRIFFING, *Proc. Phys. Soc., A* **66**, 961 (1953).
355. D. R. BATES and J. T. LEWIS, *Proc. Phys. Soc., A* **68**, 173 (1955).
356. D. R. BATES and H. S. W. MASSEY, *Phil. Trans. Roy. Soc., A* **239**, 269 (1943).
357. D. R. BATES and B. L. MOISEIWITSCH, *Proc. Phys. Soc., A* **67**, 805 (1954).
358. J. R. BATES, *J. Amer. Chem. Soc.*, **54**, 569 (1932).
359. J. R. BATES, *J. Amer. Chem. Soc.*, **55**, 426 (1933); *Proc. Nat. Acad. Sci.*, **19**, 81 (1933); *J. Chem. Phys.*, **1**, 457 (1933); *Chem. Rev.*, **17**, 401 (1935).
360. J. R. BATES and D. J. SALLEY, *J. Amer. Chem. Soc.*, **55**, 110 (1933).
361. E. BAUER, *Phys. Rev.*, **84**, 315 (1951).
362. E. BAUER, *Phys. Rev.*, **85**, 277, 707 (1952).
363. E. BAUER, *J. Chem. Phys.*, **23**, 1087 (1955).
364. E. BAUER and TA-YOU WU, *J. Chem. Phys.*, **21**, 726 (1953).
- 364a. E. BAUER and TA-YOU WU, *Canad. J. Phys.*, **34**, 1436 (1956).
365. C. E. H. BAWN and A. G. EVANS, *Trans. Faraday Soc.*, **31**, 1392 (1935).

- 365a. K. D. BAYES and G. B. KISTIAKOWSKY, *J. Chem. Phys.*, **29**, 949 (1958).
 366. K. BECHERT, *Ann. Phys.*, **4**, 191 (1949); **5**, 349 (1949); **7**, 113 (1950).
 367. R. BECKER, *Z. Phys.*, **8**, 321, (1922); *Z. Elektrochem.*, **42**, 457 (1936).
 368. J. C. BECKERLE, *J. Chem. Phys.*, **21**, 2034 (1953).
 369. O. BEECK and J. C. MOUZON, *Ann. Phys.*, **11**, 737, 858 (1931).
 370. H. BEHRENS, *Z. Phys. Chem.*, **199**, 1 (1952).
 371. L. BELCHETZ, *Trans. Faraday Soc.*, **30**, 170 (1934).
 372. L. BELCHETZ and E. K. RIDEAL, *J. Amer. Chem. Soc.*, **57**, 1168 (1935).
 373. R. P. BELL, *Proc. Roy. Soc., A* **139**, 466 (1933).
 373a. R. P. BELL, *Proc. Roy. Soc., A* **148**, 241 (1935).
 374. R. P. BELL, *Acid Base Catalysis*, Oxford (1941).
 375. R. P. BELL and E. F. CALDIN, *Trans. Faraday Soc.*, **47**, 50 (1951).
 376. T. N. BELL, P. L. ROBINSON and A. B. TRENWITH, *J. Chem. Soc.*, p. 1440 (1955).
 377. F. E. BELLES and C. O'NEAL, JR., *Sixth Symposium on Combustion*, p. 806 N.Y., (1957).
 378. P. BENDER, *Phys. Rev.*, **36**, 1535, 1543 (1930).
 379. S. W. BENSON, *J. Chem. Phys.*, **20**, 1064 (1952).
 380. S. W. BENSON, *J. Chem. Phys.*, **25**, 27 (1956).
 380a. S. W. BENSON and A. E. AXWORTHY, *J. Chem. Phys.*, **26**, 1718 (1957).
 381. S. W. BENSON and J. H. BUSZ, *J. Chem. Phys.*, **27**, 1382 (1957).
 382. S. W. BENSON and R. SRINIVASAN, *J. Chem. Phys.*, **23**, 200 (1955).
 383. J. A. BERBERET and K. C. CLARK, *Phys. Rev.*, **100**, 506 (1955).
 384. I. BERGER and G. SCHAY, *Z. phys. Chem.*, **B 28**, 332 (1935).
 385. F. BERGMANN and H. E. ESCHINAZI, *J. Amer. Chem. Soc.*, **65**, 1405 (1943).
 386. J. BERKOWITZ, W. A. CHUPKA and G. B. KISTIAKOWSKY, *J. Chem. Phys.*, **25**, 457 (1956).
 387. M. R. BERLIE and D. J. LE ROY, *J. Chem. Phys.*, **20**, 200 (1952); *Disc. Faraday Soc.*, **14**, 50 (1953).
 387a. M. R. BERLIE and D. J. LE ROY, *Canad. J. Chem.*, **32**, 650 (1954).
 388. R. B. BERNSTEIN, *J. Phys. Chem.*, **56**, 893 (1952).
 389. H. W. BERRY, R. N. VARNEY and S. NEWBERRY, *Phys. Rev.*, **61**, 63 (1942).
 390. M. BERTHELOT, *C.R. Acad. Sci., Paris*, **93**, 18 (1881).
 391. H. BEUTLER, *Z. Phys.*, **50**, 581 (1928); H. BEUTLER and E. RABINOWITSCH, *Z. Elektrochem.*, **35**, 623 (1929); *Z. phys. Chem.*, **B 8**, 231 (1930).
 392. H. BEUTLER and M. POLANYI, *Naturwissenschaften*, **13**, 711 (1925).
 393. H. BEUTLER and M. POLANYI, *Z. phys. Chem.*, **B 1**, 3 (1928).
 394. H. BEUTLER and M. POLANYI, *Z. Phys.*, **47**, 379 (1928).
 395. H. BEUTLER and E. RABINOWITSCH, *Z. phys. Chem.*, **B 8**, 403 (1930).
 395a. J. C. BEVINGTON, *Proc. Roy. Soc., A* **239**, 420 (1957).
 396. J. BIGELEISEN, *J. Chem. Phys.*, **17**, 675 (1949).
 397. J. BIGELEISEN, *J. Phys. Chem.*, **56**, 823 (1952).
 398. J. BIGELEISEN and M. GOEPPERT-MAYER, *J. Chem. Phys.*, **15**, 261 (1947).
 399. J. BIGELEISEN and M. WOLFSBERG, *J. Chem. Phys.*, **21**, 1972 (1953).
 400. M. A. BIONDI, *Phys. Rev.*, **83**, 653 (1951).
 401. M. A. BIONDI, *Phys. Rev.*, **83**, 1078 (1951).
 402. M. A. BIONDI, *Phys. Rev.*, **84**, 1072 (1951).
 403. M. A. BIONDI, *Phys. Rev.*, **88**, 660 (1952).
 404. M. A. BIONDI, *Phys. Rev.*, **89**, 337 (1953).
 405. M. A. BIONDI, *Phys. Rev.*, **93**, 650 (1954).
 405a. M. A. BIONDI and R. E. FOX, *Phys. Rev.*, **109**, 2012 (1958).
 406. F. E. BLACET and W. E. BELL, *Disc. Faraday Soc.*, **14**, 70 (1953).
 406a. V. H. BLACKMAN, *Techn. rep. 11-20, NR 061-020*, Physics Department, Princeton University, May, 1955.
 406b. V. BLACKMAN, *J. Fluid Mech.*, **1**, 61 (1956).
 407. H. BLADES, A. T. BLADES and E. W. R. STEACIE, *Canad. J. Chem.*, **32**, 298 (1954).
 408. W. BLEAKNEY, *Phys. Rev.*, **36**, 1303 (1930).
 409. J. P. BLEWETT, *Phys. Rev.*, **49**, 900 (1936).

410. F. BLOCH and N. E. BRADBURY, *Phys. Rev.*, **48**, 689 (1935).
 411. R. BLOCHMANN, *Liebigs Ann.*, **168**, 295 (1873).
 412. E. G. BLOOM, F. L. MOHLER, J. H. LENGEL and C. E. WISE, *J. Res. Nat. Bur. St.*, **41**, 129 (1948).
 413. G. BOATO, G. CARERI, A. CIMINO, E. MOLINARI and G. G. VOLPI, *J. Chem. Phys.*, **24**, 783 (1956).
 414. M. BODENSTEIN, *Z. phys. Chem.*, **13**, 56 (1894); **22**, 1 (1897); **29**, 295 (1899).
 415. M. BODENSTEIN, *Z. phys. Chem.*, **85**, 329 (1913).
 416. M. BODENSTEIN, *Z. Elektrochem.*, **22**, 53 (1916).
 417. M. BODENSTEIN, *Z. Elektrochem.*, **24**, 183 (1918); *Z. phys. Chem.*, **100**, 68 (1922).
 418. M. BODENSTEIN and G. JUNG, *Z. phys. Chem.*, **121**, 127 (1926).
 419. M. BODENSTEIN and G. B. KISTIAKOWSKY, *Z. phys. Chem.*, **116**, 371 (1925).
 420. M. BODENSTEIN and H. LÜTKEMEYER, *Z. phys. Chem.*, **114**, 208 (1925).
 421. M. BODENSTEIN and M. RAMSTETTER, *Z. phys. Chem.*, **100**, 106 (1922).
 422. M. BODENSTEIN and P. W. SCHENK, *Z. phys. Chem.*, **B 20**, 420 (1933).
 423. VON ST. BOGDANDY and M. POLANYI, *Z. Elektrochem.*, **33**, 554 (1927).
 424. VON ST. BOGDANDY and M. POLANYI, *Z. phys. Chem.*, **B 1**, 21 (1928).
 425. K. F. BONHOEFFER, *Z. phys. Chem.*, **113**, 199, 492 (1924).
 426. K. F. BONHOEFFER, *Z. phys. Chem.*, **116**, 391 (1925); *Z. Elektrochem.*, **31**, 521 (1925); *Usp. Phys. Nauk* **8**, 61 (1928).
 427. K. F. BONHOEFFER and F. HABER, *Z. phys. Chem.*, **A 137**, 263 (1928); L. FARKAS, F. HABER and P. HARTECK, *Naturwissenschaften*, **18**, 266 (1930); F. HABER, *Naturwissenschaften*, **18**, 917 (1930).
 428. K. F. BONHOEFFER and P. HARTECK, *Z. phys. Chem.*, **A 139**, Haberband, 64 (1928).
 429. K. F. BONHOEFFER and H. REICHARDT, *Z. phys. Chem.*, **A 139**, 75 (1928).
 430. W. H. BOSTICK, W. W. STRIKER and M. F. GROVER, *Phys. Rev.*, **83**, 201 (1951).
 430a. M. BOUDART, *Northwestern University Second Biennial Gas Dynamics Symposium*, Evanston, (1957).
 431. M. BOUDART and J. T. DUBOIS, *J. Chem. Phys.*, **23**, 223 (1955).
 431a. C. E. H. BAWN and G. OGDEN, *Trans. Faraday Soc.*, **30**, 432 (1934).
 432. S. F. BOYS and J. CORNER, *Proc. Roy. Soc.*, **A 197**, 90 (1949).
 432a. J. N. BRADLEY, H. W. MELVILLE and J. C. ROBB, *Proc. Roy. Soc.*, **A 236**, 318, 333, 339 (1956).
 433. L. M. BRANSCOMB, *Phys. Rev.*, **86**, 258 (1952).
 434. L. M. BRANSCOMB, *Phys. Rev.*, **86**, 587 (1952).
 435. J. BRETON, *Ann. Off. nat. des combust. liq.*, **11**, 487 (1936).
 436. A. K. BREWER and J. W. WESTHAVER, *J. Phys. Chem.*, **33**, 883 (1929).
 437. A. K. BREWER and J. W. WESTHAVER, *J. Phys. Chem.*, **34**, 1280 (1930).
 438. A. K. BREWER and P. D. KUECK, *J. Phys. Chem.*, **35**, 1293 (1931).
 439. P. BRICOUT, *J. Phys. Radium*, (VI), **9**, 88 (1928).
 440. E. BRINER, W. PFEIFFER and G. MALET, *J. Chim. Phys.*, **21**, 25 (1924).
 440a. R. K. BRINTON, *J. Chem. Phys.*, **29**, 781 (1958).
 441. D. BRITTON and N. DAVIDSON, *J. Chem. Phys.*, **23**, 2461 (1955).
 442. D. BRITTON and N. DAVIDSON, *J. Chem. Phys.*, **25**, 810 (1956).
 443. D. BRITTON, N. DAVIDSON, W. GEHMAN and G. SCHOTT, *J. Chem. Phys.*, **25**, 804 (1956).
 444. D. BRITTON, N. DAVIDSON and G. SCHOTT, *Disc. Faraday Soc.*, **17**, 58 (1954).
 445. H. P. BROIDA, *Phys. Rev.*, **82**, 765 (1951).
 446. H. P. BROIDA, *J. Chem. Phys.*, **19**, 1383 (1951).
 447. H. P. BROIDA, *J. Chem. Phys.*, **21**, 1165 (1953).
 448. H. P. BROIDA and T. CARRINGTON, *J. Chem. Phys.*, **23**, 2202 (1955).
 449. H. P. BROIDA, A. J. EVERETT and G. J. MINKOFF, *Fuel*, **33**, 251 (1954).
 450. H. P. BROIDA and A. G. GAYDON, *Trans. Faraday Soc.*, **49**, 1190 (1953).
 451. H. P. BROIDA and W. R. KANE, *Phys. Rev.*, **89**, 1053 (1953).
 452. H. P. BROIDA and H. J. KOSTKOWSKI, *J. Chem. Phys.*, **25**, 676 (1956).
 452a. H. P. BROIDA and K. E. SHULER, *J. Chem. Phys.*, **27**, 933 (1957).
 453. J. BROSSEL, *Phys. Rev.*, **83**, 210 (1951).

454. J. BROSSEL and F. BITTER, *Phys. Rev.*, **86**, 308 (1952).
 455. R. BROUT, *J. Chem. Phys.*, **22**, 1189 (1954).
 456. R. BROUT, *J. Chem. Phys.*, **22**, 934 (1954).
 457. R. BROUT, *J. Chem. Phys.*, **22**, 1500 (1954).
 458. F. B. BROWN and R. H. CRIST, *J. Chem. Phys.*, **9**, 840 (1941).
 459. H. C. BROWN, M. S. KHARASCH and T. H. CHAO, *J. Amer. Chem. Soc.*, **62**, 3435 (1940).
 460. R. D. BROWN, *Quart. Rev.*, **6**, 63 (1952).
 461. H. BRUMBERGER and R. A. MARCUS, *J. Chem. Phys.*, **24**, 741 (1956).
 461a. R. B. BRYAN, R. B. HOLT and O. OLDEMBERG, *Phys. Rev.*, **106**, 83 (1957).
 462. W. A. BRYCE and K. U. INGOLD, *J. Chem. Phys.*, **23**, 1968 (1955).
 462a. R. BUCHDAHL, *J. Chem. Phys.*, **9**, 146 (1941).
 463. E. J. BUCKLER and R. G. W. NORRISH, *Proc. Roy. Soc.*, A **167**, 318 (1938).
 463a. R. P. BUCKLEY and M. SZWARC, *Proc. Roy. Soc.*, A **240**, 396 (1957); *J. Amer. Chem. Soc.*, **78**, 5697 (1956).
 463b. E. M. BULEWICZ, C. G. JAMES and T. M. SUGDEN, *Proc. Roy. Soc.*, A **235**, 89 (1956); E. M. BULEWICZ and T. M. SUGDEN, *Trans. Faraday Soc.*, **52**, 1475 (1956).
 463c. D. L. BUNKER and N. DAVIDSON, *J. Amer. Chem. Soc.*, **80**, 5085 (1958).
 463d. D. L. BUNKER and N. DAVIDSON, *J. Amer. Chem. Soc.*, **80**, 5090 (1958).
 464. R. W. BUNSEN and H. ROSCOE, *Phil. Trans.*, 381 (1857).
 465. F. BURHORN, *Z. Phys.*, **140**, 440 (1955).
 466. S. P. BURKE and T. E. W. SCHUMAN, *Industr. Engng. Chem. (Industr.)*, **20**, 998 (1928).
 467. G. M. BURNETT and H. W. MELVILLE, *Chem. Rev.*, **54**, 225 (1954).
 468. W. G. BURNS and F. S. DAITONT, *Trans. Faraday Soc.*, **48**, 39 (1952).
 469. W. G. BURNS and F. S. DAITONT, *Trans. Faraday Soc.*, **48**, 52 (1952).
 470. M. BURTON, *J. Amer. Chem. Soc.*, **60**, 212 (1938).
 471. M. BURTON and J. L. MAGEE, *J. Chem. Phys.*, **23**, 2194 (1955).
 472. E. T. BUTLER and M. POLANYI, *Trans. Faraday Soc.*, **39**, 19 (1943).
 473. J. F. BYRNE, *Sixth Symposium on Combustion*, p. 120, N.Y., (1957).
 474. A. C. BYRNS and G. K. ROLLEFSON, *J. Amer. Chem. Soc.*, **56**, 2245 (1934).
 475. R. D. CADLE and C. SCHADT, *J. Amer. Chem. Soc.*, **74**, 6002 (1952).
 476. R. D. CADLE and C. SCHADT, *J. Chem. Phys.*, **21**, 163 (1953).
 477. H. F. CALCOTE and I. R. KING, *Fifth Symposium on Combustion*, p. 423, N.Y., (1955).
 478. A. B. CALLEAR and R. J. CVETANOVIC, *J. Chem. Phys.*, **24**, 873 (1956).
 479. H. R. CALVERT, *Z. Phys.*, **78**, 479 (1932).
 479a. J. G. CALVERT and J. T. GRUVER, *J. Amer. Chem. Soc.*, **80**, 1313 (1958).
 479b. M. CAMAC, J. CAMM, S. FELDMAN, J. KECK and C. PETTY, *Chemical Relaxation in Air, Oxygen and Nitrogen*, prepr. No. 802, Inst. of Aer. Sci., (1956).
 480. E. S. CAMPBELL, *Sixth Symposium on Combustion*, p. 213, N.Y., (1957).
 480a. T. CARRINGTON and N. DAVIDSON, *J. Phys. Chem.*, **57**, 418 (1953).
 480a'. G. CARERI, *J. Chem. Phys.*, **21**, 749 (1953).
 480a''. G. CARERI, *Nuovo Cimento*, **6**, 94 (1949); **7**, 155 (1950).
 480b. T. R. CARSON, *Proc. Phys. Soc.*, A **67**, 909 (1954).
 480c. J. K. CASHION and J. C. POLANYI, *J. Chem. Phys.*, **29**, 455 (1958).
 481. G. W. CASTELLAN and H. M. HULBURT, *J. Chem. Phys.*, **18**, 312 (1950).
 482. T. M. CAWTHON and J. D. MCKINLEY, JR., *J. Chem. Phys.*, **25**, 585 (1956).
 483. T. S. CHAMBERS and G. B. KISTIAKOWSKY, *J. Amer. Chem. Soc.*, **56**, 399 (1934).
 484. D. L. CHAPMAN, *Phil. Mag.*, (VI), **47**, 90 (1899).
 485. S. CHAPMAN and T. G. COWLING, *The Mathematical Theory of Non-Uniform Gases*, p. 248, Cambridge (1939).
 486. *Chem. and Eng. News*, **31**, 246 (1953).
 487. M. CHIO CHEN and H. A. TAYLOR, *J. Chem. Phys.*, **27**, 857 (1957).
 488. J. A. CHRISTIANSEN and H. A. KRAMERS, *Z. phys. Chem.*, **104**, 451 (1923).
 489. M. I. CHRISTIE, A. J. HARRISON, R. G. W. NORRISH and G. PORTER, *Proc. Roy. Soc.*, A **231**, 446 (1955).

490. M. I. CHRISTIE, R. G. W. NORRISH and G. PORTER, *Proc. Roy. Soc., A* **216**, 152 (1953).
491. W. CHRISTOPH, *Ann. Phys.*, **23**, 51 (1935).
492. W. W. COBLENTZ, *Ann. Phys.*, **22**, 1 (1906).
493. A. COEHN and K. STUCKARDT, *Z. Phys. Chem.*, **91**, 722 (1916).
494. C. C. COFFIN and W. B. BEAZLEY, *Canad. J. Res.*, **15-B**, 229 (1937).
495. E. COLLINSON and A. J. SWALLOW, *Chem. Rev.*, **56**, 471 (1956).
496. R. CONRAD, *Trans. Faraday Soc.*, **30**, 215 (1934).
497. J. B. CONWAY, W. F. R. SMITH, W. J. LIDDELL and A. V. GROSSE, *J. Amer. Chem. Soc.*, **77**, 2026 (1955).
498. G. A. COOK and J. R. BATES, *J. Amer. Chem. Soc.*, **57**, 1775 (1935).
499. M. A. COOK, R. T. KEYES and A. S. FILLER, *Trans. Faraday Soc.*, **52**, 369 (1956).
500. S. D. COOLEY and R. C. ANDERSON, *Industr. Engng. Chem. (Industr.)*, **44**, 1402 (1952); *J. Amer. Chem. Soc.*, **77**, 235 (1955).
501. A. S. COOLIDGE, H. M. JAMES and R. D. PRESENT, *J. Chem. Phys.*, **4**, 193 (1936).
502. J. CORNER, *Proc. Roy. Soc., A* **198**, 388 (1949).
503. C. A. COULSON, *J. Chem. Soc.*, 1435 (1955).
504. G. R. COWAN and D. F. HORNING, *J. Chem. Phys.*, **18**, 1008 (1950).
505. G. R. COWAN, D. ROTENBERG, A. DOWNIE, B. CRAWFORD, JR. and R. A. OGG, JR., *J. Chem. Phys.*, **21**, 1397 (1953).
506. G. R. COWAN, EARL VINCENT and B. CRAWFORD, JR., *J. Opt. Soc. Amer.*, **43**, 710 (1953).
507. J. D. CRAGGS, R. THORNBURN and B. A. TOZER, *Proc. Roy. Soc., A* **240**, 473 (1957).
- 507a. L. CRANBERG, G. FRYE, N. NERESON and L. ROSEN, *Phys. Rev.*, **103**, 662 (1956).
508. R. W. CROMPTON and D. J. SUTTON, *Proc. Roy. Soc., A* **215**, 467 (1952).
509. W. CRUICKSHENK, *Nicholson's J.*, **5**, 201 (1801).
510. C. F. CULLIS and C. N. HINSHELWOOD, *Disc. Faraday Soc.*, **2**, 117 (1947).
511. J. CURRY and M. POLANYI, *Z. phys. Chem.*, **B 20**, 276 (1933); A. G. EVANS and H. WALKER, *Trans. Faraday Soc.*, **40**, 384 (1944).
512. C. F. CURTISS, Univ. of Wisconsin, Naval Res. Lab., CM 476, June 8th, 1948.
513. C. F. CURTISS, *J. Chem. Phys.*, **21**, 2045 (1953).
514. C. F. CURTISS and F. T. ADLER, *J. Chem. Phys.*, **20**, 249 (1952).
515. R. J. CVETANOVIĆ, *J. Chem. Phys.*, **23**, 1375 (1955); *Canad. J. Chem.*, **33**, 1684 (1955); *J. Chem. Phys.*, **25**, 376 (1956).
516. R. J. CVETANOVIĆ, *J. Chem. Phys.*, **23**, 1208 (1955).
517. R. J. CVETANOVIĆ, *Canad. J. Chem.*, **34**, 775 (1956).
- 517a. J. DAEN and R. A. MARCUS, *J. Chem. Phys.*, **26**, 162 (1957).
518. F. S. DAINTON, *J. Phys. Coll. Chem.*, **52**, 490 (1948).
- 518a. F. S. DAINTON and D. E. McELCHERAN, *Trans. Faraday Soc.*, **51**, 657 (1955); F. S. DAINTON, K. I. IVIN and F. WILKINSON, *Trans. Faraday Soc.*, **53**, 1204 (1957).
519. A. DALGARNO, *Proc. Phys. Soc., A* **67**, 1010 (1954).
520. G. DAMKÖHLER, *Z. Elektrochem.*, **46**, 601 (1940).
521. G. DAMKÖHLER, *Z. Elektrochem.*, **48**, 62, 116 (1942).
522. G. DAMKÖHLER and W. EGGERSGÜSS, *Z. phys. Chem.*, **B 51**, 157 (1942).
523. C. J. DANBY and C. N. HINSHELWOOD, *J. Chem. Soc.*, 464 (1940).
524. F. DANIELS and E. H. JOHNSTON, *J. Amer. Chem. Soc.*, **43**, 53 (1921).
525. B. DE B. DARWENT, *J. Chem. Phys.*, **18**, 1532 (1950).
526. B. DE B. DARWENT, *J. Chem. Phys.*, **20**, 1979 (1952).
527. B. DE B. DARWENT and F. G. HURTUBISE, *J. Chem. Phys.*, **20**, 1684 (1952).
528. B. DE B. DARWENT and M. K. PHIBBS, *J. Chem. Phys.*, **22**, 110 (1954).
529. B. DE B. DARWENT, M. K. PHIBBS and F. G. HURTUBISE, *J. Chem. Phys.*, **22**, 859 (1954).
530. B. DE B. DARWENT and R. ROBERTS, *Disc. Faraday Soc.*, **14**, 55 (1953).
531. B. DE B. DARWENT and E. W. R. STEACIE, *J. Chem. Phys.*, **16**, 381 (1948).
532. A. K. DATTA, *Z. Phys.*, **77**, 404 (1932).
533. N. DAVIDSON, R. MARSHALL, A. E. LARSH, JR. and T. CARRINGTON, *J. Chem. Phys.*, **19**, 1311 (1951).

534. K. G. DENBIGH, *Trans. Faraday Soc.*, **36**, 936 (1940).
535. A. F. DEVONSHIRE, *Proc. Roy. Soc.*, A **158**, 269 (1937).
536. M. J. S. DEWAR, *J. Amer. Chem. Soc.*, **74**, 3357 (1952).
536a. V. H. DIBELER, R. M. REESE and D. E. MANN, *J. Chem. Phys.*, **27**, 176 (1957).
536b. P. G. DICKENS and J. W. LINNETT, *Proc. Roy. Soc.*, A **243**, 84 (1957).
537. R. G. DICKINSON and N. P. NIES, *J. Amer. Chem. Soc.*, **57**, 2382 (1935).
538. R. G. DICKINSON and M. S. SHERILL, *Proc. Nat. Acad. Sci.*, **12**, 692 (1926).
539. J. A. DILLON, JR., W. F. SHERIDAN, H. D. EDWARDS and S. N. GHOSH, *J. Chem. Phys.*, **23**, 776 (1955).
540. O. DIMROTH, *Z. angew. Chem.*, **46**, 571 (1933).
541. J. R. DINGLE and D. J. LE ROY, *J. Chem. Phys.*, **18**, 1632 (1950).
542. H. B. DIXON, *Phil. Trans. Roy. Soc.*, **184**, 97 (1893); **200**, 315 (1903).
542a. G. DIXON-Lewis and J. W. LINNETT, *Trans. Faraday Soc.*, **49**, 756 (1953).
543. G. DIXON-Lewis and M. J. G. WILSON, *Trans. Faraday Soc.*, **47**, 1106 (1951).
544. R. E. DODD, *Trans. Faraday Soc.*, **47**, 56 (1951).
545. J. E. DOLAN, *Sixth Symposium on Combustion*, p. 787, N.Y., (1957).
546. B. L. DONNALLY and H. E. CARR, *Phys. Rev.*, **93**, 111 (1954).
546a. R. E. DONOVAN, *J. Chem. Phys.*, **27**, 324 (1957).
547. R. DÖPEL, *Ann. Phys.*, **16**, 1 (1933).
548. W. DÖRING, *Ann. Phys.*, **43**, 421 (1943).
549. A. E. DOUGLAS, *Astrophys. J.*, **114**, 466 (1951); K. CLUSIUS and A. E. DOUGLAS, *Canad. J. Phys.*, **32**, 319 (1954).
550. J. E. DOUGLAS, B. S. RABINOVITCH and F. S. LOONEY, *J. Chem. Phys.*, **23**, 315 (1955).
551. D. A. DOWS, E. WHITTLE and G. C. PIMENTEL, *J. Chem. Phys.*, **23**, 499 (1955).
552. J. T. DUBOIS, *J. Chem. Phys.*, **25**, 178 (1956).
553. R. E. DUFF and E. HOUSTON, *J. Chem. Phys.*, **23**, 1268 (1955).
554. G. L. DUGGER, *J. Amer. Chem. Soc.*, **72**, 5271 (1950); **73**, 2398 (1951).
555. G. L. DUGGER and D. M. SIMON, *Fourth Symposium on Combustion*, p. 336, Baltimore, (1957).
556. G. L. DUGGER, R. C. WEAST and S. HEIMEL, *Fifth Symposium on Combustion*, p. 589, N.Y., (1955).
557. E. DURAND, *J. Chem. Phys.*, **8**, 46 (1940).
558. R. J. DWYER, *J. Chem. Phys.*, **7**, 40 (1939).
559. R. J. DWYER and O. OLDEMBERG, *J. Chem. Phys.*, **12**, 351 (1944).
560. C. ECKART, *Phys. Rev.*, **35**, 1303 (1930).
561. B. H. ECKSTEIN, H. A. SCHERAGA and E. R. VAN ARTSDALEN, *J. Chem. Phys.*, **22**, 28 (1954).
561a. H. EDELS and D. WHITTAKER, *Proc. Roy. Soc.*, A **240**, 54 (1957); D. WHITTAKER and H. EDELS, *Nature*, **177**, 484 (1956).
562. R. EDSE, *Third Symposium on Combustion*, p. 611, Baltimore, (1949).
563. A. EGERTON, G. J. MINKOFF and K. C. SALOOJA, *Proc. Roy. Soc.*, A **235**, 158 (1956).
564. A. EGERTON and L. M. PIDGEON, *Proc. Roy. Soc.*, A **142**, 26 (1933).
565. A. W. EHLER and G. L. WEISSLER, *Phys. Rev.*, **98**, 561 (1955).
566. A. EINSTEIN, *Sitzungsber. preuss. Akad. Wiss.*, 380 (1920).
567. O. EISENHUT and R. CONRAD, *Z. Elektrochem.*, **36**, 654 (1930).
568. G. VON ELBE, *Fifth Symposium on Combustion*, p. 79, N.Y., (1955).
569. G. C. ELTENTON, *J. Chem. Phys.*, **10**, 403 (1942); **15**, 455 (1947); *J. Phys. Coll. Chem.*, **52**, 463 (1948); *Rev. Inst. Fr. Pétr. et Ann. Comb. liq.*, **4**, 468 (1949).
570. C. ENER, A. BUSALA and J. C. HUBBARD, *J. Chem. Phys.*, **23**, 155 (1955).
571. H. ESSEX, *J. Phys. Chem.*, **58**, 42 (1954).
572. A. EUCKEN and S. AYBAR, *Z. phys. Chem.*, B **46**, 195 (1940).
573. A. EUCKEN and R. BECKER, *Z. phys. Chem.*, B **20**, 467 (1933).
574. A. EUCKEN and R. BECKER, *Z. phys. Chem.*, B **27**, 235 (1934); A. EUCKEN, *Oester. Chem. Ztg.*, **38**, 162 (1935).
575. A. EUCKEN and H. JAACKS, *Z. phys. Chem.*, B **30**, 85 (1935); A. EUCKEN, E. NÜMANN, *Z. phys. Chem.*, B **36**, 163 (1937).

576. H. G. V. EVANS, G. R. FREEMAN and C. A. WINKLER, *Canad. J. Chem.*, **34**, 1271 (1956).
577. H. G. V. EVANS and C. A. WINKLER, *Canad. J. Chem.*, **34**, 1217 (1956).
578. M. G. EVANS, *J. Chem. Phys.*, **2**, 445 (1934).
579. M. G. EVANS and M. POLANYI, *Trans. Faraday Soc.*, **31**, 875 (1935).
580. M. G. EVANS and M. POLANYI, *Trans. Faraday Soc.*, **32**, 1333 (1936).
581. M. G. EVANS and M. POLANYI, *Trans. Faraday Soc.*, **34**, 11 (1938).
582. M. W. EVANS, *Chem. Rev.*, **51**, 363 (1952).
583. A. A. EVETT and H. MARGENAU, *Phys. Rev.*, **90**, 1021 (1953).
584. H. EYRING, *J. Amer. Chem. Soc.*, **53**, 2537 (1931).
585. H. EYRING, *Chem. Rev.*, **10**, 103 (1932).
586. H. EYRING, *J. Chem. Phys.*, **3**, 107 (1935).
587. H. EYRING, H. GERSHINOWITZ and C. E. SUN, *J. Chem. Phys.*, **3**, 786 (1935).
588. H. EYRING, J. C. GIDDINGS and L. G. TENSMEYER, *J. Chem. Phys.*, **24**, 857 (1956).
589. H. EYRING, J. O. HIRSCHFELDER and H. S. TAYLOR, *J. Chem. Phys.*, **4**, 479 (1936).
590. H. EYRING, J. O. HIRSCHFELDER and H. S. TAYLOR, *J. Chem. Phys.*, **4**, 570 (1936).
591. H. EYRING and M. POLANYI, *Z. phys. Chem.*, **B 12**, 279 (1931).
592. H. EYRING and R. P. SMITH, *J. Phys. Chem.*, **56**, 972 (1952).
593. A. R. FAIRBAIRN and A. G. GAYDON, *Nature*, **175**, 253 (1955).
594. F. FAIRBROTHER and E. WARHURST, *Trans. Faraday Soc.*, **31**, 987 (1935).
595. A. C. FAIRE, O. T. FUNDINGSLAND and A. L. ADEN, *Phys. Rev.*, **93**, 650 (1954).
596. K. G. FALK, *J. Amer. Chem. Soc.*, **28**, 1517 (1906).
- 596a. C. Y. FAN, *Phys. Rev.*, **103**, 1740 (1957).
597. A. FARKAS and L. FARKAS, *Proc. Roy. Soc., A* **152**, 124 (1935).
598. A. FARKAS and P. HARTECK, *Z. phys. Chem.*, **B 25**, 257 (1934).
599. A. FARKAS and H. W. MELVILLE, *Proc. Roy. Soc., A* **157**, 625 (1936).
600. L. FARKAS, *Erg. exakt. Naturwiss.*, **12**, 163 (1933).
601. L. FARKAS and H. SACHSSE, *Z. phys. Chem.*, **B 27**, 111 (1934).
602. L. FARKAS and E. WIGNER, *Trans. Faraday Soc.*, **32**, 708 (1936).
603. J. B. FARMER, I. H. S. HENDERSON, F. P. LOSSING and D. G. H. MARSDEN, *J. Chem. Phys.*, **24**, 348 (1956).
604. J. B. FARMER, F. P. LOSSING, D. G. H. MARSDEN and E. W. R. STEACIE, *J. Chem. Phys.*, **23**, 1169 (1955).
- 604a. C. P. FENIMORE and G. W. JONES, *J. Phys. Chem.*, **61**, 651 (1957).
- 604b. C. P. FENIMORE and G. W. JONES, *J. Phys. Chem.*, **62**, 178 (1958).
- 604c. C. P. FENIMORE and G. W. JONES, *J. Phys. Chem.*, **62**, 693 (1958).
605. J. B. FENN and H. F. CALCOTE, *Fourth Symposium on Combustion*, p. 231, Baltimore, (1953).
606. R. E. FERGUSON, *J. Chem. Phys.*, **23**, 2085 (1955).
- 606a. R. E. FERGUSON, *Combustion and Flame*, **1**, 431 (1957).
607. R. E. FERGUSON and H. P. BROIDA, *Fifth Symposium on Combustion*, p. 754, N.Y., (1955).
608. E. FERMI, *Z. Phys.*, **40**, 399 (1927).
609. F. H. FIELD, J. L. FRANKLIN and F. W. LAMPE, *J. Amer. Chem. Soc.*, **78**, 5697 (1956); **79**, 2419 (1957).
610. W. FINKELNBURG, *Phys. Rev.*, **98**, 562 (1955); G. BUSZ and W. FINKELNBURG, *Z. Phys.*, **139**, 212 (1954).
611. W. FINKELNBURG, E. LAU and O. REICHENHEIM, *Z. Phys.*, **61**, 782 (1930).
612. F. FISCHER and K. PETERS, *Brennst. Ch.*, **10**, 108 (1929); K. PETERS and O. H. WAGNER, *Z. phys. Chem.*, **A 153**, 161 (1931).
613. R. G. FLUHARTY, *Nucleonics*, **3**, 46 (1948).
614. P. G. T. FOGG, P. A. HANKS and J. D. LAMBERT, *Proc. Roy. Soc., A* **219**, 490 (1953).
615. P. G. T. FOGG and J. D. LAMBERT, *Proc. Roy. Soc., A* **232**, 537 (1955).
616. S. N. FONER and R. L. HUDSON, *J. Chem. Phys.*, **21**, 1374 (1953).
617. S. N. FONER and R. L. HUDSON, *J. Chem. Phys.*, **21**, 1608 (1953).
618. S. N. FONER and R. L. HUDSON, *J. Chem. Phys.*, **23**, 1364, 1974 (1955).

619. S. N. FONER and R. L. HUDSON, *J. Chem. Phys.*, **25**, 601 (1956).
 620. G. S. FORBES, J. E. CLINE and B. C. BRADSHAW, *J. Amer. Chem. Soc.*, **60**, 1431 (1938).
 620a. H. W. FORD and N. ENDOW, *J. Chem. Phys.*, **27**, 1277 (1957).
 620b. W. FORST and P. A. GIGUÈRE, *J. Phys. Chem.*, **62**, 340 (1958).
 621. R. H. FOWLER, *Statistical Mechanics*, 2 Ed. Cambridge (1936).
 621a. R. E. FOX, *J. Chem. Phys.*, **26**, 1281 (1957).
 622. H. H. FRANCK and H. REICHARDT, *Naturwissenschaften*, **24**, 171 (1936).
 623. J. FRANCK and A. EUCKEN, *Z. phys. Chem.*, **B 20**, 460 (1933).
 624. J. FRANCK and P. JORDAN, *Anregung von Quantensprüngen durch Stöße*, Berlin (1926).
 625. J. FRANCK and R. WOOD, *Verh. deutsch. phys. Ges.*, **13**, 78 (1911); R. WOOD and J. FRANCK, *Phys. Z.*, **12**, 81 (1911).
 626. W. FRANKENBURGER, *Z. Elektrochem.*, **36**, 757 (1930).
 627. C. FRANZE, W. JOST and K. J. LESEMANN, *Z. phys. Chem., Frankf. Ausgabe*, **3**, 1 (1955).
 628. E. FREEDMAN, *J. Chem. Phys.*, **21**, 1784 (1953).
 628a. G. R. FREEMAN, C. J. DANBY and C. N. HINSHELWOOD, *Proc. Roy. Soc., A* **245**, 28 (1958); C. J. DANBY and G. R. FREEMAN, *Proc. Roy. Soc., A* **245**, 40 (1958); G. R. FREEMAN, *Proc. Roy. Soc., A* **245**, 49 (1958).
 629. E. C. FREILING, H. S. JOHNSTON and R. A. OGG, Jr., *J. Chem. Phys.*, **20**, 327 (1952).
 630. H. M. FREY, C. J. DANBY and C. N. HINSHELWOOD, *Proc. Roy. Soc., A* **234**, 301 (1956).
 631. E. FRICKE, *J. Acoust. Soc. Amer.*, **12**, 25 (1940); V.O. KNUDSEN and E. FRICKE, *J. Acoust. Soc. Amer.*, **12**, 255 (1940).
 632. H. L. FRIEDMAN, R. B. BERNSTEIN and H. E. GUNNING, *J. Chem. Phys.*, **23**, 109 (1955).
 633. L. FRIEDMAN and J. BIGELEISEN, *J. Chem. Phys.*, **18**, 1325 (1950).
 634. L. FRIEDMAN and J. BIGELEISEN, *J. Amer. Chem. Soc.*, **75**, 2215 (1953).
 635. R. FRIEDMAN, *Fourth Symposium on Combustion*, p. 259, Baltimore, (1953).
 636. R. FRIEDMAN and E. BURKE, *J. Chem. Phys.*, **21**, 710 (1953).
 637. R. FRIEDMAN and E. BURKE, *J. Chem. Phys.*, **22**, 824 (1954).
 638. R. FRIEDMAN and J. A. CYPHERS, *J. Chem. Phys.*, **23**, 1875 (1955).
 639. R. FRIEDMAN and J. A. CYPHERS, *J. Chem. Phys.*, **25**, 448 (1956).
 640. P. FRISCH and H. J. SCHUMACHER, *Z. phys. Chem.*, **B 37**, 18 (1937).
 641. C. A. FRISCHE, *Phys. Rev.*, **43**, 160 (1933).
 642. R. M. FRISTRÖM, *J. Chem. Phys.*, **24**, 888 (1956).
 642a. D. C. FROST and C. A. McDOWELL, *Proc. Roy. Soc., A* **232**, 227 (1955).
 642b. D. C. FROST and C. A. McDOWELL, *Proc. Roy. Soc., A* **241**, 194 (1957).
 642c. D. C. FROST and C. A. McDOWELL, *J. Chem. Phys.*, **29**, 964 (1958).
 642d. D. C. FROST and C. A. McDOWELL, *J. Chem. Phys.*, **29**, 503 (1958).
 643. A. A. FROST and O. OLDENBERG, *J. Chem. Phys.*, **4**, 781 (1936).
 643a. W. FORST, *Canad. J. Chem.*, **36**, 1308 (1958).
 644. K. FUKUI, T. YONEZAWA, C. NAGATA and H. SHINGU, *J. Chem. Phys.*, **22**, 1433 (1954).
 645. H. GAENSSLER and H. A. E. MACKENZIE, *J. Appl. Chem.*, **5**, 552 (1955).
 646. F. H. GARNER, R. LONG, A. J. GRAHAM and A. BADAHKSHAN, *Sixth Symposium on Combustion*, p. 802, N.Y. (1957).
 647. D. GARVIN, V. P. GUINN and G. B. KISTIAKOWSKY, *Disc. Faraday Soc.*, **17**, 32 (1954).
 648. D. GARVIN and G. B. KISTIAKOWSKY, *J. Chem. Phys.*, **20**, 105 (1952).
 649. E. GAVIOLA, *Phil. Mag.*, **6**, 1154 (1928); M. L. POOL, *Phys. Rev.*, **33**, 22 (1929).
 650. E. GAVIOLA, *Phil. Mag.*, **6**, 1167 (1928).
 651. E. GAVIOLA and R. WOOD, *Phil. Mag.*, **6**, 1191 (1928).
 652. A. G. GAYDON, *Trans. Faraday Soc.*, **42**, 351 (1946).
 653. A. G. GAYDON, *Trans. Faraday Soc.*, **42**, 292 (1946).
 654. A. G. GAYDON, *Proc. Roy. Soc., A* **183**, 111 (1944).

655. A. G. GAYDON and A. R. FAIRBAIRN, *Fifth Symposium on Combustion*, p. 324, N.Y., (1955).
656. A. G. GAYDON and N. P. W. MOORE, *Proc. Roy. Soc., A* **233**, 184 (1955).
- 656a. A. G. GAYDON, N. P. W. MOORE and J. R. SIMONSON, *Proc. Roy. Soc., A* **230**, 1 (1955).
657. A. G. GAYDON and G. WHITTINGHAM, *Proc. Roy. Soc., A* **189**, 313 (1947); A. DOOLEY and G. WHITTINGHAM, *Trans. Faraday Soc.*, **42**, 354 (1946).
658. A. G. GAYDON and H. G. WOLFHARD, *Flames, Their Structure, Radiation and Temperature*, p. 144, London (1953).
659. A. G. GAYDON and H. G. WOLFHARD, *Fuel*, **33**, 286 (1954).
660. K. H. GEIB, *Ergeb. exakt. Naturwissenschaften*, **15**, 44 (1936); *Z. phys. Chem.*, **A 169**, 161 (1934); K. H. GEIB and P. HARTECK, *Z. phys. Chem.*, **A 170**, 1 (1934).
661. K. H. GEIB, *Z. Elektrochem.*, **47**, 275 (1941).
662. K. H. GEIB and P. HARTECK, *Z. phys. Chem. (Bodenstein Festband)*, 849 (1931).
663. K. H. GEIB and P. HARTECK, *Trans. Faraday Soc.*, **30**, 131 (1934).
664. K. H. GEIB and W. M. VAIDYA, *Proc. Roy. Soc., A* **178**, 351 (1941).
665. S. GELTMAN, *Phys. Rev.*, **102**, 171 (1956).
666. E. GERJUOY and S. STEIN, *Phys. Rev.*, **97**, 1671 (1955).
667. E. GERJUOY and S. STEIN, *Phys. Rev.*, **98**, 1848 (1955).
668. H. GERSHINOWITZ, *J. Chem. Phys.*, **5**, 54 (1937).
669. H. GERSHINOWITZ and H. EYRING, *J. Amer. Chem. Soc.*, **57**, 985 (1935).
670. L. H. GEVANTMAN and R. R. WILLIAMS, *J. Phys. Chem.*, **56**, 569 (1952).
671. S. N. GHOSH and W. F. SHERIDAN, *J. Chem. Phys.*, **25**, 1076 (1956).
- 671a. S. N. GHOSH and W. F. SHERIDAN, *J. Chem. Phys.*, **26**, 480 (1957).
672. G. E. GIBSON and W. HEITLER, *Z. Phys.*, **49**, 465 (1928).
673. G. E. GIBSON, O. K. RICE and N. S. BAYLISS, *Phys. Rev.*, **44**, 193 (1933).
674. J. C. GIDDINGS, *J. Chem. Phys.*, **26**, 2210 (1957).
675. J. C. GIDDINGS and H. EYRING, *J. Chem. Phys.*, **22**, 538 (1954).
676. M. GILBERT, *Sixth Symposium on Combustion*, p. 74, N.Y., (1957).
- 676a. M. GILBERT, *Combustion and Flame*, **2**, 148 (1958).
677. M. GILBERT and D. ALTMAN, *Sixth Symposium on Combustion*, p. 222, N.Y., (1957).
678. H. B. GILBODY and J. B. HASTED, *Proc. Roy. Soc., A* **238**, 334 (1957).
- 678a. H. B. GILBODY and J. B. HASTED, *Proc. Roy. Soc., A* **240**, 382 (1957).
679. W. R. GILKERSON and N. DAVIDSON, *J. Chem. Phys.*, **23**, 687 (1955).
- 679a. E. K. GILL and K. J. LAIDLER, *Canad. J. Chem.* **36**, 1570 (1958).
680. G. GLOCKLER and S. C. LIND, *The Electrochemistry of Gases and other Dielectrics*, N.Y., (1939); E. J. B. WILLEY, *Collisions of the second kind*, London (1937).
681. S. GOLDEN, *J. Chem. Phys.*, **17**, 620 (1949).
682. S. GOLDEN and A. M. PEISER, *J. Chem. Phys.*, **17**, 630 (1949).
683. S. GOLDEN and A. M. PEISER, *J. Phys. Coll. Chem.*, **55**, 789 (1951).
684. F. GOLDMAN, *Z. phys. Chem.*, **B 5**, 307 (1929).
685. R. GOMER, *J. Chem. Phys.*, **18**, 998 (1950).
686. R. GOMER and G. B. KISTIAKOWSKY, *J. Chem. Phys.*, **19**, 85 (1951).
- 686a. C. F. GOODEVE and A. W. C. TAYLOR, *Proc. Roy. Soc., A* **152**, 221 (1935); *A* **154**, 181 (1936).
- 686b. H. F. CORDES and H. S. JOHNSTON, *J. Amer. Chem. Soc.*, **76**, 4264 (1953).
687. A. S. GORDON and R. H. KNIFE, *J. Phys. Chem.*, **59**, 1160 (1955).
688. L. G. GOUY, *Ann. Phys.*, **18**, 5 (1879); *Ann. Chim. Phys.*, **18**, 27 (1879).
689. E. GORIN, *Acta Phys.-Chim. URSS*, **9**, 681 (1938).
690. E. GORIN, *Acta Phys.-Chim. URSS*, **8**, 513 (1938); *J. Chem. Phys.*, **7**, 256 (1939).
691. E. GORIN, W. KAUFMANN, J. WALTER and H. EYRING, *J. Chem. Phys.*, **7**, 633 (1939).
692. W. M. GRAVEN, *J. Amer. Chem. Soc.*, **78**, 3297 (1956).
693. E. P. GRAY, R. W. HART and W. H. GUIER, *Phys. Rev.*, **99**, 1661 (1955).
694. J. A. GRAY, *J. Chem. Soc.*, 741 (1953).
695. P. GRAY, *Fifth Symposium on Combustion*, p. 535, N.Y. (1955).

696. P. GRAY and J. C. LEE, *Fifth Symposium on Combustion*, p. 692, N.Y., (1955); P. GRAY, J. C. LEE, H. A. LEACH and D. C. TAYLOR, *Sixth Symposium on Combustion*, p. 188, N.Y., (1957).
697. P. GRAY and G. T. ROGERS, *Trans. Faraday Soc.*, **50**, 28 (1954).
698. J. H. S. GREEN, G. D. HARDEN, A. MACCOLL and P. J. THOMAS, *J. Chem. Phys.*, **21**, 178 (1953).
699. E. F. GREENE, G. R. COWAN and D. F. HORNIG, *J. Chem. Phys.*, **19**, 427 (1951).
700. E. F. GREENE and D. F. HORNIG, *J. Chem. Phys.*, **21**, 617 (1953).
- 700a. W. D. GREENSPAN and V. H. BLACKMAN, *Bull. Amer. Phys. Soc.*, Ser. II, **2**, 217 (1957).
701. V. GRIFFING, *J. Chem. Phys.*, **23**, 1015 (1955).
702. V. GRIFFING and A. MAČEK, *J. Chem. Phys.*, **23**, 1029 (1955).
703. V. GRIFFING and J. T. VANDERSLICE, *J. Chem. Phys.*, **22**, 1142 (1954).
704. V. GRIFFING and J. T. VANDERSLICE, *J. Chem. Phys.*, **23**, 1035 (1955).
705. J. G. A. GRIFFITH and R. G. W. NORRISH, *Proc. Roy. Soc.*, A **147**, 140 (1934).
706. W. GRIFFITH, *J. Appl. Phys.*, **21**, 1319 (1950).
- 706a. A. V. GROSSE and A. D. KIRSHENBAUM, *J. Amer. Chem. Soc.*, **77**, 5012 (1955).
707. W. GROTH, *Z. phys. Chem.*, **B 37**, 315 (1937).
708. W. E. GROTH and O. OLDEMBERG, *J. Chem. Phys.*, **23**, 729 (1955).
709. A. E. GRÜN, *Z. Naturforsch.*, **9a**, 55 (1954).
- 709a. E. F. GURNEE and J. L. MAGEE, *J. Chem. Phys.*, **26**, 1237 (1957).
710. H. GUTBIER, *Z. Naturforsch.*, **12a**, 499 (1957).
711. H. GUTBIER and H. NEUERT, *Z. Naturforsch.*, **9a**, 335 (1954).
- 711a. R. HAAS, *Z. Phys.*, **148**, 177 (1957).
712. F. HABER and F. RICHARDT, *Z. anorg. Chem.*, **38**, 5 (1904).
713. H. HABER, *Phys. Z.*, **40**, 541 (1939).
714. H. D. HAGSTRUM, *Rev. Mod. Phys.*, **23**, 185 (1951).
715. A. R. HALL and H. G. WOLFHARD, *Sixth Symposium on Combustion*, p. 190, N.Y., (1957).
- 715a. A. R. HALL and H. G. WOLFHARD, *Trans. Faraday Soc.*, **52**, 1520 (1956).
716. W. H. HAMILL and R. H. SCHULER, *J. Amer. Chem. Soc.*, **73**, 3466 (1951).
717. F. HAMMETT, *Physical Organic Chemistry*, N.Y., (1940).
718. W. HANLE, *Phys. Z.*, **38**, 995 (1937).
719. W. HANLE and W. SCHAFFERNICHT, *Ann. Phys.*, **6**, 905 (1930).
720. H. G. HANSON, *J. Chem. Phys.*, **23**, 1391 (1955).
721. HANGST, E. R. STEPHENS and W. E. SCOTT, *Minneapolis Symposium* (2), No. 60, p. 25.
722. J. N. HARESNAPE, J. M. STEVELS and E. WARHURST, *Trans. Faraday Soc.*, **36**, 465 (1940).
723. W. D. HARKINS and J. M. JACKSON, *J. Chem. Phys.*, **1**, 37 (1933); W. D. HARKINS, *Trans. Faraday Soc.*, **30**, 221 (1934).
724. W. HARRIES, *Z. Phys.*, **42**, 26 (1927); W. HARRIES and G. HERTZ, *Z. Phys.*, **46**, 177 (1928).
725. P. HARTECK and S. DONDÉS, *J. Chem. Phys.*, **22**, 758 (1954).
726. P. HARTECK and S. DONDÉS, *J. Chem. Phys.*, **23**, 902 (1955).
727. P. HARTECK and S. DONDÉS, *J. Chem. Phys.*, **24**, 619 (1956).
728. P. HARTECK and U. KOPSCH, *Z. Elektrochem.*, **36**, 714 (1930).
729. P. HARTECK and U. KOPSCH, *Z. phys. Chem.*, **B 12**, 327 (1931).
- 729a. P. HARTECK, R. R. REEVES and G. MANNELLA, *J. Chem. Phys.*, **29**, 608 (1958).
730. H. VON HARTEL, *Z. phys. Chem.*, **B 11**, 316 (1931).
731. H. VON HARTEL, *Trans. Faraday Soc.*, **30**, 187 (1934).
732. H. VON HARTEL, N. MEER and M. POLANYI, *Z. phys. Chem.*, **B 19**, 139 (1932).
733. H. VON HARTEL and M. POLANYI, *Z. phys. Chem.*, **B 11**, 97 (1930).
734. J. B. HASTED, *Proc. Roy. Soc.*, A **205**, 421 (1951).
735. J. B. HASTED, *Proc. Roy. Soc.*, A **212**, 235 (1952).
736. J. B. HASTED, *Proc. Roy. Soc.*, A **222**, 74 (1954).
737. R. H. HEALEY and J. W. REED, *The Behaviour of Slow Electrons in Gases*, p. 87-102, Amalgamated Wireless, Sidney, (1941).

738. L. J. HEIDT, *J. Amer. Chem. Soc.*, **57**, 1710 (1935).
739. L. J. HEIDT and G. S. FORBES, *J. Amer. Chem. Soc.*, **56**, 2365 (1934); M. RITCHIE, *Proc. Roy. Soc., A* **146**, 848 (1934).
740. W. HEITLER and F. LONDON, *Z. Phys.*, **44**, 455 (1927).
741. W. HELLER and M. POLANYI, *Trans. Faraday Soc.*, **32**, 633 (1936).
742. G. H. HENDERSON, *Phil. Mag.*, (VI), **42**, 538 (1921).
743. V. HENRI, *Leipziger Vorträge*, p. 131, (1931).
744. D. R. HERSCHBACH, H. S. JOHNSTON, K. S. PITZER and R. E. POWELL, *J. Chem. Phys.*, **25**, 736 (1956).
745. E. HERTEL, *Z. phys. Chem.*, **B** **14**, 443 (1931); **B** **15**, 325 (1932).
746. G. HERZBERG, *Z. phys. Chem.*, **B** **17**, 68 (1932).
747. G. HERZBERG, *Astrophys. J.*, **89**, 290 (1939).
748. G. HERZBERG, *Astrophys. J.*, **96**, 314 (1942).
749. G. HERZBERG, *Rev. Mod. Phys.*, **14**, 195 (1942).
750. G. HERZBERG and D. A. RAMSAY, *Phys. Rev.*, **86**, 587 (1952).
751. G. HERZBERG and D. A. RAMSAY, *Proc. Roy. Soc., A* **233**, 34 (1955).
752. G. HERZBERG and D. A. RAMSAY, *Disc. Faraday Soc.*, **14**, 11 (1953).
753. G. HERZBERG and G. SCHEIBE, *Z. phys. Chem.*, **B** **7**, 390 (1930); N. R. DHAR, *Trans. Faraday Soc.*, **30**, 142 (1934).
754. G. HERZBERG and J. SHOOSMITH, *Canad. J. Phys.*, **34**, 523 (1956).
755. K. F. HERZFELD and F. O. RICE, *Phys. Rev.*, **31**, 691 (1928).
756. G. von HEVESY and F. PANETH, *Z. anorg. Chem.*, **82**, 223 (1913).
757. W. M. HICKAM, *Phys. Rev.*, **95**, 703 (1954).
- 757a. W. M. HICKAM and D. BERG, *J. Chem. Phys.*, **29**, 517 (1958).
758. W. M. HICKAM and R. E. FOX, *Phys. Rev.* **98**, 557 (1955).
759. W. M. HICKAM and R. E. FOX, *J. Chem. Phys.*, **25**, 642 (1956).
760. W. M. HICKAM, R. E. FOX and T. KJELDAAS, JR., *Phys. Rev.*, **96**, 63 (1954).
761. K. HILFERDING and W. STEINER, *Z. phys. Chem.*, **B** **30**, 399 (1935).
762. L. J. HILLENBRAND, JR. and M. L. KILPATRICK, *J. Chem. Phys.*, **21**, 525 (1953).
763. C. N. HINSHELWOOD, *Proc. Roy. Soc., A* **113**, 230 (1927).
764. C. N. HINSHELWOOD, K. CLUSIUS and G. HADMAN, *Proc. Roy. Soc., A* **128**, 88 (1930).
765. C. N. HINSHELWOOD and L. A. K. STAVELEY, *J. Chem. Soc.*, 818 (1936).
766. C. N. HINSHELWOOD and A. WILLIAMSON, *The Reaction between Hydrogen and Oxygen*, Oxford, (1934).
767. J. O. HIRSCHFELDER, *J. Chem. Phys.*, **26**, 271 (1957).
768. J. O. HIRSCHFELDER and C. F. CURTISS, *J. Chem. Phys.*, **17**, 1076 (1949); J. O. HIRSCHFELDER, C. F. CURTISS and D. E. CAMPBELL, *The Theory of Flame Propagation*, IV, Univ. Wisconsin Rep., No. CM 756, (1952).
769. J. O. HIRSCHFELDER, C. F. CURTISS and D. E. CAMPBELL, *J. Phys. Chem.*, **57**, 403 (1953).
770. J. O. HIRSCHFELDER, H. DIAMOND and H. EYRING, *J. Chem. Phys.*, **5**, 695 (1937).
771. J. O. HIRSCHFELDER, H. EYRING and B. TOPLEY, *J. Chem. Phys.*, **4**, 170 (1936).
772. I. C. HISATSUNE and B. CRAWFORD, JR., *J. Chem. Phys.*, **24**, 1257 (1956).
773. I. C. HISATSUNE, A. P. McHALE, R. E. NIGHTINGALE, D. L. ROTENBERG and B. CRAWFORD, JR., *J. Chem. Phys.*, **23**, 2467 (1955).
774. G. R. HOEY and D. J. LEROY, *Canad. J. Chem.*, **33**, 580 (1955).
775. T. R. HOGNESS and R. W. HARKNESS, *Phys. Rev.*, **32**, 784 (1928).
776. R. A. HOLROYD and W. A. NOYES, JR., *J. Amer. Chem. Soc.*, **76**, 1583 (1954).
777. T. HOLSTEIN, *Phys. Rev.*, **84**, 1073 (1951).
778. T. HORIE and M. OTSUKA, *J. Phys. Soc. Japan*, **9**, 219 (1954).
779. J. HORIUTI and M. POLANYI, *Acta Phys.-Chim. URSS*, **2**, 505 (1935).
780. E. I. HORMATS and E. R. VAN ARTSDALEN, *J. Chem. Phys.*, **19**, 778 (1951).
781. G. A. HORNBECK, *Third Symposium on Combustion*, Baltimore, 1949, p. 501.
782. G. A. HORNBECK, *Fifth Symposium on Combustion*, p. 790, N.Y., (1955).
783. G. A. HORNBECK and R. C. HERMAN, *Industr. Engng. Chem. (Industr.)*, **43**, 2739 (1951).
784. G. A. HORNBECK and J. P. MOLNAR, *Phys. Rev.*, **84**, 621 (1951).

- 784a. R. E. HORNIG, *J. Chem. Phys.*, **16**, 105 (1948).
 785. F. HORTON and D. M. MILLEST, *Proc. Roy. Soc., A* **185**, 381 (1946).
 786. K. E. HOWLETT, *J. Chem. Soc.*, 945 (1953).
 787. F. P. HUDSON, R. R. WILLIAMS, JR. and W. H. HAMILL, *J. Chem. Phys.*, **21**, 1894 (1953).
 788. H. H. HUPFELD, *Z. Phys.*, **54**, 484 (1929).
 789. T. A. INGLES and H. W. MELVILLE, *Proc. Roy. Soc., A* **218**, 175 (1953).
 789a. T. A. INGLES and H. W. MELVILLE, *Proc. Roy. Soc., A* **218**, 163 (1953).
 790. K. U. INGOLD and W. A. BRYCE, *J. Chem. Phys.*, **24**, 360 (1956).
 791. K. U. INGOLD, I. H. S. HENDERSON and F. P. LOSSING, *J. Chem. Phys.*, **21**, 2239 (1953).
 792. K. U. INGOLD and F. P. LOSSING, *Canad. J. Chem.*, **31**, 30 (1953).
 793. K. U. INGOLD and F. P. LOSSING, *J. Chem. Phys.*, **21**, 1135 (1953).
 794. D. J. E. INGRAM, W. G. HODGSON, C. A. PARKER and W. T. REES, *Nature*, **176**, 1227 (1955).
 795. T. INOUE and T. TAKAHASHI, *J. Phys. Soc. Japan*, **9**, 199 (1954).
 796. K. J. IVIN and E. W. R. STEACIE, *Proc. Roy. Soc., A* **208**, 25 (1951).
 797. D. S. JACKSON and H. I. SCHIFF, *J. Chem. Phys.*, **21**, 2233 (1953).
 798. J. M. JACKSON and N. F. MOTT, *Proc. Roy. Soc., A* **137**, 702 (1932).
 799. C. G. JAMES and T. M. SUGDEN, *Nature*, **175**, 252 (1955).
 799a. C. G. JAMES and T. M. SUGDEN, *Proc. Roy. Soc., A* **248**, 238 (1958); E. M. BULEWICZ and T. M. SUGDEN, *Trans. Faraday Soc.*, **52**, 1481 (1956).
 800. J. T. JEFFERIES, *Austr. J. Phys.*, **7**, 22 (1954).
 801. W. P. JESSE and J. SADAUSKIS, *Phys. Rev.*, **88**, 417 (1952).
 802. H. JOHNSTON, *J. Chem. Phys.*, **19**, 663 (1951).
 803. H. S. JOHNSTON, *J. Chem. Phys.*, **20**, 1103 (1952).
 804. H. S. JOHNSTON, *J. Amer. Chem. Soc.*, **75**, 1567 (1953).
 804a. H. S. JOHNSTON, W. A. BONNER and D. J. WILSON, *J. Chem. Phys.*, **26**, 1002 (1957).
 805. H. S. JOHNSTON and H. J. CROSBY, *J. Chem. Phys.*, **22**, 689 (1954).
 806. H. S. JOHNSTON, L. FOERING and R. J. THOMPSON, *J. Phys. Chem.*, **57**, 390 (1953).
 807. H. S. JOHNSTON and D. M. YOST, *J. Chem. Phys.*, **17**, 386 (1949).
 808. H. S. JOHNSTON and J. R. WHITE, *J. Chem. Phys.*, **22**, 1969 (1954).
 809. M. H. JONES and E. W. R. STEACIE, *J. Chem. Phys.*, **21**, 1018 (1953).
 809a. W. M. JONES, *J. Chem. Phys.*, **19**, 78 (1951).
 810. W. JOST, *Z. phys. Chem.*, **134**, 92 (1928).
 811. W. JOST, *Z. phys. Chem.*, **B** **3**, 95 (1929).
 812. W. JOST, *Z. phys. Chem.*, **A** **193**, 332 (1944).
 813. W. JOST and H. G. WAGNER, *Naturwissenschaften*, **40**, 435 (1953).
 814. E. JOUGUET, *J. Math.*, 347 (1905); 6 (1906).
 815. A. KANTROWITZ, *J. Chem. Phys.*, **14**, 150 (1946); P. W. HUBER and A. KANTROWITZ, *J. Chem. Phys.*, **15**, 275 (1947).
 815a. B. KARLOVITZ, *Selected Combustion Problems*, AGARD, London, 1954, p. 248.
 816. T. VON KÁRMÁN and S. S. PENNER, *Selected Combustion Problems*, London, 1954, p. 5.
 816a. W. E. KASKAN, *Combustion and Flame*, **2**, 229, 286 (1958).
 817. L. S. KASSEL, *J. Phys. Chem.*, **32**, 225 (1928).
 818. L. S. KASSEL, *J. Amer. Chem. Soc.*, **54**, 3949 (1932).
 819. L. S. KASSEL, *J. Amer. Chem. Soc.*, **57**, 833 (1935).
 820. L. S. KASSEL, *J. Chem. Phys.*, **5**, 922 (1937).
 821. L. S. KASSEL, *J. Chem. Phys.*, **21**, 1093 (1953).
 822. F. KAUFMAN, N. J. GERRI and R. E. BOWMAN, *J. Chem. Phys.*, **25**, 106 (1956).
 823. F. KAUFMAN, N. J. GERRI and D. A. PASCALE, *J. Chem. Phys.*, **24**, 32 (1956).
 824. F. KAUFMAN and J. R. KELSO, *J. Chem. Phys.*, **21**, 751 (1953).
 825. F. KAUFMAN and J. R. KELSO, *J. Chem. Phys.*, **23**, 602 (1955).
 826. F. KAUFMAN and J. R. KELSO, *J. Chem. Phys.*, **23**, 1702 (1955).
 826a. F. KAUFMAN, *J. Chem. Phys.*, **28**, 352 (1958).

827. J. P. KEENE, *Phil. Mag.*, **40**, 369 (1949).
 828. H. H. KELLER, *Phys. Z.*, **41**, 386 (1940).
 828a. T. B. KELLY, *J. Acoust. Soc. Amer.*, **29**, 1005 (1957).
 829. E. H. KERNER, *Phys. Rev.*, **91**, 1174; **92**, 899 (1953).
 830. E. H. KERNER, *Phys. Rev.*, **92**, 1441 (1953).
 831. G. E. KIMBALL, *J. Chem. Phys.*, **5**, 310 (1937).
 832. T. KINBARA and J. NAKAMURA, *Fifth Symposium on Combustion*, p. 285, N.Y., (1955).
 833. B. KIRSCHSTEIN, *Z. Phys.*, **60**, 184 (1930).
 834. G. B. KISTIAKOWSKY, *Z. phys. Chem.*, **117**, 337 (1925).
 835. G. B. KISTIAKOWSKY, *Photochemical Processes*, Table 39, N.Y., (1928).
 836. G. B. KISTIAKOWSKY, *J. Amer. Chem. Soc.*, **50**, 2315 (1928); **78**, 3297 (1956).
 837. G. B. KISTIAKOWSKY and H. GERSHINOWITZ, *J. Chem. Phys.*, **1**, 432, 885 (1933).
 838. G. B. KISTIAKOWSKY and P. C. MANGELSDORF, JR., *J. Chem. Phys.*, **25**, 516 (1956); G. B. KISTIAKOWSKY and P. H. KYDD, *J. Chem. Phys.*, **25**, 824 (1956).
 839. G. B. KISTIAKOWSKY and E. K. ROBERTS, *J. Chem. Phys.*, **21**, 1637 (1953).
 840. G. B. KISTIAKOWSKY and J. C. STERNBERG, *J. Chem. Phys.*, **21**, 2218 (1953); C. A. McDOWELL, *Nature*, **175**, 860 (1955).
 841. G. B. KISTIAKOWSKY and E. R. VAN ARTSDALEN, *J. Chem. Phys.*, **12**, 469 (1944).
 841a. G. B. KISTIAKOWSKY and P. WARNECK, *J. Chem. Phys.*, **27**, 1417 (1957).
 842. G. B. KISTIAKOWSKY and R. WILLIAMS, *J. Chem. Phys.*, **23**, 334 (1955).
 843. G. B. KISTIAKOWSKY and W. G. ZINMAN, *J. Chem. Phys.*, **23**, 1889 (1955).
 844. C. KITTEL, *Rep. Progr. Phys.*, **11**, 205 (1948).
 845. H. KLUMB and P. PRINGSHEIM, *Z. Phys.*, **52**, 610 (1929).
 846. R. H. KNIPE and A. S. GORDON, *J. Chem. Phys.*, **23**, 2097 (1955).
 847. H. KNOETZEL and L. KNOETZEL, *Ann. Phys.*, **2**, 393 (1948).
 848. J. H. KNOX and R. G. W. NORRISH, *Trans. Faraday Soc.*, **50**, 928 (1954).
 849. K. KNOX, R. G. W. NORRISH and G. PORTER, *J. Chem. Soc.*, 1477 (1952).
 850. V. O. KNUDSEN, *J. Acoust. Soc. Amer.*, **5**, 112 (1933); H. O. KNESER, *J. Acous. Soc. Amer.*, **5**, 122 (1933).
 851. W. KOBILITZ and H. J. SCHUMACHER, *Z. phys. Chem.*, **B 25**, 283 (1934).
 852. E. C. KOOYMAN and E. FARENHORST, *Nature*, **169**, 153 (1952).
 853. H. A. KRAMERS, *Physica*, **7**, 284 (1940).
 853a. F. KRAUS, *Z. Naturforsch.*, **12a**, 479 (1957).
 854. K. B. KRAUSKOPF and G. K. ROLLEFSON, *J. Amer. Chem. Soc.*, **56**, 327 (1934).
 855. L. KÜCHLER, *Z. phys. Chem.*, **B 41**, 199 (1938).
 856. W. B. KUNKEL and A. L. GARDNER, *Phys. Rev.*, **98**, 558 (1955).
 857. H. KWART, L. P. KUHN and E. L. BANNISTER, *J. Amer. Chem. Soc.*, **76**, 5998 (1954).
 858. J. R. LACHER, G. W. TOMPKIN and J. D. PARK, *J. Amer. Chem. Soc.*, **74**, 1693 (1952).
 859. K. J. LAIDLER, *Chemical Kinetics*, N.Y., (1950).
 860. K. J. LAIDLER, *J. Chem. Phys.*, **22**, 1740 (1954).
 861. K. J. LAIDLER, *The Chemical Kinetics of Excited States*, Oxford, (1955).
 862. K. J. LAIDLER and K. E. SHULER, *Chem. Rev.* **48**, 153 (1951).
 863. J. D. LAMBERT and J. S. ROWLINSON, *Proc. Roy. Soc.*, **A 204**, 424 (1950).
 863a. J. D. LAMBERT and R. SLATER, *Proc. Roy. Soc.*, **A 243**, 78 (1957).
 864. R. M. LANGER, *Phys. Rev.*, **85**, 740 (1952).
 865. D. LAYZER, *J. Chem. Phys.*, **22**, 222, 229 (1954).
 866. E. LEDERER and M. LEDERER, *Chromatography*, Amsterdam-Houston, London, New York, 1953.
 867. J. A. LEERMAKERS, *J. Amer. Chem. Soc.*, **55**, 3098 (1933).
 868. E. G. LEGER and C. OUELLET, *J. Chem. Phys.*, **21**, 1310 (1953).
 869. J. E. LENNARD-JONES, *Proc. Roy. Soc.*, **A 106**, 463 (1924); *Physica*, **4**, 941 (1937).
 870. D. J. LEROY, *Disc. Faraday Soc.*, **14**, 120 (1953).
 871. D. J. LEROY and E. W. R. STEACIE, *J. Chem. Phys.*, **12**, 369 (1944).
 871a. M. LETORT, *J. Chimie Phys.*, **34**, 206 (1937).

872. W. J. LEVEDAHL, *Fifth Symposium on Combustion*, p. 372, N.Y., (1955).
873. G. LEVEY and J. E. WILLARD, *J. Chem. Phys.*, **25**, 904 (1956); J. F. HORNIG, G. LEVEY and J. E. WILLARD, *J. Chem. Phys.*, **20**, 1556 (1952).
874. M. LEVY and M. SZWARC, *J. Chem. Phys.*, **22**, 1621 (1954).
875. B. LEWIS and G. VON ELBE, *J. Chem. Phys.*, **2**, 283 (1934).
876. B. LEWIS and G. VON ELBE, *J. Chem. Phys.*, **2**, 537 (1934).
877. B. LEWIS and G. VON ELBE, *Third Symposium on Combustion*, Baltimore, p. 484, (1949). G. VON ELBE and B. LEWIS, *J. Chem. Phys.*, **10**, 366 (1952).
878. R. LEWIS and J. B. FRIAUF, *J. Amer. Chem. Soc.*, **52**, 3905 (1930).
879. S. C. LIND and G. GLOCKLER, *J. Amer. Chem. Soc.*, **50**, 1767 (1928).
- 879a. S. C. LIND and P. S. RUDOLPH, *J. Chem. Phys.*, **26**, 1768 (1957).
880. F. A. LINDEMANN, *Trans. Faraday Soc.*, **17**, 598 (1922).
881. E. LINDHOLM, *Z. Naturforsch.*, **9a**, 535 (1954).
882. L. LINDNER, W. E. SCOTT and E. R. STEPHENS, *J. Chem. Phys.*, **21**, 161 (1953).
883. J. W. LINNETT, *Fourth Symposium on Combustion*, p. 20, Baltimore, 1953.
884. F. J. LIPSCOMB, R. G. W. NORRISH and B. A. THRUSH, *Proc. Roy. Soc.*, A **233**, 455 (1955).
885. F. LONDON, *Probleme der modernen Physik (Sommerfeld Festschrift)*, p. 104 (1928); *Z. Elektrochem.*, **35**, 552 (1929).
886. F. LONDON, *Z. Phys.*, **74**, 143 (1932).
887. F. P. LOSSING, K. U. INGOLD and A. W. TICKNER, *Disc. Faraday Soc.*, **14**, 34 (1953).
888. A. J. LOTKA, *J. Amer. Chem. Soc.*, **42**, 1595 (1920).
889. W. LOTMAR, *Z. Phys.*, **83**, 765 (1933).
890. W. W. LOZIER, *Phys. Rev.*, **46**, 268 (1934).
891. M. LUCQUIN and P. LAFFITTE, *Sixth Symposium on Combustion*, p. 130. N.Y., (1957).
892. E. B. LUDLAM, H. G. REID and G. S. SOUTAR, *Proc. Roy. Soc. (Edinburgh)*, **49**, 156 (1929).
- 892a. S. J. LUKASIK and J. E. YOUNG, *J. Chem. Phys.*, **27**, 1149 (1957).
893. R. LUTHER and N. A. SHILOV, *Z. phys. Chem.*, **46**, 777 (1903).
894. E. R. LYMAN, *Phys. Rev.*, **53**, 379 (1938).
895. E. R. LYMAN and F. A. JENKINS, *Phys. Rev.*, **53**, 214 (1938).
896. A. MACCOLL and P. T. THOMAS, *J. Chem. Phys.*, **19**, 977 (1951).
897. M. MAGAT and R. BONÈME, *C.R. Acad. Sci., Paris*, **232**, 1657 (1951); W. H. STOCKMAYER and L. H. PEEBLES, *J. Amer. Chem. Soc.*, **75**, 2278 (1953); E. C. KOOYMAN and E. FARENHORST, *Trans. Faraday Soc.*, **49**, 58 (1953); M. LEVY, M. STEINBERG and M. SZWARC, *J. Amer. Chem. Soc.*, **76**, 3439 (1954).
898. J. L. MAGEE, *J. Chem. Phys.*, **8**, 677 (1940).
899. J. L. MAGEE, *J. Chem. Phys.*, **8**, 687 (1940).
900. J. L. MAGEE, *Disc. Faraday Soc.*, **12**, 33 (1952); J. L. MAGEE, *J. Phys. Chem.*, **56**, 555 (1952).
- 900a. J. L. MAGEE and E. F. GURNEE, *J. Chem. Phys.*, **20**, 894 (1952).
901. J. L. MAGEE, W. SHAND and H. EYRING, *J. Amer. Chem. Soc.*, **63**, 677 (1941).
902. H. MAIER-LEIBNITZ, *Z. Phys.*, **95**, 499 (1935).
903. T. G. MAJURY and E. W. R. STEACIE, *Canad. J. Chem.*, **30**, 800 (1952).
904. E. MALLARD, *Ann. Mines*, **7**, 355 (1875).
905. E. MALLARD and H. L. LE CHATELIER, *C.R. Acad. Sci., Paris*, **93**, 145 (1881).
906. E. MALLARD and H. L. LE CHATELIER, *Ann. Mines*, **4**, 274, 379 (1883).
907. L. MANDELORN and E. W. R. STEACIE, *Canad. J. Chem.*, **32**, 474 (1954).
908. J. P. MANION and M. BURTON, *J. Phys. Chem.*, **56**, 560 (1952).
909. M. M. MANN, A. HUSTRULID and J. T. TATE, *Phys. Rev.*, **58**, 340 (1940).
910. R. MANNKOPFF, *Z. Phys.*, **36**, 315 (1926).
911. N. MANSON, *C.R. Acad. Sci., Paris*, **226**, 230 (1948); *Rev. Inst. Franc. Pétr.*, **4**, 338 (1949); *J. Chem. Phys.*, **17**, 837 (1949).
912. M. MAQUENNE, *Bull. Soc. Chim. Paris*, **40**, 60 (1883); M. BERTHELOT, *Ann. Chim. Phys.*, **12**, 463 (1887).

913. F. B. MARCOTTE and W. A. NOYES, JR., *Disc. Faraday Soc.*, **10**, 236 (1951).
 914. R. A. MARCUS, *J. Chem. Phys.*, **20**, 352 (1952).
 915. R. A. MARCUS, *J. Chem. Phys.*, **20**, 359, 364 (1952).
 916. G. V. MARR and R. W. NICHOLLS, *Canad. J. Phys.*, **33**, 394 (1955); N. H. KIESS and A. M. BASS, *J. Chem. Phys.*, **22**, 569 (1954).
 917. R. MARSHALL and N. DAVIDSON, *J. Chem. Phys.*, **21**, 659 (1953).
 918. G. R. MARTIN and H. C. SUTTON, *Trans. Faraday Soc.*, **48**, 812 (1952).
 919. R. B. MARTIN and W. A. NOYES, *J. Amer. Chem. Soc.*, **75**, 4183 (1953).
 920. C. R. MASSON and E. W. R. STEACIE, *J. Chem. Phys.*, **18**, 210 (1950).
 921. H. S. W. MASSEY, *Proc. Cambr. Phil. Soc.*, **28**, 99 (1932).
 922. H. S. W. MASSEY, *Trans. Faraday Soc.*, **31**, 556 (1935).
 923. H. S. W. MASSEY, *Negative Ions*, Cambridge, (1950).
 924. H. S. W. MASSEY and F. H. S. BURHOP, *Electronic and Ionic Impact Phenomena*, Oxford, (1952).
 924a. H. S. W. MASSEY and C. B. O. MOHR, *Proc. Roy. Soc.*, **A 139**, 187; **A 140**, 613, (1933).
 924b. H. S. W. MASSEY and R. A. SMITH, *Proc. Roy. Soc.*, **A 142**, 142 (1933).
 925. C. G. MATLAND, *Phys. Rev.*, **89**, 338 (1953).
 926. C. G. MATLAND, *Phys. Rev.*, **92**, 637 (1953).
 927. F. A. MATSEN, *J. Chem. Phys.*, **22**, 165 (1954).
 928. G. MATTON, *Sixth Symposium on Combustion*, p. 770, N.Y., (1957).
 929. W. MAURER, *Z. Phys.*, **96**, 489 (1935).
 930. W. MAURER, *Z. Phys.*, **101**, 323 (1936); **104**, 113, 658 (1937).
 931. W. MAURER, *Z. Phys.*, **40**, 161 (1939).
 932. W. MAURER and K. MEHNERT, *Z. Phys.*, **106**, 453 (1937).
 933. C. S. McCAMY, H. SHOUB and T. G. LEE, *Sixth Symposium on Combustion*, p. 795, N.Y., (1957).
 934. R. L. McCARTHY, *J. Chem. Phys.*, **22**, 1360 (1954).
 934a. J. C. MCCOUBREY and W. D. MCGRATH, *Quart. Rev.*, **11**, 87 (1957).
 935. J. C. MCCOUBREY, J. B. PARKE and A. R. UBBELOHDE, *Proc. Roy. Soc.*, **A 223**, 155 (1954); W. D. MCGRATH and A. R. UBBELOHDE, *Proc. Roy. Soc.*, **A 227**, 1 (1954).
 936. C. C. McDONALD, A. KAHN and H. E. GUNNING, *J. Chem. Phys.*, **22**, 908 (1954).
 937. G. Y. McDONALD, *J. Chem. Soc.*, 1 (1928).
 938. W. R. McDONELL and S. GORDON, *J. Chem. Phys.*, **23**, 208 (1955).
 939. C. A. McDOWELL and J. B. FARMER, *Fifth Symposium on Combustion*, p. 453, N.Y., (1955).
 940. S. P. McGLYNN, M. R. PADHYE and M. KASHA, *J. Chem. Phys.*, **23**, 593 (1955); M. R. PADHYE, S. P. McGLYNN and M. KASHA, *J. Chem. Phys.*, **24**, 588 (1956).
 940a. W. D. MCGRATH and R. G. W. NORRISH, *Proc. Roy. Soc.*, **A 242**, 265 (1957).
 941. J. D. MCKINLEY, JR., D. GARVIN and M. J. BOUDART, *J. Chem. Phys.*, **23**, 784 (1955).
 942. J. R. MCNESBY, C. M. DREW and A. S. GORDON, *J. Chem. Phys.*, **24**, 1260 (1956).
 943. J. R. MCNESBY and A. S. GORDON, *J. Amer. Chem. Soc.*, **76**, 4196 (1954).
 944. J. R. MCNESBY, A. S. GORDON and S. R. SMITH, *J. Amer. Chem. Soc.*, **78**, 1287 (1956).
 945. R. MECKE, *Naturwissenschaften*, **17**, 996 (1929).
 946. A. MECKLER, *J. Chem. Phys.*, **21**, 1750 (1953).
 947. N. MEER and M. POLANYI, *Z. phys. Chem.*, **B 19**, 164 (1932); E. HORN, M. POLANYI, *Z. phys. Chem.*, **B 25**, 151 (1934).
 948. G. G. MEISELS, W. H. HAMILL and R. R. WILLIAMS, JR., *J. Chem. Phys.*, **25**, 790 (1956).
 948a. C. E. MELTON, M. M. BRETSCHER and R. B. BALDOCK, *J. Chem. Phys.*, **26**, 1302 (1957).
 948b. C. E. MELTON and H. M. ROSENSTOCK, *J. Chem. Phys.*, **26**, 568 (1957).
 948c. C. E. MELTON and C. F. WELLS, *J. Chem. Phys.*, **27**, 1132 (1957).
 949. H. W. MELVILLE and G. M. BURNETT in A. L. FRIESS and A. WEISSBERGER, *Techniques of Organic Chemistry*, Vol. 8, p. 138, Interscience N.Y., (1953).

950. H. W. MELVILLE and J. C. ROBB, *Proc. Roy. Soc., A* **202**, 181 (1950).
 950a. D. J. MESCHI and R. J. MYERS, *J. Amer. Chem. Soc.*, **78**, 6220 (1956).
 951. H. A. MESSENGER, *Phys. Rev.*, **28**, 962 (1926); J. H. COULLIETTE, *Phys. Rev.*, **32**, 636 (1928).
 952. E. MEYER, *Z. Phys.*, **37**, 639 (1926).
 953. R. L. MILLS and H. S. JOHNSTON, *J. Amer. Chem. Soc.*, **73**, 938 (1951); see also H. S. JOHNSTON and R. L. PERRINE, *J. Amer. Chem. Soc.*, **73**, 4782 (1951); H. S. JOHNSTON and YU-SHENG-TAO, *J. Amer. Chem. Soc.*, **73**, 2948 (1951).
 954. E. A. MILNE, *J. Lond. Math. Soc.*, **1**, 1 (1926).
 955. G. J. MINKOFF and K. C. SALOOJA, *Fuel*, **32**, 516 (1953).
 956. S. K. MITRA, *Phys. Rev.*, **90**, 516 (1953).
 956a. D. E. MOE, *Phys. Rev.*, **104**, 694 (1956).
 957. E. W. MONTROLL and K. E. SHULER, *J. Chem. Phys.*, **26**, 454 (1957).
 958. G. E. MOORE, O. R. WULF and R. M. BADGER, *J. Chem. Phys.*, **21**, 2091 (1953).
 959. P. M. MORSE, *Phys. Rev.*, **90**, 51 (1953).
 959a. F. MOSELEY and J. C. ROBB, *Proc. Roy. Soc., A* **243**, 130 (1957).
 960. V. VON MUFFLING, *Handbuch der Katalyse*, **B** **6**, III, 94 (1943).
 961. W. MUND, R. LORIES and P. HUYSKENS, *Bull. Acad. Roy. Belg., Classe Sci.*, **34**, 651 (1948).
 962. R. C. MURRAY and A. R. HALL, *Trans. Faraday Soc.*, **47**, 743 (1951).
 963. E. E. MUSCHLITZ, JR., T. L. BAILEY and J. H. SIMONS, *J. Chem. Phys.*, **24**, 1202 (1956); **26**, 711 (1957).
 964. E. E. MUSCHLITZ, JR. and J. H. SIMONS, *J. Phys. Chem.*, **56**, 837 (1952).
 965. F. F. MUSGRAVE and C. N. HINSELWOOD, *Proc. Roy. Soc., A* **137**, 25 (1932).
 966. A. L. MYERSON, F. R. TAYLOR and B. G. FAUNCE, *Sixth Symposium on Combustion*, p. 154, N.Y., (1957).
 967. A. L. MYERSON, F. R. TAYLOR and PH. L. HANST, *J. Chem. Phys.*, **26**, 1309 (1957).
 968. L. S. NELSON and D. A. RAMSAY, *J. Chem. Phys.*, **25**, 372 (1956).
 969. W. NEERNST, *Z. Elektrochem.*, **24**, 335 (1918).
 970. D. NEUBERGER and A. B. F. DUNCAN, *J. Chem. Phys.*, **22**, 1693 (1954).
 971. H. NEUERT, *Z. Naturforsch.*, **8a**, 459 (1953).
 972. J. VON NEUMANN, *OSRD Report*, N **549** (1942).
 973. J. VON NEUMANN and E. WIGNER, *Phys. Z.*, **30**, 467 (1929).
 974. A. O. NIER and E. E. HANSON, *Phys. Rev.*, **50**, 722 (1936).
 975. R. E. NIGHTINGALE, G. R. COWAN and B. CRAWFORD, JR., *J. Chem. Phys.*, **21**, 1398 (1953).
 976. M. NORDMEYER, *Ann. Phys.*, **16**, 706 (1933).
 977. R. G. W. NORRISH, *Z. Elektrochem.*, **56**, 705 (1952).
 978. R. G. W. NORRISH, *Cinétique et mécanisme des réactions d'inflammation et de combustion en phase gazeuse*, Paris, 1949, p. 16 (Colloques internationaux du Centre national de la recherche scientifique. XVI).
 979. R. G. W. NORRISH, *Disc. Faraday Soc.*, No. **14**, 16 (1953).
 980. R. G. W. NORRISH and G. PORTER, *Proc. Roy. Soc., A* **210**, 439 (1952).
 981. R. G. W. NORRISH, G. PORTER and B. A. THRUSH, *Nature*, **169**, 582 (1952).
 982. R. G. W. NORRISH and B. A. THRUSH, *Quart. Rev.*, **10**, 149 (1956).
 983. W. B. NOTTINGHAM, *Phys. Rev.*, **55**, 203 (1939).
 984. W. A. NOYES, *J. Chem. Phys.*, **5**, 807 (1937); H. SPONER and L. G. BONNER, *J. Chem. Phys.*, **8**, 33 (1940).
 985. W. A. NOYES, JR., G. B. PORTER and J. F. JOLLEY, *Chem. Rev.*, **56**, 49 (1956).
 986. R. A. OGG, JR., *J. Amer. Chem. Soc.*, **56**, 526 (1934); T. W. NEWTON, *J. Chem. Phys.*, **18**, 797 (1950).
 987. R. A. OGG, JR., *J. Chem. Phys.*, **15**, 337 (1947).
 988. R. A. OGG, JR., *J. Chem. Phys.*, **21**, 2079 (1953).
 989. R. A. OGG, JR. and M. POLANYI, *Proc. Manchester Lit. Phil. Soc.*, **78**, 41 (1933); *Trans. Faraday Soc.*, **31**, 604, 1375 (1935).
 990. R. A. OGG, JR. and M. POLANYI, *Trans. Faraday Soc.*, **31**, 482 (1935).

991. R. A. OGG, JR. and W. T. SUTPHEN, *Disc. Faraday Soc.*, **17**, 47 (1954).
 992. O. OLDBERG, *Phys. Rev.*, **37**, 194 (1931).
 993. O. OLDBERG, *Phys. Rev.*, **37**, 1550 (1931).
 994. O. OLDBERG, *Phys. Rev.*, **46**, 210 (1934).
 995. O. OLDBERG, *Phys. Rev.*, **90**, 727 (1953).
 996. O. OLDBERG, *J. Chem. Phys.*, **3**, 266 (1935).
 997. O. OLDBERG and A. A. FROST, *Chem. Rev.*, **20**, 99 (1937).
 998. L. O. OLSEN and G. P. KERR, *Phys. Rev.*, **72**, 115 (1947).
 999. H. OOTUKA, *Z. phys. Chem.*, **B 7**, 422 (1930).
 1000. W. OSTWALD, *J. prakt. Chem.*, **28**, 449 (1883).
 1001. W. OSTWALD, *Lehrbuch der allgemeinen Chemie*, Bd. II, p. 635, Leipzig, (1887).
 1002. W. OSTWALD, *Z. phys. Chem.*, **34**, 248 (1900).
 1003. J. W. OTVOS and D. P. STEVENSON, *J. Amer. Chem. Soc.*, **78**, 546 (1956).
 1003'. P. J. PADLEY and T. M. SUGDEN, *Proc. Roy. Soc., A* **248**, 248 (1958); E. M. BULEVICZ and T. M. SUGDEN, *Trans. Faraday Soc.*, **54**, 1855 (1958).
 1003a. H. B. PALMER, *J. Chem. Phys.*, **26**, 648 (1957).
 1004. H. B. PALMER and D. F. HORNIG, *J. Chem. Phys.*, **26**, 98 (1957).
 1005. F. PANETH, *Trans. Faraday Soc.*, **30**, 179 (1934).
 1006. F. PANETH and W. HOFEDITZ, *Ber.*, **62 B**, 1335 (1929).
 1007. J. G. PARKER, C. E. ADAMS and R. M. STAVSETH, *J. Acoust. Soc. Am.*, **25**, 263 (1953).
 1008. W. G. PARKER and H. G. WOLFHARD, *J. Chem. Soc.*, 2038 (1950).
 1009. F. PATAT, *Z. Elektrochem.*, **42**, 85 (1936).
 1010. F. PATAT, *Anz. Akad. Wiss. Wien., Math.-naturwiss. Klasse*, 93 (1933); F. PATAT and H. HOCH, *Z. Elektrochem.*, **41**, 494 (1935).
 1011. F. PATAT, *Z. phys. Chem.*, **B 32**, 274, 294 (1936); F. PATAT and H. SACHSSE, *Z. Elektrochem.*, **41**, 493 (1935); *Nachr. Ges. Wiss. Gottingen* III, 1, 41 (1935); H. SACHSSE, *Z. phys. Chem.*, **B 31**, 79, 87 (1935).
 1012. F. PATAT and E. BARTHOLOMÉ, *Z. phys. Chem.*, **B 32**, 396 (1936).
 1013. C. R. PATRICK and J. C. ROBB, *Trans. Faraday Soc.*, **51**, 1697 (1955).
 1013a. C. R. PATRICK and J. C. ROBB, *Disc. Faraday Soc.*, **17**, 98 (1954).
 1014. W. PAYMAN and N. S. WALLS, *J. Chem. Soc.*, 420 (1923).
 1015. W. PAYMAN and R. V. WHEELER, *Fuel Sci. Pract.*, **8**, 4 (1929).
 1016. T. G. PEARSON, *J. Chem. Soc.*, 1718 (1934); N. A. PRILEZHAYEVA and A. N. TERENIN, *Trans. Faraday Soc.*, **31**, 1483 (1935); M. BURTON, *J. Amer. Chem. Soc.*, **58**, 1645 (1936).
 1017. T. G. PEARSON and R. H. PURCELL, *J. Chem. Soc.*, 1151 (1935); 253 (1936); N. H. GLAZEBROOK and T. G. PEARSON, *J. Chem. Soc.*, 1777 (1936); 567 (1937).
 1018. R. N. PEASE, *J. Amer. Chem. Soc.*, **52**, 5106 (1930).
 1019. R. N. PEASE, *J. Chem. Phys.*, **7**, 749 (1939).
 1020. H. PELZER and E. WIGNER, *Z. phys. Chem.*, **B 15**, 445 (1931).
 1021. J. P. PEMSLER, *J. Chem. Phys.*, **22**, 1834 (1954).
 1022. S. S. PENNER and E. K. BJÖRNERUD, *J. Chem. Phys.*, **23**, 143 (1955).
 1023. W. G. PENNEY, *Phys. Rev.*, **39**, 467 (1932).
 1024. F. M. PENNING, *Physica*, **5**, 286 (1938).
 1025. H. C. PENNY and H. AROESTE, *J. Chem. Phys.*, **23**, 1281 (1955).
 1026. R. L. PERRINE and H. S. JOHNSTON, *J. Chem. Phys.*, **21**, 2202 (1953).
 1027. H. S. PICKERING and J. W. LINNETT, *Trans. Faraday Soc.* **47**, 1101 (1951).
 1028. W. H. PIELMEIER, *J. Acoust. Soc. Amer.*, **15**, 22 (1943).
 1029. J. N. PITTS and F. E. BLACET, *J. Amer. Chem. Soc.*, **74**, 455 (1952).
 1029a. M. N. PLOOSTER and D. GARVIN, *J. Amer. Chem. Soc.*, **78**, 6003 (1956).
 1030. M. POLANYI, *Atomic Reactions*, London, (1932).
 1031. M. POLANYI, *Trans. Faraday Soc.*, **24**, 606 (1928); E. HORN, M. POLANYI and H. SATTLER, *Z. phys. Chem.*, **B 17**, 220 (1932).
 1031a. J. C. POLANYI, *J. Chem. Phys.*, **23**, 1505 (1955).
 1032. M. POLANYI and G. SCHAY, *Z. phys. Chem.*, **B 1**, 30 (1928).

1033. M. POLANYI and D. W. G. STYLE, *Naturwissenschaften*, **20**, 401 (1932); E. HORN, M. POLANYI and D. W. G. STYLE, *Trans. Faraday Soc.*, **30**, 189 (1934).
- 1033a. H. POLLAK and R. VAN GREEN, *Bull. Soc. Chim. Belg.*, **65**, 957 (1956).
1034. M. POOL, *Phys. Rev.*, **38**, 955 (1931).
1035. H. G. POOLE, *Proc. Roy. Soc., A* **163**, 404, 415, 424 (1937).
1036. G. PORTER, *Disc. Faraday Soc.*, **9**, 60 (1950).
1037. G. PORTER, *Proc. Roy. Soc., A* **200**, 284 (1950).
1038. G. PORTER, *Fourth Symposium on Combustion*, p. 248, Baltimore, (1953).
1039. G. PORTER and F. J. WRIGHT, *Disc. Faraday Soc.*, **14**, 23 (1953).
- 1039a. G. PORTER and F. J. WRIGHT, *Trans. Faraday Soc.*, **51**, 1201 (1955).
1040. R. F. POTTER, *Phys. Rev.*, **87**, 232 (1952); **93**, 650 (1954).
1041. R. F. POTTER, *J. Chem. Phys.*, **23**, 2462 (1955).
1042. M. PRETTRE, *Ann. Off. nat. des combust. liquides*, **6**, 7, 269, 533 (1931).
1043. M. PRETTRE, *Third Symposium on Combustion, Flame and Explosion Phenomena*, p. 397, Baltimore, (1949).
1044. I. PRIGOGINE, *J. Phys. Coll. Chem.*, **55**, 765 (1951).
1045. I. PRIGOGINE and M. MAHIEU, *Physica*, **16**, 51 (1950).
1046. I. PRIGOGINE and E. XHROUET, *Physica*, **15**, 913 (1949).
1047. H. O. PRITCHARD, *Chem. Rev.*, **52**, 529 (1953).
1048. H. O. PRITCHARD, *Rec. Trav. Chim. des Pays-Bas* **74**, 779 (1955).
1049. H. O. PRITCHARD, J. B. PYKE and A. F. TROTMAN-DICKENSON, *J. Amer. Chem. Soc.*, **76**, 1201 (1954).
1050. H. O. PRITCHARD, J. B. PYKE and A. F. TROTMAN-DICKENSON, *J. Amer. Chem. Soc.*, **77**, 2629 (1955).
1051. H. O. PRITCHARD, R. G. SOWDEN and A. F. TROTMAN-DICKENSON, *Proc. Roy. Soc., A* **217**, 563; **A 218**, 416 (1953).
- 1051a. B. S. RABINOVITCH and M. J. HULATT, *J. Chem. Phys.*, **27**, 592 (1957).
1052. E. RABINOWITSCH, *Trans. Faraday Soc.*, **33**, 283 (1937); E. RABINOWITSCH and H. L. LEHMANN, *Trans. Faraday Soc.*, **31**, 689 (1935); E. RABINOWITSCH and W. C. WOOD, *Trans. Faraday Soc.*, **32**, 907 (1936); *J. Chem. Phys.*, **4**, 497 (1936).
1053. H. RAMIEN, *Z. Phys.*, **70**, 353 (1931).
1054. D. A. RAMSAY, *J. Chem. Phys.*, **20**, 1920 (1952).
1055. D. A. RAMSAY, *J. Chem. Phys.*, **21**, 960 (1953).
1056. H. C. RAMSPERGER, *J. Amer. Chem. Soc.*, **49**, 912, 1495 (1927).
1057. O. REDLICH, *Z. phys. Chem.*, **B 28**, 371 (1935).
- 1057a. J. F. REED and B. S. RABINOVITCH, *J. Phys. Chem.*, **59**, 261 (1955).
1058. A. L. G. REES, *Proc. Phys. Soc.*, **59**, 998, 1008 (1947).
1059. L. H. REINECKE, *Z. Phys.*, **135**, 361 (1953).
1060. A. REMBAUM and M. SZWARC, *J. Chem. Phys.*, **23**, 909 (1955).
1061. F. O. RICE, *Trans. Faraday Soc.*, **30**, 152 (1934).
1062. F. O. RICE and M. D. DOOLEY, *J. Amer. Chem. Soc.*, **56**, 2747 (1934).
1063. F. O. RICE and K. F. HERZFIELD, *J. Phys. Coll. Chem.*, **55**, 975 (1951).
1064. F. O. RICE and E. TELLER, *J. Chem. Phys.*, **6**, 489 (1938).
1065. F. O. RICE and R. E. VARNERIN, *J. Amer. Chem. Soc.*, **76**, 324 (1954).
1066. F. O. RICE and F. R. WHALEY, *J. Amer. Chem. Soc.*, **56**, 1311 (1934).
1067. O. K. RICE, *J. Chem. Phys.*, **9**, 258 (1941).
- 1067a. O. K. RICE, *J. Chem. Phys.*, **21**, 730 (1953).
1068. O. K. RICE and H. C. RAMSPERGER, *J. Amer. Chem. Soc.*, **49**, 1617 (1927); **50**, 617 (1928).
1069. W. T. RICHARDS, *J. Chem. Phys.*, **4**, 561 (1936).
1070. W. T. RICHARDS, *Rev. Mod. Phys.*, **11**, 36 (1939).
1071. W. RICHARDS and J. A. REID, *J. Chem. Phys.*, **1**, 114 (1933).
1072. W. RICHARDS and J. A. REID, *J. Chem. Phys.*, **2**, 206 (1934).
1073. J. M. RICHARDSON, *Phys. Rev.*, **88**, 895 (1952).
1074. O. W. RICHARDSON, *Proc. Roy. Soc., A* **111**, 714 (1926); A. S. ROY, *Proc. Nat. Acad. Sci.*, **19**, 441 (1933).
1075. F. F. RIEKE, *J. Chem. Phys.*, **4**, 513 (1936); **5**, 831 (1937).

1076. J. K. ROBERTS, *Proc. Roy. Soc., A* **152**, 445, 464 (1935).
 1077. R. H. ROBERTS and S. E. J. JOHNSEN, *Analyst. Chem.*, **20**, 690 (1948).
 1077a. W. H. RODEBUSH and M. L. SPEALMAN, *J. Amer. Chem. Soc.*, **57**, 1474 (1935).
 1078. W. H. RODEBUSH and M. H. WAHL, *J. Chem. Phys.*, **1**, 696 (1933).
 1079. W. A. ROGERS and M. A. BIONDI, *Phys. Rev.*, **99**, 1657 (1955).
 1080. G. K. ROLLEFSON, *J. Amer. Chem. Soc.*, **55**, 148 (1933).
 1081. G. K. ROLLEFSON and M. BURTON, *Photochemistry and Mechanism of Chemical Reactions*, N.Y., (1942).
 1082. G. K. ROLLEFSON and H. EYRING, *J. Amer. Chem. Soc.*, **54**, 170 (1932).
 1083. R. ROMPE, *Z. Phys.*, **65**, 404 (1930); O. HEIL, *Z. Phys.*, **74**, 18 (1932).
 1084. J. B. ROSEN, *J. Chem. Phys.*, **22**, 733, 742, 750 (1954); *Sixth Symposium on Combustion*, p. 236, N.Y., (1957).
 1085. N. ROSEN, *J. Chem. Phys.*, **1**, 319 (1933).
 1085a. H. M. ROSENSTOCK and C. E. MELTON, *J. Chem. Phys.*, **26**, 314 (1957).
 1086. H. M. ROSENSTOCK, M. B. WALLENSTEIN, A. L. WAHRHAFTIG and H. EYRING, *Proc. Nat. Acad. Sci.*, **38**, 667 (1952).
 1087. W. A. ROSSER, JR. and H. WISE, *J. Chem. Phys.*, **24**, 493 (1956).
 1088. TH. D. ROSSING and S. LEGVOLD, *J. Chem. Phys.*, **23**, 1118 (1955); R. AMME and S. LEGVOLD, *J. Chem. Phys.*, **23**, 1960 (1955).
 1089. F. RÖSSLER, *Z. Phys.*, **96**, 251 (1935).
 1090. A. ROSTAGNI, *Nuovo Cim., Nuova Ser.*, **11**, 621 (1934); **13**, 389 (1936).
 1091. E. ROTH and G. SCHAY, *Z. phys. Chem.*, **B 28**, 323 (1935).
 1092. D. ROWLEY and H. STEINER, *Disc. Faraday Soc.*, **10**, 198 (1951).
 1093. J. S. ROWLINSON, *Quart. Rev.*, **8**, 168 (1954).
 1094. A. S. ROY and M. E. ROSE, *Proc. Roy. Soc., A* **149**, 511 (1935).
 1095. R. J. RUBIN and K. E. SHULER, *J. Chem. Phys.*, **25**, 59, 68 (1956).
 1096. K. E. RUSSELL and J. SIMONS, *Proc. Roy. Soc., A* **217**, 271 (1953).
 1097. H. SACHSSE and E. BARTHOLOMÉ, *Z. Elektrochem.*, **53**, 183 (1949).
 1098. A. SAFFER and T. W. DAVIS, *J. Amer. Chem. Soc.*, **67**, 641 (1945).
 1099. M. N. SAHA, *Phil. Mag.*, (VI), **40**, 472 (1920).
 1100. E. W. SAMSON, *Phys. Rev.*, **40**, 940 (1932).
 1101. T. M. SANDERS, JR., A. L. SCHAWLOW, G. C. DOUSMANIS and C. H. TOWNES, *J. Chem. Phys.*, **22**, 245 (1954).
 1102. E. SÄNGER, *Explosivstoffe*, **3**, 85 (1955).
 1102a. S. SATO, *J. Chem. Phys.*, **23**, 592 (1955).
 1103. K. SCHÄFER, *Z. phys. Chem.*, **B 46**, 212 (1940).
 1104. W. SCHAFFERNICHT, *Z. Phys.*, **62**, 106 (1930).
 1105. R. L. SCHALLA and G. E. McDONALD, *Fifth Symposium on Combustion*, p. 316, N.Y., (1955).
 1106. G. SCHAY, *Hochverdünnte Flammen*, Berlin (1930).
 1107. G. SCHAY, *Z. phys. Chem.*, **B 11**, 291 (1931).
 1108. M. D. SCHEER, *Fifth Symposium on Combustion*, p. 435, N.Y., (1955).
 1109. P. W. SCHENK and H. JABLONOWSKY, *Z. Elektrochem.*, **45**, 650 (1939); *Z. anorg. Chem.*, **244**, 397 (1940).
 1110. M. SCHINDLER and G. L. WEISSLER, *Phys. Rev.*, **85**, 759 (1952).
 1111. D. O. SCHISSLER and D. P. STEVENSON, *J. Chem. Phys.*, **24**, 926 (1956).
 1112. L. SCHOEN, *Fifth Symposium on Combustion*, p. 786, N.Y., (1955).
 1112a. C. C. SCHUBERT and R. N. PEASE, *J. Amer. Chem. Soc.*, **78**, 5553 (1956).
 1113. C. C. SCHUBERT and R. N. PEASE, *J. Chem. Phys.*, **24**, 919 (1956).
 1114. H. SCHÜLER, *Mem. Soc. roy. sci. Liège*, **13**, 231 (1953).
 1115. R. H. SCHULER, *J. Chem. Phys.*, **22**, 2026 (1954).
 1116. R. H. SCHULER and C. E. McCUALEY, *J. Chem. Phys.*, **25**, 1080 (1956).
 1117. J. W. SCHULTE, J. F. SUTTLE and R. WILHELM, *J. Amer. Chem. Soc.*, **75**, 2222 (1953).
 1118. R. D. SCHULTZ and H. A. TAYLOR, *J. Chem. Phys.*, **18**, 194 (1950).
 1119. H. J. SCHUMACHER, *Chemische Gasreaktionen*, Dresden u. Leipzig, (1938).

1120. H. J. SCHUMACHER, *J. Amer. Chem. Soc.*, **52**, 2377 (1930); *Z. phys. Chem.*, **B** **17**, 405 (1932); U. BERETTA and H. J. SCHUMACHER, *Z. phys. Chem.*, **B** **17**, 417 (1932).
1121. H. J. SCHUMACHER and G. SPRENGER, *Z. phys. Chem.*, **B** **12**, 115 (1931).
1122. H. J. SCHUMACHER and G. STIEGER, *Z. phys. Chem.*, **B** **12**, 348 (1931).
1123. H. J. SCHUMACHER and E. O. WIIG, *Z. phys. Chem.*, **B** **11**, 45 (1930).
1124. G. M. SCHWAB and H. FRIESS, *Z. Elektrochem.*, **39**, 586 (1933).
1125. R. N. SCHWARTZ and K. F. HERZFIELD, *J. Chem. Phys.*, **22**, 767 (1954).
1126. R. N. SCHWARTZ, Z. I. SLAWSKY and K. F. HERZFIELD, *J. Chem. Phys.*, **20**, 1591 (1952).
1127. H. A. SCHWARZ, R. R. WILLIAMS, JR. and W. H. HAMILL, *J. Amer. Chem. Soc.*, **74**, 6007 (1952).
1128. A. C. SCURLOCK and J. H. GROVER, *Fourth Symposium on Combustion*, p. 645, Baltimore, (1953).
- 1128a. A. H. SCHON, *Ann. Rev. Phys. Chem.*, **8**, 439 (1957).
1129. H. SENFTLEBEN and I. REHREN, *Z. Phys.*, **37**, 529 (1926).
1130. P. K. SEN GUPTA, *Sci. and Cult.*, **19**, 414 (1954).
1131. R. SERBER and H. S. SNYDER, *Phys. Rev.*, **87**, 152 (1952).
1132. D. SETTE, A. BUSALA and J. C. HUBBARD, *J. Chem. Phys.*, **23**, 787 (1955).
1133. D. SETTE and J. C. HUBBARD, *J. Acoust. Soc. Amer.*, **25**, 994 (1953); T. S. RAO and J. C. HUBBARD, *J. Acoust. Soc. Amer.*, **27**, 321 (1955).
- 1133a. A. SHEPP, *J. Chem. Phys.*, **24**, 939 (1956).
- 1133b. A. SHEPP and K. O. KUTSCHKE, *J. Chem. Phys.*, **26**, 1020 (1957).
1134. CH. W. SHERWIN, *Phys. Rev.*, **57**, 814 (1940).
1135. K. E. SHULER, *J. Chem. Phys.*, **21**, 624 (1953).
1136. K. E. SHULER, *Fifth Symposium on Combustion*, p. 56, N.Y., (1955).
1137. K. E. SHULER, *Sixth Symposium on Combustion*, p. 371, N.Y., (1957).
1138. D. V. SICKMAN and O. K. RICE, *J. Chem. Phys.*, **4**, 608 (1936).
1139. D. W. SIDA, *Proc. Phys. Soc.*, **A** **68**, 240 (1955).
1140. J. H. SIMONS, S. M. FONTANA, H. T. FRANCIS and L. G. UNGER, *J. Chem. Phys.*, **11**, 312 (1943).
1141. J. H. SIMONS, H. T. FRANCIS, E. E. MUSCHLITZ, JR. and G. C. FRYBURG, *J. Chem. Phys.*, **11**, 316 (1943).
1142. J. C. SLATER, *Electronic Structure of Atoms and Molecules*, Technical Report No. 3 of the Solid State and Molecular Theory Group, M.I.T.
1143. N. B. SLATER, *Proc. Cambr. Phil. Soc.*, **35**, 56 (1939).
1144. N. B. SLATER, *Proc. Roy. Soc.*, **A** **194**, 112 (1948).
1145. N. B. SLATER, *Phil. Trans.*, **A** **246**, 57 (1953).
1146. N. B. SLATER, *Proc. Roy. Soc.*, **A** **218**, 224 (1953).
1147. N. B. SLATER, *Proc. Roy. Soc. Edinburgh*, **A** **64**, 161 (1954-1955); *J. Chem. Phys.*, **24**, 1256 (1956); *Theory of Unimolecular Reactions*, Ithaca N.Y. and London, 1959.
1148. N. J. H. SMALL and A. R. UBBELOHDE, *J. Chem. Soc.*, 723 (1950).
1149. H. M. SMALLWOOD, *J. Amer. Chem. Soc.*, **56**, 1542 (1934).
1150. F. T. SMITH, *J. Chem. Phys.*, **22**, 1605 (1954).
1151. J. H. SMITH and F. DANIELS, *J. Amer. Chem. Soc.*, **69**, 1735 (1947).
1152. N. D. SMITH, *Phys. Rev.*, **49**, 345 (1936).
1153. P. SMITH, *Chem. and Ind.*, **No. 42**, 1299 (1954).
1154. P. T. SMITH, *Phys. Rev.*, **36**, 1293 (1930).
1155. R. P. SMITH and H. EYRING, *J. Amer. Chem. Soc.*, **74**, 229 (1952).
1156. R. P. SMITH, T. REE, J. L. MAGEE and H. EYRING, *J. Amer. Chem. Soc.*, **73**, 2263 (1951).
1157. S. R. SMITH and A. S. GORDON, *J. Chem. Phys.*, **22**, 1150 (1954).
1158. A. SMITHHELLS and F. DENT, *Trans. Chem. Soc.*, **65**, 603 (1894).
1159. A. SMITHHELLS and H. INGLE, *Trans. Chem. Soc.*, **61**, 216 (1892).
1160. F. F. SNOWDEN and D. W. G. STYLE, *Trans. Faraday Soc.*, **35**, 426 (1939).

1161. R. D. SOUFFIE, R. R. WILLIAMS and W. H. HAMILL, *J. Amer. Chem. Soc.*, **78**, 917 (1956).
1162. D. B. SPALDING, *Phil. Trans.*, **A 249**, 1 (1956).
1163. D. B. SPALDING, *Sixth Symposium on Combustion*, p. 12, N.Y., (1957).
- 1163a. D. B. SPALDING, *Combustion and Flame*, **1**, 296 (1957).
- 1163b. D. B. SPALDING, *Proc. Roy. Soc.*, **A 240**, 83 (1957).
1164. G. SPRENGER, *Z. Elektrochem.*, **37**, 674 (1931).
- 1164a. C. R. STANLEY, *Proc. Roy. Soc.*, **A241**, 180 (1957).
1165. R. V. ST. AUNEY, *Chimie et Industrie*, **29**, 1011 (1933).
1166. V. STANNET and R. B. MESROBIAN, *J. Amer. Chem. Soc.*, **72**, 4125 (1950).
1167. J. STARK, *Phys. Z.*, **9**, 889, 894 (1908); *Prinzipien der Atomdynamik*, Leipzig, (1911); *Ann. Phys.*, **38**, 467 (1912); A. EINSTEIN, *Ann. Phys.*, **37**, 832; **38**, 881 (1912); *J. Phys. Radium*, **3**, 277 (1913).
1168. L. A. K. STAVELEY and C. N. HINSHELWOOD, *J. Chem. Soc.*, 812 (1936).
1169. E. W. R. STEACIE, *Atomic and Free Radical Reactions*, N.Y., (1954).
1170. E. W. R. STEACIE and M. SZWARC, *J. Chem. Phys.*, **19**, 1309 (1951).
1171. E. W. R. STEACIE and R. D. McDONALD, *J. Chem. Phys.*, **4**, 75 (1936).
1172. A. E. STEARN and H. EYRING, *J. Chem. Phys.*, **3**, 778 (1935).
1173. R. P. STEIN, *Phys. Rev.*, **85**, 759 (1952).
1174. S. STEIN, E. GERJUOY and T. HOLSTEIN, *Phys. Rev.*, **93**, 934 (1954).
1175. M. STEINBERG and W. E. KASKAN, *Fifth Symposium on Combustion*, p. 664, N.Y., (1955).
1176. H. STEINER, *Trans. Faraday Soc.*, **36**, 1111 (1940).
1177. W. STEINER, *Z. phys. Chem.*, **B 15**, 249 (1932).
1178. W. STEINER, *Trans. Faraday Soc.*, **31**, 623 (1935).
1179. E. R. STEPHENS, W. E. SCOTT, J. A. GOLDEN and B. FAUNCE, *Sixth Symposium on Combustion*, p. 273, N.Y., (1957).
1180. O. STERN and M. VOLMER, *Phys. Z.*, **20**, 183 (1919).
1181. R. K. STEUNENBERG and R. C. VOGEL, *J. Amer. Chem. Soc.*, **78**, 901 (1956).
1182. B. STEVENS, *J. Chem. Phys.*, **24**, 488 (1956).
1183. B. STEVENS, *J. Chem. Phys.*, **24**, 1272 (1956).
1184. F. W. STEVENS, *J. Amer. Chem. Soc.*, **50**, 3244 (1928).
1185. D. P. STEVENSON, *J. Chem. Phys.*, **15**, 409 (1947).
1186. D. P. STEVENSON and D. O. SCHISSLER, *J. Chem. Phys.*, **23**, 1353 (1955).
- 1186'. D. P. STEVENSON and D. O. SCHISSLER, *J. Chem. Phys.*, **29**, 282, 294 (1958).
- 1186a. D. T. STEWART, *Proc. Phys. Soc.*, **B 69**, 956 (1956).
1187. J. L. STEWART, *Rev. Sci. Instr.*, **17**, 59 (1946); E. S. STEWART, *Phys. Rev.*, **69**, 632 (1946); E. S. STEWART and J. L. STEWART, *J. Acoust. Soc. Amer.*, **24**, 194 (1952).
1188. H. H. STORCH, *J. Amer. Chem. Soc.*, **54**, 4188 (1932).
- 1188a. R. L. STRONG, J. C. W. CHIEN, P. E. GRAF and J. E. WILLARD, *J. Chem. Phys.*, **26**, 1287 (1957).
1189. R. L. STRONG and J. E. WILLARD, *Abstracts Amer. Chem. Soc., Meeting*, p. 26, N.Y., (1954).
1190. H. STUART, *Z. Phys.*, **32**, 262 (1925).
1191. F. J. STUBBS, K. U. INGOLD, B. C. SPALL, C. J. DANBY and C. N. HINSHELWOOD, *Proc. Roy. Soc.*, **A 214**, 20 (1952).
1192. E. C. G. STUECKELBERG, *Helv. Phys. Acta*, **5**, 369 (1932).
1193. T. M. SUGDEN, *Fifth Symposium on Combustion*, p. 406, N.Y., (1955); H. SMITH and T. M. SUGDEN, *Proc. Roy. Soc.*, **A 219**, 204 (1953).
1194. Y. SUGIURA, *Z. Phys.*, **45**, 484 (1927).
1195. G. B. B. M. SUTHERLAND, *Proc. Roy. Soc.*, **A 141**, 342 (1933).
1196. Z. G. SZABÓ, *Acta Chim. Acad. Sci. Hung.*, **3**, 139 (1953).
1197. L. SZILLARD and T. A. CHALMERS, *Nature*, **134**, 462 (1934).
1198. M. SZWARC, *Nature*, **160**, 403 (1947); *J. Chem. Phys.*, **16**, 128, 637 (1948).
1199. M. SZWARC, *J. Chem. Phys.*, **17**, 505 (1949).
1200. M. SZWARC, *Chem. Rev.*, **47**, 75 (1950).
1201. M. SZWARC, *J. Chem. Phys.*, **23**, 204 (1955).

- 1201a. M. SZWARC and L. HERK, *J. Chem. Phys.*, **29**, 438 (1958).
1201a'. M. SZWARC, *Proc. Roy. Soc., A* **198**, 287 (1949).
1202. M. SZWARC and J. W. TAYLOR, *J. Chem. Phys.*, **23**, 2310 (1955).
1203. TA-YOU WU, *Phys. Rev.*, **71**, 111 (1947).
1204. D. TABUCHI, *J. Chem. Phys.*, **23**, 2033 (1955).
1205. TAFFANEL and LE FLOCHE, *C.R. Acad. Sci., Paris*, **156**, 1544 (1913); **157**, 469, 595 (1913); TAFFANEL, *C.R. Acad. Sci., Paris*, **157**, 714; **158**, 42 (1914).
1206. K. TAKAYANAGI, *Progr. Theor. Phys. (Japan)*, **8**, 111, 497, (1952).
1207. K. TAKAYANAGI, *Progr. Theor. Phys. (Japan)*, **11**, 557 (1954).
1208. K. TAKAYANAGI and T. KISHIMOTO, *Progr. Theor. Phys. (Japan)*, **9**, 578 (1953).
1209. F. I. TANCSOS, *J. Chem. Phys.*, **25**, 439 (1956).
1210. C. TANFORD, *J. Chem. Phys.*, **15**, 433 (1947); C. TANFORD and R. N. PEASE, *J. Chem. Phys.*, **15**, 861 (1947).
1211. C. TANFORD and R. N. PEASE, *J. Chem. Phys.*, **15**, 431 (1947).
1212. J. T. TATE and P. T. SMITH, *Phys. Rev.*, **39**, 270 (1932); **46**, 773 (1934).
1213. E. H. TAYLOR and S. DATZ, *J. Chem. Phys.*, **23**, 1711 (1955).
1214. N. TECLU, *J. prakt. Chem.*, **44**, 246 (1891).
1215. E. TELLER, *J. Phys. Chem.*, **41**, 109 (1937).
1216. S. K. THABET, Thesis, London, 1951.
1217. W. J. THALER, *J. Acoust. Soc. Amer.*, **24**, 15 (1952).
1218. O. THIEME, *Z. Phys.*, **78**, 412 (1932).
1219. C. L. THOMAS, G. EGLOFF and J. C. MORRELL, *Chem. Rev.*, **28**, 1 (1941).
1220. J. R. THOMAS and H. W. CRANDALL, *Industr. Engng. Chem. (Industr.)*, **43**, 2761 (1951).
1221. H. W. THOMPSON, *Z. phys. Chem.*, **B** **10**, 273 (1930).
1221a. H. W. THOMPSON and C. N. HINSHELWOOD, *Proc. Roy. Soc., A* **122**, 610 (1929).
1222. J. P. TOENNIS and E. F. GREENE, *J. Chem. Phys.*, **23**, 1366 (1955).
1223. R. C. TOLMAN, *The Principles of Statistical Mechanics*, Oxford, (1938).
1224. M. TRAUTZ, *Z. anorg. Chem.*, **88**, 285 (1914); M. TRAUTZ and L. WACHENHEIM, *Z. anorg. Chem.*, **97**, 241 (1916); M. TRAUTZ and F. A. HENGLEIN, *Z. anorg. Chem.*, **110**, 237 (1920); M. TRAUTZ and H. SCHLUETER, *Z. anorg. Chem.*, **136** 1 (1924).
1225. M. TRAUTZ and V. P. DALAL, *Z. anorg. Chem.*, **102**, 149 (1918).
1226. J. C. TREACY and F. DANIELS, *J. Amer. Chem. Soc.*, **77**, 2033 (1955).
1227. W. TRITTELWITZ, *Ann. Phys.*, **40**, 131 (1941).
1228. A. F. TROTMAN-DICKENSON, *Gas Kinetics*, London, (1955).
1229. A. F. TROTMAN-DICKENSON, J. R. BIRCHARD and E. W. R. STEACIE, *J. Chem. Phys.*, **19**, 163 (1951).
1230. A. F. TROTMAN-DICKENSON and E. W. R. STEACIE, *J. Chem. Phys.*, **19**, 169 (1951).
1231. A. F. TROTMAN-DICKENSON and E. W. R. STEACIE, *J. Chem. Phys.*, **19**, 329 (1951).
1232. T. TSUCHIYA, *J. Chem. Phys.*, **22**, 1784 (1954).
1233. L. A. TURNER, *Phys. Rev.*, **31**, 983 (1928); L. A. TURNER and E. W. SAMSON, *Phys. Rev.*, **37**, 1684 (1931).
1234. A. R. UBBELOHDE, *Proc. Roy. Soc., A* **152**, 378 (1935).
1235. L. UBBELOHDE and E. KOELLIKER, *J. Gasbeleucht.*, **59**, 49 (1916).
1236. H. C. UREY and J. R. BATES, *Phys. Rev.*, **34**, 1541 (1929).
1237. H. C. UREY, L. H. DAWSEY and F. O. RICE, *J. Amer. Chem. Soc.*, **51**, 1371 (1929).
1238. W. M. VAIDYA, *Proc. Roy. Soc., A* **147**, 513 (1934); *Proc. Phys. Soc., A* **64**, 428 (1951).
1239. A. VAN ITTERBEEK and P. MARIENS, *Physica*, **7**, 938 (1940).
1240. A. VAN ITTERBEEK and R. VERMAELEN, *Physica*, **9**, 345 (1942).
1241. M. VAN MEERSCHE, *Bull. Soc. Chim. Belg.*, **60**, 99 (1951).
1242. M. VANPÉE, *Bull. Soc. Chim. Belg.*, **62**, 468 (1953).
1243. M. VANPÉE and F. GRARD, *Fifth Symposium on Combustion*, p. 484, N.Y., 1955; *Fuel*, **34**, 433 (1955); M. VANPÉE, *Compt. rend.*, **242**, 373 (1956); **243**, 804 (1956).

1244. A. VAN TIGGELEN and J. VAERMAN, *Bull. Soc. Chim. Belg.*, **62**, 653 (1953).
1245. A. VAN TIGGELEN, *Mém. Acad. Roy. Belg.*, **27**, 3 (1952); A. VAN TIGGELEN and J. DECKERS, *Sixth Symposium on Combustion*, p. 61, N.Y., (1957).
1246. J. VAN WONTERGHEM and A. VAN TIGGELEN, *Fifth Symposium on Combustion*, p. 637, N.Y., (1955).
1247. R. N. VARNEY, *Phys. Rev.*, **47**, 483 (1935); **50**, 159, 1095 (1936); O. BEECK, *Phys. Z.*, **35**, 36 (1934).
1248. R. N. VARNEY, *Phys. Rev.*, **53**, 732 (1938); A. ROSTAGNI, *Phys. Rev.*, **53**, 729 (1938).
1249. R. N. VARNEY, *J. Chem. Phys.*, **23**, 866 (1955).
1250. F. H. VERHOEK, *Trans. Faraday Soc.*, **31**, 1521 (1935).
1251. R. DE VOGELAERE and M. BOUDART, *J. Chem. Phys.*, **23**, 1236 (1955).
1252. D. H. VOLMAN, *J. Chem. Phys.*, **21**, 2086 (1953); *J. Amer. Chem. Soc.*, **76**, 6034 (1954).
1253. D. H. VOLMAN, *J. Chem. Phys.*, **24**, 122 (1956).
1254. D. H. VOLMAN, *J. Chem. Phys.*, **25**, 288 (1956).
1255. D. H. VOLMAN and R. K. BRINTON, *J. Chem. Phys.*, **22**, 929 (1954).
1256. M. VOLMER and M. BOGDAN, *Z. phys. Chem.*, **B 21**, 257 (1933).
1257. G. WADDINGTON and R. C. TOLMAN, *J. Amer. Chem. Soc.*, **57**, 689 (1935).
- 1257a. L. A. WALL and W. J. MOORE, *J. Phys. Chem.*, **55**, 965 (1951).
1258. R. A. WALKER, *J. Chem. Phys.*, **19**, 494 (1951).
1259. R. A. WALKER, *Iowa State Coll. J. Sci.*, **27**, 272 (1953); R. A. WALKER, T. D. ROSSING and S. LEGVOLD, *Natl. Advisory Comm. Aeronaut. Techn. Notes.*, 3210 (1954).
- 1259a. F. T. WALL, L. A. HILLER, JR. and J. MAZUR, *J. Chem. Phys.*, **29**, 255 (1958).
1260. A. D. WALSH, *Trans. Faraday Soc.*, **43**, 297 (1947).
1261. A. D. WALSH, *J. Chem. Soc.*, 2266 (1953).
1262. A. D. WALSH, *Fuel*, **33**, 247 (1954).
1263. J. M. WALSH and F. A. MATSEN, *J. Chem. Phys.*, **19**, 526 (1951).
1264. G. H. WANNIER, *Phys. Rev.*, **90**, 817 (1953).
1265. O. H. WANSBROUGH-JONES, *Proc. Roy. Soc., A* **127**, 530 (1930).
1266. E. WARBURG, *Sitzber. Preuss. Akad. Wiss.*, **300** (1918).
1267. E. WARBURG and W. RUMPF, *Z. Phys.*, **32**, 245 (1925).
1268. E. WARHURST, *Quart. Rev.*, **5**, 44 (1951).
- 1268a. E. WARHURST, *Trans. Faraday Soc.*, **54**, 1769 (1958).
1269. H. VON WARTENBERG and G. SCHULTZE, *Z. phys. Chem.*, **B 2**, 1 (1929).
1270. A. WASSERMAN, *J. Chem. Soc.*, 612 (1942).
- 1270a. L. A. WATERMEIER, *J. Chem. Phys.*, **27**, 1118 (1957).
1271. H. WAYLAND, *Phys. Rev.*, **52**, 31 (1937).
1272. I. F. WEEKS, *Third Symposium on Combustion, Flame and Explosion Phenomena*, p. 522, Baltimore, (1949).
1273. H. G. WEISS and I. SHAPIRO, *J. Amer. Chem. Soc.*, **75**, 1221 (1953).
1274. W. WEIZEL and O. BEECK, *Z. Phys.*, **76**, 250 (1932); F. ZWICKY, *Proc. Nat. Acad. Sci.*, **18**, 314 (1932).
1275. W. WELTNER and K. PITZER, *J. Amer. Chem. Soc.*, **73**, 2606 (1951); F. A. SMITH and E. C. CREITZ, *J. Res. Nat. Bur. Stand.*, **46**, 145 (1951).
1276. W. WEST, *J. Amer. Chem. Soc.*, **57**, 1931 (1935).
1277. W. WEST and L. SCHLESSINGER, *J. Amer. Chem. Soc.*, **60**, 961 (1938).
1278. R. E. WESTON, JR., *J. Chem. Phys.*, **23**, 988 (1955).
1279. F. W. DE WETTE and Z. I. SLAWSKY, *Physica*, **20**, 1169 (1954).
1280. A. G. WHITE, *J. Chem. Soc.*, **121**, 1244 (1922).
1281. J. U. WHITE, *J. Chem. Phys.*, **8**, 79 (1940).
1282. J. U. WHITE, *J. Chem. Phys.*, **8**, 459 (1940).
1283. S. G. WHITEWAY and C. R. MASSON, *J. Chem. Phys.*, **25**, 233 (1956).
1284. E. WHITTLE and E. W. R. STEACIE, *J. Chem. Phys.*, **21**, 993 (1953).
- 1284a. K. WIBERG, *Chem. Rev.*, **55**, 713 (1955).
1285. B. WIDOM and S. H. BAUER, *J. Chem. Phys.*, **21**, 1670 (1953).

1286. K. WIELAND, *Disc. Faraday Soc.*, **2**, 172 (1947).
 1287. H. WIENER and M. BURTON, *J. Amer. Chem. Soc.*, **75**, 5815 (1953).
 1288. E. P. WIGNER, *Gött. Nachr.*, No. 4, 375 (1927).
 1289. E. P. WIGNER, *Z. phys. Chem.*, **B 19**, 203 (1932).
 1290. E. P. WIGNER, *J. Chem. Phys.*, **5**, 720 (1937); **7**, 646 (1939).
 1291. E. P. WIGNER, *Trans. Faraday Soc.*, **34**, 29 (1938).
 1292. M. H. J. WIJNEN, *J. Chem. Phys.*, **23**, 1357 (1955).
 1293. K. A. WILDE, *J. Chem. Phys.*, **22**, 1788 (1954).
 1294. A. H. WILLBOURN and C. N. HINSHELWOOD, *Proc. Roy. Soc.*, **A 185**, 353 (1946).
 1295. E. J. B. WILLEY, *Trans. Faraday Soc.*, **30**, 230 (1934).
 1295a. E. J. B. WILLEY and E. K. RIDEAL, *J. Chem. Soc.*, 669 (1927).
 1296. R. R. WILLIAMS, JR. and R. A. OGG, JR., *J. Chem. Phys.*, **15**, 691 (1947).
 1297. R. R. WILLIAMS, JR. and R. A. OGG, JR., *J. Chem. Phys.*, **15**, 696 (1947).
 1298. D. J. WILSON and H. S. JOHNSTON, *J. Amer. Chem. Soc.*, **75**, 5763 (1953).
 1299. R. H. WILSON, J. B. CONWAY, A. ENGELBRECHT and A. V. GROSSE, *Nat. Bur. Stand. Circular*, No. **523**, 111 (1954).
 1300. J. G. WINANS, *Z. Phys.*, **60**, 631 (1930).
 1301. J. G. WINANS and E. C. G. STUECKELBERG, *Proc. Nat. Acad. Sci.*, **14**, 867 (1928).
 1301a. M. W. WINDSOR, N. DAVIDSON and R. TAYLOR, *J. Chem. Phys.*, **27**, 314 (1957).
 1301b. C. A. WINKLER and H. J. SCHIFF, *Disc. Faraday Soc.*, **14**, 63 (1953).
 1302. L. WITHROW and G. M. RASSWEILER, *Industr. Engng. Chem. (Indstr.)*, **25**, 923, 1359 (1933); **26**, 1256 (1934); **27**, 872 (1935).
 1303. H. WITTE, *Z. Phys.*, **88**, 415 (1934).
 1304. K. WOHL and M. MAGAT, *Z. phys. Chem.*, **B 19**, 117 (1932).
 1305. G. WOKER, *Die Katalyse, I. Die chemische Analyse*, XI-XII, p. 117, (1910).
 1306. F. WOLF, *Ann. Phys.*, **27**, 543 (1936).
 1307. F. WOLF, *Ann. Phys.*, **28**, 361 (1937).
 1308. F. WOLF, *Ann. Phys.*, **28**, 438 (1937).
 1309. F. WOLF, *Ann. Phys.*, **30**, 313 (1937).
 1310. F. WOLF, *Ann. Phys.*, **34**, 341 (1939).
 1311. R. L. WOLFGANG, R. C. ANDERSON and R. W. DODSON, *J. Chem. Phys.*, **24**, 16 (1956).
 1312. H. G. WOLFHARDT, *Z. techn. Phys.*, **24**, 206 (1943).
 1313. H. G. WOLFHARD and W. G. PARKER, *Fifth Symposium on Combustion*, p. 718, N.Y., (1955).
 1314. M. WOLFSBERG, *J. Chem. Phys.*, **24**, 24 (1956).
 1315. R. W. WOOD, *Phil. Mag.* (VI), **23**, 469 (1912); **24**, 673 (1912); **26**, 828 (1913).
 1316. R. W. WOOD, *Proc. Roy. Soc.*, **A 97**, 455 (1920); **A 102**, 1 (1922); *Phil. Mag.*, (VI), **42**, 729 (1921); **44**, 538 (1922).
 1317. R. W. WOOD, *Phil. Mag.* (VI), **50**, 774 (1925); (VII) **4**, 446 (1927).
 1318. R. W. WOOD and J. FRANCK, *Ber. Deutsch. Phys. Ges.*, **13**, 84 (1911).
 1319. R. W. WOOD and E. GAVIOLA, *Phil. Mag.*, (VII) **6**, 271, 352 (1928).
 1320. R. W. WOOD and F. W. LOOMIS, *Phil. Mag.*, (VII) **6**, 231 (1928).
 1321. I. YASUMORI and K. FUEKI, *J. Chem. Phys.*, **22**, 1790 (1954).
 1322. A. B. ZAHLAN and B. P. BURTT, *J. Chem. Phys.*, **24**, 478 (1956).
 1323. I. ZARTMANN, *J. Acoust. Soc. Amer.*, **21**, 171 (1949).
 1324. H. ZEISE, *Thermodynamik, BIII.-I, Tabellen*, Leipzig, (1954).
 1325. M. ZELIKOFF and L. M. ASCHENBRAND, *J. Chem. Phys.*, **22**, 1680, 1685 (1954).
 1326. M. ZELIKOFF and L. M. ASCHENBRAND, *J. Chem. Phys.*, **25**, 674 (1956).
 1327. M. W. ZEMANSKY, *Phys. Rev.*, **36**, 219 (1930).
 1328. C. ZENER, *Phys. Rev.*, **37**, 556 (1931); *11th Report Comm. Contact Catalysis*, p. 103, Washington, (1935).
 1329. C. ZENER, *Phys. Rev.*, **38**, 277 (1931).
 1330. C. ZENER, *Proc. Roy. Soc.*, **A 137**, 696 (1932); **A 140**, 660 (1933).
 1331. C. ZENER, *Proc. Cambr. Phil. Soc.*, **29**, 136 (1933).
 1332. A. J. ZMUDA, *J. Acoust. Soc. Amer.*, **23**, 472 (1951).
 1333. E. G. ZUBLER, W. H. HAMILL and R. R. WILLIAMS, JR., *J. Chem. Phys.*, **23**, 1263 (1955).
 1334. B. J. ZWOLINSKY and H. EYRING, *J. Amer. Chem. Soc.*, **69**, 2702 (1947).

NAME INDEX

- Adams G. K. 720, 722
 Aden A. L. 491
 Adler F. T. 364
 Avazov B. V. 649, 650
 Alekseyev D. V. 749
 Alexander E. A. 374
 Aliyev A. A. 696
 Allen P. E. M. 97, 246-248
 Altman D. 739
 Alyea N. H. 44
 Amdur I. 339
 Amemiya T. 536
 Anderson J. M. 103, 104
 Anderson R. C. 738-741
 Andreyev D. N. 541
 Andreyev K. K. 765
 Apin A. Ya. 716, 717
 Appleyard E. T. S. 492
 Aravin G. S. 688, 689
 Arden E. A. 713
 Aroeste H. 366
 Arrhenius S. A. 14, 566
 Aschenbrand L. M. 492
 Ashmore P. G. 270
 Atkinson B. 252
 Avramenko L. I. 99-101, 105, 107, 111, 265, 408, 415, 611, 682, 724
 Aybar S. 375
 Azatyan V. V. 99, 611
- Back R. A. 105
 Badger R. M. 454
 Baeyer A. 39
 Bagdasar'yan Kh. S. 268
 Bakh A. N. 19
 Bakhareva I. F. 25
 Bannister E. L. 328, 330
 Barenblat G. I. 742
 Barr J. 671
 Barskii G. A. 726
 Bartholomé E. 401-403, 699, 704, 705, 710, 728
 Barush M. R. 69
 Bates D. R. 429, 476, 502
 Bates J. R. 448, 449, 612
 Bauer E. 207, 209, 210, 364-366
 Bauer H. J. 355, 371
 Bauer S. H. 379-381
- Bawn C. E. H. 58, 90
 Bayliss N. S. 410
 Bechert K. 745
 Becker R. 378, 379, 751
 Beckerle J. O. 354
 Beeck O. 501
 Behrens H. 672, 690
 Belchetz L. 537
 Bell K. M. 630
 Bell R. P. 210, 211
 Belyayev A. F. 673, 716-718, 765
 Benson S. W. 180, 241
 Berger I. 86
 Berlie M. R. 261
 Bernstein R. B. 60
 Berry H. W. 499
 Berthelot H. 751
 Berzelius J. J. 33
 Beutler H. 88, 230, 350, 359, 444, 662
 Bigeleisen J. 194
 Biondi M. A. 490, 491
 Björnerud E. K. 686
 Bleakney W. 475
 Blochmann R. 683
 Bodenstein M. 11, 13, 15, 24, 324, 441, 453, 459, 461, 566, 569
 Bogdan M. 62, 320
 Bogdandy St. von 79, 102, 658
 Bogoyavlenskaya M. L. 48, 586
 Bonhoeffer K. F. 80, 93, 96, 105, 536
 Born M. 201
 Boudart M. 195, 378, 394, 395
 Boyd T. J. M. 507
 Boys S. F. 731
 Bozhko N. P. 534
 Bradt P. 333
 Breton J. 757, 759
 Brewer A. K. 532
 Brinton R. K. 108
 Britton D. 333, 334
 Brodskii A. I. 55, 56, 58
 Broida H. P. 356, 360, 675, 685, 687, 688
 Brout R. 346, 354-356, 369
 Bryce W. A. 78, 112, 241, 321
 Buben N. Ya. 587, 589
 Bubnov N. N. 241, 585
 Bunker D. L. 335, 345
 Bunsen R. W. 571
 Burgess R. H. 111

- Burhop E. H. S. 384, 488
 Burhorn F. 527
 Burke E. 711, 712
 Burke S. P. 668-670
 Burnett G. M. 65, 111
 Burton M. 74, 415, 421, 449, 454, 455, 459, 538
 Butayeva F. A. 472
 Butlerov A. M. 276
- Cadle R. D. 270
 Calcote H. F. 689, 708
 Calvert J. G. 78, 109, 627, 628
 Campbell D. E. 687
 Campbell E. S. 758
 Careri G. 271
 Carrington T. 675
 Cashion J. K. 137, 568
 Castellan G. W. 364
 Chaikin A. M. 47
 Chalmers T. A. 551
 Chambers T. S. 302
 Chamugam J. 270
 Chapman D. L. 751, 754
 Chernyak N. Ya. 582
 Chirkov N. M. 42
 Christiansen J. A. 566
 Clément C. 33
 Clusius K. 35
 Coblenz W. W. 386
 Coehn A. 465
 Collinson E. 560
 Conrad R. 483, 540
 Conway J. B. 699
 Cook G. A. 612
 Cook M. A. 760
 Cooley S. D. 738-741
 Cordes H. F. 275
 Corner J. 731
 Coulson C. A. 249, 250, 276
 Cowan G. R. 69
 Crandall H. W. 69
 Crompton R. W. 483
 Crussard L. 704
 Curie M. 545
 Curtiss C. F. 364, 687, 760
 Cvetačnović R. J. 101, 431
 Cyphers J. A. 712, 726, 727
- Dainton F. S. 554
 Damköhler G. 367, 691, 744
 Dalgarno A. 507
 Danby C. J. 333
 Daniell P. J. 704
 Daniels F. 314
 Darwent B. de B. 429, 431, 446, 448
- Datz S. 90, 253
 Davidson N. 105, 333, 335, 345, 761
 de Broglie L. 118
 Denbigh K. G. 281
 Dent F. 70
 Desormes C. B. 33
 de Vogelaere R. 195
 Devonshire A. F. 383
 de Wette F. W. 375
 Dibeler V. H. 333
 Dickinson R. G. 442, 448
 Dillon J. A. 505, 507
 Dingle J. R. 247
 Dixon H. B. 756, 758
 Dixon-Lewis G. 709, 711
 Dobrinskaya A. A. 72
 Dodd A. E. 65
 Dodonova N. Ya. 387, 388, 484
 Dondes S. 314, 558
 Döpel R. 495
 Douglas A. E. 74
 Dressler K. 104
 Dubois J. T. 394, 395, 438
 Duff R. E. 105, 760
 Dugger G. L. 698, 741, 742
 Dukel'skii V. M. 490, 504, 507, 508, 511, 514
 Durand E. 392
 Dwyer R. J. 105, 388
 D'yachkovskii F. S. 241, 585
- Egerton A. 68, 69, 452
 Eggersglüß W. 691
 Egloff G. 541
 Einstein A. 366, 452
 Eisenhut O. 540
 Elbe G. von 114, 625, 691, 693, 701, 702, 706-708
 Eltenton G. C. 81
 Emanuel' N. M. 18, 47, 65, 67, 68, 606-609, 733
 Endow N. 333
 Engel A. 499
 Engler K. O. 19
 Enikolopyan N. S. 629, 693
 Eremin E. N. 534
 Essex H. 556
 Eucken A. 375, 378, 379, 381, 384, 401, 402, 405
 Evans A. G. 58, 90
 Evans H. G. V. 104
 Evans M. G. 161, 179
 Evans M. W. 744
 Evett A. A. 365
 Eyring H. 58, 114, 138, 152, 153, 172, 179, 263, 278-280, 282, 290, 303, 305, 307, 308, 326, 334-336, 379, 553

- Fabrikant V. A. 472
 Fairbairn A. R. 673, 760
 Fairbrother F. 93
 Faire A. C. 491
 Farenhorst E. 250
 Farkas A. 95, 114
 Farkas L. 94-96, 257, 333
 Faunce B. G. 729
 Fedorenko N. V. 511, 514
 Fehling H. R. 653
 Feklisov G. I. 53, 112
 Fenimore C. P. 78, 687
 Fenn J. B. 708
 Ferguson R. E. 687, 690
 Fermi E. 358
 Field F. H. 517, 518
 Filler A. S. 760
 Finkelnburg W. 523
 Fischer F. 535
 Fluharty R. G. 546
 Fok N. V. 111, 448-451
 Foner S. N. 81, 612
 Ford H. F. 333
 Fowler A. 74
 Fox R. E. 490
 Franck H. H. 106
 Franck J. 358, 378, 401, 405, 483
 Frankenburger W. 96
 Frankevich Ye. L. 486, 516, 517
 Frank-Kamenetskii D. A. 63, 105, 589, 644-646, 669, 692, 693, 699, 701, 707, 708, 710, 713, 715-719, 723, 732, 738, 741, 742, 747-749
 Franklin J. L. 333, 518
 Franze C. 733
 Friauf J. B. 756
 Fricke E. F. 372
 Friedman H. L. 60
 Friedman R. 711, 712, 726, 727
 Friess H. 80
 Frische C. A. 499, 513
 Frish S. E. 540
 Fristrom R. M. 695
 Frost A. V. 606
 Fundaminsky A. 476
 Fundingsland O. T. 491
- Gaenssen H. 66
 Garvin D. 137, 251, 389, 659
 Gaviola E. 94, 428, 444
 Gaydon A. G. 70, 71, 630, 672, 673, 691, 698, 699, 729, 744, 745, 758, 760
 Geib K. H. 98, 100, 102, 257
 Geltman S. 476
 Gerjuoy E. 485
 Gerri N. J. 320
- Gershinowitz H. 105, 172, 326, 336, 379
 Gervart Yu. G. 692
 Gevantman L. H. 559
 Ghosh S. N. 509
 Gibson G. E. 410
 Giddings J. C. 303
 Gilbert M. 275, 739
 Gilkerson W. R. 761
 Gill E. K. 302, 333, 429
 Gioumonsis G. 519
 Glasstone S. 114, 305, 307, 379
 Glick H. S. 364
 Gnyubkin V. I. 72
 Gol'braikh E. Ye. 535
 Golden J. A. 729
 Golden S. 210
 Goldmann F. 751
 Gomer R. 65, 240, 241
 Gorban N. I. 261
 Gordon A. S. 115, 230, 674
 Gordon S. 555
 Gorin E. 78, 263
 Gouy L. G. 695
 Grard F. 597
 Gray J. A. 693
 Greaves J. C. 137
 Greene E. F. 755
 Griffing G. 502
 Griffith J. G. A. 606
 Grosse A. V. 699
 Groth W. 102
 Groth W. E. 444
 Guldberg K. 3
 Gunning H. E. 60
 Gurnee E. F. 505, 506
- Haas R. 483
 Haber F. 44, 94, 680, 681
 Hadman G. 36
 Hall A. R. 718, 719
 Hamill W. H. 518, 551
 Hanle W. 495, 496, 503
 Hanst P. L. 628
 Harries W. 483, 485
 Harteck P. 80, 94, 96, 98-102, 114, 257, 314, 333, 536, 558
 Hartel H. von 89-93, 107
 Hasted J. B. 504-506, 508-510
 Heidt L. J. 459
 Heitler W. 152
 Henderson G. H. 543
 Henderson I. H. S. 241
 Henri V. 457
 Herron J. T. 333
 Herschbach D. R. 267
 Hertel E. 455

- Herzberg G. 74
 Herzfeld K. F. 45, 364, 365, 367, 375, 381, 383, 384, 387
 Hevesy G. von 49
 Hickam W. M. 490
 Hillenbrand L. J. 307
 Hinshelwood C. N. 35, 78, 286-288, 290, 293, 302, 317, 319-321, 333, 336, 599, 606, 634
 Hirschfelder J. O. 336, 553, 687, 718, 719, 760
 Hollingsworth C. A. 132
 Holstein T. 485
 Horie T. 496
 Horn E. 107
 Hornig D. F. 273
 Horton F. 498
 Hudson R. L. 81, 612
 Hugogniot J. 752, 753
 Hulbert H. M. 364
 Hurtubise F. G. 429
- Ingle H. 70, 680
 Ingold K. U. 78, 81, 112, 241, 321
 Ivin K. J. 108, 109, 241, 268
- Jablonowsky H. 98
 Jackson D. S. 103
 Jackson J. M. 383
 James C. G. 75, 679
 Jefferies J. T. 470
 Jepson D. W. 336
 Johnston E. H. 314
 Johnston H. S. 267, 275, 313-315, 397, 398
 Jones G. W. 78, 687
 Jost W. 670, 686, 695, 733, 751, 754, 756, 757, 759
 Jouguet E. 704, 751
 Jung G. 459
 Just T. 761
- Kagan Yu. M. 471, 472, 540
 Kane W. R. 360, 687
 Karlovitz B. 670
 Karman T. von 707, 708, 718, 719
 Karmilova L. V. 38, 629, 633, 679
 Karyakin A. V. 69
 Karzhavina N. A. 726
 Kaskan W. E. 687, 690, 761
 Kassel L. S. 151, 238, 239, 253, 274, 287, 290-293, 295-297, 299-303, 316, 537
 Kaufman F. 75, 104, 105, 320
 Kauzmann W. 263
 Kavadas A. V. 103
- Keller H. H. 357
 Kelly R. 333
 Kelso J. R. 104, 105
 Kerner E. H. 366, 474
 Kerr J. A. 109
 Keyes R. T. 760
 Khanova I. I. 650
 Khariton Yu. B. 594, 655
 Khitrin L. N. 726
 Kilpatrick M. L. 307
 Kimball G. E. 237-239
 Kinbara T. 690
 King I. P. 689
 King J. R. 687
 Kinsey J. L. 611
 Kirschtein B. 492
 Kistiakowsky G. B. 65, 104, 105, 146, 237, 238, 240, 241, 251, 265, 302, 441, 456, 659, 755, 761, 765
 Klein G. 742
 Klumb H. 429
 Kneser H. O. 355, 371
 Knewstubb P. F. 492
 Knipe R. H. 115, 230, 674
 Kobozev N. I. 534, 535
 Koelliker E. 725
 Kogarko S. M. 757
 Kokochashvili V. I. 738
 Kolesnikova (Lorentso) R. V. 99-101, 107, 111, 265, 724
 Koller D. K. 534
 Kolotyrkin V. M. 514
 Kondrat'ev V. N. 65, 83, 84, 88, 105, 114, 229, 230, 234, 236, 265, 408, 438, 439, 454, 551, 611, 613, 633, 662, 666, 667, 676-679
 Kondrat'eva H. I. 83, 676-678
 Konovalov D. P. 39, 40
 Kooyman E. C. 250
 Kopp D. I. 599
 Kopsch U. 80, 98-102
 Kossel W. 276
 Koval'skii A. A. 45, 47, 48, 586, 594, 599, 608, 619, 620, 622, 623, 634, 635
 Kramers H. A. 138, 566
 Krauss J. W. 109
 Kuhn L. P. 328, 330
 Kukhtenko I. I. 56
 Kuprulanov S. Ye. 514
 Kushnerev M. Ya. 98, 101
 Kwart H. 328, 330
- Lacher J. R. 252
 Laffitte P. 759
 Laidler K. J. 114, 302, 305, 307, 333, 379, 429, 447, 487, 556

- Lambert J. D. 373, 374
 Lampe F. W. 517, 518
 Landau L. D. 217, 219, 290, 294, 296,
 303, 352, 384
 Lau E. 523
 Lavrovskaya G. K. 82, 109, 415, 589
 Layzer D. 751
 Leech J. W. 476
 Le Chatelier H. L. 704, 751
 Leermakers J. A. 316
 Leipunskii A. I. 229, 230, 236, 448, 512,
 513
 Leiter A. 172
 Lennard-Jones J. E. 352
 Le Roy D. J. 247, 261, 446, 447
 Lesemann K. J. 733
 Leser T. 653
 Levedahl W. J. 693
 Levey G. 551
 Lewis B. 114, 625, 701, 702, 706-708, 756
 Liddell W. J. 699
 Lind S. C. 541, 558
 Lindemann F. A. 283, 286
 Linnett J. W. 695, 729
 Lippincott E. P. 172
 London F. 151, 152, 156-160, 218, 502,
 504
 Lorentso (see Kolesnikova)
 Lossing F. P. 81, 241
 Lotka A. J. 692
 Lovachev L. A. 722
 Lukovnikov A. F. 51-53, 108, 112
 Luther R. 33
 Lütkemeyer H. 461
 Lyman E. R. 360, 687
 Lyubimova A. K. 516
- McCarthy R. L. 526
 McDonald G. Y. 454
 McDonell W. R. 555
 McKay R. M. 103
 Mackenzie H. A. E. 66
 Magat M. 745
 Magee J. L. 88, 161, 231, 232, 258, 280,
 308, 505, 506, 538
 Mahan B. H. 365
 Mahieu M. 137
 Maizus Z. K. 18, 47, 606, 608
 Mallard E. 704, 751
 Mamotenko M. F. 244
 Manella G. 333
 Mannkopff R. 433
 Manson N. 728, 741, 742
 Marcotte F. B. 627
 Marcus R. A. 237, 239, 290
 Mardaleishvili R. Ye. 82, 109
- Margenau H. 365
 Markevich A. M. 46, 47, 452, 586, 605,
 608, 656
 Marshall R. 334
 Martin R. B. 550
 Massey H. S. W. 383, 384, 469, 470, 476,
 479, 485, 488, 502
 Masson C. R. 109
 Matland C. G. 427, 429
 Matsen F. A. 178, 194, 195
 Maurer W. 493, 494
 Medvedev S. S. 78
 Medvedeva N. I. 73
 Meer N. 92
 Meisels G. G. 509, 518, 519
 Melton C. E. 514
 Melville H. W. 65, 97, 111, 114, 246-248
 Mendeleyev D. I. 54
 Menshutkin N. A. 39
 Meschi D. J. 67
 Mesrobian R. B. 581
 Meyer E. 428
 Mikhel'son V. A. 695, 703, 751, 758, 761
 Miklukhin G. P. 54
 Millest D. M. 498
 Mills R. L. 314, 315
 Milne E. A. 433
 Mitchell A. 430, 434, 438
 Mochalov K. N. 527
 Mohr C. B. O. 469, 470, 479
 Montroll E. W. 134
 Morrell J. C. 541
 Morse P. M. 152, 485
 Mott N. F. 383
 Moore G. E. 454
 Moore N. P. W. 630, 729
 Müffling V. von 589
 Mullins B. P. 671
 Mund W. 248
 Murray R. C. 718, 719
 Muschitz E. E. 490, 491, 511
 Musgrave F. F. 320
 Myers R. J. 67
- Nagihev M. F. 311
 Nakamura J. 690
 Nalbandyan A. B. 44, 52, 53, 83, 99, 111,
 261, 270, 336, 448-451, 602, 605, 611,
 612, 624, 625, 629
 Neiman M. B. 49, 51-53, 72, 108, 112,
 586, 632, 648-650, 692, 694
 Neporent B. S. 394, 395
 Nernst W. 570, 637, 730
 Neuimin G. G. 98, 99, 107, 360, 386-388,
 403, 415, 416, 436, 437
 Newberry S. 499

- Nies N. P. 442
 Nikitin E. E. 135, 136, 272, 274, 381
 Nikitin V. A. 69
 Nordmeyer M. 504
 Norrish R. G. W. 332, 334, 335, 344,
 388-390, 424, 582, 595, 606, 629, 631,
 672, 691
 Noyes W. A. 550, 627
 Nümann E. 381, 384, 402
 Nusselt W. 704
- Obreimov I. V. 290, 298
 Ogg R. A. 260, 551
 Oldenberg O. 65, 105, 350, 359, 393, 444
 Ootuka H. 87
 Ostwald W. 34, 39, 40, 42, 276
 Otsuka M. 496
 Otvos J. W. 477
- Palmer H. B. 273
 Paneth F. 49, 79, 112
 Park, J. D. 252
 Parker J. G. 355
 Parker W. G. 684, 713
 Pascale D. A. 320
 Passauer H. 726
 Patat F. 304, 401-403
 Patrick C. R. 611
 Pauling L. 276
 Pavlov D. S. 67, 68, 733
 Payman W. 696, 697, 756
 Pearson T. G. 420
 Pease R. N. 314, 611, 645, 646, 699, 729,
 735-738, 741, 742
 Peiser A. M. 210
 Pemsler J. P. 70
 Penner S. S. 686, 707, 708, 719
 Penney W. G. 469
 Penning F. M. 484
 Peters K. 534-536
 Petukhov G. P. 54
 Pfaundler L. 4
 Pickering H. S. 729
 Pidgeon L. M. 68, 69
 Pielemeier W. H. 372, 388
 Pitzer K. S. 267
 Polanyi J. C. 114, 137, 172, 174, 568
 Polanyi M. 16, 58, 78, 79, 86, 88, 89,
 91-93, 102, 106, 107, 152, 153, 161, 172,
 179, 230, 260, 276, 658, 662
 Poltorak V. A. 606, 624
 Polyak S. S. 631, 632, 693
 Polyakov M. V. 47, 48, 586
 Poole H. G. 474
 Popov B. N. 98, 99, 414
- Popov E. I. 586
 Porter G. 103, 424, 570, 595, 672
 Potter R. F. 505, 515
 Powell R. E. 267
 Powling J. 713
 Present R. D. 133
 Prettre M. 705
 Prigogine I. 137
 Prilezhayeva N. A. 232, 234-236, 438
 Pringsheim P. 429
 Pritchard H. O. 103, 150, 253
 Pyke J. B. 103, 253
- Rabinowitsch E. 334, 335, 340, 343, 344,
 350, 359, 390, 392, 403, 444
 Ramien H. 474, 483, 484
 Ramsperger H. C. 288, 290, 295
 Rankine A. O. 752
 Rassweiler G. M. 69
 Razuvayev G. A. 54, 112
 Redlich O. 193
 Ree T. 280
 Reeves R. R. 333
 Reichardt H. 105, 106
 Reichenheim O. 523
 Reid J. A. 366
 Rekasheva A. F. 54
 Rice F. O. 45, 106, 112, 263, 367
 Rice O. K. 272, 274, 290, 295, 343-345,
 410
 Richards W. T. 366, 367, 376
 Richardson J. M. 522
 Richardt F. 680, 681
 Riemann G. F. 752
 Rivin M. A. 761
 Robb J. C. 97, 111, 246-248, 611
 Robben F. 371
 Roberts E. K. 237, 238, 240, 265
 Roberts J. K. 587
 Robinson A. L. 339
 Rodebush W. H. 75, 415
 Rogers W. A. 491
 Rollefson G. K. 334, 335, 415, 421, 449,
 454, 455, 459
 Roscoe H. 571
 Rose M. E. 354
 Rosen N. 237
 Rosenstock H. M. 290
 Rössler F. 390, 392
 Rostagni A. 497
 Roth E. 86
 Roth W. 763
 Rowlinson J. S. 373
 Roy A. S. 354
 Rozlovsckii A. I. 696, 726
 Rubin R. J. 134

- Russell K. E. 334-336, 400, 401
 Ryabinin Yu. N. 655, 656
 Rysselberghe P. Van 132
- Sabirova R. D. 310
 Sachsse H. 96, 333, 704, 705
 Sadovnikov P. Ya. 63, 105
 Saha M. N. 689
 St. Auney R. V. 536
 Salkoff M. 364, 366
 Salley D. J. 448
 Samson E. W. 427, 429
 Sato Shin 172
 Sayasov Yu. S. 617
 Schadt C. 270
 Schäfer K. 374
 Schaffernicht W. 468
 Schay G. 86, 89, 90, 658
 Schenk P. W. 98
 Schiff H. I. 103
 Schissler D. O. 517, 518
 Schlessinger L. 550
 Schoen L. 421
 Schott G. L. 611
 Schrödinger E. 119
 Schuler R. H. 549
 Schulte J. W. 554
 Schultz R. D. 550
 Schumacher H. J. 97, 98, 303, 316, 398,
 442, 454, 572
 Schumann T. E. W. 668-670
 Schwab G. M. 80
 Schwartz R. N. 364, 365, 375, 381, 383,
 387
 Schwarz H. A. 551
 Scott W. E. 729
 Semenov Ye. S. 688, 689
 Semenov N. N. 24, 36, 42, 43, 67, 68,
 111, 160, 306, 568, 573, 574, 584, 588,
 593-595, 599, 601, 602, 610, 616, 617,
 619, 623, 624, 634-637, 644, 649, 701,
 705, 706, 710, 716, 723-726, 729,
 731-734, 741, 742, 748
 Sen Gupta P. K. 103
 Shand W. 308
 Shapiro I. 63
 Shaulov Yu. Kh. 696
 Shchelkin K. I. 744
 Shekhter A. B. 98, 101, 512, 513, 533,
 587, 589
 Sheridan W. F. 509
 Sherill M. S. 448
 Sherwin C. W. 511
 Shilov A. Ye. 241, 585
 Shilov Ye. A. 310, 328, 331
 Shilov N. A. 33, 34, 39, 40, 42
- Shtern V. Ya. 108, 582, 631, 632, 693
 Shubina S. M. 44
 Shuler K. E. 134, 135, 346, 447, 568, 690,
 717, 745
 Shlyapintokh V. Ya. 111, 760
 Sida D. W. 505
 Simon D. M. 741, 742
 Simons J. 334-336, 400, 401
 Simons J. H. 504, 505, 507, 510, 511
 Sittig E. 355, 371
 Skalov B. N. 675
 Skurat V. Ye. 415
 Slater N. B. 180, 290, 296-302, 316
 Slawsky Z. I. 364, 365, 375
 Sleppy W. C. 78, 627
 Small N. J. H. 405
 Smallwood H. M. 339
 Smith F. T. 171, 659
 Smith J. H. 314
 Smith N. D. 393
 Smith P. 113
 Smith R. A. 502
 Smith R. P. 279, 280, 282
 Smith W. F. R. 699
 Smithells A. 70, 680
 Snowden F. F. 42
 Sokolik A. S. 688, 694, 761
 Sokolov N. D. 274
 Spalding D. B. 718, 720-722, 742, 743
 Spealman M. L. 75
 Sprenger G. 67, 68
 Stannet V. 581
 Stark J. 452
 Staveley L. A. K. 317
 Steacie E. W. R. 59, 77, 79-82, 93, 97,
 102, 104, 106, 108, 109, 112, 241, 242,
 261-263, 268, 311, 445-447.
 Stephens E. R. 729
 Stepukhovich A. D. 246-248, 261, 264,
 267
 Steenbeck M. 499
 Stein S. 485
 Steinberg M. 761
 Steiner W. 322, 339
 Stern O. 432
 Stevens B. 392, 419, 420
 Stevens F. W. 695
 Stevenson D. P. 477, 517-519
 Stieger G. 442
 Stocks G. W. 720, 722
 Storch H. H. 537
 Stuart H. 433
 Stuckardt S. 465
 Stueckelberg E. C. G. 504
 Style D. W. G. 42, 107
 Sugden T. M. 75, 492, 679, 684, 685
 Sugiura Y. 152

- Sullivan J. H. 175
 Sullivan J. O. 333
 Sun C. E. 172, 336
 Suttle J. F. 554
 Sutton D. J. 483
 Swallow A. J. 560
 Szabó Z. G. 113, 114
 Szwarc M. 79, 249, 263, 275, 304, 312,
 421, 585, 718
 Szillard L. 551

 Tabuchi D. 367
 Taffanel J. 746
 Talbut F. D. 761
 Tal'roze V. L. 415, 516-518, 613
 Tamm I. I. 656
 Tanczos F. I. 365
 Tanford Ch. 729, 735-738, 741, 742
 Taylor E. H. 90, 253
 Taylor H. A. 550
 Taylor H. S. 553
 Taylor J. W. 421
 Ta-You-Wu 207, 209, 210, 483-485
 Teclu N. 70, 680
 Teller E. 193, 263, 352, 384
 Terenin A. N. 107, 232, 234-236, 360,
 386-388, 403, 412, 414-417, 436, 437
 Thabet S. K. 693
 Thieme O. 494
 Thomas C. L. 541
 Thomas J. R. 69
 Thompson H. W. 44, 599
 Thomson J. J. 276, 540
 Thrush B. A. 672
 Tikhomirova N. N. 96, 261
 Tipper, C. F. H. 630
 Todes O. M. 651
 Toennis J. P. 755
 Tompkin J. W. 252
 Torsuyeva H. S. 73
 Trautz M. 324
 Trenwith A. B. 252
 Trittelwitz W. 511
 Trotman-Dickenson A. F. 103, 109, 252,
 253, 263, 268, 304, 308
 Tsirg I. 472
 Tsuchija T. 81
 Tsvet M. S. 72
 Tzepalov V. F. 111

 Ubbelohde A. R. 68, 69, 405
 Ubbelohde L. 725
 Urizko V. I. 47

 Vaerman J. 695
 Vaidya W. M. 74
 Val'ta Z. F. 594
 Van Artsdalen E. R. 264
 Vanpée M. 65, 597
 Van't Hoff J. H. 4, 14, 44, 276, 566
 Van Tiggelen A. 695, 742, 743
 Van Wonterghem J. 743
 Varney R. N. 497-499
 Vasil'ev S. S. 535
 Vedeneev V. I. 630
 Verhoeck F. H. 36
 Vieille P. 751
 Vogelaere R. de 195
 Volman D. H. 108, 429
 Volmer M. 62, 320, 432
 Volpi G. G. 104
 Voronkov V. G. 601, 731-734
 Voyevodskii V. V. 82, 96, 99, 109, 114,
 165, 166, 261, 336, 589, 606, 611-613,
 619, 624, 625, 630, 651

 Waage P. 3
 Wagner H. G. 686, 761
 Wagner O. H. 535, 536
 Wahl M. H. 415
 Wahrhaftig A. L. 290
 Walden P. I. 260
 Walker R. A. 375
 Wallenstein M. B. 290
 Walls N. S. 756
 Walsh A. D. 336, 691
 Walter J. 263
 Wannier G. H. 476
 Warhurst E. 93
 Wayland H. 498
 Weiss H. G. 63
 Wentink T., Jr. 333
 Weizel W. 501
 West W. 420, 550
 Westhaver J. W. 532
 Weston R. E. 59
 Whaley F. R. 106
 Wheeler R. V. 696, 697
 White J. U. 105, 371
 Whiteway S. G. 109
 Whittle E. 59
 Widom B. 379-381
 Wieland K. 76
 Wiener H. 538
 Wigner E. 213, 222, 257, 336, 340, 399,
 724
 Wiig E. O. 454
 Wijnen M. H. J. 265
 Wilhelm R. 554
 Willard J. E. 273, 551

- Willbourn A. H. 336
Willey E. J. B. 535
Williams R. R. 518, 551, 559
Wilson M. J. G. 709, 711
Winkler C. A. 104, 105, 333
Withrow L. 69
Wohl K. 745
Wolf F. 507, 513
Wolfhard H. G. 664, 673, 684, 698, 699,
 713, 729, 744, 745, 758
Wolfsberg M. 194
Wood R. W. 93, 358, 428, 429, 444
Wood W. C. 335
Wray K. L. 333
Wright F. F. J. 103, 570
Wulf O. R. 454
Wurster W. H. 364
- Yakovlev V. I. 645
Yavorskii B. M. 469
- Yel'yashevich M. A. 392
Zagulin A. V. 448, 599, 642, 643
Zakharova V. M. 471, 472
Zandberg E. A. 507, 508, 514
Zartmann I. 354
Zeise H. 256
Zel'dovich Ya. B. 36, 63, 105, 515, 645,
 647, 651, 701, 705, 706, 708, 710, 713,
 715-719, 723-726, 729, 732, 738, 741,
 742, 744, 746-751, 754, 755, 758, 760,
 762-765
Zelikoff M. 492
Zemansky M. W. 430, 434, 438
Zener C. 217, 219, 354, 362-364, 379,
 383, 402
Zilitinkevich S. I. 527
Zimakov P. V. 584
Zinman W. G. 755
Ziskin M. S. 65, 438, 439, 645, 646
Zwolinsky B. J. 138

S U B J E C T I N D E X

- Acceptor 29
Adiabatic
explosion 650
processes 117, 124-127, 200
Autocatalysis 40-43, 624
Born method (Born approximation)
201-204, 470
Bremsstrahlung 547
Catalytic recombination method 80
Chain breaking
quadratic 587
linear 588
Chains
completely branched 593
energy 568
mixed 568
Characteristic reaction time 5, 55
Charge transfer (exchange)
asymmetrical 505, 507-511
symmetrical 505-507
Chemical induction 29-34
Chemiluminescence 75, 84, 88
Collision stabilization of the quasimolecule
228, 229
Collisions of the first and second kind
168, 169
Complex radicals 113, 114
Coupled reactions 29-32
Degenerate
branching 601-603
explosion 595, 634
Delta distribution of energy 135
Diffusion
of radiation 433
propagation of flames 718, 728-742
Discharge
arc 526
condensed 520
corona 520
electrodeless 525
glow 521-525
high-frequency 525
microwave 526
silent 519
spark 520
torch 527
Dispersion of ultrasonic waves 366-379
Disproportionation 7, 108, 268, 582, 587
Dissociative recombination 491
Equilibrium
in flames 684-690
radiation 75
Factor
excitation 75
induction 29, 34
Flame
candle 671, 672
front structure 687, 711-713
Flames
cool 690-694
diffusion 657-673
flat 711
highly-rarefied 84-92, 658-662
hot 679-690
rarefied 673-677
separated 70, 680
turbulent 670
Flash photolysis 107, 413, 424
Franck-Condon principle 529
Function
excitation 467-474, 493-495
ionization 467, 474-480, 496-500
Morse 152, 209
Gas-kinetic cross section 146
Homogeneous catalysis 32-38
Hot particles 549-551, 568
Hugoniot's curve and equation 735-755,
760-762
Ignition peninsula 594-599
Impact parameter 139
Induction period 571, 633, 63,
Inductor 29, 34
Inhibitor 38, 423, 606, 750
Interaction of chains 601-603
Intermediate substances 17, 30, 32, 35,
61, 66-84, 561
Isotope effect 56-60
Isotopic exchange 49, 54, 81
Koval'skii's method 45-48

- Labelled-atom method 48-60
 Law
 autocatalytic 39-42
 Lambert-Beer 406-409
 of mass action 3, 4, 17
 Semenov 595, 617, 636
 Limiting process 59, 64, 320
 Limits
 ignition 594, 597-599, 609, 617-619
 624-627, 732
 of flame propagation 731-734
 London equation 152, 157-160, 216, 244
 Mass-spectrometric method 81
 Method
 of distorted waves 201, 205, 206
 of isotopic exchange 49, 54, 81
 of partial stationary concentrations 24, 616
 of quasi-stationary concentrations, see
 Steady-state method
 Mirror method 79
 Normal vibrations 162, 170
 Non-adiabatic processes 117, 124-127, 200
 Para-ortho
 conversion 77, 95
 method 77
 Path length of ionized particles 542-547
 Periodic chemical processes 691-693
 Peroxide theory of oxidation 19, 20
 Photo-ionization 414
 Plasmas 524, 527
 Poisson's curve 753, 755
 Polarographic method 71
 Predisociation 417, 418, 425, 441, 455, 457
 induced 408, 418, 441
 Pre-explosion heating up 640
 Proton transfer 515-519
 Pseudo-Boltzmann distribution of energy 133-138
 Quenching method 67
 Racemic mixture 260
 Radiation stabilization of molecules 228-230, 235
 Radiochromatography 72
 Reaction region
 diffusion 588-590
 kinetic 590
 Relaxation time, thermal 132, 135, 365, 367, 372, 394
 Steady-state method 24, 32, 621, 720
 Stepwise excitation 472
 Steric factor 16, 200, 663
 Stern-Volmer formula 432-434
 Stoichiometric concentrations 3
 equation of reaction 2, 36
 order of reaction 4
 Temperature coefficient of reaction rate 15
 "electronic" 524, 527
 ignition 647
 "rotational" 133, 392, 486, 686, 687
 "translational" 133, 392
 "vibrational" 133, 392
 Thermal chromatography 72
 neutrons 548
 radiation 75
 relaxation 346
 Third ignition limit 624-627
 Toluene method 310
 Transmission coefficient 176, 180, 194-196
 True activation energy 16, 253, 266, 461
 Tunnel effect 210, 295
 Turbulent reactor 692
 Two-stage ignition 648-649
 Walden inversion 260
 Wigner's principle 222
 Zero-point energy 155